GM 56134

PROGRAMME DE TRAVAUX, PROJET ARGILE, EAU, MER

PROGRAMME DE TRAVAUX POUR LE RENOUVELLEMENT DES PERMIS DE RECHERCHE DE SUBSTANCES MINÉRALES DE SURFACE : PRS 0002039-0002040-0002041-0002042-0002043-0002044

1) DESCRIPTION DU PROJET

Les concepts généraux de ce projet sont l'argile, l'eau et la mer d'où la raison sociale de la corporation *Argile Eau Mer* qui s'est donnée comme objectif principal de caractériser l'argile marine ou fluviale de Baie Saint-Ludger, plus particulièrement celle qui est en liquéfaction, pour déterminer des usages en cosmétique et en thérapeutique.

Baie Saint-Ludger .est située à environ 20 kilomètres à l'ouest de Baie-Comeau. Ce petit village forme la baie de la péninsule Manicouagan laquelle a été constituée par le rejet des sédiments de la rivière aux Outardes et de la rivière Manicouagan. L'accès au secteur se fait aisément à partir de la route 138 par une voie secondaire pavée qui longe la rive du fleuve Saint-Laurent sur une distance d'environ 13 kilomètres.

Ce village, qui a un sol presque entièrement argileux, présente des caractéristiques géophysiques et synergiques intéressantes en raison de sa rive sud qui s'ouvre sur le fleuve Saint-Laurent dans lequel viennent se déverser ruisseaux, rivières et eaux d'infiltration des tourbières qui habitent sa surface en son centre et sur sa rive nord.

Ces tourbières, qualifiées de savane, sont présentes sur les terrains réservés par le Ministère des ressources naturelles à l'entreprise *Argile Eau mer* pour lui permettre d'exercer des recherches sur l'argile par le biais de six titres miniers de permis de recherche de substances minérales de surface, (PRS) totalisant cinq cent quatre-vingts (580) hectares. Les terrains désignés par les permis de recherche sont situés sur le rang 1 (PRS 0002039-0002040) et le rang Pointe-aux- Outardes (PRS 0002041-0002042-0002043-0002044)

L'argile, qui forme la presque totalité des couches du sol par interstratification, est visible à partir de la plage. Cette argile est traversée par trois eaux : celle de la savane, celle de la mer-fleuve et à certains endroits par celle des rivières. Cet alliage d'eau salée, d'eau douce et de savane renforce l'hypothèse de base que l'argile présente des propriétés spécifiques pour des usages en thalassothérapie et en cosmétique.

2) MÉTHODE ET CONNAISSANCES

Deux méthodes sont suivies pour réaliser ce projet. D'abord, pour caractériser l'argile c'est la dialectique qui est utilisée parce qu'elle part du principe des interrelations qui existent dans la matière énergétique. Ces relations permettent d'expliquer le particulier par rapport au général, la partie par rapport au tout, le local par rapport au global, la contradiction par rapport à la différence et à la synthèse. Ensuite, pour connaître les propriétés spécifiques de l'argile de Baie Saint-Ludger, la méthode expérimentale est privilégiée dans le sens que la recherche est construite dans l'objectif d'analyser systématiquement les données afin de vérifier l'hypothèse de base.

La connaissance des argiles relève des sciences de la nature telles que la physique, la chimie, la géologie, la minéralogie et la granulométrie.
Des consultations auprès d'experts et de spécialistes de différents ministères, institutions universitaires aident a inventorier des manières de procéder pour faire la recherche. Des analyses de laboratoire sur des échantillons d'argile, des recherches documentaires, des stages de formation et des participations à des congrès contribuent également à orienter le projet de recherche quant aux technologies qui doivent être développées.

L'ensemble de ces connaissances technologiques et scientifiques seront ensuite soumises à l'expérimentation pour vérifier les caractéristiques spécifiques de l'argile de Baie Saint-Ludger en fonction de concevoir des « prototypes » en cosmétique et en thérapeutique.

Finalement, une vision environnementaliste anime cette recherche puisque le projet d'*Argile eau mer* veut contribuer au renforcement des rives de Baie Saint-Ludger.

Les «catégories suivantes»: la caractérisation de l'argile sensible et du gisement, la transformation de l'argile en produits et les modalités d'exploitation représentent les différents champs d'activités du présent programme des travaux de recherche et se retrouveront plusieurs fois au travers le présent texte.

3) TRAVAUX

Ce programme des travaux est décrit à partir des quatre «catégories» suivantes : caractérisation de l'argile et du gisement, moyens d'extraction des argiles et produits d'argile pour les usages cosmétiques et thérapeutiques

3.1 La caractérisation de l'argile

La formule chimique, la minéralogie et la granulométrie de l'argile de Baie Saint-Ludger sont, en partie, connues ce qui représente un avancement puisqu'aucun travail antérieur n'avait été fait pour caractériser le type d'argile dans la région concernée (voir le rapport relatif aux travaux miniers)

La synthèse des connaissances théoriques générales appliquées au secteur de Baie Saint-Ludger représente également un progrès puisqu'on sait maintenant qu'il existe un niveau d'argile épais d'au moins 5 mètres, s'étendant sur plusieurs kilomètres. On peut l'observer d'ailleurs sur un bonne partie de ses berges.

On sait également que les argiles en liquéfaction se retrouvent dans les couches profondes du sous-sol entre 30 et 35 pieds. Or, ce sont ces argiles qui présentent les caractéristiques requises pour les usages en cosmétique et en thérapeutique en raison de leur couleur, de leur texture et de leur contenu aqueux. On peut donc procéder à des échantillonnages pour caractériser l'eau interstitielle afin de faire ressortir la spécificité des argiles de Baie Saint-Ludger puisque celles-ci, tout comme d'autres argiles en liquéfaction du Québec, ont le niveau de sensibilité le plus élevé au monde. Leur caractérisation en fonction de leurs utilisations cosmétiques et thérapeutiques ferait progresser la connaissance de cette sorte d'argile et pourrait servir à découvrir de nouveaux usages.

Ce qui détermine l'orientation pour faire les analyses sur des échantillons d'argile ce sont les caractéristiques et propriétés recherchées dans la matière première. Étant donné que la couleur, la texture et l'homogénéité de certaines couches d'argile de Baie Saint-Ludger semblent convenir à des usages de soins corporels, les analyses préfigurées pour vérifier cette hypothèse sont les suivantes :

L'analyse chimique pour obtenir une formule moyenne type par l'identification des éléments présents dans les échantillons. Cette formule est établie en :

- comparant les divers résultats des analyses effectuées sur les échantillons prélevés dans les différentes couches du gisement et à la surface;

- analysant l'homogénéité et les variations des éléments chimiques;

- vérifiant la présence ou l'absence de substances toxiques pour l'organisme humain tels que le plomb, le mercure et les éléments radioactifs lourds comme le radium ou le strontium;

- identifiant le pourcentage de silice libre et la présence d'iode puisqu'il s'agit d'une argile

L'analyse physique pour connaître la plasticité, la résistance mécanique, la gamme de vitrification, la nature réfractaire, la couleur de surface cuite et l'absorption de l'argile.

L'analyse de la granulométrie pour connaître la taille des particules.

L'analyse de l'eau interstitielle ou l'analyse de la chimie des eaux pour déterminer le contenu aqueux de l'argile sensible. Comme l'argile est une matière qui a une intimité avec l'eau et que celle qui existe dans une couche inférieure du terrain devient liquide lorsqu'elle est maniée, il faut aussi analyser la teneur d'eau de l'argile pour :

❋ connaître les caractéristiques physiques, chimiques et minéralogiques de cette eau. Ces analyses sont très importantes pour distinguer les argiles du Québec des autres argiles puisque ce sont les aspects physico-chimiques de l'eau qui la différencie. C'est également l'eau interstitielle qui fait que les argiles des basses terres du Saint-Laurent ont le niveau de sensibilité le plus élevé au monde;

❋ classifier l'argile selon sa cohésion (de très molle à molle);

L'analyse du contenu organique pour repérer les micro-organismes s'ils sont présents ce qui serait probable compte tenu de la présence des tourbières à la surface des terrains.

Cette caractérisation étant réalisée, il y aurait un progrès puisque les propriétés chimiques et physiques de l'argile de Baie Saint-Ludger seraient, pour la première fois, connues ce qui pourrait permettre d'en déterminer les usages les plus prometteurs. De plus, le contenu aqueux de l'argile fluviale sensible n'a jamais été analysé au Québec en fonction des usages cosmétiques et thérapeutiques. L'analyse des eaux interstitielles serait donc, aussi, une première et cela pourrait conduire à des avancées technologiques intéressantes.

Ces différentes analyses seront ensuite comparées aux autres déjà analysés effectuées (voir le rapport des travaux relatif aux travaux miniers).

C'est M. Jean-François Wilhelmy, du Centre de recherches minérales, qui effectuera ces analyses. Mme Jeanne Percival, de la Commission géologique du Canada, sera également consulter pour donner son expertise.

3.2. La transformation de l'argile en produits cosmétiques et thérapeutiques

L'ensemble des connaissances issues des différentes recherches, enquêtes et formations ont permis de déterminer le type de produits d'argile qui serait le plus intéressant à commercialiser. Comme l'argile est fort peu connue dans les centres de beauté et de santé du Québec son plein potentiel d'utilisation reste à développer. Son origine marine ainsi que sa liquéfaction la positionne avantageusement dans la tradition thermaliste du réseau québécois puisque l'eau de mer a la réputation d'avoir un effet bienfaisant dans ce type de traitement. Les thérapeutes sont à la recherche de nouvelles façons d'intégrer les produits de la mer dans leurs soins.

Toutes ces raisons font que le prototype d'un produit de boue thérapeutique ayant conservé son contenu aqueux est retenu comme produit utilisable dans les centres de beauté et de santé.

Cette boue d'argile pourrait remplacer les algues dans les traitements puisque celles-ci contiennent de l'iode et qu'un certain nombre de clients et clientes en sont allergiques. Ce produit d'argile peut contribuer à donner de nouveaux bienfaits aux traitements lorsqu'utilisée en synergie avec d'autres produits et thérapies parce ses propriétés absorbantes-adsorbantes tirent les substances malsaines, fixent les enveloppements sur la peau et y fait pénétrer les minéraux réparateurs. De plus, ses propriétés cicatrisantes pourraient augmenter les bienfaits procurés par les masques de beauté et les sablages corporels. Ses propriétés de conducteur peuvent également contribuer au bien-être des enveloppements. Son contenu aqueux (l'eau interstitielle) peut procurer les avantages qu'offre la thalassothérapie par l'usage de l'eau de mer.

En ce qui concerne les relais de santé, le développement d'une thalassothérapie à Baie Saint-Ludger est la stratégie qui s'avère la plus réalisable pour promouvoir le produit en permettant de créer une appellation d'origine. Ce centre pourrait devenir une sorte de laboratoire pour le développement de produit à «conditionner» pour la distribution.

Dans les centres de produits naturels, l'argile est beaucoup plus connue tant au niveau de ses propriétés qu'au niveau de ses usages comme produit naturel et comme produit transformé. On retrouve de l'argile dans plusieurs produits comme les savons, masques de beauté, shampooings, crèmes... etc. À l'état naturel, elle est présentée en cataplasmes, en bandes ou encore dans des sacs de papier.

Les centres de produits naturels pourraient devenir un créneau important pour la commercialisation de l'argile de Baie Saint-Ludger en raison de leur potentiel d'utilisation et aussi leur permettre de réaliser des économies sur le transport puisque l'argile qu,ils utilisent est importée. Son origine fluviale et ses propriétés spécifiques pourraient aussi contribuer à son succès si elle était vendue à l'état naturel.

Le produit-type retenu pour ces centres est donc une argile présentée à l'état liquide, plutôt qu'à l'état de poudre, dans des contenants de verre. De plus, cette présentation ferait sa différence et sa nouveauté par rapport aux autres argiles offertes sur le marché.

Dans le secteur des pharmacies qui dominent nettement la distribution des cosmétiques et produits de toilette incluant les produits pour les soins de la peau, un produit « grand public » est projeté sous la forme d'un pansement (de différentes grandeurs) et de ses dérivées : le cataplasme et la compresse.

Une perspective à envisager serait de diversifier l'utilisation de l'argile pour rentabiliser son extraction et sa transformation.

Cependant, pour réaliser ces produits, les analyses mentionnées dans la caractérisation de l'argile s'avèrent indispensables puisqu'il faut s'assurer que cette argile soit de bonne « qualité ». Par le fait même, il faut aussi connaître les règlements et lois qui régissent l'utilisation des argiles en thalassothérapie et en esthétique.

La prochaine étape consiste donc à prélever quelques échantillons représentatifs sur le terrain ainsi qu'à réaliser les tests et analyses nécessaires pour déterminer si ces argiles rencontrent les conditions de qualité pour le marché des produits en thalassothérapie et en cosmétique. Il faudra, entre autres, procéder à des analyses chimique des éléments, de l'eau interstitielle et des micro-organismes pour repérer, s'il y en a, les composés toxiques, la teneur en bactéries, et les éléments traces... etc.

Dans une deuxième étape, il faudra s'assurer d'un bon produit sur le marché : couleur, douceur, teneurs en certains minéraux.... etc. Si les argiles rencontrent ces conditions et critères, alors les actions pour caractériser le dépôt d'argile
pourront être entreprises.

Monsieur Patrice Hildgen de l'École supérieure de pharmacie de l'Université de Montréal, ainsi qu'une personne rattachée à Santé Canada aideront à orienter les travaux de ce secteur d'activités.

3.3. La caractérisation du gisement

Des études géologiques ont démontrées que les dépôts meubles de la région sont en grande partie deltaïques ; ils comprennent du sable, du silt et de l'argile. La stratigraphie est complexe parce que les sédiments deviennent plus grossiers ou plus fins, selon qu'on se rapproche ou qu'on s'éloigne de l'ancienne embouchure de la rivière aux Outardes. Cette embouchure est située au niveau des dépôts meubles et du socle précambrien. La surface du delta est parsemée d'anciens chenaux remplis de dépôts de sable et de gravelle, généralement recouverts de tourbe et de matière organique.

Par rapport à la région, le gisement est défini sur le territoire par les dimensions déterminées par les PRS. La caractérisation du gisement se fait par le prélèvement d'échantillons dans la profondeur des terrains et à leur surface soit manuellement, soit par des forages. Pour échantillonner sur toute la surface et dans toute la profondeur, il faut considérer la diversité des couches de terrain ainsi que la présence des différentes substances minérales et organiques. Les échantillons prélevés sont ensuite acheminés vers des laboratoires pour être analysés.

La liste de paramètres à suivre pour caractériser le gisement est la suivante :

■ Trouver les limites physiques du dépôt d'argile à l'aide d'une cartographie de surface et de tranchées, de sondages géophysiques et de forages (carottiers) : forme générale du dépôt, longueur, largeur, épaisseur, présence de lentilles d'argile ... etc.

■ Déterminer le nature et l'épaisseur de la couche de stérile recouvrant le dépôt d'argile.

■ Estimer le tonnage total des réserves d'argile de type commercial : un programme d'échantillonnage et de caractérisation (géotechnique, minéralogique et chimique) des échantillons devra être exécuté afin de bien définir la valeur économique du projet. Les résultats des essais de caractérisation serviront autant pour établir la valeur marchande du dépôt que pour l'étude des conditions d'exploitation et de sécurité du chantier. Certains résultats, en particulier les données géotechniques, pourront servir dans l'évaluation des travaux de restauration du site.

■ Tracer, à partir des critères de qualité retenus, des frontières (iso-contours) sur les plans d'exploitation afin de bien limiter les zones riches, moyennes et passables.

Monsieur Camil Kobzi, expert géologue, agira comme conseiller dans cette démarche

3.4. Les moyens d'extraction des argiles liquides

Le mode d'exploitation envisagé est conditionné par la nature du territoire de la péninsule

Manicouagan entourée d'eau, composée presque exclusivement d'argile et comportant plusieurs savanes à sa surface.

La transformation que les produits cibles devront subir pour les rendre conformes aux exigences de la mise en marché implique des études de faisabilité quant aux méthodes, aux techniques, aux équipements et aux installations nécessaires à l'extraction et à la transformation de l'argile. Ces études doivent aussi inclure le niveau de compétence technique et théorique du personnel.

L'érosion qui frappe durement et régulièrement les berges de la péninsule Manicouagan provoque des coulées d'argile qui sont dues à la sensibilité de ces matériaux (Chagnon, 1968). Le degré de sensibilité de cette sorte d'argile fait qu'elle perd complètement de sa résistance pour se transformer en liquide lorsqu'elle est maniée. Il faut tenir compte de cette formation géologique pour développer des méthodes d'extraction et d'installations sécuritaires.

Les études effectuées au Québec et dans les pays scandinaves ont démontré l'efficacité des méthodes de calcul de glissement de terrain utilisées en géotechnique par la mesure des caractéristiques mécaniques des sols et de la connaissance de la nature de ceux-ci. La recherche sur l'argile de Baie Saint-Ludger mentionne plusieurs facteurs pouvant contribuer à l'érosion des rives mais parmi ceux-ci, la sensibilité des argiles semble être le facteur le plus important. Or, les argiles de Baie Saint-Ludger sont reconnues pour être, à certains endroits, extrêmement sensibles. On sait aussi qu'à ce degré de sensibilité l'argile perd complètement de sa résistance pour devenir liquide. Il faut donc tenir compte de cette formation géologique pour développer des méthodes d'extraction et d'installation efficaces.

Bjerrum, un célèbre géotechnicien de Norvège a écrit : « Nous devons vivre avec l'argile sensible, construire nos industries sur le dépôt, apprendre à résoudre les problèmes qu'elle pose ». La Norvège est l'endroit au monde où la connaissance de la mécanique des sols est la plus avancée en raison des travaux de recherche qui ont permis de comprendre les causes des glissements de terrain. Ces études pourront être consultées pour déterminer le mode d'exploitation, les méthodes d'extraction et d'installation. On pourra également consulter l'étude effectuée par M. Serge Hüppé du CRIQ pour le compte *d'Argile eau mer* qui mentionne plusieurs moyens d'extraction des argiles et plusieurs moyens de stabilisation des rives après l'extraction.

Les méthodes d'extraction présentement envisagées sont le **pompage** et/ou la **succion** ainsi que des moyens d'extraction sur pneumatique. Cependant, ces méthodes devront être étudiées par un ingénieur géologue et/ou une firme d'ingénieurs expérimentés qui pourront alors faire des recommandations concernant la stabilité et l'intégrité des terrains concernés. Les données fournies par ces études nous permettront de :

❖ vérifier s'il est possible techniquement d'extraire et de raffiner l'argile ;

❖ évaluer l'ampleur des investissements requis ;

❖ juger si ces exigences techniques et financières sont toujours compatibles avec les objectifs du projet. S'il y a compatibilité, il s'agira ensuite d'élaborer un plan d'affaire.

Plusieurs facteurs écologiques, géologiques et techniques doivent également être considérés pour déterminer de façon plus précise le mode d'exploitation. Des hypothèses sont déjà envisagées. À court et moyen terme, il faut attendre les résultats des travaux de caractérisation du gisement pour continuer la recherche sur les techniques d'exploitation. Si ces résultats sont positifs, on pourra procéder aux actions suivantes :

■ Choisir les équipements d'exploitation en fonction du niveau de production désiré (T.m./jour), des propriétés physico-chimiques de l'argile, de l'environnement physique de surface, de la nature des sols contenant l'argile, des contraintes environnementales spécifiques et de l'ampleur, des dimensions, de la forme et de la position du dépôt d'argile par rapport à la surface du sol.

■ Déterminer si l'argile extraite nécessitera un traitement ou une série de traitements avant son utilisation. Si oui, il faudra établir le schéma de traitement et déterminer les équipements requis.

■ Déterminer le moyen de transport de l'argile vers la station ou l'usine de traitement.

■ Déterminer les coûts d'exploitation, de transport, de traitement... etc. Effectuer une étude de préfaisabilité, incluant un « cash flow ».

Monsieur Denis Lessard, ingénieur géologue, du Centre de recherche minérale qui est déjà intervenu dans ce dossier poursuivra le travail déjà amorcé.

comportement des sols à Chute-aux-Outardes en fonction de la construction du barrage Outardes II.

✓Contacts auprès de l'Association des relais de santé, des centres de thalassothérapie et des instituts esthétiques pour bénéficier des informations récentes sur le marché en vue de l'élaboration du plan d'affaires pour le centre de thalassothérapie.

✓Discussion avec la Dr Jeanne Percival de la Commission géologique au sujet des analyses sur les échantillons d'argile et sur la travail de recherche. Elle doit produire le rapport de recherche bientôt.

✓Première Lettre de Monsieur Huppé annonçant la réorientation des actions dans les études sur les moyens d'extraction. Sa deuxième lettre fait état de la seconde rencontre avec M. Denis Lessard, ing.,M.Sc. du Centre de recherches minérales du Québec. Celui-ci avait été consulté pour offrir son expertise au sujet de l'investigation requise, des actions à poser et des paramètres à connaître pour caractériser le gisement d'argile à Baie Saint-Ludger. Dans sa lettre M. Huppé décrit la nature et la portée des gestes à effectuer.

✓ Rencontre à Québec avec M. Jean François Bertrand, directeur de la Station de recherche sur la pomme de terre des Buissons, au sujet du site pour la construction du centre de thalassothérapie. Contact avec M. Mercier de l'Hydro-Québec à ce même sujet.

Octobre 1997

✓Demande d'appui au conseil municipal pour l'achat d'une partie de lot et pour la mise sur pied du centre de thalassothérapie.

✓ Discussions avec M. Dominic Ménard pour savoir s'il est possible d'augmenter l'assistance financière dans le cadre de l'entente Canada-Québec pour des travaux technico-économiques afin de tenir compte des nouveaux développements survenus dans la recherche du CRIQ. Je lui soumettrai une proposition à ce sujet.

✓ Conversation téléphonique avec Mme Lynda Duchesne du MRN du Canada pour l'informer des nouveaux développements dans la recherche

Novembre - décembre 1997

✓ Réception d'une copie préliminaire du rapport de Mme Percival. Cette copie contient seulement les données des analyses minéralogiques semi-quantitatives. Plusieurs autres informations s'ajouteront dans le rapport que doit remettre Mme Parcival au mois de novembre.

✓ Demande d'une offre de service à M.Denis Lessard du CRM du Québec pour une recherche sur la caractérisation du gisement en fonction de déterminer de façon plus rigoureuse les critères de qualité des argiles sensibles de Baie Saint-Luger, de connaître le tonnage total des réserves d'argile de type commercial et de savoir si l'argile extrait nécessitera un traitement ou une série de traitements avant son utilisation. Le moyen de transport de l'argile vers la station ou l'usine de traitement ainsi qu'une estimation des coûts liés à l'exploitation, au transport et au traitement seront aussi examinés.

C'est cette demande d'offre de service qui sera soumise à M. Ménard pour une assistance financière.

✓ Discussions téléphoniques avec M. Luc Arsenault du FREM de la Côte-Nord et envoi de la documentation faisant état des développements récents dans la recherche. Demande d'une aide financière et de l'assistance géologique du FREM pour trouver les limites physiques d'une partie du dépôt d'argile à l'aide d'une cartographie de surface et de tranchées, de sondages géophysiques et de forages.

ACTIVITÉS CONNEXES

Cette description du travail technique effectué durant la période relative à la réclamation ne comprend pas les activités connexes telles que :

✗ Les rencontres avec des personnes qui ne sont pas directement impliquées dans la recherche mais qui servent soit à inventorier des pistes de recherche, soit à trouver des sources de financement. Ces rencontres ont lieu avec des représentants des institutions municipales, régionales et gouvernementales.

✗ L'abondante correspondance nécessaire pour présenter et faire comprendre le projet.

✗ Les nombreuses conversations téléphoniques pour réaliser l'ensemble des démarches.

✗ La consultation des livres, journaux et revues spécialisées et ce à chaque étape de la recherche.

✗ La participation à des séminaires, colloques, conférences et associations professionnelles.

✗ Les enquêtes sur le terrain et l'élaboration de stratégies d'action et d'interventions.

✗ Le travail de bureau pour la correspondance et la recherche.

✗ Les voyages et les déplacements.

RECHERCHES ET ÉTUDES

◆ **Recherche sur l'argile à partir de deux grands secteurs d'activité : la cosmétologie et la médecine**, Chantal Giroux G., Groupe matériaux et procédés, CRIQ, juillet 1993

◆ **Recherche préliminaire sur l'argile de Baie Saint-Ludger**, Denise Saulnier, été 1994

Cette recherche explique la formation de la péninsule Manicouagan à partir d'études géologiques. Elle expose également les propriétés chimiques et physiques de l'argile marine ainsi que sa structure en référant aux études de Jean-Yves Chagnon sur *Les coulées d'argile dans la Province de Québec* lesquelles étudient aussi le phénomène de la liquéfaction des argiles. Les coulées argileuses sur la rive gauche de la Rivière aux Outardes à partir des travaux de J.D. Allard sur les *Zones exposées aux mouvements de terrain dans la région de Chutes-aux-Outardes* sont ensuite commentées au niveau régional pour rendre compte de la formation géologique de Baie Saint-Ludger. Finalement, elle qualifie l'argile que l'on retrouve sur les terrains où s'effectue la recherche à partir d'analyses sur des échantillons observés dans les laboratoires.

◆ **Recherche documentaire sur l'emploi en thérapeutique et en cosmétique, sur les propriétés de l'argile en général et sur l'argile marine** par Marie-Hélène Dupuis du service de la Bibliothèque de l'École polytechnique de l,Université de Montréal.

Cette recherche a été effectuée à partir des banques de données Electre, Chemical abstracts, Pascal ainsi que sur les catalogues de bibliothèques de l'Université de Montréal et sur l'index papier « Repère ». Se joignent à cette documentation des références aux argiles en général et aux argiles marines dans les domaines de la géologie et de la minéralogie. Plusieurs études sur l'environnement des argiles : les « facies » sont aussi mentionnées ainsi que sur les produits d'argile de consommation.

Cette recherche documentaire s'ajoute aux ouvrages théoriques spécialisées sur les argiles qui avaient été consultées et sur les brochures concernant les directives de la direction des médicaments du Ministère de la santé du Canada. Elle contient les titres de livres, études et articles sur les multiples usages des argiles thérapeutiques et cosmétiques et sur les produits composés d'argile.

◆ **Étude de marché**, déposée au MICSTQ, secteur de la pétrochimie, par Pierre Hubert, Firme Topomarketing, août 1995 .

Cette étude est de nature qualitative. Plusieurs chapitres portent sur des recherches sur les produits d'argile en cosmétique et en thérapeutique. L'étude déborde donc le cadre du marché.

Programmes

◆ **Programme de travaux de recherche** pour l'obtention de PRS déposé au service des titres miniers MRNQ, Denise Saulnier, janvier 1994.

◆ **Programme de travaux de recherche** pour l'obtention de PRS soumis au service des titres miniers MRNQ, Denise Saulnier,janvier 1996.

◆ **Programme** d'incitation concernant des projets de recherche scientifique et de développement expérimental, Denise Saulnier, présenté aux Ministères du Revenu, novembre 1997.

Rapports

◆ **Rapport sur l'argile de Baie Saint-Ludger**, Luc Arsenault et Bertrand Brassard, FREM de la Côte Nord.

◆ **Rapport** des analyses des échantillons, André Chagnon , CRSQ, mars 1996

◆ **Rapport des travaux de recherche** (janvier 1994 - janvier 1996), Denise Saulnier, déposé au service des titres miniers, MRNQ.

◆ **Rapports sur les entrevues** réalisées avec Henri Pisani et Nadia Tchernenko, Denise Saulnier, août 1995

◆ **Devis** du CRIQ sur les **Techniques d'extraction des argiles souterraines**, mars 97.

◆ **Preliminary Report**, Semi-quantitive Clay Mineralogical and Particle Size Analyses, Christine Burton and Jeanne Percival, novembre 1997.

◆ **Rapport** sur les Techniques d'extraction des argiles souterraines, Serge Huppé, CRIQ, novembre 1997.

Correspondance

Toute la correspondance impliquée dans ce dossier peut être consultée sur demande

Personne responsable de la recherche

La personne responsable de la recherche est Denise Saulnier, présidente de la compagnie *Argile eau mer.*

Diplômes

Baccalauréat ès arts de l'Université Laval à Québec (1964-1968)

Maîtrise en philosophie de l'Université de Montréal (1969-1972)

Certificat en informatique appliqué à l'éducation de l'Université du Québec à Montréal (1982-1987) et des crédits pour un certificat de perfectionnement en enseignement de l'Université de Sherbrooke (1988-1996)

Certificat en enseignement de l'anglais (à compléter par 3 crédits) de l'Université de Montréal (1989-1991) et de l'Université Mc Gill (1991-1994)

Expérience

Vingt-deux (22) ans d'expérience dans l'enseignement de la philosophie au CEGEP Lionel-Groulx, Sainte-Thérèse de Blainville et de multiples expériences dans la défense de causes sociales.

Habiletés

La formation philosophique et pédagogique ainsi que l'expérience dans l'enseignement rendent la personne apte à :

⊗ exercer un travail de recherche en utilisant diverses habiletés intellectuelles telles que l'analyse, la synthèse, l'induction, la déduction et la logique ;

⊗ analyser les structures sous-jacentes de la société afin de comprendre les événements sociaux, politiques et économiques en relation avec ces structures ce qui lui permet de les situer dans le contexte actuel de mondialisation ;

⊗ comprendre les exigences de la rationalité pour les appliquer à la rationalité scientifique ce qui rend possible la théorisation, l'expérimentation et la vérification des hypothèses de départ ;

⊗ coordonner une recherche multidisciplinaire en ayant la formation pour comprendre la synthèse des résultats des sciences de la nature, sociales, humaines et appliquées. La mise en relation de ces résultats permet de tracer les orientations dans la recherche ;

⊗ écrire et communiquer chacune des étapes du processus de la connaissance et de la recherche ;

⊗ former du personnel en ayant recours aux principes et méthodes pédagogiques ;

⊗ intervenir publiquement pour communiquer la vision générale et les éléments plus particuliers du projet.

La formation en informatique appliquée à l'éducation fait:

La formation en informatique appliquée à l'éducation fait:

⊗ comprendre les grands enjeux technologiques actuels ;

⊗ inventorier des procédés technologiques liés à l'information et à la robotisation ;

⊗ chercher des applications technologiques liées au développement durable et environnemental.

La formation en anglais permet d' :

⊗ utiliser cette langue lorsqu'elle est nécessaire à la lecture et aux communications.

Autres

Les nombreux voyages à l'étranger et le fait d'être originaire de Baie Saint-Ludger permettent de faire des contacts avec des personnes qui sont d'importantes sources d'informations et de communications, et confèrent des connaissances de l'environnement physique, social et humain.

Échanges avec des spécialistes

❊ Monsieur Alain Andersen, B.Sc., M.Sc. conseiller en technologie industrielle, CNRC

❊ Monsieur Luc Arsenault, géologue, FREM de la Côte-Nord

❊ Monsieur Bertrand Brassard, géologue, FREM de la Côte-Nord

❊ Monsieur Jacques Chiasson, représentant du MICSTQ, bureau régional de Baie-Comeau

❊ Monsieur Daniel Danis, Géologue, FREM de la Côte-Nord

❊ Monsieur Claude Deschênes, analyste, Laboratoire Environnement SNC, Sept-Iles

❊ Monsieur Joseph Hammagi, géologue à l'Hydro-Québec

- Madame Doris Harrisson, auteur du livre *Les relais de santé au Québec*

- Monsieur Serge Huppé, technicien senior en technologie et données industriellles, CRIQ.

- Monsieur A. Kévreau, technicien en laboratoire, Laboratoire Kélab, Baie-Comeau

- Monsieur Camille Kobzi, expert géologue, Entreprises Bruneau

- Monsieur Yves Leroux, CRIQ

- Monsieur Denis Lessard, ingénieur-géologue, Centre de recherches minérales du Québec

- Monsieur Ingo Medvescek, Ph.D.,Commission géologique du Canada.

- Monsieur Patrick Morel à L'Huissier, dr, économiste minier, MRNC.

- Monsieur Christian Morin, ingénieur, service des titres miniers, MRNQ

- Monsieur François Morneau, géomorpholoque, section environnement du MTQ

- Madame Raymonde Ouellet, secteur pétrochimie, MICSTQ

- Madame Jeanne Percival, Ph.D., Commission géologique du Canada

- Monsieur Henri Pisani, technicien des argiles, *Les argiles de Haute-Provence*

- Monsieur Mohammad Hosseini, Ph.D, dr.,ingénieur en géotechnique

- Monsieur Michel Tessier, agronome, département de phytobiologie, faculté d'agronomie, Université Laval

- Monsieur Rock Thibert, Ph.D. École supérieure de pharmacie, Université de Montréal

- Monsieur Richard Voyer, Ph.D, CRIQ

- Madame Nadia Tchernenko, auteur du livre *Les sept couleurs de l'argile.*

IDENTIFICATION ET SYNTHÈSE DES TRAVAUX

Rapport expliquant les dépenses déclarées dans les *Travaux d'échantillonnage et d'analyses* (annexe 5) et dans la partie *Évaluation technique et autres types de travaux* (annexe 6)

Le renouvellement des Permis de recherche de substances minérales de surface (PRS 0002039-0002040-0002041-0002042-0002043-0002044) a pour objectif de permettre à l'entreprise *Argile eau mer* de mener son projet à terme.

Le projet d' *Argile eau mer* consiste à caractériser l'argile sensible et le gisement de Baie Saint-Ludger, gisement délimité par les permis de recherche de substances minérales (PRS), dans le but d'exploiter cette argile à des fins cosmétiques et/ou thérapeutiques et à la commercialiser. La commercialisation se fera d'abord , à petite échelle, via le centre de thalassothérapie qui sera mis sur pied à Baie Saint-Ludger puis ensuite pourra rejoindre un marché plus vaste.

Pour vous permettre de bien comprendre la nature des travaux qui ont été effectués du 16 janvier 1996 au 16 janvier 1998 et les dépenses qui leurs sont associés, je vais rappeler brièvement les grands axes de la recherche.que vous pouvez retrouver, plus détaillés, dans le document intitulé *Argile eau mer : chronologie du travail effectué,* inclus dans cet envoi.

Ces grands axes sont la caractérisation de l'argile et du gisement dont les coûts de recherche sont détaillés dans l'annexe 5 : Travaux d'échantillonnage et d'analyse du document intitulé : *Rapport relatif aux travaux miniers.* Les méthodes d'extraction des argiles sensibles et la transformation de l'argile en produits cosmétiques et thérapeutiques, qui constituent les autres axes de la recherche, sont traités dans l'annexe 6 : Évaluation technique et Autres types de travaux.

1.La caractérisation de l'argile et du gisement.

1.1. Les analyses de M.André Chagnon du Centre de recherche scientifique

Les deux forages effectués en décembre 1995 sous la direction de Messieurs Luc Arsenault et Bertrand Brassard du Fond régional d'exploration minière de la côte Nord (FREM) sur le terrain désigné par le PRS 0002041,ont permis de prélever 5 échantillons qui ont ensuite été analysés par M. Chagnon du CRG.

Les coûts relatifs aux forages et à la prise d'échantillons ont été déclarés pour le renouvellement du PRS 0002041 en janvier 1996 mais les coûts pour l'analyse des échantillons ne l'ont pas été puisque le rapport de ces analyses m'a été remis le 7-15-96. Comme j'avais bénéficié d'une aide financière du FREM pour faire effectuer ces travaux et analyses, je ne dispose pas de factures pour attester le coût de ces travaux.

Je vous envoie donc une copie du rapport de Messieurs Arsenault et Brassard qui contient en annexe 3 le détail des analyses minéralogique, chimique (incluant les éléments traces) et granulométrique de 5 échantillons. Les prix affectés à chacune de celles-ci ont été estimés à partir du document *Tarification* du Centre de recherche minérale, avril 1997 et des suggestions de Mme Jeanne Percival de la Commission géologique du Canada.

Le total des dépenses pour ces analyses est de 1 660 $. Ce montant est reporté dans la section 3, pour le PRS 0002041, puisque c'est sur ce lot que les échantillons ont été prélevés.

1.2. Les analyses de Mme Jeanne Percival de la Commission géologique du Canada

Suite aux recommandations contenues dans le rapport de Messieurs Arsenault et Brassard, j'ai demandé à Mme Jeanne Percival de la Commission géologique du Canada d'analyser des échantillons, provenant du dépôt d'argile qui affleure sur toute la rive, échantillons prélevés sur chaque lot identifié à des PRS. Cet échantillonnage réalisé à moindre coût permettait en outre, d'aller chercher l'argile liquide qui, il me semble, peut répondre le mieux aux critères de qualité pour des soins corporels.

Mme Percival m'a fait parvenir, fin novembre 1997, un rapport intitulé : "PRELIMINARY REPORT Semi-Quantitative Clay Mineralogical and Particle Size Analyses" de ces échantillons . Compte tenu que le Dr Percival est une chercheure scientifique du Gouvernement fédéral, elle ne m'a pas facturé de montant pour les analyses puisque la recherche a été faite pour le bénéfice de la science. C'est ce qu'elle explique à la page 2 de son rapport que j'inclus dans cet envoi.

Elle mentionne cependant que 20 analyses minéralogiques et granulométriques ont été faites et que le coût de chacune est de 150 $. Le coût total de ces analyses est donc de 150 $ x 20 = 6 000 $ alors que le coût du moyen de transport pour lui remettre les échantillons est de 265 $ (.34 ¢ par kilomètre, selon le prix admis au

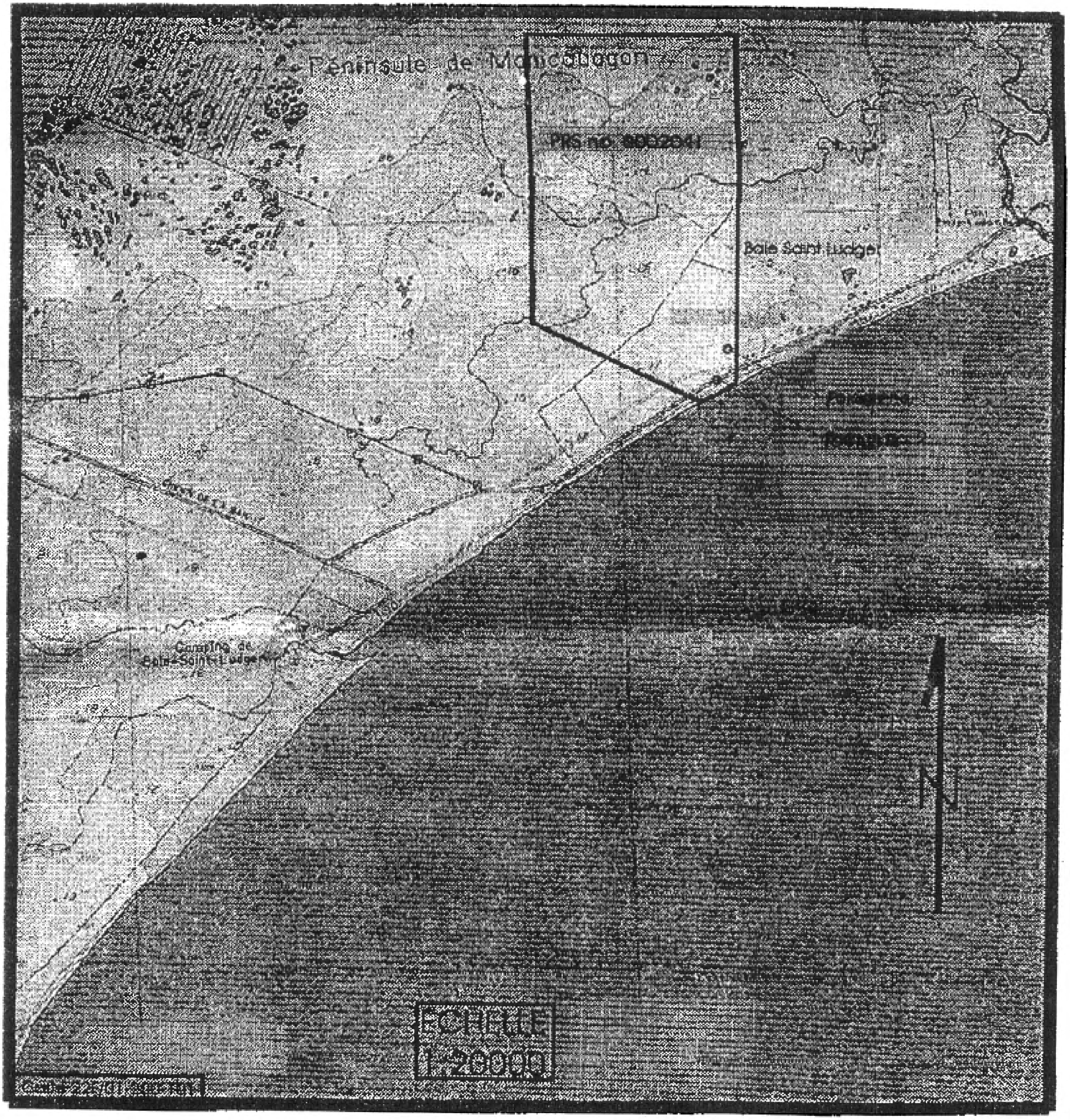

Carte de localisation du PRS 2041, péninsule Manicouagan, région de Baie Comeau

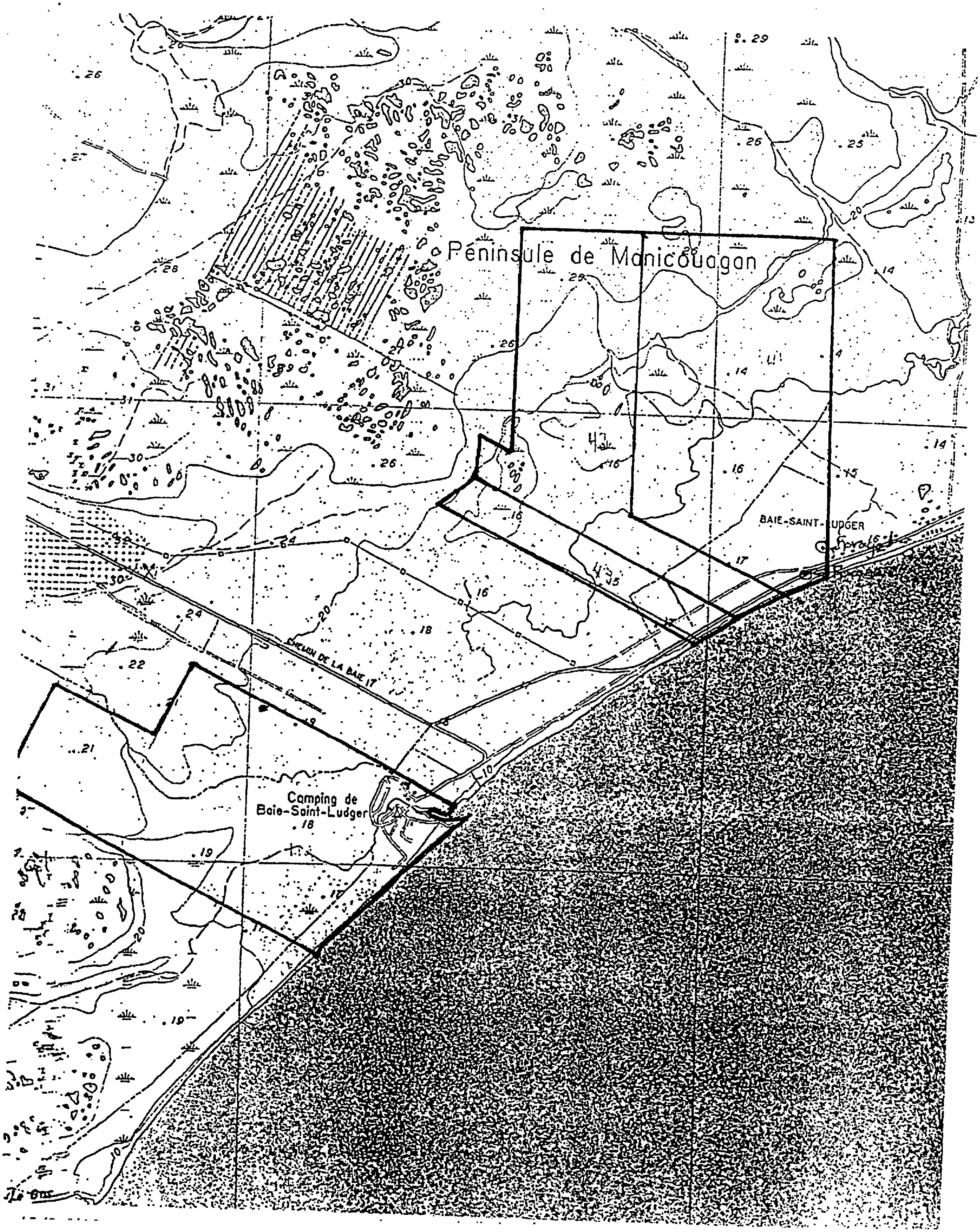
Péninsule de Manicouagan
BAIE-SAINT-LUDGER
Camping de Baie-Saint-Ludger
CHEMIN DE LA BAIE 17
4.7
4.35
29
26
25
28
31
30
24
22
21
20
19
18
17
16
15
14
10

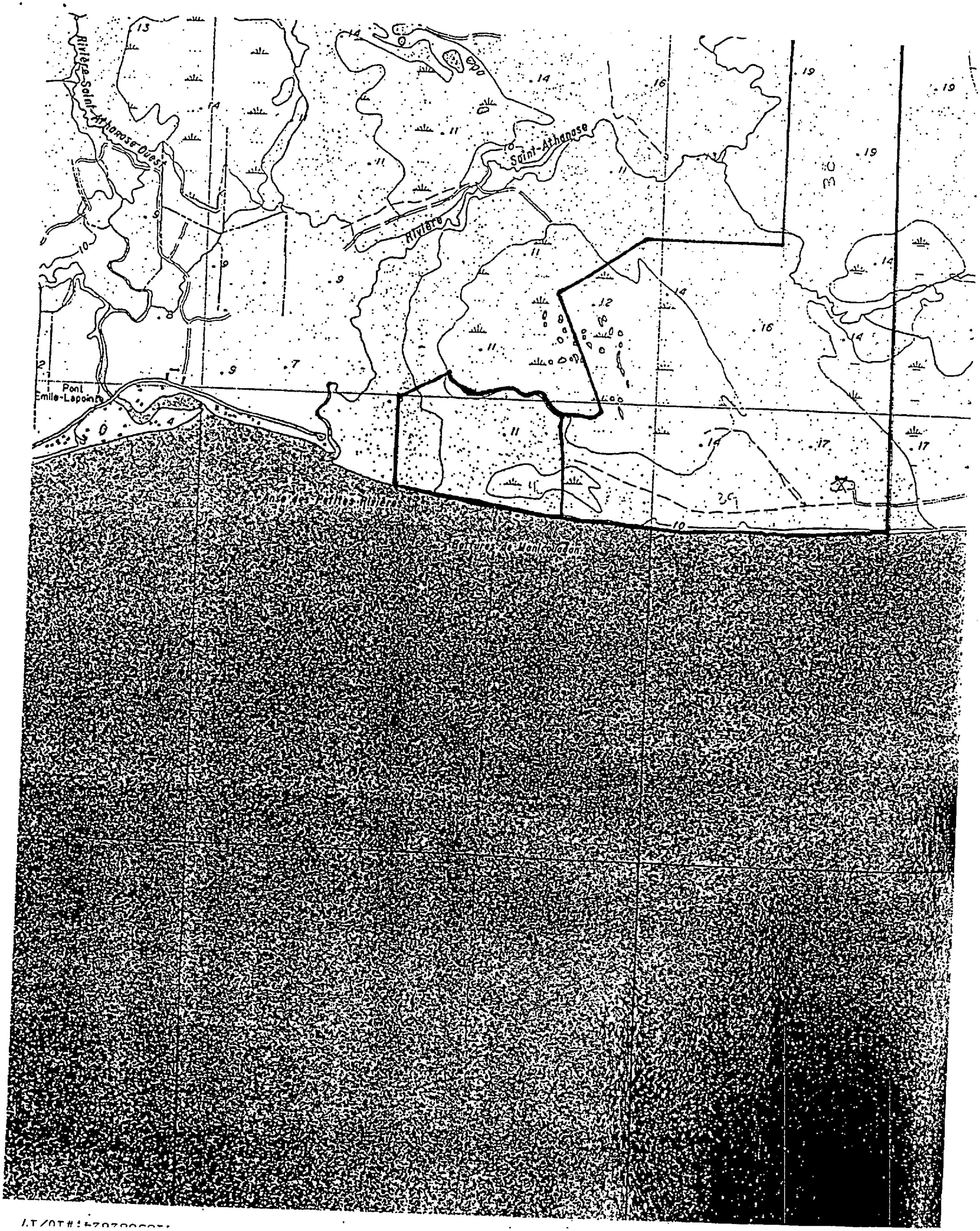
Rivière Saint-Athanase-Ouest
Rivière
Saint-Athanase
Pont Emile-Lepointe
Anse des Petites Rivières
Battures de Manicouagan
13
14
14
14
16
19
19
19
11
11
11
11
11
11
10
10
9
9
9
8
7
4
2
12
14
16
14
14
17
17
10
39

PRS 000 2043

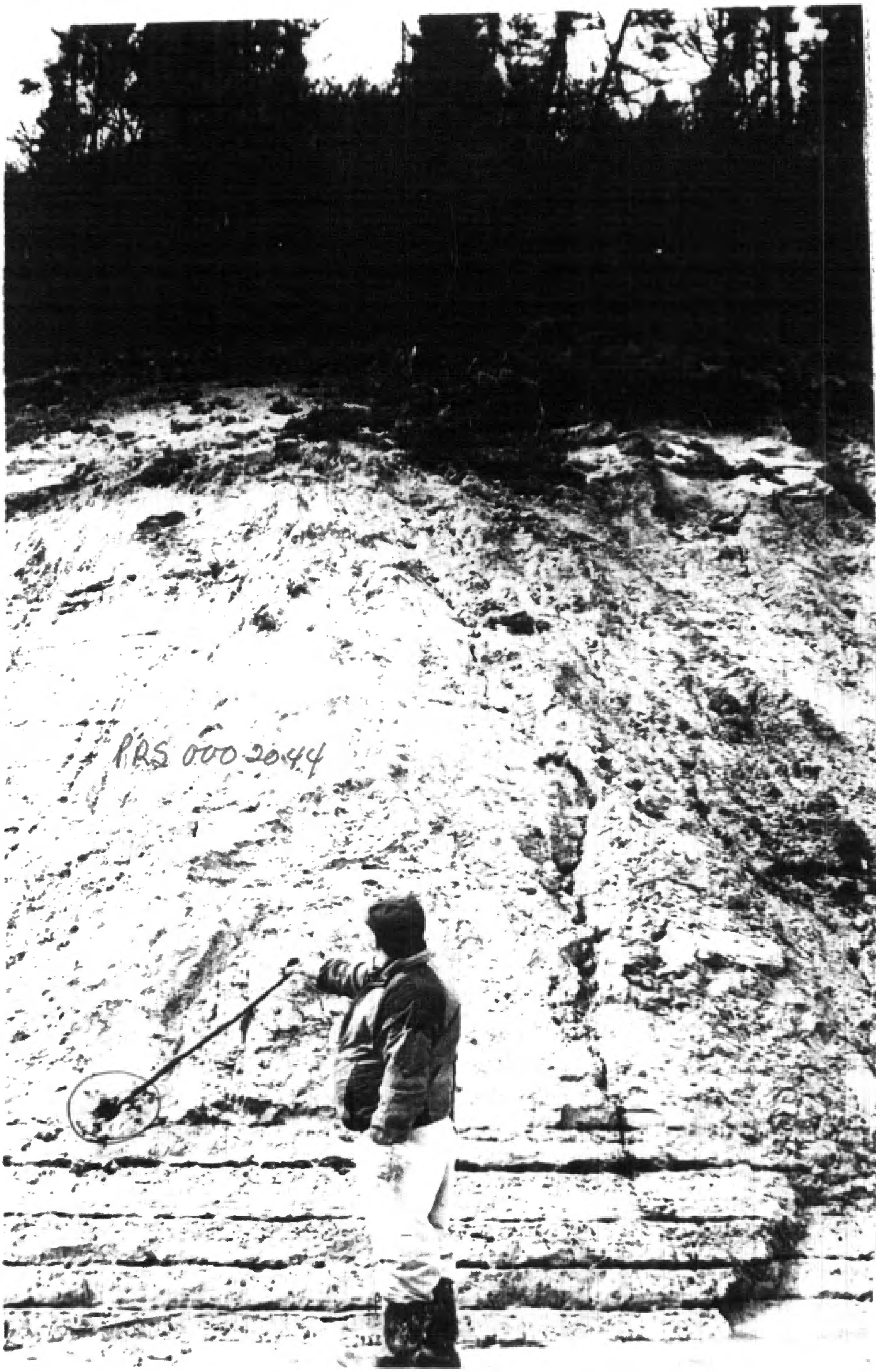

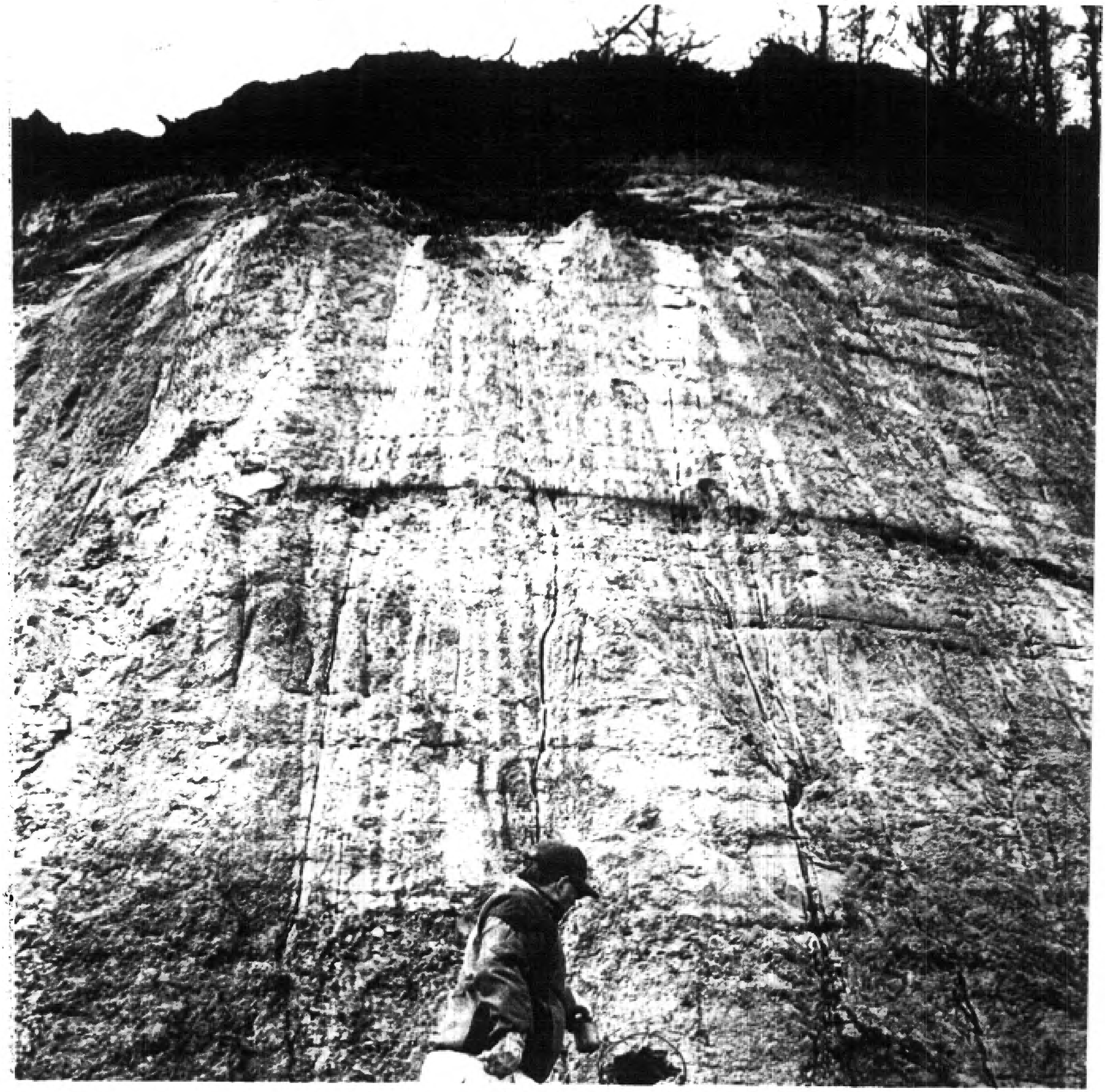

PRS 0002044

PRS0002040

PRS000 2039

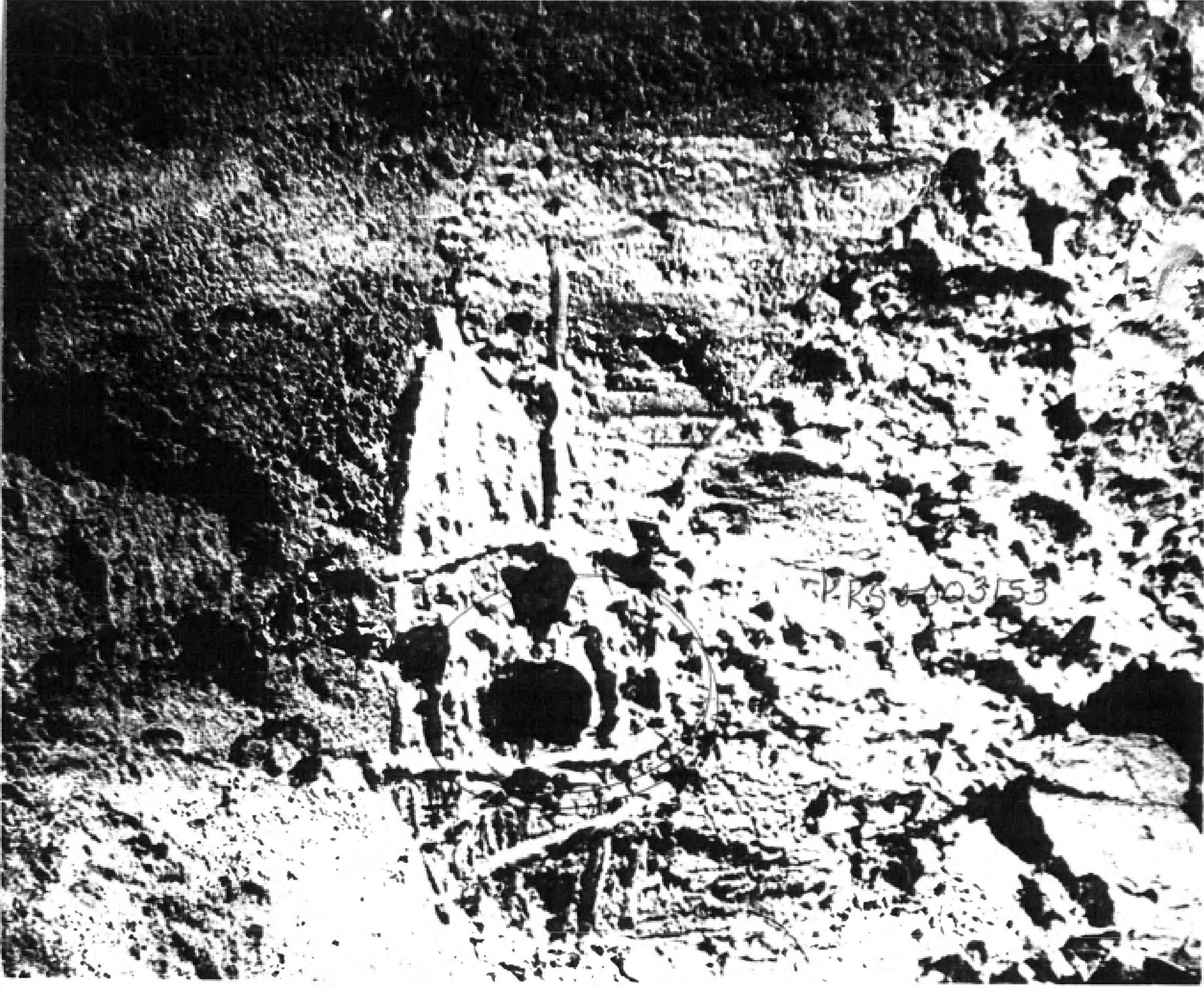

PRS 000 2040

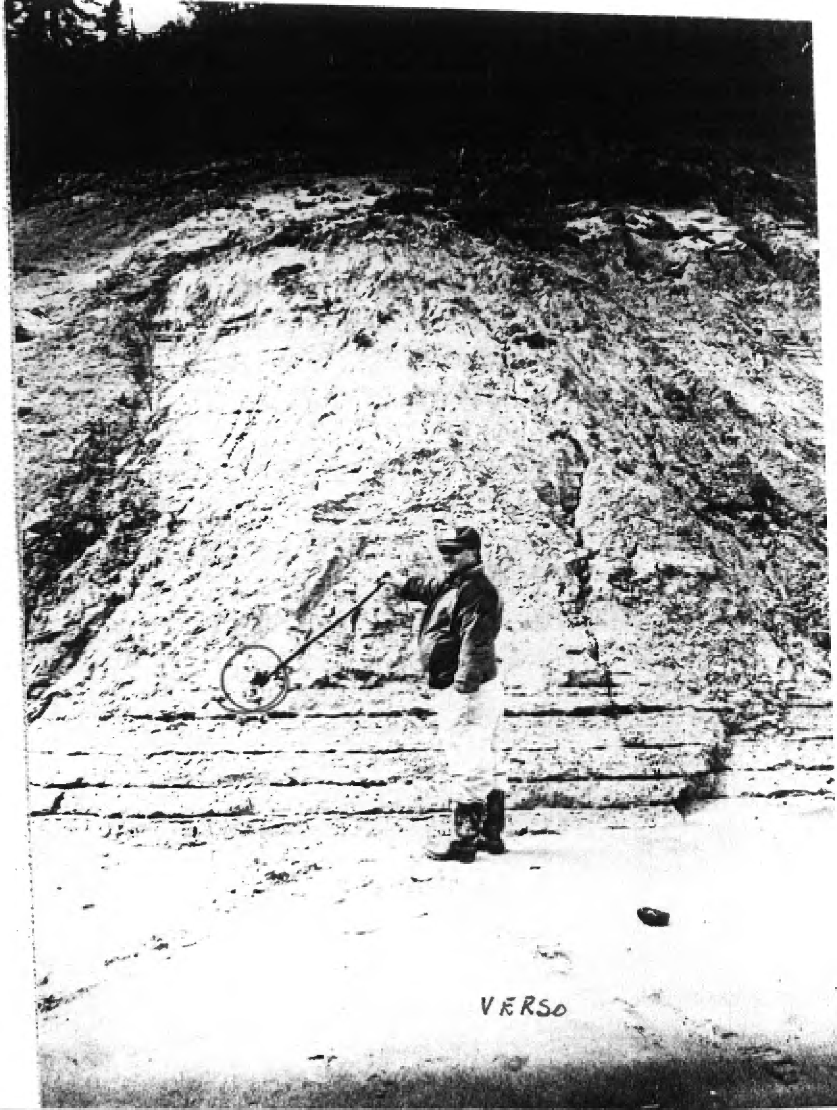

VERSO

PRS 0002044

VERSO

VERSO

PRS 0002041 et 0002042

entre les 2

PRS 0002043 - 0002042

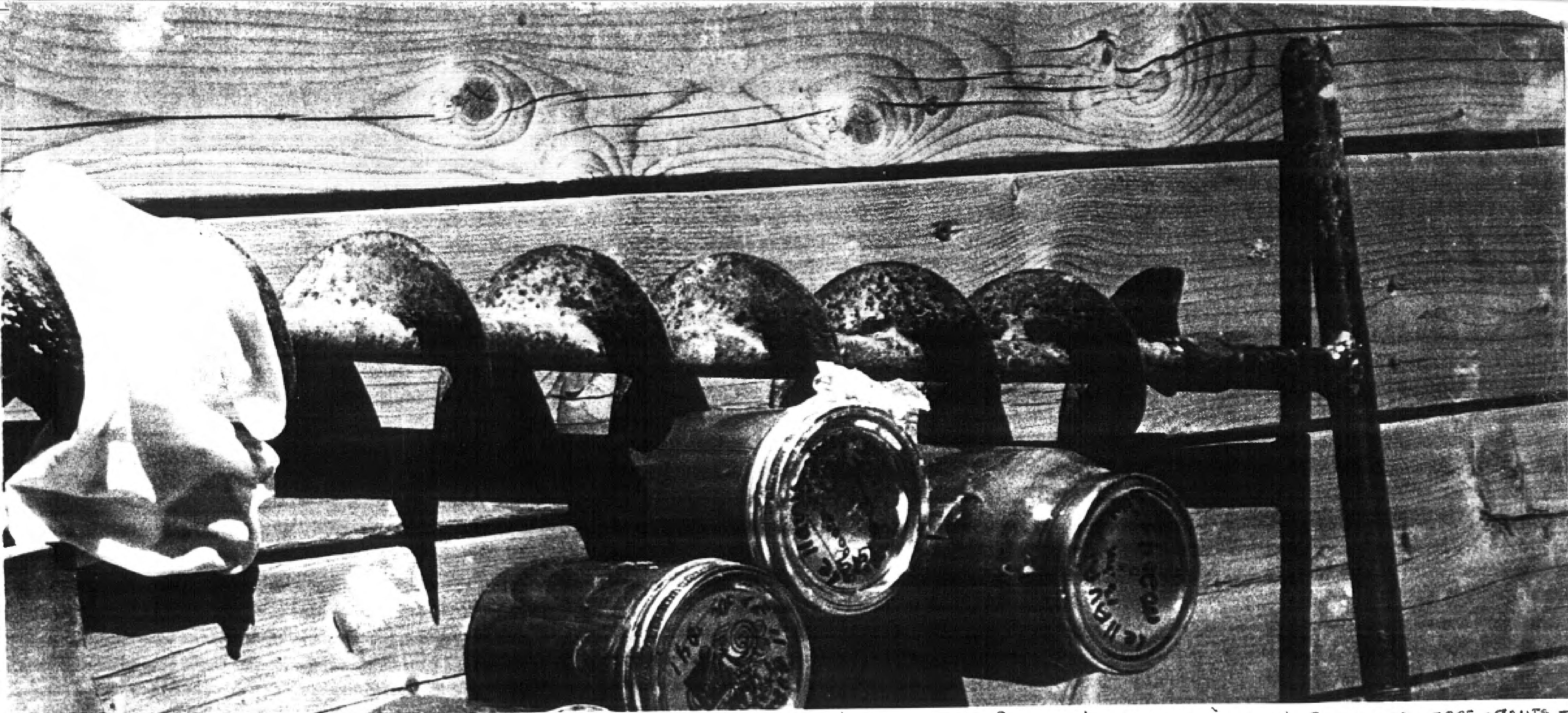

INSTRUMENTS POUR LE PRÉLÈVEMENT D'ÉCHANTILLONS : MÈCHE 48' - Bocaux DE VERRE - GANTS - CUILLERE DE BOIS - DE CAOUTCHOUC

DESCRIPTION DES ÉCHANTILLONS D'ARGILE MARINE

POUR FINS D'ANALYSE

LIEU : Baie Saint-Ludger, Péninsule Manicouagan, Côte-Nord du Québec

DATE : 16 mai 1997

NUMÉRO de permis de recherche de substances minérales de surface **(P.R.S.) :** 000-2042. Rang Point-aux-Outardes, Canton Manicouagan

MANIÈRE D'ÉCHANTILLONNER : A partir de la plage, en creusant manuellement un trou d'environ 6 pouces de diamètre avec une cuillère de bois pour ne pas mettre l'argile en contact avec du métal. La profondeur du trou est d'environ 12 pouces de la rive de façon à éliminer les substances de surface qui pourraient altérer l'argile. L'argile est prélevée en introduisant un bocal de verre au fond du trou dans lequel on introduit l'argile à l'aide de la main recouverte d'un gant de fin caoutchouc.

HAUTEUR DE LA RIVE : La hauteur de la rive varie d'un lieu à l'autre. Les lots identifiés aux différents P.R.S. ont donc une hauteur différente. Chacun d'eux sera donc évalués approximativement quant à la hauteur de la rive où l'échantillon a été prélevé. Pour ce qui est du lot désigné par le P.R.S. 0002042 la hauteur de la rive est de : 50 pieds environ

HAUTEUR DU TROU À PARTIR DE LA PLAGE : 4 pieds environ

REMARQUES : Cette argile était très liquide .

DESCRIPTION DES ÉCHANTILLONS D'ARGILE MARINE

POUR FINS D'ANALYSE

LIEU : Baie Saint-Ludger, Péninsule Manicouagan, Côte-Nord du Québec

DATE : 17 mai 1997

NUMÉRO de permis de recherche de substances minérales de surface **(P.R.S.) :** 000-2041. Rang Pointe-aux-Outardes, Canton Manicouagan

MANIÈRE D'ÉCHANTILLONNER : A partir de la plage, en creusant manuellement un trou d'environ 6 pouces de diamètre avec une cuillère de bois pour ne pas mettre l'argile en contact avec du métal. La profondeur du trou est d'environ 12 pouces de la rive de façon à éliminer les substances de surface qui pourraient altérer l'argile. L'argile est prélevée en introduisant un bocal de verre au fond du trou dans lequel on introduit l'argile à l'aide de la main recouverte d'un gant de fin caoutchouc.

HAUTEUR DE LA RIVE : La hauteur de la rive varie d'un lieu à l'autre. Les lots identifiés aux différents P.R.S. ont donc une hauteur différente. Chacun d'eux sera donc évalués approximativement quant à la hauteur de la rive où l'échantillon a été prélevé. Pour ce qui est du lot désigné par le P.R.S. 0002041 la hauteur de la rive est de : 30 pieds environ

HAUTEUR DU TROU À PARTIR DE LA PLAGE : 8 pieds environ

REMARQUES : Cette argile était très liquide .

DESCRIPTION DES ÉCHANTILLONS D'ARGILE MARINE

POUR FINS D'ANALYSE

LIEU : Baie Saint-Ludger, Péninsule Manicouagan, Côte-Nord du Québec

DATE : 17 mai 1997

NUMÉRO de permis de recherche de substances minérales de surface **(P.R.S.) :** 000-2040. Rang 1, Canton Manicouagan

MANIÈRE D'ÉCHANTILLONNER : A partir de la plage, en creusant manuellement un trou d'environ 6 pouces de diamètre avec une cuillère de bois pour ne pas mettre l'argile en contact avec du métal. La profondeur du trou est d'environ 12 pouces de la rive de façon à éliminer les substances de surface qui pourraient altérer l'argile. L'argile est prélevée en introduisant un bocal de verre au fond du trou dans lequel on introduit l'argile à l'aide de la main recouverte d'un gant de fin caoutchouc.

HAUTEUR DE LA RIVE : La hauteur de la rive varie d'un lieu à l'autre. Les lots identifiés aux différents P.R.S. ont donc une hauteur différente. Chacun d'eux sera donc évalués approximativement quant à la hauteur de la rive où l'échantillon a été prélevé. Pour ce qui est du lot désigné par le P.R.S. 0002040 la hauteur de la rive est de : 25 pieds environ

HAUTEUR DU TROU À PARTIR DE LA PLAGE : 2 pieds environ

REMARQUES : Le matériel n'était pas liquide, il était plutôt sableux .

DESCRIPTION DES ÉCHANTILLONS D'ARGILE MARINE

POUR FINS D'ANALYSE

LIEU : Baie Saint-Ludger, Péninsule Manicouagan, Côte-Nord du Québec

DATE : 17 mai 1997

NUMÉRO de permis de recherche de substances minérales de surface **(P.R.S.) :** 000-2039. Rang 1, Canton Manicouagan

MANIÈRE D'ÉCHANTILLONNER : A partir de la plage, en creusant manuellement un trou d'environ 6 pouces de diamètre avec une cuillère de bois pour ne pas mettre l'argile en contact avec du métal. La profondeur du trou est d'environ 12 pouces de la rive de façon à éliminer les substances de surface qui pourraient altérer l'argile. L'argile est prélevée en introduisant un bocal de verre au fond du trou dans lequel on introduit l'argile à l'aide de la main recouverte d'un gant de fin caoutchouc.

HAUTEUR DE LA RIVE : La hauteur de la rive varie d'un lieu à l'autre. Les lots identifiés aux différents P.R.S. ont donc une hauteur différente. Chacun d'eux sera donc évalués approximativement quant à la hauteur de la rive où l'échantillon a été prélevé. Pour ce qui est du lot désigné par le P.R.S. 0002039 la hauteur de la rive est de : 20 pieds environ

HAUTEUR DU TROU À PARTIR DE LA PLAGE : 4 pieds environ

REMARQUES : Le matériel n'était pas liquide, il était plutôt sableux .

DESCRIPTION DES ÉCHANTILLONS D'ARGILE MARINE

POUR FINS D'ANALYSE

LIEU : Baie Saint-Ludger, Péninsule Manicouagan, Côte-Nord du Québec

DATE : Le 15 mai 1997

NUMÉRO de permis de recherche de substances minérales de surface **(P.R.S.) :** 0002044 (Rang Pointe-aux-Outardes, Canton Manicouagan

MANIÈRE D'ÉCHANTILLONNER : A partir de la plage, en creusant manuellement un trou d'environ 6 pouces de diamètre avec une cuillère de bois pour ne pas mettre l'argile en contact avec du métal. La profondeur du trou est d'environ 12 pouces de la rive de façon à éliminer les substances de surface qui pourraient altérer l'argile. L'argile est prélevée en introduisant un bocal de verre au fond du trou dans lequel on introduit l'argile à l'aide de la main recouverte d'un gant de fin caoutchouc.

-

HAUTEUR DE LA RIVE : La hauteur de la rive varie d'un lieu à l'autre. Les lots identifiés aux différents P.R.S. ont donc une hauteur différente. Chacun d'eux sera donc évalués approximativement quant à la hauteur de la rive où l'échantillon a été prélevé. Pour ce qui est du lot désigné par le P.R.S. 0002044 la hauteur de la rive est de : 50 pieds environ

HAUTEUR DU TROU À PARTIR DE LA PLAGE : 5 pieds environ

REMARQUES : Cette argile était très liquide

PRS 0002038

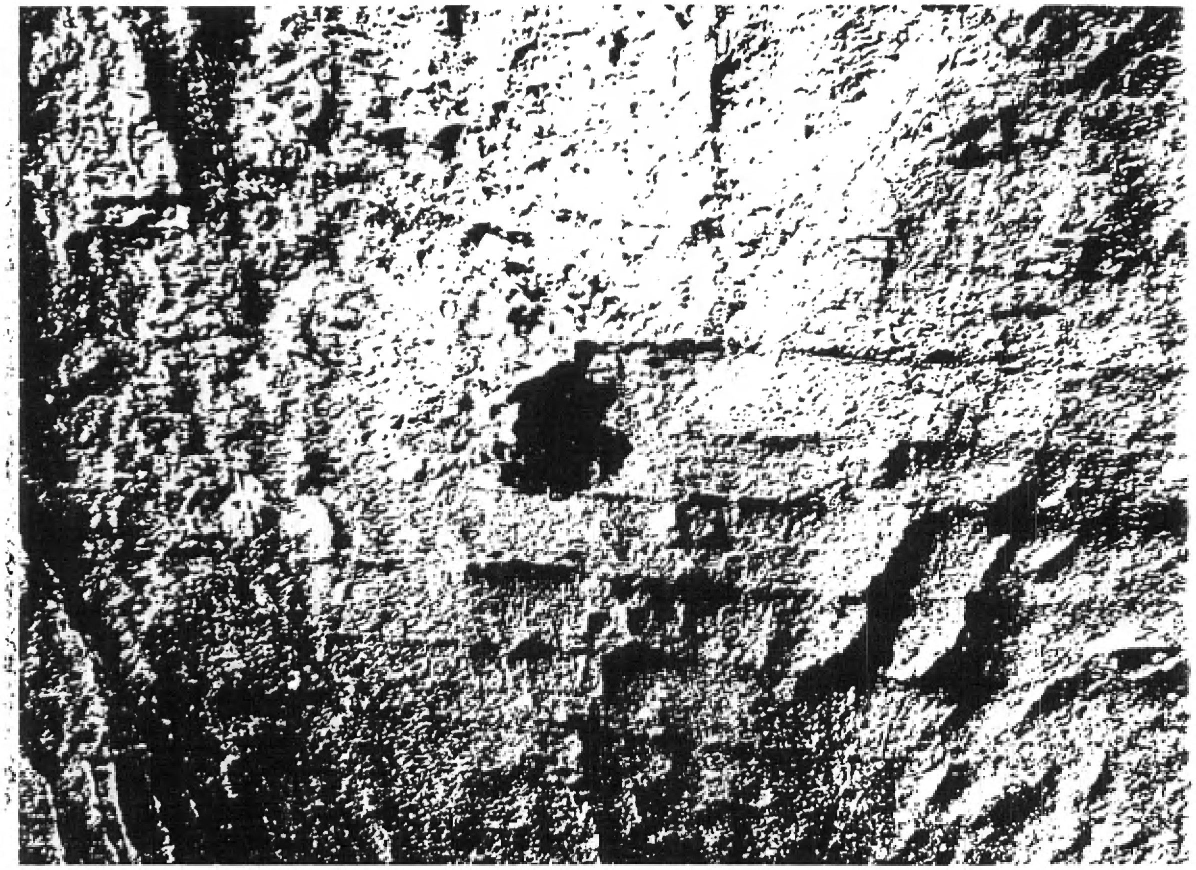

Argile eau mer

Rapport contenant les certificats de laboratoires donnant les résultats d'analyse des échantillons prélevés

20 JANVIER 1999

À l'attention de Denise Saulnier
Client Argile-Eau-Mer
5594 Waverly
Montréal, Qc.
H2T 2Y1

No de certificat 3986-98
Date d'émission 98-05-22
Date de réception 98-05-08
No. demande 98-39411
Bon de commande NA

Identification	1 Composite (0002041, 0002042, 0002043)
Référence	Argile Eau Mer
Matrice	Sol
Date de prélèvement	NA
Lieu du prélèvement	S-980424-BS1
Prélevé par	Denise Saulnier
No de laboratoire	180894
Date de préparation	98-05-13
Date d'analyse	98-05-13
HAP-T-S-13	mg/kg
Naphtalène	< 0.1
Acénaphthylène	< 0.1
Acénaphtène	< 0.1
Fluorène	< 0.1
Phénanthrène	< 0.1
Anthracène	< 0.1
Fluoranthène	< 0.1
Pyrène	< 0.1
7,12-Diméthylbenzoanthracène	< 0.1
Benzo (g,h,i) pérylène	< 0.1
Benzo (c) phénanthrène	< 0.1
Chrysène	< 0.1
Benzo (a) anthracène	< 0.1
Benzo (b,j,k) fluoranthène	< 0.1
Benzo (a) pyrène	< 0.1
3-Méthylcholanthrène	< 0.1
Indéno (1,2,3-cd) pyrène	< 0.1
Dibenzo (ah) anthracène	< 0.1
Dibenzo (a,l) pyrène	< 0.1
Dibenzo (a,i) pyrène	< 0.1
Dibenzo (a,h) pyrène	< 0.1
Total	ND
%Récupération	
D10-Fluorène	100
D10-pyrène	100
D12-Benzo[a]pyrène	100

Non-conformité(s):
Commentaire(s):
Note: Ces résultats ne se rapportent qu'aux échantillons soumis pour analyse.

CHIMISTE
Martin Brunet
91-37?
QUÉBEC

Chimiste
Martin Brunet

À l'attention de Denise Saulnier
Client Argile-Eau-Mer
5594 Waverly
Montréal, Qc.
H2T 2Y1

No de certificat 3986-98
Date d'émission 98-05-22
Date de réception 98-05-08
No. demande 98-39411
Bon de commande NA

Identification	1 Composite (0002041, 0002042, 0002043)
Référence	Argile Eau Mer
Matrice	Sol
Date de prélèvement	NA
Lieu du prélèvement	S-980424-BS1
Prélevé par	Denise Saulnier
No de laboratoire	180894
Date de préparation	98-05-12
Date d'analyse	98-05-12
BPC-A-S-13	mg/kg
Aroclor 1242	< 0.1
Aroclor 1248	< 0.1
Aroclor 1254	< 0.1
Aroclor 1260	< 0.1
Total	ND
%Récupération	
Décachlorobiphényle	92

Non-conformité(s):
Commentaire(s):
Note: Ces résultats ne se rapportent qu'aux échantillons soumis pour analyse.

Martin Brunet
94-076

Chimiste
Martin Brunet

Certificat d'analyse – Certificate of Analysis

À l'attention de Denise Saulnier
Client Argile-Eau-Mer
5594 Waverly
Montréal, Qc.
H2T 2Y1

No de certificat 3986-98
Date d'émission 98-05-22
Date de réception 98-05-08
No. demande 98-39411
Bon de commande NA

Identification	1 Composite (0002041, 0002042, 0002043)
Référence	Argile Eau Mer
Matrice	Sol
Date de prélèvement	NA
Lieu du prélèvement	S-980424-BS1
Prélevé par	Denise Saulnier
No de laboratoire	180894
Date de préparation	98-05-13
Date d'analyse	98-05-14
HGM-C10-50-S-13	mg/kg
Hydrocarbures Pétroliers C10-C50	110
%Récupération	

Non-conformité(s):
Commentaire(s):
Note: Ces résultats ne se rapportent qu'aux échantillons soumis pour analyse.

Martin Brunet
94-076

Chimiste
Martin Brunet

Division de Roche ltée
Groupe-conseil
1818, rte de l'Aéroport
Sainte-Foy (Québec)
Canada, G2G 2P8
Téléphone:
(418) 871-8722
Télécopieur:
(418) 871-9556

Sujet : ANALYSE DE SOL

Client : BODYCOTE TECHNITROL INC.
Responsable : M.MARTIN BRUNET
Prélevé par : VOTRE REPRESENTANT

Votre référence : CT-02740

Echantillon(s) recu(s) le : 98/05/12

		No Labo:	107033			
		V/Réf:	39411-180 894			
PARAMETRE	Unité	D.Pr.: H.Pr.:				
Pesticides organochlorés						
Alpha-BHC	mg/kg		<0.0003			
Hexachlorobenzène (HCB)	mg/kg		<0.0003			
Béta-BHC	mg/kg		<0.0006			
Gamma-BHC(lindane)	mg/kg		<0.0020			
Delta-BHC	mg/kg		<0.0008			
Heptachlore	mg/kg		<0.0005			
Aldrine	mg/kg		<0.0030			
Heptachlore époxide	mg/kg		<0.0004			
Gamma-chlordane	mg/kg		<0.0004			
o,p'-DDE	mg/kg		<0.0010			
Endosulfan I	mg/kg		<0.0002			
Alpha-chlordane	mg/kg		<0.0002			
p,p'-DDE	mg/kg		<0.0005			
Dieldrine	mg/kg		<0.0004			
o,p'-DDD (TDE)	mg/kg		<0.0010			
Endrine	mg/kg		<0.0020			
Endosulfan II	mg/kg		<0.0002			
p,p'-DDD (TDE)	mg/kg		<0.0010			
o,p'-DDT	mg/kg		<0.0010			
Endrine aldéhyde	mg/kg		<0.0006			
Endosulfan sulfate	mg/kg		<0.0010			
p,p'-DDT	mg/kg		<0.0020			
Endrine cétone	mg/kg		<0.0009			
Méthoxychlore	mg/kg		<0.0090			

Division de Roche ltée
Groupe-conseil
1818, rte de l'Aéroport
Sainte-Foy (Québec)
Canada, G2G 2P8
Téléphone:
(418) 871-8722
Télécopieur:
(418) 871-9556

		No Labo: V/Réf: D.Pr.: H.Pr.:	107033 39411-180 894			
PARAMETRE	Unité					
Mirex	mg/kg		<0.0015			
Récupération			-			
1,2,4,5-tétrabromobenzène	%		98			
Décachlorobiphényle	%		110			
Pesticides phénoxyacides						
Dicamba	mg/kg		<0.20			
MCPP (Mécoprop)	mg/kg		<0.02			
MCPA	mg/kg		<0.02			
2,4-DP (Dichloprop)	mg/kg		<0.02			
2,4-D	mg/kg		<0.02			
2,4,5-TP (Silvex)	mg/kg		<0.02			
2,4,5-T	mg/kg		<0.02			
MCPB	mg/kg		<0.02			
2,4-DB	mg/kg		<0.02			
Piclorame	mg/kg		<0.02			
Pesticides organophosphorés						
Diuron	mg/kg		<0.3			
EPTC	mg/kg		<0.2			
Tébuthiuron	mg/kg		<0.1			
Déisopropyl atrazine	mg/kg		<0.3			
Déethyle atrazine	mg/kg		<0.1			
Bromoxynil	mg/kg		<0.6			
Bendiocarbe	mg/kg		<0.1			
Trifluraline	mg/kg		<0.1			
Phorate	mg/kg		<0.2			

PARAMETRE	Unité	No Labo: V/Réf: D.Pr.: H.Pr.:	107033 39411-180 894			
Diméthoate	mg/kg		<0.1			
Simazine	mg/kg		<0.1			
Carbofurane	mg/kg		<0.1			
Atrazine	mg/kg		<0.2			
Terbufos	mg/kg		<0.2			
Diazinon	mg/kg		<0.1			
Dinoseb	mg/kg		<0.8			
Triallate	mg/kg		<0.1			
Métobromuron	mg/kg		<0.1			
Pirimicarb	mg/kg		<0.1			
Diméthénamide	mg/kg		<0.1			
Métribuzine	mg/kg		<0.1			
Méthyl parathion	mg/kg		<0.1			
Carbaryl	mg/kg		<0.1			
Fénitrothion	mg/kg		<0.1			
Linuron	mg/kg		<0.3			
Malathion	mg/kg		<0.1			
Métolachlore	mg/kg		<0.2			
Chlorpyrifos	mg/kg		<0.1			
Cyanazine	mg/kg		<0.2			
Parathion	mg/kg		<0.1			
Dichlofop-méthyl	mg/kg		<0.1			
Azinphos-méthyl	mg/kg		<0.3			
Téméphos	mg/kg		<2.0			
Récupération			-			

		No Labo:	107033			
		V/Réf:	39411-180 894			
		D.Pr.:				
PARAMETRE	Unité	H.Pr.:				
Propoxur	%		90			

Ce rapport est pour l'usage exclusif du client et ne peut être reproduit, sinon en entier, sans une permission écrite d'Envirolab

Approuvé par:

MARC PAQUET, Chim., M.Sc.

Marc Paquet
90-090

À l'attention de Denise Saulnier
Client Argile-Eau-Mer
5594 Waverly
Montréal, Qc.
H2T 2Y1

No de certificat 3986-98
Date d'émission 98-05-22
Date de réception 98-05-08
No. demande 98-39411
Bon de commande NA

No. de laboratoire	183016	180894	183018	183017	
Type de contrôle	Blanc	Echantillon	Duplicata	Contrôle Certifié	
Matrice	Sol	Sol	Sol		
Date de prélèvement		00-01-01	00-01-01		
Lieu du prélèvement		S-980424-BS1	S-980424-BS1		
Prélevé par		Denise Saulnier	Denise Saulnier		
Référence				Obtenu	Écart acceptable
Date de préparation	98-05-19	98-05-19	98-05-19	98-05-19	
Date d'analyse	98-05-19	98-05-19	98-05-19	98-05-19	
HMA-T-S-13	mg/kg	mg/kg	mg/kg	ng	ng
Benzène	< 0.1	< 0.1	< 0.1	340	(269 - 437)
Ethylbenzène	< 0.1	< 0.1	< 0.1	210	(180 - 292)
Chlorobenzène	< 0.1	< 0.1	< 0.1	81	(67 - 101)
Toluène	< 0.1	< 0.1	< 0.1	110	(95 - 144)
Xylènes	< 0.1	< 0.1	< 0.1	340	(307 - 505)
Styrène	< 0.1	< 0.1	< 0.1	(-)	(-)
1,2-Dichlorobenzène	< 0.1	< 0.1	< 0.1	250	(183 - 307)
1,3-Dichlorobenzène	< 0.1	< 0.1	< 0.1	280	(181 - 311)
1,4-Dichlorobenzène	< 0.1	< 0.1	< 0.1	660	(460 - 760)
Total	ND	ND	ND		
%Récupération					
Dibromofluorométhane	97	59	66	110	
D8-Toluène	82	78	79	89	
1-Bromo-4-fluorobenzène	83	80	82	93	

Non-conformité(s):
Commentaire(s):
Note: Ces résultats ne se rapportent qu'aux échantillons soumis pour analyse.

CHIMISTE
Martin Brunet
94-076
QUÉBEC

Certificat d'analyse • Certificate of Analysis

À l'attention de Denise Saulnier
Client Argile-Eau-Mer
5594 Waverly
Montréal, Qc.
H2T 2Y1

No de certificat 3986-98
Date d'émission 98-05-22
Date de réception 98-05-08
No. demande 98-39411
Bon de commande NA

No. de laboratoire	181874			181877	
Type de contrôle	Blanc	Echantillon	Duplicata	Contrôle Certifié	
Matrice					
Date de prélèvement					
Lieu du prélèvement					
Prélevé par					
Référence				Obtenu	Écart acceptable
Date de préparation	98-05-13			98-05-13	
Date d'analyse	98-05-13			98-05-13	
PHE-CL-T-S-13	mg/kg			mg/kg	mg/kg
2-Chlorophénol	< 0.1			5.0	(2 - 6.1)
3-Chlorophénol	< 0.1			(-)	(-)
4-Chlorophénol	< 0.1			(-)	(-)
2,3-Dichlorophénol	< 0.1			(-)	(-)
2,4-Dichlorophénol	< 0.1			(-)	(-)
2,5-Dichlorophénol	< 0.1			(-)	(-)
2,6-Dichlorophénol	< 0.1			(-)	(-)
3,4-Dichlorophénol	< 0.1			(-)	(-)
3,5-Dichlorophénol	< 0.1			(-)	(-)
2,3,4-Trichlorophénol	< 0.1			(-)	(-)
2,3,5-Trichlorophénol	< 0.1			(-)	(-)
2,3,6-Trichlorophénol	< 0.1			(-)	(-)
2,4,5-Trichlorophénol	< 0.1			9.0	(1.5 - 9.6)
2,4,6-Trichlorophénol	< 0.1			(-)	(-)
3,4,5-Trichlorophénol	< 0.1			(-)	(-)
2,3,4,5-Tétrachlorophénol	< 0.1			(-)	(-)
2,3,4,6-Tétrachlorophénol	< 0.1			(-)	(-)
2,3,5,6-Tétrachlorophénol	< 0.1			(-)	(-)
Pentachlorophénol	< 0.1			7.3	(2.6 - 9.2)
Total	ND				
%Récupération					
D3-2,4-dichlorophénol	100			100	
C13-Pentachlorophénol	100			100	
D2-2,4,6-Trichlorophénol	85			120	

Non-conformité(s):
Commentaire(s):
Note: Ces résultats ne se rapportent qu'aux échantillons soumis pour analyse.

CHIMISTE
Martin Brunet
94-076
QUÉBEC

À l'attention de Denise Saulnier
Client Argile-Eau-Mer
5594 Waverly
Montréal, Qc.
H2T 2Y1

No de certificat 3986-98
Date d'émission 98-05-22
Date de réception 98-05-08
No. demande 98-39411
Bon de commande NA

No. de laboratoire	181875			181876	
Type de contrôle	Blanc	Echantillon	Duplicata	Contrôle Certifié	
Matrice					
Date de prélèvement					
Lieu du prélèvement					
Prélevé par					
Référence				Obtenu	Écart acceptable
Date de préparation	98-05-13			98-05-13	
Date d'analyse	98-05-13			98-05-13	
PHE-NCL-T-S-13	mg/kg			mg/kg	mg/kg
Phénol	< 0.1			(-)	(-)
o-Crésol	< 0.1			0.8	(0.8 - 7.2)
m-Crésol	< 0.1			(-)	(-)
p-Crésol	< 0.1			(-)	(-)
2-Nitrophénol	< 0.1			(-)	(-)
2,4-Diméthylphénol	< 0.1			(-)	(-)
2,4-Dinitrophénol	< 0.1			(-)	(-)
4-Nitrophénol	< 0.1			(-)	(-)
2-Méthyl-4,6-dinitrophénol	< 0.1			(-)	(-)
Total	ND				
%Récupération					
D3-2,4-dichlorophénol	100			100	
C13-Pentachlorophénol	100			100	
D2-2,4,6-Trichlorophénol	85			120	

Non-conformité(s):
Commentaire(s):
Note: Ces résultats ne se rapportent qu'aux échantillons soumis pour analyse.

Martin Brunet
94-076

Certificat d'analyse • Certificate of Analysis

À l'attention de Denise Saulnier
Client Argile-Eau-Mer
5594 Waverly
Montréal, Qc.
H2T 2Y1

No de certificat 3986-98
Date d'émission 98-05-22
Date de réception 98-05-08
No. demande 98-39411
Bon de commande NA

Identification	1 Composite (0002041, 0002042, 0002043)
Référence	Argile Eau Mer
Matrice	Sol
Date de prélèvement	NA
Lieu du prélèvement	S-980424-BS1
Prélevé par	Denise Saulnier
No de laboratoire	180894
Date de préparation	98-05-13
Date d'analyse	98-05-13
PHE-NCL-T-S-13	mg/kg
Phénol	< 0.1
o-Crésol	< 0.1
m-Crésol	< 0.1
p-Crésol	< 0.1
2-Nitrophénol	< 0.1
2,4-Diméthylphénol	< 0.1
2,4-Dinitrophénol	< 0.1
4-Nitrophénol	< 0.1
2-Méthyl-4,6-dinitrophénol	< 0.1
Total	ND
%Récupération	
D3-2,4-dichlorophénol	93
C13-Pentachlorophénol	94
D2-2,4,6-Trichlorophénol	88

Non-conformité(s):
Commentaire(s):
Note: Ces résultats ne se rapportent qu'aux échantillons soumis pour analyse.

Martin Brunet
94-076

Chimiste
Martin Brunet

Certificat d'analyse – Certificate of Analysis

À l'attention de Denise Saulnier
Client Argile-Eau-Mer
5594 Waverly
Montréal, Qc.
H2T 2Y1

No de certificat 3986-98
Date d'émission 98-05-22
Date de réception 98-05-08
No. demande 98-39411
Bon de commande NA

Identification	1 Composite (0002041, 0002042, 0002043)
Référence	Argile Eau Mer
Matrice	Sol
Date de prélèvement	NA
Lieu du prélèvement	S-980424-BS1
Prélevé par	Denise Saulnier
No de laboratoire	180894
Date de préparation	98-05-13
Date d'analyse	98-05-13
PHE-CL-T-S-13	mg/kg
2-Chlorophénol	< 0.1
3-Chlorophénol	< 0.1
4-Chlorophénol	< 0.1
2,3-Dichlorophénol	< 0.1
2,4-Dichlorophénol	< 0.1
2,5-Dichlorophénol	< 0.1
2,6-Dichlorophénol	< 0.1
3,4-Dichlorophénol	< 0.1
3,5-Dichlorophénol	< 0.1
2,3,4-Trichlorophénol	< 0.1
2,3,5-Trichlorophénol	< 0.1
2,3,6-Trichlorophénol	< 0.1
2,4,5-Trichlorophénol	< 0.1
2,4,6-Trichlorophénol	< 0.1
3,4,5-Trichlorophénol	< 0.1
2,3,4,5-Tétrachlorophénol	< 0.1
2,3,4,6-Tétrachlorophénol	< 0.1
2,3,5,6-Tétrachlorophénol	< 0.1
Pentachlorophénol	< 0.1
Total	ND
%Récupération	
D3-2,4-dichlorophénol	93
C13-Pentachlorophénol	94
D2-2,4,6-Trichlorophénol	88

Non-conformité(s):
Commentaire(s):
Note: Ces résultats ne se rapportent qu'aux échantillons soumis pour analyse.

Chimiste
Martin Brunet
94-076

Certificat d'analyse - Certificate of Analysis

À l'attention de Denise Saulnier
Client Argile-Eau-Mer
5594 Waverly
Montréal, Qc.
H2T 2Y1

No de certificat 3986-98
Date d'émission 98-05-22
Date de réception 98-05-08
No. demande 98-39411
Bon de commande NA

Identification	1 Composite (0002041, 0002042, 0002043)
Référence	Argile Eau Mer
Matrice	Sol
Date de prélèvement	NA
Lieu du prélèvement	S-980424-BS1
Prélevé par	Denise Saulnier
No de laboratoire	180894
Date de préparation	98-05-19
Date d'analyse	98-05-19
HHT-T-S-13	mg/kg
Chloroforme	< 0.1
1,1-Dichloroéthane	< 0.1
1,1-Dichloroéthène	< 0.1
1,2-Dichloroéthane	< 0.1
1,2-Dichloroéthène (t+c)	< 0.1
1,2-Dichloropropane	< 0.1
1,3-Dichloropropène (t+c)	< 0.1
Dichlorométhane	< 0.1
1,1,2,2-Tétrachloroéthane	< 0.1
Tetrachloroéthène	< 0.1
Tetrachlorure de Carbone	< 0.1
1,1,1-Trichloroéthane	< 0.1
1,1,2-Trichloroéthane	< 0.1
Trichloroéthène	< 0.1
Total	ND
%Récupération	
Dibromofluorométhane	59
D8-Toluène	78
1-Bromo-4-fluorobenzène	80

Non-conformité(s):
Commentaire(s):
Note: Ces résultats ne se rapportent qu'aux échantillons soumis pour analyse.

Martin Brunet
94-076

Chimiste ____________
Martin Brunet

À l'attention de Denise Saulnier
Client Argile-Eau-Mer
5594 Waverly
Montréal, Qc.
H2T 2Y1

No de certificat 3986-98
Date d'émission 98-05-22
Date de réception 98-05-08
No. demande 98-39411
Bon de commande NA

Identification	1 Composite (0002041, 0002042, 0002043)
Référence	Argile Eau Mer
Matrice	Sol
Date de prélèvement	NA
Lieu du prélèvement	S-980424-BS1
Prélevé par	Denise Saulnier
No de laboratoire	180894
Date de préparation	98-05-19
Date d'analyse	98-05-19
HMA-T-S-13	mg/kg
Benzène	< 0.1
Ethylbenzène	< 0.1
Chlorobenzène	< 0.1
Toluène	< 0.1
Xylènes	< 0.1
Styrène	< 0.1
1,2-Dichlorobenzène	< 0.1
1,3-Dichlorobenzène	< 0.1
1,4-Dichlorobenzène	< 0.1
Total	ND
%Récupération	
Dibromofluorométhane	59
D8-Toluène	78
1-Bromo-4-fluorobenzène	80

Non-conformité(s):
Commentaire(s):
Note: Ces résultats ne se rapportent qu'aux échantillons soumis pour analyse.

CHIMISTE Martin Brunet 94-076 QUÉBEC

Chimiste
Martin Brunet

H9R 4P3

INVOICE PORT A

PAGE

FACTURÉ À / INVOICED TO

ARGILE-EAU-MER
5594 WAVERLY
MONTREAL, QC
H2T 2Y1
Canada
ATTENTION: DENISE SAULNIER

REQUIS PAR / REQUESTED BY

ARGILE-EAU-MER
5594 WAVERLY
MONTREAL, QC
H2T 2Y1
Canada
ATTENTION: DENISE SAULNIER

Nº CLIENT CUSTOMER NO.	VOTRE Nº COMMANDE YOUR ORDER NO.	Nº PROJET PROJETCT NO.	DATE RAPPORT REPORT DATE	AUTRES OTHERS	TERR.
MTSCAA		98-39411	06/26/98		

QUANTITÉ QUANTITY	ARTICLE ITEM	DESCRIPTION	PRIX UNITAIRE UNIT PRICE	MONTANT AMOUNT
1.00		PESTICIDE-BPC-EMA HRT-PHENOLS-HYDR. PETROLIERS-HAP.	$1305.00	$1305.00

PAYER PAR CHEQUE #0043

MERCI!

Notre numéro de référence: [illegible]

[illegible]

SOUS-TOTAL SUB-TOTAL	[illegible]
T.P.S./G.S.T. 105156822RT	$91.35
T.V.Q./Q.S.T. 1000448890	$104.73

H9H 4P3

INVOICE RAPPORT A

PAGE	

FACTURÉ À / INVOICED TO

ARGILE-EAU-MER
5594 WAVERLY
MONTREAL, QC
H2T 2Y1
Canada
ATTENTION: DENISE SAULNIER

REQUIS PAR / REQUESTED BY

ARGILE-EAU-MER
5594 WAVERLY
MONTREAL, QC
H2T 2Y1
Canada
ATTENTION: DENISE SAULNIER

Nº CLIENT CUSTOMER NO.	VOTRE Nº COMMANDE YOUR ORDER NO.	Nº PROJET PROJETCT NO.	DATE RAPPORT REPORT DATE	AUTRES OTHERS	TERR.
MISCAA		98-39411	06/26/98		

QUANTITÉ QUANTITY	ARTICLE ITEM	DESCRIPTION	PRIX UNITAIRE UNIT PRICE	MONTANT AMOUNT
1.00		PESTICIDE-BPC-HMA-HRT-PHENOLS-HYDR. PETROLIERS-HAP.	$1305.00	$1305.00

PAYER PAR CHEQUE #0043

MERCI!

Notre numéro de référence: 002627

MB/CB/CM

SOUS-TOTAL SUB-TOTAL $1305.00	$1305.00
T.P.S./G.S.T. 105156822RT	$91.35
T.V.Q./Q.S.T. 1000448890	$104.73

À l'attention de Denise Saulnier
Client Argile-Eau-Mer
5594 Waverly
Montréal, Qc.
H2T 2Y1

No de certificat 3986-98
Date d'émission 98-05-22
Date de réception 98-05-08
No. demande 98-39411
Bon de commande NA

No. de laboratoire	181790			181791	
Type de contrôle	Blanc	Echantillon	Duplicata	Contrôle Certifié	
Matrice					
Date de prélèvement					
Lieu du prélèvement					
Prélevé par					
Référence				Obtenu	Écart acceptable
Date de préparation	98-05-12			98-05-12	
Date d'analyse	98-05-12			98-05-12	
BPC-A-S-13	mg/kg			mg/kg	mg/kg
Aroclor 1242	< 0.1			(-)	(-)
Aroclor 1248	< 0.1			18	(13 - 31)
Aroclor 1254	< 0.1			(-)	(-)
Aroclor 1260	< 0.1			(-)	(-)
Total	ND				
%Récupération					
Décachlorobiphényle	76			90	

Non-conformité(s):
Commentaire(s):
Note: Ces résultats ne se rapportent qu'aux échantillons soumis pour analyse.

Martin Brunet
94-076

À l'attention de Denise Saulnier
Client Argile-Eau-Mer
5594 Waverly
Montréal, Qc.
H2T 2Y1

No de certificat 3986-98
Date d'émission 98-05-22
Date de réception 98-05-08
No. demande 98-39411
Bon de commande NA

No. de laboratoire	181873			181878	
Type de contrôle	Blanc	Echantillon	Duplicata	Contrôle Certifié	
Matrice					
Date de prélèvement					
Lieu du prélèvement					
Prélevé par					
Référence				Obtenu	Écart acceptable
Date de préparation	98-05-13			98-05-13	
Date d'analyse	98-05-13			98-05-13	
HAP-T-S-13	mg/kg			mg/kg	mg/kg
Naphtalène	< 0.1			11	(5.8 - 14)
Acénaphthylène	< 0.1			(-)	(-)
Acénaphtène	< 0.1			10	(4.5 - 11)
Fluorène	< 0.1			(-)	(-)
Phénanthrène	< 0.1			(-)	(-)
Anthracène	< 0.1			4.2	(0.6 - 6)
Fluoranthène	< 0.1			(-)	(-)
Pyrène	< 0.1			5.3	(1.5 - 6.3)
7,12-Diméthylbenzoanthracène	< 0.1			(-)	(-)
Benzo (g,h,i) pérylène	< 0.1			(-)	(-)
Benzo (c) phénanthrène	< 0.1			(-)	(-)
Chrysène	< 0.1			2.6	(1.1 - 3.4)
Benzo (a) anthracène	< 0.1			(-)	(-)
Benzo (b,j,k) fluoranthène	< 0.1			6.4	(1.2 - 6.7)
Benzo (a) pyrène	< 0.1			(-)	(-)
3-Méthylcholanthrène	< 0.1			(-)	(-)
Indéno (1,2,3-cd) pyrène	< 0.1			(-)	(-)
Dibenzo (ah) anthracène	< 0.1			(-)	(-)
Dibenzo (a,l) pyrène	< 0.1			(-)	(-)
Dibenzo (a,i) pyrène	< 0.1			(-)	(-)
Dibenzo (a,h) pyrène	< 0.1			(-)	(-)
Total	ND				
%Récupération					
D10-Fluorène	95			100	
D10-pyrène	85			80	
D12-Benzo[a]pyrène	100			100	

Non-conformité(s):
Commentaire(s):
Note: Ces résultats ne se rapportent qu'aux échantillons soumis pour analyse.

Martin Brunet
94-076

Certificat d'analyse – Certificate of Analysis

À l'attention de Denise Saulnier
Client Argile-Eau-Mer
5594 Waverly
Montréal, Qc.
H2T 2Y1

No de certificat 3986-98
Date d'émission 98-05-22
Date de réception 98-05-08
No. demande 98-39411
Bon de commande NA

No. de laboratoire	181869			181871	
Type de contrôle	Blanc	Echantillon	Duplicata	Contrôle Certifié	
Matrice					
Date de prélèvement					
Lieu du prélèvement					
Prélevé par					
Référence				Obtenu	Écart acceptable
Date de préparation	98-05-13			98-05-13	
Date d'analyse	98-05-13			98-05-13	
HGM-C10-50-S-13	mg/kg			mg/kg	mg/kg
Hydrocarbures Pétroliers C10-C50	< 100			1900	(1370 - 2930)
%Récupération					

Non-conformité(s):
Commentaire(s):
Note: Ces résultats ne se rapportent qu'aux échantillons soumis pour analyse.

Martin Brunet
94-076

À l'attention de Denise Saulnier
Client Argile-Eau-Mer
5594 Waverly
Montréal, Qc.
H2T 2Y1

No de certificat 3986-98
Date d'émission 98-05-22
Date de réception 98-05-08
No. demande 98-39411
Bon de commande NA

No. de laboratoire	183023	180894	183020	183022	
Type de contrôle	Blanc	Echantillon	Duplicata	Contrôle Certifié	
Matrice	Sol	Sol	Sol		
Date de prélèvement		00-01-01	00-01-01		
Lieu du prélèvement		S-980424-BS1	S-980424-BS1		
Prélevé par		Denise Saulnier	Denise Saulnier		
Référence				Obtenu	Écart acceptable
Date de préparation	98-05-19	98-05-19	98-05-19	98-05-19	
Date d'analyse	98-05-19	98-05-19	98-05-19	98-05-19	
HHT-T-S-13	mg/kg	mg/kg	mg/kg	ng	ng
Chloroforme	< 0.1	< 0.1	< 0.1	230	(196 - 298)
1,1-Dichloroéthane	< 0.1	< 0.1	< 0.1	430	(406 - 625)
1,1-Dichloroéthène	< 0.1	< 0.1	< 0.1	(-)	(-)
1,2-Dichloroéthane	< 0.1	< 0.1	< 0.1	790	(675 - 1095)
1,2-Dichloroéthène (t+c)	< 0.1	< 0.1	< 0.1	(-)	(-)
1,2-Dichloropropane	< 0.1	< 0.1	< 0.1	(-)	(-)
1,3-Dichloropropène (t+c)	< 0.1	< 0.1	< 0.1	(-)	(-)
Dichlorométhane	< 0.1	< 0.1	< 0.1	130	(94.5 - 239)
1,1,2,2-Tétrachloroéthane	< 0.1	< 0.1	< 0.1	(-)	(-)
Tetrachloroéthène	< 0.1	< 0.1	< 0.1	460	(359 - 580)
Tetrachlorure de Carbone	< 0.1	< 0.1	< 0.1	830	(620 - 1075)
1,1,1-Trichloroéthane	< 0.1	< 0.1	< 0.1	320	(247 - 434)
1,1,2-Trichloroéthane	< 0.1	< 0.1	< 0.1	280	(218 - 393)
Trichloroéthène	< 0.1	< 0.1	< 0.1	400	(394 - 625)
Total	ND	ND	ND		
%Récupération					
Dibromofluorométhane	97	59	66	110	
D8-Toluène	82	78	79	89	
1-Bromo-4-fluorobenzène	83	80	82	93	

Non-conformité(s):
Commentaire(s):
Note: Ces résultats ne se rapportent qu'aux échantillons soumis pour analyse.

CHIMISTE
Martin Brunet
94-076
QUÉBEC

Le 24 avril 1998.

Madame Denise Saulnier
Argile - Eau - Mer
273-3573

FAX: 273-9373

OBJET: **Offre de services analytiques numéro S - 980424 -BS-1**
Analyse d'argile

Madame Saulnier,

La présente est pour faire suite à notre conversation téléphonique d'aujourd'hui relativement à l'objet cité en rubrique. Vous trouverez sur le tableau ci-dessous les tarifs reliés à ces paramètres.

PROPOSITION TARIFAIRE

Paramètre	Tarif unitaire[1,2]
Hydrocarbure Pétrolier C10-C50	70.00 $
Hydrocarbure Aromatique Monocyclique et Hydrocarbure Halogéné Totaux (HAM et HHT), composés volatiles	130.00 $
Hydrocarbures Aromatique Polycyclique (HAP) et Phénols	190.00 $
Biphényle Polychloré (Aroclor)	90.00 $
Pesticides Organochloré (note 3)	145.00 $
Pesticides Organophosphorés (note 3)	260.00 $
Pesticides Phénoxyacide (note 3)	190.00 $
Pesticides Diquat et Paraquat (note 3)	230.00 $

1305
91.35 (T.P.S
104.72 (T.V.Q

1501,07
txes Incluses

Note 1:	Taxe et transport en sus, terme net 30 jours, tarif valable jusqu'au 31 décembre 1998. Délai d'analyse de 5 jours ouvrables. Contrôle de qualité normal. Facturation minimale de 65.00 $ par expédition.
Note 2:	**Veuillez mentionner le numéro de l'offre pour que ces tarifs soient appliqués.**
Note 3:	Analyses faite en sous-traitance, délai d'analyse de 10 jours ouvrables

Espérant le tout conforme à vos attentes, recevez Madame Saulnier, mes salutations les meilleures.

Benoît Saumure M. Sc. Chimiste
Directeur de projets

I:\LAB_MGR\PROP\PROP98\PRIV~1\ARGILE~1\80424BS2.DOC

NO. DE COMPTE T.P.S - T.V.Q

Montréal, le 22 juin 1998

Rapport no. 131-EL-1078-2

Madame Denise Saulnier
Argile eau mer
5594, rue Waverly
Montréal (Québec) H2T 2Y1

A l'attention de Madame Denise Saulnier

Objet : Essais de limites de consistance
Utilisation thérapeutique des argiles

Madame,

Suite à votre demande, nous avons effectué deux essais de limites de consistance et deux essais de teneur en eau sur deux échantillons que vous nous avez apportés. Le tableau suivant donne les résultats obtenus.

Tableau : résultats des essais de limites de consistance sur les échantillons nos. 2041 et 2043.

Échantillon no.	Teneur en eau (%)	Limite de liquidité (%)	Limite de plasticité (%)	Indice de plasticité (%)
2043	32	24	18	6
2041	28	22	Proche de 17	Proche de 5

Nous espérons ce rapport à votre entière satisfaction et nous demeurons à votre disposition pour tout renseignement additionnel. Veuillez agréer, Madame, l'expression de nos salutations distinguées.

Consultant Sol-Géo inc.

M. Hosseini
100226

Mohammad Hosseini, ing., Ph.D., Dr.
Président

En duplicata

RAPPORT SUR L'ARGILE
DE BAIE-SAINT-LUDGER
(SNRC 22 F/1)

PAR :

Bertrand Brassard
Directeur général F.R.E.M.
géologue, M. Sc.

Luc Arsenault
géologue de projet

POUR :

Denise Saulnier

DÉCEMBRE 1995

TABLE DES MATIÈRES

1. OBJECTIF

L'objectif visé par ce présent rapport est de résumer les travaux exécutés dans le secteur de Baie-Saint-Ludger, ainsi que de discuter des résultats des analyses faites sur l'argile.

2. BUTS

Le but des travaux était de caractériser l'argile provenant d'un des six permis de recherche de substance minérale appartenant à Mme Denise Saulnier. Ceci, afin de déterminer à quelles utilisations pourrait être associées cette argile, en vue d'en faire l'exploitation économique.

3. LOCALISATION ET ACCÈS

Le secteur de Baie-Saint-Ludger se situe à environ 20 km à l'ouest de Baie-Comeau. Plus précisément, les permis (PRS) de Mme Saulnier se trouvent entre les longitudes 68°15' et 68°23' et les latitudes 49°04' et 49°07'. On accède aisément le secteur à partir de la route 138 par une voie secondaire pavée qui longe la rive du St-Laurent sur une distance d'environ 13 km.

4. TRAVAUX ANTÉRIEURS

À notre connaissance, aucun travail n'a été fait afin de caractériser le type d'argile dans la région de Baie-Saint-Ludger. Le secteur est bien connu pour le problème d'érosion de ses berges. Conséquemment, seuls des travaux portant sur la stabilité de celle-ci ont été exécutés.

5. PRS
PERMIS DE RECHERCHE DE SUBSTANCE MINÉRALE DE SURFACE

Un total de six permis de recherche de substance minérale de surface ont été acquis par Mme Saulnier.

TABLEAU
DES PRS DE MME SAULNIER

PRS	0002039	
PRS	0002040	
PRS	0002041	2 forages
PRS	0002042	
PRS	0002043	
PRS	0002044	

Leur validité est d'une durée de deux ans à partir du 17 janvier 1994.

Les résultats discutés dans ce rapport proviennent essentiellement de deux forages effectués sur le PRS 0002041.

6. GÉOLOGIE DES DÉPÔTS MEUBLES (tiré de Allard 1984)

Les dépôts meubles de la région sont en grande partie des dépôts deltaïques; ils comprennent du sable, du silt et de l'argile. La stratigraphie est complexe; les sédiments deviennent plus grossiers ou plus fins, selon qu'on se rapproche ou qu'on s'éloigne de l'ancienne embouchure de la rivière aux Outardes, embouchure située au niveau de la limite des dépôts meubles et du socle précambrien. La surface du delta est parsemée d'anciens chenaux remplis de dépôts sablo-graveleux, généralement recouverts de tourbe et de matière organique.

7. TRAVAUX SUR LE TERRAIN

Les travaux de forage ont été faits sur le permis numéro 0002041 du 13 au 14 décembre 1995.

Les travaux ont été exécutés par la firme SEDAC inc. L'équipement utilisé était une foreuse pour dépôts meubles ainsi qu'un échantillonneur de type cuillère fendue de 18 pouces de long.

En tout, deux forages ont été complétés soit un de 45 pieds et un autre de 34.5 pieds.

L'emplacement du forage numéro 1 se trouve à moins de 100 mètres au nord du chemin et le forage numéro 2 se trouve à 50 mètres le long de l'ancien chemin, aujourd'hui désaffecté.

8. ANALYSES CHIMIQUES

En tout, cinq échantillons ont été envoyés pour fin d'analyses au Centre géoscientifique de Québec (C.G.Q.). Conséquemment, les commentaires inclus dans cette section proviennent en partie de M. André Chagnon du C.G.Q. et en partie des géologues du F.R.E.M.

8.1 MINÉRALOGIE

L'analyse minéralogique a été effectuée par diffraction aux rayons-X sur l'échantillon global, sans fractionnement granulométrique. Les résultats sont présentés en annexe 3. Les proportions des minéraux sont estimées à partir de l'intensité des pics de diffraction corrigée par l'effet d'orientation et de masse.

Il y a très peu de phyllosilicate dans les échantillons qui sont surtout formés de quartz et de feldspath. Le mica est une biotite et la chlorite est magnésienne. L'amphibole est de type hornblende. Cet assemblage ressemble beaucoup à ceux déjà observés dans les argiles de la mer de Champlain des Basses-Terres. Les minéraux sont peu ou pas altérés. Si l'on regarde les analyses granulométriques, on se rend compte qu'une partie de la masse de ces sédiments doit être amorphe. C'est la règle dans ce genre de matériaux.

2 GRANULOMÉTRIE

Les analyses effectuées au granulomètre à laser nous montre un matériau silteux ayant une proportion faible de particules plus fines que deux microns. De plus, ces analyses indiquent que l'ensemble des particules ont une granulométrie variant entre 3.99 et 17.87 microns. La distribution est plutôt bimodale. Les paramètres statistiques des courbes de distribution accompagnent le graphique et nous indiquent un très mauvais trie des particules.

9. CONCLUSION

Les deux forages effectués sur le PRS no. 0002041 nous permettent de déduire qu'un horizon d'argile se trouve sous une couverture de sable d'environ 20 pieds (6.1 m.). Selon ces forages, le niveau d'argile est épais d'au moins cinq mètres et semble s'étendre sur plusieurs kilomètres puisqu'il est observé sur une bonne partie des berges de Baie Saint-Ludger.

Il est à noter que les travaux d'échantillonnage ont été rendus difficiles dû à la liquéfaction de l'argile. Celle-ci semble avoir une quantité d'eau assez importante soit d'environ 50%.

Les resultats d'analyses minéralogiques nous permettent de conclure qu'en moyenne, les minéraux présents dans cet argile sont : 44%

quartz, 36% feldspath-Na, 6,2% feldspath-K, 7,2% amphibole, 6,6% biotite et 2% chlorite. Selon M. Chagnon, cet assemblage a été observé à plusieurs endroits, typiquement dans les dépôts de la mer de Champlain des Basses-Terres.

En ce qui a trait aux éléments traces, on note des valeurs relativement basses sauf pour deux des éléments soit le barium (723 à 803 ppm) et le strontium (419 à 459 ppm).

10. RECOMMANDATIONS

Les conclusions tirées dans ce rapport ne nous permettent pas d'évaluer le juste potentiel de l'argile de Baie-Saint-Ludger pour les fins de thalassothérapie et industrielles. Toutefois, les résultats fragmentaires obtenus jusqu'à présent semblent indiquer que la composition minéralogique ainsi que la granulométrie ne semblent pas conformes à ce type d'utilisation. Par conséquent, nous recommandons que les résultats soient analysés par des spécialistes dans ce domaine.

RÉFÉRENCES

ALLARD, J.D. - 1984 - Zones exposées aux mouvements de terrain dans la région de Chûte-aux-Outardes. Ministère des Richesses Naturelles, Québec, DV 83-01

BRADY, J.G. et Dean, R.S. - Composition et propriétés des argiles et des schistes argileux à céramique du Québec. Ministère de L'Énergie, des Mines et des Ressources, Ottawa, R 187

FRANCONI, A.-SHARMA, K.N.M.- LAURIN, A.F. - 1975 - Région des rivières Betsiamites et Moisie (Grenville 1968-1969). Ministère des Richesses naturelles, Québec. RG-162

M.R.N.Q. - 1969 - Carte aéromagnétique 22G/14. Ministère des Richesses naturelles, Québec. Carte 4996G.

NEWMAN, A.C.D. - 1987 - Chemistry of clays and clay minerals, Mineralogical Society monograph, No. 6

ANNEXE I

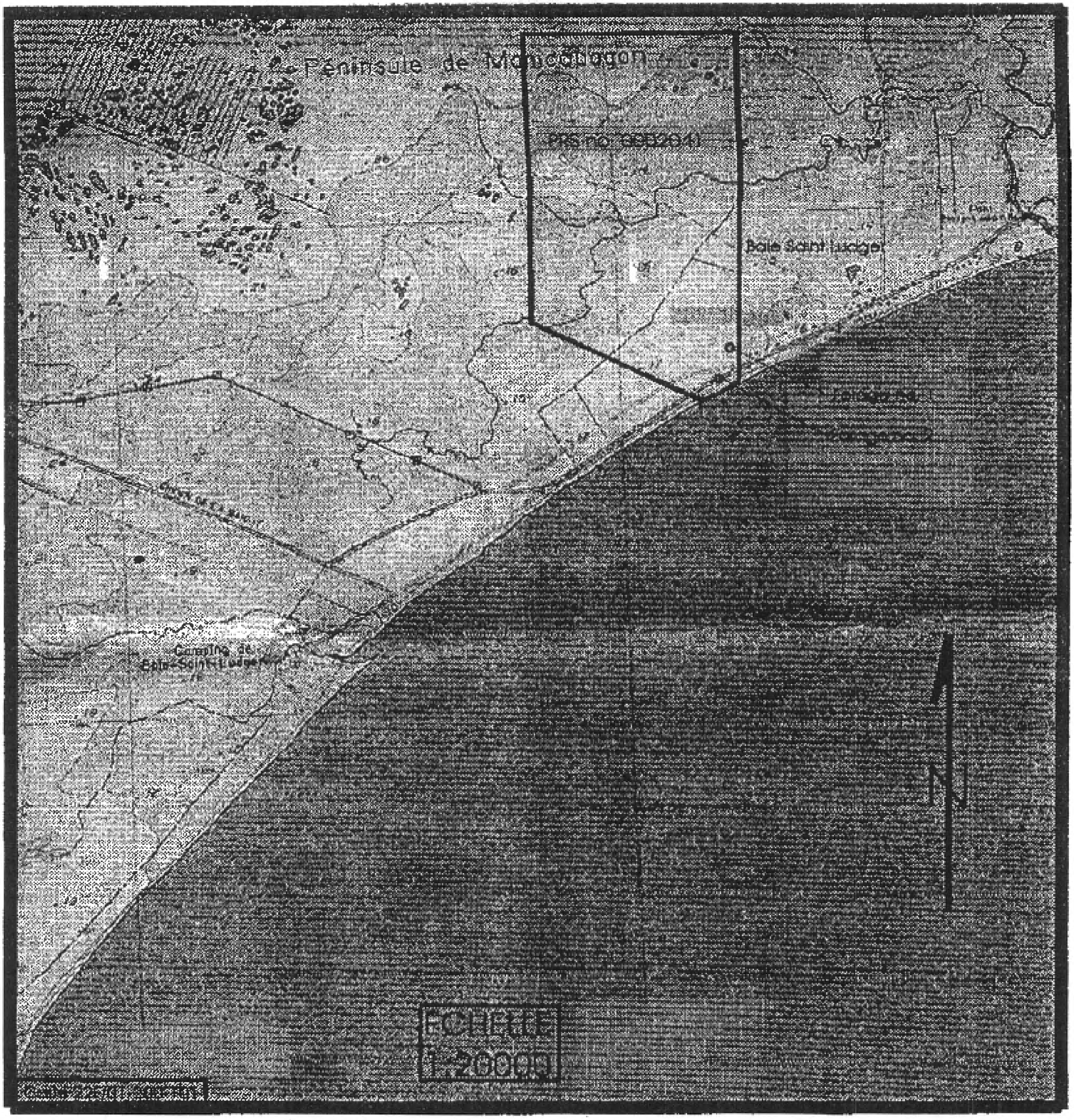

Carte de localisation du PRS 2041, péninsule Manicouagan, région de Baie Comeau

ANNEXE II

Forage no. 1 Baie-Saint-Ludger

Régistre de sondage, trou numéro 1	
Profondeur	Description
0 à 20 pieds	sable fin de couleur brun à brun-pâle
20 à 25 pieds	sable fin de couleur brun-pâle, mouillé (nappe)
25 à 45 pieds	sable fin gris-pâle et argilleux

ANNEXE III

Tableau 1. Résultats de l'analyse semie-quantitative par diffraction aux rayons-X de 5 échantillons d'argile. QTZ.: quartz; NA-FELD.: feldspath plagioclase; K-FELD.: feldspath potassique; AMPH.: amphibole; CHLOR.: chlorite

NO. INRS	ECHANT.	MINÉRALOGIE						
		QTZ	NA-FELD	K-FELD	AMPH.	MICA	CHLOR.	TOTAL
28695	1 À 2	50	30	5	8	7	2	100
28696	3 À 4	40	40	5	8	7	2	100
28697	5 À 6	40	40	7	10	3	2	100
28698	7 À 8	45	35	7	5	8	2	100
28699	9 À 10	45	35	7	5	8	2	100
moyenne		44	36	6.2	7.2	6.6	2	100

QTZ : quartz; NA-FELD : feldspath plagioclase; K-FELD : feldspath potassique; AMPH : amphibole ;

HY964RAP

Centre Géoscientifique de Québec
Laboratoire de fluorescence X

Nom du clie	Héroux Yvon
Projet	Frem argiles
Imputation	15242840
Nom du lot	HY964
Nombre	5

Code	Échantillon	Na2O	MgO	Al2O3	SiO2	P2O5
Cal	1YH29695	3,87	3,01	16,43	60,25	0,2
Cal	2YH29696	3,91	3,4	16,88	60,32	0,21
Cal	3YH29697	3,96	3,37	16,78	60,07	0,21
Cal	4YH29698	3,73	3,17	15,79	56,67	0,21
Cal	5YH29699	3,9	3,16	16,71	60,35	0,23

Échantillon	S	K2O	CaO	TiO2	MnO	Fe2O3
1YH29695	0	2,65	4,1	0,62	0,09	5,6
2YH29696	0	2,76	3,93	0,65	0,1	6,09
3YH29697	0	2,59	4,1	0,66	0,09	5,96
4YH29698	0	2,56	6,01	0,62	0,19	5,87
5YH29699	0	2,67	4,35	0,67	0,1	6,05

Échantillon	Ba	Co	Cr	Cu	Ga	Nb
1YH29695	756	19	97	40	19	< 3
2YH29696	748	23	105	48	19	< 3
3YH29697	723	21	101	36	18	5
4YH29698	726	21	98	32	19	< 3
5YH29699	803	20	102	37	15	3

Échantillon	Ni	Pb	Rb	Sr	V	Y
1YH29695	63	< 5	78	429	88	14
2YH29696	73	11	91	419	97	16
3YH29697	59	7	84	432	95	19
4YH29698	58	13	82	459	88	17
5YH29699	61	11	89	439	91	19

Échantillon	Zn	Zr	PfF	Total
1YH29695	72	156	1,55	98,55
2YH29696	77	134	1,7	100,14
3YH29697	83	167	1,5	99,47
4YH29698	77	151	3,61	98,61
5YH29699	78	175	1,55	99,96

```
FRITSCH Particle Sizer Analysette 22

ZDDDDDDDDDDDDDDDDDDDDDDDDDDDDDDDDDDDDDDDDDDDDDDDDDDDDDDDDDDDDDDDDDDDDDDDDDDDDDDDDDDDDDDDDDDDDDDDDDDDDDD?
3Measure Numb    23Date 02-12-953Time 16:193Iteration Resid. 0.0148 %3  Overl  3Iteration    56 3Beam obscu   10.00 %  3
CDDDDDDDDDDDDDDDDDDDDDDDDDDDDDDDDDDDDDDDDDDDDDDDDDDDDDDDDDDDDDDDDDDDDDDDDDDDDDDDDDDDDDDDDDDDDDDDDDDDDDD4
3 Argiles 28695                          Fraction 37u < >150u                                                 3
3 Fraunhofer                              n =   fnhf * Fraunhofer                       n =   fnhf ' = 0.0000 3
CDDDDDDDDDDDDDDDDDDDDDDDDDDDDDDDDDDDDDDDDDDDDDDDDDDDDDDDDDDDDDDDDDDDDDDDDDDDDDDDDDDDDDDDDDDDDDDDDDDDDDD4
3    95.02% >    1.00 f     87.34% >    2.00 f     77.05% >    4.00 f     52.49% >   16.00 f     34.23% >   32.00 f    3
3    14.51% >   63.00 f      7.08% >  125.00 f    ******% >  250.00 f    ******% >  500.00 f    ******% > 1000.00 f    3
CDDDDDDDDDDDDDDDDDDDDDDDDDDDDDDDDDDDDDDDDDDDDDDDDDDDDDDDDDDDDDDDDDDDDDDDDDDDDDDDDDDDDDDDDDDDDDDDDDDDDDD4
3    90.00% >    1.64 f     80.00% >    3.30 f     70.00% >    6.27 f     60.00% >   11.11 f     50.00% >   17.87 f    3
3    40.00% >   26.34 f     30.00% >   36.66 f     20.00% >   50.47 f     10.00% >   88.31 f     Volume Distribution    3
@DDDDDDDDDDDDDDDDDDDDDDDDDDDDDDDDDDDDDDDDDDDDDDDDDDDDDDDDDDDDDDDDDDDDDDDDDDDDDDDDDDDDDDDDDDDDDDDDDDDDDDY
ZDDDDDDDDDDDDDDDDDDDDDDDDDDDDDDDDDDDDDDDDDDDDDDDDDDDDDDDDDDDDDDDDDDDDDDDDDDDDDDDDDDDDDDDDDDDDDDDDDDDDDD?
3 Arithm. mean diameter :    32.08 um   Variance              :       38.47 sqr(um)   Skewness   :            399.60 3
3 Geom mean diameter    :    13.92 um   Standard Deviation    :        6.20 um        Curtosis   :           7386.973
3 Qadr.Sq. mean diam.   :    49.94 um   Mean Deviation        :       28.27 um        Span       :              4.85 3
3 Harmonic mean diam.   :     4.48 um   Coefficient Variance:        119.93 %         Uniformity :              1.45 3
3 Mode                  :   148.63 um   Median                    :   17.87 um        Mean/Median Ratio    :    1.79 3
3                           Spec. surface area          1.3407 sqr(m)/cc          Form factor    1                     3
@DDDDDDDDDDDDDDDDDDDDDDDDDDDDDDDDDDDDDDDDDDDDDDDDDDDDDDDDDDDDDDDDDDDDDDDDDDDDDDDDDDDDDDDDDDDDDDDDDDDDDDY
```

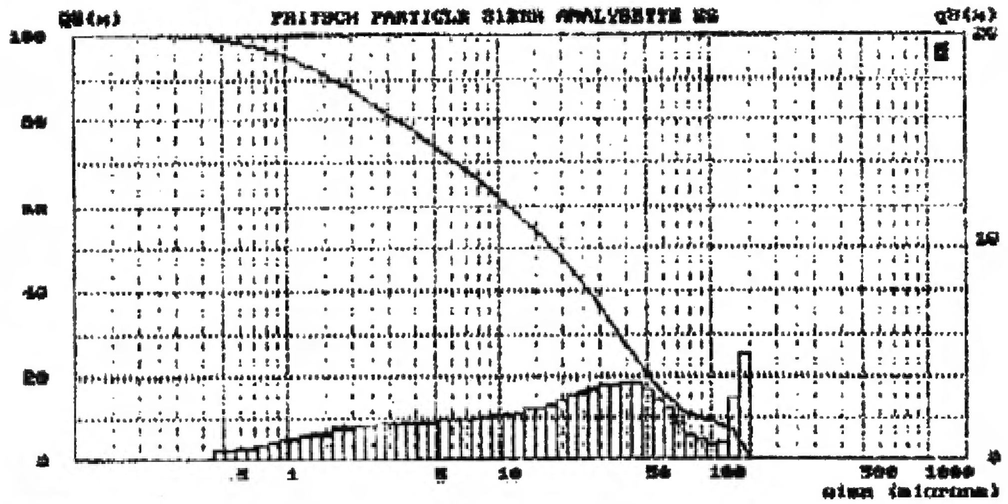

1   2   Argiles 28695   Fraction 37u < >150u

1-2

```
FRITSCH Particle Sizer Analysette 22

IDDDDDDDDDDDDDDDDDDDDDDDDDDDDDDDDDDDDDDDDDDDDDDDDDDDDDDDDDDDDDDDDDDDDDDDDDDDDDDDDDDDDDDDDDDDDDDDDDDDDD?
3Measure Numb    37Date 02-12-953Time 16:293Iteration Resid. 0.0188 %3  Overl  3Iteration    56 3Beam obscu   11.00 %  3
CDDDDDDDDDDDDDDDDDDDDDDDDDDDDDDDDDDDDDDDDDDDDDDDDDDDDDDDDDDDDDDDDDDDDDDDDDDDDDDDDDDDDDDDDDDDDDDDDDDDDDD4
3 Argiles 28696                          Fraction 37u ( )150u                                          3
3 Fraunhofer                              n =   fnhf * Fraunhofer                        n =   fnhf ' = 0.0000 3
CDDDDDDDDDDDDDDDDDDDDDDDDDDDDDDDDDDDDDDDDDDDDDDDDDDDDDDDDDDDDDDDDDDDDDDDDDDDDDDDDDDDDDDDDDDDDDDDDDDDDDD4
3    91.79% >    1.00 f     79.13% >    2.00 f     61.93% >    4.00 f     25.26% >   16.00 f     7.31% >   32.00 f    3
3     0.16% >   63.00 f      0.00% >  125.00 f    ######% >  250.00 f    ######% >  500.00 f   ######% > 1000.00 f    3
CDDDDDDDDDDDDDDDDDDDDDDDDDDDDDDDDDDDDDDDDDDDDDDDDDDDDDDDDDDDDDDDDDDDDDDDDDDDDDDDDDDDDDDDDDDDDDDDDDDDDDDD4
3    90.00% >    1.14 f     80.00% >    1.92 f     70.00% >    2.92 f     60.00% >    4.31 f    50.00% >    6.38 f    3
3    40.00% >    9.34 f     30.00% >   13.49 f     20.00% >   19.42 f     10.00% >   28.53 f    Volume Distribution  3
@DDDDDDDDDDDDDDDDDDDDDDDDDDDDDDDDDDDDDDDDDDDDDDDDDDDDDDDDDDDDDDDDDDDDDDDDDDDDDDDDDDDDDDDDDDDDDDDDDDDDDDY
IDDDDDDDDDDDDDDDDDDDDDDDDDDDDDDDDDDDDDDDDDDDDDDDDDDDDDDDDDDDDDDDDDDDDDDDDDDDDDDDDDDDDDDDDDDDDDDDDDDDDD?
3  Aritha. mean diameter :   11.07 um   Variance              :      11.80 sqr(um)   Skewness   :            63.12 3
3  Geom mean diameter    :    5.96 um   Standard Deviation    :       3.44 um        Curtosis   :           726.963
3  Quadr.Sq. mean diam.  :   16.13 um   Mean Deviation        :       9.11 um        Span       :             4.30 3
3  Harmonic mean diam.   :    2.83 um   Coefficient Variance:       106.62 %         Uniformity :             1.31 3
3  Mode                  :   14.75 um   Median                :       6.38 um        Mean/Median Ratio  :     1.74 3
3                      Spec. surface area          2.1196 sqr(m)/cc          Form factor   1                   3
@DDDDDDDDDDDDDDDDDDDDDDDDDDDDDDDDDDDDDDDDDDDDDDDDDDDDDDDDDDDDDDDDDDDDDDDDDDDDDDDDDDDDDDDDDDDDDDDDDDDDDDY
```

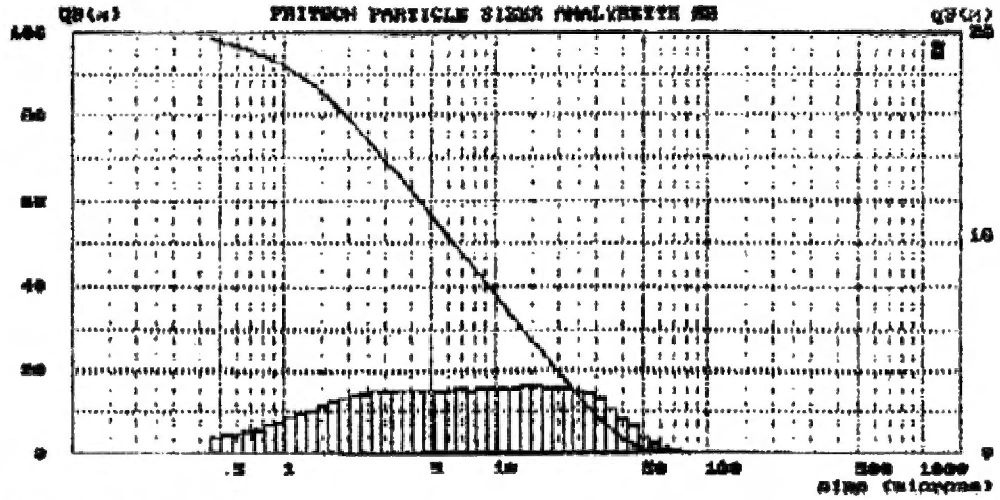

1   3   Argiles 28696   Fraction 37u ( )150u

3-4

FRITSCH Particle Sizer Analysette 22

```
ZDDDDDDDDDDDDDDDDDDDDDDDDDDDDDDDDDDDDDDDDDDDDDDDDDDDDDDDDDDDDDDDDDDDDDDDDDDDDDDDDDDDDDDDDDDDDDDDDDDDDDDDDDDDDDDDDD?
3Measure Numb    49Date 02-12-953Time 16:4231teration Resid. 0.0137 13  Overl  3Iteration    56 3Beam obscu   11.00 %  3
CDDDDDDDDDDDDDDDDDDDDDDDDDDDDDDDDDDDDDDDDDDDDDDDDDDDDDDDDDDDDDDDDDDDDDDDDDDDDDDDDDDDDDDDDDDDDDDDDDDDDDDDDDDDDDDDDD4
3 Argiles 28697                       Fraction 37u < >150u                                                        3
3 Fraunhofer                            n =   fnhf ' Fraunhofer                          n =   fnhf ' = 0,0000 3
CDDDDDDDDDDDDDDDDDDDDDDDDDDDDDDDDDDDDDDDDDDDDDDDDDDDDDDDDDDDDDDDDDDDDDDDDDDDDDDDDDDDDDDDDDDDDDDDDDDDDDDDDDDDDDDDDD4
3    93.41% >    1.00 /     83.19% >    2.00 /     68.88% >    4.00 /     34.75% >   16.00 /     13.16% >   32.00 /    3
3     0.73% >   63.00 /      0.00% >  125.00 /    ******% >  250.00 /    ******% >  500.00 /    ******% > 1000.00 /    3
CDDDDDDDDDDDDDDDDDDDDDDDDDDDDDDDDDDDDDDDDDDDDDDDDDDDDDDDDDDDDDDDDDDDDDDDDDDDDDDDDDDDDDDDDDDDDDDDDDDDDDDDDDDDDDDDDD4
3    90,00% >    1.32 /     80.00% >    2.37 /     70.00% >    3.80 /     60.00% >    5.97 /     50.00% >    9.10 /    3
3    40.00% >   13.29 /     30.00% >   18.71 /     20.00% >   25.78 /     10.00% >   35.70 /    Volume Distribution    3
@DDDDDDDDDDDDDDDDDDDDDDDDDDDDDDDDDDDDDDDDDDDDDDDDDDDDDDDDDDDDDDDDDDDDDDDDDDDDDDDDDDDDDDDDDDDDDDDDDDDDDDDDDDDDDDDDDY
ZDDDDDDDDDDDDDDDDDDDDDDDDDDDDDDDDDDDDDDDDDDDDDDDDDDDDDDDDDDDDDDDDDDDDDDDDDDDDDDDDDDDDDDDDDDDDDDDDDDDDDDDDDDDDDDDDD?
3  Arithm. mean diameter :    14.42 um   Variance              :      14.61 sqr(um)   Skewness    :          78.65 3
3  Geom mean diameter    :     7.75 um   Standard Deviation    :       3.82 um        Curtosis    :        1060.953
3  Qadr.Sq. mean diam.   :    20.48 um   Mean Deviation        :      11.52 um        Span        :           3.78 3
3  Harmonic mean diam.   :     3.39 um   Coefficient Variance:       101.30 %         Uniformity :            1.19 3
3  Mode                  :    26.43 um   Median                  :     9.10 um        Mean/Median Ratio    :  1.58 3
3                           Spec. surface area        1.7704 sqr(m)/cc          Form factor   1                    3
@DDDDDDDDDDDDDDDDDDDDDDDDDDDDDDDDDDDDDDDDDDDDDDDDDDDDDDDDDDDDDDDDDDDDDDDDDDDDDDDDDDDDDDDDDDDDDDDDDDDDDDDDDDDDDDDDDY
```

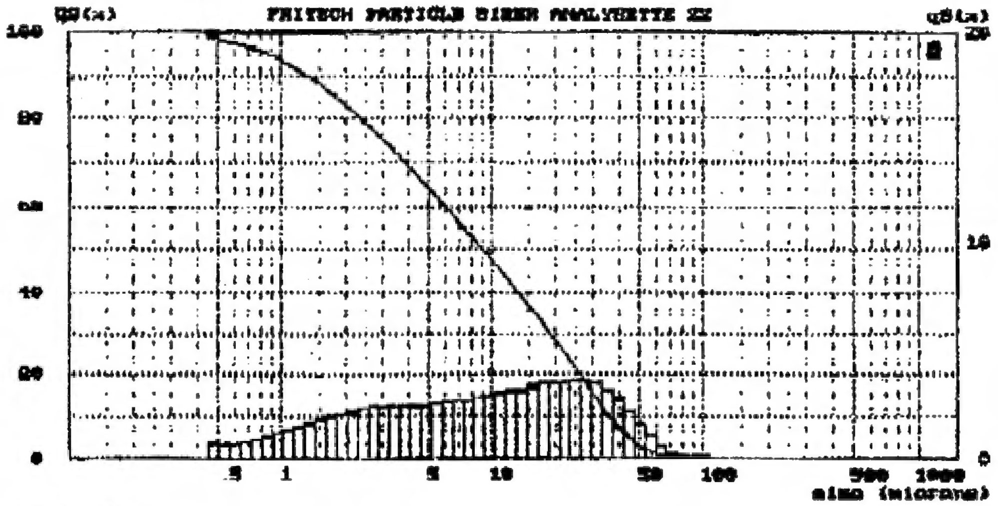

1 4 Argiles 28697 Fraction 37u < >150u

5-6

```
FRITSCH Particle Sizer Analysette 22

ZDDDDDDDDDDDDDDDDDDDDDDDDDDDDDDDDDDDDDDDDDDDDDDDDDDDDDDDDDDDDDDDDDDDDDDDDDDDDDDDDDDDDDDDDDDDDDDDDDDDDDD?
3Measure Numb    53Date 02-12-953Time 18:353Iteration Resid. 0.0255 %3  Overl  3Iteration    56 3Beam obscu   15.00 %  3
CDDDDDDDDDDDDDDDDDDDDDDDDDDDDDDDDDDDDDDDDDDDDDDDDDDDDDDDDDDDDDDDDDDDDDDDDDDDDDDDDDDDDDDDDDDDDDDDDDDDDDDD4
3 Argiles 28698                        Fraction 37u < >150u                                               3
3 Fraunhofer                            n =   fnhf ~ Fraunhofer                          n =   (nnf ' = 0.0000 3
CDDDDDDDDDDDDDDDDDDDDDDDDDDDDDDDDDDDDDDDDDDDDDDDDDDDDDDDDDDDDDDDDDDDDDDDDDDDDDDDDDDDDDDDDDDDDDDDDDDDDDDD4
3   89.13% >   1.00 f     73.11% >   2.00 f     49.92% >   4.00 f      5.20% >  16.00 f      0.05% >  32.00 f   3
3    0.05% >  63.00 f      0.00% > 125.00 f    ******% > 250.00 f    ******% > 500.00 f    ******% > 1000.00 f  3
CDDDDDDDDDDDDDDDDDDDDDDDDDDDDDDDDDDDDDDDDDDDDDDDDDDDDDDDDDDDDDDDDDDDDDDDDDDDDDDDDDDDDDDDDDDDDDDDDDDDDDDD4
3   90.00% >   0.95 f     80.00% >   1.56 f     70.00% >   2.21 f     60.00% >   2.96 f     50.00% >   3.99 f   3
3   40.00% >   5.44 f     30.00% >   7.31 f     20.00% >   9.67 f     10.00% >  13.15 f     Volume Distribution 3
@DDDDDDDDDDDDDDDDDDDDDDDDDDDDDDDDDDDDDDDDDDDDDDDDDDDDDDDDDDDDDDDDDDDDDDDDDDDDDDDDDDDDDDDDDDDDDDDDDDDDDDDY
ZDDDDDDDDDDDDDDDDDDDDDDDDDDDDDDDDDDDDDDDDDDDDDDDDDDDDDDDDDDDDDDDDDDDDDDDDDDDDDDDDDDDDDDDDDDDDDDDDDDDDDD?
3  Aritha. mean diameter :    5.79 um   Variance             :       5.39 sqr(um)   Skewness   ;            32.09 3
3  Geom mean diameter    :    3.76 um   Standard Deviation   :       2.32 um        Curtosis   :           700.113
3  Qadr.Sq. mean diam.   :    7.89 um   Mean Deviation       :       4.07 um        Span       :             3.06 3
3  Harmonic mean diam.   :    2.21 um   Coefficient Variance:      93.07 %          Uniformity :             0.96 3
3  Mode                  :    9.03 um   Median                :      3.99 um        Mean/Median Ratio    :   1.45 3
3                         Spec. surface area         2.7164 sqr(m)/cc         Form factor   1                      3
@DDDDDDDDDDDDDDDDDDDDDDDDDDDDDDDDDDDDDDDDDDDDDDDDDDDDDDDDDDDDDDDDDDDDDDDDDDDDDDDDDDDDDDDDDDDDDDDDDDDDDDDY
```

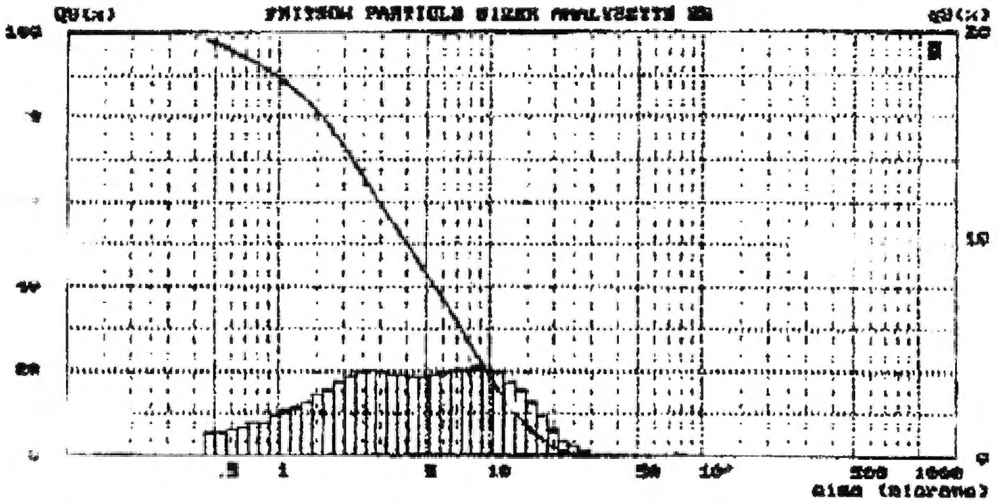

```
1     5   Argiles 28698                   Fraction 37u < >150u
```

7-8

DESCRIPTION DES ÉCHANTILLONS D'ARGILE MARINE

POUR FINS D'ANALYSE

LIEU : Baie Saint-Ludger, Péninsule Manicouagan, Côte-Nord du Québec

DATE : Le 15 mai 1997

NUMÉRO de permis de recherche de substances minérales de surface **(P.R.S.) :** 0002044 (Rang Pointe-aux-Outardes, Canton Manicouagan

MANIÈRE D'ÉCHANTILLONNER : A partir de la plage, en creusant manuellement un trou d'environ 6 pouces de diamètre avec une cuillère de bois pour ne pas mettre l'argile en contact avec du métal. La profondeur du trou est d'environ 12 pouces de la rive de façon à éliminer les substances de surface qui pourraient altérer l'argile. L'argile est prélevée en introduisant un bocal de verre au fond du trou dans lequel on introduit l'argile à l'aide de la main recouverte d'un gant de fin caoutchouc.

HAUTEUR DE LA RIVE : La hauteur de la rive varie d'un lieu à l'autre. Les lots identifiés aux différents P.R.S. ont donc une hauteur différente. Chacun d'eux sera donc évalués approximativement quant à la hauteur de la rive où l'échantillon a été prélevé. Pour ce qui est du lot désigné par le P.R.S. 0002044 la hauteur de la rive est de : 50 pieds environ

HAUTEUR DU TROU À PARTIR DE LA PLAGE : 5 pieds environ

REMARQUES : Cette argile était très liquide

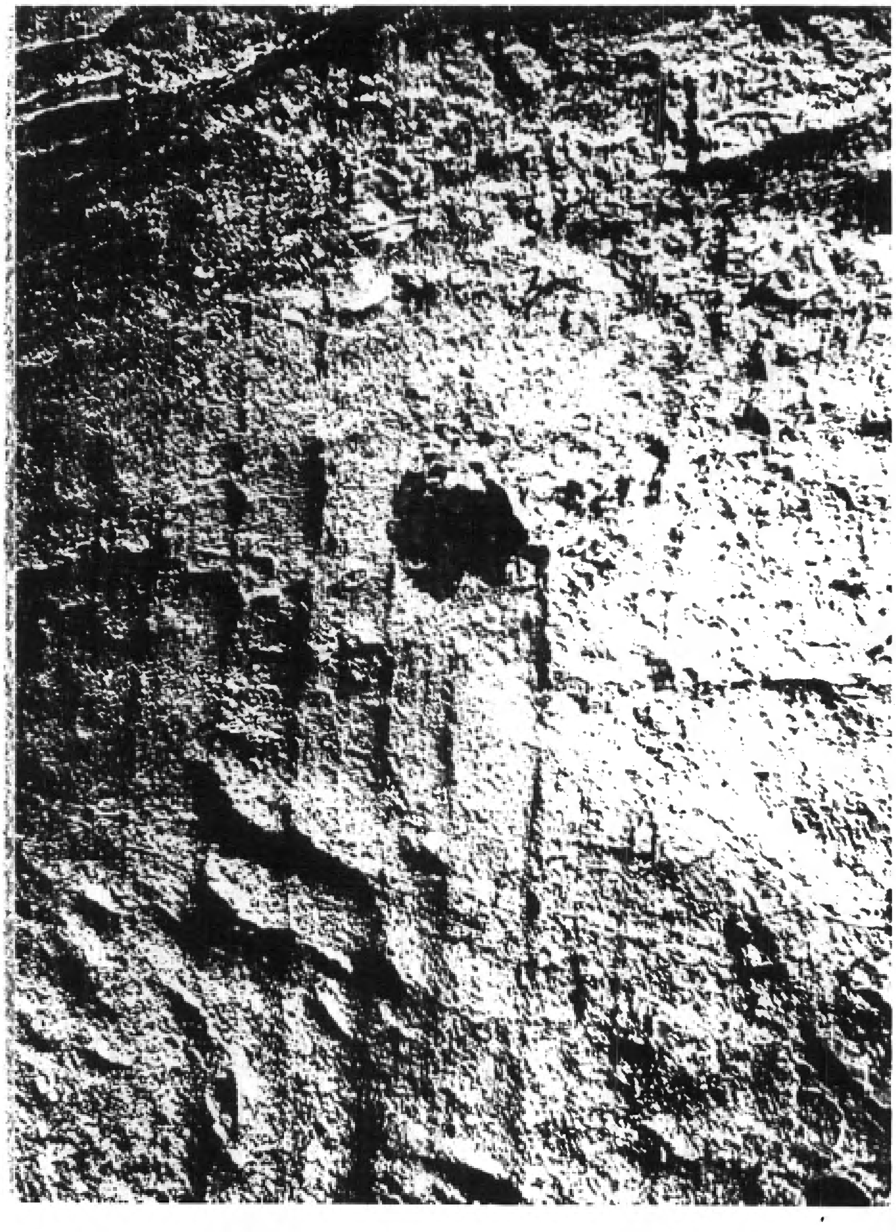

DESCRIPTION DES ÉCHANTILLONS D'ARGILE MARINE

POUR FINS D'ANALYSE

LIEU : Baie Saint-Ludger, Péninsule Manicouagan, Côte-Nord du Québec

DATE : 16 mai 1997

NUMÉRO de permis de recherche de substances minérales de surface **(P.R.S.) :** 000-2043. Rang Point-aux-Outardes, Canton Manicouagan

MANIÈRE D'ÉCHANTILLONNER : A partir de la plage, en creusant manuellement un trou d'environ 6 pouces de diamètre avec une cuillère de bois pour ne pas mettre l'argile en contact avec du métal. La profondeur du trou est d'environ 12 pouces de la rive de façon à éliminer les substances de surface qui pourraient altérer l'argile. L'argile est prélevée en introduisant un bocal de verre au fond du trou dans lequel on introduit l'argile à l'aide de la main recouverte d'un gant de fin caoutchouc.

HAUTEUR DE LA RIVE : La hauteur de la rive varie d'un lieu à l'autre. Les lots identifiés aux différents P.R.S. ont donc une hauteur différente. Chacun d'eux sera donc évalués approximativement quant à la hauteur de la rive où l'échantillon a été prélevé. Pour ce qui est du lot désigné par le P.R.S. 0002043 la hauteur de la rive est de : 30 pieds environ

HAUTEUR DU TROU À PARTIR DE LA PLAGE : 4 pieds environ

REMARQUES : Cette argile était plus ou moins liquide .

DESCRIPTION DES ÉCHANTILLONS D'ARGILE MARINE

POUR FINS D'ANALYSE

LIEU : Baie Saint-Ludger, Péninsule Manicouagan, Côte-Nord du Québec

DATE : 16 mai 1997

NUMÉRO de permis de recherche de substances minérales de surface **(P.R.S.) :** 000-2042. Rang Point-aux-Outardes, Canton Manicouagan

MANIÈRE D'ÉCHANTILLONNER : A partir de la plage, en creusant manuellement un trou d'environ 6 pouces de diamètre avec une cuillère de bois pour ne pas mettre l'argile en contact avec du métal. La profondeur du trou est d'environ 12 pouces de la rive de façon à éliminer les substances de surface qui pourraient altérer l'argile. L'argile est prélevée en introduisant un bocal de verre au fond du trou dans lequel on introduit l'argile à l'aide de la main recouverte d'un gant de fin caoutchouc.

HAUTEUR DE LA RIVE : La hauteur de la rive varie d'un lieu à l'autre. Les lots identifiés aux différents P.R.S. ont donc une hauteur différente. Chacun d'eux sera donc évalués approximativement quant à la hauteur de la rive où l'échantillon a été prélevé. Pour ce qui est du lot désigné par le <u>P.R.S. 0002042</u> la hauteur de la rive est de : 50 pieds environ

HAUTEUR DU TROU À PARTIR DE LA PLAGE : 4 pieds environ

REMARQUES : Cette argile était très liquide .

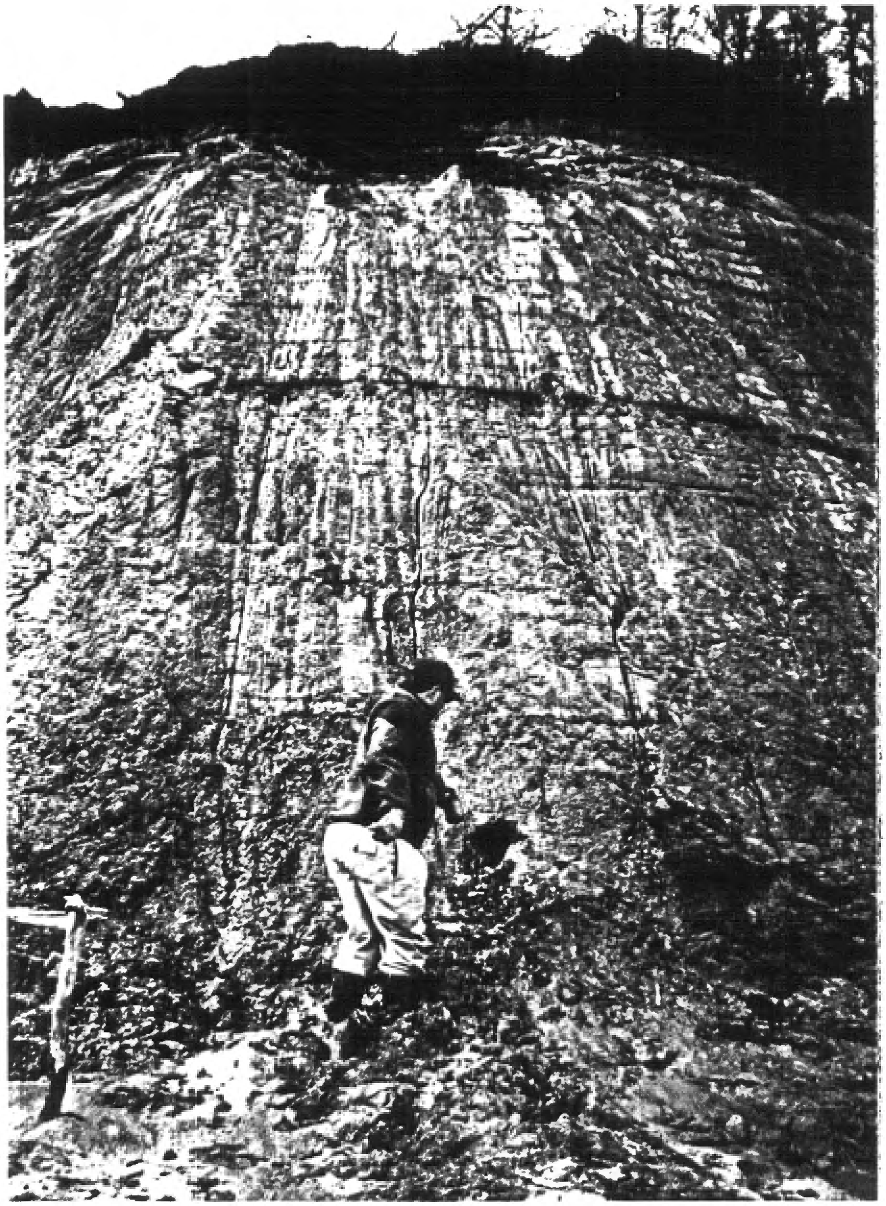

DESCRIPTION DES ÉCHANTILLONS D'ARGILE MARINE

POUR FINS D'ANALYSE

LIEU : Baie Saint-Ludger, Péninsule Manicouagan, Côte-Nord du Québec

DATE : 17 mai 1997

NUMÉRO de permis de recherche de substances minérales de surface **(P.R.S.) :** 000-2041. Rang Pointe-aux-Outardes, Canton Manicouagan

MANIÈRE D'ÉCHANTILLONNER : A partir de la plage, en creusant manuellement un trou d'environ 6 pouces de diamètre avec une cuillère de bois pour ne pas mettre l'argile en contact avec du métal. La profondeur du trou est d'environ 12 pouces de la rive de façon à éliminer les substances de surface qui pourraient altérer l'argile. L'argile est prélevée en introduisant un bocal de verre au fond du trou dans lequel on introduit l'argile à l'aide de la main recouverte d'un gant de fin caoutchouc.

HAUTEUR DE LA RIVE : La hauteur de la rive varie d'un lieu à l'autre. Les lots identifiés aux différents P.R.S. ont donc une hauteur différente. Chacun d'eux sera donc évalués approximativement quant à la hauteur de la rive où l'échantillon a été prélevé. Pour ce qui est du lot désigné par le P.R.S. 0002041 la hauteur de la rive est de : 30 pieds environ

HAUTEUR DU TROU À PARTIR DE LA PLAGE : 8 pieds environ

REMARQUES : Cette argile était très liquide .

DESCRIPTION DES ÉCHANTILLONS D'ARGILE MARINE

POUR FINS D'ANALYSE

LIEU : Baie Saint-Ludger, Péninsule Manicouagan, Côte-Nord du Québec

DATE : 17 mai 1997

NUMÉRO de permis de recherche de substances minérales de surface **(P.R.S.) :** 000-2040. Rang 1, Canton Manicouagan

MANIÈRE D'ÉCHANTILLONNER : A partir de la plage, en creusant manuellement un trou d'environ 6 pouces de diamètre avec une cuillère de bois pour ne pas mettre l'argile en contact avec du métal. La profondeur du trou est d'environ 12 pouces de la rive de façon à éliminer les substances de surface qui pourraient altérer l'argile. L'argile est prélevée en introduisant un bocal de verre au fond du trou dans lequel on introduit l'argile à l'aide de la main recouverte d'un gant de fin caoutchouc.

HAUTEUR DE LA RIVE : La hauteur de la rive varie d'un lieu à l'autre. Les lots identifiés aux différents P.R.S. ont donc une hauteur différente. Chacun d'eux sera donc évalués approximativement quant à la hauteur de la rive où l'échantillon a été prélevé. Pour ce qui est du lot désigné par le P.R.S. 0002040 la hauteur de la rive est de : 25 pieds environ

HAUTEUR DU TROU À PARTIR DE LA PLAGE : 2 pieds environ

REMARQUES : Le matériel n'était pas liquide, il était plutôt sableux .

DESCRIPTION DES ÉCHANTILLONS D'ARGILE MARINE

POUR FINS D'ANALYSE

LIEU : Baie Saint-Ludger, Péninsule Manicouagan, Côte-Nord du Québec

DATE : 17 mai 1997

NUMÉRO de permis de recherche de substances minérales de surface **(P.R.S.) :** 000-2039. Rang 1, Canton Manicouagan

MANIÈRE D'ÉCHANTILLONNER : A partir de la plage, en creusant manuellement un trou d'environ 6 pouces de diamètre avec une cuillère de bois pour ne pas mettre l'argile en contact avec du métal. La profondeur du trou est d'environ 12 pouces de la rive de façon à éliminer les substances de surface qui pourraient altérer l'argile. L'argile est prélevée en introduisant un bocal de verre au fond du trou dans lequel on introduit l'argile à l'aide de la main recouverte d'un gant de fin caoutchouc.

HAUTEUR DE LA RIVE : La hauteur de la rive varie d'un lieu à l'autre. Les lots identifiés aux différents P.R.S. ont donc une hauteur différente. Chacun d'eux sera donc évalués approximativement quant à la hauteur de la rive où l'échantillon a été prélevé. Pour ce qui est du lot désigné par le P.R.S. 0002039 la hauteur de la rive est de : 20 pieds environ

HAUTEUR DU TROU À PARTIR DE LA PLAGE : 4 pieds environ

REMARQUES : Le matériel n'était pas liquide, il était plutôt sableux .

Argile eau mer

Rapport
et
Résultats des analyses

par Jeanne Percival et
Catharine Burton

ommission GÉOLOGIQUE DU CANADA

20 JANVIER 1999

PRELIMINARY REPORT

Semi-Quantitative Clay Mineralogical and Particle Size Analyses

November 1997

Catharine Burton
and
Jeanne Percival
Geological Survey of Canada

Answers to questions:

a) Mineralogy will not provide you with the answer re: therapeutic/cosmetic use. When my student calls I will ask her if there was any information from the internet (I assume no-she would have written it up if it was available). The therapeutic use can only be determined through, I believe, the "skin test" with rabbits (as discussed in June). I had hoped that Dr. Murray would contact me in early October but he has no to date. I have contacted him again, and I hope to find a lab for analysis and the cost. I have contacted another US person, but he did not know of any commercial labs to do these analyses. However, I will try to find you a contact person at Health Canada who can advise you on how to proceed in testing your material for commercial use.

b) We did not analyze for major and trace elements, not within my mandate or budget, as we (the GSC) would send these out for commercial analyses. This should be done by your company- I can have the samples sent to a lab for analyses if you like, estimated cost is about $120/sample.

Collecting interstitial water is extremely difficult, especially for chemical analysis. This is difficult for lake sediments that are highly saturated, more so for your samples which are not highly saturated. If it is only water content that is needed, then this is done usually when chemical analyses is conducted (as Loss on Ignition, LOI).

Yes the samples were compared to the cosmetic samples you sent (I do not have the info on their product names-will ask my student). As these only represent a few of the commercially available materials, it is not a complete comparison. Also, there was no standard protocol used to select products nor the actual samples, thus a bias may have been introduced. These comparisons provide a small amount of information for your benefit only.

c) As I have not charged you for these analyses this puts me and you into a precarious position. As government research scientist I am not in the business to help with mine permits etc. and do analyses for free (to compete with the private sector). As I see this as a joint research project (in a very loose way) and I am only able to assess the quality of the clay deposit through its mineralogy (not final use). I would like to be able to retain this information on file, and possibly publish (with you) the information in a future open-file report. If this is allowable in the future, more data will be required to complete it.

The worth of the analyses, on a commercial basis, is considerable. You can estimate that each XRD analysis costs about $150 per sample and each particle size analysis (this was a complete analysis with substantially more data in hand) is about the same ($150/sample). Thus the total cost is in the order of $6000.

I trust this information will be of assistance to you this week. We can pursue continued collaboration following more discussion if you are interested.

Jeanne Percival
November 17, 1997

Table 1: Semi-quantitative clay mineralogical results using X-ray powder diffraction analyses and JADE® software.

Sample No	Qtz	Kfs	Pl	Chl	Ill	Kao	Sm	ML	Cal	Comments
Field Samples										
001	13	18	36	4	26	2				possible amphibole
002	10	18	36	3	33				tr	possible amphibole
003	17	23		7	50				3	minor amphiboles
0041A	17		44	5	32					trace of anhydrite
0041B	14	16	39	2	27					trace of anhydrite
0042A	17		47	3	30	3				
0042B	17	19	43	4	17					trace of amphibole
0043	8		33	4	48	6				
0044	18		42	3	30	1			1	minor amphibole
Other Samples										
AVGC	7	17		7	56	12		m-tr	3	
ANI	3		2	10	10	74	tr			
AVC	5			6	68	16		tr	5	
CVH-1					13	87				
CVH-2	tr			10	13	77	tr			
CPN						100				
KIC	8		30	28	33				tr	

Sample No	Qtz	Kfs	Pl	Chl	Ill	Kao	Sm	ML	Cal	Comments
M100	8		15	23	26	28	M			
PEO	2	26	27	15	22	6	tr			trace of Anhydrite
ESM			98							dolomite (1.5%) and anhydrite ((0.5%)

Qtz = quartz; Kfs = K Feldspar; Pl = plagioclase feldspar; Chl = chlorite; Ill = illite; Kao = kaolinite; SM = smectite (expandible clay mineral); ML = mixed-layer clay mineral; Hem = hematite; Cal = calcite; M= major; m = minor; tr = trace.

Note: Most samples contain some anhydrite and an amorphous component. ML component may be an illite-smectite or chlorite-smectite mixed-layer mineral; these cannot be quantified at this time. Thus these estimates are only semi-quantitative with a large error (e.g., ~15-20%).

Table 2: Particle size analysis of field and other cosmetic samples.

Sample No.	%Pebbles	%Sand	%Silt	%Clay
Field Samples				
001	0.00	44.12	53.85	2.03
002	0.00	18.18	77.95	3.86
003	0.00	54.09	43.58	2.33
0041A	0.00	0.17	85.26	14.58
0041B	0.00	0.76	88.91	10.33
0042A	0.00	5.77	83.95	10.29
0042B	0.00	4.09	86.12	9.78
0043	0.00	2.24	83.76	13.98
0044	0.00	4.63	86.64	8.74
Other Samples				
AVGC	0.00	2.32	86.35	11.30
ANI	0.00	2.82	82.80	14.36
AVC	1.03	1.10	85.15	13.75
CVH	0.00	0.00	86.55	13.44
CPN	0.00	0.00	68.74	31.26
ABP	0.00	0.00	90.23	9.78
KIC	0.00	8.34	83.23	8.42
AB/WC	0.00	0.00	68.68	31.32
M100	0.00	6.80	90.20	2.99
PEO	0.00	8.45	89.23	2.32
ESM	0.00	10.67	86.91	2.42

Table 3: Mean sand, silt and clay content of field and other samples.

No. Samples	% Sand	% Silt	% Clay
Field Samples			
9	14.89	76.67	8.44
6 (excl. 001-003)*	2.94	85.77	11.28
Other Samples			
11	3.68	83.46	12.85
8 (excl. M100-esm)*	1.82	81.46	16.70

Field Samples

All field samples are dominated by illite and plagioclase feldspar with subordinate amounts of K feldspar and quartz (see Table 1). Chlorite tends to occur only in minor to trace amounts and kaolinite is observed in a few samples as a very minor component. Most samples do contain some amphibole, others may contain trace amounts of anhydrite and calcite. The mineralogy reflects the mineralogy of Precambrian rocks that would occur in the area. Samples 001 to 003 are sand-rich with up to 54% sand-size material. The remaining samples are dominated by silt-sized particles (Table 2).

Other Samples

Disclaimer: These samples were provided by Denise Saulnier for comparative analysis; they do not represent all available, commercial materials.

AVGC: This is a mica-rich (illite 56%) sample with minor amounts of kaolinite, plagioclase feldspar, chlorite and quartz. It also contains minor to trace amounts of calcite and a mixed-layer clay mineral (probably illite/smectite). It is silt-rich with only a minor amount of clay-size material present.

ANI: This sample is dominated by kaolinite (74%) with minor amounts of illite and chlorite. It is also silt-rich with a minor amount of clay-size material present.

AVC: This is an illite-rich (68%) sample with minor amounts of kaolinite and less amounts of chlorite and quartz. It is silt-rich with minor clay, but does contain a very small amount of pebbles (> 2 mm).

CVH: Two samples were analyzed for their mineralogy. Both were kaolinite rich with minor amounts of illite and for the second sample chlorite. The sample is silt-rich with minor clay-size material and no sand.

CPN: This sample is pure kaolinite. It is dominated by silt-size particles but the clay-content has increased (double) relative to the samples listed above.

ABP: No XRD reported. Sample is very silt-rich (90%) with the remaining particles being clay-size.

KIC: This sample contains subequal amounts of illite, chlorite and plagioclase feldspar and a minor amount of quartz. It is silt-rich but also contains sub-equal amounts of clay and sand-size particles.

AB/WC: No XRD reported in Table 1. Qualitative data show that it is dominated by kaolinite and a minor amount of illite. This sample is clay-rich relative to others (similar to CPN) as well as silt-rich.

M100: This sample contains subequal amounts of kaolinite, illite and chlorite with minor amounts of plagioclase feldspar and quartz. It also contains a major amount of smectite which cannot be quantified using this process. Smectite is an expanding mineral of variable composition. This sample is also silt-rich but contains a larger amount of sand-sized particles relative to the other samples and therefore much less clay content.

PEO: This sample contains subequal amounts of plagioclase feldspar, K feldspar and illite and minor amounts of chlorite and kaolinite. Particle size data is similar to sample M100 with an increase in the sand content relative to the clay content.

ESM: This sample contains plagioclase feldspar with a trace amount of anhydrite and dolomite. It is silt-rich with a minor amount of sand.

Comparison of Field and Other Samples

The other (cosmetic) samples tend to contain more kaolinite and less non-clay silicates than the field samples. The mean clay content is 12.8% for the cosmetic samples, and 16.7% if samples M100, PEO and ESM are excluded from the calculation due to their low clay content (Table 3). In contrast, the mean content of clay-sized material for the field samples is 8.4% for all samples, and 11.3% if samples 001, 002 and 003 are excluded from the calculation due to their low clay content. Thus if the low clay content samples are excluded the particle size data is relatively comparable. The data of the cosmetic samples shows that these products are dominated by silt-sized particles with minor clay. The main difference between the field samples and the cosmetic samples if based on their mineralogy, mainly the kaolinite content.

PRELIMINARY REPORT

Semi-Quantitative Clay Mineralogical
and
Particle Size Analyses

November 1997

Catharine Burton
and
Jeanne Percival
Geological Survey of Canada

Answers to questions:

a) Mineralogy will not provide you with the answer re: therapeutic/cosmetic use. When my student calls I will ask her if there was any information from the internet (I assume no-she would have written it up if it was available). The therapeutic use can only be determined through, I believe, the "skin test" with rabbits (as discussed in June). I had hoped that Dr. Murray would contact me in early October but he has no to date. I have contacted him again, and I hope to find a lab for analysis and the cost. I have contacted another US person, but he did not know of any commercial labs to do these analyses. However, I will try to find you a contact person at Health Canada who can advise you on how to proceed in testing your material for commercial use.

b) We did not analyze for major and trace elements, not within my mandate or budget, as we (the GSC) would send these out for commercial analyses. This should be done by your company- I can have the samples sent to a lab for analyses if you like, estimated cost is about $120/sample.

Collecting interstitial water is extremely difficult, especially for chemical analysis. This is difficult for lake sediments that are highly saturated, more so for your samples which are not highly saturated. If it is only water content that is needed, then this is done usually when chemical analyses is conducted (as Loss on Ignition, LOI).

Yes the samples were compared to the cosmetic samples you sent (I do not have the info on their product names-will ask my student). As these only represent a few of the commercially available materials, it is not a complete comparison. Also, there was no standard protocol used to select products nor the actual samples, thus a bias may have been introduced. These comparisons provide a small amount of information for your benefit only.

c) As I have not charged you for these analyses this puts me and you into a precarious position. As government research scientist I am not in the business to help with mine permits etc. and do analyses for free (to compete with the private sector). As I see this as a joint research project (in a very loose way) and I am only able to assess the quality of the clay deposit through its mineralogy (not final use). I would like to be able to retain this information on file, and possibly publish (with you) the information in a future open-file report. If this is allowable in the future, more data will be required to complete it.

The worth of the analyses, on a commercial basis, is considerable. You can estimate that each XRD analysis costs about $150 per sample and each particle size analysis (this was a complete analysis with substantially more data in hand) is about the same ($150/sample). Thus the total cost is in the order of $6000.

I trust this information will be of assistance to you this week. We can pursue continued collaboration following more discussion if you are interested.

Jeanne Percival
November 17, 1997

Field Samples

All field samples are dominated by illite and plagioclase feldspar with subordinate amounts of K feldspar and quartz (see Table 1). Chlorite tends to occur only in minor to trace amounts and kaolinite is observed in a few samples as a very minor component. Most samples do contain some amphibole, others may contain trace amounts of anhydrite and calcite. The mineralogy reflects the mineralogy of Precambrian rocks that would occur in the area. Samples 001 to 003 are sand-rich with up to 54% sand-size material. The remaining samples are dominated by silt-sized particles (Table 2).

Other Samples

Disclaimer: These samples were provided by Denise Saulnier for comparative analysis; they do not represent all available, commercial materials.

AVGC: This is a mica-rich (illite 56%) sample with minor amounts of kaolinite, plagioclase feldspar, chlorite and quartz. It also contains minor to trace amounts of calcite and a mixed-layer clay mineral (probably illite/smectite). It is silt-rich with only a minor amount of clay-size material present.

ANI: This sample is dominated by kaolinite (74%) with minor amounts of illite and chlorite. It is also silt-rich with a minor amount of clay-size material present.

AVC: This is an illite-rich (68%) sample with minor amounts of kaolinite and less amounts of chlorite and quartz. It is silt-rich with minor clay, but does contain a very small amount of pebbles (> 2 mm).

CVH: Two samples were analyzed for their mineralogy. Both were kaolinite rich with minor amounts of illite and for the second sample chlorite. The sample is silt-rich with minor clay-size material and no sand.

CPN: This sample is pure kaolinite. It is dominated by silt-size particles but the clay-content has increased (double) relative to the samples listed above.

ABP: No XRD reported. Sample is very silt-rich (90%) with the remaining particles being clay-size.

KIC: This sample contains subequal amounts of illite, chlorite and plagioclase feldspar and a minor amount of quartz. It is silt-rich but also contains sub-equal amounts of clay and sand-size particles.

AB/WC: No XRD reported in Table 1. Qualitative data show that it is dominated by kaolinite and a minor amount of illite. This sample is clay-rich relative to others (similar to CPN) as well as silt-rich.

M100: This sample contains subequal amounts of kaolinite, illite and chlorite with minor amounts of plagioclase feldspar and quartz. It also contains a major amount of smectite which cannot be quantified using this process. Smectite is an expanding mineral of variable composition. This sample is also silt-rich but contains a larger amount of sand-sized particles relative to the other samples and therefore much less clay content.

PEO: This sample contains subequal amounts of plagioclase feldspar, K feldspar and illite and minor amounts of chlorite and kaolinite. Particle size data is similar to sample M100 with an increase in the sand content relative to the clay content.

ESM: This sample contains plagioclase feldspar with a trace amount of anhydrite and dolomite. It is silt-rich with a minor amount of sand.

Comparison of Field and Other Samples

The other (cosmetic) samples tend to contain more kaolinite and less non-clay silicates than the field samples. The mean clay content is 12.8% for the cosmetic samples, and 16.7% if samples M100, PEO and ESM are excluded from the calculation due to their low clay content (Table 3). In contrast, the mean content of clay-sized material for the field samples is 8.4% for all samples, and 11.3% if samples 001, 002 and 003 are excluded from the calculation due to their low clay content. Thus if the low clay content samples are excluded the particle size data is relatively comparable. The data of the cosmetic samples shows that these products are dominated by silt-sized particles with minor clay. The main difference between the field samples and the cosmetic samples if based on their mineralogy, mainly the kaolinite content.

Table 1: Semi-quantitative clay mineralogical results using X-ray powder diffraction analyses and JADE® software.

Sample No	**Qtz**	**Kfs**	**Pl**	**Chl**	**Ill**	**Kao**	**Sm**	**ML**	**Cal**	**Comments**
Field Samples										
001	13	18	36	4	26	2				possible amphibole
002	10	18	36	3	33				tr	possible amphibole
003	17	23		7	50				3	minor amphiboles
0041A	17		44	5	32					trace of anhydrite
0041B	14	16	39	2	27					trace of anhydrite
0042A	17		47	3	30	3				
0042B	17	19	43	4	17					trace of amphibole
0043	8		33	4	48	6				
0044	18		42	3	30	1			1	minor amphibole
Other Samples										
AVGC	7	17		7	56	12		m-tr	3	
ANI	3		2	10	10	74	tr			
AVC	5			6	68	16		tr	5	
CVH-1					13	87				
CVH-2	tr			10	13	77	tr			
CPN						100				
KIC	8		30	28	33				tr	

Sample No	Qtz	Kfs	Pl	Chl	Ill	Kao	Sm	ML	Cal	Comments
M100	8		15	23	26	28	M			
PEO	2	26	27	15	22	6	tr			trace of Anhydrite
ESM			98							dolomite (1.5%) and anhydrite ((0.5%)

Qtz = quartz; Kfs = K Feldspar; Pl = plagioclase feldspar; Chl = chlorite; Ill = illite; Kao = kaolinite; SM = smectite (expandible clay mineral); ML = mixed-layer clay mineral; Hem = hematite; Cal = calcite; M= major; m = minor; tr = trace.

Note: Most samples contain some anhydrite and an amorphous component. ML component may be an illite-smectite or chlorite-smectite mixed-layer mineral; these cannot be quantified at this time. Thus these estimates are only semi-quantitative with a large error (e.g., ~15-20%).

Table 3: Mean sand, silt and clay content of field and other samples.

No. Samples	**% Sand**	**% Silt**	**% Clay**
Field Samples			
9	14.89	76.67	8.44
6 (excl. 001-003)*	2.94	85.77	11.28
Other Samples			
11	3.68	83.46	12.85
8 (excl. M100-esm)*	1.82	81.46	16.70

Table 2: Particle size analysis of field and other cosmetic samples.

Sample No.	%Pebbles	%Sand	%Silt	%Clay
Field Samples				
001	0.00	44.12	53.85	2.03
002	0.00	18.18	77.95	3.86
003	0.00	54.09	43.58	2.33
0041A	0.00	0.17	85.26	14.58
0041B	0.00	0.76	88.91	10.33
0042A	0.00	5.77	83.95	10.29
0042B	0.00	4.09	86.12	9.78
0043	0.00	2.24	83.76	13.98
0044	0.00	4.63	86.64	8.74
Other Samples				
AVGC	0.00	2.32	86.35	11.30
ANI	0.00	2.82	82.80	14.36
AVC	1.03	1.10	85.15	13.75
CVH	0.00	0.00	86.55	13.44
CPN	0.00	0.00	68.74	31.26
ABP	0.00	0.00	90.23	9.78
KIC	0.00	8.34	83.23	8.42
AB/WC	0.00	0.00	68.68	31.32
M100	0.00	6.80	90.20	2.99
PEO	0.00	8.45	89.23	2.32
ESM	0.00	10.67	86.91	2.42

Table 1: Semi-quantitative clay mineralogical results using X-ray powder diffraction analyses and JADE® software.

Sample No	**Qtz**	**Kfs**	**Pl**	**Chl**	**Ill**	**Kao**	**Sm**	**ML**	**Cal**	**Comments**
Field Samples										
001	13	18	36	4	26	2				possible amphibole
002	10	18	36	3	33				tr	possible amphibole
003	17	23		7	50				3	minor amphiboles
0041A	17		44	5	32					trace of anhydrite
0041B	14	16	39	2	27					trace of anhydrite
0042A	17		47	3	30	3				
0042B	17	19	43	4	17					trace of amphibole
0043	8		33	4	48	6				
0044	18		42	3	30	1			1	minor amphibole
Other Samples										
AVGC	7	17		7	56	12		m-tr	3	
ANI	3		2	10	10	74	tr			
AVC	5			6	68	16		tr	5	
CVH-1					13	87				
CVH-2	tr			10	13	77	tr			
CPN						100				
KIC	8		30	28	33				tr	

Sample No	Qtz	Kfs	Pl	Chl	Ill	Kao	Sm	ML	Cal	Comments
M100	8		15	23	26	28	M			
PEO	2	26	27	15	22	6	tr			trace of Anhydrite
ESM			98							dolomite (1.5%) and anhydrite ((0.5%)

Qtz = quartz; Kfs = K Feldspar; Pl = plagioclase feldspar; Chl = chlorite; Ill = illite; Kao = kaolinite; SM = smectite (expandible clay mineral); ML = mixed-layer clay mineral; Hem = hematite; Cal = calcite; M= major; m = minor; tr = trace.

Note: Most samples contain some anhydrite and an amorphous component. ML component may be an illite-smectite or chlorite-smectite mixed-layer mineral; these cannot be quantified at this time. Thus these estimates are only semi-quantitative with a large error (e.g., ~15-20%).

Table 2: Particle size analysis of field and other cosmetic samples.

Sample No.	%Pebbles	%Sand	%Silt	%Clay
Field Samples				
001	0.00	44.12	53.85	2.03
002	0.00	18.18	77.95	3.86
003	0.00	54.09	43.58	2.33
0041A	0.00	0.17	85.26	14.58
0041B	0.00	0.76	88.91	10.33
0042A	0.00	5.77	83.95	10.29
0042B	0.00	4.09	86.12	9.78
0043	0.00	2.24	83.76	13.98
0044	0.00	4.63	86.64	8.74
Other Samples				
AVGC	0.00	2.32	86.35	11.30
ANI	0.00	2.82	82.80	14.36
AVC	1.03	1.10	85.15	13.75
CVH	0.00	0.00	86.55	13.44
CPN	0.00	0.00	68.74	31.26
ABP	0.00	0.00	90.23	9.78
KIC	0.00	8.34	83.23	8.42
AB/WC	0.00	0.00	68.68	31.32
M100	0.00	6.80	90.20	2.99
PEO	0.00	8.45	89.23	2.32
ESM	0.00	10.67	86.91	2.42

Table 3: Mean sand, silt and clay content of field and other samples.

No. Samples	% Sand	% Silt	% Clay
Field Samples			
9	14.89	76.67	8.44
6 (excl. 001-003)*	2.94	85.77	11.28
Other Samples			
11	3.68	83.46	12.85
8 (excl. M100-esm)*	1.82	81.46	16.70

Field Samples

All field samples are dominated by illite and plagioclase feldspar with subordinate amounts of K feldspar and quartz (see Table 1). Chlorite tends to occur only in minor to trace amounts and kaolinite is observed in a few samples as a very minor component. Most samples do contain some amphibole, others may contain trace amounts of anhydrite and calcite. The mineralogy reflects the mineralogy of Precambrian rocks that would occur in the area. Samples 001 to 003 are sand-rich with up to 54% sand-size material. The remaining samples are dominated by silt-sized particles (Table 2).

Other Samples

Disclaimer: These samples were provided by Denise Saulnier for comparative analysis; they do not represent all available, commercial materials.

AVGC: This is a mica-rich (illite 56%) sample with minor amounts of kaolinite, plagioclase feldspar, chlorite and quartz. It also contains minor to trace amounts of calcite and a mixed-layer clay mineral (probably illite/smectite). It is silt-rich with only a minor amount of clay-size material present.

ANI: This sample is dominated by kaolinite (74%) with minor amounts of illite and chlorite. It is also silt-rich with a minor amount of clay-size material present.

AVC: This is an illite-rich (68%) sample with minor amounts of kaolinite and less amounts of chlorite and quartz. It is silt-rich with minor clay, but does contain a very small amount of pebbles (> 2 mm).

CVH: Two samples were analyzed for their mineralogy. Both were kaolinite rich with minor amounts of illite and for the second sample chlorite. The sample is silt-rich with minor clay-size material and no sand.

CPN: This sample is pure kaolinite. It is dominated by silt-size particles but the clay-content has increased (double) relative to the samples listed above.

ABP: No XRD reported. Sample is very silt-rich (90%) with the remaining particles being clay-size.

KIC: This sample contains subequal amounts of illite, chlorite and plagioclase feldspar and a minor amount of quartz. It is silt-rich but also contains sub-equal amounts of clay and sand-size particles.

AB/WC: No XRD reported in Table 1. Qualitative data show that it is dominated by kaolinite and a minor amount of illite. This sample is clay-rich relative to others (similar to CPN) as well as silt-rich.

M100: This sample contains subequal amounts of kaolinite, illite and chlorite with minor amounts of plagioclase feldspar and quartz. It also contains a major amount of smectite which cannot be quantified using this process. Smectite is an expanding mineral of variable composition. This sample is also silt-rich but contains a larger amount of sand-sized particles relative to the other samples and therefore much less clay content.

PEO: This sample contains subequal amounts of plagioclase feldspar, K feldspar and illite and minor amounts of chlorite and kaolinite. Particle size data is similar to sample M100 with an increase in the sand content relative to the clay content.

ESM: This sample contains plagioclase feldspar with a trace amount of anhydrite and dolomite. It is silt-rich with a minor amount of sand.

Comparison of Field and Other Samples

The other (cosmetic) samples tend to contain more kaolinite and less non-clay silicates than the field samples. The mean clay content is 12.8% for the cosmetic samples, and 16.7% if samples M100, PEO and ESM are excluded from the calculation due to their low clay content (Table 3). In contrast, the mean content of clay-sized material for the field samples is 8.4% for all samples, and 11.3% if samples 001, 002 and 003 are excluded from the calculation due to their low clay content. Thus if the low clay content samples are excluded the particle size data is relatively comparable. The data of the cosmetic samples shows that these products are dominated by silt-sized particles with minor clay. The main difference between the field samples and the cosmetic samples if based on their mineralogy, mainly the kaolinite content.

Dr. J.B. Percival
Geological Survey of Canada
601 Booth St.
Ottawa, Ontario
K1A 0E8

December 2, 1997

Mme. Denise Saulnier
Presidente de Argile Eau Mer
5594 Waverly
Montreal Quebec
Canada H2T 2H1

Dear Denise,

Thank you for your fax of November 27th. I have delayed answering you as I am still trying to locate the correct person at Health Canada for you to contact. I am close, but have not spoken directly with him to confirm that this is indeed the place to contact (Product Safety Division). Once I actually confirm this, I will fax you his/her name and phone number for your reference.

In terms of the cosmetic products that we analyzed. As we have no permission from the original companies, it is best not to know which one is represented by those letters. In order to do that, I would have to contact them all and obtain permission for such a study. For your information, however, the letters were taken from the original product names; I do not have the original bags. Thus if you know what was sent you probably can figure this out for yourself.

As a geologist working in the federal government I also must do things in a public way. Thus I do not want to jeopardize your position in developing your deposit. You must know that terminology concerning clay must be understood. Clay has two meanings. The first is in terms of grain size. A clay size material is less than 0.002 mm or less than 2 microns. Your deposit is mostly silt-rich (greater than 2 microns) with a small amount of sand and clay. I believe this deposit, geologically, is likely a marine sediment or a glacial till but I would need to look at the geology of the area to confirm this idea. The other meaning of the term clay is mineralogical, i.e., clay minerals. The other products analyzed contain high amounts of clay minerals, your samples only contain about 50% clay minerals. This does not mean to say your product is not good, that is for Health Canada ultimately to decide, but it may not be for the same use as some of the others. I do not know the other products and there use, and thus cannot state it any further than what was written in my preliminary report.

Best regards,

Jeanne B. Percival

Natural Resources Canada
Geological Survey of Canada

Ressources naturelles Canada
Commission géologique du Canada

FAX (613) 943-1286
Télécopieur

Mineralogy & Chemistry Subdivision
Room 759 - 601 Booth
Ottawa, Ontario CANADA
K1A 0E8

Sous division de la minéralogie etr de la chimie
pièce 759, 601 rue Booth
Ottawa, Ontario CANADA
K1A 0E8

TO: Denise Saulnier **FAX NO:** 514-273-~~33~~73 93
à

FROM: Jeanne Percival **FAX 613-943-1286 MIN & CHEM GSC**
de

DATE: Jan. 6/98

NUMBER of pages, including this one: (2)
PAGES, celle-ci incluse:

Message:

Dear Denise

Happy New Year. I received this information just before the holidays. Hope it helps. I will also give you the contact at Health Canada: Bob Greene 613-941-6058 He will direct you. I believe no tests are really required by them. Good luck.

Jeanne

If there is a problem with this transmission, call:
Pour tout problème concernant cette transmission, telephonez: 613-996-2323

Canada

Argile
eau
mer

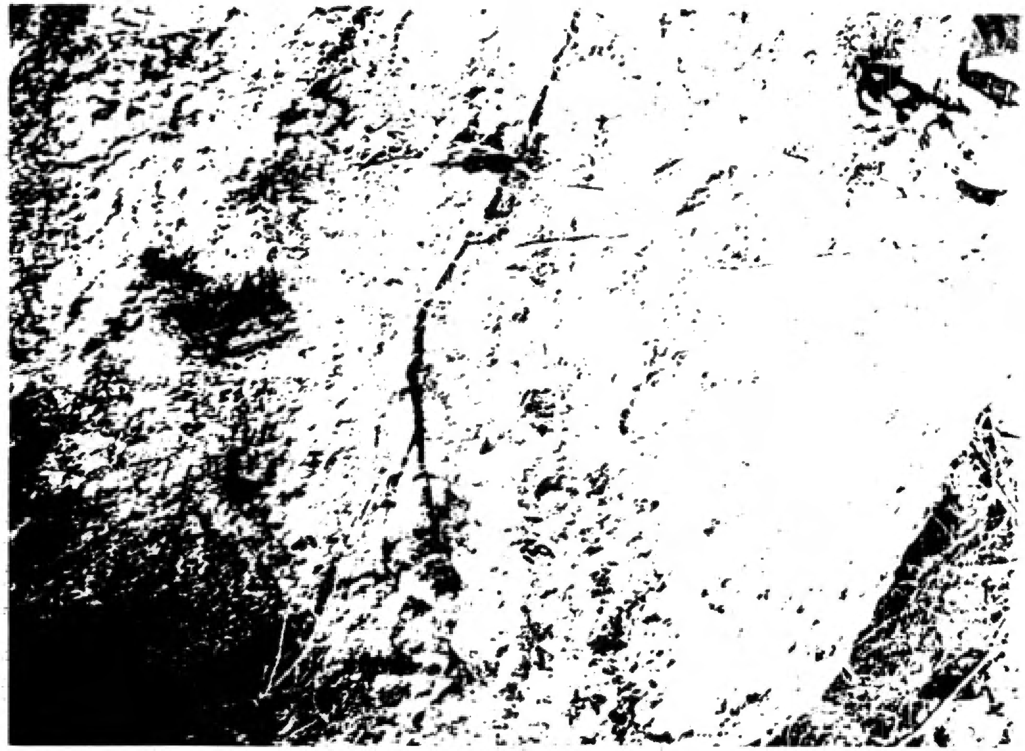

Rapport des

Analyses et échantillons d'argile

par André Chagnon
CRSQ (janvier 1996)

20 JANVIER 99

Sainte-Foy, le 26 mars 1996

M. Luc Arsenault
Fonds Régional d'Exploration Minière de la Côte-Nord
456, avenue Arnaud,
Bureau RC. 07
Sept-Îles Qc.
G4R 3B1
Télécopieur; (418) 968-2624

Cher Luc

Je te transmet les résultats préliminaires de l'analyse de 5 échantillons d'argile que tu m'as fait parvenir.

MINÉRALOGIE

L'analyse minéralogique a été effectuée par diffraction aux rayons-X sur l'échantillon global, sans fractionnement granulométrique. Les résultats sont présentés au tableau annexé à la présente. Les proportions des minéraux sont estimées à partir de l'intensité des pics de diffraction corrigée pour l'effet d'orientation et de masse.
Il y a très peu de phyllosilicate dans les échantillons qui sont surtout formés de quartz et de feldspath. Le mica est une biotite et la chlorite est magnésienne. L'amphibole est de type hornblende. Cet assemblage ressemble beaucoup à ceux que j'ai déjà observés dans les argiles de la mer de Champlain des Basses-Terres. Les minéraux sont peu ou pas altérés. Si l'on regarde les analyses granulométriques, on se rend compte qu'une partie de la masse de ces sédiments doit être amorphe. C'est la règle dans ce genre de matériaux.

ANALYSES GRANULOMÉTRIQUES.

Les analyses effectuées au granulomètre à laser nous montre un matériau silteux ayant une proportion faible de particules plus fines que 2 microns. La distribution est plutôt bimodale. Les paramètres statistiques des courbes de distribution accompagnent le graphiques et nous indiquent un très mauvais trie des particules.

Je te ferai parvenir les résultats de la chimie dès que je les aurai, normalement d'ici la fin de semaine. Si tu as des questions, n'hésites pas à communiquer avec moi.

Salut et à bientôt

André Chagnon.

ANNEXE II

Forage no. 1 Baie-Saint-Ludger

Régistre de sondage, trou numéro 1	
Profondeur	Description
0 à 20 pieds	sable fin de couleur brun à brun-pâle
20 à 25 pieds	sable fin de couleur brun-pâle, mouillé (nappe)
25 à 45 pieds	sable fin gris-pâle et argilleux

Tableau 1. Résultats de l'analyse semie-quantitative par diffraction aux rayons-X de 5 échantillons d'argile. QTZ.: quartz; NA-FELD.: feldspath plagioclase; K-FELD.: feldspath potassique; AMPH.: amphibole; CHLOR.: chlorite

NO. INRS	ECHANT.		MINERALOGIE					
		QTZ	NA-FELD	K-FELD	AMPH.	MICA	CHLOR.	TOTAL
28695	1 A 2	50	30	5	8	7	2	100
28696	3 À 4	40	40	5	8	7	2	100
38697	5 À 6	40	40	7	10	3	2	100
28698	7 À 8	45	35	7	5	8	2	100
28699	9 À 10	45	35	7	5	8	2	100

QTZ.: quartz; NA-FELD.: feldspath plagioclase; K-FELD.: feldspath potassique; AMPH.: amphibole ;

ANNEXE III

Tableau 1. Résultats de l'analyse semie-quantitative par diffraction aux rayons-X de 5 échantillons d'argile. QTZ.: quartz; NA-FELD.: feldspath plagioclase; K-FELD.: feldspath potassique; AMPH.: amphibole; CHLOR.: chlorite

NO. INRS	ECHANT.	MINÉRALOGIE						
		QTZ	NA-FELD	K-FELD	AMPH.	MICA	CHLOR.	TOTAL
28695	1 À [illegible]	50	30	5	8	7	2	100
28696	3 À 4	40	40	5	8	7	2	100
28697	5 À 6	40	40		10	3	2	100
28698	7 À 8	45	35		5	8	2	100
28698	9 À 10	45	35		5	8	2	100
moyenne		44	36	6.2	7.2	6.6	2	100

QTZ : quartz; NA-FELD : feldspath plagioclase; K-FELD : feldspath potassique; AMPH : amphibole ;

HY964RAP

Centre Géoscientifique de Québec						
Laboratoire de fluorescence X						
	Nom du clie	Héroux Yvon				
	Projet	Frem argilec				
	Imputation	15242840				
	Nom du lot	HY964				
	Nombre	5				
Code	Échantillon	Na2O	MgO	Al2O3	SiO2	P2O5
Cal	1YH29695	3,87	3,01	16,43	60,25	0,2
Cal	2YH29696	3,91	3,4	16,88	60,32	0,21
Cal	3YH29697	3,96	3,37	16,78	60,07	0,21
Cal	4YH29698	3,73	3,17	15,79	56,67	0,21
Cal	5YH29699	3,9	3,16	16,71	60,38	0,23
Échantillon	S	K2O	CaO	TiO2	MnO	Fe2O3
1YH29695	0	2,65	4,1	0,62	0,09	5,6
2YH29696	0	2,76	3,93	0,65	0,1	6,09
3YH29697	0	2,59	4,1	0,66	0,09	5,96
4YH29698	0	2,56	6,01	0,62	0,19	5,87
5YH29699	0	2,67	4,35	0,67	0,1	6,05
Échantillon	Ba	Co	Cr	Cu	Ga	Nb
1YH29695	756	19	97	40	19	< 3
2YH29696	748	23	105	48	19	< 3
3YH29697	723	21	101	36	18	5
4YH29698	726	21	98	32	19	< 3
5YH29699	803	20	102	37	16	3
Échantillon	Ni	Pb	Rb	Sr	V	Y
1YH29695	63	< 5	78	429	88	14
2YH29696	73	11	91	419	97	16
3YH29697	59	7	84	432	95	19
4YH29698	58	13	82	459	88	17
5YH29699	61	11	89	439	91	19
Échantillon	Zn	Zr	PfF	Total		
1YH29695	72	156	1,55	98,55		
2YH29696	77	134	1,7	100,14		
3YH29697	83	167	1,5	99,47		
4YH29698	77	151	3,61	98,61		
5YH29699	78	175	1,55	99,96		

FRITSCH Particle Sizer Analysette 22

```
ZDDDDDDDDDDDDDDDDDDDDDDDDDDDDDDDDDDDDDDDDDDDDDDDDDDDDDDDDDDDDDDDDDDDDDDDDDDDDDDDDDDDDDDDDDDDDDDDDDDD?
3Measure Numb    2 3Date 02-12-953Time 16:193Iteration Resid. 0.0148 %3  Overl  3Iteration   56 3Beam obscu   10.00 %  3
CDDDDDDDDDDDDDDDDDDDDDDDDDDDDDDDDDDDDDDDDDDDDDDDDDDDDDDDDDDDDDDDDDDDDDDDDDDDDDDDDDDDDDDDDDDDDDDDDDDD4
3 Argiles 28635                          Fraction 37u ( )150u                                    3
3 Fraunhofer                             n =   fnhf * Fraunhofer                 n =   fnhf ' = 0.0000 3
CDDDDDDDDDDDDDDDDDDDDDDDDDDDDDDDDDDDDDDDDDDDDDDDDDDDDDDDDDDDDDDDDDDDDDDDDDDDDDDDDDDDDDDDDDDDDDDDDDDD4
3    95.02% )    1.00 f     87.34% )    2.00 f     77.05% )    4.00 f     52.49% )   16.00 f     34.23% )   32.00 f     3
3    14.51% )   63.00 f      7.08% )  125.00 f     ******% )  250.00 f     ******% )  500.00 f     ******% ) 1000.00 f     3
CDDDDDDDDDDDDDDDDDDDDDDDDDDDDDDDDDDDDDDDDDDDDDDDDDDDDDDDDDDDDDDDDDDDDDDDDDDDDDDDDDDDDDDDDDDDDDDDDDDD4
3    90.00% )    1.64 f     80.00% )    3.30 f     70.00% )    6.27 f     60.00% )   11.11 f     50.00% )   17.87 f     3
3    40.00% )   26.34 f     30.00% )   36.66 f     20.00% )   50.47 f     10.00% )   88.31 f     Volume Distribution   3
@DDDDDDDDDDDDDDDDDDDDDDDDDDDDDDDDDDDDDDDDDDDDDDDDDDDDDDDDDDDDDDDDDDDDDDDDDDDDDDDDDDDDDDDDDDDDDDDDDDDY
ZDDDDDDDDDDDDDDDDDDDDDDDDDDDDDDDDDDDDDDDDDDDDDDDDDDDDDDDDDDDDDDDDDDDDDDDDDDDDDDDDDDDDDDDDDDDDDDDDDDD?
3 Arithm. mean diameter :    32.08 um   Variance             :      38.47 sqr(um)   Skewness   :          399.60 3
3 Geom mean diameter    :    13.92 um   Standard Deviation   :       6.20 um       Curtosis   :          7386.973
3 Qadr.Sq. mean diam.   :    49.94 um   Mean Deviation       :      28.27 um       Span       :            4.85 3
3 Harmonic mean diam.   :     4.48 um   Coefficient Variance:      119.93 %        Uniformity :            1.45 3
3 Mode                  :   148.63 um   Median                 :    17.87 um       Mean/Median Ratio   :   1.79 3
3                           Spec. surface area         1.3407 sqr(m)/cc         Form factor   1                  3
@DDDDDDDDDDDDDDDDDDDDDDDDDDDDDDDDDDDDDDDDDDDDDDDDDDDDDDDDDDDDDDDDDDDDDDDDDDDDDDDDDDDDDDDDDDDDDDDDDDDY
```

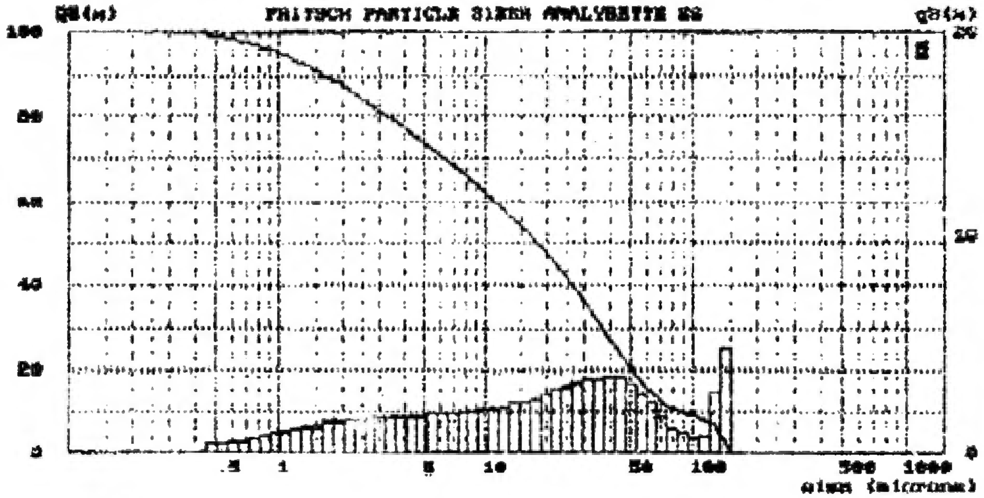

1 2 Argiles 28635 Fraction 37u ( )150u

1-2

FRITSCH Particle Sizer Analysette 22

```
ZDDDDDDDDDDDDDDDDDDDDDDDDDDDDDDDDDDDDDDDDDDDDDDDDDDDDDDDDDDDDDDDDDDDDDDDDDDDDDDDDDDDDDDDDDDDDDD?
3Measure Numb    37Date 02-12-953Time 16:293Iteration Resid. 0.0188 %3  Overl  31teration    56 3Beam obscu   11.00 %  3
CDDDDDDDDDDDDDDDDDDDDDDDDDDDDDDDDDDDDDDDDDDDDDDDDDDDDDDDDDDDDDDDDDDDDDDDDDDDDDDDDDDDDDDDDDDDDDD4
3 Argiles 28896                    Fraction 37u ( )150u                                            3
3 Fraunhofer                       n =   fnht * Fraunhofer                      n =   fnhf ' = 0.0000 3
CDDDDDDDDDDDDDDDDDDDDDDDDDDDDDDDDDDDDDDDDDDDDDDDDDDDDDDDDDDDDDDDDDDDDDDDDDDDDDDDDDDDDDDDDDDDDDD4
3    91.79% >    1.00 f     79.13% >    2.00 f     61.93% >    4.00 f     25.26% >   16.00 f      7.31% >   32.00 f    3
3     0.16% >   63.00 f      0.00% >  125.00 f    ******% >  250.00 f    ******% >  500.00 f    ******% > 1000.00 f   3
CDDDDDDDDDDDDDDDDDDDDDDDDDDDDDDDDDDDDDDDDDDDDDDDDDDDDDDDDDDDDDDDDDDDDDDDDDDDDDDDDDDDDDDDDDDDDDD4
3    90.00% >    1.14 f     80.00% >    1.92 f     70.00% >    2.92 f     60.00% >    4.31 f     50.00% >    6.38 f    3
3    40.00% >    9.34 f     30.00% >   13.49 f     20.00% >   19.42 f     10.00% >   28.53 f     Volume Distribution  3
@DDDDDDDDDDDDDDDDDDDDDDDDDDDDDDDDDDDDDDDDDDDDDDDDDDDDDDDDDDDDDDDDDDDDDDDDDDDDDDDDDDDDDDDDDDDDDDY
ZDDDDDDDDDDDDDDDDDDDDDDDDDDDDDDDDDDDDDDDDDDDDDDDDDDDDDDDDDDDDDDDDDDDDDDDDDDDDDDDDDDDDDDDDDDDDDD?
3 Aritha. mean diameter :   11.07 um   Variance           :      11.80 sqr(um)   Skewness  :          63.12 3
3 Geom mean diameter    :    5.96 um   Standard Deviation :       3.44 um       Curtosis  :          726.963
3 Quadr.Sq. mean diam.  :   16.13 um   Mean Deviation     :       9.11 um       Span      :           4.30 3
3 Harmonic mean diam.   :    2.83 um   Coefficient Variance:    106.62 %        Uniformity :          1.31 3
3 Mode                  :   14.75 um   Median             :       6.38 um       Mean/Median Ratio  :  1.74 3
3                        Spec. surface area       2.1196 sqr(m)/cc        Form factor   1                        3
@DDDDDDDDDDDDDDDDDDDDDDDDDDDDDDDDDDDDDDDDDDDDDDDDDDDDDDDDDDDDDDDDDDDDDDDDDDDDDDDDDDDDDDDDDDDDDDY
```

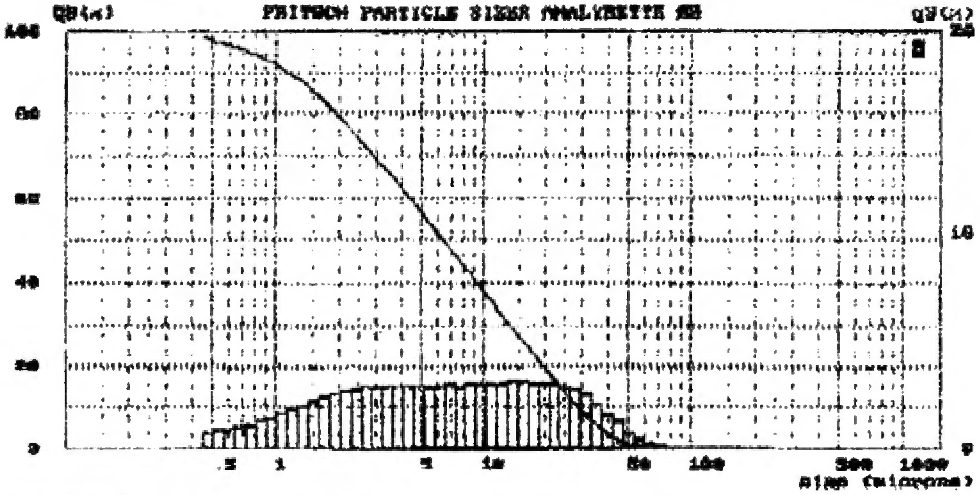

3   Argiles 28896   Fraction 37u ( )150u

3-4

```
FRITSCH Particle Sizer Analysette 22

ZDDDDDDDDDDDDDDDDDDDDDDDDDDDDDDDDDDDDDDDDDDDDDDDDDDDDDDDDDDDDDDDDDDDDDDDDDDDDDDDDDDDDDDDDDDDDDDDDDDDD?
3Measure Numb    43Date 02-12-953Time 16:423Iteration Resid. 0.0137 %3  Overl  3Iteration    56 3Beam obscu   11.00 %  3
CDDDDDDDDDDDDDDDDDDDDDDDDDDDDDDDDDDDDDDDDDDDDDDDDDDDDDDDDDDDDDDDDDDDDDDDDDDDDDDDDDDDDDDDDDDDDDDDDDDDDD4
3 Argiles 28697                      Fraction 37u ( )150u                                          3
3 Fraunhofer                          n =   fnhf ' Fraunhofer                      n =   fnhf ' = 0.0000 3
CDDDDDDDDDDDDDDDDDDDDDDDDDDDDDDDDDDDDDDDDDDDDDDDDDDDDDDDDDDDDDDDDDDDDDDDDDDDDDDDDDDDDDDDDDDDDDDDDDDDDD4
3    93.41% )   1.00 f    83.19% )   2.00 f    68.88% )   4.00 f    34.75% )  16.00 f    13.16% )   32.00 f   3
3     0.73% )  63.00 f     0.00% ) 125.00 f   ######% ) 250.00 f   ######% ) 500.00 f   ######% ) 1000.00 f   3
CDDDDDDDDDDDDDDDDDDDDDDDDDDDDDDDDDDDDDDDDDDDDDDDDDDDDDDDDDDDDDDDDDDDDDDDDDDDDDDDDDDDDDDDDDDDDDDDDDDDDD4
3    90.00% )   1.32 f    80.00% )   2.37 f    70.00% )   3.80 f    60.00% )   5.97 f    50.00% )    9.10 f   3
3    40.00% )  13.29 f    30.00% )  18.71 f    20.00% )  25.78 f    10.00% )  35.70 f    Volume Distribution   3
@DDDDDDDDDDDDDDDDDDDDDDDDDDDDDDDDDDDDDDDDDDDDDDDDDDDDDDDDDDDDDDDDDDDDDDDDDDDDDDDDDDDDDDDDDDDDDDDDDDDDDY
ZDDDDDDDDDDDDDDDDDDDDDDDDDDDDDDDDDDDDDDDDDDDDDDDDDDDDDDDDDDDDDDDDDDDDDDDDDDDDDDDDDDDDDDDDDDDDDDDDDDDDD?
3  Arithm. mean diameter :   14.42 um   Variance              :     14.61 sqr(um)   Skewness    :          78.65 3
3  Geom mean diameter    :    7.75 um   Standard Deviation    :      3.82 um        Curtosis    :         1060.953
3  Qadr.Sq. mean diam.   :   20.48 um   Mean Deviation        :     11.52 um        Span        :           3.78 3
3  Harmonic mean diam.   :    3.39 um   Coefficient Variance: :    101.30 %         Uniformity :            1.19 3
3  Mode                  :   26.43 um   Median                  :    9.10 um        Mean/Median Ratio   :   1.58 3
3                         Spec. surface area        1.7704 sqr(m)/cc          Form factor   1                     3
@DDDDDDDDDDDDDDDDDDDDDDDDDDDDDDDDDDDDDDDDDDDDDDDDDDDDDDDDDDDDDDDDDDDDDDDDDDDDDDDDDDDDDDDDDDDDDDDDDDDDDY
```

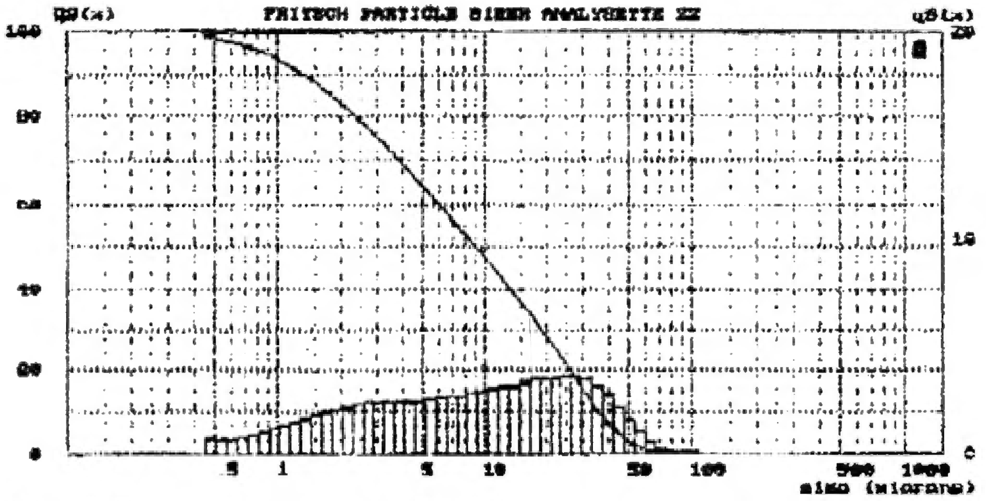

1 4 Argiles 28697 Fraction 37u ( )150u

5-6

FRITSCH Particle Sizer Analysette 22

```
ZDDDDDDDDDDDDDDDDDDDDDDDDDDDDDDDDDDDDDDDDDDDDDDDDDDDDDDDDDDDDDDDDDDDDDDDDDDDDDDDDDDDDDDDDDDDDDDDDDDDDDD?
3Measure Numb    53Date 02-12-953Time 18:353Iteration Resid. 0.0255 13  Overl  3Iteration    56 3Beam obscu   15.00 % 3
CDDDDDDDDDDDDDDDDDDDDDDDDDDDDDDDDDDDDDDDDDDDDDDDDDDDDDDDDDDDDDDDDDDDDDDDDDDDDDDDDDDDDDDDDDDDDDDDDDDDDDD4
3 Argiles 28698                   Fraction 37u < >150u                                              3
3 Fraunhofer                       n =   fnhf ^ Fraunhofer                          n =   (nnf ' = 0.0000 3
CDDDDDDDDDDDDDDDDDDDDDDDDDDDDDDDDDDDDDDDDDDDDDDDDDDDDDDDDDDDDDDDDDDDDDDDDDDDDDDDDDDDDDDDDDDDDDDDDDDDDDD4
3    89.13% >   1.00 /    73.11% >   2.00 /    49.32% >   4.00 /     5.20% >  16.00 /     0.05% >  32.00 /    3
3     0.03% >  63.00 /     0.00% > 128.00 /   ******% > 250.00 /   ******% > 500.00 /   ******% > 1000.00 /   3
CDDDDDDDDDDDDDDDDDDDDDDDDDDDDDDDDDDDDDDDDDDDDDDDDDDDDDDDDDDDDDDDDDDDDDDDDDDDDDDDDDDDDDDDDDDDDDDDDDDDDDD4
3    90.00% >   0.95 /    80.00% >   1.56 /    70.00% >   2.21 /    60.00% >   2.96 /    50.00% >   3.99 /    3
3    40.00% >   5.44 /    30.00% >   7.31 /    20.00% >   9.67 /    10.00% >  13.15 /   Volume Distribution  3
@DDDDDDDDDDDDDDDDDDDDDDDDDDDDDDDDDDDDDDDDDDDDDDDDDDDDDDDDDDDDDDDDDDDDDDDDDDDDDDDDDDDDDDDDDDDDDDDDDDDDDDY
ZDDDDDDDDDDDDDDDDDDDDDDDDDDDDDDDDDDDDDDDDDDDDDDDDDDDDDDDDDDDDDDDDDDDDDDDDDDDDDDDDDDDDDDDDDDDDDDDDDDDDDD?
3 Aritha. mean diameter :    5.79 um   Variance             :      5.39 sqr(um)   Skewness    :        32.09 3
3 Geom mean diameter    :    3.76 um   Standard Deviation   :      2.32 um        Curtosis    :        700.113
3 Qadr.Sq. mean diam.   :    7.89 um   Mean Deviation       :      4.07 um        Span        :         3.06 3
3 Harmonic mean diam.   :    2.21 um   Coefficient Variance:      93.07 %         Uniformity  :         0.56 3
3 Mode                  :    9.03 um   Median                :      3.99 um       Mean/Median Ratio  :  1.45 3
3                         Spec. surface area       2.7164 sqr(m)/cc         Form factor   1                  3
@DDDDDDDDDDDDDDDDDDDDDDDDDDDDDDDDDDDDDDDDDDDDDDDDDDDDDDDDDDDDDDDDDDDDDDDDDDDDDDDDDDDDDDDDDDDDDDDDDDDDDDY
```

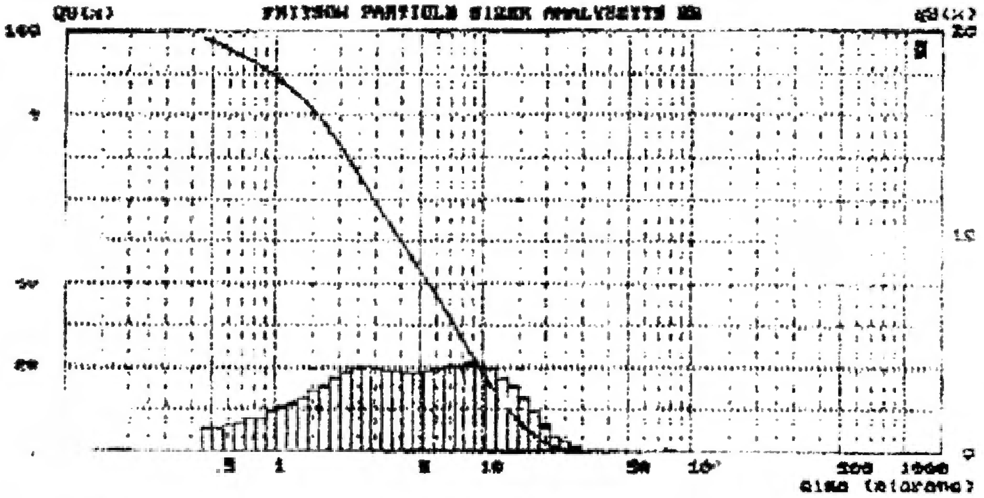

1   3   Argiles 28698   Fraction 37u < >150u

7-2

Argile eau mer

Rapport de recherche
documentaire par

Marie-Hélène Dupuis
de
l'École polytechnique de
l'Université de
MONTRÉAL

20 JANVIER 1999

ÉCOLE
POLYTECHNIQUE

12 février 1996

**Service d'information
documentaire de
l'École Polytechnique
(SIDEP)**

Mme Denise Saulnier
5594 Waverly
Montréal QC H2T 2Y1

Chère Madame,

A la suite de notre rencontre de ventdredi dernier, veuillez trouver ci-joint d'autres références aux argiles marines (format titre et mots-clés). Vous avez donc des références dans les domaines de la géologie, plus celles trouvées dans une banques sur les produits de consommation avec l'expression "sea or marine" "clays". J'attire votre attention également sur la table des matières ci-jointe (Géologie des argiles, livre disponible à notre bibliothèque), dont un chapître couvre les argiles de sédiments marins.

N'hésitez pas à communiquer avec moi si vous voulez plus de détails, ou si vous avez des questions sur les résultats. Veuillez agréer, Madame Saulnier, l'expression de mes sincères salutations.

Marie-Hélène Dupuis

Marie-Hélène Dupuis
340-4213

**École affiliée à
l'Université de Montréal**
Campus de l'Université de Montréal
2900, boul. Édouard-Montpetit
Montréal (Québec)

Case postale 6079, succursale A
Montréal (Québec), Canada
H3C 3A7
Tél.: (514) 340-4213
Télécop.: (514) 340-4026

Argile thérapeutique et cosmétique

Préparé pour
Mme Denise Saulnier
Argile Eau Mer

par
Marie-Hélène Dupuis,
Service d'information documentaire
École Polytechnique

1

Livres (pour commande ou emprunt)

DATE DE PUBLICATION : 1986
DESCRIPTION : 96 p. ; 22 x 14 cm
ISBN : 2-85012-018-9
PRIX : Br. 60.00 FRF
MOTS-MATIERES : Argile médicinale
RUBRIQUES DEWEY : 615.43

AUTEURS : Clergeaud, Chantal*Clergeaud, Lionel
TITRE : L'Argile
AUTEURS, COLLABORATIONS : C. et L. Clergeaud
ill. Laurent et Lionel Clergeaud
EDITEUR : Vie claire
DATE DE PUBLICATION : 1984
DESCRIPTION : 194 p. : ill. ; 21 x 14 cm
ISBN : 2-86540-028-X
PRIX : Br. 98.00 FRF
RESUME : Cet ouvrage, à but d'utilisation thérapeutique et domestique, traite des différentes propriétés de l'argile.
MOTS-MATIERES : Argile médicinale
RUBRIQUES DEWEY : 616.2

AUTEURS : Guenot, Jean-Pierre
TITRE : Les Argiles
10 propriétés, 50 alliés, 100 utilisations
AUTEURS, COLLABORATIONS : Jean-Pierre Guenot
préf. Maurice Mességué
LIEU DE PUBLICATION : Paris
EDITEUR : Chiron
DATE DE PUBLICATION : 1987
DESCRIPTION : 190 p. ; 24 x 17 cm
ISBN : 2-7027-0367-4
PRIX : Br. 98.00 FRF
RESUME : Présentation simple et précise des diverses méthodes qui permettent d'utiliser à bon escient les différentes qualités d'argile que l'on peut trouver. Les plantes à associer.
MOTS-MATIERES : Argile médicinale
RUBRIQUES DEWEY : 615.45

DATE DE PUBLICATION : 1988
DESCRIPTION : 190 p. ; 21 x 13 cm
ISBN : 2-7337-7016-0
PRIX : Br. 75.00 FRF
RESUME : Guide pratique qui permet de choisir une argile particulière pour agir dans un domaine spécifique : digestion, voies respiratoires, circulation sanguine, etc. Indique également les adjuvants naturels agissant en synergie avec l'argile.
MOTS-MATIERES : Argile médicinale
RUBRIQUES DEWEY : 615.1
614.1

AUTEURS : Olivier, Jean François
TITRE : La Puissance naturelle des argiles
AUTEURS, COLLABORATIONS : Jean François Olivier
EDITEUR : Encre
DATE DE PUBLICATION : 1988
DESCRIPTION : 64 p. : ill. en coul. ; 28 x 21 cm
ISBN : 2-7337-7015-2
PRIX : Br. 49.00 FRF
RESUME : Comment choisir et utiliser l'argile pour une meilleure santé. Les différentes techniques d'utilisation. Comment les argiles se sont formées.
MOTS-MATIERES : Argile médicinale
RUBRIQUES DEWEY : 615.1
614.1

AUTEURS : Mathieu, Gustave
TITRE : Guérissez par l'argile
AUTEURS, COLLABORATIONS : Gustave Mathieu
LIEU DE PUBLICATION : Paris
EDITEUR : Plon
DESCRIPTION : 278 p. ; 23 x 14 cm
ISBN : 2-268-00958-0
PRIX : Br. 78.00 FRF
RESUME : En spécialiste de l'argilothérapie, sachez préparer l'argile et connaissez les pouvoirs, les dangers et les limites de l'argile.
MOTS-MATIERES : Argile médicinale

DATE DE PUBLICATION : 1990
DESCRIPTION : 125 p. ; 23 x 14 cm
COLLECTION : Equilibre
ISBN : 2-268-00965-3
PRIX : Br. 78.00 FRF
RESUME : Examine l'action protectrice des oligo-éléments, celle des vitamines et le traitement spécifique de chaque affection.
MOTS-MATIERES : Argile médicinale

AUTEURS : Passebecq, André
TITRE : L'Argile pour votre santé
applications thérapeutiques et esthétiques,
dictionnaire de naturopathie
AUTEURS, COLLABORATIONS : André Passebecq
EDITION : 12e éd.
LIEU DE PUBLICATION : Saint-Jean-de-Bray (Loiret)
EDITEUR : Dangles
DATE DE PUBLICATION : 1990
DESCRIPTION : 136 p. : ill. ; 18 x 14 cm
COLLECTION : Santé naturelle
ISBN : 2-7033-0192-8
PRIX : Br. 85.00 FRF
MOTS-MATIERES : Médecine naturelle

AUTEURS : Carité, Jean-Marc
TITRE : L'Argile médicinale
AUTEURS, COLLABORATIONS : Jean-Marc Carité
EDITION : Nouv. éd. rev. et corr.
LIEU DE PUBLICATION : Bats (Landes)
EDITEUR : Utovie
DATE DE PUBLICATION : 1990
DESCRIPTION : 32 p.
COLLECTION : L'Encyclopédie d'Utovie
ISBN : 2-86819-102-9
PRIX : Br. 20.00 FRF
MOTS-MATIERES : Argile médicinale
RUBRIQUES DEWEY : 615.43

DESCRIPTION : 93 p. : ill. ; 21 x 15 cm
COLLECTION : Bien-être et santé
ISBN : 2-87724-029-0
PRIX : Br. 41.00 FRF
RESUME : Donne la description des diverses utilisations de l'argile et, par ordre alphabétique, un index thérapeutique.
MOTS-MATIERES : Argile médicinale
RUBRIQUES DEWEY : 615.35

AUTEURS : Dextreit, Raymond
TITRE : L'Argile qui guérit
mémento de médecine naturelle
AUTEURS, COLLABORATIONS : Raymond Dextreit
EDITION : Nouv. éd.
EDITEUR : Vivre en harmonie
DATE DE PUBLICATION : 1993
DESCRIPTION : 217 p. ; 21 x 14 cm
COLLECTION : La Voie de la santé
ISBN : 2-7155-0067-X
PRIX : Br. 85.00 FRF
RESUME : Ouvrage essentiellement pratique résultant de plus de 20 années d'observations et d'expérience personnelle.
MOTS-MATIERES : Argile médicinale

EDITEUR : Carrère-Lafon
DATE DE PUBLICATION : 1985
DESCRIPTION : 300 p. : ill. en coul. ; 23 x 15 cm
PRIX : Cart 67.00 FRF
RESUME : Un guide sur les bienfaits de l'argile pour la vie quotidienne tant sur le plan médical et philosophique que sur le plan pratique.
MOTS-MATIERES : Argile
RUBRIQUES DEWEY : 615.35

B) Radar 1990-1995

(juniper, cataplasms contg. green montmorillonite clay)
IT Essential oils
RL: THU (Therapeutic use); BIOL (Biological study); USES (Uses)
(lavender, cataplasms contg. green montmorillonite clay)
IT Essential oils
RL: THU (Therapeutic use); BIOL (Biological study); USES (Uses)
(mint, Mentha, cataplasms contg. green montmorillonite clay)
IT ***Clays*** , biological studies
RL: ***THU (Therapeutic use)*** ; BIOL (Biological study); USES (Uses)
(montmorillonitic, cataplasms contg. green montmorillonite clay)
IT Essential oils
RL: THU (Therapeutic use); BIOL (Biological study); USES (Uses)
(rosemary, cataplasms contg. green montmorillonite clay)
IT Essential oils
RL: THU (Therapeutic use); BIOL (Biological study); USES (Uses)
(sassafras, cataplasms contg. green montmorillonite clay)
IT Essential oils
RL: THU (Therapeutic use); BIOL (Biological study); USES (Uses)
(sweet marjoram, cataplasms contg. green montmorillonite clay)
IT 76-22-2, Camphor 89-78-1, Menthol 7647-14-5, Sea salt, biological studies
RL: THU (Therapeutic use); BIOL (Biological study); USES (Uses)
(cataplasms contg. green montmorillonite clay)

L5 6 ANSWERS CA COPYRIGHT 1996 ACS
IC ICM C07C319-28
ICS C07C323-52; C07C323-58; C07C323-25; A61K007-09; A61K007-155
CC ***62-3*** (Essential Oils and Cosmetics)
TI Deodorant compositions for extracting malodorous compounds comprising a thiol group-containing compound and an absorbant powder
ST deodorant malodor thiol compd absorbant powder; thioglycolic acid active carbon deodorant
IT Deodorants
Sawdust
(deodorant compns. for extg. malodorous compds. comprising thiol group-contg. compd. and absorbant powder)
IT Kieselguhr
RL: BUU (Biological use, unclassified); BIOL (Biological study); USES (Uses)
(deodorant compns. for extg. malodorous compds. comprising thiol group-contg. compd. and absorbant powder)
IT Odor and Odorous substances
(malodors; deodoranw copn~. for extg. malodorous compds. comprising thiol group-contg. compd. and absorbant powder)
IT ***Clays*** , biological studies
RL: BUU (Biological use, unclassified); BIOL (Biological study); USES (Uses)
(argils, deodorant compns. for extg. malodorous compds. comprising thiol group-contg. compd. and absorbant powder)
IT 7440-44-0, Carbon, biological studies
RL: BUU (Biological use, unclassified); BIOL (Biological study); USES (Uses)
(active; deodorant compns. for extg. malodorous compds. comprising thiol group-contg. compd. and absorbant powder)
IT 52-90-4, Cystein, biological studies 60-23-1, Cysteamine 60-23-1D, Cysteamine, C2-5 acyl derivs. 68-11-1, Thioglycolic acid, biological studies 79-42-5, Thiolactic acid 107-96-0, 3-Mercapto-propionic acid 471-34-1, Calcium carbonate, biological studies 2485-62-3, Methyl cysteinate 3411-58-3, Ethyl cysteinate 14807-96-6, Talc, biological studies 68148-42-5, Glycerol monothioglycolate 134367-07-0 161765-51-1
RL: BUU (Biological use, unclassified); BIOL (Biological study); USES (Uses)
(deodorant compns. for extg. malodorous compds. comprising thiol group-contg. compd. and absorbant powder)

```
L5   6 ANSWERS   CA  COPYRIGHT 1996 ACS
IC   ICM  A61K033-06
     ICS  A61K035-02
CC   63-6 (Pharmaceuticals)
TI   Pharmaceutical compositions based on clay
ST   pharmaceutical compn clay infection; cataplasm illite uterine
     infection
IT   Diarrhea
       (inhibitors; pharmaceutical compns. based on clay)
IT   Bactericides, Disinfectants, and Antiseptics
     Infection
     Wound
       (pharmaceutical compns. based on clay)
IT   Smectite-group minerals
     RL: BAC (Biological activity or effector, except adverse); THU
     (Therapeutic use); BIOL (Biological study); USES (Uses)
       (pharmaceutical compns. based on clay)
IT     ***Clays***   , biological studies
     RL:   ***THU (Therapeutic use)***   ; BIOL (Biological study); USES
     (Uses)
       (pharmaceutical compns. based on clay)
IT   Inflammation inhibitors
       (antirheumatics, pharmaceutical compns. based on clay)
IT   Bladder
       (disease, cystitis, pharmaceutical compns. based on clay)
IT   Ear
       (disease, otitis, pharmaceutical compns. based on clay)
IT   Medical goods
       (poultices, pharmaceutical compns. based on clay)
IT   Pharmaceutical dosage forms
       (powders, pharmaceutical compns. based on clay)
IT   1318-74-7, Kaolinite, biological studies   12173-60-3, Illite
     12174-11-7, Attapulgite
     RL: BAC (Biological activity or effector, except adverse); THU
     (Therapeutic use); BIOL (Biological study); USES (Uses)
       (pharmaceutical compns. based on clay)
```

L5 6 ANSWERS CA COPYRIGHT 1996 ACS
IC ICM A61K007-06
CC ***62-4*** (Essential Oils and Cosmetics)
TI Detergent cosmetic compositions containing silicones
ST detergent cosmetic silicone clay
IT Cosmetics
Detergents
Hair preparations
Shampoos
Surfactants
(detergent cosmetic compns. contg. silicones and ***clays***)
IT Chlorite-group minerals
Clays , biological studies
Kaolin, biological studies
Siloxanes and Silicones, biological studies
RL: BUU (Biological use, unclassified); BIOL (Biological study);
USES (Uses)
(detergent cosmetic compns. contg. silicones and ***clays***)
IT Cyclosiloxanes
RL: BUU (Biological use, unclassified); BIOL (Biological study);
USES (Uses)
(di-Me, detergent cosmetic compns. contg. silicones and
clays)
IT 1318-00-9, Vermiculite 1318-93-0, Montmorillonite, biological
studies 9016-00-6, Polydimethyl siloxane 11138-66-2, Xanthan gum
12172-85-9, Beidellite 12173-47-6, Hectorite 12298-43-0,
Halloysite 12417-86-6, Stevensite 14807-96-6, Talc, biological
studies 31900-57-9, Polydimethyl siloxane 61076-98-0, Antigorite
63800-37-3, Sepiolite 66732-77-2, Saponite
RL: BUU (Biological use, unclassified); BIOL (Biological study);
USES (Uses)
(detergent cosmetic compns. contg. silicones and ***clays***)

L5 6 ANSWERS CA COPYRIGHT 1996 ACS
IC ICM A61K007-043
ICS C08L001-18
CC ***62-4*** (Essential Oils and Cosmetics)
TI Toluene-free nail polish gels
ST camphor nitrocellulose nail polish solvent
IT Thickening agents
Wetting agents
(nail polish compns. contg. nitrocellulose and camphor and)
IT Alkyd resins
Acrylic polymers, uses
Clays , uses
RL: BIOL (Biological study)
(nail polish compns. contg. nitrocellulose and camphor and)
IT Alcohols, biological studies
Esters, biological studies
RL: BIOL (Biological study)
(solvent-diluent systems contg., for nail polish compns.)
IT Polysulfonamides
RL: BIOL (Biological study)
(arom., nail polish compns. contg. nitrocellulose and camphor and)
IT Cosmetics
(nail lacquers, nitrocellulose and camphor in)
IT 9004-70-0, Nitrocellulose
RL: BIOL (Biological study)
(nail polish compns. contg. camphor and)
IT 76-22-2, Camphor
RL: BIOL (Biological study)
(nail polish compns. contg. nitrocellulose and)
IT 1318-93-0D, Montmorillonite ((Al1.33-1.67Mg0.33-0.67)(Ca0-1Na0-1)0.33Si4(OH)2O10.xH2O), benzyldodceyltrimethylam}onium complexes 9003-63-8, Polybutylmethacrylate 10328-35-5D, montmorillonite complexes
RL: BIOL (Biological study)
(nail polish compns. contg. nitrocellulose and camphor and)
IT 67-63-0, Isopropanol, biological studies 84-74-2, Dibutyl phthalate 123-86-4, Butyl acetate 141-78-6, Ethyl acetate, biological studies
RL: BIOL (Biological study)
(solvent-diluent systems contg., for nail polish compns.)
IT 77-92-9, Citric acid, biological studies
RL: BIOL (Biological study)

(thickener, nail polish compns. contg. nitrocellulose and camphor
and)

IT 7664-38-2, Phosphoric acid, miscellaneous
RL: MSC (Miscellaneous)
(thickener, nail polish compns. contg. nitrocellulose and camphor
and)

Références en anglais (38)

L6 38 ANSWERS CA COPYRIGHT 1996 ACS

IC ICM A61B005-055
ICS A61K033-04; A61K033-06

CC 8-9 (Radiation Biochemistry)

TI Magnetic resonance imaging agent comprising barium sulfate and a clay

ST barium sulfate clay MRI agent; bentonite barium sulfate MRI agent

IT Digestive tract
(magnetic resonance imaging agent with barium sulfate and a clay)

IT Bentonite, biological studies
Clays , biological studies
RL: ***THU (Therapeutic use)*** ; BIOL (Biological study); USES (Uses)
(magnetic resonance imaging agent with barium sulfate and a clay)

IT Imaging
(NMR, contrast agents, magnetic resonance imaging agent with barium sulfate and a clay)

IT ***Clays*** , biological studies
RL: ***THU (Therapeutic use)*** ; BIOL (Biological study); USES (Uses)
(smectitic, magnetic resonance imaging agent with barium sulfate and a clay)

IT 7727-43-7, Barium sulfate
RL: THU (Therapeutic use); BIOL (Biological study); USES (Uses)
(magnetic resonance imaging agent with barium sulfate and a clay)

```
L6   38 ANSWERS   CA  COPYRIGHT 1996 ACS
IC  ICM  A61K007-02
    ICS  A61K007-48
CC     ***62-4***   (Essential Oils and Cosmetics)
TI  Cosmetic makeup compositions containing pre-emulsified lubricants
ST  makeup cosmetic silicone polyglyceryl methacrylate lubricant
IT  Emulsifying agents
    Humectants
    Sunscreens
      (cosmetic makeup compns. contg.)
IT  Lanolin
    Esters, biological studies
    Polyoxyalkylenes, biological studies
    RL: BIOL (Biological study)
      (cosmetic makeup compns. contg., as emollients)
IT  Lecithins
    Glycerides, biological studies
    RL: BIOL (Biological study)
      (cosmetic makeup compns. contg., as emulsifiers)
IT  Waxes and Waxy substances
    RL: BUU (Biological use, unclassified); BIOL (Biological study);
    USES (Uses)
      (cosmetic makeup compns. contg., as emulsifiers)
IT     ***Clays***   , biological studies
    RL: BIOL (Biological study)
      (cosmetic makeup compns. contg., as stabilizer)
IT  Siloxanes and Silicones, biological studies
    RL: BIOL (Biological study)
      (mixts. with poly(glyceryl methacrylate), cosmetic makeup compns.
      contg., as lubricant)
IT  Cyclosiloxanes
    RL: BIOL (Biological study)
      (di-Me, cosmetic makeup compns. contg., as emollients)
IT  Fatty acids, biological studies
    RL: BUU (Biological use, unclassified); BIOL (Biological study);
    USES (Uses)
      (esters, cosmetic makeup compns. contg., as emollients)
IT  Polyoxyalkylenes, biological studies
    RL: BUU (Biological use, unclassified); BIOL (Biological study);
    USES (Uses)
      (ethers, cosmetic makeup compns. contg., as emollients)
IT  Steroids, biological studies
    RL: BUU (Biological use, unclassified); BIOL (Biological study);
```

USES (Uses)
(hydroxy, ethoxylated, cosmetic makeup compns. contg., as emulsifiers)
IT Lecithins
RL: BIOL (Biological study)
(hydroxylated, cosmetic makeup compns. contg., as emulsifiers)
IT Hydrocarbons, biological studies
RL: BIOL (Biological study)
(long-chain, cosmetic makeup compns. contg., as emollients)
IT Cosmetics
(makeups, silicone/polyglyceryl methyacrylate lubricant in)
IT 31566-31-1, Glyceryl monostearate
RL: BIOL (Biological study)
(cosmetic makeup compns. contg.)
IT 142-16-5, Dioctyl maleate
RL: BIOL (Biological study)
(cosmetic makeup compns. contg., as emollient)
IT 9016-00-6, Dimethyl siloxanes
RL: BIOL (Biological study)
(cosmetic makeup compns. contg., as emollients)
IT 57-10-3D, Palmitic acid, reaction products with triethanolamine
57-11-4D, Octadecanoic acid, reaction products with triethanolamine
102-71-6D, reaction products with stearic acid 111-42-2D,
Diethanolamine, reaction product wiwh alkyl phosphate 7664-38-2D,
Phosphoric acid, alkyl esters, reaction products with diethanolamine
RL: BIOL (Biological study)
(cosmetic makeup compns. contg., as emulsifiers)
IT 56-81-5, 1,2,3-Propanetriol, biological studies
RL: BIOL (Biological study)
(cosmetic makeup compns. contg., as humectant)
IT 156229-00-4, Lubrasil
RL: BIOL (Biological study)
(cosmetic makeup compns. contg., as lubricant)
IT 1327-43-1, Magnesium aluminum silicate 9004-34-6, Cellulose,
biological studies 9004-62-0, Hydroxyethyl cellulose 11138-66-2,
Xanthan gum
RL: BIOL (Biological study)
(cosmetic makeup compns. contg., as stabilizer)
IT 28474-30-8, Polyglyceryl methacrylate
RL: BIOL (Biological study)
(mixts. with silicones, cosmetic makeup compns. contg., as lubricant)

L6 38 ANSWERS CA COPYRIGHT 1996 ACS
IC ICM A61K007-16
CC ***62-7*** (Essential Oils and Cosmetics)
TI an abrasive mouthwash in the form of a pourable suspension
ST abrasive mouthwash suspension surfactant
IT Gums and Mucilages
Humectants
Surfactants
(abrasive mouthwash suspension contg.)
IT Smectite-group minerals
Clays , biological studies
RL: BIOL (Biological study)
(abrasive mouthwash suspension contg.)
IT Abrasives
(mouthwash suspension contg.)
IT Mouthwashes
(suspension, abrasives and suspending agents and surfactants in)
IT Resins
RL: BIOL (Biological study)
(synthetic, abrasive mouthwash suspension contg.)
IT Surfactants
(amphoteric, abrasive mouthwash suspension contg.)
IT Surfactants
(anionic, abrasive mouthwash suspension contg.)
IT ***Clays*** , biological studies
RL: BIOL (Biological study)
(montmorillonitic, abrasive mouthwash suspension contg.)
IT Surfactants
(nonionic, abrasive mouthwash suspension contg.)
IT 56-81-5, Glycerin, biological studies 79-10-7D, Acrylic acid,
copolymers 151-21-3, Sodium lauryl sulfate, biological studies
471-34-1, Calcium carbonate, biological studies 1344-28-1,
Alumina, biological studies 7440-70-2D, Calcium, salts
7631-86-9, Silica, biological studies 7664-93-9D, Sulfuric acid,
higher alkyl esters 9003-04-7, Sodium polyacrylate 9005-64-5,
Tween 20 11138-66-2, Xanthan gum 13463-67-7, Titanium dioxide,
biological studies 15435-29-7, Bromochlorophene
RL: BIOL (Biological study)
(abrasive mouthwash suspension contg.)

L6 38 ANSWERS CA COPYRIGHT 1996 ACS
IC ICM A61K007-32
CC ***62-4*** (Essential Oils and Cosmetics)
TI Low residue antiperspirant creams
ST antiperspirant cream Cyclomethicone
IT Thickening agents
(antiperspirant cream contg.)
IT Paraffin waxes and Hydrocarbon waxes, biological studies
RL: BIOL (Biological study)
(antiperspirant cream contg.)
IT Hydrocarbons, biological studies
RL: BIOL (Biological study)
(branched C16-68, antiperspirant cream contg.)
IT ***Clays*** , compounds
RL: BIOL (Biological study)
(reaction product with Quaternium-18, antiperspirant cream contg.)
IT Quaternary ammonium compounds, compounds
RL: BIOL (Biological study)
(bis(hydrogenated tallow alkyl)dimethyl, chlorides, reaction products with ***clays*** , antiperspirant cream contg.)
IT Antiperspirants
(creams, Cyclomethicone- and clay thickening agent-contg.)
IT Cyclosiloxanes
RL: BIOL (Biological study)
(di-Me, antiperspirant cream contg.)
IT Castor oil
RL: BIOL (Biological study)
(hydrogenated, antiperspirant cream contg.)
IT 56-40-6D, Glycine, complexes with aluminum zirconium trichlorohydrate 64-17-5, Ethanol, biological studies 67-56-1, Methanol, biological studies 108-32-7, Propylene carbonate 1327-41-9, Aluminum chlorohydrate 98106-53-7D, Aluminum zirconium chloride hydroxide ($Al_4ZrCl_3(OH)_{13}$), glycine complexes
RL: BIOL (Biological study)
(antiperspirant cream contg.)

L6 38 ANSWERS CA COPYRIGHT 1996 ACS
IC ICM A61L009-01
CC ***62-1*** (Essential Oils and Cosmetics)
TI Sodium bicarbonate-containing powdered deodorant composition for shoes, in particular for sporting shoes
ST shoe deodorant sodium bicarbonate
IT Shoes
(deodorant for, sodium bicarbonate-contg.)
IT Deodorants
(for shoes, sodium bicarbonate-contg.)
IT ***Clays*** , biological studies
RL: BIOL (Biological study)
(shoe deodorant contg. sodium bicarbonate and)
IT 144-55-8, Sodium bicarbonate, biological studies
RL: BIOL (Biological study)
(shoe deodorant contg.)
IT 546-93-0, Magnesium carbonate 1314-13-2, Zinc oxide, biological studies 10043-35-3, Boric acid, biological studies
RL: BIOL (Biological study)
(shoe deodorant contg. sodium bicarbonate and)

L6 38 ANSWERS CA COPYRIGHT 1996 ACS
IC ICM A61L009-01
ICS A61L009-04; B01J007-00; A61K007-46
NCL 422305000
CC ***62-7*** (Essential Oils and Cosmetics)
TI Perfumed stable gel composition
ST deodorant perfume gel glycol surfactant

IT Apple
Gardenia
Jasmine
Spices
(flavor; perfumed stable gel compns. for deodorants)
IT Odor and Odorous substances
Perfumes
(perfumed stable gel compns. for deodorants)
IT Kieselguhr
Petroleum spirits
Sand
Soaps
Clays , biological studies
Glycols, biological studies
Hydrocarbons, biological studies
RL: BUU (Biological use, unclassified); BIOL (Biological study);
USES (Uses)
(perfumed stable gel compns. for deodorants)
IT Deodorants
(air fresheners, perfumed stable gel compns. for deodorants)
IT Flavoring materials
(cherry, perfumed stable gel compns. for deodorants)
IT Deodorants
(gels, perfumed stable gel compns. for deodorants)
IT Flavoring materials
(lemon, perfumed stable gel compns. for deodorants)
IT Surfactants
(nonionic, perfumed stable gel compns. for deodorants)
IT Flavoring materials
(spearmint, perfumed stable gel compns. for deodorants)
IT 56-81-5, Glycerol, biological studies 57-55-6, Propylene glycol,
biological studies 64-17-5, Ethanol, biological studies
107-41-5, Hexylene glycol 822-16-2, Sodium stearate 7631-86-9,
Silica, biological studies 25154-52-3, Nonylphenol 25322-68-3,
Polyethylene glycol

RL: BUU (Biological use, unclassified); BIOL (Biological study);
USES (Uses)
* Illite et usage therapeutique (en anglais)

L4 1 ANSWERS CA COPYRIGHT 1996 ACS
IC ICM A61K007-38
CC ***62-4*** (Essential Oils and Cosmetics)
TI Deodorants comprising layered silicates
ST deodorant cosmetic layered silicate
IT Smectite-group minerals
Bentonite, biological studies
RL: BIOL (Biological study)
(deodorant cosmetics contg.)
IT Deodorants
(layered silicates-contg.)
IT Silicates, biological studies
RL: BIOL (Biological study)
(layered, deodorant cosmetics contg.)
IT 1318-74-7, Kaolinite (Al2(Si2O7).2H2O), biological studies
1318-93-0, Montmorillonite ((Al1.33-1.67Mg0.33-0.67)(Ca0-1Na0-1)0.33Si4(OH)2O10.xH2O), biological studies 1319-41-1, Saponite ((Mg0.5-1Fe0-0.5)3(Si3.67Al0.33)(Na0-0.33Ca0-0.17)(OH)2O10.4H2O)
12172-85-9, Beidellite (Al2(Si3.67Al0.33)(Na0-0.33Ca0-0.17)(OH)2O10.xH2O) 12173-47-6, Hectorite ((Mg2.67Li0.33)Si4Na0.33[F0.5-1(OH)0-0.5]2O10) ***12173-60-3*** ,
* Illite ([Al1.75(Fe0-1Mg0-1)0.25]K0.75(Si3.5Al0.5)[(OH)0.5-1F0-0.5]2O10) 12174-06-0, Nontronite (Fe2(Si3.67Al0.33)Na0.33(OH)2O10.xH2O)
RL: BIOL (Biological study)
(deodorant cosmetics contg.)

Montmorillonite et usage cosmétique, en français :

L10 3 ANSWERS CA COPYRIGHT 1996 ACS
IC ICM A61K007-00
ICS A61K009-107
CC ***62-4*** (Essential Oils and Cosmetis)~
TI Cosmetic compositions containing microspheres dispersed in aqueous gel
ST cosmetic compn microsphere aq gel; aftershave gel acrylic copolymer Expancel EL23
IT Gums and Mucilages
Sunscreens
(cosmetic compns. contg. microspheres dispersed in aq. gel)
IT Acrylic polymers, biological studies
Silica gel, biological studies
Silicates, biological studies
RL: BUU (Biological use, unclassified); BIOL (Biological study); USES (Uses)
(cosmetic compns. contg. microspheres dispersed in aq. gel)
IT Polysaccharides, biological studies
RL: BUU (Biological use, unclassified); BIOL (Biological study); USES (Uses)
(derivs.; cosmetic compns. contg. microspheres dispersed in aq. gel)
IT Silsesquioxanes
RL: BUU (Biological use, unclassified); BIOL (Biological study); USES (Uses)
(Me, cosmetic compns. contg. microspheres dispersed in aq. gel)
IT Shaving preparations
(aftershaves, cosmetic compns. contg. microspheres dispersed in aq. gel)
IT Gelation
(agents, cosmetic compns. contg. microspheres dispersed in aq. gel)
IT Cosmetics
(cleansing, cosmetic compns. contg. microspheres dispersed in aq. gel)
IT Cosmetics
(eye shadows, cosmetic compns. contg. microspheres dispersed in aq. gel)
IT Ceratonia siliqua

(flour, cosmetic compns. contg. microspheres dispersed in aq.
gel)

IT Cosmetics
(foundations, cosmetic compns. contg. microspheres dispersed in
aq. gel)

IT Cosmetics
(gels, cosmetic compns. contg. microspheres dispersed in aq. gel)

IT Carboxylic acids, biological studies
RL: BUU (Biological use, unclassified); BIOL (Biological study);
USES (Uses)
(poly-, cosmetic compns. contg. microspheres dispersed in aq.
gel)

IT ***1318-93-0*** , Montmorillonite, biological studies 1398-61-4D,
Chitin, derivs. 9000-30-0, Guar gum 9003-39-8, Pvp 9004-34-6D,
Cellulose, derivs. 9004-61-9, Hyaluronic acid 9004-61-9D,
Hyaluronic acid, salts 9004-64-2, Hydroxypropyl cellulose
9005-25-8D, Starch, derivs. 9005-32-7D, Alginic acid, salts
9007-28-7, Chondroitin sulfate 11138-66-2, Xanthan gum
25322-68-3, Peg 25618-55-7, Polyglycerin 27756-15-6, Acrylic
acid-stearyl methacrylate copolymer 28474-30-8,
Polyglycerylmethacrylate 52357-35-4 71010-52-1, Gellan gum
96949-21-2, Rhamsan gum 134499-37-9, Carbopol 954 158885-77-9,
Expancel E 14 158885-78-0, Expancel E 116 158885-79-1, Expancel
E 123
RL: BUU (Biological use, unclassified); BIOL (Biological study);
USES (Uses)
(cosmetic compns. contg. microspheres dispersed in aq. gel)

L10 3 ANSWERS CA COPYRIGHT 1996 ACS
IC ICM A61K007-021
CC ***62-3*** (Essential Oils and Cosmetics)
TI Cosmetic liquids containing trimethylsiloxysilicic acid and volatile
silicone and fatty acid esters with saccharose
ST cosmetic liq trimethylsiloxysilicic acid silicone; fatty acid ester
saccharose cosmetic liq
IT Clay minerals
Bentonite, biological studies
Siloxanes and Silicones, biological studies
RL: BUU (Biological use, unclassified); BIOL (Biological study);
USES (Uses)
(cosmetic liqs. contg. trimethylsiloxysilicic acid and volatile
silicone and fatty acid esters with saccharose)
IT Siloxanes and Silicones, biological studies
RL: BUU (Biological use, unclassified); BIOL (Biological study);
USES (Uses)
(Me hydrogen, cosmetic liqs. contg. trimethylsiloxysilicic acid
and volatile silicone and fatty acid esters with saccharose)
IT Quaternary ammonium compounds, biological studies
RL: BUU (Biological use, unclassified); BIOL (Biological study);
USES (Uses)
(alkylbenzyldimethyl, chlorides, cosmetic liqs. contg.
trimethylsiloxysilicic acid and volatile silicone and fatty acid
esters with saccharose)
IT Surfactants
(cationic, cosmetic liqs. contg. trimethylsiloxysilicic acid and
volatile silicone and fatty acid esters with saccharose)
IT Siloxanes and Silicones, biological studies
RL: BUU (Biological use, unclassified); BIOL (Biological study);
USES (Uses)
(di-Me, cosmetic liqs. contg. trimethylsiloxysilicic acid and
volatile silicone and fatty acid esters with saccharose)
IT Siloxanes and Silicones, biological studies
RL: BUU (Biological use, unclassified); BIOL (Biological study);
USES (Uses)
(di-Me Ph, cosmetic liqs. contg. trimethylsiloxysilicic acid and
volatile silicone and fatty acid esters with saccharose)
IT Fatty acids, biological studies
RL: BUU (Biological use, unclassified); BIOL (Biological study);

2

Livres repérés dans les catalogues de bibliothèques québécoises (pour emprunt)

A) Réseau des Cegeps

```
<Page suiv.>: Titre suivant


                               Recherche
                         Recherche par sujet
Nigelle, Eric, 1915-                                               --- 5 ---
      Pouvoirs merveilleux de l'argile : en association avec l'eau et les
   plantes : fangothrapie,bains de boue / Eric Nigelle. -- 5e ed. -- Soissons,
   France : Andrillon, 1976.
      196p.

      1. Argile--Emploi en thrapeutique.  2. Naturopathie.  I. Titre.

1 document(s):
Cgep de Limoilou
    X02616297    RM666C545 N684 1976





PF1: Terminer PF3: Notice complte <Page prc.>: Titre prcdent
<Page suiv.>: Titre suivant


                               Recherche
                         Recherche par sujet
Masson, Robert.                                                    --- 7 ---
      La sant par l'argile / Robert Masson ; dessins originaux de Valrie-
   Catherine Richez. -- Nouv. d. rev. -- Paris : M.A. ditions, 1986, c1983.
      127 p. : ill. ; 22 cm. -- (L'Aide-nature ; 1)

      ISBN 2-86676-047-6
      Type de documents: livre.

      1. Argile--Emploi en thrapeutique.  I. Titre.  II. Titre: L'Argile.
   III. Collection.

1 document(s):
Cgep de Jonquire - Collection gnrale
    X00164634    RM 666 C545M38 1986




PF1: Terminer PF3: Notice complte <Page prc.>: Titre prcdent
<Page suiv.>: Titre suivant
```

```
<Page suiv.>: Titre suivant

                                    Recherche
                               Recherche par sujet
Nigelle, Eric, 1915-                                                  --- 5 ---
       Pouvoirs merveilleux de l'argile : en\association avec l'eau et les
   plantes : fangothrapie,bains de boue / Eric Nigelle. -- 5e ed. -- Soissons,
   France : Andrillon, 1976.
       196p.

       1. Argile--Emploi en thrapeutique.  2. Naturopathie.   I. Titre.

1 document(s):
Cgep de Limoilou
    X02616297    RM666C545 N684 1976




PF1: Terminer PF3: Notice complte <Page prc.>: Titre prcdent
<Page suiv.>: Titre suivant
```

```
                                    Recherche
                               Recherche par sujet
Masson, Robert.                                                       --- 7 ---
       La sant par l'argile / Robert Masson ; dessins originaux de Valrie-
   Catherine Richez. -- Nouv. d. rev. -- Paris : M.A. ditions, 1986, c1983.
       127 p. : ill. ; 22 cm. -- (L'Aide-nature ; 1)

       ISBN 2-86676-047-6
       Type de documents: livre.

       1. Argile--Emploi en thrapeutique.  I. Titre.  II. Titre: L'Argile.
   III. Collection.

1 document(s):
Cgep de Jonquire - Collection gnrale
    X00164634    RM 666 C545M38 1986



PF1: Terminer PF3: Notice complte <Page prc.>: Titre prcdent
<Page suiv.>: Titre suivant
```

B) Bibliothèques de l'Université de Montréal

```
                          ATRIUM - AFFICHAGE ABREGE            (1 de 1 notices)
                                                         Nbre d'exemplaires :1
         [Auteur]  Valnet, Jean, 1920-
          [Titre]  Traitement des maladies par les legumes, les fruits et les
                   cereales / Jean Valnet.
        [Edition  8e ed. revue et augmentee.
  [Adresse bibl.]  Paris : Maloine, 1982.
    [Description]  527 p., 16 p. de planches : ill. en coul.
         [Sujets]  Dietotherapie
                   Vegetarisme
                   Argile -- Emploi en therapeutique

    Biblioth eque Collection/Cote
    ------------  -----------------------
 1. Sante         WB 430 V197t 1982                          ***



 Derni ere Page
Ordres :    Voir l'ecran precedent
 [Etape precedente] eXplorer]   [Affichage complet]   [Imprimer]
 [MARC]   [Historique]    [confiGurer]    [Nouvelle recherche]   [Finir]
 [? aide]
```

```
                          ATRIUM - AFFICHAGE ABREGE            (1 de 1 notices)
                                                         Nbre d'exemplaires :2
         [Auteur]  Donadieu, Yves
          [Titre]  L'argile : therapeutique naturelle / Yves Donadieu.
  [Adresse bibl.]  Paris : Maloine, 1980.
    [Description]  147 p.
     [Collection]  Les Therapeutiques naturelles;
         [Sujets]  Argile
                   Argile -- Emploi en therapeutique

    Biblioth eque Collection/Cote
    ------------  -----------------------
 1. Para-med.     WB 935 D674a                               ***
 2. Sante         WB 935 D674a ex.2                          ***



 Derni ere Page
Ordres :    Voir l'ecran precedent
 [Etape precedente] eXplorer]   [Affichage complet]   [Imprimer]
 [MARC]   [Historique]    [confiGurer]    [Nouvelle recherche]   [Finir]
 [? aide]
```

```
                          ATRIUM - AFFICHAGE ABREGE            (1 de 1 notices)
                                                         Nbre d'exemplaires :1
         [Auteur]  Holtzapffel, Thierry
          [Titre]  Les mineraux argileux : preparation, analyse
                   diffractometrique et determination / Thierry Holtzapffel.
  [Adresse bibl.]  Villeneuve d'Ascq : S.G.N., 1985.
    [Description]  136 p. : ill.
```

```
        [Collection]  Publication (Societe geologique du Nord);  no 12
            [Sujets]  Mineraux argileux

      Biblioth eque Collection/Cote
      ------------  -----------------------
   1. Geologie      QE 65 S63 no.012 1985                       ***



   Derni ere Page
  Ordres :    Voir l'ecran precedent
   [Etape precedente] eXplorer]   [Affichage complet]   [Imprimer]
   [MARC]   [Historique]   [confiGurer]   [Nouvelle recherche]   [Finir]
   [? aide]
```

```
                              ATRIUM - AFFICHAGE ABREGE          (1 de 1 notices)
                                                            Nbre d'exemplaires :1
            [Auteur]  Velde, Bruce
             [Titre]  Introduction to clay minerals : chemistry, origins, uses,
                      and environmental significance / B. Velde.
           [Edition  1st ed.
    [Adresse bibl.]  London ; New York : Chapman & Hall, 1992.
      [Description]  vii, 198 p. : ill. ; 24 cm.
            [Sujets]  Argile -- Analyse
                      Mineraux argileux

      Biblioth eque Collection/Cote
      ------------  -----------------------
   1. Geographie    QE 471 .3 V44 1992                          ***



   Derni ere Page
  Ordres :    Voir l'ecran precedent
   [Etape precedente] eXplorer]   [Affichage complet]   [Imprimer]
   [MARC]   [Historique]   [confiGurer]   [Nouvelle recherche]   [Finir]
   [? aide]
```

C) Institut Canadien de l'information scientifique et technique

```
(P)recedent  (S)uivant  commande (R)eguliere  commande (U)rgente  (Q)uitter
s

     3 / 5
RE - 13906602
TI - Summary report. No. 17, Bentonite, Fuller's earth and kaolinitic clays
AT - Additional Title: Rapport sommaire. No 17, Bentonite, argile smectique et
     argiles kaolinitiques.
     Additional Title: Bentonite, Fuller's earth and kaolinitic clays.
AU - Andrews, P. R. A.
DA - 1992
CE - MAIN Ser TN496 R22e no. MSL 92/52




(P)recedent  (S)uivant  commande (R)eguliere  commande (U)rgente  (Q)uitter


(P)recedent  (S)uivant  commande (R)eguliere  commande (U)rgente  (Q)uitter
s

     3 / 16
RE - 6986083
TI - The clay products industry : a market profile for industrial minerals in
     Canada's manufacturing sectors
AT - Additional Title: L'industrie des produits d'argile : profil du marche
     des mineraux industriels dans les secteurs manufacturiers au Canada.
AU - Prud'homme, Michel.; Francis, Diana.
DA - 1986
CE - MAIN Ser TN1 I618 MRI 86/3
```

aussi aux HEC - voir ci-joint

```
(P)recedent  (S)uivant  commande (R)eguliere  commande (U)rgente  (Q)uitter


(P)recedent  (S)uivant  commande (R)eguliere  commande (U)rgente  (Q)uitter
s

     3 / 5
AN - 595754
RE - 13906602
TI - Summary report. No. 17, Bentonite, Fuller's earth and kaolinitic clays
```

```
AT - Additional Title: Rapport sommaire. No 17, Bentonite, argile smectique et
     argiles kaolinitiques.
     Additional Title: Bentonite, Fuller's earth and kaolinitic clays.
AU - Andrews, P. R. A.
CS - Mineral Sciences Laboratories (Canada)
PU - [Ottawa] : Mineral Sciences Laboratories, [1992] ix, 185 p.
CP - Ontario [ONC]
DA - 1992
SE - Division report (Mineral Sciences Laboratories (Canada)) ; MSL 92-52 (R)
NU - MSL 92-52 (R
LA - English
SL - French
NO - Summary in French.
DT - Report; Government Publication: Federal/National
CC - Local LC class: TN496
(P)recedent  (S)uivant  commande (R)eguliere  commande (U)rgente  (Q)uitter
```

```
(P)recedent  (S)uivant  commande (R)eguliere  commande (U)rgente  (Q)uitter
s
DT - Report; Government Publication: Federal/National
CC - Local LC class: TN496
CE - MAIN Ser TN496 R22e no. MSL 92/52
```

```
(P)recedent  (S)uivant  commande (R)eguliere  commande (U)rgente  (Q)uitter
```

D) Bibliothèque de l'École des Hautes Études Commerciales

```
                           Recherche
                       Recherche par sujet
01-3019062                                                   --- 1 ---
Prud'homme, Michel.
     Profil du march des minraux industriels dans les secteurs
  manufacturiers au Canada : l'industrie des produits d'argile / Michel
  Prud'homme, Diana Francis. -- [Ottawa] : nergie, mines et ressources Canada,
   [1986].
     vi, 19, 19, vi p. -- (Rapport interne / Secteur de la politique minrale
  ; MRI 86/3)

     Titres de la couverture: L'industrie des produits d'argile = The clay
     products industry.
     Textes en franais et anglais disposs tte-bche avec page de titre
     additionnelle en anglais : A market profile for industrial minerals in
     Canada's manufacturing sectors : the clay products industry.
     Bibliogr.
     ISBN 0-662-54846-9




                     A suivre ... Taper une touche pour afficher la page suivante
```

3

Liste d'articles

13/8/8
DIALOG(R)File 144:(c) 1996 INIST/CNRS. All rts. reserv.

11617386 PASCAL No.: 94-0399780
Dermatophytes, virus et boues thermales

English Descriptors: Medicinal mud; Virus; Bacteria; Bacteriology; Parasitology; Mycosis; Skin disease; Grey literature
Broad English Descriptors: Infection

French Descriptors: Boue medicinale; Virus; Bacterie; Bacteriologie; Parasitologie; Mycose; Peau pathologie; Litterature grise; Maturation boue

Classification Cods:~f0230A11

13/8/9
DIALOG(R)File 144:(c) 1996 INIST/CNRS. All rts. reserv.

11617058 PASCAL No.: 94-0399452
Etude sur les boues de DAX : leur emploi en therapeutique

English Descriptors: Medicinal mud; Treatment; Chemical analysis; Mud; Microbiology; Grey literature; Efficiency; Landes
Broad English Descriptors: Frankreich; Europa

French Descriptors: Boue medicinale; Traitement; Analyse chimique; Boue; Microbiologie; Litterature grise; Efficacite; Landes; Station thermale

Classification Codes: 002B30A11

13/8/10

11617057 PASCAL No.: 94-0399451

Elaboration d'une base de donnees bibliographiques sur les boues thermales (Methodes experimentales d'etude)

English Descriptors: Computer science; Databank; Medicinal mud; Grey literature; Bibliography

French Descriptors: Informatique; Banque donnee; Boue medicinale; Litterature grise; Bibliographie

Classification Codes: 002B30A11

14/8,K/1
DIALOG(R)File 144:(c) 1996 INIST/CNRS. All rts. reserv.

11619486 PASCAL No.: 94-0401880
La pelotherapie a l'hopital thermal des armees VICTOR DE CASTELLANE

English Descriptors: Thermal cure; Mineral water; Osteoarthritis; Medicinal mud; Diseases of the osteoarticular system; Pyrenees-Orientales
Broad English Descriptors: Frankreich; Europa

French Descriptors: Cure thermale; Eau mineralisee; Arthrose; Boue medicinale; Systeme osteoarticulaire pathologie; Pyrenees Orientales

Classification Codes: 002B30A11

...des Armees Victor de Castellane resulte d'un contact prolonge (5 mois) entre de l' argile d'une carriere enrichie en humus vegetal et de l'eau bicarbonatee sulfuree. Utilisee dans...

French Descriptors: Cure thermale; Eau mineralisee; Arthrose; Boue medicinale ; Systeme osteoarticulaire pathologie; Pyrenees Orientales

---

14/8,K/2
DIALOG(R)File 144:(c) 1996 INIST/CNRS. All rts. reserv.

11608712 PASCAL No.: 94-0391106
Determination d'un peloi-de destine a la station thermale d'Amneville. Etude des echanges transcutanes de calcium lors de son application experimentale

English Descriptors: Medicinal mud; Calcium; Research; Crenotherapy

French Descriptors: Boue medicinale; Calcium; Recherche; Crenotherapie

Classification Codes: 002B30A11

Les types d' argiles pouvant servir a confectionner un peloi-de avec l'eau d'Amneville. Etude sur 6 sujets du passage transcutane de l'ion calcium apres application d'une argile dont la capacite cationique d'echange est saturee a plus de 94% par du calcium

French Descriptors: Boue medicinale ; Calcium; Recherche; Crenotherapie

14/8,K/3
DIALOG(R)File 144:(c) 1996 INIST/CNRS. All rts. reserv.

11608676 PASCAL No.: 94-0391070
L"embrocation" thermale de Rochefort-sur-mer

English Descriptors: Medicinal mud; Crenotherapy; Skin disease

French Descriptors: Boue medicinale; Crenotherapie; Peau pathologie

Classification Codes: 002B30A11

L'"embrocation" thermale de Rochefort-sur-mer est preparee a l'aide d'une argile saturee en eau thermale et enrichie avec le floculat obtenu a partir de cette eau...

French Descriptors: Boue medicinale ; Crenotherapie; Peau pathologie

---

14/8,K/4
DIALOG(R)File 144:(c) 1996 INIST/CNRS. All rts. reserv.

11608670 PASCAL No.: 94-0391064
Choix et controle des matieres premieres dans la preparation des boues thermales : approche galenique

English Descriptors: Medicinal mud; Crenotherapy; Quality control

French Descriptors: Boue medicinale; Crenotherapie; Controle qualite

Classification Codes: 002B30A11

... rigoureuse. Etude du comportement mecanique et thermique de 7 roches argileuses. Modalites de controle des argiles

French Descriptors: Boue medicinale ; Crenotherapie; Controle qualite

14/8,K/5
DIALOG(R)File 144:(c) 1996 INIST/CNRS. All rts. reserv.

11604219 PASCAL No.: 94-0386613
Argiles et peloi-des. Manifestations des echanges cationiques

English Descriptors: Medicinal mud; Crenotherapy

French Descriptors: Boue medicinale; Crenotherapie

Classification Codes: 002B30A11

Argiles et peloi-des. Manifestations des echanges cationiques

French Descriptors: Boue medicinale ; Crenotherapie

14/8,K/6
DIALOG(R)File 144:(c) 1996 INIST/CNRS. All rts. reserv.

11604218 PASCAL No.: 94-0386612
Pelotherapie. Engouement et contraintes
Thermalisme de l'est de la France

English Descriptors: Medicinal mud; Crenotherapy

French Descriptors: Boue medicinale; Crenotherapie

Classification Codes: 002B30A11

...d'action des boues. L'efficacite risque d'etre moindre si l'on utilise des argiles pures sans bioglee d'algues et de micro-organismes, peloi-des artificiels a envisager

French Descriptors: Boue medicinale ; Crenotherapie

Exemple de format complet (incluant le résumé et la source)

14/7/6
DIALOG(R)File 144:Pascal
(c) 1996 INIST/CNRS. All rts. reserv.

11604218 PASCAL No.: 94-0386612
Pelotherapie. Engouement et contraintes
Thermalisme de l'est de la France
COLLIN JF
Journal: PRESSE THERMALE ET CLIMATIQUE, 1984, 121 (3) 121-122
ISSN: 0032-7875 Availability: BDSP/ISMH-RAM540200048
No. of Refs.: 15 ref.
Document Type: P (Serial) ; A (Analytic)
Country of Publication: France
Language: French
Les differents types de boues thermales. Reflexion sur les modes d'action des boues. L'efficacite risque d'etre moindre si l'on utilise des argiles pures sans bioglee d'algues et de micro-organismes, peloi-des artificiels a envisager

A) Banques de données

Chemical abstracts :

1989-1996, en français: (format titre et mots-clés)

brevet

CA COPYRIGHT 1996 ACS
IC ICM A61K007-06
CC ***62-3*** (Essential Oils and Cosmetics)
TI Cosmetic composition for capillary care based on emulsion of clay, = titre :
oil, and/or fatty substance.
ST capillary hair cosmetic clay lipid; oil fat clay capillary hair
cosmetic
IT Coconut oil
Fats and Glyceridic oils Index terms : It=
Olive oil
Vitellins
RL: BIOL (Biological study)
(hair capillary care compn. contg.)
IT Lipids, biological studies
RL: BIOL (Biological study)
(hair capillary care compn. contg., of plant)
IT Hair preparations
(with clay and lipid components, for uncurled hair)
IT ***Clays*** , biological studies
RL: BIOL (Biological study)
(red, hair capillary care compn. contg.)
IT Fats and Glyceridic oils
RL: BIOL (Biological study)
(shea butter, hair capillary care compn. contg.)
IT Fats and Glyceridic oils
RL: BIOL (Biological study)
(wheat germ, hair capillary care compn. contg.)
IT 77-92-9, Citric acid, biological studies
RL: BIOL (Biological study)
(hair capillary care compn. contg.)

L5 6 ANSWERS CA COPYRIGHT 1996 ACS
IC ICM A61F007-02
ICS B01F009-02
CC 63-6 (Pharmaceuticals)
TI Cataplasms containing green montmorillonite clay
ST pharmaceutical cataplasm montmorillonite clay essential oil; plant ext pharmaceutical cataplasm montmorillonite clay; sea salt pharmaceutical cataplasm montmorillonite clay; Plasmarglyl cataplasm montmorillonite clay essential oil
IT Pharmaceutical dosage forms
(cataplasms contg. green montmorillonite clay)
IT Essential oils
RL: THU (Therapeutic use); BIOL (Biological study); USES (Uses)
(cataplasms contg. green montmorillonite clay)
IT Arnica
Birch
Chamomile
Cypress
Goatsbeard
Hamamelis
Harpagophytum
Horse chestnut
Mallow
St.-John's-wort
Willow
(exts.; cataplasms contg. green montmorillonite clay)
IT Viola tricolor
(wild, exts.; cataplasms contg. green montmorillonite clay)
IT Essential oils
RL: THU (Therapeutic use); BIOL (Biological study); USES (Uses)
(cajuput, cataplasms contg. green montmorillonite clay)
IT Essential oils
RL: THU (Therapeutic use); BIOL (Biological study); USES (Uses)
(citrus, cataplasms contg. green montmorillonite clay)
IT Essential oils
RL: THU (Therapeutic use); BIOL (Biological study); USES (Uses)
(coriander, cataplasms contg. green montmorillonite clay)
IT ***Clays*** , biological studies
RL: ***THU (Therapeutic use)*** ; BIOL (Biological study); USES (Uses)
(green, cataplasms contg. green montmorillonite clay)
IT Oils
RL: THU (Therapeutic use); BIOL (Biological study); USES (Uses)

Banques sur les produits de consommation: références en anglais

2/8/1 (Item 1 from file: 9)
DIALOG(R)File 9:(c) 1996 Resp. DB Svcs. All rts. reserv.

01382950
Ciminelli Sea Clay Mask; Sea Mineral Mask; Eye and Wrinkle Cream; Super Hydrating Cream; Calming Day Cream; Eye and Neck Gel; Body Lotion; Revitalizing Face Cream; Revitalizing Body Cream; Revitalizing Eye and Lip Mask; Marine Body Lotion
WORD COUNT: 124

COMPANY NAMES: SUSAN CIMINELLI SIN ARuc
INDUSTRY NAMES: Pharmaceutical; Personal care products
PRODUCT NAMES: Dermatologicals, except sunscreen and sunburn remedies (283439); Facial scrubs and masks (284430)
CONCEPT TERMS: All product and service information; Product introduction
BRAND NAMES: Susan Ciminelli Skin Care
GEOGRAPHIC NAMES: North America (NOAX); United States (USA)

2/8/2 (Item 2 from file: 9)
DIALOG(R)File 9:(c) 1996 Resp. DB Svcs. All rts. reserv.

01239892
Ocean Potion Bath & Body Thalassotherapy Sea Clay Mud Pack
WORD COUNT: 144

COMPANY NAMES: BURT'S BEES INC
INDUSTRY NAMES: Personal care products
PRODUCT NAMES: Facial scrubs and masks (284430)
CONCEPT TERMS: All product and service information; Product introduction
BRAND NAMES: Ocean Potion Bath & Body Thalassotherapy; Sea Clay Mud Pack
GEOGRAPHIC NAMES: North America (NOAX); United States (USA)

2/8/3 (Item 3 from file: 9)
DIALOG(R)File 9:(c) 1996 Resp. DB Svcs. All rts. reserv.

01028730

Aphrodisia Naturals Facial Steaming Herbs; Facial Care Oil - Normal/Combination Skin; Dry/Mature Skin; Sensitive Skin; Rosewater; Natural Mineral Clay - White; French Green; Morroccan Red; Fuller's Earth; Facial Care Sampler; Moisturizing Body Scrub; Sea Clay Body Mask; Body Care Sampler; Essential Oil - Allspice; Anise; Balsam Fir; Basil; Bay; Bergamot; Birch; Cajeput; Camphor; Cardamom; Carrot; Thuja Cedarleaf; Cedarwood; Cinnamon; Citronella; Clary Sage; Clove; Cypress; Eucalyptus; Fennel Seed; Frankincense; Egyptian Geranium; Ginger; Grapefruit; Juniper; French Lavender; Spanish Lavender; Lemon; Lemongrass; Lime; Wild Marjoram; Natural Myrrh; Nutmeg; Sweet Orange Oil; Mandarin Orange; Palmarosa; East Indian Patchouly; Pennyroyal; Black Pepper; Peppermint; Pine Needle; Rosemary; Rosewood; Sage; Mysore Sandalwood; Sassafras; Spearmint; Marigold Tagetes; Tangerine; Tea Tree; White Thyme; Vetivert; Wintergreen; Ylang Ylang; Regular Precious Oil - Blue Chamomile; Jasmine Absolute; Neroli; Otto of Rose; 7% Sol
WORD COUNT: 150

COMPANY NAMES: APHRODISIA PRODUCTS INC
INDUSTRY NAMES: Personal care products
PRODUCT NAMES: Cremes, lotions and oils (other than bath) for facial and body care (284415)
CONCEPT TERMS: All product and service information; Product introduction
GEOGRAPHIC NAMES: North America (NOAX); United States (USA)

2/8/5 (Item 2 from file: 16)
DIALOG(R)File 16:(c) 1996 Information Access Co. All rts. reserv.

01168322
New finding backs idea that life started in clay rather than sea.

PRODUCT: *Biology (8522100)
EVENT: *Science & Research (31)
COUNTRY: *United States (1USA)

Argiles marines, en français, dans Pascal, 1985:1996

2/8/1 (Item 1 from file: 144)
DIALOG(R)File 144:(c) 1996 INIST/CNRS. All rts. reserv.

12324018 PASCAL No.: 95-0563052
Authigenese et evolution d'argiles hydrothermales oceaniques : exemples des monts de la ride des Galapagos et des sediments de la ride de Juan de Fuca
(Formation and evolution of oceanic hydrothermal clay minerals (mounds form the Galapagos Spreading Center and sediments of the Juan de Fuca Ridge))

English Descriptors: clay minerals; marine sediments; hydrothermal conditions; Deep Sea Drilling Project; Ocean Drilling Program; Juan de Fuca Ridge; East Pacific

French Descriptors: Argile mineral; Sediment marin; Condition hydrothermale ; DSDP; ODP; Dorsale Juan de Fuca; Ocean Pacifique Est; DSDP Leg 70; ODP Leg 139

Classification Codes: 226C02; 223B; 001E01P02; 001E01H

2/8/2 (Item 2 from file: 144)
DIALOG(R)File 144:(c) 1996 INIST/CNRS. All rts. reserv.

12303811 PASCAL No.: 95-0537379
Construction de la digue nord de l'amenagement La Grande 1
(Construction of the north dyke of the La Grande 1 project)

English Descriptors: Dike; Cut off wall; Sensitive clay; Marine clay; Excavations; Design; Wall; Grout; Cement; Bentonite; Foundations; Sand; Construction works; Canada
Broad English Descriptors: Nordamerika

French Descriptors: Digue; Parafouille; Argile sensible; Argile marine; Fouille genie civil; Conception; Paroi; Coulis; Ciment; Bentonite; Fondation ouvrage; Sable; Travaux construction; Canada

Classification Codes: 001D14L03; 295

2/8/3 (Item 3 from file: 144)
DIALOG(R)File 144:(c) 1996 INIST/CNRS. All rts. reserv.

11534245 PASCAL No.: 94-0377992
Les mecanismes d'alimentation du plateau de Thermaikos (N.O. Mer Egee) par les couches nepheloides
(Alimentation mechanisms of the Thermaikos plateau (NW Egean sea) by nepheloid layers)

English Descriptors: susendd materials; nepheloid layer; clay minerals; Aegean Sea; Greece
Broad English Descriptors: East Mediterranean; Mediterranean Sea; Europe

French Descriptors: Matiere en suspension; Couche nepheloide; Argile mineral; Mer Egee; Grece; Golfe Thermaikos

Classification Codes: 226C02; 001E01P02

2/8/4 (Item 4 from file: 144)
DIALOG(R)File 144:(c) 1996 INIST/CNRS. All rts. reserv.

11283998 PASCAL No.: 94-0103574
Authigenese et evolution d'argiles hydrothermales oceaniques. (Exemples des monts du centre d'expansion des Galapagos et des sediments de la Ride de Juan de Fuca)
(Authigenesis and evolution of oceanic hydrothermal clays (Case of Mounts from the Galapagos expansion center and sediments of Juan de Fuca rise))

English Descriptors: clay minerals; marine sediments; halmyrolysis; hydrothermal alteration; Southeast Pacific

French Descriptors: Argile mineral; Sediment marin; Alteration sous marine; Alteration hydrothermale; Pacifique Sud Est

Classification Codes: 226C02; 223B; 001E01P02; 001E01H

2/8/5 (Item 5 from file: 144)
DIALOG(R)File 144:(c) 1996 INIST/CNRS. All rts. reserv.

11283985 PASCAL No.: 94-0103561
La sedimentation marine des mineraux argileux
(Clay minerals marine sedimentation)

English Descriptors: review; clay minerals; marine sedimentation; diagenesis; mineralized mud; paleoclimatology; structural controls

French Descriptors: Synthese bibliographique; Argile mineral; Sedimentation marine; Diagenese; Boue mineralisee; Paleoclimat; Controle tectonique

Classification Codes: 223A01; 001E01G01

2/8/6 (Item 6 from file: 144)
DIALOG(R)File 144:(c) 1996 INIST/CNRS. All rts. reserv.

11162533 PASCAL No.: 93-0671740
Resistance au cisaillement sous faivble consolidation et structuration des ragiles marines
(Shear streength under low consolidation and structuration of marine clays)

English Descriptors: strength; clay; marine sediments; Holocene; shear; undrained soil test; consolidation; thixotropy; Quebec
Broad English Descriptors: clastic sediments; sedimentary rocks; Quaternary ; Eastern Canada; North America

French Descriptors: Resistance mecanique; Argile; Sediment marin; Holocene; Cisaillement; Essai non draine; Consolidation; Thixotropie; Quebec

Classification Codes: 226B01; 001E01O01

2/8/7 (Item 7 from file: 144)
DIALOG(R)File 144:(c) 1996 INIST/CNRS. All rts. reserv.

10900214 PASCAL No.: 93-0409578
Kystes de Dinoflagelles et palynofacies: indicateurs des variations bathymetriques dans le bassin de Guercif (Maroc) au Jurassique (Bathonien terminal-Oxfordien basal)
(Dinoflagellate cysts and palynofacies : evidence of bathymetric variations in the basin of Guercif (Morocco) during the Jurassic (late Bathonian-early Oxfordian))

English Descriptors: Morocco; Tethys; Middle Jurassic; Bajocian; Bathonian; Upper Jurassic; dinoflagellates; bathymetry; silt; sandstone; biostratigraphy; clay; marine environment; shallow-water environment; foraminifers; eustacy; depth indicators; boreholes; cores; Oxfordian; pollen diagrams; paleogeography
Broad English Descriptors: North Africa; Mesozoic; clastic sediments; sedimentary rocks; clastic rocks

French Descriptors: Maroc; Tethys; Jurassique moyen; Bajocien; Bathonien; Jurassique sup; Flore dinoflagelle; Bathymetrie; Silt; Gres; Biostratigraphie; Argile; Milieu marin; Milieu eau peu profonde; Faune foraminifere; Eustatisme; Indicateur bathymetrique; Sondage; Carotte; Oxfordien; Palynodiagramme; Paleogeographie

Classification Codes: 224A; 227A02; 001E01I; 001E01Q02

2/8/8 (Item 8 from file: 144)
DIALOG(R)File 144:(c) 1996 INIST/CNRS. All rts. reserv.

10890199 PASCAL No.: 93-0399563
Apports mineraux argileux neogenes et pleistocenes dans le bassin Indien Central
Programme dynamique et bilans de la Terre. Resultats des travaux 1988 - 1992
(Neogene and Pleistocene clay mineral fluxes in the Central Indian basin)

English Descriptors: clay minerals; marine sediments; Neogene; Pleistocene; Indian Ocean
Broad English Descriptors: Tertiary; Quaternary

French Descriptors: Argile mineral; Sediment marin; Neogene; Pleistocene; Ocean Indien

Classification Codes: 223A01; 226C02; 001E01G01; 001E01P02

2/8/9 (Item 9 from file: 144)
DIALOG(R)File 144:(c) 1996 INIST/CNRS. All rts. reserv.

10213517 PASCAL No.: 92-0419419
Utilisation des mineraux sedimentaires argileux pour la reconstitution des variations paleoclimatiques a court terme en Mer d'Arabie
(Use of sedimentary clay minerals for the reconstitution of periodic paleoclimatic variations in the Arabian Sea)

English Descriptors: Arabian Sea; clay; paleoclimatology; Neogene; Ocean Drilling Program; illite; palygorskite; sedimentation rates
Broad English Descriptors: Indian Ocean; clastic sediments; sedimentary rocks; Tertiary

French Descriptors: Mer d'Oman; Argile; Paleoclimat; Neogene; ODP; Illite; Palygorskite; Taux sedimentation; Ride Owen; ODP site 721 leg 117

Classification Codes: 224A; 001E01I

2/8/10 (Item 10 from file: 144)
DIALOG(R)File 144:(c) 1996 INIST/CNRS. All rts. reserv.

09748923 PASCAL No.: 91-0546057
Sedimentologie et palynologie du Neogene du Bassin de Boudinar. Implications paleogeographiques et paleoclimatiques (Rif Nord-Oriental, Maroc)

English Descriptors: Theses; Sections; Neogene; Conglomerate; Marl; Fluvial sedimentation; Nearshore sedimentation; Marine sedimentation; Clay minerals; Pollen analysis; Paleoclimatology; Paleogeography; Rif; Thesis; Geological section; Paleoclimate
Broad English Descriptors: Tertiary; Clastic rocks; Sedimentary rocks; Morocco; North Africa

French Descriptors: These; Coupe geologique; Neogene; Conglomerat; Marne; Sedimentation fluviatile; Sedimentation littorale; Sedimentation marine; Argile mineral; Analyse pollinique; Paleoclimat; Paleogeographie; Domaine Rifain; Fan delta; Bassin Boudinar; Stratigraphie sequentielle

Classification Codes: 224A; 227A02; 001E01I; 001E01Q02

2/8/11 (Item 11 from file: 144)
DIALOG(R)File 144:(c) 1996 INIST/CNRS. All rts. reserv.

09405230 PASCAL No.: 91-0195608
L'Argile de La Perade; nouvelle unitemarine anterieure au Wisconsinien superieur, vallee du Saint-Laurent, Quebec
(The La Perade Clay; a new marine unit older than late Wisconsinan, Saint Lawrence Valley, Quebec)

English Descriptors: Saint Lawrence Valley; Quebec; Clay; Marine sediments; Fossils; Saint Lawrence River; Upper Pleistocene; Absolute age; Paleoenvironment; Upper Wisconsinan; Cartier Sea; Sainte-Anne-de-la-Perade; Saint-Pierre-les-Becquets; La Perade Clay; Fossil; Age estimation
Broad English Descriptors: Eastern Canada; North America; Clastic sediments ; Sedimentary rocks; Quaternary; Canada; America

French Descriptors: Vallee Saint Laurent; Quebec; Argile; Sediment marin; Fossile; Saint Laurent; Pleistocene sup; Datation; Paleoenvironnement

Classification Codes: 226C02; 001E01P02

2/8/12 (Item 12 from file: 144)
DIALOG(R)File 144:(c) 1996 INIST/CNRS. All rts. reserv.

09302777 PASCAL No.: 91-0093151
Mecanismes de formation des argiles des halos noirs de basaltes oceaniques
(Formation mechanisms of clays in the oceanic basalt black halos)

English Descriptors: Pliocene; Pleistocene; Seawater; Mixture; Phyllosilicate; Chemical analysis; Galapagos Islands; Mid-ocean ridges; X ray diffraction; Tholeiitic basalt; Deep Sea Drilling Project; Clay minerals; Hydrothermal alteration; Fluid phase; Melange; Iron-rich

composition; Smectite; Glauconite; Celadonite; Sheet silicates; TEM data; Chemical composition; X-ray diffraction analysis
Broad English Descriptors: Pacific Ocean Islands; Neogene; Tertiary; Quaternary; East Pacific Ocean Islands

French Descriptors: Pliocene; Pleistocene; Eau mer; Melange; Phyllosilicate ; Analyse chimique; Galapagos; Dorsale oceanique; Diffraction RX; Leg 54; Leg 70; Site 424; Site 425; Site 510; MORB; Halos; Basalte tholeitique; DSDP; Argile mineral; Alteration hydrothermale; Phase fluide; Composition riche en fer; Smectite; Glauconite; Celadonite; Donnee MET

Classification Codes: 001E01A02; 001E01B03; 220A02; 220B03

2/8/13 (Item 13 from file: 144)
DIALOG(R)File 144:(c) 1996 INIST/CNRS. All rts. reserv.

09128085 PASCAL No.: 90-0296465
Correlations entre la masse volumique et la resistivite d'un sediment marin
(Correlation between the bulk density and the electrical resistivity of a marine clay)

English Descriptors: Marine sediments; Clay; Porosity; Resistivity; Electrical methods; Kaolinite; Sand; Laboratory studies; Electric resistivity; Electrical method; Laboratory test
Broad English Descriptors: Clastic sediments; Sedimentary rocks

French Descriptors: Sediment marin; Argile; Porosite; Resistivite electrique; Methode electrique; Kaolinite; Sable; Essai laboratoire; Teneur eau

Classification Codes: 226B01; 223B; 001E01O01

2/8/14 (Item 14 from file: 144)
DIALOG(R)File 144:(c) 1996 INIST/CNRS. All rts. reserv.

09124080 PASCAL No.: 90-0292460
Interaction des accumulations terrigenes et oceaniques dans le Quaternaire moyen et superieur des marges profondes du Gabon et de la ride medio-guineenne

English Descriptors: Theses; Marine sediments; Quaternary; Clay minerals; Foraminifers; Stable isotopes; O-18/O-16; Carbonates; Paleoclimatology; Paleo-oceanography; Southeast Atlantic; Thesis; Paleoclimate
Broad English Descriptors: South Atlantic; Atlantic Ocean

French Descriptors: These; Sediment marin; Quaternaire; Argile mineral; Faune foraminifere; Isotope stable; O 18-O 16; Carbonate; Paleoclimat; Paleooceanographie; Atlantique Sud Est; Bassin Angolais

Classification Codes: 226C02; 001E01P02

2/8/15 (Item 15 from file: 144)
DIALOG(R)File 144:(c) 1996 INIST/CNRS. All rts. reserv.

09086014 PASCAL No.: 90-0254373
Sedimentation argileuse plio-quaternaire sur la marge armoricaine (Leg 80 DSDP)

English Descriptors: Clay minerals; Marine sediments; Shelf environment; Upper Pliocene; Quaternary; Factor analysis; Paleoclimatology; North American Atlantic; Paleoclimate
Broad English Descriptors: Neogene; Tertiary; North Atlantic; Atlantic Ocean

French Descriptors: Argile mineral; Sediment marin; Milieu marge continentale; Pliocene sup; Quaternaire; Analyse factorielle; Paleoclimat ; Atlantique Nord Ouest; DSDP Site 548; DSDP Site 549; Goban Spur

Classification Codes: 223A01; 226C02; 001E01G01

2/8/16 (Item 16 from file: 144)
DIALOG(R)File 144:(c) 1996 INIST/CNRS. All rts. reserv.

08979835 PASCAL No.: 90-0147982
Repartition des mineraux argileux sur une marge a maree : exemple sud Gascogne

English Descriptors: Clay minerals; Marine sediments; Shelf environment; Bay of Biscay
Broad English Descriptors: North Atlantic; Atlantic Ocean

French Descriptors: Argile mineral; Sediment marin; Milieu marge continentale; Golfe de Gascogne

Classification Codes: 226C02

2/8/17 (Item 17 from file: 144)
DIALOG(R)File 144:(c) 1996 INIST/CNRS. All rts. reserv.

08922527 PASCAL No.: 90-0090588
Voies et mecanismes de cristallogenese des mineraux argileux, ferriferes en milieu marin: le processus de glauconitisation, evolutions minerales, structurales et geochimiques
(Ways and mechanism of crystallogenesis of ferriferous clay minerals under sea conditions, the glauconitization process: mineralogical, structural and geochemical evolution)

English Descriptors: Paleocene; Ivory Coast; Genesis; Clay minerals; Smectite; Iron-rich composition; Stability; Thermodynamic properties; Thermodynamics
Broad English Descriptors: Paleogene; Tertiary; West Africa; Africa

French Descriptors: Paleocene; Cote d'Ivoire; Genese; Argile mineral; Smectite; Composition riche en fer; Stabilite; Thermodynamique

Classification Codes: 223A04; 001E01G04

2/8/18 (Item 18 from file: 144)
DIALOG(R)File 144:(c) 1996 INIST/CNRS. All rts. reserv.

08919151 PASCAL No.: 90-0087202
Genese et evolution des argiles vertes hydrothermales oceaniques : Les "Monts" du rift des Galapagos (Pacifique equatorial)

English Descriptors: Theses; Clay; Marine environment; Hydrothermal conditions; Smectite; Glauconite; Major elements; Stable isotopes; O-18/O-16; Isotopes; Sr-87/Sr-86; North American Pacific; North Atlantic Ridge; Thesis; Hydrothermal condition
Broad English Deslrip:ors: Clastic sediments; Sedimentary rocks; Pacific Ocean; North Atlantic; Atlantic Ocean

French Descriptors: These; Argile; Milieu marin; Condition hydrothermale; Smectite; Glauconite; Analyse majeurs; Isotope stable; O 18-O 16; Isotope ; Sr 87-Sr 86; Pacifique Nord Est; Dorsale Atlantique Nord; Halo noir; TAG

Classification Codes: 223B; 220C01; 001E01H

2/8/19 (Item 19 from file: 144)
DIALOG(R)File 144:(c) 1996 INIST/CNRS. All rts. reserv.

08835369 PASCAL No.: 90-0003232
Sedimentation argileuse au Cenozoique superieur dans l'Ocean Indien nord-oriental
(Late Cenozoic clay sedimentation in the North-eastern Indian Ocean)

English Descriptors: Indian Ocean; Cores; Deep Sea Drilling Project; Marine sedimentation; Clay minerals; Spatial distribution; Early diagenesis; Climate effects; Neogene; Quaternary
Broad English Descriptors: Tertiary

French Descriptors: Ocean Indien; Carotte; DSDP; Sedimentation marine; Argile mineral; Distribution spatiale; Diagenese precoce; Action climatique; Neogene; Quaternaire; Repartition spatiale

Classification Codes: 223B; 001E01H

2/8/20 (Item 20 from file: 144)
DIALOG(R)File 144:(c) 1996 INIST/CNRS. All rts. reserv.

08648977 PASCAL No.: 89-0198197
Note sur les variations du niveau marin relatif a l'Holocene, a Riviere-Ouelle, cote sud du Saint-Laurent

(Note on relative Holocene sea level fluctuations at Riviere-Ouelle, south shore of the Saint Lawrence, Quebec)

English Descriptors: Holocene; Changes of level; Saint Lawrence River; Quebec; Clay; Sand; Silt; Riviere Ouelle; Goldthwait Sea Clay
Broad English Descriptors: Quaternary; Eastern Canada; North America; Clastic sediments; Sedimentary rocks

French Descriptors: Holocene; Variation niveau; Saint Laurent; Quebec; Argile; Sable; Silt; Argile Goldthwait Sea

Classification Codes: 226C02

2/8/21 (Item 21 from file: 144)
DIALOG(R)File 144:(c) 1996 INIST/CNRS. All rts. reserv.

08617116 PASCAL No.: 89-0166258
Etude de la sedimentation argileuse tertiaire dans le bassin belgo-franco-anglais : comparaison avec l'Ocean Atlantique nord
(A study of Tertiary argillaceous sedimentation in the Belgo-Franco-English basin. A comparison with the North Atlantic Ocean)

English Descriptors: Tertiary; Belgium; France; England; North Atlantic; Clay minerals; Marine environment; Paleoenvironment; Paleoclimatology; Paleoclimate
Broad English Descriptors: Europe; United Kingdom; Atlantic Ocean; Great britain

French Descriptors: Tertiaire; Belgique; France; Angleterre; Ocean Atlantique Nord; Argile mineral; Milieu marin; Paleoenvironnement; Paleoclimat

Classification Codes: 223A01; 001E01G01

2/8/22 (Item 22 from file: 144)
DIALOG(R)File 144:(c) 1996 INIST/CNRS. All rts. reserv.

08614507 PASCAL No.: 89-0163608
Diagenese d'enfouissement et diagenese thermique. Effets sur les silicates argileux
(Effects of burial and thermal diagenesis on clay silicates)

English Descriptors: Senegal Basin; Senegal; Tyrrhenian Sea; Clay minerals; Mixed-layer minerals; Diagenesis; Heat flow; Geothermal flow
Broad English Descriptors: West Africa; West Mediterranean; Mediterranean Sea; Africa

French Descriptors: Bassin Senegal; Senegal; Mer Tyrrhenienne; Argile mineral; Mineral interstratifie; Diagenese; Flux geothermique; ODP; Site 652; Forage Kafountine; Diagenese enfouissement; N125534N125534W0164347W0164347; N402130N402130E0120859E0120859

Classification Codes: 223A01; 001E01G01

2/8/23 (Item 23 from file: 144)
DIALOG(R)File 144:(c) 1996 INIST/CNRS. All rts. reserv.

08611036 PASCAL No.: 89-0160137
Les apports du diapirisme argileux dans la sedimentation d'un prisme d'accretion: la Ride de la Barbade, au sud-est des Petites Antilles
(Diapiric mud in the growth of an accretionary complex: the southern Barbados ridge, Lesser Antilles arc)

English Descriptors: Barbados Ridge; Guyanese Atlantic; Quaternary; Marine sediments; Clay minerals; Diapirs; Diapir
Broad English Descriptors: North Atlantic; Atlantic Ocean

French Descriptors: Dorsale Barbade; Atlantique Guyanes; Quaternaire; Sediment marin; Argile mineral; Diapir; Campagne Caracolante; Sediment superficiel; Diapir boue; Argilocinese; Prisme accretion

Classification Codes: 223B; 001E01H

2/8/24 (Item 24 from file: 144)
DIALOG(R)File 144:(c) 1996 INIST/CNRS. All rts. reserv.

08606025 PASCAL No.: 89-0155113
Les argiles et les composes silico-ferriques des sediments metalliferes de la fosse Atlantis II (Mer Rouge)
(Clays and Silico-ferric compounds of metalliferous sediments from Atlantes II Deep (Red Sea))

English Descriptors: Red Sea; Clay; Potential deposits; New minerals; Smectite; Ferruginous composition; Isotopes; Mossbauer spectroscopy; X-ray diffraction analysis; Mineral deposits, genesis; Zoning; New mineral; Moessbauer spectrometry; X ray diffraction
Broad English Descriptors: Indian Ocean; Clastic sediments; Sedimentary rocks

French Descriptors: Mer Rouge; Argile; Gisement potentiel; Mineral nouveau; Smectite; Composition ferrugineuse; Isotope; Spectrometrie Moessbauer; Diffraction RX; Génese gite; Zonalite; Fosse Atlantis II; Ferripyrophyllite; Hisingente; Ferrihydrite; Feroxyhyte

Classification Codes: 221A02; 223B; 001E01E02

2/8/25 (Item 25 from file: 144)
DIALOG(R)File 144:(c) 1996 INIST/CNRS. All rts. reserv.

08442858 PASCAL No.: 88-0443747
Influences continentales et marines dans les sediments cenozoiques de 'Ocean Indien nord oriental
(Continental and marine influences in Cenozoic sediments from the Northeastern Indian Ocean)

English Descriptors: Indian Ocean; Tertiary; Quaternary; Clay minerals; Provenance; Marine transport; Terrigenous materials; Structural controls; Climate effects; Early diagenesis; Origin

French Descriptors: Ocean Indien; Tertiaire; Quaternaire; Argile mineral; Origine; Transport marin; Matiere terrigene; Controle tectonique; Action climatique; Diagenese precoce; Argile lattee

Classification Codes: 223B; 220C02; 001E01H

2/8/26 (Item 26 from file: 144)
DIALOG(R)File 144:(c) 1996 INIST/CNRS. All rts. reserv.

08390997 PASCAL No.: 88-0391751
Enseignements generaux de l'extreme constance de la sequence argile-halite du Carnien de bassins distants et isoles d'Europe du Nord-Ouest

English Descriptors: Carnian; Jura Mountains; Saone-Rhone Basin; Lorraine; Paris Basin; North Sea; Clay; Halite; Salt; Arid environment; Humid environment; Stratigraphic wedges
Broad English Descriptors: Upper Triassic; Mesozoic; Europe; France; North Atlantic; Atlantic Ocean; Clastic sediments; Sedimentary rocks

French Descriptors: Carnien; Jura Chaine; Bassin Saone et Rhone; Lorraine; Bassin Parisien; Mer du Nord; Argile; Halite; Sel; Milieu aride; Milieu humide; Biseau

Classification Codes: 224A

2/8/27 (Item 27 from file: 144)
DIALOG(R)File 144:(c) 1996 INIST/CNRS. All rts. reserv.

08288889 PASCAL No.: 88-0289439
Teneurs en metaux lourds des sediments fins de la baie de Fort-de-France, Martinique, Petites Antilles francaises
(Heavy metal concentrations in fine-grained sediments of the bay of Fort-de-France, Martinique, French Lesser Antilles)

English Descriptors: Martinique; Marine sediments; Clay minerals; Major elements; Heavy metals; Enrichment; Pollution; Environmental geology; Heavy metal
Broad English Descriptors: West Indies; Central America; America

French Descriptors: Martinique; Sediment marin; Argile mineral; Analyse majeurs; Metal lourd; Enrichissement; Pollution; Geologie environnement; Baie Fort de France

Classification Codes: 226B; 220B03; 001E01O

2/8/28 (Item 28 from file: 144)
DIALOG(R)File 144:(c) 1996 INIST/CNRS. All rts. reserv.

08041753 PASCAL No.: 88-0043607
Mineraux argileux lattes : les smectites du domaine atlantique
(Lathed-shape clay minerals: smectites of the Atlantic area)

English Descriptors: Smectite; Clay minerals; Marine environment; Upper Jurassic; Cretaceous; Tertiary; Quaternary; Early diagenesis; TEM data; Atlantic Ocean
Broad English Descriptors: Mesozoic

French Descriptors: Smectite; Argile mineral; Milieu marin; Jurassique sup; Cretace; Tertiaire; Quaternaire; Diagenese precoce; Donnee MET; Ocean Atlantique

Classification Codes: 223B; 001E01H

2/8/29 (Item 29 from file: 144)
DIALOG(R)File 144:(c) 1996 INIST/CNRS. All rts. reserv.

07904639 PASCAL No.: 87-0384425
Echanges entre particules et fluide interstitiel. Information apportee par l'etude des argiles lattees

English Descriptors: Pore water; Diagenesis; Ion exchange; Clay; Permeability; Marine sedimentation; Europe; America; Atlantic Ocean
Broad English Descriptors: Clastic sediments; Sedimentary rocks

French Descriptors: Eau interstitielle; Diagenese; Echange ion; Argile; Permeabilite; Sedimentation marine; Europe; Amerique; Ocean Atlantique; Argile lattee

Classification Codes: 223A01

2/8/30 (Item 30 from file: 144)
DIALOG(R)File 144:(c) 1996 INIST/CNRS. All rts. reserv.

07904194 PASCAL No.: 87-0383980
Transport particulaire actuel du fleuve Congo et de quelques affluents; enregistrement quaternaire dans l'eventail detritique profond (Sedimentologie, mineralogie et geochimie)

English Descriptors: Theses; Stream transport; Suspended materials; Organic materials; Clay minerals; Marine sediments; Submarine fans; West Africa; Congo Basin; Southeast Atlantic; Thesis; Organic matter
Broad English Descriptors: South Atlantic; Atlantic Ocean; Africa

French Descriptors: These; Transport fluviatile; Matiere en suspension; Matiere organique; Argile mineral; Sediment marin; Cone sous marin; Afrique Ouest; Bassin Congo; Atlantique Sud Est

Classification Codes: 226C01; 001E01Q01

2/8/31 (Item 31 from file: 144)
DIALOG(R)File 144:(c) 1996 INIST/CNRS. All rts. reserv.

07556348 PASCAL No.: 87-0393600
Les sediments metalliferes oceaniques actuels et anciens: Caracterisation, comparaisons

English Descriptors: Theses; Mineralized mud; Marine sediments; Clay; Coarse-grained materials; Fine-grained materials; Cores; Mud; X-ray data; East Pacific Rise; Southeast Pacific; Red Sea; Cyprus; Troodos Massif; Uniformitarianism; Hydrothermal processes; Halmyrolysis; Diagenesis; Major elements; Thesis; Microfauna; Ooze
Broad English Descriptors: Clastic sediments; Sedimentary rocks; Pacific Ocean; Indian Ocean; Middle East; Asia

French Descriptors: These; Boue mineralisee; Sediment marin; Argile; Fraction grossiere; Fraction fine; Carotte; Vase; Donnee RX; Dorsale Pacifique Est; Pacifique Sud Est; Mer Rouge; Chypre; Massif Troodos; Actualisme; Gite hydrothermal; Alteration sous marine; Diagenese; Analyse majeurs; Fosse Shaban; Terre ombre; Microfaune

Classification Codes: 223B; 226C02; 221A02; 001E01I

2/8/32 (Item 32 from file: 144)
DIALOG(R)File 144:(c) 1996 INIST/CNRS. All rts. reserv.

07437165 PASCAL No.: 87-0068074
L'enregistrement des paleocirculations et des paleoclimats dans les depots neogenes de l'Atlantique Est subtropical et equatorial: apports du Leg O.D.P. 108 (Ocean Drilling program)
(Neogene paleocirculation and paleoclimat record of O.D.P. Leg 108 (Tropical and subtropical East Atlantic))

English Descriptors: Paleo-oceanography; Neogene; Paleoclimatology; Deep-sea environment; Clay; Carbonates; Deep-sea sedimentation; Southeast Atlantic; Paleoclimate
Broad English Descriptors: Tertiary; Clastic sediments; Sedimentary rocks; South Atlantic; Atlantic Ocean

French Descriptors: Paleooceanographie; Neogene; Paleoclimat; Milieu mer profonde; Argile; Carbonate; Sedimentation mer profonde; Atlantique Sud Est; Ocean Drilling Program Leg 108; Argile rouge

Classification Codes: 224A; 001E01J

2/8/33 (Item 33 from file: 144)
DIALOG(R)File 144:(c) 1996 INIST/CNRS. All rts. reserv.

07228213 PASCAL No.: 86-0117013
Decouverte d'Oligocene marin fossilifere pres de Saint-Jean-de-Monts (Vendee)
(Discovery of fossiliferous marine Oligocene near Saint-Jean-de-Monts (Vendee))

English Descriptors: Borehole sections; Stampian; Clay; Foraminifers; Marine environment; Grabens; Vendee; Borehole cross-setio; Graben
Broad English Descriptors: Oligocene; Paleogene; Tertiary; Clastic sediments; Sedimentary rocks; Armorican Massif; France; Europe; Pays de Loire; France; Europe

French Descriptors: Coupe sondage; Stampien; Argile; Faune foraminifere; Milieu marin; Graben; Vendee; Saint Jean de Monts

Classification Codes: 224A; 001E01J

2/8/34 (Item 34 from file: 144)
DIALOG(R)File 144:(c) 1996 INIST/CNRS. All rts. reserv.

07214848 PASCAL No.: 86-0103627
Quelques relations entre certaines proprietes geotechniques pour les argiles molles de la region de Montreal (Quebec, Canada)

English Descriptors: Soil mechanics; Quebec; Soft clays; Marine sediments; Engineering properties; Shear strength
Broad English Descriptors: Eastern Canada; North America

French Descriptors: Mecanique sol; Quebec; Argile molle; Sediment marin; Propriete geotechnique; Resistance cisaillement; Region Montreal

Classification Codes: 226B

2/8/35 (Item 35 from file: 144)
DIALOG(R)File 144:(c) 1996 INIST/CNRS. All rts. reserv.

06073775 PASCAL No.: 85-0335364
Application des caracteristiques geoacoustiques d'une argile artificielle a l'etude du champ acoustique d'une antenne multi-elements
(Application of artificial clay geoacoustic parameters to the study of the acoustic field of a multi array transducer)

English Descriptors: Acoustic detection; Marine sediments; Clay; Focusing; Transducer; Acoustic antenna; Antenna array; Acoustic field; Digital simulation; Engineering geology; Target detection; Performance; Underwater acoustics; Instrumentation

French Descriptors: Detection acoustique; Sediment marin; Argile; Focalisation; Transducteur; Antenne acoustique; Antenne reseau; Champ acoustique; Simulation numerique; Geotechnique; Detection cible; Performance; Acoustique sous marine; Appareillage

Classification Codes: 001B05D

énas - Québec - La Baie

aréna qui se métamorphose / Jean-Pierre mard. – *La Revue municipale et des travaux blics*, 71, no 3, mars 1993, p. 17-18, 22-23.

tapes de la transformation de l'aréna de la Ville La Baie pour les besoins de la présentation de la ce de théâtre *La fabuleuse histoire d'un royaume* Ghislain Bouchard.

gent (Métal) *voir* **Argent**

gent (Monnaie) - Aspect psychanalytique

couple et l'argent / Juliette Loppé, Natacha tu, François Reynaert, André Burguière. -- *Le uvel Observateur*, no 1510, 14 oct. 1993, p. 13. (dos sond ill stat graph entr)

ossier: résultats d'un sondage réalisé auprès des nçais sur les désaccords relatifs aux questions gent dans le couple et la famille; reportage et té- ignages sur la gestion de l'argent dans le couple intérêt des contrats de mariage; entrevue avec I. iss-Schimmel sur l'aspect psychanalytique des mportements des couples envers l'argent; les its civils donnés aux femmes lors de la Révolution nçaise.

gent (Monnaie) - Blanchissage *voir* **Blan- chissage de l'argent**

gent (Monnaie), Attitude envers l'

re qui roule... / Pierre Bourgault. – *L'Actua-* 18, no 8, 15 mai 1993, p. 20-22. (ill biogr)

opos de Pierre Bourgault sur son rapport à l'ar-

gent (Monnaie), Attitude envers l'- Qué- bec

rgent et vous / Jean Paré. – *L'Actualité*, 18, 8, 15 mai 1993, p. 24-36. (dos sond ill stat)

ossier: les résultats d'un sondage sur les attitu- s, les opinions et les habitudes des Québécois ce à l'argent; leurs dons à des oeuvres de charité.

rgent - Minerais - Etats-Unis - Nevada - Histoire

écouverte de minerai argentifère par le Cana- ien Henry Comstock [au Nevada en 1859] / ichel Gagné. -- *Philatélie Québec*, no 170, ept. 1992, p. 42-43. (ill)

Rappel de cette découverte et de l'exploitation de mine; timbre-poste américain émis pour commé- orer cet événement.

rgent - Mines et extraction - Etats-Unis - Nevada - Histoire

écouverte de minerai argentifère par le Cana- ien Henry Comstock [au Nevada en 1859] / ichel Gagné. – *Philatélie Québec*, no 170, ept. 1992, p. 42-43. (ill)

Rappel de cette découverte et de l'exploitation de mine; timbre-poste américain émis pour commé- orer cet événement.

rgent de poche

os bons coups pour 1993 / Carole Hébert. -- *rotégez-vous*, janv. 1993, p. 33-36. (rens)

Conseils aux jeunes consommateurs pour mieux érer leur argent de poche.

rgent de voyage

eut-on partir sans elles? / Christine Baberger. -- *L'Actualité*, 18, no 4, 15 mars 1993, p. 40. rens ill)

Que faut-il apporter en voyage: argent, chèques de voyage ou cartes de crédit?

Argent électronique *voir* **Monnaie électronique**

Argent, Travail de l' *voir* **Orfèvrerie**

Argenterie - Entretien

L'argenterie argentée : [son entretien] / Louise Saint-Pierre. – *Décormag*, no 226, nov. 1993, p. 104. (ill rens)

Argentine - Constitution

Dans une Argentine où l'argent fait la loi..., M. [Carlos] Menem empoche les dividendes de la stabilité / Bernard Cassen. – *Le Monde diplomatique*, no 475, oct. 1993, p. 22. (anal ill)

Stabilité monétaire, libéralisation de l'économie et bonne performance du commerce extérieur valent au président argentin un large appui dans le pays; mais sa réélection ne peut se faire que s'il réussit à faire amender la constitution, ce qui n'est pas acquis.

Argentine - Economie

[Fiche sur l']Argentine : [histoire, géographie, population et économie]. – *Les Débrouillards*, no 123, avril 1993, p. 27. (ill)

Dans une Argentine où l'argent fait la loi..., M. [Carlos] Menem empoche les dividendes de la stabilité / Bernard Cassen. – *Le Monde diplomatique*, no 475, oct. 1993, p. 22. (anal ill)

Stabilité monétaire, libéralisation de l'économie et bonne performance du commerce extérieur valent au président argentin un large appui dans le pays; mais sa réélection ne peut se faire que s'il réussit à faire amender la constitution, ce qui n'est pas acquis.

Argentine - Elections, 1993

Dans une Argentine où l'argent fait la loi..., M. [Carlos] Menem empoche les dividendes de la stabilité / Bernard Cassen. – *Le Monde diplomatique*, no 475, oct. 1993, p. 22. (anal ill)

Stabilité monétaire, libéralisation de l'économie et bonne performance du commerce extérieur valent au président argentin un large appui dans le pays; mais sa réélection ne peut se faire que s'il réussit à faire amender la constitution, ce qui n'est pas acquis.

Argentine - Emigration et immigration - Histoire

La cavale des maudits / Eric Conan. – *L'Express*, no 2197, 19 août 1993, p. 24-33. (ill)

Récit de l'exode en Argentine de centaines de Français fuyant la justice de la Libération à la fin des années 1940.

Argentine - Géographie

[Fiche sur l']Argentine : [histoire, géographie, population et économie]. – *Les Débrouillards*, no 123, avril 1993, p. 27. (ill)

Argentine - Histoire

[Fiche sur l']Argentine : [histoire, géographie, population et économie]. – *Les Débrouillards*, no 123, avril 1993, p. 27. (ill)

Argentine - Politique économique

Dans une Argentine où l'argent fait la loi..., M. [Carlos] Menem empoche les dividendes de la stabilité / Bernard Cassen. – *Le Monde diplomatique*, no 475, oct. 1993, p. 22. (anal ill)

Stabilité monétaire, libéralisation de l'économie et bonne performance du commerce extérieur valent au président argentin un large appui dans le pays; mais sa réélection ne peut se faire que s'il réussit à faire amender la constitution, ce qui n'est pas acquis.

Argentine - Politique et gouvernement

Dans une Argentine où l'argent fait la loi..., M. [Carlos] Menem empoche les dividendes de la stabilité / Bernard Cassen. – *Le Monde diplomatique*, no 475, oct. 1993, p. 22. (anal ill)

Stabilité monétaire, libéralisation de l'économie et bonne performance du commerce extérieur valent au président argentin un large appui dans le pays; mais sa réélection ne peut se faire que s'il réussit à faire amender la constitution, ce qui n'est pas acquis.

Argentine - Politique monétaire

Dans une Argentine où l'argent fait la loi..., M. [Carlos] Menem empoche les dividendes de la stabilité / Bernard Cassen. – *Le Monde diplomatique*, no 475, oct. 1993, p. 22. (anal ill)

Stabilité monétaire, libéralisation de l'économie et bonne performance du commerce extérieur valent au président argentin un large appui dans le pays; mais sa réélection ne peut se faire que s'il réussit à faire amender la constitution, ce qui n'est pas acquis.

Argentine - Relations - OTAN

L'Argentine se rapproche de l'OTAN / Alberto Miguez. – *Revue de l'OTAN*, 41, no 3, juin 1993, p. 28-30. (anal ill)

Axes majeurs de la politique extérieure de l'Argentine; son rapprochement avec l'OTAN et l'éventualité de la mise sur pied d'un organisme de sécurité dans l'Atlantique Sud.

Argentine - Relations extérieures

L'Argentine se rapproche de l'OTAN / Alberto Miguez. – *Revue de l'OTAN*, 41, no 3, juin 1993, p. 28-30. (anal ill)

Axes majeurs de la politique extérieure de l'Argentine; son rapprochement avec l'OTAN et l'éventualité de la mise sur pied d'un organisme de sécurité dans l'Atlantique Sud.

Argentoratum (Ville ancienne) *voir* **Strasbourg (France)**

Argile - Emploi en thérapeutique

La boue qui soigne / Marie Gros. – *Santé*, no 92, oct. 1993, p. 50-54. (rens)

Les vertus médicinales de la boue; à quoi ressemble un traitement en fangothérapie; les centres européens et québécois qui offrent ce type de traitement.

La boue qui soigne / Marie Gros. – *Santé*, no 92, oct. 1993, p. 50-54. (rens)

Les vertus médicinales de la boue; à quoi ressemble un traitement en fangothérapie; les centres européens et québécois qui offrent ce type de traitement.

L'argile pour votre beauté / Hélène Chimier. – *Vie et santé*, no 1185, nov. 1992, p. 52-53. (rens)

L'utilisation de l'argile pour désintoxiquer notre système digestif et pour les soins de la peau et des cheveux.

L'argile pour votre beauté / Hélène Chimier. – *Vie et santé*, no 1185, nov. 1992, p. 52-53. (rens)

L'utilisation de l'argile pour désintoxiquer notre système digestif et pour les soins de la peau et des cheveux.

Argile dans les soins de beauté

L'argile pour votre beauté / Hélène Chimier. – *Vie et santé*, no 1185, nov. 1992, p. 52-53. (rens)

L'utilisation de l'argile pour désintoxiquer notre système digestif et pour les soins de la peau et des cheveux.

Argilothérapie *voir* **Argile - Emploi en thérapeutique**

Argoud, Antoine

La dictature de la graphologie / François Cavigliol, Gwenaëlle Aubry, Frédéric Douzet. – *Le Nouvel Observateur*, no 1494, 24 juin 1993, p. 4-11. (dos ill entr)

Dossier: enquête sur l'utilisation de la graphologie dans la sélection du personnel en France; histoire de cette discipline; entretien avec le graphologue et ancien colonel Antoine Argoud.

Arida, Zeina

[L'amour] : carte blanche à dix écrivains / André Brink, Henri Lopes, Tahar Ben Jelloun, Zeina Arida, Luisa Futoransky, J. M. G. Le Clézio. – *Le Courrier de l'Unesco*, 46, avril 1993, p. 9-24 (A suivre). (dos ill)

Essais et textes de fiction sur l'amour par six écrivains contemporains.

Aridité *voir* **Sécheresses**

Aristide, Jean-Bertrand

Haïti : le jour où "Titid" reviendra... / Vincent Hugeux. – *L'Express*, no 2198, 26 août 1993, p. 40-45. (anal ill carte)

Le point sur la situation politique en Haïti.

Argile - Emploi en thérapeutique

Argile : la santé par la terre / Ronald Mary, Florence D'Artell, André Pharon. – *Psychologies*, no 53, avril 1988, p. 66-74. (d i r)

Dossier: emploi de l'argile en thérapeutique; le masque d'argile; différents types d'argile.

Argilothérapie *voir* **Argile - Emploi en thérapeutique**

Argumentation

Le crible dialectique : approche de l'argumentation traduite en termes de système expert / Pierre Boudon. – *Protée*, 15, no 3, automne 1987, p. 21-31. (r)

Stratégies morpho-syntaxiques et argumentatives [du discours : analogie de structure] / Alain Berrendonner. – *Protée*, 15, no 3, automne 1987, p. 48-58. (r)

Aria (Film : Grande-Bretagne)

"Aria" / Patrick Schupp. – *Séquences*, no 137, nov. 1988, p. 85-86. (i)

Commentaire sur ce film constitué de dix courts métrages réalisés par Nicolas Roeg, Charles Sturridge, Jean-Luc Godard, Julien Temple, Bruce Beresford, Robert Altman, Franc Roddam, Ken Russell, Derek Jarman et Bill Bryden.

Ariane (Fusée)

Europe : le ciel ne peut pas attendre / Sylvie O'Dy, Françoise Harrois-Monin. – *L'Express*, no 1896, 13 nov. 1987, p. 35-38. (i)

Enjeux du sommet des Etats membres de l'Agence spatiale européenne, tenu à La Haye, en novembre 1987; programme relié à la trilogie Ariane 5, Hermès et Colombus.

Ariane le titan / Sylvie O'Dy. – *L'Express*, no 1940, 16 sept. 1988, p. 18.

La fusée européenne met sur orbite les satellites américains.

Ariane sur sa lancée / Jean-Claude Grenier, Cédric Philibert. – *Géo*, no 105, nov. 1987, p. 78-97. (i)

Sueurs froides sur orbite : [lancement d'un satellite de télécommunications français par la fusée Ariane] / Gérard Petitjean. – *Le Nouvel observateur*, no 1250, 21 oct. 1988, p. 46-47.

TDF 1 : la solitude des grands espaces / Patrick Bonazza. – *Le Nouvel observateur*, no 1252, 3 nov. 1988, p. 25. (i)

Manque de téléspectateurs malgré la réussite du lancement d'Ariane 2 à Kourou.

Les 30 défis d'Ariane [pour résister aux fusées concurrentes] / Albert Ducrocq. – *Sciences et avenir*, no 489, nov. 1987, p. 28-34. (i)

L'Europe sur orbite : [un pas en avant vers la construction d'une future station spatiale] / Albert Ducrocq. – *Sciences et avenir*, no 490, déc. 1987, p. 24-30. (i)

Ariane, le grand essor : [les atouts majeurs de la fusée européenne] / Albert Ducrocq. – *Sciences et avenir*, no 498, août 1988, p. 18-23. (i)

Le dernier lancement de la fusée Ariane en Guyane : tir réussi. Kourou est au septième ciel ... / Philippe Demenet, Eric Planchard. – *La Vie*, no 2240, 4 août 1988, p. 16-21. (i)

Arianespace (Firme)

Fusées en Chine : l'espace au rabais. – *L'Express*, no 1941, 23 sept. 1988, p. 22.

La Chine solde les lancements de satellites.

L'Européen de l'année, Frédéric D'Allest / Aimé Savard, Christian Troubé. – *La Vie*, no 2209, 31 déc. 1987, p. 24-27. (i)

Portrait et carrière du président du Centre national d'études spatiales et patron de la firme Arianespace.

Arias, Oscar

Oscar Arias, don Quichotte de la paix / Jean-Pierre Boris. – *L'Express*, no 1916, 1er avril 1988, p. 42-43.

Portrait du président du Costa Rica, récipiendaire du prix Nobel de la paix en 1987.

Le Nicaragua face au plan de paix [signé en août 1987 à Esquipulas] / Philippe Burin des Roziers. – *Notes et études documentaires*, no 4850, 1987, p. 129-134.

Oscar Arias, l'homme du cessez-le-feu / Aimé Savard. – *La Vie*, no 2199, 22 oct. 1987, p. 55-57.

Réalisation du président du Costa Rica pour son pays et pour la paix en Amérique centrale.

Ariel (Firme)

Ariel : regroupement et financement / François Riverin. – *Finance*, 9, no 30, 9 mai 1988, p. 10.

Sphinx poursuit sa croissance malgré le krach et les fausses rumeurs / François Riverin. – *Finance*, 9, no 44, 29 août 1988, p. 7. (i)

Aristote

La "rhétorique" d'Aristote et les études de droit / Denis Le May. – *Les Cahiers de droit*, 29, no 1, mars 1988, p. 247-263. (r)

Mimèsis et catharsis : de la représentation à la dénégation du réel chez Aristote, Artaud et Brecht / Alain Bernard Marchand. – *Philosophiques*, 15, no 1, printemps 1988, p. 107-127. (r)

Arithmétique - Problèmes et exercices

Jeux mathématiques : [exercices commentés d'arithmétique] / Denis Bresson. – *Pour la science*, no 126, avril 1988, p. 102-107. (i r)

Arizona Jojoba (Firme)

Les Canadiens : rois et maîtres du jojoba aux Etats-Unis / Pierre Boutin. – *Finance*, 9, no 4, 26 oct. 1987, p. 60.

Réussite de la firme Arizona Jojoba, inscrite à la Bourse de Vancouver.

Arizona Junior (Film : Etats-Unis)

Baby boom / Jean A. Gili, Michel Ciment, Hubert Niogret. – *Positif*, nos 317-318, juil.-août 1987, p. 60-65. (e i)

Commentaire sur le film *Arizona Junior*, de Joel Coen; entretien avec le réalisateur et avec Ethan Coen, le producteur.

Arkey (Logiciel)

Arkey : [logiciel de CAO en] architecture sur Atari ST / P. Cabon. – *Micro-Systèmes*, no 82, janv. 1988, p. 83-86. (i p)

Arletty (Actrice)

Arletty, 90 ans d'atmosphère / Gilbert Perrin. – *La Vie*, no 2225, 21 avril 1988, p. 62-64. (i r)

ARM (Microprocesseur) *voir* **Acorn Risc Machine (Microprocesseur)**

Armada (Flotte)

L'invincible Armada : tout est soumis au prince hors le vent / Jean-Marie Constant, James McCearney. – *Historama*, no 53, juil. 1988, p. 10-17. (i)

Causes de la défaite de cette flotte espagnole en 1588.

Armani, Giorgio

Cinq grands maîtres de la séduction : [les couturiers italiens Armani, Ferre, Krizia, Valentino et Versace] / Jacqueline Pinard. – *Châtelaine*, 29, no 10, oct. 1988, p. 92-101. (i)

Vie et carrière de chacun; quelques éléments de leur collection de mode.

Armée républicaine irlandaise *voir* **IRA (Groupe politique : Irlande du Nord)**

Armée rouge japonaise (Groupe politique : Japon)

Attentats : le dernier carré de l'"Armée rouge" [japonaise] / Claude Moniquet. – *L'Express*, no 1921, 6 mai 1988, p. 38-39. (i)

Portrait d'une nouvelle organisation terroriste née au Japon.

Armées - Amérique latine

Amérique latine : l'armée ne désarme pas / Christian Rudel. – *Croissance des jeunes nations*, no 300, déc. 1987, p. 19.

Les violations des droits de l'homme par l'armée perdurent dans les démocraties nouvellement installées.

Armement

Le grand bazar aux canons dans le tiers-monde / Alain Gresh. – *Le Monde diplomatique*, no 408, mars 1988, p. 9. (s)

Le marché de l'armement dans le tiers-monde et le rôle des nombreux marchands.

Le big bang technologique : [le Canada et le marché de l'armement] / Lyne Fréchet. – *Revue Commerce*, 90, no 5, mai 1988, p. 34-46. (i)

Armement - Coopération internationale

La coopération en matière d'armements classiques : mettre la charrue avant les boeufs / Mack F. Mattingly. – *Revue de l'OTAN*, 35, no 5, oct. 1987, p. 26-30. (i)

Argentine (Roman)

Zones et zonards / Philippe Curval. – *Magazine littéraire*, no 264, avril 1989, p. 144. (des livre)
Commentaire sur deux romans de science-fiction: *O-Zone* de Paul Theroux et *Argentine* de Joël Houssin.

Argentine - Descriptions et voyages - Histoire

[Emile] Daireaux au Far East [au 19e siècle] / Chantal Edel. – *Grands reportages*, no 90, avril 1989, p. 106-109. (ill)
Description de l'Argentine.

Argentine - Elections, 1989

Elections et démocratie au Salvador et en Argentine / Yvon Grenier. – *L'Analyste*, no 27, automne 1989, p. 36-40. (anal)
Analyse des résultats des élections de 1989 dans ces deux pays.

[Pour les élections de mai 1989 en] Argentine, la fibre péroniste vibre toujours / Christian Rudel. – *Croissance des jeunes nations*, no 316, mai 1989, p. 36-38. (anal carte ill)

Argentine : raz-de-marée péroniste ; Carlos Menem, fils d'immigrés syriens, succédera en décembre à Raúl Alfonsín / Jean-Louis Buchet. – *Jeune Afrique*, no 1481, 24 mai 1989, p. 14. (anal ill)
Les résultats des élections en Argentine.

Un péroniste [Carlos Menem] élu président de l'Argentine / Catherine Derivery, Denis Hautin-Guiraut. – *Le Monde*, no 2115, 11 mai 1989, p. 1-2. (biogr anal)
Analyse de la situation après l'élection d'un péroniste à la tête de l'Argentine et portrait de Carlos Menem et du mouvement justicialiste qu'il représente.

Argentine - Etat d'urgence

Argentine : le président [Raul] Alfonsin décrète l'état de siège dans tout le pays [après le pillage des commerces] / Denis Hautin-Guiraut. – *Le Monde*, no 2117, 25 mai 1989, p. 3. (nouv)

Argentine - Forces armées

Le tangage argentin / Jacques Girardon. – *L'Express*, no 1953, 15 déc. 1988, p. 22-24. (ill)
Regard sur la mutinerie dans les forces armées en Argentine.

Le goûter des généraux [argentins] / Jacques Girardon. – *L'Express*, no 1956, 6 janv. 1989, p. 16. (anal ill)
Raul Alfonsin fait des cadeaux à l'armée qui risque de menacer à nouveau la démocratie.

Argentine - Politique et gouvernement

Turbulences politiques en Argentine : l'épiscopat garde une attitude prudente / Juan Navarro Floria. – *L'Actualité religieuse dans le monde*, no 65, 15 mars 1989, p. 15-16. (ill nouv)

L'épiscopat argentin pense retrouver son influence. – *L'Actualité religieuse dans le monde*, no 68, 15 juin 1989, p. 6-7. (nouv)
Suite à la victoire des péronistes aux élections de mai 1989.

Elections et démocratie au Salvador et en Argentine / Yvon Grenier. – *L'Analyste*, no 27, automne 1989, p. 36-40. (anal)
Analyse des résultats des élections de 1989 dans ces deux pays.

[Pour les élections de mai 1989 en] Argentine, la fibre péroniste vibre toujours / Christian Rudel. – *Croissance des jeunes nations*, no 316, mai 1989, p. 36-38. (anal carte ill)

Argentine : vers le retour du péronisme? / Victor Sukup. – *Etudes*, t. 370, févr. 1989, p. 149-162. (anal bibl)

Le goûter des généraux [argentins] / Jacques Girardon. – *L'Express*, no 1956, 6 janv. 1989, p. 16. (anal ill)
Raul Alfonsin fait des cadeaux à l'armée qui risque de menacer à nouveau la démocratie.

Argentine : le scrutin de la débâcle / Jacques Girardon. – *L'Express*, no 1975, 19 mai 1989, p. 22-24. (anal ill)
Regard sur la situation politique et popularité du candidat Carlos Saul Menem aux élections présidentielles.

[Nouveau président argentin, Carlos Saul] Menem : une histoire d'amour / Jacques Girardon. – *L'Express*, no 1992, 15 sept. 1989, p. 54-55. (ill anal)

Argentine : raz-de-marée péroniste ; Carlos Menem, fils d'immigrés syriens, succédera en décembre à Raúl Alfonsín / Jean-Louis Buchet. – *Jeune Afrique*, no 1481, 24 mai 1989, p. 14. (anal ill)
Les résultats des élections en Argentine.

[Terrorisme, malaise de l'armée, marasme économique] : le président [Raul] Alfonsin est mobilisé sur tous les fronts / Charles Vanhecke, Catherine Derivery. – *Le Monde*, no 2100, 26 janv. 1989, p. 5. (nouv des)

M. [Raul] Alfonsin jette l'éponge. – *Le Monde*, no 2119, 8 juin 1989, p. 1. (nouv)
L'Argentine n'a plus de président: Raul Alfonsin démissionne avant l'entrée en fonction de son successeur Carlos Saul Menem.

Passation des pouvoirs en Argentine : Carlos Menem, l'"esperanza" du désespoir / Eduardo Febbro. – *Le Monde*, no 2123, 6 juil. 1989, p. 3. (anal ill)
Les raisons pour lesquelles les Argentins ont choisi Carlos Menem comme président.

Tant d'espoirs déçus en Argentine / Carlos Gabetta. – *Le Monde diplomatique*, no 422, mai 1989, p. 23. (anal ill)
Crise économique, recul de Raul Alfonsin devant les militaires et affrontement entre péronistes et radicaux lors de l'élection présidentielle.

Un macho au volant : [Carlos Menem, président de l'Argentine] / Pierre Blanchet. – *Le Nouvel Observateur*, no 1280, 18 mai 1989, p. 36-37. (ill)

Argentine - Relations extérieures - Grande-Bretagne

Malouines, l'archipel blessé / Jan Krauze. – *Géo*, no 115, sept. 1988, p. 146-159. (carte ill entr)
Description; entretiens avec les ambassadeurs d'Argentine et de Grande-Bretagne en France concernant les positions de leurs gouvernements dans la question de la souveraineté sur ce territoire.

Argentine - Relations extérieures - Mali

Moussa Traoré, [président de l'Organisation de l'unité africaine] en Amérique latine / Zyad Limam. – *Jeune Afrique*, no 1470, 8 mars 1989, p. 32-34. (ill)
Commentaire sur la tournée du président malien en Argentine et à Cuba.

Argile

La beauté et l'argile : soins du visage / Isabelle Gremeaux. – *Vie et santé*, no 1147, mai 1989, p. 25. (rens)

Argile - Emploi en thérapeutique

L'argile, une alliée / Andrée Charles. – *Vie et santé*, no 1139, sept. 1988, p. 30-34. (anal ill)
Les vertus thérapeutiques de l'argile.

L'argile pour [traiter] les animaux / Andrée Charles. – *Vie et santé*, no 1150, sept. 1989, p. 48.

Argilothérapie *voir* **Argile - Emploi en thérapeutique**

Arhasino, Alberto

Jeux de miroirs / Frédéric Vitoux. – *Le Nouvel Observateur*, no 1261, 5 janv. 1989, p. 73. (livre)
Commentaire sur deux romans d'Albert Arbasino *Les petites vacances* et *Miroir, gentil miroir*.

Ariane (Fusée)

L'Europe sur orbite : un contrat de 2 milliards de francs pour Ariane / Jean-François Augereau. – *Le Monde*, no 2112, 20 avril 1989, p. 12. (nouv)
Succès actuel des Européens dans le domaine spatial; regard sur les difficultés des premières années.

Arias Calderon, Ricardo

Panama : l'agonie d'une dictature / Michel Peyrard. – *Paris-Match*, no 2087, 25 mai 1989, p. 28-35. (ill)
Un climat de violence sans précédent règne dans la capitale depuis que le général Manuel Antonio Noriega, battu aux élections par l'opposition, a décidé de s'accrocher au pouvoir.

Aridité *voir* **Sécheresses**

Ariel (Film : Finlande)

Plein sud / Jean A. Gili. – *Positif*, no 344, oct. 1989, p. 72-73. (ill critiq)
Commentaire sur le film *Ariel* d'Aki Kaurismäki.

Ariel Capital Management (Firme)

Les black yuppies de Chicago / Dominique Nora. – *Le Nouvel Observateur*, no 1283, 8 juin 1989, p. 18-19. (ill)
Le succès de quelques gens d'affaires noirs.

Aristegui, Pedro Manuel de

Beyrouth : l'ambassadeur pour cible / Pour Damas, il fallait que la mission française soit un échec : "Liban, chasse gardée" / Patrick Forestier. – *Paris-Match*, no 2083, 27 avril 1989, p. 54-59. (ill)
Les circonstances de la mort de Pedro Manuel de Aristegui, ambassadeur d'Espagne au Liban, victime des bombardements syriens.

Aresponsabilité *voir* **Responsabilité**

Argent (Monnaie) - Aspect religieux - Christianisme

L'argent sale / Bernard Vaudour-Faguet. -- *Economie et humanisme*, no 310, nov.-déc. 1989, p. 70-72.
Parallèle entre le discours de l'Eglise du Moyen Age sur l'argent et le discourss actuel des socialistes français sur le profit.

Argent (Monnaie) - Aspect social - France

L'argent diabolique / Anthony Rowley. -- *L'Histoire*, no 132, avril 1990, p. 76. (ill opin)
Le rapport des Français avec l'argent.

Argent (Monnaie) - Blanchissage *voir* **Blanchissage de l'argent**

Argent de poche

Les jeunes et l'argent / Gilles Massé. -- *A+, le magazine affaires +*, 13, no 5, juin 1990, p. 12-23. (anal graph entr)
L'éducation économique des enfants et des adolescents.

"J'ai mon compte en banque" / Françoise Genest. -- *Châtelaine*, 31, no 11, nov. 1990, p. 174. (des rens)
L'enfant et l'épargne.

Comment se procure-t-on de l'argent de poche? / Francine Gagnon. -- *Vidéo-presse*, 19, no 9, mai 1990, p. 8-11. (ill opin)
Opinion de jeunes sur ce sujet.

Argent électronique *voir* **Monnaie électronique**

Argent et enfant *voir* **Enfants et argent**

Argent et les lettres : histoire du capitalisme d'édition, 1880-1920 (Livre)

Comptes rendus / Béatrice Craig, Reed G. Geiger. -- *Histoire sociale*, 23, no 45, mai 1990, p. 195-199. (livre)
Critique de *Family, Class and Ideology in Early Industrial France : Social Policy and the Working-Class Family, 1825-1848* de K. A. Lynch; *Women, Work and the French State : Labour Protection and Social Patriarchy, 1879-1919* de M. L. Stewart; *L'argent et les lettres : histoire du capitalisme d'édition, 1880-1920* de J.-Y. Mollier.

Argent fou (Livre)

Pour une morale de l'argent / Christian Rioux. -- *L'Actualité*, 15, no 6, 15 avril 1990, p. 52-53. (entr ill)
Entretien avec Alain Minc au sujet de son livre *L'argent fou*, sur le capitalisme et les changements politiques mondiaux.

Les nouveaux réseaux de la gauche [en France] / Sylvie Pierre-Brossolette, Sabine Delanglade, Alain Minc. -- *L'Express*, no 2009, 12 janv. 1990, p. 26-36. (ill graph livre dos)
Dossier: Lien entre les grands leaders socialistes et les managers d'entreprise; liens entre le président Mitterrand et le chef d'entreprise Pierre Bergé; entrevue avec Thierry Pfister; extrait du livre *L'argent fou* d'Alain Minc.

De la Révolution à la catastrophe / François Ewald. -- *Magazine littéraire*, no 277, mai 1990, p. 96-97. (des livre)
Analyse de quatre ouvrages: *Lignes d'horizon* de J. Attali; *Manifeste pour une fin de siècle obscure* de M. Gallo; *Le génie de la liberté* de J. Julliard; *L'argent fou* d'A. Minc.

Un cri d'alarme / Jacques Decornoy. -- *Le Monde diplomatique*, no 431, févr. 1990, p. 23. (livre)
Compte rendu de *L'argent fou* d'Alain Minc.

A Monsieur le directeur des R. G. [Renseignements généraux] / Jacques Julliard. -- *Le Nouvel Observateur*, no 1326, 5 avril 1990, p. 80. (livre ill)
Commentaire sur le livre d'Alain Minc, *L'argent fou*.

Argentine - Conditions économiques

Sauve qui peut l'Argentine / Sophie Durocher. -- *L'Actualité*, 15, no 17, 1er nov. 1990, p. 60-63. (anal ill)
La situation de ce pays, un an après la prise du pouvoir par C. Menem.

Argentine - Desriptions et voyages

Buenos Aires : quai des brumes / Jacques Tiano. -- *Grands reportages*, no 101, avril 1990, p. 40-43. (ill rens)
Description de cette ville.

Argentine - Economie

La veillée d'armes des carapintadas / Jacques Girardon. -- *L'Express*, no 2016, 2 mars 1990, p. 24-27. (anal ill)
La crise économique en Argentine; la menace d'un coup d'Etat militaire.

Argentine - Histoire

L'Argentine. -- *Missi*, no 520, avril 1990, p. 112-138. (dos carte ill)
Dossier sur l'évolution socio-politique de ce pays et l'action menée par l'Eglise catholique.

Argentine - Histoire - Comptes rendus de livres

[Domingo Faustino] Sarmiento, le "Michelet argentin" / Pierre Lepape. -- *Le Monde*, no 2181, 16 août 1990, p. 12. (livre)
Compte rendu du livre de D. F. Sarmiento, *Facundo*.

Argentine - Politique économique

L'Argentine se décompose / Alexandre Valente. -- *Le Monde diplomatique*, no 433, avril 1990, p. 9. (anal bibl des)
Bilan des tentatives du nouveau président argentin Carlos Menem pour sortir son pays de la crise économique.

Argentine - Politique et gouvernement

Sauve qui peut l'Argentine / Sophie Durocher. -- *L'Actualité*, 15, no 17, 1er nov. 1990, p. 60-63. (anal ill)
La situation de ce pays, un an après la prise du pouvoir par C. Menem.

L'Argentine au bord de la dictature? / Sophie Durocher. -- *L'Actualité*, 15, no 18, 15 nov. 1990, p. 66. (anal)
Les ambitions politiques du général Antonio Bussi.

La veillée d'armes des carapintadas / Jacques Girardon. -- *L'Express*, no 2016, 2 mars 1990, p. 24-27. (anal ill)
La crise économique en Argentine; la menace d'un coup d'Etat militaire.

L'Argentine. -- *Missi*, no 520, avril 1990, p. 112-138. (dos carte ill)
Dossier sur l'évolution socio-politique de ce pays et l'action menée par l'Eglise catholique.

Buenos Aires : les mariés de l'enfer / Chantal de Rudder. -- *Le Nouvel Observateur*, no 1344, 9 août 1990, p. 16-20. (anal biogr ill)
Les problèmes économiques et politiques en Argentine; portrait du président et de sa femme.

Argentine - Relations extérieures - Grande-Bretagne

Histoire secrète de la guerre des Malouines, [1982] / Bruno de Cessole. -- *Historama*, no 75, mai 1990, p. 88-94. (ill)

Argile

Les argiles en chimie organique [pour accélérer les réactions] / Pierre Laszio. -- *La Recherche*, no 219, mars 1990, p. 314-323. (bibl graph ill)

Argile - Emploi en thérapeutique

[La firme] Argiletz : les pionniers de l'argile : [et] l'argile, à quoi ça sert? / Marlyse Bleeckx. -- *Vie et santé*, no 1152, nov. 1989, p. 38-40.

Argiletz (Firme)

[La firme] Argiletz : les pionniers de l'argile : [et] l'argile, à quoi ça sert? / Marlyse Bleeckx. -- *Vie et santé*, no 1152, nov. 1989, p. 38-40.

Argilothérapie *voir* **Argile - Emploi en thérapeutique**

Argos (Système de localisation et de collecte de données)

Dans le sillage des oiseaux / Natalie Levisalles. -- *Sciences et avenir*, no 519, mai 1990, p. 44-49. (ill)
Grâce aux satellites et à des balises miniatures, on peut suivre les oiseaux dans leurs lointains voyages.

Argot - Etude et enseignement - France

La Sorbonne se met à l'argot / Sylvie Halpern. -- *L'Actualité*, 15, no 19, 1er déc. 1990, p. 105-106.
Présentation d'un centre d'étude de l'argot à la Sorbonne, en France.

Argovie (Suisse) - Economie

Au coeur de la Suisse, l'Argovie. -- *Paris-Match*, no 2132, 5 avril 1990, encart, p. i-xvi. (ill profil pub)
Public-reportage: regard sur l'économie de ce canton et présentation de quelques industries.

Arguin, Maurice

Occasion manquée / Jean-François Chassay. -- *Spirale*, no 98, été 1990, p. 16. (livre)
Critique du livre *Le roman québécois de 1944 à 1965* de Maurice Arguin.

Ariane (Fusée)

Révélations sur 3 accidents [de la fusée] Ariane / Jean-Michel Caradec'h, Gilbert Charles. -- *L'Express*, no 2026, 11 mai 1990, p. 10-13. (anal ill)

L'Europe à la conquête de l'espace / Jean-Claude Grenier. -- *Géo*, no 139, sept. 1990, p. 128-156. (anal ill)
Les succès du programme spatial européen; le projet de la station orbitale Columbus; les réussites de l'industrie aérospatiale européenne.

L'odyssée [de la fusée] Ariane / Jean-François Augereau. -- *Le Monde*, no 2147, 21 déc. 1989, p. 14. (des ill)
Rappel historique du lancement de la fusée Ariane; le programme spatial français.

Argentine - Politique économique

La résurrection de l'Argentine / Pierre Lacerte. — *Magazine affaires plus*, 16, no 8, oct. 1993, p. 18-23. (dos ill entr)

Principaux éléments de la politique économique de l'Argentine de 1989, qui amena une réforme majeure de l'économie; bilan de cette politique; entrevue avec le ministre de l'économie, Domingo Cavallo.

Les miracles du "sorcier" argentin / Patrick Bonazza. — *Le Point*, no 1125, 9 avril 1994, p. 70-75. (biogr dos ill)

Portrait du ministre argentin de l'Economie, Domingo Cavallo; les méthodes qu'il utilise pour redresser l'économie de son pays.

Argentine - Politique et gouvernement

Le mystère Carlos Menem / Christophe Guibéléguiet. — *Croissance : le monde en développement*, no 370, avril 1994, p. 18-21. (ill)

Parcours et stratégie politiques du chef d'Etat argentin; la situation économique difficile qui prévaut dans ce pays.

Argento, Dario

IIe Festival international du cinéma fantastique, [Montréal, 1993] / Martin Girard, Johanne Larue, Elie Castiel. — *Séquences*, no 167, nov.-déc. 1993, p. 8-10. (ill entr critiq)

Critique de quelques films présentés lors de ce festival; entrevue avec le cinéaste italien Dario Argento sur sa carrière et ses films.

Argentoratum (Ville ancienne) *voir* **Strasbourg (France)**

Argile - Emploi en thérapeutique

Le pansement à l'argile / Auffret. — *La Revue de l'infirmière*, no 13, sept. 1994, p. 10-12. (ill rens)

Les différentes argiles; leur composition; leurs propriétés thérapeutiques; indications et préparation d'un pansement.

Argilothérapie *voir* **Argile - Emploi en thérapeutique**

Argot

Les Français parlent comme ça... / Jean-Marie Bretagne. — *Ça m'intéresse*, no 155, janv. 1994, p. 64-67. (ill bibl)

Comment évolue le vocabulaire; le développement de l'argot; le langage "politiquement correct".

Argoud, Antoine

Quand [Pierre] Messmer fait enlever le colonel [Antoine] Argoud, [l'un des chefs de l'Organisation Armée secrète, en 1963] / Rémi Kauffer. — *Historia*, no 569, mai 1994, p. 52-58. (ill)

Rappel des faits et explications sur cette affaire d'Etat qui consacra la défaite des derniers activistes se réclamant de l'Algérie française.

Ariane (Fusée)

Bon anniversaire, Ariane / Jean Lopez. — *Science & vie junior*, no 54, déc. 1993, p. 60-61. (ill carte)

Evolution de la fusée Ariane depuis 1979; son profil de vol; la participation des pays européens à sa construction.

Les stars de la conquête spatiale / Jean Lopez. — *Science & vie junior*, no 62, sept. 1994, p. 82-91. (ill carte dos graph)

Dossier: le rôle de la fusée dans la mise en orbite d'un satellite; les composantes d'une fusée; carte des sites de lancement spatial; les différents lanceurs et leurs caractéristiques; le principe du moteur-fusée; la chronologie d'un lancement d'Ariane.

Aridité *voir* **Sécheresses**.

Aris, Michael

[L'amour sous les balles, 2e partie] : les deux passions de Suu Kyi / Jean-Paul Mari. — *Le Nouvel Observateur*, no 1550, 21 juill. 1994, p. 28. (biogr ill)

Le parcours de la dissidente birmane; sa vie avec son mari, Michael Aris.

Aristide, Jean-Bertrand

Les conditions d'un retour / Yves Hardy. — *Croissance : le monde en développement*, no 364, oct. 1993, p. 10-11. (ill entr)

Entretien avec le président haïtien Jean-Bertrand Aristide.

Aristide l'indésirable / Christian Rudel. — *Croissance : le monde en développement*, no 366, déc. 1993, p. 19. (anal ill)

L'appui de la CIA et du Vatican aux opposants au retour du président Aristide; interrogation sur l'impact du blocus naval décrété par le président américain.

Good morning Haiti! / Christian Hoche, Jean Lesieur, Philippe Coste, Vincent Hugeux. — *L'Express international*, no 2255, 29 sept. 1994, p. 26-29. (ill chron)

Regard sur la politique extérieure des États-Unis envers Haïti sous Bill Clinton; le débarquement pacifique des Marines à Haïti.

Titid II : prophète sous influence / Vincent Hugeux. — *L'Express international*, no 2259, 27 oct. 1994, p. 33-35. (ill biogr)

Portrait politique de Jean-Bertrand Aristide à son retour de trois années d'exil; son nouveau message de réconciliation; brève biographie.

"Titid" et les vengeurs / Chantal de Rudder. — *Le Nouvel Observateur*, no 1563, 20 oct. 1994, p. 32-33. (ill)

La situation politique tendue aux lendemains du retour du président Aristide en Haïti.

Arithmétique

Pythagore / Jean Lopez. — *Science & vie junior*, no 54, déc. 1993, p.-78-81. (ill graph)

Rappel des travaux du mathématicien Pythagore; l'école pythagorienne.

Arles (France) - Descriptions et voyages - Récits - Histoire

Les merveilles du royaume d'Arles / Annie Duchesne. — *L'Histoire*, no 169, sept. 1993, p. 86-93. (ill carte bibl anal)

Histoire et description de ce royaume à partir du *Livre des merveilles : divertissement pour un empereur* écrit par Gervais de Tilbury au début du 13e siècle.

Arles (France) - Histoire

Les merveilles du royaume d'Arles / Annie Duchesne. — *L'Histoire*, no 169, sept. 1993, p. 86-93. (ill carte bibl anal)

Histoire et description de ce royaume à partir du *Livre des merveilles : divertissement pour un empereur* écrit par Gervais de Tilbury au début du 13e siècle.

Arman (Sculpteur)

Arman / Virginie Merlin. — *Paris-Match*, no 2338, 17 mars 1994, p. 32-35. (entr biogr ill)

Entretien avec ce sculpteur français, naturalisé américain, sur sa vie et sa carrière.

Armani, Giorgio

Parfum de femme / Ginette Haché. — *Elle Québec*, no 50, oct. 1993, p. 84-85. (ill)

Le lancement du parfum Giò du couturier Giorgio Armani; la carrière de ce dessinateur de mode italien.

Armateurs - Taïwan - Biographies

Comment Evergreen a coulé l'Occident / Bruno Birolli. — *Le Nouvel Observateur*, no 1526, 3 févr. 1994, p. 20-21. (biogr ill graph stat)

Parcours de l'armateur taïwanais, Chang Yung-fa, propriétaire de la compagnie de transport maritime Evergreen.

Armée américaine *voir* **Etats-Unis - Forces armées**

Armée canadienne *voir* **Canada. Forces armées**

Armée de l'air française *voir* **France - Armée de l'air**

Armée et population *voir* **Forces armées et population**

Armée française *voir* **France - Forces armées**

Armée islamique du salut (Algérie)

Algérie : le jeu secret de la France / Yves Cuau, Xavier Raufer, André Pautard, Vincent Hugeux. — *L'Express international*, no 2249, 18 août 1994, p. 4-14. (dos anal ill entr)

Dossier: attitude de la France à l'égard du problème algérien et face aux menaces de terrorisme en sol français proférées par l'Armée islamique du salut; rôle de Charles Pasqua dans la politique algérienne de la France; inquiétudes au Maghreb; tolérance des autorités britanniques envers le Parti de libération islamique présent à Londres; forces et faiblesses du FIS selon Olivier Roy.

Enquête sur le FIS / Farid Aïchoune, René Backmann. — *Le Nouvel Observateur*, no 1553, 11 août 1994, p. 22-25. (anal ill graph)

Attentats contre les étrangers en Algérie; les différentes factions issues du Front islamique du salut; la montée du Groupe islamique armé; attitude de la France à l'égard du problème algérien.

Armée républicaine irlandaise *voir* **IRA (Groupe politique : Irlande du Nord)**

Armée zapatiste de libération nationale (Mexique)

Pourquoi les Indiens [du Mexique] n'en peuvent plus / Christian Rudel. — *Croissance : le monde en développement*, no 368, févr. 1994, p. 12-15. (ill anal)

Les raisons qui ont poussé les rebelles zapatistes à l'insurrection.

Ce que Zedillo doit changer / Corine Chabaud. — *Croissance : le monde en développement*, no 374, sept. 1994, p. 16-20. (anal carte ill)

Commentaires de quelques Mexicains sur la victoire du candidat du Parti révolutionnaire institutionnel aux élections présidentielles de 1994; la révolte des Zapatistes comme réaction au danger d'exclusion associé aux accords de libre-échange nord-américain.

Les enfants perdus de Zapata / Vincent Hugeux. — *L'Express international*, no 2219, 20 janv. 1994, p. 18-21. (ill carte)

L'insurrection des Indiens du Chiapas, au Mexique, sous la bannière de l'Armée zapatiste de libération nationale; les conditions économiques dans la région.

La révolte des enfants de Zapata / François Reynaert. — *Le Nouvel Observateur*, no 1523, 13 janv. 1994, p. 39. (ill)

Les causes de la révolte des Amérindiens du Chiapas, au Mexique.

Le "réformisme armé" du major Mario / René Backmann. — *Le Nouvel Observateur*, no 1525, 27 janv. 1994, p. 34-36. (ill)

Reportage sur l'Armée zapatiste de libération nationale et sur son chef, "major Mario"; les conditions économiques et les revendications des Amérindiens du Chiapas.

Chiapas : lumière sur des massacres / René Backmann. — *Le Nouvel Observateur*, no 1527, 10 févr. 1994, p. 39. (ill)

Les témoignages accablants contre l'armée et la police mexicaines lors de la guérilla dans le Chiapas.

Les enfants perdus de Zapata / Francis Pisani. — *Le Nouvel Observateur*, no 1533, 24 mars 1994, p. 62-63. (ill)

Point de vue d'écrivains et d'intellectuels mexicains sur la révolte des Amérindiens du Chiapas.

Don Samuel, l'âme du Chiapas / Philippe Demenet. — *La Vie*, no 2535, 31 mars 1994, p. 14-20. (carte ill)

Le soutien de l'évêque Samuel Ruiz Garcia aux Indiens du Chiapas entrés en révolte en janvier 1994.

Marked Record

AN: 91-23222
TI: Determination of clay size fraction of marine clays.
AU: Sridharan-A; Jose-Babu-T; Abraham-Benny-Mathews
OS: Indian Inst. Sci. Mech. Sci. Div., Bangalore, India; Cochin Univ. Sci. and Technol., India
SO: ASTM-Geotechnical-Testing-Journal. 14. (1). p. 103-107.
6 Refs.
CO: GTJODJ
YR: 1991
PD: illus., 1 table
LA: English
DE: India-; engineering-geology; soil-mechanics; experimental-studies; clay-; clastic-sediments; marine-environment; environment-; Indian-Peninsula; Asia-; Cochin-; granulometry-; hydrometers-
DT: Analytic; Serial
CC: 22-Engineering-and-environmental-geology
SB: B; Bibliography and Index of Geology (1969-present)
IS: 0149-6115

3 of 3
Marked Record

AN: 68-55465
TI: Geochemistry of niobium and tantalum.
AU: Parker-Raymond-L; Fleischer-Michael
SO: U.-S.-Geological-Survey-Professional-Paper. 43 p.
PB: U. S. Geological Survey, Reston, VA
YR: 1968
PD:
tables
LA: English
AB: This report summarizes work on the geochemistry of niobium and tantalum published since Rankama's treatise. A glossary and bibliography are included. The abundance of niobium and tantalum in the Earth's crust is about 20 and 2 ppm respectively. Abundance tables for different rocks show that niobium is most abundant in alkalic rocks, and alkalic mafic and ultramafic rocks. Tantalum generally accompanies niobium in an abundance of one-tenth to one-fifteenth that of niobium, although it is extremely low in some niobium-rich alkalic complexes. The highest content of niobium in sedimentary deposits is in deep-sea manganese nodules and in bauxites, whereas the highest tantalum content is in marine clays and bauxite. Niobium and tantalum in meteorites are a fraction of their clarke values, although tektites have a tantalum content similar to that of the Earth's crust.
DE: bibliography-; niobium-; geochemistry-; tantalum-; abundance-; mineral-data; Niobium-minerals; Glossary-; Tantalum-minerals; crust-; summary-; classification-by-chemical-type; occurrence-; USGS-
DT: Monographic; Serial; Report
SB: N; Bibliography of North American Geology (1785-1970)

Marked Record

AN: 95-29303

TI: Geochemical and mineralogical characteristics of some fine post-glacial marine deposits in the St. Lawrence Lowlands.

AU: Ramesh-Ramachandran

OS: McGill University, Canada; Doctoral

SO: 185 p.

YR: 1991

PD:

illus.

LA: English

AB: The post-glacial marine transgressive days of the St. Lawrence Lowlands constitute a major source of chemical elements to the suspended and dissolved loads of the lower St. Lawrence River. In order to better understand the nature of this source and its contributions, the present study investigates the mineralogy and the geochemistry of fine-grained deposits from the Champlain Sea and Goldthwait Sea deep-water facies. Sediments from land sites and from horizons submerged under the estuary, and suspended matter from the lower river and estuary, are analyzed, An attempt is made to reconsider the chemical nature, the concentration as well as the distribution and origin of an "amorphous" phase reported eartier in the sensitive marine clays. Two different extraction methods are applied to two distinct fine (<2mu m) size fractions. The extraction capacity differs with particle size and with the method used. However, the results from both methods correlate well, indicating a total amorphous content below 5% to 6% by weight, mainly composed of silica and of Fe and Al hydroxides. Irregular aggregates are observed under transmission electron microscopy. This amorphous phase represents a non-negligible contribution to the major element flux of the St. Lawrence. Long-term experiments keeping the sediments in suspension show that the release of silica, Fe and Al takes place preferentially in fresh water, and is inversely related to the salinity. In nature, contributions of dissolved silica by this mechanism would be minor (<3% of the total silica load). The relationships between the mineral content and the chemical composition of the post-glacial clays, as well as their variations with depth, particle size and location are examined. In the colloid-size fraction, an increase in illite and a decrease in feldspars with depth along two sections and one core raise the possibility of mild weathering in situ. This is supported by trends of indices for mineralogical and chemical maturity. Compared to indices calculated for sediments in other major rivers, those for the post-glacial marine clays of the St. Lawrence are low.

DE: bedload-; Cenozoic-; Champlain-Sea; clastic-sediments; clay-; clay-minerals; glacial-environment; glaciation-; Goldthwait-Sea; grain-size; mineral-composition; North-America; outwash-; Pleistocene-; provenance-; Quaternary-; Saint-Lawrence-Lowlands; Saint-Lawrence-River; sediments-; sensitive-clays; sheet-silicates; silicates-

DT: Monographic; Thesis

CC: 02-Geochemistry; 24-Surficial-geology-Quarternary-geology

SB: B; Bibliography and Index of Geology (1969-present)

2 of 3

IS: 1044-9612
RN: P 0612

Marked Record

AN: 91-23222
TI: Determination of clay size fraction of marine clays.
AU: Sridharan-A; Jose-Babu-T; Abraham-Benny-Mathews
OS: Indian Inst. Sci. Mech. Sci. Div., Bangalore, India; Cochin Univ. Sci. and Technol., India
SO: ASTM-Geotechnical-Testing-Journal. 14. (1). p. 103-107.
6 Refs.
CO: GTJODJ
YR: 1991
PD: illus., 1 table
LA: English
DE: India-; engineering-geology; soil-mechanics; experimental-studies; clay-; clastic-sediments; marine-environment; environment-; Indian-Peninsula; Asia-; Cochin-; granulometry-; hydrometers-
DT: Analytic; Serial
CC: 22-Engineering-and-environmental-geology
SB: B; Bibliography and Index of Geology (1969-present)
IS: 0149-6115

---

3 of 3
Marked Record

AN: 68-55465
TI: Geochemistry of niobium and tantalum.
AU: Parker-Raymond-L; Fleischer-Michael
SO: U.-S.-Geological-Survey-Professional-Paper. 43 p.
PB: U. S. Geological Survey, Reston, VA
YR: 1968
PD:
tables
LA: English
AB: This report summarizes work on the geochemistry of niobium and tantalum published since Rankama's treatise. A glossary and bibliography are included. The abundance of niobium and tantalum in the Earth's crust is about 20 and 2 ppm respectively. Abundance tables for different rocks show that niobium is most abundant in alkalic rocks, and alkalic mafic and ultramafic rocks. Tantalum generally accompanies niobium in an abundance of one-tenth to one-fifteenth that of niobium, although it is extremely low in some niobium-rich alkalic complexes. The highest content of niobium in sedimentary deposits is in deep-sea manganese nodules and in bauxites, whereas the highest tantalum content is in marine clays and bauxite. Niobium and tantalum in meteorites are a fraction of their clarke values, although tektites have a tantalum content similar to that of the Earth's crust.
DE: bibliography-; niobium-; geochemistry-; tantalum-; abundance-; mineral-data; Niobium-minerals; Glossary-; Tantalum-minerals; crust-; summary-; classification-by-chemical-type; occurrence-; USGS-
DT: Monographic; Serial; Report
SB: N; Bibliography of North American Geology (1785-1970)

1 of3
Marked Record

AN: 95-29303
TI: Geochemical and mineralogical characteristics of some fine post-glacial marine deposits in the St. Lawrence Lowlands.
AU: Ramesh-Ramachandran
OS: McGill University, Canada; Doctoral
SO: 185 p.
YR: 1991
PD:
illus.
LA: English

AB: The post-glacial marine transgressive days of the St. Lawrence Lowlands constitute a major source of chemical elements to the suspended and dissolved loads of the lower St. Lawrence River. In order to better understand the nature of this source and its contributions, the present study investigates the mineralogy and the geochemistry of fine-grained deposits from the Champlain Sea and Goldthwait Sea deep-water facies. Sediments from land sites and from horizons submerged under the estuary, and suspended matter from the lower river and estuary, are analyzed, An attempt is made to reconsider the chemical nature, the concentration as well as the distribution and origin of an "amorphous" phase reported eartier in the sensitive marine clays. Two different extraction methods are applied to two distinct fine (<2mu m) size fractions. The extraction capacity differs with particle size and with the method used. However, the results from both methods correlate well, indicating a total amorphous content below 5% to 6% by weight, mainly composed of silica and of Fe and Al hydroxides. Irregular aggregates are observed under transmission electron microscopy. This amorphous phase represents a non-negligible contribution to the major element flux of the St. Lawrence. Long-term experiments keeping the sediments in suspension show that the release of silica, Fe and Al takes place preferentially in fresh water, and is inversely related to the salinity. In nature, contributions of dissolved silica by this mechanism would be minor (<3% of the total silica load). The relationships between the mineral content and the chemical composition of the post-glacial clays, as well as their variations with depth, particle size and location are examined. In the colloid-size fraction, an increase in illite and a decrease in feldspars with depth along two sections and one core raise the possibility of mild weathering in situ. This is supported by trends of indices for mineralogical and chemical maturity. Compared to indices calculated for sediments in other major rivers, those for the post-glacial marine clays of the St. Lawrence are low.

DE: bedload-; Cenozoic-; Champlain-Sea; clastic-sediments; clay-; clay-minerals; glacial-environment; glaciation-; Goldthwait-Sea; grain-size; mineral-composition; North-America; outwash-; Pleistocene-; provenance-; Quaternary-; Saint-Lawrence-Lowlands; Saint-Lawrence-River; sediments-; sensitive-clays; sheet-silicates; silicates-
DT: Monographic; Thesis
CC: 02-Geochemistry; 24-Surficial-geology-Quarternary-geology
SB: B; Bibliography and Index of Geology (1969-present)

2 of3

Ministère du Transport du Québec.) soit .34¢ x 390= 265 $. La distance entre Ottawa et Montréal est de 195 kilomètre x 2= 390.

Le montant total de 6265 $ a été divisé en 6 et reparti, dans la section 3, entre les 6 PRS puisque les échantillons analysés provenaient de chacun des terrains affectés à ceux-ci.

1.3 Échantillonnage

Parce que je ne pouvais pas payer d'autres forages, j'ai échantillonné moi-même et fait parvenir les échantillons au Dr Percival. Je lui ai remis une description de cet échantillonnage et des photos pour confirmer la valeur de la méthode et les lieux où les échantillons ont été prélevés. J'inclus cette description dans le présent envoi et des photocopies des photographies.

Je ne déclare pas de salaire pour cet échantillonnage même si le travail a duré 3 jours, soit du 15 au 19 mai 1997, et que j'ai reçu l'aide d'une autre personne pour l'effectuer.Je déclare seulement :
✱ le transport de Montréal à Baie Saint-Ludger (671 kilomètres x 2 x .34 ¢)= 456.28
✱ le prix de certains repas = 42.92 $
✱ le prix du matériel (bocaux, pelle, gants, photos, sacs...)= 100 $
(Voir les factures de restaurants et d'essence qui confirment les dates de ce travail).

Le total des dépenses est donc de 600 $ (599.20 $) . Ce montant a été divisé en 6 et reparti ensuite dans la section 3 pour les 6 PRS (100 $ chacun) puisque c'est sur les 6 terrains couverts par les PRS que les échantillons ont été prélevés.

2. Les moyens d'extraction

En mars 1997, j'ai demandé au Centre de recherche industrielles du Québec (CRIQ) une étude pour identifier les méthodes et équipements les plus efficaces et les moins dommageables pour le milieu. Cette recherche avait pour objectifs de me permettre de juger des implications techniques des systèmes à l'étude, de connaître les orientations prises par la recherche et l'industrie et aussi de m'éclairer quant aux éventuelles décisions concernant le transfert de technologie ou de savoir-faire, l'achat d'équipements, la conception d'un appareil dédié ou autres options.

C'est dans le cadre de cette étude que M. Denis Lessard du Centre de recherche minérale du Québec a été sollicité comme expert en exploitation minière pour donner son avis avant de pousser plus loin les contacts hors Québec. M. Lessard, après avoir consulté l'ensemble des documents que j'ai remis au CRIQ, recommande une liste de paramètres à connaître concernant la zone d'exploitation du dépôt d'argile puisque plusieurs données techniques visant la **caractérisation globale** du gisement sont absentes ou incomplètes.

En effet, une infime partie de l'ensemble du territoire convoité (il couvre environ 500 hectares) est connue et cela à partir de deux forages seulement. Ces résultats fragmentaires rendent donc difficile l'étude de stabilisation du site et le choix des équipements nécessaires à son exploitation commerciale.

Ces raisons font que l'étude a été temporairement suspendue pour déterminer des critères de qualité à l'argile et pour caractériser le gisement. Le montant de l'étude du CRIQ est de 12 700 $ et il a été entièrement payé. (Voir les chèques annexés). Comme cette étude a été subventionnée de 6 350 $ dans le cadre de l'Entente Canada-Québec pour le développement minéral, (voir la lettre ci-incluse attestant cette aide financière) j'ai demandé à M Dominic Ménard du Service de développement minéral, MERQ, d'affecter le montant restant pour des analyses des eaux interstitielles, des micro-organismes et de éléments chimiques. M. Jean François Wilhelmy , du Centre de recheche minérale, effectura ces analyses.

Le total de 12 700 $ de cette étude a été reparti, dans la section 3, pour chaque PRS.

3. La transformation de l'argile en produits cosmétiques et/ou thérapeutiques

3.1. La 11 Conférence internationale sur les Argiles du 15-21 juin à Ottawa

J'ai participé à cette conférence pour avoir des informations générales et scientifiques sur les argiles et pour développer des contacts au niveau international. La participation à cette conférence a coûté 1 3 18 $. Ce montant couvre :

✱ Les repas et le stationnement : 173 $
✱ L'inscription et l'hébergement : 850 $
✱ L'abonnement à la société minérale des argiles : 30$
✱ Le voyage Montréal-Ottawa (aller-retour) : 265$

2.2 Recherche documentaire sur les argiles en cosmétique et thérapeutique effectuée par Marie-Hélène Dupuis de la bibliothèque de l'École polytechnique de l'Université de Montréal. Cette recherche a couté 250 $

Les factures de ces frais de participation à la conférence et pour la recherche documentaire sont annexées et les côuts sont repartis sur l'ensemble des PRS.

Canton: MANICOUAGAN 22F01

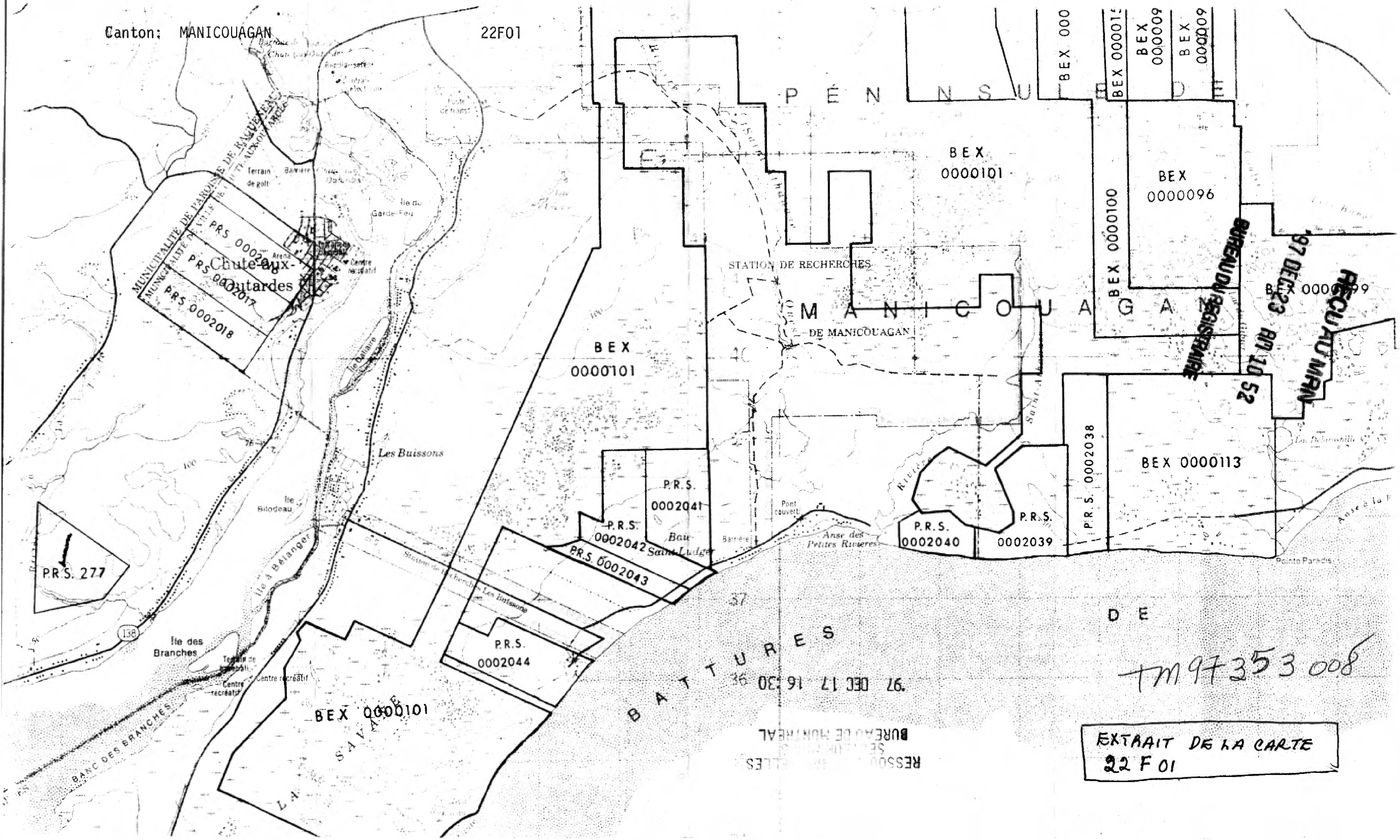

BUREAU DU REGISTRAIRE '97 DEC 23 AM 10 52

REÇU AU MRN

TM 97 353 008

EXTRAIT DE LA CARTE 22 F 01

Argile eau mer

Rapport

de

caractèrisation du
gisement et des analyses
pour dèterminer les critères
de qualité de l'argile

Centre de recherche minèrale

20 janvier 1999

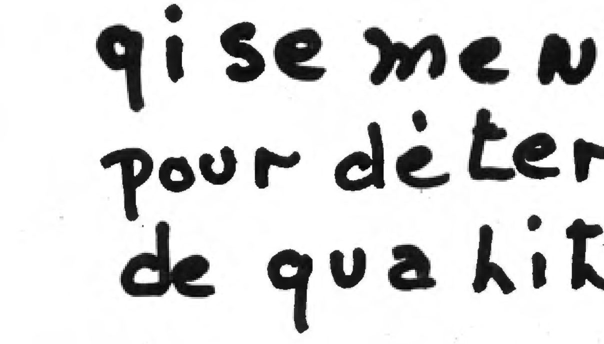

Gouvernement du Québec
Ministère des
Ressources naturelles

Sainte-Foy, le 28 août 1997

Monsieur Serge Huppé
Aviseur technique
CRIQ
333 rue Franquet
Ste-Foy QC
G1P 4C7

OBJET : Exploitation d'un dépôt d'argile sensible

Monsieur Huppé,

Suite à notre rencontre d'hier, vous trouverez ci-dessous une liste de paramètres à connaître afin de bien définir les grandes lignes du projet d'exploitation du dépôt d'argile sensible que vous m'avez décrit sommairement.

- Trouver les limites physiques du dépôt d'argile à l'aide d'une cartographie de surface et de tranchées, de sondages géophysiques et de forages (carottiers) : forme générale du dépôt, longueur, largeur, épaisseur, présence de lentilles d'argile...
- Déterminer la nature et l'épaisseur de la couche de stérile recouvrant le dépôt d'argile.
- Estimer le tonnage total des réserves d'argile de type commercial : un programme d'échantillonnage et de caractérisation (géotechnique, minéralogique et chimique) des échantillons devra être exécuté afin de bien définir la valeur économique du projet. Les résultats des essais de caractérisation serviront autant pour établir la valeur marchande du dépôt que pour l'étude des conditions d'exploitation et de sécurité du chantier. Certains résultats, en particulier les données géotechniques, pourront servir dans l'évaluation des travaux de restauration du site.
- Tracer, à partir des critères de qualité retenus par votre cliente, des frontières (iso-contours) sur les plans d'exploitation afin de bien délimiter les zones riches, moyennes et passables.
- Choisir les équipements d'exploitation en fonction du niveau de production désiré par votre cliente (t.m./jour), des propriétés physico-chimiques de l'argile, de l'environnement physique de surface, de la nature des sols contenant l'argile, des contraintes environnementales spécifiques et de l'ampleur, des dimensions, de la forme et de la position du dépôt d'argile par rapport à la surface du sol.

- Déterminer si l'argile extrait nécessitera un traitement ou une série de traitements avant son utilisation. Si oui, il faudra établir le schéma de traitement et déterminer les équipements requis.
- Déterminer le moyen de transport de l'argile vers la station ou l'usine de traitement.
- Déterminer les coûts d'exploitation, de transport, de traitement... Effectuer une étude de préfaisabilité, incluant un «cash flow».

Tel que je vous le mentionnais lors de notre rencontre, les analyses chimiques, les essais de microcaractérisation et le développement de procédés de traitement peuvent être effectués au C.R.M.

Les travaux relatifs à la mise en valeur et à l'exploitation d'un dépôt ne font pas partie des activités couvertes par le C.R.M. Si vous le désirez, je peux vous donner les coordonnées de consultants qui peuvent réaliser les travaux suivants : estimation des réserves, conception de plans d'exploitation, étude de stabilité des pentes et étude technico-économique sur l'exploitation d'un dépôt.

N'hésitez pas à me contacter pour de plus amples informations.

Veuillez accepter, M. Huppé, l'expression de mes sentiments les meilleurs.

Denis Lessard, ing. M.Sc.
Chargé de projet
Centre de recherche minérale

C.C. M. Alain Claveau, ing., Ph.D.
Directeur de la recherche

CRM
ISO 9001
CENTRE DE RECHERCHE MINÉRALE
Tél.: (418) 643-4540
Téléc.: (418) 643-6706
http:www.crm.gouv.qc.ca/

Gouvernement du Québec
Ministère des
Ressources naturelles

Madame Denise Saulnier
Argile Eau de mer inc.
5594 Waverly
Montréal (Québec)
H2T 2Y1
FAX: (514) 273-9373

Résultat d'une étude minéralogique

Date :	28 mai 1998
Sujet :	Nature de deux échantillons d'argile
V/Réf.:	Client #30343
N/Réf.:	98-001174

Madame,

Veuillez trouver ci-joints les résultats de l'interprétation modale effectuée sur les échantillons soumis (#2042 et #2043). Les certificats d'analyse granulométrique par microtrac, les diffractogrammes (#980078 et #980079) de rayons X ainsi que le certificat d'analyse sont annexés à la présente.

Les portions solide et liquide ont d'abord été séparées dans chacun des échantillons (#2042 et #2043) dans le but d'analyser chacune des phases. Aucun minéral des argiles n'a été détecté par diffraction des rayons X dans la phase solide. Ces échantillons correspondent à des argiles au sens granulométrique du terme et non au sens minéralogique. En effet, l'analyse par microtrac a permis de déterminer que 43 % du matériel correspond granulométriquement à une argile (< 3,9 µm) pour l'échantillon #2042 et 40 % pour l'échantillon #2043.

Ces deux échantillons d'argile contiennent jusqu'à 20 % de quartz dont la présence dans les produits cosmétiques peut engendrer des problèmes d'abrasion lorsque ceux-ci sont utilisés sur la peau et ce, à cause de la dureté élevée de ce minéral.

***

Espérant ces quelques résultats conformes à vos attentes, veuillez agréer, Monsieur, l'expression de mes sentiments les meilleurs.

Sylvie Lévesque
Sylvie Lévesque

2700, rue Einstein
Sainte-Foy (Québec)
Canada
G1P 3W8

Station d'essais:
1180, Place Dufresne, Québec
(Québec) Canada
G1N 1X7

<980079.MDI> 0002043 argile [JADE - Search/Match Report]

Client Information	Analyst Information
Name = ARGILE EAU DE MER INC. Voice = Fax = Sample ID = 0002043 argile	Name = DANIEL MOISAN Voice = (418) 643-4540 POSTE 250 Fax = (418) 646-6080 Sample ID = 980079.MDI

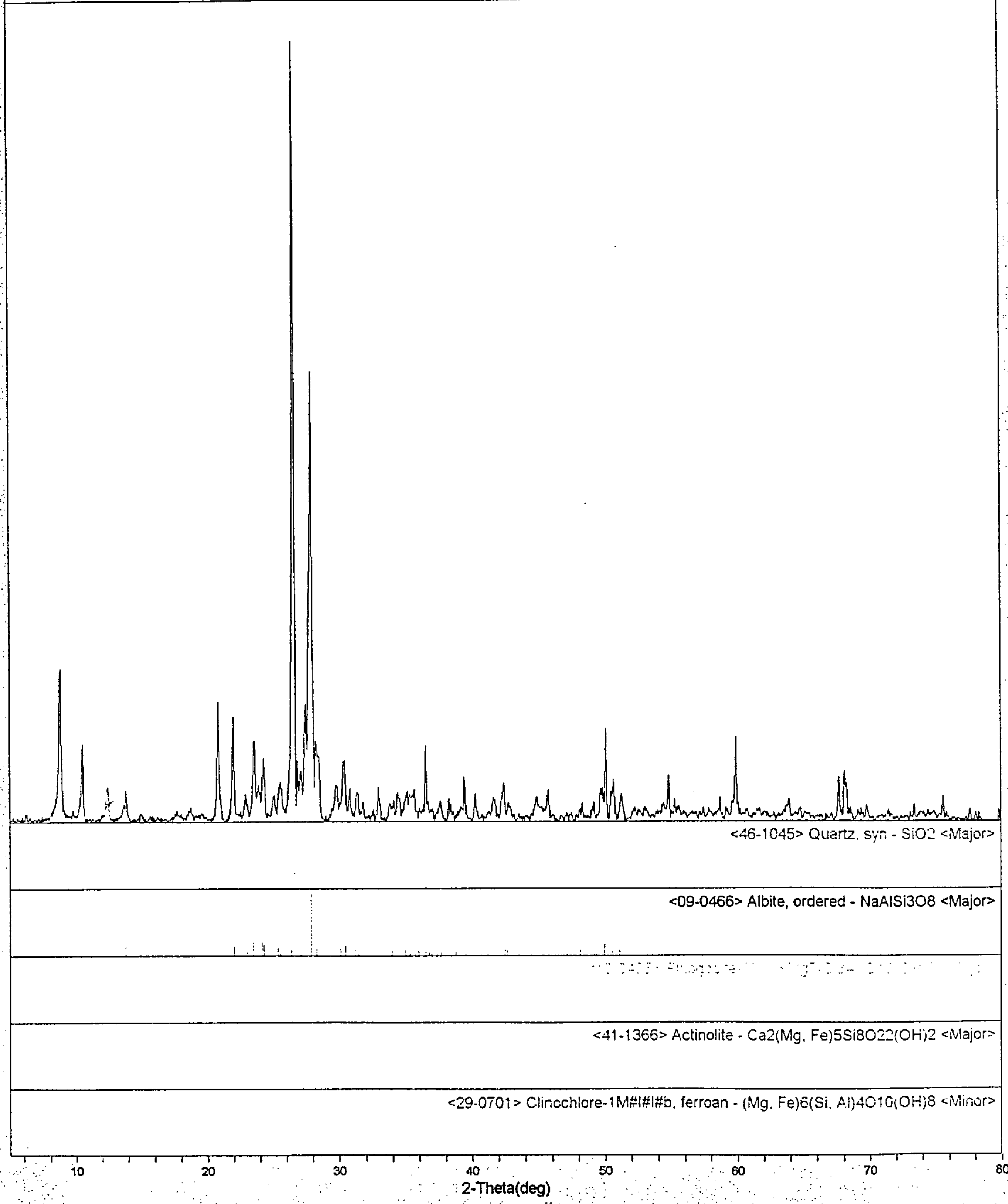

<980078.MDI> 0002042 argile [JADE - Search/Match Report]

Client Information	Analyst Information
Name = ARGILE EAU DE MER INC.	Name = DANIEL MOISAN
Voice = Fax =	Voice = (418) 643-4540 POSTE 250 Fax = (418) 646-6080
Sample ID = 0002042 argile	Sample ID = 980078.MDI

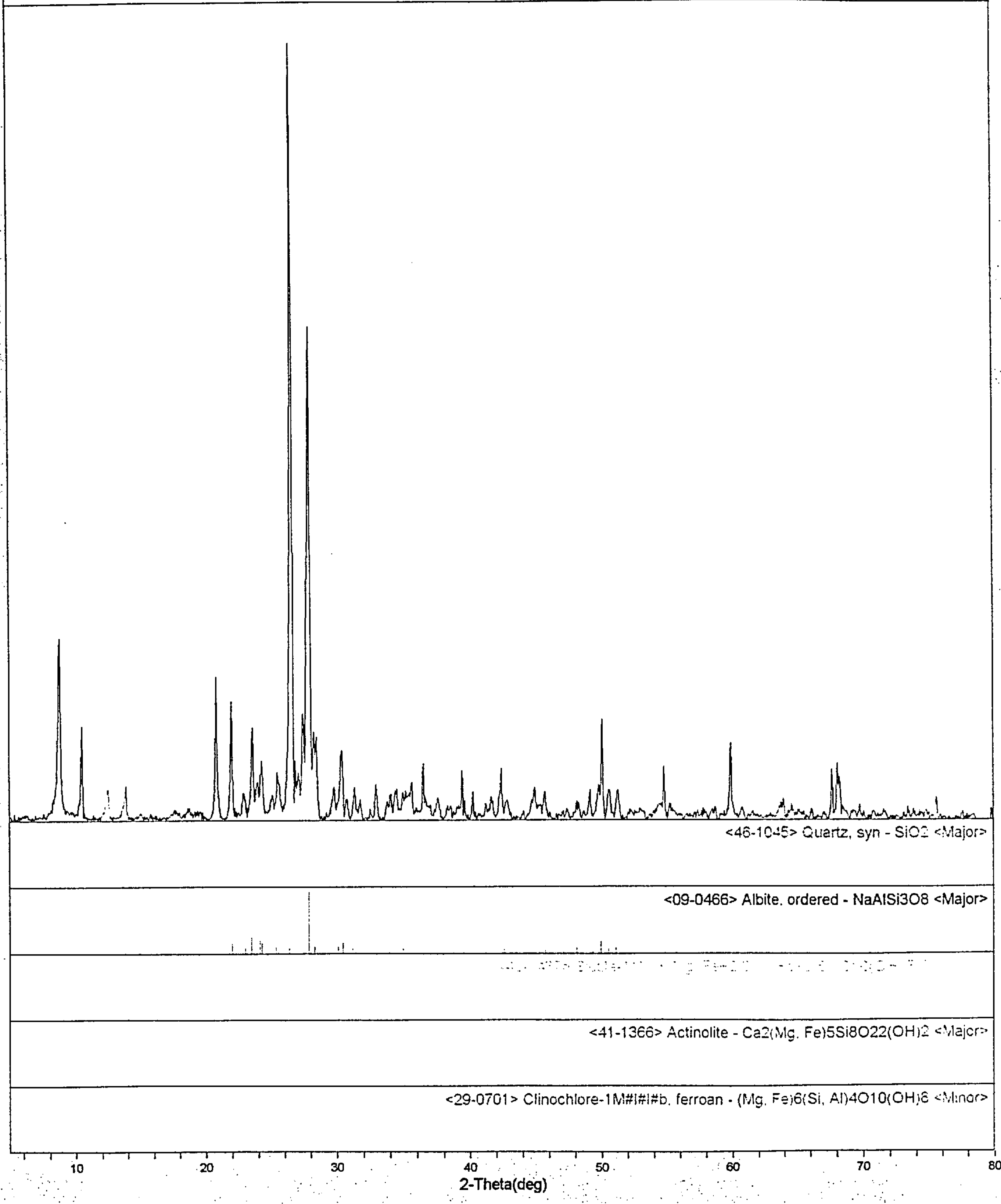

Centre de recherche minérale

Thursday, Apr 23, 1998 @03:39p

Interprétation modale de l'échantillon d'argile #2042

Diffractogramme: #98-0078

	Analyse souche	Analyse calculée	Quartz	Albite	Biotite	Actinolite	Chlorite	Apatite
Proportion			21,36	29,00	31,16	15,06	1,50	0,50
SiO_2	59,80	59,8	100,0%	68,0%	34,0%	51,0%	30,0%	
Al_2O_3	16,20	16,2		20,0%	30,0%	5,0%	20,0%	
Fe_2O_3	6,25	6,3			18,0%	3,0%	16,0%	
MgO	3,34	3,2			2,0%	15,0%	22,0%	
CaO	3,92	3,9				24,0%	1,0%	58,0%
Na_2O	3,80	3,8		12,0%	1,0%			
K_2O	2,81	2,8			9,0%			
TiO_2	0,66	0,6			2,0%			
MnO	0,09	0,0						
P2O5	0,21	0,2						42,0%
Cr2O3	0,02	0,0						
PAF	1,78	1,7			4,0%	2,0%	11,0%	
C_{total}	0,22	0,0						
Total	98,88	98,6	100,0%	100,0%	100,0%	100,0%	100,0%	100,0%
Modale	98,57							

CENTRE DE RECHERCHE MINÉRALE
Direction du laboratoire d'analyse

Interprétation modale de l'échantillon d'argile #2043

Diffractogramme: #98-0079

	Analyse souche	Analyse calculée
Proportion		
SiO_2	60,00	60,0
Al_2O_3	16,20	16,2
Fe_2O_3	6,00	6,5
MgO	3,30	3,3
CaO	4,17	4,2
Na_2O	3,83	3,9
K_2O	2,76	2,7
TiO_2	0,66	0,6
MnO	0,10	0,0
P2O5	0,22	0,2
Cr2O3	0,02	0,0
PAF	1,91	1,4
C_{total}	0,33	0,0
Total	99,17	99,1
Modale	99,05	

Quartz	Albite	Biotite	Actinolite	Chlorite	Apatite
20,66	30,00	30,33	16,05	1,50	0,52
100,0%	68,0%	34,0%	51,0%	30,0%	
	20,0%	30,0%	5,0%	20,0%	
		19,0%	3,0%	16,0%	
		2,0%	15,0%	22,0%	
			24,0%	1,0%	58,0%
	12,0%	1,0%			
		9,0%			
		2,0%			
					42,0%
		3,0%	2,0%	11,0%	
100,0%	100,0%	100,0%	100,0%	100,0%	100,0%

CRM
ISO 9001
CENTRE DE RECHERCHE
MINÉRALE

DATE: 98/05/21

A:

Madame Denise Saulnier
Argile Eau de mer Inc.
5594, Waverly
MONTREAL (Québec)

H2T 2Y1

Télécopieur : 514-273-9373

Numéro de dossier: 6997
Numéro de projet : 30343
Numéro de demande: 98 04 22 004

R E S U L T A T

	DESIGN:	0002042 solide	0002043 solide	0002042 sol'n	0002043 sol'n
	NO.LAB:	98 001105	98 001106	98 001107	98 001108
A01	SiO2	59,8 %	60,0 %		
	Al2O3	16,2 %	16,2 %		
	Fe2O3t	6,25 %	6,00 %		
	MgO	3,34 %	3,30 %		
	CaO	3,92 %	4,17 %		
	Na2O	3,80 %	3,83 %		
	K2O	2,81 %	2,76 %		
	TiO2	0,66 %	0,66 %		
	MnO	0,09 %	0,10 %		
	P2O5	0,21 %	0,22 %		
	Cr2O3	0,02 %	0,02 %		
	PAF	1,78 %	1,91 %		
B12	Cor&gr	0,03 %	0,04 %		
B13	Ct:CO2	0,22 %	0,33 %		
B41	S tot	0,05 %	0,04 %		
B66	Mtrac	*	*		
B74	Cl %	<0,10 %	<0,10 %		
G04	TT.ext			*	*
L03	As			Ech.insuf.	Ech.insuf.
L12	Cl ppm			2,6 mg/L	14,6 mg/L
L19	F			0,5 mg/L	0,5 mg/L
L43	S tot.			2,4 ppm	4,0 ppm
M01	pH eau			8,8	9,0
M04	Alc.			57 mg/L de CaCO3	92 mg/L de CaCO3
M32	Al			60,2 ppm	37,3 ppm
	Ba			487 ppb	279 ppb
	Ca			9,9 ppm	5,8 ppm
	Cd			<2 ppb	<2 ppb
	Cr			149 ppb	96 ppb
	Cu			492 ppb	321 ppb
	Fe			56,7 ppm	36,6 ppm

Centre de recherches minérales
Service du Laboratoire d'analyse
2700, rue Einstein
SAINTE-FOY, (Québec), G1P 3W8
Téléphone : (418) 643-4504
Télécopieur: (418) 643-6706

```
             * * * * * * * * * * * * * * * * * * * *  R E S U L T A T * * * * * * * * * * * * * * * * * *
             *                                                                                          *
             *                                                                                          *
             *     DESIGN: 0002042 solide 0002043 solide 0002042 sol'n  0002043 sol'n                   *
             *     NO.LAB: 98 001105      98 001106      98 001107      98 001108                       *
             *                                                                                          *
             *                                                                                          *
             * A01 SiO2      59,8  %        60,0  %                                                     *
             *     Al2O3     16,2  %        16,2  %                                                     *
             *     Fe2O3t     6,25 %         6,00 %                                                     *
             *     MgO        3,34 %         3,30 %                                                     *
             *     CaO        3,92 %         4,17 %                                                     *
             *     Na2O       3,80 %         3,83 %                                                     *
             *     K2O        2,81 %         2,76 %                                                     *
             *     TiO2       0,66 %         0,66 %                                                     *
             *     MnO        0,09 %         0,10 %                                                     *
             *     P2O5       0,21 %         0,22 %                                                     *
             *     Cr2O3      0,02 %         0,02 %                                                     *
273-9373     *     PAF        1,78 %         1,91 %                                                     *
             *                                                                                          *
             * B12 Cor&gr     0,03 %         0,04 %                                                     *
             * B13 Ct:CO2     0,22 %         0,33 %                                                     *
             * B41 S tot      0,05 %         0,04 %                                                     *
 22 004      * B66 Mtrac       *              *                                                         *
             * B74 Cl %      <0,10 %        <0,10 %                                                     *
             * G04 TT.ext                                    *              *                           *
             * L03 As                                    Ech.insuf.     Ech.insuf.                      *
             * L12 Cl ppm                                  2,6 mg/L      14,6 mg/L                      *
             * L19 F                                       0,5 mg/L       0,5 mg/L                      *
             * L43 S tot.                                  2,4  ppm       4,0  ppm                      *
             * M01 pH eau                                  8,8            9,0                           *
             *                                                                                          *
             * M04 Alc.                                   57   mg/L      92   mg/L                      *
             *                                             de CaCO3       de CaCO3                      *
             *                                                                                          *
             *                                                                                          *
             * M32 Al                                     60,2  ppm      37,3  ppm                      *
érales       *     Ba                                    487    ppb     279    ppb                      *
'analyse     *     Ca                                      9,9  ppm       5,8  ppm                      *
             *     Cd                                     <2    ppb      <2    ppb                      *
 3W8         *     Cr                                    149    ppb      96    ppb                      *
304          *     Cu                                    492    ppb     321    ppb                      *
706          *     Fe                                     56,7  ppm      36,6  ppm                      *
             *                                                                                          *
             * * * * * * * * * * * * * * * * * * * * * * * * * * * * * * * * * * Page   1 de   2  * *
```

ISO 9001
CENTRE DE RECHERCHE
MINÉRALE

DATE: 98/05/21

A:

Madame Denise Saulnier
Argile Eau de mer Inc.
5594, Waverly
MONTREAL (Québec)

H2T 2Y1

Télécopieur : 514-273-9373

Numéro de dossier: 6997
Numéro de projet : 30343
Numéro de demande: 98 04 22 004

	DESIGN:	0002042 solide	0002043 solide	0002042 sol'n	0002043 sol'n
	NO.LAB:	98 001105	98 001106	98 001107	98 001108
A01	SiO2	59,8 %	60,0 %		
	Al2O3	16,2 %	16,2 %		
	Fe2O3t	6,25 %	6,00 %		
	MgO	3,34 %	3,30 %		
	CaO	3,92 %	4,17 %		
	Na2O	3,80 %	3,83 %		
	K2O	2,81 %	2,76 %		
	TiO2	0,66 %	0,66 %		
	MnO	0,09 %	0,10 %		
	P2O5	0,21 %	0,22 %		
	Cr2O3	0,02 %	0,02 %		
	PAF	1,78 %	1,91 %		
B12	Cor&gr	0,03 %	0,04 %		
B13	Ct:CO2	0,22 %	0,33 %		
B41	S tot	0,05 %	0,04 %		
B66	Mtrac	*	*		
B74	Cl %	<0,10 %	<0,10 %		
G04	TT.ext			*	*
L03	As			Ech.insuf.	Ech.insuf.
L12	Cl ppm			2,6 mg/L	14,6 mg/L
L19	F			0,5 mg/L	0,5 mg/L
L43	S tot.			2,4 ppm	4,0 ppm
M01	pH eau			8,8	9,0
M04	Alc.			57 mg/L de CaCO3	92 mg/L de CaCO3
M32	Al			60,2 ppm	37,3 ppm
	Ba			487 ppb	279 ppb
	Ca			9,9 ppm	5,8 ppm
	Cd			<2 ppb	<2 ppb
	Cr			149 ppb	96 ppb
	Cu			492 ppb	321 ppb
	Fe			56,7 ppm	36,6 ppm

Centre de recherches minérales
Service du Laboratoire d'analyse
2700, rue Einstein
SAINTE-FOY, (Québec), G1P 3W8
Téléphone : (418) 643-4504
Télécopieur: (418) 643-6706

ISO 9001
CENTRE DE RECHERCHE
MINÉRALE

DATE: 98/05/21

A:

Madame Denise Saulnier
Argile Eau de mer Inc.
5594, Waverly
MONTREAL (Québec)

H2T 2Y1

Télécopieur : 514-273-9373

Numéro de dossier: 6997
Numéro de projet : 30343
Numéro de demande: 98 04 22 004

Responsables:

M. Desgagné, chim.: ______
R. Gagné, chim.: ______
Y. Couture, chim.: ______
G. Gosselin, chim.: ______
Marc Bisson, chim.: ______________
directeur

Centre de recherches minérales
Service du Laboratoire d'analyse
2700, rue Einstein
SAINTE-FOY, (Québec), G1P 3W8
Téléphone : (418) 643-4504
Télécopieur: (418) 643-6706

SLA-F-33 (95-03)

Mn	738	ppb	455	ppb
Na	34,5	ppm	57,0	ppm
Ni	112	ppb	70	ppb
P	1,7	ppm	1,0	ppm
Pb	117	ppb	57	ppb
Zn	160	ppb	101	ppb

P01 Séch.
Z07 QAN

Argile
eau
mer

Rapport du

Centre de recherches
industrielles du Québec
d'une étude sur les moyens
d'extraction des argiles
Souterraines

20 JANVIER 1999

TECHNIQUES D'EXTRACTION
DES ARGILES SOUTERRAINES

Dossier Client n° 712-AP-20478
Plan de travail n° PT-20478

MARS 1997

CLIENT : ARGILE EAU MER
554, rueWaverly
Montréal (Québec) H2T 2Y1

À l'attention de madame Denise Saulnier
Tél. : (514) 273-3573

C.D. : Claude Raymond

RESPONSABLE DE PROJET :

Serge Huppé
Direction de l'information industrielle et
technologique

DIRECTEUR :
Claude Jacques

Sainte-Foy, le 05 mars 1997

CRIQ
CENTRE DE RECHERCHE
INDUSTRIELLE DU QUÉBEC

TABLE DES MATIERES

1.0 LE CONTEXTE

Consciente du potentiel économique que représentent les argiles marines ou fluviales de Baie Saint-Ludger, madame Denise Saulnier, de la compagnie *Argile eau mer*, travaille depuis plusieurs années à la concrétisation de son projet d'extraction et de transformation de l'argile en produits cosmétiques et thérapeutiques.

Trois des six étapes menant à la concrétisation finale de son projet sont pratiquement terminées. Il s'agit de la détermination des applications potentielles de l'argile et des propriétés requises, la comparaison entre les propriétés des argiles actuellement commercialisées sur le marché et celles présentes à Baie Saint-Ludger, la sélection des applications les plus prometteuses en regard des aspects techniques, économiques et environnementaux.

Sur la base des actions entreprises antérieurement, madame Saulnier aborde maintenant une phase critique dans le cheminement de son projet, c'est-à-dire l'identification et l'évaluation des méthodes d'extraction de l'argile souterraine présente à Baie Saint-Ludger. M^{me} Denise Saulnier souhaite faire le point sur les technologies respectueuses du milieu, existantes ou à l'étude, à même d'être utilisées dans le cadre de ses opérations d'extraction.

Pour orienter ses actions et garantir la réussite de son entreprise, M^{me} Denise Saulnier se doit de trouver réponse aux questions suivantes : quelles sont les approches mises de l'avant à l'échelle internationale au cours des dernières années? Existe-t-il des données techniques particulières portant sur leur utilisation à l'échelle industrielle? Quels peuvent être leurs coûts moyens d'obtention? Quels sont les moyens susceptibles de réduire l'impact négatif de ces techniques sur les sols sensibles et friables? Quelles sont les entreprises privées ou les experts qui ont oeuvré à leur élaboration? Quels sont les intervenants privés ou publics disposés à partager leur savoir-faire? Etc.

C'est pour trouver réponse à ces interrogations et d'accompagner madame Saulnier dans ses démarches que les services de la **Direction de l'information industrielle et technologique** du *Centre de recherche industrielle du Québec (CRIQ)* sont sollicités.

2.0 L'OBJECTIF

Cette investigation a pour objectif principal d'assister madame Saulnier dans la cueillette de données lui permettant de prendre connaissance des éléments pouvant orienter ses décisions. De manière plus précise, il s'agit d'identifier les moyens d'extraction (méthodes ou équipements) les plus efficaces et les moins dommageables pour le milieu. À partir de ces éléments, madame Saulnier sera à même de juger quelles sont les implications techniques des systèmes à l'étude et, par le fait même, de connaître les orientations prises par la recherche et l'industrie. Sur ces bases, il lui sera possible de prendre une décision éclairée quant à la suite à donner à ce dossier, soit le transfert de technologie ou de savoir-faire, l'achat d'équipements, la conception d'un appareil dédié, etc.

3.0 LA MÉTHODOLOGIE

Pour mener à bien ces travaux, des spécialistes en information feront le point de la situation internationale en ce qui concerne les technologies visées.

Pour y parvenir, ils mettront à contribution l'ensemble des moyens dont disposent les services de la **Direction de l'information industrielle et technologique** du ***Centre de recherche industrielle du Québec.*** Ceux-ci se composent de références spécialisées, de publications scientifiques et techniques, de sources électroniques de pointe rattachées aux technologies de l'information et d'un réseau international d'alliances avec des groupes ou organisations reconnues pour leurs compétences techniques.

3.1 RECHERCHE SUR MÉDIAS ÉLECTRONIQUES ET DANS LA LITTÉRATURE

Banques de données informatisées

Les spécialistes en information travaillant sur le projet consulteront les principales banques de données versées dans le secteur de la géologie, des mines, de l'environnement et de l'ingénierie. Cette recherche englobera la littérature scientifique, technique et commerciale des cinq dernières années. Compte tenu des particularités techniques de certains équipements, les banques de brevets seront aussi mises à contribution afin de retracer des précisions pertinentes à ce sujet.

Lors de cette recherche, notre mandat sera de retracer toute information utile sur les systèmes mis en place, ou à l'étude, à l'échelle internationale, pouvant convenir à l'extraction des argiles liquides souterraines. Notre investigation portera également sur les technologies développées pour d'autres produits ayant des caractéristiques proches de celles de l'argile.

INTERNET : Sites Web, groupes de discussions et babillards électroniques

À l'aide des informations que nous aurons recensées à l'étape précédente, nous recueillerons de plus amples détails sur les institutions d'enseignement, les organisations, les fournisseurs ou manufacturiers, les experts étrangers, etc. avec lesquels communiquer par la suite. Nous visiterons leur site Web, lorsque disponible, et vérifierons si leurs orientations cadrent avec la nature des informations que nous recherchons. Il en va de même en ce qui concerne les groupes de discussions et les babillards électroniques. Concernant ce dernier point, comme l'ensemble de nos actions se fera sous le nom du ***Centre de recherche industrielle du Québec***, nous aurons ainsi la reconnaissance nécessaire pour participer à des forums spécialisés et destinés aux milieux universitaires ou de la recherche.

3.2 CONTACTS AUPRÈS DES FOURNISSEURS D'ÉQUIPEMENTS

Nous identifierons, à l'aide de guides d'achats et de répertoires spécialisés, les fournisseurs d'équipements susceptibles de nous proposer le matériel recherché.

Ces démarches couvriront les principaux pays européens reconnus pour leur expertise dans le domaine ainsi que le territoire nord-américain. Toutefois, cette limitation ne se veut aucunement restrictive : nous pourrons ainsi retenir des firmes en place dans tout autre pays jugé d'intérêt.

Cette investigation ne se restreint pas qu'aux simples manufacturiers de matériel destiné à l'extraction des terres argileuses. Nous élargirons notre champ d'action à d'autres entreprises offrant des équipements industriels pour des utilisations connexes. Avec une telle approche, nous serons en mesure de prendre connaissance de voies de solution émanant de différentes sphères de l'industrie.

Pour chacun de nos contacts, une lettre personnalisée leur sera adressée. Au sein de celle-ci, nous mentionnerons le pourquoi de notre requête et les données que nous escomptons recevoir d'eux. Le tout sera acheminé par télécopie automatique, courrier électronique ou par courrier postal.

3.3 CONTACTS AUPRÈS D'EXPERTS OU D'ORGANISMES RECONNUS

Des échanges, à l'échelle internationale, seront réalisés par courrier électronique, téléphone, télécopieur ou courrier postal, auprès des gens reconnus pour leurs compétences dans le domaine de l'extraction des argiles. Pour y parvenir, l'ensemble des données cumulées à l'étape 3.1 sera consulté afin d'y puiser les contacts les plus utiles à initier en premier lieu. Ceci inclut également les renseignements figurant à l'intérieur des brevets identifiés et retenus pour leur pertinence. Le tout sera complété par la consultation de répertoires spécialisés recensant l'ensemble des institutions de recherche, associations et bureaux d'experts-conseils. L'objectif de ces démarches est d'en savoir plus sur les approches existantes ou à l'étude et les orientations prises par l'industrie et la recherche à l'échelle internationale.

L'essentiel de nos discussions abordera des thèmes similaires à ceux discutés avec les fournisseurs et manufacturiers d'équipements.

3.4 ANALYSE DES INFORMATIONS ET PRÉSENTATIONS DES RÉSULTATS

À la suite de cette collecte exhaustive d'information, nous serons en mesure de synthétiser et de vous présenter l'ensemble des méthodes ou technologies en lien avec vos préoccupations. De plus, ce travail permettra d'avoir une idée valable des équipements requis, des particularités techniques à considérer, de prendre connaissance de certaines données rattachées aux coûts d'obtention et d'opérationalisation des appareils et de connaître les meilleurs acteurs, nationaux ou internationaux, détenant les compétences recherchées pour vous aider à mener à bien votre projet. Se joindront, en annexe, l'ensemble des références bibliographiques les plus intéressantes, la documentation technique sélectionnée et retenue pour analyse, la liste complète des manufacturiers, organismes ou experts contactés, les fiches techniques des équipements obtenus auprès des manufacturiers ainsi que les avis techniques que nous aurons recueillis auprès des spécialistes.

C'est alors, après que madame Denise Saulnier ait pris connaissance de ces informations et si les approches techniques retenues présentent des particularités technologiques notables ou font l'objet d'une protection légale quelconque, que des entretiens seront initiés avec les détenteurs de ces technologies. Nous verrons alors à sonder leur intérêt face à la vente de leurs équipements, à un transfert technique ou de savoir-faire ou à l'allocation d'une licence exclusive d'exploitation.

Cette dernière intervention, ainsi que toute autre portant sur une étude approfondie de la rentabilité d'une technologie ou approche fera l'objet de travaux ultérieurs non prévus au sein de l'actuelle proposition.

Pour écarter les informations inutiles, aucune action ne sera entreprise avant d'avoir consulté les données que madame Denise Saulnier a déjà à sa disposition. Des entretiens auront donc lieu en début de mandat afin de préciser adéquatement l'orientation de nos recherches. Nous nous efforçons, de cette manière, à éviter les activités n'apportant pas ou peu de valeur ajoutée à l'information recueillie.

4.0 LES RESSOURCES ET LES ÉCHÉANCIERS

Les coûts reliés à la réalisation de ces travaux se chiffrent à 12 700 $ et permettent de couvrir les frais de banques de données, l'achat de documents, le temps du personnel technique relié à la cueillette de l'information et à son analyse et les frais de communication. Les travaux s'échelonneront sur une période de douze (12) semaines.

Ce délai de réalisation est en grande partie attribuable au temps de réponse des divers contacts initiés à l'étranger et aux échanges qui s'en suivront. En ce qui a trait au début des travaux, il sera déterminé après entente entre les parties.

5.0 LES RÉSULTATS ESCOMPTÉS

La poursuite des démarches entreprises à ce jour par madame Denise Saulnier et l'atteinte de ses objectifs passent par une synthèse objective des informations internationales recueillies lors des actions décrites antérieurement. Les techniques d'extraction qui seront retenues nécessiteront des déboursés appréciables pour leur obtention (achats, implantation, ajustement, équipements périphériques, etc.). Ceci est sans compter la connaissance et la maîtrise qu'elles requièrent pour une utilisation optimale et en accord avec la fragilité du milieu. Il est donc important de s'assurer des bons choix et de se doter, pour y parvenir, des informations nécessaires. Les argents ainsi investis permettront, de plus, de bâtir une argumentation solide lors de discussions avec les experts techniques, les fournisseurs de ces technologies ou les équipes appelées à modifier ou à concevoir un nouvel appareil. M^{me} Saulnier évitera ainsi bien des tracas et des dépenses inutiles.

6.0 LES CONDITIONS DU SUCCÈS DE LA DÉMARCHE

Afin de rencontrer les résultats attendus, il est important qu'une synergie s'installe entre le responsable du projet et la cliente. Des échanges téléphoniques entre les parties seront établis sur une base régulière et des rencontres seront tenues si cela s'avèrent nécessaires.

C'est dans cette optique que le **CRIQ** se veut partenaire dans la réussite de cette démarche.

ANNEXE

CURRICULUM VITAE

CURRICULUM VITAE

Serge Huppé	Technicien senior en technologie et données industrielles Direction de l'information industrielle et technologique

---

FORMATION

1995-	UNIVERSITÉ LAVAL Maîtrise en sciences et technologies des aliments
1991-1994	UNIVERSITÉ LAVAL Certificat en sciences et technologies des aliments
1986	MINISTÈRE DE L'AGRICULTURE, DES PÊCHERIES ET DE L'ALIMENTATION (en collaboration avec le ministère de l'Éducation) Cours d'inspection et triage des produits marins
1983-1985	CÉGEP DE STE-FOY A.E.C. en sciences universelles (Sciences pures et sciences santé)
1980-1983	CÉGEP D'ALMA D.E.C. en technologie agricole
Langue première	UNIVERSITÉ LAVAL, études en langue française CÉGEP DE STE-FOY, cours de français écrit et littéraire.
Langue seconde	UNIVERSITÉ LAVAL, programme spécial de langue anglaise niveaux 3 et 4 UNIVERSITÉ DU QUÉBEC, anglais 1001, 1002, 1003 et 1004 ATELIERS DE CONVERSATION ANGLAISE DU QUÉBEC INC. cours niveau avancé II.
Langue étrangère	UNIVERSITÉ DU QUÉBEC, cours d'espagnol 1001.
Technique	Séminaires de stratégie de recherche avancée pour interrogation de serveurs de bases de données : DIALOG, QUESTEL, ORBIT, DATASTAR, CAN/OLE, INSIGHT, FOODLINE, etc. Formations particulières sur les brevets, leur interprétation, leur recherche au sein des banques de DERWENT, CLAIMS, INPADOC, JAPIO, etc. Formations sur l'utilisation optimale de L'INTERNET en agro-alimentaire.

Cours spéciaux en vente, service à la clientèle, gestion des priorités, rôle conseil et prise des besoins, qualité totale, etc.

Journées d'information et de perfectionnement technique sur : INTERNET, les nouveaux pathogènes, l'étiquetage nutritionnel, le commerce international des denrées alimentaires, les normes ISO 9000 en alimentaire, les protéines fonctionnelles, les amidons modifiés, l'irradiation des aliments, le développement durable dans le secteur bioalimentaire,les neutraceutiques, HACCP «principes généraux», HACCP «la mécanique du système», etc.

Sessions de formation sur DOS, W-P 5,0, W-P 5,1, NATUREL, LOTUS 1-2-3, WINDOWS, WORD, etc.

EXPÉRIENCE

1989- CENTRE DE RECHERCHE INDUSTRIELLE DU QUÉBEC

Technicien senior en technologie et données industrielles au sein de la Direction de l'information industrielle et technologique
Spécialisation : Industries agro-alimentaire.

- Recherche, analyse et diffusion de l'information technologique et industrielle.
- Mise en place pour la petite et grande entreprise de plans de surveillance continue de l'information technologique et commerciale.
- Recherche de normes, de brevets.
- Service d'aide technique auprès de consultants canadiens en poste à l'étranger (technologies adaptées au milieu).
- Recherches de procédés, de protocoles expérimentaux, de nouvelles technologies, de nouveaux produits.
- Recherches d'équipements, de matières premières, de fournisseurs.
- Dossiers : étude de faisabilité, profil d'intérêts, ...
- Recherches approfondies sur banques de données informatisées.

1988-1989 MINISTÈRE DE L'AGRICULTURE, DES PÊCHERIES ET DE L'ALIMENTATION DU QUÉBEC

Inspecteur en alimentation au niveau des produits carnés; région agricole 04.

1987

Centre spécialisé des Pêches,
Collège de Grande-Rivière, Gaspésie

Élaboration d'un plan de cours et formation des inspecteurs provinciaux et des contrôleurs de la qualité devant oeuvrer dans les usines de transformation de produits marins.

1986-1988

Ministère de l'Agriculture, des Pêcheries et de l'Alimentation du Québec

Inspecteur en alimentation au niveau des produits marins; secteurs Basse, Moyenne et Haute Côte-nord.

1985-1986

Groupe Biocontrôle

Technicien conseil en fertilisation et entretien.

DIVERS

1996-

Participe à la mise en place des outils et élabore la stratégie de recherche d'information pour alimenter, sur une base continuelle, les veilleurs du CVC Chimie sur le sujet des composés chimiques d'origine végétale.

1996

Anime les rencontres et présente les services en information du CRIQ lors de la 4e Édition du Carrefour des biotechnologies du Québec - 1996, St-Hyacinthe.

1996

Réalise une investigation en territoire coréen : discussions d'affaires, avec les représentants technique et commercial, aux bureaux chef des firmes Miwon Farm Co., Ltd. et Korea Livestock Trading Corporation; analyse de la situation avec les officiels de la Délégation du Québec et de l'Ambassage canadienne en place à Séoul; visites organisées des principaux points de vente pour la cueillette de données (recherche et analyse d'information stratégique et technologique pour clients industriels).

1996

Réalise une investigation en territoire nippon : discussions d'affaires, avec les représentants technique et commercial, aux bureaux chef des firmes Canada Beef Export Federation, Japan Meat Conference, Japan Ham and Sausage Processors Cooperative Association, Japan External Trade Organisation, Japan Meat Traders Association, Ajinomoto Co., Inc., Kanebo, Ltd, Takanashi Milk Products Co.,

	Ltd., Takanashi Milk Products Sales Co., Ltd., Morinaga Milk Industry Co., Ltd., Kyodo Milk Industry Co., Ltd, Nutrition Science Institute Meiji Milk Products Co., Ltd.; couverture du salon alimentaire internationale FOODEX JAPON 1996; visites organisées de six principaux points de vente au détail pour la cueillette de données (recherche et analyse d'information stratégique et technologique pour clients industriels).
1995	Forme, dans les bureaux du SENAI de l'État du Pernambuco (Recife, Brésil) et du CERTA (Pétrolina, Brésil), les équipes techniques en place appelées à offrir des services d'information industrielle et technologique aux industries agro-alimentaire du Nord-Est du Brésil. Présente des séminaires et rencontres les responsables d'organismes brésiliens intéressés à la diffusion d'information industrielle et technologique: CIET (Rio), CIAT (Brasilia), IBICT (Brasilia), SEBRAE (Brasilia).
1995-1996	Oeuvre, en collaboration avec le CINTECH AA, l'Université Laval et le CRDA, à la mise en place des structures et à l'opérationnalisation du Réseau de veille stratégique bioalimentaire.
1994	Présente une conférence sur l'évolution et les tendances technologiques internationales dans le secteur des additifs, lors du colloque sur les additifs alimentaires : une occasion d'affaires; organisé pour les industriels de la chimie, des ingrédients et de la transformation alimentaires par le groupe de travail sur les additifs alimentaires (CRIQ, MAPAQ, CRDA, Santé-CANADA et MICST).
1994	Réalise une investigation en territoire français : discussions d'affaires, avec le docteur J.L. Maubois, directeur de recherche à l'INRA de Rennes, les représentants techniques et commercials de l'Association de la transformation laitière française, le chef du Bureau des industries laitières françaises; couverture des salons alimentaires internationaux SIAL, GIA, MATIC et SIEL, FRANCE (recherche d'information stratégique et technologique pour clients industriels).
1994	Réalise une investigation en territoire britannique : couverture de l'exposition alimentaire internationale FIE, EUROPE, ANGLETERRE (recherche d'information stratégique et technologique pour clients industriels).
1994	Réalise une investigation en territoire nippon : couverture de l'exposition alimentaire internationale FOODEX JAPON 1994, rencontre avec la direction du Japan Food Industry Center (recherche d'information stratégique et technologique pour clients industriels).

1993-	Travaille à la mise en place des produits touchant l'analyse continue de l'information concurrentielle, commerciale, environnementale et technique (veille technologique).
1992-	Élabore les structures d'accueil, recueille les informations techniques, planifie les visites, s'occupe du suivi, participe à la formation, etc. lors de la prise en charge de stagiaires étrangers (Maroc, Brésil, Rwanda, Mali, Mauritanie, Trinidad and Tobago, Ghana, Côte-d'Ivoire, etc.).
1991-1992	Collabore avec le journal «Pêche Impact». Rédaction de la rubrique Nouveaux produits et Nouvelles technologies.
1991	Anime les rencontres et présente les services en information du CRIQ au Congrès annuel de l'ICSTA, Montréal.
1991	Donne une conférence, portant sur les nouveautés rencontrées à ANUGA 1991, aux membres de l'ICSTA du chapitre de Québec.
1991	Réalise une investigation en territoire allemand : couverture de l'exposition alimentaire internationale ANUGA 1991, RFA (recherche d'information technologique pour clients industriels).
1990	Anime les rencontres et présente les services en information du CRIQ à la Soirée des fournisseurs de l'ICSTA, Montréal.
1990	Réalise une investigation en territoire américain : couverture de l'exposition alimentaire internationale «Boston Seafood Show», USA (recherche d'information technologique pour clients industriels).

ASSOCIATIONS PROFESSIONNELLES ET AUTRES

1994-	Membre de la Fondation du Conseil des gouverneurs du Centre de recherche et de développement sur les aliments (CRDA).
1994-	Membre de l'Association des diplômés de sciences et technologies des aliments de l'Université Laval (ADISTA).
1995-1996	Membre du conseil d'administration du Centre d'innovation technologique agro-alimentaire (CINTECH AA).
1996-	Membre de l'Association des manufacturiers (AMPAQ).

Montréal, le 24 février 1997

Centre de Recherche Industrielle du Québec
Parc technologique du Québec métropolitain
333 rue Franquet, Case postale 9038
Sainte-Foy (Québec)
G1V 4C7

Par télécopieur et par courrier

Monsieur Claude Raymond,

Cette lettre a pour objectif de solliciter l'expertise du CRIQ en vue d'effectuer une recherche sur les moyens technologiques nécessaires afin d'extraire une couche d'argile très sensible du sous-sol de lots situés à Baie Saint-Ludger sur la péninsule Manicouagan de la Côte Nord du Québec.

L'extraction de l'argile représente une autre phase du dossier que j'ai déjà présenté au CRIQ le 3 décembre 1992 et qui avait alors été soumis à Monsieur Richard Voyer, Ph.D. qui y a fait suite par lettre le 22 décembre 1992. Cette lettre a été déterminante dans la poursuite de mon projet parce que Monsieur Voyer y a tracé les étapes à suivre pour le concrétiser :

- déterminer les applications potentielles de l'argile et les propriétés requises ;
- comparer les propriétés de l'argile commercialisée avec l'argile de Baie Saint-Ludger ;
- sélectionner les applications prometteuses considérant les aspects techniques, économiques et environnementaux de même que le marché potentiel ;
- évaluer les méthodes d'extraction de l'argile ;
- évaluer les procédés d'extraction en considérant les applications retenues ;
- réaliser une étude de faisabilité visant la mise sur pied d'un centre de thalassothérapie à Baie Saint-Ludger, sur la Côte Nord.

Jusqu'à maintenant les trois premières étapes sont, en partie, réalisées. Le coup d'envoi a été donné par l'élaboration d'un travail de recherche sur banque de données informatisées effectuée par Madame Chantal Giroux du CRIQ du Groupe des matériaux et procédés. Par l'intermédiaire du CRIQ, j'ai été référée au Conseil national de recherche du Canada (CNRC), Programme Pari, lequel a subventionné cette recherche. Cette dernière portait sur les utilisations commerciales et industrielles de l'argile dans deux grands secteurs d'activité : la cosmétologie et la médecine. Des documents issus de cette recherche m'ont été transmis ainsi que les comptes rendus des converversations les plus pertinentes engagées auprès de manufacturiers de produits cosmétiques et de produits pharmaceutiques ou biomédicaux. De ces documents et conversations téléphoniques, Madame Giroux en ressort que :

- le marché de la cosmétologie semble le plus accessible à cause de la place déjà acquise qu'occupe l'argile dans ce secteur d'activité ;
- le secteur de la santé demeure une avenue qui devra être davantage approfondie au Québec

étant donné que, du côté de l'Europe, il y a déjà une ouverture certaine pour cette matière première ;

❀ le potentiel du produit de l'argile a assurément une place sur le marché.

La phase suivante a consisté à présenter une demande de permis de recherche de substances minérales de surface au Service des titres miniers, Ministère des Ressources naturelles (MER) que j'ai obtenue et renouvelée sur 580 hectares de terrain afin d'étudier et caractériser l'argile (Voir copies de 2 segments de cartes géographiques ci-incluses qui situent l'emplacement des permis de recherche à Baie Saint-Ludger).

Par la suite, une étude de marché, des forages, des analyses de laboratoire, des rencontres et contacts avec les experts concernés ainsi que la consultation et la production d'une abondante documentation ont permis la reconnaissance *d'ARGILE EAU MER* par le Ministère du Revenu du Canada comme entreprise pouvant bénéficier de crédits d'impôts à la recherche scientifique et du développement expérimental. Soulignons les conseils et recommandations de Monsieur Alain Andersen du CNRC.

La prochaine étape vise une étude de faisabilité concernant l'extraction de l'argile à Baie Saint-Ludger d'autant plus que le MER offre une subvention pour un Programme d'assistance aux études technico-économiques et travaux d'expérimentation. **C'est ce qui m'amène à demander, de nouveau l'assistance du CRIQ pour produire cette étude de faisabilité.**

Comme cette demande d'assistance financière doit être présentée au MER avant le 31 mars 1997 et que je dois bénéficier d'un certain temps pour la réaliser, je souhaiterais avoir la réponse du CRIQ le plus rapidement possible. Cette réponse concerne les études nécessaires à faire pour trouver les moyens d'extraction les plus écologiques et les plus sécuritaires pour entreprendre l'extraction de l'argile de Baie Saint-Ludger. Elle doit donc contenir un devis d'étude c'est-à-dire une estimation des coûts associés à ces procédés technologiques et aux études pour les déterminer. Il est évident que ce programme de coûts peut être établi par étapes. Les moyens d'extraction ayant été déterminés, la recherche sur les produits pourra alors commencer.

Pour vous permettre d'avoir un aperçu du travail qui a été accompli depuis Juillet 1993, je joins à cette lettre le document qui décrit le travail de recherche pour le développement de produits d'argile qui a été présenté au MRC pour acquérir des crédits d'impôt à la recherche scientifique et au développement expérimental. Vous pourrez également prendre connaissance des subventions gouvernementales déjà obtenues, y lire la description générale du projet en terme d'objectifs scientifiques et technologiques ainsi que découvrir la méthode qui a été utilisée.

À la lecture de ce document vous constaterez le travail qui a été réalisé et celui qui reste à faire. Il est important de savoir que ce texte est construit autour de *3 grandes catégories de recherches qui sont la caractérisation de l'argile, la transformation de l'argile en produits thérapeutiques et cosmétiques et finalement les modalités d'exploitation.* Celles-ci se retrouvent à la fois dans le chapitre traitant de l'avancement scientifique et technologique recherché et dans celui portant sur les incertitudes technologiques. Vous aurez une vision plus globale de ce qui a été déjà accompli dans la partie chronologique des événements.

Pour en savoir d'avantage sur les principales recherches, études, programmes et rapports produits sur l'argile de même que sur les ouvrages théoriques et techniques consultés et finalement sur les échanges avec des spécialistes vous n'aurez qu'à vous référez à la dernière partie du document.

Si toutefois ce rapport de recherche était insuffisant ou encore si vous voulez examiner d'autres écrits n'hésitez pas à m'en faire la demande, cela me fera plaisir d'y répondre le plus rapidement possible.

Ces études sur la faisabilité touchent la partie la plus concrète et la plus sensible de mon projet. C'est avec beaucoup d'enthousiasme que je l'entreprends et que je demande l'assistance du CRIQ pour la réaliser.

Je vous remercie de votre attention et soyez assuré, Monsieur Raymond, de mon entière disponibilité.

Denise Saulnier
pour ARGILE EAU MER
5594 Waverly,
Montréal (Québec)
H2T2Y1
Tél. : (514) 273-3573
Fax : (514) 273-9373

p.j. Demande de réclamation : programme d'incitation concernant des projets de recherche scientifique et de développement expérimental

2 segments de cartes géographiques

DS/mb

CRIQ

CENTRE DE RECHERCHE
INDUSTRIELLE DU QUÉBEC

Le 30 septembre 1997

Madame Denise Saulnier
ARGILE EAU MER
554, rue Waverly
Montréal (Québec) H2T 2Y1

OBJET : ***Seconde rencontre avec M. Denis Lessard, ing., M.Sc.***

Madame,

Voici, comme je vous en avais informé, un compte rendu des points importants soulevés lors de l'analyse de l'ensemble des informations techniques que vous nous avez soumises à ce jour. Ces données furent examinées par M. Denis Lessard, chargé de projet au Centre de recherche minérale. Par cet exercice, nous tentions, tous deux, de nous assurer que vous possédiez toutes les données de base nécessaires à la poursuite de la présente investigation. Dans le cas contraire, nous devions identifier les démarches à entreprendre de manière à atteindre les résultats souhaités.

La consultation des écrits sur lesquels nous nous penchions a mis clairement en lumière le manque de données techniques nécessaires à la prise de vos décisions. En effet, il est difficile, voire inutile, de songer à exploiter pareils sites sur la base des résultats fragmentaires obtenus à l'aide des deux forages effectués sur le permis de recherche de substance minérale numéro 0002041. L'investigation requise nécessite une série d'actions sur l'ensemble du territoire convoité et touche bon nombre de paramètres tous aussi importants les uns que les autres. Ce n'est pas la qualité des tests effectués qui est ici en cause mais, surtout, le nombre limité des échantillons prélevés. Un tel échantillonnage ne permet pas d'obtenir un portrait réel de la situation. Trop d'inconnus demeurent, inconnus qui empêchent d'évaluer les dépôts d'argile à leur juste valeur. Ces inconnus pourraient compromettre le succès de votre entreprise par des investissements en temps et en argent inappropriés.

À titre d'exemple de paramètre, les commentaires provenant de M. André Chagnon du Centre géoscientifique de Québec (C.G.Q.) et des géologues du F.R.E.M. indiquent qu'il s'agit d'une argile au sens granulométrique du terme puisqu'elle est composée majoritairement de débris rocheux. Une trop grande variation de cette granulométrie peut jouer sur la qualité de la matière première et sur son utilisation. Il y a une limite critique à ne pas dépasser. Généralement, les farines de roches possèdent peu de propriétés thérapeutiques. Il est donc nécessaire de connaître la proportion des vrais minéraux argileux ici en présence.

Il n'y a pas de grandes nouveautés à propos des gestes à poser. Ces derniers vous ont été présentés dans la lettre que M. Denis Lessard m'a adressée le 28 août dernier. Les lignes qui suivent visent toutefois à en préciser davantage la nature et la portée.

En ce qui a trait à la cartographie de surface, aux sondages géophysiques et aux forages, les tests doivent être réalisés par des firmes spécialisées en la matière. De plus, ces dernières doivent être reconnues pour leur expertise dans les sédiments meubles.

La première action vise à dresser une bonne cartographie de surface et de tranchées. Les travaux et les coûts approximatifs qui en découlent se subdivisent de la façon suivante :

- cartographie sur le terrain : durée : une semaine; coût : 2 000 $
- interprétation des cartes : 2 000 $
- travaux de surface : excavation en surface, etc. : 2 000 $
- prise d'échantillons de surface et leur analyse : nombre : 100 échantillons; coût : 5 000 $

De la conclusion tirée de la cartographie de surface, une évaluation de l'étendue réelle du gisement doit être entreprise. Des tests de sismique/réfraction permettront d'obtenir plus de détails sur la situation spatiale et sur l'épaisseur de ce, ou ces, dépôt(s) d'argile. Les coûts minimaux, engendrés par ces travaux, sont d'environ 4 000 $.

Des données cumulées lors des actions entreprises antérieurement, il sera possible de déterminer le nombre ainsi que la localisation des forages en profondeur à réaliser. Ces derniers apporteront des précisions sur la composition, le pH, la granulométrie, la teneur en eau, etc. des carottes ainsi recueillies. De plus, ces prélèvements apporteront plus de précision sur la profondeur du gisement et sur l'emplacement de la nappe phréatique. Ces renseignements influenceront grandement la manière dont sera exploité ce dépôt d'argile (pente des abords, mode d'extraction par pompes ou pelles sur pneumatiques, etc.) et le niveau de difficulté pour y parvenir (pompe de surface, puits d'assèchement, mode de stabilisation, etc.). La somme à débourser pour une trentaine de ces forages, exécutés à l'aide d'un tube carottier double et à une profondeur moyenne de 35 pieds, peut atteindre facilement les 25 000 $ (36 $/pied linéaire).

Puis, les carottes ainsi extraites subiront un ensemble d'analyses visant à les caractériser et à les **comparer avec vos propres critères de qualité.** Plusieurs analyses minérales sont déjà clairement identifiées pour les argiles. Pour ces 30 échantillons, il faut prévoir un montant d'environ 10 000 $.

Une fois l'ensemble de démarches complétées, toute l'information doit être présentée à un bureau d'ingénierie expérimenté en la matière. Ce dernier mettra tous ces renseignements en relation et tirera des conclusions en fonction de la quantité, de la qualité, du mode d'exploitation et de la viabilité du gisement d'argile de Baie-Saint-Ludger.

Bien que ces travaux peuvent sembler onéreux à première vue, leur exécution s'avère incontournable pour vous assurer de la viabilité de ce projet.

Nous avons tenté de vous présenter un portrait succinct mais juste de la situation. Si des interrogations demeurent, n'hésitez pas à communiquer avec nous pour obtenir plus de précisions.

Nous vous prions de croire, Madame, à notre entière collaboration et à l'expression de nos meilleurs sentiments.

Serge Huppé
Responsable de projet
Direction de l'information
industrielle et technologique

p.j. : tarification pour analyse minérale

c.c. : Claude Raymond, CRIQ
Denis Lessard, C.R.M.
Fichier central (n° PE 20478)

CRIQ

CENTRE DE RECHERCHE
INDUSTRIELLE DU QUÉBEC

Le 10 septembre 1997

Madame Denise Saulnier
ARGILE EAU MER
5594, rue Waverly
Montréal (Québec) H2T 2Y1

Objet : Réorientation de nos actions; Projet PE-20478

Madame,

Comme nous en avions soulevé la possibilité lors de nos discussions antérieures, je vous confirme, par la présente, que nous reconduisons la date de remise des résultats des travaux en cours, dans le cadre de l'étude citée en rubrique, dans la semaine du 14 novembre prochain.

Ce report s'explique, en partie, par la période estivale qui s'avérait peu propice à la réalisation des contacts que nous avions planifiés antérieurement. Mais ce choix s'avère surtout dicté par les échanges que nous avons eus avec M. Denis Lessard, du Centre de recherche minérale du Québec. Ces entretiens ont mis en lumière un nombre important de paramètres à connaître avant de songer à pousser plus avant nos contacts hors Québec. En effet, un certain nombre de données techniques, visant la caractérisation exacte de la zone d'exploitation de votre dépôt d'argile, semblent incomplètes. Sans ces dernières, il sera difficile de recueillir les informations recherchées sur la stabilisation du site ainsi que sur les équipements nécessaires à son exploitation commerciale. La pertinence des données souhaitées est donc tributaire de la connaissance des informations techniques qui semblent nous faire présentement défaut.

Nous nous accordons un temps de réflexion afin de faire le point sur la situation pour ainsi déterminer la meilleure orientation à donner au présent dossier.

Veuillez, s'il y a lieu, nous aviser de tout désaccord avec ces modalités d'ici le 21 septembre. Autrement, nous considérerons alors que l'échéancier vous convient. Pour tout commentaire, veuillez communiquer avec M. Claude Raymond qui assurera le suivi de ce dossier au cours des deux prochaines semaines.

.../2

J'espère le tout conforme à vos attentes. Si d'autres renseignements vous étaient nécessaires, n'hésitez pas à communiquer avec moi ou M. Raymond au 1-800-667-2386, poste 289 ou 222.

Recevez, Madame, mes salutations les plus cordiales.

Serge Huppé, R.P.
Direction de l'information
industrielle et technologique

SH/jad

c. c. : Claude Raymond, CDT, CRIQ
Fichier central (n° PE 20478)

TECHNIQUES D'EXTRACTION
DES ARGILES SOUTERRAINES

Dossier Client n° 700-PE-20478
Rapport technique n° RT-20478

NOVEMBRE 1997

CLIENT : ARGILE EAU MER
5594, rue Waverly
Montréal QC H2T 2Y1

À l'attention de madame Denise Saulnier
Tél. : (514) 273-3573
Baie Saint-Ludger (418) 567-8127

C.D. : Claude Raymond

RESPONSABLE DE PROJET :

Serge Huppé
Direction de l'information
industrielle et technologique

DIRECTEUR :
Claude Jacques

Sainte-Foy, le 25 novembre 1997

CRIQ
CENTRE DE RECHERCHE
INDUSTRIELLE DU QUÉBEC

TABLE DES MATIÈRES

1.0 CONTEXTE

Consciente du potentiel économique que représentent les argiles marines ou fluviales de Baie Saint-Ludger, M^{me} Denise Saulnier, de la compagnie ***Argile eau mer***, travaille depuis plusieurs années à la concrétisation de son projet d'extraction et de transformation de l'argile en produits cosmétiques et thérapeutiques.

M^{me} Saulnier désire identifier et évaluer les méthodes d'extraction pouvant convenir le mieux à l'exploitation des argiles souterraines présentes à Baie Saint-Ludger. M^{me} Saulnier souhaite également faire le point sur les technologies ou méthodes respectueuses du milieu, existantes ou à l'étude, susceptibles d'être utilisées dans le cadre de ses opérations d'extraction.

Pour orienter ses actions et garantir la réussite de son entreprise, M^{me} Denise Saulnier se doit de trouver réponse aux questions suivantes : Quelles sont les approches mises de l'avant à l'échelle internationale au cours des dernières années? Existe-t-il des données techniques particulières portant sur leur utilisation à l'échelle industrielle? Quels peuvent être leurs coûts moyens d'obtention? Quels sont les moyens susceptibles de réduire l'impact négatif de ces techniques sur les sols sensibles et friables ? Quelles sont les entreprises privées ou les experts qui ont oeuvré à leur élaboration? Quels sont les intervenants privés ou publics disposés à partager leur savoir-faire? Etc.

C'est dans le but de trouver réponse à ces interrogations et d'accompagner M^{me} Saulnier dans ses démarches que les services de la Direction de l'information industrielle et technologique du *Centre de recherche industrielle du Québec (CRIQ)* furent retenus.

2.0 OBJECTIF

Cette investigation a pour objectif principal d'assister M^{me} Saulnier dans la cueillette de données lui permettant de prendre connaissance des éléments pouvant orienter ses décisions. De manière plus précise, il s'agit d'identifier les moyens d'extraction (méthodes ou équipements) les plus efficaces et les moins dommageables pour le milieu. À partir de ces éléments, M^{me} Saulnier sera à même de juger quelles sont les implications techniques des systèmes à l'étude et, par le fait même, de connaître les orientations prises par la recherche et l'industrie. Sur ces bases, il lui sera possible de prendre une décision éclairée quant à la suite à donner à ce dossier, soit le transfert de technologie ou de savoir-faire, l'achat d'équipements, la conception d'appareils dédiés, etc.

3.0 DESCRIPTION DES TRAVAUX RÉALISÉS

3.1 RECHERCHE SUR MÉDIAS ÉLECTRONIQUES ET DANS LA DOCUMENTATION

Banques de données informatisées

Cette première recherche d'information porte sur les banques de données couvrant le domaine de la propriété intellectuelle et celui plus large des écrits à caractère technique et commercial. Cette investigation en est une internationale et couvre majoritairement la documentation publiée au cours des cinq dernières années.

Nous avons, dans un premier temps, pris connaissance des données que M^{me} Saulnier a mises à notre disposition. Sur la base de ces informations, nous avons retenu les banques les plus aptes à fournir les informations souhaitées, parfait les stratégies de recherche et les avons exécutées. De ces actions, il fut conservé plusieurs centaines de résumés d'articles ayant un intérêt dans le présent dossier.

Un tri a par la suite été accompli afin de ne garder que les écrits apparaissant comme les plus pertinents. Des informations plus complètes, sur chacun des documents préalablement retenus, ont été recherchées.

Sites WWW sur Internet

Au sein des informations recueillies sur banques de données, nous avons ciblé bon nombre d'institutions universitaires, d'entreprises, d'organisations publiques ou privées et d'experts étrangers avec lesquels nous désirions communiquer subséquemment. Nous avons donc recherché et consulté leur site WWW, lorsque disponible, vérifié les ouvrages identifiés à leur nom, cumulé plus de données sur les entités ou les personnes ayant eu des relations avec leurs travaux, etc. Nous désirions, de cette manière, en connaître plus sur ceux qui ont gravité autour des centres d'intérêt que sont les technologies d'extraction des argiles sensibles et la stabilisation des sites d'exploitation.

3.2 IDENTIFICATION D'EXPERTS OU D'ORGANISMES RECONNUS POUR LEUR COMPÉTENCE

Dans le but d'initier des échanges auprès de gens reconnus pour leur compétence dans le domaine, et ce, dans les pays visés par notre étude (Europe, Canada, Nouvelle-Zélande, États-Unis et Australie), l'ensemble des données cumulées à l'étape 3.1 fut consulté afin d'y puiser les contacts les plus utiles à initier en premier lieu. Ceci inclut également les renseignements figurant à l'intérieur des brevets que nous avions identifiés et conservés pour leur pertinence. Le tout fut complété par la consultation de répertoires spécialisés recensant l'ensemble des institutions de recherches, ou des bureaux d'ingénieurs-conseils spécialisés dans le secteur qui nous intéresse. L'objectif de ces démarches était de recenser les meilleurs acteurs avec lesquels transiger pour en savoir plus sur les approches à l'étude et les orientations prises par la recherche et l'industrie à l'échelle internationale. Au total, 164 experts ou organismes ont ainsi été identifiés par notre personnel.

3.3 IDENTIFICATION DE FOURNISSEURS D'ÉQUIPEMENTS

Par ces contacts, sous souhaitions retracer, à l'aide de guides d'achat et de répertoires spécialisés, les fournisseurs d'équipements les plus susceptibles de nous proposer les technologies ou méthodes respectueuses du milieu et pouvant convenir à l'exploitation des argiles souterraines présentes à Baie Saint-Ludger.

Ces démarches couvraient les principaux pays européens reconnus pour leur expertise dans le domaine ainsi que les sociétés actives dans ce domaine, présentes sur le territoire nord-américain.

Cette investigation ne s'est pas restreinte qu'aux simples manufacturiers de matériel destinés à l'extraction des terres argileuses. Notre recherche englobait également des entreprises offrant des équipements industriels pour des utilisations connexes. Avec une telle approche, nous étions en mesure de prendre connaissance de voies de solution émanant de différentes sphères de l'industrie.

Cette investigation a nécessité des travaux de même nature que ceux décrits au point 3.2. Dans le cadre de cette recherche 67 fabricants ou fournisseurs ont ainsi été localisés par notre service.

4.0 RÉSULTATS OBTENUS

Des centaines de références que nous avons consultées, seules les plus pertinentes furent retenues pour vous être présentées. Nous n'aborderons pas tous ces points en détail au sein de ce bref rapport. Seuls la correspondance et les écrits les plus importants seront ici discutés. **Nous vous invitons à vous référer aux annexes pour de plus amples détails. Les informations périphériques qu'elles contiennent sauront apporter d'autres données qui vous seront profitables.**

Suite aux actions décrites aux points 3.1, 3.2 et 3.3, et ce, tel que prévu au plan de travail PT-20478, nous devions initier un nombre considérable de contacts afin de compléter les données déjà en notre possession et de valider les avenues de solution auprès de gens reconnus pour leurs connaissances dans le domaine. Dans un premier temps, nous escomptions acheminer, aux personnes ou organismes préalablement identifiés, une lettre personnalisée par télécopieur, courrier électronique ou courrier postal. Au sein de notre correspondance, nous leur mentionnions le pourquoi de notre requête et les données que nous désirions recevoir d'eux. Puis des discussions plus étoffées, avec les meilleurs acteurs nationaux et internationaux, nous auraient permis de cumuler le maximum d'information pouvant orienter M^{me} Denise Saulnier dans son projet.

Pour nous assurer de présenter l'ensemble des paramètres techniques, nécessaires à la bonne compréhension de notre demande, nous avons discuté du contenu de notre requête avec M. Denis Lessard, ingénieur au Centre de recherche minérale du Québec. Ce dernier, possédant une expérience dans l'extraction et la valorisation des argiles, fut identifié comme expert lors des actions décrites à l'étape 3.2 du présent rapport. Bien que l'ensemble des actions que notre direction a entrepris jusqu'à maintenant s'avérait justifié, il est apparu, comme nous vous l'avons par la suite exposé au sein de nos correspondances des 28 août et

30 septembre derniers, que les déductions avancées sur la base des deux forages effectués sur le permis de recherche de substance minérale numéro 0002041, ne permettaient pas de dresser une représentation exacte de la situation. Trop d'inconnus demeurent, inconnus qui empêchent d'évaluer la nature et la valeur réelle des dépôts d'argile en question. Ce manque de données, touchant la caractérisation de l'ensemble du site d'exploitation de Baie Saint-Ludger et la méconnaissance de la nature exacte des argiles qu'il pourrait contenir, est susceptible de compromettre le succès de cette entreprise par des investissements en temps et en argent inappropriés.

De l'avis même de M. Lessard, il est pour l'instant impossible de recevoir des avis d'experts ou de manufacturiers sans en connaître davantage sur le tonnage total des réserves d'argile de type commercial en présence, le niveau de production désiré (t.m./jour), les propriétés physico-chimiques exactes de l'argile recherchée, l'environnement physique de surface, la nature des sols contenant l'argile, les contraintes environnementales spécifiques et leur ampleur, les dimensions, la forme et la position des dépôts d'argile par rapport à la surface du sol, etc.

À la lumière de ces constatations, et suite aux entretiens que nous avons eus M^{me} Denise Saulnier, M. Claude Raymond, conseiller en développement technologique au CRIQ, et moi-même, le 8 octobre dernier, il a été convenu, d'un commun accord, de suspendre les actions entreprises dans le cadre du présent dossier et de clore l'actuel projet. Néanmoins, l'ensemble des données cumulées jusqu'à ce jour demeure la propriété de la demanderesse. Ces informations seront de nouveau utiles une fois mieux définies la totalité des paramètres de base à connaître, touchant le dépôt d'argile sensible de Baie Saint-Ludger. Ces données en main, le CRIQ, ou tout autre intervenant ayant les compétences recherchées, pourra relancer le dossier sur des bases solides.

Nous avons, au sein de ce mandat, recensé l'information, trouvé de plus amples données pour en évaluer la pertinence et établir divers contacts pour obtenir l'avis de professionnels du milieu et déceler les acteurs futurs avec lesquels M^{me} Denise Saulnier pourra transiger. Nous avons donc suivi et réalisé les étapes décrites au sein de notre proposition du 5 mars 1997.

Même si le présent travail ne se veut pas exhaustif, il regroupe le maximum d'information qu'il nous a été donné de cumuler sur le sujet, dans le cadre des contraintes rencontrées et des budgets qui nous ont été alloués par M^{me} Saulnier. Nous sommes convaincus qu'il sera un outil précieux dans la planification des actions à venir.

ANNEXE A

BREVETS RETENUS (RÉSUMÉ)

United States Patent **4,759,664**

Deal **Jul. 26, 1988**

Method of building or restoring marshes and beaches

Inventors: **Deal; Troy M.** (277 Trismen Ter., Winter Park, FL 32789).

Appl. No.: **724,251**

Filed: **Apr. 17, 1985**

Related U.S. Application Data

Continuation-in-part of Ser No. 681,071, Dec. 12, 1984, which is a continuation of Ser. No. 579,805, Feb. 17, 1984, abandoned, which is a continuation of Ser. No. 221,219, Dec. 30, 1980, abandoned.

Intl. Cl. :	**E02D 3/00**, E02D 17/00, E02F 5/00, E02F 3/88
Current U.S. Cl.:	405/258; 37/195; 37/317; 405/117; 405/303
Field of Search:	405/15, 52, 74, 217, 258, 107, 222, 263; 299/9; 37/54, 195, 66

References Cited | [Referenced By:]

U.S. Patent Documents

1,404,112	Jan., 1922	Goebl et al.	405/258
1,844,348	Feb., 1932	Claybourn et al.	406/97
2,158,046	May, 1939	Prendergast	405/74
2,191,845	Feb., 1940	Bretting	405/258
2,818,682	Jan., 1958	Finn	405/258
2,926,437	Mar., 1960	Ellicott, Jr.	37/72
3,521,387	Jul., 1970	Degelman	37/66
3,638,432	Feb., 1972	Schoonmaker	405/74
3,786,639	Jan., 1974	Pineno et al.	405/267
3,842,607	Oct., 1974	Kelseaux et al.	405/217
4,261,117	Apr., 1981	Van Der Peyl	37/58
4,397,587	Aug., 1983	Op den Velde et al.	405/217
4,523,879	Jun., 1985	Finucane et al.	405/217
4,567,731	Feb., 1986	Horan	405/217
4,614,458	Sept., 1986	Austin	405/74

Other References

J. G. Riley, How Imperial Built First Arctic Island, 1974.

Articles from Various Florida Newspapers, 1979.

"New Machine Clears Weed-Choked waterways", North Port News, Feb. 15, 1979.

Primary Examiner: Reese; Randolph A.
Assistant Examiner: Ricci; John A.
Attorney, Agent or Firm: Beaman & Beaman

Abstract

The invention pertains to a method for the building or restoration of marshes and beaches wherein a slurry of solid material and water is formed at one location and pumped to a remote location for uniform distribution of the slurry over a large area to substantially increase the elevation for the purpose of building a marsh, restoring a beach, or the like. The slurry is distributed by a high pressure nozzle uniformly directing a spray which falls in a mist over the area on which the slurry is deposited to produce a significant elevational increase in the area. The nozzle may make alternate directional sweeps, or rotate in a common direction to cover a circular area, with various adjustable vertical angles and pressure variations to control distribution.

16 Claims, 5 Drawing Figures

[USPTO] [CNIDR]

3,080,256	Mar., 1963	Bundy	501/148
3,252,757	May, 1966	Granquist	
3,298,849	Jan., 1967	Dohman et al.	501/148
3,586,478	Jun., 1971	Neumann	
3,666,407	May, 1972	Orlemann	
3,671,190	Jun., 1972	Newuman	
3,844,978	Oct., 1974	Hickson	423/331
3,844,979	Oct., 1974	Hickson	423/331
3,852,405	Dec., 1974	Granquist	423/118
3,855,147	Dec., 1974	Granquist	252/317
3,892,587	Jul., 1975	Abercrombie, Jr.	501/148
3,961,979	Jun., 1976	Abercrombie, Jr.	106/487
4,017,324	Apr., 1977	Eggers	106/487
4,078,941	Mar., 1978	Bundy	106/487
4,359,339	Nov., 1982	Van Fisk et al.	501/127
4,695,402	Sept., 1987	Finlayson et al.	252/315.2
5,015,334	May, 1991	Derrick	162/168.1
5,057,467	Oct., 1991	Croft	106/487
5,075,033	Dec., 1991	Cody et al.	106/487
5,223,098	Jun., 1993	Cluyse et al.	162/181.2
5,266,538	Nov., 1993	Knudson et al.	501/145
5,279,664	Jan., 1994	Robinson et al.	106/487

Foreign Patent Documents

92/11218	Jul., 1992	WO

Primary Examiner: Bell; Mark L.
Assistant Examiner: Marcheschi; Michael
Attorney, Agent or Firm: Klauber & Jackson

Abstract

An aqueous slurry of smectite clay of elevated solids content, comprising an aqueous solution or emulsion of from about 0.5 to about 13% by weight of said slurry of a salt of a low molecular weight amine salt, in which is dispersed from about 10 to 47% by weight of the slurry, of a smectite clay. The amine salt is effective to prevent the smectite from swelling appreciably, whereby the slurry can be shipped and stored without creating a gelling problem. The inhibiting or suppressing effect of the amine salt on the swelling of the clay and on gelling of the slurry is reversible upon subsequent dilution with water, thereby facilitating use of the smectite in typical applications, e.g. as a retention aid in paper making, or as a viscosifier.

30 Claims, No Drawings

United States Patent **5,466,28**
Derr **Nov. 14, 1995**

Material for use as soil stabilizer and as soil substit

Inventors:	**Derr; John D.** (Akron, OH).
Assignee:	**Wessco, Inc.** (Norton, OH).
Appl. No.:	**319,133**
Filed:	**Dec. 5, 1994**

Related U.S. Ap

Division of Ser No. 206,739, Mar. 7, 1994, Pat. No

Intl. Cl. :	**C04B 14/10**
Current U.S. Cl.:	106/487; 106/900; 264/176.1; 405/258; 405/263
Field of Search:	487, DIG. 4, 900; 264/176.1; 405/258, 263

References Cited | [

U.S. Patent D

Re15,829	May, 1924	Er	106/811
3,082,111	Mar., 1963	M	106/286
3,607,339	Sept., 1971	D	106/309
3,661,604	May, 1972	A	106/98
4,523,755	Jun., 1985	T	272/3
4,822,420	Apr., 1989	B	106/74
4,824,810	Apr., 1989	L	501/84
5,175,131	Dec., 1992	L	501/84
5,264,029	Nov., 1993	K	106/287.17

Foreign Patent

36644	Sept., 1981

Primary Examiner: Bell; Mark L.
Assistant Examiner: Marcheschi; Michael
Attorney, Agent or Firm: Renner, Kenner, Greive, Bo

2 of

Abstract

A soil substitute material includes from about 2 to about 9 parts by weight of crushed brick; from about 5 to about 25 parts by weight of a filler material; from about 60 to about 90 parts by weight of raw clay; and, from about 0 to about 3 parts by weight of a hydrating material. The material is compacted at from about 3500 to about 5000 pounds per square inch. A method of preparing a soil substitute includes admixing the components with from about 5 to about 18 parts by weight of water and compressing the hydrated mixture at from about 3500 to about 5000 pounds per square inch.

8 Claims, No Drawings

[USPTO] [CNIDR]

▲

(1 of 1)

United States Patent **5,1**

Patel, et. al. **Sept. 22,**

Drilling fluid additive and method for inhibiting hy

Inventors: **Patel; Arvind D.** (Houston, TX); **McLa**ty, TX).

Assignee: **M-I Drilling Fluids Company** (Houston

Appl. No.: **783,368**

Filed: **Oct. 28, 1991**

Intl. Cl. : **C09K 7/02**

Current U.S. Cl.: **507/131**

Field of Search: **507/131**

References Cited | [

U.S. Patent D

3,127,344	Mar., 1964	De	507/131
3,200,106	Aug., 1965	Di	507/131 X
4,148,736	Apr., 1979	M	507/131 X

Primary Examiner: Stoll; Robert L.
Assistant Examiner: Geist; Gary L.
Attorney, Agent or Firm: Arnold, White & Durkee

Abstr

This invention relates to drilling fluid additives that sup within a subterranean well and to methods for controlling clay swelling during the drill well. Aliphatic polyamines and aliphatic acids react to form polyamides and polya ater soluble, that have molecular weights of less than about 1000, and that ha. The polyamides and polyamino acids are added to water base drilling fluids throughout a well.

When X in the acid is a hydroxyl group, the polyamide llowing general structure: ##STR1## When X in the acid is a halogen such as chl acid products have the following general structure: ##STR2## The drilling flu method of controlling clay swelling provide for improved control of the rheologic g fluids along with an increased environmental compatibility.

12 Claims, 4 Dra

United States Patent **5,558,171**
McGlothlin, et. al. **Sept. 24, 1996**

Well drilling process and clay stabilizing agent

Inventors: **McGlothlin; Raymond E. (Houston, TX); Woodworth; Frank B. (Houston, TX).**
Assignee: **M-I Drilling Fluids L.L.C. (Houston, TX).**
Appl. No.: **232,386**
Filed: **Apr. 25, 1994**

Intl. Cl. : C09K 7/02, E21B 21/00
Current U.S. Cl.: 175/64; 175/65; 175/72; 507/128; 507/129; 507/131
Field of Search: 507/128, 129, 131, 904; 175/64, 65, 72

References Cited | [Referenced By]

U.S. Patent Documents

2,761,835	Sept., 1956	Brown	
2,761,843	Sept., 1956	Brown	
2,873,251	Feb., 1959	Jones	
3,127,344	Mar., 1964	DeGroote	
3,200,106	Aug., 1965	Dickson	
4,782,120	Nov., 1988	Rousset et al.	525/326.6
4,816,551	Mar., 1989	Oehler et al.	528/295.3
4,853,465	Aug., 1989	Cowan et al.	530/506
4,957,639	Sept., 1990	Fox	166/275 X
5,149,690	Sept., 1992	Patel	507/131

Primary Examiner: Suchfield; George A.
Attorney, Agent or Firm: Arnold, White & Durkee

Abstract

The invention relates to clay stabilizing agents for use in an alkaline water-base fluid such as a drilling mud and the use of such clay stabilizing agents in the drilling of wells. The clay stabilizing agent comprises a polyfunctional polyamine reaction product prepared by the reaction of a polyamine base

reactant with urea or a dialkylcarbonate or by reaction with urea and a dialkylcarbonate. The stabilizing agent is subject to subsequent acidification to reduce the pH thereof to a value of about 7 or less. The polyamine base reactant is selected from the group consisting of an aliphatic polyamine, a polyaliphatic polyamine, a heterocyclic polyamine, an alkylalkanol polyamine and mixtures thereof. Specifically, the base reactant comprises an aliphatic polyamine selected from the group consisting of ethylenediamine, diethylenetriamine, tetraethylenetetramine, and tetraethylenepentamine and mixtures thereof. Preferably the base reactant has at least three amino groups and a molecular weight within the range of 100-300 and more preferably 100-200. A low molecular weight alkyl acid phosphate, specifically, ethyl acid phosphate, propyl acid phosphate, butyl acid phosphate and mixtures thereof, can also be used. Preferably this supplement comprises ethyl acid phosphate. The alkyl acid phosphate may be added to the stabilizing agent in an aqueous solution subsequent to acidification of the product.

14 Claims, No Drawings

[USPTO] [CNIDR]

(1 of 1)

United States Patent **5,603,744**
K urner **Feb. 18, 1997**

Process for establishing optimum soil conditions by naturally forming tilth

Inventors: **K urner; Rudolf** (Hessigheimer Strasse 22, D-70437 Stuttgart, DE).
Appl. No.: **211,801**
Filed: **Nov. 15, 1994**
PCT Filed: **Oct. 13, 1992**
PCT No: **PCT/EP92/02356**
371 Date: **Nov. 15, 1994**
102(e) Date: **Nov. 15, 1994**
PCT Pub. No.: **WO93/08143**
PCT Pub. Date: **Apr. 29, 1993**

Foreign Application Priority Data

Oct. 14, 1991 [DE]	41 33 984.3

Intl. Cl. : C05F 3/00, C05F 5/00, C05F 9/04, C05F 11/02
Current U.S. Cl.: 71/9; 71/13; 71/15; 71/23; 71/24; 71/25; 71/62; 71/63
Field of Search: 71/1, 8, 9, 10, 13, 15, 23-25, 62, 63

References Cited | [Referenced By]

U.S. Patent Documents

3,944,408	Mar., 1976	Postrihac	71/13
4,559,073	Dec., 1985	Minato et al.	71/15

Foreign Patent Documents

419899	Feb., 1937	BE
0221219A1	Apr., 1987	EP
0444392A3	Sept., 1991	EP
2023318	Aug., 1970	FR
283369	Oct., 1990	DE

Primary Examiner: Lander; Ferris
Attorney, Agent or Firm: Bardehle, Pagenberg, Dost, Altenburg, Frohwitter, Geissler and Partners

---

Abstract

A process is disclosed for establishing optimum soil conditions by biologically disintegrating minerals in the presence of Ca compunds, clay and protein- and lignocellulose-containing organic vegetable waste, as well as protein-containing organic animal waste. The process includes the following steps: a) finely crushing a mixture of minerals containing at least potassium, magnesium, phosphate and silicate, all in insoluble form; b) subjecting the vegetable and animal organic waste to an usual preliminary crushing step; c) micronizing the organic waste, preferably while homogeneously mixing it with the mixture of minerals; and d) fermenting the mixture of micronized organic waste and finely crushed minerals in the presence of finely crushed Ca-compound and clay, in microbially appropriate conditions.

17 Claims, No Drawings

[USPTO] [CNIDR]

▲

(1 of 1)

(1 of 1)

United States Patent **5,607,902**

Smith, et. al. **Mar. 4, 1997**

Method of treating shale and clay in hydrocarbon f

Inventors: **Smith; Kevin W.** (McMurray, PA); **Tho** aopolis, PA).

Assignee: **ClearWater, Inc.** (Pittsburgh, PA).

Appl. No.: **610,739**

Filed: **Mar. 4, 1996**

Related U.S. App

Continuation of (including streamline cont.) Ser. N , 1993, abandoned.

Intl. Cl. : C09K 7/02

Current U.S. Cl.: 9; 507/121; 507/225; 507/226

Field of Search: 507/119, 120, 225, 226, 121

References Cited | [

U.S. Patent D

2,761,835	Sept., 1956	Brown	252/8.55
4,100,079	Jul., 1978	Sinkovitz et al.	252/8.55
4,225,445	Sept., 1980	Dixon	252/8.55
4,293,427	Oct., 1981	Lucas et al.	252/8.5
4,305,860	Dec., 1981	Iovine et al.	260/29.6
4,374,739	Feb., 1983	McLaughlin et al.	252/8.55R
4,393,939	Jul., 1983	Smith et al.	166/293
4,447,342	May, 1984	Borchardt et al.	252/8.55D
4,455,240	Jan., 1984	Costello	507/119
4,460,627	Jul., 1984	Weaver et al.	427/212
4,476,931	Oct., 1984	Boles et al.	507/119
4,533,708	Aug., 1985	Costello	526/295
4,536,292	Aug., 1985	Matz	210/701
4,652,623	Mar., 1987	Chen et al.	526/287
4,690,996	Sept., 1987	Shih et al.	527/312
4,726,906	Feb., 1988	Chen et al.	252/8.514
4,772,462	Sept., 1988	Boothe et al.	424/70
4,842,073	Jun., 1989	Himes et al.	166/294
5,013,456	May, 1991	St. John et al.	210/734
5,032,295	Jul., 1991	Matz et al.	252/8.51
5,207,924	May, 1993	Reed et al.	210/734
5,209,854	May, 1993	Reed et al.	210/734

Primary Examiner: Tucker; Philip
Attorney, Agent or Firm: Krayer; William L.

Abstract

Swelling and migration of subterranean clay is inhibited during drilling for and stimulation of the production of hydrocarbon fluids, and preparation therefor, by treating said formations with a copolymer of about 5% to about 50% of an anionic monomer such as acrylic acid, methacrylic acid, or 2-acrylamido-2-methyl propane sulfonic acid and the balance a cationic monomer selected from dimethyl diallyl ammonium chloride, or acryloxy or methacryloxy ethyl, propyl or 3-methyl butyl trimethyl ammonium chlorides or methosulfates. Permeability damage to the formation is reduced in the presence of the copolymer; it is particularly effective in spite of the presence of a foaming agent.

15 Claims, No Drawings

[USPTO] [CNIDR]

(1 of 1)

(1 of 1)

United States Patent **5,616,235**
Acar, et. al. **Apr. 1, 1997**

Electrochemical stabilization of soils and other porous media

Inventors: **Acar; Yalcin B.** (Baton Rouge, LA); **Gale; Robert J.** (Baton Rouge, LA).

Assignee: **Board of Supervisors of Louisiana State University and Agricultural and Mechanical College** (Baton Rouge, LA).

Appl. No.: **655,709**

Filed: **Jun. 3, 1996**

Intl. Cl. : C25C 1/22

Current U.S. Cl.: 205/766; 204/450; 204/515

Field of Search: 204/515, 450; 205/766

References Cited | [Referenced By]

U.S. Patent Documents

5,137,608	Aug., 1992	Acar et al.	204/130

Foreign Patent Documents

1-52906	Mar., 1989	JP

Other References

Jacobs et al., "Model and Experiments on Soil Remediation by Electric fields," Sep. 1993.

Sutton et al., "Soil Improvement Committee-Admixtures Report" in a Symposium entitled Soil Improvement-A Ten year update Apr. 1987 pp. 120-135.

P. Madshus et al., "Improvement of Quick Clay by Electrolysis," Scandinavian Geotechnical Meeting, Sweden, Bulletin 17, Dept. of Geotechnical Engineering, Norwegian Institute of Technology (1984) (English Translation).

I. Casagrande, "Electro-osmosis in Soils," Geotechnique, vol. 1, pp. 159-177 (1949).

Acar et al., "Fundamentals of Extracting Species From Soils by Electrokinetics," Waste Mngmnt., vol. 13, pp. 141-151 (1993).

Soil Improvement: History, Capabilities, and Outlook, Amer. Soc. Civ. Eng., pp. 46-47 (Feb.

1978).

Soil Improvement Methods and Their Applications in Civil Engineering, Dept. Civ. Eng., North Carolina State University, Raleigh, NC, pp. 44-49, 56-59, 62-71 (1981).

Acar et al., "Electrokinetic remediation: Basics and technology status," J. Haz. Mat., vol. 40, pp. 117-137 (1995).

Segall et al., "Electroosmotic Contaminant-Removal Process," ASCE J. Env. Eng., vol. 118, pp. 84-100 (1992).

Oldham et al., Materials Evaluated as Potential Soil Stabilizers, Misc. Paper S-77-15, U.S. Army Engineer Waterways Experiment Station, pp. A7, A9, A132, A137, A189, and A194 (1977).

Sutton et al., "Soil Improvement Committee -Admixtures Report," pp. 121-125, 128-135 in Welsh (ed.) Soil Improvement -A Ten Year Update (1987).

van Impe, Improvement Techniques and Their Evolution, A.A. Balkema/Rotterdam/Brookfield, pp. 42-47, 89, 91, and 93 (1993).

Anderson, et al., Soil Improvement History, Capabilities, and Outlook, American Society of Civil Engineers, pp. 46-47, Feb., 1978.

Soil Improvement--A Ten Year Update, Geotechnical Special Publication No. 12, pp. 120-135, Apr., 1987.

Jacobs et al., Model and Experiments on Soil Remediation by Electric Fields, Presented at ACS Emerging Technologies in Hazardous Waste Management V, pp. 1-15, Sep. 1993.

Primary Examiner: Phasge; Arun S.
Attorney, Agent or Firm: Runnels; John H.

Abstract

Suitable electrolyte conditioning at the electrodes greatly facilitates the transport of desired ions through soil, enhancing the ability of electrokinetic processes to stabilize the soil through cementing reactions. Cationic species are injected at the anode, and anionic species at the cathode, with suitable electrolyte conditioning. For example, if acid or base formation negatively affects transport, chemical conditioning is used to neutralize the acid or base products of electrolysis. Ionic species can be transported through soil at rates of several centimeters a day, even in soils such as clays having a low hydraulic conductivity. Electroosmotic transport can be minimized by appropriate conditioning of the pore fluid chemistry. For example, placement of chemical conditioners with smaller cations at the anode compartment and larger anions at the cathode compartment, or increasing the ion content of the pore fluid (e.g. by acidification) can help minimize electroosmotic transport and any of its adverse effects on species transport. The cations and anions are preferably selected to form cementatious precipitates in the soil. Thus when cationic species are injected at the anode and anionic species are injected at the cathode, stabilization reactions can prevail in the soil as the result of cross-transport of species, and a homogenous and uniform cementation and stabilization can be achieved in a short time.

United States Patent **5,616,235**
Acar, et. al. **Apr. 1, 1997**

Electrochemical stabilization of soils and other porous media

Inventors: **Acar; Yalcin B.** (Baton Rouge, LA); **Gale; Robert J.** (Baton Rouge, LA).

Assignee: **Board of Supervisors of Louisiana State University and Agricultural and Mechanical College** (Baton Rouge, LA).

Appl. No.: **655,709**

Filed: **Jun. 3, 1996**

Intl. Cl. : **C25C 1/22**

Current U.S. Cl.: 205/766; 204/450; 204/515

Field of Search: 204/515, 450; 205/766

References Cited | [Referenced By:]

U.S. Patent Documents

5,137,608	Aug., 1992	Acar et al.	204/130

Foreign Patent Documents

1-52906	Mar., 1989	JP

Other References

Jacobs et al., "Model and Experiments on Soil Remediation by Electric fields," Sep. 1993.

Sutton et al., "Soil Improvement Committee-Admixtures Report" in a Symposium entitled Soil Improvement-A Ten year update Apr. 1987 pp. 120-135.

P. Madshus et al., "Improvement of Quick *Clay* by Electrolysis," Scandinavian Geotechnical Meeting, Sweden, Bulletin 17, Dept. of Geotechnical Engineering, Norwegian Institute of Technology (1984) (English Translation).

I. Casagrande, "Electro-osmosis in Soils," Geotechnique, vol. 1, pp. 159-177 (1949).

Acar et al., "Fundamentals of *Extracting* Species From Soils by Electrokinetics," Waste Mngmnt., vol. 13, pp. 141-151 (1993).

Soil Improvement: History, Capabilities, and Outlook, Amer. Soc. Civ. Eng., pp. 46-47 (Feb.

1978).

Soil Improvement Methods and Their Applications in Civil Engineering, Dept. Civ. Eng., North Carolina State University, Raleigh, NC, pp. 44-49, 56-59, 62-71 (1981).

Acar et al., "Electrokinetic remediation: Basics and technology status," J. Haz. Mat., vol. 40, pp. 117-137 (1995).

Segall et al., "Electroosmotic Contaminant-Removal Process," ASCE J. Env. Eng., vol. 118, pp. 84-100 (1992).

Oldham et al., Materials Evaluated as Potential Soil Stabilizers, Misc. Paper S-77-15, U.S. Army Engineer Waterways Experiment Station, pp. A7, A9, A132, A137, A189, and A194 (1977).

Sutton et al., "Soil Improvement Committee -Admixtures Report," pp. 121-125, 128-135 in Welsh (ed.) Soil Improvement -A Ten Year Update (1987).

van Impe, Improvement Techniques and Their Evolution, A.A. Balkema/Rotterdam/Brookfield, pp. 42-47, 89, 91, and 93 (1993).

Anderson, et al., Soil Improvement History, Capabilities, and Outlook, American Society of Civil Engineers, pp. 46-47, Feb., 1978.

Soil Improvement--A Ten Year Update, Geotechnical Special Publication No. 12, pp. 120-135, Apr., 1987.

Jacobs et al., Model and Experiments on Soil Remediation by Electric Fields, Presented at ACS Emerging Technologies in Hazardous Waste Management V, pp. 1-15, Sep. 1993.

Primary Examiner: Phasge; Arun S.
Attorney, Agent or Firm: Runnels; John H.

Abstract

Suitable electrolyte conditioning at the electrodes greatly facilitates the transport of desired ions through soil, enhancing the ability of electrokinetic processes to stabilize the soil through cementing reactions. Cationic species are injected at the anode, and anionic species at the cathode, with suitable electrolyte conditioning. For example, if acid or base formation negatively affects transport, chemical conditioning is used to neutralize the acid or base products of electrolysis. Ionic species can be transported through soil at rates of several centimeters a day, even in soils such as clays having a low hydraulic conductivity. Electroosmotic transport can be minimized by appropriate conditioning of the pore fluid chemistry. For example, placement of chemical conditioners with smaller cations at the anode compartment and larger anions at the cathode compartment, or increasing the ion content of the pore fluid (e.g. by acidification) can help minimize electroosmotic transport and any of its adverse effects on species transport. The cations and anions are preferably selected to form cementatious precipitates in the soil. Thus when cationic species are injected at the anode and anionic species are injected at the cathode, stabilization reactions can prevail in the soil as the result of cross-transport of species, and a homogenous and uniform cementation and stabilization can be achieved in a short time.

Found Terms:

US4230183

S2: 1 of 1

US4230183 Method for treating subterranean, clay-containing earth formations

---

United States Patent

Patent Number: US4230183

Kalfoglou; George

Date of Patent: Oct. 28, 1980

METHOD FOR TREATING SUBTERRANEAN, CLAY-CONTAINING EARTH FORMATIONS

Inventor:

Kalfoglou; Geo(Houston, TX)

Assignee:

Texaco Inc(White Plains, NY; Assignee type: U.S. Company or Corpor

Appl. Number: 78US-968314
Filed: Dec. 11, 1978

Int. Cl.-2

2-E21B-043-0022

U.S. Cl.

166274000,6630500000R, 25285500000D

Field of Search

166273000, 166274000, 166275000, 16630500R, 25285500D

Found Terms:

US4230183

S2: 1 of 1

US4230183 Method for treating subterranean, clay-containing earth formations

---

United States Patent

Patent Number: US4230183

Kalfoglou; George

Date of Patent: Oct. 28, 1980

METHOD FOR TREATING SUBTERRANEAN, CLAY-CONTAINING EARTH FORMATIONS

Inventor:

Kalfoglou; Geo(Houston, TX)

Assignee:

Texaco Inc(White Plains, NY; Assignee type: U.S. Company or Corpor

Appl. Number: 78US-968314
Filed: Dec. 11, 1978

Int. Cl.-2

2-E21B-043-0022

U.S. Cl.

166274000,16630500000R, 25285500000D

Field of Search

166273000, 166274000, 166275000, 16630500R, 25285500D

United States Patent **5,075,033**
Cody, et. al. **Dec. 24, 1991**

Processes for preparing organophilic clay gellants

Inventors: **Cody; Charles A.** (Robbinsville, NJ); **Kemnetz; Steven J.** (Trenton, NJ).
Assignee: **Rheox, Inc.** (Hightstown, NJ).
Appl. No.: **430,162**
Filed: **Nov. 1, 1989**

Related U.S. Application Data

Division of Ser No. 109,393, Oct. 19, 1987, Pat. No. 4,894,182.

Intl. Cl. : **B01J 13/00**
Current U.S. Cl.: 252/315.2; 106/487; 252/28; 507/100; 507/910; 523/445; 523/447; 556/173
Field of Search: 252/8.515, 315.2, 28; 106/487; 556/173

References Cited | [Referenced By]

U.S. Patent Documents

3,228,969	Jan., 1966	Kerr	556/173
4,040,974	Aug., 1977	Wright et al.	252/315.2
4,382,868	May, 1983	House	252/315.2 X
4,412,018	Oct., 1983	Finlayson et al.	252/315.2 X
4,434,075	Feb., 1984	Mardis et al.	252/315.2
4,605,621	Aug., 1986	Pinnavaia et al.	435/190 X
4,664,820	May, 1987	Magauran et al.	252/315.2 X
4,695,402	Sept., 1987	Finlayson et al.	252/315.2
4,742,098	May, 1988	Finlayson et al.	252/315.2 X
4,894,182	Jan., 1990	Cody et al.	252/315.2

Primary Examiner: Lovering; Richard D.
Attorney, Agent or Firm: Burns, Doane, Swecker & Mathis

Abstract

An improved organophilic clay gellant which is the reaction product of a smectite-type clay, an organic cation and, optionally, an organic anion. The cation from the smectite-type clay, the anion from the organic cation and, if present, the cation form the organic anion form a by-product which is water, a gas, an insoluble compound or a mixture thereof. The organophilic clay gellant can exhibit improved efficiency and dispersibility. In a process for preparing an organophilic clay gellant which constitutes a further aspect of the present invention, significant advantages can be observed since the liquid remaining after the organophilic clay gellant is separated from the reaction mixture can be recycled for further use without detrimental effect on the quality of the organophilic clay gellant thereafter produced.

14 Claims, No Drawings

[USPTO] [CNIDR]

References Cited

U.S. PATENT DOCUMENTS

US2238930	4/1941	Chamberlain et al	166305000R
US2771138	11/1956	Beeson	166274000
US2947360	8/1960	Bernard	166274000
US3701384	10/1972	Routson et al	166273000
US3762485	10/1973	Chesser et al	166305000R
US3827977	8/1974	Miles et al	166305000R
US3843524	10/1974	Perricone et al	166305000R
US3926258	12/1975	Hessert et al	166275000
US4129183	12/1978	Kalfoglou	166305000R

Primary Examiner Novosad; Stephen J.
Assistant Examiner Suchfield; George A.
Attorney, Agent, or Firm Ries; C. G., Kulason; Robert A., Park; Jack H.

ABSTRACT

Disclosed is a method for treating subterranean earth formations conta
water-sensitive clays, including petroleum-containing formations, in o
the formation less sensitive to swelling and other phenomena which cau
the earth formation when the clay content is contacted with relatively
contacting the clay with an aqueous solution of a chelated polyvalent
transition metal ions, including magnesium, vanadium, chromium, mangan
zinc, ruthenium, rhodium, silver, cadmium, iridium, platinum, gold, me
organic ligands are ethylene diamine, diaminopropane, diaminobutane, d
triethylenetetraamine, tetraethylenepentamine, pentaethylenehexamine,
triaminopropane, diaminoaminoethylpropane, diaminomethylpropane, diami
dipyridylamine, phenanthroline, aminoethylpyridine, terpyridine, bigua

14 Claims

* * * * *

(1 of 1)

United States Patent **5,349,118**

Davidovits **Sept. 20, 1994**

Method for obtaining a geopolymeric binder allowing to stabilize, solidify and consolidate toxic or waste materials

Inventors: Davidovits; Joseph (16 rue Galilee, Saint Quentin, FR), F-02100 .

Appl. No.: 90,950

Filed: **Jul. 13, 1993**

Related U.S. Application Data

Division of Ser No. 855,633, May 1, 1992, abandoned.

Foreign Application Priority Data

Sept. 4, 1990 [FR] 90
109

Intl. Cl. : **B09B 1/00, C01B 33/26**

Current U.S. Cl.: 588/252; 106/624; 106/707; 106/900; 405/128; 588/257

Field of Search: 106/624, 626, 707, 900; 405/128, 129, 263-266; 588/249, 252, 256, 257

References Cited | [Referenced By]

U.S. Patent Documents

4,028,454	Jun., 1977	Davidovits et al.	264/82
4,349,368	Sept., 1982	Davidovits	106/84
4,377,415	Mar., 1983	Johnson et al.	524/4
4,472,199	Sept., 1984	Davidovits	106/813
4,509,985	Apr., 1985	Davidovits et al.	106/624
4,537,710	Aug., 1985	Komarneni et al.	252/631
4,640,715	Feb., 1987	Heitzmann et al.	106/706
4,642,137	Oct., 1987	Heitzmann et al.	106/607
4,842,649	Jun., 1989	Heitzmann et al.	106/707
4,859,367	Aug., 1989	Davidovits	252/628
5,114,622	May, 1992	Funabashi et al.	252/629

Other References

D. C. Comrie et al., "Geopolymer Technologies in Toxic Waste Management," Geopolymer '8, vol. 1, pp. 107-123, Universite de Technologie, Compiegne, France, (1988).

Davidovits et al., "Long Term Durability of Hazardous Toxis and Nuclear Waste Disposals." Geopolymer '88, vol. 1, pp. 125-134, Universite de Technologie, Compiegne, France, (1988).

Sang et al., "Aluminum-27 and Silicon-29 MAS-NMR Study of the Kaolinite-Mullite Transformation," J. Am. Cearm. Soc., 71 (10), C418-C421 (1988).

Regourd, "Microanalytical Studies of Surface Hydration Reactions of Cement Compounds." Phil. Tran. R. Soc. Land. A 310, 85-92 (1983).

Skibsted, "High-speed (^*29*) Si and (^*27*) Al MAS NMR Studies of Portland and High Alumina Cements," Geopolymer '88, vol. 3, pp. 179-196, Universite de Technologie, Compiegne, France 1988.

MacKenzie et al., "Outstanding Problems in the Kaolinite-Mullite Reaction Sequence Investigated by (^*29*) Si and (^*27*) Al Solid State NMR," J. Am. Cearm. Soc., 68 (6), 293-297 (1985).

Primary Examiner: Taylor; Dennis L.
Assistant Examiner: Ricci; John A.
Attorney, Agent or Firm: Browdy and Neimark

Abstract

The method of the invention provides a geopolymeric binder in powder, used for the ultra rapid treatment of materials, soils or mining tailings, containing toxic wastes. The geopolymeric binder has a setting time equal to or greater than 30 minutes at a temperature of 20 *deg.* C. and a hardening rate such as to provide compression strengths (Sc) equal to or greater than 15 MPa, after only 4 hours at 20 *deg.* C., when tested in accordance with the standards applied to hydraulic binder mortars having a binder/sand ratio equal to 0.38 and a water/binder ratio between 0.22 and 0.27. The preparation method includes the following three reactive constituents:

a) an alumino-silicate oxide (Si(*2*) O(*5*),Al(*2*) O(*2*)) in which the Al cation is in (IV-V) coordination as determined by MAS-NMR analytical spectroscopy for (^*27*) Al;

b) a disilicate of sodium and/or potassium (Na(*2*),K(*2*))(H(*3*) SiO(*4*))(*2*) ;

c) a silicate of calcium where the molar ratios between the three reactive constituents being equal to or between ##EQU1## where Ca(^++) designates the calcium ion belonging to a weakly basic silicate of calcium whose atomic ratio Ca/Si is lower than 1.

5 Claims, No Drawings

[USPTO] [CNIDR]

United States Patent **5,211,239**
Thomas, et. al. **May 18, 1993**

Method of maintaining subterranean formation permeability and inhibiting clay swelling

Inventors: **Thomas; Todd R.** (Coroapolis, PA); **Smith; Kevin W.** (McMurray, PA).
Assignee: **Clearwater, Inc.** (Pittsburgh, PA).
Appl. No.: **835,602**
Filed: **Feb. 13, 1992**

Intl. Cl. : **E21B 43/22, E21B 43/26**
Current U.S. Cl.: **166/308**; 166/305.1; 507/240; 507/922
Field of Search: 166/294, 305.1, 308, 275; 405/264; 252/8:551, 8.554

References Cited | [Referenced By]

U.S. Patent Documents

2,761,835	Sept., 1956	Brown	
3,422,890	Jan., 1969	Durley	
4,374,739	Feb., 1983	McLaughlin et al.	252/8.551
4,447,342	May, 1984	Borchardt et al.	252/8.554
4,842,073	Jun., 1989	Himes et al.	166/294
4,974,678	Dec., 1990	Himes et al.	166/308
4,977,962	Dec., 1990	Himes et al.	166/305.1
5,097,904	Mar., 1992	Himes	166/305.1
5,099,923	Mar., 1992	Aften et al.	166/294

Other References

Donald G. Hill, "Clay Stabilization--Criteria for Best Performance" Mar. 24-25, 1982, SPE 10656 pp. 127-138.

Himes, Vinson & Simon "Clay Stabilization in Low-Permeability Formations" SPE Production Engineering, Aug. 1991 pp. 252-258.

Primary Examiner: Suchfield; George A.

Attorney, Agent or Firm: Krayer; William L.

Abstract

Moulding and migration of subterranean clay is inhibited during stimulation of the production of hydrocarbon fluids, and preparation therefor, by treating said formations with a compound of the formula (CH(*2*) .dbd.CH-CH(*2*))(*n*) N+(CH(*3*))(*4-n*) X(^-) where X may be any anion which does not adversely react with the formation or treatment fluid and n is an integer from 1 to 4.

18 Claims, 7 Drawing Figures

[USPTO] [CNIDR]

(1 of 1)

United States Patent **5,099,923**
Aften, et. al. **Mar. 31, 1992**

Clay stabilizing method for oil and gas well treatment

Inventors: **Aften; Carl W.** (Sugarland, TX); **Gabel; Robert K.** (Sugarland, TX).
Assignee: **Nalco Chemical Company** (Naperville, IL).
Appl. No.: **661,429**
Filed: **Feb. 25, 1991**

Intl. Cl. :	**E21B 43/25**
Current U.S. Cl.:	**166/294**; 166/305.1; 166/307; 166/308; 405/264; 507/240; 507/935
Field of Search:	166/271, 275, 281, 294, 305.1, 307, 308; 106/900; 252/8.551, 8.553, 8.554; 405/264

References Cited | [Referenced By]

U.S. Patent Documents

2,713,033	Jul., 1955	Cardwell et al.	252/8.553 X
2,761,835	Sept., 1956	Brown	252/8.554
3,349,032	Oct., 1967	Krieg	252/8.554 X
3,412,019	Dec., 1968	Hoover et al.	210/54
4,366,071	Dec., 1982	McLaughlin	166/305.1 X
4,366,074	Dec., 1982	McLaughlin et al.	166/305.1 X
4,462,718	Jul., 1984	McLaughlin et al.	166/305.1 X
4,526,693	Jul., 1985	Son et al.	175/65
4,580,633	Apr., 1986	Watkins et al.	166/295
4,703,803	Nov., 1987	Blumer	166/307 X
4,842,073	Jun., 1989	Himes et al.	166/294

Other References

Sax, N. Irving et al, Hawley's Condensed Chemical Dictionary, eleventh edition, 1987, Van Nostrand Reinhold Comany, New York, p. 343.

Primary Examiner: Suchfield; George A.
Attorney, Agent or Firm: Lundeen; Daniel N., Miller; Robert A., Epple; Donald G.

Abstract

A clay swelling inhibitor additive for oil and gas well treatment is disclosed. The additive comprises an aqueous solution of tetraalkylammonium chloride, preferably tetramethylammonium chloride and a quaternary amine-based cationic polyelectrolyte, such as methyl chloride quaternary salt of ethylene-ammonia condensation polymer. The additive composition synergistically retards water absorption by the down-hole clay formation.

10 Claims, 2 Drawing Figures

[USPTO] [CNIDR]

United States Patent **5,097,904**
Himes **Mar. 24, 1992**

Method for clay stabilization with quaternary amines

Inventors: **Himes; Ronald E.** (Duncan, OK).
Assignee: **Halliburton Company** (Duncan, OK).
Appl. No.: **657,700**
Filed: **Feb. 28, 1991**

Intl. Cl. :	**E21B 33/138,** E21B 43/26, E21B 43/27
Current U.S. Cl.:	**166/294**; 166/305.1; 166/307; 166/308; 507/240
Field of Search:	166/271, 294, 305.1, 307, 308; 252/8.551, 8.553, 8.554; 106/900

References Cited | [Referenced By]

U.S. Patent Documents

2,761,835	Sept., 1956	Brown	252/8.554
2,761,840	Sept., 1956	Brown et al.	252/8.554 X
2,761,843	Sept., 1956	Brown	252/8.554 X
3,349,032	Oct., 1967	Krieg	252/8.554 X
3,768,566	Oct., 1973	Ely et al.	166/308
4,462,718	Jul., 1984	McLaughlin et al.	166/305.1 X
4,842,973	Jun., 1989	Himes et al.	166/294
4,974,678	Dec., 1990	Himes et al.	166/308

Primary Examiner: Suchfield; George A.
Attorney, Agent or Firm: Weaver; Thomas R.

Abstract

A method of treating a clay-containing subterranean formation with an aqueous fluid is disclosed. The method features the use of quaternary ammonium compounds as additives to control formation damage caused by contacting the formation with the aqueous fluid.

14 Claims, 1 Drawing Figures

United States Patent **5,197,544**
Himes **Mar. 30, 1993**

Method for clay stabilization with quaternary amines

Inventors: **Himes; Ronald E. (Duncan, OK).**
Assignee: **Halliburton Company (Duncan, OK).**
Appl. No.: **809,783**
Filed: **Dec. 18, 1991**

Related U.S. Application Data

Continuation of (including streamline cont.) Ser. No. 657,700, Feb. 28, 1991, Pat. No. 5,097,904.

Intl. Cl. :	**E21B 33/138**, E21B 43/26, E21B 43/27
Current U.S. Cl.:	**166/294**; 166/305.1; 166/307; 166/308; 507/240; 507/922
Field of Search:	166/271, 294, 305.1, 307, 308; 106/900; 252/8.551, 8.553, 8.554

References Cited | [Referenced By]

U.S. Patent Documents

2,761,835	Sept., 1956	Brown	252/8.554
2,761,840	Sept., 1956	Brown et al.	252/8.554 X
2,761,843	Sept., 1956	Brown	252/8.554 X
3,349,032	Oct., 1967	Krieg	252/8.554 X
3,768,566	Oct., 1973	Ely et al.	166/308
4,462,718	Jul., 1984	McLaughlin et al.	166/305.1 X
4,842,073	Jun., 1989	Himes et al.	166/294
4,974,678	Dec., 1990	Himes et al.	166/308

Primary Examiner: Suchfield; George A.
Attorney, Agent or Firm: Weaver; Thomas R.

Abstract

A method of treating a clay-containing subterranean formation with an aqueous fluid is disclosed. The

method features the use of quaternary ammonium compounds as additives to control formation damage caused by contacting the formation with the aqueous fluid.

16 Claims, 1 Drawing Figures

[USPTO] [CNIDR]

▲

(1 of 1)

United States Patent **5,160,642**

Schield, et. al. **Nov. 3, 1992**

Polyimide quaternary salts as clay stabilization agents

Inventors:	**Schield; John A.** (Chesterfield, MO); **Naiman; Michael I.** (St. Louis, MO); **Scherubel; Gary A.** (St. Louis, MO).
Assignee:	**Petrolite Corporation** (St. Louis, MO).
Appl. No.:	**529,026**
Filed:	**May 25, 1990**

Intl. Cl. :	**E21B 43/26**, C07D 207/452, C08F 26/02
Current U.S. Cl.:	**507/222**; 166/281; 166/294; 166/305.1; 166/308; 507/118; 507/922; 525/66; 526/262; 548/521; 548/522
Field of Search:	526/262; 525/66; 252/8.551; 548/521, 522

References Cited | [Referenced By]

U.S. Patent Documents

3,291,679	Dec., 1966	O'Brien	526/262 X
3,778,416	Dec., 1973	Zoller et al.	8/181 X
4,366,071	Dec., 1982	McLaughlin et al.	252/8.551
4,366,072	Dec., 1982	McLaughlin et al.	252/8.551
4,366,073	Dec., 1982	McLaughlin et al.	252/8.551
4,366,074	Dec., 1982	McLaughlin et al.	252/8.551
4,374,739	Feb., 1983	McLaughlin et al.	252/8.551
4,434,076	Feb., 1984	Mardis et al.	252/8.551 X
4,440,649	Apr., 1984	Loftin et al.	252/8.551 X
4,460,483	Jul., 1984	Weaver	252/8.551
4,497,596	Feb., 1985	Borchardt et al.	252/8.551 X
4,505,833	Mar., 1985	Lipowski et al.	252/8.551 X
4,536,303	Aug., 1985	Borchardt	252/8.551
4,536,304	Aug., 1985	Borchardt	252/8.551
4,536,305	Aug., 1985	Borchardt et al.	252/8.551
4,563,292	Jan., 1986	Borchardt	252/8.551
4,626,363	Dec., 1986	Gleason et al.	252/8.551 X
4,627,926	Dec., 1986	Peiffer et al.	252/8.551
4,652,621	Mar., 1987	Kadono et al.	252/8.551 X
4,693,639	Sept., 1987	Hollenbeak et al.	252/8.551 X
4,828,726	May, 1989	Himes et al.	252/8.551 X
4,842,073	Jun., 1989	Himes et al.	252/8.551 X
4,959,163	Sept., 1990	Holtmyer et al.	252/8.551

Foreign Patent Documents

WO88/04680	Jun., 1988	WO

Primary Examiner: Stoll; Robert L.
Assistant Examiner: Geist; Gary L.
Attorney, Agent or Firm: Boone; Jeffrey S., Solomon; Kenneth

Abstract

A clayish formation, such as encountered in rock surrounding an oil well bore, is stabilized with a quaternary ammonium salt of an imide of polymaleic anhydride. The invention is particularly relevant to hydraulic fracturing fluids used for enhanced oil recovery.

22 Claims, No Drawings

[USPTO] [CNIDR]

United States Patent **4,959,163**
Holtmyer, et. al. **Sept. 25, 1990**

Polyampholytes-high temperature polymers and method of use

Inventors: **Holtmyer; Marlin D.** (Duncan, OK); **Hunt; Charles V.** (Duncan, OK).
Assignee: **Halliburton Company** (Duncan, OK).
Appl. No.: **267,489**
Filed: **Nov. 3, 1988**

Intl. Cl. : **E21B 43/26**
Current U.S. Cl.: 507/203; 166/283; 166/305.1; 166/308; 507/222; 507/225; 507/226; 507/260; 507/267; 507/903; 507/922
Field of Search: 252/8.551; 166/305.1, 308, 283

References Cited | [Referenced By]

U.S. Patent Documents

2,087,506	Aug., 1936	DeGroote	
2,692,285	Oct., 1954	Robinson	
2,775,617	Dec., 1956	Shapiro	
3,297,706	Jul., 1967	Sobolev	
3,813,441	May, 1974	Mueller-Schiedamayer	
3,826,311	Jul., 1974	Szabo et al.	166/305.1 X
3,868,328	Feb., 1975	Boothe et al.	166/308 X
3,943,060	Mar., 1976	Martin et al.	166/308 X
4,056,496	Nov., 1977	Mancini	
4,147,681	Apr., 1979	Lim	
4,152,274	May, 1979	Phillips et al.	166/308 X
4,209,651	Jun., 1980	Prichard	
4,224,150	Sept., 1980	Buriks	
4,319,013	Mar., 1982	Cabestany	
4,435,528	Mar., 1984	Domina	
4,460,758	Jul., 1984	Peiffer et al.	526/287
4,462,917	Jul., 1984	Conway	
4,464,270	Aug., 1984	Hollenbeak	
4,470,915	Sept., 1984	Conway	
4,477,360	Oct., 1984	Almond	
4,502,967	Mar., 1985	Conway	
4,520,210	May, 1985	Schneider	
4,552,670	Nov., 1985	Lipowski	
4,563,292	Jan., 1986	Borchardt	166/305.1 X
4,605,718	Aug., 1986	Jansma	
4,610,305	Sept., 1986	Martin	
4,627,926	Dec., 1986	Peiffer et al.	166/308 X
4,699,722	Oct., 1987	Dymond et al.	252/8.551
4,730,081	Mar., 1988	Holtmyer	
4,767,550	Aug., 1988	Hanlon	

Foreign Patent Documents

926540	May, 1973	CA	166/308
0115836	Jan., 1984	EP	
60-212590	Oct., 1985	JP	166/305.1

Other References

Conway, Journal of Petroleum Technology, Feb. 315-320 (1983).

Doe, et al., "Development and Evaluation of EOR Polymers Suitable for Hostile Environments: Copolymers of Vinylpyrrolidone and Acrylamide," SPE 14233 (1985).

Primary Examiner: Stoll; Robert L.
Assistant Examiner: Geist; Gary L.
Attorney, Agent or Firm: Kent; Robert A.

Abstract

A method and composition for stimulating high temperature subterranean formations. The composition comprises a novel crosslinkable polymer containing anionic and cationic functional groups (a polyampholyte). The polyampholyte comprises a mixture of at least one from each of the following groups:

Group I acrylamide, partially hydrolyzed acrylamide, N,N-dimethylacrylamide, N-substituted-(N'-dialkylaminoalkyl) acrylamides, aminoalkylacrylates, dialkylaminoalkylacrylates or mixtures thereof;

Group II 2-acrylamido-2-methylpropane sulfonic acid, sodium salt, vinylphosphonic acid, partially hydrolyzed acrylamide or mixtures thereof; and

Group III methacrylamidopropyldimethyl-2,3-dihydroxypropylammonium sulfate having the formula ##STR1## In the performance of the method, the polyampholyte is inverted into an aqueous liquid to form a viscous liquid which is buffered to about 4 to 6.5 and admixed with a crosslinking agent capable of crosslinking dihydroxypropyl functionalities. The crosslinked fluid then is introduced into a formation at a rate and pressure sufficient to fracture the formation.

16 Claims, No Drawings

[USPTO] [CNIDR]

United States Patent **5,328,880**

Lampert, et. al. **Jul. 12, 1994**

Fluidity of slurries of kaolin clay using tetraalkylammonium compounds

Inventors: **Lampert; Jordan K. (Metuchen, NJ); Slepetys; Richard A. (Brick, NJ); Dombrowski; Thomas (Fanwood, NJ).**

Assignee: **Engelhard Corporation (Iselin, NJ).**

Appl. No.: **139,297**

Filed: **Oct. 19, 1993**

Intl. Cl. : **C09K 7/06**

Current U.S. Cl.: **501/148; 501/146**

Field of Search: 501/145, 146, 148; 162/181.8; 106/486, 487

References Cited | [Referenced By]

U.S. Patent Documents

2,950,983	Aug., 1960	Rowland	106/308
2,982,665	May, 1961	Wilcox	106/308
2,994,616	Aug., 1961	Rowland	106/308
2,995,458	Aug., 1961	Murray	106/288
3,236,666	Aug., 1966	Sawyer	106/72
3,266,917	Feb., 1966	Sawyer et al.	106/72
3,282,715	Nov., 1966	Sawyer et al.	106/72
3,394,022	Jul., 1967	Lyons et al.	106/288
3,464,634	Jul., 1969	Brociner	241/4
3,663,461	May, 1972	Dover	260/2.BP
3,674,521	Jul., 1972	Noble	106/72
3,797,574	Mar., 1974	Feverbacher et al.	166/274
3,849,151	Nov., 1974	Abercrombie, Jr.	106/288.B
3,961,979	Jun., 1976	Abercrombie, Jr.	106/308.N
4,030,941	Jun., 1977	Kunkle et al.	106/309
4,045,235	Aug., 1977	Bidwell et al.	106/72
4,105,466	Aug., 1978	Kunkle et al.	106/309

4,106,949	Aug., 1978	Malden	106/288.B
4,144,083	Mar., 1979	Abercrombie, Jr.	106/288.B
4,144,084	Mar., 1979	Abercrombie, Jr.	106/288.B
4,144,085	Mar., 1979	Abercrombie, Jr.	106/288.B
4,314,919	Feb., 1983	Washabaugh et al.	260/22.CB
4,477,422	Aug., 1984	Ginn	423/327
4,572,296	Feb., 1986	Watkins	166/303
4,631,091	Dec., 1986	Goodman	501/148 X
4,738,726	Apr., 1988	Pratt et al.	106/308.N
4,772,332	Sept., 1988	Nemeh et al.	106/487
4,804,416	Feb., 1989	Jepson et al.	106/468
4,828,726	May, 1989	Himes et al.	252/8.553
4,842,073	Jun., 1989	Himes et al.	166/294
4,843,048	Jun., 1989	House et al.	501/148
4,974,678	Dec., 1990	Himes et al.	166/308
5,061,461	Oct., 1991	Sennett et al.	423/112
5,089,151	Feb., 1992	Hall et al.	252/8.557
5,097,904	May, 1992	Himes	252/8.551
5,110,501	May, 1992	Knudson, Jr. et al.	252/315.2
5,128,027	Jul., 1992	Halaka et al.	229/5
5,152,906	Oct., 1992	Aften et al.	252/8.551
5,160,642	Nov., 1992	Schield et al.	252/8.551
5,198,415	Mar., 1993	Stieger	507/103

Other References

Theng, et al., "The Effect of Exchangeable Alkyl-Ammonium Ions On The Swelling of Montmorillonite In Water", Clay Minerals 7, pp. 271-293 (1968), no month.

Theng, et al., "Adsorption of Alkylammonium Cations By Montmurillonite", Clay Minerals 7, pp. 1-17 (1967) no month.

Weiss, "Organic Derivatives of Mica Type Layer Silicates", Angew. Chem. internat. Edit./vol. 2 (1963) No. 3 pp. 134-144 no month.

Primary Examiner: Group; Karl
Assistant Examiner: Gallo; Chris
Attorney, Agent or Firm: Moselle; Inez L.

Abstract

The present invention relates to a process for reducing the inherent low shear viscosity of kaolin clays contaminated with expandable layer minerals. A water soluble tetraalkyl ammonium compound is contacted with the clay during conventional wet processing.

17 Claims, No Drawings

[USPTO] [CNIDR]

▲

(1 of 1)

United States Patent **5,120,344**

Libor, et. al. **Jun. 9, 1992**

Method for producing a barrier layer in soil

Inventors: **Libor; Oszkar** (Budapest, HU); **Nagy; Gabor** (Budapest, HU); **Szekely; Tamas** (Budapest, HU); **Mester; Rudolf** (Budaors, HU); **Kazareczki; Kalman** (Budapest, HU); **Muller; Tibor** (Szolnok, HU); **Kiss; Jeno** (Budapest, HU); **Saghi; Zoltan** (Szekesfehervar, HU); **Hosszu; Adam** (Budapest, HU).

Assignee: **Altalanos Iparfejlesztesi Rt.** (Budapest, HU); **Vizepitooipari Troszt** (Budapest, HU).

Appl. No.: **747,467**

Filed: **Aug. 13, 1991**

Related U.S. Application Data

Continuation of (including streamline cont.) Ser. No. 306,031, Feb. 2, 1989, abandoned.

Intl. Cl. : **C05G 3/00**, C05G 3/04, C09K 17/00

Current U.S. Cl.: 71/27; 106/900; 405/264; 504/116; 524/446; 71/903; 71/904; 71/DIG 1

Field of Search: 71/1, 3, 11, 27, 903, 904; 524/446, 448; 405/263, 264; 106/287.1, 900; 97/57.6, 9

References Cited | [Referenced By]

U.S. Patent Documents

3,772,893	Nov., 1973	Eilers	61/36.R
4,600,744	Jul., 1986	Libor et al.	524/446
4,669,920	Jun., 1987	Dymond	252/8.551 X

Primary Examiner: Lander; Ferris
Attorney, Agent or Firm: Schweitzer Cornman & Gross

Abstract

The present invention relates to a method for producing a closing layer which improves the water and nutrient retention of soils, particularly of sandy soils, characterized in that a layer of clay mineral/polymer gel capable of binding and releasing water in a reversible manner is introduced into the soil, preferably 20-60 cm below the soil surface, in such a way that a clay mineral is reacted either before or after or

during activation in the presence of water, with 0.5-30% by weight, calculated for the weight of the clay mineral, of one or more water-soluble polymer capable of reacting with the clay mineral, the water content of the resulting gel is adjusted either before or after or during the reaction to a value at which the resistance of medium of the gel is at least three times higher than that of a polymer-free suspension containing the same amount of the clay mineral, if a non-activated clay mineral has been applied as starting substance, the clay mineral is activated with an alkaline activating agent after reacting it with the polymer, and, if desired, further amounts of a water-soluble polymer, one or more water-insoluble swelling xerogel capable of at least 100% water uptake and forming swollen particles less than 1 mm in diameter and/or one or more chemical for agricultural use, preferably a plant nutrient, a fungicidal substance acting against soil-borne fungi and/or a plant growth increasing substance, is added to the gel either before or after or during the reaction with the polymer, and/or, if desired, the gel and the non-reacted polymer molecules are cross-linked with an aldehyde, and finally the thus-formed gel layer is covered with a soil layer.

13 Claims, No Drawings

[USPTO] [CNIDR]

(1 of 1)

United States Patent **5,604,168**
Libor **Feb. 18, 1997**

Clay-containing mixture and blend capable of forming a moisture resistant gel, and use of that mixture and blend

Inventors:	**Libor; Oszkar** (Budapest, HU).
Assignee:	**Aannemingsbedrijf Van Der Biggelaar Limburg B.V.** (Wessem, NL).
Appl. No.:	**495,511**
Filed:	**Nov. 17, 1995**
PCT Filed:	**Jan. 25, 1994**
PCT No:	**PCT/NL94/00017**
371 Date:	**Nov. 17, 1995**
102(e) Date:	**Nov. 17, 1995**
PCT Pub. No.:	**WO94/18284**
PCT Pub. Date:	**Aug. 18, 1994**

Foreign Application Priority Data

Feb. 3, 1993 [HU]	2960/93
Jul. 16, 1993 [HU]	20361/93

Intl. Cl. :	C04B 33/00, C09K 17/00
Current U.S. Cl.:	501/141; 106/900; 252/315.5; 71/64.09; 71/903
Field of Search:	501/141; 252/315.5; 71/62, 64.09, 903; 106/900

References Cited | [Referenced By]

U.S. Patent Documents

3,736,758	Jun., 1973	Dolfing et al.	61/36.R
4,669,920	Jun., 1987	Dymond	405/264
4,753,908	Jun., 1988	Kawase et al.	502/63
5,120,344	Jun., 1992	Libor et al.	71/27
5,407,480	Apr., 1995	Payton et al.	106/487

Foreign Patent Documents

0244981	Nov., 1987	EP
0335653	Oct., 1989	EP
0495108	Jul., 1992	EP
2127991	Oct., 1972	FR
1439734	Jun., 1976	GB

Primary Examiner: Group; Karl
Attorney, Agent or Firm: Seed and Berry LLP

Abstract

A dry mixture of (a) powdered or ground smectite and/or a smectite-containing natural rock, wherein the smectite is in an inactive state, (b) 1-10% by weight of a water-soluble polymer and (c) 0.8-6.0% by weight of a powdered activating agent can be combined with soil and water to provide a gel which is a barrier composition. The mixture may additionally contain a diluting agent, so as to form a dry blend, where the blend may likewise be combined with soil and water to provide a gel which is a barrier composition. The blend may be used to provide for water-tight insulation of vasins, damps and other objects exposed to damaging effects of water, and may also be used as a sealing for deponies, as a protecting layer for articles exposed to acidic liquids, and as a filling agent for cavities and cracks on articles exposed to water.

7 Claims, No Drawings

[USPTO] [CNIDR]

▶ ▲

(1 of 6)

United States Patent **5,436,218**

Hausberg **Jul. 25, 1995**

Agglomerates for reclaiming uncultivated soils comprising superabsorbent polymers and polybutadiene oil adhesive

Inventors: **Hausberg; Egbert** (Schermbeck, DE).

Assignee: **Huels Aktiengesellschaft** (Marl, DE).

Appl. No.: **103,228**

Filed: **Aug. 9, 1993**

Foreign Application Priority Data

Nov. 6, 1992 [DE] 42 37

Intl. Cl. : A01N 25/08, A01N 25/26, A01N 63/00, C09K 17/40

Current U.S. Cl.: 504/101; 424/421; 424/93.4; 424/93.5; 504/116; 504/117; 514/949; 71/903; 71/DIG 1

Field of Search: 71/DIG. 1, 903; 504/116, 101, 117; 424/93 D, 93 Q, 421; 514/949

References Cited | [Referenced By]

U.S. Patent Documents

4,015,970	Apr., 1977	Hennart	71/11
5,057,326	Oct., 1991	Sampson	424/711
5,120,344	Jun., 1992	Libor et al.	71/27

Foreign Patent Documents

0072213	Feb., 1983	EP
0475433	Mar., 1992	EP
0495108	Jul., 1992	EP
2635333	Feb., 1990	FR

Primary Examiner: Clardy; S. Mark
Attorney, Agent or Firm: Oblon, Spivak, McClelland, Maier & Neustadt

---

Abstract

The invention relates to agglomerates which are permeable to gas, absorbs and stores liquids and comprises:

A) a mineral carrier material,

B) a water-insoluble polymer which absorbs and stores liquids,

C) an adhesive and

D) optionally appropriate additives and adjuvants.

The agglomerates are outstandingly suitable for reclaiming uncultivated soils, in particular slopes, landfill sites, arid areas as well as golf courses and the like.

20 Claims, No Drawings

[USPTO] [CNIDR]

(6 of 6)

United States Patent **4,906,142**
Taki, et. al. **Mar. 6, 1990**

Side cutting blades for multi-shaft auger system and improved soil mixing wall formation process

Inventors: **Taki; Osamu** (Belmont, CA); **Takeshima; Shigeru** (San Mateo, CA).
Assignee: **S.M.W. Seiko, Inc.** (Redwood City, CA).
Appl. No.: **389,546**
Filed: **Aug. 2, 1989**

Related U.S. Application Data

Division of Ser No. 172,401, Mar. 23, 1988.

Intl. Cl.:	**E02D 17/13**, E02D 5/18
Current U.S. Cl.:	**405/267**; 405/233; 405/241; 405/269
Field of Search:	405/267, 266, 258, 263, 269, 232, 231, 233, 239, 240, 241

References Cited | [Referenced By]

U.S. Patent Documents

2,048,710	Jul., 1936	Ranney	405/267
2,950,902	Aug., 1960	Olds	175/323 X
3,023,585	Mar., 1962	Livey	405/269 X
3,139,729	Jul., 1964	Miotti	405/267
3,422,913	Jan., 1969	Young	175/323 X
4,036,529	Jul., 1977	Hawthorne et al.	175/323 X
4,043,909	Aug., 1977	Endo et al.	210/49
4,063,424	Dec., 1977	Takagi et al.	
4,065,928	Jan., 1978	Takagi et al.	
4,065,933	Jan., 1978	Katayama	
4,069,678	Jan., 1978	Miura et al.	
4,084,383	Apr., 1978	Kukino et al.	
4,089,183	May, 1978	Endo et al.	
4,189,239	Feb., 1980	Miyaguchi et al.	366/169
4,212,548	Jul., 1980	Miyaguchi et al.	366/348
4,402,630	Oct., 1983	Miura et al.	405/266
4,436,453	Mar., 1984	Miura et al.	405/263
4,449,856	May, 1984	Tokoro et al.	405/269
4,475,847	Oct., 1984	Cornely et al.	405/264
4,662,792	May, 1987	Gessay	405/233

Foreign Patent Documents

51-71605	Jun., 1976	JP
52-78302	Jun., 1977	JP
52-152608	Dec., 1977	JP
55-44812	Nov., 1980	JP
58-29374	Jun., 1983	JP
58-29375	Jun., 1983	JP

Other References

"S.M.W. Machine," Product Brochure of S.M.W. Seiko, Inc.

"Teno Column Method" Product Brochure of the Tenox Corporation (publication date unknown).

"Just One of Our Fleet," Product Advertisement (publication date unknown).

"The Soil Mixing Wall (SMW Technique)-Guidelines for its Design and Implementation," Japanese Materials Institute.

"In Situ Soil Improvement Techniques", Lime Columns (dated Mar. 1987).

Jasperse and Ryan, "Geotech Import: Deep Soil Mixing," Civil Engineering (Dec. 1987), pp. 66-68.

Primary Examiner: Taylor; Dennis L.
Attorney, Agent or Firm: Workman, Nydegger & Jensen

Abstract

The present invention is directed to side cutting blades for use with multi-shaft auger machines which mix soil with a chemical hardener in situ to form soilcrete columns. The side cutting blades includes two parallel blades which cut the soil between the adjacent columns along planes approximately tangential to the periphery of adjacent columns. As the soil is cut by the cutting blades, the soil is thoroughly mixed with a chemical hardening agent. Adjacent soilcrete columns are integrally connected by substantial column overlap without physically moving the columns closer together or performing multiple borings on the soil adjacent to the columns formed by the initial boring.

The side cutting blades are particularly suited for use with a multi-shaft auger machine which has minimal column overlap. A multi-shaft auger machine equipped with side cutting blades may be used to construct continuous in situ wall formations which are homogeneous in composition and have a minimum thickness approximately equal to the diameter of the auger shafts.

32 Claims, 23 Drawing Figures

[USPTO] [CNIDR]

(1 of 1)

Found Terms:

US4227575

S3: 1 of 1

US4227575 Reservoir stabilization by treating water sensitive clays

United States Patent

Patent Number: US4227575

Nooner; Daryl W.

Date of Patent: Oct. 14, 1980

RESERVOIR STABILIZATION BY TREATING WATER SENSITIVE CLAYS

Inventor:

Nooner; Daryl W(Houston, TX)

Assignee:

Texaco Inc(White Plains, NY; Assignee type: U.S. Company or Corpor

Appl. Number: 78US-920881
Filed: Jun. 30, 1978

Int. Cl.-2

2-E21B-043-0024

U.S. Cl.

166303000,166288000

Field of Search

166272000, 166273000, 166274000, 166275000, 166288000, 166303000, 16630500R

References Cited

U.S. PATENT DOCUMENTS

US2761843	9/1956	Brown	25200855D
US3087539	4/1963	Maurer, Jr.	25200855D
US3237692	3/1966	Wallace et al	166303000
US3347313	10/1967	Matthews et al	166272000
US3360043	12/1967	Braden, Jr. et al	166272000
US3444931	5/1969	Braden, Jr.	166305000R
US3476183	11/1969	Haynes, Jr. et al	166275000
US3491833	1/1970	Braden, Jr.	166272000
US3847222	11/1974	Braden, Jr.	166272000

Primary Examiner Novosad; Stephen J.
Assistant Examiner Suchfield; George A.
Attorney, Agent, or Firm Ries; Carl G., Kulason; Robert A., Young; James F.

ABSTRACT

A method of treating subterranean formations containing water-sensitiv contacting the formation with an aqueous solution of nitrogen containi temperatures whereby the montmorillonite is transformed into other cla to swelling when contacted with water.

3 Claims

* * * * *

S4: 1 of 1

US4164979 Reservoir stabilization by treating water sensitive clays

---

United States Patent

Patent Number: **US4164979**

Nooner; Daryl W.

Date of Patent: **Aug. 21, 1979**

RESERVOIR STABILIZATION BY TREATING WATER SENSITIVE CLAYS

Inventor:

Nooner; Daryl W. (Houston, TX)

Assignee:

Texaco Inc. (White Plains, NY; Assignee type: U.S. Company or Corporation)

Appl. Number: 78US-920882
Filed: **Jun. 30, 1978**

Int. Cl.-2

2-E21B-043-0022, 2-E21B-043-0024

U.S. Cl.

166288000, 166303000, 25285500000D

Field of Search

166272000, 166273000, 166274000, 166275000, 166288000, 166303000, 16630500R

References Cited

U.S. PATENT DOCUMENTS

US2761843	9/1956	Brown	25200855D
US3087539	4/1963	Maurer, Jr	25200855D
US3237692	3/1966	Wallace et al	166303000
US3347313	10/1967	Matthews et al	166272000
US3360043	12/1967	Braden, Jr. et al	166272000
US3444931	5/1969	Braden, Jr	166305000R
US3476183	11/1969	Haynes, Jr. et al	166275000
US3491833	1/1970	Braden, Jr	166272000
US3847222	11/1974	Braden, Jr	166303000

Primary Examiner - **Novosad; Stephen J.**
Assistant Examiner - **Suchfield; George A.**
Attorney, Agent, or Firm - **Whaley; Thomas H., Ries; Carl G.**

ABSTRACT

A method of treating subterranean formations containing water-sensitive montmorillonite clays by contacting the formation with an aqueous solution of potassium salts of organic acids at elevated temperatures whereby the montmorillonite is transformed into other clay minerals which are less sensitive to swelling when contacted with water.

7 Claims

* * * * *

Found Terms:

US3796263

S5: 1 of 1

US3796263 TREATMENT OF AN UNDERGROUND FORMATION

United States Patent

Patent Number: **US3796263**

Hudson; Phillip E., et. al.

Date of Patent: **Mar. 12, 1974**

TREATMENT OF AN UNDERGROUND FORMATION

Inventors:

Hudson; Phillip E. (Austin, TX)

Braden, Jr.; William B. (Houston, TX)

Assignee:

Texaco Inc. (New York, NY; Assignee type: U.S. Company or Corporation)

Appl. Number: **72US-263063**
Filed: **Jun. 15, 1972**

U.S. Cl.

166295000

Field of Search

166292000, 166295000

References Cited

U.S. PATENT DOCUMENTS

US3393737	7/1968	Richardson	166292000
US3438440	4/1969	Richardson	166292000
US3285339	11/1966	Walther et al	166295000
US3297086	1/1967	Spain	166295000

Primary Examiner - **Novosad; Stephen J.**

ABSTRACT

A method of treating underground formations, especially those containing clays or clay-like materials which are sensitive to fresh water, to desensitize the clays so they will not swell or disperse on contact with fresh water. The treatment consists of contacting the clay-containing formation with solutions which accomplish the electroless deposition of metal on the clay particles. Optionally, the formation can be resin coated prior to electroless plating.

9 Claims

* * * * *

Found Terms:

US3847222

S6: 1 of 1

US3847222 TREATMENT OF AN UNDERGROUND FORMATION CONTAINING WATER-SENSITIVE CLAYS

United States Patent

Patent Number: **US3847222**

Braden, Jr.; William B.

Date of Patent: **Nov. 12, 1974**

TREATMENT OF AN UNDERGROUND FORMATION CONTAINING WATER-SENSITIVE CLAYS

Inventor:

Braden, Jr.; William B. (Houston, TX)

Assignee:

Texaco Inc. (New York, NY; Assignee type: U.S. Company or Corporation)

Appl. Number: **73US-410721**
Filed: **Oct. 29, 1973**

U.S. Cl.

166303000, 166272000

Field of Search

166272000, 166303000, 166274000, 166273000, 16630500R

References Cited

U.S. PATENT DOCUMENTS

US3064732	11/1962	Bernard et al	166305000R
US3236306	2/1966	Atwood	166305000R
US3360043	12/1967	Braden Jr. et al	166272000
US3444931	5/1969	Braden, Jr	166303000
US3610338	10/1971	Harnsberger	166272000
US3621913	11/1971	Braden, Jr	166272000
US3710863	1/1973	Webster et al	166272000

Primary Examiner - **Novosad; Stephen J.**
Attorney, Agent, or Firm - **Whaley; Thomas H., Ries; C. G.**

ABSTRACT

Method of treating an underground formation containing water sensitive clays and sand to stabilize and/or improve same employing a prescribed volume of steam followed by contact with a guanidine salt in a prescribed type of hydrocarbon solvent.

10 Claims

* * * * *

Found Terms:

US3822749

S7: 1 of 1

US3822749 METHOD OF TREATING SUBTERRANEAN FORMATIONS TO IMPROVE PERMEABILITY

United States Patent

Patent Number: **US3822749**

Thigpen, Jr.; Arnold B.

Date of Patent: **Jul. 9, 1974**

METHOD OF TREATING SUBTERRANEAN FORMATIONS TO IMPROVE PERMEABILITY

Inventor:

Thigpen, Jr.; Arnold B. (Houston, TX)

Assignee:

Texaco Inc. (New York, NY; Assignee type: U.S. Company or Corporation)

Appl. Number: **72US-301904**
Filed: **Oct. 30, 1972**

U.S. Cl.

166303000, 16630500000R

Field of Search

166272000, 166275000, 166303000, 16630500R, 25200855000R

References Cited

U.S. PATENT DOCUMENTS

US2761836	9/1956	Brown et al	25200855R
US2761837	9/1956	Brown et al	25200855R
US2947360	8/1960	Bernard	166305000R
US3349032	10/1967	Krieg	25200855R
US3353593	11/1967	Boberg	166272000
US3379249	4/1968	Gilchrist et al	166303000
US3422890	1/1969	Darley	166305000R
US3444931	5/1969	Braden	166303000
US3454095	7/1969	Messenger et al	166303000
US3603396	9/1971	Braun	166305000R
US3610338	10/1971	Payton et al	166272000

Primary Examiner - **Novosad; Stephen J.**
Assistant Examiner - **Ebel; Jack E.**
Attorney, Agent, or Firm - **Whaley; T. H., Reis; C. G.**

ABSTRACT

A method of treating wells drilled in the earth and the subterranean formation surrounding and in fluid communication with the wells by injecting into the wells and surrounding formation a gaseous mixture comprising steam and an aliphatic polyamine such as ethylenediamine, diethylenetriamine, triethylenetetramine, or piperazine, to increase the fluid permeability of the formation, especially formations which have sustained a permeability decline due to contacting water sensitive clay with fresh water.

18 Claims, 3 Drawing Figures

* * * * *

Found Terms:

US3807500

S8: 1 of 1

US3807500 METHOD OF TREATING SUBTERRANEAN FORMATIONS TO IMPROVE PERMEABILITY

United States Patent

Patent Number: **US3807500**

Thigpen, Jr.; Arnold B., et. al.

Date of Patent: **Apr. 30, 1974**

METHOD OF TREATING SUBTERRANEAN FORMATIONS TO IMPROVE PERMEABILITY

Inventors:

Thigpen, Jr.; Arnold B. (Houston, TX)

Tate; Jack F. (Houston, TX)

Assignee:

Texaco Inc. (New York, NY; Assignee type: U.S. Company or Corporation)

Appl. Number: **73US-340504**
Filed: **Mar. 12, 1973**

U.S. Cl.

166303000, 166307000

Field of Search

166303000, 166312000, 166305000, 166307000

References Cited

U.S. PATENT DOCUMENTS

US3208528	9/1965	Elliot	166305000R
US3444931	5/1969	Braden	166305000R
US3621913	11/1971	Braden, Jr	166305000R
US3710863	1/1973	Webster	166303000

OTHER PUBLICATIONS

Smith et al., Potassium, Calcium Treatments Inhibit Clay Swelling, Nov. 30, 1964, The Oil and Gas Journal, pages 80, 81.

Primary Examiner - **Leppink; James A.**
Attorney, Agent, or Firm - **Whaley; T. H., Ries; C. G.**

ABSTRACT

A method for treating subterranean formations containing water sensitivity clays which have sustained permeability damage due to contact with fresh water, to increase the permeability of the subterranean formations, comprising injecting into the formation via wells drilled into such formations a solution of potassium chloride followed by treating with a heated fluid including steam having a temperature of at least 300 *deg.* F. for several hours, followed by treating the formation with mud acid or retarded mud acid.

11 Claims, 3 Drawing Figures

* * * * *

Found Terms:

US3807500

S8: 1 of 1

US3807500 METHOD OF TREATING SUBTERRANEAN FORMATIONS TO IMPROVE PERMEABILITY

United States Patent

Patent Number: **US3807500**

Thigpen, Jr.; Arnold B., et. al.

Date of Patent: **Apr. 30, 1974**

METHOD OF TREATING SUBTERRANEAN FORMATIONS TO IMPROVE PERMEABILITY

Inventors:

Thigpen, Jr.; Arnold B. (Houston, TX)

Tate; Jack F. (Houston, TX)

Assignee:

Texaco Inc. (New York, NY; Assignee type: U.S. Company or Corporation)

Appl. Number: **73US-340504**
Filed: **Mar. 12, 1973**

U.S. Cl.

166303000, 166307000

Field of Search

166303000, 166312000, 166305000, 166307000

References Cited

U.S. PATENT DOCUMENTS

US3208528	9/1965	Elliot	166305000R
US3444931	5/1969	Braden	166305000R
US3621913	11/1971	Braden, Jr.	166305000R
US3710863	1/1973	Webster	166303000

OTHER PUBLICATIONS

Smith et al., Potassium, Calcium Treatments Inhibit Clay Swelling, Nov. 30, 1964, The Oil and Gas Journal, pages 80, 81.

Primary Examiner - **Leppink; James A.**
Attorney, Agent, or Firm - **Whaley; T. H., Ries; C. G.**

ABSTRACT

A method for treating subterranean formations containing water sensitivity clays which have sustained permeability damage due to contact with fresh water, to increase the permeability of the subterranean formations, comprising injecting into the formation via wells drilled into such formations a solution of potassium chloride followed by treating with a heated fluid including steam having a temperature of at least 300 *deg.* F. for several hours, followed by treating the formation with mud acid or retarded mud acid.

11 Claims, 3 Drawing Figures

* * * * *

Found Terms:

US4478283

S9: 1 of 1

US4478283 Process for improving waterflood performance in heterogeneous clay-sensitive formations

United States Patent

Patent Number: US4478283

Sydansk; Robert D.

Date of Patent: Oct. 23, 1984

PROCESS FOR IMPROVING WATERFLOOD PERFORMANCE IN HETEROGENEOUS CLAY-SENSITIVE FORMATIONS

Inventor:

Sydansk; Robert(Dittleton, CO)

Assignee:

Marathon Oil Compan(Findlay, OH; Assignee type: U.S. Company or Co

Appl. Number: 83US-510126
Filed: Jul. 1, 1983

Int. Cl.-3

3-E21B-033-0138

U.S. Cl.

166292000,166273000

Field of Search

166292000, 166273000, 166274000, 166275000, 16630500R

References Cited

U.S. PATENT DOCUMENTS

US2941597	6/1960	O'Brien	166305000R
US3208528	9/1965	Elliott et al.	166273000
US3371710	3/1968	Harvey et al.	166273000
US3470956	10/1969	Boston et al.	166273000
US3580337	5/1971	Gogarty et al.	166274000
US3581824	6/1971	Hurd	166273000
US3637015	1/1972	Holm	166273000
US3677344	7/1972	Hayes et al.	166273000
US3710863	1/1973	Webster et al.	166274000
US3827500	8/1974	Reed	166274000
US4230183	10/1980	Kalfoglou	166274000

OTHER PUBLICATIONS

Moore, "How to Combat Swelling Clays", The Petroleum Engineer, Mar. 1960, pp. 78-100.

Smith et al., "Potassium, Calcium Treatments Inhibit Clay Swelling", The Oil And Gas Journal, Nov. 30, 1964, pp. 80-81.

Slobod, "Restoring Permeability to Water-Damaged Clays", The Oil and Gas Journal, vol. 68 No. 5, Feb. 2, 1970, pp. 104-108.

Primary Examiner: Burchfield; George A.
Attorney, Agent, or Firm: Hummel; Jack L., Brown; Rodney F.

ABSTRACT

A freshwater containing polyvalent cations and relatively few or no monovalent cations is injected into a heterogeneous clay-sensitive subterranean hydrocarbon-bearing formation via a well. The polyvalent cation solution displaces the saline connate water in the near wellbore environment and contacts a first water-sensitive clay. The polyvalent cation solution exchanges polyvalent cations for monovalent cations in the first clay causing little clay damage while producing a monovalent cation solution which is thereafter displaced into the far wellbore environment. The monovalent cation solution contacts a second water-sensitive clay in the relatively highly permeable zones of the far well-bore environment to effect clay damage and reduce the permeability of the highly permeable zones in the far wellbore environment. The process results in improved waterflood sweep efficiency.

12 Claims, 1 Drawing Figure

* * * * *

United States Patent **5,282,694**

Kovacs, et. al. **Feb. 1, 1994**

Method of reclaiming abandoned settling ponds

Inventors:	**Kovacs; Mihaly** (Plant City, FL); **Kovacs; Peter** (Plant City, FL); **Kovacs; Endro** (Plant City, FL).
Assignee:	**Kempco, Inc.** (Ft. Meade, FL).
Appl. No.:	**977,612**
Filed:	**Nov. 17, 1992**

Intl. Cl. :	**F02B 11/00**
Current U.S. Cl.:	405/36; 210/170; 37/317; 37/337; 405/258; 405/303; 405/52
Field of Search:	405/258, 52, 36, 73, 74, 303; 37/69, 70, 71, 75-78, 58-60, 62; 210/170

References Cited | [Referenced By]

U.S. Patent Documents

1,432,489	Oct., 1922	Osterberg	405/36
1,460,558	Jul., 1923	Olden	37/70
1,760,314	May, 1930	Murrey	210/170 X
2,786,284	Mar., 1957	Todd	37/70 X
4,016,073	Apr., 1977	Jordan	405/129 X
4,276,164	Jun., 1981	Marione et al.	210/170
4,759,664	Jul., 1988	Deal	405/258

Primary Examiner: Taylor; Dennis L.
Attorney, Agent or Firm: Dowell & Dowell

Abstract

Settling ponds used in strip mining are reclaimed using lightweight amphibious vehicles which are capable of traversing land, water or clay surfaces and wherein the method consists of pumping clay settled in subsurface areas and spreading the clay remotely over crusted surface areas to thereby create stabilized low profile drainage ditches which extend from low level areas of the ponds to the perimeters thereof to allow water drain off to the perimeter.

United States Patent **4,759,664**

Deal **Jul. 26, 1988**

Method of building or restoring marshes and beaches

Inventors: **Deal; Troy M.** (277 Trismen Ter., Winter Park, FL 32789).

Appl. No.: **724,251**

Filed: **Apr. 17, 1985**

Related U.S. Application Data

Continuation-in-part of Ser No. 681,071, Dec. 12, 1984, which is a continuation of Ser. No. 579,805, Feb. 17, 1984, abandoned, which is a continuation of Ser. No. 221,219, Dec. 30, 1980, abandoned.

Intl. Cl. :	**E02D 3/00, E02D 17/00, E02F 5/00, E02F 3/88**
Current U.S. Cl.:	**405/258; 37/195; 37/317; 405/117; 405/303**
Field of Search:	405/15, 52, 74, 217, 258, 107, 222, 263; 299/9; 37/54, 195, 66

References Cited | [Referenced By]

U.S. Patent Documents

1,404,112	Jan., 1922	Goebl et al.	405/258
1,844,348	Feb., 1932	Claybourn et al.	406/97
2,158,046	May, 1939	Prendergast	405/74
2,191,845	Feb., 1940	Bretting	405/258
2,818,682	Jan., 1958	Finn	405/258
2,926,437	Mar., 1960	Ellicott, Jr.	37/72
3,521,387	Jul., 1970	Degelman	37/66
3,638,432	Feb., 1972	Schoonmaker	405/74
3,786,639	Jan., 1974	Pineno et al.	405/267
3,842,607	Oct., 1974	Kelseaux et al.	405/217
4,261,117	Apr., 1981	Van Der Peyl	37/58
4,397,587	Aug., 1983	Op den Velde et al.	405/217
4,523,879	Jun., 1985	Finucane et al.	405/217
4,567,731	Feb., 1986	Horan	405/217
4,614,458	Sept., 1986	Austin	405/74

Other References

J. G. Riley, How Imperial Built First Arctic Island, 1974.

Articles from Various Florida Newspapers, 1979.

"New Machine Clears Weed-Choked waterways", North Port News, Feb. 15, 1979.

Primary Examiner: Reese; Randolph A.
Assistant Examiner: Ricci; John A.
Attorney, Agent or Firm: Beaman & Beaman

Abstract

The invention pertains to a method for the building or restoration of marshes and beaches wherein a slurry of solid material and water is formed at one location and pumped to a remote location for uniform distribution of the slurry over a large area to substantially increase the elevation for the purpose of building a marsh, restoring a beach, or the like. The slurry is distributed by a high pressure nozzle uniformly directing a spray which falls in a mist over the area on which the slurry is deposited to produce a significant elevational increase in the area. The nozzle may make alternate directional sweeps, or rotate in a common direction to cover a circular area, with various adjustable vertical angles and pressure variations to control distribution.

16 Claims, 5 Drawing Figures

[USPTO] [CNIDR]

United States Patent **5,616,235**
Acar, et. al. **Apr. 1, 1997**

Electrochemical stabilization of soils and other porous media

Inventors: **Acar; Yalcin B.** (Baton Rouge, LA); **Gale; Robert J.** (Baton Rouge, LA).

Assignee: **Board of Supervisors of Louisiana State University and Agricultural and Mechanical College** (Baton Rouge, LA).

Appl. No.: **655,709**

Filed: **Jun. 3, 1996**

Intl. Cl. : **C25C 1/22**

Current U.S. Cl.: 205/766; 204/450; 204/515

Field of Search: 204/515, 450; 205/766

References Cited | [Referenced By]

U.S. Patent Documents

5,137,608	Aug., 1992	Acar et al.	204/130

Foreign Patent Documents

1-52906	Mar., 1989	JP

Other References

Jacobs et al., "Model and Experiments on Soil Remediation by Electric fields," Sep. 1993.

Sutton et al., "Soil Improvement Committee-Admixtures Report" in a Symposium entitled Soil Improvement-A Ten year update Apr. 1987 pp. 120-135.

P. Madshus et al., "Improvement of Quick Clay by Electrolysis," Scandinavian Geotechnical Meeting, Sweden, Bulletin 17, Dept. of Geotechnical Engineering, Norwegian Institute of Technology (1984) (English Translation).

I. Casagrande, "Electro-osmosis in Soils," Geotechnique, vol. 1, pp. 159-177 (1949).

Acar et al., "Fundamentals of Extracting Species From Soils by Electrokinetics," Waste Mngmnt., vol. 13, pp. 141-151 (1993).

Soil Improvement: History, Capabilities, and Outlook, Amer. Soc. Civ. Eng., pp. 46-47 (Feb.

1978).

Soil Improvement Methods and Their Applications in Civil Engineering, Dept. Civ. Eng., North Carolina State University, Raleigh, NC, pp. 44-49, 56-59, 62-71 (1981).

Acar et al., "Electrokinetic remediation: Basics and technology status," J. Haz. Mat., vol. 40, pp. 117-137 (1995).

Segall et al., "Electroosmotic Contaminant-Removal Process," ASCE J. Env. Eng., vol. 118, pp. 84-100 (1992).

Oldham et al., Materials Evaluated as Potential Soil Stabilizers, Misc. Paper S-77-15, U.S. Army Engineer Waterways Experiment Station, pp. A7, A9, A132, A137, A189, and A194 (1977).

Sutton et al., "Soil Improvement Committee -Admixtures Report," pp. 121-125, 128-135 in Welsh (ed.) Soil Improvement -A Ten Year Update (1987).

van Impe, Improvement Techniques and Their Evolution, A.A. Balkema/Rotterdam/Brookfield, pp. 42-47, 89, 91, and 93 (1993).

Anderson, et al., Soil Improvement History, Capabilities, and Outlook, American Society of Civil Engineers, pp. 46-47, Feb., 1978.

Soil Improvement--A Ten Year Update, Geotechnical Special Publication No. 12, pp. 120-135, Apr., 1987.

Jacobs et al., Model and Experiments on Soil Remediation by Electric Fields, Presented at ACS Emerging Technologies in Hazardous Waste Management V, pp. 1-15, Sep. 1993.

Primary Examiner: Phasge; Arun S.
Attorney, Agent or Firm: Runnels; John H.

Abstract

Suitable electrolyte conditioning at the electrodes greatly facilitates the transport of desired ions through soil, enhancing the ability of electrokinetic processes to stabilize the soil through cementing reactions. Cationic species are injected at the anode, and anionic species at the cathode, with suitable electrolyte conditioning. For example, if acid or base formation negatively affects transport, chemical conditioning is used to neutralize the acid or base products of electrolysis. Ionic species can be transported through soil at rates of several centimeters a day, even in soils such as clays having a low hydraulic conductivity. Electroosmotic transport can be minimized by appropriate conditioning of the pore fluid chemistry. For example, placement of chemical conditioners with smaller cations at the anode compartment and larger anions at the cathode compartment, or increasing the ion content of the pore fluid (e.g. by acidification) can help minimize electroosmotic transport and any of its adverse effects on species transport. The cations and anions are preferably selected to form cementatious precipitates in the soil. Thus when cationic species are injected at the anode and anionic species are injected at the cathode, stabilization reactions can prevail in the soil as the result of cross-transport of species, and a homogenous and uniform cementation and stabilization can be achieved in a short time.

United States Patent **5,137,608**
Acar, et. al. **Aug. 11, 1992**

Electrochemical decontamination of soils or slurries

Inventors:	**Acar; Yalcin B.** (Baton Rouge, LA); **Gale; Robert J.** (Baton Rouge, LA).
Assignee:	**Board of Supervisors of Louisiana State University and Agricultural and Mechanical College** (Baton Rouge, LA).
Appl. No.:	**443,936**
Filed:	**Nov. 30, 1989**
Intl. Cl. :	**C25C 1/22**
Current U.S. Cl.:	205/688; 204/515; 205/702; 205/756; 205/766; 205/771
Field of Search:	204/182.2, 130, 180.1

References Cited | [Referenced By]

U.S. Patent Documents

2,831,804	Apr., 1958	Collopy	204/131
4,453,594	Jun., 1984	Patton et al.	204/130
4,479,857	Oct., 1984	Barton, Jr.	204/130
5,074,986	Dec., 1991	Probstein et al.	204/130

Other References

Daniel et al., Electrokinetic Decontamination of soil, Biennium progress report (Oct. 30, 1989).

Putnam, Determination of pH gradients in the Electrochemical Processing of Kaolinite (Dec. 1988).

Mitchell, Fundamentals of Soil Behavior, pp. 353-370 (1976).

Segall et al., Electro-Osmosis Chemistry and Water Quality, J. Geotech. Engr. Div., ASCE, Technical Notes, vol. 106, No. GT10, pp. 1148-1152 (1980).

Bruch, Electroosmosis in Ground Water Pollution Control, U.S. Dept. Commerce PB-273 377 (1976).

Probstein et al., Quantification of Fluid & Chemical Flow in Electrokinetics, draft position paper presented at Workshop on Electro-Kinetic Treatment and its Application in Environmental-Geotechnical Engineering for Hazardous Waste Site Remediaton (University of Washington, Seattle, Wash., Aug. 4-5, 1986).

Mitchell, Potential Uses of Electrokinetics for Hazardous Waste Site Remediation, presented at Workshop on Electro-Kinetic Treatment and its Application in Environmental-Geotechnical Engineering for Hazardous Waste Site Remediation (University of Washington, Seattle, Wash., Aug. 4-5, 1986).

Runnells et al., A Laboratory Study of Electromigration as a Possible Field Technique for the Removal of Contaminants from Ground Water, Groundwater Monitoring Review, pp. 85-91 (Summer 1986).

Daniel et al., Electrokinetic Decontamination of Soil, Biennium Progress Report Presented to Gulf Coast Hazardous Substance Research Center, Beaumont, Tex. (Oct. 30, 1989).

Lageman et al., Theory and Practice of Electro-Reclamation, presented at Forum on Innovative Hazardous Waste Treatment Technologies, Atlanta, Ga. (Jun. 19-21, 1989).

Putnam, Determination of pH Gradients in the Electrochemical Processing of Kaolinite, M. S. Thesis Louisiana State University, Baton Rouge, La. (Dec. 1988).

Acar et al., Decontamination of Soils Using Electro-Osmosis, Abstract and Slides of Presentation at First Annual Symposium on Hazardous Waste Research (Hazardous Waste Research Center, Baton Rouge, La., (Oct. 20-21, 1987).

Acar et al., Decontamination of Soils Using Electro-Osmosis, Research Proposal submitted to Louisiana Board of Regents (Jan. 9, 1987).

Primary Examiner: Neibling; John
Assistant Examiner: Phasge; Arun S.
Attorney, Agent or Firm: Runnels; John H.

Abstract

The electrochemical decontamination of soil or slurries through the use of an inert anode, a nonreactive cathode, and supplying water to the soil near the anode.

33 Claims, 14 Drawing Figures

[USPTO] [CNIDR]

ANNEXE B

DOCUMENTATION TECHNIQUE RETENUE (COMPLÈTE)

92-H-114

Closure of LG-1 Reservoir Across a Sensitive Clay Terrace

by
P. Langlois and C. E. Schneeberger
both of Tecsult Inc.

and

J. Levay and B. Boncompain
both of Société d'Energie de la Baie James

Presented to

HYDRAULIC POWER SECTION

CANADIAN ELECTRICAL ASSOCIATION

MONTREAL, QUEBEC

SEPTEMBER 1991

RÉSUMÉ

La réalisation du projet hydroélectrique LG-1 implique la construction d'une digue de 2 km de longueur à travers la terrasse argileuse située en rive nord. Le niveau de la crête de la digue est fixé à 35 m en vue de créer un réservoir à la cote 32 m. Dans sa majeure partie, la digue est de type revanche sauf à son extrémité nord où elle atteint une hauteur de 10.5 m.

La nature sensible de la fondation d'argile molle a conduit le concepteur à incorporer dans le projet des travaux de stabilisation des berges tant en aval qu'en amont dans le but d'éviter que des glissements de type coulée n'aient lieu entrainant des conséquences possiblement désastreuses pour la digue. De telles coulées sont typiques des berges argileuses de La Grande Rivière, elles peuvent atteindre des reculs de 1 à 2 km.

Cette contribution décrit les conditions géotechniques de la terrasse argileuse et identifie les principaux critères de conception qui furent adoptés.

SUMMARY

The development of the LG-1 hydroelectric project requires the construction of a 2 km long dyke across a clay terrace. The nominal crest elevation of the dyke is 35 m and will confine the proposed LG-1 reservoir at elevation 32 m. Most of the dyke is of the freeboard type except for its northern extremity where the dyke reaches a height of 10.5 m.

The sensitive nature of the soft clay foundation has called for several design features to assure the stability of the dyke along with both upstream and downstream bank stabilization work in order to avoid the occurrence of potentially disastrous retrogressive slides. Such slides are typical of La Grande River clay banks and may reach 1-2 km in lateral extent.

The paper describes the geotechnical conditions of the clay terrace and presents the most significant design criteria that were adopted.

INTRODUCTION

The development of the LG-1 hydroelectric complex is currently underway in northern Quebec. The powerhouse is a run-of-the-river type with a total installed capacity of 1 368 MW. The project is located (Figure 1) on La Grande River approximately 37 km upstream from the mouth of the river at James Bay.

In addition to the powerhouse, the development includes the construction of a 17 200 m^3/s capacity spillway, a small rockfill dyke on the south shore and a 2,4 km long dyke on the north shore. The general arrangement for LG-1 is shown on Figure 2. The nominal reservoir level is at elevation 32 m while the crest level of the dyke is set at elevation 35 m for sections on till and rock foundation and 36 m for sections on the north terrace.

Additional information on the LG-1 hydroelectric development are given in an accompanying paper (Bouchard et al, 1991).

From a geotechnical standpoint the most interesting feature of the LG-1 development is the presence of a wide sensitive clay terrace along the north bank of the river. The ground elevation across this terrace varies from elevation 31 to 33 m except for its northern reach where a little stream has partially eroded the surficial material down to elevation 26 m. The terrace is constituted of sensitive clay and silt materials partly covered by a fine sand and silty sand deposit. The potential development of retrogressive slides in the sensitive clayey silt as well as the potential for seismic liquefaction of the fine sand layers are elements of concern for the design of the LG-1 dykes.

Historically large slides have always existed in the La Grande River clay banks. Such slides may reach 1-2 km in size (SEBJ, 1991). A recent slide occurred in September 1987, (Figure 3) at km 82.5 involving a total volume of around 3 000 000 m^3 of clay and silt material.

Since the LG-1 terrace conditions are similar to the ones where flowslides occurred, the design of the North Dyke had to incorporate appropriate bank stabilization work both upstream and downstream of the proposed dyke. The aim of this paper is to present and describe the features incorporated in the design which assure the long term integrity of the closure work.

EARTHWORK DESCRIPTION

The North Dyke is divided into three sections. The first section of the dyke is 640 m long, and is built on rock and till foundation and extends from the concrete gravity dam up to a rock knob on the north bank. The second section, 1 200 m in length, is of the freeboard type across the terrace. Finally, the third and last section is 600 m long and is constructed in the eroded depression that borders the clay terrace along its northern limit. Typical cross-sections of the dyke are illustrated in Figure 4. The bank stabilization work is divided into upstream stabilization work and downstream stabilization work. Typical cross-sections are illustrated in Figure 5.

North Dyke on Rock and Till Foundation

This section of the North Dyke has a maximum height of 22 m. The design is standard (SEBJ, 1987 and Paré et al., 1978) and includes a total volume of 436 000 m^3 of earth and rockfill material. The dyke is designed as a rockfill embankment on a till foundation with a core keyed down to bedrock. The design requires the complete excavation of the clayey overburden. The dyke comprises a vertical central till core flanked by granular filters and transitions with rockfill shoulders.

The North Dyke axis was located so that it crosses the river bank where the bedrock is the shallowest.

North Dyke on Terrace

This section of the North dyke is of the freeboard type, its maximum height reaches 5 m and includes an additional 1 m freeboard protection against seismically induced settlements. The dyke construction will require a total volume of 204 000 m^3 of earth material. The dyke is designed as a sand and till embankment on sand foundation. It incorporates a vertical cutoff through the permeable foundation which, as discussed further, constitutes an important element of the downstream stabilization.

North Dyke in the Depression

This section of the North dyke has a maximum height of 10.5 m. It is designed as a granular material embankment on a soft clay and peat foundation. The total volume of required backfill material is around 385 000 m^3. Berms are provided on both sides of the dyke to assure its stability. The lower berm is 50 m wide at an average elevation of 31 m. The upper berm is 45 m wide at an average elevation of 33 m. The wide central core of the dyke is made of till and is founded on clay whereas the sand shoulders are founded directly on peat.

A description of the stability and settlement assessments that were carried out for this dyke is beyond the scope of this paper.

For the last two sections of the North Dyke the sand fill is constituted of fine alluvial sand deposited over the upstream part of the terrace.

Upstream Stabilization

The upstream stabilization includes the construction of a draining rockfill blanket on the existing slope. The blanket has a minimum width of 12 m and extends up to the terrace level. This blanket is provided for a bank length of 1 100 m. The work was carried out in the spring of 1990 with material obtained from the powerhouse excavation.

The upstream stabilization also includes the excavation of a 700 m long trench across the terrace. The bottom of the trench is 40 m wide. An excavation of 250 000 m^3 of sand and silt is required. About 50% of this volume is made up of sand that will be used in the dyke construction.

Downstream Stabilization

The downstream stabilization includes the construction of a series of three staged rockfill berms over a total bank length of 1 200 m. The lower berm is at elevation 5 m to provide access to the river during the summer period. The intermediate berm is set at elevation 9.5 m to resist ice thrust during high winter flow conditions. Finally, the upper berm is at elevation 19.5 m for seismic stability reasons. The lower and intermediate berms were constructed in 1990 when large rockfill volumes were readily available from the powerhouse excavation. The upper berm is presently under construction.

For the control of ground water flow:

- The downstream stabilization also includes the installation of 22 large diameter relief wells that extend to the underlying till stratum.
- Drainage trenches were excavated downstream of the dyke in order to reduce the rainfall infiltration recharge and to support the favourable effect of the cut-off under the dyke.

GEOLOGICAL AND GEOTECHNICAL CONDITIONS

Bedrock Conditions

Figure 6 is a plot of bedrock contours and outcrops across the terrace at LG-1. The general bedrock pattern exhibits a deep buried valley located in the middle of the terrace. The deepest bedrock elevation is at elevation -40 m which represents a total overburden thickness of 70 m.

The buried valley is slightly curved. It intersects the present river bed both upstream and downstream of the LG-1 area. The bedrock valley is separated from the present river valley by a rock ridge which culminates at elevation +30 m. As noted previously, this rock knob was considered in the selection of the closure axis.

Figure 7 is a stratigraphic cross-section along the closure axis and Figure 8 is a section across the terrace in the upstream/downstream direction.

Glacial Deposit

The bedrock is covered by a layer of glacial till of variable thickness. The maximum till thickness of 30 m is found in the deepest section of the bedrock valley. The till layer is more permeable than the overlying clay, so that is was necessary to determine whether or not the till was connected to both the upstream and the downstream river water levels.

Drilling data conclusively indicate that the till is connected with the upstream river bed. It actually outcrops over an island located less than 1 km upstream of the LG-1 powerhouse. The till layer will therefore be considered as hydraulically connected with the future LG-1 reservoir.

In the downstream area the till layer is deeper and covered by a thick clay layer over a long section so that outcropping of the till in the river bed is at some distance from the bank.

Marine Clay Deposit

About 8 000 years ago the waters of the Tyrrell Sea invaded the eastern reaches of James Bay as the Wisconsin glacier retreated to the East. At that time the LG-1 area was located below sea level so that a thick marine clay layer was deposited on top of the existing till and bedrock. The bedrock then slowly rose as a result of the isostatic process that followed the ice retreat.

As shown in Figure 7, the marine clay stratum is presently found throughout the terrace with a rather uniform 20 to 30 m thickness. The clay deposit is however thinner where approaching the outcrops due to recent river erosion.

The clay layer is found near the surface immediately below the surficial peat bog in the northern depression where a 10.5 m high dyke is to be built. The geotechnical characteristics of the clay in this area are described below.

The water content of the clay increases with depth from 35 to 60% within the top 8 m thick transition layer where material varies from clayey silt to silty clay. It then decreases very gradually to about 50% at 20 m depth. The liquid limit varies from 25 to 35 and the plastic limit is equal to around 20. Because of its high liquidity index, the clay exhibits sensitivities in excess of 400 when measured in the laboratory using the Swedish Fall Cone. The marine clay is of soft to medium consistency. The top 5 m thick layer is characterized by an undrained shear strength of around 15 kPa. Below that stratum the shear strength gradually increases with depth up to around 50 kPa at 20 m depth.

Deltaic and River Deposits

Deltaic and river deposits are found on top of the marine clay layer in the middle of the northern terrace. They vary in gradation from fine to medium, compact sand including some silt layers on the upper part of the deposit to loose silty sand and thinly interbedded silts in the bottom part of the deposit.

The thickness of the surficial sand layer (river deposit) appears to increase from the upstream bank towards the downstream bank. The sand actually constitutes most of the northern terrace. It has been eroded along the northern depression by a secondary stream thus forming a 3 m high sand rim.

Peat Deposit

The only significant peat deposit that is of significance to the design of the closure dykes at LG-1 is located in the depression along the northern edge of the sand terrace. The peat layer is variable in thickness reaching a maximum of 3.2 m along the sand terrace. The peat is fibrous with an average water content of around 1200%.

Piezometric Conditions

Three main hydrogeological units across the north terrace are as follows :

- an upper water bearing stratum of deltaic and river deposits;
- an intermediate aquiclude of marine clay;
- a lower water bearing stratum contained in the glacial till deposit and possibly the upper fractured part of the bedrock.

These hydrogeological units were monitored for one year prior to construction.

The piezometric conditions in the upper water bearing stratum are characterized by a near surface water level. In this stratum, the permeability varies from 10^{-2} to 10^{-6} cm/s. The higher permeabilities are generally measured at shallow depths of 3 to 4 m. However, localized pervious sand layers are also found at greater depth. Permeability values of around 10^{-3} cm/s were in fact obtained at depths of 6 to 8 m.

The upper water level appears to be drained by the stream flowing in the northern depression and by the La Grande River. Along the downstream river bank, a series of springs confirm the draining effect of the river bank.

The piezometric conditions in the lower water bearing stratum are apparently characterized by a much lower water head than the upper aquifer as shown on Figure 9. On the downstream section, the head differential between both strata is as high as 20 m. The piezometric levels in the glacial till show the influence of seasonal variations in the river level as induced by the LG-2 powerhouse regulation. Recharge comes from the inland outcrop as in some areas water levels are higher than upstream river levels. Permeabilities in the till are in the range 10^{-3} to 10^{-6} cm/s. This range is quite similar to the range of permeabilities measured in the upper part of the bedrock.

DESIGN CRITERIA

General

The stability of the earth works required to close the LG-1 reservoir across the clayey terrace has to be assured against a variety of conditions.

Firstly, under normal operating conditions, the reservoir level is maintained at a constant elevation of +32 m. The stability of the downstream clay bank may be diminished as a result of a potential rise

in pore pressures in the underlying till or in the surficial sand. The occurrence of a slide at the downstream river bank may trigger a large retrogressive flowslide that could reach the closure dyke.

Secondly, under exceptional drawdown conditions, the upstream clay bank may be destabilized. Any failure of the upstream bank could similarly trigger a major flowslide.

Thirdly, under seismic loading conditions, the closure dykes as well as the bank stabilization work have to remain stable.. The potential for a seismically induced liquefaction of the surface sand layers had to be accounted for in the design of the North Dyke across the sand terrace.

Downstream Bank Stabilization

The river bank downstream of LG-1 is locally unstable. In this area the clayey silt layer which is a transition layer between the marine and deltaic deposits intersects the slope near its toe which corresponds to a depth of about 22 m. This silt material is most susceptible to retrogress over distances as large as 1 500 m. This corresponds to a distance/depth ratio (R/D) of 70 which is on the upper range of recorded data from natural slides (Mitchell and Markell, 1974). There is consequently a risk that such a slide could reach the dyke. Some positive action was deemed necessary to stabilize the river bank.

The river water level downstream of the LG-1 powerhouse will vary depending on the river discharge and ice conditions. The maximum river water level of +9 m occurs in December or January during a very cold winter, when an ice cover is forming in the lower reach of the river and the river flow is maximum. The minimum river water level of +2.0 m occurs in April or May, before the spring thaw.

The critical section of the river bank occurs between 1.5 and 2.7 km downstream of the LG-1 axis where the slopes are steeper, in the order of 1.8H:1V to 2.2H:1V. A typical cross section of the bank is shown in Figure 5c. The terrace is at elevation +28 m and the beach at the toe of the slope at about +3 m. The various soil layers encountered from the surface down are as follows :

- a 20 m thick stratified sand and silty sand;
- a 7 m thick clayey silt layer;
- a 20 m thick marine clay layer;
- a 1 m to 20 m thick glacial till layer.

The stability of the river bank is precarious under present conditions. Recent slides are abundant and conditions will likely deteriorate as a result of the following factors :

- wave and ice action from the river;
- increased water seepage from the upper sand deposit due to the presence of the reservoir;
- increased water pressure in the deeper till deposit due to recharge of the till by impounded water.

The adopted stabilizing measures achieve an adequate stability of the river bank in this area and eliminate the risk of a major retrogressive slide. They include the construction of staged rockfill berms along the toe of the bank. Control of groundwater pressures in the lower aquifer involve the installation of a series of 30 cm diameter relief wells down to the till through the clay layer. The purpose of these wells is to cope with a possible rise of 2 to 3 times the existing head. Also, a positive cutoff wall will be provided along the axis of the dyke through the deltaic and river deposits. This cut-off together with drainage trenches ensures that the stability of the downstream slope is also improved in regard to eventual liquefaction during an earthquake.

Stability analyses were performed using effective strength parameters ($c' = 7$ kPa and $\phi' = 28°$) and actual pore pressure data. The steepest stable section of the downstream bank was assumed to be of marginal stability. The actual pore pressure assumptions were therefore adjusted until a safety factor of 1.0 is obtained.

The predicted long term groundwater conditions in the upper sand were assumed to remain unchanged. The predicted long term groundwater conditions in the till take into account the effect of the relief wells. For these conditions, the required safety factor was determined to be 1.3. Under static conditions, it was found that the crest of the upper rockfill berm should be set at elevation +14 m. However, assuming that the deepest sand layer would liquefy under seismic conditions, an increase in the rockfill crest elevation was required. The residual strength of a partly liquefied sand was assumed to be as low as 25 kPa. The critical safety factor under seismic conditions was found to be approximately 1.1 for a berm elevation set at +19.5 m.

Upstream Bank Stabilization

High and steep clay slopes exist upstream of the LG-1 closure axis. Two distinct zones may be identified. The first zone, approximately 1 200 m long, is characterized by the presence of a rocky hill between the clay slope and the river. The clay slope is 16 m high and is located immediately upstream of the closure axis. Slope failure in this zone may induce a retrogressive slide that could potentially destroy the freeboard dyke and allow the flow to bypass the LG-1 dam. Some positive action is therefore considered necessary in this area.

The second zone is located further upstream of the first one. It is approximately 1 500 m in length. The 24 m high clay slope in this zone has its toe in the river. Since it is located at more than 1 km from the closure axis, it is unlikely that a retrogressive slide originating in this zone would reach the closure dyke. However, in order to limit the extent of any potential slide, a wide trench was proposed across the sand terrace to stop the progress of a slide.

In both zones, the slopes culminates at elevation +32 m which means that they would be completely submerged by the LG-1 reservoir. The slopes would therefore be stabilized under normal operating conditions. However, exceptional events such as sudden drawdown or an earthquake may threaten their stability. In this case, the drawdown conditions are by far the most critical design conditions. The selected design drawdown conditions are such that the reservoir level would be lowered from a normal pool level of +32 m to a spillway sill elevation of +12.35 m in less than 5 days. Considering the clayey nature of the soils, such a drawdown rate represents the worst case of a sudden and near complete drawdown.

The clay slope in the first zone indicated above is composed of a top 5 m thick silty sand layer which is typically underlain by a 14 m thick silt and clayey silt layer. The deeper marine clay deposit appears at an elevation that roughly corresponds to the toe of the slope. The method adopted for stabilizing the slope in this zone involves the construction of a free draining rockfill berm that provides a minimum safety factor of 1.2 during specified drawdown conditions.

In the second zone, the toe of the bank is presently attacked by river flow at elevation +10 m. The slope is cut by numerous slides, some of them being quite recent. In this zone, the slope is topped by a 3 m thick silty sand layer, underlain by a 10 m thick clayey silt layer and a 20 m thick marine clay layer. Typically, the bottom of the slope is steeper than the average due probably to the presence of the clay. Most of the slides have occurred in the upper two-thirds of the slope, where silt and clayey silt are exposed. The likelihood of a retrogressive slide in this zone must be envisaged.

The cost of stabilizing this zone of the river bank was found prohibitive due to the very large volumes of material required. It was decided not to stabilize the slope but rather to accept the risk of a retrogressive slide and to limit its potential extent before it reaches the closure dyke. The idea is to create a topographic depression across the terrace which would stop a retrogressive flow in progress. The trench solution is based on the fact that most natural earthflows in sensitive clays actually terminate in natural gullies. The excavated trench is designed to remain stable when reached by the retrogressive flow.

In the design of the trench, it was assumed that a retrogressive slide had started on the river bank at elevation +15 m at the interface between the clayey silt and the marine clay. The assumed slip surface is at an angle of 1.4% which, according to Mitchell and Markell (1974), corresponds to the worst case of observed slides. The cross section of the stabilizing trench that is used for stability computations was shown in Figure 5b.

The trench geometry was determined so as to provide a safety factor of 1.4. The trench has a depth of 6 m and a base width of 40 m. The trench location was selected to minimize the initiated earthflow volume.

Freeboard Dyke on Terrace

The presence, in the middle of the terrace, of a 24 m thick deposit of fine sand and silt has posed two serious design considerations. The first concern is related to potential ground liquefaction during a seismic event. The second is related to modification of the ground water regime in the sand deposit with potential increase in water level near the downstream river bank. Both concerns are reviewed as follows :

a) Seismic conditions

The selection of the Maximum Credible Earthquake (MCE) for the LG-1 project was based on data provided by Energy, Mines and Resources Canada. The results of this analysis led to the following two seismic events :

- A magnitude 7.5 earthquake occurring 850 km away in the Charlevoix seismic province (see Figure 1)
- A magnitude 5.0 earthquake occurring 30 km away along the James Bay shoreline

Both events would produce a ground acceleration of 0.06 g at the LG-1 site accounting for ground amplification due to the presence of the thick clay overburden.

An initial evaluation of the liquefaction potential was made using the relationship proposed by Yoshimi (1977). According to this author, a seismic event of magnitude M would not create any liquefaction at a distance greater than R where :

$$\log R\ (\mathrm{km}) = 0.77\ M \quad - 3.6$$

Using this equation, it was calculated that the 7.5 magnitude event would not produce liquefaction beyond a distance of 150 km. Similarly a 5.0 magnitude event would not induce liquefaction beyond a 2 km distance. Moreover, a magnitude 5 earthquake would not be critical for liquefaction analysis because it corresponds to only two cycles of vibrations.

It could tentatively be concluded that no liquefaction would be induced at LG-1 under the postulated MCE. In order to substantiate this preliminary conclusion, the approach proposed by Seed and al. (1976) was also used. The cyclic stress ratio τ/σ'_v determined by using this method for a series of sand samples are in the order of 0.07. As shown in Figure 10 they consistently fall in the safe zone as determined by Seed for a magnitude 7.5 earthquake. Penetration data obtained with piezocone equipment have indicated a higher degree of safety.

However, recent earthquake events (Mexico 1985, Saguenay 1987) have raised questions about the amplification properties of thick soft clay deposits. For this reason, it was considered safer to incorporate in the dyke design some additional protection against any loss of freeboard.

The proposed engineering solution is to provide for an additional 1.0 m freeboard. By raising the crest elevation to +36 m, the dyke would be adequately protected against seismically induced ground settlements.

b) Ground water flow conditions

The creation of the LG-1 reservoir at elevation +32 m will induce downward ground water flow in the sand and silty sand deposit underlying the dyke. The adopted design criteria was to make sure that no increase in water level would occur near the downstream end of the terrace.

The ground water flow below the freeboard dyke and through the downstream part of the terrace was modelled using a 2-dimensional finite element computer programm. Various cutoff depths were considered as well as various downstream drainage elements. It was decided to provide for a complete cutoff through the 24 m deep river and deltaic deposits. As shown in Figure 2 it was also decided to provide for two parallel drainage trenches across the terrace to eliminate any recharge of the water level in the terrace.

The cutoff total area is 18 000 m^2. The deepest sections of the cutoff will be constructed using the "plastic diaphragm" technique in order to limit the amount of excavated area so as to avoid sliding in the loose silty sands. In shallower sections of the cutoff, the more conventional slurry trench technique will be used.

CONCLUSIONS

The presence of a 2 km wide sensitive clay terrace located immediately north of the LG-1 development has necessitated important stabilization works.

Large retrogressive slides have occured along the La Grande River in similar clay banks. One such slide encompassed a total volume of clayey material in excess of 3 millions cubic metres. The existence of an unstable bank area downstream of LG-1 indicated that if a large retrogressive slide occured at LG-1 the permanent closure works could be destroyed. In order to fully eliminate such a risk, very significant bank stabilization works have been constructed along the unstable clayey bank area downstream of LG-1. These works include the construction of a staged rockfill berm and the installation of a series of large diameter relief wells.

Sudden and complete drawdown conditions were accounted for in the design with the consequence that existing clay slopes located upstream of the LG-1 axis were stabilized. One area will be stabilized by constructing a free draining rockfill blanket. However, the river bank located further upstream also posed the threat of being destabilized during sudden drawdown. Slope failure in this area could also trigger a major retrogressive slide with, however, less catastrophic consequences. It was decided to accept this risk but to limit the extent of the slide by excavating a wide trench across the terrace in between the upstream river bank and the closure works.

Seismic conditions at LG-1 are far from being severe. However, the presence of a deep fine sand deposit on top of the clay required the potential for ground liquefaction to be studied. Eventhough current design methods showed only a marginal risk of liquefaction, some precautions were taken such as the allowance for an additional freeboard to the dyke.

The bulk of the upstream and downstream stabilization work was constructed during the 1990 season using rockfill materials from specified excavations. The downstream drainage trenches were also excavated in 1990 to provide sand for the early stage of dyke construction. The excavation of the upstream trench as well as the completion of the downstream stabilization work are currently (1991) underway. Despite the large quantities of materials involved in stabilizing the sensitive clay terrace, the costs of these works were maintained at relatively low levels by judiciously combining these works with the powerhouse excavation and dyke construction.

The impoundment of the LG-1 reservoir is scheduled for December 1993.

ACKNOWLEDGMENTS

The authors wish to thank the Société d'énergie de la Baie James for permission to publish this paper and the Tecsult staff in the preparation of this paper. They are indebted to the Board of Engineering Experts of the SEBJ for continued support and advice from the early development of the concepts to the detailed design and drafting of the earth works presented in this paper. The Board is chaired by Dr. R.B. Peck, and comprises D.D. Campbell, G.S. Larocque, J.T. Madill and W. F. Swiger.

REFERENCES

BOUCHARD, M., TREMBLAY, P.R., PERREAULT, J. (1991) "L'aménagement hydroélectrique de La Grande 1". Canadian Electrical Association, Hydraulic Power Section, September, 1991.

MITCHELL, R.J. and MARKELL, A.R. (1974) "Flowsliding in Sensitive Soils", Canadian Geotechnical Journal, Vol. 11, No 1, pp. 11-31.

PARÉ, J.J., LAROCQUE, G.S. and SCHNEEBERGER, C.E. (1978) "Design of Earth and Rockfill Dams for La Grande", Water Power and Dam Construction Journal, Vol. 32, No 1, pp. 38-44, London, January, 1978.

SEED, H.B., Muraka, R., Lysmer, J. and Idriss, I.M. (1976) "Relationships of Maximum Acceleration, Maximum Velocity, Distance from Source and Local Site Conditions for Moderately Strong Earthquake", Bulletin of the Seismological Society of America, Vol. 66, No 4, August, pp. 1323-1342.

SEBJ (1987) "Le Complexe hydroélectrique de La Grande Rivière - Réalisation de la première phase", Publication de la SEBJ.

SEBJ (1991) "Dynamique des berges de La Grande Rivière - Caractérisation de l'état de référence (1989) avant l'exploitation des centrales de La Grande 2A et de La Grande 1", Publication du Service Géologie et Mécanique des Sols de la SEBJ, juin 1991.

YOSMIMI, Y. (1977) "Soil Dynamics and its Application to Foundation Engineering", Proc. 9th Int. Conf. Soil Mechanics and Foundation Engineering, Tokyo, Vol. II.

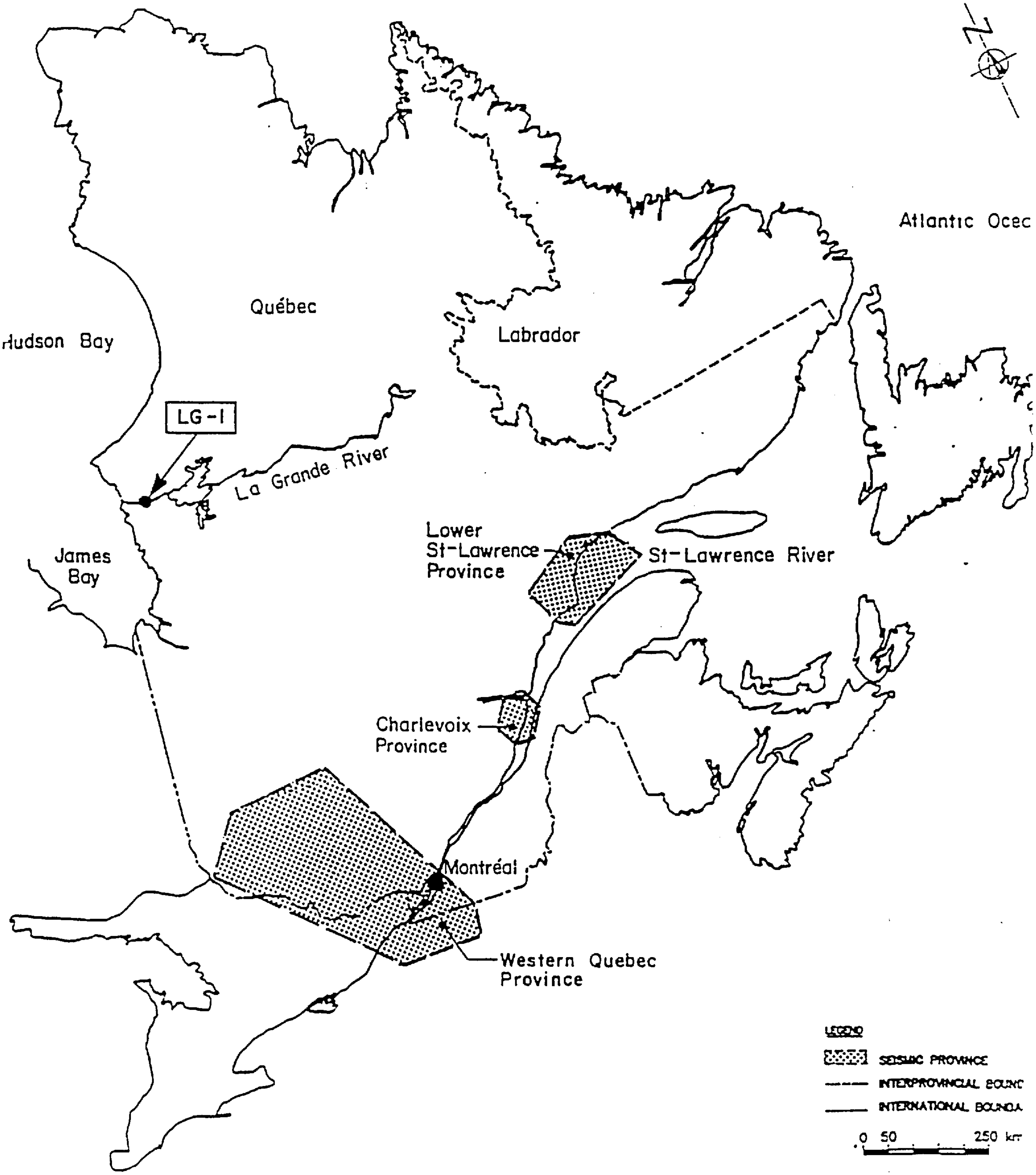

FIGURE 1
LOCATION OF THE LG-I PROJECT

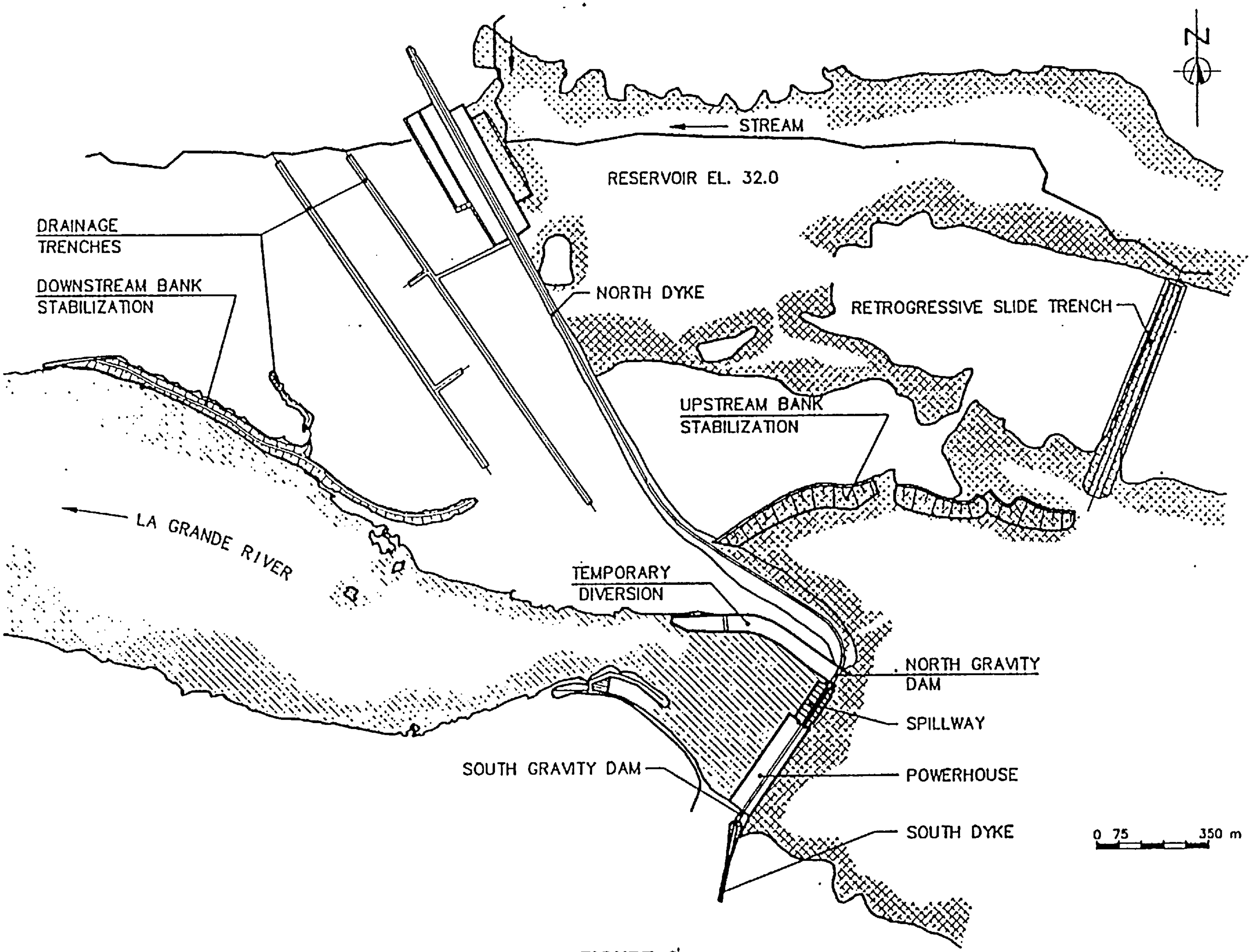
N
STREAM
RESERVOIR EL. 32.0
DRAINAGE TRENCHES
DOWNSTREAM BANK STABILIZATION
NORTH DYKE
RETROGRESSIVE SLIDE TRENCH
UPSTREAM BANK STABILIZATION
LA GRANDE RIVER
TEMPORARY DIVERSION
NORTH GRAVITY DAM
SPILLWAY
SOUTH GRAVITY DAM
POWERHOUSE
SOUTH DYKE
0 75 350 m

FIGURE 2

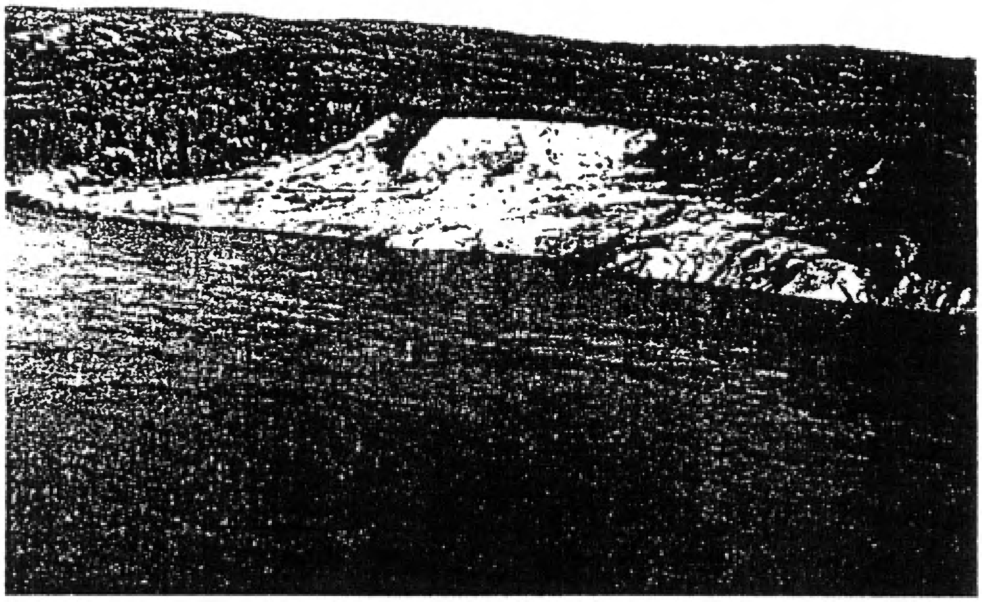

Km 82.5 SEPTEMBER 1987

FIGURE 3

AERIAL VIEW OF FLOWSIDE
IN SENSITIVE CLAY TERRACE
ALONG THE LA GRANDE RIVER

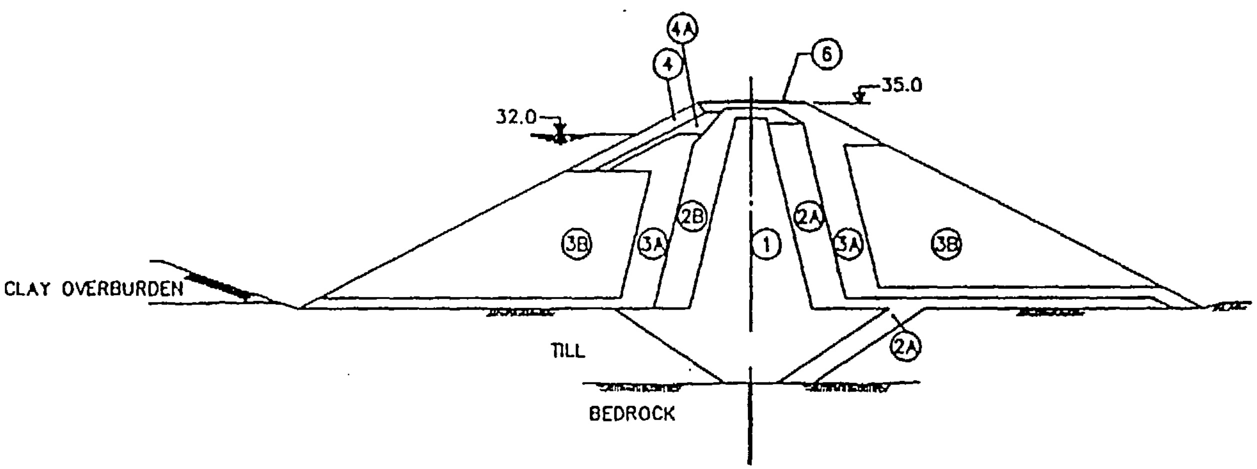

A) NORTH DYKE ON ROCK AND TILL FOUNDATION

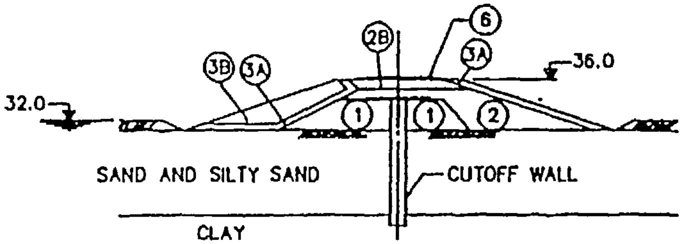

B) NORTH DYKE ON TERRACE

LEGEND

①	TILL
②	PITRUN SAND
②A	SAND AND GRAVEL
②B	SAND AND GRAVEL
②E	SELECTED PITRUN SAND
③A	CRUSHED STONE
③B	ROCKFILL
④	RIP-RAP
④A	BEDDING
⑥	CRUSHED STONE

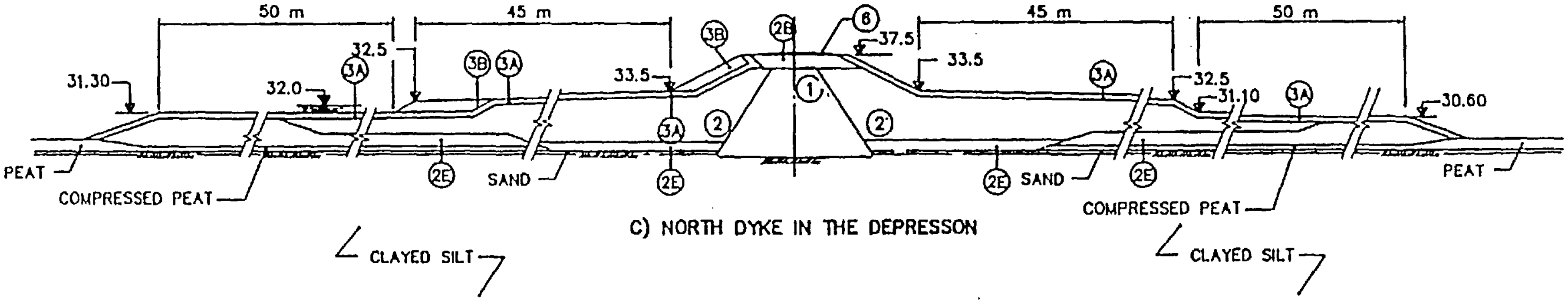

C) NORTH DYKE IN THE DEPRESSON

FIGURE 4

TYPICAL CROSS-SECTIONS UTILIZED FOR DYKE CONSTRUCTION

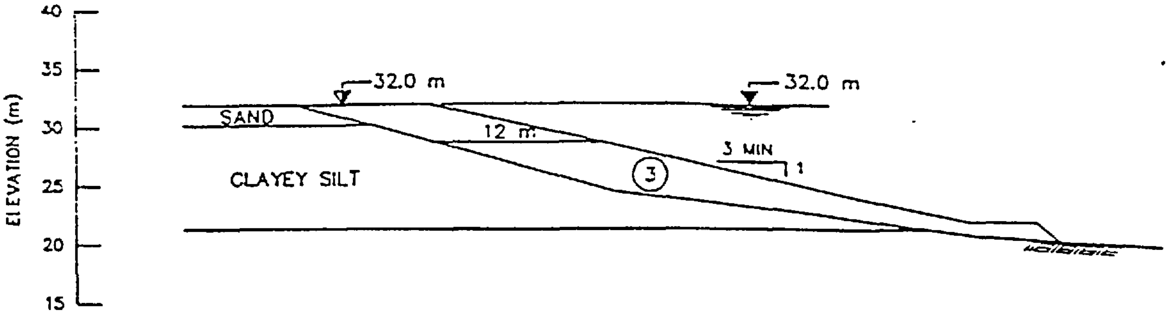

A) UPSTREAM BANK STABILIZATION

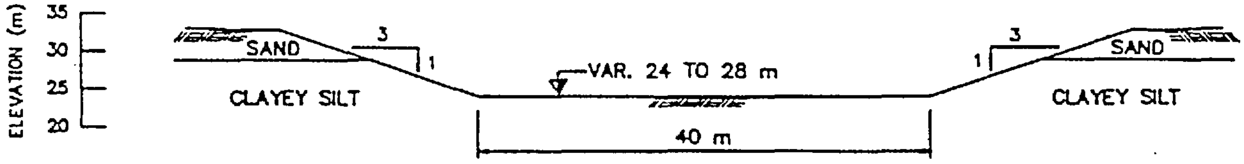

B) UPSTREAM TRENCH AGAINST RETROGRESSIVE SLIDES

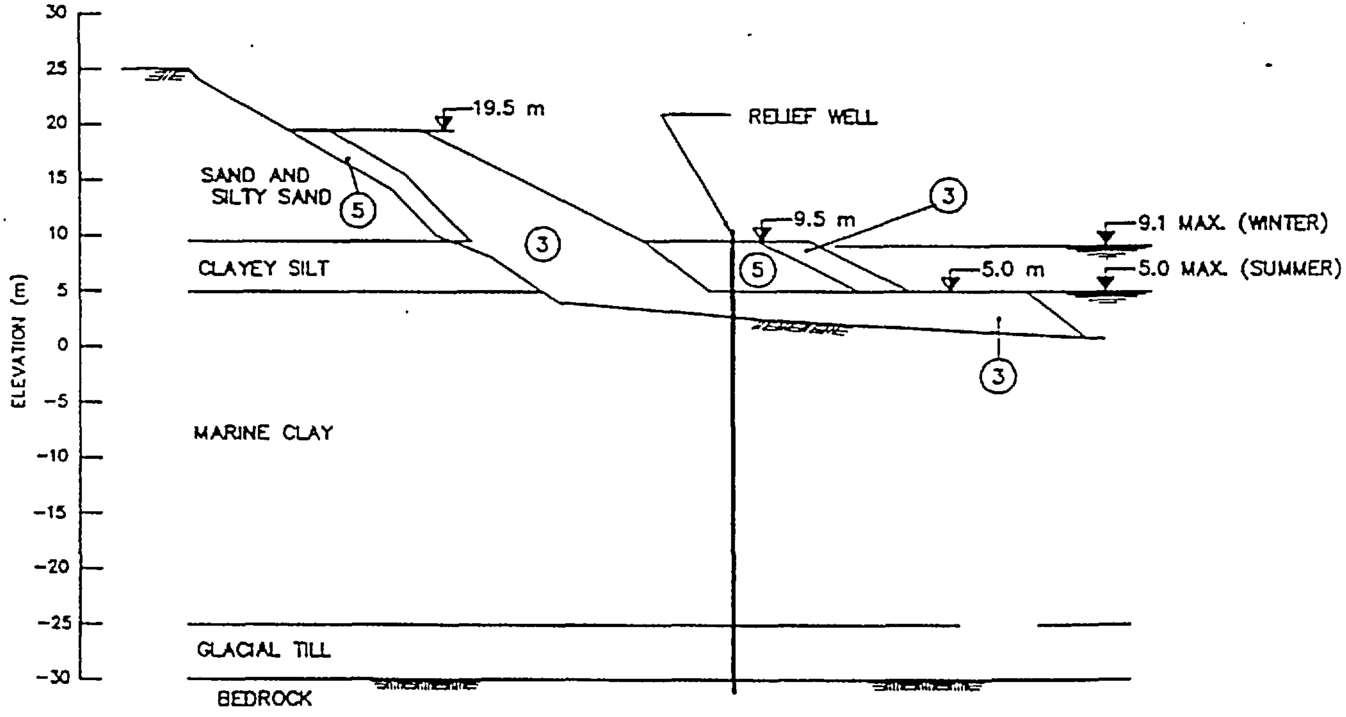

C) DOWNSTREAM BANK STABILIZATION

LEGEND

③ ROCKFILL

⑤ PITRUN SAND AND GRAV

FIGURE 5

TYPICAL CROSS-SECTIONS
USED FOR BANK STABILIZATION

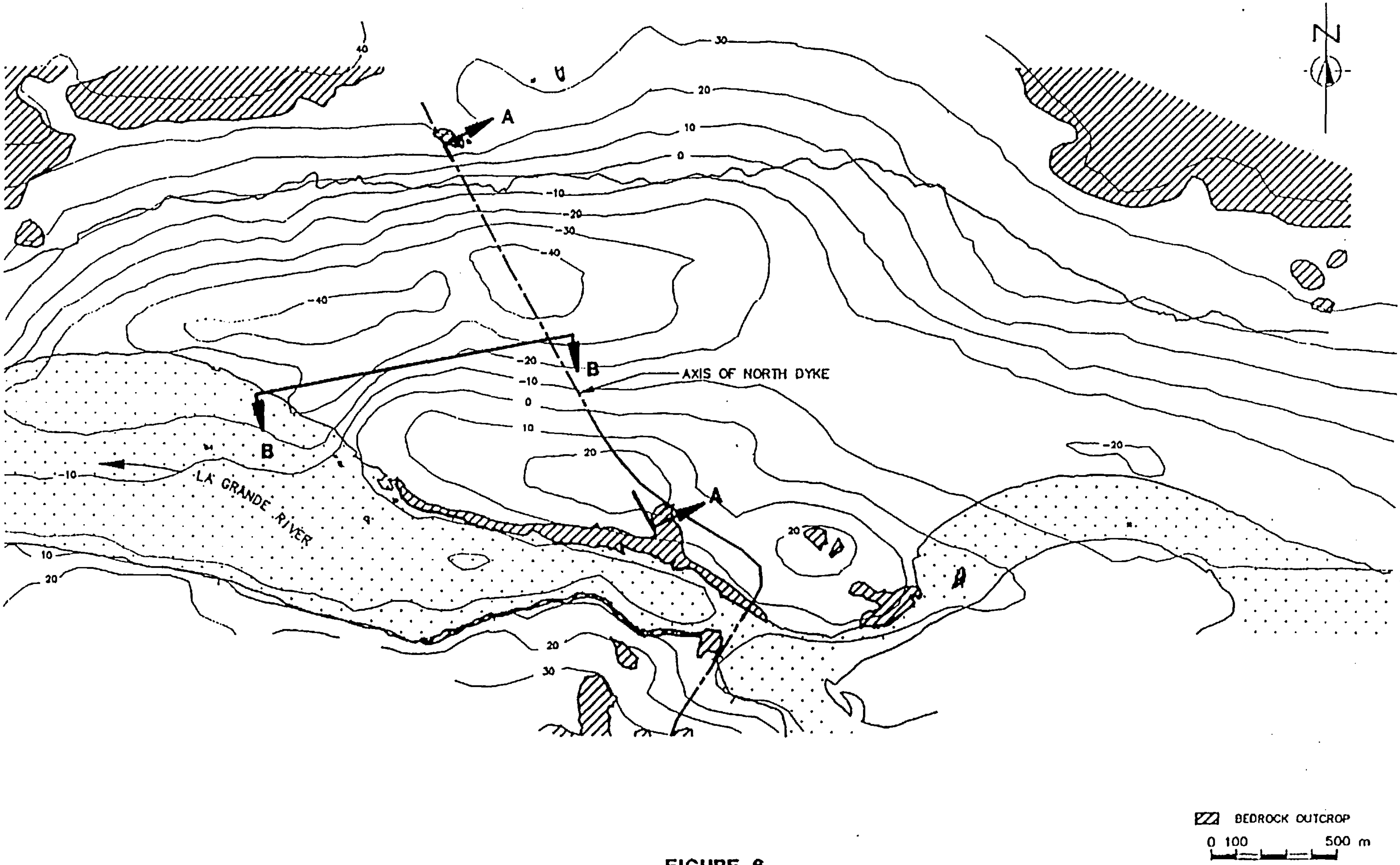

FIGURE 6

BEDROCK CONTOURS

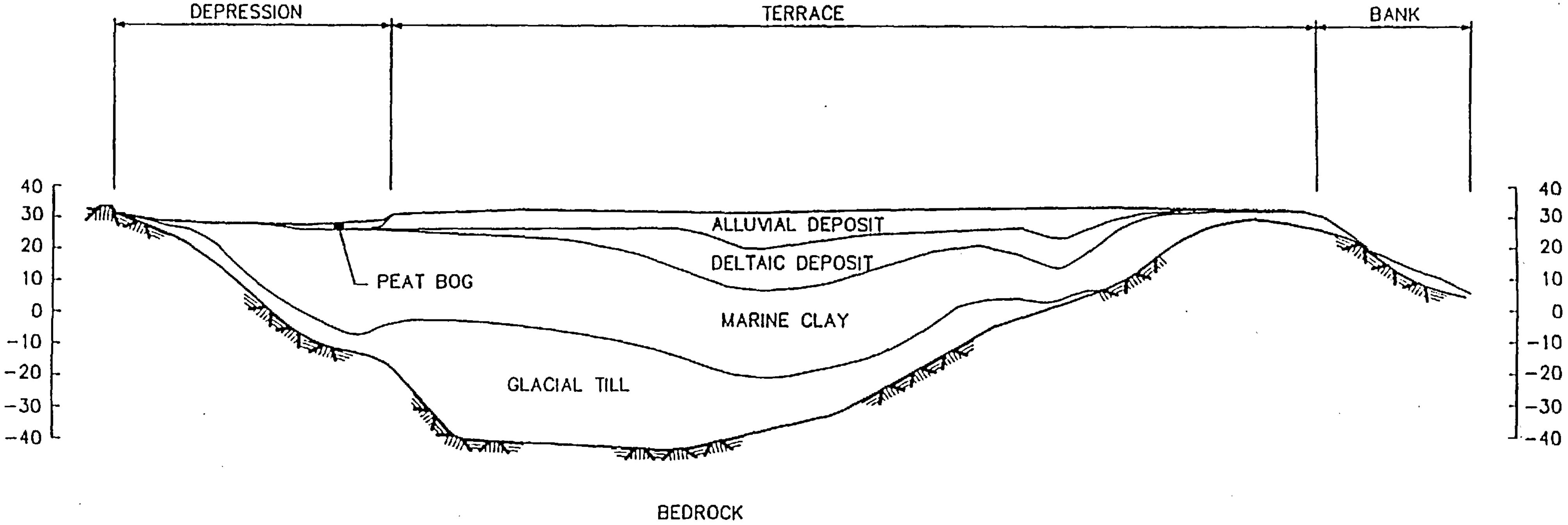

FIGURE 7

LONGITUDINAL SECTION A–A.
ALONG CLOSURE AXIS (NORTHERN TERRACE)
AT LG–1

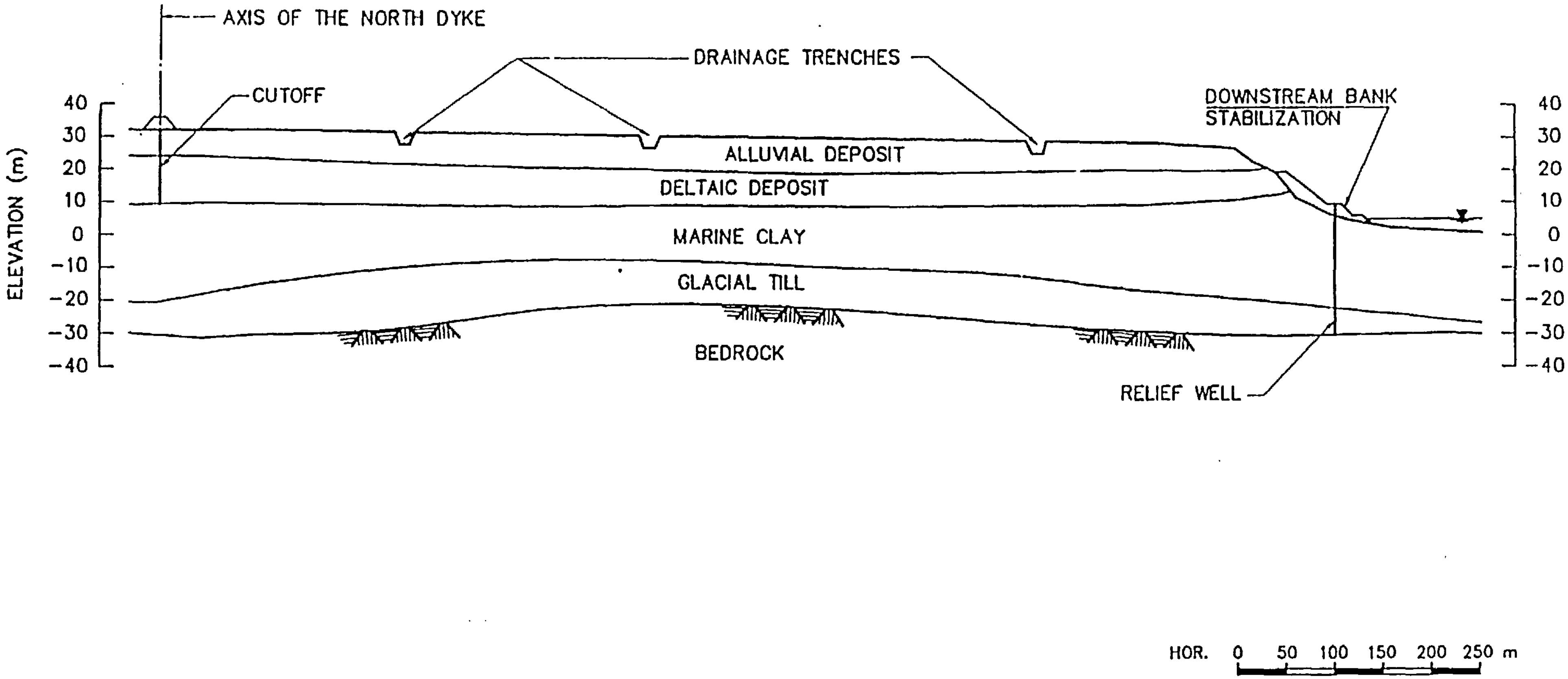

FIGURE 8

LONGITUDINAL SECTION B-B
ACROSS TERRACE AT LG 1

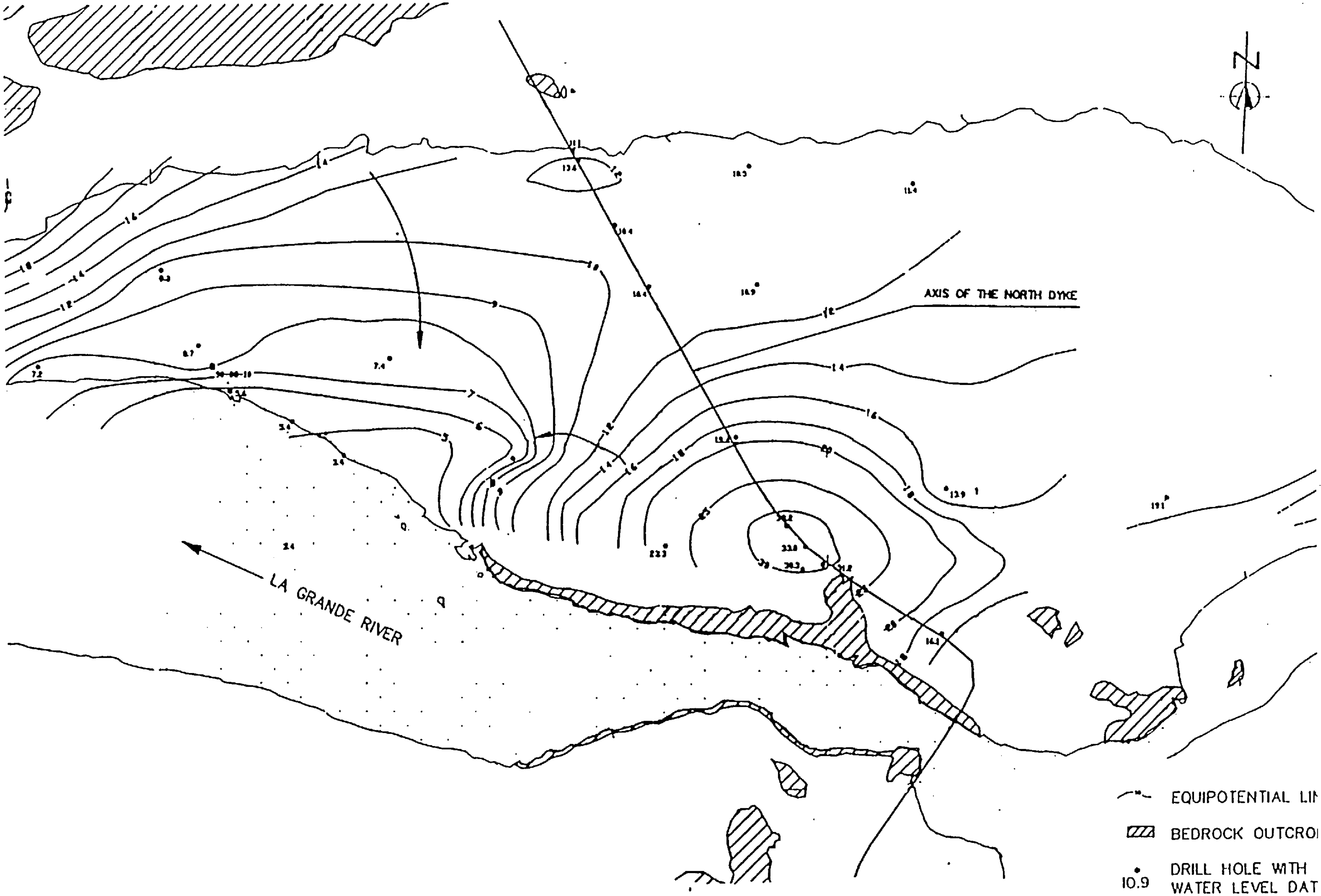

FIGURE 9

EQUIPOTENTIAL LINES IN

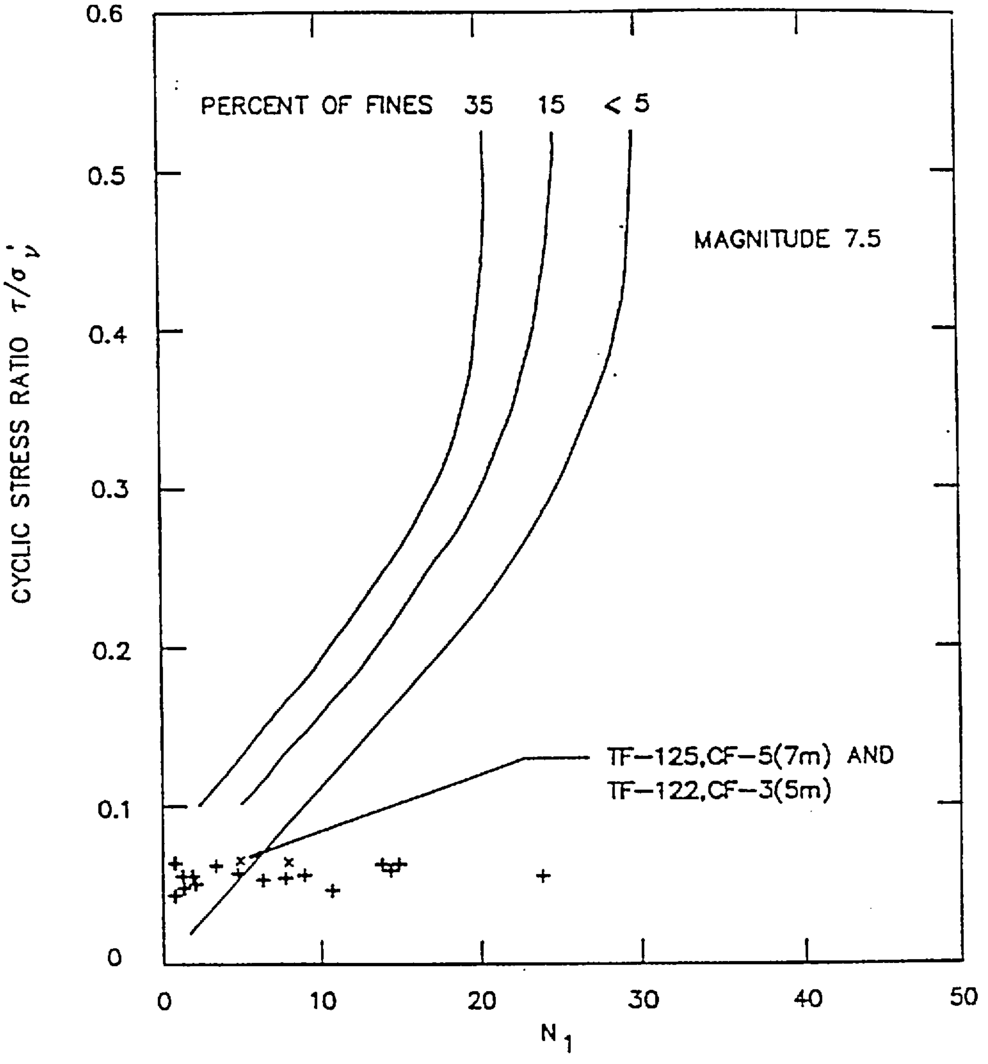

+ FINES CONTENT > 6%
× FINES CONTENT ≤ 6%

FIGURE 10

LIQUEFACTION ANALYSIS
OF SAND AT LG-1

GEOTECHNICAL ENGINEERING
Emerging Trends in Design and Practice

Editor
K.R. SAXENA

A.A. BALKEMA/ROTTERDAM
1994

12

The State of the Art of Geosynthetic Reinforced Soil Structures

T. Yamanouchi and N. Fukuda

INTRODUCTION

Since ancient times natural geotextiles such as timber, bamboo, twigs, reeds, jute, hemp, and palm fibre have been used for the reinforcement of the earth together with the enrichment of it with additional bending and tensile strength in the construction of embankments, stabilisation of weak foundations, and flood control. In some cases these materials are employed to achieve structural effectiveness by means of laying them in the earth in one or multiple layers or by integrating the earth and gravels within mats, cells, and gabions (Yamanouchi 1992). These techniques were handed down from generation to generation and they are, at present, replaced by methods using steel and synthetic materials. However, in some countries the natural geotextiles are still used as effective reinforcing materials (Datye 1987). The use of soil walls for housing construction that gives the earth tensile strength by composing it with straw is known, at present, as the art of Texsol (Leflaive 1982); it integrates the earth by means of long filaments.

The reticulated root pile method and the soil nailing method that increase the stability of the earth structure by insertion of steel bars into the ground are supposed to originate from the idea of stabilising the earth with roots of growing trees.

As to most of these methods the design procedure using limit equilibrium method has been proposed in accordance with the industrially specified reinforcing materials and the mechanical characteristics of the soil and foundation, and thus numerous cases of construction achievement have been reported.

These methods, however, do not necessarily fully reflect the reinforcing mechanism and they are designed adopting high safety factors to compensate for the discrepancy between the design assumptions and the actual performance of the structure. The results of numerous experiments and the structure's actual instrumented observation show that the present design method is so much on the conservative side that it is to be considered uneconomical. Moreover, some are of the opinion that the design will become more rational if the necessary measures for permanent or temporary structure, measures for vitality and safety, and measures for seismic design are taken into consideration. Thus, various future works should be carried out by adopting the approach from the research point of view.

In the present report the fundamental concepts of the reinforcement technique are first compiled and then the present state of the art of design based upon the testing and analysis of geotextile-reinforced embankments and soil walls is described with an emphasis on Japan's research and achievement in the earth reinforcement field.

TYPE OF EARTH REINFORCEMENT METHOD AND PREVAILING CONDITIONS

Table 1 shows types of reinforcement methods and their functions. The reinforcement is expected to achieve tensile resistance, anchor resistance, shear resistance, and bending resistance resulting from the interaction between soil and reinforcement, and in some cases compression resistance is also expected. In some methods multiple effects can be achieved from reinforcement.

The research and development activities on all methods of reinforced embankment construction that are described in Table 1 are compiled in Table 2.

PRESENT DESIGN METHOD FOR GEOSYNTHETIC REINFORCED EMBANKMENTS AND WALL STRUCTURES

Corresponding Reinforced Soil Structures

In this section the present design method of reinforced embankments or walls that have facings from gentle slopes to almost vertical ones (Fig.1) is described.

General Outline of the Design Method

In conducting stability analysis based on limit equilibrium method of reinforced embankment or reinforced wall, Tatsuoka (1986) has classified stability into two kinds, as shown in Table 3. I-B and II are, in some case, called 'internal stability analysis'. I-B is a stability analysis method like Coulomb's earth pressure theory that takes into account the overall limit equilibrium state. On the other hand, II is a method like Rankine's earth pressure theory that takes into consideration the local or partial limit equilibrium state relating to the strain and displacement of localised soil and reinforcement. In I-A the stabilities against sliding, overturning and lack of bearing capacity are checked. And in II-A, the partial limit equilibrium state is checked for all reinforcement members

Table 1. Classification of soil reinforcement construction methods

Group	Sub-group	Representative method	Function of reinforcement
Embankment reinforcement and soil wall	With discrete facing	Terre Armee method	Tensile reinforcement due to friction, partly shear reinforcement
		York method	Ditto
		Geogrid reinforcement method	Ditto
		Websol system	Ditto, partly anchor resistance
		TRRL method	Anchor resistance against thrust
		Multi-anchor method	Ditto
	With rigid facing	RRR method	Tensile reinforcement and retaining wall effect
	Without facing (gentle slope)	Steel mesh reinforcement	Tensile reinforcement, partly shear reinforcement
		Non-woven fabric reinforcement	
		Geonet reinforcement	
		Geogrid reinforcement	
	Without facing (steep slope)	Geogrid reinforcement	Tensile reinforcement, partly shear reinforcement (non-woven: drainage effect)
		Woven fabric reinforcement	
		Non-woven fabric reinforcement	
Foundation reinforcement	Without rigidity	Sheet laying method	Tensile reinforcement, separation
		Geonet laying method	Ditto, restraining
		Geogrid laying method	Ditto
		Steel mesh laying method	Ditto
	With rigidity	Mattress reinforcement	Tensile and bending reinforcement
		Multi-anchored bars	Ditto
Natural slope reinforcement	Short steel bars	Soil nailing	Tensile, shear, and bending reinforcement
	Long steel bars	Reticulated root pile	Tensile, shear, bending, and compression reinforcement

that can stand against the pull out and rupture conditions under the exerting forces.

The procedure for stability analysis is generally classified into three types as follows.

A) The method of approach from the point of partial internal stability

1) Determine the resultant of horizontal external forces, $(\sigma T_{req})_{max}$, required to make the reinforced embankment stable.

Table 2. Chronology of activities on development of reinforced soil structures and their environs

Year	Events
1952	Reticulated root piles were developed in Italy (adopted according to underpinning)
1959	Woven fabrics were laid for rehabilitation works of Isewan Typhoon disasters (Japan)
1962	Development of non-woven fabrics of continuous fibres by spun bond method (USA)
1963	Development of Terre Armee (France) by Vidal (patent 1966)
1968	Development of woven sheets (Fukuzumi) or geonet laying method (Yamanouchi) for weak ground (Japan)
1970s	Development of soil nailing method for underground excavation (France and Germany)
1974	Development of reticulated root piles for slope stabilisation works
1977	The use of geosynthetics to reinforce the backfill behind retaining walls (US Forest Service and Sweden)
	Int. Conf. the Use of Geotextiles (1st Int. Geotextiles Conf.) (Paris)
1978	Symp. Reinforced Soil Structures by ASCE, Pittsburgh, Pennsylvania (USA)
	Development of a temporary support system for excavation by soil nailing system (Shen *et al.*)
1979	Development of polymer grid reinforcement (UK)
1980	Successful construction of Websol system (UK)
1981	State of the art report on reinforced soil structures (J.K. Mitchell *et al.*), 10th Int. Conf. SMFE, Stockholm, Sweden.
1982	2nd Int. Geotextile Conf., Las Vegas (USA)
	Continuous synthetic fiber method for granular soil reinforcement by E. Leflaive
1983	Session on Reinforced Soil Structures, 8th Symp. European Society of SMFE (Helsinki)
	Case study of embankment construction using polymer grids, UK's success story
1984	Symp. Polymer Grid Reinforcement in Civil Engineering (London)
	Announcement of Steep Reinforced Embankment Design by Jewell *et al.* (London)
	Symp. Geomembranes (Denver)
	Int. Geotextile Society (IGS) founded (presided over by J.P. Giroud)
	Geotextiles and Geomembranes, an Int. Jour. Publication (Ed. by T.S. Ingold)
	Geotextiles and Geomembranes by Int. Information Source (Ed. by J.D. Scott and E.A. Ricards)
1985	Technical Committee on Geotextiles, ISSMFE (TC9) established
	11th Int. Conf. SMFE, Geotextiles sectional meeting (chaired by J.P. Giroud, San Francisco) *Earth Reinforcement and Soil Structures* (Ed. by C.J.F.P. Jones)
1986	3rd Int. Geotextile Conf. (Vienna)
	Geotextile Testing, an Inventory of Current Geotextile Test Method and Standard (Ed. IGS)
1987	Publication of *Guide to Design and Construction on Reinforced Slope with Steel Bars* (Japan Highway Public Corporation)
1988	Publication of *ASTM Standards on Geosynthetics* (1st ed., 2nd ed. in 1991)
	Report on Strengthened Reinforced Soils and Other Fills by British Standards Institute
	Int. Symp. Theory and Practice of Earth Reinforcement (chaired by T. Yamanouchi, Fukuoka, Japan)
1990	*Specification for the Use of Geotextiles and Related Materials* by Ground Engineering Group Board, ICE
	4th Int. Geotextile Conf. (Hague)

Contd.

Table 1. Classification of soil reinforcement construction methods

Group	Sub-group	Representative method	Function of reinforcement
Embankment reinforcement and soil wall	With discrete facing	Terre Armee method	Tensile reinforcement due to friction, partly shear reinforcement
		York method	Ditto
		Geogrid reinforcement method	Ditto
		Websol system	Ditto, partly anchor resistance
		TRRL method	Anchor resistance against thrust
		Multi-anchor method	Ditto
	With rigid facing	RRR method	Tensile reinforcement and retaining wall effect
	Without facing (gentle slope)	Steel mesh reinforcement Non-woven fabric reinforcement Geonet reinforcement Geogrid reinforcement	Tensile reinforcement, partly shear reinforcement
	Without facing (steep slope)	Geogrid reinforcement Woven fabric reinforcement Non-woven fabric reinforcement	Tensile reinforcement, partly shear reinforcement (non-woven: drainage effect)
Foundation reinforcement	Without rigidity	Sheet laying method	Tensile reinforcement, separation
		Geonet laying method	Ditto, restraining
		Geogrid laying method	Ditto
		Steel mesh laying method	Ditto
	With rigidity	Mattress reinforcement	Tensile and bending reinforcement
		Multi-anchored bars	Ditto
Natural slope reinforcement	Short steel bars	Soil nailing	Tensile, shear, and bending reinforcement
	Long steel bars	Reticulated root pile	Tensile, shear, bending, and compression reinforcement

that can stand against the pull out and rupture conditions under the exerting forces.

The procedure for stability analysis is generally classified into three types as follows.

A) The method of approach from the point of partial internal stability

1) Determine the resultant of horizontal external forces, $(\sigma T_{\mathrm{req}})_{\mathrm{max}}$, required to make the reinforced embankment stable.

Table 2. *Contd.*

Year	Events
1991	Successful Construction of Geosynthetic-reinforced Soil Retaining Wall (RRR method) for Railway by Railway Technical Research Institute (Japan) Publication of *Recommandations Clouterre* by Ponts et Chaussees (France) Int. Symp. Geosynthetic-reinforced Soil Retaining Walls (chaired by Wu, Denver, Colorado) ASTM standards on geosynthetics (USA)
1992	Publication of *Manual for Design and Construction of Geotextile Reinforced Soil Method*, Public Works Research Institute (Japan) Int. Symp. Earth Reinforcement Practice (chaired by Ochiai *et al.*, Fukuoka. Japan)

Table 3. General outline of the method of stability analysis for reinforced earth structure (after Tatsuoka, 1986)

I. Checking of overall stability	I-A. Check external stability assuming the reinforced zone as a rigid body	
	I-B. Check overall stability assuming not only the reinforced zone as a rigid body, but also slip circle passing the inner part of reinforced zone	Checking internal stability
II. Checking of partial stability	II-A. Determine the forces acting on each reinforcement using equilibrium condition of section-area around the reinforcement and check its stability	
	II-B. Check against sectional extra-deformation and sectional repture	

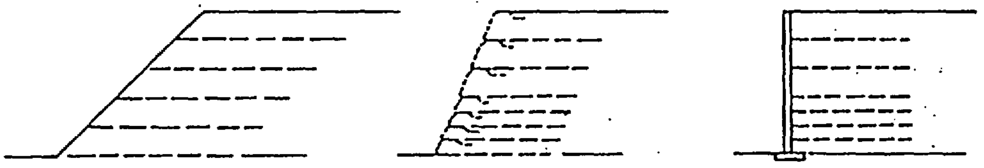

(a) Reinforcement of gentle-slope embankments

(b) Reinforcement of steep-slcpe embankments

(c) Reinforcement of wall structures

Fig. 1. Various kinds of reinforced embankments and walls

2) Compute the required tension (T_{req}) for each reinforcement member from the assumption that the tensile forces are distributed in the depth direction and resisting the required external resultant obtained from (1).
3) Secure the fixing length and the material strength to keep the material stable under the T_{req} determined in (2).
4) The above is the partial internal stability of the reinforcement members and from this condition the laying pattern of the reinforcements is determined.

5) Check the overall external stability of the reinforced zone (slipping, sliding, and overturning).
6) Check the overall internal stability (slipping) for the area other than the slip area that has the maximum value of ΣT_{req}.

B) The method of approach from the overall internal stability of reinforced zone

1) Assume the strength and the layout of the reinforcements.
2) Check the integration of the reinforced zone by checking the overall internal stability as to various slipping surfaces that pass through the reinforced zone.
3) Check the overall stability of the reinforced zone (slipping, sliding, and overturning).

C) The method of approach from the external stability of reinforced zone

This method is similar to method (A). According to step (5), the required width of reinforced zone is first determined and then the internal stability is checked in this method.

The representative method of (A) is the method of Terre Armee, and the Design and Construction Manual (1992) of geotextile reinforcement method by Public Works Research Institute, Ministry of Construction, in Japan (hereinafter PWRI) also corresponds to this method (A).

On the other hand method (B) is adopted in the Reinforced Embankment Manual (1992) for Railway Structures by the Railway Technical Institute in Japan. This method positively uses the integration of the zone reinforced by laying of reinforcements. For this integration effect, not only the reinforcements but also the treatments for rigid facing are the predetermined conditions.

Moreover, the representative method (C) is used for the design of geogrid-reinforced wall by Jones (1984).

Besides the above-mentioned basic design method, the kind of failure mode, the form or pattern of the slip-failure plane, the definition of safety factor and design method, and the way of thinking for the tension-distribution of the reinforcement should be taken into consideration.

Table 4 gives comparative design considerations of the reinforced embankments or reinforced walls. In that Table, the failure mode of Jones (1984) coherent gravity method is the same as that of Terre Armees.

Figure 2 shows the comparison of how the coefficient of earth pressure, K, is affected by the type of slip failure mode and the kind of stability analysis method. The value of K is calculated by the following equation:

$$K = \frac{2\Sigma T_{req}}{\gamma H^2}$$

where ΣT_{req} is the total required reinforcement's tensile force and H is height of embankment.

Different slip failure modes, such as two-part wedge of Jewell *et al.* (1984), Schmertmann *et al.* (1987), Fukuda *et al.* (1989b) (a part of Geogrid Research

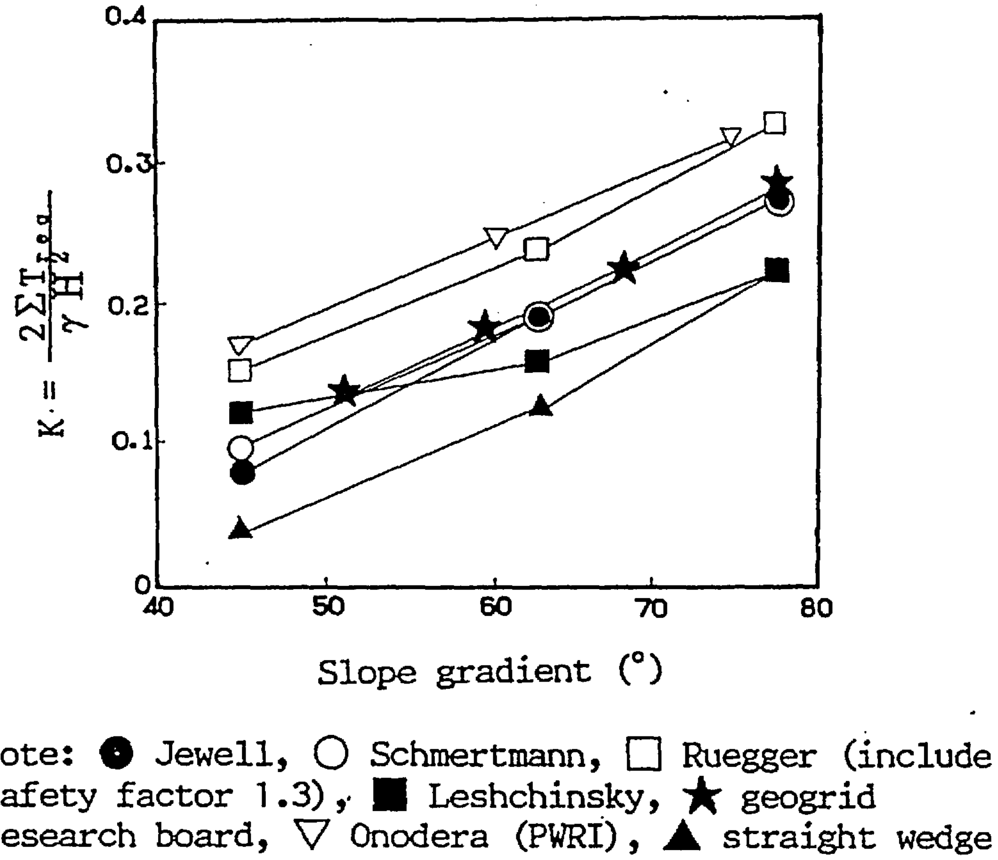

note: ● Jewell, ○ Schmertmann, □ Ruegger (include safety factor 1.3), ■ Leshchinsky, ★ geogrid research board, ▽ Onodera (PWRI), ▲ straight wedge

Fig. 2. Comparison of K values of various proposed design methods. (Modified version of Fukuda *et al.* 1989a)

Board's proposal 1990) and the slip circle of Ruegger (1986) and Onodera *et al.* (originated from PWRI proposal 1992), log spiral of Leshchinsky *et al.* (1987), are proposed and adopted. These are also added by the linear failure mode of Fukuda *et al.* (1989a). In the case of slip circle method, the safety factor is adopted as 1.2 by Onodera *et al.* (1992). This value is higher than that of any other method. From this fact it can be inferred that the required quantity of reinforcements is different from one method to another under similar design conditions.

PRACTICAL PERFORMANCE OF REINFORCED SOIL STRUCTURES

Steep-slope reinforced embankments or walls have been constructed at numerous sites. There are more than 16,000 cases of practical reinforced soil wall construction based on the Terre Armee method, which is considered the principle of all reinforced soil wall construction techniques. The number of achievements in soil structure construction using geosynthetic reinforcement is also increas-

Table 4. Development of design methods for embankment structures reinforced with polymer grids or other geotextiles

Author	Reinforce material (RM)	Length of RM	Strength of RM	Soil constant	Pore water pressure $\gamma_u = u/\gamma z$	Interacting friction coefficient	Slope angle (°)	Ultimate equilibrium model	Layer spacing	Crest surcharge	Notes
Ingold (1982) (design chart)	Geotextile	Parallel, same length	—	ϕ'	—	—	30–80	Endless slope slip circle	Constant	—	Safety of slope
Jewell *et al.* (1984) (design chart)	Geogrid	Parallel, same length	Safe design strength at end of design	ϕ'_c	$\delta = 0.5\phi'_c$ $0, 025, 0.5$	(Pullout) $\delta = 0.8\phi c'$	30–80	Two-part wedge	Arbitrary	Uniform distribution	Most used chart (design method) Safe design strength = specified inservice-strength/safety factor = $f_k/\gamma_u F_s$
Jones *et al.* (1984) (design chart)	Geogrid	Parallel, same length	Same as Jewell's	ϕ'	—	*Refer to notes	90	Slip plane	Arbitrary	Uniform distribution	Design procedure Coherent gravity and tie-back wedge
Yamanouchi *et al.* (1986)	Geogrid	Parallel, same length	40% of tensile strength	Shirasu ϕ' $\tan^{-1}\left[\frac{\phi'}{1.5}\right]$	—	Same as Jewell's	30–80	Two-part wedge	Arbitrary	Uniform distribution	• Basically same as Jewell's method • Apply Richardson's method for seismic design • Tensile strength during earthquake = 1.4 × that of static condition

Bonoparte *et al.* (1986) (design chart)	Geogrid Geotextile	Parallel, same length	50% of maximum strength	ϕ'_{cr}	—	Determine by shear box test	45–90	Two-part wedge	Constant	—	Seismic design based on static design method (charting the ratio of dynamic force/static force)
Hirota and Yamaoka (1986) (design chart)	Geotextile	Parallel	Long-term tensile strength	ϕ'	Arbitrary γ_u	$\delta = 2/3\phi'$	Steep slope	Slip circle log-spirial	Constant	Uniform distribution	Proposed the safety factor map
Schneider and Holtz (1986) (design chart)	Geogrid Geotextile	Parallel	Strength determined from test	ϕ' c'	0.35	$0.5\phi' < \delta < \phi'$	0–40	Two-part wedge	—	—	Extension of Murray's research, consider the cohesion
Leshchinsky and Perry (1987) (design chart)	Geotextile	Parallel	25–50% of tensile strength	ϕ'	—	$\delta = 2/3\phi'$	15–90	Plane slip log-spirial	Constant	Uniform distribution	Refer to the report of Delaware University, 1985
Schmertmann *et al.* (1987) (design chart)	Geogrid	Parallel, different length	< 20–40% of tensile strength	ϕ'_f $\tan^{-1}\left[\frac{\phi'}{1.5}\right]$	—	0.9 times shear strength of soil	30–80	Two-part wedge slip plane	Arbitrary	Uniform distribution	Extension of Jewell's research

ing steadily. These earth structures are designed on the principles of classical mechanics taking large safety factors including long-term durability problems on the conservative side. Various laboratory tests, prototype model tests, and instrumented measurement of completed structures are conducted with a view to checking the viability of design method, realising the reinforcement mechanism, and monitoring the structure during and after construction. Several design methods proposed on the basis of the available data do not necessarily reflect the real reinforcing mechanism of reinforced soil structure and some structures are to be assessed as over-designed or very conservative designs. At present, consequently, a series of researches are conducted with the objective of establishing a rational approach to design with practical consideration of reinforcing mechanism and also an economic design. Here some differences between the design and the constructed structure are described on the basis of results from several research works.

Behaviour of Geosynthetic Reinforced Soil Structures

It is clear from the results of field measurement that the tensions in the reinforcements of reinforced soil structures tend to be less than those of the design computation (Fukuda *et al.* 1986 and others).

Field measurements and their comparisons of partial factors of safety were conducted by Rimoldi (1988) on two types of steep-slope reinforced embankments, by Yamanouchi *et al.* (1986a, Kagoshima) and Cazzuffi *et al.* (1988, Modena) on five types of concrete-face reinforced soil walls, by Berg *et al.* (1986, Tucson, Lithonia, Gaspe) on three types of reinforced embankments, and by Christopher (1987, Cascade) and Bathurst *et al.* (1987, Kingston) on two types of reinforced embankments (Table 5). Rowe and Ho (1992) also compared the measured tensions and the results computed by 12 proposed design methods for four types of wall. The 12 proposed design methods are Jewell (1987), Schlosser (1990), Bonaparte *et al.* (1987), Forest Service (1983), Broms (1978), Collin (1986), Tensar Corporation (1986), Murray (1980), Simac *et al.* (1990), Leschinsky and Perry (1989), Schmertmann *et al.* (1987), and Ruegger (1986). As to walls 1 to 3, the designed values are 1.6 to 2.5 times larger than the measured values and hence the design parameters are overestimated. As to wall 4 with plywood facing, 4 m high test wall by Minami *et al.* (1987), the designed values are equal to the measured values.

The above-mentioned trend shows the same result even if the designed parameters of fill material are taken on the safe side. Thus, caution is necessary in the evaluation of reinforcement effect.

Reduction of Earth Pressure on the Wall

In a reinforced soil wall the earth pressure acting on the facing is generally taken at active state. And the reinforced wall with reinforcements of high-tensile stiffness is designed with earth pressure at rest acting at the upper section of the

Table 5. Partial factors of safety for eight instrumented reinforced soil walls steep slopes (Rimoldi 1988, modified by Rowe and Ho 1992)

Factor of safety	Kagoshima	Tucson	Lithonia	Caspe	Cascade	Kingston′	Kingston″	Modena
FS1	0.9–2.3	0.9–3.2	—	1.05–2.4	0.75	2.16	1.93	2.9
FS2	2.7	1.2	11.6	1.21	1.14	—	—	3.6
FS3	2.5–6.1	1.2	—	1.28 · 2.9	0.85	—	—	10.9
FS4	11.3–27.0	11.5·32.0	—	9.1–21.0	3.0	32.0	11.4	27.2
FS5	4.5–10.8	4.2·11.6	—	2.4–5.6	2.4	11.6	4.1	13.6

FS1 = α_c/α_m FS2 = α_d/α_c FS3 = α_d/α_m FS4 = α_f/α_m FS5 = α_a/α_m

α_c = average tensile force using *in situ* parameters
α_m = measured tensile force or tensile force deduced from strain
α_d = average tensile force calculated using design parameters
α_f = peak tensile strength
α_a = allowable tensile strength
′ full panel, ″ discrete panel

wall. Broms (1978) has taken into consideration the earth-pressure reduction effect of fabric-reinforced retaining wall on the basis of limit equilibrium condition of fill material sandwiched between the reinforcements. The integration effect that results from the interaction of soil and reinforcement is not taken into consideration in design methods, except in Broms'. The more flexible the wall facing, the more the earth pressure on the wall is likely to be reduced, taking the tensile stiffness of reinforcement and the soil's strength-deformation characteristics as governing factors.

Fukuda *et al.* (1984) compared active earth pressures and the observed horizontal earth pressures that result from the forward-inclined facing when grids are fixed or not fixed to the rigid wall of 1 m height in the soil-container test. From this comparison it is learnt that Rankine's active earth pressure is in equilibrium in the case of geogrids fixed to the wall, and the earth pressure reduction which corresponds to the pullout resistance of reinforcements can be achieved when the grids are not fixed to the wall.

Rowe and Ho (1992) show the relationship between the height ratio and normalised horizontal soil stress (K/Ka) for four types of walls (Balzer *et al.* 1990, Berg *et al.* 1986, Simac *et al.* 1990) and Yamanouchi *et al.*'s prototype test wall (1986b, height 6.4 m, discrete concrete panel facing, geogrid SR-2) as shown in Fig. 3.

From these results it is verified that earth-pressure reduction can be expected when the wall facing has some allowance for deformation. With this idea in mind Yeo *et al.* (1992) proposed the reinforced soil structure that makes use of compressible boundary between the facing and the fill material. Research on simulation of earth-pressure reduction effect by numerical analysis was also conducted (Ogisako *et al.* 1988, Hada *et al.* 1988).

Vertical Pressure Distribution at Bottom of Reinforced Zone

In the design of reinforced soil structures based on limit equilibrium method, the external stability is checked by the equilibrium condition of surcharge load, earth pressure in the rear section, and dead load of the structure assuming the reinforced zone as a pseudo-gravity wall and the width of reinforced zone is determined. The vertical pressure acting on the bottom of reinforced zone thus derived is assumed to be of trapezoidal and Meyerhof's distribution pattern. The measured vertical soil pressures of constructed reinforced wall by Berg *et al.* (1986) and also a comparative study by Bolton and Pang (1982) reveal that the Meyerhof's assumption, i.e., the uniform distribution, is more representative than the trapezoidal distribution. These results demonstrate that assuming the reinforced zone as showing the rigid behaviour is not necessarily appropriate for the reinforced soil structure.

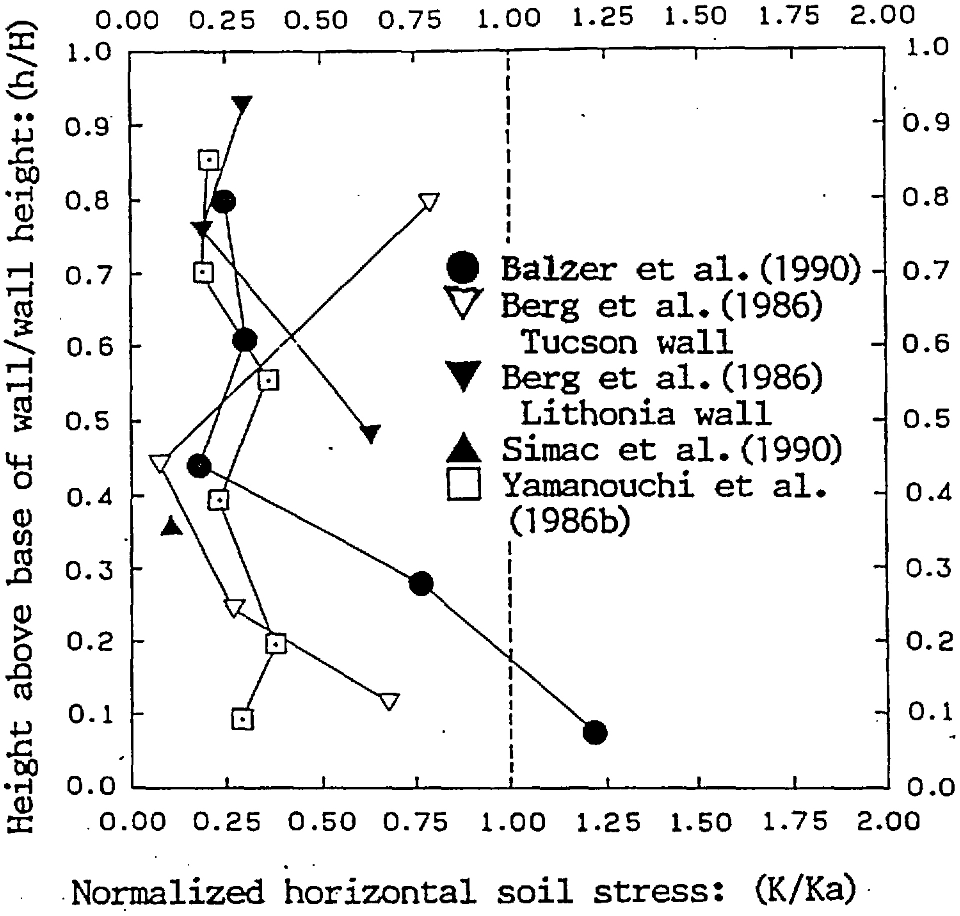

Fig. 3. Field observations of horizontal soil stress at wall face (after Rowe and Ho 1992; additional work by Yamanouchi *et al.* 1986b)

The Required Laying Length of Reinforcements for Steep-Slope Embankment and Wall

The laying length of reinforcements is generally basically taken to be uniform throughout on the principle of the pseudo-retaining wall assumption. Minami *et al.* (1987) carried out the tests on a prototype model of geogrid-reinforced earth wall and found the required reinforcement .length. The apparatus set up for testing is as shown in Fig. 4 and in this test the minimum reinforcement length required for the embankment stability is determined by cutting the geogrids serially as the electricity is passed through the wires wound around the geogrids. Figure 4 shows the occurrence of slip surface approximately equal to Rankine's potential failure plane in time of the embankment rupture. From the tests it was verified that the wall structure is kept stable if the minimum required laying length is taken as a bond length determined on the basis of the active failure plane.

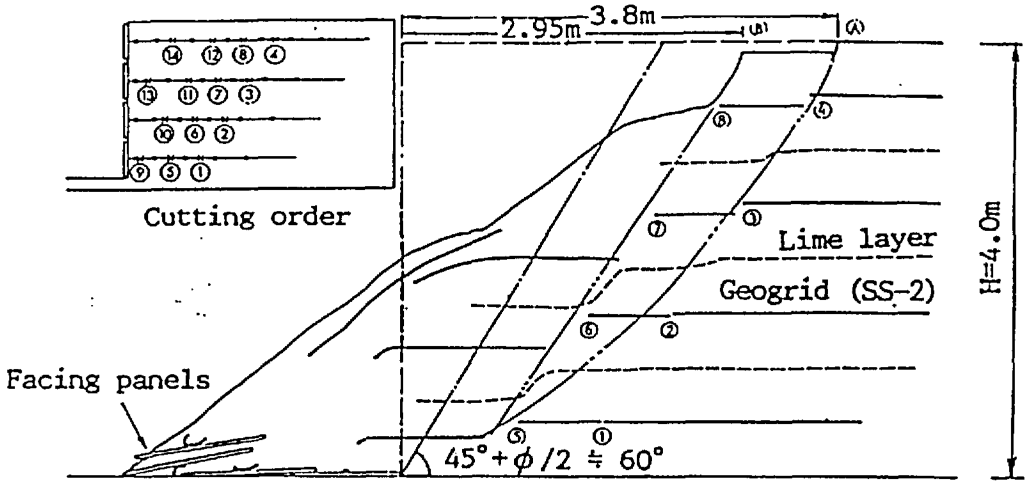

Fig. 4. Geometry of reinforced wall and locations of observed failure plane (after Minami *et al.* 1987)

Yamanouchi *et. al.* (1986b) has conducted tests on 6.4 m high geogrid-reinforced prototype retaining wall and compared the results of two cases, one with uniform reinforcement length 4.5 m, and the other with length 2.5 m at 2 m height from the bottom. The design is done in accordance with the tie-back-wedge theory, and as shown in Fig. 5 both walls are confirmed stable. With uniform reinforcement length the strain or tension does not take place at the inner geogrids of the lower section and thus it is clear that these reinforcements do not contribute to the stability of the wall.

As stated above, the reinforcement laying length required for the stability of reinforced earth wall should be equal to the bond length that satisfies the resisting force of the potential failure line at active state. Thus, Japan's design procedure for reinforced earth structure is developed on the basis of Terre Armee's method.

THE ROLE OF WALL FACING IN REINFORCED SOIL WALL

In considering the reinforcing mechanism of the conventional reinforced soil wall the wall facing bears the earth prèssure acting on it, and the design is based on the principle that the resistance against the earth pressure is secured by the pullout resistance of the reinforcements. In fact the wall facing is expected to display its efficiency in aesthetics and stability to protect the wall from local failure at upper wall section and from degradation of reinforcement members of slope surface and their damage. The role of the reinforcement effect on the overall reinforced earth wall is not taken into consideration.

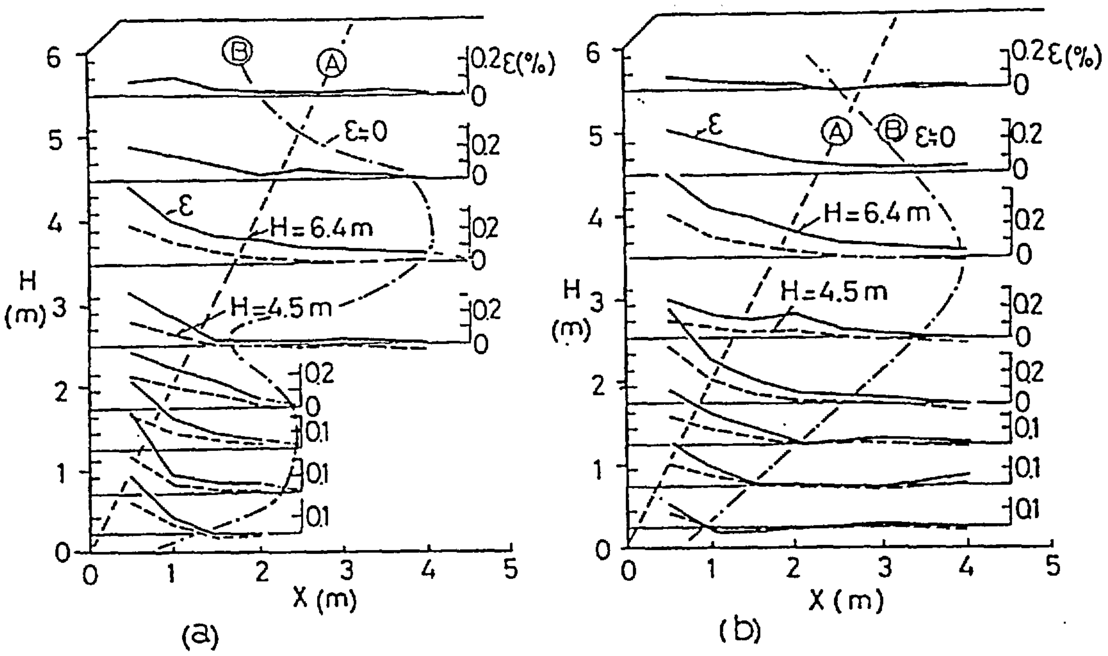

Fig. 5. Strain distribution of polymer grids during constructing prototype test wall, (A) potential failure plane in active state, (B) locus of zero-strain in reinforcements (after Yamanouchi *et al.* 1986b). (a) reinforcement length 4.5 and 2.5 m, (b) reinforcement length 4.5 m

Tatsuoka (1992) has classified the wall of the reinforced earth structure into the types shown in Fig. 6 and Table 6. The effectiveness of the contribution of the wall type (local rigidity, overall axial rigidity, overall shear rigidity, overall bending rigidity, gravity resistance) toward stability is discussed.

Out of the various types, E type satisfies all kinds of facing rigidity and requires some change of pattern for efficient display of the effect of reinforce-

Table 6. Classification of facing types according to the facing rigidity (after Tatsuoka, 1992)

Facing rigidity	Facing type								
	A	B1	B2	B3	C	C′	C″	D	E
Local rigidity	×	△	□	○	○	○	○	○	○
Overall axial rigidity	×	×	×	×	○	×	○	○	○
Overall shear rigidity	×	×	×	×	○	○	×	○	○
Overall bending rigidity	×	×	×	×	×	×	×	○	○
Gravity resistance	×	×	×	×	×	×	×	×	○

× : Lacks of facing rigidity
△ : Slightly having facing rigidity
□ : Moderately having facing rigidity
○ : Sufficiently having facing rigidity

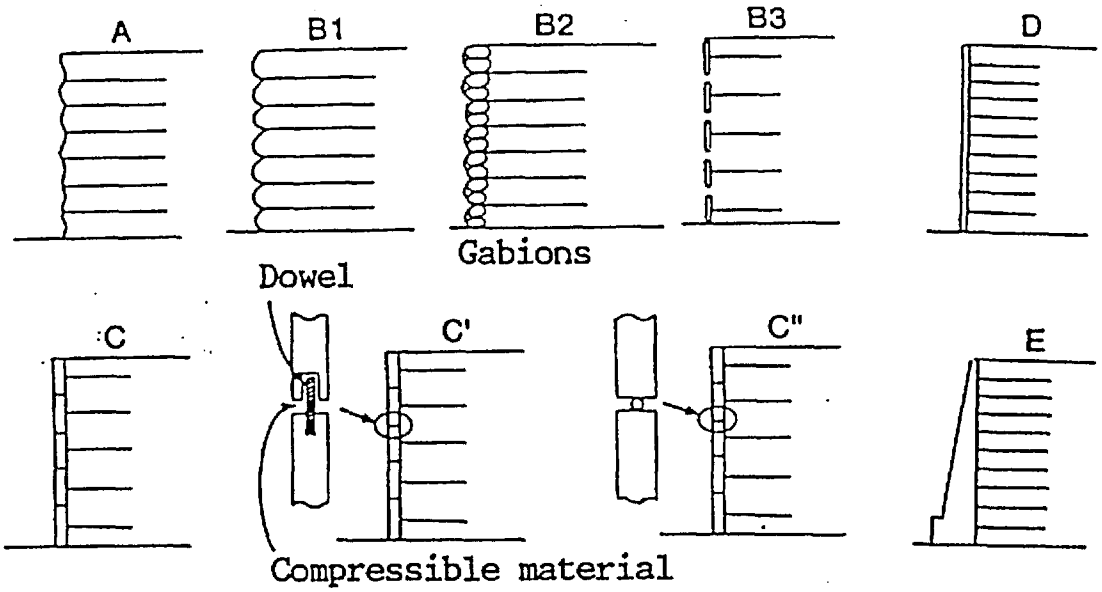

Fig. 6. Schematic diagram showing various facing types for vertical walls (after Tatsuoka *et al.* 1992)

ment. The method of retaining wall construction, first the vertical slope formed by geogrid reinforcement and then the cast-in-place concrete facing at the front, has been developed as shown in Fig. 7 against the paradox of the gravity-type facing that restrains the deformation of the fill body. As the integration of reinforcements and wall facing can be achieved by this method, it is confirmed by means of loading tests that the reinforcement length can be shortened. The author suggests the reinforcing mechanism that takes into consideration the gravity facing's resistance as shown in Fig. 8. According to this method the deformation of fill material is already completed and a high bearing capacity can be obtained with a very small deformation under additional load. Hence, this construction method is applied to railway embankment construction such as that in Shinkansen and the total extended length of such embankment construction runs more than 7 km. Moreover, the application of this method to bridge footing is also successful.

On the other hand, Miki *et al.* (1992) have demonstrated that the pile of sand bags used for slope surface treatment proves to be quite effective as a retaining structure by means of the destruction tests on geogrid-reinforced embankment of height 6.0 m and face slope horizontal (H): Vertical (V) = 0.2 : 1

This means that the embankment failure test is conducted with a variation of spacing and length of grids that are disconnected by means of passing electricity through nichrome wires prewound at 27 cm interval on grids (25 cm spacing) as shown in Fig. 9. The critical grid laying spacing is found to be 1-2 m according to the prediction analysis by circular method and two-part wedge method; eventually the embankment collapses 70 cm grid spacing with sand-bag pile-up.

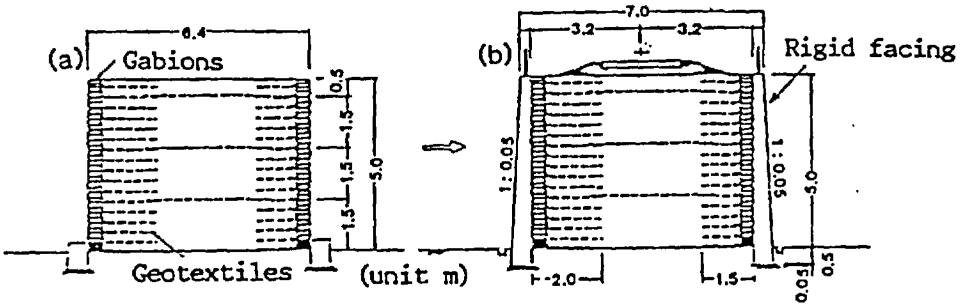

1st stage: construct vertical embankment with multilayered short reinforcements and sand bags

2nd stage: construct cast-in-place concrete facing

Fig. 7. Reinforced soil wall method with rigid facing and short reinforcements for railway embankment (Murata *et al.* 1991)

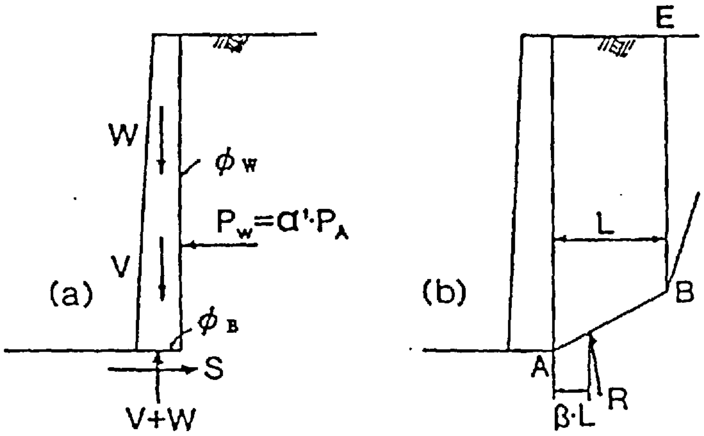

W:Weight of facing
$V=\alpha P_W \tan\phi_W$
P_A=Active earth pressure when unreinforced
$S=(V+W)\tan\phi_B$
$P_W=\alpha' P_A$

Fig. 8. Coefficients α, α', and β to take into account the contribution of the facing's rigidity to the stability of the wall (after Tatsuoka *et al.* 1992)

From the test the effectiveness of the reinforced zone (width 70 cm) as a retaining structure is analysed by force polygon method and it is clear that the reinforcement mechanism displays its utmost efficiency as a retaining structure when the result of vertical forces and earth pressure of the rear section is within the reinforced zone with an appropriate inclination. Figure 10 shows the relationship between the safety factors with and without the resistance of retaining structure. Figure 11 shows how each force (sliding force, shearing resistance of soil, reinforcing strength, and resisting force by wall structure) changes at each stage of wire cutting to maintain the stability of the steep reinforced embankment ($F_s = 1.0$).

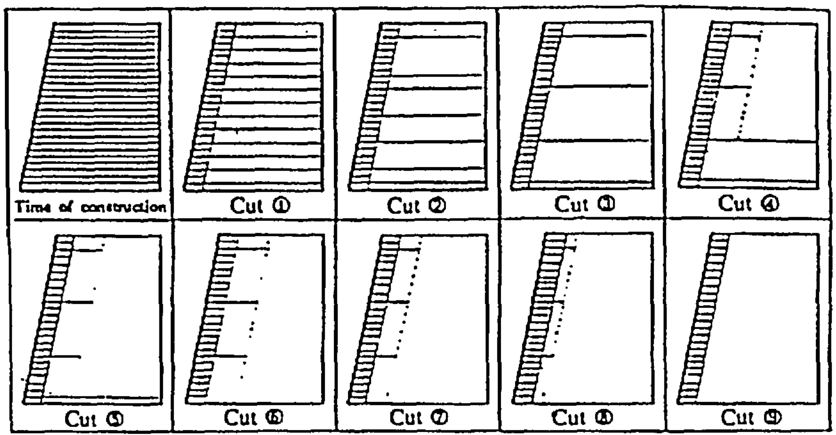

Fig. 9. Cutting stages of geogrids (after Miki *et al.* 1992)

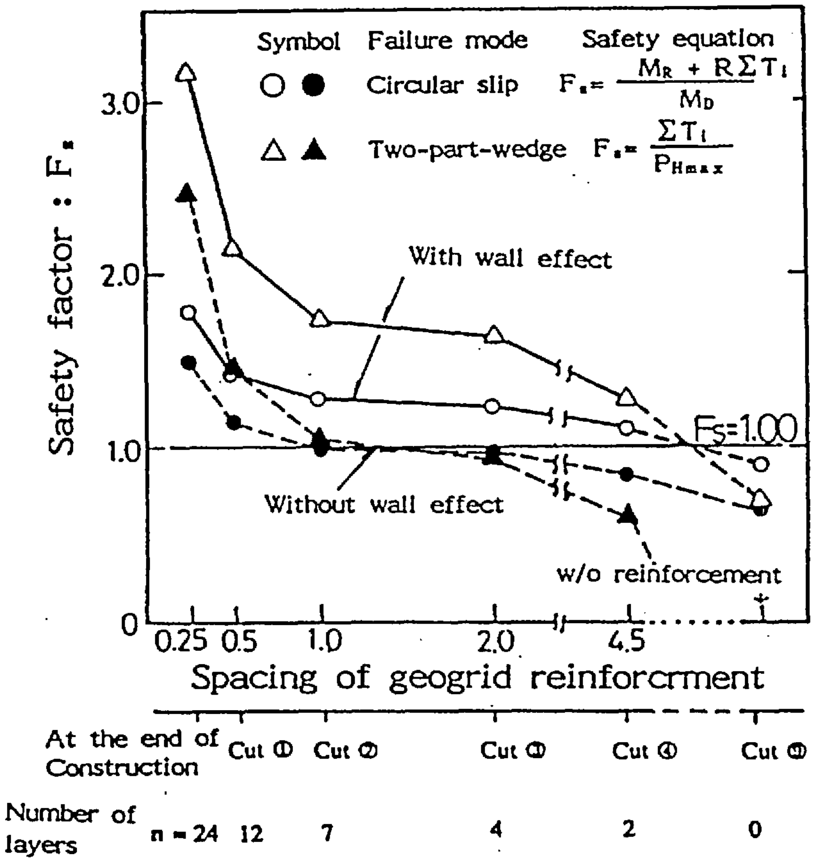

Fig. 10. Transition of safety factors based on measured tensile resisting force, with and without retaining wall effect (after Miki *et al.* 1992)

The retaining effect thus obtained from slope structure proves that the measured tensions of grid are lower than the computed ones.

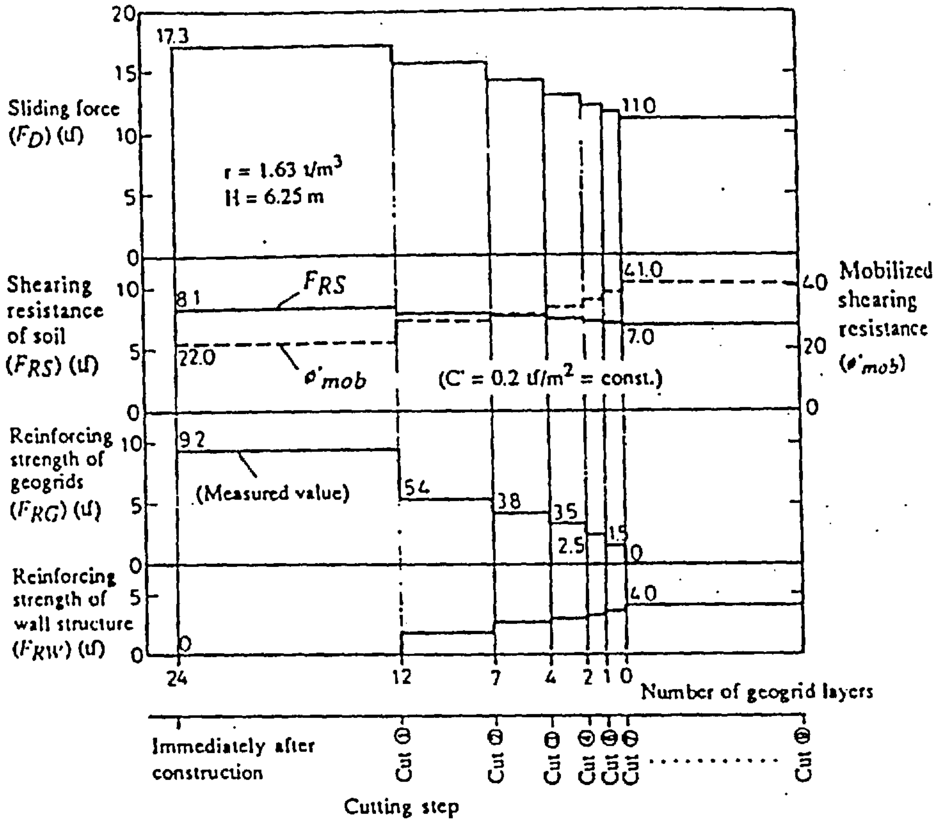

Fig. 11. Relationship between cutting steps and sliding force of soil mass, shearing resistance of soil and reinforcing strength of geogrids and wall structure (after Miki *et al.* 1992)

Recently the construction of wall facing by precast concrete block has been proposed (Jones *et al.* 1988, Knutson 1990, Rimoldi and Cambiaghi 1992).

From the above-mentioned results it can also be inferred that the design of reinforced embankment can be established taking into consideration the retaining effect of facing.

NUMERICAL ANALYSIS ON REINFORCED SOIL STRUCTURE

In considering the reinforcing mechanism of earth structures the most fundamental problem of deformation is ignored completely as engineering ideas such as limit equilibrium concept and safety factor are given priority. Jewell (1988) has proposed the limit equilibrium concept that predicts the facing's deformation. The numerical analysis method was found to be the most appropriate.

As to the numerical analysis method, there are the finite element method (FEM) and rigid body and spring model (RBSM) method proposed by Kawai (1977). The RBSM is developed to express the discontinuous phenomenon of soil mass that occurs at the time of slope failure and that cannot be analysed by the FEM, an exclusive method based on continuity of soil (Fig. 12). The

RBSM transmits the stresses from the soil-mass interface as a rigid body through the normal and shear spring. Hada *et al.* (1992) conducted tests on the model shown in Fig. 13 for the geotextile-reinforced embankment. Reliable results are obtained from the simulation of the laboratory model wall and practical steep reinforced embankment. As to the application of the FEM to reinforced earth structure, Al-Hussaini and Johnson (1978) and Herrmann and Al-Yassin (1978) conducted research on Terre Armee, Yamanouchi *et al.* (1986a) on geotextile, and others on numerous applications to tests and simulation of structures.

The FEM is applied to numerous tests and simulation of practical structures and its applicability or viability has been reported. How a reliable prediction and

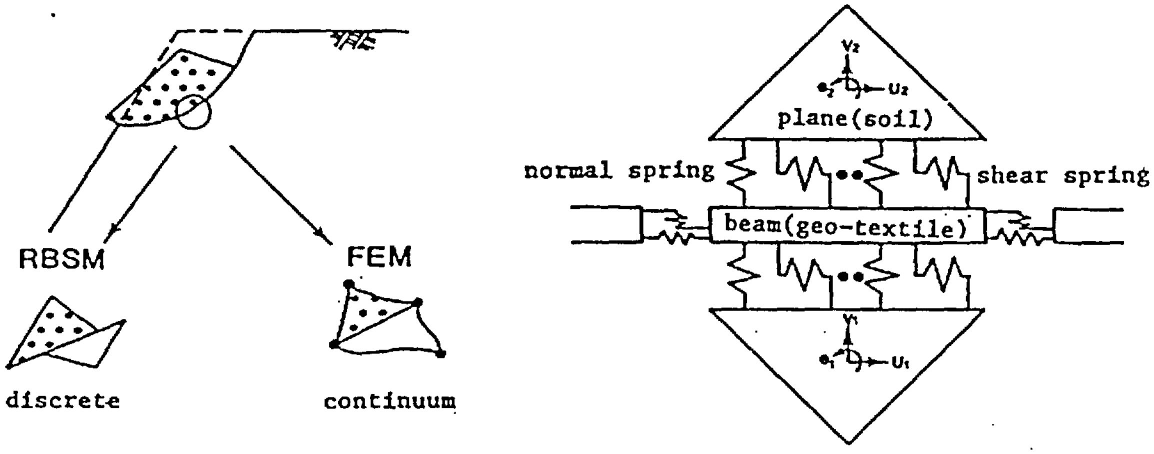

(a) Difference between RBSM and FEM

(b) Model of interface

Fig. 12. Basic concept and interface of rigid body and spring model (after Hada *et al.* 1988)

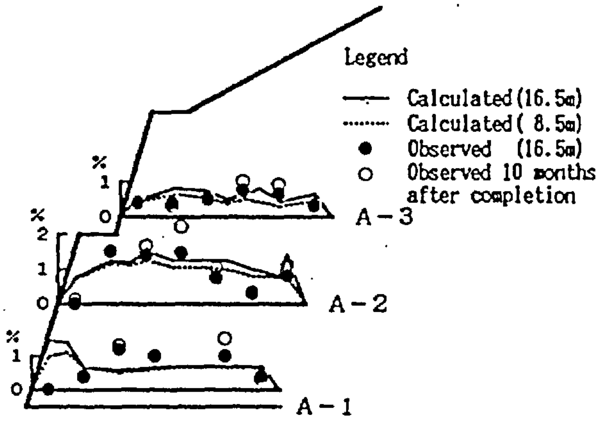

Fig. 13. Comparison of computed values with the strain by deducing the long-term deformation (Hada *et al.* 1992)

reflection of it to the design can be achieved and how the interface model can be constructed for soil, reinforcement material, and wall facing are, however, not yet clarified.

The International Symposium on Geosynthetic Reinforced Retaining Wall sponsored by Wu was held in 1991 in Denver to predict the deformation and rupture or failure according to the loading tests on Denver Wall constructed with non-woven fabric and timber facing as shown in Fig. 14. It was quite interesting but the prediction proves very difficult. The prediction is made as to the deformation and failure of the sand and clay embankment or wall for the cases after construction, after loading by surcharge load of 15 psi, and 100 hours after loading.

The participants of the symposium were grouped into 15 teams; three teams were assigned to the limit equilibrium method and strain compatibility analysis, one team to centrifugal test method, and 11 teams to the FEM method. The soil constitutive law used in FEM is concerned with Duncan-Chang model (elasto-viscoplastic model), generalised plasticity model, etc. The predictions were done for the sand and clayey soil embankments at 29 psi and 33 psi and the results are shown in Table 7. Few teams predicted correctly; most under-predicted or over-predicted.

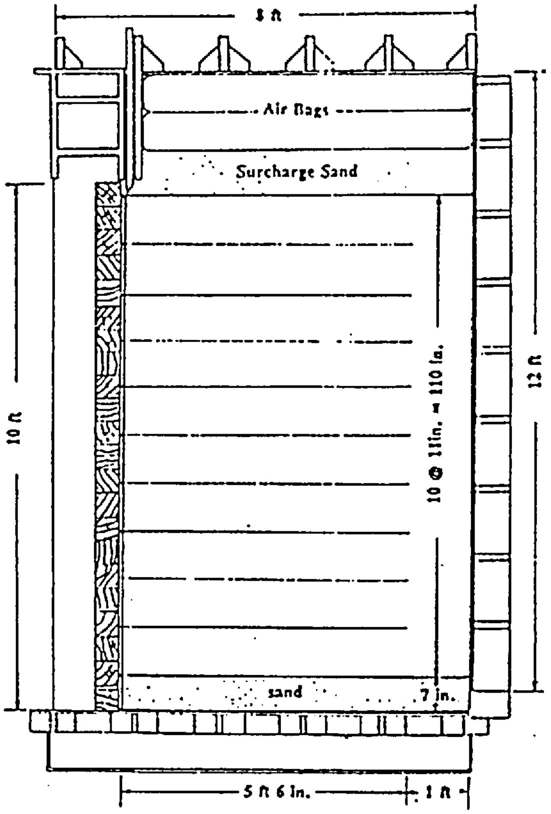

Fig. 14. Configuration of the Denver walls (after Wu 1992)

Table 7. Predicted failure surcharge pressure on Denver wall (after Wu *et al.* 1992)

Predictor	Predicted P (failure) (psi)	
	Granular backfill	Cohesive backfill
U. of Delaware	1.5–3.0	3.0–6.0
CU Denver	43	13
U. of Strathclyde	>75	>15
Hohai U.	>50	>30
Polytech. U. and LTR	6	—
Osaka U.	29	21
PWRI	18	30
U. of Tokyo	—	10.9
WES	—	—
Geosyntech and Tensar	13–16	—
CDOT	12	27
RMCC	19	11
Exxon	24	—
CU Boulder	55–59	—
U. of Newcastle upon Tyne	20+	20+
Measured	29	>33

Claybourn and Wu (1992) have applied various limit equilibrium design methods to the model constructed of the same sand and demonstrated that the predictions done by researchers were underestimating: namely Forest Service 0.7 psi, Broms 6.3 psi, Collin 7.3 psi, Bonaparte *et al.* 0.9 psi, Leshchinsky *et al.* 5.2 psi, Schmertmann *et al.* 6.0 psi, Geoservices 0 psi. This is considered to be due to the fact that each design method is not taking into consideration the rigidity of the wall facing which is encountered in practice.

APPROACHES ON SEISMIC DESIGN

The usual practice adopted for earthquake-proof embankment construction is either to decrease the slope of the embankment or to protect the slope failure by means of retaining wall. The method of reinforcing the soil structures by reinforcements is also considered efficient, economical, and easy to construct with a high degree of earthquake resistance. However, it requires prior investigation into the structure's behaviour during earthquake and the proper use of the reinforcement for an earthquake-proof embankment construction. The knowledge gained from the experimental studies, the concept of the seismic design, and the assessment of actual seismic resistance in view of the earth-reinforced soil structures is summarised as follows.

Model Studies on Seismic Resistance of Reinforced Soil Structures

To clarify the seismic-resistance efficiency of the reinforced soil structures, model vibration tests are being conducted at various research laboratories and institutes. The behaviour of an earth structure is generally affected by its size or dimension. However, it is possible to qualitatively assess the seismic-resistance efficiency to formulate a reliable design method.

To assess seismic earth pressure on the facing panels, Richardson and Lee (1975) conducted small-scale shaking model tests on Terre Armee and investigated the failure modes due to pullout forces and the rupture of the reinforcements and also the tensile properties of the reinforcements during the accelerated vibration. The results are presented in Fig. 15 and show the distribution of tensile stresses during the accelerated vibration. Richardson *et al.* (1977) confirmed by shaking table tests on prototype wall that the relationship of Fig. 15 is satisfactory. In accordance with this way of thinking Yamanouchi *et al.* (1986) has conducted evaluation studies on the seismic resistance of geogrid-reinforced steep slope.

To test seismic resistance efficiency, Koga *et al.* (1988) undertook shaking table model studies in the case of inclined foundation since severe damages are reported to occur at the road embankment section in mountainous areas during earthquake. From the relationship between the excitation acceleration and the cumulative average settlement of fill crest the main results of the tests can be summarised as follows.

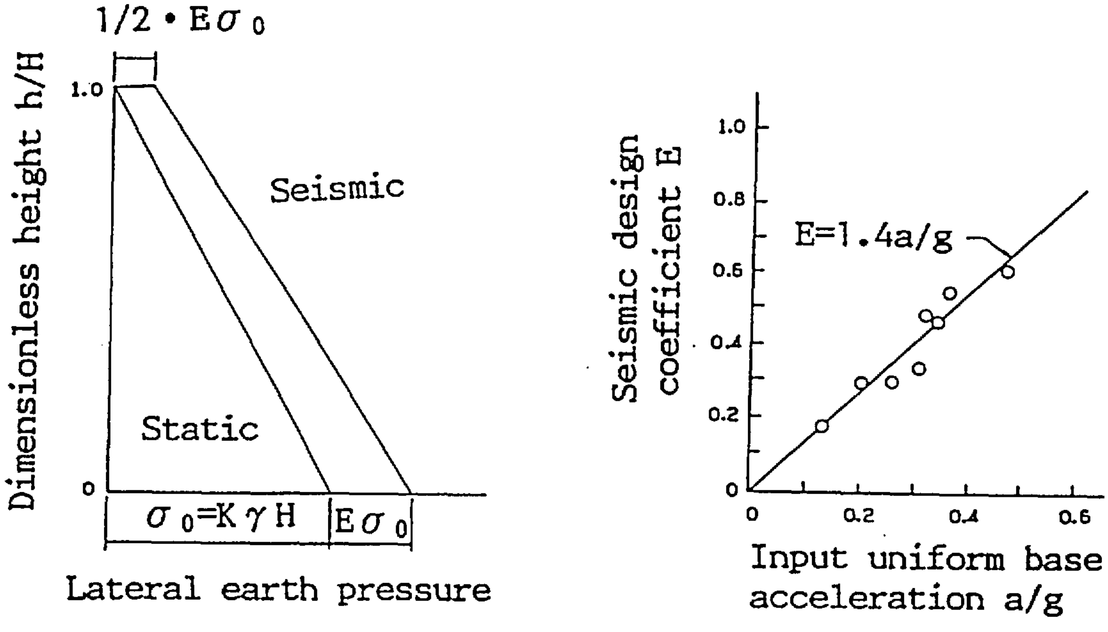

Fig. 15. Design envelope for maximum seismic earth pressure on reinforced earth wall (after Richardson *et al.* 1975)

1) In the case of unreinforced embankment the gentler the slope, the higher the seismic resistance, but the failure will take place all of a sudden. When the embankment is reinforced there is some deformation of the embankment, such as bulging and crest settlement, without failure.
2) The settlement of the fill crest is comparatively small in the case of reinforcement laid in a smaller spacing.
3) With equal spacing the embankment reinforced by laying high-stiffness reinforcements has a lower crest settlement.
4) The steeper the slope the bigger the settlement, but it is not so significant.
5) The longer the laying length of non-woven reinforcements, the smaller the settlement of the embankment.

Koga *et al.* (1986) conducted shaking table tests using a model embankment (height 30 cm) to investigate the behaviour of a steep reinforced embankment on a flat foundation during earthquake. Main results of the model studies are as follows.

1) The failure pattern of the reinforced embankment is such that the reinforced zone is integrated and pushed forward showing the behaviour of a gravity-type retaining wall. And accompanying this the wedge-like soil block is formed at the back of the reinforced zone. The embankment collapses in the pattern of overturning in case of the vertical wall and sliding of the reinforced zone.
2) When the laying length is longer the overturning does not take place even if the main failure lines appear on the embankment body. This result is not so much affected by the slope gradient.
3) The response magnification is bigger at the slope surface than inside the embankment. And the response magnification gets bigger with the increase of height. At a point under the active sliding plane the response magnification is 1.0 and the soil grains work as the inertia force.

Murata *et al.* (1992) conducted tests on the shaking table models to assess the earthquake resistance efficiency using the rigid face reinforced earth wall. The model test conditions are as shown in Fig. 16.

The accumulated horizontal outward displacement of facing that shows the wall's stability is much larger for case 5 than for case 1 (Fig. 17), apparently due to its low facing's rigidity. The wall also becomes more stable by the use of longer reinforcement (case 2) and by the use of an inclined facing (case 3), but becomes less stable by the use of a smaller number of reinforcement layers (case 4).

From the results of seismic-resistance tests it is confirmed that the rigidity of facing greatly contributes to the stability of the reinforced soil wall.

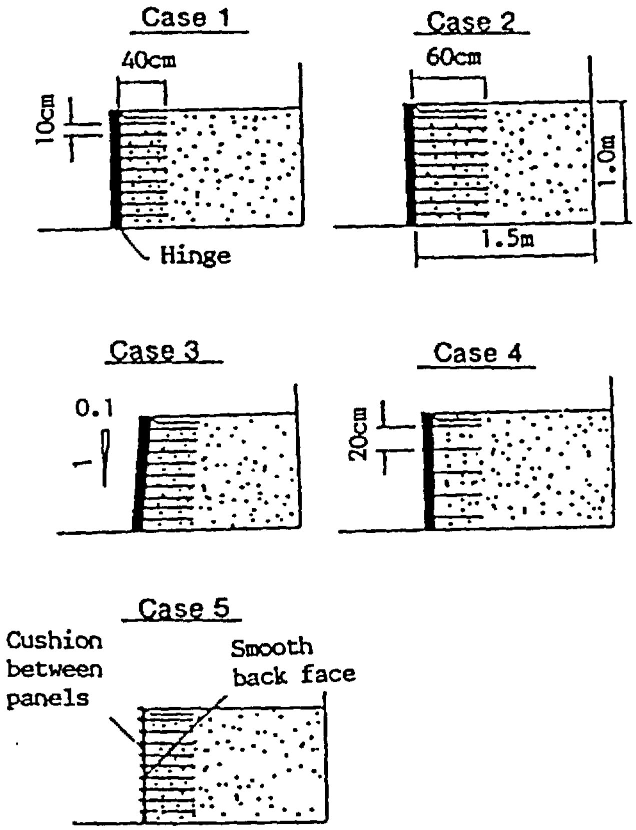

Fig. 16. Models for dynamic loading tests (after Murata *et al.* 1992)

Design Method and Stability Analysis of Reinforced Soil Structures under Seismic Loading

As stated above the model studies on the earthquake efficiency of reinforced embankment are considered still insufficient. However, by combining these limited test results and available know-how the seismic stability analysis and design method are supposed to be formulated.

The conventional stability analysis methods of soil structures under seismic forces are the method based upon the limit equilibrium method and FEM method. The commonly used design method is based upon the former. And the seismic forces are treated by the seismic coefficient method (Mononobe, 1933) that converts the vibrational forces into static inertia. Thus, when the limit equilibrium method and the seismic coefficient method are combined the stability analysis during earthquake can be considered in terms of static inertia problem and basically the seismic coefficient method is derived by extending the commonly used stability analysis method.

On the basis of the seismic resistance method, PWRI adopted the slip circle analysis, and Bonaparte *et al.* (1986) and Yamanouchi *et al.* (1991) applied the two-part wedge method to the slope stability analysis. Moreover the Railway

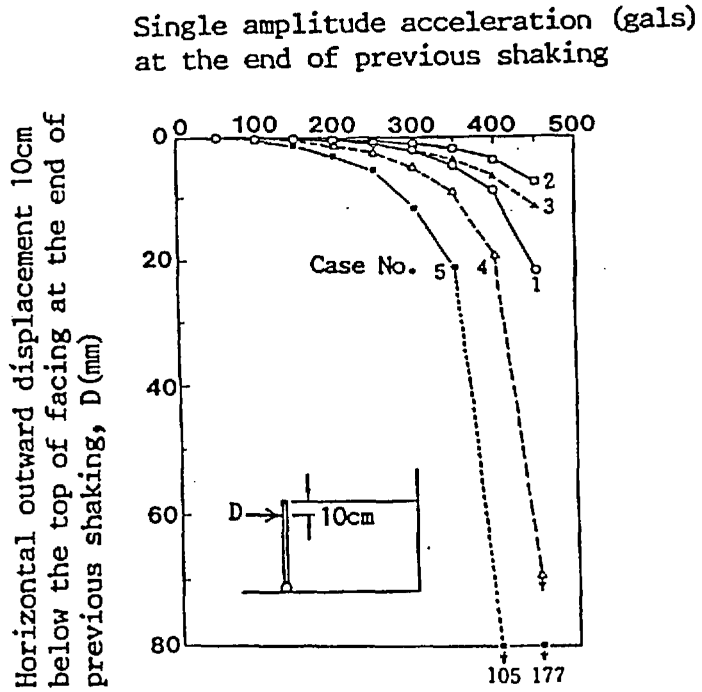

Fig. 17. Results of dynamic tests (after Murata *et al.* 1992)

Technical Research Institute (1992) adopted the slip circle method for the external stability analysis and two-part wedge method with seismic conditions for internal stability analysis.

Case Study on Earthquake Resistance of Reinforced Embankment

Since the 1980s a considerable number of earth structures reinforced by geotextiles have been constructed. No particular case of embankment damaged by earthquake was reported. The validity of the design method is still to be verified. However, some geogrid-reinforced embankments or walls have, for the first time, suffered damages in the Loma Prieta earthquake that occurred in 1989 around San Francisco (M7.1). After this earthquake Collin *et al.* (1992) have confirmed, as a result of field studies, the safety of all the cases of reinforced structures and verified that reinforced soil structures are excellent at resisting earthquake forces.

CONCLUSION

The function of reinforcement is mainly for tensile resistance and shear strength can be expected in the case of reinforcement with shear resistance. The most suitable reinforcement material, a topic of heated discussion in this field (see, for example, Godfrey, 1984), is the material that has high-elongation stiffness characteristics with high tensile strength in case it is used for reinforced soil wall. When the reinforced soil effect is to be considered as an integration effect the concentrated laying of low-strength reinforcements is, in some case, considered more effective for a particular reinforcement that requires stability. However, as to the commonly used design method it is difficult to assess the reinforced soil effect since the tensile strength only is taken into consideration on the basis of frictional resistance between soil and reinforcement.

Most of the reinforcement methods of today have undergone some stages of change as a result of research and development activities (see Fig. 18). This means that the stability analysis is proposed on the basis of the existing theories on soil mechanics and foundation engineering such as the limit equilibrium method, the earth pressure theory, and the theory of plasticity, with a view to formulating the general concept of the method. The next step is to research the salient feature of the reinforcing material and the friction and pullout characteristics of the material in the soil as well. Using these results the research on how to determine the design parameters required for the stability analysis (stage I), the verification of the design concept by means of the model tests and prototype tests (stage II), and the reinforcing mechanism by means of numerical analyses or centrifugal model tests (stage III) is conducted. While various applications of the methods are under scrutiny the research on the new technique is in progress.

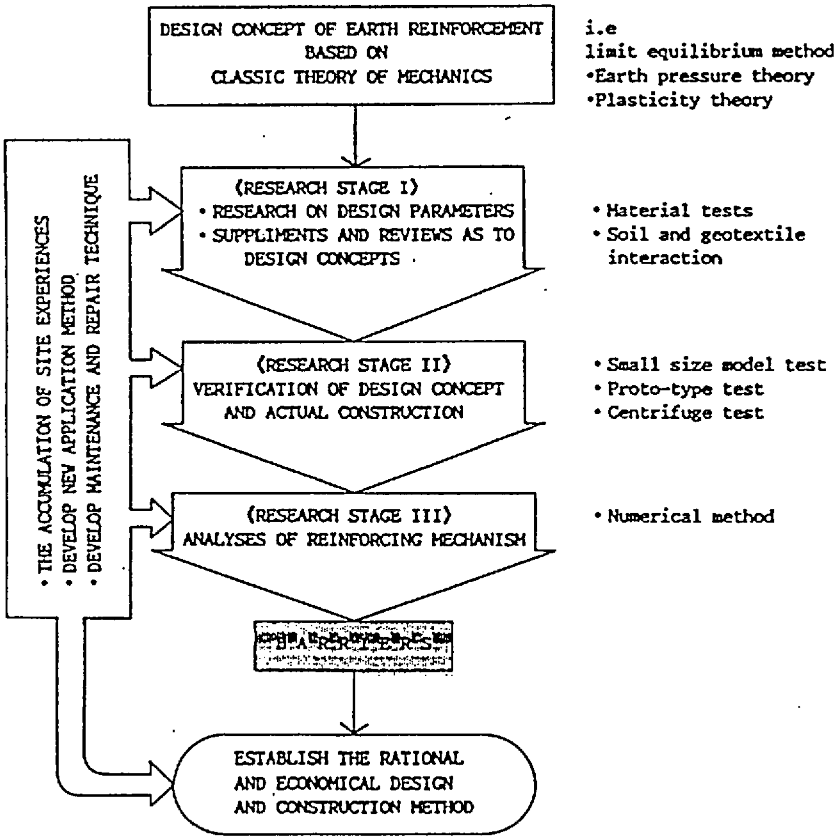

Fig. 18. Trends on research and development of earth reinforcement

All these activities are conducted with the final objective of making further progress on earth reinforcement technique by establishing the design and construction method for a more rational and more economical earth reinforcement. This is the present state of the art of earth reinforcement.

REFERENCES

Al-Hussaini, M.M. and L.D. Johnson (1978). Numerical analysis of a reinforced earth wall. *Symp. Earth Reinforcement*, ASCE Annu. Conv. Pittsburgh, Pennsylvania, pp. 98–126.

Balzer, E., P. Delmas, Y. Matichard and B.R. Thamm (1990). Geotextile reinforced abutment: full scale test and theory. Proc. Int. Reinforced Soil Conf.: Performance of reinforced soil structures. British Geotechnical Society: 47–52.

Bathurst, R.J., W.F. Wawrychuk and P.M. Jarret (1987). Laboratory investigation of two large-scale geogrid reinforced soil walls. *Proc. NATO A.R.W. on Application of Polymeric Reinforcement in Soil Retaining Structures*, RMC. Kingston, pp. 71–125.

Berg, R.R., R. Bonaparte, R.P. Anderson and V.E. Chouery (1986). Design construction and performance of two geogrid reinforced soil walls *Proc. 3rd Int Conf. Geotextiles*. Vienna, pp. 401–406.

Bolton, M.D. and P.L.R. Pang (1982). Collapse limit states of reinforced earth walls. *Geotechnique*, 32 (4): pp. 349–367.

Bonaparte, R., G.R. Schmertmann and N.D. Williams (1986). Seismic design of slope reinforced with geogrids and geotextiles. *Proc. 3rd Int. Conf. Geotextiles*, Vienna, Vol. 1, pp. 273–278.

Bonaparte, R., R.P. Holz and J.P. Giroud (1987). Soil reinforcement design using geotextiles and geogrids. *Geotextile Testing and Design Engineer*, ASTM STO 952, pp. 69–116.

Broms, B.B. (1978). Design of fabric reinforced retaining structures. *Proc. Symp. Earth Reinforcement*, ASCE, Pittsburg, pp. 282–303.

Cazzuffi, D., A. Pagotto and P. Rimoldi (1988). Behavior of a geogrid reinforced embankment over waste material. *Proc. 2nd Int. Conf. Case Histories in Geotechnical Engineering*, St. Louis.

Christopher, B.R. (1987). Geogrid reinforced soil retaining wall to widen an earthdam and support high live loads. *Proc. Geosynthetic '87 Conf.*, New Orleans.

Claybourn, A.F. and J.T.H. Wu (1992). Failure loads of the Denver walls by current design methods. *Geosynthetic-Reinforced Soil Retaining Walls*. J.T.H. Wu (ed.). Balkema, Rotterdam, pp. 61–77.

Collin, J.G. (1986). Earth wall design. Ph.D. thesis, University of California at Berkeley.

Collin, J.G., V.E. Chouery-Curtis and R.R. Berg (1992). Field observation of reinforced soil structures under seismic loading. *Proc. Int. Symp. Earth Reinforcement Practice*, Fukuoka, Japan, Vol. 1, pp. 223–228.

Datye, K.R. (1987). Geotextile use in India—Recent experience and suggested developments. *Proc. Post Vienna Conf. Geotextiles*, Singapore, pp. 33–47.

Fukuda, N., N. Miura and T. Yamanouchi (1984). Reduction of earth pressure acting on a retaining wall by reinforcing with elongating-processed plastic grid, Tsuchi-To-Kiso, *JSSMFE*, 32 (6): 21–26 (in Japanese).

Fukuda, N., V. Takahashi, J. Ohtani, M. Ohuchi, J. Nishimura, E. Kinoshita and M. Yoshizawa (1989a). A comparative study of proposed design method of geotextile reinforced steep embankment. *24th Conf. JSSMFE*, pp. 5–8 (in Japanese).

Fukuda, N., Y. Takahashi, J. Ohtani, J. Nishimura, M. Ohuchi, M. Yoshizawa and E. Kinoshita (1989b). Proposals on the design method for geogrid reinforced steep embankments. *Proc. 4th IGS Japan Chapter Symp.*, Tokyo, pp. 133–139 (in Japanese).

Fukuda, N., T. Yamanouchi and N. Miura (1986). Comparative studies of design and construction of steep reinforced embankment. *Geotextiles and Geomembranes*, 4: 269–284.

Geogrid Research Board (1990). *Guidelines for Geogrids*, Vols. 1 and 2. 244 pp. and 150 pp. (in Japanese).

Godfrey, K.A., Jr. (1984). *Retaining Walls: Competition or Anarchy*? Civil Engineering ASCE, pp. 48–52.

Hada, M., K. Kagawa and S. Fukushima (1992). Field measurement of reinforcement strain and discrete limit analysis. *Int. Symp. Earth Reinforcement Practice*, Fukuoka, Japan, pp. 241–244.

Hada, M., Y. Yaguchi and K. Kagawa (1988). Application of RBSM analysis to earth reinforced method. *Int. Symp. Theory and Practice of Earth Reinforcement*, Fukuoka, Japan, pp. 395–400.

Herrmann, L.R. and Z. Al-Yassin (1978). Numerical analysis of reinforced soil systems. *Symp. Earth Reinforcement*, ASCE Annu. Conv., Pittsburgh, Pennsylvania, pp. 428–457.

Hirota, Y. and I. Yamaoka (1986). Studies on the slope stability of geotextile reinforced wall using slip plane method. *Proc. 1st IGS Japan Chapter Symp.*, Tokyo, pp. 101–106 (in Japanese).

Ingold, T.S. (1982). An analytical study of geotextile reinforced embankment *2nd Int. Conf. Geotextiles*, Las Vegas, pp. 683–688.

Jewell, R.A. (1987). Reinforced soil wall analysis and behavior, Application of polymeric reinforcement in soil retaining structures. NATO ASI Series E: Applied Science, Vol. 147, Kluwer, pp. 365–408.

Jewell, R.A. (1988). Compatibility, serviceability and design factors for reinforced soil walls. *Int. Symp. Theory and Practice of Earth Reinforcement*, Fukuoka, Japan, pp. 611–616.

Jewell, R.A., N. Paine and R.I. Woods (1984). Design method for steep reinforced embankments. *Polymer Grid Reinforcement*, Thomas Telford, pp. 70–81.

Jones, C.J.F.P. (1984). Design and construction methods. *Proc. Symp. Polymer Grid Reinforcement*, ICE, London, No. 6.1, 8 pp.

Jones, C.J.F.P., A. McGown and D.J. Varney (1988). Construction methods, economics and specifications. *The Application of Polymeric*, NATO ASI Series, Kluwer Academic Publishers, pp. 573–611.

Kawai, T. (1977). A new discrete model for analysis of solid mechanics problems. *Seisan-Kenkyu*, 29 (4): 14–16.

Knutson, A.F. (1990). Reinforced soil retaining structures, Norwegian experience. *Proc. 4th Int. Conf. Geotextiles, Geomembranes and Related Products*, Vol. 1, The Hague, pp. 87–91.

Koga, Y., Y. Itoh, S. Washida and T. Shimazu (1988). Seismic resistance of reinforced embankment by model shaking table tests. *Int. Symp. Theory and Practice of Earth Reinforcement*, Fukuoka, Japan. Balkema, Rotterdam, pp. 413–418.

Koga Y., E. Taniguchi, Y. Itoh, M. Sakaguchi, A. Nakanishi and T. Sakami (1986). Shaking model tests on geotextile reinforced embankment. *1st IGS Japan Chapter Symp.*, Tokyo, pp. 57–60 (in Japanese).

Leflaive, E. (1982). The reinforcement of granular materials with continuous fibers. *2nd Int. Conf. Geotextiles*, Las Vegas, pp. 721–726.

Leshchinsky, D. and E.B. Perry (1987). A design procedure for geotextile-reinforced walls. *Geotech. Fabrics Rep.*, pp. 21–27.

Leshchinsky, D. and E.B. Perry (1989). On the design of geosynthetic-reinforced soil walls. *Geotextiles and Geomembranes*, 10: 53–63.

Miki, H., K. Kudo, M. Taki, N. Fukuda, K. Iwasaki and J. Nishimura (1992). Experimental study on full scale geogrid reinforced embankment model. *Int. Symp. Theory and Practice of Earth Reinforcement*, Fukuoka, Japan, pp. 269–274.

Minami, K., H. Nakata, I. Shimada, S. Uehara, S. Maruo and A. Nakane (1987). Large-scale failure experiments on geotextile-reinforced retaining wall. *Proc. IGS—Geotextiles and Geomembranes*, Japan Chapter of IGS, Kyoto, pp. 81–92.

Mononobe, N. (1933). *Theory of Earthquake Resistant Civil Structures*. Tokiwa Pub. Co., Tokyo, 308 pp. (in Japanese).

Murata, O., M. Tateyama and F. Tatsuoka (1992). Loading tests of geosynthetic-reinforced soil retaining walls and their stability analyses. *Int. Symp. Earth Reinforcement Practice*, Fukuoka. Balkema, Rotterdam, pp. 385–390.

Murata, O., M. Tateyama, F. Tatsuoka, K. Nakamura and Y. Tamura (1991). A reinforcing method for earth retaining walls using short reinforcing members and a continuous rigid facing. *Proc. ASCE Geotech. Engg. Cong., Geotech.* Special Publication 27, pp. 953–956.

Murray, R.T. (1980). Fabric reinforced earth walls, development of design equations. *Ground Eng.*, 13 (7): 29–36.

Ogisako, E., H. Ochiai, S. Hayashi and A. Sakai (1988). FEM analysis of polymer grid reinforced-soil retaining walls and its application to the design method. *Int. Symp. Theory and Practice of Earth Reinforcement*, Fukuoka. Balkema, Rotterdam, pp. 559–564.

Onodera, S., S. Naemura, A. Nakane and S. Maruo (1992). A design method for sleep reinforced embankments with geotextiles. *Proc. Int. Symp. Earth Reinforcement Practice*, Fukuoka. Balkema, Rotterdam, pp.391–396.

Public Works Research Institute (1992). Manual for design and construction of reinforced soil structures constructed using geotextiles. Report by Research Institute of Public Works, No. 3007, 40 pp. (in Japanese).

Railway Technical Research Institute (1992). Design standard of railway structures: Earth structures.

Rimoldi, P. (1988). A review of field measurements of the behavior of geogrid reinforced slopes and walls. *Proc. Int. Symp. Theory and Practice of Earth Reinforcement*, Fukuoka. Balkema, Rotterdam, pp. 571–576.

Rimoldi, P. and A. Cambiaghi (1992). The use of geogrids in road applications in Italy. *Int. Symp. Earth Reinforcement Practice*, Fukuoka. Balkema, Rotterdam, pp. 397–402.

Richardson, G.N. and K.L. Lee (1975). Seismic design of reinforced earth walls. *J. Geotech. Engg. Div., Proc. ASCE*, 101 (GT2): 167–188.

Richardson, G.N., D. Feger, A. Fong and K.L. Lee (1977). Seismic testing of reinforced earth wall. *J. Geotech. Engg. Div., Proc. ASCE*, 103 (GTI): 1–17.

Rowe, R.K. and S.K. Ho (1992). A review of the behaviour of reinforced soil walls. *Int. Symp. Earth Reinforcement Practice*, Keynote Lectures, Fukuoka, pp. 47–76.

Ruegger, R. (1986). Geotextile reinforced soil structures on which vegetation can be established. *Proc. 3rd Int. Conf. Geotextiles*, Vienna, Vol. 2, pp. 451–458.

Schlosser, F. (1990). Mechanically stabilized earth retaining structures in Europe, design and performance of earth retaining structures. ASCE Geotech. Special Publication No. 25, pp. 347–378.

Schmertmann, G.R., V.E. Chouery-Curtis, R.D. Johnson and R. Bonaparte (1987). Design charts for geogrid-reinforced soil slopes. *Geosynthetic '87 Conf.*, New Orleans, pp. 108–120.

Schneider, H.R. and R.D. Holtz (1986). Design of slopes reinforced with geotextiles and geogrids. *Geotextiles and Geomembranes*, 3: 29–51.

Simac, M.R., B.R. Christopher and C. Bonczkiewicz (1990). Instrumented field performance of 6m geogrid soil wall. *Proc. 4th Int. Conf. Geotextiles, Geomembranes and Related Products*, The Hague, Vol 1, pp. 53–59.

Tatsuoka, F. (1986). Principle of mechanism and design, reinforced soil method. JSSMFE, Tokyo, 25–165 (in Japanese).

Tatsuoka, F. (1992). Roles of facing rigidity in soil reinforcing. *Int. Symp. Earth Reinforcement Practice*, Keynote Lectures, Fukuoka, pp. 77–115.

Tensor Corporation (1986). Guidelines for the design of Tensar geogrid reinforced soil retaining walls. Tensar technical note, TTN: RWI.

Wu, J.T.H, X. Qi, N. Chou, I. Ksouri, M.B. Helwany and C. Huang (1992). Comparisons of predictions for Denver walls. In *Geosynthetic-Reinforced Soil Retaining Walls*. J.T.H. Wu (ed.), Balkema, Rotterdam, pp. 43–60.

Yamanouchi, T. (1992). Historical review of geotextiles for reinforcement of earth works in Asia. *Proc. Int. Symp. Earth Reinforcement Practice*, Fukuoka, 2: 735–749.

Yamanouchi, T., N. Fukuda and M. Ikegami (1986a). Design and techniques of steep reinforced embankments without supportings. *Proc. 3rd Int. Conf. Geotextiles*, Vienna, Vol. 1, pp. 199–204.

Yamanouchi, T., N. Fukuda, H. Oda, K. Maruyama, T. Nagata, Y. Kobayashi and T. Morihata (1986b). Test construction work for polymer grid reinforced retaining wall. *21th Conf. JSSMFE*, pp. 1433–1434 (in Japanese).

Yamanouchi, T., H. Ochiai, N. Fukuda and K. Takaoka (1991). A proposal of seismic design method of steep reinforced embankments. *Proc. 26th JSSMFE Conf.*, Nagano, pp. 2117–2120. (in Japanese).

Yeo, K.C., K.Z. Andrawes and M.A. Saad (1992). The use of a compressible boundary layer in reinforced soil structures. *Proc. Int. Symp. Earth Reinforcement Practice*, Fukuoka, Japan. Balkema, Rotterdam, pp. 449–454.

15

Slope Stabilization Using Vegetation

Tien H. Wu

INTRODUCTION

The use of vegetation for slope stabilization started in ancient times. A fine historical review may be found in Greenway (1987). Krabel (1936) was among the first to use soil-biotechnical construction in the United States. In more recent times, the roles played by vegetation in some specific geotechnical processes have been recognised. Vegetation may affect slope stability in many ways. Comprehensive reviews may be found in Gray (1970), Gray and Leiser (1982), Greenway (1987), and Coppin and Richards (1990). The stability of slopes is governed by the load, which is the driving force that causes failure, and the resistance, which is the strength of the soil-root system. The weight of trees growing on a slope adds to the load but the roots of trees may serve as a soil reinforcement and increase the resistance. Vegetation may influence slope stability indirectly through its effect on the soil moisture regime. Vegetation intercepts rainfall and draws water from the soil via evapotranspiration. This reduces soil moisture and pore pressure, increases the shear strength of the soil, and increases the resistance. Vegetation roots tend to increase soil permeability and increase infiltration and soil moisture, while the organic layer associated with vegetative cover tends to retard infiltration. The objective of this paper is to outline the methods that may be used to evaluate the influence of these factors on slope stability. Emphasis is placed on the mechanics of slope stability.

CONDITIONS FOR STABILITY

Stability analysis allows one to evaluate an existing condition or a proposed solution to determine if it meets the requirements of safety. The most common methods are based on limit equilibrium, which considers the shear strength and shear stress on potential surfaces of failure.

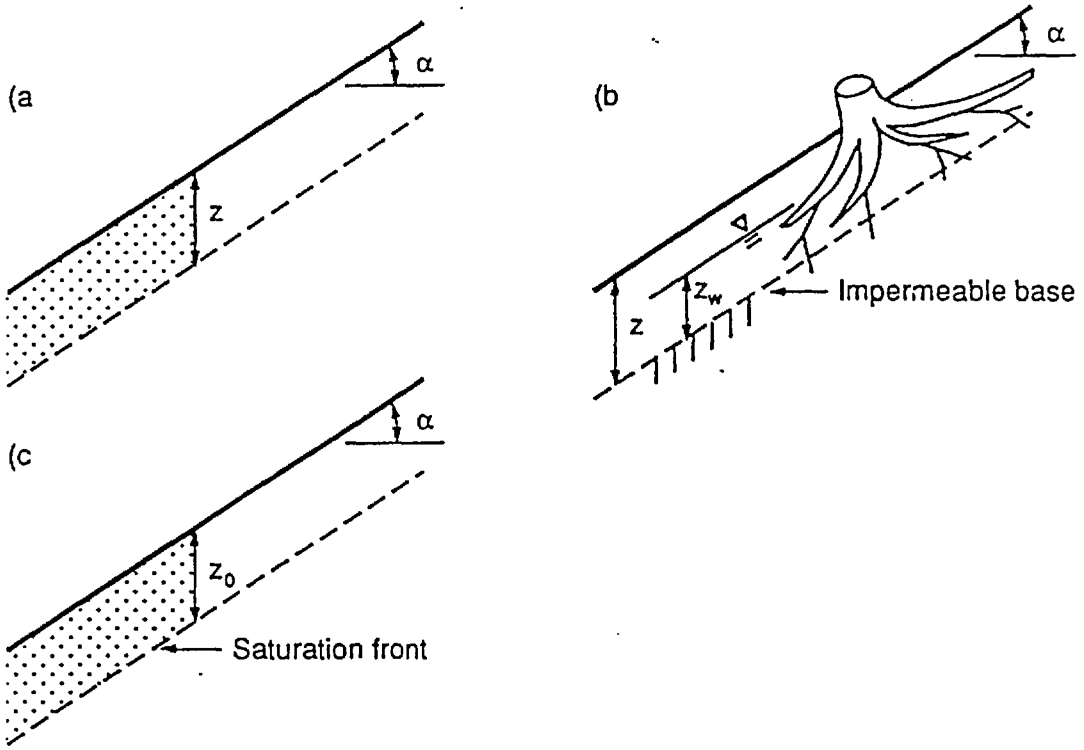

Fig. 1. Slope stability: (a) finite slope, (b) seepage parallel to slope, (c) saturation from surface

The above relations are sufficient to show the influence of the various factors on stability. To emphasise the key issues, the results of a simple parametric study are given in Fig. 2 for two sets of soil strength, $\phi' = 27°$, $c' = 0$, and $\phi' = 40°$, $c' = 0$. The former represents a plastic cohesive soil in the drained condition and the latter a cohesionless soil. The figure shows the influence of s_r on the safety factor for various z. It is important to note that the effect of s_r is largest at small z, that is when the failure surface is at a shallow depth. Comparison of Figs. 2a and b shows the important role of the seepage force. Vegetation also effects stability indirectly through its effect on seepage. If it can reduce the vertical infiltration, it will reduce z_0, the depth of the saturated zone in Fig. 1c. For seepage parallel to the slope, reduced infiltration will reduce z_w in Fig. 1b. Fig. 2c shows the influence of the surcharge p due to the weight of the trees and of w, the shear force due to wind. The effect of p and w is small for z exceeding 1 m, although the effect also depends on α and ϕ'. More detailed examination of these issues may be found in Brown and Sheu (1975) and Coppin and Richards (1990). Stability analysis with a circular arc as slip surface and with s_r acting over part of the slip surface has been described by Wu (1984a).

The shear strength of soils, s_s, is described by the Mohr-Coulomb criterion:

$$s_s = c + \sigma \tan \phi \tag{1a}$$

In terms of effective stress, the shear strength is (Terzaghi 1936):

$$s_s = c' + \sigma' \tan \phi' = c' + (\sigma - u) \tan \phi' \tag{1b}$$

where c = cohesion, σ = normal stress, and ϕ = angle of internal friction; the prime denotes effective stress, and u = pore pressure.

Where the soil contains roots, shear failure would involve failure of the soil-root system. A simple approach is to consider the root as a reinforcement which increases the shear strength by s_r. Then

$$s = s_s + s_r \tag{2}$$

This value of s may then be used in the conventional methods of stability analysis. Procedures for evaluation of s_r are presented in a subsequent section.

A variety of failure modes are possible. In this paper, we present the basic issues using the simple case of an infinite slope, Fig. 1a. The safety factor is

$$F_s = \frac{s}{\gamma z \sin \alpha \cos \alpha} \tag{3}$$

where γ = unit weight of the soil, z = depth of the slip surface, and α = slope angle. If a shallow soil layer lies over an impermeable base and seepage occurs parallel to the slope, Fig. 1b, the pore pressure is

$$u_s = \gamma_w z_w \cos^2 \alpha \tag{4a}$$

where γ_w = unit weight of water. In effective stress analysis, assuming 0 excess hydrostatic pore pressure,

$$F_s = \frac{c' + [z_w(\gamma_s - \gamma_w) + (z - z_w)\gamma] \cos^2 \alpha \tan \phi'}{[z_w \gamma_s + (z - z_w)\gamma] \sin \alpha \cos \alpha} \tag{4b}$$

where γ_s = saturated unit weight of soil. If the soil has low permeability, saturation due to rainfall may proceed from the surface downward. Then a saturated zone forms below the surface as shown in Fig. 1c. The pore pressure in the saturated zone is 0, then

$$F_s = \frac{c' + \gamma_s z_0 \cos^2 \alpha \tan \phi'}{\gamma_s z_0 \sin \alpha \cos \alpha} \tag{5}$$

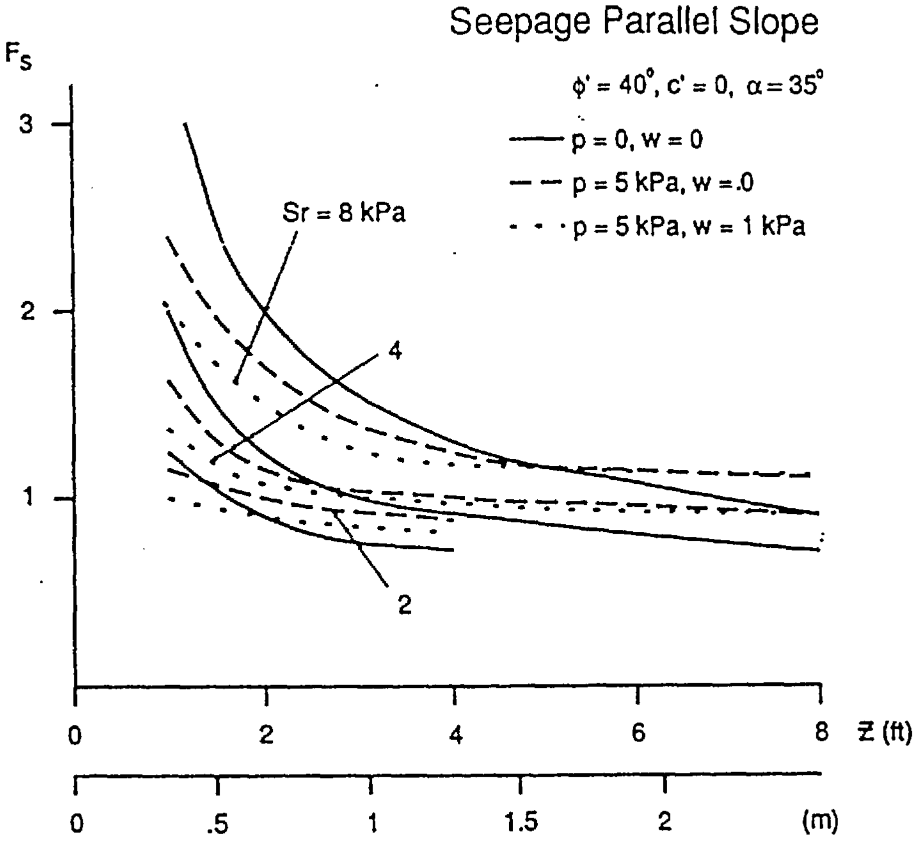

Fig. 2. (continued)

EFFECT OF VEGETATION ON PORE PRESSURE

Vegetation affects pore pressure by intercepting precipitation and by removing water through evapotranspiration. In principle, the equation for saturated-unsaturated flow (Philip 1957, 1969) can be solved with the appropriate boundary conditions and material parameters (e.g., Freeze 1971). However, it is often difficult to estimate accurately the many parameters that are needed for the solution. Also, complexities near the surface, such as shrinkage cracks and root holes, are difficult to quantify. For purposes of comparison, simplified models based on mass balance may be used instead, as shown in Fig. 3a. Precipitation (q) enters at the top and (d) is the discharge, which is the sum of evapotranspiration (e) and drainage by gravity flow (f). A variety of models have been proposed for calculation of the flow through the partly saturated zone and the drainage (Bevan 1982, Sangrey *et al.* 1984, Greenway *et al.* 1984, Reddi and Wu 1991).

An example that illustrates the effect of various parameters on the piezometric level in a slope is shown in Fig. 4. The infiltration and drainage were

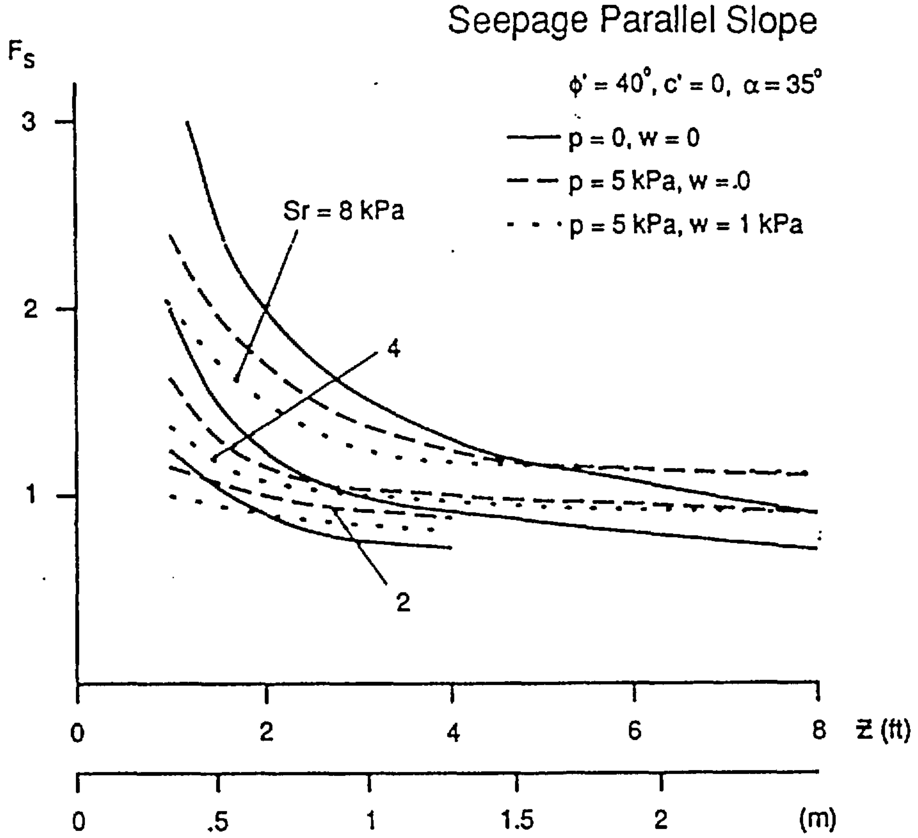

Fig. 2. (continued)

EFFECT OF VEGETATION ON PORE PRESSURE

Vegetation affects pore pressure by intercepting precipitation and by removing water through evapotranspiration. In principle, the equation for saturated-unsaturated flow (Philip 1957, 1969) can be solved with the appropriate boundary conditions and material parameters (e.g., Freeze 1971). However, it is often difficult to estimate accurately the many parameters that are needed for the solution. Also, complexities near the surface, such as shrinkage cracks and root holes, are difficult to quantify. For purposes of comparison, simplified models based on mass balance may be used instead, as shown in Fig. 3a. Precipitation (q) enters at the top and (d) is the discharge, which is the sum of evapotranspiration (e) and drainage by gravity flow (f). A variety of models have been proposed for calculation of the flow through the partly saturated zone and the drainage (Bevan 1982, Sangrey *et al.* 1984, Greenway *et al.* 1984, Reddi and Wu 1991).

An example that illustrates the effect of various parameters on the piezometric level in a slope is shown in Fig. 4. The infiltration and drainage were

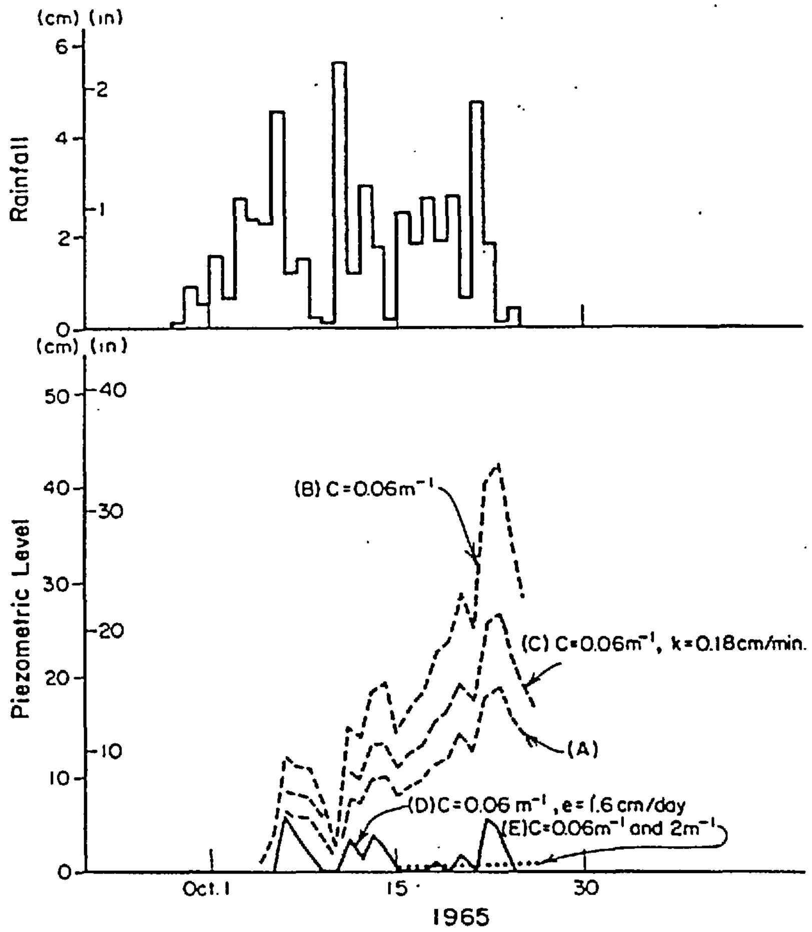

Fig. 4. Computed pore pressure, Maybeso Valley (Wu 1984a)

to a narrow zone with thickness t (Fig. 5). The root is represented by a bar which is initially straight (broken line) and is displaced into the position shown by the solid line. The displacement introduces an axial force, T, as well as a shear and a bending moment in the bar. The addition to the shear strength is

$$s_r = \frac{T_z}{A} \tan \phi + T_x \tag{6}$$

where A = area of the section. For a given shear displacement, x, the deformation of the bar, the axial force, and the shear and moment will depend on the relative stiffness of the bar with respect to the soil and the initial position and length of the bar. A complete solution requires treatment of the soil-bar interaction as a three-dimensional problem in continuum mechanics. To date, only two-dimensional solutions have been obtained for large displacements and inelastic soil behaviour (Juran *et al.* 1981). However, simplified decoupled solutions are available for several special cases. These are described in the following sections.

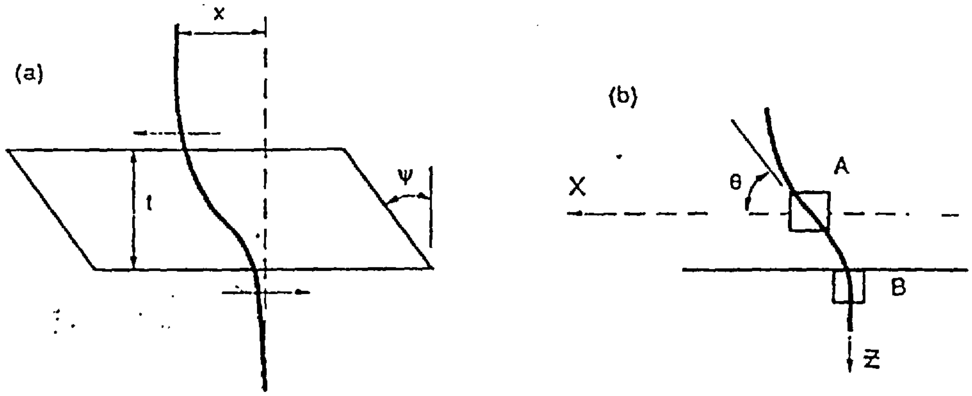

Fig. 5. Displacement in Shear zone

To evaluate the force T in Eq. (6), it is necessary to consider the soil-root interaction. The simplest interaction model is to assume that the soil deforms in simple shear and the root deforms with the soil through the angle ψ, Fig. 6a. The second assumption would be true for a perfectly flexible root. Then,

$$\theta = \tan^{-1}\left(\frac{1}{\frac{x}{t}+\frac{1}{\tan\alpha}}\right) \tag{7a}$$

$$s_r = \left\{T\cos\left(\frac{\pi}{2}-\theta\right)\tan\phi + T\sin\left(\frac{\pi}{2}-\theta\right)\right\}/A \tag{7b}$$

Where there are more than one root,

$$s_r = \left\{\sum_{i=1}^{n} T_i\cos\left(\frac{\pi}{2}-\theta_i\right)\tan\phi + T_i\sin\left(\frac{\pi}{2}-\theta_i\right)\right\}/A \tag{7c}$$

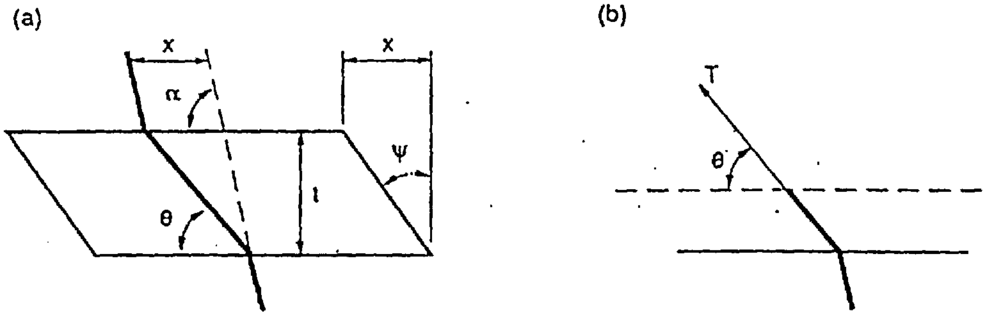

Fig. 6. Soil-root interaction model

where n = number of roots in area A and ϕ may be in terms of either total or effective stress, but should correspond to the method used in stability analysis.

For values of $\left(\frac{\pi}{2} - \theta\right)$ between 48° and 72° and ϕ between 30° and 40°, s_r in Eq. (7c) is insensitive to θ and may be approximated by (Wu *et al.* 1979),

$$s_r = 1.2 \sum_{i=1}^{n} T_i / A \tag{8a}$$

If it is assumed that the different roots are loaded to approximately the same stress σ_r, then Eq. (8a) becomes

$$s_r = 1.2 \frac{\sigma_r A_r}{A} = 1.2 \sigma_r a_r \tag{8b}$$

where A_r = sum of cross-sectional areas of all roots in area A, and $a_r = A_r / A$.

Model tests by Shewbridge and Sitar (1989) show that the shape of the displaced reinforcement depends on the stiffness of the reinforcements. If it is assumed that the soil displacement is equal to the reinforcement displacement, then an approximate relation between t and the reinforcement stiffness $E_r I_r$ can be obtained with Shewbridge's (Shewbridge and Sitar, 1989) data. This is shown in Fig. 7. For comparison, t was also estimated from the measured soil displacements outside the shear box in *in situ* tests (Wu *et al.* 1988a). These are also shown in Fig. 7. The boundary conditions and E_s for the *in situ* test are not the same as those in Shewbridge's tests. However, the general agreement is encouraging. Thus, for a given stiffness and shear displacement, x, t and θ in Eq. (7a) can be estimated. A more refined solution is to estimate the deformed shape of the reinforcement from the results of Shewbridge's tests and derive the work required to produce the deformation. The axial and shear forces in the reinforcement are then calculated from the work (Shewbridge and Sitar 1990).

At the other extreme, stiff roots that are nearly perpendicular to the shear zone $\left(\theta \approx \frac{\pi}{2}\right)$ may be analysed as laterally loaded piles. The ultimate resistance for a short root (Fig. 8a) is (Broms 1964a)

$$T_{x,f} = \frac{c N_c D L}{2.4} \tag{9}$$

for cohesive soils ($\phi = 0$) and (Broms 1964b)

$$T_{x,f} = \frac{1}{2} \gamma D L^2 \tan^2 \left(\frac{\pi}{4} + \frac{\phi}{2}\right) \tag{10}$$

for cohesionless soils ($c = 0$), where $N_c \approx 7$ (Wu *et al.* 1988c). If the root is long, bending failure could occur. The solutions may be found in Broms (1964a, 1964b). If the root is oriented almost parallel to the shear zone ($\theta \to 0$), the

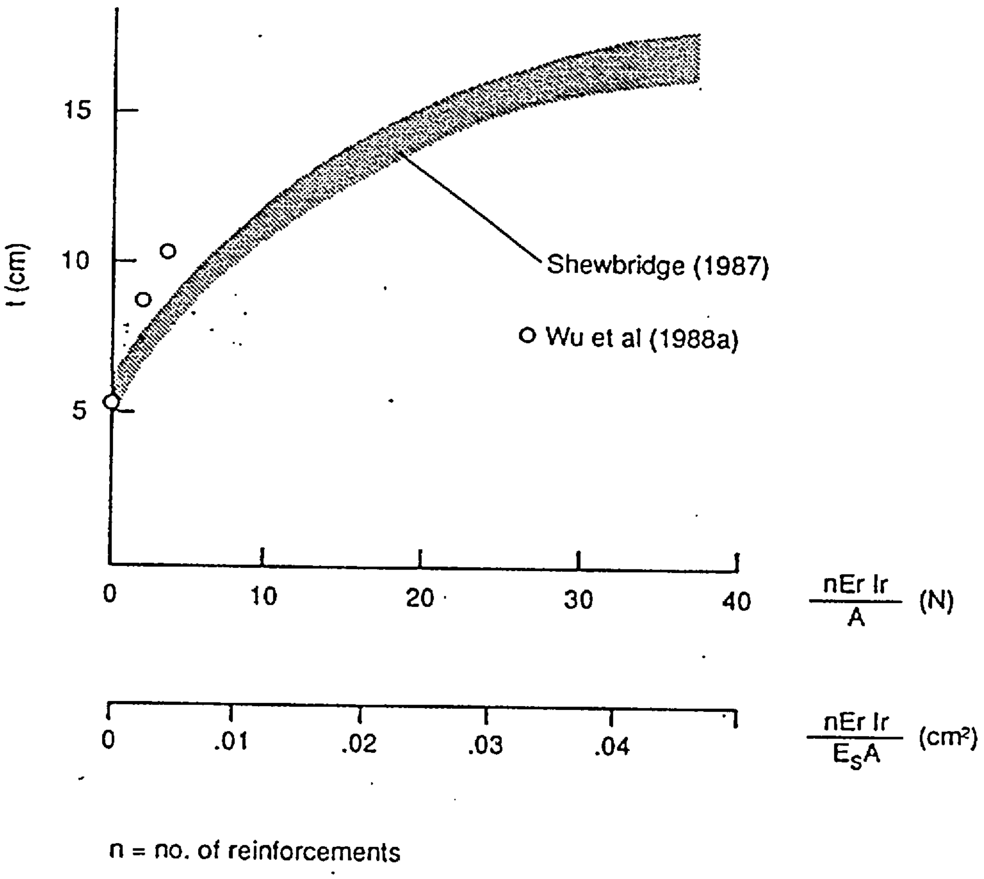

Fig. 7. Relation between thickness of shear zone and reinforcement stiffness, $E_s = 8000$ kPa, $n =$ number of reinforcements

ultimate resistance is close to the ultimate tensile resistance (Fig. 8b). For a root segment, the ultimate tensile resistance is

$$T_f = \sigma_t A_r \tag{11a}$$

where σ_t = tensile strength, or the shearing resistance along the soil-root interface

$$T_f = \pi D f L \tag{11b}$$

where f = interface resistance.

ROOT PROPERTIES

The root properties that are needed for the computation of soil-root interaction include the root geometry and the strength properties. While data are available for a number of species, these are limited to the sites from which the data were obtained. It is known that root properties depend on site conditions but

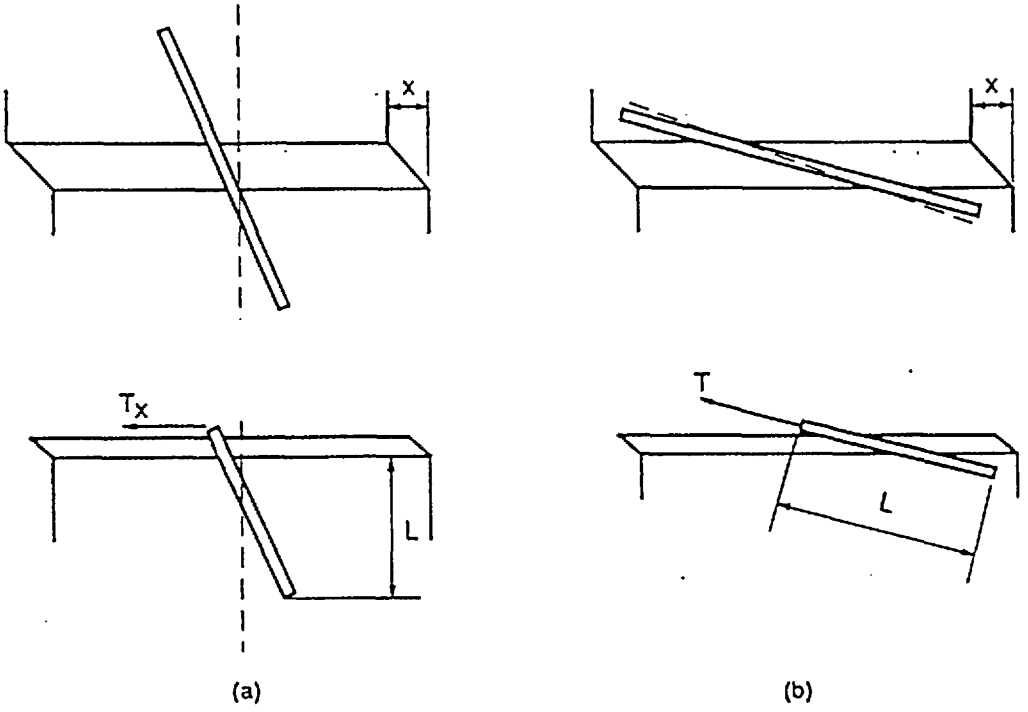

Fig. 8. Simplified models for soil-root interaction

the relations are not well established. Hence, extrapolation of data from one site to another involves uncertainties. However, available data are sufficient for approximate calculations in a number of cases. These should be verified by *in situ* tests whenever possible. Most of the data collected pertain to tree roots. Data on roots of shrubs and grasses are more limited.

Root Geometry

In the comprehensive sense, root geometry denotes all the properties that are necessary to define the positions and dimensions of the roots in the system. Comprehensive descriptions of root morphology of trees have been given by Stout (1956), Sutton (1969), Kozlowski (1971), and others.

Data from excavated roots have been used to establish the dimensions of components of a root system and their relations with environmental factors. It is known that the depth of a root system is strongly influenced by soil moisture and soil profile. Most of the root system is found within the zone of aeration and few roots extend into impermeable soils or bedrock. Where not limited by the above factors, the root crown and lateral roots of deciduous trees in the eastern United States usually extend to depths up to 0.5 m (Stout 1956). Sinker roots and taproots may extend to greater depths. In arid regions, some trees and shrubs may grow taproots as long as 27 m to reach water (Williams and Pidgeon 1983, Coatsworth and Evans 1984).

Data available from excavated roots are summarised in Table 1. The growth of roots from cuttings used in soil-biotechnical systems may be expected to be different from that of natural seedlings. Ultimately, the root system of the established plant may approach that of a plant that grows from natural seedlings. Data on the rate of growth are scarce. Studies were made on roots of cuttings of willows and poplars, one year after planting, by Hathaway (1973), and the results are included in Table 1. The maximum depth of roots of grass and forbs in temperate zones is usually 0.5 m. Root area ratios of grass and forbs on horizontal planes estimated from drawings are also given in Table 1.

Strength Properties of Roots

We consider first the strength of roots in tension. The strength of the root material may be measured by performing the simple tension test on a root segment. Available data on tensile strength are summarised in Table 2. The detailed summary by Greenway (1987) shows that differences between root strengths of species of the same family can be very large. There also may be large differences between root strengths of one species growing in different locations. Also, the tensile strength decreases with diameter for a given species (Burroughs and Thomas 1977). Considering the wide range of strengths, the values given in Table 2 may only serve as a rough guide in the estimation of root strength. Data on roots of shrubs are scarce, but the available data indicate that the range is not significantly different from that of trees. A distinction should be made on whether the root was tested with or without the bark and whether or not the diameter includes the thickness of the bark. The Young's modulus is less frequently used than the tensile strength. Limited available data are also given in Table 2.

It is necessary to distinguish between the tensile strength of a root segment and the tensile resistance of a root system. Most roots contain branch roots such as the root which passes through the shear box in Fig. 9. Since the diameter of a branch root may be smaller than that of the main root, there is the possibility that a branch may fail first. Progressive failure occurs with successive failure of other branches. The system fails when all branches that support the main root fail. The load displacement relation is strongly dependent on the number and orientation of branch roots with respect to the direction of the applied force. The tensile resistance and the load-displacement relation of root systems may be measured by *in situ* pullout tests. Test methods have been described by Wu *et al.* (1979) and Riestenberg (1987).

Examples of typical load displacement curves from pullout tests are shown in Fig. 10 with the root geometry. The white ash root consisted of a nearly straight main root with two branches. The peak resistance was reached when the main root failed near the branch point, at the top of the segment shown in Fig. 10a. This case approaches the tensile test on a root segment and the strength, $\sigma_{p'}$, in the pullout test would be close to the tensile strength of the root

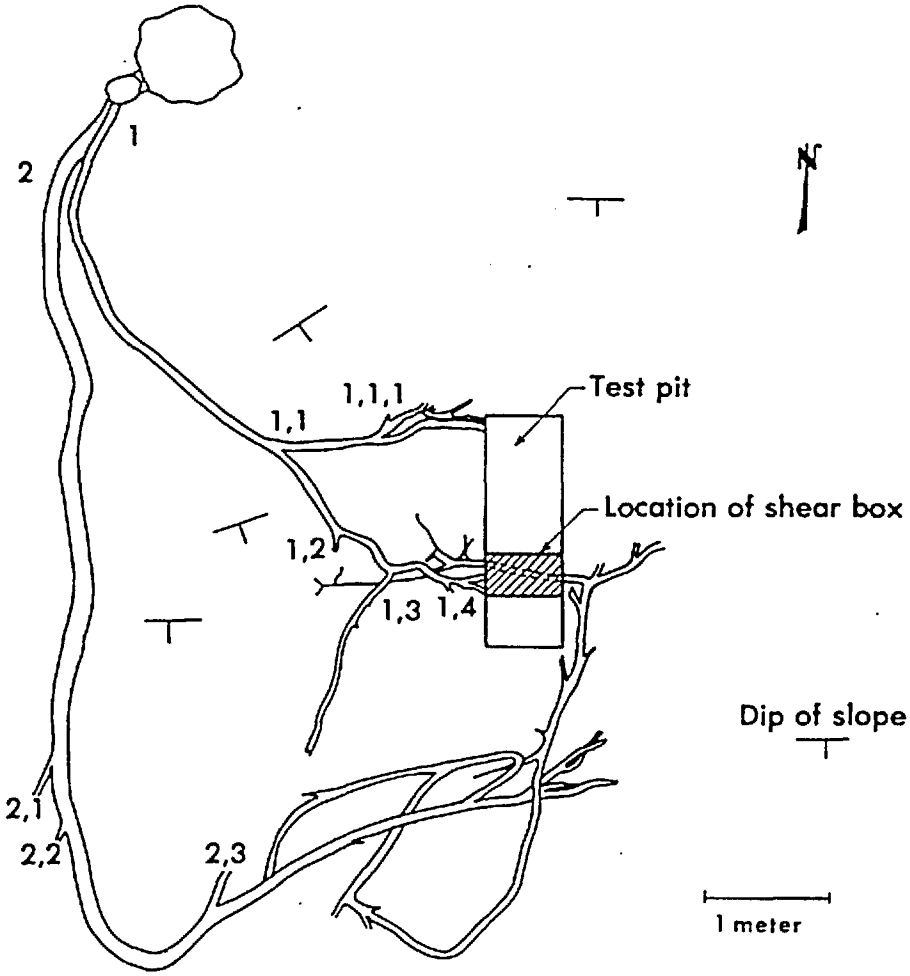

Fig. 9. Root system of a western hemlock (Wu *et al.* 1988a)

σ_t. In contrast, the sugar maple root is not straight and has many branches. The many peaks in the load-displacement curve, Fig. 10b, reflect points at which different branch roots failed. Eventually, all the branches failed. The resistance of such a system may be considerably less than that of the main root segment. Figure 11 shows plots of peak and ultimate resistances against diameter of the root at the pulled end. The ultimate resistance is that just before the root system failed, which occurred at axial displacement of 10 cm or greater. Also shown in Fig. 11 is the curve for Eq. (11a). This relation gives a reasonable prediction of the resistance of the root system for diameters less than 1 cm. This is because the smaller roots have fewer branches than the large ones and resemble the white ash root in Fig. 10a. Thus, for larger roots Eq. (11a) overestimates the tensile resistance. Similar conclusions may be drawn from the results of pullout tests by Wu *et al.* (1979) on Sitka spruce, western hemlock, and Alaska yellow cedar.

Table 1. Root area and roots' contribution to shear strength

Site	Soil	Species	Depth	Diam (cm)	$a_r = \frac{A_r}{A}$	s_r(kPa)	θ	$\frac{s_r}{a_r}$ (kPa)	References
(a) Estimated from a_r									
Cincinnati, Ohio	Colluvium, Eden silty clay loam	Sugar maple	Slip surface, above boundary between B and C horizons, 0.5 m	<2.5	1.4×10^{-4}	5.70 4.30^x	90°	2.8×10^4	Riestenberg and Sovonick-Dunford (1983)
Maybeso Valley, Alaska	Till, colluvium	Sitka spruce, western hemlock, Alaska cedar	Slip surface, boundary between B and C horizons, 0.5–1 m	<1.3	$3.7–10.0 \times 10^{-4}$	4.3–12.6	90°		Wu (1984a)
					3.7×10^{-4}	5.0^x		1.4×10^4	Wu *et al.* (1979)
						$3.4–4.4^x$			Swanston (1970)
Hong Kong	Decomposed granite		0–1.5 m	<1.0	$0.5–15 \times 10^{-4}$	0.5–10.0**		10^4	Greenway (1987)
New Zealand		Willow, poplar cuttings (1 yr old)		<1.0	$A_r = 5.2$ cm^2				Hathaway (1973)
Netherlands		Marram grass	15 cm	<0.3	$1.5–15 \times 10^{-4}$	1.5–15**	−90°–90°		Wu (1984a)
Alps		Grass	25–75 cm	<1	$2–8 \times 10^{-4*}$	2–8**	−90°–90°		Schiechtl (1980)
		Willow	1 m	<2	$6 \times 10^{-4*}$	6**			Schiechtl (1980)
		Poplar	0.5 m	<1	$2 \times 10^{-4*}$	2**			Schiechtl (1980)

(b) *In situ* shear tests								
Oregon	Slickrock Preacher Loam	Hemlock	0.3–0.6 m	<3.0	$10–80 \times 10^4$	1–8	0.1×10^4	Wu *et al.* (1988a)
California		*Pinus contorta*					0.1×10^4	Ziemer (1981)
Japan	Loam	Alder			$0–2 \times 10^4$	0–1	0.05×10^4	Endo and Tsuruta (1969)
(c) Laboratory Shear Tests								
California		Barley	30 cm	<.05	$0.2–0.8 \times 10^4$	0.6–2.6	3×10^4	Waldron (1977)
Temascal Ranch, California	Castaic silty clay loam	Chaparral +	20–45 cm			−0.6–3.0		Terwilliger (1988)
		Grassland +	20–45 cm			−0.9–2.4		Terwilliger (1988)

\+ see Terwilliger (1988) for species inventory

x calculated from slope failures

* area is estimated from drawings and photographs of excavated roots

**s_r is calculated with $\sigma_r = 10$ MPa

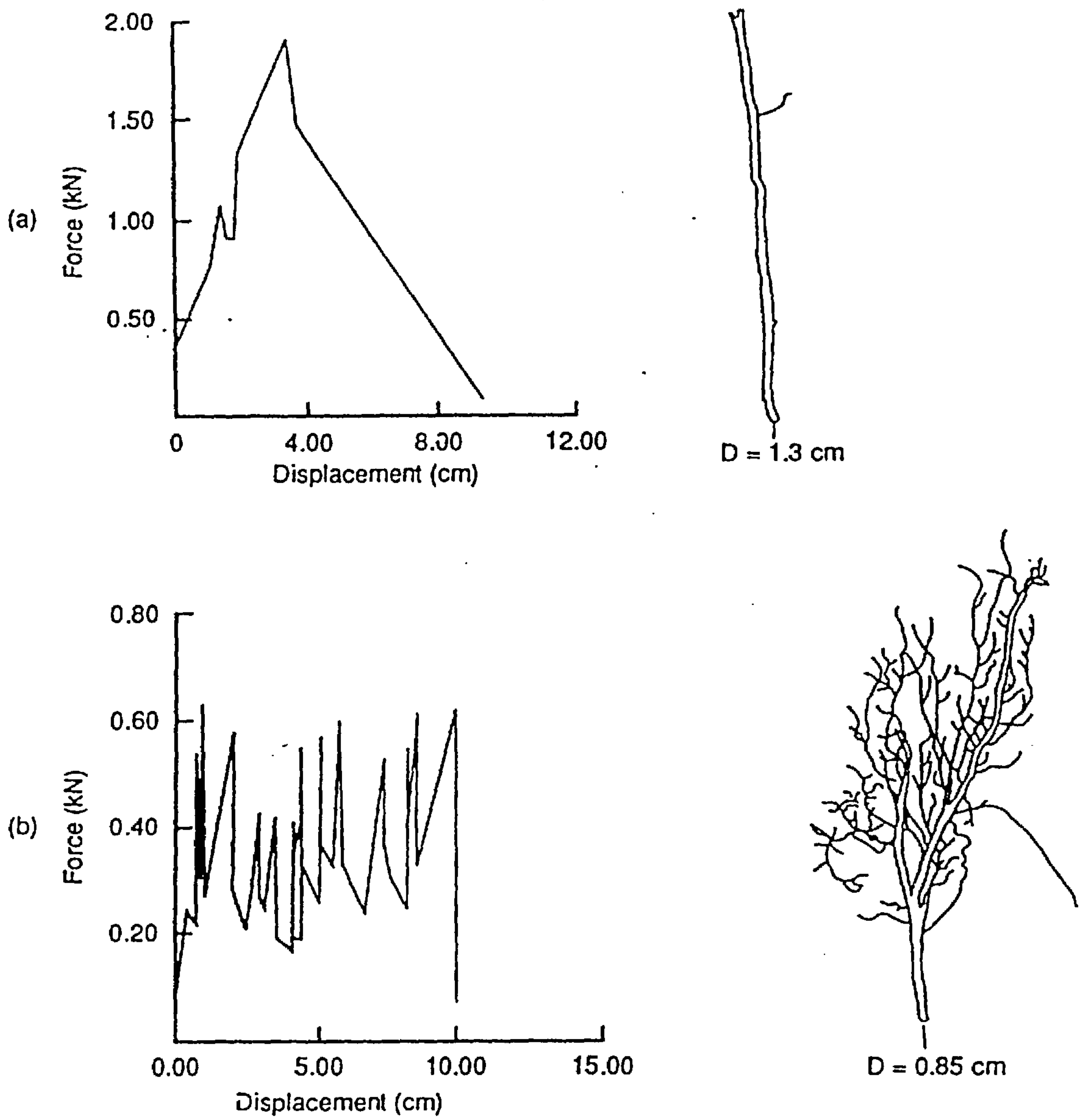

Fig. 10. Typical load displacement relations: (a) white ash, (b) sugar maple (from Riestenberg 1987)

Contribution to Shear Strength

If a root is flexible and the tensile force in the root can be estimated, Eq. (8) may be used to calculate s_r. One procedure is to obtain a_r from measurements. If the root diameters are less than 1 cm, use Eq. (11a) to get T and then Eq. (8b). Values of s_r estimated from a_r are summarised in Table 1a. The values of s_r for Cincinnati and Maybeso Valley were calculated with σ_t and σ_p, respectively, but were also checked against the values of $s = s_s + s_r$ at failure of the slopes. Tables 1b and 1c show the values obtained from *in situ* shear tests and labora-

Table 2. Tensile strength of roots

		Tensile strength (MPa)	Young's modulus (MPa)	Reference
Salix	Willows	9–36	200–300*	Hathaway and Penny (1975)
Populus	Poplars	5–38	200–300*	Hathaway and Penny (1975)
Alnus	Alders	4–74		
Pseudotsuga	Douglas fir	19–61		
Acer sacharinum	Silver maple	15–30**	600**	Beal (1987)
Tsuga heterophylia	Western hemlock	27	170**	Beal (1987)
Vaccinum	Huckleberry	16		
Hordeum vulgare	Barley	15–31	40–90	Waldron and Dakessian (1981)
	Grass, forbs	2–20		
	Moss	2–7 kPa		Wu (1984b)

Data are from Schiechtl (1980), except where otherwise noted.

* values were estimated from stress-strain curves

** roots were tested without removing bark; cross-sectional area includes area of bark

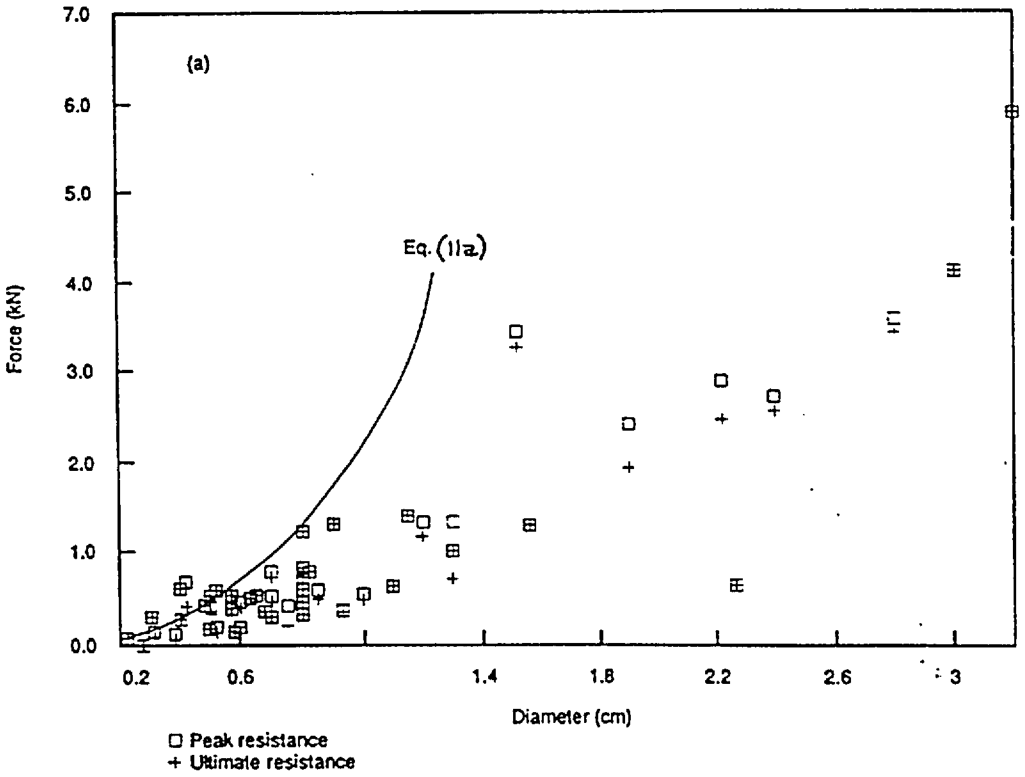

Fig. 11. Tensile resistance versus root diameter for white ash (from Riestenberg 1987)

tory shear tests on soil-root systems, respectively. These results are plotted in Fig. 12 for comparison. The wide spread in the data is reflected in the large differences between values of s_r/a_r in Table 1. The difference between slope failures and *in situ* shear tests should be noted. Observations of slip surfaces at Cincinnati and Maybeso Valley showed that most of the roots, including those with diameter up to 2.5 cm, failed by tension. On the other hand, the *in situ* tests at Oregon contained many roots that were cut off by the shear box and many roots, especially those with diameters larger than 1 cm, did not fail by tension. This condition probably also holds for other *in situ* shear tests. Clearly, Eq. (11a) is not applicable to roots that did not fail in tension.

Field observations of failures of roots with diameters much larger than 2.5 cm are scarce. Because of the extensive branching often associated with roots of larger diameters, progressive failure of the root system, as described in the preceding section, will control the tensile resistance of the larger roots. Because the root geometry is usually not well known without extensive excavation, the progressive failure cannot be calculated. Hence, *in situ* tests of the type described by Wu *et al.* (1988a) may be used to determine the relation between T and the shear displacement x. The measured T at a given x may be used in Eq. (6) to compute s_r at that x. If *in situ* tests could not be performed, it may be necessary to estimate T from available test data, such as those shown in Fig. 11.

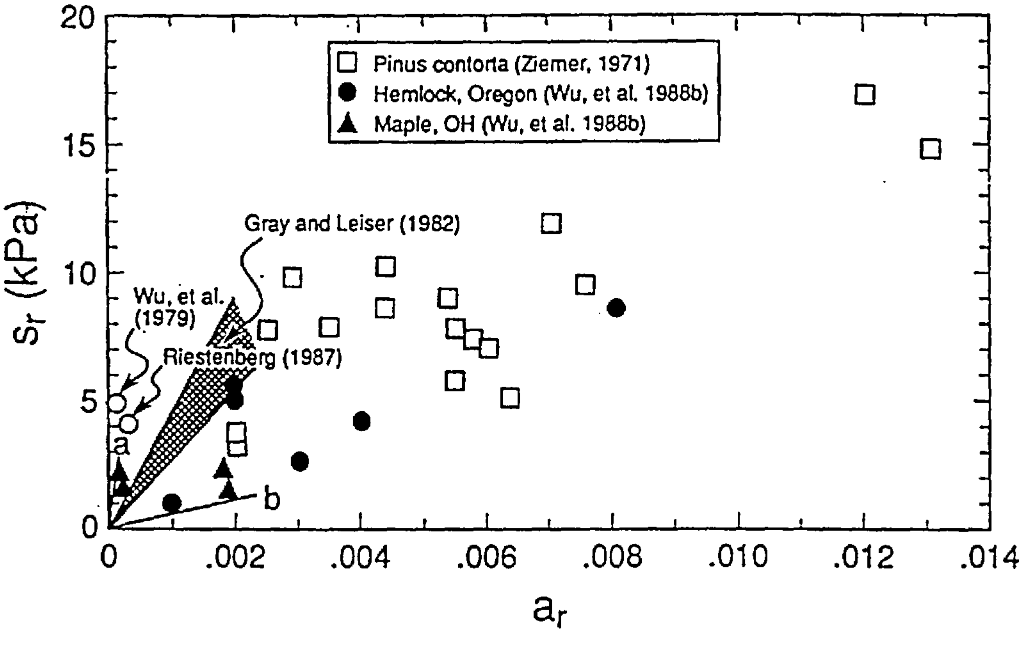

Fig. 12. Root strength versus area ratio: line a = barley (Waldron 1977), line b = alder (Endo and Tsuruta 1969)

EXAMPLES OF SLOPE STABILISATION

Vegetation has been used for slope stabilisation under a variety of conditions. The following examples illustrate use of stability analysis on some recent applications of soil-biotechnical construction.

Slopes of embankments and cuts are subjected to infiltration of precipitation. If the soil has a low permeability and the ground water is located at some depth below the surface, saturation during periods of prolonged rainfall progresses from the surface downward. Because the suction is reduced to zero in the saturated zone, Eq. (5) shows that a shallow slide would occur if ϕ' is equal to or less than the slope angle α. For many clays of low plasticity, the softened strength (Skempton 1964) is around $\phi' = 30°$ and $c' = 0$. Hence, it is not surprising that shallow slips are frequently found on clay slopes with α close to 30°. Vegetation roots increase the shear strength by s_r, which can significantly increase the safety factor if the roots extend below the slip surface.

An example is the embankment failure on interstate route I-77, near Caldwell, Ohio, shown in Fig. 13 (Wu *et al.* 1993). During wet seasons, the slope was found to be saturated to a depth of up to 0.6 m. Shallow slips and their dates of occurrence are also shown. The embankment material consisted of a clay derived from weathering of a red Conemaugh shale. The shear strength of the clay was approximately $\phi' = 30°$ and $c' = 0$. The slope of the embankment is approximately 27°. Thus, if the slope is saturated by infiltration from the surface, the safety factor would be close to 1, according to Eq. (5). If seepage parallel to the slope should occur, the safety factory, according to Eq. (4b), is less than 1. Results of suction measurements and permeability tests indicate that the soil near the surface could have a much higher permeability than the soil below. Then, seepage parallel to the slope could occur through the surface layer.

One measure for repair of the embankment was to use live planting on the slopes. Black locust (*Robinia pseudoacacia*) seedlings were planted at 1.2 m spacings. No information was available on roots of black locusts. The contribution of the tree roots to the shear strength could only be estimated. The data given in Table 1 show that a_r for most species is greater than 10^{-4}. Using $a_r = 2 \times 10^{-4}$ and $\sigma_r = 20$ MPa in Eq. (9b) gives $s_r = 4$ kPa. Using this in Eq. (5) gives an adequate safety factor.

To evaluate the effectiveness of the construction, roots of several seedlings were excavated after one year (Fig. 14). The value of a_r was found to be around 0.4×10^{-5} at 0.3 m. This is too small to have an influence on stability. The question is whether the slope can remain stable until sufficient roots are developed.

An advantage of soil-biotechnical construction is that the cuttings serve as reinforcement even before roots are developed. A combination of soil-biotechnical systems and mechanical reinforcement was used in the construction of an embankment slope on State Highway 126, near Marion, North Carolina (Soil Bioengineering Corp. 1986). Most of the slides consisted of shallow

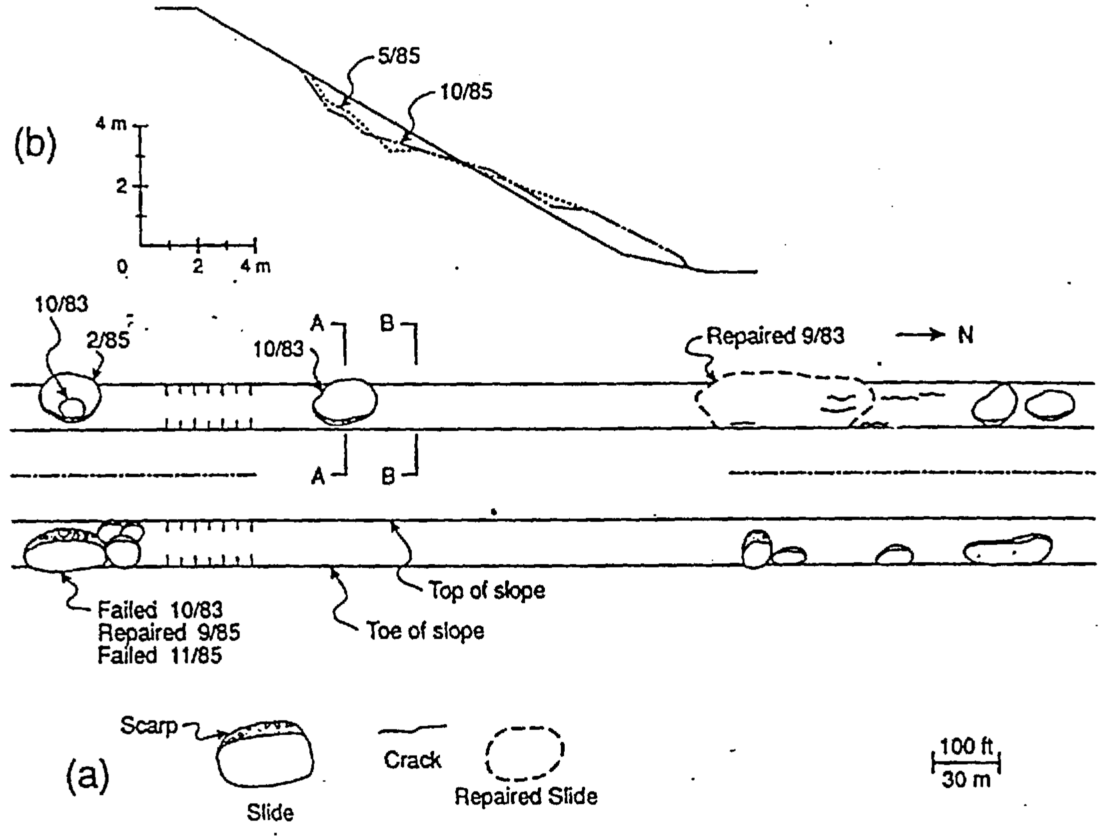

Fig. 13. Embankment failure, I-77, Ohio: (a) plan, (b) section A-A (Wu *et al.* 1993)

slips that extended to depths of 1–1.5 m. The embankment material consisted primarily of clayey to sandy silt, ML and SM, according to the Unified Classification system. The shear strength, as measured in triaxial tests, was variable and $c' = 0$, $\phi = 30°$ were considered representative of the average. Since the embankment slope was also 30°, the failure mechanism was believed to be similar to that in the preceeding example. Live brush layers consisting of stems 1.25 to 5 cm in diameter were placed in three directions as shown in Fig. 15, with about 15 stems/m in each direction. These layers were placed at 0.75 m spacing vertically. Between Sta. 21 + 00 and 23 + 00, Tensar SS2 geogrids were placed at 1.5–3 m spacing vertically, in addition to the brush layers, Fig. 15a. The woody species used in brush-layer and live facine construction were: black willow (*Salix nigra*), willow (*Salix* sp.), redtwig dogwood (*Cornus* sp.), river birch (*Betula* sp.), and privet (*Ligustum* sp.).

To evaluate the soil reinforcement, the stems in a brush layer are analysed as the stiff rod in Fig. 8c. Immediately after installation, the stems have no roots and the maximum tension is equal to the bond between soil and stem. Assuming

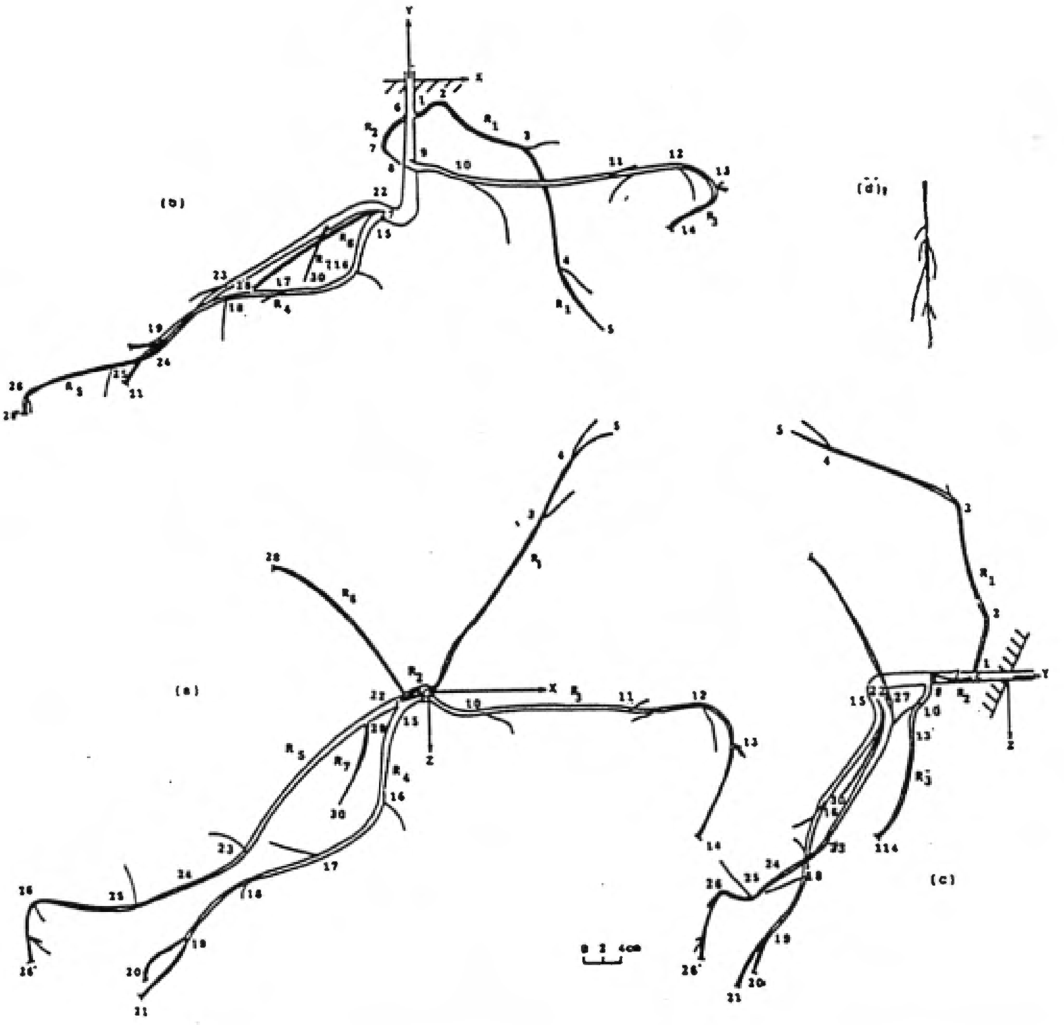

Fig. 14. Roots of black locust seedlings, I-77, Ohio: (a), (b), (c) one year after planting, (d) seedling at time of planting

that the suction is zero, the interface resistance in Eq. (11b) is

$$f = \gamma z \tan \delta \tag{12}$$

where δ = friction between soil and stem. A conservative estimate is $\tan \delta = \frac{1}{2} \tan \phi$. Assuming that only the portion below the potential slip surface, Fig. 15b, contributes to s_r, $L = 1.5$ m. For $D = 1.27$ cm, $T = 596$ N, Eq. (11b) and Eq. (8a) give $s_r = 2.67$ kN/m of slip surface. Eq. (5) gives $F_s = 1.68$. For comparison purposes, the contribution of the geogrid is computed in the same

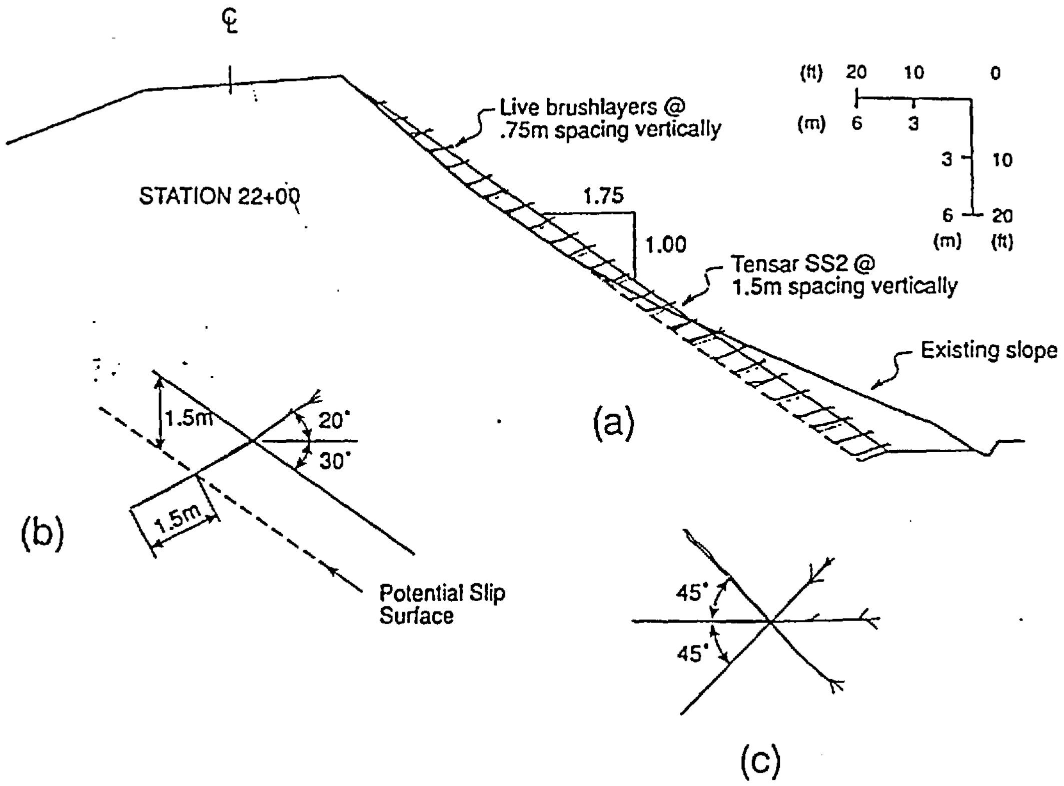

Fig. 15. Cross-section of embankment on Route NC126 (from Soil Bioengineering Corp.)

way. The creep strength of Tensar SS2 is about 7.41 kN/m (Tensar Corp. 1987). When the geogrids are placed at 0.75 m spacings vertically, $s_r = 2.37$ kN/m and $F = 1.4$. When the geogrids are placed at 1.5 m spacings in combination with the live brush layers at 0.75 m spacings, $s_r = 3.56$ kN/m and $F_s = 1.9$.

To study the long-term performance, segments of buried willow stems were excavated in 1991, about four years after construction. Figure 16 shows the roots on a stem that was only a few cm below the ground surface. It was found that $A_r = 1$ cm^2/m of stem. When δ is substituted for ϕ, Eq. (7c) can be used to calculate s_r, which is equal to f in Eq. (12). Using $\sigma_r = 20$ MPa, $T = 30$ kN. On the other hand, willow stems excavated from depths of 1–1.5 m were partly decayed and had few roots, Fig. 17. It is questionable whether roots at such depths may be expected to survive as naturally grown willows do not have roots that extend more than 0.6 m below the surface.

SUMMARY AND CONCLUSIONS

Theory and observations show that vegetation can contribute effectively to slope stability by reducing the pore pressure and by reinforcing the soil. Their effectiveness is most significant for shallow slides. The reduction in pore pressure is difficult to predict because of the complexities of moisture flow near the surface. *In situ* measurements are needed for reliable estimates. Approximate estimates

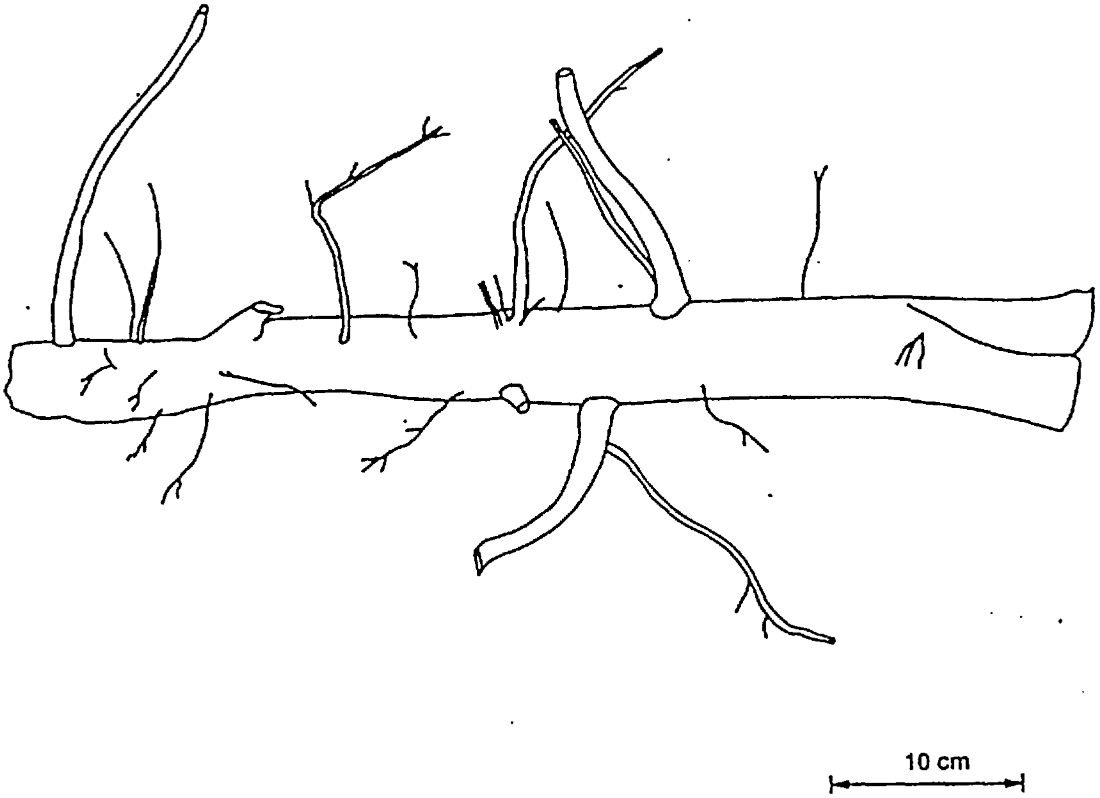

Fig. 16. Excavated stem of willow just below ground, Route NC126

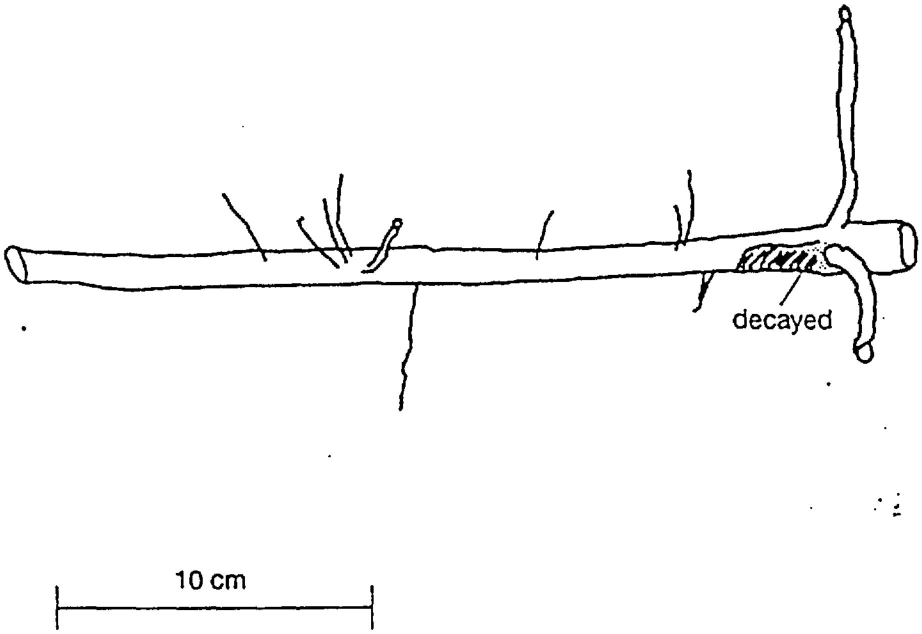

Fig. 17. Excavated stem of willow, 1.5 m below ground, Route NC126

of soil reinforcement by roots can be made for cases where the root diameters are less than 1 cm. For larger roots, more needs to be known about the root geometry and failure modes before reliable procedures for prediction can be formulated.

In practical applications, prediction of the effectiveness of live plantings requires estimates of the growth rate of roots, which are often not available. Soil biotechnical construction can provide adequate reinforcement prior to root growth. The question is whether there is a maximum depth below which the cuttings will not develop roots. More research in this direction, especially well-documented case histories, will help to promote the use of biotechnical methods.

ACKNOWLEDGEMENTS

I wish to thank R.B. Sotir, M.M. Riestenberg, W.L. Moore, E.D. Penny, and R.R. Ziemer for providing some of the information used in this paper. A large part of the writer's research described here was supported by grants or contracts from the National Science Foundation, U.S. Forest Service, and U.S. and Ohio Departments of Transportation. This paper was derived from a position paper for the Workshop on Biotechnical Stabilization, University of Michigan, 1991.

REFERENCES

Beal, P.E. (1987). Estimation of the shear strength of root reinforced soils. M.S. Thesis, Ohio State University, Columbus, Ohio.

Bevan, K. (1982). On subsurface storm flow: Predictions with simple kinematic theory for saturated and unsaturated flows. *Water Resources Res.*, 18: 1627–1633.

Broms, B. (1964a). Lateral resistance of piles in cohesive soils. *J. Soil Mech. Foundation Division*, ASCE, 90(SM2): 27–63.

Broms, B. (1964b). Lateral resistance of piles in cohesionless soils. *J. Soil Mech. Foundation Division*, ASCE, 90(SM3): 123–156.

Brown, C.B. and M.S. Sheu (1975). Effects of deforestation on slopes. *J. Geotech. Division*, ASCE, 101(GT2): 147–165.

Burroughs, E.R. and B.R. Thomas (1977). Declining root strength in Douglas-fir after felling as a factor in slope stability. Research paper INT-90, Intermountain Forest and Range Experiment Station, U.S. Forest Service, Ogden, Utah, 27 pp.

Coatsworth, A. and J. Evans (1984). Discussion on influence of vegetation on shrinking and swelling of clays. *Geotechnique*, 34: 154–155.

Coppin, N.J. and I.G. Richards (1990). *Use of Vegetation in Civil Engineering*, Butterworths, London, 272 pp.

Endo, T. and T. Tsuruta (1969). The effect of tree roots upon the shearing strength of soil. Annual Report, Hokkaido Branch, Tokyo Forest Experiment Sta., 18: 168–179.

Freeze, R.A. (1971). Three-dimensional, transient, saturated-unsaturated flow in a groundwater basin. Water Resources Research, 7: 347–366.

Gray, D.H. (1970). Effect of forest clear-cutting on the stability of natural slopes. *Bull. Assn. Engg. Geol.*, 7(1): 45–66.

Gray, D.H. and A.T. Leiser (1982). *Biotechnical Slope Protection and Erosion Control.*, Van Norstrand Reinhold Co., New York, 271 pp.

Greenway, D.R. (1987). Vegetation and slope stability. In: *Slope Stability* (M.G. Anderson and K.S. Richards, eds.). John Wiley and Sons Ltd., New York, pp. 187–230.

Greenway, D.R., M.G. Anderson and K.C. Brain-Boys (1984). Influence of vegetation on slope stability in Hong Kong. *4th Int. Symp. Landslides*, Toronto, Vol. 1 pp. 399–404.

Hathaway, R.L. and D. Penny (1975). Root strength in some *Populus* and *Salix* clones. *New Zealand J. Bot.*, 13: 333–344.

Hathaway, R.L. (1973). Factors affecting the soil binding capacity of the root systems of some *Populus* and *Salix* clones. M.S. Thesis, Massey Univ., Palmerston North, 161 pp.

Juran, I., F. Schlosser, C. Louis, M. Kemos and B. Eckmann (1981). Le reinforcement des sols par barres passives, *Proc. 10th Int. Conf. Soil Mechanics and Foundation Engineering*, Vol. 3. pp. 713–716.

Kozlowski, T.T. (1971). *Growth and Development of Trees*. Academic Press, New York, 443 pp.

Krabel, C.J. (1936). Erosion control on mountain roads. Circular 380, U.S. Dept. of Agriculture, Washington, D.C., 44 pp.

Philip, J.R. (1957). The theory of infiltration. 1. The infiltration equation and its solution. Soil Science, 83: 345–357.

Philip, J.R. (1969). Theory of infiltration. In: *Advances in Hydroscience*, (V.T. Chow, ed.)., Academic Press, New York, NY, 5: 215–295.

Reddi, L.N. and T.H. Wu (1991). Probabilistic analysis of groundwater levels in hillside slopes. *J. Geotech. Engg.*, ASCE, 117(6): 872–890.

Riestenberg, M.M. (1987). Anchoring of thin colluvium on hillslopes by roots of sugar maple and white ash. Ph.D. Dissertion, University of Cincinnati, Ohio.

Riestenberg, M.M. and S. Sovonick-Dunford (1983). The role of woody vegetation in stabilizing slopes in the Cincinnati area, Ohio. *Geol. Soc. Amer. Bull.*, 94: 506–518.

Sangrey, D.A., K.O. Harrop-Williams and J.A. Klaiber (1984). Predicting groundwater response to precipitation. *J. Geotech. Engg. Division*, ASCE, 110: 957–975.

Schiechtl, H.M. (1980). Bioengineering for Land Reclamation and Conservation. University of Alberta Press, Edmonton, 404 pp.

Shewbridge, S.E. and N. Sitar (1989). Deformation characteristics of reinforced sand in direct shear. *J. Geotech. Engg.*, ASCE, 115: 1134–1147.

Shewbridge, S.E. and N. Sitar, (1990). Deformation-based model for reinforced sand. *J. Geotech. Engg.* ASCE, 116: 1153–1170.

Skempton, A.W. (1964). Long-term stability of clay slopes. *Geotechnique*, 14: 75–101.

Soil Bioengineering Corp. (1986). Failure fill slope stabilization using soil bioengineering technology on State Highway NC 126, McDowell Co., North Carolina. Soil Bioengineering Corp. (now Robbin B. Sotir and Assoc.,) Marietta, Georgia.

Stout, B.B. (1956). Studies of the root systems of deciduous trees. Black Rock Forest Bulletin No. 15, Harvard University, Cambridge, Massachusetts, 44 pp.

Sutton, R.F. (1969). Form and development of conifer root systems. Tech. Comm. No. 7, Commonwealth Forestry Bureau, Oxford.

Swanston, D.N. (1970). Mechanics of debris avalanching in shallow till soils of southeastern Alaska, Research Paper PNW 103, Forest Service, U.S. Dept. of Agriculture.

Tensar Corp. (1987). Slope reinforcement with Tensar geogrids, Design and Construction Guideline, Tech. Note TTN: SS1, Tensar Corp., Morrow, Georgia.

Terwilliger, V.J. (1988). Mechanical effects of chaparral disturbances on soil slip patterns in the Transverse Ranges of Southern California. Ph.D. Dissertation, University of California, Los Angeles, 200 pp.

Terwilliger, V.J. (1990). Effects of vegetation on soil slippage by pore pressure modification. *Earth Surface Processes and Landforms*, 15: 553–570.

Terzaghi, K. (1936). The shearing resistance of saturated soils and the angle between planes of shear. *Proc. 1st Int. Conf. Soil Mechanics and Foundation Engineering*, Vol. 1 p. 54.

Waldron, L.J. (1977). The shear resistance of root-permeated homogeneous and stratified soil. *J. Soil Sci. Soc. Amer.*, 41: 843–849

Waldron, L.J. and S. Dakessian, (1981). Soil reinforcement by roots: Calculation of increased shear resistance from root properties. *Soil Sci.*, 132: 427–435.

Williams, A.A.B. and J.T. Pidgeon, (1983). Evapotranspiration and heaving clays in South Africa. *Geotechnique*, 33: 141–150.

Wu, T.H. (1984a). Effect of vegetation on slope stability. In: *Soil Reinforcement and Moisture Effects in Slope Stability*. Transportation Research Record 965, Transportation Research Board, Washington, D.C.

Wu, T.H. (1984b). Soil movements on permafrost slopes near Fairbanks, Alaska. *Canadian Geotech. J.*, 21: 699–709.

Wu, T.H., P.E. Beal and C. Lan (1988a). *In situ* shear tests of soil root systems. *J. Geotech. Engg.*, ASCE, 114: 1376–1394.

Wu, T.H., W.P. Mckinnell III and D.N. Swanston (1979). Strength of tree roots and landslides on Prince of Wales Island, Alaska. *Canadian Geotech. J.*, 16: 19–33.

Wu, T.H., R.M. McOmber, R.T. Erb and B.E. Beal (1988c). A study of soil root interaction. *J. Geotech. Engg.*, ASCE, 114: 1351–1375.

Wu, T.H., B. Randolph and C.S. Huang (1993). Stability of shale embankments. *J. Geotech. Engg.*, ASCE (in press).

Wu, T.H. and D.N. Swanston (1980). Risk of landslides in shallow soils and its relation to clear-cutting in southeastern Alaska. *For. Sci.*, 26: 495–510.

Ziemer, R.R. (1981). Roots and the stability of forested slopes. In: *Erosion and Sediment Transport in Pacific Rim Steeplands*, Publ. 132. International Assoc. of Hydrological Science, London, pp. 343–361.

1995 ANNUAL CONFERENCE OF THE CANADIAN SOCIETY
FOR CIVIL ENGINEERING
CONGRÈS ANNUEL DE LA SOCIÉTÉ CANADIENNE DE
GÉNIE CIVIL 1995
JUNE 1-3, 1995, OTTAWA, ONTARIO

STABILISATION DE LA BERGE AVAL DE L'AMÉNAGEMENT LA GRANDE 1

Michel Massiéra*
École de génie, Université de Moncton, Moncton, N.-B. E1A 3E9

Jerry Levay
Société d'énergie de la Baie James, Montréal, Québec H2Z 1Z9

RÉSUMÉ

Dans le cadre de la réalisation de l'aménagement hydro-électrique La Grande 1 (LG-1) du complexe La Grande, au nord du Québec, une digue de 2 444 m de long a été construite sur la rive nord. La présence d'argile sensible, d'origine marine, recouverte de dépôts alluviaux et deltaïques de sable et silt, a nécessité une conception particulière faisant appel à des travaux de stabilisation de la berge aval pour éviter que des glissements de type coulée puissent affecter l'intégrité de la digue. Cet article présente les conditions géotechniques de la terrasse rive nord en insistant sur les travaux de stabilisation et les méthodes de contrôle des sous-pressions par l'installation de puits de relâche dans l'aquifère captif sous la berge aval.

ABSTRACT

LG-1 hydroelectric project, part of the La Grande Complex in Northern Quebec, required the construction of a 2 444 m long dyke on the north bank. The presence of sensitive marine clay, covered with deltaic sand, river sand and silt deposits, called for special design features such as the downstream bank stabilization work to avoid the occurrence of potentially disastrous retrogressive slides. This paper describes the geotechnical conditions of the northern terrace and presents the different construction phases of the river bank stabilization with emphasis on the control of groundwater pressures in the lower aquifer by the installation of relief wells.

* Adresse antérieure
Société d'énergie de la Baie James, chantier de LG-1, Baie James, Québec J0Y 3P0

INTRODUCTION

Dans le cadre de la phase II du développement hydro-électrique du complexe La Grande à la Baie James, l'aménagement La Grande 1 (LG-1) a nécessité la stabilisation des berges aval et amont de La Grande Rivière. En effet, les berges le long de La Grande Rivière, entre son embouchure et l'aménagement LG-2, sont localement instables (SEBJ, 1991). Elles comportent des talus d'argile et de silt d'une grande hauteur qui sont susceptibles de subir une rétrogression typique des argiles sensibles. En rive droite, en aval de la centrale LG-1, la rétrogression peut atteindre la digue de revanche qui constitue la partie centrale de la digue nord (fig. 1).

En rive gauche, les rétrogressions éventuelles ne mettent pas en péril les ouvrages permanents. C'est pourquoi la rive droite a été l'objet d'études particulières qui ont mené à des travaux de stabilisation.

Après une description des conditions de fondations de la berge aval, rive droite, et des choix possibles pour stabiliser cette berge aval, l'article présente les différentes phases de construction des travaux de stabilisation (fig. 2). Il insiste plus particulièrement sur les procédés de construction, l'instrumentation installée et les essais de contrôle effectués.

LES CONDITIONS DE FONDATIONS

Terrasse aval

En surface, la terrasse aval est caractérisée par des dépôts fortement stratifiés de sable et silt d'origine alluvionnaire et deltaïque. Ces dépôts forment une dépression dont la profondeur maximale atteint près de 24 m sous l'axe de la digue nord pour ensuite remonter progressivement jusqu'à 18 m sur la berge aval (fig. 3). Sous ces dépôts, se retrouvent successivement jusqu'à 30 m de silt argileux et d'argile silteuse d'origine marine, suivis d'une épaisseur maximale de 37 m de moraine qui comble une vallée rocheuse.

Les dépôts alluviaux de surface ont une perméabilité de l'ordre de 10^{-2} à 10^{-4} cm/s dans les sables propres et de 10^{-3} à 10^{-5} cm/s pour les sables silteux. A l'intérieur des dépôts deltaïques, la perméabilité se situe entre 10^{-4} et 10^{-6} cm/s.

Pour les dépôts argileux, les profils de résistance au cisaillement indiquent que la cohésion non drainée tombe sous la ligne $\gamma H/6$, γ étant la poids volumique de sol et H la profondeur. Cette ligne représente le critère généralement admis pour évaluer le potentiel de rétrogression, c'est-à-dire zone qui est susceptible de subir une rupture non drainée par rétrogression, à partir du moment où le talus devient instable (Mitchell et Markell, 1974). Au bord de la rivière, les résultats sont plus dispersés avec des valeurs de la cohésion non drainée inférieures à la tendance générale. De plus, l'argile ne démontre pas où très peu, de gain de résistance avec la profondeur. Les valeurs observées à cet endroit oscillent entre 45 et 80 kPa.

La compacité de la moraine est généralement dense à très dense. Les valeurs de perméabilité obtenues dans la moraine sont généralement de l'ordre de 10^{-4} à 10^{-6} cm/s. Les forages montrent un toit du rocher d'excellente qualité sous la terrasse et un rocher fissuré pour le premier demi mètre le long de la berge aval.

Berge aval

La berge aval a une pente raide sur une longueur d'environ 1000 m, entre les kilomètres 34 et 35. Dans ce secteur, l'épaisseur du sable et silt est plus importante. La pente de la berge est généralement de l'ordre de 1,8H: 1V à 2,2H: 1V. La partie supérieure de la berge est souvent plus raide, jusqu'à 1,5H: 1V. Les venues d'eau à la base de la couche superficielle de sable et silt ont provoqué des glissements superficiels par érosion. L'examen des talus existants de la berge indique que les portions raidies à 1,5H: 1V sont instables et subissent des glissements superficiels. Les sections à 1,8H: 1V peuvent être considérées à la limite de la stabilité.

Le pied de la berge est généralement constitué d'argile marine dénudée par érosion sur une hauteur maximale de 10 m. Ce dépôt argileux se prolonge sur une épaisseur de plus de 40 m sur le bord de la rivière aux environs du PM 00 et diminue d'épaisseur vers les PM croissants. Il n'atteint plus qu'une épaisseur d'une dizaine de mètre au PM 700. Au dessous de ce dépôt argileux, la couche de moraine est d'épaisseur variable (voir fig. 4).

Conditions hydrogéologiques

Les conditions hydrogéologiques qui existent en rive droite sont très particulières et constituent l'une des données importantes dans la conception de la digue nord de revanche et la stabilisation de la berge aval (Tecsult, 1991). Elles peuvent être schématisée de la façon suivante (fig. 3):

- un aquifère libre ou nappe phréatique près de la surface dans les dépôts alluviaux et deltaïques dont l'alimentation est assurée par les précipitations et le drainage est contrôlé par le ruisseau nord et les résurgences dans les talus en bordure de la rivière (voir fig. 1).

- un aquifère captif profond dans la moraine et le toit du rocher fissuré dont l'alimentation se fait principalement par les affleurement de moraine et le roc au nord de la dépression où coule le ruisseau. Le drainage se fait par la rivière tant en amont qu'en aval de l'axe de la digue nord.

- un aquitard dans les dépôts argileux. Sous la terrasse, le sous-drainage de la nappe de surface par l'aquifère profond provoque un gradient hydraulique vers le bas. Sur la berge aval, l'encaissement de la rivière provoque une inversion du gradient hydraulique vers le haut.

CONCEPTION DE LA STABILISATION DE LA BERGE AVAL

Globalement, la nature sensible de la fondation d'argile molle a conduit le concepteur à incorporer, dans le projet, des travaux de stabilisation des berges tant en aval qu'en amont (fig. 1), dans le but d'éviter que des glissements de type coulée n'aient lien, entrainant des conséquences possiblement désastreuses pour la digue (Schneeberger et al. 1991).

Pour la berge aval, les études ont porté entre autres sur les écoulements souterrains sous la terrasse et la stabilité sous des conditions sismiques (Tecsult, 1991). La présence de dépôts perméables dans la fondation de la digue de revanche a soulevé certaines questions relatives aux débits de fuite à travers la fondations après la mise en eau du réservoir au niveau 32 m. En effet, tout changement notable des conditions hydrogéologiques naturelles sur la terrasse affecterait la stabilité de la berge aval et favoriserait une rétrogression potentielle. L'étude des écoulements sous la terrasse a mis en évidence qu'il était nécessaire d'avoir une coupure totale (écran d'étanchéité) jusqu'au silt argileux dans l'axe de la digue de revanche (voir fig. 3).

Sur la terrasse, les écoulements de surface en direction de la berge aval sont contrôlés par 3 tranchées de drainage (fig. 1). Les tranchées no. 1 et no. 2 rejoignent le ruisseau nord. La tranchée no. 3, en bordure du talus de la rivière, permet d'assécher un petit lac qui recueille une partie des précipitations de la terrasse aval et d'intercepter certaines résurgences dans le talus.

En vue de dissiper l'éventuel excès de pression interstitielle généré dans la couche de moraine (aquifère captif) suite au remplissage du réservoir LG-1, il était prévu de réaliser 22 puits de relâche sur la berge aval entre le PM 132 et le PM 762. Les puits de relâche sont installés de façon à s'assurer que la mise en eau du réservoir, au niveau 32 m, ne modifiera pas les sous-pressions qui existent, sous la berge aval, dans la couche de moraine sous-jacente aux dépôts argileux, par rapport aux conditions naturelles (fig. 3).

Les analyses de stabilité ont été réalisées en utilisant les paramètres au contraintes effectives relativement conservateurs ($c' = 7$ kPa et $\phi' = 28°$) et les conditions piézométriques naturelles. Deux types de confortement de la berge aval ont été analysés: adoucissement du talus ou butée drainante en enrochement. La solution qui a été finalement retenue est celle d'une butée drainante. Celle-ci comporte deux bermes de pied en enrochement aux niveaux 5 m et 9,5 m ainsi qu'un masque granulaire drainant et de l'enrochement jusqu'au niveau 19,5 m (fig. 2). Avec cette alternative, les coefficients de sécurité minimum obtenus sont respectivement de 1,71 dans le cas de l'analyse statique et de 1,3 pour l'analyse en liquéfaction (Tecsult, 1991).

DESCRIPTION DES TRAVAUX DE STABILISATION

Sur la rive droite, la berge aval d'une hauteur d'environ 28 m a été stabilisée au moyen d'une butée drainante d'environ 1 160 m de longueur qui est constituée de façon suivante (fig. 2):

- une berme de pied en enrochement de 10 m de largeur au niveau 5 m entre le point métrique (PM) 132 et le PM 1160.
- une berme de 14,5 m de largeur, constituée de matériaux granulaires (zone 5) de 10 m de largeur et protégée par un perré en enrochement tout-venant (zone 3) de 4,5 m de largeur, entre le PM 00 et le PM 785. Au delà du PM 785 et jusqu'au PM 1160, la berme est constituée d'enrochement tout-venant.
- une berme de 12 m de largeur minimum, constituée d'un masque de matériaux granulaires drainants (zone 5) de 3 m de largeur au minimum. Ce masque est protégé par un enrochement tout-venant de 9 m de largeur au minimum au niveau 19,5 m, entre le PM 132 et les environs du PM 800.

En vue de dissiper les sous-pressions qui pourraient se créer dans la couche de moraine suite au remplissage du réservoir LG-1, 24 puits de relâche ont été forés et installés à partir de la berme située au niveau 5 m, entre le PM 00 et le PM 702 (fig. 3 et 4). Pour contrôler les écoulements de surface, 3 tranchées de drainage ont été excavées (fig. 1). Ces tranchées de drainage ont respectivement 1337 m, 1165 m et 220 m de longueur et une largeur minimale de 2 m à la base et une profondeur d'environ 3 m en moyenne.

TRAVAUX DE STABILISATION DE LA BERGE AVAL

Écran d'étanchéité et tranchées de drainage

Les travaux de construction de l'écran d'étanchéité de 1030 m de longueur et de 17,7 m de profondeur en moyenne sous l'axe de la digue nord de revanche, ont été décrits par Massiéra et Levay (1994).

Les tranchées de drainage no. 1 et no. 2 ont été excavées en deux phases distinctes car le sable excavé a été utilisé, d'une part, pour la construction de deux planches d'essai sur tourbe situées à l'amont de la digue nord sur argile et, d'autre part, pour la construction des épaulements sur tourbe de la digue nord dans le même secteur. L'excavation des tranchées a fourni 56 127 m^3 de sable fin à moyen pour la réalisation des zones 2 et 2E des planches d'essai et des épaulements. Le volume de mort-terrain non utilisable pour la construction a été de 40 426 m^3. Les contrôles ont porté principalement sur la profondeur minimum des tranchées: 3 m; la pente minimum des talus 3H: 1V; et la pente pour permettre le drainage des eaux de surface vers le ruisseau nord.

Butée drainante

La butée drainante a été réalisée en deux saisons. D'abord, du 30 mai au 26 juillet 1990, la berme au niveau 5 m a été construite, en presque totalité, entre le PM 00 et le PM 1160. Une autre berme a été réalisée, en partie, jusqu'aux environs du niveau 9,5 m entre le PM 00 et le PM 1160 pour commencer les travaux de stabilisation du talus de la berge aval (voir fig. 2). Ces bermes ont été construites en enrochement tout-venant (zone 3) qui provenait directement du site d'excavation des fondations de la centrale LG-1 (fig. 1).

L'enrochement a été déversé par des camions de 35 t de capacité, à partir d'une plate-forme située à 1 m au-dessus du niveau de la rivière, puis par la suite, épandu en couches de 1,5 m d'épaisseur. Au total, 191 598 m^3 d'enrochement ont été mis en place en 1990.

La mise en place des remblais a repris le 17 mai 1991. La berme au niveau 5 m entre le PM 00 et le PM 825 et la berme au niveau 9,5 m entre le PM 132 et le PM 825 ont été complétées, par la mise en place de l'enrochement tout-venant (zone 3) et des matériaux granulaires (zone 5). La berme entre le niveau 9,5 m et le niveau 19,5 m a été réalisée, entre le PM 132 et le PM 800, en mettant contre la pente naturelle un géotextile et une couche drainante de matériaux granulaires (zone 5) sur laquelle s'appuit l'enrochement tout-venant (voir fig. 2). Le niveau de cette berme décroit de 19,5 m (PM 132) à 9,5 m (PM 00). Une couche de roulement en pierre concassée 80-0 mm (zone 6) a été mise en place au niveau 9,5 m. Tous ces travaux ont été complétés le 5 décembre 1991. Au total 199 752 m^3 d'enrochement (zone 3), 70 138 m^3 de matériaux granulaires (zone 5) et 2 788 m^3 de pierre concassée (zone 6) ont été mis en place en 1991. La mise en place des matériaux constituant les différentes zones et les contrôles s'y rapportant se sont effectués selon les procédures normalisées par la Société d'énergie de la Baie James qui ont été décrites par Paré et al. (1978).

Puits de relâche

Les 24 puits de relâche ont été forés et installés à partir de la berme située au niveau 5 m. Pour s'adapter aux conditions stratigraphiques rencontrées (niveaux du toit de la moraine et du toit du roc), les puits PR 21 (PM 732) et PR 22 (PM 762) ont été supprimés et 4 puits (PR 23 à PR 26) ont été ajoutés à l'extrémité ouest de la butée drainante entre le PM 00 et le PM 99 (fig. 4). Les travaux d'installation et de développement se sont déroulés en deux phases. Tout d'abord, 7 puits de relâche (PR 23, PR 24, PR 01, PR 02, PR 08, PR 09 et PR 18) ont été installés et développés entre le 21 mai et le 12 juin 1991 pour pouvoir effectuer les essais de pompage dans les puits PR 23, PR 02, PR 08 et PR 18. Par la suite, les 17 autres puits de relâche ont été installés et développés entre le 1 juillet et le 29 juillet 1991.

Les puits de relâche ont été forés en un diamètre de 305 mm à l'aide d'un tricône. La boue de forage utilisée est une boue "Revert" qui ne colmate pas les filtres des crépines. Dans chaque puits, une crépine de 152 mm de diamètre en acier inoxydable a été installée sur une longueur d'environ 1 m dans le roc et sur toute l'épaisseur de la couche de moraine. Ces puits de relâche ont été développés en utilisant la méthode à forage ouvert. La durée de développement des puits a varié de 16 h à 58 h. Elle a été en moyenne de 30 h 12 min par puits. A la fin de chaque développement, la teneur en sable était inférieure à 10 ppm après 15 min de pompage. Ces puits ont été raccordés à des tuyaux collecteurs en polyéthylène à haute densité (PEHD) de 315 mm de diamètre qui ont été eux-mêmes raccordés à 3 exutoires de même diamètre qui se déversent dans La Grande Rivière.

Pour déterminer les caractéristiques de l'aquifère profond, 4 essais de pompage ont été réalisés entre le 26 juin et le 12 juillet 1991. Les conductivités hydrauliques globales estimées de la couche de moraine située dans le sillon ouest entre le PM 00 et le PM 342 et, probablement jusqu'aux environs du PM 500 sont de l'ordre de 1.5 x 10^{-3} à 5,8 x 10^{-2} cm/s. Dans le sillon est, la conductivité hydraulique globale trouvée pour la couche de moraine est de l'ordre de 3 x 10^{-4} cm/s.

Instrumentation

L'instrumentation permanente installée sur la terrasse aval comporte 30 piézomètres hydrauliques (à tube ouvert). Celle installée sur la berge aval (fig. 4) comprend 17 piézomètres dont 10 piézomètres scellés (PS) et 7 piézomètres hydrauliques (PH). Ces piézomètres ont permis de vérifier les conditions hydrogéologiques naturelles qui existaient sous la terrasse aval avant installation des puits de décharge. Ils ont été aussi utilisés lors de la réalisation des essais de pompage. Ces piézomètres ont permis aussi de constater que le comportement des ouvrages de stabilisation, depuis la mise en eau en novembre 1992 et l'exploitation du réservoir, est très satisfaisant.

REMERCIEMENTS

Les auteurs remercient la Société d'énergie de la Baie James (SEBJ) d'avoir permis la publication de cette communication. La conception de la digue nord a été le fruit d'une collaboration étroite entre les spécialistes de la SEBJ, le Comité des experts de la SEBJ et la firme d'ingénieurs-conseils TECSULT Inc.

RÉFÉRENCES

MASSIÉRA, M. et LEVAY J. 1994. La paroi au coulis ciment-bentonite de la digue nord de l'aménagement LG-1. Comptes rendus, congrès annuel de la Société canadienne de génie civil, vol. 1, pp. 679-688.

MITCHELL, R.J. et MARKELL, A.R. 1974. Flowsliding in sensitive soils. Canadian geotechnical journal, 11 (1), pp. 11-31.

PARÉ, J.-J. LAROCQUE, G.S. et SCHNEEBERGER, C.E. 1978. Design of earth and rockfill dams for La Grande. Water Power and Dam Construction, 30 (1), pp. 38-45.

SCHNEEBERGER, C.E., LANGLOIS, P., LEVAY, J. et BONCOMPAIN, B. 1991. Closure of LG-1 reservoir across a sensitive clay terrace. Canadian Electrical Association, Hydraulic Power Section, 26 p.

SEBJ. 1991. Dynamique des berges de La Grande Rivière. Caractérisation de l'état de référence (1989) avant l'exploitation des centrales de La Grande 2A et de La Grande 1. Société d'énergie de la Baie James, 45 p.

TECSULT INC. 1991. Complexe La Grande, Projet LG-1 (1986). Rapport de conception, conception des ouvrages, vol. 2a, 184 p.

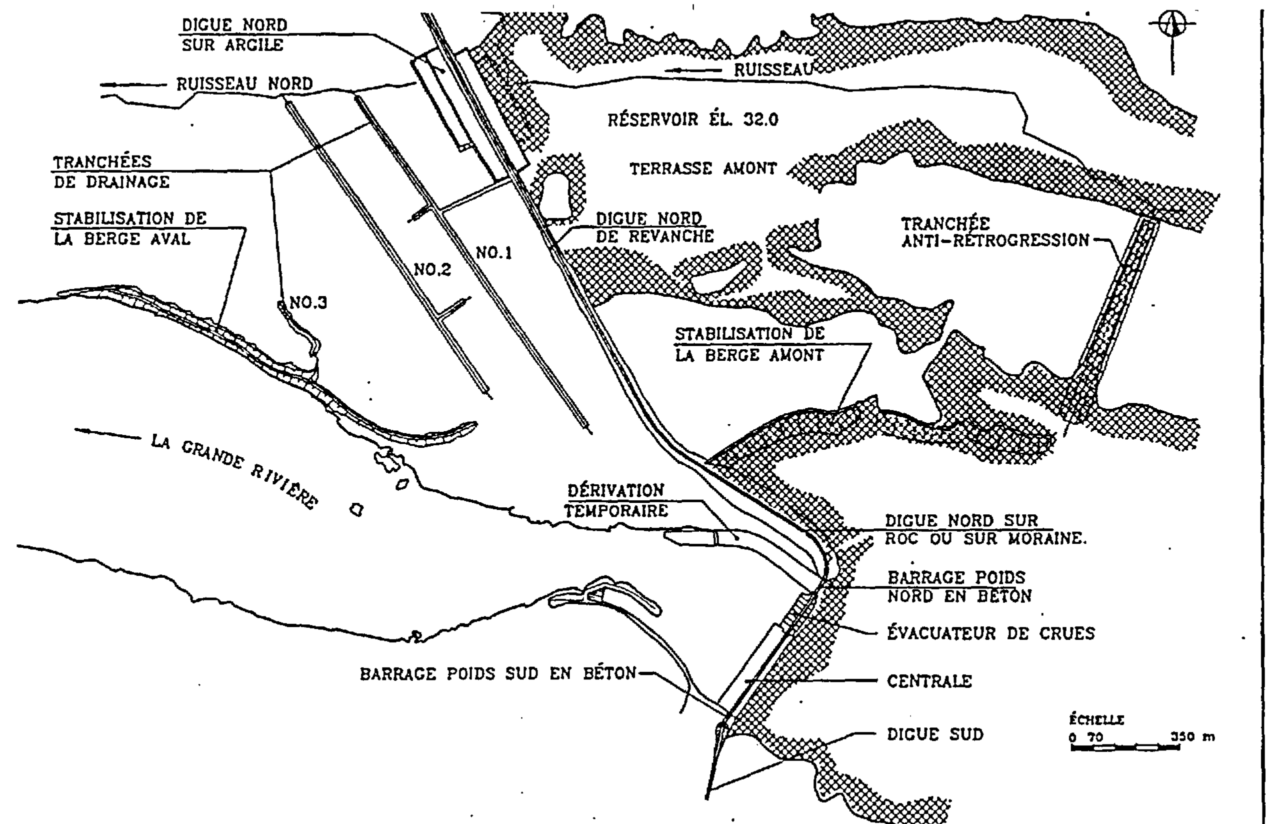

AMÉNAGEMENT GÉNÉRAL DU PROJET LG -1
FIGURE 1

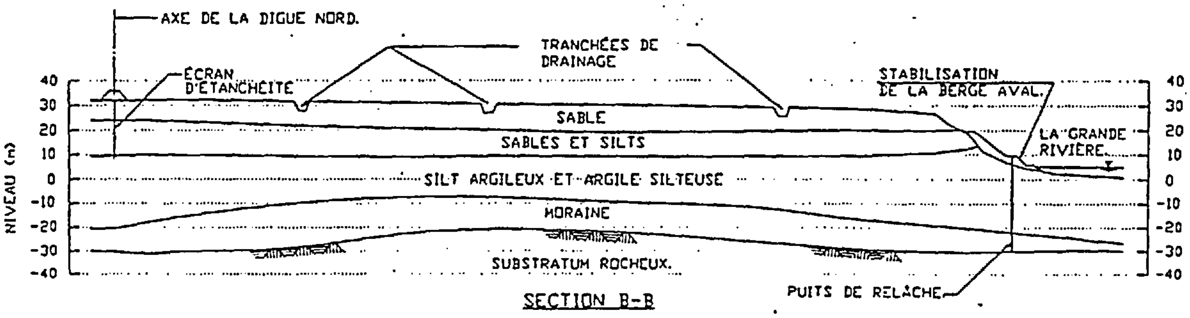

SECTION B-B

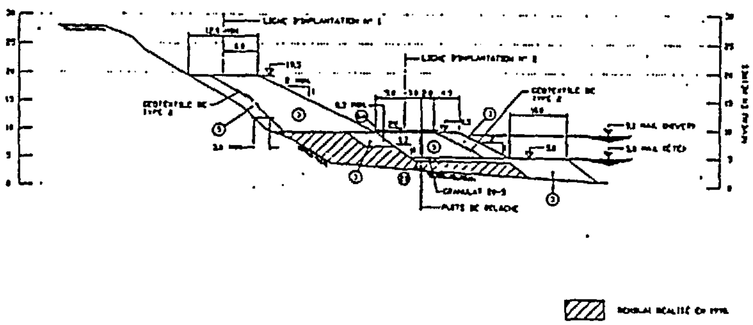

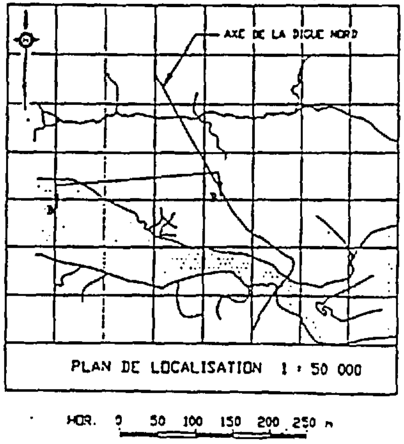

BERGE AVAL - STABILISATION
COUPE TYPE DU PM 132 AU PM 785
FIGURE 2

COUPE STRATIGRAPHIQUE
DE LA TERRASSE AVAL (SECTION B-B)
FIGURE 3

LEGENDE

③ -ENROCHEMENT TOUT-VENANT.

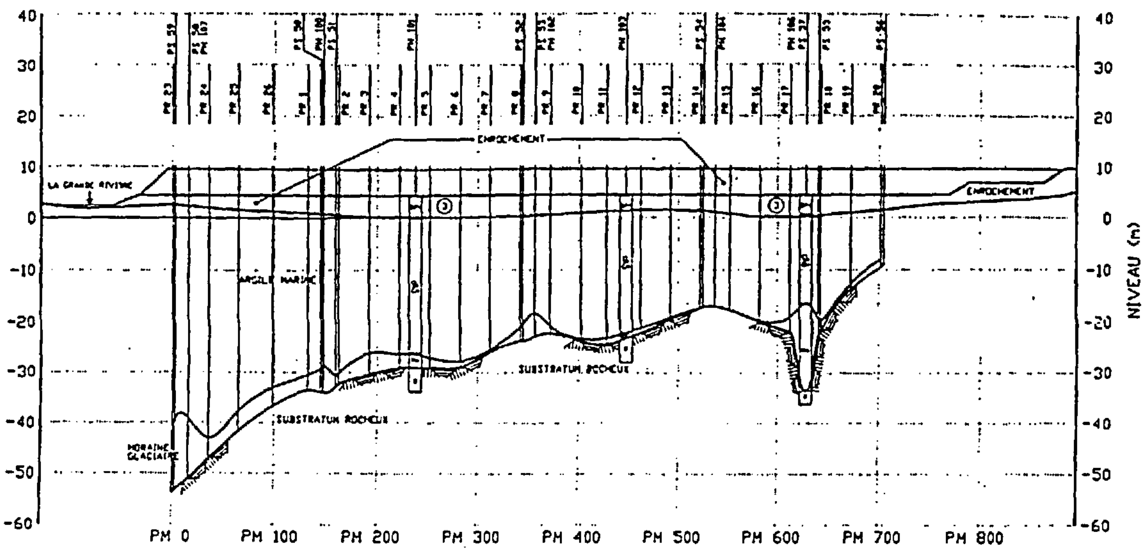

STABILISATION DE LA BERGE AVAL
PUITS DE RELACHE ET INSTRUMENTATION
FIGURE 4

Developments in Geotechnical Aspects of Embankments, Excavations and Buried Structures, Balasubramaniam et al. (eds)
© 1991 Balkema, Rotterdam. ISBN 90 5410 019 2

Mechanically stabilized earth (MSE) and other ground improvement techniques for infrastructure constructions on soft and subsiding ground

D.T.Bergado, C.L.Sampaco, M.C.Alfaro & R.Shivashankar & A.S.Balasubramaniam
Asian Institute of Technology, Bangkok, Thailand

SUMMARY: The presence of thick deposits of soft clay and the effect of ground subsidence due to the excessive pumping of groundwater cause numerous foundation problems to infrastructure constructions in Chao Phraya Plain, Thailand in the form of large subsoil compressions and the associated differential settlements as well as slope instability. To mitigate such natural hazards, several schemes of mechanically stabilized earth (MSE) are proposed for such constructions as underground pipeline, road culverts, road embankments, dikes along irrigation canals, and approach embankments to overpasses and viaducts. The MSE method can be also combined most appropriately with the subsoil improvement using either lime/cement piles, granular piles, or vertical band drains. The combined improvement schemes can increase shear strength, reduce total and differential settlements, and minimize lateral spreading. Moreover, the aforementioned improvement schemes can be a viable alternative to the existing method of using precast, reinforced concrete pile foundation.

1 INTRODUCTION

Most major cities in the Southeast Asian region are located in the coastal plains with thick deposits of soft clays. These deposits are found in most countries of the region (Fig. 1) such as the Chao Phraya Plain in Thailand, Mekong Delta in Cambodia and Vietnam, Malaysian Coastal Plain, Philippine Central Plain, and Indonesian Coastal Plain. Majority of the infrastructure constructions in the coastal plains are road embankments, flood control dikes, landfills, embankments along irrigation canals, underground pipelines, road culverts, etc.

For the usual constructions on soft and subsiding ground, pile foundations are commonly used. This results in more expensive project costs and large differential settlements between pile supported structures and the ground supported structures. As an alternative, mechanically stabilized earth (MSE) using geogrid reinforcements is proposed. This method consists of reinforcing the soil using steel or polymer (plastic) ma-

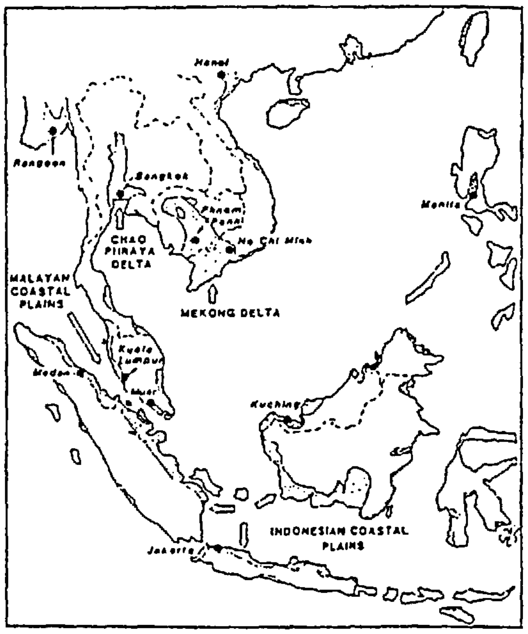

Fig. 1. The distribution of recent clays in Southeast Asia (After Cox, 1970)

erials. The reinforcement which is trong in tension combines with the oil which is strong in compression, orming a very strong and semi-rigid omposite material. The tension in he reinforcement is mobilized by the nteraction between the reinforcement nd the soil in the form of friction r adhesion and bearing resistances. he grid reinforcement usually generates pullout resistance up to 6 times igher than the strip reinforcement Nielsen and Anderson, 1984). Among he grid reinforcement, steel grids re found to be superior than the polymer grid in terms of low extensibiity and higher tensile strengths Fowler et al, 1986). Since the mobiization of the interaction between he soil and reinforcement depends on he relative strains generated in he reinforcement, the steel grid renforcement is preferable. The scheme or this method is shown in Fig. 2.

To obtain the necessary data for nalysis, full scale laboratory and ield load tests as well as laboratoy pullout tests were performed. The est results are presented together ith the modeling and prediction of soil-geogrid interaction including applications of MSE constructions. Part of the data were obtained during the sabbatical leave of the first author at Saga University, Japan. At the later part of this paper, several ground improvement techniques that can be combined with the MSE construction are described and presented.

2 LOAD TESTS ON UNREINFORCED AND REINFORCED GRAVEL

The load test set-up on both unreinforced and reinforced gravel using either double reinforcement or geocell are shown in Fig. 3 (Bergado et al, 1986b). Types 1, 2, and 3 refer to the unreinforced, geocell, and double reinforcements, respectively. The schematic diagrams for Types 4 and 5, which are also shown in Fig. 3, refer to the geocell and double reinforced gravel, respectively, resting on the reconstituted soft clay. The reinforcement consisted of Tensar polymer grids. The gravel specimen has plan dimensions of 150 cm by 150

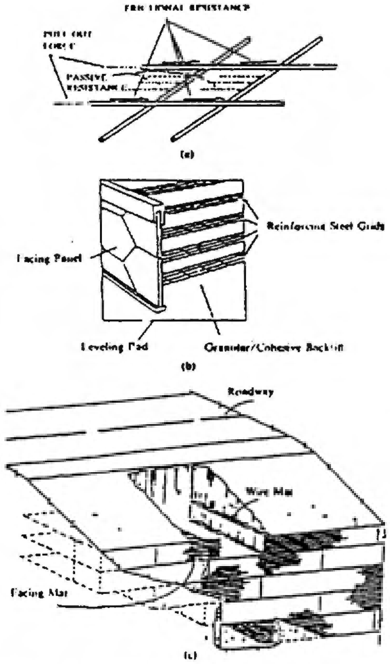

ig. 2. Welded steel bar mesh, steel grids reinforcement with concrete facing and welded wire wall.

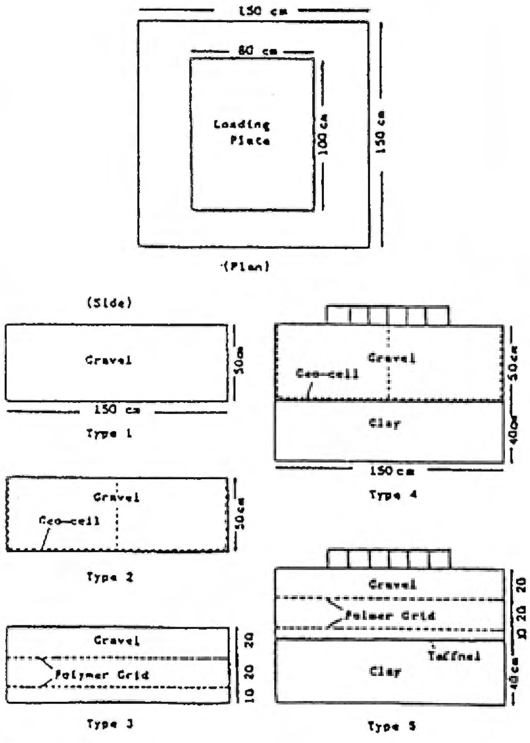

Fig. 3. Load tests on unreinforced and reinforced gravel.

Ca
weight
at 1.
result
ships
and su
with
formed
compact
the co
too la
dimens
gravel
format
mended

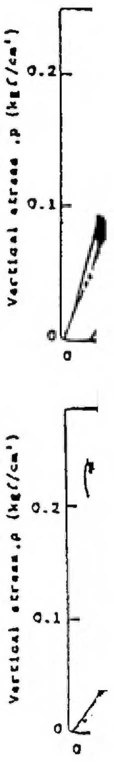

Fig. 4

3 FUL
PIP

The ce
sewage
ground
pile f
Sa) o
with a
nite b

cm and a height of 50 cm. The unit weight of the gravel was maintained at 1.8 t/m^3 as much as possible. The resulting load-settlement relationships from the load tests are plotted and summarized in Fig. 4. The gravel with geocell yielded the largest deformation due to the difficulty of compacting the corner sections. Also, the cell sizes of the geocell maybe too large in relation to its whole dimensions. The double reinforced gravel performed better with less deformation and was subsequently recommended.

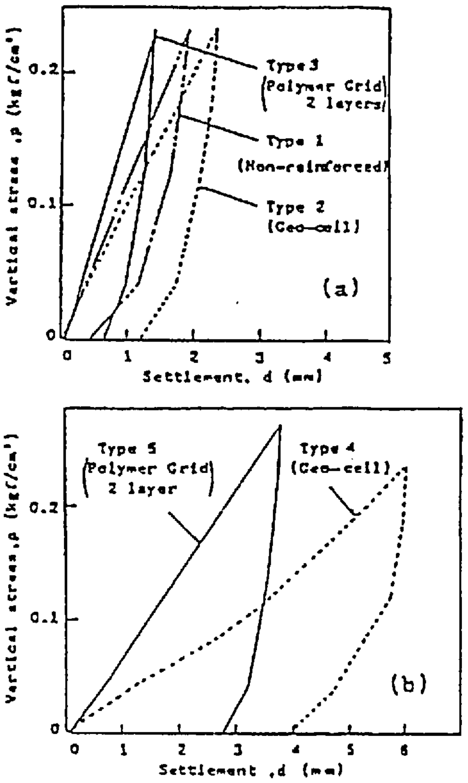

Fig. 4. Load-settlement curves from the load tests.

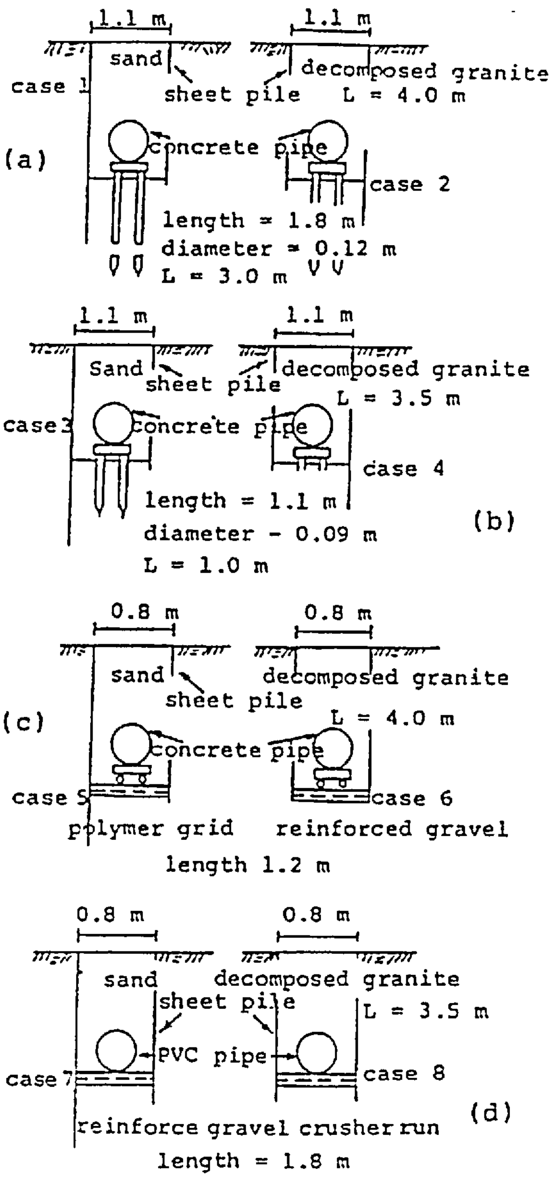

Fig. 5. Sewage pipeline on soft and subsiding ground with reinforced foundations.

3 FULL SCALE TEST ON UNDERGROUND PIPELINE CONSTRUCTION

The usual foundation of underground sewage pipeline on soft and subsiding ground consists of concrete pipe on pile foundations of either long (Fig. 5a) or short (Fig. 5b) dimensions with either sand or decomposed granite backfill (Bergado et al, 1988c). Alternative designs consist of concrete pipes (Fig. 5c) or PVC pipes (Fig. 5d) resting on mechanically stabilized earth (MSE). Full scale field tests were done on cases 1 to 8 as shown in Fig. 5 wherein the movements at the top of the pipeline were monitored. The measured movements as plotted in Fig. 6a indicate the applicability of the mechanically stabilized gravel foundation. The MSE foundation in this case consisted of Tensar polymer geogrids with crusher run gravel backfill. The movements of the more expensive scheme of pile supported pipeline (Figs. 6a and 6b) are not much different from the corresponding amounts using the much cheaper MSE foundation scheme. The field loading tests were done on the soft Ariake clay, Saga City, Japan.

4 PULLOUT TESTS AND APPLICATIONS USING TENSAR AND BAMBOO GEOGRIDS AT AIT

For the internal stability of reinforced soil structures, there are two failure modes, namely: tensile failure of the wires and pullout failure of the reinforcement from the soil. It is necessary to know the pullout resistance of the reinforcement in designing against pullout failure. As pointed out by Ingold (1983), the pullout test is the most realistic model for assessing the performance of low extensibility geogrids.

A type of pullout apparatus was developed at the Asian Institute of Technology (AIT) by Bergado et al (1987) based on the model of Peterson and Anderson (1980). The cell was made of reinforced concrete which was open at the top and front. The cell was approximately 0.8 m wide by 1.0 m long and 0.9 m high with two steel columns fixed on each side as shown in Fig. 7a. The normal pressure was applied by means of hydraulic jack reacting against a steel reaction beam simulating the desired overburden pressure. The reinforcement was clamped by two steel angles and the pullout force was applied by another hydraulic jack reacting against the steel supporting frame which was fixed in front as shown in Fig. 7b.

Both the weathered clay and lateritic soil backfills were compacted inside the pullout cell to 95% of standard proctor density at optimum moisture content with lift thickness of 15 cm. The desired normal pressure was applied and allowed to come to equilibrium for about 10 minutes. The pullout force was applied at a dis-

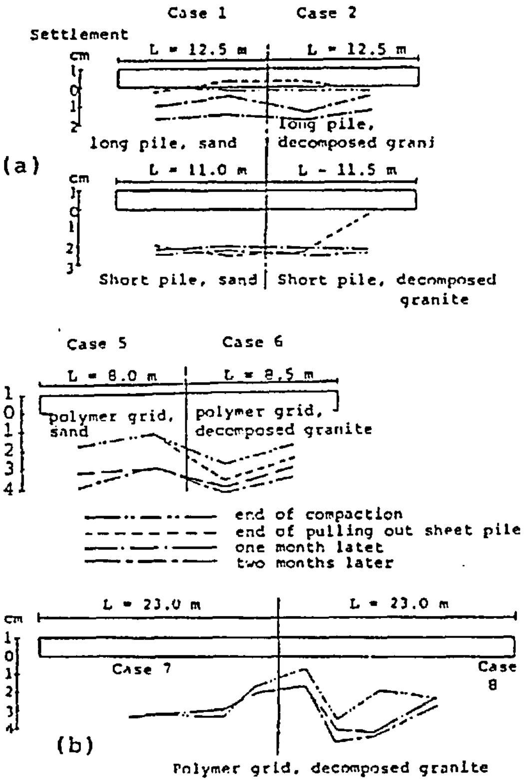

Fig. 6. Settlements of sewage pipeline on reinforced foundations.

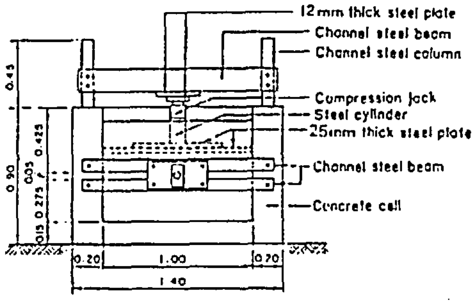

(a) Front view

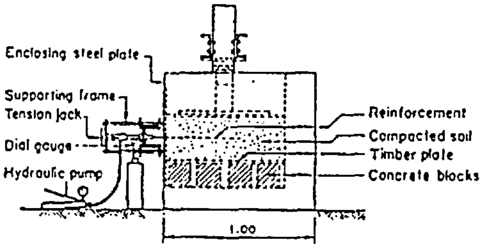

(b) Side view

Fig. 7. The pullout test cell (Dimension in meters).

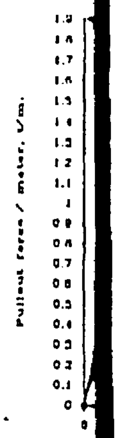

Fig.

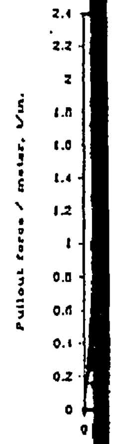

Fig.

place
out f
ments
terva
pulle
The n
10 ts
The
0.46
were
0.60
of 0.
dual
cm by

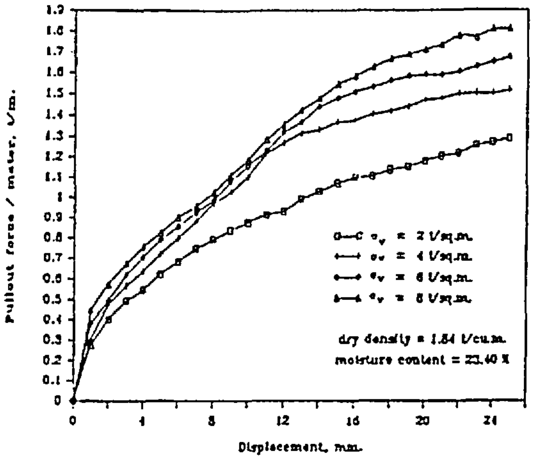

Fig. 8. Force-displacement curves for pullout test no. 3 of Tensar SS2 geogrids with weathered clay backfill.

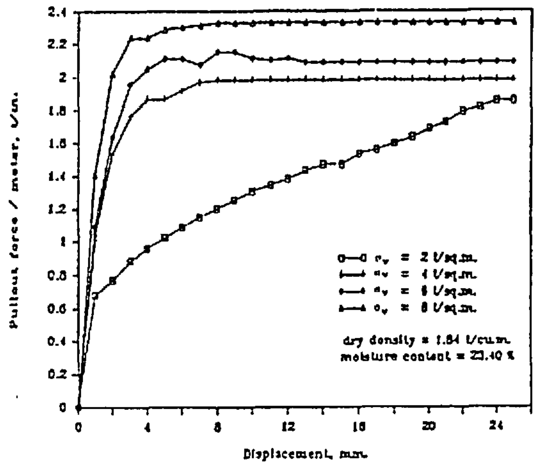

Fig. 9. Force-displacement curves for pullout test no. 1 of bamboo grids with weathered clay backfill.

placement rate of 1 mm/min. The pullout force and horizontal displacements were recorded at one minute interval until the reinforcement was pulled to a displacement of 2.5 cm. The normal pressure ranged from 2 to 10 tsm.

The size of the Tensar geogrids was 0.46 m by 0.46 m. The bamboo grids were having dimensions of 0.275 m by 0.60 m with cross-sectional dimension of 0.5 cm by 1.0 cm for each individual member. The mesh geometry was 10 cm by 15 cm.

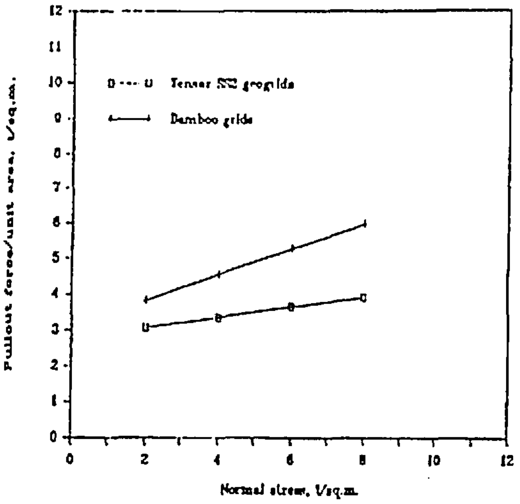

Fig. 10. Comparison of pullout test results for Tensar SS2 geogrids and bamboo grids with clayey sand backfill.

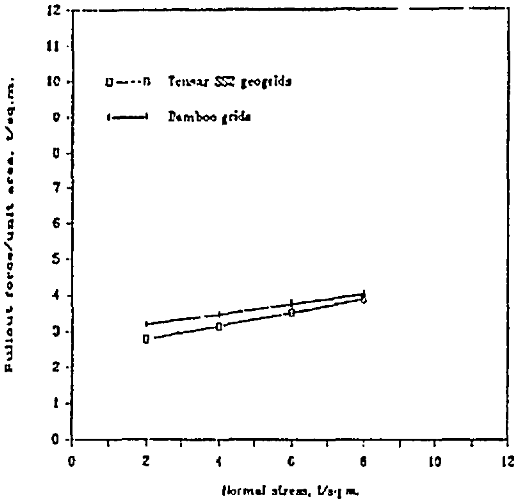

Fig. 11. Comparison of pullout test results for Tensar SS2 geogrids and bamboo grids with weathered clay backfill.

Using bamboo grids, the force-displacement curves had more well-defined peaks than those using Tensar geogrids as shown in Figs. 8 and 9, respectively. Moreover, it was found that the bamboo grids have higher pullout resistance than Tensar SS2 geogrids provided that each has the same plan area as shown in Figs. 10 and 11, for lateritic soil and weathered clay soil, respectively.

The total pullout resistance of the geogrids reinforcement, F_t, can be expressed as:

$$F_t = F_f + F_b \quad . . . . \quad (1)$$

where: F_f is the adhesion resistance of longitudinal member and F_b is the bearing resistance of the transverse member. Bergado et al (1987) derived the following:

$$F_t = (2\mu A_f + mA_bN_c)\ C_u \quad . . . \quad (2)$$

where: μ is the adhesion factor between soil and reinforcement, A_f is the total plan area of the geogrid only, C_u is the undrained cohesive shear strength of the soil as defined by Ingold (1983), m is the total number of the transverse members, N_c is the bearing capacity factor for a strip footing embedded in the soil which is equal to 7.5 (Ingold, 1983), and A_b is the cross-sectional area perpendicular to the direction of pull of the individual members.

The predicted and observed pullout resistance are compared in Figs. 12 and 13 using lateritic soil and weathered clay, respectively. The predicted results agreed well with the experimental results. For the bamboo grids, the predicted pullout resistance with adhesion factor of unity using both soil types, agreed fairly well with the experimental results as shown in Figs. 14 and 15.

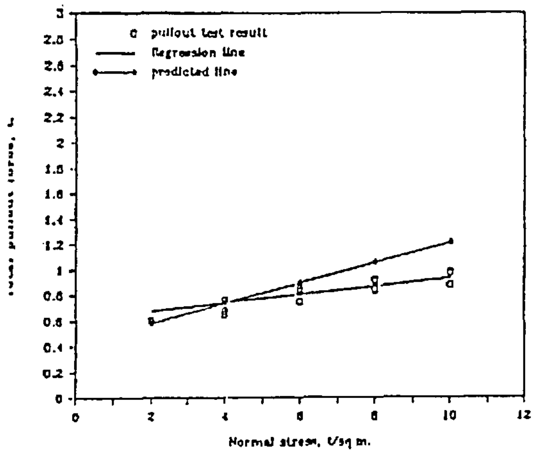

Fig. 12. Comparison of predicted and observed pullout force for Tensar SS2 geogrids with clayey sand backfill.

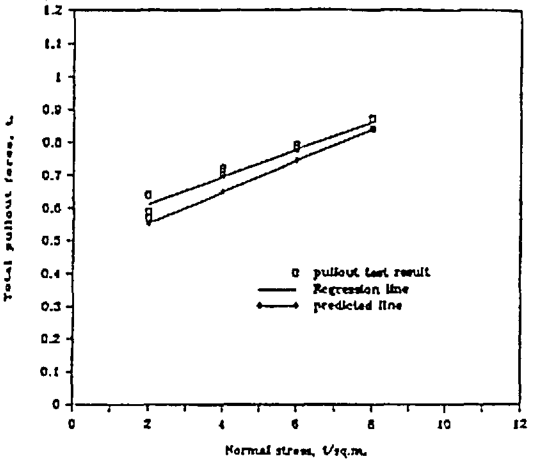

Fig. 13. Comparison of predicted and observed pullout force for Tensar SS2 geogrids with weathered clay backfill.

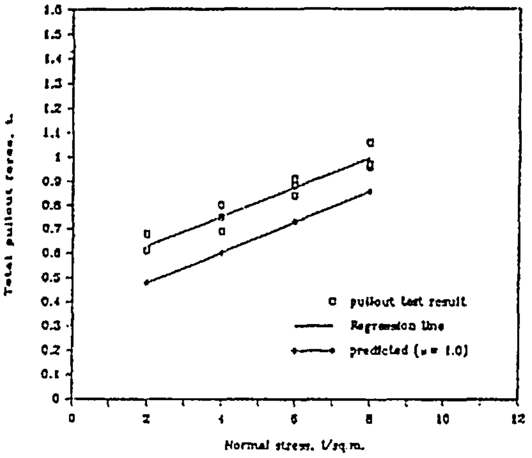

Fig. 14. Comparison of predicted and observed pullout force for bamboo grids tested with lateritic soil (μ = 1.0).

5 REINFORCED CANAL ENBANKMENT, PATHUM THANI, THAILAND

A case study on the application of the aforementioned pullout test results was done in Amphor Nong Sua, Pathumthani Province, Thailand. The infrastructure is a road embankment on the bank of an irrigation canal. The difference of water level in the irrigation canal during the rainy and dry seasons is 2 m. The slip failure occured during low water level as

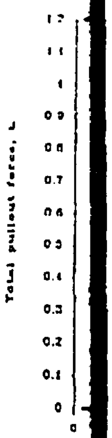

Fig. 1

shown
Depart
emban
forced
design
the r
Tensar
Netlo
mechan
done
soil p
soil p

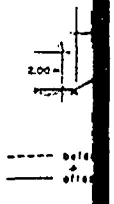

Fig. 1

Fig. 17

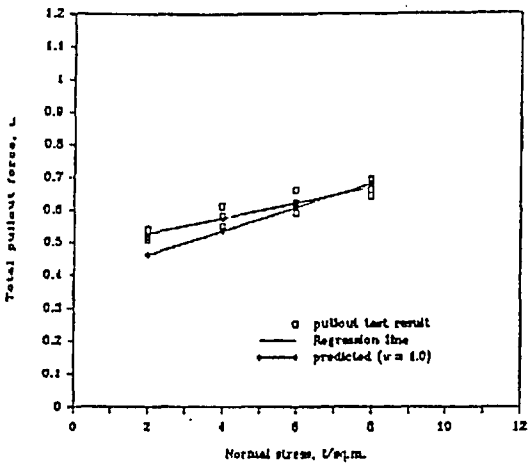

Fig. 15. Comparison of predicted and observed pullout force for bamboo grids tested with weathered clay (μ = 1.0).

shown in Fig. 16. The Public Works Department of Thailand repaired the embankment by using geogrids reinforced soil as shown in Fig. 17. The design of the remedial measures and the reinforcement consisting of Tensar SS2 geogrids were donated by Netlon Ltd. A reanalysis of the mechanical stabilization scheme was done by Bergado et al (1987). The soil profile together with the basic soil properties are shown in Fig. 18.

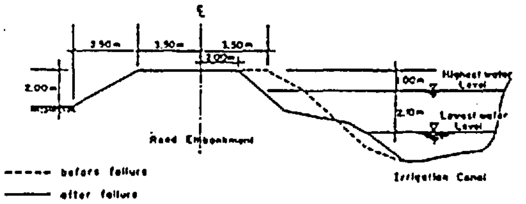

Fig. 16. Geometry of embankment before and after failure.

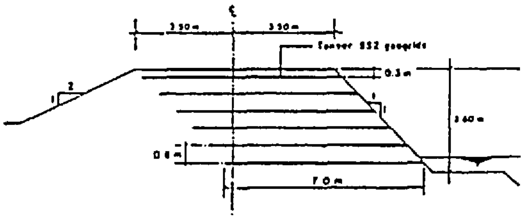

Fig. 17. Tensar SS2 geogrids layout as proposed by Netlon Limited.

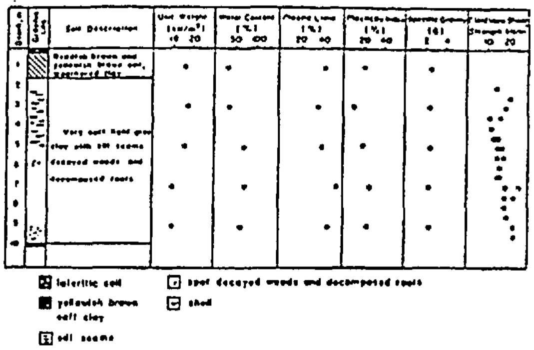

Fig. 18. Soil profile at the site of case study.

The field vane shear strength slightly increased with depth. The total stress analysis was employed in conjunction with the Modified Bishop Method of slope stability analysis at various conditions and the results are tabulated in Table 1.

Table 1. Summary of reanalysis of a case study

	Analysis	*Factor of safety*
Unreinforced embankment (consider tension crack)	slope failure side slope 2:1 (H:V) w/o surcharge	0·98
	slope failure side slope 2:1 (H:V) w/ surcharge	0·69
	slope failure side slope 1:1 (H:V) w/ surcharge	0·69
Reinforced embankment	bearing capacity failure	2·02
	slope failure side slope 1:1 (H:V) w/ surcharge	1·44
	tension failure	2·40
	pull-out failure	8·74

The external stability of the embankment was analyzed by checking the factor of safety against bearing capacity failure and deep slope stability, yielding values of factor of safety of 2.00 and 1.44, respectively. The slope failure analysis was carried out using the method suggested by Jones (1985). For the internal stability, the tensile force in the reinforcement and the pullout resistance were evaluated. The factor of safety against tensile failure was 2.40 and the corresponding value for the pullout resistance was 8.74 as shown in Table 1.

6 PULLOUT TEST USING TENSAR GEOGRIDS AT SAGA UNIVERSITY, SAGA CITY, JAPAN

The apparatus for the pullout test is shown in Fig. 19 which was designed by the first author during his sabbatical in Saga University, Saga, Japan (Bergado et al, 1988c). The size of the geogrid reinforcement was 80 cm by 75 cm. A total of 14 strain gages were bonded to the geogrid in two lines. For the gravel backfill, a total of 4 tests were performed, namely: GM1 with 6 and 8 tsm normal pressure, SR2 with 6 tsm, and SS35 with 6 tsm. For decomposed granite, SS35 was used under vertical stresses of 2, 4, and 6 tsm for a total of 3 tests.

Fig. 19. Pullout test set-up.

When the geogrid is pulled out from the backfill soil, the pullout resistance is mobilized in both grid junction and ribs as shown in Fig. 20a. The pullout resistance on both sides of the geogrid are modelled to be concentrated at the grid junctions as shown in Fig. 20b (Ochiai and Sakai, 1987). The pullout force, F_t, exerted on the polymer grid, produces displacement, X_i, at each grid junction.

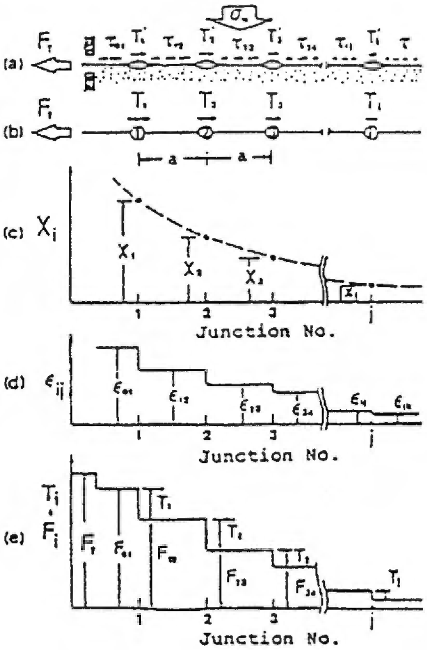

Fig. 20. Analytical procedure of pullout test results.

The displacements of the grid junctions (Fig. 20c) can be measured in the pullout test under constant vertical stress. The strains of the geogrid between junctions can be calculated by:

$$\varepsilon_{ij} = (X_i - X_j)/a \quad . \ . \ . \ . \ . \ . \ (3)$$

where a is the distance between grid junctions. Figure 20d shows the strain plots. The axial force between grid junctions that cor-respond to the strain, ε_{ij}, is determined using the standard stress-strain curves of the geogrids provided by Netlon (1984). The plot of the axial force $(F_i - F_{i+1})$ represents the pullout resistance, T_i, mobilized at each grid junction. The shear stiffness, k_s, can be obtained from the plot of T_i versus displacement, u, by the following equation:

$$2\tau = 2k_s u \quad . \ . \ . \ . \ . \ . \ . \ . \ . \ . \ (4)$$

where τ is the shear resistance.

The pullout force, F_t, for gravel backfill with Tensar GM1 reinforcement was plotted against strain. Figure 21 shows the strain plots under normal stress of 6 tsm at

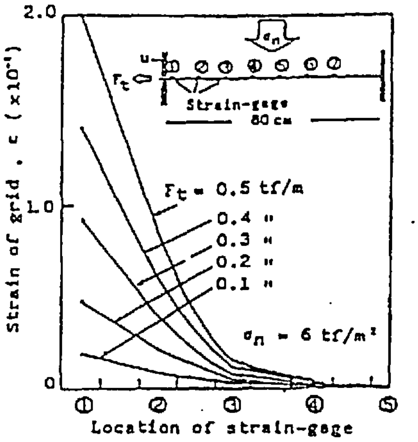

Fig. 21. Typical strain plots from pullout test.

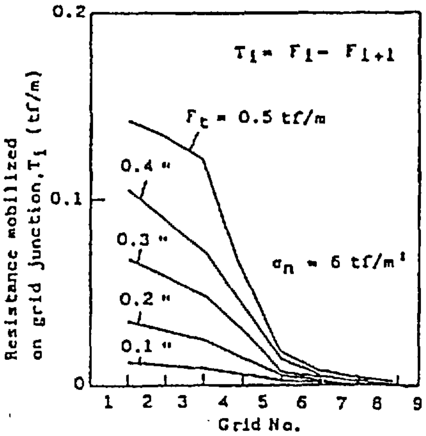

Fig. 22. Typical pullout resistance mobilized on grid junctions.

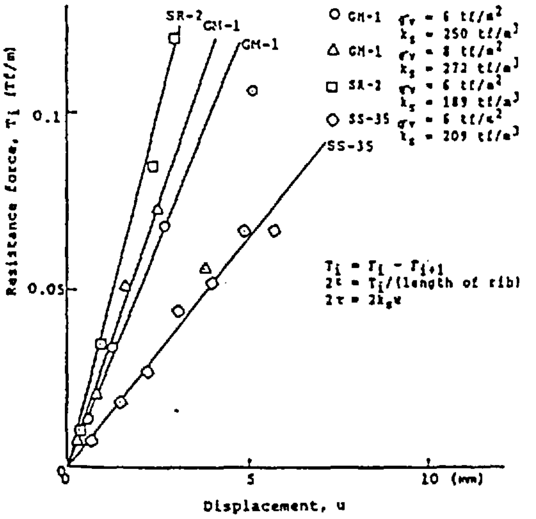

Fig. 23. Shear stiffness for gravel backfill.

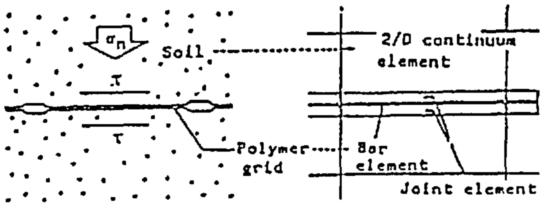

Fig. 24. FEM model of reinforced soil.

different pullout force, F_t. The calculated pullout resistance, T_i, is plotted in Fig. 22 and the shear stiffness, k_s, derived from the pullout resistance is plotted in Fig. 23 versus displacements for GM1, SR2, and SS35. The k_s value obtained for SR2 was the highest followed by GM1 and SS35. The above process demonstrated the calculation of k_s.

Figure 24 shows the finite element model of the reinforced soil (Ochiai et al, 1988). The geogrid is transformed into a joint element on both sides representing the interface with the soil and a truss element in the middle transmitting axial force only. The joint element expresses the transmission of the compressive force and sliding against shear displacement. The relationship between shear displacement $\{u\}_{s,n}$ of the joint element (length=ℓ) and the incremental loading $\{F\}_{s,n}$ is given in the following expression:

$$\{F\}_{s,n} = [K]_{s,n} \{u\}_{s,n} \quad . \; . \; . \quad (5)$$

where the stiffness matrix $[K]_{s,n}$ is expressed by

$$[K]_{s,n} = 1/4\ell \begin{bmatrix} k_s & 0 & k_s & 0 & -k_s & 0 & -k_s & 0 \\ & 2k_s & 0 & 0 & 0 & 0 & 0 & -2k_n \\ & & k_s & 0 & -k_s & 0 & -k_s & 0 \\ & & & 2k_n & 0 & -2k_n & 0 & 0 \\ & & & & k_s & 0 & k_s & 0 \\ & & (sym) & & & 2k_n & 0 & 0 \\ & & & & & & k_s & 0 \\ & & & & & & & 2k_n \end{bmatrix} \quad (6)$$

The joint element has two unit stiffness, a normal stiffness, k_n, and a shear stiffness, k_s. The shear stiffness can be determined from the results of the laboratory pullout test.

7 REINFORCED GRAVEL FOUNDATION FOR CULVERT CONSTRUCTION, JAPAN

A project of Japan Ministry of Construction consisted of a box culvert construction along the road crossing a canal in Saga Plain, Kyushu Island, Japan. The culvert structure is founded on a 15 m thick, soft and compressible Ariake clay on subsiding ground. Ordinarily, pile foundation is used in this type of construction. However, in this study, it was recommended to use the cheaper reinforced gravel foundation using two layers of Tensar GM1 geogrids (Fig. 25) so that the differential settlements will be minimized. The FEM model described earlier was used for the analysis. The parameters used are tabulated in Table 2. As shown in Fig. 25, the double reinforced gravel foundation has a thickness of 50 cm whose bottom is located 2.75 m below the ground level (line A-A in Fig. 25).

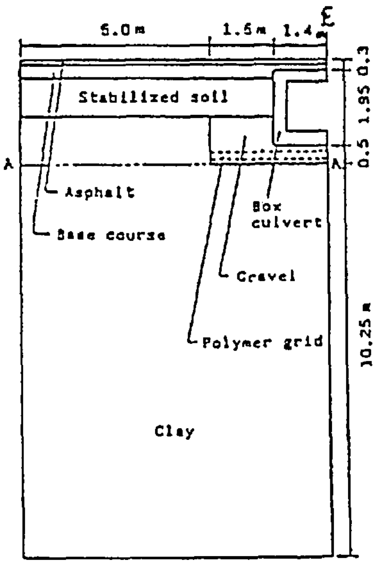

Fig. 25. Box culvert construction with reinforced gravel foundation on soft Araike clay.

Table 2. Parameters used in the FEM analysis

	E(t/m')	ν	γ(t/m')
Asphalt	2.0x10'	0.30	2.3
Base course	1.75x10'	0.43	1.8
Stabilized soil	1.0x10'	0.40	1.8
Gravel	1.5x10'	0.43	0.8
Cloy	3.0x10'	0.45	0.6
Culvert	3.0x10'	0.17	2.5
	k_s(t/m')	k_n(t/m')	
Joint element	2.50x10'	1.0x10'	
	E(t/m')	A(m')	
Bar element	1.8x10'	1.3x10⁻'	

The results of the FEM analysis are plotted in Figs. 26 and 27 whose reference is line A-A of Fig. 25. The settlements resulting from the body force plus external force are shown in Fig. 26 for both unreinforced and reinforced cases at a uniform load of 6 tsm. The reinforced case yielded less differential settlements. A different scheme was used in Fig. 27 wherein the culvert was excluded from the external force application. The settlements with reference to line A-A (Fig. 25) resulting from external loads only as shown in Fig. 27 indicate less differential settlements in the mechanically stabilized case.

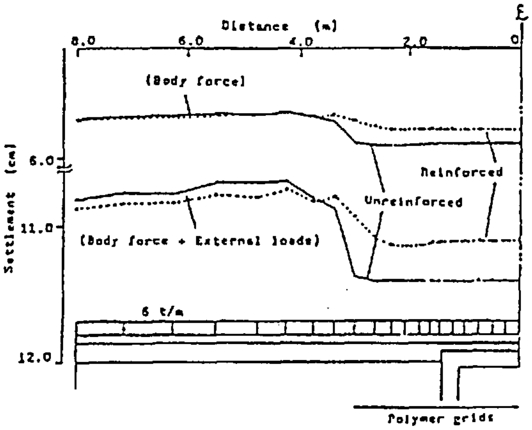

Fig. 26. Settlements at line A-A under uniform loading.

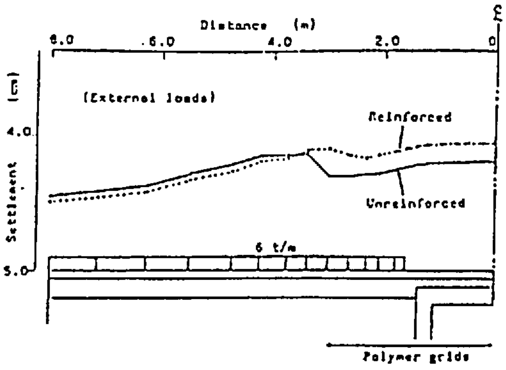

Fig. 27. Settlements at line A-A without load in the box culvert.

8 PULLOUT TESTS AND APPLICATIONS OF WELDED WIRE MECHANICALLY STABILIZED EARTH

Welded wire steel grids generate frictional resistance in its longitudinal member and passive resistance in front of the trans-verse member. Chang et al. (1977) was the first to report that the pullout resistance of the welded wire grid was approximately six times greater than for strip reinforcements. In this study, the pullout tests were conducted using a 50"x30"x20" (LxWxH) test cell designed and manufactured at the Asian Institute of Technology (Bergado et al, 1989). The schematic diagram of the pullout apparatus is shown in Fig. 28. The vertical stress was supplied by air bags sandwiched between flexible, 1/4" thick metal plates. The pullout force, measured by means of an electrical load cell, was applied by means of an electrically-controlled hydraulic cylinder with a maximum capacity of 50,000 lbs (22,730 kg). The horizontal displacement of the mat was monitored using a linear variable differential transformer (LVDT) and the pulling rate was 1 mm/min. The data acquisition system consisting of the 21X micrologger recorded both the mat displacement and the axial strains in the longitudinal and transverse members through bonded electrical resistant strain gages. A typical instrumented mat used in the pullout tests is shown in Fig. 29. The reinforcement used were fabricated locally using the readily available mild steel bars. Tensile strength tests conducted axially on these bars indicate the occurrence of yield stresses at low strains in the order of 0.4 to 0.5%. A modulus of elasticity of 194,737 MPa was calculated corresponding to 0.70 of the yield strength. The backfill materials consist of weathered Bangkok clay and lateritic residual soil whose properties are tabulated in Table 3. The backfill materials were compacted at 95% standard Proctor densities at both dry and wet sides of optimum.

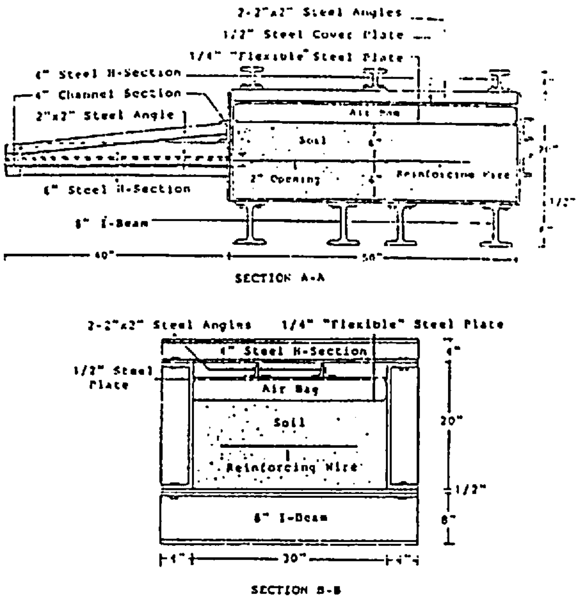

Fig. 28. Different views of the pull-out testing cell along the longitudinal (section A-A) and transverse (section B-B) directions.

Typical stress-strain relationships for dry and wet side compactions are shown in Figs. 30 and 31, respectively. It can be observed that the pullout strength in the wet side compaction is very much lower compared to the dry side. The plots of strain with distance from the facing are typically shown in Figs. 32 and 33 for the dry and wet side compactions, respectively. The results indicate linear variation of strains along the longitudinal members ranging from 0.01% to 0.2%. The levels of strains reduced when the backfill compaction varies from dry side to wet side of optimum. The dry side exhibited steeper slope of strain variation with distance.

Table 3. Summary of basic soil properties

soil Description	Gs	Wp (%)	Wl (%)	Ip (%)	% Passing No.200	γd max (t/m³)	Wopt (%)	Direct Shear Test				UU Triaxial Test (95%)	
								Dry Side (95%)		Wet Side (95%)		c (t/m²)	ϕ (degree)
								c (t/m²)	ϕ (degree)	c (t/m²)	ϕ (degree)		
Redish Gray Weathered Clay (CL)	2.67	21	45	24	83	1.60	23.3	8.3	32.2	7.3	16.5	11.80	31.5
Lateritic Residual Soil (GC)	2.61	39	23	16	18	1.93	11.5	3.54* (8.30)#	56.83* (40.20)#	1.43*	47.47*	8.0	32.5

* Low Normal Pressure (0.2 to 1.8 t/m²) # High Normal Pressure (1 to 13 t/m²)

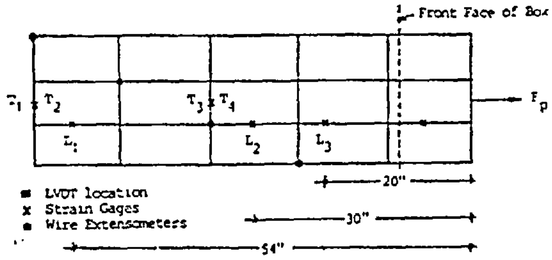

Fig. 29. Typical schematic diagram of an instrumented mat.

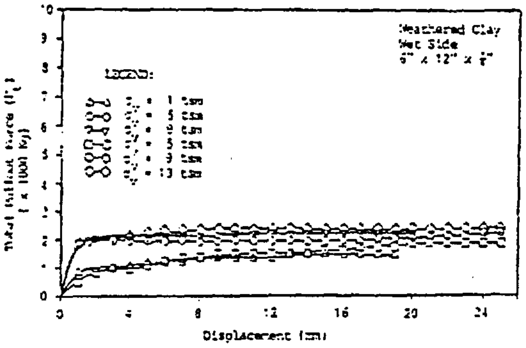

Fig. 31. Typical load-displacement curve for weathered clay compacted at the wet side of optimum.

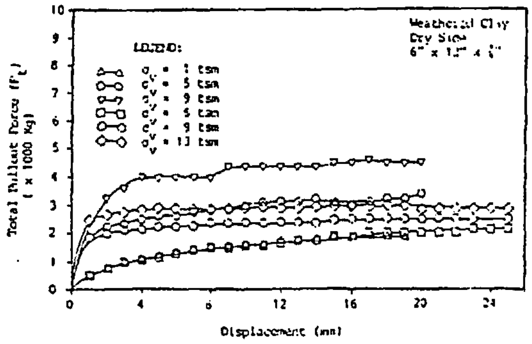

Fig. 30. Typical load-displacement curve for weathered clay compacted at the dry side of optimum.

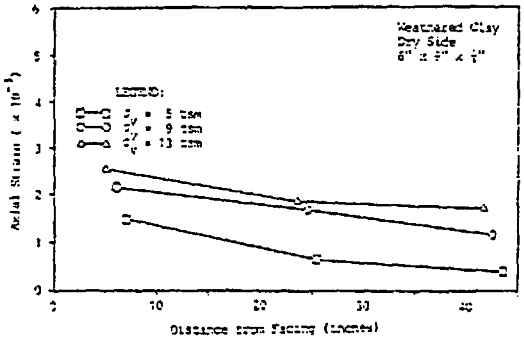

Fig. 32. Variation of axial strain with distance from the facing for weathered clay compacted at the dry side of optimum.

Having stronger soil, the dry side compaction generated higher strains in the reinforcements and lower mat displacements than in the wet side compaction.

Peterson and Anderson (1980) proposed that there is frictional or adhesion resistance at the longitudinal member and bearing resistance in front of the transverse members. The passive resistance generated is similar to that of a strip footing rotated to the horizontal direction (Fig. 34a). The frictional or adhesion resistance, F_f, is taken as:

$$F_f = 2\mu\sigma_v A_f \quad . \ . \ . \ . \ . \ . \ . \quad (7)$$

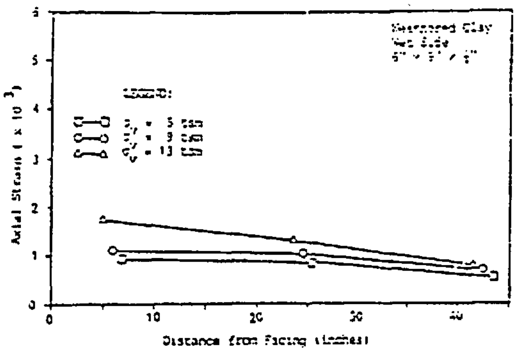

Fig. 33. Variation of axial strain with distance from the facing for weathered clay compacted at the wet side of optimum.

where µ is the adhesion factor between the soil and reinforcement, and A_f is the total surface area of the longitudinal member outside the failure plane. The bearing resistance, F_b, was derived by Peterson and Anderson (1980) as follows:

$$F_b/(Nwd) = cN_c + \sigma_v N_q \quad . . . . (8)$$

where N is the number of transverse wires, w is the width of the reinforcing mats, d is the diameter of the wire and N_c and N_q are Terzaghi's bearing capacity factors.

Jewell et al (1984) suggested to base the failure mechanism for low strains to failure mechanism associated with punching failure mode in the soil as shown in Fig. 34b. Rowe and Davis (1982) have studied the bearing stresses on vertical surfaces loaded horizontally for the case of anchor plates embedded in the soil using elasto-plastic finite element analysis. The bearing stress of the soil on grid members is assumed to be similar to the base pressure on deep foundations. For cohesive-frictional soil, the equation derived by Rowe and Davis (1982) can be expressed as:

$$F_b/(Nwd) = C_u F_c{}' + hF_\gamma{}' \quad . . . (9)$$

where C_u is the soil adhesion which is computed to include the effect of surcharge, $F_c{}'$ is the factor to account for the effect of cohesion on anchor behaviour, and $F_\gamma{}'$ is the factor for the effect of soil weight.

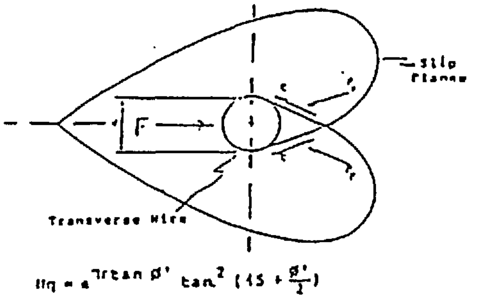

(a) Bearing Capacity Failure Mode
(after Peterson & Anderson 1980)

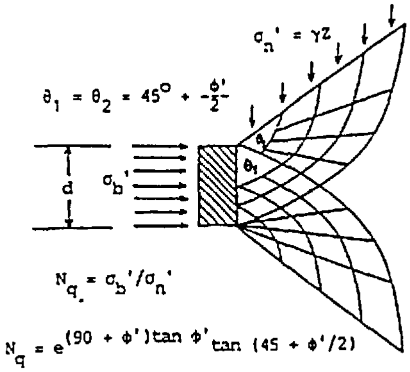

(b) Punching Failure Mode
(after Jewell et al 1984)

Fig. 34. Failure mechanisms with respective expressions for N_q.

The prediction of passive resistance of the transverse members proposed by Peterson and Anderson (1980) seemed to overestimate in the dry side compaction (Fig. 35). The model, however, yielded good agreement with the experimental results for the wet

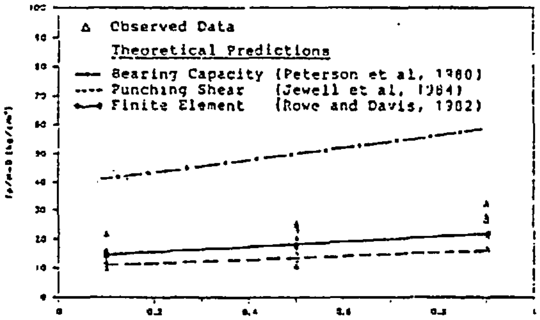

Fig. 35. Experimental vs. theoretical passive resistance of transverse members for weathered clay compacted at the dry side of optimum.

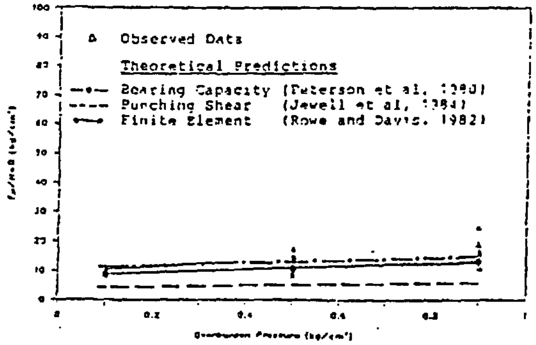

Fig. 36. Experimental vs. theoretical passive resistance of transverse members for weathered clay compacted at the wet side of optimum.

side compaction (Fig. 36). The closer prediction in the wet side compaction reflected the full mobilization of the passive resistance due to larger mat displacements during the pullout test. It was also observed that full mobilization of passive resistance occurred for smaller diameter bars. The punching failure mode proposed by Jewell et al (1984), which can develop for smaller mat displacements, seems to closely predict the actual behaviour of the soil-grid interaction in the dry side compaction (Fig. 35). The model slightly underestimated the passive resistance in the wet side compaction (Fig. 36). The prediction using finite elements according to Rowe and Davis (1982) seems to yield the best agreement for both dry side and wet side compactions (see Figs. 35 and 36).

A welded wire mechanically stabilized earth (MSE) embankment was constructed inside the campus of the Asian Institute of Technology in conjunction with the USAID Research Project. The experimental embankment was divided into three sections, each about 16 ft long (4.88 m), and utilizing three different backfill materials, namely: clayey sand, lateritic soil, and weathered clay (Fig. 37). The parts of the welded wire wall reinforcements are shown in Fig. 38. It consisted of a vertical welded wire MSE wall facing on one side and a sloping unreinforced wall in the opposite side as shown in Fig. 39. A minimum of about 7 instrumented layers for each backfill soil types were provided. The reinforcement mats consisted of W4.5 x W3.5 wires with 6"x9" grid openings and were instrumented with strain gages at various locations as shown in Fig. 39. Each reinforcement units has dimension of 8' wide and 18'9" long. A schematic layout of the typical instrumentation of the test embankment is shown in Fig. 40.

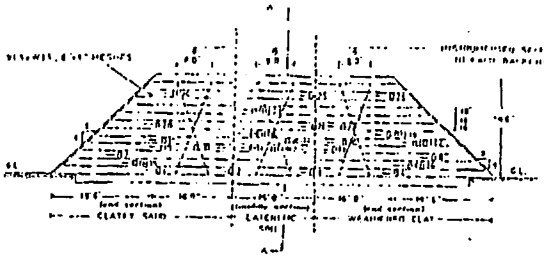

Fig. 37. Front section of the welded wire wall.

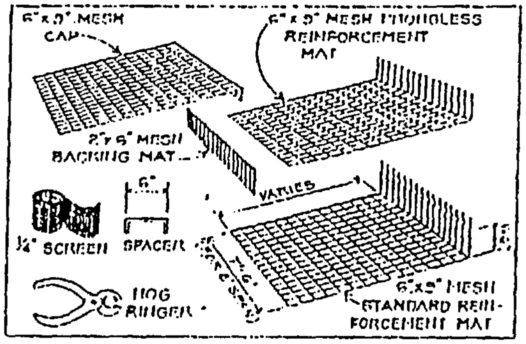

Fig. 38. Accessories used for the construction of welded wire wall (after Hilfiker Co., 1988).

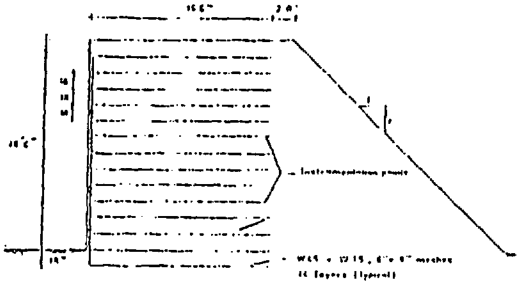

Fig. 39. View of welded wire wall along section A-A showing the instrumented welded wire mat layers.

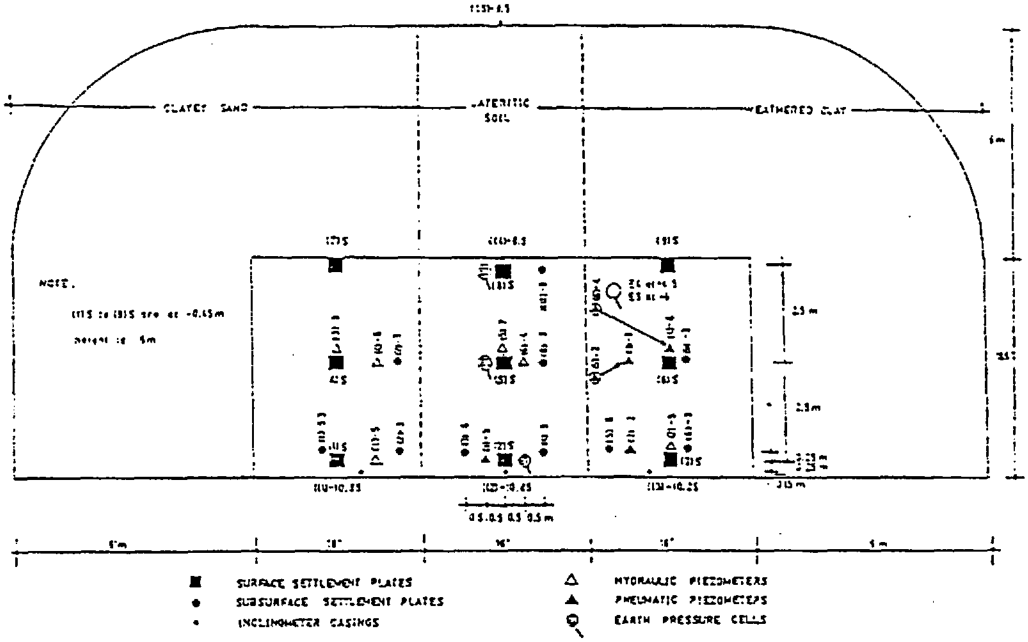

Fig. 40.

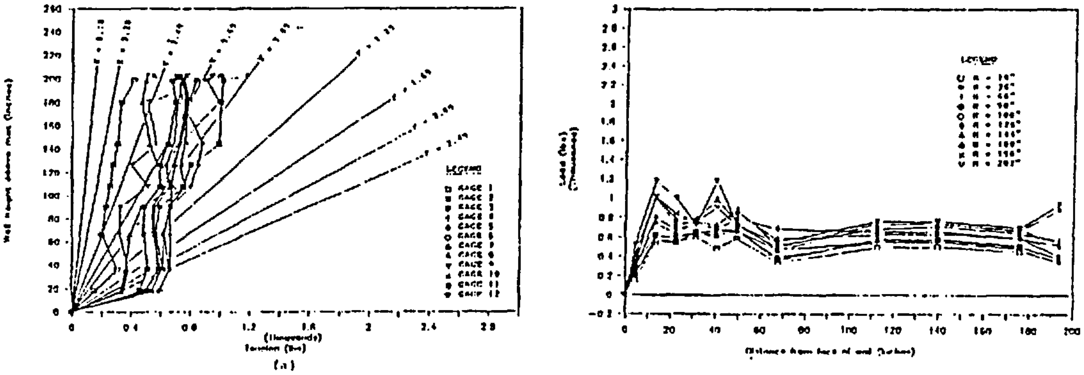

Fig. 41. (a) Plot of tension against wall height above mat for weathered clay (Mat No. 2).

(b) Plot of tension against distance from the face of the wall for weathered clay (Mat No. 2).

From the measured strains, the tension in the wire can be computed, given the modulus of elasticity of steel, and the cross-sectional area of the wire. The computed tensions are plotted for each mat as typically shown in Fig. 41 for the weathered clay backfill in relation to embankment height and distance from the face.

Lateral movements of the subsoil and the embankment were measured using a Digitilt inclinometer. Three of these (I1 to I3) were installed vertically near the face. Two others were installed in the opposite side (Fig. 40). The plots of the lateral movements are given for inclinometer I2 in Fig. 42. The maximum lateral movement in the subsoil occurred at 3.0 m depth, the weakest part. After 29 days since the end of construction, the lateral movements ranged from 110 to 120 mm. The lateral move-

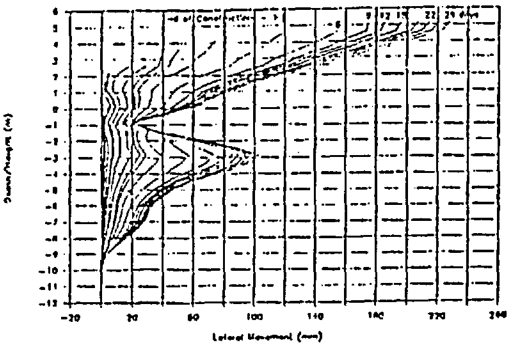

Fig. 42. Plots of depth/height against lateral movement for inclinometer no. 2

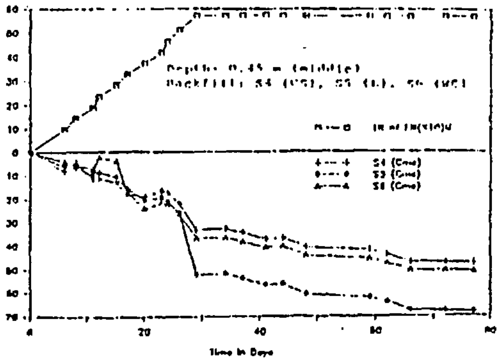

Fig. 44. Observed surface settlements at the center of each section of the wall (S4 to S6).

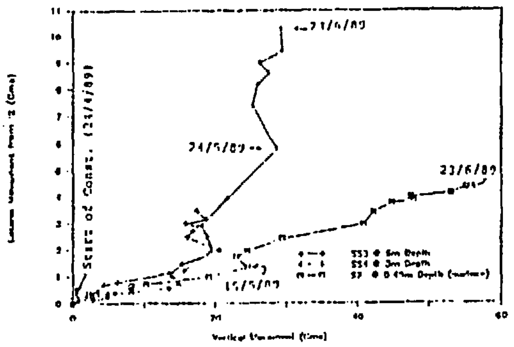

Fig. 43. Lateral movement plotted against the vertical movement of wall (inclinometer no. 2).

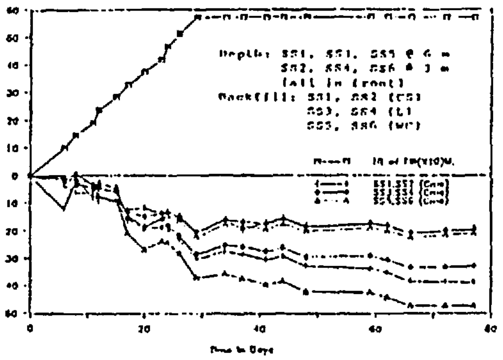

Fig. 45. Observed subsurface settlements of the soft clay foundation (SS1 to SS6).

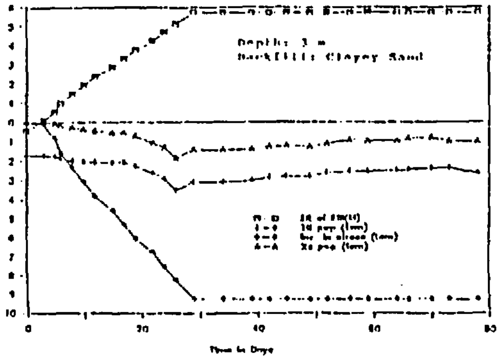

Fig. 46. Measured excess porewater pressure developed in the soft clay foundation (hydraulic piezometer no. 3).

ment plotted against vertical settlements is shown in Fig. 43. This indicates that the soft clay subsoil is being squeezed out from beneath the embankment, simultaneously with the dissipation of excess pore pressures.

Settlements were measured by levelling survey with reference to a benchmark. The surface settlements at the front near the face have been more or less identical. However, the observed maximum surface settlement occurred at the very center (S5) as plotted in Fig. 44 and the shape of the settlement surface is somewhat like a bowl shape. The subsurface settlements are plotted in Fig. 45.

Pneumatic and hydraulic piezometers were used to measure excess pore pressures. These piezometers were installed at different locations (Fig. 40). The excess pore water pressure decreased at a very slow rate immediately after the end of construction (Figs. 46 and 47). The dissipation of excess pore pressure

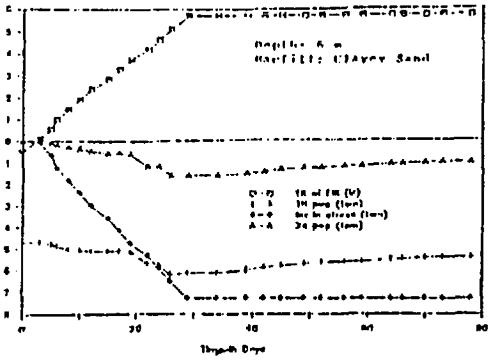

Fig. 47. Measured excess porewater pressure developed in the soft clay foundation (hydraulic piezometer no. 4).

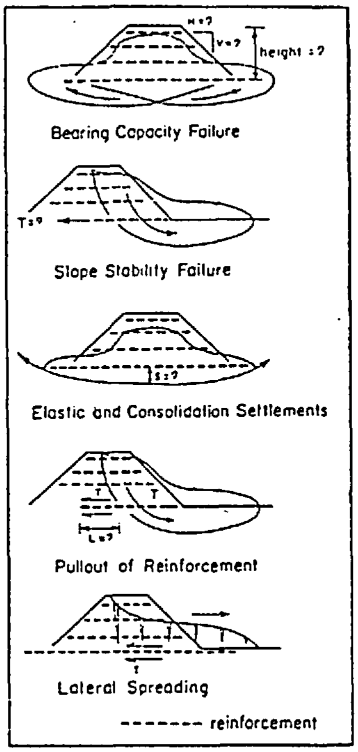

Fig. 48. Design of mechanically stabilized embankment on soft ground.

indicated the occurrence of the process of consolidation. Also shown in these figures were the increase in vertical stress as calculated by the method of Poulos and Davis (1974). In all cases, the excess pore pressures were found to be far below the surcharge load. The excess pore pressures were also affected by the seasonal fluctuation of the groundwater level.

To determine the vertical pressure distribution along the base of the wall, SINCO pneumatic total earth pressure cells were installed along the centerline of the embankments perpendicular to the wall face beneath the lateritic soil backfill. The cell was 9 inch in diameter and 0.434 inch thick, made of stainless steel. The vertical pressure distribution as observed from the three cells in the front (E1), middle (E2), and back (E3) during the embankment construction varied according to the changes in the loads during the different stages of construction.

9 ADVANTAGES OF MSE CONSTRUCTION ON SOFT GROUND

As stated previously, the main foundation problem in coastal plain areas is the presence of thick, soft clay deposits which is very weak and compressible material. Associated with the low strength of the subsoil is the problem of low bearing capacity and slope instability. To solve these problems, the conventional approach is to use very gentle slope of 3H to 1V. Moreover, the embankments cannot be constructed very high because of slope instability or sliding problems (see Fig. 48). Mechanical stabilization by reinforcing the embankment will allow steeper slope of 1H to 1V which entails less volume of fill and savings in material costs as well as construction of higher embankments. Due to the compressible clay foundation, earth structures on soft clays such as road embankments can be subjected to large settlements to as much as 2 m in 10 years. These settlements are caused by compression of the soft clay due to the imposed loads of the embankments as well as the ground subsidence due to pumping of groundwater. Since the embankments cannot be constructed very high because of stability problems, costly reconstruction is needed to raise the embankments above maximum flood level after 10 years. Utilizing reinforced earth embankment, the stability will be improved. Thus, higher embankments can be constructed extending the design life of earth structures to as much as 30 years. Another problem occurring on earth structures resting on soft clay foundation such as road embankments is the phenomenon of lateral spreading of the embankment that will contribute to large total differential settlements (Fig. 49). This problem can be prevented by utilizing reinforced earth construction. Furthermore, reinforced earth construction can tolerate differential movements common in areas of subsiding ground. Reinforced earthfills will function as a stiff raft floating over compressible stratum with the reinforcements providing tensile strength to the earthfills. This method of construction also redistributes the load to become more uniform, thereby, reducing differential settlements. Thus, reinforced earthfill can also form as an alternative foundation for residential houses, industrial buildings, oil storage tanks, and other lightly-loaded structures. The present state-of-practice utilizes precast, reinforced concrete pile foundation which can create differential movements between the pile supported structures and the surrounding soil due to the consolidation or compression of the clay and ground subsidence.

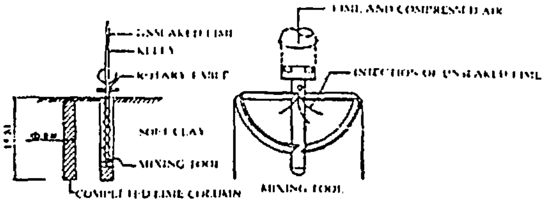

(A) LIME-CEMENT PILE INSTALLATION BY SWEDISH METHOD

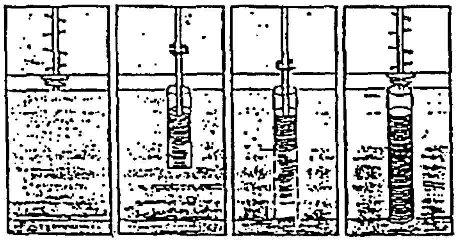

(B) LIME/CEMENT PILE INSTALLATION BY JAPANESE METHOD

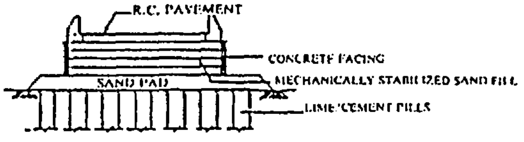

(C) TYPICAL COMBINATIONS

Fig. 49. Installation of lime/cement piles.

10 IN-SITU GROUND IMPROVEMENT TECHNIQUES

The MSE constructions can be effectively combined with other in-situ underground improvement techniques for maximum efficiency. Several below ground improvements have been studied, namely: lime/cement piles, granular piles, and vertical drains and are described below.

Lime/cement piles operate on the principle that the calcium ions in both lime and cement react with the clay through the processes of ion exchange and flocculation as well as pozzolanic reaction. The divalent calcium ions replace the monovalent sodium and hydrogen ions in the double layer surrounding each clay mineral. Thus, fewer number of divalent calcium ions is needed to neutralize the net negative charge of each clay minerals reducing the size of the double layer and increasing the attraction of the clay particles leading to flocculated soil structure. Furthermore, the silica and alumina in the clay react with the lime, forming such cementing agents such as calcium silicates and calcium aluminate hydrates in a process called pozzolanic reaction. The organic content of the soft Bangkok clay seemed to vary from 2 to 5% with occasional value of 9 % while the salt contents can be as much as 0.5 to 2 % (5 to 20 g/ℓ). The results of the testing program at the Asian Institute of Technology have found that adding 5 to 10 % of quicklime is the optimum mix proportion (Balasubramaniam et al, 1988). The addition of quicklime increased the unconfined compressive strength to about 5 times as much and increased the preconsolidation pressure by 3 times as much. The coefficient of consolidation also increased by 10 to 40 times and the effective strength parameters also in-creased, especially the angle of internal friction from 24° to 40°. Moreover, it was found from actual experiments that the admixtures in the clay did not diffuse into the surrounding soil and thus, preventing pollution of the ground. Mixing 10% cement with the soft Bangkok clay increased the unconfined compressive strength up to 10 times and increased the preconsolidation pressures by 2 to 4 times as much. An increase in the coefficient of consolidation by about 10 to 40 times was also observed (Law, 1989). Usually, cement is more effective than lime when the organic content in the clay exceeds 8%. Lime/cement piles are constructed either by dry jet mixing or wet jet mixing method (Miura et al, 1987). In the former, the cement or quicklime powder is injected into the deep ground through a pipe with the aid of compressed air and then the powder is mixed with the clay mechanically by means of the rotating wings as demonstrated in Fig. 49. In the latter method, the slurry cement is jetted into the clay by a pressure of about 20 MPa from a rotating nozzle.

Granular piles are composed of compacted sand and gravel inserted into the soft clay foundation by displacement method. It has the main advantage over the reinforced concrete pile in that it redistributes the stresses to the surrounding ground but still retaining some form of stress concentration in the more stiffer material of the granular pile. The pile deforms by bulging into the clay and distributes the stresses at the uppper portion of the subsoil strata rather than transferring the stresses to the deeper layers, thus causing it to reinforce the soft ground and at the same time causing the soil to support it (Bergado et al, 1988e). Results of the laboratory and field tests conducted at the Asian Institute of Technology (Bergado et al, 1988a), indicated that the stress concentration factor which is the ratio between the stresses in the pile and the clay, varies from about 2 to 5. The strength and bearing capacity increased by 4 to 5 times and the settlement was reduced by 30 to 50%. Typical applications of granular piles on soft ground are illustrated in Fig. 50.

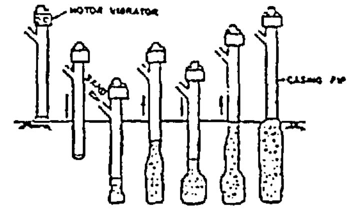

(A) INSTALLATION OF GRANULAR PILES

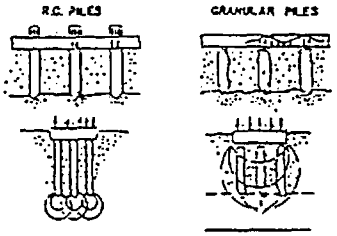

(B) COMPARISON OF CONCRETE AND GRANULAR PILES

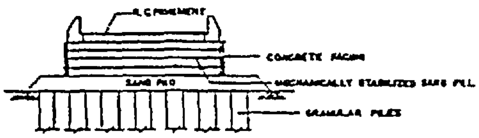

(C) TYPICAL COMBINATIONS

Fig. 50. Granular piles (sand or gravel piles).

Vertical drains served to shorten the paths of drainage for the less permeable soft clay, accelerating the rate of consolidation such that most of the settlements occur before or during construction stage. Vertical drainage can be made by inserting sand drains or prefabricated band drains into the soft clay. Preloading is required to create hydraulic gradients for the pore water in the clay to follow into the drains and can be applied by means of embankment surcharge or by the use of vacuum pressure (Moh et al, 1987). This method has been successfully tested at the Asian Institute of Technology in both the laboratory and field conditions (Bergado et al, 1988d). In this case, most of the subsoil compression due to the embankment loading is completed in the first 6 to 10 months with only negligible amounts remaining for the rest of the project life. The typical highway applications of prefabricated vertical drains are illustrated in Fig. 51.

11 RESEARCHES ON GROUND IMPROVEMENT TECHNIQUES

Current researches on different techniques of ground improvement is currently going on at the Geotechnical and Transportation Engineering Division of AIT to mitigate such natural hazards such as ground subsidence and compressible foundation subsoil. Among the soil improvement techniques

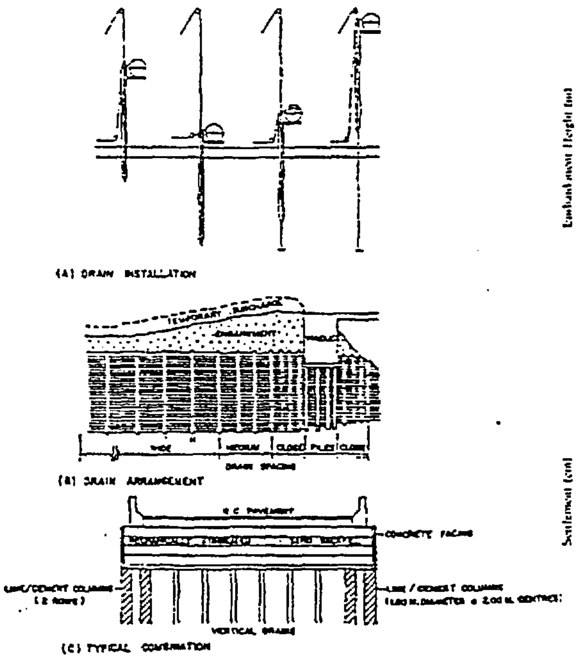

Fig. 51. Vertical drains with preloading and lime/cement piles.

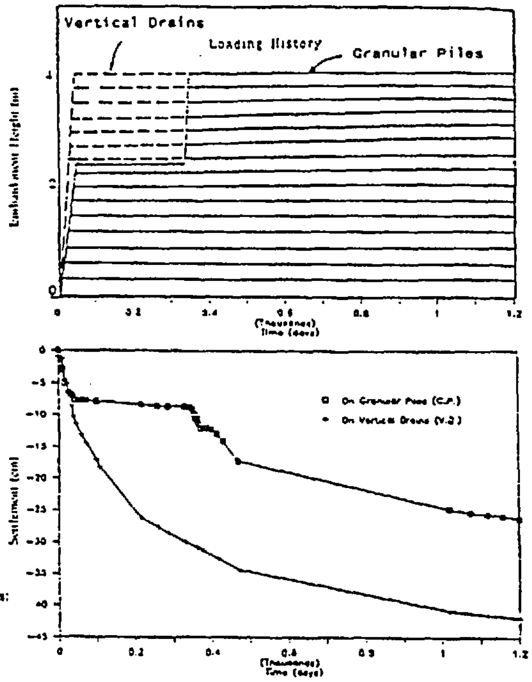

Fig. 52. Settlement behavior of embankments on granular piles and on vertical drains.

that can be applicable are reinforced earth (mechanically stabilized earth), granular piles, vertical drains, and lime or cement piles. Already, test embankments have been constructed on soft Bangkok clay improved with granular piles (Bergado et al, 1988a) and vertical Mebra band drains (Bergado et al, 1988d) inside the AIT campus. A comparison of the settlement behaviour of the two embankments on granular piles and on Mebra drains is shown in Fig. 52. A third test embankment was recently completed using a different type of vertical band drains (Alidrain) which was installed using both large and small mandrel sizes. Figures 53 and 54 show the section view and plan view of the embankment, respectively. The observed time-settlement is shown in Fig. 55. Meanwhile, prototype models are being tested in the AIT soil engineering laboratory concerning reinforced earth, granular piles, vertical drains, and lime/cement stabilized soil.

The U.S. Agency for International Development (USAID) through USAID (Thailand) under the Program on Science and Technology Cooperation has granted the Asian Institute of Technology a three-year research project with total cost of US$150,000.00 through Dr. Dennes T. Bergado of the Geotechnical and Transportation Engineering Division as the principal investigator. The main objective of this research project is to develop the design and construction guidelines for using locally available weathered Bangkok clays including lateritic soils and clayey sands, which are classified as cohesive soils to

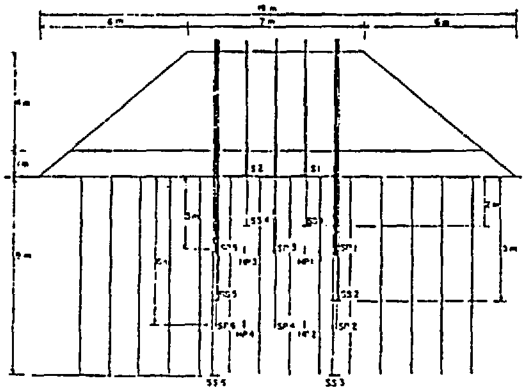

Fig. 53. Section view of embankment on prefabricated Alidrains.

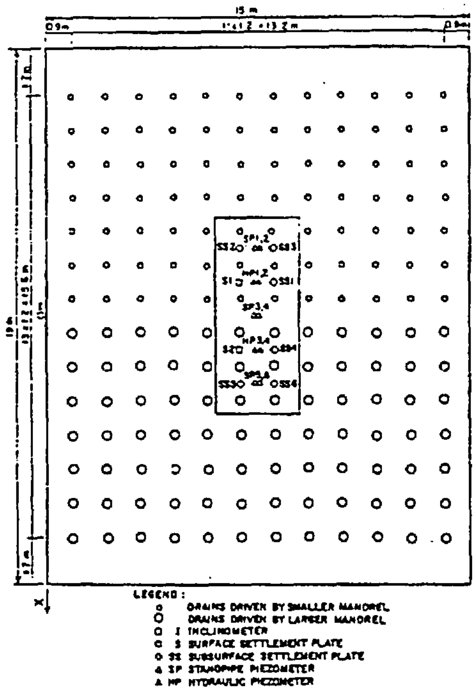

Fig. 54. Plan view of embankment on prefabricated Alidrains.

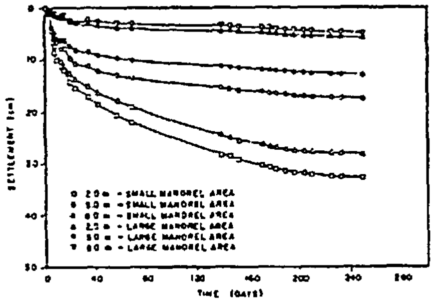

Fig. 55. Observed time-settlement curve for embankment on prefabricated Alidrains.

be used as backfill materials with welded steel bars as grid reinforcement. The main work includes construction of large scale pullout box in the laboratory for pullout tests to study the interaction between the backfill soil and the reinforcement using advanced electronic data measurements and collection. Preliminary results and analyses of the data on pullout tests have been published (Bergado et al, 1989). Also, a full scale welded wire wall embankment system with a height of 5.5 m was recently constructed at the campus of AIT. The wall is shown in Fig. 37 and consists of a vertical face with sloping sides. Field pullout tests will be performed on dummy reinforcements embedded at different depths of the wall. The corrosion rate will also be monitored on buried dummy reinforcements. This research work forms a logical extension to the current knowledge on soil reinforcement as understood for granular soils, which develop high frictional resistance between the soil and reinforcement elements.

12 CONCLUSIONS

The existing natural hazards in coastal plain areas such as the presence of soft ground and the effect of ground subsidence due to excessive pumping of groundwater, require different schemes of soil and ground improvements for infrastructure constructions to prevent slope instability and minimize total and differential settlements. It is concluded that the appropriate scheme will be a combination of either lime/cement piles or granular piles for improvement in the subsoil with overlying mechanically stabilized (reinforced earth) embankment fill. It is noted that both lime/cement piles and granular piles are also basically a form of earth reinforcement. The vertical drains combined with preloading are quite effective in precompression and preconsolidation of the soft clay subsoil but this scheme often needs some time to execute. The various soil/ground improvement techniques described in this paper are economical and viable alternatives to the existing method of using precast, reinforced concrete piles to support embankments, especially in the transition units between the pile-supported viaducts (overpasses) and the at-grade road embankments.

REFERENCES

Balasubramaniam, A.S., Bergado, D.T., Buensuceso, B. and Yang, C.W. (1988). Ground Improvement Techniques for Approach Road Design and Rehabilitation of Road Embankment. Proc. Symp. on Roads, Bridges and Highways for 21st Century, Bangkok, 14 pp.

Bergado, D.T., Bukkanasuta, A. and Balasubramaniam, A.S. (1987). Laboratory Pullout Tests Using Bamboo and Polymer Geogrids Including a Case Study. Geotextiles and Geomembranes Journal, Vol. 5, pp. 153-189.

Bergado, D.T., Miura, N., Panichayatum, B. and Sampaco, C.L. (1988a). Reinforcement of Soft Bangkok Clay Using Granular Piles. Proc. Intl. Geotech. Symp. on Theory and Practice of Earth Reinforcement, Fukuoka, Japan, pp. 179-184.

Bergado, D.T., Sampaco, C.L., Miura, N. and Sakai, A. (1988b). Reinforced Gravel Foundations for Box Culvert and Sewage Pipeline Construction on Soft and Subsiding Ground. Proc. 1st Indian Geotextiles Conference, Bombay, India.

Bergado, D.T., Sampaco, C.L., Miura, N. and Onitsuka, K. (1988c). Interaction of Geogrid Reinforcement with Gravel and Decomposed Granite Backfill with Applications. Proc. Intl. Conf. on Geomechanics of Tropical Soils, Singapore, pp. 351-357.

Bergado, D.T., Miura, N., Singh, N. and Panichayatum, B. (1988d). Improvement of Soft Bangkok Clay Using Vertical Band Drains Based on Full Scale Test. Proc. Intl. Conf. on Eng'g. Problems of Regional Soils, Beijing, China, pp. 379-384.

Bergado, D.T., Singh, N., Sim, S.H., Panichayatum, B. and Sampaco, C.L. (1988e). Improvement of Soft Bangkok Clay Using Vertical Drains Compared with Granular Piles. Geotextiles and Geomembranes Journal (in press).

Bergado, D.T., Cisneros, C.B., Shivashankar, R., Alfaro, M.C. and Sampaco, C.L. (1989). Pullout Resistance of Steel Geogrids with Weathered Clay Backfill. Proc. Symp. on the Application of Geosynthetic and Geofibre in SE Asia, Kuala Lumpur, Malaysia.

Chang, J.C., Hannon, J.B. and Forsyth, R.A. (1977). Pull Resistance and Interaction of Earthwork Reinforcement and Soil. Transportation Research Board, 56th Annual Meeting.

Cox, J.B. (1970). The Distribution and Formation of the Recent Sediments in Southeast Asia. Proc. 2nd Southeast Asian Conference on Soil Eng'g., Singapore, pp. 29-47.

Fowler, J., Peters, J. and Franks, L. (1986). Influence of Reinforcement Modulus on Design and Construction of Mohicanville Dike No. 2. Proc. 3rd Intl. Conf. on Geotextiles, Vienna, Austria, pp. 267-271.

Ingold, T.S. (1983). Laboratory Pullout Testing of Grid Reinforcement in Clay. Geotechnical Testing Jour., Vol. 6, No. 3, pp. 112-119.

Jewell, R.A., Milligan, G.W.A., Sarsby, R.W. and Dubois, D. (1984). Interaction Between Soil and Geogrids. Proc. Symp. on Polymer Grid Reinforcement. Thomas Telford Ltd., London.

Jones, C.J.F.P. (1985). Earth Reinforcement and Soil Structures. Butterworths Book Co., London.

Law, K.H. (1989). Strength and Deformation Characteristics of Cement-Treated Clay. M.Eng. Thesis No. GT-88-6, AIT, Bangkok.

Miura, N., Bergado, D.T., Sakai, A. and Nakamura, R. (1987). Improvement of Soft Marine Clay by Special Admixtures Using Dry and Wet Mixing Methods. Proc. 9th Southeast Asian Geotech. Conf., Bangkok, Thailand.

Moh, Z.C. and Woo, S.M. (1987). Preconsolidation of Soft Bangkok Clay by Non-Displacement Sand Drains and Surcharge. Proc. 9th Southeast Asian Geotech. Conf., Bangkok, Thailand.

Netlon Ltd. (1984). Test Methods and Physical Properties of Tensar Geogrids. Technical Guideline of Netlon Ltd., England.

Nielsen, M.R. and Anderson, L.R. (1984). Pullout Resistance of Wire Mats Embedded in Soil. Report Submitted to the Hilfiker Co., Utah State University, Logan, Utah.

Ochiai, H., Hayashi, S., Ogisaku, E. and Sakai, A. (1987a). Analysis of Polymer Grid Reinforced Soil Retaining Wall. Proc. 8th Asian Regional Conference, Tokyo, Japan.

Ochiai, H. and Sakai, A. (1987b). Analytical Method for Geogrid Reinforced Soil Structures. Proc. 8th Asian Regional Conference, Tokyo, Japan, pp. 483-486.

Peterson, L.M. and Anderson, L.R. (1980). Pullout Resistance of Welded Wire Mats Embedded in Soil. Utah State University, Logan, Utah.

Poulos, H.G. and Davis, E.H. (1974). Elastic Solutions for Soil and Rock Mechanics. John Wiley & Sons Inc., New York.

Rowe, R.K. and Davis, E.H. (1982). The Behaviour of Anchor Plates in Sand. Geotechnique, Vol. 32, No. 1, pp. 25-41.

Developments in Geotechnical Aspects of Embankments, Excavations and Buried Structures, Balasubramaniam et al. (eds)
© 1991 Balkema, Rotterdam. ISBN 90 5410 019 2

Interaction of steel geogrids and low-quality, cohesive-frictional backfill and behavior of mechanically stabilized earth (MSE) wall on soft ground

D.T. Bergado, A.S. Balasubramaniam, K.H. Lo, R. Shivashankar, C.L. Sampaco & M.C. Alfaro
GTE Division, Asian Institute of Technology, Bangkok, Thailand

ABSTRACT: This paper deals with the behavior of MSE test wall consisting of steel grids reinforcement embedded in cohesive-frictional backfill soil that was constructed on soft Bangkok clay. The mechanism of interaction between steel grids reinforcement and low-quality, cohesive-frictional backfill is being modelled and analyzed. Laboratory pullout tests were performed using large pullout box designed for this study. Field pullout tests were also conducted on dummy reinforcements embedded in a full scale mechanically stabilized earth wall utilizing three different backfill materials, namely: clayey sand, lateritic residual soil, and weathered clay backfill. The magnitude of mobilized pullout resistance as well as the strains induced in the reinforcing elements were strongly influenced by the variation of the base pressure of the wall which is, in turn, affected by the arching effects of the reinforcements and the pattern of deformation of the soft clay foundation. Laboratory pullout tests generally provided conservative approximation of actual pullout resistance in comparison to the field pullout test results. Finite element analyses were also done to simulate and verify the load-displacement of the reinforcements and the behavior of the MSE wall. The overall agreement between the experimental and theoretical results were quite satisfactory. The measured wall settlements and lateral movements, after more than a year, were quite excessive but were found to have no adverse effects on the overall wall performance. Thus, it can be concluded that MSE wall and embankment systems using steel grids reinforcements embedded in locally-available, cohesive-frictional backfill soils is a viable and economical alternative scheme for infrastructure construction on soft ground.

1 INTRODUCTION

Most major cities in the Southeast Asian region are located in the coastal plains with thick deposits of soft clays. These deposits are found in most countries of the region (Fig. 1) such as the Chao Phraya Plain in Thailand, Mekong Delta in Cambodia and Vietnam, Malaysian Coastal Plain, Philippine Central Plain, and Indonesian Coastal Plain. Most of these coastal plains are characterized by a recent deposit of marine sediments consisting of a topmost layer of compressible clay underlain by alternating layers of stiff clay and dense sand with gravel. Typical of these features is the flat, deltaic-marine deposit of the Chao Phraya Plain in Thailand, wherein Bangkok metropolis is located, which covers a width of about 200 km and a north-south dimension of about 300

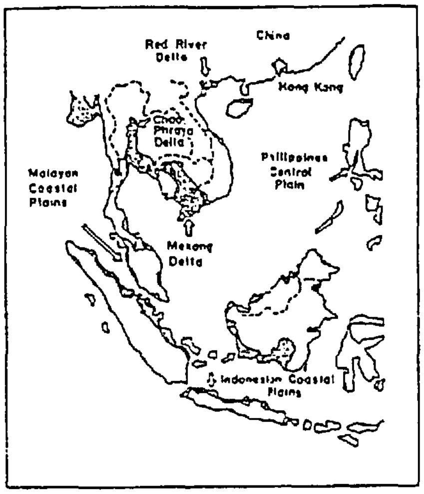

Fig. 1 The distribution of recent clays in Southeast Asia.

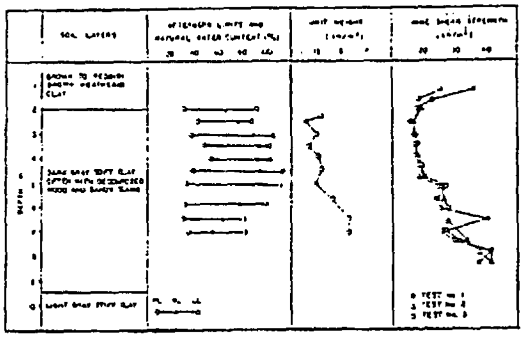

Fig. 2 Typical subsoil profile and geotechnical properties at AIT campus.

km. The typical near surface subsoil profile at the campus of the Asian Institute of Technology (AIT), located about 45 km north of Bangkok is shown in Fig. 2 with the corresponding geotechnical properties. The presence of a thick layer of soft clay can pose considerable problems to infrastructure constructions within the coastal plains because of its high compressibility and low strength. Majority of these infrastructure constructions are road embankments, flood control dikes, landfills, embankments along irrigation canals, etc. In the case of road embankments, such infrastructures are subjected to height restrictions of about 3.4 m with a gentle slope of 3H to 1V to avoid stability failures. But even with this height, highway embankments can undergo excessive settlements of about 2 m in about 10 years time, sinking below their maximum flood level, and thus, requiring costly reconstruction and maintenance works (Bergado et al, 1990a). On the other hand, rapid expansion and high cost of land often compels for steep and high embankments without the normally wide and flat slopes. To alleviate such problems, mechanical stabilization by earth reinforcement (mechanically stabilized earth) can be a viable alternative. The technique offers specific technical, economic, and aesthetic advantages compared to the more conventional methods, making the principle to be presently adopted for construction of retaining walls, embankment slope repairs, retention of excavations and in-situ slope stabilization. The deformation response characteristics of mechanically stabilized earth structures often provide technically attractive solutions on sites with poor foundation soils owing to their extreme tolerance of large deformations, both laterally and vertically, compared to conventional retaining walls. Their flexibility also allows the use of lower factor of safety for bearing capacity design. Moreover, the reinforcement in the soil tend to distribute the stresses in the foundation subsoil, hence, eliminating the use of concrete piles for lightly-loaded structures. Furthermore, mechanical stabilization by steel grids reinforcement will minimize differential movements within the earthfill, reducing the occurrence of cracking in the pavements.

Mechanically stabilized earth (MSE) consists of reinforcing the soil using steel or polymer (plastic) grid materials. The reinforcement which is strong in tension combines with the soil which is strong in compression, forming a very strong and semi-rigid composite material. The tension in the reinforcement is mobilized by the interaction between the reinforcement and the soil in the form of friction or adhesion and bearing resistances. The grid reinforcements usually generates pullout resistance up to 6 times higher than the strip reinforcements (Nielsen and Anderson, 1984). Among the grid reinforcement, steel grids are found to be superior than the polymer grid in terms of low extensibility and higher tensile strengths (Fowler et al. 1985). Since the mobilization of the interaction between the soil and reinforcement depends on the relative strains generated in the reinforcement, steel grids are preferable.

High quality granular backfill materials are suitable for mechanically stabilized earth constructions. However, these backfill materials are not often readily available especially within the coastal plains and thus, are expensive due to high transportation cost. The use of locally-available, poor-quality, cohesive-frictional backfill materials is, therefore, imperative for economic reasons. Granular backfill materials are considered high in quality and suitable for such construction because they are free-draining and consequently the stress transfer between the reinforcement and soil backfill is said to be immediate as lift of the backfill is placed, and shear strength increase will not lag behind vertical loading. They usually behave as elastic materials in the load level of practical interest such that no post construction movements associated with internal yielding or readjustments are anticipated. On the contrary, fine-grained materials are considered as poor in quality for use in mechanically stabilized earth constructions owing to their poor drainage characteristics and often exhibit elastoplastic or plastic behavior which increases the

: the
:aring
:orce-
: the
:ence.
: for
more,
grids
ntial
ucing
ements.
con-
steel
The
nsion
g in
and
nsion
the
and
adhe-
grid
llout
the
erson,
steel
the
lity
: et
the
force-
rains
steel

rials
ized
back-
dily
stal
to
of
ive-
ere-
ons.
ered
con-
ning
be-
fill
the
ngth
ical
stic
ical
tion
lding
the
con-
in
tions
ris-
or
the

possibility of post-construction movements due to creep. In addition, as soils become more fine-grained, their resistivity, which is an important factor controlling the rate of galvanic corrosion, generally decreases which is indicative for aggressive soils. With the introduction of grid reinforcements and modern methods of corrosion protection, the use of poor quality backfill materials in mechanically stabilized earth construction has gradually attracted much attention in the recent years due to their added economic advantages and feasibility in other places especially those situated within coastal plains.

The basic design criteria for MSE structures involves satisfying: (i) external stability and (ii) internal stability (Lee et al, 1973; McKittrick, 1978; Anderson et al, 1986a,b; Mitchell and Villet, 1987). External stability is evaluated by considering the entire reinforced soil mass as a semi-rigid structure which is checked for with the conventional criteria such as (a) overturning, (b) sliding, (c) bearing capacity, and (d) deep stability (conventional slope stability with a failure surface below the reinforced mass). The internal stability of reinforced soil structures requires an evaluation of: (a) tension in the reinforcing elements and (b) pullout resistance of reinforcing elements. As pointed out by Ingold (1983), the pullout test is the most realistic model to study the soil-reinforcement interaction problems.

This paper is a partial result of the on-going research project at the Asian Institute of Technology, concerning the investigation of the potential use of widely available, but poorer in quality, backfill materials in walls and embankments stabilized mechanically by welded wire mesh (steel geogrids) reinforcements. The research project involves the construction of a full-scale welded wire wall/embankment system on compressible foundation and the study of the soil-reinforcement interaction by laboratory and field pullout tests. Results of the laboratory pullout tests have been published earlier (Bergado et al, 1989a,b; Bergado et al, 1990b,c,d,e).

2 THE MECHANICALLY STABILIZED EARTH (MSE) TEST WALL

2.1 Description, construction and instrumentation Program

The test embankment is divided into 3 sections along its length, consisting of about 14.64 m long at the top, and

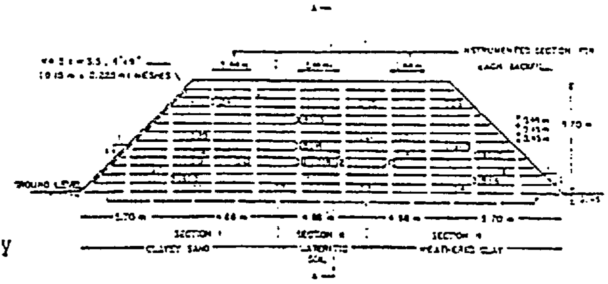

Fig. 3 Front sectionof the mechanically stabilized earth (MSE) wall.

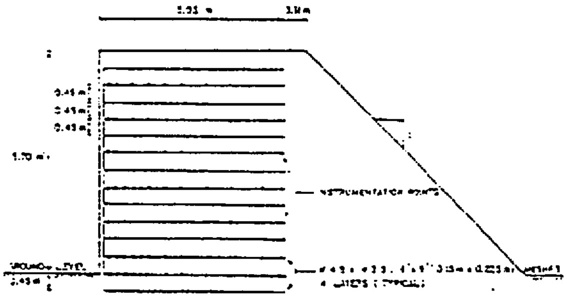

Fig. 4 Typical cross-section of the wall showing instrumentation points in the reinforcing mats.

composed of 3 different backfill materials (Fig. 3). It has a vertical welded-wire reinforced wall with a wire mesh facing unit on one side, and a sloping, unreinforced embankment along the opposite side as shown in the section view in Fig. 4. Table 1 summarizes the relevant geotechnical properties of the backfill materials used in the embankment. The reinforcing mats used were 2.44 m wide by 5.0 m long galvanized, welded wire mesh of W4.5 x W3.5 (diameter of 6.0 mm and 5.40 mm, respectively) wires on a 6 x 9 inches (0.15 x 0.225 m) grid openings. Seven of these mats were instrumented with strain gages for each section as shown in Fig. 4. The embankment construction involved the placement of the reinforcement, with the bent-up portion forming a part of the facing elements. The first layer of the reinforcement mats was laid 0.45 m below the ground level. Backing mats and screens were provided along the vertical side of the wall and backfilled with pea gravel which extended up to 0.45 m towards the embankment to prevent erosion of the cohesive backfill soil. The fill layers between reinforcing mats were placed and

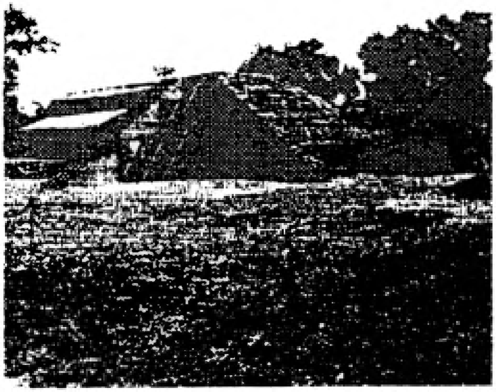

Fig. 5 Photograph of the mechanically stabilized earth (MSE) wall (a) front view and (b) oblique view

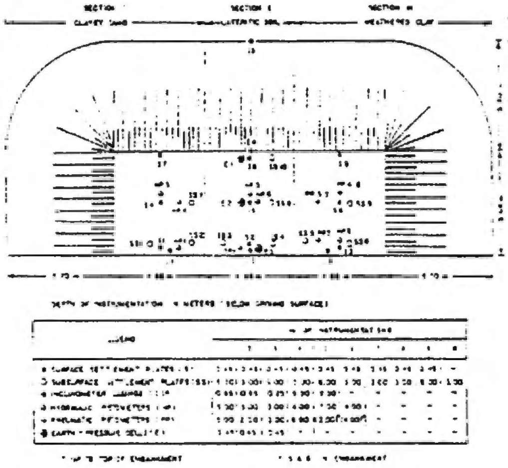

Fig. 6 Schematic layout of field instrumentation for the MSE wall.

compacted in 3 equal compaction lifts up to a total thickness of about 0.45 m corresponding to the vertical spacing of the reinforcing grids. Each lift was compacted by a combination of a hand tamper and a roller to the specified density of about 95% standard Proctor compaction. The placement moisture content was maintained within 1-2% on the dry side of optimum as verified by the Troxler nuclear densitometer. Figure 5 shows a photograph of the completed MSE test embankment. An instrumentation program, primarily consisting of strain measurements on the seven instrumented blayers in each section, was developed to evaluate the performance of the MSE test embankment. In addition, dummy reinforcing mats as shown in Fig. 3 were also instrumented and embedded at different levels of each section for field pullout tests. Additional dummy reinforcing mats for corrosion observation were embedded at different locations for later retrieval. The schematic layout of the field instrumentation is given in Fig. 6.

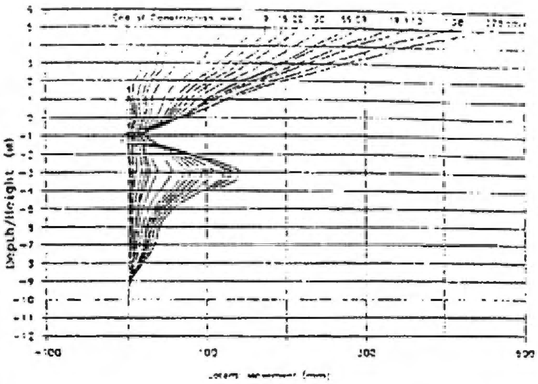

Fig. 7 Typical plots of wall lateral movement against depth or height (Inclinometer No. 2).

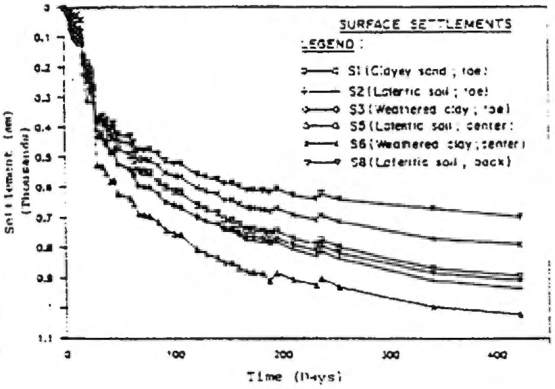

Fig. 8 Plots of surface settlemetns with time.

2.2 Lateral displacements, settlements, and excess pore pressure

The typical plots of the lateral movements for inclinometer I2 are shown in Fig. 7 which is similar to that of inclinometers I1 and I3. After 228 days from the end of construction period, the maximum outward lateral movement measured at the top of the wall face was about 300 mm. The maximum lateral movement in the subsoil at 3 m depth was about 110 mm, which indicated the potential location of shear failure surface corresponding to the weakest soft clay layer. The rate of lateral movement in the subsoil was, however, observed to be decreasing with time. The direction of the subsoil lateral movements in I4 and I5 are opposite and of smaller magnitudes compared to that near the face which seems to indicate that the soil is being squeezed out from the front and from the back, but predominantly from the front corresponding to the heavier load. The surface settlement-time relationships at different sections of the embankment are shown in Fig. 8. The surface settlements at the front along the longitudinal section beneath the interconnected wire mesh facing of the wall (S1,S2,S3) have been almost identical with a magnitude of 0.90 m. Similarly, the subsurface settlements at 6 m depth were also found to be nearly identical at 0.25 m. However, at 3 m depth below the same longitudinal section, settlement plate SS4 at the middle section settled an amount of 0.51 m which is comparably lower than its adjacent settlement plates SS2 and SS6 which settled at 0.67 m and 0.75 m, respectively. The maximum surface settlement occurred at the center plate S5 below the middle section (lateritic residual soil) such that the overall settlement pattern at the surface indicates a dish-like configuration. The vertical (d) and lateral (δ) deformations were plotted in d-(δ/d) coordinates, similar similar to the diagram for construction control of embankments on soft ground (Matsuo and Kawamura, 1977). As shown in Fig. 9, the plots are way below the critical boundary curves of p_j/p_f = 0.90 which was the suggested failure criterion for assessing the safety of embankments. Piezometer readings taken at different locations beneath the wall indicated that the porewater pressures continued to dissipate, though at a very slow rate as typically shown in Fig. 10.

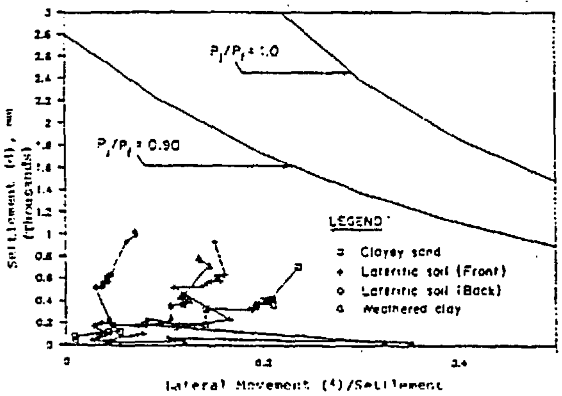

Fig. 9 Safety assessment of wall performance during construction.

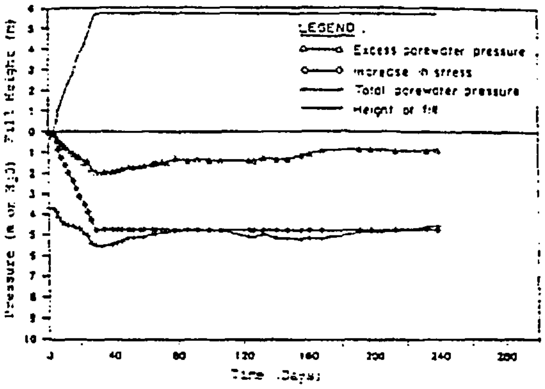

Fig. 10 Typical plots of excess pore pressure with time.

2.3 Earth pressure at the base of the wall

To determine the vertical pressure distribution at the bottom of the wall, SINCO pneumatic total pressure cells were used (Fig. 6). During the construction of the first 4 layers, the base pressure at 0.50 m behind the face (E1) was increasing (from 1 to 29 kN/m²) and higher than E2 and E3 (each recorded a constant pressure of 1 kN/m²), implying that the center of pressure is located near the face. After 8 layers, the center of pressure tends to have been shifted backwards as observed from the base pressure readings, probably due to the increase in embankment weight, and with it, the increase in the surface settlements at the center. By the end of the twelfth layer, the base pressures recorded in all the three cells were nearly the same at 55 kN/m². The surface settlements near these points were also about the same at 26 mm. However, towards the end of construction, E2 recorded a base pressure of 70 kN/m² which is greater than 63 kN/m² at E1, and much greater than the pressure of 50 kN/m² at E3, resulting to the drastic increase of settlement at S5. It has been observed throughout the post-construction phase that any abrupt increase in E2 is followed construction period, the maximum outward lateral movement measured at the top of the wall face was about 300 mm. The maximum lateral movement in the subsoil at 3 m depth was about 110 mm, which indicated the potential location of shear failure surface corresponding to the weakest soft clay layer. The rate of lateral movement in the subsoil was, however, observed to be decreasing with time. The direction of the subsoil lateral movements in I4 and I5 are opposite and of smaller magnitudes compared to that near the face which seems to indicate that the soil is being squeezed out from the front and from the back, but predominantly from the front corresponding to the heavier load. The surface settlement-time relationships at different sections of the embankment are shown in Fig. 8. The surface settlements at the front along the longitudinal section beneath the interconnected wire mesh facing of the wall (S1,S2,S3) have been almost identical with a magnitude of 0.90 m. Similarly, the subsurface settlements at 6 m depth were also found to be nearly identical at 0.25 m. However, at 3 m depth below the same longitudinal section, settlement plate SS4 at the middle section settled an amount of 0.51 m which is comparably lower than its adjacent settlement plates SS2 and SS6 which settled at 0.67 m and 0.75 m, respectively. The maximum surface settlement occurred at the center plate S5 below the middle section (lateritic residual soil) such that the overall settlement pattern at the surface indicates a dish-like configuration. The vertical (d) and lateral (δ) deformations were plotted in d-(δ/d) coordinates, similar similar to the diagram for construction control of embankments on soft ground (Matsuo and Kawamura, 1977). As shown in Fig. 9, the plots are way below the critical boundary curves of $p_j/p_f = 0.90$ which was the suggested failure criterion for assessing the safety of embankments. Piezometer readings taken at different locations beneath the wall indicated that the porewater pressures continued to dissipate, though at a very slow rate as typically shown in Fig. 10.

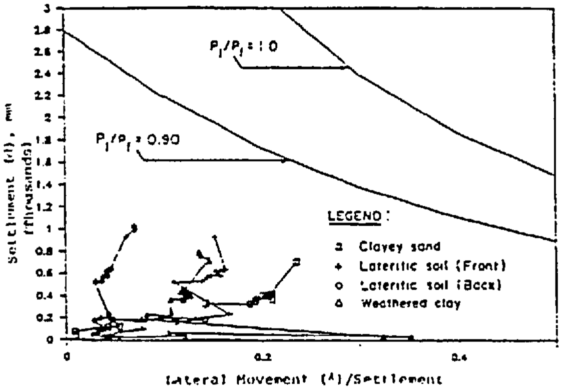

Fig. 9 Safety assessment of wall performance during construction.

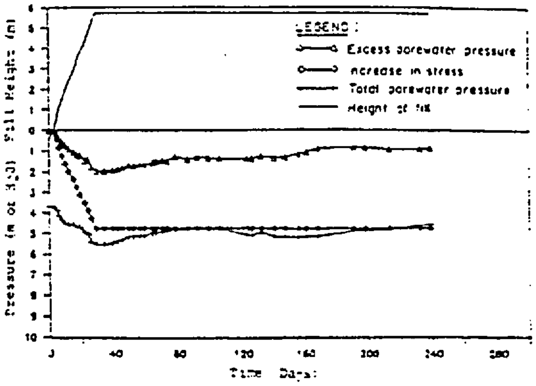

Fig. 10 Typical plots of excess pore pressure with time.

2.3 Earth pressure at the base of the wall

To determine the vertical pressure distribution at the bottom of the wall, SINCO pneumatic total pressure cells were used (Fig. 6). During the construction of the first 4 layers, the base pressure at 0.50 m behind the face (E1) was increasing (from 1 to 29 kN/m²) and higher than E2 and E3 (each recorded a constant pressure of 1 kN/m²), implying that the center of pressure is located near the face. After 8 layers, the center of pressure tends to have been shifted backwards as observed from the base pressure readings, probably due to the increase in embankment weight, and with it, the increase in the surface settlements at the center. By the end of the twelfth layer, the base pressures recorded in all the three cells were nearly the same at 55 kN/m². The surface settlements near these points were also about the same at 26 mm. However, towards the end of construction, E2 recorded a base pressure of 70 kN/m² which is greater than 63 kN/m² at E1, and much greater than the pressure of 50 kN/m² at E3, resulting to the drastic increase of settlement at S5. It has been observed throughout the post-construction phase that any abrupt increase in E2 is followed by a release of pressure at E1. When E1 starts increasing from its lowest value, there will be at first a slight release in the value of E2, and thereafter, E2 again starts increasing gradually at first for a while and then at some stage, an abrupt increase. This whole process seems to develop a cyclic variation in the base pressures caused by arching effects due to interconnection of reinforcements at the facing units of the wall. This process is expected to continue until consolidation of the subsoil is completed. Any abrupt increase in the value of E2 coupled with large settlement therein at the center, was also reflected by the sharp increase in porewater pressures at the center and the variable mode of strain generation in the reinforcing mats as discussed in the next section. The base pressure distributions are plotted in Fig. 11.

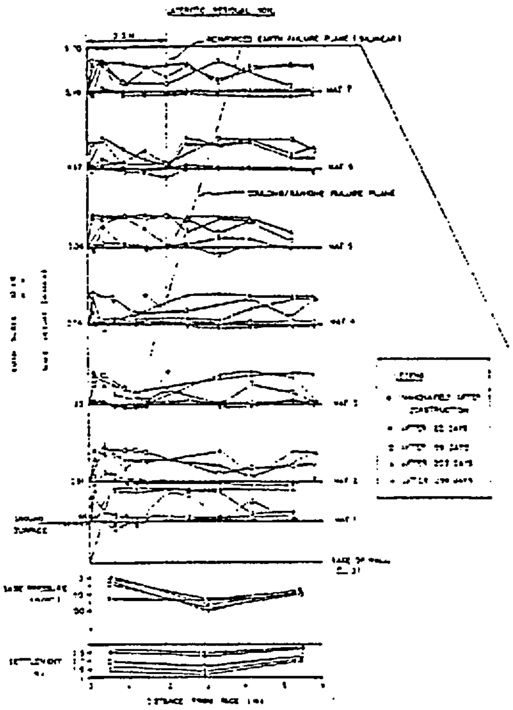

Fig. 11 Variations of reinforcement tension, base pressure, and settlements at different periods for the middle section.

2.4 Tension in the reinforcing wires

The 21X datalogger with a multiplexer and storage module was used to store the data from the temperature compensating electrical-resistant strain gages which were mounted diametrically opposite each other. The reinforcement tensions immediately after construction and four other periods after construction, are depicted in Fig. 13 for the middle section of the test embankment, including the settlement profiles and base pressures. After 22 days from the end of construction, it is seen that some reinforcing mats displayed a sudden release of stresses in all sections corresponding to the abrupt decrease in earth pressure near the face (E1) to almost a zero value, with E2 and E3, retaining almost the same magnitude. After 89 days, the earth pressures at 3 locations were all found to increase drastically at almost the same rate which subsequently increased the strains in the reinforcement for all layers. The maximum lateral pressures immediately after construction are plotted with depth in Fig. 12 for the middle section, and were compared to existing earth pressure theories on reinforced soil structures as discussed by Jones (1985). The measured values immediately after construction were higher than the coherent gravity and tie-back structure hypotheses but seems to be closely predicted by the compaction theory proposed by Ingold (1983). It is interesting to note how arching effect has altered the lateral pressures in the lateritic soil section, which is supposed to be the strongest backfill used in the wall, by yielding lower measured lateral pressures than the other 2 sections. This

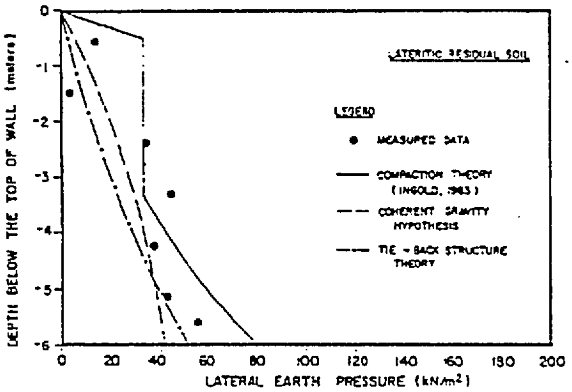

Fig. 12 Comparison between the measured lateral earth pressures immediately after construction, and the various theoretical expressions (middle section).

effect was verified from field pullout tests on dummy reinforcing mats located at the center section which indicated contrasting results with theoretical expectations in terms of lower pullout resistances than both weathered clay and clayey sand, and strikingly, decreasing pullout resistances with increasing overburden pressures. On the other hand, the pullout resistances from laboratory pullout tests show increasing pullout capacity with increasing normal pressures (Bergado et al, 1989a,b; 1990b,c,d,e).

2.5 Lateral earth pressure coefficient, K

Typical variations of reinforcement tension during construction as each lift of the backfill was placed above the mat are given in Fig. 13 for the middle section.

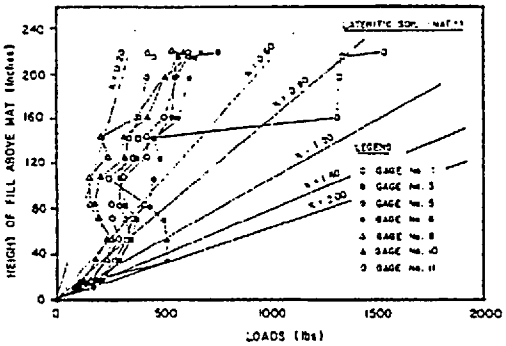

Fig. 13 Variation of wire tensions with height of fill for mat no. 1 in the middle section of the wall.

The graphs were replotted to show the variation of tension with distance from the face of the wall as shown in Fig. 14. The maximum value of K was obtained corresponding to the height of the backfill above each reinforcing mat and plotted as shown in Fig. 15 for the lateritic residual soil at the middle section of the wall. The plots of K indicate an increasing trend as we approach the top of the wall, with most of these values way above the limiting active value (K_a). Similar trend was obtained for the other 2 sections of the wall. This variation is significantly different from those reported for welded wire walls with high quality backfill on comparatively hard foundations (Anderson et al, 1987) as well as for reinforced earth walls (McKittrick, 1978). These deviations may be attributed to the flexibility of the foundation subsoil and to the residual pressures induced by compaction.

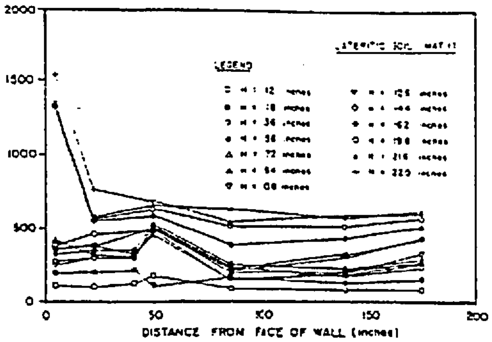

Fig. 14 Variation of reinforcement tension with distance from the face of wall at different fill heights for mat no. 1 in the middle section of the wall.

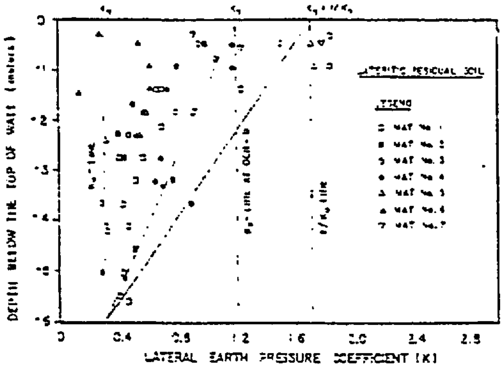

Fig. 15 Measured lateral earth pressure coefficient (K) during construction of the wall at the middle section.

Foundation compressibility can enhance lateral displacement of the wall face as the test embankment is constructed. The lateral movement necessary to develop the fully active case (K_a) had been reported by Terzaghi (1934) to be only a minimal fraction of the wall height (H/1000). Any further movement of the face will increase the lateral pressure (Carder et al, 1977,1980; Terzaghi, 1934). In this study, the maximum lateral movement measured for the wall, immediately after construction, amounted to about 0.15 m which is much higher than the required displacement of 0.0057 m to develop the fully active case. For a grid-reinforced soil wall, this continuous outward wall movement may cause the full mobilization of the passive resistance of transverse members, thereby inducing larger strains in the longitudinal members. On the other hand, experimental evidence using compacted sand and silty clay backfills have shown that the maximum lateral earth pressures throughout the height of the wall are significantly higher than were calculated from the at-rest (K_o) values, especially at the top meter of the wall (Carder et al, 1977, 1980; Murray and Boden, 1979; Ingold, 1983). These high values were attributed to the residual stresses induced by compaction as was also found by Murray and Farrar (1990). Although these magnitude of residual stresses depend on the type and size of the compaction plant employed, the maximum stresses at the very top of the wall cannot exceed the lateral pressure calculated using the coefficient of earth pressure for unloading, K_o'(Broms, 1974; Rowe, 1954). Carder et al (1977, 1980) assumed K_o' to have a value of $1/K_o$, where K_o was calculated from the Jaky (1948) equation ($K_o = 1-\sin \phi'$). Figure 15 typically shows the envelopes of K for the middle section which appeared to have a similar trend as the other 2 sections of the wall. The K-envelope varying from K_a to K_o' may be taken as the upperbound. The other envelope which varies from K_a to K_o, where K_o was calculated assuming that the compacted backfill is overconsolidated with an OCR of 3, seems to be more appropriate. These recommended envelopes for K may be applicable to walls constructed up to 6 m height on soft and compressible foundation, and utilizing poor quality backfill materials having both friction and cohesion. This result may also be overconservative for walls which will undergo only very small lateral movements. In addition, the values of K reported herein were calculated from the construction data of the wall and did not take into account the increase in vertical pressures due to overturning moment. If such a factor is considered, lower back-figured values of K will result.

2.6 Maximum tension line

The response generated by the wall due to foundation compressibility creates a unique situation wherein existing theories on earth pressures may not be directly applicable. Current design methods use either classical earth pressure theories such as those of Coulomb and Rankine, or an empirical design method which usually involves the assumption of an equivalent fluid pressure distribution. While this situation is seldom, if not encountered in practice, it can be said that the present design method presupposes the very specific combinations of a rigid wall rotating actively about its toe with a backfill acted on by gravitational forces only. For reinforced soil walls, the maximum tension line was reported to define a failure surface or wedge of a Coulomb/Rankine type failure plane, bilinear failure plane, or the log spiral failure plane. Any of these conditions may not be satisfied if foundation flexibility gets into the picture as in the case of the base pressure distributions cited earlier. It was, however, found that even with this variable mode of earth pressure at the base of the wall, the maximum tension line for this study (Fig. 11) seems to closely conform to the log spiral failure plane (farther from the face than the Coulomb/Rankine failure plane) at the lower half of the wall, and conform to the reinforced earth failure plane (closer to the face than the Coulomb/Rankine failure plane) for the upper half of the wall, especially at the two outer sections (I and III).

3 LABORATORY AND FIELD PULLOUT TESTS

Laboratory and field pullout tests were carried out to study the interaction between the steel geogrids reinforcement and the poor quality backfill materials consisting of weathered Bangkok clay, clayey sand, and lateritic residual soil.

3.1 Laboratory pullout tests

In the laboratory, pullout tests were conducted using a 50"x30"x20" (LxWxH) test cell made up of 1/2" thick steel plates and was designed and fabricated at the Asian Institute of Technology. The schematic diagram of the pullout apparatus is shown in Fig. 16. The vertical stress was supplied by an air bag located between the 1/4 " thick, flexible metal plates. The pullout force, measured by means of a load cell, was applied to the test specimen using an electrically-controlled hydraulic cylinder mounted against the supporting frame of the pullout cell. The horizontal displacement of the mat was monitored using the linear variable differential transformer (LVDT) and was pulled out at the rate of 1 mm/min. The data acquisition system (21X micrologger with AM416 multiplexer) recorded both the mat displacement and the axial strains in the longitudinal and transverse members by means of strain gages. The tests were performed on varying wire sizes, mesh geometry and compaction conditions of the backfill materials. The reinforcements used in this study were fabricated locally using

iting
fill
. For
ision
ilure
type
e, or
these
inda-
s as
ribu-
ever.
le of
wall,
study
the
n the
ilure
and
ilure
the
the
the

were
tion
ment
ials
lay,
oil.

were
test
ates
the
The
atus
ress
ween
tes.
f a
test
lled
the
The
was
able
was
The
gger
the
in
s by
were
mesh
the
used
using

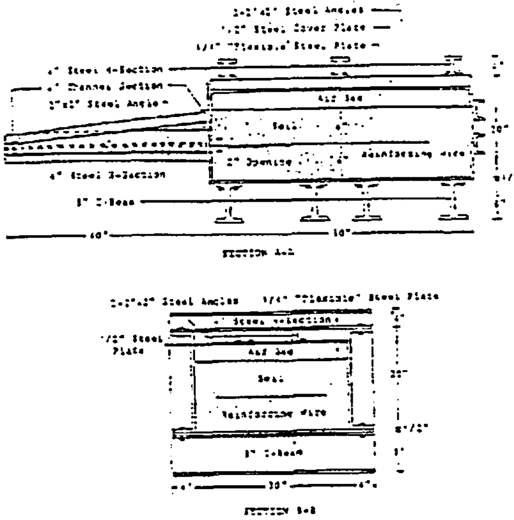

Fig. 16 The pullout testing cell used in laboratory pullout tests.

readily available mild steel bars. Tensile strength conducted on these bars indicated occurrence of yield stresses at low strains in the order of 0.2% to 0.3% and a modulus of elasticity of 30 x 10 psi. The rein-forcements consisted of 1/4", 3/8", and 1/2" diameter steel bars with varying aperture sizes of 6"x9", 6"x12" and 6"x18". The backfill materials were compacted at 95% standard Proctor densities at both dry and wet sides of optimum. Typical stress-strain relationships for dry and wet sides of optimum compaction for the weathered clay backfill are shown in Figs. 17 and 18, respectively. It can be observed that the pullout resistance in the wet side compaction is very much lower compared to the dry side although both conditions was found to increase with increasing confining normal stresses, as observed for good quality granular backfill materials. The same trend was also found for the other types of backfill materials used in this study. However, lateritic residual soil backfill seems to have higher pullout resistance than the clayey sand and weathered clay backfills, in descending order. Reinforcements with their transverse members removed were also tested to determine the contribution of the longitudinal members through adhesion/ friction with the soil. In all the tests conducted, the soil-reinforcement interaction indicated the dominant role of passive resistance contributed by the transverse members to the total pullout resistance. The friction resistance of the longitudinal members was found to have a minimal contribution to the total pullout resistance. It was also found that the mobilized interaction depends on the relative displacements between the reinforcement and the backfill, wherein the smaller diameter bars were effective in enhancing the full mobilization of passive resistance. The 6"x9" mesh geometry seems to be the most efficient of all the grid sizes that were used. The steel grids pulled out with linearly decreasing axial strains from the point of load application, in the order of 0.01 to 0.02% as expected for inextensible reinforcements.

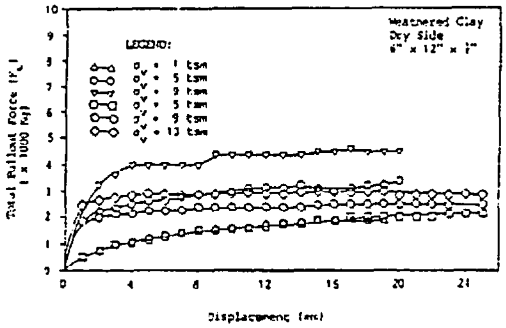

Fig. 17 Typical load-displacement curves for weathered clay compacted at the dry side of optimum.

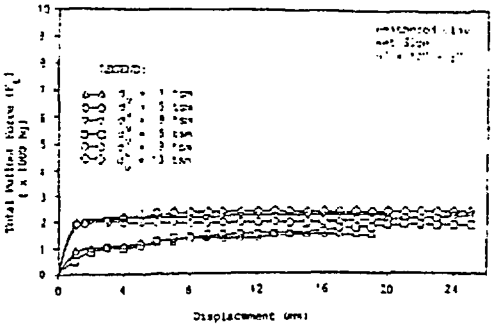

Fig. 18 Typical load-displacement curves for weathered clay compacted at the wet side of optimum.

3.2 Field pullout tests

Field pullout tests were carried out in conjunction with laboratory tests to verify the soil-reinforcement interaction under actual soil condition using field prototypes. The tests were conducted on dummy reinforcing mats embedded at different locations along the vertical face of the wall as shown in Fig. 3 and were performed in the same manner as in the laboratory, utilizing the same pulling machine and data acquisition system. Typical field pullout test set-up is shown in Fig. 19. The typical stress-strain relationship for the weathered clay backfill is shown in Fig. 20. The pullout resistance is seen to increase with increasing overburden pressure which confirms the laboratory tests and theoretical expectations. The same trend was observed with the clayey sand backfill. On the contrary, the lateritic residual soil backfill showed a decrease in pullout resistance with increasing overburden pressure. This is attributed to the arching effects due to the interconnection of the interface of the reinforcements and higher subsoil deformations at the middle section. This was verified when the pullout resistance of dummy reinforcements embedded at the lower parts of the wall was considerably less compared with the clayey sand and weathered clay backfill sections with the same overburden pressures as well as the same reinforcement geometry and size. Without arching effects, this should unlikely to happen considering that lateritic residual soil has higher strength which consequently could give higher pullout resistance as observed in laboratory tests.

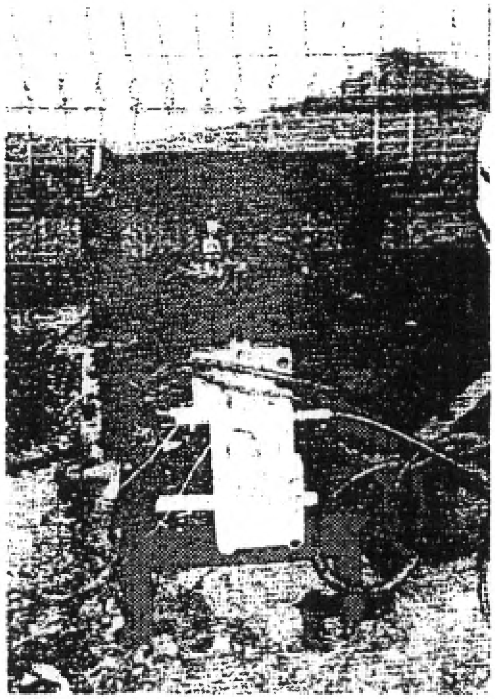

Fig. 19 Typical set-up of pullout test in the field.

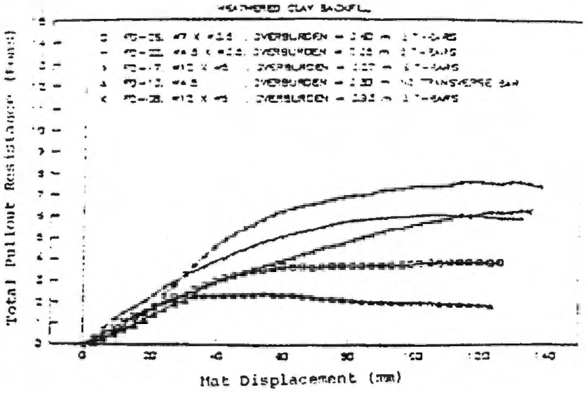

Fig. 20 Summary plots of field pullout resistance versus the mat displacement for the weathered clay backfill.

3.3 Comparison of laboratory and field pullout tests

It was observed that the pullout resistance produced in the field pullout tests were higher than in the laboratory under the same backfill and overburden pressure conditions. One reason could be due to the embedment length of the reinforcement employed in the field pullout test, which is double than that in the laboratory. Longer reinforcements have higher peak pullout resistance for the same overburden pressure (Chang et al, 1977). Other reasons could be the variation in sample compaction, effects of pea gravel near the wall face, boundary conditions and scale effects. As the reinforcement is pulled out from the pullout box, lateral pressure can develop against the rigid front face, leading to arching of the soil over the inclusion which reduces the vertical stress on the reinforcement, and consequently, decrease the pullout resistance (Juran et al, 1988; Palmiera and Milligan, 1989). It was also observed that the laboratory pullout tests yielded a peak pullout resistance at relatively low displacement compared to the field pullout tests. This is attributed to the fact that more elongation in longer reinforcement will result in more displacement to reach the yield load for the same overburden pressure.

4 NUMERICAL MODELLING OF MSE WALL/EMBANKMENT SYSTEM

4.1 Computer program description and modifications

The NONLIN1 computer program was written and developed to analyze numerically the soil-structure interaction problems and permits solution to problems involving relative movements between structural media such as concrete and steel as well as soil media. The program implements the analytical method suggested by Ochiai and Sakai (1987) which combines the joint element expressing the property of the discontinuous plane, with the bar element transmitting axial force only. Material nonlinearity is considered in the program and the "initial stress" iterative technique for solving nonlinear problems as proposed by Zienkiewicz et al (1969) is adopted. The program was specifically designed for modelling the soil-reinforcement interaction in a pullout test and can be used efficiently to predict pullout resistance of the reinforcement of a given geometry. Necessary debugging modifications were also made to use the program in IBM/3080 mainframe computer system. Modifications were also made in this study so that it can be used to analyze the MSE test embankment and to model the pullout tests in the laboratory (Lo, 1990). Consequently, the vertical facing of the welded wire wall subjected to a transverse load was modelled by using a special 2 or 3-node one-dimensional bending element (Hermitian element), having a length L and a section property EI that combines elastic modulus E with the area moment I. Two degrees of freedom that are both translational and rotational were assumed at each node of the element. By considering the behavior as linearly elastic, the constitutive matrix $[D]^e_B$ for the Hermitian element can be expressed as:

$$[D]^e_B = EI \tag{1}$$

For such an element, the element stiffness matrix $[K]^e_B$ is given by Cheung and Yeo (1979) as:

$$[K]^e_B = EI \begin{bmatrix} 12/L^3 & 6/L^2 & -12/L^3 & 6/L^2 \\ 6/L^2 & 4/L & -6/L^2 & 2/L \\ -12/L^3 & -6/L^2 & 12/L^3 & -6/L^2 \\ 6/L^2 & 2/L & -6/L^2 & 4/L \end{bmatrix} \tag{2}$$

A subroutine SMATBN was then developed to form the element stiffness matrix $[K]^e_B$ of the Hermitian element and was added to the program NONLIN1. Subroutines were also developed to calculate the shape functions and their derivatives for 2- and 3-node bending elements.

4.2 Input parameters for the model elements

The following input parameters were employed to define the material properties of all the model elements:

Soil Elements. The three types of backfill material used in the wall were included and were represented by an elasto-plastic material model obeying a Mohr-Coulomb failure criterion. Hyperbolic parameters suggested by Duncan and Chang (1970) were also adopted in the analyses. Stress-strain parameters of the soils from UU triaxial tests were used to account for partial saturation and the short-term undrained loading condition. A constant value of 0.36 was assumed for the Poisson's ratio of the backfill materials. The undrained elastic modulus E_u of the foundation subsoil was assumed to be a function of the undrained field vane shear strength, Su, i.e. $E_u = \alpha S_u$, where lies between 70 and 250 for Bangkok clay (Balasubramaniam and Brenner, 1981). From correlations on pressuremeter and the vane shear tests, a value of α of 145 was obtained by Bergado et al (1986). The undrained Poisson's ratio was taken as 0.49.

Interface Elements. The interface between the soil and structure was represented by one-dimensional joint elements to allow for relative displacement between the soil and structure if the mobilized shear stress at the interface equals or exceeds that obtained from Mohr-Coulomb strength theory. The shear stiffness of the joint element was estimated based on the method recommended by Ochiai and Sakai (1987). Figure 21 shows the variation of

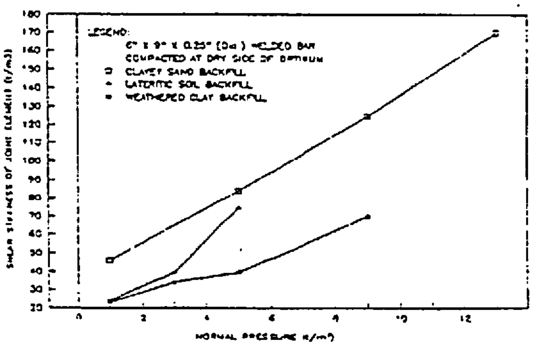

Fig. 21 Variation of shear stiffness of joint element with normal pressures.

the estimated values of the shear stiffness of joint element for all the backfills. The normal stiffnesses of the joint elements were assumed to be a higher value of 100 times their shear stiffnesses. The material parameters c and ϕ of the interface were set to be the same as those of the surrounding backfill.

Reinforcing Elements. Three parameters were required to define the bar material representing the steel bar mat reinforcements. The modulus of elasticity and yield stress were set equal to the known value for steel. The area per unit length of the wall face was calculated based on the actual cross-sectional area of longitudinal steel per bar mat and the horizontal center-to-center spacing between bar mats to convert the three-dimensional discrete bar mats into two-dimensional representation.

Beam Elements. The modulus of elasticity, yield stress, and sectional area per unit width of wall were taken equal to the value used in reinforcing elements, while the moment of inertia was assumed to be 3.8×10^{-10} m^4/m for W4.5 bars.

4.3 Finite element mesh and boundary idealization

The finite element mesh was established based on the geometry of the structure under consideration, the zones of expected high stress gradients, the zones of interest for computed stresses and deformations, the practical limitations of program capacity and the required running times. Mesh boundary conditions were selected to appropriately model the expected deformations and were set far enough from the reinforced soil zone so as to have negligible influence on the problem. The typical finite element meshes used for the pullout tests and in analyzing the welded wire reinforced wall are shown in Figs. 22 and 23, respectively.

4.4 Results of numerical modelling

Only the end-of-construction behavior of the mechanically stabilized wall was modelled based on total stress finite element method which takes into account the nonlinear inelastic behavior of the soil and slippage between soil and reinforcement. An elasto-perfectly plastic model using Mohr-Coulomb yield criterion was used to describe the soil behavior in the analysis. The interface between soil and reinforcement and soil-wall facing were represented by a joint element of zero thickness and with slip behavior being defined by a Mohr-Coulomb failure criterion. The reinforcement was considered as a linear elastic material with axial stiffness but negligible flexural rigidity. One dimensional bending element was employed to model the face of the wall. In addition, the effects of material nonlinearity were incorporated into the numerical algorithm by adjusting the initial stress matrix.

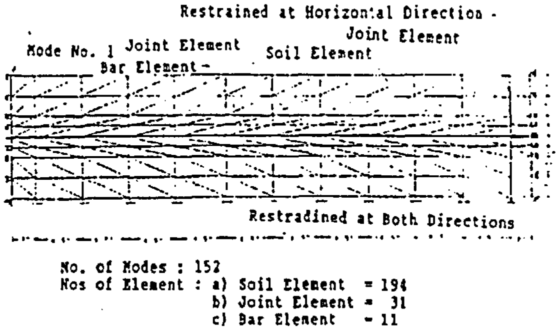

Fig. 22 Typical finite element mesh for numerical modelling of soil-reinforcement interaction in the pullout test.

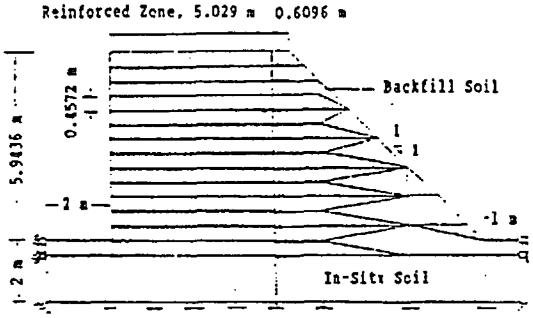

Fig. 23 Typical finite element mesh for numerical modelling of the MSE wall/embankment system.

Load-Displacement Response. The comparison between the predicted load-displacement curves and experimental results for 6"x9"x 1/4" diameter steel mesh is typically shown in Fig. 24. The results show a good agreement between the experimental and analytical values from finite element analysis. The maximum difference in pullout load between the experiment and prediction was about 15%. In order to define completely the load-displacement response in the pullout test, five displacement increments were applied to the nodal point at the free end of the reinforcement just in front of the pullout box.

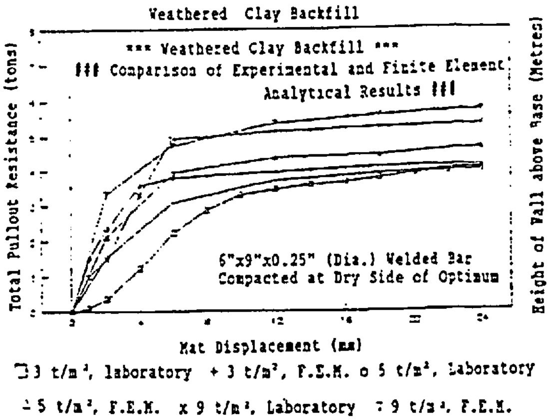

Fig. 24 Comparison of experimental and FEM prediction of load-displacement curves for weathered clay backfill.

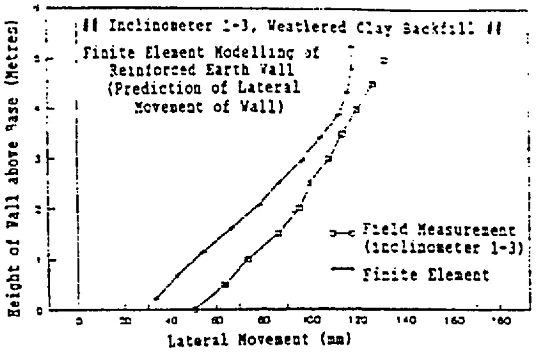

Fig. 25 Comparison of the measured and FEM prediction of wall lateral movements at inclinometer station I3.

Lateral Movement of the Wall Face. The MSE test embankment was constructed such that each section of the facing panel that was added to form the facing element was held in place to prevent lateral movement, while the corresponding level of backfill was added. Appropriate modelling of the facing element is considered as the main factor for the lateral deformations. One-dimensional bending (Hermitian) elements were properly introduced to simulate the typical facing units of the welded wire wall, i.e. bent pronged mats, backing mats, and screens as adopted in the field. The typical profile of lateral movements of the wall face at the end of construction stage from the finite element results is illustrated in Fig. 25 for the middle section. For comparison, the measured lateral movements at inclinometer I3 is also shown. Generally, the shape of the finite element result profiles agreed well with the measured profiles for all sections along the wall. The higher values measured in the field maybe attributed to the partial drainage in the soft clay foundation at the early stage of construction. In other words, a certain amount of consolidation settlement had already taken place prior to the completion of the MSE test embankment. The incremental sequence of reinforced soil wall construction also caused each new soil layer and facing panel to be placed on a previous layer that had already undergone some lateral deformations. In general, the maximum lateral movement predicted by the finite element method occurred at some 4 to 5 m above the base of wall while the actual lateral movement profile gradually increases to a maximum value at the top of the wall.

Tension Along the Longitudinal Members. The FEM prediction of the tension force distribution along the longitudinal bar for mat #2 in the weathered clay section during the end of construction is shown in Fig. 26. The plot was produced after plotting the points representing the predicted bar element tension at the center of each bar element, and then connecting the points with a smooth curve. The tensile stress obtained by FEM, which was based on a continuous reinforcing sheet covering the entire area at a given reinforcement level of the wall, was converted to actual tensile stress in the discrete bar-mat by multiplying it with the horizontal center-to-center spacing of the reinforcements, and dividing by the longitudinal cross-sectional steel area

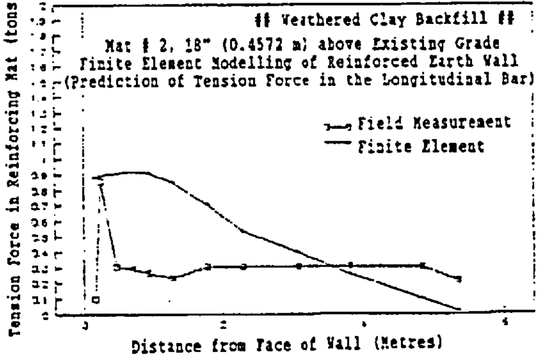

Fig. 26 Comparison of the measured and FEM prediction of reinforcement tension in the weathered clay section (Mat No. 2).

per bar mat (Schmertmann et al, 1989). The general distribution pattern was zero tension at the free end of the reinforcement, with steadily increasing tension up to a maximum value, then slightly decreasing tension towards the wall face. Comparison of the tension force from FEM and field measurements (Fig. 26) shows that the FEM results are somewhat higher than the field measurements. The crude approximation of the shear stiffness on the interface element between reinforcement and the backfill material could have contributed to the difference in the results.

5 CONCLUSIONS

The MSE test wall/embankment with its stability never endangered, both during construction and post-construction phases inspite of the excessive settlements and lateral movements, is an ample proof that mechanically stabilized system can be effectively used to reinforce poor quality and marginal quality backfill materials on soft foundations as was also confirmed from laboratory and field pullout tests conducted in this study. Laboratory pullout tests on the three backfills with normal presures up to 130 kN/m^2 proved that even with such poor quality backfill materials, the pullout resistances increased with increasing confining normal pressures as observed for good quality backfill materials, but were much affected by the moisture content and degree of compaction of the soil. The laboratory pullout test generally provided conservative approximation of the actual pullout resistance. The overall agreement between the experimental and theoretical results were quite satisfactory. Furthermore, if the subsoil was also stabilized by some effective method, it would have drastically reduced the total and differential settlements and lateral movements, resulting in improved stability of the embankment system. The variation of earth pressure at the base of the wall, the strains in the reinforcing members, the lateral earth pressure coefficient K, and the location of maximum tension line were found to be strongly affected by foundation compressibility and the effects of backfill compaction, which subsequently caused the overall behavior to deviate from those observed on reinforced walls with granular backfill and constructed on a relatively good foundation subsoils.

6 ACKNOWLEDGMENTS

Grateful acknowledgments are extended to USAID (Thailand) for providing the necessary funds to support our present research activities.

7 REFERENCES

Anderson, L.R., Sharp, K.D. & Harding, O.T. (1987). Performance of a 50-ft. High Welded Wire Wall. Geotech. Spec. Publication No. 12 (ASCE), Ed JP Welsh. pp. 280-308.

Anderson, L.R., Sharp, K.D., Woodward, B.L. & Winward, R.F. (1986a). Performance of the Rainier Avenue Welded Wire Retaining Wall. Dept. of Civil Eng'g., Utah State Univ., Logan, Utah, U.S.A.

Anderson, L.R., Liu, J. & Bay, J.A. (1986b). Experimental Evaluation and Design Recommendations for Syro Anchored Retaining Wall System. Syro Steel Company, Centerville, Utah, U.S.A.

Balasubramaniam, A.S. & Brenner, R.P. (1981). Consolidation and Settlement of Soft Clay. Soft Clay Engineering. Brand, E.W. & Brenner, R.P. (eds.), Elsevier Scientific Publishing Company.

Bergado, D.T., Khaleque, M.A., Neeyapan, R. & Chang, C.C. (1986). Correlations of In-situ Tests in Bangkok Subsoils. Geotechnical Engineering Journal, Vol. 17, pp.1-37.

Bergado, D.T., Cisneros, C.B., Shivashankar, R., Alfaro, M.C. & Sampaco, C.L. (1989a). Pullout Resistance of Steel Geogrids with Weathered Clay Backfill. Proc. Symp. App. Geosynthetic and Geofibre in SE Asia, Petaling Jaya, Selangor Darul Ehsan, Malaysia, pp. 1-26-1-34.

Bergado, D.T., Sampaco, C.L., Alfaro, M.C., Shivashankar, R. & Balasubramaniam, A.S. (1989b). Welded Wire Wall and Embankment System with Poor Quality Backfills on Soft Clay. Third Progress Report Submitted to the U.S. Agency for Intl. Development, Bangkok, Thailand, 109 pp.

Bergado, D.T., Ahmed, S., Sampaco, C.L. & Balasubramaniam, A.S. (1990a). Settlements of Bangna-Bangpakong Highway on Soft Bangkok Clay. J. Geotech. Eng. Div. (ASCE), 116(1), pp. 136-155.

Bergado, D.T., Sampaco, C.L., Alfaro, M.C., Shivashankar, R. & Balasubramaniam, A.S. (1990b). Welded Wire Wall and Embankment System with Poor Quality Backfills on Soft Clay. Fourth Progress Report Submitted to the U.S. Agency for Intl. Development, Bangkok, Thailand. 134 pp.

Bergado, D.T., Sampaco, C.L., Shivashankar, R., Alfaro, M.C., Anderson, L.R. & Balasubramaniam, A.S. (1990c). Interaction of Welded Wire Reinforcement with Poor Quality Backfill. Proc. 10th Southeast Asian Geotech. Conf. (1), Taipei, pp. 29-34.

Bergado, D.T., Cisneros, C.B., Sampaco, C.L., Alfaro, M.C. & Shivashankar, R. (1990d). Effect of Compaction Moisture Contents on Pullout of Steel Geogrids with Weathered Clay Backfill. Proc. 4th Intl. Conf. on Geotextiles and Geomembranes, The Hague, Netherlands.

Bergado, D.T., Sampaco, C.L., Shivashankar, R. & Balasubramaniam, A.S. (1990e). Welded Wire Wall and Embankment System with Poor Quality Backfills on Soft Clay. Fifth Progress Report Submitted to the U.S. Agency for Intl. Development, Bangkok, Thailand.

Broms, B.B. (1974). Lateral Earth Pressures due to Compaction of Cohesionless Soils. Proc. 4th Budapest Conf. on SMFE, pp. 373-384.

Carder, D.R., Pocock, R.G. & Murray, R.T. (1977). Experimental Retaining Wall Facility-Lateral Stress Measurements with Sand Backfill. Rep. No. LR 766, Trans. and Road Res. Lab., Crowthorne, 19 pp.

Carder, D.R., Murray, R.T. & Krawczyk, J.V. (1980). Earth Pressures Against an Experimental Retaining Wall Backfilled with Silty Clay. Rep. No. LR 946, Trans. and Road Res. Lab., Crowthorne, 21 pp.

Chang, J.C., Hannon, J.B. & Forsyth, R.A. (1977). Pullout Resistance and Interaction of Earthwork Reinforcement and Soil. Trans. Res. Record 640, Trans. Res. Board, National Research Council, Washington, D.C., pp. 1-7.

Duncan, J.M. & Chang, C.Y. (1970). Nonlinear Analysis of Stress-Strain in Soils. Journal of Soil Mechanics and Foundation Div., ASCE, Vol. 96, No. SM5, pp. 1629-1653.

Fowler, J., Peters, J. & Franks, L. (1985). Influence of Reinforcement Modulus on Design and Construction of Mohicanville Dike No. 2. ICG, Vienna, Austria, pp. 267-271.

Ingold, T.S. (1983). The Design of Reinforced Soil Walls by Compaction Theory. The Structural Engineer, 61A(7), pp. 205-211.

Jones, C.J.F.P. (1985). Earth Reinforcement and Soil Structures. Butterworks and Co. Ltd., London, U.K.

Juran, I., Knochennus, G., Acar, Y.B. & Arman, A. (1988). Pullout Response of Geotextiles and Geogrids (Synthesis of Available Experimental Data). Geosynthetics for Soil Improvement, Geotechnical Special Publication No. 18, ASCE, pp. 92-111.

Lee, K.L., Adams, B.D. & Vagneron, J.J. (1973). Reinforced Earth Retaining Walls. J. of the Soil Mech. and Found. Div., ASCE, Vol. 99, No. SM10.

Lo, K.H. (1990). Modelling of Laboratory and Field Pullout Test of Steel Geogrid Reinforcements. M.Eng. Thesis, Asian Institute of Technology, Bangkok, Thailand.

Matsuo, M. & Kawamura, K. (1977). Diagram for Construction Control of Em-bankment on Soft Ground. Soils and Foundations, Vol. 17, No. 3, pp.37-52.

McKittrick, D.P. (1978). Reinforced Earth: Application of Theory and Research to Practice. Proc. Symp. on Soil Reinforcing and Stabilizing Techniques, Sydney, Australia.

Mitchell, J.K. & Villet, W.C.B. (1987). Reinforcement of Earth Slopes and Embankments. National Cooperative Highway Research Program Report 290, Trans. Research Board, National Research Council, Washington, D.C.

Murray, R.T. & Boden, J.B. (1979). Reinforced Earth Wall Constructed with Cohesive Fill. Proc. Intl. Conf. Soil Reinf., Vol. 2, Paris, pp. 569-577.

Murray, R.T. & Farrar, D.M. (1990). Reinforced Earth Wall on the M25 Motorway at Waltham Cross. Proc. Instn. Civil Engrs., Part I, Vol. 88, pp. 261-282.

Nielsen, M.R. & Anderson, L.R. (1984). Pullout Resistance of Wire Mats Embedded in Soil. Report Submitted to the Hilfiker Company, Utah State University, Logan, Utah, U.S.A.

Ochiai, H. & Sakai, A. (1987). Analytical Method for Geogrid-Reinforced Soil Structures. Proc. 8th Asian Reg. Conf., Kyoto, Japan, pp. 483-486.

Palmiera, E.M. & Milligan, G.W.E. (1989). Scale and Other Factors Affecting the Results of Pullout Tests of Grids Buried in Sand. Geotechnique, Vol. 34, No. 3, pp. 515-524.

Rowe, P.W. (1954). A Stress-Strain Theory for Cohesionless Soil with Application to Earth Pressure At-Rest and Moving Walls. Geotechnique, Vol. 4, No. 2, pp. 70-88.

Schmertmann, G.R., Chew, S.H. & Mitchell, J.K (1989). Finite Element Modelling of Reinforced Soil Wall Behavior. Geotechnical Engineering Report No. UCB/GT/89-01, Univ. of California, Berkeley, U.S.A.

Terzaghi, K. (1934). Large Retaining Wall Tests (I): Pressure of Dry Sand, Engineering News Record, Vol. 112,, 136-140.

Zienkiewicz, O.C., Valliappan, S. & King, G.P. (1969). Elasto-plastic Solutions of Engineering Problems: Initial Stress, Finite Element Approach. Intl. J. for Num. Methods in Engineering, Vol. 1, pp. 75-100.

Index des auteurs
Author index

An investigation of the roadway through drilling showed the soils to be fairly dry though wetter than optimum at some locations. At first it was felt that there was seepage from the uphill ground but this was ruled out from a study of the topography. The problem was diagnosed to be a loss of bearing capacity through degradation of the sideslope due to runoff from the pavement structure. Some areas where this problem did not occur were associated with areas where pavement runoff was towards the backslope ditch.

To prevent deterioration of the roadway stone columns were utilized at all distressed locations. The need to undertake some repair was generated by the fact that this roadway was too important to the travelling public and the constraints for repair, should slipouts occur, would be great. Also, the repair techniques resulting for a slipout would not be easily undertaken.

The scheme used is shown in Figure 10. As shown, the columns were cemented only in the top 3 m following which plain stone columns were used below to the depth of treatment. The idea was to improve the overall resistance of the subsoils in the top 3 m where the traffic stresses were greatest. In addition, a series of curbs and catchbasins were designed to prevent the water running off the pavement onto the shoulder, weakening same thereby leading to overall pavement deterioration.

The stone-cement mix was initially mixed insitu but was later done in the Maintenance Operations Yards using the mixing arrangement used for mixing gravel and salt for winter maintenance of roadways. A cement content of about 5% by weight was used along with fairly clean gravel aggregate. To this mix a small amount of water was added so that the mix formed a cohesive mass when squeezed with the hands. Where the mix appeared dry some water was added into the holes as the columns were constructed.

Compaction of the columns was done using a plate tamper. Since construction of these columns there has been no visible signs of any further increase in pavement distress and the remedy is considered to be performing well.

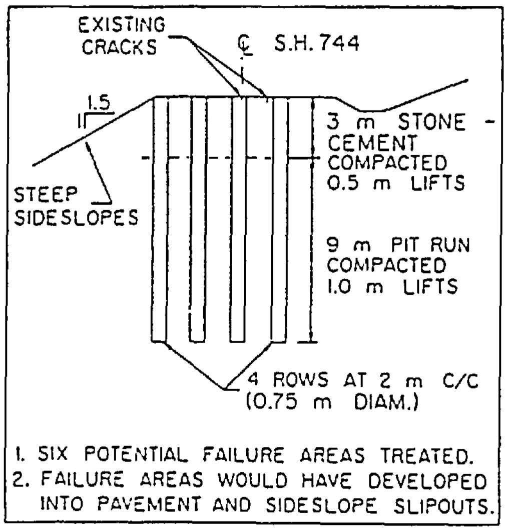

Figure 10: Layout of Stone Cement Columns

PROJECT EXPENDITURES

Table 1 provides summary statistics on the treated sites showing the total lengths drilled and the costs expended at each site as well as the cost per metre. The total expenditure for the eight sites amounts to $467,060 with an average cost of $42.09 per metre.

Table 1

SITE	DESIGN	M	COST	COST /M	AVE DEPTH/ COL.	DATE
1.	Stone	685	33,346	48.80	8	Sept. '80
2	Stone-Lime	1258	48,900	38.85	6	May '88
3	Stone	869	33,389	38.42	8	April '88
4	Stone-Lime	2714	149,644	55.14	13	Sept. '88
5	Stone-Lime	275	9837	35.77	6	Oct. '88
6	Stone-Lime	367	20,524	55.92	5	Nov. '88
7	Stone-Lime	732	11,335	15.50	6	Nov. '88
8	Stone-Lime	3313	160,085	48.32	6	Dec. '88
Totals		10,213	467,060	42.09	7	

Note: Data has been rounded off.

SUMMARY

Alberta Transportation and Utilities has experimented with the use of "drilled stone columns" as a remedial measure for problems of slope stability, bearing capacity, and settlement along highways within the Province of Alberta. So far, none of the sites treated have given any problems requiring further treatment. Alberta Transportation and Utilities will continue to utilize this method of remediation where it is deemed to be appropriate and cost effective compared to other possible methods. The Geotechnical Section will continue to monitor the performance of these sites and report at a later date on future performance. Interested readers requiring further details on the approach can contact the authors.

ACKNOWLEDGEMENTS

The execution of the remedial measures at the various sites was undertaken by the Geotechnical Field Services Section under the general direction of geotechnical staff engineers assigned to these projects. Many of the variations to the installation approach regarding mixing and compacting were provided by field staff and their keen interest in this technique was very beneficial. The authors also like to thank Les Appleby and Gisele Chartrand for their patience and cooperation in drafting the diagrams and typing the manuscript, respectively.

The information presented does not constitute a standard or regulation and are not necessarily the views of Alberta Transportation and Utilities.

FIELD TEST OF ELECTRO-OSMOTIC STRENGTHENING OF SOFT SENSITIVE CLAY

K. Y. LO*
I. I. INCULET**
K. S. HO*

* Civil Engineering, University of Western Ontario, London, Ontario
** Electrical Engineering, University of Western Ontario, London, Ontario

ABSTRACT

A field test was undertaken to assess the effectiveness of the electro-osmosis method in strengthening the soft sensitive (Leda) clay in Gloucester Test Fill site. Specially designed copper electrodes were installed to prevent gas accumulation around the electrode and to allow pore water in the soil to flow out from the cathode without pumping. The variation of settlement, shear strength and voltage distribution during treatment was monitored and tube samples were recovered before and after treatment for laboratory test. The results of field vane tests at different locations within the treated area and at different times indicate that the undrained shear strength increased uniformly by approximately 50 % for a period of 32 days throughout the depth of the electrodes. Concurrently, the surface settlements of 50 mm were achieved. The total power consumption was less than 1 % of the total project cost, indicating that the design of the treatment system was efficient. It is evident, therefore, that substantial increase in strength as well as general improvement in soil properties may be achieved by this improved version of electro-osmosis. The elimination of pumping improved the economy of the process considerably. It is expected that the process may receive wider application as a result of these improvements.

NTRODUCTION

Although the fundamental aspect of the complexities of soil-water-electricity interaction was not thoroughly known, electro-osmosis was applied in the field and was proven to work very well in silt, sensitive silt, silty clay and soft sensitive clay in a number of projects for the stabilization and improvement of soils (Casagrande 1948, 1949, 952, Soderman and Milligan 1961, Bjerrum et al 1967, Fetzer 1967, Wade 1972). However, unsuccessful application was also reported Caron 1971a,b). In most cases electro-osmosis was only used for temporary stabilization such as excavation or dewatering. It has often been considered that, in spite of the successful case histories, the process was economically impractical and retained as the last resort until field problem was encountered.

Deposits of soft sensitive clay (Champlain Sea or Leda Clay) cover a large proportion of the lowlands of the St. Lawrence River and ttawa Valleys. Extensive networks of past and future constructions such as highway embankments, bridges, earth dams of major hydro-electric generating facilities are ocated in this area. It is therefore of ngineering and economic importance to improve the soil properties of the soft sensitive clay.

It was shown by the laboratory investigation (Lo, Inculet and Ho 1990) that the electro-osmosis method was effective in strengthening the soft sensitive clay and the mechanism of the process was also studied. A field test was therefore proposed and undertaken in July-August 1989 to assess the effectiveness of the treatment in strengthening the soft sensitive clay in Gloucester Test Fill site. The objectives of the field tests are,

(a) to verify the applicability of the process for strengthening of the soft sensitive clay in the field,
(b) to develop an efficient and economical version of electro-osmosis method for engineering practice, and,
(c) to study the limitations of the process.

DESCRIPTION OF THE TEST AREA

The field test was performed in the Gloucester test fill site at Canada Forces Station (C.F.S.) in which a test embankment was constructed in 1967 by the Division of Building Research, National Research Council of Canada, at a location of 21 km south-east of Ottawa. The purpose of this test embankment was to study the field performance of the soft sensitive clay. The initial performance of the

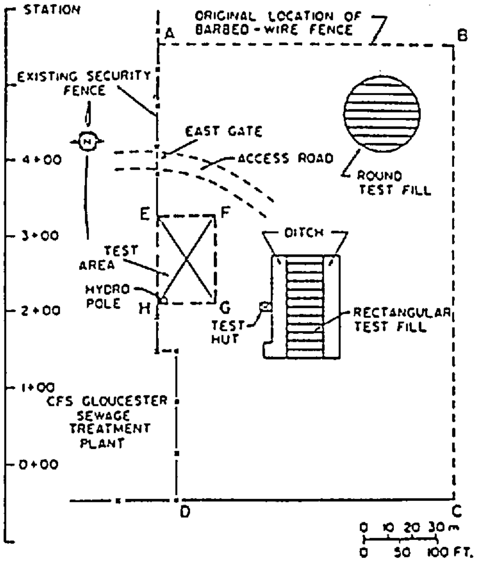

Figure 1 General Layout of The Gloucester Test Fill Site

embankment was described and analyzed by Bozozuk and Leonards (1972). Subsequent study was carried out by Lo, Bozozuk and Law (1976) to analyze the long-term settlement of the embankment. The test fill site (which has been designated as "National Test Site") is surrounded by security fence with a locked entrance, providing an enclosed area for security. The field test area was approximately 15 m west of the test embankment as shown in figure 1 (area enclosed by EFGH). The dimensions of the field test area was 40.25 m by 29.87 m (132 ft by 98 ft) with the south and west sides surrounded by security fence and the other two sides by snow fence.

The electric potential for electro-osmosis was supplied by the direct current rectifier with power rating of 120 V and 60 A, housed inside a ventilated metallic transport container of size 3 m by 6 m. A main power supply of two phases, 220 V, 60 A were obtained from the nearby office of the Royal Canadi Legion, Branch 627. The metallic container and rectifier were electrically grounded to the adjacent grounding rods to avoid electric hazard. A security guard was employed duri the treatment period to look after the fie test area at night and in the weekends.

A detailed geotechnical profile is sho in figure 2 (Bozozuk and Leonards 1972). F the present investigation (July-August 198 field vane tests and moisture content tests were carried out inside the test area before treatment and the test results are plotted the same figure for comparison. It may be se that the field vane strengths were simila The average moisture content of the pre-treatment test is about 80 % compared to an average of 60 % by Bozozuk and Leonards (1972 However, the trends of moisture conte variation in both cases are similar.

As can be seen from the soil profile in figure 2, the average vane shear strength the soil above 5.5 m (18 ft) was lower than kPa while that below this level was higher than 30 kPa. It was therefore decided to treat the soft soil between 1.5 m and 5.5 m levels. T total length of the electrode was 6.1 m (20 f and the length of the electrode embedded in the soil was 5.5 m (18 ft).

ELECTRODE DESIGN AND INSTALLATION

In most past applications, with the exception of Bjerrum et al (1967), the desi of cathode usually consisted of iron pipe a eductor pipe installed in a pre-drilled hole o substantial size (about 400 mm diameter) and filled up with clean filter sand. Th installation and material costs of electrod are therefore quite high and particularl pumping of expelled water is usually required. The anode is usually made of iron pipe, rail or steel bar and the product of the electr chemical reaction is the formation of the ir oxide and hydroxide of high electrica resistance which decreases the efficiency of the treatment. Furthermore, such design of

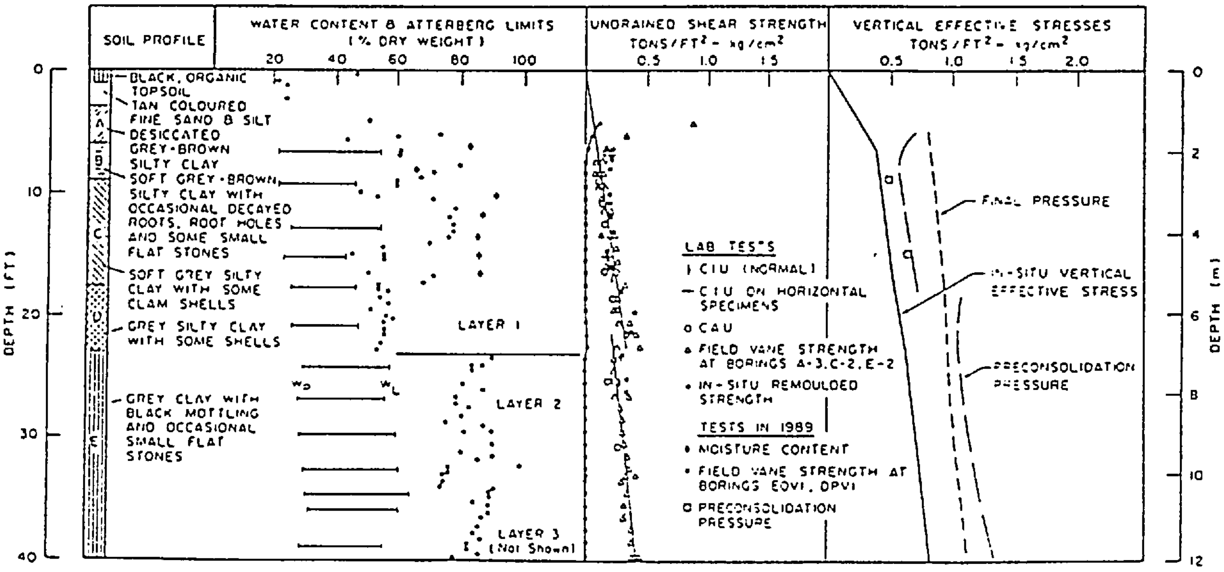

Figure 2 Geotechnical Profile of Subsoil Condition in Gloucester Test Fill Site. Profile Updated During Field Test (after Bozozuk and Leonards, 1972; part of profile not shown)

thode and anode prohibited the application of ectrode polarity reversal.

From laboratory and model tests, it was own that the use of perforated copper pipe s more effective (Ho 1990). It provided passage for expelled water and gas to flow into the cathode and out to the surface during eatment and no pumping of water was required. e undesirable effect of high resistance tallic oxide and hydroxide was also eliminated due to the replacement by copper oxide and hydroxide of high conductivity. With is electrode design, both the anode and thode are identical and the manufacturing and stallation costs of the electrodes are therefore reduced. The detail of the electrode designed for the field test is shown in figure . A 50.8 mm nominal diameter copper pipe .D. 60.3 mm, I.D. 52.4 mm and wall thickness .97 mm) was used as electrode with 9.5 mm holes drilled at 50.8 mm spacing along the ipe. For the ease of pushing the electrode to the ground, a cone-shaped steel shoe was stalled at the tip of electrode.

From the unsuccessful application reported y Caron (1971a,b), it is deduced that ontinuous sand and silt layers in the subsoil re not favourable for the process. Due to the relatively high conductivity of such layers, it would cause short circuiting of the system. If e groundwater table is higher than these ayers, water from these layer will flow into e perforated electrode and affect the efficiency of the treatment. In view of this observation, the subsoil condition of the field est area was carefully studied and it was ound that the top 1.22 m of crust (top soil, ine sand and silt) would have adverse effect to the treatment. It was therefore necessary o insulate that part of electrode by putting everal layers of varnish coating onto the pipe urface, as shown in figure 3. To avoid short circuiting of the system due to heavy rainfall and flooding of the ground surface, the top 0.3 of the electrode was also insulated. urthermore, no hole was drilled along the nsulated portion of the electrode to avoid any groundwater and rain water from flowing into the electrode. The total length of the lectrode was 6.1 m with an embedded length of .5 m to treat the top 5.5 m of soft soil excluding the crust. Four weep-holes were drilled at 0.3 m below the top of electrode to llow water flowing out from the pipe and to void corrosion of the contact of the electric able and copper pipe. Several trenches were dug to divert the expelled water from the treatment area.

The electrode was then pushed into the oil by a drilling rig and care was taken to install the electrode vertically. Due to disturbance of the highly sensitive clay, the lectrodes were filled with slurry (remoulded lay) during pushing. The interior of the lectrodes were cleaned by flushing water into the copper pipes.

ELECTRODE LAYOUT

In the electro-osmotic test area, nine lectrodes were installed in a 9.15 m square rid configuration, as shown in figure 4. Two square grids of 3.05 m and 6.1 m were formed by

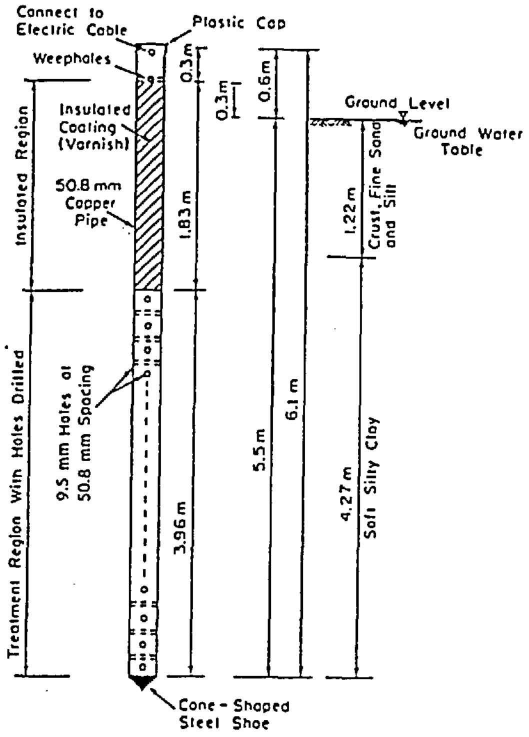

Figure 3 Details of Electrode for Electro-Osmosis

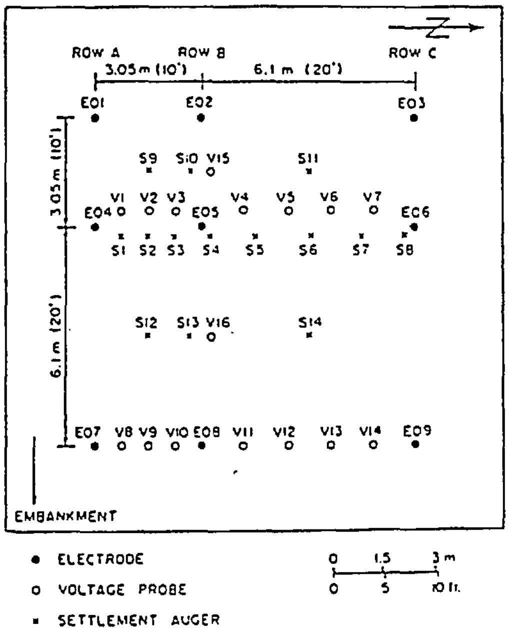

Figure 4 General Layout of Electrodes, Voltage Probes and Settlement Augers

electrodes E01-E02-E05-E04 and electrodes E05-E06-E09-E08 respectively so that the effect of spacing on the treatment could be studied. The electrical circuiting was arranged so that the Row A electrodes (E01-E04-E07) were of the same polarity (positive) while the Row B electrodes (E02-E05-E08) were of opposite polarity (negative). The Row C electrodes (E03-E06-E09) were of the same polarity (positive) as Row A. The polarity of the electrodes was then reversed midway in the treatment period. It is therefore expected from this electrode configuration that water will flow out from the centre row of electrodes during treatment with normal polarity and from the two outer rows of electrodes when the polarity is reversed.

INSTRUMENTATION AND MONITORING

During the electro-osmotic treatment, the variation of ground settlement, vane shear strength and voltage distribution with treatment time were monitored. The settlement was monitored by means of steel settlement auger of 0.61 m length with 0.15 m embedded in the soil and the settlement was measured by means of surveying instruments. The layout of the settlement augers is shown in figure 4.

The variation of field vane shear strength with treatment time was measured by means of the Norwegian field vane apparatus with vane size of 55 mm by 110 mm. Tests were carried out before, during and after treatment. The vane was pushed manually to the required depths for testing.

Fourteen voltage probes were installed to measure the voltage distribution as shown in figure 4. The voltage probe was made of 12.7 mm diameter copper pipe, with 1.33 m embedded in the soil. The surface of the copper pipe was covered by a layer of insulation coating with only the bottom 0.3 m uncoated. The purpose was to limit the measurement of the voltage distribution in the soft clay but not in the crust layer.

TEST PROCEDURES AS PERFORMED

At the beginning of treatment, Row A and Row C electrodes were connected to the positive terminal of the rectifier and the Row B electrodes were connected to the negative terminal. On day 1 (July 24, 1989), a voltage of 25 volts was applied. As water was expelled from the soil, the electrical resistance of the soil increased and consequently decreased the current flow. The applied electrical potential was therefore regulated periodically in order to maintain a relatively constant level of current flow of approximately 40 A (ampere). The variations of applied voltage and current with time are shown in figure 5. Due to the thunderstorm in day 4 and for safety reason, the power was switched off and re-started on day 5 morning. On day 18 (August 10, 1989), based on the field vane test results (to be discussed later), it was decided to reverse the current flow. In this treatment, the polarities of Row A and Row C electrodes were negative and Row B were positive. The maximum applied voltage was 120 V.

During the treatment, the following quantities were measured daily except in weekends:

(a) settlement of soil surface
(b) field vane strength at different locations, test performed as required
(c) voltage distribution in the soil between electrodes
(d) current and voltage variation of power supply
(e) collection of water samples for laboratory analysis.

After the treatment, nine field vane test profiles were performed at different locations to determine the post-treatment shear strength increase and to investigate the uniformity of treatment. Two boreholes to recover 127 mm (5") diameter samples were drilled, halfway between two 3.05 m electrodes and two 6.1 m electrodes for detailed laboratory tests.

The installation was completed in two weeks. Treatment lasted 32 days with 17 days of normal polarity and 15 days of reversed polarity.

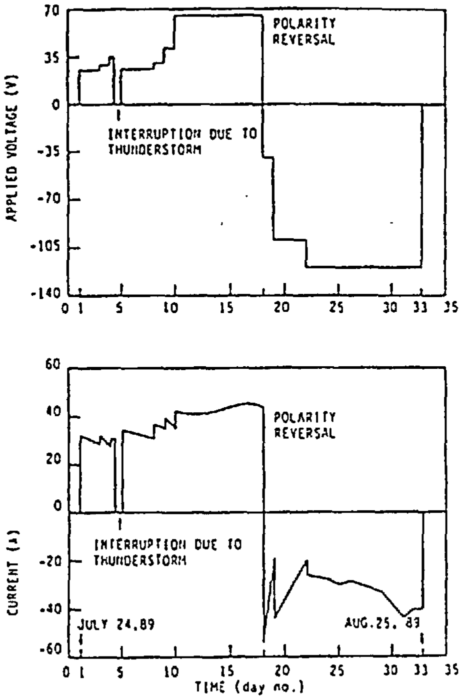

Figure 5 Applied Voltage and Current Variation with Treatment Time

RESULTS OF FIELD TESTS

A substantial amount of data has been obtained from the field test. In presentation the results of settlement, strength changes and voltage distribution, only those that highlight the process are presented. The results of laboratory tests on samples recovered from the field after treatment will be discussed in a separate paper. Complete results of both field and laboratory tests may be found in Ho (1990).

(a) Observations at Electrodes

On day 1 of treatment, a direct voltage of 25 volts was applied and the effect of electro-osmosis was observed immediately. About 50 minutes after the application of electric potential, water started to flow out from the cathodes, as shown in the photo in figure 6. Gas bubbles were also observed in the expelled water and they were expected to be hydrogen due to electrolysis of water. At anode, the copper pipe electrode was initially filled with water up to the level of groundwater table. When the electric power was on, no water was found inside the pipe.

Figure 6 Photo Showing Water Flowing out from the Cathode during Treatment and No Pumping is Required

(b) Settlement Measurement

The results of settlement measurement are plotted in figures 7 and 8. For clarity of presentation, only the settlement with treatment time curves of augers S2, S4, S6 and S8 are shown in figure 7. The settlement curves for S2, S6 and S8 indicate that during the treatment with normal polarity, the average settlement rate was about 3.3 mm/day. The maximum settlement up to day 18 was 62 mm. For settlement curve S4, since the auger was installed near to electrode E05 which was a cathode during normal polarity, it recorded the upward movement of the ground surface between day 1 and day 8 to a maximum value of 50 mm. From day 9 onward, the soil commenced to settle and up to day 18 the soil settled by 32 mm, resulting in a net heave of 18 mm. When the electrode polarity was reversed on day 18, the augers S2, S6 and S8 showed no appreciable further settlement while auger S4 recorded a constant rate of settlement of about 1.6 mm/day, with a further settlement of 24 mm. At the end of treatment, with the exception of auger S4, the settlement of the treated area is 38 to 68 mm, with an average settlement of 51 mm. Figure 8 shows the settlement-time profiles recorded by the three rows of settlement augers.

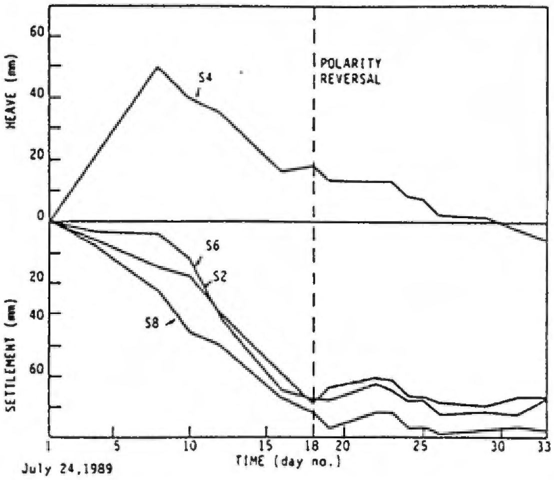

Figure 7 Measured Settlement with Time

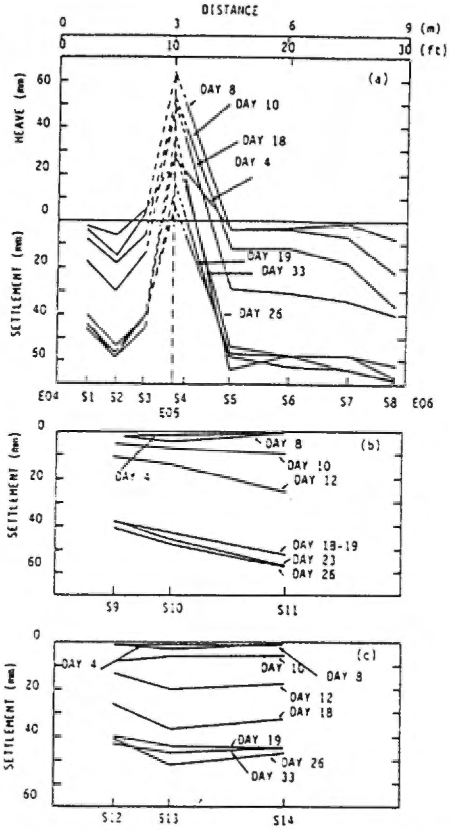

Figure 8 Settlement Profiles for (a) along Electrodes E04-E05-E06, (b) Augers S9-S10-S11, and (c) Augers S12-S13-S14

(c) Field Vane Test

A total of 26 vane test profiles were performed during and after treatment, with the test locations as shown in figure 9. The tests were carried out between 2 m and 6 m depth to investigate the shear strength changes in the soft clay layer and the effects of treatment on the clay below electrode tips, if any. Five strength profiles were carried out at 43 and 44 days after treatment (day 76 and 77) to check the long term effect of the treatment. Tests were also carried out in the "inactive zone" where the electric field intensity was expected to be minimal. Table 1 summarizes the test results. Typical profiles of vane shear strength at different times of treatment are shown in Fig. 10. Using the initial vane shear strength profile, the percentage increases of shear strength with depth at different times of treatment are shown in Fig. 11. The average final strength increase between the electrodes and average shear strength variation with time are plotted in figures 12 and 13 respectively.

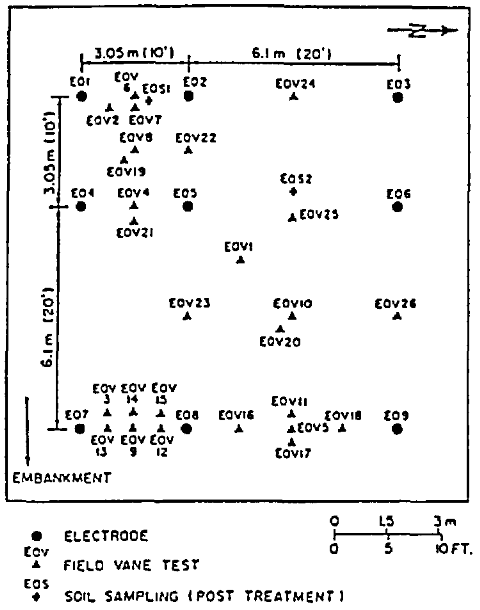

Figure 9 Layout of Field Vane Test and Sampling

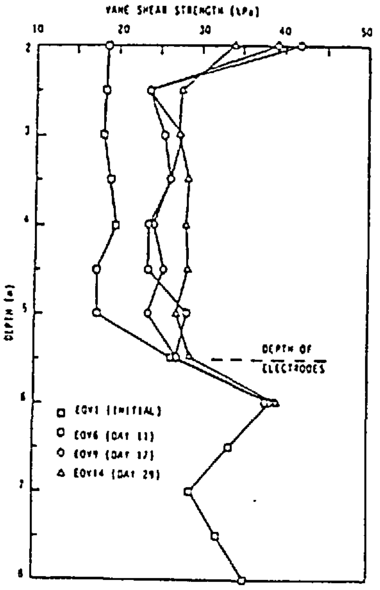

Figure 10 Variation of Vane Shear Strength Profiles with Time at Halfway of Electrodes of 3.05 m Spacing

Table 1 Summary of Field Vane Test Results

Location	Day No.	Average Shear Strength (kPa)	Average Shear Strength Increase (%)
EOV1[(a)]	---	18.2	0
EOV2	3	21.1	16.2
EOV3	9	24.3	33.7
EOV4	11	21.2	16.1
EOV5	11	20.1	10.7
EOV6	11	24.9	36.6
EOV7	17	22.2	22.0
EOV8	17	22.0	20.8
EOV9	17	24.7	35.5
EOV10	18	21.5	18.4
EOV11	18	23.2	27.7
EOV12	24	23.8	30.5
EOV13	29	29.5	62.2
EOV14	29	27.4	50.8
EOV15	29	26.1	43.6
EOV16	32	23.5	29.2
EOV17	32	24.8	36.5
EOV18	32	25.5	40.1
EOV19	33	23.2	27.5
EOV20	33	22.4	23.1
EOV21	31	26.3	44.6
EOV22[(b)]	76	20.2	11.1
EOV23	77	19.6	7.6
EOV24	76	25.3	38.8
EOV25	76	25.0	37.5
EOV26	77	19.7	8.3

Notes:-
(a) pre-treatment test
(b) 43 days after treatment

The average vane shear strength before treatment of the upper layer of soft clay between 2 m and 5.5 m is 18.2 kPa. From Table 1, the maximum average shear strength increase is 62 % (day 29) in test EOV13. The average shear strength increase of the soil after treatment halfway between a pair of electrodes of 3.05 m spacing is 50 % (day 29) and that of 6.1 m spacing is 36 % (day 32), as shown in figures 11a and 11b. In the centres of 3.05 m and 6.1 m square grids, which are considered to be the inactive zone of the treatment area, the average shear strength increase is 27 % and 23 % respectively (figures 11c and 11d), amounting to more than half of the shear strength increase of the corresponding increase in midway of the two electrodes. Another inactive zones of the test area are in the tests EOV22, EOV23 and EOV26 where the shear strengths increase are 11 %, 7.6 % and 8.3 % respectively. The uniformity of electro-osmotic treatment to the shear strength increase was also investigated by performing vane tests at different locations between two pair of electrodes. Vane tests EOV13, EOV14 and EOV15 were carried out after treatment between electrodes EO7 and EO8 (3.05 m spacing), and tests EOV16, EOV17 and EOV18 between electrodes EO8 and EO9 (6.1 m spacing), with the test holes located evenly between two electrodes. The average shear strength increase between electrodes is presented in figure 12. The results show that the shear strength increased rather uniformly, to a value of 50 % for 3.05 m electrode spacing and 36 % for 6.1 m electrode spacing.

The increase of shear strength with treatment time is presented in figure 13. It may be seen that for the 3.05 m electrode spacing, a rapid increase in shear strength occurred in the first few days of treatment, with 16 % increase on day 3. The rate of strength increase gradually diminishes with time up to day 18. When the electrode polarity was reversed, the rate of strength increase picked up again and showed a trend of further strength increase beyond day 33, if the

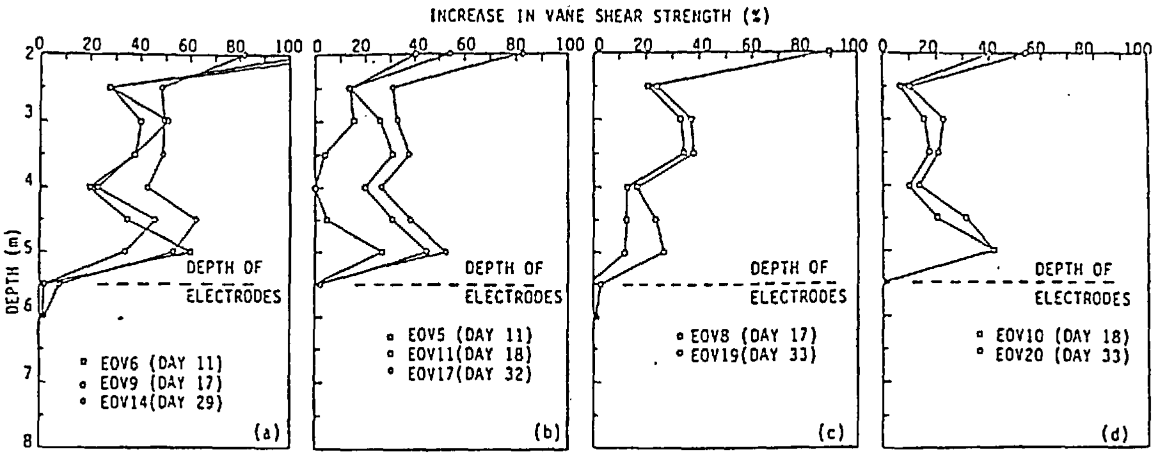

Figure 11 Profiles of Vane Shear Strength Increase with Time at (a) Halfway of 3.05 m Electrode Spacing, (b) Halfway of 6.1 m Electrode Spacing, (c) Centre of 4 Electrodes of 3.05 m Square Grid, and (d) Centre of 4 Electrodes of 6.1 m Square Grid.

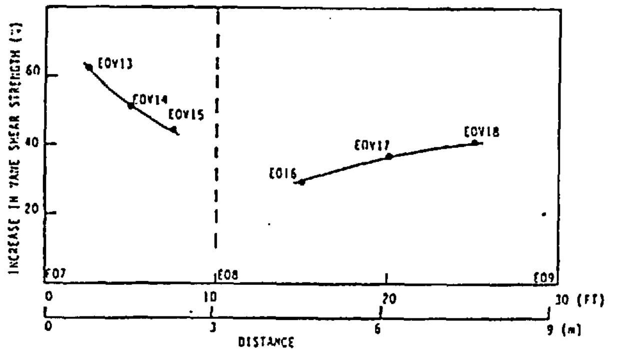

Figure 12 Variation of Average Shear Strength Between Electrodes E07-E08-E09 after Treatment

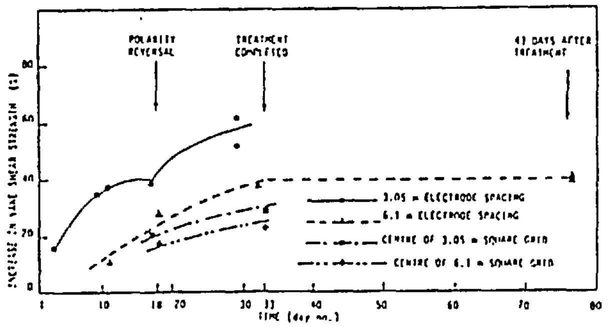

Figure 13 Percentage Increase in Average Shear Strength with Treatment Time

treatment had been continued. The curves for the other three regions (6.1 m electrode spacing, centre of 3.05 m square grid and centre of 6.1 m square grid) show the steady increase in shear strengths with relatively constant rates and there are trends of further shear strength increase beyond day 33 as well. The long term effect of the process was also investigated by carrying out two vane test profiles (EOV24 and EOV25) on day 76, 43 days after power was switched off. The shear strength increase remains at 38.8 % and 37.5 % respectively. Further tests will be carried out to verify the permanent effect of treatment.

(d) Voltage Distribution and Power Consumption

As a result of pore water being extracted from the soil, the electrical resistance of the soil increased, and the current density would vary at an applied potential difference. As shown in figure 5, there was a variation in applied voltage and current during the period of treatment. During the first 3 days the applied voltage was set at 25 V in order to examine how the current dropped due to the increase in resistance. The current dropped from 31.9 A to 28 A corresponding to a 12 % reduction. From then on the current was kept to a level of 35 to 40 A and the applied voltage was regulated periodically. The maximum voltage applied in normal treatment was 65 V with a current flow of 44.8 A. On day 18, the electrode polarity was reversed and the applied voltage was set to -40 V with a current flow of -53.9 A. The magnitude of current dropped to -19.6 on day 19 and the applied voltage was adjusted to -100 V in order to maintain a current flow of -44.4 A. The magnitude of current dropped again on day 22 to -19.8 A. The applied voltage was then set to the maximum capacity of the rectifier of 120 V and the magnitude of current increased to -26.1 A. From then on the applied voltage was constant while the magnitude of current flow increased gradually to a maximum of -43.4 A. On day 33, the current was -39.6 A just before power shut off.

Sixteen voltage probes were installed with the locations as shown in figure 4 to measure the voltage distribution in the test area. The voltage variation in soil between electrodes EO4-EO5-EO6 is plotted in figure 14 respectively. It may be seen that the potential drop between the anode and the nearest voltage probe at 0.76 m was high while that at halfway between electrodes is low. This indicates that the power consumption at vicinity to anode is quite high.

ADVANTAGES OF THE IMPROVED VERSION FOR ELECTRO-OSMOSIS

As discussed in the preceding sections, several modifications have been made in the design of electrodes and techniques of

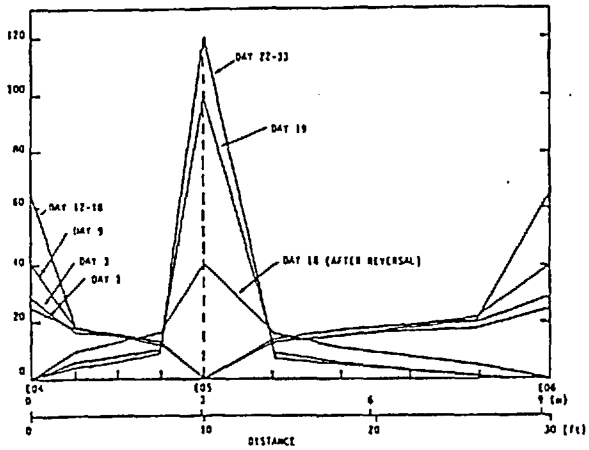

Figure 14 Voltage Variation in Soil between Electrodes E04-E05-E06

treatment. From the test results presented, it appears that these modifications improved the effectiveness of the electro-osmosis process. The advantages of the improved version are discussed in this section.

(a) <u>Effects of New Electrode Design</u>

One of the reasons of the slow development of the electro-osmotic strengthening method is due to the high electricity consumption for the process and for water pumping. In the field test, the effect of electro-osmosis was so obvious that water flowed out from the cathodes 50 minutes after power was switched on. This shows an improvement of the electrode design that water can flow out from the cathode without pumping and as a result, the installation and electricity cost can be reduced drastically. Another advantage of the new electrode design is the release of water around cathode that reduces the development of excess positive pore water pressure in the soil at the vicinity of the cathode and therefore reduces the risk of shear strength decrease, as reported in Bjerrum et at (1967).

The electrodes developed also eliminates the problem of gas accumulation around electrodes. Due to electrolysis of water, hydrogen and oxygen are produced at cathode and anode respectively and the gas formation increases the electrical resistance of the system and decreases the efficiency of electro-osmotic treatment. In the present field test, the holes in the electrodes provide the passage for the gas generated into the electrode, together with the flow of expelled water. This results in the better soil conductivity and the reduction of gas pressure development in the soil. The electrode-soil contact and consequently treatment efficiency are improved.

As a result of the electrical insulation of part of the electrode in the pervious crust, no short circuiting problem occurred during treatment. It is therefore demonstrated by the field test that the adverse effects of any undesirable soil layer can be avoided by insulation. It also emphasizes the need to investigate and interpret the subsoil conditions carefully to ensure the success of the process.

(b) <u>Heave at Cathode</u>

As described in previous section, the settlement auger S4 near the cathode shows upward and then downward ground movement an the heave was reduced to settlement afte polarity reversal (figure 7). This shows a improvement in the effectiveness of treatment compared with the problem reported b Casagrande (1952) that the soil near to cathod had considerable upward movement. Thi observation also suggests that the soil could be treated relatively uniformly by using the technique of polarity reversal. The problem o differential settlement may be reduced particularly if the reversal of polarity ha been undertaken earlier than day 18. The uniformity of treatment as obtained may be assessed in figures 8a to 8c in which th profile of ground settlement of three section of the test area are plotted. With th exception of auger S4 which is close to the cathode, the three settlement profiles at the end of treatment show maximum differentia settlement approximately ± 20 % of the averag final settlement. In future applications, this amount may be reduced by a judicious usage of the technique of polarity reversal.

(c) <u>Undrained Shear Strength</u>

The field test showed that the shea strength increased substantially in relatively short period of 32 days (figures 1 and 12). The results also indicate that the 6.1 m electrode spacing can also increase the shear strength significantly by 40 %, implyin that a wider electrode spacing may be used The increase in shear strengths in the inactive zones was not expected in the past applications and very close electrode spacing was used i order to improve the shear strength in thes areas. In this field test, the shear strength in these zones increased significantly, especially in the centre of the square grids. This further shows the effectiveness of th process with the special electrode design.

With regarding to achieving uniformity of shear strength increase, the electrode polarit reversal appears to be an useful technique. A reported previously (Bjerrum et al 1967), th treatment of soil was nonuniform in that the shear strength decreased from anode to cathode with no strength increase at the cathode. Th field test shows that the soil can be treate more uniformly by reversing the electro polarity as shown in figure 12.

From the plot of shear strength increas with treatment time in figure 13, it appea that the soil between 3.05 m electrode spacin was slightly over-treated. The resistance o the over-treated soil increased significant and hence decrease the efficiency of th process at the later stage of treatment wi normal polarity. However, this situation was improved when the electrode polarity wa reversed. For the curve corresponding to 6 m electrode spacing, due to a wider spacin the soil was treated slowly and no sign over-treatment was detected. This result indicates an advantage of using wider electrod spacing, and is further supported by t results plotted in figure 12. For long te effects, two vane test profiles were performe 43 days after treatment and no further chang in shear strength was found indicating the shear strength improvement due to the electro-osmotic treatment tends to be permanent. This behaviour can be explained by the results of laboratory consolidation test (Lo, Inculet and Ho 1990) that the soil is over-consolidated by the electric potential and the preconsolidation pressure increased after treatment. The situation of switching off the electric power is similar to the unloading stage of the consolidation test and by the principle of classical soil mechanics, the change in void ratio in rebound of soil due to unloading is small. Hence the electro-osmotic treatment may be expected to be permanent.

In the case record reported by Bjerrum et al (1967), the embedded depth of the electrodes was 9.6 m. It was observed, however, that the shear strength increased to a depth of about 6 m, and no effect was detected below this depth. A possible reason for this "depth effect" is that gas was formed at the electrodes during treatment. Due to the soil over-burden pressure, it was difficult for the gas to escape to the atmosphere and eventually accumulated at the lower part of the electrode. This results in the increase of resistance of the system and decrease in efficiency of the process. The electrode used in the field test are of different design and as can be seen from the shear strength profiles (Fig 11a to 11d), no such phenomenon of "depth effect" was observed and the strength increased throughout the depths of the electrodes.

(d) Power Consumption

The total power consumption in the field test was 2136 kWh, approximately 1 % of the total project cost. This may be compared with the case reported by Bjerrum et al (1967) in which the cost of electricity was as high as 25 % of the total project cost. The present version of electro-osmotic treatment may therefore be considered to be relatively efficient and economical. It is expected that the electricity cost of a project of similar size to that in Norway would be slightly higher due to a higher resistance and power loss in a larger treatment area. Unfortunately, comparison with other reported cases in clays could not be made because cost and consumption were seldom reported.

CONCLUSIONS

To study the applicability of the electro-osmosis process for increasing the strength of soft sensitive Champlain Sea clay, a field test was performed at the national test site. The electrodes were designed to reduce or eliminate some inherent undesirable features of the process so as to improve the efficiency of treatment. From the results of this investigation, the following conclusions may be drawn.

(a) The soft sensitive Champlain Sea clay, with an average initial undrained strength of 18 kPa, can be treated effectively by the electro-osmosis process. The increase in undrained shear strength was 60 % between electrodes of 3 m spacing and 40 % between electrodes of 6.1 m spacing in a treatment period of 32 days with a current of 40 amperes.

(b) The increase in strength is uniform throughout the entire depth of the electrodes and no "depth effect" was observed, as in some previous applications.

(c) Results of field vane tests at different times during treatment indicate that strength increase can be enhanced both in magnitude and uniformity by the technique of polarity reversal. This technique also eliminates the problem of no strength increase at cathode.

(d) Vane tests performed 43 days after treatment show that the strengths gained remain constant.

(e) The final settlement of the test area is approximately 50 mm, with a differential settlement of ± 20 %. The technique of electrode reversal is therefore a useful tool to reduce differential settlement.

(f) No pumping of expelled water is required in this "improved version" of electro-osmosis. Water flows out of the electrode 50 minutes after "switch-on". Both installation and electricity costs are reduced substantially with the electrodes developed.

From the results of this field test, it is evident that substantial increase in strength can be achieved within a practical time period with concurrent reduction in cost. It is hoped that this effective and versatile process may receive wider application in soft sensitive clays.

ACKNOWLEDGEMENTS

The research performed was supported by the National Science and Engineering Research Council of Canada under Grants No. OPG0007745 and No OPG0002743 and by a research grant from Ontario Hydro. The authors wish to express their thanks to Dr. M. Bozozuk, Dr. J.H.L. Palmer and Dr. K.T. Law of the National Research Council of Canada for their co-operation of conducting the field test, and to their technical staff for the assistance of installation of electrodes and soil sampling.

REFERENCES

Bjerrum, L., Moum, J. and Eide, O. 1967. Application of electro-osmosis to a foundation problem in a Norwegian quick clay. Geotechnique, Vol. 17, pp.214-235.

Bozozuk, M. and Leonards, G.A. 1972. The Gloucester test fill. Special Conference on Performance of Earth and Earth-Supported Structures, ASCE, Purdue University, Vol. 1, Part 1, pp.299-317.

Caron, C. 1971a. Consolidation électrochimique du sol de la Culée Rive Droite du Pont de la Basse-Chaine a Angers. Annales I.T.B.T.P., Paris, France, No. 66, pp.11-13.

Caron, C. 1971b. Consolidation des terrains argileus par électro-osmose. Annales I.T.B.T.P., Paris, France, No. 82, pp.75-92.

Casagrande, L. 1948. Electro-osmosis. Proceedings of the Second International Conference on Soil Mechanics and Foundation Engineering. Rotterdam, Vol. 1, pp.218-223.

Casagrande, L. 1949. Electro-osmosis in Soils. Geotechnique, Vol. 1, No. 3, pp.159-177.

Casagrande, L. 1952. Electro-osmosis stabilization of soils. Journal of Boston Society of Civil Engineers, January, Vol. 39, pp.51-83.

Fetzer, C.A. 1967. Electro-osmotic stabilization of West Branch Dam. Journal of the Soil Mechanics and Foundations Division, ASCE, Vol.93, SM4, pp.85-106.

Ho, K.S. 1990. Electrical strengthening of soft sensitive clays. Ph.D. Thesis. The University of Western Ontario, London, Ontario.

Lo, K.Y., Bozozuk, M. and Law, K.T. 1976. Settlement analysis of the Gloucester test fill. Canadian Geotechnical Journal, Vol. 13, pp.339-354.

Lo, K.Y., Inculet, I.I. and Ho, K.S. 1990. Electro-osmotic strengthening of soft sensitive clays. Canadian Geotechnical Journal, to be published.

Soderman, L.G. and Milligan, V. 1961. Capacity of friction piles in varved clay increased by electro-osmosis. Proceedings, 5th International Conference on Soil Mechanics and Foundation Engineering, Vol.II, Paris, pp.143-147.

Wade, M.H. 1976. Slope stability by electro-osmosis. Proceedings, 29th Canadian Geotechnical Conference, Vancouver, Section X, pp.44-66.

ATSF 1980 EL DORADO LINE CHANGE FAILURE/REHABILITATION

By Gerald P. Raymond,[1] Member, ASCE

ABSTRACT: Track support failure and rehabilitation of 14 km of railway mainline built in 1980 over a compacted clay (liquid limit 50–70) is presented. The failed construction substituted a 300-mm thick 5% lime stabilized layer for subballast. Ballast, 300-mm thick below the tie base, supported prestressed concrete ties of similar design to those used in the Northeast Corridor reconstruction. Rehabilitation addressed the problems associated with subgrade pumping, track stiffness/softness, internal and external drainage, equivalent granular cover (total depth), and the compatibility of the ballast's toughness and mineral hardness in relation to the aggregate in the concrete ties. Reconstruction used inexpensive, locally available sand-sized material for the subballast. A custom made geotextile was incorporated for extra safety. The rehabilitated track, carried out in 1984, has performed excellently.

INTRODUCTION

The Atchison, Topeka and Santa Fe Railway Company's (ATSF) mainline between Ellinor and El Dorado, Kansas, which for the most part followed the valley of the Walnut River, was first put into service in 1924. Due to increased flooding of valley farmland and the increasing threat of flooding to local towns the U.S. Army Corps of Engineers decided to construct a dam for flood control. The new dam's conservation pool, shown in Fig. 1, would cause flooding of a portion of the mainline track. To maintain service after construction of the dam a line change of about 14.5 km (9.03 mi) to higher ground was required. To eliminate delays that would occur from a long-term environmental impact study all local soil borrows, for any relocations and for the dam, were taken from areas near the riverbed that would be covered by the conservation pool.

The U.S. Army Corps of Engineers requested the ATSF railway to undertake the railway relocation design, subject to final review by the Corps of Engineers. The ATSF railway employed a consulting engineering firm and a geotechnical engineering subconsultant to design to at least the then current recommendations of the American Railway Engineering Association's (AREA's) *Manual for Railway Engineering* (1979).

The line change, as built, is 1.14 km (0.713 mi) longer than the original track, has a maximum curvature of 1°, a maximum grade of 0.37%, and averages 6.5 m (21.5 ft) higher in elevation than the abandoned track. The track was constructed with 68-kg/m (136-lb/yd) rails and Northeast Corridor (NEC) concrete type ties and NEC hard tie pads. The riverbed borrow area used for the line change was composed of silty clay with liquid limits, in the range of 50 and as high as 70. The compacted densities of the fill were not less than 95% Standard Proctor up to a depth 1.6 m below formation level (i.e., 1.6 m below the subgrade/track support interface). For

---

[1] Prof., Dept. of Civ. Engrg., Queens Univ., Kingston, Ontario, Canada K7L 3N6.

Note. Discussion open until January 1, 1992. To extend the closing date one month, a written request must be filed with the ASCE Manager of Journals. The manuscript for this paper was submitted for review and possible publication on May 15, 1990. This paper is part of the *Journal of Geotechnical Engineering*, Vol. 117, No. 8, August, 1991. ©ASCE, ISSN 0733-9410/91/0008-1191/$1.00 + $.15 per page. Paper No. 26063.

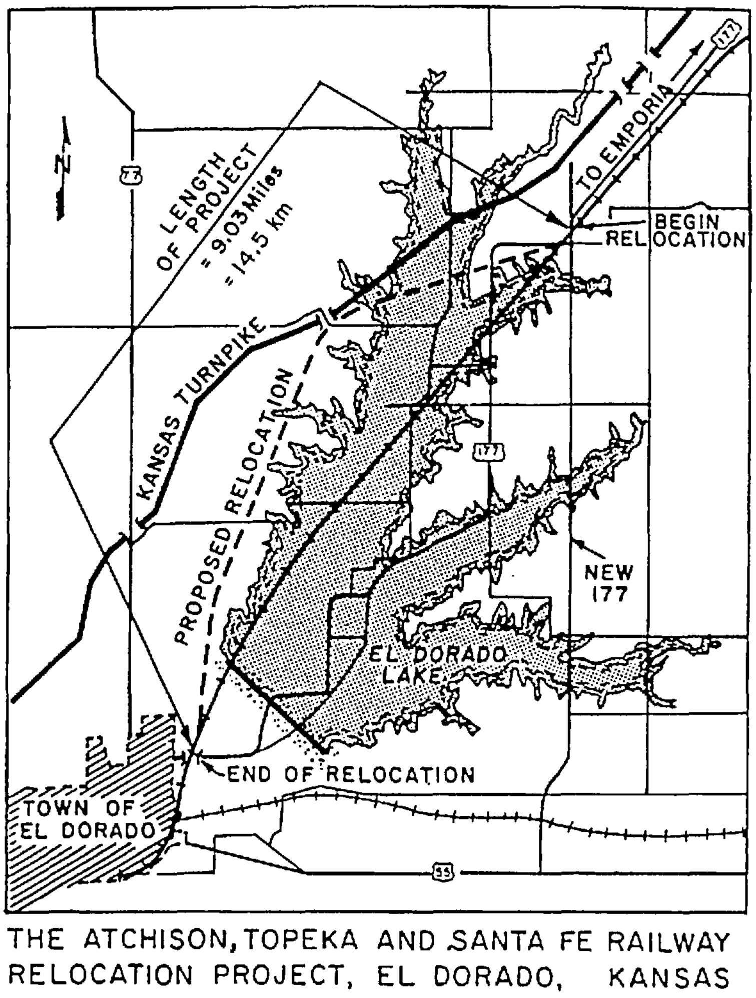

FIG. 1. Map of Line Change and El Dorado Lake

the last 1.6 m compaction was not less than 100% Standard Proctor. Because of possible artesian conditions all rock cuts were covered with a 0.3-m (12-in.) compacted layer of borrow soil to formation level.

From the formation level the track support structure, which is shown in Fig. 2, consisted of a 0.3-m (12-in.) 5% lime-stabilized borrow material layer covered by a 0.3-m (12-in.) ballast layer graded AREA No. 4 (*Manual* 1979) below the concrete crosstie base. A 0.15-m to 0.3-m (6-in. to 12-in.) lime-stabilized layer was, at the time, the standard method used by the ATSF railway as subballast for new construction (mainly branchlines) using timber crossties. The El Dorado project was the first time concrete crossties were used by ATSF on a major length of track. An access road of 0.3-m (12-in.) lime-stabilized wearing surface was located next to the track. While the ac-

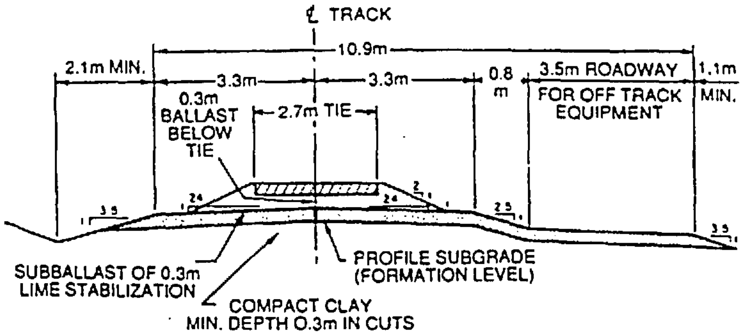

FIG. 2. Typical Cross Section of Line Change (1 m = 3.3 ft)

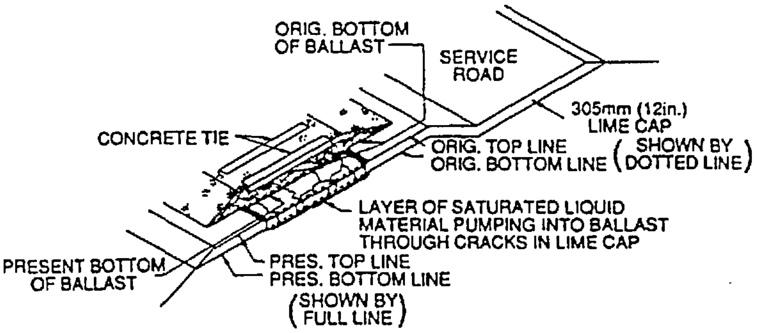

FIG. 3. Conceptual Condition of Failed Track

cess road remained intact its surface became muddy in wet weather and dusty in dry weather. As seen in Fig. 2 the access road's top elevation was at formation level.

The line change track was placed into revenue service on May 14, 1980, and the speed was gradually increased over three days reaching up to 125 km/hr (79 mph) on straight track sections. Annual tonnage was in the range of 55,000,000 gross T (60 MGT) and was from mixed traffic. Deviations of line and level were recorded in the spring of 1981 after some heavy rainstorms and the deviations increased during the year, requiring major slow orders as low as 16 km/hr (10 mph) by January 1982. A number of investigations were initiated in 1981 followed by a 0.2-m (8-in.) raise of ballast in January 1982 over the whole line change. The track raise initially allowed speeds to be increased to 65 km/hr (40 mph). Unfortunately it was only of temporary value and in October of 1982 the writer was requested to suggest possible solutions.

PRIOR INVESTIGATIONS

During the spring and summer of 1981 the ATSF conducted investigations in conjunction with Maxim Engineering (Perdue 1981) and the Association of American Railways (AAR) ("The El Dorado").

Maxim Engineering established that the limecap had fractured without loss of compressive strength and that the upper surface of the compacted clay formation had softened, mixed with rainwater, forming a slurry that migrated under traffic loading through the limecap fractures, fouling the ballast. A minimum limecap unconfined compression strength of 360 kPa (7,200 lb/sq ft) was measured. Strengths ranged up to 1,260 kPa (25,200 lb/sq ft). Conceptually their conclusions are shown in Fig. 3. The migration of clay solids had resulted in the top of the limecap surface area directly below the ties settling to an elevation of about 30 mm (1.2 in.) less than the adjoining shoulder surface area. This allowed trapping of rainwater, which aggravated the pumping phenomenon.

The AAR instrumented the line change in September 1981 at mile post (MP) 167.8 and that of the adjacent unchanged track having wooden crossties at MP 162.9. The AAR instrumentation involved placement of settlement meters and pressure cells on the surface of the limecap plus pressure cells in the unchanged track. The settlement readings were taken weekly by the ATSF personnel. In addition, load/deformation readings sufficient to calculate track moduli were taken.

The settlement meters at MP 167.8 (five in total) were placed directly below a rail on the limecap in a rock cut where the rock had initially been covered with 0.3 m (12 in.) of compacted clay plus the limecap. Readings observed to the time of the writer's investigation are shown in Fig. 4. Fig. 4 shows the settlement of: (a) The base of the rail; (b) the average settlement of the three settlement meters placed below the same rail and midpoint between the ties; and (c) the average settlement of two settlement meters placed below the same rail and below the ties. Monthly rainfalls have been added at the top of Fig. 4. As seen, during the time of the plotted readings over 125 mm (5 in.) of limecap settlement was recorded. This is also seen as the main cause of rail settlement. No settlements were taken on the old existing wood tie track, which showed no major distress. A subsequent excavation of this track, requested by the writer, revealed about 1.5 m (5 ft) of granular fill overlying the original clay embankment. Extensive grout injection was evident within the granular layers, indicating past instability problems.

In January 1982 two further sections were instrumented with settlement meters by the ATSF railway and the results are shown in Fig. 5. Both instrumented sections were on fill, one of approximately 6-m (20-ft) thickness and the other of approximately 9 m (30 ft). The results shown in Fig. 5 are not significantly different from the results recorded over the same time period (weeks 17–54) shown in Fig. 4. These results confirm, in the writer's opinion, the conceptual failure mechanism shown in Fig. 3. That is, the large settlements were due to erosion of the surface of the untreated clay fill at the interface with the limecap rather than settlement of the underlying compacted materials or its underlying foundations.

The AAR pressure cell instrumentation involved four test configurations. For all configurations the pressure cells were placed directly below a rail. One cell was below a tie (i.e., rail seat) and another was placed below the same rail at the centerline of the crib. For all four configurations an excavation, two-cribs and one-tie wide, made to 0.3 m (12 in.) below the existing base of the tie (on the line change this was to the top of the limecap), was the method of installation. For three configurations the track was recon-

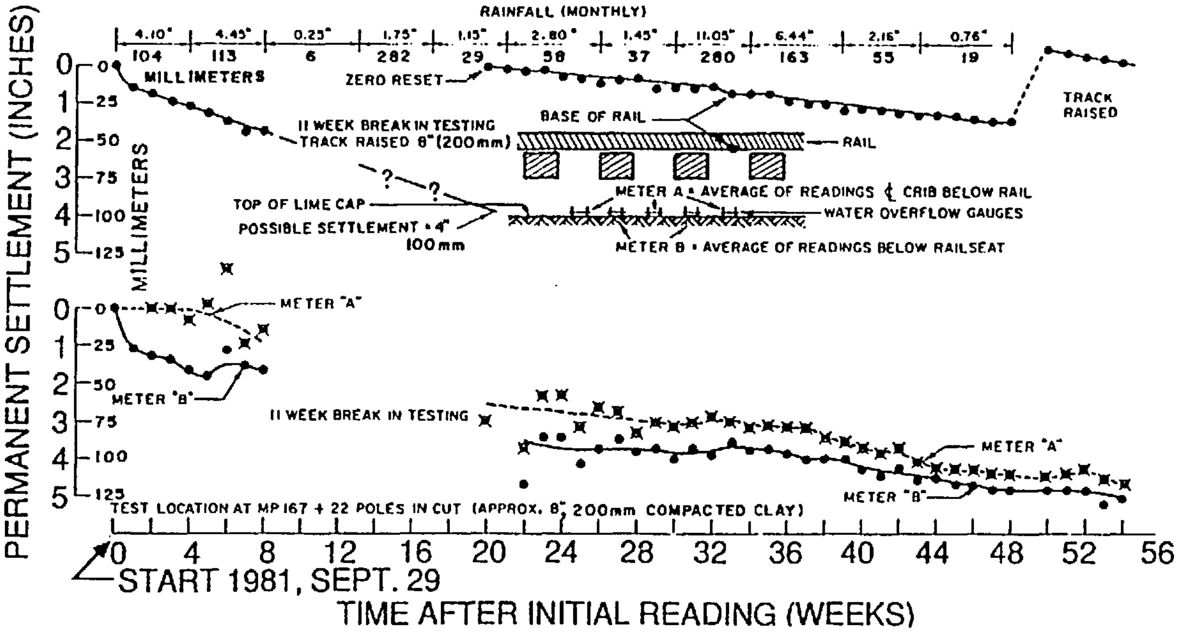

FIG. 4. Settlements from Cut Location

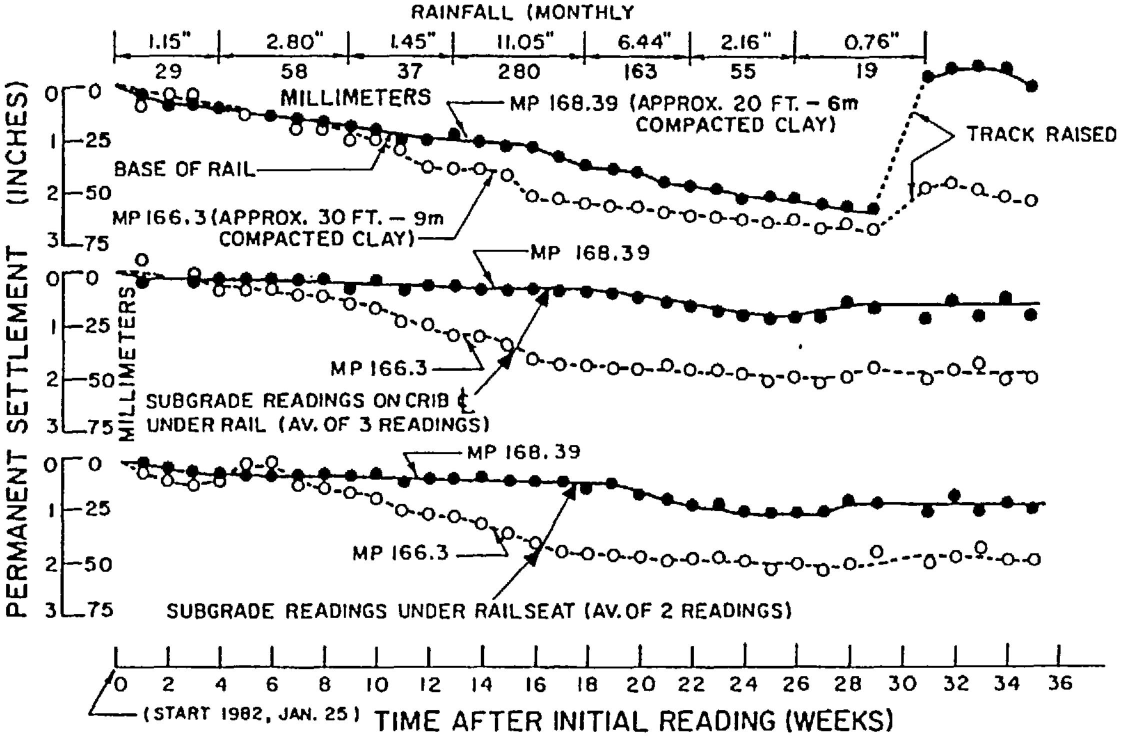

FIG. 5. Settlements from Embankment Locations

TABLE 1. El Dorado Static Loading Test Results

Configuration (1)	Rail deflection (mm) (2)	Track modulus (MN/m/m) (3)	Vertical Stress Measured (Calculated at Top of Limecap)	
			Rail seat (4)	Crib (5)
Wood-tie track	4.14	19	43 (93)	24 (66)
Concrete Northeast Corridor hard pad	0.84	110	59 (115)	23 (61)
Concrete Northeast Corridor soft pad	0.97	93	55 (112)	29 (60)
Concrete hard pad plus raise 200-mm ballast	1.60	52	46 (73)	28 (63)

Note: 1 mm = 0.04 in; 1 MN/m/m = 143 lb/in./in.; 1 kPa = 20 lb/sq ft.

structed on the cells with a 0.3-m (12-in.) ballast cover below the base of the tie (i.e., refilling the excavation and tamping the track). One was on the 1924 built (wood tie) track, while the other two were on the line change. The two configurations on the line change involved the same track with the only difference in these two tests being a change of the tie pad between the rail and the tie's rail seat. The harder pads used were those installed during the line change construction and had properties identical to those used initially on the Northeast Corridor (NEC). The softer pads used were those selected as standard for all further NEC installations at the time when about 50% of the NEC concrete ties had been installed. The fourth configuration was on the line change and involved the same track as just mentioned using the hard pads but with 0.5 m (20 in.) of ballast below the base of the concrete ties (i.e., a raise of 0.2 m or 8 in.).

The rail deformation and pressure cell readings measured by the AAR below a tie loaded with the central axle of the front truck of a GE type U36c locomotive are given in Table 1 along with the writer's estimated value of track modulus and calculated vertical stresses based on the methods outlined in detail elsewhere (Raymond 1985a). Clearly, the calculated stresses are much greater than actually measured; however, this may be due to differences in the compressibility of the cells in comparison with the ballast or due to arching across the sides of the excavations into which the cells were placed. While the theoretically calculated and measured stresses may not agree they nevertheless show similar trends insofar as the lower the track modulus the lower the stresses at the same depth below the tie base. Similarly, a greater depth of ballast reduces the track modulus and also reduces the vertical stresses. What is the optimum value of track modulus, however, is a debatable question for which there are varying opinions.

SITE VISIT OF OCTOBER 9, 1982—IN CUT

The day of the writer's site visit was sunny and dry; however, the ground was saturated with rain, which had been heavy during the previous day. At MP 167.8 in cut territory a tie was pulled and an excavation made. The

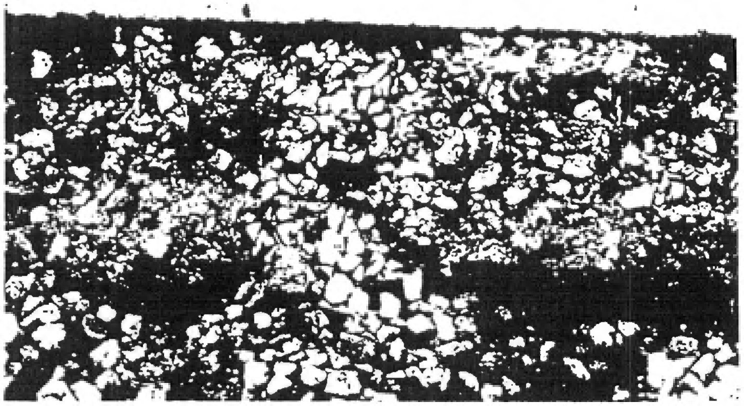

FIG. 6. Example of Ballast Grinding at Contact Face with Concrete Ties

ballast was 0.33-m (13-in.) deep and there was a clear division between the original badly degraded and subgrade fouled ballast and the recent 0.2-m (8-in.) ballast raise. The new ballast was excessively degraded due to the high loads and abrasive environment of the concrete ties on the limestone/dolomite ballast that had been used. A typical example of this degradation is seen in Fig. 6. Most of the small particles on the excavation face dropped down from the tie/ballast contact area during excavation. Concrete ties are invariably manufactured using silica sands whose Moh's hardness approximates 6.5–7. Limestone has as its primary mineral calcite, which has a Moh's hardness of 3 while dolomites are composed of minerals having a Moh's hardness of 3.5. As previously stated elsewhere by the writer (Raymond 1985b) such large differences are bound to cause major abrasion to the softer minerals—in this case the ballast.

The excavation, from the centerline to some 0.6 m (24 in.) beyond one end of the removed tie, was taken down to below the limecap. The limecap was 0.33-m (13-in.) thick on the centerline. Below the limecap were thin voids the thickness of a knife blade from which slurried clay flowed. A typical example of the slurry flow is shown in Fig. 7. The limecap 0.4 m (16 in.) beyond the end of the removed tie was 0.36-m (14-in.) thick and was firmly bedded on the underlying compacted clay.

Below the rail seat the compacted clay was measured to be 0.2-m (8-in.) thick and was founded on a bedrock. A Torvane was used to measure the shear strength of the compacted clay (i.e., half the unconfined compression strength). This was 70 kPa (1,000 lb/sq ft) on the surface below the slurry and 100 kPa (2,000 lb/sq ft) 25 mm (1 in.) below this surface. At the depth of 25 mm (1 in.) below the slurry six 25-mm (1-in.) thick consolidometer rings were pushed into the compacted clay and carefully excavated to give six undisturbed ring samples. These were protected in plastic seal wrap for laboratory testing.

While the excavation was open the inspection was interrupted by the pas-

FIG. 7. Example of Slurry at Formation Level

sage of two trains. During the passing of the first train, mud flowed out of the east face from a location just below the limecap while on the west face mud flowed out from about the midheight (construction plane) of the limecap. During the passage of the second train, a second west face outlet developed. This was below the limecap at the limecap/clay interface.

In addition to the observations in the excavation it was noted that considerable ditch infilling with soil had occurred in the cut area. Standing water existed at an elevation close to the bottom of the limecap.

SITE VISIT OF OCTOBER 9, 1982—EMBANKMENT

A second tie was pulled and excavation made at MP 169.15. At this location the embankment consisted of over 6 m (20 ft) of compacted clay.

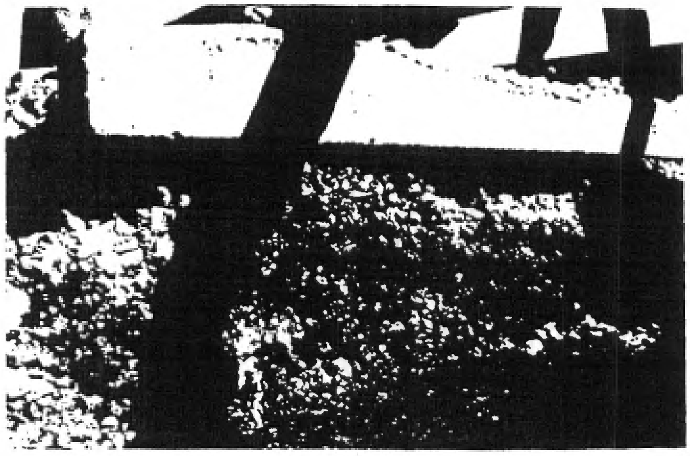

FIG. 8. Example of Pumping below Railseat

Excavation was first made to the top of the limecap. Below the railseat of the east side the mud had pumped right up to the face of the tie base while at the centerline of the track the mud interface was 225 mm (9 in.) below the tie base. The pumped mud below the railseat was typically pyramid shaped as would be given by theory assuming higher stressed areas pump faster. A typical observation is shown in Fig. 8. Below the rail seat of the west side the mud had pumped up to 150 mm (6 in.) below the tie base and at the centerline the mud was 225 mm (9 in.) below the base of tie. The measured depth to the top of the limecap from the base of tie was 0.53 m (21 in.) at both the centerline and rail seat of both excavated faces. On the excavated surface of the limecap a seepage hole was clearly evident where mud was pumping and eroding through the limecap.

The excavation was then extended through the limecap. The measured limecap thickness was 0.3 m (12 in.) below both the centerline and rail seat of both sidewalls. At this point the work was stopped for the passage of two trains. During the passage of these trains, mud was gushing out (pumping several centimeters into the air) at a location directly below the railseat of the east wall tie. As far as could be determined, this mud was coming from the limecap/clay interface.

After the passage of these two trains, the excavated surface was taken down another 25 mm (1 in.) by hand and consolidation ring samples taken in the same manner as at the previous site.

LABORATORY TESTS

Several of the consolidation ring samples were trimmed, immediately immersed in water and loaded via a porous stone to uniform loads as small as 3 kPa (60 lb/sq ft). After soaking for 4 days these samples all had shear strengths measured with the Torvane greater than 100 kPa (2,000 lb/sq ft).

A second test involved trimming pairs of ring samples, then extruding them, immersing one immediately in water while allowing the second to air

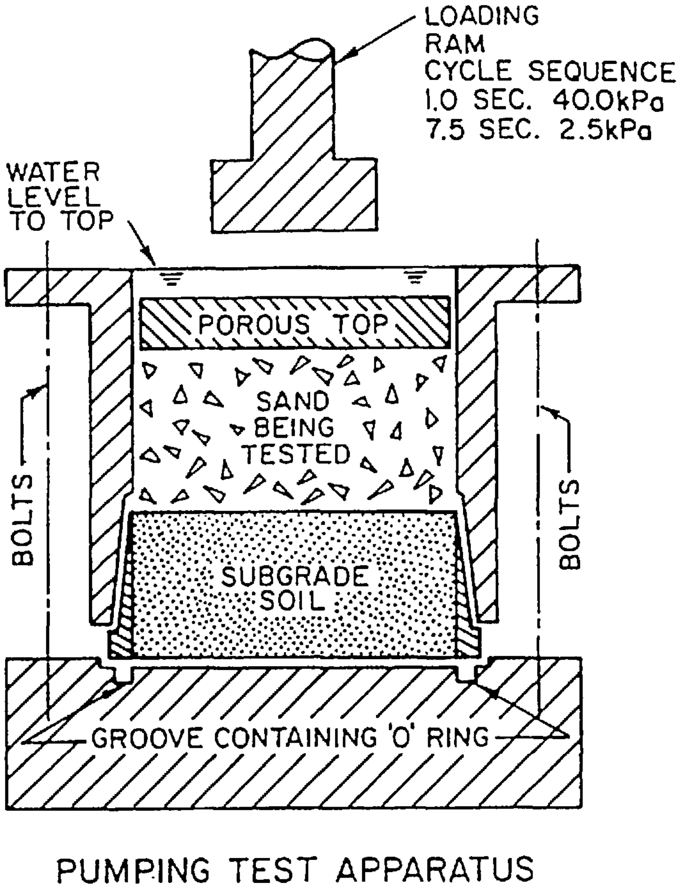

FIG. 9. Apparatus for Repeated Load Tests (1 kPa = 20 lb/sq ft)

dry for 24 hours and then immersing it. In each case the air dried sample collapsed within 24 hours of immersion while the other sample remained intact and maintained a high strength. This suggests that much of the slurry formed in the field occurred due to drying and wetting at the limecap-compacted clay interface after the limecap fractured.

Pairs of ring samples obtained from below the rail seat of each location were trimmed, immersed in water, or partially air-dried and immersed in water, while being confined in the apparatus shown in Fig. 9. Each sample was covered with a presieved local sand from the El Dorado area. The presieve involved sieving through a No. 10 (2-mm) sieve to remove any plus-2-mm size particles. The grain sizes of the two sands, the test sand samples and the clay samples are shown in Fig. 10. A set of results of the repeated load tests is shown in Fig. 11. It may be seen that the clay failed to penetrate the finer so-called quartzite sand—a quarry crusher waste material, while the so-called filter sand was completely fouled with clay despite its name. As seen in Fig. 10 the quarry waste consisted of about 5% material passing

TABLE 2. Shear Box Tests σ_n = 50 kPa (1,000 lb/sq ft)

Compaction (1)	ϕ (dry soil)		e_0	
	Quartzite (2)	Filter (3)	Quartzite (4)	Filter (5)
Loose	32.6	39.6	0.67	0.57
Dense	42.4	58.9	0.55	0.42

shown in Table 2. The low strength obtained with the quartzite material points to the importance of good compaction when using this material.

PROBLEMS TO BE SOLVED

The major problems requiring solutions were:

1. Stop the subgrade clay from migrating (pumping).
2. Ensure sufficient granular cover so that the subgrade is not overstressed.
3. Ensure the track stiffness is soft enough to prevent tie damage from impact loading and stiff enough to keep cyclic maintenance low.
4. Ensure good internal and external drainage so the rainfall can get out faster than it can get in, and so that the ditches do not contain standing water.
5. Ensure compatibility of the ballast used with concrete ties.

PROBLEM SOLUTIONS

From the laboratory test results shown in Fig. 11 clay particle migration may be stopped by using a layer of well-compacted quartzite sand. This material was cheap, costing $1.10 per tonne ($1.00 per ton). This was about 20 times cheaper than a graded highway granular A. Its grading is also less likely to result in segregation of particles.

The field investigations failed to locate any shear failures in the subgrade soil, suggesting that 0.6 m (24 in.) of granular cover or granular-plus-limecap cover should be adequate for the existing traffic; however, much of the traffic passed under conditions of imposed slow orders. Impact loading is known to increase with speed (*Manual* 1979; Raymond 1985a). An increase in granular cover above 0.6 m was justified after consideration of the higher-impact loadings probable from higher speeds.

Track modulus has an important effect on the design of a concrete tie track structure. With wood tie construction it is commonly stated that the stiffer the track the better. This statement is reasonable because the compressibility of the wooden ties allows them to absorb impact loadings. Concrete is much stiffer than wood and also easier to damage. The significance of stiffness and impact loading is illustrated in Fig. 12 where, for the same impact, it is seen that the spring (track support) force is related directly to the square root of its stiffness. Typical calculations for different track constructions have been done previously (Raymond 1985a) and are shown again in Fig. 13 to illustrate herein the immense increases that can occur in the track support stresses from realistic wheel impacts on too stiff a track. Careful consideration was therefore given to track modulus determination using the methods outlined previously (Raymond 1985a).

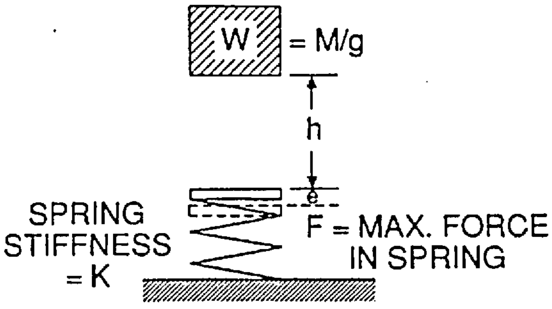

ENERGY FROM FALL = W (h+e)

ENERGY ABSORBED BY SPRING = F.e/2

= F (F/K)/2

$$\therefore F = [K.M]^{0.5} [2(h+e)/g]^{0.5}$$

FIG. 12. Example Showing Importance of Track Stiffness on Support Forces from Impact Loading

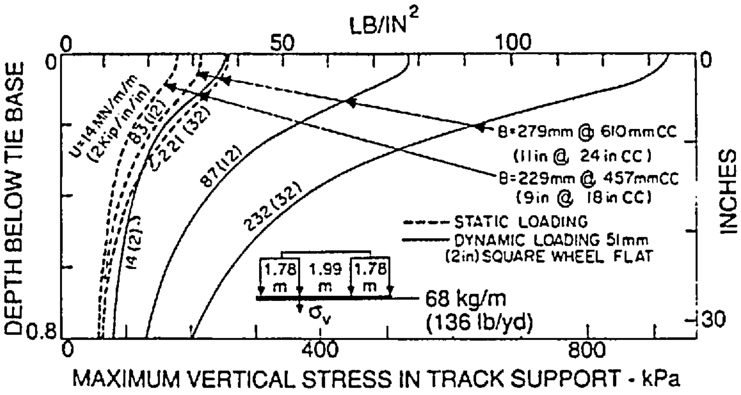

FIG. 13. Example of Estimated Vertical Stresses in Track Support for Static Loading and Severe Impact Loading for Track of Different Stiffness (Raymond 1985a)

The track modulus has to lie within a given range to minimize cyclic maintenance and tie damage. This range varies with different personal opinions but is generally in the range of 14 MN/m/m (2,000 lb/in./in.) of rail to 46 MN/m/m (8,000 lb/in./in.) of rail. Using methods outlined previously (Raymond 1985a), it was estimated that using 100 mm (4 in.) of quartzite sand, 100 mm (4 in.) of filter sand, 100 mm (4 in.) of 3 mm (0.125 in.) plus screenings from the ballast waste, and 300 mm (12 in.) of AREA No. 4 graded Ballast supported on a rigid base (assumed rigid limecap) would give a track modulus in the range of 28 MN/m/m (4,000 lb/in./in.) of rail. These quantities placed on the access road plus the use of a 1,050 g/m^2 (30

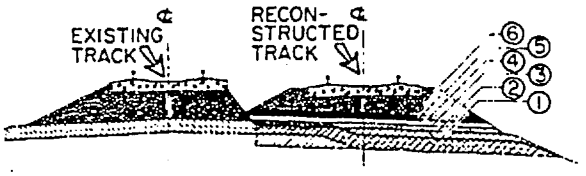

ALL INTERFACED LAYERS WITH 1:24 SLOPE

①-RECONSTRUCTED LIME CAP; ②-FINE SAND; ③-COARSE SAND; ④-GEOTEXTILE; ⑤-FINE GRAVEL SIZED SCREENINGS; ⑥-BALLAST

FIG. 14. Rehabilitation Cross Section

oz/sq yd) custom-made resin-treated geotextile to CN rail specification (Raymond 1988; Raymond and Bathurst 1990) between the sand and screenings represented the final granular or granular equivalent cover solution. The geotextile was selected, based on its excellent performance in CN track, and the writer's observations that no standard manufactured geotextile then available performed satisfactorily in a track situation. The geotextile was used as a safety measure against ballast fouling from either the subgrade or sand layers. This decision was based on the importance of the track and ATSF's request to be conservative in the design to ensure no future failures. The geotextile also facilitated construction as the sand layers showed considerable rutting where construction equipment was allowed to traffic the compacted surface prior to the geotextile placement. After geotextile placement little rutting was observed.

Internal drainage was designed for by using a 4% slope on all granular layer interfaces and by placement of the geotextile below the crushed screenings and above the local sands. The screenings and ballast are crushed, controlled, graded material free of fines, which should drain easily to the geotextile while the sands would be obtained as found. External drainage was already existing once the infilled ditches were cleaned out.

Good-quality ballast aggregate in the mid-United States is scarce. After examination of several aggregates, ballast aggregate/concrete tie compatibility was ensured by the use of a hard dark grey fine igneous rock. Thin section analysis indicated fine platey feldspar crystals that were evenly distributed with pyroxene crystals. They had no preferential orientation. There were no visible microfractures on any of the thin sections examined although one macrofracture was evident. Such an intensity of fractures was judged to be insufficient to cause major degradation of a railway ballast. The ballast's mineralogy was judged to be of stable character and unlikely to weather quickly. The compatible hardness of the minerals with that of typical concrete sands along with the above characteristics judged the basalt to be both suitable and the best ballast material examined.

The final section design, having thicknesses as recommended earlier in this section, is shown in Fig. 14. The track was rebuilt on the access road to minimize traffic interruption. The ATSF chose to remake the access road limecap by scarification and mixing with sand and fly ash for a remade limecap thickness of 0.45 m (18 in.).

POSTREHABILITATION PERFORMANCE

Reconstruction of the line-change track became necessary after numerous ballast lifts had been applied to maintain the track open to traffic. Fouled ballast depths of over 650 mm (28 in.) existed on many areas of the track prior to rehabilitation. The track was reconstructed in the summer of 1984 using the section shown in Fig. 14. Details of the reconstruction methods have been published elsewhere ("El Dorado" 1984; "El Dorado" 1985).

In April 1985, after one of the wettest winter/early springs on record, a site visit was made to assess the geotextile's performance. It was noted that as each set of coupled freight car wheels of a passing train traversed a given point water was pumped horizontally along the geotextile and was discharged from the geotextile's edge to the ditch. This illustrated the value of the geotextile in facilitating internal drainage and the importance of installing geotextiles, when used, so that water drains by gravity through the geotextile away from the load-bearing area of the track to the ditch. If, as seems reasonable, the water has come from the sand below the geotextile then water drainage under rapid loading was upwards. The geotextile is an extremely effective separator to prevent sand particle migration from fouling the ballast. The same is true should ice lensing occur in the sand during freezing weather.

Since being placed into service in August 1984 mixed traffic totaling annually about 55,000,000 gross T (60 MGT) has traversed the rehabilitated track at the design speeds without any out-of-face cyclic maintenance. Furthermore no out-of-face cyclic maintenance is presently (April 1990) planned. Over 300,000,000 gross T (330 MGT) of traffic have not caused sufficient track deviations to require any out-of-face cyclic maintenance. This is a very large amount of traffic compared with most track in revenue service [see Raymond (1985b)] and is a testament to the quality of the rehabilitation design and construction. Although it cannot be proven the writer is of the opinion that the large maintenance cycle is in part due to the geotextile's function of facilitating drainage and maintaining a separation face between the manufactured graded granular layers and the obtained (as found) granular layers.

SUMMARY AND CONCLUSION

The failure of a recently designed mainline railway track has been presented along with investigations and instrumentation used to establish a rehabilitation design. The investigations established the necessity of: (a) Preventing pumping by a material other than a lime-stabilized layer; (b) ensuring a sufficient granular cover to protect the subgrade that gave a soft enough track modulus to prevent high-impact loadings, but stiff enough to give a high cyclic maintenance cycle; (c) ensuring good internal and external drainage; and (d) selecting a ballast whose minerology was compatible with that of the sands used for concrete aggregate.

The case study establishes the importance of a granular layer, graded to prevent subgrade pumping, in railway track-support design involving stabilized soil layers. The postconstruction behavior of the incorporated geotextile clearly indicates the importance of installing geotextiles to facilitate internal drainage and its preferred transmissibility over the installed sand.

The rehabilitation cross section is shown in Fig. 14 and has proven to give excellent service without requiring out-of-face cyclic maintenance after more than 300,000,000 gross Tonnes (330 MGT) of traffic.

ACKNOWLEDGMENTS

The El Dorado investigations were done with the cooperation of Mr. Keith Pottorff, district engineer in 1982, and Mr. Leroy Draper, division engineer in 1982 of the ATSF Railway. Their cooperation is gratefully acknowledged as is the Atchison, Topeka and Santa Fe Railway Companies' permission to publish this article.

APPENDIX. REFERENCES

"El Dorado Line: Why good track turned sour." (1984). *Railw. Track Struct.*, 80(1), 22–26.

"El Dorado Line: Why good track turned sour." (1985). *Railw. Track Struct.*, Jan., 23–28.

Manual for railway engineering. (1979). American Railway Engrg. Association, Washington, D.C.

Perdue, G. W. (1981). *Geotechnical investigation for field and engineering evaluation El Dorado Lake track relocation project, El Dorado, Kansas.* Maxim Engineering Inc., Dallas, Tex., Oct. 26, 1981.

Raymond, G. P. (1985a). "Analysis of track support and determination of track modulus." *Transp. Res. Rec.*, 1022, 80–90.

Raymond, G. P. (1985b). "Research on railroad ballast specifications and evaluation." *Transp. Res. Rec.*, 1006, 1–8.

Raymond, G. P. (1988). "Railway track geotextiles." *Proc. Third Canadian Symp. on Geosynthetics*, Committee on Geosynthetics of the Canadian Geotechnical Society.

Raymond, G. P., and Bathurst, R. J. (1990). "Test results on exhumed railway track geotextiles." *Proc. Fourth Int. Conf. on Geotextiles and Related Produces.* International Geotextile Society, 1, 197–202.

The El Dorado Line change field test results. (1982). Association of American Railroads, Chicago, Ill., Jan.

FIELD BEHAVIOR OF EXCAVATION STABILIZED BY DEEP SOIL MIXING

By T. D. O'Rourke,[1] Member, ASCE, and C. J. O'Donnell,[2] Associate Member, ASCE

ABSTRACT: This paper describes the performance of a tiedback excavation with a soil mixed wall in Boston where underlying marine clay was stabilized by deep soil mixing (DSM) and jet grouting. Lateral and vertical soil displacements, soil strains, and tieback loads are evaluated. The interaction between the retained soil and a reinforced concrete box culvert, supported on drilled shafts, is described. Piezometer measurements behind the wall are summarized. They show pore-water pressures in marine clay substantially less than the hydrostatic pressures assumed in design.

INTRODUCTION

Deep soil mixing (DSM) involves the in-situ mixing of soil and cement with special equipment, frequently using rigs with counterrotating augers [e.g., Taki and Yang (1991)]. The method (Terashi and Tanaka 1981) has been applied extensively for stabilization of natural and dredged marine clays, and has been used to strengthen clays at the base of braced excavations (Tanaka 1993).

Despite the growing use of DSM, there are many questions regarding its field strength and deformation characteristics, its influence on ground displacement patterns, and its effect on pore-water pressure and loads conveyed to excavation support systems. This paper presents a case history of DSM and jet grouting to stabilize a tiedback excavation in Boston. This paper presents and interprets field measurements of soil displacements, tieback loads, and pore-water pressures, providing field evidence essential for clarifying the performance of excavations stabilized by these procedures.

SITE DESCRIPTION

The tiedback excavation is described by O'Rourke and O'Donnell (1997) in a companion paper. The excavation location and plan view are presented in Figs. 1 and 2, respectively. Cut-and-cover techniques were used at this site to construct a reinforced concrete structure for Highway I-90. Temporary support was provided by means of a soil mixed wall (SMW) with earth-anchored tiebacks. The SMW was installed by means of a triple auger rig, with 860-mm diameter overlapping soil mixed columns. Structural reinforcing for the wall was provided by steel sections (W21 × 50) on 1.22-m spacings. Tiebacks were postgrouted typically 24 h after initial grouting with a process similar to the tube-a-manchette method [e.g., Xanthakos et al. (1994)].

Cross-section A-A marks the location where excavation performance prior to DSM is described by O'Rourke and O'Donnell (1997). Cross-section B-B′ marks the location of interest in the present paper. The final excavation depth was 15.25 m. Temporary support was provided by six levels of tiebacks, five of which were anchored in marine clay; the lowest level was anchored in dense glacial deposits, 30 m below ground surface.

DEEP SOIL MIXING AND JET GROUTING

DSM and jet grouting were used to reinforce the excavation base against deep rotational failure. These measures were taken after the excavation had achieved a depth of 8.1–10.9 m. Hence, the SMW buttresses and jet grout zones were installed under conditions where there was differential vertical loading and potential horizontal stress imbalance. The combined DSM and jet grout made up 35% of the soil volume in the treated zone, as shown in Fig. 3.

The primary component of the system was a series of parallel DSM buttresses on 2.4-m centers. The buttresses were composed of a single line of interlocking DSM columns connected near the wall to three rows of DSM columns.

Unconfined compression tests were performed on specimens sampled at depths of 6–12 m in uncured DSM panels. Tests were performed on cylindrical specimens of two different sizes: (1) 150-mm diameter by 300 mm high; and (2) 75-mm diameter by 150 mm high (GeoTesting 1994). Specimens were cured for 7–56 d, and only a small or negligible increase in strength was observed after 7 d curing. The mean strength of 37, 150-mm diameter and 51, 75-mm diameter specimens was each 3.83 MN/m^2, with coefficients of variation of 0.49 and 0.47, respectively.

Jet grout was placed between the wall and the buttresses. A two fluid system of grouting was used in which a high pressure jet of grout penetrates the soil within an envelope of compressed air. Three pairs of grout columns were injected at each buttress location.

The construction sequence is illustrated in Fig. 4. Construction began on the DSM buttresses when the excavation was

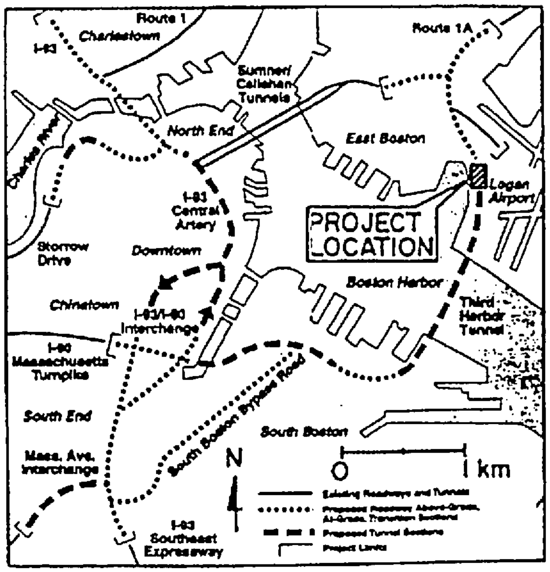

FIG. 1. Plan View of Boston CA/T Project with Location of BIF Site

---

[1] Prof., School of Civ. and Envir. Engrg., Cornell Univ., Hollister Hall, Ithaca, NY 14853.

[2] Engr., Mueser Rutledge Consulting Engrs., New York, NY 10017.

Note. Discussion open until November 1, 1997. Separate discussions should be submitted for the individual papers in this symposium. To extend the closing date one month, a written request must be filed with the ASCE Manager of Journals. The manuscript for this paper was submitted for review and possible publication on December 14, 1995. This paper is part of the *Journal of Geotechnical and Geoenvironmental Engineering*, Vol. 123, No. 6, June, 1997. ©ASCE, ISSN 1090-0241/97/0006-0516–0524/$4.00 + $.50 per page. Paper No. 12237.

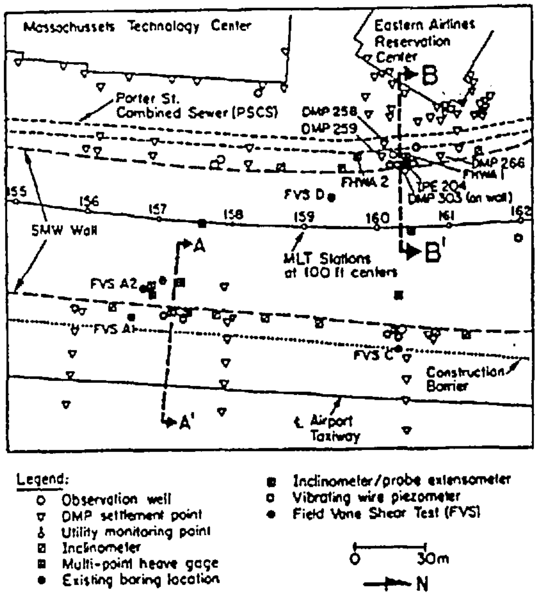

FIG. 2. Plan View of BIF Excavation and Instrumentation

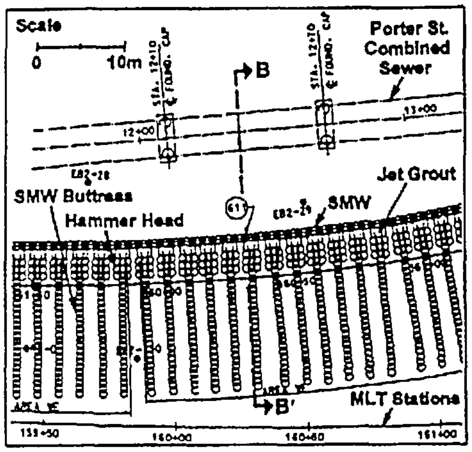

FIG. 3. Plan View of Base Stabilization Scheme

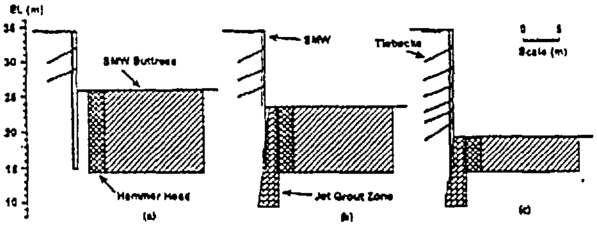

FIG. 4. Construction Sequence for Base Stabilization Scheme: (a) Construction of SMW Buttress; (b) Jet Grouting; (c) Final Subgrade

at elevation 25.9 m. At this location the buttresses were 16.2 m long and were installed to elevation 14.3 m, just 0.6 m below the bottom of the wall. The buttresses were terminated in marine clay to avoid creating zones of substantially different stiffness and settlement characteristics beneath the permanent highway structure to be built within the excavation.

The excavation was taken to elevation 23.5 m before jet grouting. Grout was injected to elevation 9.4 m, 5.5 m below the bottom of the wall. Inclined grout columns were used to provide vertical as well as lateral support of the wall.

SOIL CONDITIONS

The soil conditions have been described by O'Rourke and O'Donnell (1996). The soil profile at station 160 + 30 (see Fig. 5) consists of approximately 7 m of granular and cohesive fill underlain by a 1-m thick layer of organic silt and a 23-m thick deposit of marine clay. The water table was 3 m deep, and the marine clay is underlain by a 10-m thick deposit of glacial soils overlying bedrock. Table 1 summarizes the characteristics and relevant properties of each soil layer. Fig. 5 shows the soil profile relative to the excavation support system and structures adjacent to the deep cut, as described in the next section.

MEASUREMENTS OF EXCAVATION PERFORMANCE

A plan view of the instrumentation at and near the Mainline Tunnel (MLT) Station 160 + 30 is shown in Fig. 2. Of particular interest are three inclinometer/probe extensometers (IPEs), labeled IPE 204, Federal Highway Administration (FHwA-1), and FHwA-2, which were installed at distances of 0.6, 3.66, and 6.71 m behind the wall. An IPE is an inclinometer equipped with extensometer magnets that are used to measure settlements at various depths. The close proximity of the IPEs along the excavation alignment and the similarity in depths, support installation, and excavation operation at the IPE locations makes it possible to use the instruments to estimate strains from soil deformations within approximately the same plane perpendicular to the wall.

The array of instrumentation at cross-section B-B' is illustrated in Fig. 5(a). The locations of deformation measurement points (DMP) are also included in this figure. As can be seen in Fig. 5(a), the excavation was adjacent to the Porter Street Combined Sewer (PSCS), a posttensioned reinforced concrete box culvert supported by twin 1.22-m diameter drilled shafts on 18.3-m centers. The support for the culvert is included in Fig. 5(a) for illustrative purposes but is omitted in the other figures because cross-section B-B' was located along the span between supports, as shown in Fig. 3.

O'Rourke and O'Donnell (1996) provide a detailed evaluation of the excavation, which was separated into five principal stages, as listed in Table 2. Cumulative ground movements for the last three stages are presented in Figs. 5(b)–5(d) in which the soil strata, excavation support system, and PSCS are drawn to scale. The tiebacks shown in the figures were instrumented with load cells, and the bond zones and free lengths in the figures represent the as-built dimensions taken from the proof test records. The length of every other tieback at a given level was staggered by approximately 6 m to avoid concentrating anchors within a relatively small zone. The tiebacks shown in Figs. 5(b)–5(d) were of maximum length, with the exception of the fifth level where tiebacks were 6 m shorter than those on either side. The displacements shown in Figs. 5(b)–5(d) are described under the subsections that follow.

Stage 3

Fig. 5(b) shows the excavation after completion of the DSM buttresses. Incremental lateral wall movements, as large as 50 mm, were observed during the construction of the SMW buttresses. Immediately after installation and before curing, the buttresses apparently did not possess sufficient strength or stiffness to resist lateral earth pressures at depth. Therefore, their installation led to a reduction in soil resistance, which allowed the wall to move laterally. It is interesting to note that settlements of 40 mm were recorded adjacent to the PSCS, yet none were measured above the culvert, even though 50 mm of lateral movement took place.

Stage 4

Between stages 3 and 4 the excavation was taken to a depth of 10.9 m. The third-level tiebacks were installed, and jet

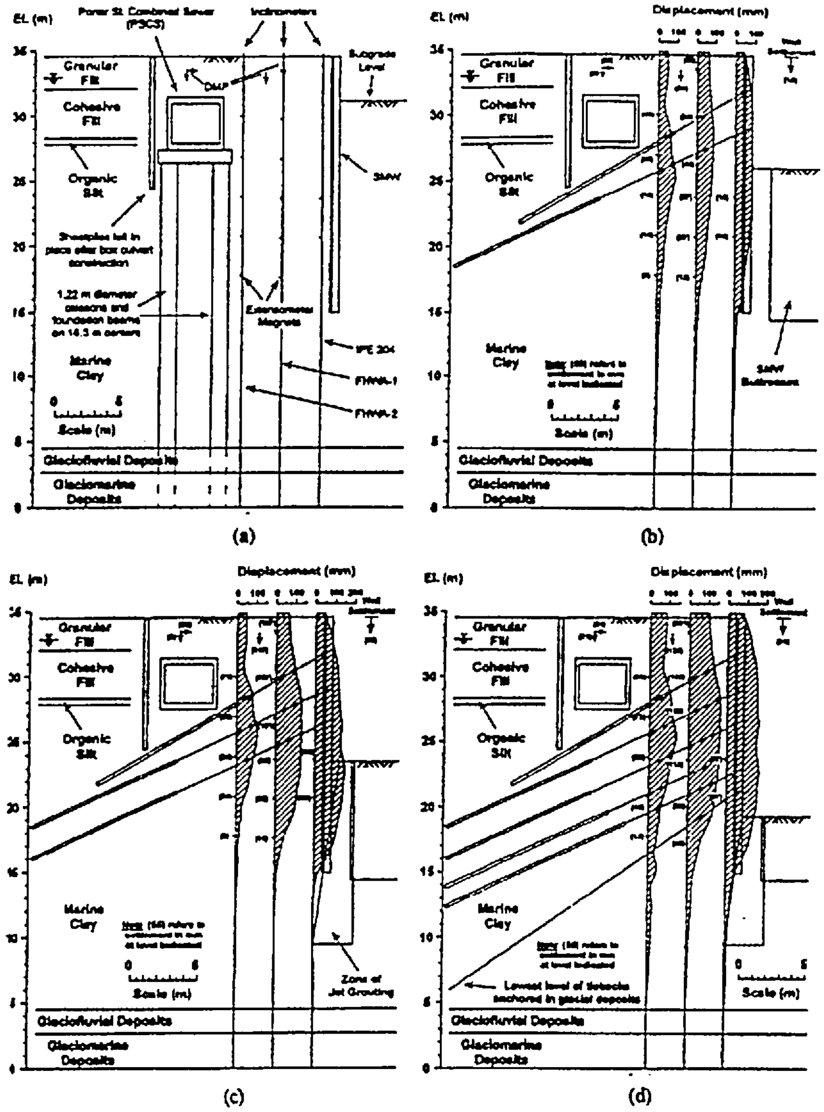

FIG. 5. Cross Sections of Instrumentation and Displacement Measurements for Principal Construction Stages: (a) Instrumentation; (b) Stage 3; (c) Stage 4; (d) Stage 5

grouting between the wall and buttresses was completed. Significant movements occurred during this period, as shown in Fig. 5(c). The majority of the movements took place during jet grouting. As a result, incremental displacements as high as 70 mm were measured at the base of the excavation, and the cumulative lateral wall movement increased to 153 mm. SMW settlement increased from 18 to 69 mm.

Stage 5

During this stage, the excavation was brought to final subgrade at a depth of 15.25 m. Three levels of tiebacks were installed, the lowest of which was anchored in the glacial deposits as indicated in Fig. 5(d). There was a modest increase in lateral displacement near the top of the SMW during this stage. By the final stage of excavation, the maximum lateral movements measured by IPE 204, FHwA-1, FHwA-2 were 70, 167, and 140 mm, respectively.

STRAIN FIELD COMPUTATIONS

Assuming plane strain conditions, soil strains were computed from the instrumentation measurements in a manner similar to that performed by Finno and Nerby (1989), as illustrated in Fig. 6. The horizontal strains ε_h were computed from inclinometer measurements by dividing the differential horizontal displacement between two points at a given elevation by the initial horizontal distance between them [see Fig. 6(a)]. The vertical strains ε_v were computed from multiple-point extensometer and surface DMPs by dividing the differential vertical movement between adjacent measurement points by the initial vertical distance between them [see Fig. 6(b)]. The horizontal and vertical angular distortions, $\partial u/\partial y$ and $\partial v/\partial x$, were calculated by dividing the differential horizontal and vertical displacements by the vertical and horizontal distances separating adjacent measurement points [see Fig. 6(c)]. They were used to calculate pure shear strain ε_{hv} according to

$$\varepsilon_{hv} = \frac{1}{2}\left(\frac{\partial u}{\partial y} + \frac{\partial v}{\partial x}\right) \quad (1)$$

Engineering shear strain is equivalent to the sum of angular shear distortions $\partial u/\partial y$ and $\partial v/\partial x$, or simply twice the pure shear strain. Maximum shear strain γ_{max} is equal to the diameter of the Mohr's circle of strain, calculated by

$$\gamma_{max} = [\gamma_{hv}^2 + (\varepsilon_h - \varepsilon_v)^2]^{1/2} \quad (2)$$

where

TABLE 1. Summary of Soil Characteristics and Properties at Case History Site

Soil type (1)	Description (2)	Unit weight (kN/m³) (3)	Drained angle of shearing resistance (4)	Undrained shear strength[a] (kN/m²) (5)
Granular fill: elevation 32.0–34 6	Brown coarse to fine sand, trace of silt and cinders with fragments of brick, wood, and concrete.	18.9	30°	—
Cohesive fill: elevation 28.5–32.0	Pebble to head-size clay fragments with infilling of subangular to angular coarse sand and gravel.	18.0	30°	0.3–0.4 σ'_{vo}[b]
Organic silt: elevation 27.5–28.5	Slightly to moderately overconsolidated medium stiff dark brown to black organic silt, little fine sand, trace of shells, and clay.	17.3	30°	33–53[c]
Marine clay	Gray clay and silt with seams and partings of fine sand.			
Elevation 25.0–27.5	Overconsolidated crust	18.5	—	119
Elevation 21.0–25.0	Upper zone	18.5	—	119–41[d]
Elevation 12.0–21.0	Middle zone	18.5	—	46
Elevation 4.5–12.0	Lower zone	18.5	—	56
Glaciofluvial deposits: elevation 2.5–4.5	Gray coarse to fine sand, little coarse to fine gravel, trace of silt with cobbles.	21.2	42°	—
Glaciomarine deposits: elevation −5.0–2.5	Gray silt, little coarse to fine sand, clay, trace of fine gravel with cobbles.	23.1	—	96–383[e]

[a] Strengths of marine clay are corrected from VST values according to Bjerrum (1972).

[b] s_u expressed as a function of vertical effective stress σ'_{vo}.

[c] Average strength ± one standard deviation.

[d] Linearly decreasing with depth.

[e] Assumed to increase linearly with depth from devation of 27.4–−3.1 m.

TABLE 2. Excavation Stages at MLT Station 160 + 30

Stage (1)	Construction activities (2)
1	Excavation at elevation of 31 m; first-level tiebacks installed (contract day 622).
2	Excavation at elevation of 25.9 m; second-level tiebacks installed (contract day 687).
3	Deep soil mixing buttresses constructed; excavation at elevation of 25.9 m (contract day 703).
4	Excavation at elevation of 23.5 m; third-level tiebacks installed; jet grouting completed (contract day 738).
5	Excavation at final subgrade (elevation of 19.2 m) (contract day 792).

$$\gamma_{hv} = 2\varepsilon_{hv} = \frac{\partial u}{\partial y} + \frac{\partial v}{\partial x} \qquad (3)$$

Maximum shear strain contours were developed in this manner for each principal stage of construction.

SOIL SHEAR STRAIN CONTOURS

Maximum strain contours are presented and described under the headings that follow. A cross section of the displacement instruments is provided in Fig. 7(a) to assist in the interpretation of the results.

Stage 3

This stage of the excavation corresponds to the installation of SMW buttresses, during which resistance to lateral pressures was reduced and the wall translated horizontally towards the excavation. As illustrated in Fig. 7(b), lateral wall movement below the excavation base resulted in a concentration of shear strain at elevation 22.5 m. Above the excavation base, shear strains were concentrated near the PSCS, indicating differential settlement between the PSCS and SMW. Shear strains were also concentrated adjacent to the tieback bond zone as a result of shear transfer from the anchors into the surrounding soil.

Stage 4

Maximum shear strain increased to more than 5.0% adjacent to the PSCS [see Fig. 7(c)], which indicates that a vertical shear plane developed and the SMW and adjacent soil mass settled relative to the PSCS. Close to the base of the wall, a zone of shear concentration developed at an angle of approximately 35° with respect to the horizontal. This shear zone marks the lower displacement boundary of the soil mass.

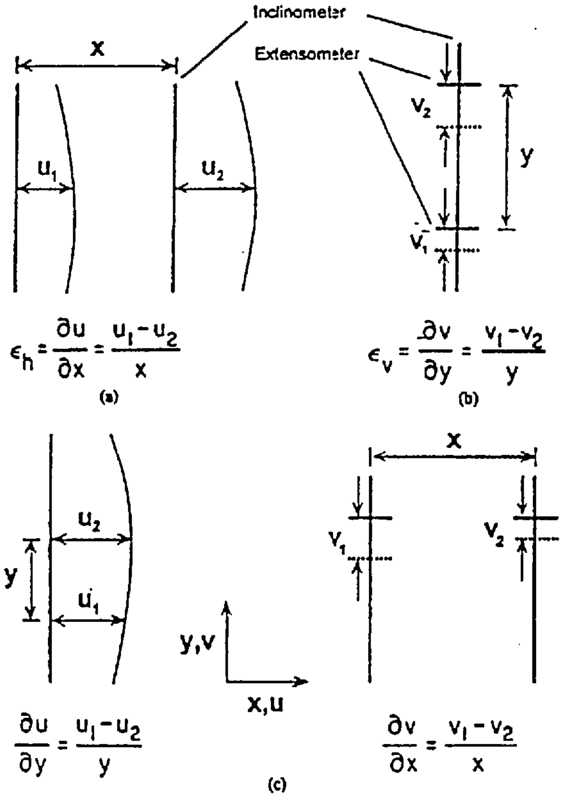

FIG. 6. Determination of Horizontal and Vertical Strains and Angular Distortions: (a) Horizontal Strain; (b) Vertical Strain; (c) Angular Distortions

Stage 5

The maximum shear strains at the final stage of excavation are presented in Fig. 7(d). Essentially, the strain pattern is sim-

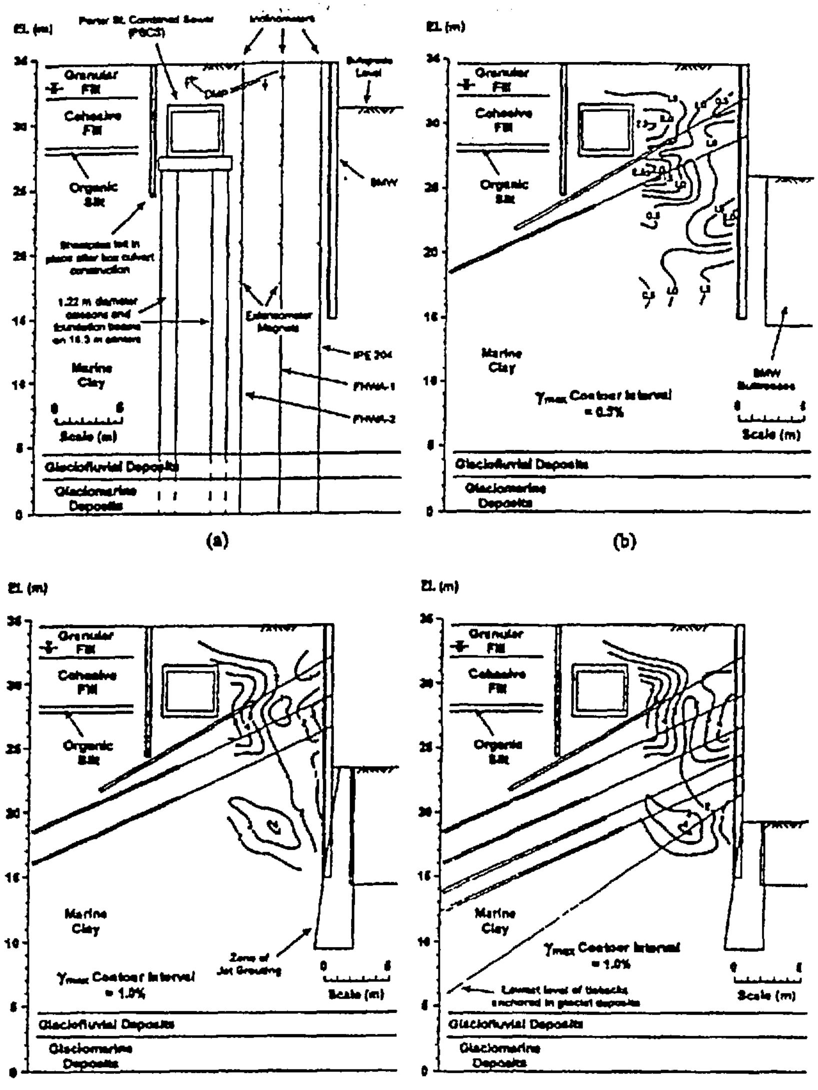

(a)

(b)

(c)

(d)

FIG. 7. Cross Section of Instrumentation and Maximum Shear Strain Contours for Principal Construction Stages: (a) Instrumentation; (b) Stage 3; (c) Stage 4; (d) Stage 5

ilar to that of the previous stage. There was no further development of the lower shear zone, which formed during jet grouting, presumably because of the stabilizing effects of the hardened DSM and jet grout in combination with the installation of the lower three tieback levels.

SOIL DEFORMATION CHARACTERISTICS

Fig. 8 shows the horizontal displacement profiles at the SMW for the principal stages of construction. Only a small amount of lateral movement occurred after DSM installation in response to 2.4 m of excavation from stage 3 to stage 3*. The volume of ground movement associated with stages 3 and 4, pertaining to DSM and jet grout applications, represents approximately 60% of the total volume of movement when the excavation reached subgrade. After DSM and jet grouting, the excavation was advanced to subgrade, and three more levels of tiebacks were installed. Only a modest amount of additional lateral movement occurred.

Fig. 9 shows the maximum shear strain contours at stage 4 after jet grouting. The deformed shape of the wall and settlement profile adjacent to the wall are plotted as dashed lines, and the planes of concentrated shear are shown by solid lines. Blocktype deformation of the soil and SMW occurred. Substantial settlement developed at the surface, with sharp differential settlement near the inboard edge of the PSCS. Asphalt, as thick as 150 mm, was placed in zones of surface settlement to maintain a serviceable road west of the excavation.

TIEBACK LOADS

Fig. 10(a) presents a plot of loads in the upper five tieback levels at station 160 + 35 as a function of time. Cross sections of the instrumented tiebacks, delineating the bond zone and free length of each tieback, are presented in Figs. 5 and 7. Tiebacks were installed on 1.5–1.8-m horizontal separations. No load cell was installed on the sixth-level tieback, which was anchored in soil below the marine clay.

The axial load in the first-level tieback decreased steadily with time as lateral wall movement at the first level increased. Load reduction may have been related to the location of the bond zone, which was situated to avoid obstructions relatively close to the wall (see Figs. 5 and 7).

The second- and third-level tieback loads increased after prestressing, whereas the fourth- and fifth-level tieback loads decreased after prestressing. Load decreased in all tieback loads immediately after the next lower tieback was prestressed and locked off. This is especially evident in the fifth level where loads decreased significantly at about day 780 in response to prestressing the sixth-level tiebacks.

counts for forces generated by the weight of the retained soil and ground-water pressure. The design diagram was divided into a hydrostatic component to account for water pressure behind the SMW and a trapezoidal component to account for horizontal effective stresses in the soil. The unit weight of seawater was used in design calculations.

The analytical procedure to determine the tieback forces has been referred to as the staged excavation-continuous beam method (Tamaro and Gould 1993). The method represents the wall as a continuous beam and analyzes for equilibrium at each stage in the excavation process. At the area of interest, hydrostatic and trapezoidal pressures, similar to those in Fig. 11(a), were used above the excavation base for each excavation stage after the first-level tieback installation. Rankine active and passive earth pressures were assumed outside and inside the excavation below the base of the cut. Horizontal pressure generated by construction equipment was accounted for, but is not shown in the figure.

Fig. 11(b) compares the apparent earth pressures evaluated from the measured tieback loads with those calculated from the design tieback forces. The sixth-level tiebacks are not included in the comparison because these support members were designed to promote deep rotational stability in addition to achieving equilibrium of lateral earth pressures. Accordingly, tieback loads measured just before installation of the sixth-level tiebacks were used in assessing apparent earth pressures. The excavation was approximately 14.7 m deep at this time, as indicated in the figure.

The measured apparent earth pressures are generally smaller than those determined from design values, especially for the first-, fourth-, and fifth-level tiebacks. Because the tiebacks were locked off at 100% design load, the measured apparent pressures are primarily a reflection of the design pressures. To evaluate the validity of the hydrostatic pressure assumed in design, it was necessary to measure directly the pore-water pressure in the soil adjacent to the wall.

WATER PRESSURE

There were four vibrating wire piezometers (VWPs) and one open standpipe observation well near station 160 + 30

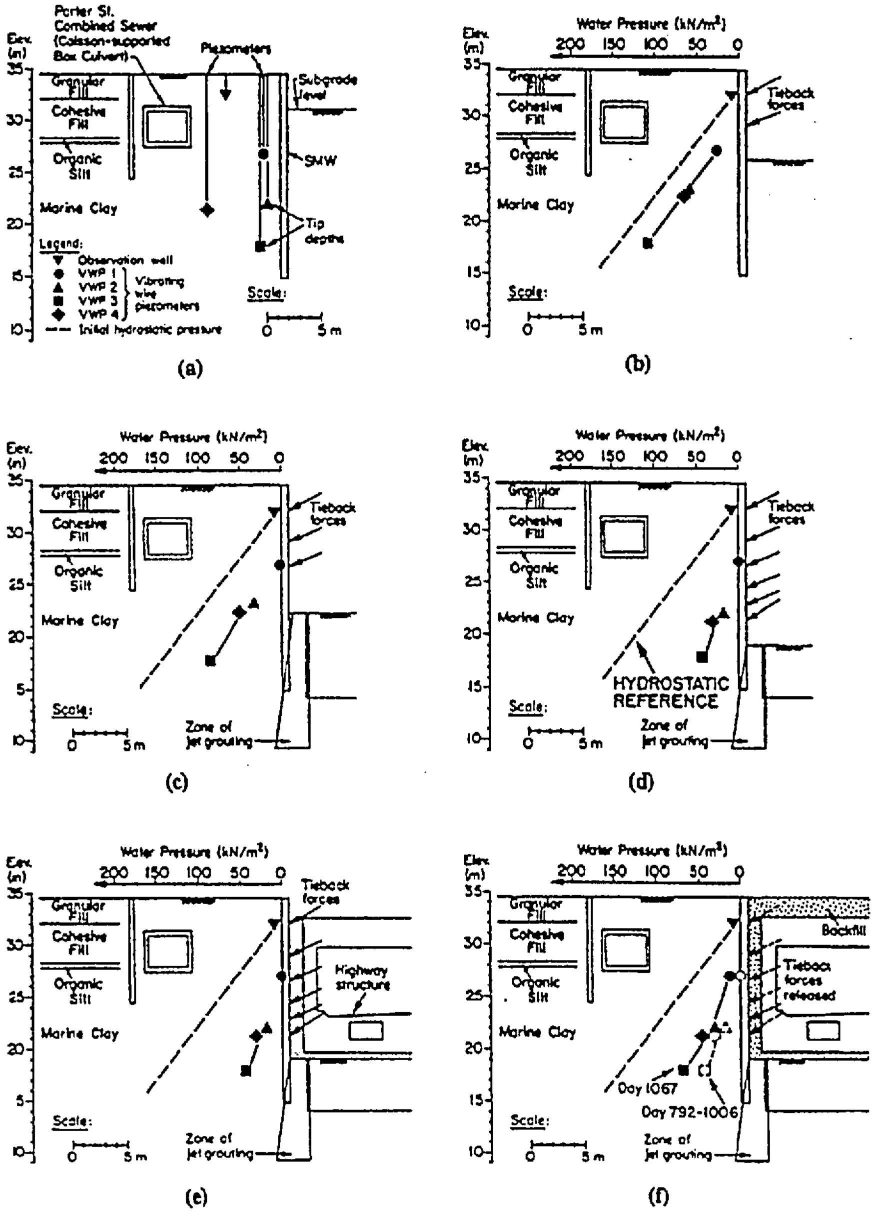

FIG. 12. Piezometer and Observation Well Measurements Adjacent to Excavation: (a) Piezometers; (b) Stage 2; (c) Stage 4; (d) Stage 5 (Day 792); (e) Day 1,006; (f) Day 1,067

[see Figs. 2 and 12(a)]. Three VWPs were installed approximately 1.5 m from the SMW in the marine clay at depths of 8.2, 11.5, and 16.8 m. An additional VWP was installed about 7.5 m from the wall at a depth of 12.4 m. Because the observation well was not cased through the granular and underlying cohesive fill, it is assumed that well measurements are representative of the most pervious material penetrated by the well. Accordingly, piezometric surfaces measured at the observation well are referenced with respect to the base of the granular fill.

Figs. 12(b)–12(f) show measured water pressures at various construction stages. For reference, a hydrostatic pressure distribution similar to the one assumed in design is presented in each figure as a dashed line. At all stages, measured water pressures in the marine clay were significantly lower than hydrostatic pressure. The water level in the granular fill dropped only about 300 mm from its initial level, implying that recharge in the fill occurred at a rate sufficient to keep pace with drainage through the underlying soils and SMW.

Fig. 12(f) shows the water pressures measured on day 1,067 after the release of all tieback loads and placement of granular backfill between the highway structure and SMW. Piezometric pressures increased steadily in response to backfilling from day 1,006 to 1,067 until they attained the levels depicted in the figure.

Fig. 13 presents piezometric heads at VWP 2 and VWP 3 as a function of time. These data are typical of all VWP measurements. The plot shows distinct increments of positive pore pressure each time a tieback level was prestressed. These pore pressures, however, drained rapidly. The drop-off in pore pressure is especially evident for VWP 3 after prestressing tieback levels 4, 5, and 6. In each case, a decay time of approximately 10–15 d was required to return water pressure to the general trend line.

Pore pressure measurements at a slurry wall excavation of similar depth in similar Boston soils (Jaworski 1973) show nearly identical trends of initial hydrostatic conditions, relatively rapid water pressure reduction during excavation, and partial recovery during subsurface construction and backfilling. Jaworski (1973) attributed most of the water pressure reduction to drainage abetted by seepage through separations at joints in the slurry wall. He showed that the measured water pressures conform with those for steady-state seepage and that the steady-state seepage pressures were not changed substantially for walls with effective hydraulic conductivities equal to and as much as 10 times less than the vertical hydraulic conductivity of adjacent clay.

Soil mixed walls have hydraulic conductivities, k, of roughly 1×10^{-6}–1×10^{-7} cm/s [e.g., Taki and Yang (1991)], which is roughly equivalent to the horizontal k of marine clay. Moreover, the large number of tiebacks installed at the site would have created, in effect, a series of weep holes. These tieback penetrations of the wall in combination with thin sand and silt layers, which are present in marine clay, apparently played a significant role in promoting drainage.

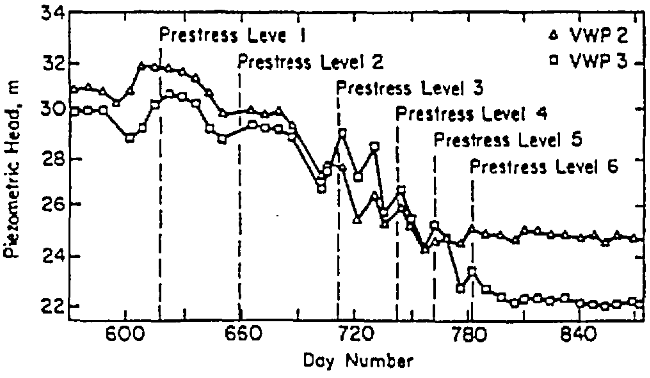

FIG. 13. Piezometric Head versus Time

DEEP ROTATIONAL STABILITY

Deep rotational stability (DRS) was evaluated at this location according to the procedures described by O'Rourke and O'Donnell (1996, 1997). In essence, critical circular arc failure surfaces were determined in accordance with simplified Bishop limiting equilibrium analyses, and the safety factor for deep rotational stability was calculated.

Fig. 14 shows the critical slip circle for conditions prior to the installation of the sixth-level tiebacks. Because there was no resisting moment from the sixth-level tiebacks, the safety factor was lowest at this stage. Because of its vertical caisson support, the PSCS reduces the driving moment by an amount equivalent to the moment generated by the hatchured portion of soil shown in the figure. Accounting for moment reduction from the vertically supported PSCS and the variations in soil strength discussed by O'Rourke and O'Donnell (1996, 1997), the safety factor was between 1.03 and 1.13. Because relatively short distances were excavated and supported before additional soil was removed at the same base level, it is likely that the actual safety factor during construction was somewhat higher.

The incremental lateral deformation between stage 4, just after jet grouting, and a time just before installation of the sixth-level tiebacks on day 780 are shown at an expanded horizontal scale in Fig. 15. These displacements indicate that a zone of incremental shear strain of approximately 0.5% developed at depth during this period. The results of DSS tests

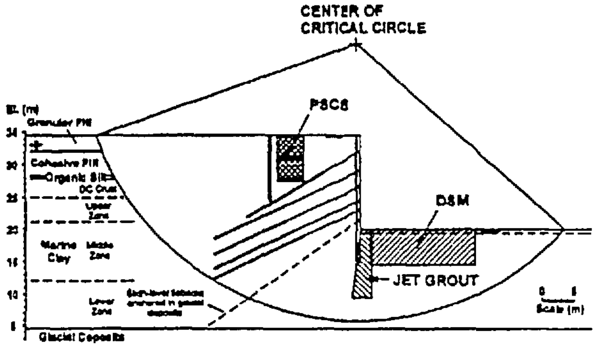

FIG. 14. Critical Slip Surface for Deep Rotational Stability

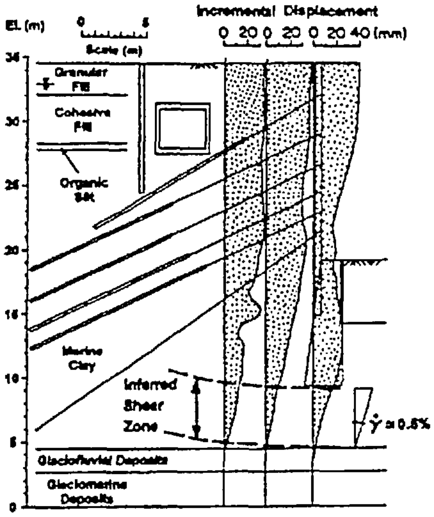

FIG. 15. Incremental Lateral Displacements between Stages 4 and 5

on marine clay similar to that at the BIF site (Haley 1995) show that a strain increment of 0.5% is sufficient to mobilize as much as 50% of the undrained strength if deformation is imposed near the initial portion of the stress-strain plot.

The DRS analyses show that soil stabilization, in combination with the tiebacks, resulted in critical slip circles that penetrated into the deepest zones of the marine clay at the final stages of excavation. There was sufficient shear resistance along these slip surfaces to promote deep rotational stability of the excavation.

CONCLUSIONS

Field measurements show that DSM and jet grouting were successful in promoting deep rotational stability at the 15.25-m deep excavation in marine clay at the case history site. DSM and jet grouting caused a temporary softening of soil in front of the excavation wall, which apparently was related to the reduced strength and stiffness of soil mix and jet grout before curing. As a consequence, soil resistance was reduced and the wall translated toward the excavation.

Soil movement and load cell measurements indicate that the soil in which the tiebacks were anchored displaced laterally approximately 75 mm during excavation. Lateral displacement of the tieback anchor zone contributed directly to lateral wall movement and implies that tiebacks in marine clay should be evaluated carefully with respect to acceptable levels of deformation.

An SMW has a hydraulic conductivity either approximately equal to or slightly larger than that of marine clay. Moreover, multiple tieback penetrations of the wall will promote seepage. Accordingly, an SMW in marine clay tends to act as a free drainage surface. With time, the initial hydrostatic pore-water pressures in the clay dissipate until reduced water pressures compatible with steady-state seepage conditions are established. Piezometer measurements indicate that steady-state seepage conditions at the case history site were established relatively rapidly at a rate consistent with the rate of excavation. Accordingly, water pressures in marine clay behind the SMW and above the base of excavation were significantly less than the hydrostatic conditions assumed in design.

ACKNOWLEDGMENTS

This paper was prepared as part of research sponsored by FHwA under Contract No. 15-0532082-A4. The writers thank A. DiMillio and J. Cooper of the FHwA for their assistance. Brian Kelly of D'Appolonia Engineering made valuable contributions in the form of site observations and acquisition of case history information. Joan-marie Dewsnap helped in performing limiting equilibrium analyses and summarizing clay strength data. The writers also thank the Nicholson Construction Company, McPhail Associates, Mueser Rutledge Consulting Engineers, and Bechtel/Parsons Brinckerhoff Joint Venture for their assistance in acquiring field measurements and soil characterization data. Laurie McCall typed the manuscript, and Ali Avcisoy helped prepare the figures.

APPENDIX. REFERENCES

Bjerrum, L. (1972). "Embankments on soft ground." *Proc., Spec. Conf. on Perf. of Earth-Supported Struct.*, ASCE, New York, N.Y., Vol. II, 1–54.

Finno, R. J., and Nerby, S. M. (1989). "Saturated clay response during braced cut construction." *J. Geotech. Engrg.*, ASCE, 115(8), 1065–1084.

GeoTesting Express. (1994). "Strength of cement-soil at C07A2." *Rep. Prepared for Nicholson Constr. Co.*, Acton, Mass.

Haley & Aldrich. (1995). "Draft supplemental geotechnical data report, central artery (I-93)/tunnel (I-90) project, design section D009A, Boston, MA." *Rep. Prepared for Maguire/Harris Joint Venture, File No. 11220-052*, Cambridge, Mass., Vols. 1–4.

Jaworski, W. E. (1973). "An evaluation of the performance of a braced excavation," PhD thesis, Massachusetts Inst. of Technol., Cambridge, Mass.

O'Rourke, T. D., and O'Donnell, C. J. (1996). "Case history studies of deep excavations in clay." *Rep. No. DTFH61-95-P-00776, Prepared for Fed. Hwy. Admin.*, Cornell Univ., Ithaca, N.Y.

O'Rourke, T. D., and O'Donnell, C. J. (1997). "Deep rotational stability of tiedback excavations in clay." *J. Geotech. and Geoenvir. Engrg.*, ASCE, 123(6), 506–515.

Taki, O., and Yang, D. S. (1991). "Soil-cement mixed wall technique." *Geotechnical engineering congress 1991: geotechnical special publication no. 27*, ASCE, New York, N.Y., Vol. 1, 298–309.

Tamaro, G. J., and Gould, J. P. (1993). "Analysis and design of cast insitu walls (diaphragm walls)." *Retaining structures*, C. R. I. Clayton, ed., Thomas Telford, London, England, 343–352.

Tanaka, H. (1993). "Behavior of braced excavations stabilized by deep mixing method." *Soils and Found.*, 33(2), 105–115.

Terashi, M., and Tanaka, H. (1981). "Ground improvement by deep mixing method." *Proc., 10th Int. Conf. on Soil Mech. and Found. Engrg.*, A. A. Balkema, Rotterdam, The Netherlands, Vol. 3, 191–194.

Xanthakos, P., Abramson, L. W., and Bruce, D. A. (1994). *Ground control and movement*, John Wiley & Sons, Inc., New York, N.Y.

modifications were made to the nodes at the soil-drain interface in order to achieve good matching of analysis and field deformation behavior?

2. How much have the pore-pressure predictions improved in Figs. 8 and 9 after allowing for nonzero excess pore-pressure dissipation at the soil-drain interface?

APPENDIX. REFERENCE

Tan, S. A. (1993). "Ultimate settlement by hyperbolic plot for clays with vertical drains." *J. Geotech. Engrg.*, ASCE, 119(5), 950–956.

Closure by B. Indraratna,[7] Member, ASCE

RESPONSE TO DISCUSSION BY D. RUSSEL AND C. C. HIRD

The use of a reduced permeability zone adjacent to the drains is the common technique of modeling smear effects in finite analysis. However, for the stabilised Muar clay foundation, Fig. 10 indicates clearly that the effects of both smear and well resistance are negligible. Therefore, the smaller settlements observed in the field are related to retarded rate of pore-pressure dissipation at the drain boundary or simply drain clogging. Experience with various types of synthetic vertical drains has shown that clogging is not uncommon when installed in soft clays, depending on the apparent opening size (AOS) of the geofabric apertures.

The evaluation of "drain clogging" introduced by the authors was based on a back-analysis approach where nonzero excess pore pressures are introduced at the drain boundaries to match the centerline settlements (Fig. 12). This was carried out by using a subroutine to introduce further pore-pressure shape functions (Ratnayake 1991). At the centerline, the single-drain analysis can be directly related to the one-dimensional consolidation settlements. Also, as explained in the paper, the assumption of plane strain at the embankment centerline has not contributed to excessive settlements. The magnitude of undissipated excess pore pressures at the drain boundaries (Table 6) are used to determine the drain efficiency, hence the degree of clogging. If the efficiency of the drains is 100%, then the computed consolidation settlements should coincide with the values obtained from perfect drain analysis. Using the back-calculated undissipated pore pressures, good predictions could be obtained for settlements and lateral displacements at other locations. Perfect drain conditions were approached only after a period of 400 days.

The authors agree with the discussers that errors can occur due to the assumption of plane strain in the modeling of vertical drains. In fact, a subsequent analysis was conducted (Sivaneswaran 1993) where the rows of drains were converted to equivalent drain walls to be more compatible with plane strain modeling. The analytical formulation of the equivalent drain walls and their application in finite-element analysis will be presented in a future paper. Converting the actual drain pattern to equivalent drain walls was effective in decreasing the settlements only slightly, still overpredicting the rate of consolidation. The authors agree without hesitation that conversion to equivalent drain walls is more realistic in the case of plain strain modeling, along similar concepts proposed by Cheung et al. (1991), Hird et al. (1992) and Zeng et al. (1989). Nevertheless, none of these methods would explain or evaluate clogging of drains, although smear and well-resistance effects could be incorporated.

It is well known that the permeability decreases with increasing consolidation. However, the authors do not believe that empirical relationships developed elsewhere for other types of soils should be readily adopted for soft marine clays. In addition to the extensive field permeability tests, the authors have conducted detailed consolidation tests under various stress levels (depending on depth), from which the average permeability for each soil layer was determined (Indraratna et al. 1992). These values were employed in the CRISP finite-element program. By comparing the analyses A, B, and C given by the discussers in their settlement-time curves, it

TABLE 6. Undissipated Excess Pore Pressures at Drain Boundaries

Loading stage (1)	Time (days) (2)	Undissipated pore pressures (%) (3)
1st	0	100
1st	44	81
1st	105	16
2nd	129	100
2nd	159	80
2nd	413	18

---

[7] Sr. Lect., Dept. of Civ. and Min. Engrg., Univ. of Wollongong, NSW 2522, Australia.

APPENDIX. REFERENCES

Hird, C. C., Pyrah, I. C., and Russell, D. (1992). "Finite element analysis of soil containing vertical drains." *Géotechnique*, London, England, 42(3), 381–538.

Muir Wood, D. (1990). *Soil behaviour and critical state soil mechanics*. Cambridge University Press, Cambridge, U.K.

Russell, D. (1990). "An element to model thin, highly permeable materials in two-dimensional finite element consolidation analyses." *2nd Specialty Conf. on Numer. Methods in Geotech. Engrg.*, CEDEX, Santander, Spain, 303–310.

Russell, D. (1992a). "Finite element analysis of soil containing vertical drains." *Ground Engrg.*, Thomas Telford, London, England, August.

Russell, D. (1992b). "Finite element analyses of embankments on soft ground incorporating reinforcement and drains." PhD thesis, University of Sheffield, Sheffield, U.K.

Tavenas, F., Jean, P., Leblond, P., and Leroueil, S. (1983). "The permeability of natural soft clays, part II: Permeability characteristics." *Can. Geotech. J.*, 17(2), 236–260.

Taylor, D. W. (1948). *Fundamentals of soil mechanics*. McGraw-Hill, New York, N.Y.

Discussion by Siew-Ann Tan,[6] Member, ASCE

The authors have presented an interesting and useful case history involving the application of flexible vertical drains to accelerate the consolidation of the soft clays for safe construction of highway embankments on soft clays. Judging from the wealth of laboratory and field data available, the detailed finite-element analysis performed using the modified Cam-clay constitutive model in the CRISP program is justifiable. However, in day-to-day engineering design work, such data is not easily obtainable, and therefore judgment is required to identify the correct set of parameters to use for making reasonable prediction of field behavior. Thus, the writer seeks clarification of the values of λ and κ used in the analysis as stated in Table 2.

The oedometer tests are constant (q/p) ratio tests, for which the compression constant of the normally consolidated line (NCL) that is the compression index C_c and the recompression line C_r can be obtained as the slope of (e, log σ'_o) plots, whereas the Cam-clay parameters λ and κ are obtained from triaxial isotropic consolidation tests by plotting in (e, ln p) space. Thus, there exist simple relationships between C_c and λ, and C_r and κ as given by Britto and Gunn (1987)

$$\lambda = \frac{C_c}{2.303} \text{ and } \kappa = \frac{C_r}{2.303} \qquad (5a,b)$$

Using the above relationships and the data from Fig. 3, the following are the writer's estimates for λ and κ for various depths of clays as compared to the authors' values in Table 2.

From Table 5, it is evident that the values of κ from oedometer tests are very close to that of isotropic triaxial consolidation tests. But, the values of λ from oedometer tests are consistently very much larger than those from triaxial tests. This may be expected for the overconsolidated upper clay up to a depth of 8 m, where overconsolidation ratios of 1–2 can cause a significant reduction in λ as compared to the λ from the NCL. Thus, the use of a much reduced pseudo-λ would enable a better match between the modified Cam-clay yield locus and the actual yield locus obtained experimentally. But below the depth of 8 m, we are dealing with a normally consolidated clay, so what could be the cause of the significant reduction in λ as shown in Table 5?

It is commonly known that the Cam-clay parameters of λ, κ, and M are influenced by the nature of stress path testing. But, to make finite-element analysis practical in the absence of stress path testing facility, we need to relate these parameters reasonably accurately to simple oedometer and triaxial tests that are readily available in most laboratories.

On the prediction of vertical settlements, it is apparent that from the embankment width to clay depth ratio, we have a case of one-dimensional compression near the centerline of the embankment. This could be verified by the inclinometer data of S4, S5, and S6, which were

TABLE 5. Comparison of κ and λ from Oedometer and Triaxial Data

Depth (m) (1)	Authors' Data		Discusser's estimates from Fig. 3					
	κ (2)	λ (3)	w_n (%) (4)	e_o (5)	$C_r/(1 + e_o)$ (6)	$C_c/(1 - e_o)$ (7)	κ (8)	λ (9)
2–6	0.06	0.16	90	2.39	0.05	0.37	0.07	0.54
6–11	0.05	0.13	70	1.86	0.05	0.27	0.06	0.33
11–18	0.035	0.09	60	1.59	0.05	0.20	0.05	0.22

---

[6] Sr. Lect., Dept. of Civ. Engrg., Nat. Univ. of Singapore, 10 Kent Ridge Crescent, Singapore 0511.

not given in the paper. Applying the hyperbolic method (Tan 1993) to the ground surface settlement for the first stage loading of 100 days (Fig. 10), with the soil and drain parameters given in the paper, the plots in Fig. 18 are obtained. From the hyperbolic plot, the predicted t_{60} is 37 days, and t_{90} is 98 days. Using the single-drain theory of Barron (1948) combined with Terzaghi's theory, the back-calculated value of c_v is 4.5 m^2/hr, and the corresponding c_h is 6.2 m^2/hr, which compares very well with the mean values of 4.6 m^2/hr and 6.3 m^2/hr for c_v and c_h as obtained from Table 1.

Using the parameters obtained from the hyperbolic method, the computed settlement by the single-drain theory with drain smearing compares well with the field data as shown in Fig. 19, predicting an ultimate settlement of 0.47 m in agreement with the authors' finite-element analysis. However, from the compressibility data of Fig. 3, the estimated ultimate settlement is about 0.6 m; thus, single-drain theory would predict a much faster settlement rate than observed, as also shown in Fig. 19. Therefore, the authors' finite-element analysis using a nonzero excess pore pressure at the soil-drain interface provides a rational explanation for the much slower settlement and pore pressure dissipation observed in the field.

In this regard, the writer seeks two further points of clarification:

1. Without actual measurements of pore pressures at the soil-drain interface, what specific

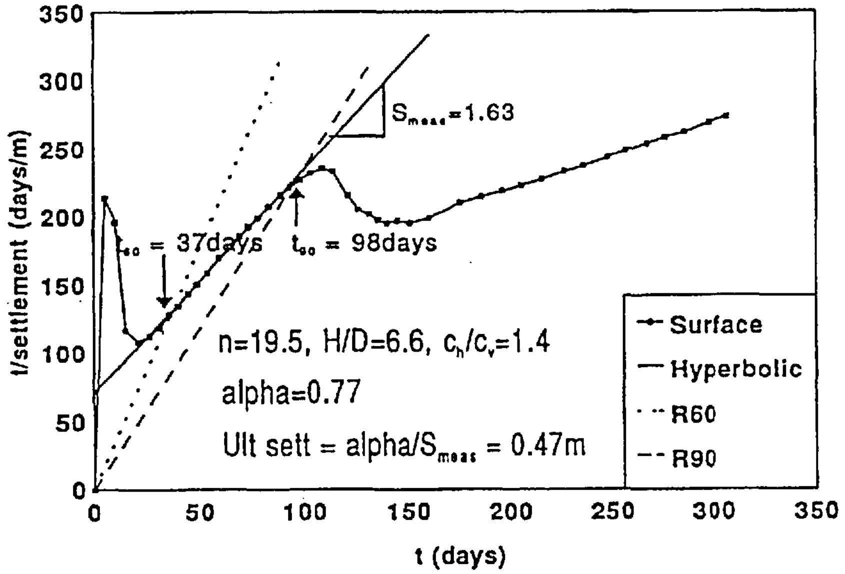

FIG. 18. Hyperbolic Plot of Muar Surface Settlement

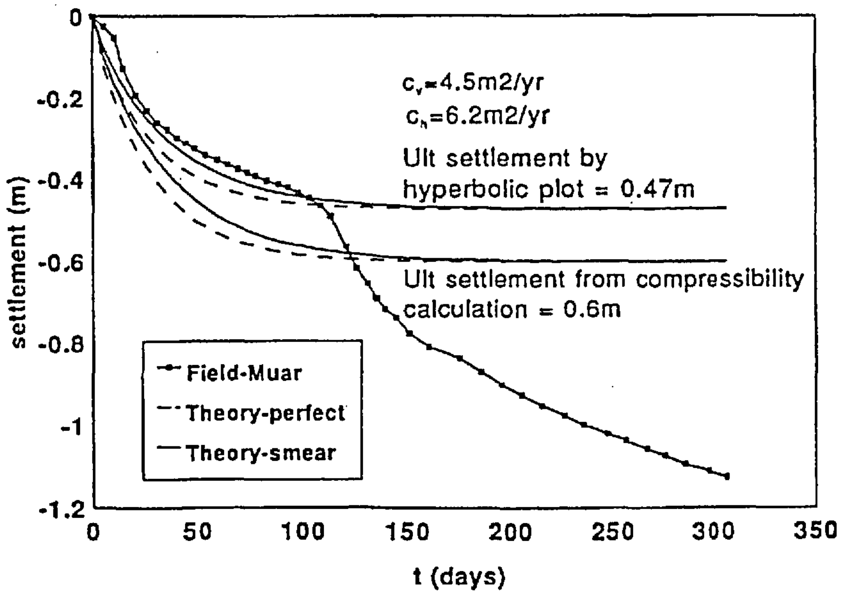

FIG. 19. Muar Surface Settlement (Drain Spacing 1.3-m Triangle)

PERFORMANCE OF EMBANKMENT STABILIZED WITH VERTICAL DRAINS ON SOFT CLAY

By B. Indraratna,[1] Member, ASCE, A. S. Balasubramaniam,[2] Fellow, ASCE, and P. Ratnayake[3]

ABSTRACT: This study describes the performance of a full-scale embankment raised on a soft marine clay, stabilized with vertical band drains in Malaysia. The finite element code CRISP, which is based on critical-state soil mechanics, has been employed to investigate the performance of the embankment and the underlying soft clay. Predictions of the excess pore pressures and both vertical and lateral displacements are made and compared with field observations. The limited use of closed-form solutions for the prediction of settlements at the line of symmetry of the embankment is also discussed. The effectiveness of the prefabricated drains has been evaluated according to the rate of excess-pore-pressure dissipation at the soil-drain interface. The numerical approach is based on a coupled consolidation analysis rather than on a conventional, purely undrained analysis. The numerical analysis reveals that for efficient vertical drains, the influence of smear and well resistance can be ignored. While the assumption of perfect drains may be acceptable in the long term, the short-term settlements are governed by the drain efficiency.

INTRODUCTION

This study is concerned with the behavior of a full scale embankment with vertical band drains, constructed by the Malaysian Highway Authority (*Proceedings* 1989) on the Muar coastal plain, slightly north of the Malaysian North-South Expressway (Fig. 1). In fact, a comprehensive array of 14 such embankments was built in the same site with nine different ground-improvement techniques to assess the relative merits of various soil-stabilization schemes. One embankment was constructed to failure without any soil-improvement techniques for the purpose of comparison. Its behavior was analyzed and discussed in detail in a previous paper (Indraratna et al. 1992).

The current study provides a means of evaluating the effectiveness of vertical band drains in improving soft soil foundations subjected to embankment loading. The maximum completed height of the embankment was 4.75 m, and it was constructed over a period of four months. The embankment fill consisted of a granitic residual soil compacted to a unit weight of 25 kN/m^3. Underneath the embankment, fully penetrating vertical band drains were installed in a triangular pattern. The prefabricated drains consisted of polyolefine cores (rectangular cross section) with 24 channels. The sides of the drains were perforated with 0.2-mm-diameter holes at 2-mm centers. A cross section through the center of the embankment is shown in Fig. 2. The drain parameters relevant for the analysis are summarized as follows.

---

[1] Lect., Dept. of Civ. and Mining Engrg., Univ. of Wollongong, P.O. Box 1144, Northfields Avenue, Wollongong, New South Wales 2500, Australia.

[2] Prof., Div. of Geotech. Engrg., Asian Inst. of Tech., G.P.O. Box 2754, Bangkok, Thailand.

[3] Lect., Dept. of Civ. Engrg., Univ. of Peradeniya, Sri Lanka.

Note. Discussion open until July 1, 1994. To extend the closing date one month, a written request must be filed with the ASCE Manager of Journals. The manuscript for this paper was submitted for review and possible publication on May 15, 1992. This paper is part of the *Journal of Geotechnical Engineering*, Vol. 120, No. 2, February, 1994. ©ASCE, ISSN 0733-9410/94/0002-0257/$1.00 + $.15 per page. Paper No. 4065.

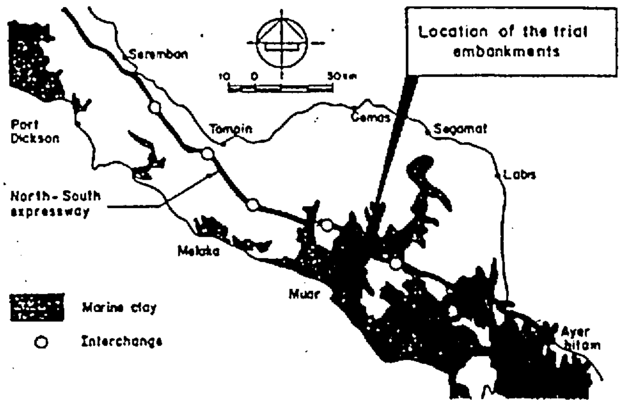

FIG. 1. Location of Marine Clay Deposits and Trial Embankments

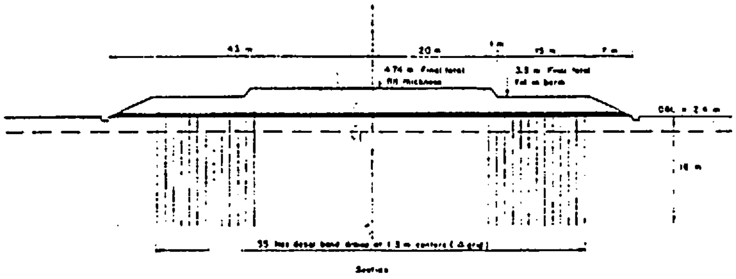

FIG. 2. Cross Section through Centerline of Embankment with Vertical Drains

- Drain pattern: triangular
- Maximum length: 18.0 m
- Drain spacing: 1.30 m
- Cross section: 95 mm × 2 mm^2
- Equivalent diameter: 70 mm
- Influence-zone diameter: 1.365 m
- Smeared-zone diameter: 400 mm

The paper describes the predicted and measured behavior of the embankment and the underlying soft clay foundation. The effectiveness of the band drains is evaluated on the basis of excess-pore-pressure dissipation and both vertical and lateral displacements. The foundation response is modeled according to the modified cam-clay theory, incorporated in the finite element method. The relevant soil parameters were determined by undrained, K_0-consolidation triaxial tests. In the finite element code (CRISP), the field behavior was simulated using a coupled (Biot) consolidation model, rather than a purely undrained analysis, which proved to be more realistic for this particular soil (Indraratna et al. 1992). The compression of the soft clay with vertical drains was also determined by the analytical solution proposed by Barron (1948), which combines the radial and vertical consolidation phases. The predictions made from these different methods were compared with the observed field measurements. It is shown that the discrepancy between the observations and predictions is acceptable, and that the vertical drains are effective in accelerating the stabilization of the soft clay.

SOIL CONDITIONS IN TEST SITE

A detailed soil profile including the grain size distribution and mineralogy was given by Indraratna et al. (1992). Therefore, only a summary is presented here. The clays along the west coast of peninsular Malaysia constitute a coastal plain of marine clay up to 20 m thick, with an average lateral extent of about 25 km. The subsurface geology data at the site reveal the existence of a weathered crust of about 2.0 m above a 16.5-m-thick layer of soft silty clay. The soft silty clay can be further divided into an upper very soft layer and a lower soft silty clay. Immediately beneath this lower clay layer is a 0.3–0.5-m-thick peaty soil followed by a stiff sandy clay. The clay ends at a dense sand layer beyond 22.5 m below ground level, although a distinct interface cannot be identified. The variations of the water content, liquid and plastic limits, and consolidation parameters with depth are presented in Fig. 3. Although many soft clays in Southeast Asian countries are generally normally consolidated, light overconsolidation caused by surface desiccation and weathering is sometimes exhibited toward the surface, as shown by this marine clay. It was also determined that the unit weight of the clay with depth was fairly consistent between 15–16 kN/m^3, except at the topmost crust, where the unit weight approached 17 kN/m^3. The field permeability varied from 1–2 × 10^{-9} m/s with increasing depth within the soft clay layer.

The undrained shear strength, as measured by the field vane, had a

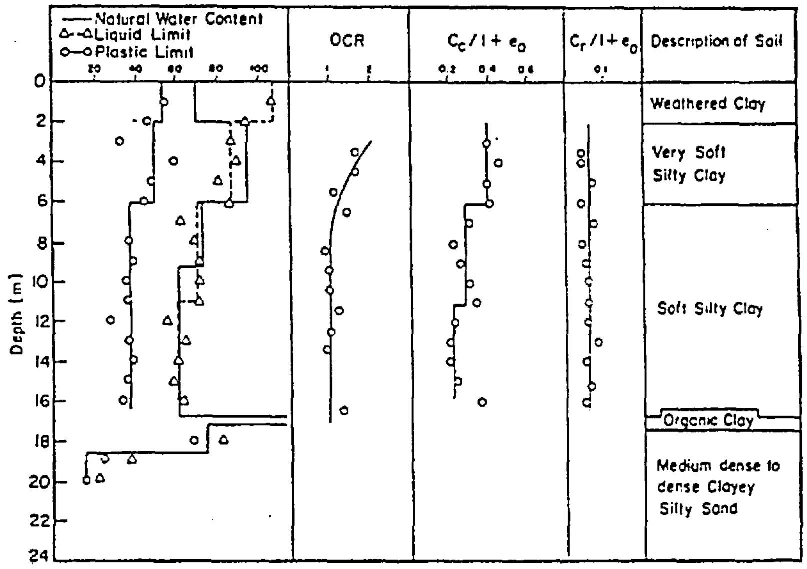

FIG. 3. Geotechnical Properties of Muar Clay (Data Provided by Malaysian Highway Authority, Kuala Lumpur, Malaysia)

TABLE 1. Variation of Strength and Consolidation Parameters

Depth (m) (1)	E_u (kPa) (2)	c' (kPa) (3)	ϕ' (degrees) (4)	$c_v \times 10^{-4}$ (cm²/s) (5)	$c_h \times 10^{-4}$ (cm²/s) (6)
0–2	25,500	8	12.5	7.5	10.0
2–5	6,600	14	14	30.0	40.0
5–8	8,933	22	7	15.0	23.5
8–11	9,120	9	20	13.0	15.0
11–14	6,593	16	17	16.0	22.0
14–18	5,884	14	21.5	5.5	8.5

TABLE 2. Modified Cam-Clay Parameters Required for Numerical Analysis (CRISP)

Depth (m) (1)	κ (2)	λ (3)	e_{cs} (4)	M (5)	v (6)	K_w ($\times 10^4$) (7)	γ_s (kN/m³) (8)	k_h (m/s) (9)	k_v (m/s) (10)
0–1.75	0.06	0.16	3.10	1.19	0.29	4.4	16.5	6.4×10^{-9}	3.0×10^{-9}
1.75–5.50	0.06	0.16	3.10	1.19	0.31	1.1	15.0	5.2×10^{-9}	2.7×10^{-9}
5.50–8.0	0.05	0.13	3.06	1.12	0.29	2.4	15.5	3.1×10^{-9}	1.4×10^{-9}
8.0–18.0	0.035	0.09	1.61	1.07	0.26	22.7	16.0	1.3×10^{-9}	0.6×10^{-9}

minimum value of about 8 kPa at a depth of 3 m, and this increased approximately linearly with depth. The corrected field-vane strengths as proposed by Bjerrun (1973) have been used in the numerical analysis. Only limited information was available with regard to the thin peaty soil layer (less than 0.5 m thick) at a depth of about 18 m below the ground level. Consequently, for the purpose of analysis, the effect of this peat layer has been ignored. In addition to the in situ data, a considerable amount of laboratory information was acquired for the subsurface clay deposits prior to the construction of the test embankment. These included oedometer consolidation tests and unconsolidated undrained (UU), consolidated isotropically undrained (CIU), and consolidated drained (CD) triaxial tests. The undrained modulus (E_u), effective strength parameters (c' and ϕ'), and the vertical and horizontal coefficient of consolidation (c_v and c_h) are summarized in Table 1. Consolidation tests were done on both vertically and horizontally oriented specimens (Ratnayake 1991). Furthermore, a series of specialized triaxial tests were also conducted, including constant stress ratio tests, effective and total stress path tests, and anisotropically consolidated undrained (CU) tests. The results of these tests provided the appropriate modified cam-clay model parameters of the subsoils (Table 2), for the prediction of displacements and pore-pressure changes beneath the test embankment. The cam-clay parameters (Roscoe and Burland 1968) include the gradients of volume against log pressure relations for consolidation and swelling (λ and κ, respectively); slope of the critical state line based on effective stresses (M); void ratio at unit consolidation pressure (e_{cs}); bulk modulus (K); horizontal and vertical permeabilities (k_h and k_v); and Poisson's ratio (v).

NUMERICAL ANALYSIS

The critical-state finite element program CRISP was developed at Cambridge University, Cambridge, England. It incorporates the modified cam-clay constitutive model and enables coupled (Biot) consolidation analysis to be carried out, in addition to the purely undrained or drained analysis. The coupled behavior includes both undrained deformations and the drained settlements. It has been shown earlier that the modified cam-clay model is accurate in representing the undrained deformation behavior of soft Muar clay (Balachandran 1990). In the past, CRISP has proved to be accurate and consistent for predicting the deformation response of normally consolidated to lightly overconsolidated soils (Britto and Gunn 1987).

The horizontal permeability of the soft Muar clay foundation exceeds the vertical permeability. The results predicted using CRISP were subsequently compared with the actual field observations. The performance of the vertical drains was evaluated as discussed in the following.

As a preliminary finite-element-method (FEM) exercise, the settlements based on a single vertical drain under embankment loading were analyzed using the coupled consolidation model for an axisymmetric, perfect drain. Comparison of these results with the analytical solutions enabled the proper calibration of CRISP. The diameter of the individual influence-zone diameter for this triangular pattern of drains is 1.365 m (Ratnayake 1991). As the in situ horizontal (lateral) permeability for the subsoils is at least double the permeability in the vertical direction, the total compression is a function of both vertical and radial drainage. The extent of the smeared zone was estimated according to Hansbo (1981), and was 0.4 m, or almost twice the equivalent diameter of the mandrel. For the finite element analysis, the horizontal permeability of the smeared zone was reduced to equal the vertical permeability.

To compute lateral and vertical displacements, excess pore-water pressures, and surface settlements corresponding to the sequential construction of the embankment, linear-strain-quadrilateral (LSQ) elements were used in the finite element discretization of the clay foundation (Fig. 4). The eight-node LSQ elements are characterized by additional pore pressure degrees of freedom at the four corner nodes; the pore pressures vary linearly over the element. For the influence zone of the vertical drains, the finite element mesh was made relatively fine (Fig. 4). The axes of drains coincide with every other vertical line of this fine mesh, where the spacing between the drains consists of two rows of LSQ elements. In the case of perfect drains (no clogging and smearing), excess pore pressures at the drain boundaries are considered to be zero. Nevertheless, partial clogging of synthetic drains retards the rate of dissipation of excess pore pressures. In this analysis, the undissipated excess pore pressures were computed using additional pore-pressure shape functions applied to nodes along the drain boundaries. For the case of perfect drains, the excess pore pressures at these nodes would be always set to zero. The modified pore-pressure subroutines used in conjunction with CRISP are discussed in detail by Ratnayake (1991).

A foundation depth of 18.0 m was considered to be sufficient, as the soil layers beyond this depth were considerably stiffer than the upper soft clay

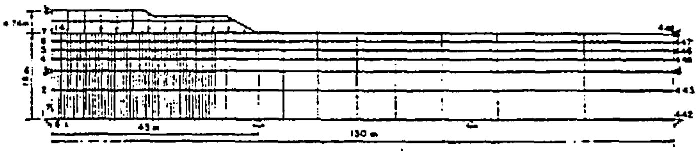

FIG. 4. Finite Element Discretization of Embankment and Subsoils with Vertical Drains

layer. This assumption was justified independently by Balachandran (1990) and Ratnayake (1991). The lateral boundary of the finite element mesh is defined at a distance of seven times the vertical depth from the centerline or three times the vertical depth from the embankment toe. The clay foundation is divided into six horizontal layers, representing the variation of soil properties within the subsurface deposits. The actual performance of the drains could be evaluated comparing the FEM results with the field measurements. In addition, along the centerline of the embankment, Barron's (1948) consolidation theory with radial flow was also employed. The surface loading imposed by the embankment is assumed to be rigid in Barron's (1948) solution; thus, the equal strain solution is considered to be appropriate. The performance of the embankment on the improved foundation could be evaluated with respect to perfect drains, drains with smeared zones, and well resistance.

The associated soil deformation can be simulated by determining the relevant critical-state parameters correctly. The laboratory procedure for the determination of the fundamental cam-clay parameters by triaxial tests is discussed in detail by Britto and Gunn (1987). The values of modified cam-clay parameters obtained from CK_0U triaxial tests and employed in the analysis are summarized in Table 2. The variations of the unit weight (γ_t) as well as horizontal and vertical permeabilities (k_x and k_y) with depth as obtained from in situ tests are also tabulated. The cam-clay properties of the thin weathered crust have been assumed to be the same as those obtained for the silty clay layer just beneath it, in the absence of sufficient data for surface samples.

The surcharge loading imposed on the soft foundation by the compacted embankment is based on a unit weight of 20.5 kN/m^3. The rate of loading is a function of the construction history of the embankment as summarized in Table 3. The geotechnical properties of the fill are as follows.

- Bulk density: 20.4–20.9 kN/m^3
- Dry density: 17.5–18.6 kN/m^3
- Liquid limit: 96–117%
- Plastic limit: 38–46%
- Plasticity index: 56–71%
- Consolidated drained (CD) triaxial tests: c'_d = 14.2 kPa, and ϕ'_d = 31.3°

The enhanced shear strength of the compacted residual fill (sandy clay) is evident from the results of consolidated drained triaxial tests, which indicate a friction angle (ϕ') of 31°. The in situ stress conditions required in the numerical analysis are presented in Table 4, including the effective stresses (σ'_{xo} and σ'_{yo}), isotropic preconsolidation pressure (p_c), and the variation of ground-water pressure (u) with depth.

TABLE 3. Construction History of Embankment

Stage (1)	Fill period (days) (2)	Fill thickness (m) (3)	Rate of filling (m/day) (4)	Rest period (days) (5)
1	1–14	0.0–2.57	0.18	14–105
2	105–129	2.57–4.74	0.09	129–present

TABLE 4. In Situ Stress Conditions at Muar Embankment Site

Depth (m) (1)	σ_{ho} (kPa) (2)	σ_{vo} (kPa) (3)	u (kPa) (4)	p_c (kPa) (5)
0	0	0	0	110
1.75	17.3	28.9	0.0	95
5.5	29.1	48.4	36.7	44
8.0	37.6	62.6	61.3	60
18.0	74.8	124.6	159.3	65

FIELD MEASUREMENTS AND PREDICTIONS

Certain simplifications have been made in the numerical analysis. For instance, some soil properties of the topmost crust have been assumed to be the same as those of the upper-clay-layer deposit, in the absence of reliable laboratory or field data. Also, the effect of the thin peat layer has been ignored due to its considerable depth below the ground level. The test embankment is compacted with a residual fill prone to tensile cracking at certain differential settlements, regardless of its enhanced shear resistance (Indraratna et al. 1990). The effect of the tensile properties of the embankment fill on the numerical predictions was ignored, as the embankment fill was considered as a surcharge loading applied on the foundation surface in two stages of construction (Fig. 4). Furthermore, the excess pore pressures at the drain-soil interfaces for perfect drains at any given time are considered to be zero. In practice, the pore-pressure dissipation may not be instantaneous, due to partial clogging among other factors. The lateral fixity of the finite element mesh (boundary) and the assumption of plane strain cause inevitable deviations from the actual three-dimensional state.

The soft clay foundation was extensively instrumented to monitor the lateral and vertical movements and the development of excess pore-water pressures. The settlements beneath the embankment were measured with the aid of extensometers and settlement gages, while the lateral displacements were determined from the inclinometer readings (Fig. 5). The pore pressures were measured with pneumatic piezometers, and their locations are shown in Fig. 6. The positions of the vertical band drains (shown earlier in Fig. 2) are not marked in Figs. 5 and 6 for diagramatic clarity.

Pore Pressures beneath Embankment

The time-dependent pore-pressure variations along the centerline of the embankment (P4–P7) and 23.3 m to the left of the centerline (P1–P3) were monitored by pneumatic piezometers (Fig. 6). These instruments were located within the influence zone, i.e., triangular grid pattern (1.3-m spacing) of the vertical drains. In the two-dimensional plane strain analysis, the finite element predictions are computed at the corresponding depth, but not necessarily at the exact location (in plan) of the piezometers. As a result, the two-dimensional predictions can deviate from accuracy. However, as the piezometers are located within the influence zone of the closely spaced drains, the error can be considered to be small.

Since the soft clay below a depth of 8 m from the original ground surface is normally consolidated (Fig. 3), the prediction of excess pore pressures by modified cam-clay can be regarded as reliable for these soil layers. For the deposits close to the ground surface, the overconsolidation ratio ap-

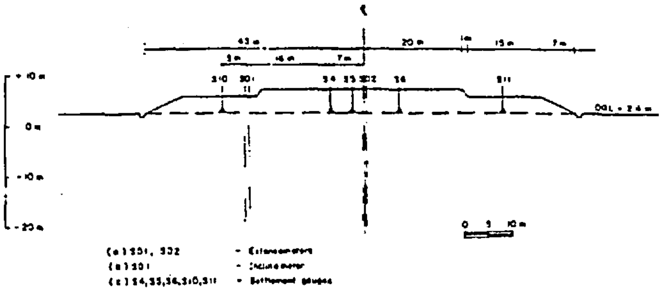

FIG. 5. Location of Settlement Gages and Inclinometers

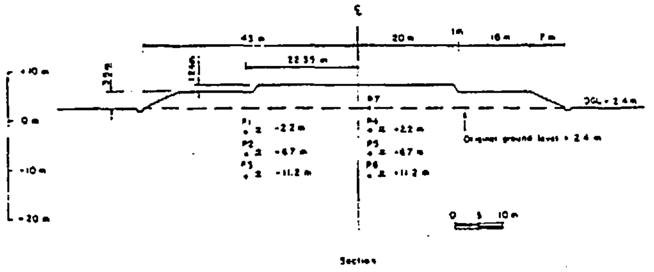

FIG. 6. Location of Pneumatic Piezometers

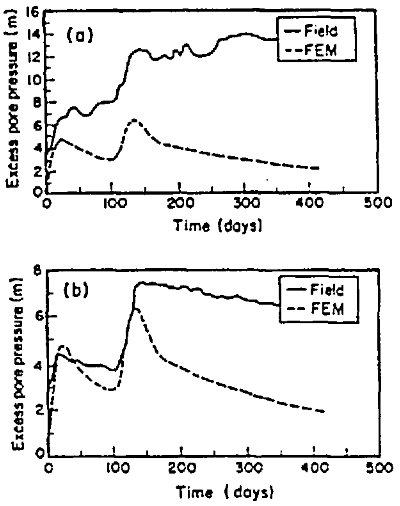

FIG. 7. Variation of Excess Pore Pressures at Embankment Centerline for Piezometers: (*a*) P5 at 9.1 m below Ground Level; and (*b*) P6 at 13.6 m below Ground Level

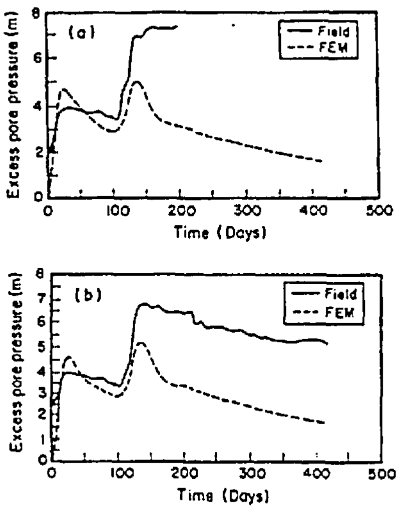

FIG. 8. Variation of Excess Pore Pressures, 23 m Away from Embankment Centerline for Piezometers: (*a*) P5 at 9.1 m below Ground Level; and (*b*) P6 at 13.6 below Gound Level

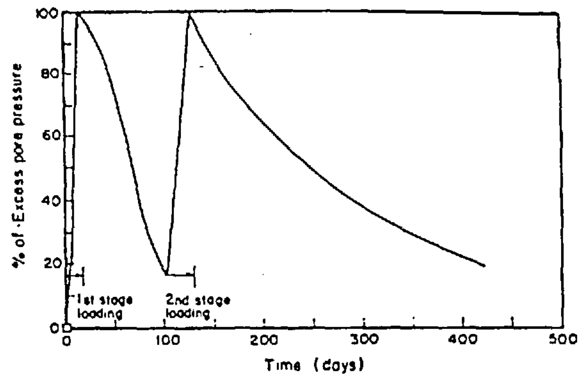

FIG. 9. Percentage of Undissipated Excess Pore Pressures at Drain-Soil Interfaces

proaches 2, hence the predictions from the modified cam-clay model may deviate from accuracy. Figs. 7 and 8 illustrate the typical variation of the excess pore pressures with time along the centerline (P5 and P6) and 23 m to its left (P2 and P3), respectively.

Although the general trends between the finite element results and field data are in agreement especially during the initial stages, the marked discrepancy beyond 100 days is too large to be attributed solely to the plane strain assumption. These excess pore-pressures reflect the retarded efficiency of the vertical drains (partial clogging). Alternatively, the average undissipated excess pore pressures could be estimated by finite element back-analysis of the settlement data at the centerline of the embankment (Fig. 9). In this plot, 100% represents zero dissipation when the drains are fully loaded. Accordingly, at the end of the first stage of construction (i.e., 2.5 m of fill after 105 days), the undissipated pore pressures decrease from 100% to 16%. For the second stage of loading, the corresponding magnitude decreases from 100% to 18% after a period of 284 days, during which the height of the embankment has already attained the maximum of 4.7 m. It can be deduced from Fig. 9 that perfect drain conditions are approached only after a period of 400 days.

Surface Settlement—Analytical Predictions

The centerline is also the line of symmetry of the embankment on which the lateral displacements are zero. Consequently, the analytical or numerical procedures can often be simplified at the line of symmetry. In this section, the predictions are based on the assumption of zero excess pore pressures at the drain boundaries. In other words, the drains are considered to be 100% efficient at all times. The consolidation settlement at ground surface was predicted from the equal strain solution for a single-drain model, which also incorporates the effect of smearing and well resistance (Barron 1948). Since the single-drain analysis assumes zero lateral deformation, it is justified only at the centerline of the embankment. In contrast, the settlments without drains were computed from the one-dimensional consolidation theory (Terzaghi 1943). The field measurements and the predictions from these simplified methods are illustrated in Fig. 10.

It is obvious that the installation of vertical band drains has a considerable

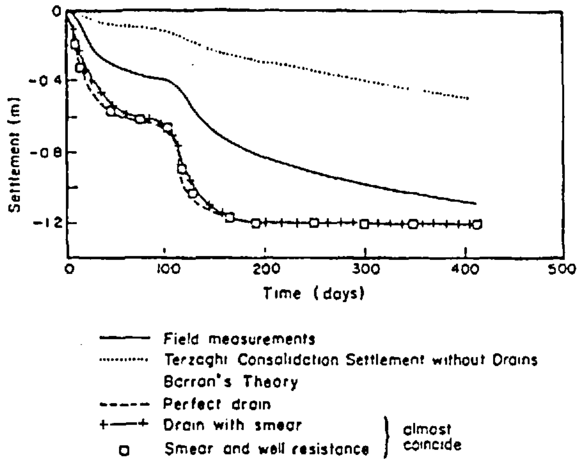

FIG. 10. Comparison of Consolidation Settlement at Ground Surface at Embankment Center

effect on the surface settlements. For instance, at the end of 400 days, the field measurements approach 90% consolidation, and its magnitude is a factor of 2.5 greater than the corresponding surface settlement without drains. However, in comparison with Barron's (1948) solution where complete consolidation is achieved in less than 250 days, the field measurements certainly indicate retarded pore-pressure dissipation at the drain boundaries, as illustrated earlier (Fig. 9). Fig. 10 further reveals that the influence of smearing is small (less than 10%), and is negligible beyond 200 days. The inclusion of well resistance does not seem to have any further effect. This is not surprising, as noticeable well resistance is generally encountered for much longer drains (Ratnayake 1991).

Settlements and Heave—Finite Element Analysis

The single-drain analysis and one-dimensional consolidation analysis are not sufficient to investigate the overall behavior of the soft clay foundation. An extensive consolidation analysis of the clay layers below the entire embankment (including all vertical band drains) is required for the prediction of settlements and lateral displacements away from the centerline. A few very important assumptions have been made in this finite element analysis. To execute CRISP within its limitations: (1) Plane strain conditions were assumed; and (2) the stiffness of the drain was considered to be the same as that of the adjacent soil element. As the effect of smearing and well resistance was not substantial, the detailed finite element analysis was performed for the two extreme cases: with perfect drains and without drains. For perfect drains, the excess pore pressures at the drain boundaries were assumed to be zero.

The consolidation settlements determined by the finite element analysis are illustrated in Fig. 11, together with the predictions for an identical embankment without drains. The field data and numerical predictions are plotted for the ground surface, and at depths of 5.5 m and 12 m, respectively, along the centerline. As a supplementary exercise, a simplified finite element analysis was also conducted for an axisymmetric single drain, including the bank-

;, the
: is a
thout
com-
nents
aries,
ce of
The
This
d for

s are
tion.
: em-
ction
, few
lysis.
were
same
well
per-
ains.
were

ılysis
ıtical
s are
vely,
nent
g the

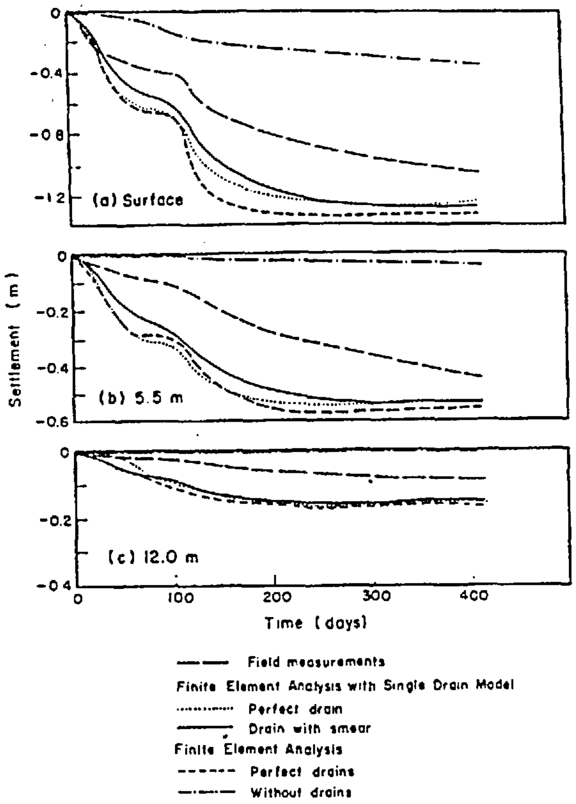

FIG. 11. Consolidation Settlement along Centerline of Embankment at Various Depths

smear effect. In this analysis, the discretized mesh was confined within the influence zone of a single drain, without allowing lateral deformations at the boundaries. The corresponding predictions are also plotted in Fig. 11. The single-drain analysis confirms that the effect of smearing is insignificant particularly after 250 days, which is in accordance with Barron's (1948) solution.

The settlement rates obtained for the complete embankment with perfect drains are only slightly greater than the single-drain analysis. In other words, the assumption of plane strain at the center of embankment has not contributed to excessive settlements. However, both finite element solutions give significantly higher settlements than the field measurements. In particular, at a depth of 12 m, the predicted settlements have reached the utlimate stage, whereas the measurements are still increasing. At the end of the first loading stage (105 days), the field data indicate a surface settlement of 0.4 m, which is only about 60% of the predicted value. However, at the end of 400 days, the predicted and measured surface settlements are 1.28 m and 1.13 m, respectively, giving a more acceptable drain efficiency of 87% in the longer term. The high initial settlements shown by perfect drains is due not only to the assumption of zero excess pore pressures but also to the plane strain condition, which indirectly considers drains in the third dimension. The assumption of the associated flow rule (normality condition) in the cam-clay model also contributes to increased displacements.

To conduct an accurate numerical analysis, the excess pore pressures remaining at the drain boundaries at a given time must be incorporated in the analysis rather than assuming perfect drains. For this purpose, additional subroutines were developed and used in conjunction with CRISP (Ratnayke 1991). In this modification, the nonzero excess pore pressures were computed via additional pore-pressure shape functions applied at the relevant nodes of the LSQ elements along the vertical dissipation boundaries. Figs. 12 and 13 illustrate the corrected settlements along the centerline and at a distance of 23 m to its left. As expected, the modified results provide an excellent match with the field response from the ground surface up to a depth of 12 m.

Although the analysis of perfect drains generally indicates higher initial settlements, the ultimate settlements are reasonably close to the field values. In contrast, 23 m away from the centerline, the field settlements after the second stage of embankment loading exceed the finite element predictions, and beyond 400 days, the field settlements are even greater than the predictions based on perfect drains. One probable reason for this may be the

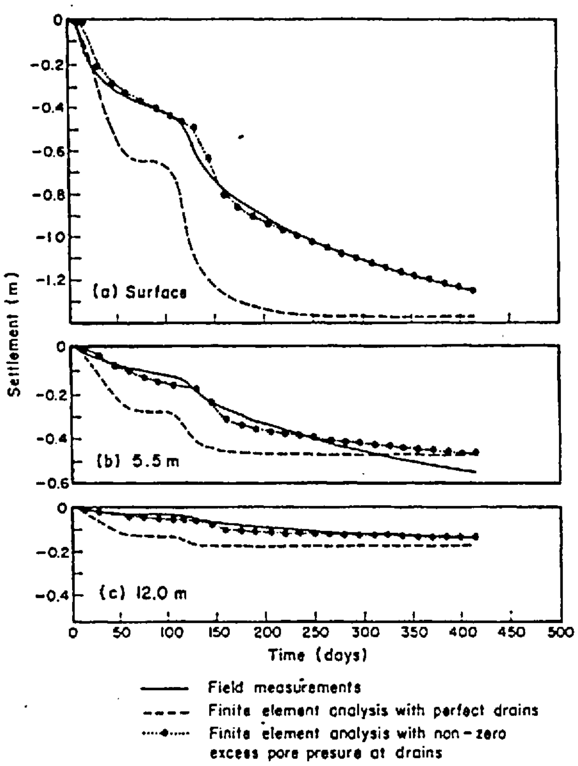

FIG. 12. Comparison of Finite Element Analysis with Field Measurements along Embankment Centerline

s in the
ɔrmality
isplace-

ːessures
rated in
ditional
atnayke
re com-
'elevant
:s. Figs.
ınd at a
vide an
up to a

r initial
values.
fter the
ictions,
he pre-
be the

ʒ along

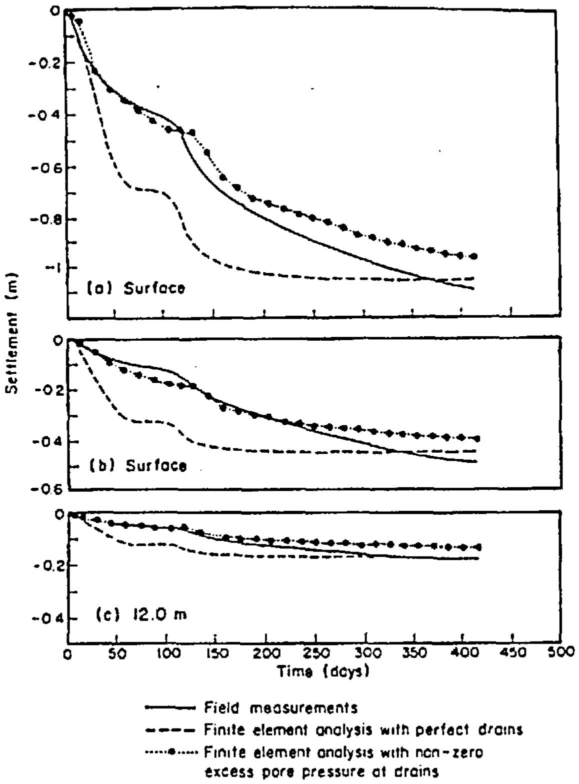

FIG. 13. Comparison of Finite Element Analysis with Field Measurements 23 m from Embankment Centerline

overestimation of heave by the finite element method beyond the toe of the embankment (43 m from the centerline), as shown in Fig. 14 for selected time periods. The maximum predicted heave of 0.1 m may be somewhat higher than the actual values, but as the heave measurements away from the toe are not available, definite conclusions cannot be made. In general, there is no doubt that the modified cam-clay theory is sufficient in predicting the surface settlement profile, if the undissipated excess pore pressures at the drain boundaries are accounted for, as verified in Fig. 14. As the actual field conditions are partially drained, realistic prediction of surface settlements should be anticipated from a coupled consolidation analysis rather than from a purely undrained or purely drained analysis.

Lateral Displacements

The variation of in situ lateral displacements with time at the location of the inclinometer (SD1) is illustrated in Fig. 15. These lateral displacements can be considered as incremental or creep, as the initial lateral movement due to surcharge loading has been subtracted from the total lateral displacements observed at any given time. As expected, the maximum displacements are measured within the upper soft clay layer, whereas within the deeper (stiffer) deposits, the lateral movements are severely curtailed.

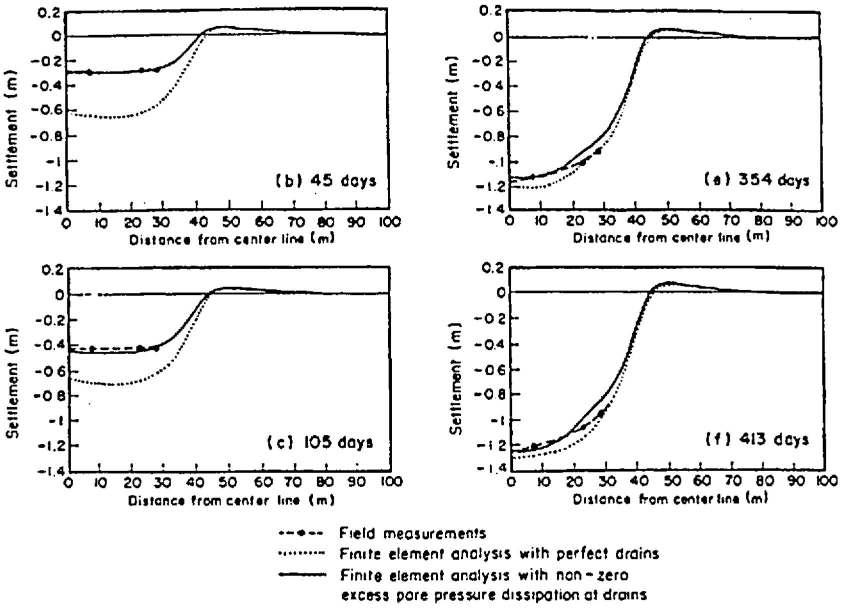

FIG. 14. Surface Settlement Profiles at Selected Time Periods

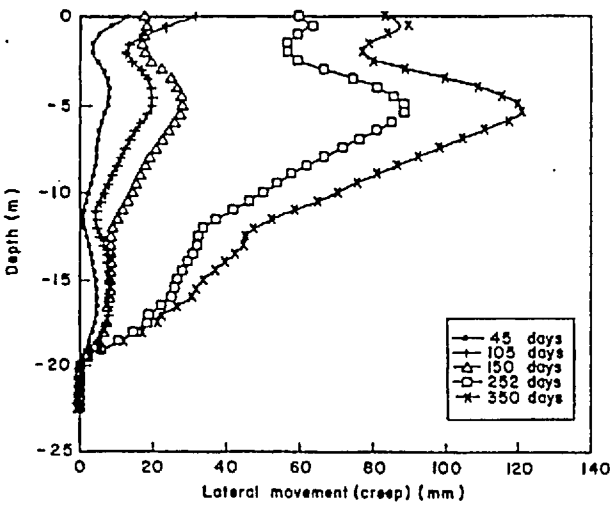

FIG. 15. Development of Lateral Movements at Various Time Periods

However, it is of interest to note the effect of the overconsolidated crust on the lateral displacements within the uppermost 2 m of the foundation. It is obvious from Fig. 15 that the incremental lateral movements at a depth of 5 m are considerably larger than the measurements at any other depth, which is indicative of the probable development of a slip surface at this

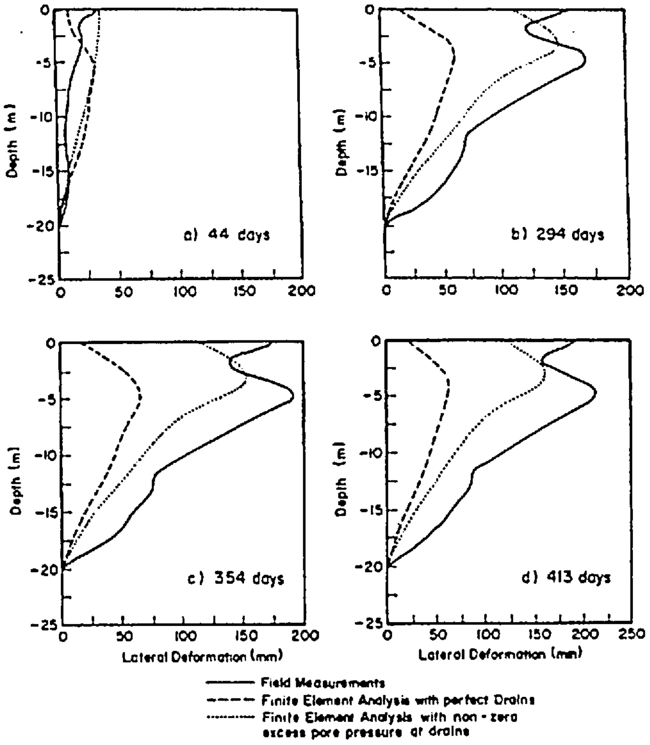

FIG. 16. Lateral Deformation Profiles at Inclinometer Location (23 m from Centerline)

depth if the embankment has been constructed to failure. Total lateral displacements as measured in the field are plotted with the finite element predictions in Fig. 16, for time periods of 44, 294, 354, and 413 days, respectively. As expected, the predictions based on perfect drains are considerably lower than the field measurements, while the recognition of nonzero excess pore pressures at the drain boundaries provides a more realistic comparison.

Previous studies on embankments have shown that the accurate prediction of lateral displacements is a formidable task, in comparison with vertical displacements (Poulos 1972; Indraratna et al. 1992). The errors made in the prediction of lateral movements can be numerous. For instance, the stiff surficial crust restricts the lateral deformation just beneath the embankment to some extent. This process could not be accurately modelled in the analysis, due to the absence of geotechnical data for the overconsolidated crust. In this finite element analysis (CRISP), the modified cam-clay parameters have been obtained from triaxial CK_0U stress-strain behavior. The magnitudes of soil parameters determined in the laboratory are influenced by the initial stress history and the subsequent stress paths followed under given loading-unloading conditions. Although the cam-clay theory proposes the soil parameters (λ, κ, and M) to be unique for a specific yield surface, the laboratory determination of their magnitudes can be influenced by the nature of stress path testing.

CONCLUSIONS

The performance of an embankment constructed on a soft foundation stabilized with vertical band drains was analyzed in this study. The effectiveness of the vertical band drains could be evaluated by considering the excess pore-water pressures, vertical and lateral displacements, and the surface settlement profile in relation to the consolidation behavior of the soft clay. For efficient vertical drains, this case study reveals that the effect of smear and well resistance is generally negligible. In the short term, the rate of dissipation of the excess pore pressures at the drain-soil boundaries controls the drain efficiency, and hence the consequent settlements. In the long term (more than 400 days), the assumption of perfect drain seems to be realistic.

In the short term, the assumption of zero excess pore pressures at the drain boundaries overestimates vertical settlements but underestimates the lateral yield. For perfect drains, although the prediction of initial or short-term vertical settlements is conservative, significant underprediction of the lateral movements is of greater concern. This is because the propagation of failure surface is mainly a function of the incremental lateral displacements within the upper soft clay (Donald and Giam 1989; Indraratna et al. 1992). Therefore, to evaluate the stability of a rapidly built embankment on soft clay, the excess-pore-pressure conditions at the drain boundaries must be correctly incorporated into the finite element analysis at any given time. This study has shown that unless the undissipated excess pore pressures along the drain boundaries are correctly accounted for, the vertical settlements and lateral displacements cannot be predicted to an acceptable degree of accuracy. In this respect, the addition or modification of the pore-pressure shape functions of the elements along the soil-drain boundaries is desirable.

The accurate prediction of lateral displacements require careful assessment of soil parameters corresponding to the actual stress path response in the field, during embankment loading. The installation of vertical band drains curtails the lateral displacements substantially, thereby minimizing the risk of shear failure (slip surface). The existence of a rigid crust just beneath the embankment can also resist lateral displacements, facilitating the construction of higher embankments.

The use of a plane strain finite element analysis (CRISP) cannot be regarded superior to a more powerful three-dimensional analysis of flow into vertical drains. Nevertheless, considering the relative simplicity of the modified cam-clay theories and the user-friendly CRISP, the current analysis is justified in terms of both computational effort and the acceptable quality of predictions.

ACKNOWLEDGMENTS

The writers gratefully appreciate the support of the Malaysian Highway Authority. The writers wish to extend their thanks to Robert Hudson and Ted Brand (Geotechnical Control Office, Hong Kong) for their advice and technical assistance. The assistance of A. Britto and S. Balachandran (Cambridge University, Cambridge, England) is appreciated. Useful comments made by R. N. Chowdhury (University of Wollongong, Wollongong, New South Wales, Australia) are also acknowledged.

ɔy the na-

ɔundation
'he effec-
:ering the
and the
or of the
the effect
term, the
ɔundaries
ts.·In the
seems to

es at the
nates the
or short-
ɔn of the
gation of
ıcements
ıl. 1992).
t on soft
must be
en time.
ɔressures
al settle-
.e degree
·pressure
esirable.
ıl assess-
ponse in
:al band
nimizing
rust just
:ilitating

.nnot be
of flow
ty of the
analysis
: quality

ɪighway
son and
vice and
n (Cam-
mments
ıg, New

APPENDIX. REFERENCES

Balachandran, S. (1990). "Simulation of a test embankment failure (Muar flood plain, Malaysia) using finite element techniques coupled with critical state soil mechanics." MS thesis, Asian Institute of Technology, Bangkok, Thailand.

Barron, R. A. (1948). "Consolidation of fine-grained soils by drain wells." *Trans.*, ASCE, 113, 714–742.

Bjerrum, L. (1973). "Problems of soil mechanics and construction on soft clays." *Proc., 8th Int. Conf. Soil Mech. and Found. Engrg.*, International Society of Soil Mechanics and Foundation Engineering, 3, 111–159.

Britto, A. M., and Gunn, M. J. (1987). *Critical state soil mechanics via finite elements*. Ellis Horwood, Chichester, U.K.

Donald, I. B., and Giam, P. S. K. (1989). "Improved comprehensive limit equilibrium stability analysis." *Civil Engineering Research Report No. 1/1989*, Monash Univ., Melbourne, Australia.

Hansbo, S. (1981). "Consolidation of fine-grained soils by prefabricated drains." *Proc., 10th Int. Conf. Soil Mech. and Found. Engrg.*, International Society of Soil Mechanics and Foundation Engineering, 3, 677–682.

Indraratna, B., Balasubramaniam, A. S., and Balachandran, S. (1982). "Performance of test embankment constructed to failure on soft marine clay." *J. Geotech. Engrg.*, ASCE, 118(1), 12–33.

Indraratna, B., Dilema, E. L. G., and Nutalaya, P. (1990). "Stability of lateritic residual soil for core compaction and design of appropriate granular filters." *Dam Engrg.*, 1(3), 201–220.

Poulos, H. G. (1972). "Observed and predicted behavior of two embankments on clay." *Geotech. Engrg. J. Southeast Asian Geotech. Soc.*, Hong Kong, 3(1), 1–20.

Proceedings of International Symposium on Trial Embankments on Malaysian Marine Clays. (1989). Vols. 1 and 2, Malaysian Highway Authority, Kuala Lumpur, Malaysia.

Ratnayake, A. M. P. (1991). "Performance of test embankments with and without vertical drains at Muar Flats site, Malaysia." MS thesis, Asian Institute of Technology, Bangkok, Thailand.

Roscoe, K. H., and Burland, J. B. (1968). "On the generalized stress strain behavior of wet clay." *Engineering plasticity*. Cambridge Univ. Press; Cambridge, U.K., 535–609.

Terzaghi, K. (1943). *Theoretical soil mechanics*. John Wiley and Sons, New York, N.Y.

Bergado, D. T., Shivashankar, R., Alfaro, M. C., Chai, J.-C. & Balasubramaniam, A. S. (1993). *Géotechnique* 43, No. 4, 589–603

Interaction behaviour of steel grid reinforcements in a clayey sand

D. T. BERGADO,* R. SHIVASHANKAR,† M. C. ALFARO,* JIN-CHUN CHAI*
and A. S. BALASUBRAMANIAM*

The interaction behaviour between steel grid reinforcements and a clayey sand has been studied in laboratory and field pullout tests. The clayey sand is potentially useful as cheap, low quality, locally available and cohesive-frictional backfill in the construction of mechanically stabilized earth walls and embankments, especially in coastal areas. The laboratory tests were conducted under undrained conditions at three compaction moisture conditions. The field tests were conducted on dummy reinforcements embedded at different elevations in a full-scale test embankment resting on soft clay foundation. The laboratory tests revealed that the moisture content of the compacted soil, compaction stress, applied normal stress level, diameter and spacing to diameter ratios of the transverse members of the steel grid, all affect the soil–reinforcement interaction, and thereby, also the magnitudes of the pullout resistances. Interferences between the bearing transverse members of the grid were found to be less significant for spacing to diameter ratios above 75. The laboratory tests, in general, gave conservative values of the pullout resistances as compared with the field tests. The proposed prediction equations agreed well with the experimental data.

KEYWORDS: bearing capacity; compaction; earthfill; full-scale tests; laboratory tests; reinforced soils.

L'interaction entre les renforcements par treillis métalliques et les sables argileux a été étudiée à l'aide d'essais de traction en laboratoire et sur chantier. Le sable argileux est utilisé pour construire des murs en terre mécaniquement stabilisés et des remblais, dans les zones littorales notamment. Ce type de matériau est en effet un matériau de remplissage cohérent-frottant bon marché, de qualité médiocre et disponible localement. Les essais de laboratoire ont été menés, dans des conditions non-drainées, avec trois teneursen eau de compactage. Les essais de chantier ont été réalisés sur des renforcements ancrés à différentes profondeurs dans un remblai grandeur nature reposant sur des argiles molles. Les essais de laboratoire ont montré que la teneur en eau du sol compacté, la contrainte de compaction, le niveau de contrainte normale, le diamètre et les rapports espacement-diamètre des composants transversaux du treillis métallique jouent sur les interactions renforcement-sol, et par conséquent, sur la grandeur de la résistance à la traction. Les interférences entre les éléments porteurs transversaux du treillis semblent moins importantes pour des rapports espacement–diamètre supérieurs à 75. Les essais de laboratoire donnent, en général, des valeurs de résistance en traction plus reproductibles que celles obtenues dans les essais de chantier. Les équations proposées pour la prédiction du comportement sont en bon accord avec les données expérimentales.

INTRODUCTION

The use of cheaper and locally available soils as backfills in mechanically stabilized earth (MSE) constructions, although these may be of low quality, is necessary in regions where good quality granular backfill soils are not readily available at a reasonable cost. MSE is a composite construction material formed by the inclusion of tension resistant materials in the backfill soils to impart tensile strength to the soil and to improve its engineering properties. In its modern form, MSE was first applied for retaining walls that utilized granular backfills and horizontally laid steel strip reinforcements connected to concrete facing units, and was called 'reinforced earth' (Vidal, 1969). Since then, soil reinforcement techniques have developed greatly through the use of various forms of reinforcement of different materials and in different applications. The use of low quality, locally available and cohesive-frictional backfills in MSE constructions has attracted much attention in recent years with the advent of the grid type of reinforcement, and

---

Discussin on this Paper closes 5 April 1994; for further details see p. ii.

* Asian Institute of Technology, Bangkok.

† Saga University, Japan.

especially the welded wire reinforcements. Chang, Hannon & Forsyth (1977) observed that the steel grid reinforcements generated about 5–6 times more pullout resistance than steel strip reinforcements of equivalent area, and that about 85–90% of the total pullout resistance F_t of the steel grid reinforcements comes from the passive resistance F_b due to the soil bearing in front of the transverse members of the grid.

The transverse members of a grid reinforcement can be considered analogous to a series of strip footings in succession which have been rotated through 90° to the horizontal and pulled through the soil. Two types of bearing capacity failure mechanism in front of the transverse members of the grid reinforcement have been proposed. The first is the general bearing capacity failure mechanism (Peterson & Anderson, 1980) in which the slip planes are fully developed (Fig. 1). The prediction equation for the pullout resistance in this case is based on the Terzaghi–Buisman bearing capacity equation as follows

$$F_b/NWD = CN_c + \sigma_v\ N_q \qquad (1)$$

where N, W and D are the number, width and diameter respectively of the transverse wires of the grid reinforcement, C is the cohesion intercept of the backfill soil, σ_v is the vertical normal stress and

$$N_q = e^{\pi \tan\phi} \tan^2 (45 + \phi/2) \qquad (2)$$

$$N_c = (N_q - 1) \cot \phi \qquad (3)$$

where ϕ is the angle of internal friction of the backfill soil. This prediction gives an apparent upper bound envelope for the pullout capacities of the grid reinforcements (Palmeira & Milligan, 1989; Jewell, 1990; Shivashankar, 1991). The second mechanism, proposed by Jewell, Milligan, Sarsby & Dubois (1984) is based on the punching shear failure mode of deeply embedded foundations (Fig. 2). The equation for calculating the pullout bearing resistance has the same form as equation (1), but the bearing capacity factors are expressed as N_{q1} and N_{c1} where

$$N_{q1} = e^{(\pi/2 + \phi)\tan\phi} \tan (45 + \phi/2) \qquad (4)$$

$$N_{c1} = (N_{q1} - 1) \cot \phi \qquad (5)$$

This prediction gives an apparent lower bound envelope for the pullout capacities of the grid reinforcements (Palmeira & Milligan, 1989; Jewell, 1990; Shivashankar, 1991).

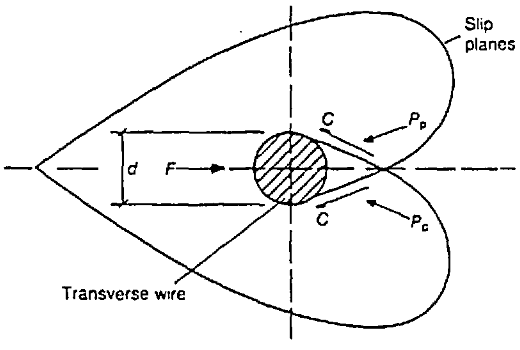

Fig. 1. General bearing capacity failure mechanism (Peterson & Anderson, 1980): see equation (2)

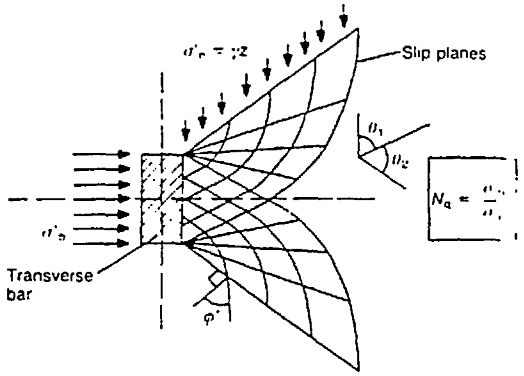

Fig. 2. Punching shear failure mechanism (Jewell *et al.*, 1984): see equation (4)

Ospina (1988) observed that in the case of dry sands, at low confining pressures the failure was close to the punching shear failure mode, whereas at higher confining normal pressures the failure approached a general bearing failure. Using radiography, Ospina observed a general bearing failure with backfill soils comprising uniformly graded fine sand (sand A) and well graded coarse-to-fine sand (sand B) in their loose states. In the dense state, sand A predominantly showed a punching failure; sand B showed a combination of punching and general bearing failures. For the dry Leighton Buzzard sands used in their pullout tests, Palmeira & Milligan (1989) observed that the interference becomes negligible for S/D values above 50, where S is the spacing between the grid bearing members. The data and analyses presented in this Paper were obtained by Shivashankar (1991).

CLAYEY SAND BACKFILL

The index properties of the clayey sand backfill are given in Table 1. The results of the direct and the triaxial shear tests are summarized in Table 2. Direct shear tests were conducted at three moisture conditions: at the dry and wet sides of optimum moisture content (OMC) compacted so

Clay	Silt	Sand			Gravel	
		Fine	Medium	Coarse	Fine	Coarse
33	11	41	14	1	0	0

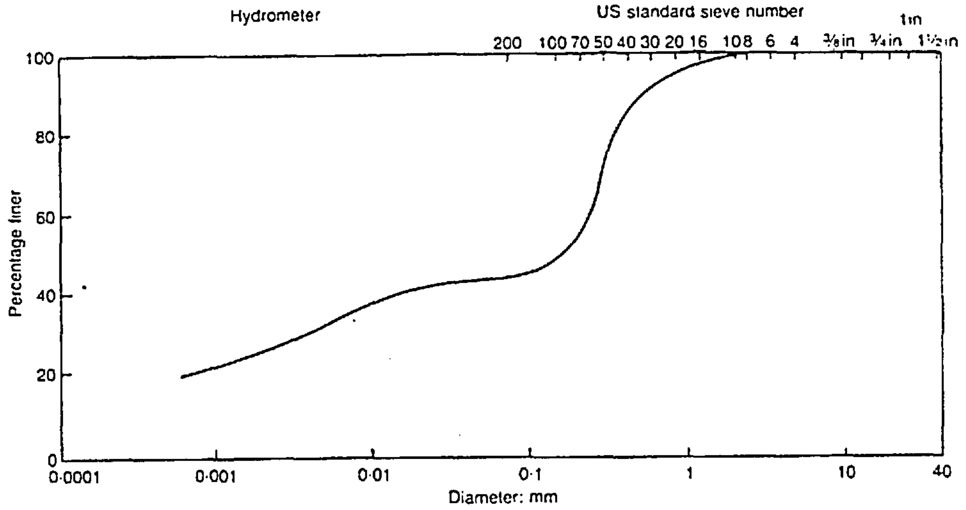

Fig. 5. Grain size distribution of clayey sand (1 in = 25·4 mm)

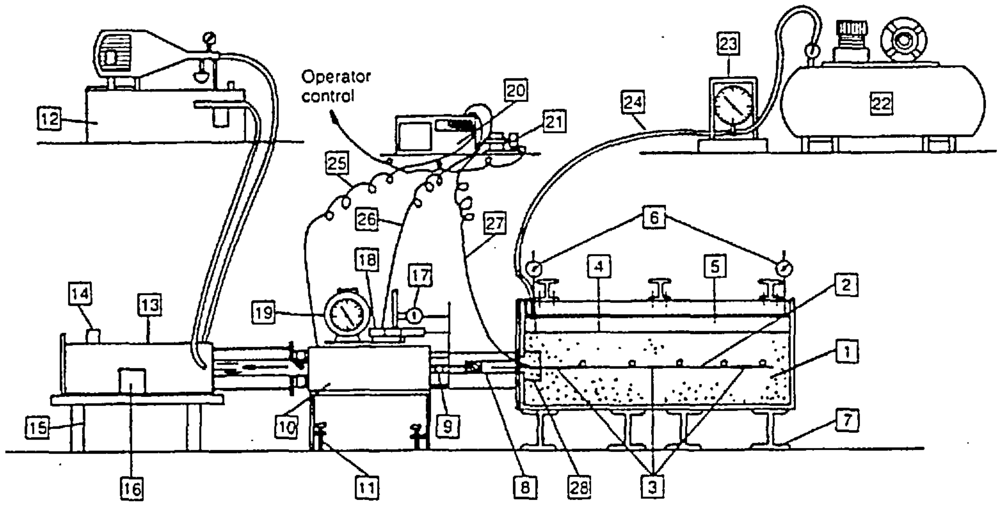

1 Compacted soil in pullout box
2 Grid specimen
3 Strain gauges
4 Flexible plate placed over compacted soil
5 Air bags for applying normal pressures
6 Dial gauges at top to measure dilatancy
7 Airlock pads
8 Clamping mechanism
9 Swivel joint
10 Load cell
11 Mount load for load cell of adjustable height
12 Piston pump and motor with filters and valves
13 Hydraulic cylinder
14 Servo valve
15 Mount for cylinder
16 Analogue output module
17 Front dial gauges
18 LVDT for measuring front displacements
19 Stop clock
20 21X data logger with multiplexer
21 EMRS power supply module and EMD amplifier module
22 Air compressor
23 Regulator
24 Stiff tubing
25 Lead wire connecting load cell to data logger
26 Lead wire connecting LVDT to data logger
27 Lead wires connecting all strain gauges to data logger through multiplexer
28 Two horizontal sleeves 100 mm apart

Fig. 6. Laboratory pullout test set-up

Table 1. Index properties of clayey sand

Colour	Brownish
Percentage passing US standard sieve 200	45%
Atterberg limits Liquid limit Plastic limit	 32% 12%
Standard Proctor compaction test OMC Maximum dry density	 14·4% 17·9 kN/m^3
Specific gravity of soil particles	2·55

that the dry density corresponded to 95% of standard Proctor density, and at OMC compacted to 100% of standard Proctor density (Table 2). The direct shear specimen is 150 mm long, 150 mm wide and 127 mm high. The air dried soil sample was mixed with the appropriate amount of water, then sealed in a plastic bag and kept in a humid room for 24 h. The specimen was compacted to the desired degree in the direct shear box in four layers. Normal pressure was applied and the specimen was sheared at a constant shear displacement rate of 1 mm/min. The tests were conducted in unconsolidated–undrained conditions to simulate the shear condition of the soil during the pullout test. However, the triaxial tests were conducted only at a moisture content of 13·2%, about 1% on the dry side of optimum, and compacted to 95% of standard Proctor density. The specimen was 102 mm in diameter and 204 mm high, and was compacted in a mould by a static compaction machine. The tests were conducted in unconsolidated–undrained conditions with a constant axial strain rate of 0·019%/min (0·38 mm/min). The strength parameters in Table 2 were determined by total stress analysis. Typical stress–strain curves from the direct and the triaxial shear tests are shown in Figs 3(a) and 4. Fig. 3(b) shows the failure envelopes from the direct shear tests at all three moisture conditions. The typical grain size distribution of the clayey sand used in this study is shown in Fig. 5.

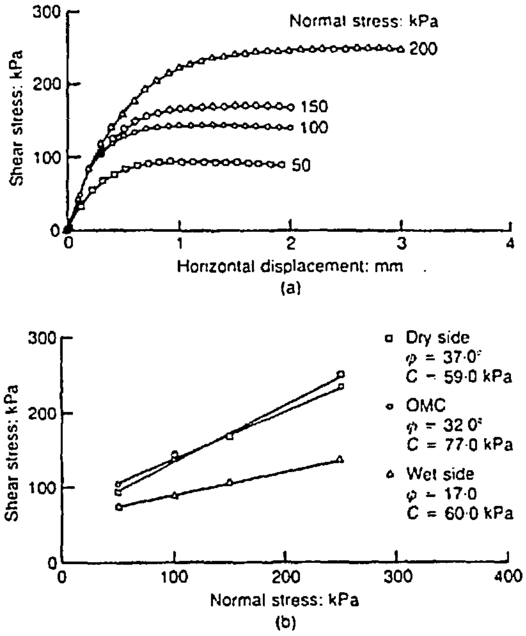

Fig. 3. (a) Typical stress–strain curves from the direct shear tests (clayey sand (95%) on dry side); (b) failure envelopes from the direct shear tests at various compaction moisture conditions

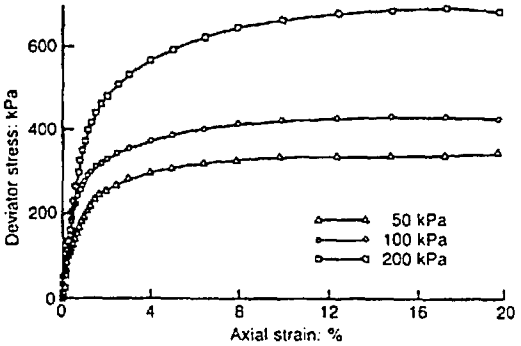

Fig. 4. Typical stress–strain curves from triaxial shear tests: clayey sand (95%) on dry side

Table 2. Direct and triaxial shear results for clayey sand

Standard Proctor density	Water content: %	Dry unit weight: kN/m^3	ϕ: degrees	C: kPa
Direct shear test				
95% dry side	10·0	17·0	37·0	59·0
100% (OMC)	14·4	17·9	32·0	77·0
95% wet side	20·2	17·0	17·0	60·0
Triaxial test				
95% dry side	13·2	17·0	33·0	56·0

sand. An inflated air bag was placed over this plate to take reaction from I-beams above it which were bolted onto the top of the pullout box, through an upper top cover plate.

FULL-SCALE TEST EMBANKMENT

A full-scale wall/embankment MSE system with welded steel geogrid reinforcements as shown in Fig. 9 was constructed inside the campus of the Asian Institute of Technology 42 km north of Bangkok. It has a vertical welded steel grid facing the front and a sloping back (Fig. 8(b)): the unreinforced slope can be built as 1 : 1 because of the effect of cohesion of backfill soil. It comprises three sections corresponding to the three different backfill materials used, i.e. clayey sand in section I, lateritic residual soil in section II and weathered Bangkok clay in section III (Fig. 9(a)). The backfill materials were compacted to 95% standard Proctor (ASTM D698) densities on the dry side of optimum (see Fig. 9). Details of the performance of this MSE wall/embankment have been given by Bergado, Sampaco, Shivashankar, Alfaro, Anderson & Balasubramaniam (1991), and Bergado, Shivashankar, Sampaco, Alfaro & Anderson (1991).

Related laboratory and field pullout test results using steel grid reinforcements in conjunction with this full-scale test embankment have been given by Bergado, Hardiyatimo, Cisneros, Chai, Alfaro, Balasubramaniam & Anderson (1992) and Bergado, Lo, Chai, Shivashankar, Alfaro & Balasubramaniam (1992). Dummy reinforcement specimens protruding ~0·35 m from the vertical face of the wall/embankment system were installed during construction, at different levels in each of the three sections, for field pullout tests. The foundation subsoil consists of a layer of soft clay ~6 m thick sandwiched between a surficial 2 m thick layer of weathered Bangkok clay and an underlying layer of stiff clay.

FIELD TESTS AND RESULTS

Constant strain field pullout tests were conducted about eight months after the construction of the test embankment. By this time, both the foundation subsoil and the wall/embankment system had undergone vertical and lateral movements. Five dummy reinforcement specimens embedded in the clayey sand section (see Fig. 9(a)) were pulled out. A typical dummy reinforcement is shown in Fig. 10. The pullout test procedure was the same as adopted in the laboratory pullout tests; the dummy reinforcements were pulled out at 1 mm/min. The pullout force was applied by means of a specially designed reaction frame butting against the wall face. A wooden platform was built to support the pullout equipment.

Figure 11 shows a typical set-up for the field pullout test. Figs 12 and 13 show the load–displacement and strain–displacement curves for the field pullout tests in clayey sand. These figures show that for dummy mats 7 and 9, the pullout resistance was not fully mobilized even at a pullout displacement of 125 mm. However, the increase in pullout resistance rate was reduced starting at a pullout displacement of 80 mm. Dummy mat 10 has longitudinal bars with ribs only (25 mm long) with 225 mm spacing. The

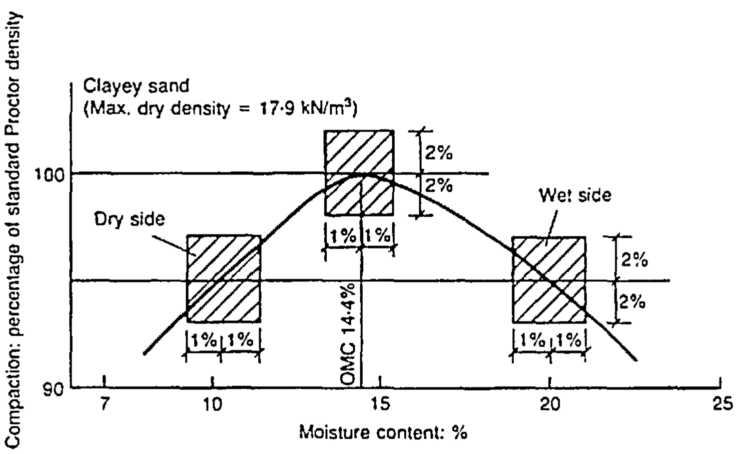

Fig. 8. Compaction curve of the clayey sand showing ranges of the moisture contents and the dry densities used in the laboratory pullout tests and the direct shear tests

LABORATORY TESTS

Pullout tests were conducted in the laboratory using a pullout box 1·25 m long, 0·75 m wide and 0·51 m deep (inside dimensions), made of steel plates and steel beams welded and bolted together (Fig. 6). A multi-stage pullout testing procedure was followed. Three pullout tests in three corresponding loading stages were conducted at each set-up. The vertical confining normal stress was increased at each stage. In the first stage, the reinforcing mat was pulled out under a given normal stress, then the pulling force was released and the normal stress was increased. After allowing the normal stress to stabilize for ~30 min, the mat was again pulled out. This constituted the second stage, and was followed by a similar third stage. At each stage the mat was pulled out by 25 mm.

Two diametrically opposed strain gauges were fixed at each instrumentation point on the grid specimen to cancel any bending stresses. Before the start of the actual pullout test, a seating load of ~2 kN was applied to remove any slack in the system. During the pullout test, a uniform pullout rate of 1 mm/min was maintained with the help of electronic controls. All the pullout tests were conducted under unconsolidated–undrained conditions. The clayey sand on the dry side of optimum and at the OMC was actually in the partially saturated state. Two types of pullout test (or reinforcement) were conducted.

(*a*) *friction pullout tests:* conducted using a reinforcement system with the four longitudinal bars spaced laterally at 0·15 m and no transverse bars embedded in the soil (Fig. 7(a))

(*b*) *grid pullout tests:* conducted using welded wire grid reinforcements of varying bar sizes and mesh geometries (Fig. 7(b), Table 3); the contribution of the bearing resistances in front of the transverse members was estimated by subtracting from the results of the grid pullout test (total pullout resistance) the frictional pullout resistance derived from the corresponding friction pullout test in (*a*) above.

Table 3. Diameter of welded wires

Wire size number	Nominal diameter: mm
W3·5	5·359
W4·5	6·071
W5	6·502
W7	7·595
W12	9·931

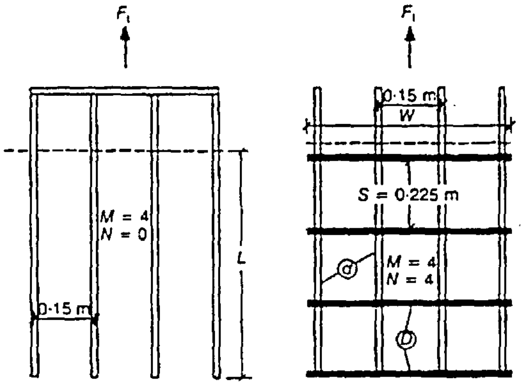

Fig. 7. Types of reinforcement used in the laboratory pullout tests

In each set-up, the soil in the pullout box was compacted in two equal lifts, each 0·15 m thick, using a hand-operated impact (Wacker) tamper. After compaction of the first lift, the level of the compacted soil surface reached almost up to the centre of the pullout slot where the reinforcement was placed. The grid specimen was then placed in position at the centre of the slot and its level and alignment were checked. The second lift of the backfill soil was placed over it and compacted again. The uniformity in the degree of compaction and the moisture contents in both lifts was checked by use of a nuclear gauge densitometer.

Pullout tests were conducted at the same three compaction moisture conditions as for the direct shear test specimens. A variation of ±2% about the mean value was observed in the degree of compaction; a corresponding variation of ±1% was recorded in the moisture content (Fig. 8). The clayey sand used was found to be very sensitive to changes in moisture content only on the wet side of optimum, where there was a sharp decrease in shear strength (Fig. 3(b)).

Two horizontal metal plates were used as sleeves on the inside part of the opening of the pullout box, extending 0·15 m behind the face. The purpose of these was to decrease the horizontal stresses on the front face near the slot during the pullout and also to minimize the arching effects over the grid specimens. The sleeves were positioned across the full width of the pullout box, above and below the reinforcements. This also kept the normal loads off the front 0·15 m. The two sleeves were separated by spacers 0·1 m high at the front corners of the pullout box to avoid any contact with the reinforcements as shown in Fig. 6.

A layer of fine sand ~30 mm thick was laid out on top of the compacted soil to distribute the normal pressure uniformly. The lower top cover plate, 6·35 mm thick, was then placed over the

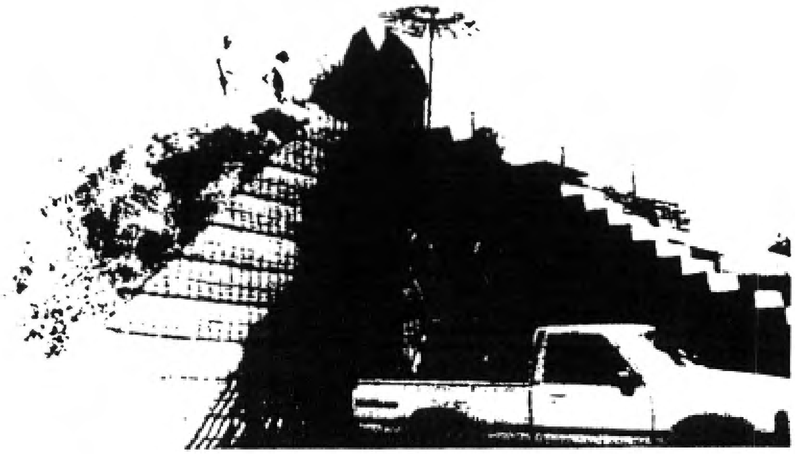

Fig. 11. Typical field pullout test set-up

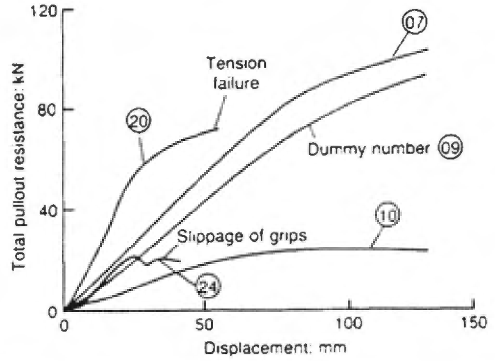

Fig. 12. Load–displacement curves from field pullout tests in clayey sand

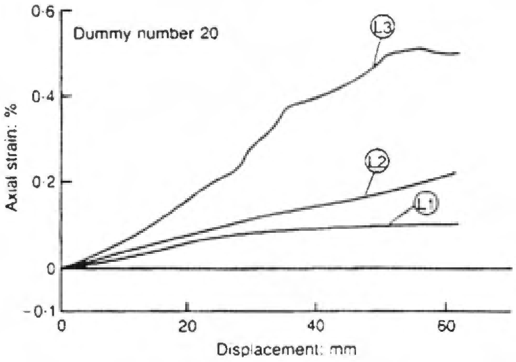

Fig. 13. Strain–displacement curves from field pullout tests in clayey sand

total resistance was fully mobilized at a pullout displacement of 60 mm. A comparison of the results from dummy mats 9 and 10 shows that most pullout resistance was derived from bearing resistance of grid transverse members. To be mobilized, the pullout bearing resistance needs larger pullout displacements.

LABORATORY TEST RESULTS

Friction pullout tests

Figure 14 shows the results of the friction pullout tests at various compaction moisture conditions. The frictional resistances $F_f/\pi LMd$ were found to increase slightly with increasing applied normal stress at all moisture conditions.

Apparent friction coefficient

The apparent friction coefficient on the longitudinal wires has been defined as

$$\mu^* = f/\sigma_{\text{ave}} \quad (6)$$

$$f = F_f/M\pi dL \quad (7)$$

where μ^* is the apparent friction coefficient, f is the frictional resistance over the longitudinal wires, σ_{ave} is the average overburden pressure on the members of the grid reinforcement, F_f is the maximum pullout force from the frictional pullout tests at the end of a 25 mm pull, M and D are the number and diameter of longitudinal wires in the grid reinforcement and L is the length of embedment of the grid reinforcement in the backfill soil. μ^* was found to decrease with the increase in the applied normal stress level. Fig. 15

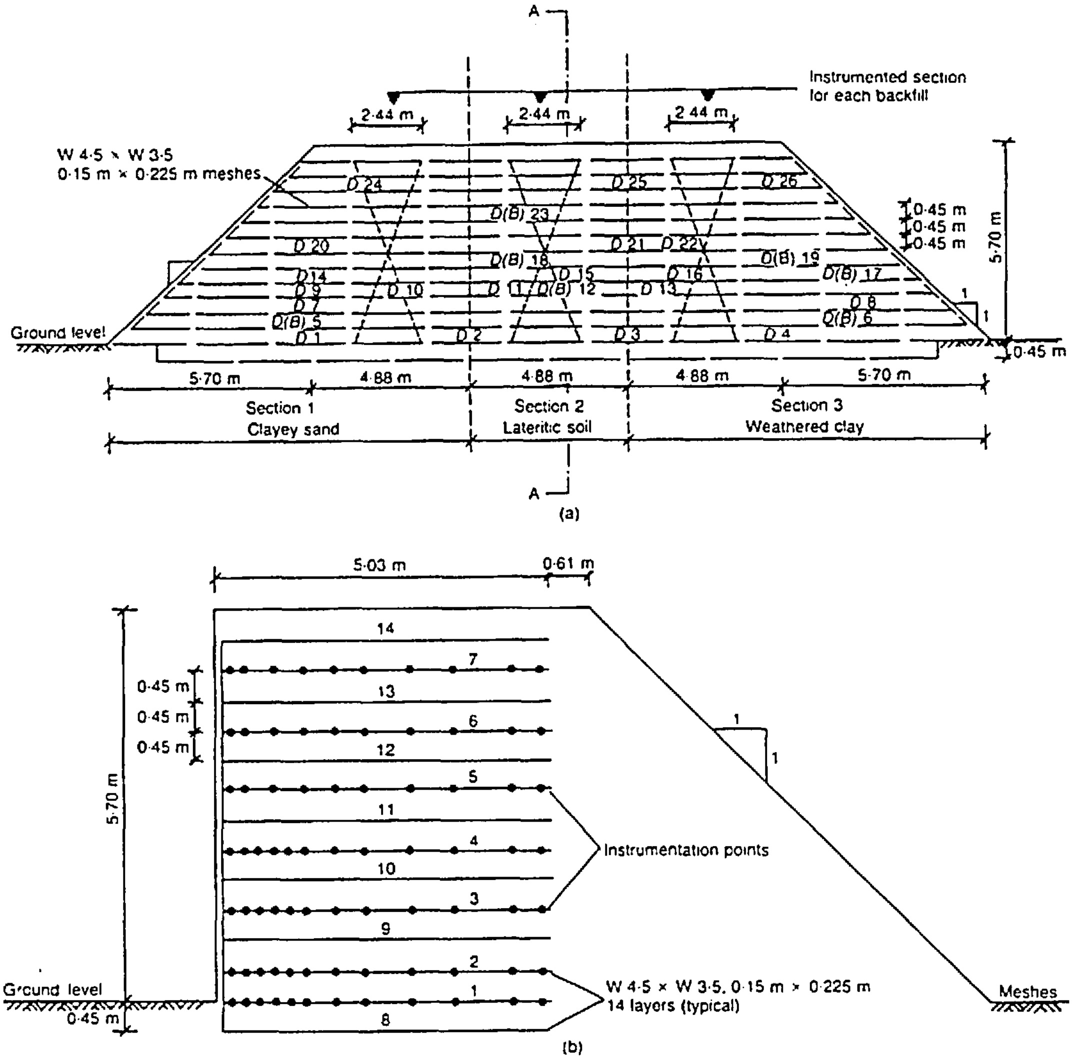

Fig. 9. Views of the welded wire wall: (a) front-sectional; (b) cross-sectional (only mats 1–7 are instrumented)

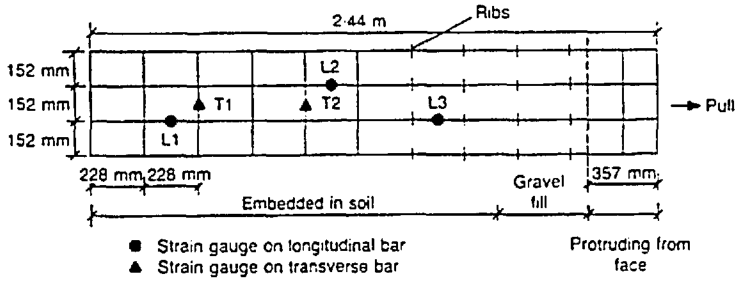

Fig. 10. Typical dummy reinforcement used in field pullout test

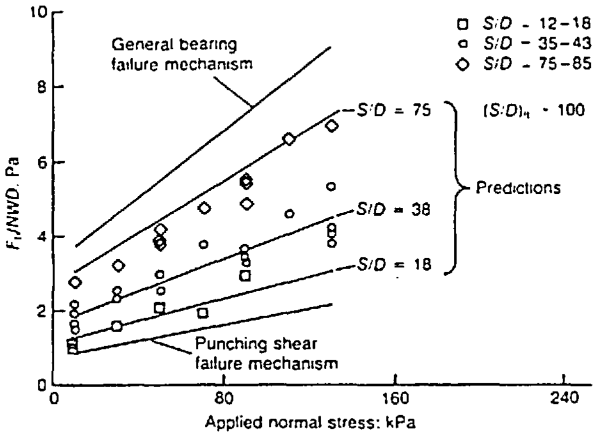

Fig. 17. Grid pullout test results on the dry side of OMC (laboratory, clayey sand)

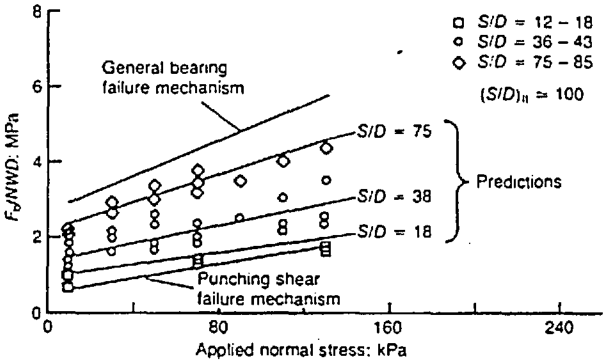

Fig. 18. Grid pullout test results at OMC (laboratory, clayey sand)

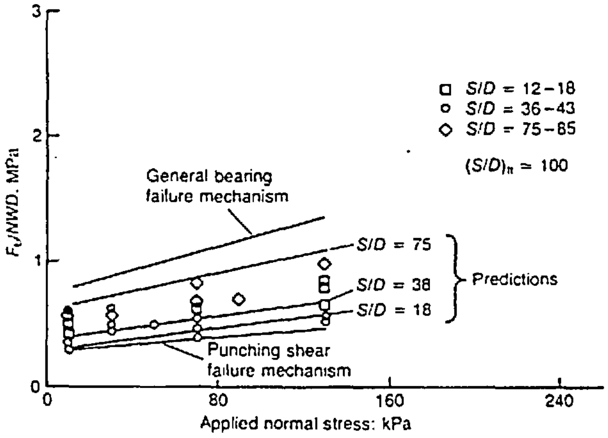

Fig. 19. Grid pullout test results on the wet side of OMC (laboratory, clayey sand)

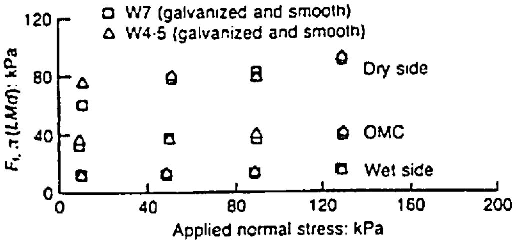

Fig. 14. Friction pullout test results for clayey sand at various moisture conditions (laboratory)

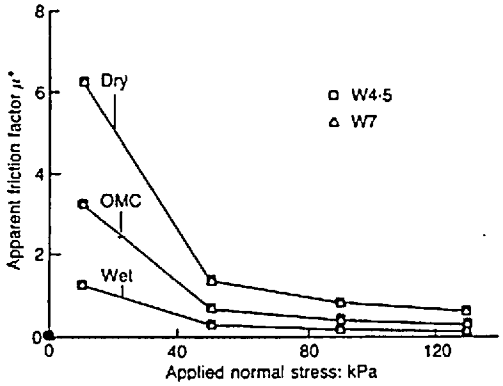

Fig. 15. Variation of the apparent friction coefficient with the applied normal stress level at various moisture conditions (laboratory, clayey sand)

shows that the curves flatten out beyond a normal stress level of ~100 kPa. These results are similar to those obtained by Schlosser & Elias (1978) for pullout tests of strip reinforcements from reinforced earth walls.

The average overburden pressure σ_{ave}, i.e. stress normal to the surface of the wires, was taken as 1·15 times σ_v (see Fig. 16) to account for the compaction induced stresses and the circular cross-section of the longitudinal wires. Compaction effects can be a form of overconsolidation. An assumed overconsolidation ratio of 8 was found to be appropriate for the compacted clayey sand used in this study: this value corresponds to a lightly overconsolidated soil (Dunn, Anderson & Kiefer, 1980; Bergado, Sampaco *et al.*, 1991), giving a coefficient of lateral earth pressure at rest K_0 value of 1·3.

Grid pullout tests

The contribution of the frictional resistance over the longitudinal wires to the total pullout resistance of the grid reinforcement was found on average to be only about 10–15%. The pullout resistance of the grid reinforcements was found to vary considerably with the *S/D* ratios of the transverse members of the grid. The results of this study agreed essentially with the apparent upper and lower bound envelopes mentioned above, and agreed well with the findings of Ospina (1988). At lower confining normal stresses the failure was closer to the punching shear failure mode; at higher confining normal stresses it was closer to the general bearing failure. For the smaller diameter transverse bars at larger spacings (larger *S/D* values), especially at higher confining normal stresses, the pullout resistances after 25 mm of pull tended to approach the prediction of the general bearing failure mechanism. In the case of the grid mats with closely spaced and larger diameter transverse wires, the pullout resistances after 35 mm pull tended to approach the prediction of the punching shear failure mechanism, especially at low confining normal stresses (Figs 17–19).

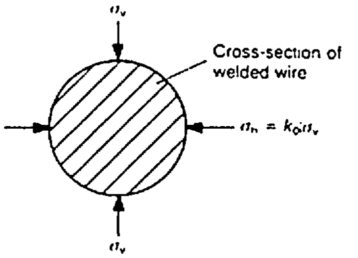

Compacted soil ≡ Overconsolidated soil
(OCR = 8, K_0 = 1·3 for weathered clay)

Fig. 16. Average overburden pressure on members of grid reinforcement: $\sigma_{ave} = (\sigma_v + \sigma_h)/2 = 1{\cdot}15\sigma_v$

On the wet side of OMC, the total pullout resistances were found to be very small. This is reflected by the low values of the shear strength parameters of clayey sand backfill on the wet side (Table 2). Moreover, the clayey sand backfill on the wet side was found to be fully saturated. The increase in the moisture content seems to incline the pullout failure mechanism in front of the transverse bars towards the general bearing failure mechanism (Fig. 19). The pullout behaviour of the grid reinforcements in compacted cohesive-frictional soils on the wet side is comparable with that in loose and dry sands.

Effect of stage loading

The rate of increase in the total pullout resistance with the grid displacement was higher in the earlier part of the laboratory grid pullout tests. After this initial phase, i.e. after about 8–12 mm displacement of the grid specimen, the rate of increase slowed down considerably and the can interfere with each other (Palmeira & Milligan, 1989). In the calculation of the values of the degree of interference (DI) from the grid pullout test data, the maximum bearing resistance that can be generated in front of the transverse bars with no interference $(F_b/NWD)_{lt}$ was obtained from equations (1)–(3), which give the apparent upper bound value. The DI from the grid pullout test data was thus calculated as

$$\mathrm{DI} = 1 - \frac{(F_b/NWD)_{ave}}{(F_b/NWD)_{lt}} \qquad (8)$$

where $F_b/NWD)_{ave}$ is the average bearing resistance mobilized in front of all the transverse bars of the grid reinforcement obtained from the grid pullout test. The first transverse bar was assumed to have no interference effects; the bearing resistances mobilized in front of all the other transverse bars were assumed to be proportional to the S/D ratios of the grid reinforcement. Therefore, the DI can also be expressed in terms of the grid parameters as

$$\mathrm{DI} = 0{\cdot}8 - \frac{(S/D)}{(S/D)_{lt}} \qquad (9)$$

where DI > 0 and $(S/D)_{lt}$ is the limiting value of (S/D) such that for $(S/D) > (S/D)_{lt}$ there will be no more interference effects and the bearing resistances mobilized in front of the transverse members are the maximum possible values. $(S/D)_{lt}$ for clayey sand at all moisture conditions was found to be ~100. Equation (9) is valid only for S/D >10: this was the lower limit value used in the study. The linear relationship of DI and S/D indicated by equation (8) at different compaction moisture conditions is shown in Fig. 22, which also shows that at all moisture conditions, and normal stress levels of 10–130 kPa, the interference between bearing members of the steel grid reinforcements becomes less significant (< ~25%) for S/D >75. Although there is considerable scatter in the data, the trend is clear.

PREDICTION EQUATIONS FOR LABORATORY TESTS

The frictional resistance F_f, is given by

$$F_f = \pi LMd[C_a{}^p + \sigma_{ave} \tan (\delta^p)] \qquad (10)$$

Dividing both sides by NWD

$$F_f/NWD = \pi S_f[C_a{}^p + \sigma_{ave} \tan (\delta^p)] \qquad (11)$$

The terms $C_a{}^p$ and $\tan \delta^p$ were obtained by a simple linear regression of the friction pullout test data with F_f/NWD as the dependent variable and the average overburden pressure, $\sigma_{ave} = 1{\cdot}15\sigma_v$, as the independent variable. The values of $C_a{}^p$ and $\tan \delta^p$ obtained for clayey sand were 70 kPa and 0·18 on the dry side, 37 kPa and 0·05 at OMC and 14 kPa and 0·04 on the wet side.

The bearing resistance in front of the transverse bars has been expressed in general form as

$$F_b/NWD = (CN_c + \sigma_v N_q)(1 - \mathrm{DI}) \qquad (12)$$

The term F_b/NWD represents the bearing resistance per unit area of the transverse members normal to the direction of pullout. The bearing capacity factors N_q and N_c were obtained from equations (2) and (3) respectively. The shear strength parameters were derived from the direct shear tests. The DI in equation (12) can be estimated from equation (9) by considering a suitable value of $(S/D)_{lt}$. The prediction lines are shown in Figs 17–19; these agree well with the experimen-

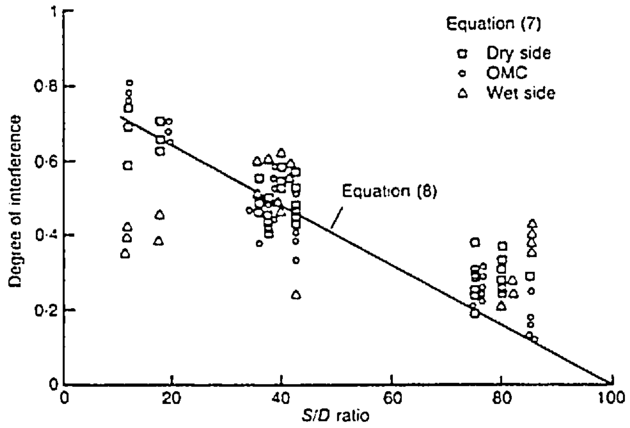

Fig. 22. Variation of degree of interference with S/D (laboratory)

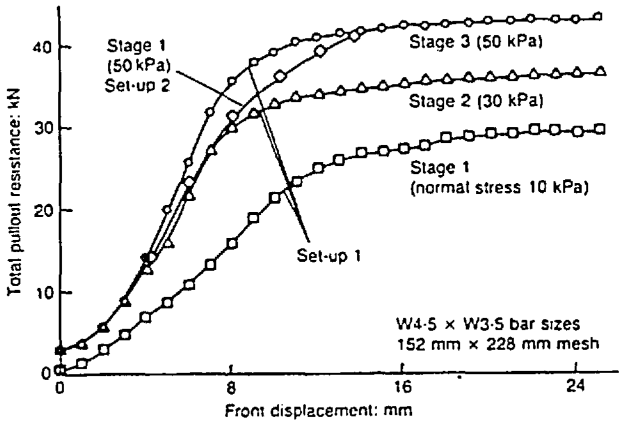

Fig. 20. Typical load–displacement curves from laboratory pullout tests (clayey sand, dry side of OMC)

pullout resistances attained approximately constant values (Fig. 20). For a given displacement at a given normal stress and compaction moisture condition, the laboratory pullout resistance of the grid reinforcements during the first stage loading, especially on the dry side of OMC, was lower than during the later stages (Fig. 20). However, the difference in the maximum pullout resistances at the end of 25 mm of pull was found to be very small. It was therefore concluded from this study that for every stage in a multi-stage pullout testing programme, the maximum pullout resistance at the end of 25 mm of pull for a given normal stress and moisture condition was about the same. The only difference was in the manner in which these peak values were attained. The peak values comprised the maximum pullout resistances of the grid reinforcements at the end of 25 mm of pull, for any set-up at a given moisture condition, adopting the three-stage pullout testing programme for each set-up. The first stage load–displacement curves were found to be flatter and smoother than the later stages, indicating a lower modulus (Fig. 20). The second stage loading results were found to lie on the regression line for the total pullout resistances at that moisture condition (Fig. 21). Motaleb & Anderson (1988) concluded that the load–displacement curves for the multi-stage tests were continuations of the post-yield portion of the first stage curve, which was also found to be relevant to the results of this study.

Degree of interference

Grid members may be considered as a succession of bearing elements buried in the soil that

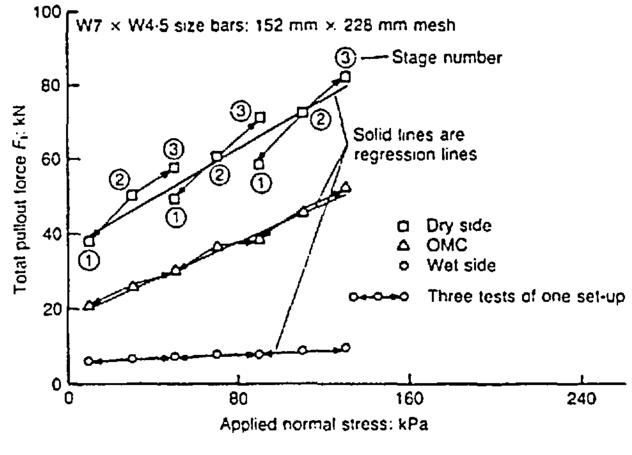

Fig. 21. Effect of moisture content and stage loading on the laboratory pullout capacities (clayey sand)

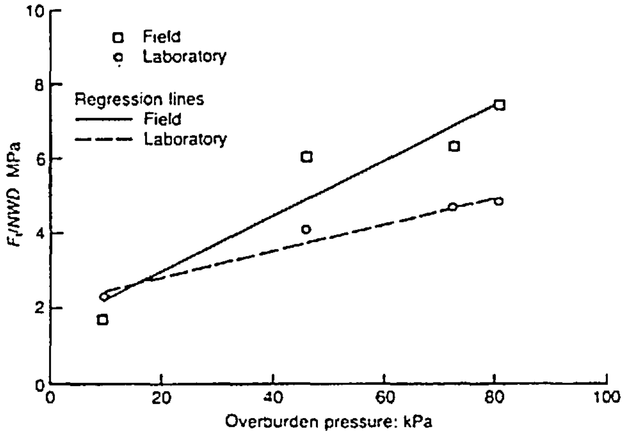

Fig. 23. Comparison of laboratory and field pullout test results (clayey sand)

box, expecially the front face in the small scale tests, can affect the generated pullout resistances. Compaction and moisture can be controlled better in the laboratory.

CONCLUSIONS

The pullout failure mechanisms in front of the transverse members of the grid, and hence the magnitude of the total pullout resistance, were found to be a function of both soil and grid parameters.

Either the general bearing failure mechanism or the punching shear failure mechanism is possible at any time in front of the transverse of the grid during pullout, depending on the grid and soil parameters.

The pullout failure mechanism was found to be a function of the *S/D* ratios of the transverse bars, the compaction moisture content of the soil and the stiffness of the soil as compared with that of the transverse member. An increase in the moisture content, the vertical normal stresses or the *S/D* ratios was found to steer incline pullout failure mechanism towards a general bearing failure mechanism.

The bearing resistances in front of the transverse bars of the steel grid constitute about 85–90% of the total pullout resistance; the frictional resistances over the longitudinal wires contribute the rest.

Interference between the passive resistant zones of the successive transverse members in a steel grid reinforcement becomes less significant for *S/D* ratios greater than ~75. However, bar diameters of ~6·35 mm for both longitudinal and transverse bars forming mesh openings of about 0·15 × 0·225 m to 0·15 × 0·3 m have been found to be the most convenient in practice. The vertical spacing can be provided according to the design requirements.

Cohesive-frictional soils compacted to 95% of standard Proctor's density on the dry side of OMC can generate pullout capacities comparable to those of the good quality granular backfill soils.

The welded-wire mats can be used effectively to reinforce low quality cohesive-frictional backfill soils.

ACKNOWLEDGEMENTS

This work was done as a part of a three-year USAID sponsored research project conducted at the Asian Institute of Technology (AIT), Bangkok, Thailand. Thanks are due to Professor Loren R. Anderson and Casan L. Sampaco of Utah State University, Logan, Utah, USA, for their help as research collaborators. Dr Shivashankar was supported by the Japanese Government for the first three years of his study at AIT.

NOTATION

C	cohesion intercept of the backfill soil
D	diameter of the transverse wires of the grid reinforcement
d	diameter of the longitudinal wires of the grid reinforcement
F_b	bearing resistance (force) in front of the transverse wires
F_f	frictional resistance (force) over the longitudinal wires
F_t	total pullout resistance (force) of the grid reinforcement
f	frictional resistance over the longitudinal wires

tal data. The total pullout resistance can be expressed in general form as

$$F_t/NWD = [(CN_c + \sigma_v N_q)(1 - \mathrm{DI})] + \pi S_f[C_a{}^p + \sigma_{ave} \tan(\delta^p)] \qquad (13)$$

COMPARISON OF LABORATORY AND FIELD RESULTS

The reinforcement mats used in both the laboratory and the field pullout tests had 0·15 × 0·225 m mesh openings with various bar diameters, and most of them had five transverse bars. The length of embedment of the reinforcements in the laboratory pullout tests was ~1·0 m; that of the dummy reinforcements in the field pullout tests was ~2 m. Regular dummy mats 0·15 m × 0·225 m and 2·0 m long were used with some of the transverse bars clipped, and only five or six transverse bars remaining.

Direct comparison of the pullout resistance–pullout displacement curves for field and laboratory pullout tests is difficult because the grid geometry, applied normal pressure, etc. were not exactly the same. Generally, laboratory pullout test curves show a higher resistance mobilization rate and the maximum pullout resistance was mobilized for a pullout displacement of ~20 mm (see Fig. 20). The field pullout tests (see Fig. 12) show a gradual and continuous increase of pullout resistance up to a pullout displacement of more than 50 mm, except for dummy mats 20 and 24. Dummy mat 20 had a higher rate of increase of pullout resistance initially and failed by tension failure of the steel bar. The test results for dummy mat 24 were influenced by slippage of the grips, as indicated in Fig. 12. This difference in pullout resistance mobilization rate is partly because in the field all the transverse members were more than 1 m away from the wall face (the transverse members near the wall face were cut according to the capacity of the pullout machine and to avoid the active zone of the MSE wall), and the formation of the shear surface may need a larger pullout displacement; in the laboratory the pullout box was only 1·25 m long.

For comparison of the field and laboratory maximum pullout resistance per unit bearing area (from transverse members), the resistance for ~1 m ribbed longitudinal members of the field dummy mats in the field was subtracted from total pullout resistance by use of the apparent friction coefficient between ribbed steel bar and clayey sand, which was determined only from field pullout tests with ribbed longitudinal members: the value was 2·77. The field pullout tests yielded higher pullout resistances than the laboratory pullout tests (Table 4, Fig. 23). There are two possible reasons for this

(*a*) the boundary effect as discussed above with reference to the pullout test curves: the first transverse member in the field pullout tests may not be influenced by other transverse members, and may yield a higher bearing resistance (a lower degree of interference)

(*b*) vertical stress redistribution within the reinforced wall/embankment system due to differential settlement of the foundation soil and the bending rigidity of the steel grids. The interconnection of all the reinforcement layers at the facing for the full length and height of the wall, and the fact that the settlements at the middle lateritic soil section were higher than at the two end (clayey sand and weathered clay) sections, might have caused arching effects. These effects might in turn have caused the vertical stresses or the overburden pressures from the middle section to be redistributed to the two end sections. During the laboratory pullout tests, the interaction of the soil/reinforcement system and the rigid boundaries of the laboratory pullout

Table 4. Laboratory and field pullout resistances: mesh 152 mm × 228 m

	Dummy mat number (see Fig. 9(a))				
	24	20	10	9	7
Mat	W7 × W4·5	W4·5 × W3·5	W4·5 × W3·5	W12 × W5	W7 × W4·5
$M \times N$*	4 × 5	4 × 5	4 × 0	4 × 5	4 × 5
Overburden: m	0·50	2·40	3·75	3·80	4·23
Pullout: mm/s	46·0	61·5	127·0	126·0	127·5
Embedment: m	2·086	2·078	2·045	2·046	2·045
P_t‡ (field): kN	23·66‡	73·82¶	24·66	94·0	103·52
P_t‡ (laboratory): kN	31·90	50·4	20·9	69·6	67·2

* M is number of longitudinal bars, N is number of transverse bars.

† P_t is total pullout force.

‡ Not a peak value.

¶ Tension failure at grips.

L	length of embedment of the grid reinforcement in the backfill soil
M	number of longitudinal wires in the grid reinforcement
N	number of transverse wires in the grid reinforcement
N_c, N_q	bearing capacity factors
S	spacing between grid bearing members
W	width of each transverse wire
δ	angle of friction between the reinforcement and the soil
ϕ	angle of internal friction of the backfill soil
μ^*	apparent friction coefficient
σ_{ave}	average overburden pressure on members of grid reinforcement
σ_h	horizontal normal stress
σ_v	vertical normal stress

REFERENCES

Bergado, D. T., Sampaco, C. L., Shivashankar, R., Alfaro, M. C., Anderson, L. R. & Balasubramaniam, A. S. (1991). Performance of a welded wire wall with poor quality backfills on soft clay. *Proc. Geotech. Eng. Congr., Boulder*, pp. 909–922. New York: American Society of Civil Engineers.

Bergado, D. T., Shivashankar, R., Sampaco, C. L., Alfaro, M. C. & Anderson, L. R. (1991). Behavior of welded wire with poor quality, cohesive-frictional backfills on soft Bangkok clay (a case study). *Can. Geotech. J.* 28, No. 6, 860–880.

Bergado, D. T., Hardiyatimo, H. C., Cisneros, C. B., Chai, J. C., Alfaro, M. C., Balasubramaniam, A. S. & Anderson, L. R. (1992). Pullout resistance of steel geogrids with weathered clay as backfill material. *Geotech. Testing J.* 15, No. 1, 33-46.

Bergado, D. T., Lo, K. H., Chai, J. C., Shivashankar, R., Alfaro, M. C. & Balasubramaniam, A. S. (1992). Pullout tests using steel grids reinforcement with low-quality backfill. *J. Geotech. Engng. Div. Am. Soc. Civ. Engrs* 118, No. 7, 1047–1063.

Chang, J. C., Hannon, J. B. & Forsyth, R. A. (1977). *Pullout resistance and interaction of earthwork reinforcement and soil.* Transportation Research Record 640, pp. 1–7. Washington, D.C.: National Research Council.

Dunn, I. S., Anderson, L. R. & Kiefer, F. W. (1980). *Fundamentals of geotechnical analysis.* New York: Wiley.

Jewell, R. A., Milligan, G. W. E., Sarsby, R. W. & Dubois, D. (1984). Interaction between soil and geogrids. *Polymer grid reinforcement*, pp. 18-30. London: Thomas Telford.

Jewell, R. A. (1990). Reinforcement bond capacity. *Géotechnique* 40, No. 3, 513–518.

Motaleb, A. A. A. & Anderson, L. R. (1988). *Pullout resistance of welded wire mats embedded in clayey silt backfill.* MS thesis, Utah State University.

Ospina, R. I. (1988). *An investigation on the fundamental interaction mechanism of non-extensible reinforcement embedded in sand.* MS thesis, Georgia Institute of Technology.

Palmeira, E. M. & Milligan, G. W. E (1989). Scale and other factors affecting the results of the pullout tests of grids buried in sand. *Géotechnique* 39, No. 3, 551–584.

Peterson, L. M. & Anderson, L. R. (1980). *Pullout resistance of welded wire mesh embedded in soil.* Research report, Utah State University.

Schlosser, F. & Elias, V. (1978). Friction in reinforced earth. *Proc. Symp. Earth Reinforcement, Pittsburg*, pp. 735–762. New York: American Society of Civil Engineers.

Shivashankar, R. (1991). *Behavior of a mechanically stabilized earth (MSE) embankment and wall system with poor quality backfills on soft clay deposits, including a study of the pullout resistances.* Doctoral dissertation submitted, Asian Institute of Technology, Bangkok.

Vidal, M. H. (1969). *The principle of reinforced earth.* Highway Research Record 282, pp. 1–16. Washington, D.C.: National Research Council.

BY STEVE NOVOTNY
ROGER BARR

Geotextiles Help Stabilize Reservoir Floor

The Seneca Station Hydro Electric plant lies adjacent to the Allegheny Reservoir in Warren, Pa. The station is owned jointly by the Pennsylvania Electric Co. and Cleveland Electric Illuminating Co., and operated by the Pennsylvania Electric Co. (Penelec). Though in no danger of failure, after more than 15 years of service, the entire floor of the reservoir needed routine resurfacing and resealing.

Since the reservoir stores water pumped nightly from the Allegheny Reservoir, which is released the next day to drive the turbines of the adjacent hydro plant, the project had to be completed quickly to cut lost generation costs. Subgrade stabilization and resurfacing of the 74-foot deep basin floor had to be completed during a five week period.

Background

Completed in 1969, the basin floor was built with an asphaltic liner, a bituminous pavement which had a higher than normal asphalt content and aggregate gradation to provide a low permeability. A portion of the reservoir floor known as the bent run depression, however, was constructed of clay fill covered with a layer of cold-mix asphalt. With the passage of time, this area of the reservoir floor had become saturated.

Cold-mix asphalt was never designed to inhibit seepage, and, therefore, water readily moved down into the clay fill. The well saturated clay provided an extremely unstable subgrade for an asphalt overlay. This area of clay was originally constructed in some spots to depths of more than 20 feet.

Removal of the clay was not considered an alternative because of the projected cost and schedule constraints. An option of rolling uniformly graded coarse aggregate into the soft clay until it stabilized and then placing a geotextile on the subgrade was presented to the contractor. The contractor elected to place a double layer of geotextile to achieve the same result. ▶

After the reservoir was pumped dry stabilization of the floor began.

The cement/aggregate was delivered by truck and spread by motor grader.

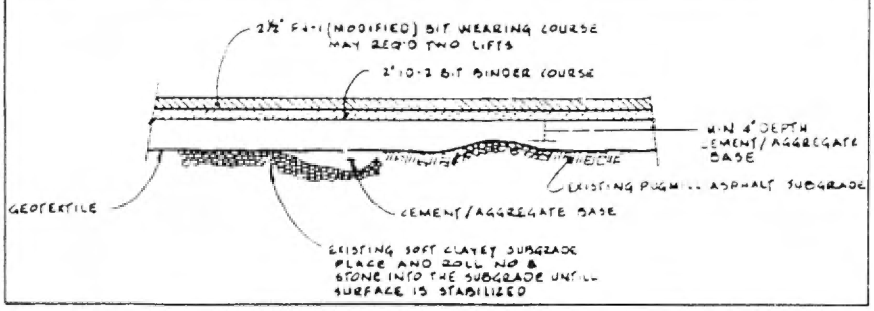

Figure 1: Typical Pavement Section (bent run area only).

The original design utilized a geotextile in order to improve the bearing capacity of the subgrade. Penelec engineers, who served as project designers, specified a necessary elongation factor of 70 percent (ASTM D1682) for the geotextile so it could conform to irregularities in the subgrade, preventing puncture during and after installation. A burst strength of 400 psi (ASTM D751) was specified to provide a stable subgrade in order that the cement/aggregate base could be compacted to the required density atop the subgrade.

The project contractor, L. C. Whitford Co., Wellsville, New York, selected Trevira 1115 manufactured by Hoechst Celanese Textile Fibers Group, Charlotte, N.C., because it was deemed technically acceptable. Timeliness of delivery was also a factor in the selection of this geotextile.

Installation

Construction commenced in the spring of 1986, as soon as weather and a scheduled outage permitted. The contractor began by pumping the reservoir dry. After pumping was completed, preparation and stabilization work began in the saturated areas, which comprised just under 10 percent of the total area of the reservoir. Simultaneous paving of stable areas proceeded with the placing of 2½ inches of asphaltic surface course to seal it against seepage.

In the unstable area, the geotextile was installed by the contractor over the exposed saturated clay. In the most unstable areas, a double layer of geotextile was installed. The first layer was put in place with 1 foot overlaps, and the second layer was laid directly on top of the first. In some areas a single layer of geotextile was determined to be sufficient.

As installation of 70,000 yards of geotextile progressed, 16,000 cubic yards of cement/aggregate were delivered by truck, spread by motor grader on the geotextile to a maximum depth of 12 inches and compacted with vibratory rollers. The geotextile helpe keep the cement/aggregate intact under the compressive forces exerted by compaction equipment during construction.

The entire reservoir was then overlaid with 2½ inches of a modified asphalt-sand surface course to seal i against seepage.

After curing for three days, the cement/aggregate was sprayed with a tac coat and then overlaid with a 2-inc asphaltic binder course and the 2½ inch asphaltic surface course.

Even with 10 of the 29 days allote to complete this job rained out, the contractor was able to complete the job on time.

Results

The reservoir has been monitored an after nearly four years, appears to b performing satisfactorily. In the areas known as the bent run depression geotextiles were used successfully to provide a stable subgrade for constructio purposes, allowing installation of th pavement and cement/aggregate whic provides the water retention capabilities.

Steve Novotny is senior engineer I for the Pennsylvania Electric Co. He is a graduate of the University of Pittsburgh, Johnstown, and has worked for Penelec for seven years. Roger Barr is director of publications for the Industrial Fabrics Association International, publishers of Geotechnical Fabrics Report.

Geotextiles and Geomembranes 13 (1994) 357–369
1994 Elsevier Science Limited
Printed in Ireland
0266-1144/94/$7.00

Geotextile–Bamboo Fascine Mattress for Filling over Very Soft Soils in Malaysia

C. T. Toh,[a] S. K. Chee,[a] C. H. Lee[a] & S. H. Wee[b]

[a]Geotechnical Engineering Consultants, 34-3 Medan Setia, 2 Bukit Damansura, 50490 Kuala Lumpur, Malaysia

[b]Polyfelt Geosynthetics Sdn Bhd, No. 2 Jln SS21/62, Damansara Utama, 47400 Petaling Jaya, Malaysia

ABSTRACT

Very soft deposits such as peat, marine clays and tin mining slime are found extensively in Malaysia. Severe problems are encountered when filling over such deposits. Woven and nonwoven geotextiles have been used to assist in fill deposition over such very soft deposits. This paper describes the desired properties of geotextiles for this purpose, methods of placing the geotextile and deposition of the fill. A nonwoven geotextile with a bamboo fascine mattress is found to be most effective.

INTRODUCTION

This paper pertains to the use of geotextiles as a separator and bamboo fascine mattress as a reinforcement to enable controlled fill deposition over very soft deposits. In Malaysia, such deposits take the form of peat, very soft marine clays, and unconsolidated silty clays (slime) found in disused tin mining land.

Different types of geotextiles and methods of laying have been attempted. Highly extensible nonwovens placed over a bamboo fascine mattress was found to be the most appropriate and economical method.

SOFT DEPOSITS

Peat which is mainly found in low-lying poorly drained depressions or basins in the coastal areas occur over a total of 2.6 million ha corresponding to 8% of the total land area of Malaysia. Approximately 1·7 million ha of peat are found in the state of Sarawak (Mutalib *et al.*, 1991).

The peat is characterized by:

(i) high and variable water contents ranging over 200–2000%;
(ii) low bulk densities of the order of 10 kN/m^3; and
(iii) low shear strengths generally of the order of 5–10 kPa.

Soft marine clays of Quartenary age are found throughout the coastal plains of Malaysia, giving rise to broad structures of flat to gently undulating terrain. Descriptions and properties of soft clays in Malaysia are given by Ting *et al.* (1988), Malaysian Highway Authority (1989), Raj and Singh (1990), Chee (1991) and Chee *et al.* (1992). Generally, the vane shear strengths of the upper regions range over 8–15 kPa with the strength increasing with depth. The thickness of the soft clay deposits may extend to more than 30 m.

Unconsolidated silty clays (slime) are the end result of tin mining activity. Such activities were concentrated mainly in the Kinta Valley and the Kuala Lumpur–Langat tin fields, resulting in significant areas in and around present day Ipoh and Kuala Lumpur being underlain by tin tailings. Methods for reclaiming disused tin tailings are given by Toh (1989) and Toh *et al.* (1992). These unconsolidated sediments found within tailing ponds are generally characterized by very low to low undisturbed vane shear strengths typically less than 5 kPa.

DEPOSITION OF FILL

Deposition of fill into very soft deposits often results in the following problems:

(i) excessive lateral movements;
(ii) remoulding of the very soft deposits with heave of remoulded material and the formation of mud waves;
(iii) mixing of fill with the very soft material and the trapping of soft clay pockets within the fill; and
(iv) consequential significant differential settlement.

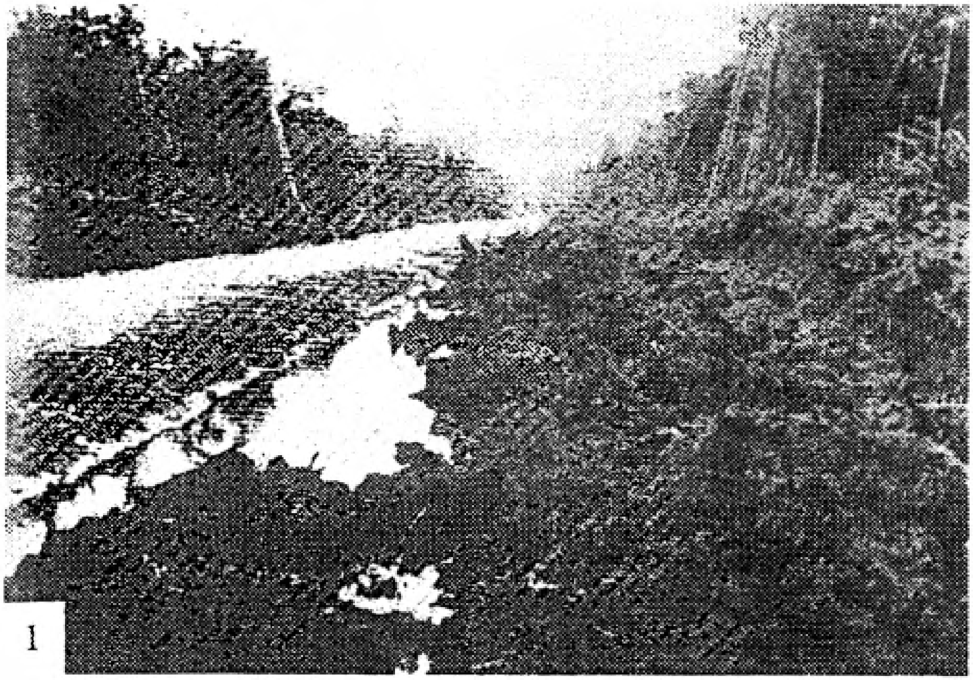

Fig. 1. Heave and displacement from end tipping into peat.

The above problems are more severe for peat and unconsolidated mining slimes than marine and alluvial clays.

Figure 1 illustrates the results of end tipping into peat. The tilting of the trees on both sides of the fill indicates excessive lateral movements. Toh *et al.* (1990) demonstrated the effectiveness of lowering the ground water table to improve the peat for the purpose of fill placement without the problems described above. However, in areas where drainage for the purpose of lowering the water table cannot be effected, a geotextile on a bamboo fascine mattress as described in the following sections of this paper has been found to be very effective. Other methods for filling over peat include the use of planks and timber placed side by side to form a continuous mat.

Figures 2 and 3 illustrate the end results of uncontrolled filling by end tipping into a disused tin mining slime pond. The resulting heave causes soft material to rise to occupy the remainder of the pond. Unless the pond water depth is significant and structures exist near to the pond, dewatering is normally carried out before placement of fill. Working in the dry permits speedier operations, compaction of fill by normal compaction plant and the use of residual soil fill, sand fill being more expensive. Dewatering, however, poses difficulties in the laying of geotextiles since

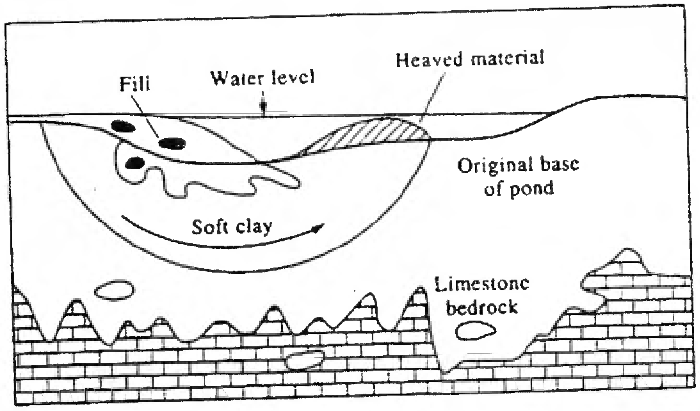

Fig. 2. Heave and displacement of soft material from uncontrolled filling of a slime pond.

3

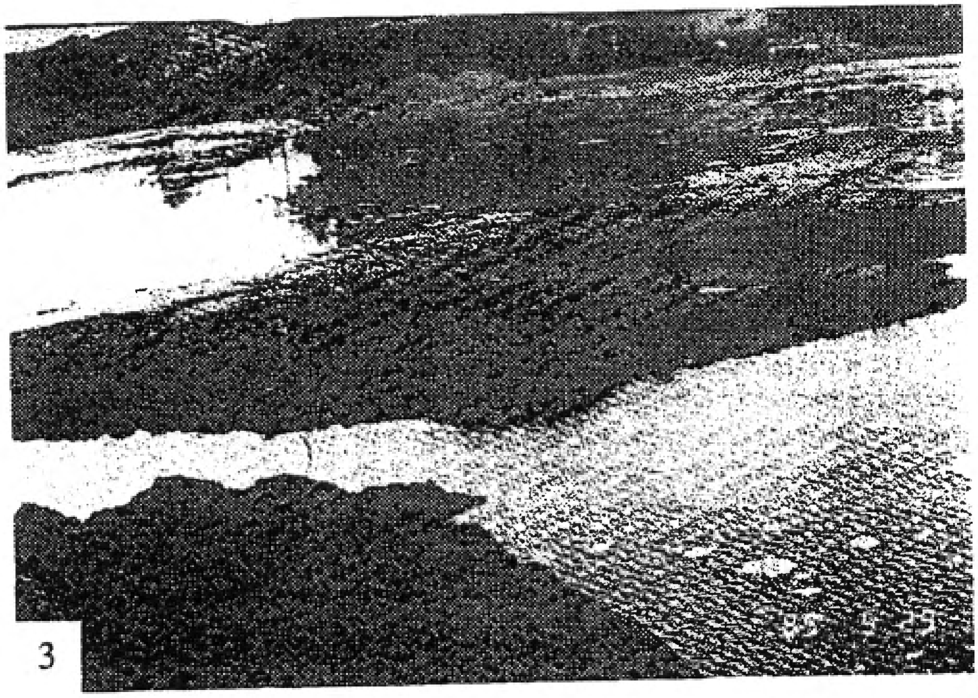

Fig. 3. Mud waves from end tipping into a disused tin-mining slime pond.

the very soft consistency of the slime does not permit access by plant, machinery or human beings. Further geotextiles cannot be rolled directly on to the slime without the roll sinking into the very soft material. As for peat areas, a geotextile placed over a bamboo fascine was found to be the most effective method of overcoming the above problems.

GEOTEXTILE

The geotextile for use with a bamboo fascine mattress for filling over soft material is intended to serve as a separator to prevent fill mixing with the soft deposits causing remoulding and excessive heave and thereby resulting in loss of control of the filling process. Intermixing of fill and soft deposits will also result in the loss of mechanical properties of the fill material. In order for the geotextile to serve effectively as a separator, it must be able to withstand the construction stresses caused by the filling operation. Hence, the selection of the appropriate type and grade of geotextile must take into consideration the survivability criteria.

The geotextile properties necessary for the fulfilment of the above function and survivability criteria are:

(i) a high puncture resistance. Puncture can be a common occurrence caused by debris at the base of the pond and wood pieces in peat areas. Resistance to puncture may be best achieved by use of nonwoven geotextiles with continuous filaments which serve to provide a compact and entangled structure. Geotextiles with low puncture resistance would require a high tearing resistance;
(ii) a high percentage elongation at break because of the large strains due to heave ahead of the filling front;
(iii) a high resistance against bursting due to the upward pressure on the geotextile caused by the mud wave ahead of the filling front;
(iv) high permeability to enable rapid dissipation of pore pressures of the mud wave built up by the filling operation;
(v) strength isotropy to ensure against weakness in any particular direction.

While high tensile strength is an added advantage, such increased strengths are generally associated with significantly higher costs. Due to the possibility of prolonged exposure on site, the geotextile should have a high UV resistance.

SEWN SEAMS

Tearing whenever encountered invariably occurred along the sewn seams and attention had to be focussed on achieving high seam efficiencies.

'Flat' or 'Prayer' type seams sewn in two rows are prefered over 'Butterfly' or 'J' seams (Dias, 1985) due to ease of sewing on site especially for thicker geotextiles.

Polyester threads with dtex 3 × 1100 with break strength of 19 kg was

Table 1
Seam Strength Tests

Test no.	*Strength (N/200 mm)*	*Observations*
1	3 754	Rupture of fabric
2	4 558	Rupture of thread
3	3 170	Rupture of fabric
4	4 200	
5	4 038	
Average	3 944	

found to be satisfactory. Polyester threads are prefered due to higher UV resistance and better resistance to effects of prolonged exposure to moisture.

'101' Single Thread Chainstitch sewn in two rows or '401' Two-Thread Chainstitch (Dias, 1985) sewn in one row both with stitch densities of 3·5 stitches/in were found to be adequate. Seam strength tests (ASTM, 1990) were carried out on Polyfelt TS720 geotextile samples sewn together using a '401' Two-Thread Chainstitch with a stitch density of 3·5 stitches/in. The test results summarized in Table 1 indicate seam efficiencies of 100%.

BAMBOO FASCINE MATTRESS

It is not possible to lay and to effectively connect together sheets of geotextile over large areas for which access is a major difficulty.

The functions of the bamboo mattress are:

(i) to enable the initial necessary human access into the pond; and
(ii) to provide a platform for laying and sewing the geotextile. The configuration of the bamboo fascine must be such that the geotextile may be rolled directly on to it.

The bamboo fascine mattress also serves as a reinforcement at the base of the fill by providing bending and tensile resistances, and by so doing:

(a) increases the factor of safety against bearing capacity failure;
(b) reduces the magnitude of mud waves ahead of the filling front; and
(c) allows the machinery access after deposition of about 300–500 mm of sands or gravels.

Some laboratory tests demonstrating the enhanced bearing capacity of footings on soft clay by use of rods possessing both tensile and bending stiffness with a geotextile were reported by Yusuf *et al.* (1989).

ıer UV
.ure to

Thread
s of 3·5
:, 1990)
:r using
'in. The
)%.

ıeets of

and
.ile. The
.hat the

: base of
ing:

:e;
ont; and
)0 mm of

pacity of
bending

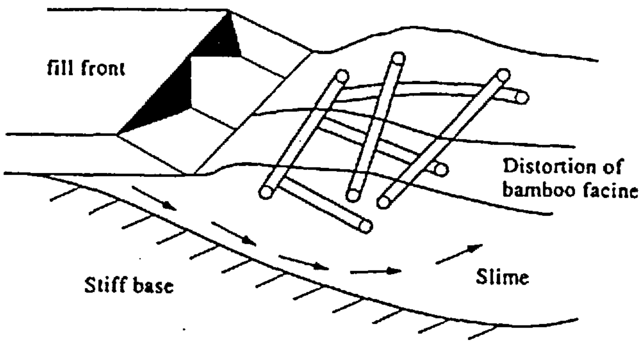

Fig. 4. Distortion and displacement of bamboo fascine.

The bamboo pieces must be properly tied together by wire to form a rigid and secure frame and properly anchored in place at the edges to prevent the lateral movements of the soft deposit displacing and distorting the bamboo frame away from the geotextile in the manner illustrated in Fig. 4.

INITIAL LAYER OF FILL

The first fill layer should preferably be sand and be of a thickness which ranges over 300–600 mm in order to ensure against excessive stresses on the geotextile due to earthworks equipment as well as to ensure against bearing capacity failure and excessive heave. Spreading of the initial sand layer is best done by use of light equipment such as backpushers. The fill stockpile should be kept a minimum distance of 20 m behind the filling front in order to avoid bearing capacity failure.

CASE HISTORIES

Case 1

Figures 5–7 illustrate the first use of a nonwoven geotextile sheet with a bamboo fascine mattress to enable earth filling over a 30 000 m^2 initially inaccessible slime pond at Sungei Besi on the outskirts of Kuala Lumpur. The thickness of slime was generally 20 m but was up to 33 m in localized areas. The undisturbed vane shear strength of the slime was about 5 kPa.

The geotextile used was Polyfelt TS700, a nonwoven continuous filament needle-punched geotextile with a strip tensile strength of 18 kN/m and an elongation at break of 50–80%. Approximately 3 000 m^2 of geotextiles with bamboo fascine mattress was layed in a 10 h working day.

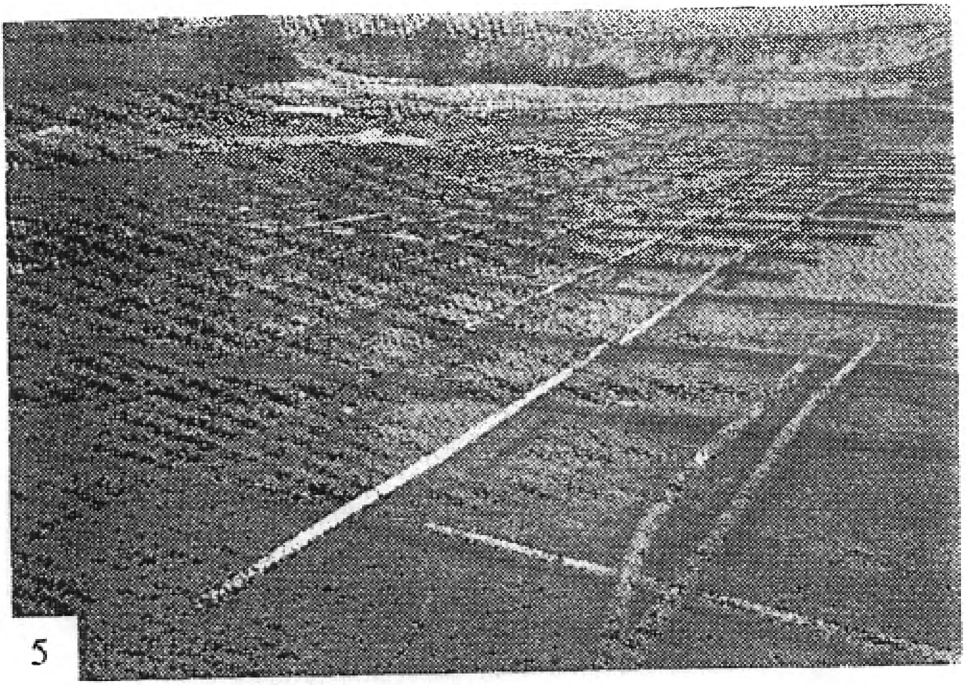

Fig. 5. Bamboo fascine mattress on a slime pond.

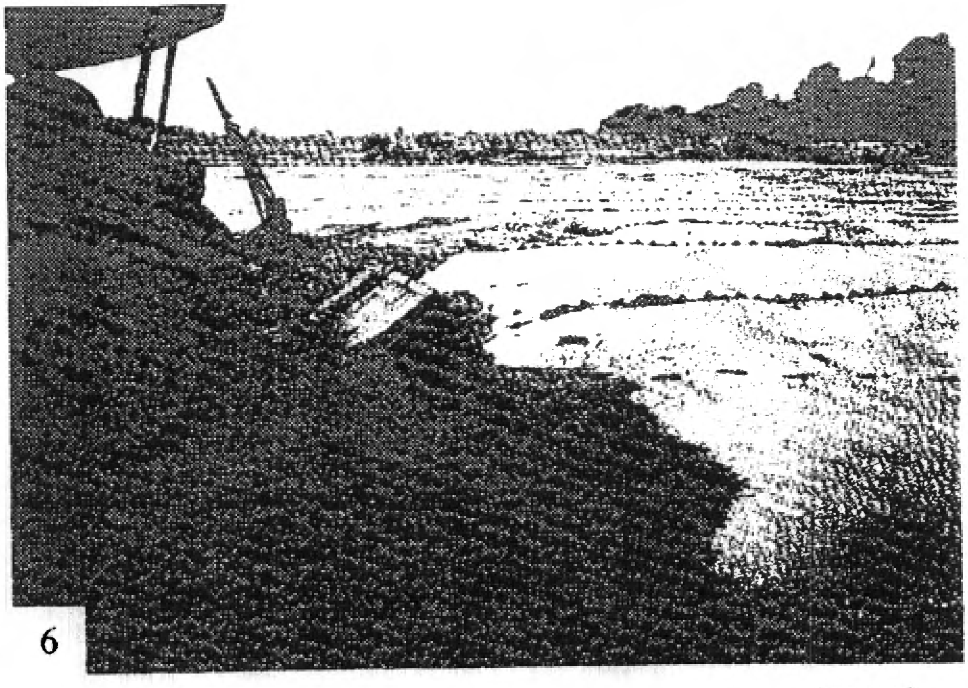

Fig. 6. Sand deposition onto geotextile–bamboo fascine mattress over a slime pond.

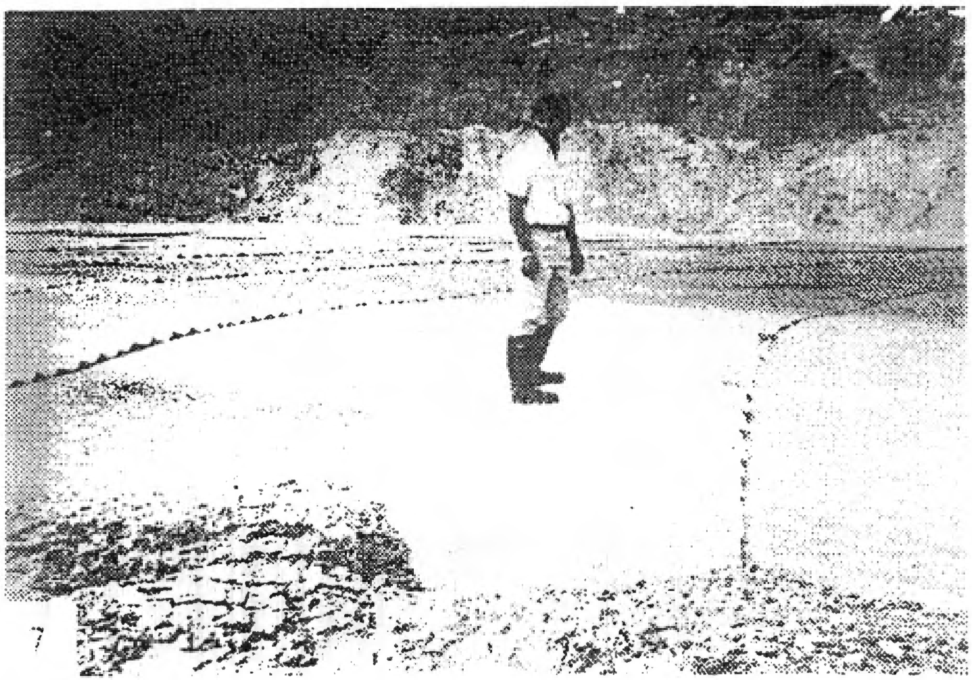

Fig. 7. Controlled heave ahead of filling front on a slime pond.

Tearing of the geotextile did not take place despite the relatively low tensile strength of 18 kN/m. However, seam tearing did take place (Fig. 8) and this led to the improvements to seam sewing discussed earlier.

Puncture of the geotextile due to distorted bamboo pieces did occur at several places but propagation of tear did not take place due to the mitigating effects of the entangled structure of the needle-punched nonwoven filaments.

Case 2

Figures 9 and 10 illustrate earthfilling operations over a geotextile bamboo fascine mattress at the 5 km Ring Road, Kuching. The subsurface takes the form of peat (moisture contents 200–600%) over soft clays.

Delays in the commencement of earthwork resulted in the geotextiles being exposed for a period of about 3 months. Tensile tests (ASTM, 1986) were carried out on samples of the geotextile, Polyfelt TS700, after that period of exposure to sunlight: the results are summarized in Table 2.

The strength after about 3 months exposure is still higher than the strength value recommended by the manufacturer, viz 18 kN/m. The results show that the recommended values are conservative and that the

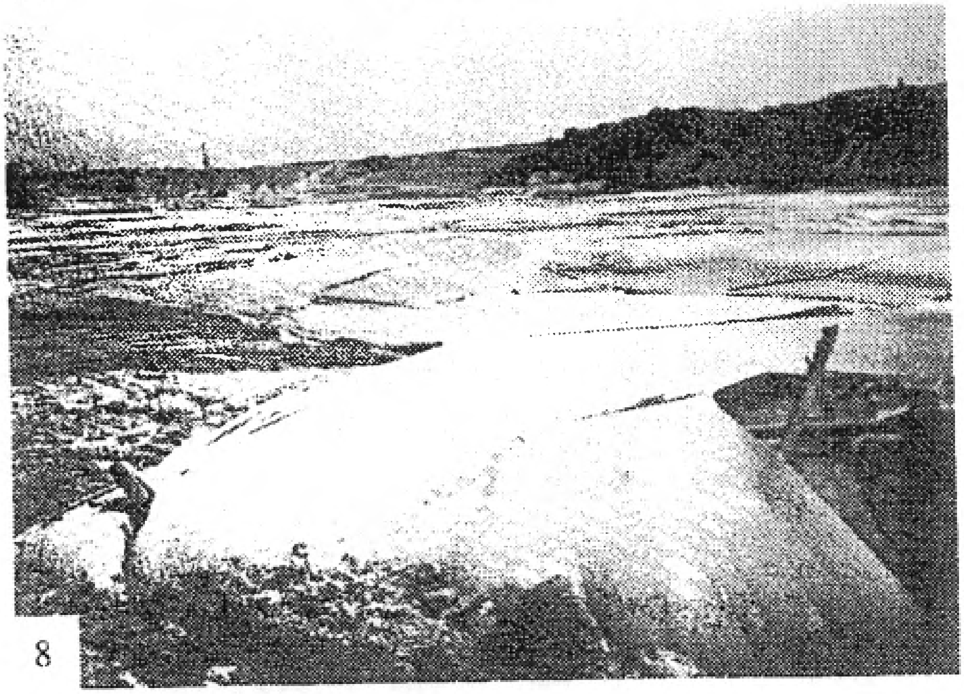

8

Fig. 8. Seam tearing and puncture of geotextile.

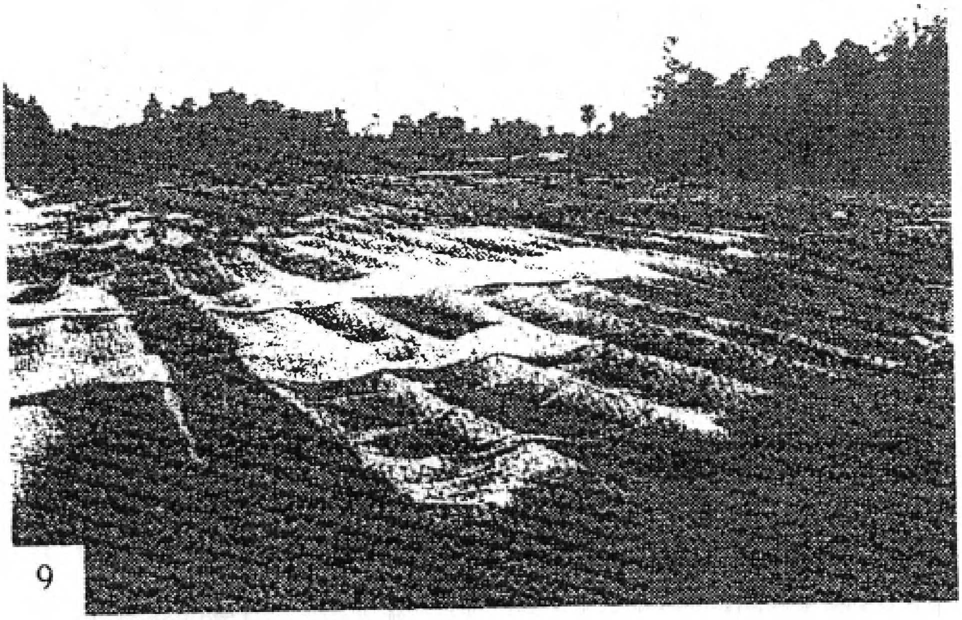

9

Fig. 9. Geotextile–bamboo fascine mattress over peat.

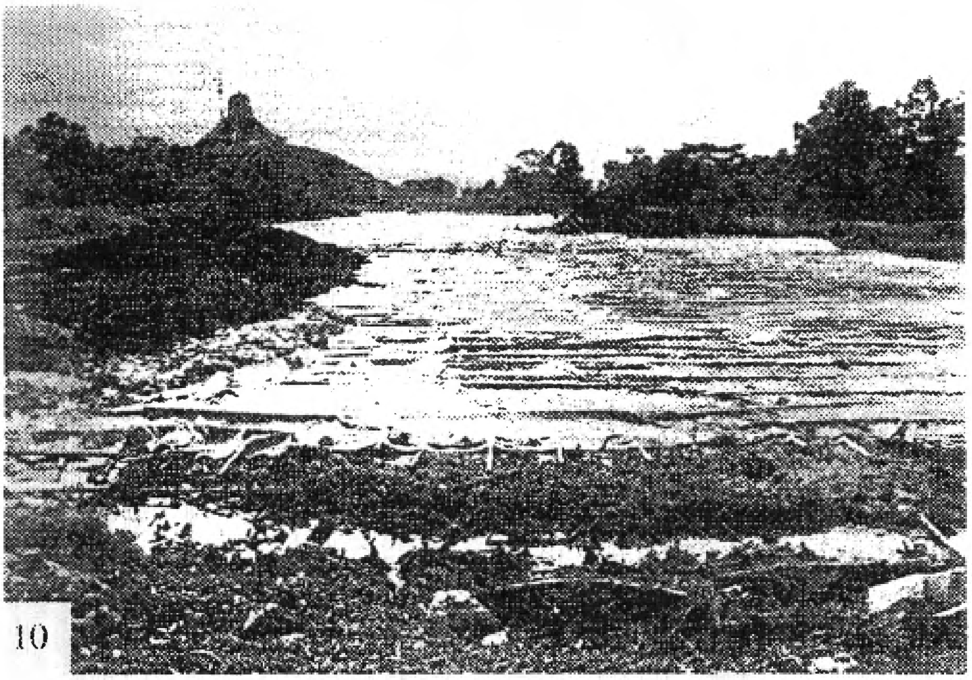

Fig. 10. Geotextile bamboo fascine mattress over peat.

Table 2
Strength Tests on Geotextiles (3 months exposure to sunlight)

Test no.	*Direction*	*Tensile strength*		*Elongation at break (%)*
		(N/200 mm)	*(kN/m)*	
1	1st direction	4 223	21·1	78·0
2	2nd direction (perpendicular to 1st direction)	4 528	22·6	41·0

hindered amine light (HAL) stabilizer used by the manufacturer to mitigate the degradative effects of UV rays is effective.

An initial sand fill of 300 mm was placed over the geotextile–bamboo fascine before placement of compacted residual soil fill. Minimal heave was reported throughout the filling process which was entirely within control.

Case 3

Figure 11 illustrates the laying of the bamboo fascine mattress on amorphous peat and organic clays after excavation of 3 m of the more fibrous

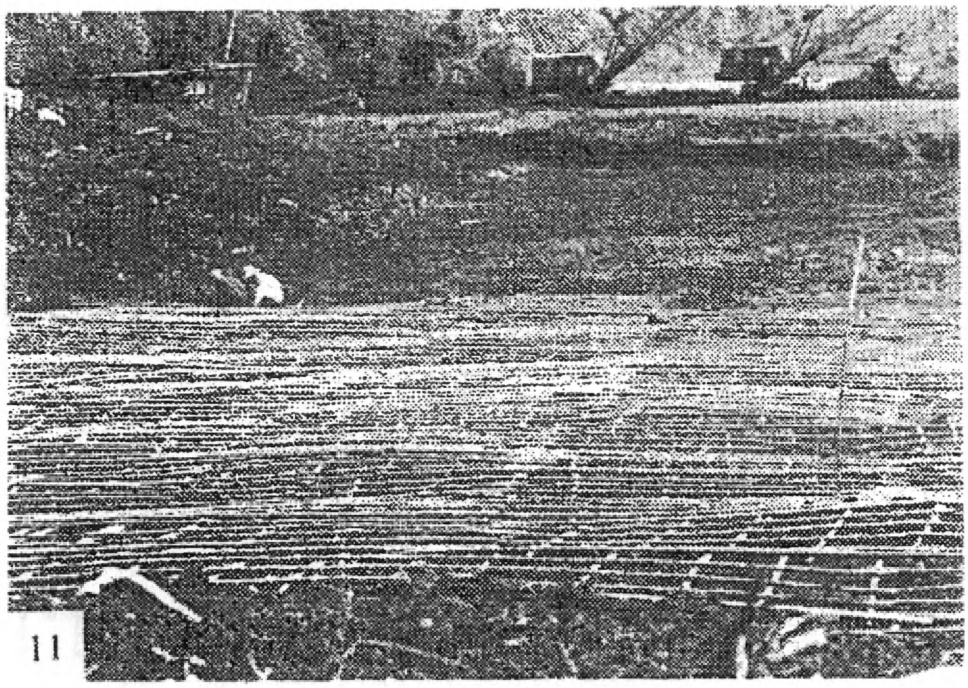

Fig. 11. Bamboo fascine over peat.

peat. Polyfelt TS720 (tensile strength of 19·5 kN m) was placed over the bamboo fascine mattress. A 300 mm thick gravel layer placed over the geotextile was sufficient to support heavy equipment for installation of prefabricated vertical drains through the geotextile and soft clays beneath.

SUMMARY AND CONCLUSION

The geotextile bamboo fascine mattress has been successfully used to enable deposition of fill over very soft deposits such as slimes and peat without the problems of mixing of fill with soft deposits, remoulding, mud waves and general loss of control of the filling process.

The bamboo fascine mattress facilitates access, provides a platform for rolling on and sewing geotextiles, increases bearing capacity and significantly reduces mud waves. These properties permit the use of a relatively low strength nonwoven geotextile. It is important that the geotextile used be of high extensibility, possess a high resistance to bursting, be able to mitigate tear on puncture, and be of high permeability. Care should be exercised when sewing the geotextile sheets to ensure a high level of seam efficiency.

over the
over the
ation of
beneath.

used to
and peat
ing, mud

:form for
d signifi-
relatively
xtile used
e able to
hould be
l of seam

REFERENCES

ASTM (1990). Standard test method for sewn strength of sewn geotextiles wide width method. ASTM D4883-90.

ASTM (1986). Standard test methods for tensile properties of geotextiles by the wide width strip method. ASTM D4595-86.

Chee. S. K. (1991). Embankments on Malaysian marine clays A case study of instability. Proc. 1st Young Geotechnical Engineers Conference. Bangkok.

Chee. S. K.. Loh. M. H. & Toh. C. T. (1993). Stability of embankment on soft clay. Proc. Sarawak Road Conference.

Dias. V. (1985). Thread selector for geotextiles. *Geotech. Fabrics Rep.*. 3(1). IFAI. 15-19.

Malaysian Highway Authority (1989). *Proc. Int. Symp. on Trial Embankments on Malaysian Marine Clays. Vols 1 & 2.* ed. R. R. Hudson. C. T. Toh & S. F. Chan.

Mutalib. A. A.. Lim. J. S.. Wong. M. H. & Koonvai. L. (1991). Characterisation. distribution and utilisation of peat in Malaysia. Proc. Int. Symp. Tropical Peatland. Kuching. Malaysia. May.

Raj. J. K. & Singh. M. C. (1990). Clay mineralogy of holocene marine clays along the north–south expressway. Proc. Seminar on Geotechnical Aspects of the North-South Expressway. Juala Lumpur. 5–6 Nov.

Ting. W. H.. Wong. T. F. & Toh. C. T. (1988). Design Parameters for soft ground in Malaysia. *Geotech. Engng.* 19(1) 95–126.

Toh. C. T. (1989). Reclamation of disused tin-mining land and mining ponds. Internal report submitted to Pengurus Lebuhraya Malaysia Berhad.

Toh. C. T.. Chua. S. K.. Chee. S. K.. Yeo. S. C. & Chock. E. T. (1990). Peat replacement trial at Machap Proc. Seminar on Geotechnical Aspects of the North–South Expressway. Kuala Lumpur. 5–6 Nov.

Toh. C. T.. Chee. S. K.. Lee. C. H. & Wee. S. H. (1992). Geotextiles for reclamation of disused tin mining ponds. Proc. Int. Symp. on Applications of Geosynthetic Technology. INA-JGS. Jakata. 23–24 Nov.

Yusuf. M. Z.. Werner. G. & McGrown. A. C. (1989). The bearing capacity of bamboo and geotextile reinforced sand on soft clay. Symp. on the Applications of Geosynthetic and Geofibre in SE Asia. Petaling Jaya. Malaysia.

Proceedings of the Fourth (1994) International Offshore and Polar Engineering Conference
Osaka, Japan, April 10-15, 1994

ISBN 1-880653-10-9 (Set); ISBN 1-880653-11-7 (Vol. I)

Permeability Studies in Marine Clays Stabilized with Lime Column

S. Narasimha Rao and Paul K. Mathew
Ocean Engineering Centre, Indian Institute of Technology
Madras, India

ABSTRACT

Soft marine clays are very sensitive to changes in tress system, moisture content and system chemistry of he pore fluid. There is a necessity to improve the behaviour of these deposits using any one of the available ground improvement techniques. In the present nvestigation an attempt is made to improve the ermeability using lime column techniques in marine clays. The experimental programme was carried out with model lime columns installed in two test setups. In the irst setup a central lime column was installed in a ircular tank and in the second setup number of columns ere installed in a rectangular tank. A marine clay from east coast of India was used as a test bed. Number of samples were taken at different radial distances and ime periods. From the tests conducted on these amples, it has been established that lime has seeped into the surrounding soil for large distances and this is indicated by pH values and XRD analysis. There is normous improvement in permeability and the k values re improved by 10 to 15 times. This shows a good omise for improving the reclaimed coastal soft deposits and offshore deposits.

EY WORDS: aggregation, diffusion, flocculation, lime, arine clay, permeability

INTRODUCTION:

Weak marine deposits have been found both on the oast and in several offshore areas spread over many arts of the world. There are problems associated with these fine grained soils deposited at a soft consistency. Fine grained soils are very sensitive to hanges in stress system, moisture content, and system hemistry of the pore fluid. In addition to these, the problems arising out of high compressibility and low shear strength of these weak marine deposits expose eotechnical engineers to considerable challenge in the onstruction of various coastal and offshore tructures. The performance of these soft fine grained deposits under different conditions of environment varies between wide limits.

In order to improve the engineering behaviour of soils several improvement techniques are available in soil engineering practice. The selection of any one of these methods for any problem can only be made after a comparison with other techniques proves a particular method is well suited for a particular system. In fine grained soils chemical stabilization methods are well suited. Of the several chemical methods available for altering soil properties, the addition of lime in one form or the other to soft and expansive soils has been effectively used in improving the soil characteristics.

The influence of lime on the various soil properties has been reported by many investigators. Some of the earlier investigators (Clare and Cruchley, 1957; Mateous, 1964) suggested that the addition of lime to the soil caused considerable reduction in the plasticity index of high plasticity soils and it improves the workability of the soils. The work of Thompson (1964) indicated considerable improvement in the engineering properties of lime treated soils and these beneficial changes are explained through mechanisms viz. namely (i). cation exchange (ii) flocculation and (iii) aggregation. Many investigators supported these mechanisms and recommended lime stabilization in improving the soil characteristics especially for subgrade soils in highway and air field pavements. Quite a good number of investigators (Glenn, 1967; Kawamura and Diamond, 1975; Willoughby et. al., 1968) identified the reaction products and these reaction products are mainly the cementation compounds like calcium aluminate hydrate (CAH), calcium silicate hydrate (CSH) and many other calcium compounds and these are like pozzolanic compounds in portland cement. The cementation compounds aggregate the particles together and as a result of which large floccules are formed and this almost amounts to effective particle growth. With increase in the particle size considerable increase in the permeability is expected. Based on the success of lime stabilization in the field of highways, efforts are now being made to extend this as an in-situ ground improvement technique through lime column and lime injections. Broms and Boman (1975) brought out the concepts of lime columns and in this method preformed bores were made and filled with soil lime mix. It was believed that this improved soil lime column could support the superstructure. Okumura and Terashi (1975) reported a method of lime injection for improving the soft submarine soils in Japanese harbors. Based on these early works of lime column / lime injections, some investigators (Brandl, 1981; Broms, 1984; Narasimha Rao and Somayazulu, 1984) suggested methods to install lime columns and the work of Narasimha Rao et. al. (1991) and Narasimha Rao et. al. (1993) brought out that lime diffuses into the surrounding soils for a considerable distance and improves the soil characteristics.

In all the above afore mentioned works it was brought out that the lime columns - lime injections techniques brings in considerable improvements in strength and reduces the compressibility of the surrounding soils. In this investigation an attempt is made to show that the diffusion of lime from the column or from the injection points not only improves the strength and compressibility behaviour of the soil but also significantly improves the permeability. This improvement in permeability is studied mainly to propose that it can also help in improving the drainage characteristics of the soils and the lime column can also act as a small drain.

PERMEABILITY

Permeability is a measure of the ease with which a fluid passes through a material and is one of the engineering properties of soils. The knowledge of permeability is necessary in all the problems dealing with seepage, settlements and stability analysis. The coefficient of permeability for a given soil depends on particle diameter, properties of the pore fluid, the void ratio, the shape and the arrangements of the pores and of the soil particles and the amount of undissolved gas in the pore water. The coefficient of permeability as explained by Darcy's Law is

$$v = k\,i \qquad (1)$$

where

v = velocity

k = the coefficient of permeability (or hydraulic conductivity or permeability)

i = the hydraulic gradient

The changes in the permeability in the surrounding soil due to the installation of lime columns are studied through an experimental programme whose details are presented in the next section.

EXPERIMENTAL WORKS

In the present study, bulk samples of marine clay were collected from a site near Madras in the east coast of India. The physical properties of the soil are given in Table 1. The clay minerals were identified using X-ray diffraction analysis as per the ASTM X-ray card file index (1991). The X-ray diffraction pattern of the untreated soil is shown in Fig. 1.

The testing program was planned in two phases. In the first phase, model single lime column of 40mm diameter was installed at the centre of the test tank of 600mm in diameter and 500mm depth. The tests were carried out for columns installed under both fresh water and sea water conditions. For the determination of permeability undistributed samples were collected at radial distances of 50mm, 150mm and 250mm from a depth of 250mm from the top of the soil bed. Fig. 2 shows the details of single column setup. In the second phase several lime columns were installed in a test tank having dimensions 1000mm x 1000mm and 750mm depth. In this setup the marine clay was mixed with sea water to the required consistency. Fig. 3 shows the details of setup with group of lime columns. In this setup, undistributed samples were collected at depths of 200mm and 500mm from the top of soil bed at the sampling points shown in Fig. 3.

To install the lime columns at the predetermined position, PVC tubes of 40mm internal diameter, open at both ends were placed in position. The soil prepared at a consistency suitable to field conditions was packed around the PVC tubes. Fully saturated soil was placed in the test tank in layers of about 50 to 75mm thickness under soft to medium stiff consistency. Each layer was first hand packed and then pressed with a wooden template to remove entrapped air and to ensure homogeneous packing. Soil beds having thicknesses of 450mm for single column setup and 700mm for setup with group of lime columns where thus prepared. After the soil bed was placed, the lime columns were formed by introducing quick lime (Calcium oxide) into the pipe and was compacted with a tamping rod. Simultaneous withdrawal of the guide pipe was done. In this way, the lime columns were formed. In order to avoid free swelling condition of the soil, a nominal surcharge pressure of 5 kPa was applied. After the installation of the column was completed, a standing water of 50mm height was maintained at the top of the soil bed throughout the period of testing.

The permeability was mainly determined from consolidation tests. The test apparatus used was a standard oedometer (ASTM, 1989) in which there was a consolidation ring of 60mm in diameter and 20mm in height. Soil from an undistributed sampler was pushed into the ring and the soil sample was placed in between two porous stones. The tests were conducted as per the specifications, ASTM (1989).

RESULTS AND DISCUSSIONS

DETERMINATION OF pH VALUES

From the literature, it is clear that the lime seeped into the soil system improves the permeability. In view of this it is necessary to confirm the penetration of lime into the surrounding soil. pH measurements are normally used to indicate the alkalinity or acidity in a particular environment. In order to have a quick appraisal of the lime induced alkalinity into the surrounding soil, a number of pH measurements were carried out on a good number of samples from various test setups. The procedure followed is standard procedure as described by Jackson (1958). The pH of suspensions was determined by glass calomel combined electrodes using a pH digital meter.

The pH of the untreated soil mixed in pure water is 7.15 and in sea water it is 6.15. Samples were collected from different radial distances of 50, 100, 150, 200 and 250mm from the columns and also at different time periods ranging from 2 to 60 days. The pH values measured from these samples are presented in figs. 4 and 5. The pH of the samples collected from the edge of the column is 10.85 to 11.20. Fig. 6 shows the variation of pH with time for the setup with group of lime columns.

It could be seen that there is a gradual decrease in pH value with radial distance and even at a radial distance of 250mm the pH measured at an initial stage (2 days) is about 7.5 and at the same distance it improves to 8.89 after a time period of 45 days. This clearly brings out that considerable lime has seeped into the system. A similar set of measurements carried out from the samples taken from the setup containing group of columns also show a similar variation in pH values. The stabilized values of pH up to 8.89 at a distance corresponding to six times the diameter of the column confirms that a good volume of soil is stabilized by the seeping lime. Before the results of permeability tests are presented this phenomena of the seeping lime is further confirmed by the X-ray diffraction analysis and the results presented in the next section.

X-RAY DIFFRACTION (XRD) ANALYSIS

Lime reactivity of a soil is generally influenced by three factors, viz. (i) the amount and type of clay (ii) the increase in pH and (iii) the amount of silica and alumina present for the formation of cementing compounds. The improved values of pH have already confirmed the penetration of lime. The solubility of silica and alumina in the system also increases with the increase in pH furnishing maximum opportunity for pozzolanic reactions to occur. In the present study the new pozzolanic compounds formed were identified by X-ray diffraction analysis. Figs. 7 and 8 show XRD patterns for treated samples. From these diffractogrammes, one could observe new peaks indicating the formation of new reaction products. In a XRD analysis the diffractogrammes obtained are matched with the standard diffractogrammes available in the ASTM X-ray card file index (1991). The new cementation compounds identified are calcium silicate hydrate (CSH), calcium aluminate (CA), albite, tobermorite, anorthite etc. These new compounds are responsible for the aggregation of soil particles and consequent improvement in permeability.

PERMEABILITY STUDIES

From the tests carried out using oedometer, permeability values were computed. The permeability (k) of untreated marine clay was found to be 23.5 x 10^{-9} cm/sec at a pressure range of 50 kPa to 100 kPa. From the tests carried out on various samples taken at different radial distances and time periods the values were computed and are shown in Figs. 9&10. Fig. 9 refers to the results obtained from single setup in fresh water whereas fig.10 refers to the results obtained from column with sea water. With time there is an improvement in the permeability at all the radial distances. These results are tallying with pH values reported earlier. As it is known that higher penetration of lime is reflected in higher values of pH and at higher values, obviously particle growth is better. Hence the variation in the permeability with the radial distance and with the pH value are quite expected. A similar set of observations are obtained from the samples tested from the setup containing the group of columns are also presented in Fig. 11. This also confirm with time, the permeability values are improved by nearly 15 times. All these results clearly bring out that there is enormous improvement in the permeability. Hence this type of technique can be conveniently used to improve not only the strength but also the drainage characteristics. The improvement in the drainage characteristics finds a good potential use in reclaiming large tracts of coastal soft clay deposits. Further even in under water deposits it is possible to make use of this technique along with preloading technique to improve the strength behaviour. There could be enormous reduction in time period required in preloading technique. The increase in permeability can also be due to the exchange of calcium ions giving rise to improved flocculation and reduction in double layer thickness. Aggregation combined with flocculation alters the normal pore size distribution in clay. A number of substantially larger pores are created adjacent to the flocs and this is proved by the improvement in the permeability.

CONCLUSIONS

1. With the installation of lime columns, there is a considerable improvement in the alkalinity of the surrounding soil and the improvements in the pH from 6.15 to 8.89 is a clear indication of seeping lime.
2. The seeping lime brings in many improvements and this results in the aggregation of the soil particles. The X-ray diffraction analysis confirm several cementation compounds.
3. With improvements in alkalinity and aggregation of soil particles there is enormous increase in the coefficient of permeability. The improvements in permeability are in the range of 10 to 15 times. These are confirmed from the tests on both single column and multi column setups using both fresh water and sea water. These studies brings out a potential application for improving the drainage characteristics of coastal deposits and in preloading of offshore deposits.

REFERENCES

ASTM X-ray card file and index (1991). Annual Book of ASTM Standards, Philadelphia Pa.

ASTM D 2435 - 80 (1989). "Standard test method for one-dimensional consolidation properties of soils," Annual Book of ASTM Standards, Vol 04.08, pp 283-287.

Brandl, H (1981). "Alteration of soil parameters by stabilization with lime," Proc 10th Int Conf on Soil Mech and Found Engg, Stockholm, Sweden, Vol 3, pp 587-594.

Broms, B B (1984). "Stabilization of soil with lime columns," Proc Seminar on soil Improvement and Construction Technique in Soft Ground, Singapore, pp 120-133.

Broms, B B, and Boman, P (1975). "Lime stabilized columns," Fifth Asian Regional Conf on Soil Mech and Found Engg, Bangalore, India, Vol 1, pp 227-234.

Clare, K E, and Cruchley, A F (1957). "Laboratory experiments in the stabilizations of clays with hydrated lime," Geotechnique, Vol 7, pp 97-111.

Glenn, G R (1967). "X-ray studies of lime bentonite reaction products," Jl of the American Ceramic Society, Vol 50, No 6, pp 312-326.

Jackson, M L (1958). Soil Chemical Analysis, Prentice - Hall International, London.

Kawamura, M, and Diamond, S (1975). "Stabilization of clay soils against erosion loss," Clays and Clay Minerals, Vol 23, pp 443-451.

Mateous, M (1964). "Soil-Lime research at Iowa State University," Jl of Soil Mech and Found Div, ASCE, Vol 90, No SM2, pp 127-153.

Narasimha Rao, S, Rajasekaran, G, and Prasad, C V (1993). "Lime column method of stabilization in marine clay," Eleventh South East Asian Geotechnical Conf, Singapore, pp 397-402.

Narasimha Rao, S, Somayazulu, J R, and Ramesh, N V (1984). "The use of lime columns in soft clays," Proc Indian Geotechnical Conference, Calcutta, India, Vol 1, Section V, pp 39-44.

Narasimha Rao, S, Somayazulu, J R, and Rajasekaran, G (1991). "Stabilization of soft marine clay using deep in-situ lime column method," Tenth Int Conf on Offshore Mech and Artic Engg, No 91-388, Vol 1, Norway.

Okumura, T, and Terashi, M (1975). "Deep lime mixing method of stabilization of marine clays," Fifth Asian Regional Conf on Soil Mech and Found Engg, Vol 1, pp 69-75.

Thompson, M R (1964). 'The significance of soil properties in lime soil stabilization," Highway Engg Series No 13, Illinois Co-op Highway Program, Illinois.

Willoughby, D R, Gross, K A, Ingles, O G, Silva, S R, and Spiers, V M (1968). "The identification of reaction products in alkali stabilized clay by electron microscopy, X-ray and electron diffraction," Paper no 430, reprinted from the Proc of the fourth Conf of the Australian Road Research Board, Vol 4, Part 2, pp 1386-1408.

Table 1.

Physical Properties of Marine Clay

1. Natural moisture content	= 59%
2. Liquid limit	= 62%
3. Plastic limit	= 22%
4. Plasticity Index	= 40%
5. Unified Classification	= C H
6. Grain size distribution	
Clay size fraction	= 48%
Silt size fraction	= 37%
Sand size fraction	= 15%
7. Specific gravity	= 2.64
8. Field density	= 1.646 gm/cc

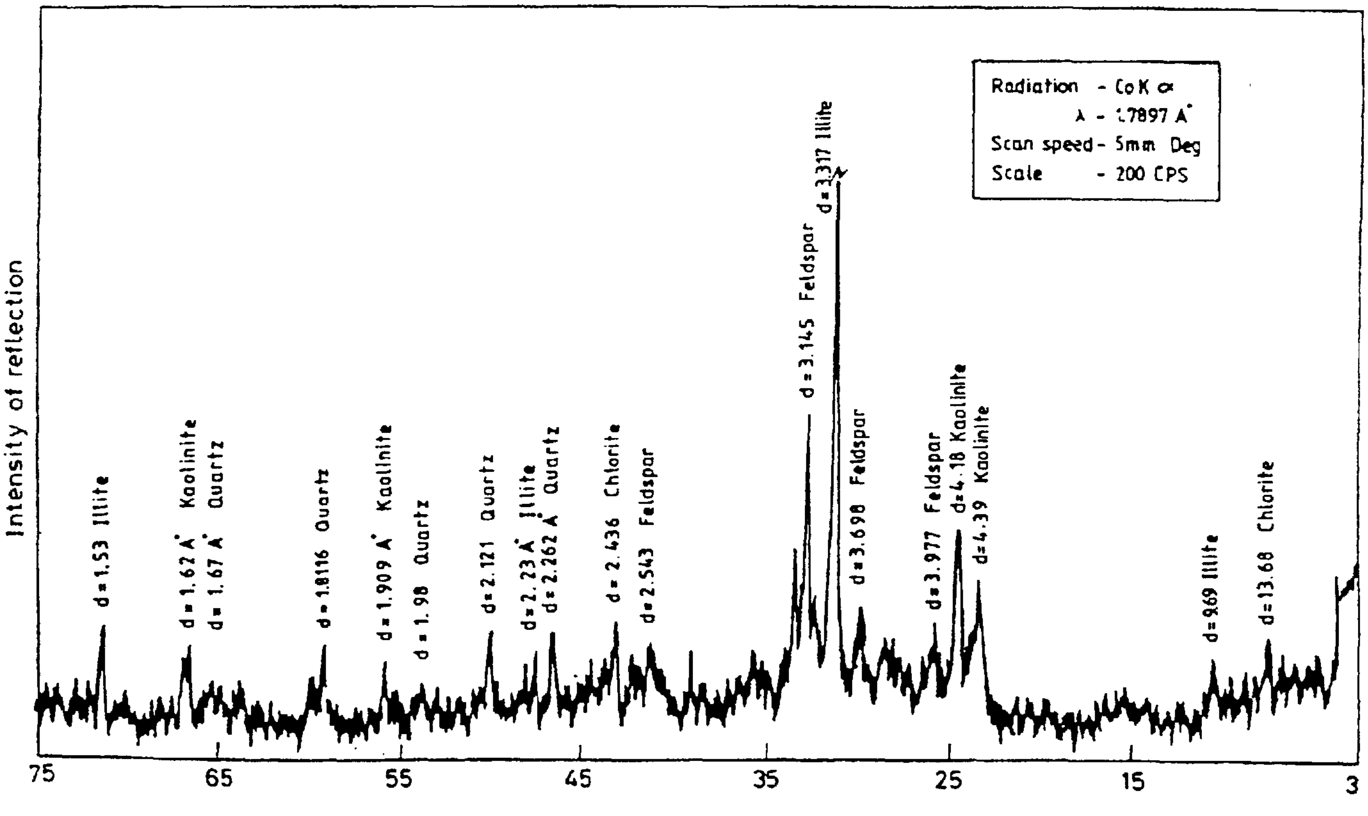

Fig. 1. X-ray Diffractogramme for untreated sample - sieved through 425 μ - Powder sample.

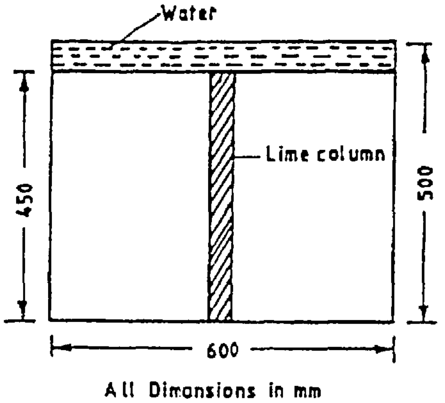

Fig. 2 . Details of single Column setup

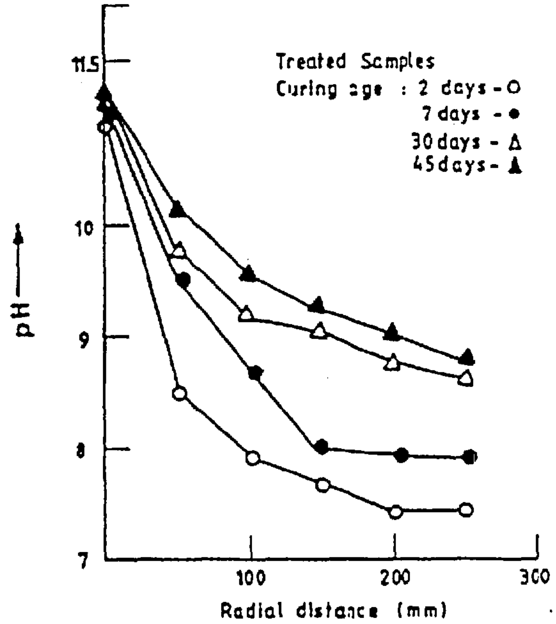

Fig. 4. Variation of pH with time along Radial distance-(Lime Column with pure water.)

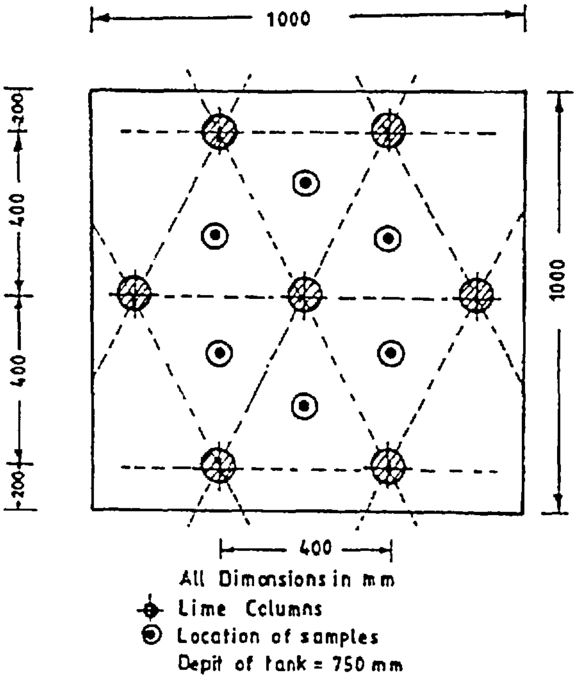

Fig. 3. Details of setup- Lime Column Group.

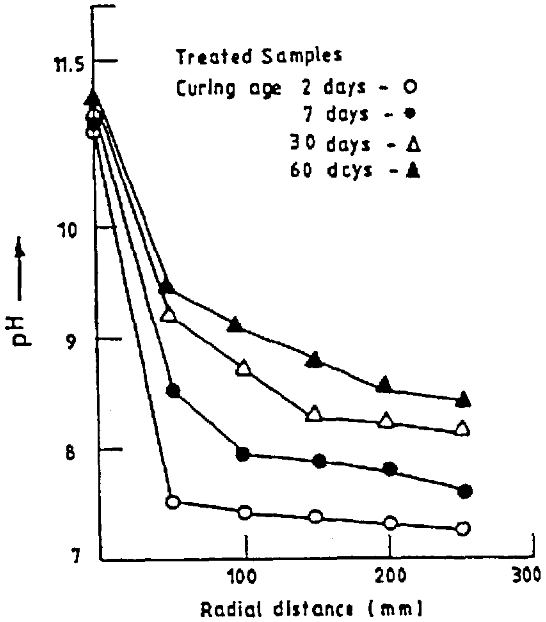

Fig. 5 Variation of pH with time along Radial distance-(Lime Column with Sea water.)

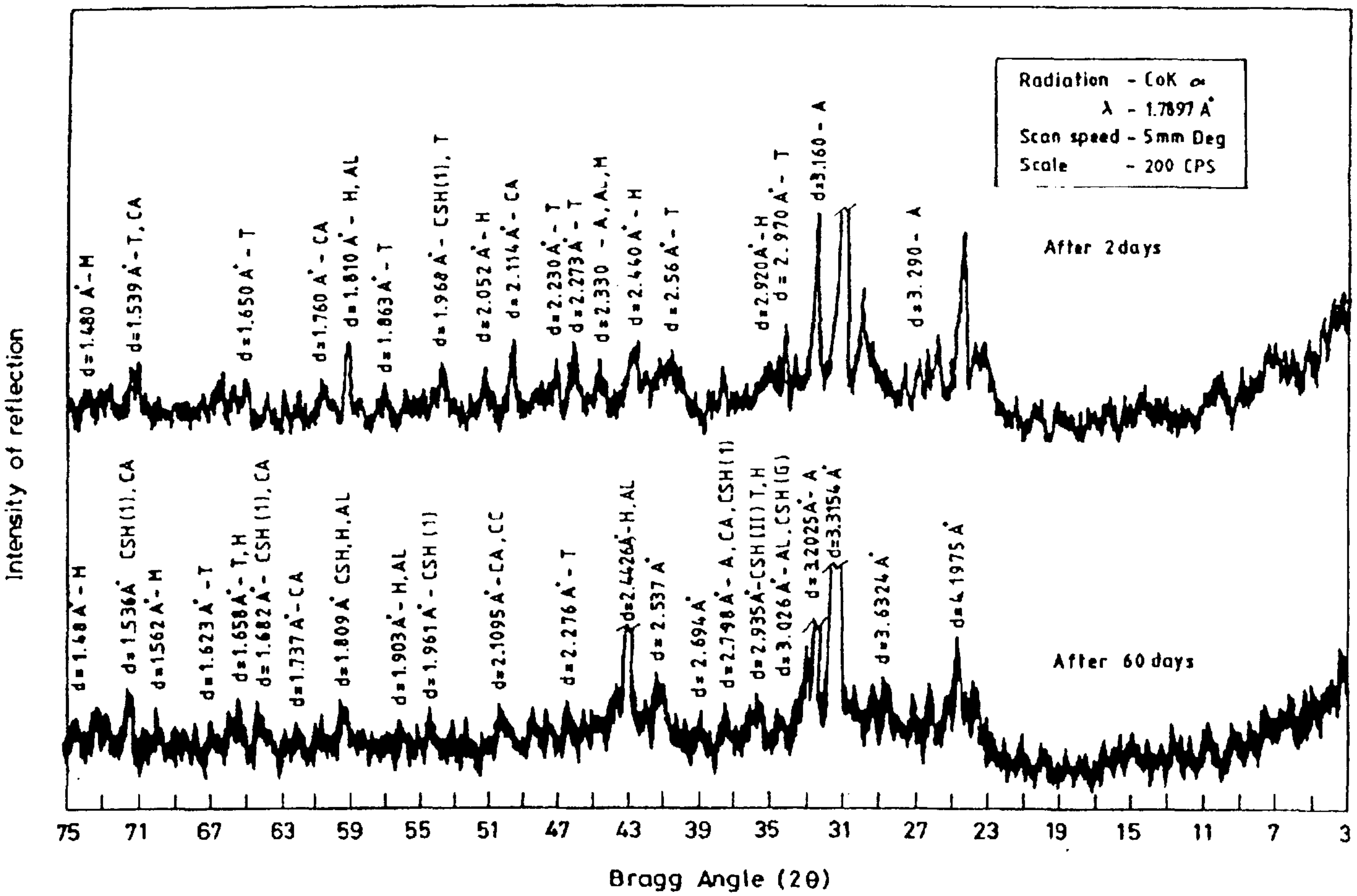

Fig. 7 XRD patterns of lime treated samples - Lime column with pure water.

A - Anorthite, T - Tobermorite, AL - Albite, CA - Calcium Aluminate, H - Hillebrandite,
M - Margarite, CC - Calcium Carbonate, CSH - Calcium Silicate Hydrate.

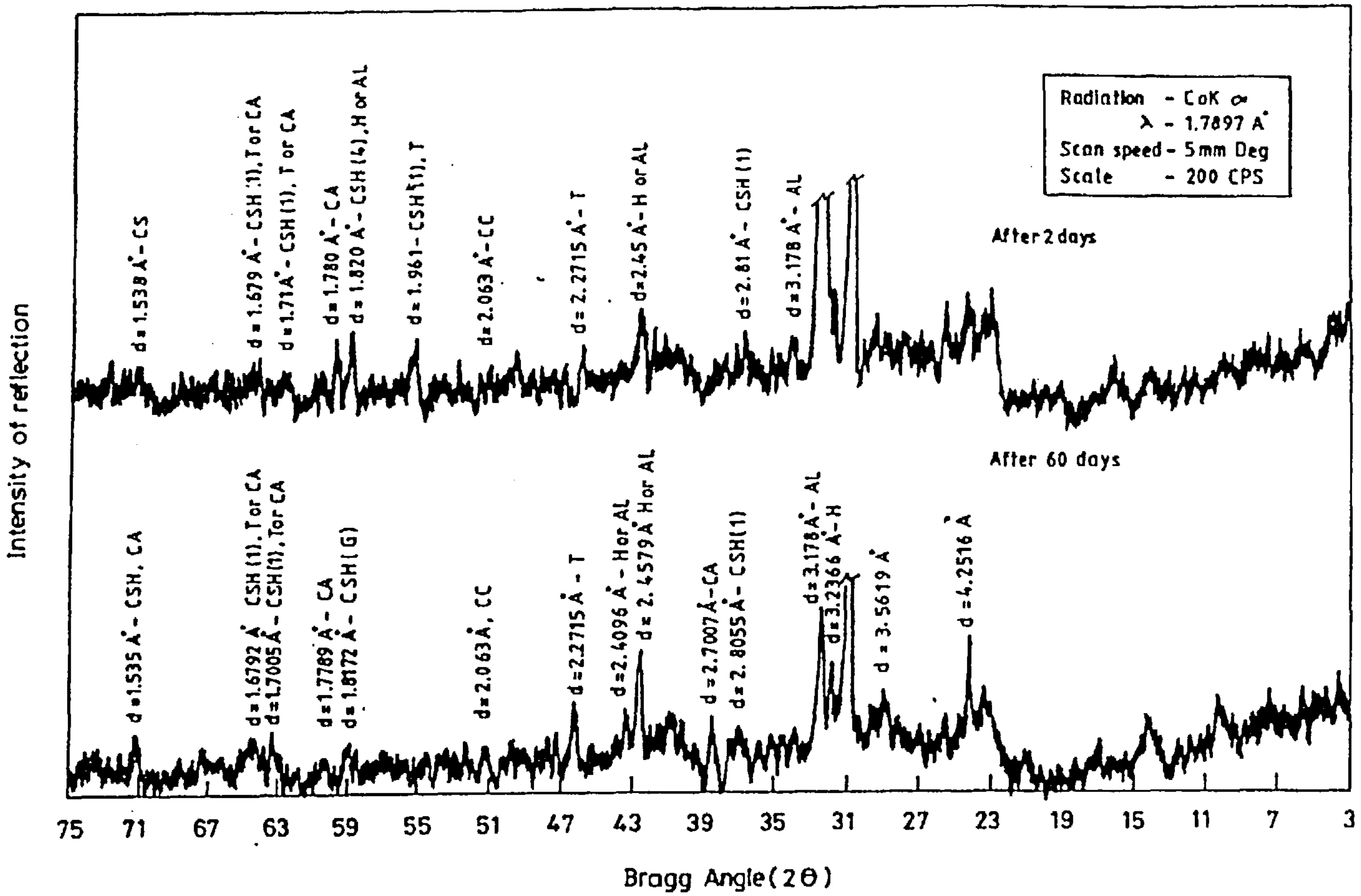

Fig. 8. XRD Patterns of lime treated samples - Lime column with sea water

A - Anorthite, T - Tobermorite, AL - Albite, CA - Calcium Aluminate, H - Hillebrandite, M - Margarite, CC - Calcium Carbonate, CSH - Calcium Silicate Hydrate.

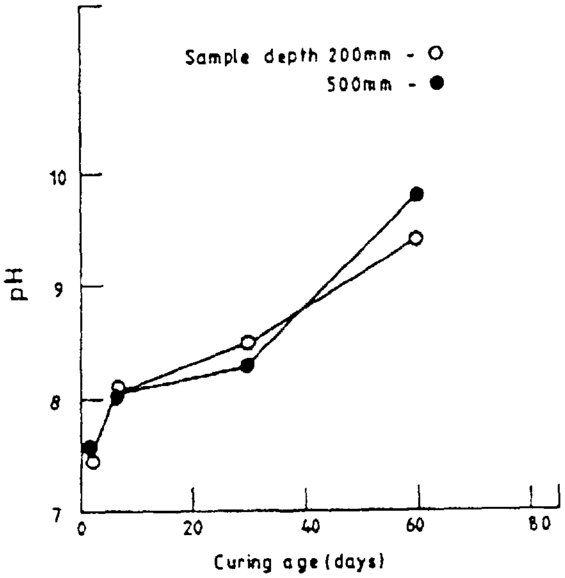

Fig.6 Variation of pH - (Lime column - group).

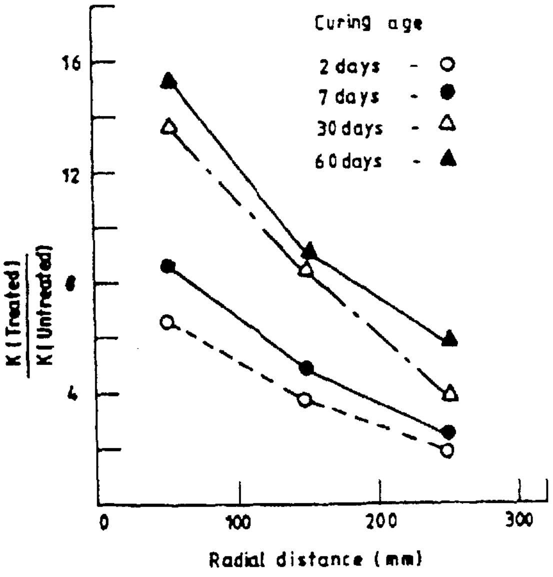

Fig.9 Variation of $\frac{K(\text{Treated})}{K(\text{Untreated})}$ with time along radial distance(lime column with pure water.)

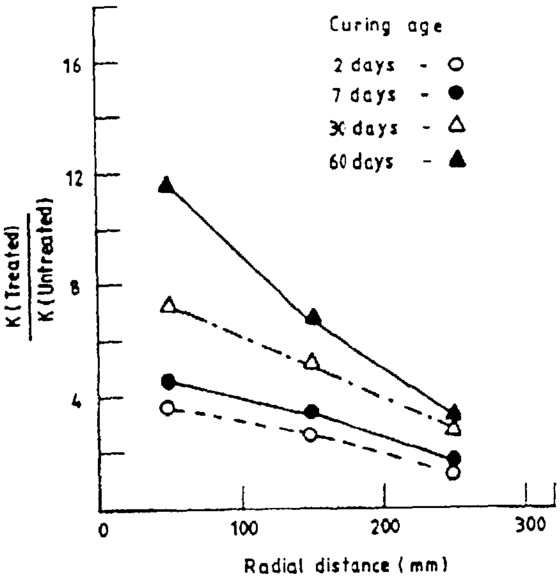

Fig.10 Variation of $\frac{K(\text{Treated})}{K(\text{Untreated})}$ with time along radial distance(lime column with sea water.)

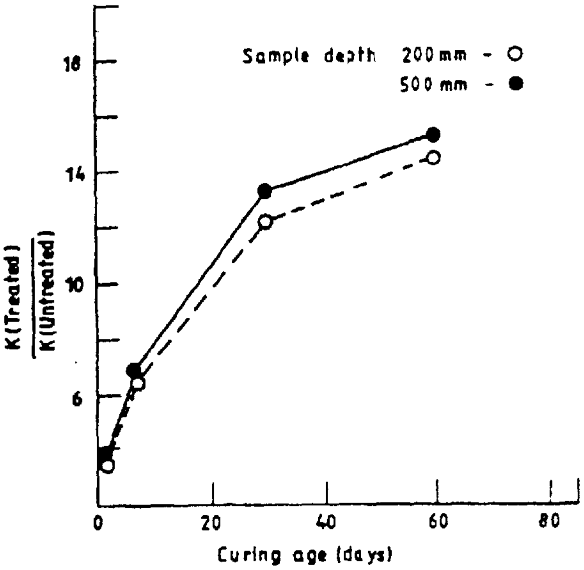

Fig.11 Variation of $\frac{K(\text{Treated})}{K(\text{Untreated})}$ (Lime column group)

SEISMIC REHABILITATION OF SARDIS DAM

Said Salah-Mars[1], Lelio H. Mejia[1], Robert Fleming[2], Wayne Forrest[2], Samuel Stacy[2]

Abstract

Extensive subsurface investigation of the embankment dam revealed the existence of a weak layer of silt and soft clay in the original topstratum clay underlaying the upstream shell of Sardis Dam (Mississippi). Based on the evaluation of the ground motions at the site due to an earthquake on the New Madrid source region, it was estimated that the weak layer would suffer substantial strength loss. The potential strength loss of the weak layer could trigger a slope failure of the upstream shell of the dam. Different alternatives to improve the shear strength of the weak layer were investigated. They included deep soil-cement mixing, stone columns and vibro-compaction, drilled piers, and driven piles.

A dam rehabilitation scheme based on reinforcing the upstream shell of the dam and its foundation using driven piles is presented herein. Compared to the other alternatives, driven prestressed concrete piles offered the most reliable and practical remediation; better quality control; and had potentially less uncertainty of the composite strength obtained. Prestressed concrete piles have a higher strength and more shear resistance compared to other alternatives. Based on fluctuations in reservoir level, the reinforcement technique would need to be installed from floating plant. Driven piles offer the most feasible alternative based on the difficulties of installing reinforcements such as piers and stone columns underwater. In addition, driven piles had the added benefit of some densification of the upper sand shell as a result of pile driving operations. The remediation procedure consists of driving piles through the sand shell and weak layer and into the dense substratum sand. The piles will provide resistance to the potential sliding mass (triggered by liquefaction of the weak layer) by transmitting the loads to the dense substratum sand. Two- and three-dimensional nonlinear finite element analyses were performed to analyze the soil-pile behavior and interaction effects.

---

[1] Woodward-Clyde Consultants, 500 12th St., Suite 100, Oakland, California

[2] US Army Corps of Engineers, Vicksburg, Mississippi

The soil-pile interaction, the pile embedment length into the dense substratum sand, the pile shear and moment distributions induced by the potentially sliding mass, and the pile group effect are presented.

Description of Sardis Dam

Sardis Dam is located in Northwestern Mississippi, on the Little Tallahatchie River, a tributary of the Yazoo River. The dam was built in the late 1930's by the US Army Corps of Engineers (COE) for flood control, however, it also provides recreational opportunities. The total length of the dam is approximately 15,000 feet with a maximum height of 117 feet. The central portion of the dam, located in the floodplain of the Little Tallahatchie River, ranges in height from 90 to 117 feet, and is approximately 8,500 feet long. The central portion of the dam was constructed by hydraulic filling. The dam has a watershed area of approximately 1,500 square miles and a reservoir volume at flood control pool (Elevation 281.4 feet) of 1.46 million acre-feet. The embankment dam consists of a clayey silt core flanked on both sides by sand shells. A rolled clay cap forms the crest section of the dam. The foundation material consists of a 15-foot thick clay and silt stratum, underlain by a 25-foot thick dense silty sand and sand substratum over an older stiff to very stiff Tertiary clay formation. A plan view and typical cross-section of the dam are shown in Figures 1 and 2, respectively.

Recently, an extensive subsurface investigation program conducted by the COE, indicated that the clay and silt topstratum contains an average 5-foot-thick weak layer, beneath the upstream shell of the dam, which may liquefy during a large earthquake in the New Madrid seismic source region. The peak ground acceleration (PGA) at the site during this event is estimated to be about 0.2g. The location of the weak layer varies both in thickness and in elevation, and is discontinuous along the dam alignment. A typical profile of standard penetration tests (SPT) performed along the upstream section of the dam is shown in Figure 3.

Based on the field subsurface investigations and laboratory testings performed by the COE, it was estimated that post-earthquake residual shear strength ratio (Su/P) defined as the ratio of the undrained shear strength (Su) over the effective overburden pressure (P), is about 0.075 for the weak layer . Limit equilibrium analyses indicated that the upstream shell of the dam presents a potential for post-earthquake failure, where the weak layer underlies the sand shell.

Numerical Analyses of the Soil-Pile Interaction

This section presents an analytical evaluation of the deformation behavior of the reinforced zone (Figure 4) under lateral loading resulting from the potential sliding of the upper shell upon liquefaction of the weak clayey silt in the foundation. The work included the development of finite element models to analyze the behavior of the pile-reinforced zone assuming post-liquefaction conditions in the weak layer. Both a three-dimensional (3-D) analysis of a pile with its tributary soil mass, assumed to be one of a large group of piles subjected to direct shear loading, and a two-dimensional (2-D) analysis of the reinforced zone in the dam were performed.

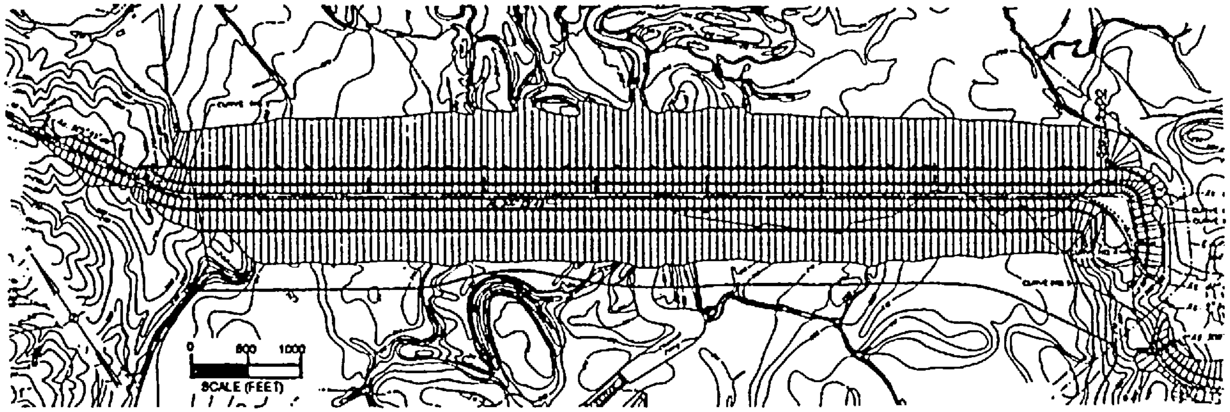

Figure 1: Sardis Dam plan view

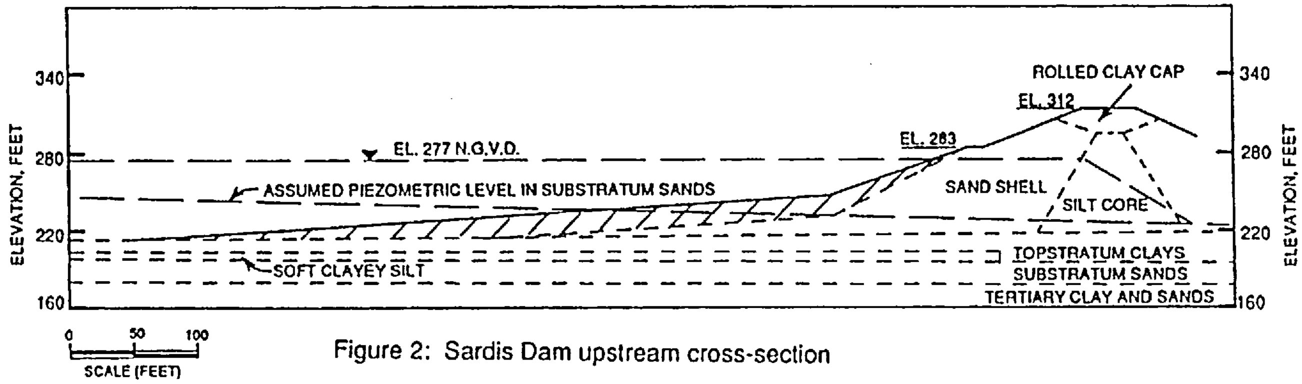

Figure 2: Sardis Dam upstream cross-section

Table 1: Hyperbolic soil parameters used in analysis

Material	γ (pcf)	ø (deg.)	c (psf)	K	n	Rf	Kb	m	Kur	Ko
Sand Shell	125	30	0	400	0.7	0.75	600	0.30	600	0.50
Topstratum Stiff Clay	120	0	2000	350	0.7	0.70	700	0.10	525	0.70
Weak Clayey Silt	120	0	230	4	0.7	0.70	8	0.10	10	0.60
Substratum Sand	125	35	0	500	0.7	0.70	750	0.30	750	1.00

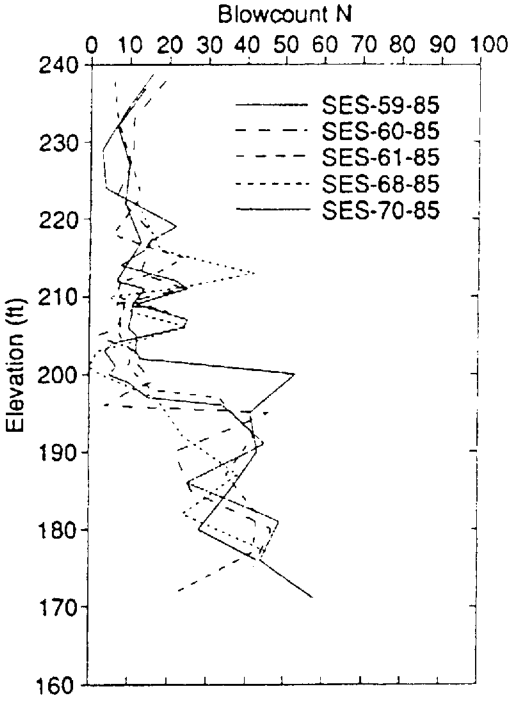

Figure 3: SPT blowcount along the 350-foot-line upstream of the dam

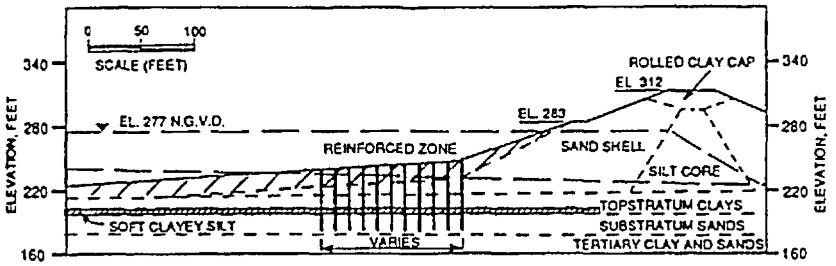

Figure 4: Sardis Dam upstream cross-section and reinforced zone

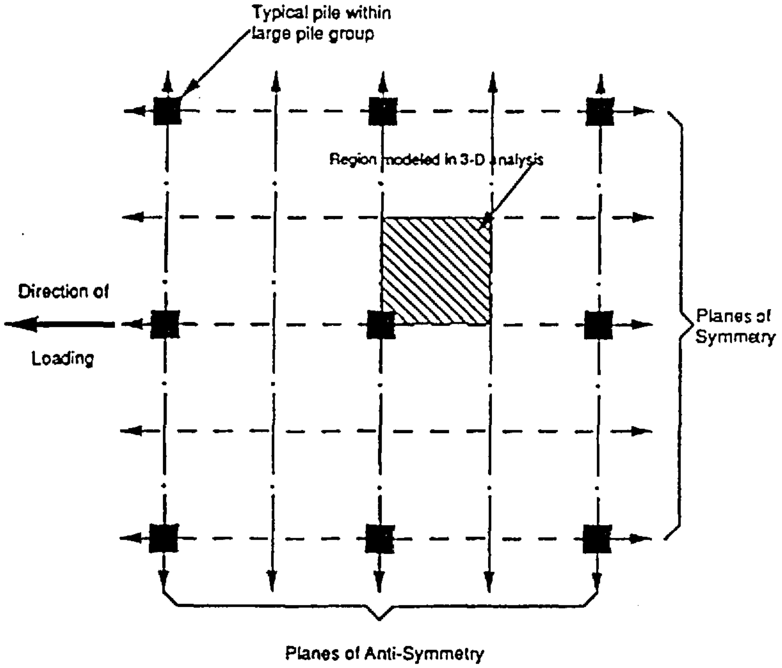

Figure 5: Plan view of portion of large pile group used in 3-D analysis

Three finite element computer codes were used in the study. NONSAP, a nonlinear static and dynamic code, was used to analyze the three-dimensional behavior of the single pile representative of a large number of piles. SSCOMP, an incremental elasticity nonlinear static code, was used to analyze the single pile case and the reinforced zone. DYSLAND, a nonlinear static and dynamic code, was used to analyze the single pile case.

The shear stress-strain behavior of the soils was represented by the hyperbolic model developed by Duncan and his co-workers (1980). The soil parameters used in the hyperbolic model are shown in Table 1. These parameters were assumed to represent the stress-strain behavior of the materials after liquefaction of the soft clayey silt has occurred. They were selected based on parameters previously used by the District to evaluate the post-earthquake stability of the dam (U.S. Army COE, 1988), on parameters published for similar materials (Duncan et al. 1980), and judgement. The post earthquake loading is then applied assuming the undrained shear strength of the soil and the resistance of the pile within the soil mass. As the weak layer reaches its residual strength, the upstream shell may undergo a slope failure whose plane of failure would likely extend through the weak layer. The loading resulting from the soil mass which will tend to move down-slope, will generate pressure on the soil-pile system acting down-slope and increasing with depth.

Single Pile Analysis

A detailed evaluation of the deformation behavior of the piles in the reinforced zone (see Figure 4) would require an extensive 3-D analysis of the entire reinforced zone and the dam. To simplify the problem and to evaluate the local behavior of a "typical" pile within the reinforced zone (including the effects of nearby piles), it is assumed that the ground surface is horizontal and that the reinforced zone consists of a very large group of piles as shown in plan view in Figure 5. It is also assumed that the reinforced zone is in a global state of direct shear in the direction shown in Figure 5. Under these conditions, deformations of the soil-pile system will be symmetrical with respect to planes parallel to the direction of the load and anti-symmetrical with respect to planes transverse to the load. Thus, the behavior of the large group of piles can be analyzed with a model of a one-quarter section of a single pile and its tributary soil volume, corresponding to the shaded area in Figure 5, and as illustrated in Figure 6. Such a model permits efficient evaluation of the effects of various parameters including pile spacing, pile diameter, embedment length, material property variation, etc.

A triangular lateral pressure distribution increasing with depth was assumed to act on the soil which exerts its pressure on the piles. This stress distribution is consistent with the distribution of at-rest pressures up-slope of the reinforced zone. Recent analyses conducted by the Waterways Experiment Station (WES) using 2-D finite element simulation of the entire dam and the piles using the computer program TARA-3 (Finn et al., 1986) yielded a triangular lateral stress distribution along the front pile, as assumed herein.

A "baseline" case was selected as a reference for parametric studies. The parameters corresponding to the baseline case are presented in Table 1 and Figure 6.

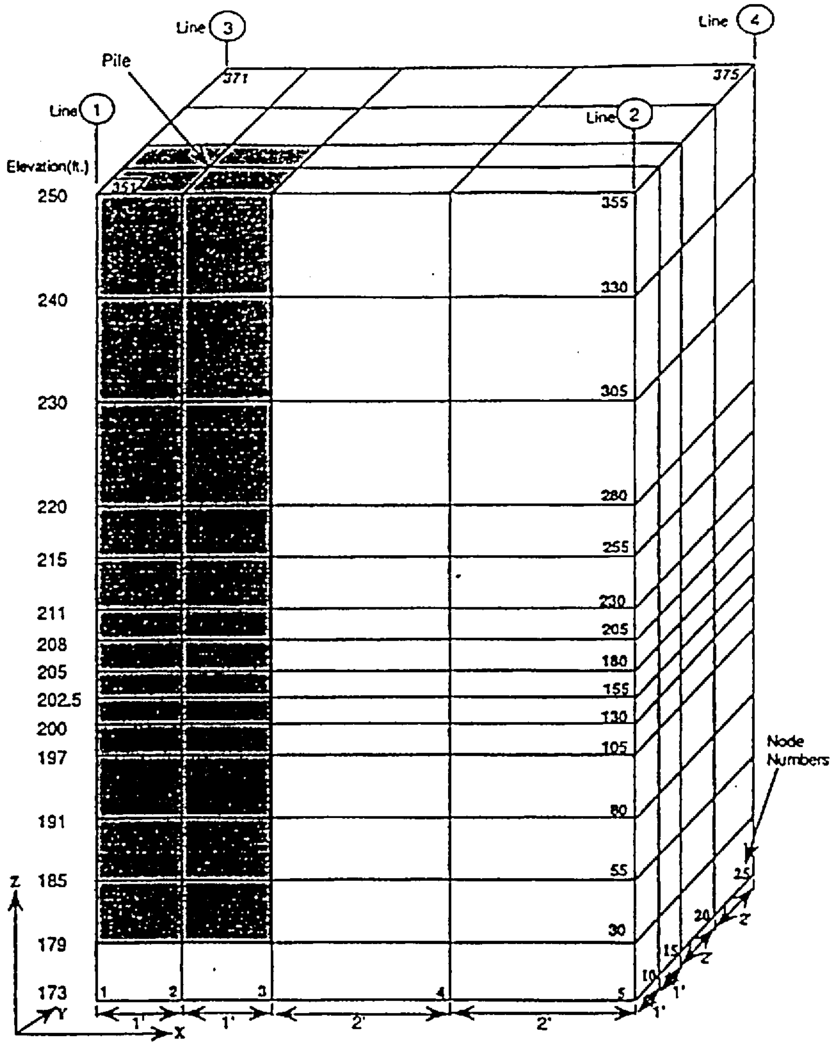

Figure 6: Finite element mesh used to model the soil and pile system

The reference to lateral load, however, deserves further explanation. The baseline lateral load is defined as the lateral load which causes an average shear stress in the weak layer equal to the shear strength of this layer. Thus, the baseline load results in an average shear stress of 230 psf in the weak layer and below.

The baseline case consists of a 24-inch-square prestressed concrete pile embedded 15 feet into the dense substratum sand with a pile centerline-to-centerline spacing of 12 feet. The driving lateral load corresponds to the baseline load as defined above. The calculated deflections of the model along lines 1, 2, 3 and 4 (see Figure 6), are shown in Figure 7. The pile centerline (line 1) deflects with a smooth "S" shape and bridges across the weak layer. A tendency for "shearing" of the weak layer is seen in lines 3 and 4 away from the pile. In addition, there is a tendency for the tip of the pile to "kick back". The calculated deflection at the top of the pile is about 0.53 inches.

Similar deformation analyses were performed for lateral pressures equal to 2, 8, and 16 times the baseline load, corresponding to an average shear stresses in the weak layer of 460 psf, 1840 psf, and 3680 psf, respectively. The calculated deformations at the top of the pile were 1.15, 7.2, and 32 inches, respectively, indicating a highly nonlinear behavior. Although the load deformation relationship is nonlinear, the deflected shapes of the pile are relatively similar for all load cases. At 16 times the baseline load, the soil-pile system is in a state of failure.

The distribution of bending moments and shear forces along the pile for the above four loads are shown in Figures 8 and 9, respectively. The bending moments in Figure 8 are normalized by the maximum moment of the baseline case. The shear diagrams in Figure 9 are normalized by the maximum shear of the baseline case. The calculated maximum shear in the pile for the baseline case is 32.4 kips. This value was obtained directly from the calculated shear stress in the pile. Since the baseline load is 33.1 kips, the pile carries approximately 98 percent of the applied load while the weak clayey silt carries the remaining 2 percent. The maximum bending moment in the pile for the baseline case is 1330 kip-inches. While the 8-node isoparametric solid element has adequate shear characteristics and provides reliable estimates of shear in the pile, it has relatively poor bending properties. Accordingly, the maximum bending moment for the baseline case was obtained from the above calculated maximum shear and the ratio between maximum moment and shear given by the deflected shape of the pile.

Figures 8 and 9 show that the calculated shapes of the bending moment and shear diagrams are essentially independent of the load level. The bending moments and shear forces in the pile are approximately proportional to the applied load. Figure 8 indicates that the highest moment occurs at the boundary between the substratum sand and the weak clayey silt. The shear force diagrams in Figure 9 show that the highest shear occurs in the weak layer below the stiff clay layer.

Several parameters were varied in the analyses to evaluate their effects on the behavior of the pile-soil system. These parameters included pile spacing, pile width, pile embedment into the substratum sand, soil properties, and load distribution. Only a very succinct description of some of the salient results are presented herein. The analysis indicated that generally the moments and shear forces are proportional to the tributary

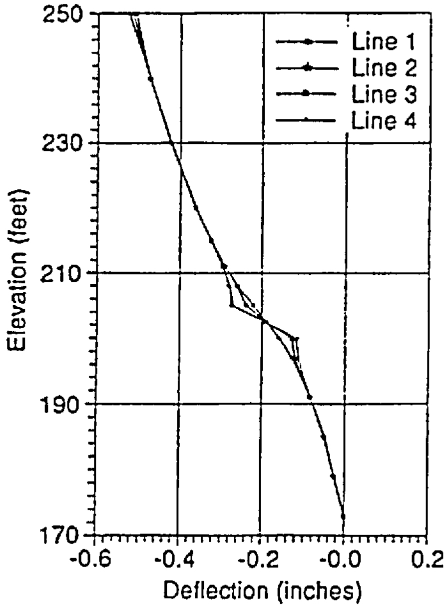

Figure 7: Lateral deflection of soil and pile under baseline load

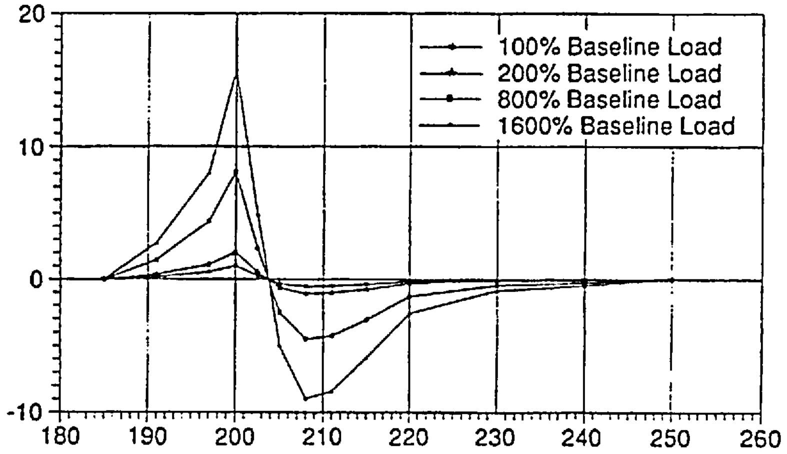

Figure 8: Normalized moment distribution along the pile

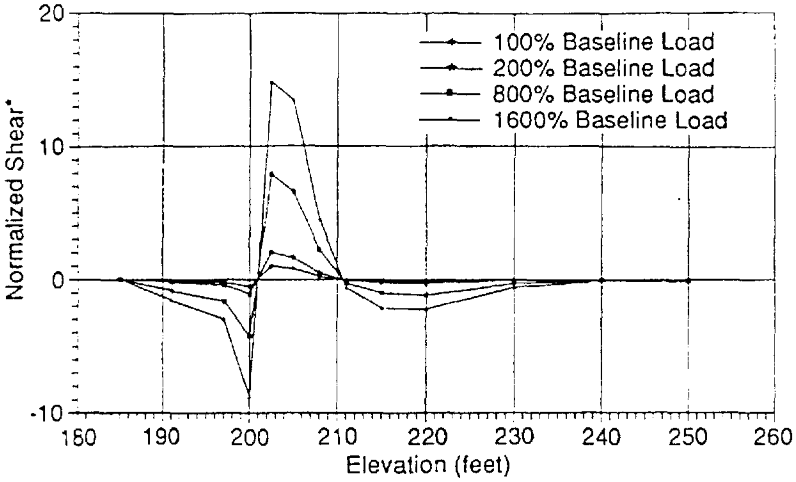

Figure 9: Normalized shear force distribution along pile

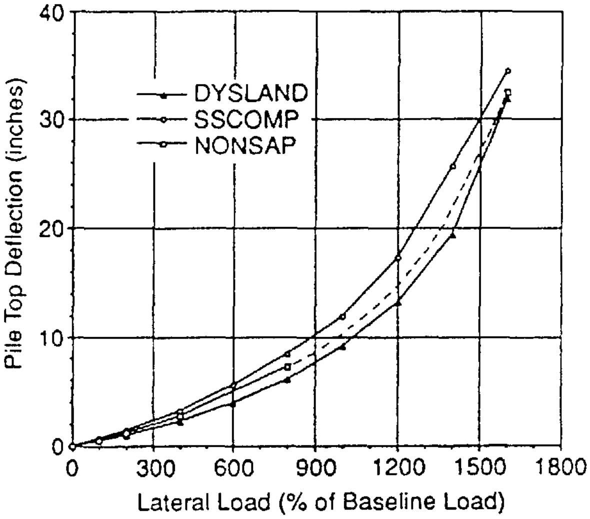

Figure 10: Load deflection curves for different methods of analysis

area which is directly related to the pile spacing. The embedment length into the substratum sand was varied from 3 feet to 21 feet. At about 15 feet into the substratum sand, the moment and shear diagrams tend to become stationary. The shape of the moment and shear diagrams appear to be unaffected by the pile size. The deflection at the top of the pile under the baseline load is about 0.58 inch for the 18-inch square pile, about 0.53 inches for the 24-inch pile and about 0.38 inches for the 48-inch pile. The lack of correlation between the pile deflection and the pile rigidity is a result of the capacity of the substratum sand to carry the pile lateral load. This outcome is useful because it indicates that stronger piles do not necessarily provide a higher composite shear strength in the weak layer. The desired composite shear strength in the weak layer is conditioned by the ability of the substratum sand to carry the pile load. Indeed an increase of the shear strength of the substratum sand resulted in a substantial reduction in the pile head deflection. The pile bending moment and shear force appear to be unaffected by the increase of the weak layer parameter K from 4 to 40 (as defined in Table 1). However, the thickness of the weak layer seems to induce a significant increase in the pile top deflection and moment while the shear force is unaffected. For an 8-foot weak layer, the moment was estimated to be about 1.5 times that of the baseline case.

The single pile analysis was also evaluated using 2-D finite element simulation with the computer codes SSCOMP and DYSLAND. The results of the 2-D simulations yielded similar results to those of the 3-D analysis. For comparison purposes, the results of the 3-D and the two 2-D simulations are shown in Figure 10.

Pile Group Analysis

The program SSCOMP was used to analyze the zone of the dam shown in Figure 11. A zone with 11 rows of piles spaced at 12 feet on centers in both directions was assumed. The finite element mesh used in the analyses is shown in Figure 11. The analysis was performed for four load levels, corresponding to 1, 2, 8, and 16 times the baseline load. The soil and pile parameters are the same as those used for the single pile analysis.

The calculated pile deflections, moments, and shears for the front pile (line 1), the middle pile (line 6), and the last pile (line 11), were similar in shape to those obtained in the 3-D analysis. However, the magnitude of the deformation among the piles in the group were substantially different. The moment and shear diagrams of the piles were normalized with respect to their corresponding maximum moment and shear for the different load levels analyzed. The results indicated that the normalized family of curves fall within a narrow range. This finding is useful because the moment and shear diagrams for different loads can be generated from the single average normalized curves for both moment and shear.

The pairs of maximum moment and corresponding maximum shear were compared for all the parametric case analyzed in this study. The data points fall within a narrow band, indicating a linear relationship between the maximum moment and the corresponding maximum shear force as shown in Figure 12. As an example, the average ratio of moment over shear for the 5-foot weak layer appears to be about 50 inches. This

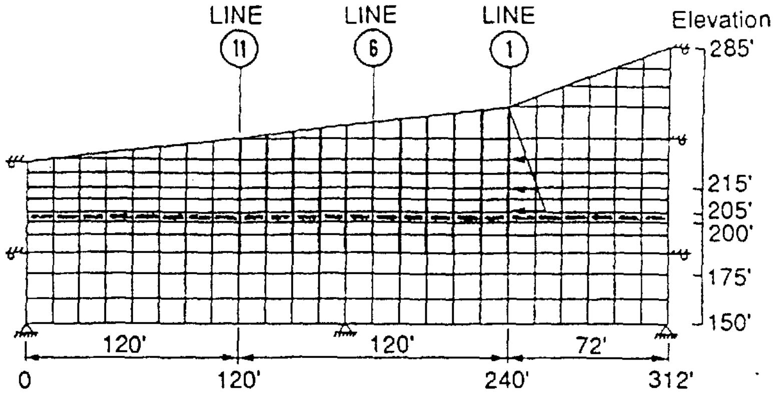

Figure 11: Finite element mesh and loading conditions for pile group analysis

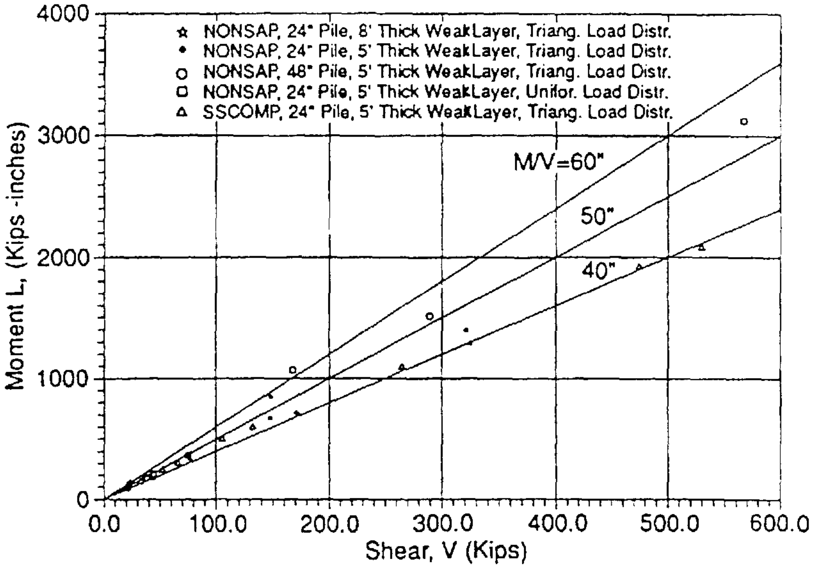

Figure 12: Maximum moment verses maximum shear in pile

relationship can be useful in generating the design moment in the pile once the required shear strength of the reinforced weak layer is established. The required shear strength of the reinforced weak layer should satisfy the stability and deformation criteria.

Despite the similarity in the shape of the moment and shear diagrams, the results of the group analyses indicate that the back (downslope) piles deflect less than the front (upslope) piles and slightly more than the middle piles. The front piles, facing the driving load, carry relatively more load than the back piles which in turn carry slightly more load than the middle piles. A typical distribution of maximum moment among the piles in the group is illustrated in Figure 13. Similar load distribution was also obtained for the maximum shear. These group effects on the load distribution among the piles can also be useful in assessing the design load level for the pile subgroups, or alternatively, rearranging the pile spacing (i.e. tighter pile spacing in the front) to accommodate a more "uniform" load distribution among the piles in the group.

Finally, stress mappings of the reinforced zone were generated to observe the behavior of the group of piles within the soil mass. Maximum and horizontal shear stress and stress level contours in the reinforced zone were mapped for several load levels. For illustration, Figure 14 shows the contours of horizontal shear stress within the reinforced zone for a load corresponding to 12 times the baseline load. The largest horizontal shear stresses occur within the substratum sand near the tip of the piles. There is a significant amount of stress transfer upstream and downstream of the reinforced zone. Within the reinforced zone the maximum shear stresses (not shown here) are nearly equal to the horizontal shear stresses. The stress level (i.e., mobilized strength or ratio of stress to strength) contours within the reinforced zone indicate that the highest stress levels (over 0.8) occur within the reinforced zone above and below the weak layer. The results of the analyses for 16 times the baseline load indicate that stress levels of over 0.8 develop throughout the reinforced zone and they approach 1.0 within a major portion of this zone, indicating development of a global state of failure.

Summary and Conclusions

Driving piles to reinforce the weak layer of silt and clay underlying the upstream shell of Sardis Dam is a viable option because the well controlled strength of the piles can be used to improve with reliable accuracy the shear resistance along the weak layer. Pile driving also provides a potential densification of the upper sand shell as a result of the driving vibrations. A test section performed at the site did provide evidence of densification of the upper shell like material as a result of pile driving. A detailed analysis of the soil-pile system is a necessary tool to help evaluate the controlling parameters specific to the site under study.

The variation of parameters such as: pile spacing, pile width, pile embedment in the substratum sand, soil properties, and load distribution indicated that:

(1) The average shear strength capacity of the reinforced weak layer is controlled mostly by the strength of the substratum sand. The shape of the bending moment and shear diagram along the length of the pile are relatively insensitive to the various

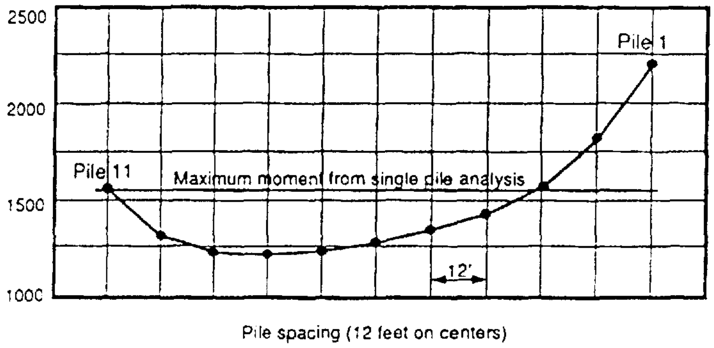

Figure 13: Maximum moment distribution across the pile group

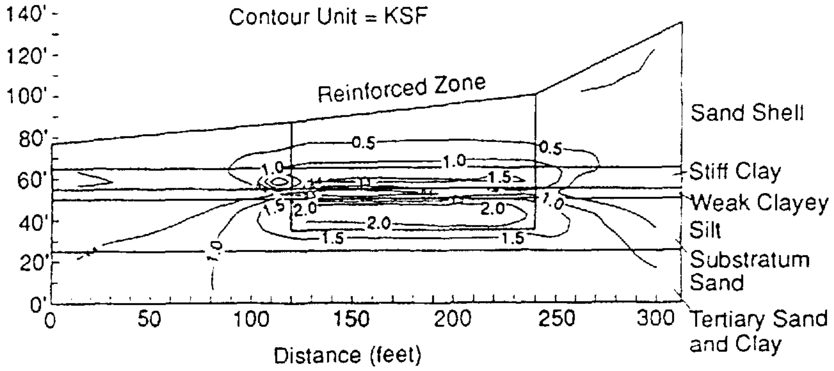

Figure 14: Horizontal shear stress in reinforced zone

parameters considered above. The maximum bending moment is roughly proportional to the maximum shear.

(2) A minimum pile embedment of 15 feet into the substratum sands appears sufficient to develop the optimum bending and shear capacity for the 24-inch pile. Shallower embedments are likely to result in excessive rotation at the pile tips and deflection at the pile tops.

(3) The maximum shear and bending moment will vary with the locations of the piles within the reinforced zone. To estimate the shear and bending moments within the pile group, data similar to those shown in Figure 13 should be used as a guide.

Acknowledgment

The studies summarized in this paper were funded by the U.S. Army Corps of Engineers, Vicksburg, Mississippi. Woodward-Clyde Consultants provided support for the preparation of this paper through the Professional Development Program. This support is gratefully acknowledged. Our thanks are also extended to Mr. Robert K. Green who provided valuable comments.

References

Bathe, K-J, Wilson, E.L., Iding R.H., (1975), "NONSAP, A Structural Analysis Program for Static and Dynamic Response of Nonlinear Systems", Report No. VC SESM 74-3, College of Engineering, University of California, Berkeley, California, February.

Duncan, J.M., Seed, R.B., Wong, K.S., and Ozawa Y., (1984), "Feadam 84: A Computer Program for Finite Element Analysis of Dams", Report No. SU/GT/84-03, Department of Civil Engineering, Stanford University, Stanford, California, November.

Duncan, J.M., Seed, R.B., (1984), "SSCOMP: A Finite Element Analysis Program for Evaluation of Soil-Structure Interaction and Compaction Effects", Report No. UCB/GT/84-02, Department of Civil Engineering, University of California, Berkeley, California.

Duncan, J.M., Byrne, P., Wong, K.S., and Mabry P. (1980), "Strength, Stress-Strain and Bulk Modulus Parameters for Finite Element Analyses of Stresses and Movements in Soil Masses", Report No. UCB/GT/80-01, College of Engineering, University of California, Berkeley, California, August.

Finn, W. E. Liam, Yogendrakumar, M., Yoshida, N. and Yoshida, H. (1986), "TARA-3: A Program to Compute the response of 2-D Embankments and Soil Structure Interaction Systems to seismic Loadings," Dept. Of Civil Eng., University of British Columbia, Vancouver, Canada.

Salah-Mars, S., (1989), "A Multiple Yield Surface Plasticity Model for Response of Dry Soil to Impact Loading", Ph.D. Dissertation, Department of Civil Engineering, Stanford University, California, June.

Ocean Engng, Vol. 21, No 2, pp. 207–219, 1994.
Printed in Great Britain.

0029–8018/94 $6.00 + .00
Pergamon Press Ltd

ELECTRO-OSMOTIC STABILIZATION OF MARINE CLAY WITH CHEMICAL PILES

R. SRINIVASARAGHAVAN* and G. RAJASEKARAN†

*Geotechnical Division, Structural Engineering Department, Annamalai University, Tamil Nadu, India;
†Ocean Engineering Centre, Indian Institute of Technology, Madras 600 036, India

Abstract—Weak marine clay deposits exist all along the seacoast of many parts of the world. Due to the poor engineering characteristics of these deposits, they pose several foundation problems to various coastal structures. Because of the high salt content in these deposits, the electro-osmotic technique has been effectively adopted to stabilize these deposits with some inorganic additives. In this investigation, the physico-chemical changes that occurred in a marine clay with various inorganic additives are presented and discussed. The improvement in the strength and plasticity characteristics of the soil have also been studied and reported. The newly formed reaction products arising out of the diffusion of lime are identified using X-ray diffraction technique (XRD). The present study indicates great promise regarding the use of electro-osmotic technique with inorganic additives as a quick remedial measure for the *in-situ* stabilization of coastal marine clay deposits.

1. INTRODUCTION

EXTENSIVE soft clay deposits are often encountered all along the coastal regions in several parts of the world. These soft deposits occur in layers ranging from a few metres in thickness to depths of 30 m below the sea-bed level along the coastal region. They are characterized by low shear strength and high compressibility properties. Because of the increased construction activities in these areas, there is a necessity to improve the engineering properties of these deposits. Treatment of the fine grained soils with chemical additives to improve their properties has been in vogue for several years. These marine deposits respond very well to electro-osmotic technique with chemical additives because of their high salt concentration [Katti (1967); Katti and Pavate (1980)]. In this paper, an attempt has been made to investigate the beneficial changes in the engineering properties of a marine clay using electro-osmotic technique with three inorganic additives such as sodium chloride (NaCl), potassium chloride (KCl) and calcium chloride ($CaCl_2$).

Several mechanisms such as cation exchange, flocculation, aggregation, carbonation and pozzolanic reactions are responsible for the beneficial effects induced in the soil system as a result of chemical stabilization and the use of various chemicals for the treatment of weak clay deposits is widely practiced. Because of the proven success of lime in the field of soil stabilization, this method has also been extended to deep *in-situ* treatment of soft marine clays (Yanase, 1968; Okumara and Terashi, 1975). Broms and Boman (1975, 1976) used lime piles for stabilizing weak Swedish soils. They used mechanically operated equipment to install these lime piles. A similar technique has been used by Okumara and Terashi (1975) for stabilizing thick soft marine deposits and reclaimed soils of a Japanese harbour area. The use of lime with chemical additives such as sodium chloride (NaCl) to stabilize kaolinite and montmorillonite mixtures has been reported by Lees *et al.* (1983).

Casagrande (1952) and Casagrande *et al.* (1961) have effectively used the electro-osmotic technique to stabilize the weak soils underneath Canadian railway lines. Bjerrum (1967) and Mitchell (1970) have reported that under the normal potential difference in the soil system, a considerable amount of current passes through the salt-saturated soil media. Mitchell *et al.* (1980) have evaluated the volume change properties of the electro-osmotically stabilized soils. Lo *et al.* (1991) have carried out a comprehensive experimental investigation on the electro-osmotic strengthening of soft sensitive clay and studied the mechanism of the electro-osmosis process.

In India, Balasubramanian (1969) studied the electro-kinetic behaviour of the Bombay marine clay. Patwardhan (1977) has studied the effect of electro-chemical hardening of a marine clay with calcium chloride piles. Katti *et al.* (1980) had used the electro-chemical hardening technique for stabilizing Bombay marine clay. The aim of the present experimental work is to evaluate the beneficial effects that occurred in the soil system due to the electro-osmotic technique in the presence of inorganic additives. The changes occurring in the plasticity and strength properties of the soil were studied by conducting consistency and unconfined compressive strength tests. The newly formed cementation compounds have also been examined using the XRD patterns of soil samples and are reported.

2. EXPERIMENTAL WORK

2.1. *Soil used*

The soil used in this experimental investigation is a marine clay obtained from the coastal basin behind Port Nova, Tamil Nadu, India. Bulky soil samples were taken at a depth of 1.5 m below the ground level and these samples were air-dried and stored correctly. The physical and chemical properties of the untreated soil are given in Table 1.

TABLE 1. UNTREATED SOIL PROPERTIES

Sample No.	Physical and chemical properties	Test values
1.	Liquid limit	55%
2.	Plastic limit	22%
3.	Shrinkage limit	8%
4.	Specific gravity	2.6
5.	Free swell index	54%
6.	Cation exchange capacity	39 m. eq/100 g of soil
7.	pH	8.1
8.	Conductivity of the soil	4.3×10^{-3} ℧ mV
9.	Total soluble salts	2%
10.	Chlorides	0.04%
11.	Sulphates	0.01%
12.	Organic matter	0.7%
13.	Unconfined compressive strength of the soil	0.11 N/mm^2

2.2. *Test programme*

In the present investigation, the effect of electro-osmotic stabilization of lime and lime-gypsum piles with different inorganic additives in a marine clay has been studied and discussed. The details of the experimental set-up are shown in Fig. 1. A perspex tank of size 300 × 250 × 300 mm was filled with silty clay in layers of 20 mm thickness at a moisture content close to its liquid limit and care was taken to remove air voids by slight tamping of the soil. A homogeneous soil bed was thus prepared up to a height of 250 mm. Two holes of 20 mm diameter and 200 mm height were made in

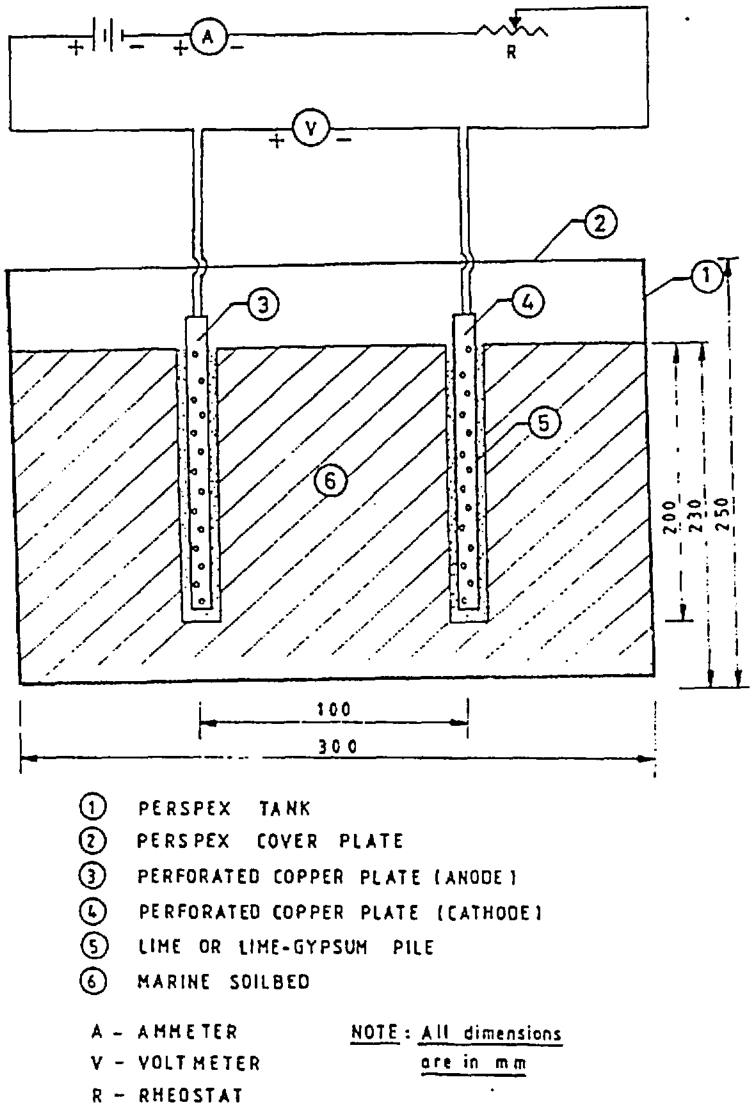

Fig. 1. Details of experimental set-up.

the soil bed at a spacing of 100 mm. Perforated copper electrodes of size 220 × 20 mm were installed in the holes. These holes were backfilled with any one of the three inorganic additives, namely sodium chloride (NaCl) or potassium chloride (KCl) or calcium chloride ($CaCl_2$) mixed with lime and lime-gypsum. The composition of the different chemicals used is given in Table 2. The addition of the chemical mixture for lime and lime-gypsum piles varied by 2 and 4% of the dry weight of the soil. The percentage of the salts, NaCl or KCl or $CaCl_2$, added with lime and lime-gypsum filling as piles varied by 1:1 ratio. A constant potential of 30 V was applied between the electrodes and was maintained for a period of 72 hr. Direct current of 5 A was varied between the electrodes to accelerate the diffusion of chemicals into the soil. Thus, a total number of 24 different tests were carried out in the first phase to study the effect of different chemicals on the electro-osmotic stabilization. It was found that the combination of calcium chloride with lime-gypsum piles was most effective in improving the strength and plasticity properties of soil. This is mainly due to the easy replacement of monovalent cations present in the soil by the divalent calcium ions from the lime-gypsum mixture. Hence, in the second phase with the lime-gypsum and calcium chloride mixture, studies on the effect of electro-osmotic treatment with time were made for different treatment periods of 3, 7, 14, 21, 28 and 35 days.

In the first phase, after 72 hr of treatment, the current supply was stopped and the samples were taken in-between the chemical piles at a depth of 100 mm. In the second phase, after each period of treatment such as 3, 7, 14, 21, 28 and 35 days, the current supply was stopped and the samples were taken in the same way as mentioned above. The beneficial changes occurring in the soil due to the effect of electro-osmotic treatment with inorganic additives have been studied by conducting Atterberg limit and strength tests. The diffusion of chemicals from the chemical piles into the soil has been studied with pH measurements. The formation of the cementation compounds such as Calcium

TABLE 2. COMPOSITION OF CHEMICALS USED

Sample No.	Chemical used	Composition	
1.	Lime (unhydrated)	Calcium	= 56%
		Silica	= 36%
		Iron oxide	= 4%
		Phosphorous	= 0.1%
2.	Gypsum	Minimum assay	= 96%
		Chloride	= 0.002%
		Magnesium and alkali salts	= 0.20%
3.	Sodium chloride	Minimum assay (after ignition)	= 99%
		Bromide and iodide	= 0.01%
		Nitrate	= 0.001%
		Phosphate	= 0.005%
		Sulphate	= 0.002%
		Potassium	= 0.01%
4.	Potassium chloride	Minimum assay (after ignition)	= 99.5%
		Sulphate	= 0.03%
		Iron	= 0.002%
		Sodium	= 0.01%
5.	Calcium chloride	Minimum assay	= 98%
		Heavy metals	= 0.002%

TABLE 3. EFFECT OF LIME PILES ON SOIL PROPERTIES

Sample No.	Soil properties	Percentage of chemicals added					
		NaCl		KCl		$CaCl_2$	
		1%	2%	1%	2%	1%	2%
1.	Liquid limit (%)	46	42	43	38	40	38
2.	Plastic limit (%)	23	24	25	28	25	29
3.	Shrinkage limit (%)	9	10	9	11	10	12
4.	pH	8.3	8.4	8.3	8.4	8.4	8.4
5.	Unconfined compressive strength (N/mm^2)	0.50	0.71	0.58	0.74	0.61	0.82

Silicate Hydrate (CSH) and Calcium Aluminate Hydrate (CAH) has been studied using the X-ray diffraction technique (XRD).

3. RESULTS AND DISCUSSION

3.1. *Variation of Atterberg limits*

Atterberg limit tests were determined for the soil samples taken after the first and second phases of treatment to study the changes in the consistency of soil due to the penetration of inorganic additives into the soil. In the first phase, the liquid limit of the soil reduced from 55 to 36%, the plastic limit increased on average from 23 to 29%, and the shrinkage limit value increased from 8 to 12% (see Tables 3 and 4).

In the second phase, the liquid limit of the soil was found to decrease from 55 to 31%, whereas the plastic and shrinkage limits of the soil increased from 23 to 33% and from 8 to 15%, respectively (see Table 5).

Any increase in the salt concentration or substitution of divalent cations for monovalent cations resulted in the decrease of repulsive force in the soil system. There is thus a reduction in the interparticle force between the soil particles resulting in the formation of flocculated structure leading to reduction in the plasticity characteristics of the soil.

TABLE 4. EFFECT OF LIME-GYPSUM PILES ON SOIL PROPERTIES

Sample No.	Soil properties	Percentage of chemicals added					
		NaCl		KCl		$CaCl_2$	
		1%	2%	1%	2%	1%	2%
1.	Liquid limit (%)	44	40	41	40	40	36
2.	Plastic limit (%)	24	26	26	29	26	29
3.	Shrinkage limit (%)	9	10	9	10	11	12
4.	pH	8.3	8.6	8.5	8.7	8.9	8.95
5.	Unconfined compressive strength (N/mm^2)	0.60	0.73	0.61	0.88	0.68	0.91

TABLE 5. EFFECT OF LIME-GYPSUM PILES ON SOIL PROPERTIES (LONG DURATION TEST—PHASE II)

Sample No.	Soil properties	Duration of treatment (days)					
		3	7	14	21	28	35
1.	Liquid limit (%)	36	35	33	33	31	31
2.	Plastic limit (%)	28	28	30	32	33	33
3.	Shrinkage limit (%)	12	12	14	14	15.5	15.5
4.	pH	8.9	9.0	9.1	9.1	9.15	9.15
5.	Unconfined compressive strength (N/mm^2)	0.91	0.92	0.92	0.93	0.95	0.95

3.2. *Variation of pH*

Tests were carried out with the soil samples to study the variation of pH with time due to the diffusion of inorganic additives as per the procedure suggested by Jackson (1958). The test results clearly indicate that there was a marked increase in the pH values from 8.1 to 9.1. The test results are given in Tables 3–5. The above changes that occurred in the soil are understood to be due to the diffusion of chemicals into the soil and this is indicated by the increased values of pH.

3.3. *Variation of strength*

Undisturbed samples were taken in-between the chemical piles after electro-osmotic treatment for conducting unconfined compressive strength tests. These test results clearly indicate that there is a threefold to tenfold improvement in the strength of the soil with time. This is mainly due to the removal of water from the soil bed under the potential difference and also due to the formation of cementation products such as Calcium Silicate Hydrate (CSH) and Calcium Aluminate Hydrate (CAH). These cementation compounds bind the clay particles together and hence there is an increase in the particle size of the clay particles forming into silt or sand size particles. From the earlier works, it has been established that these newly formed cementation compounds are stable and cannot be leached out easily (Subba Rao, 1979; Somayazulu, 1987).

3.4. *X-ray diffraction studies*

The minerals present in the untreated soil have been investigated completely for the proper identification of the various cementation compounds due to the soil–inorganic additives reactions. An automatic X-ray diffractometer of Philips make was used for the identification of all clay minerals and cementation compounds. X-ray diffractogrammes were obtained using Cu-Kα (nickel filter) with an input voltage of 34 kV and 24 mA. A scan speed of 3° per minute has generally been used for the identification of minerals and cementation products due to seeping of the inorganic additives from the chemical piles and their reaction with the soil. The air-dried untreated and treated soil powders were used for obtaining the XRD patterns of soil samples.

The X-ray diffractogramme of the untreated soil is shown in Fig. 2. This clearly indicates the presence of swelling clay mineral montmorillonite with appreciable quantities of quartz and feldspar. The presence of montmorillonite was confirmed by hydrochloric acid and glycerolated treatments. The montmorillonite peak was unaffected by

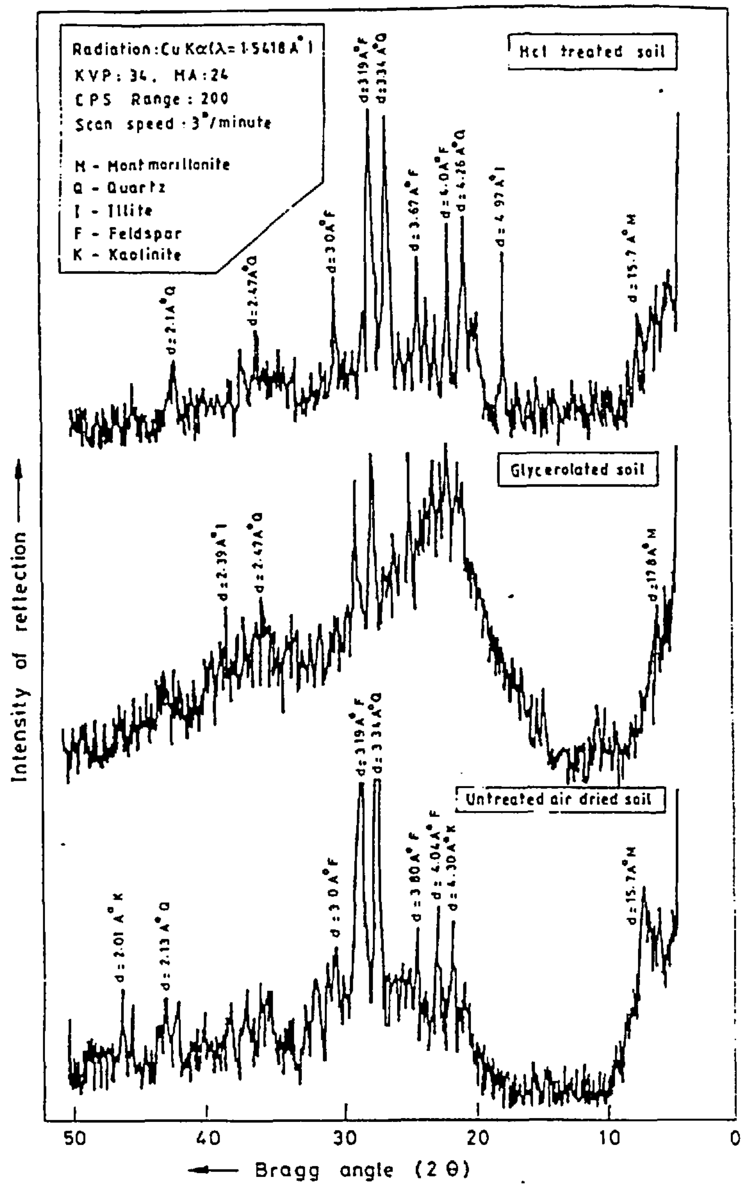

FIG. 2. X-ray diffractogramme of untreated soil.

heating the soil to 60°C for 1 hr with 1N hydrochloric acid. This has been further confirmed by the shift of the montmorillonite peak from 15.7 to 17.8 Å due to glycerolated treatment. The very high influenced peaks of 3.19 and 2.99 Å show the presence of feldspar and the presence of 3.34 and 4.3 Å peaks indicates quartz. Glenn (1967) identified the lime–bentonite reaction products. Lees *et al.* (1983) identified the cementation products present in the lime–sodium chloride treated soils. The XRD pattern of treated samples is shown in Figs 3–5. Due to the diffusion of various inorganic additives under the effect of electro-osmotic stabilization, many cementation compounds such as CSH, CAH, Hillebrandite, Tobermorite, Albite, etc. (see Tables 6 and 7) have been formed. These compounds bind the clay particles together and aggregation of soil particles takes place, thus resulting in an enormous increase in the strength of the soil with time.

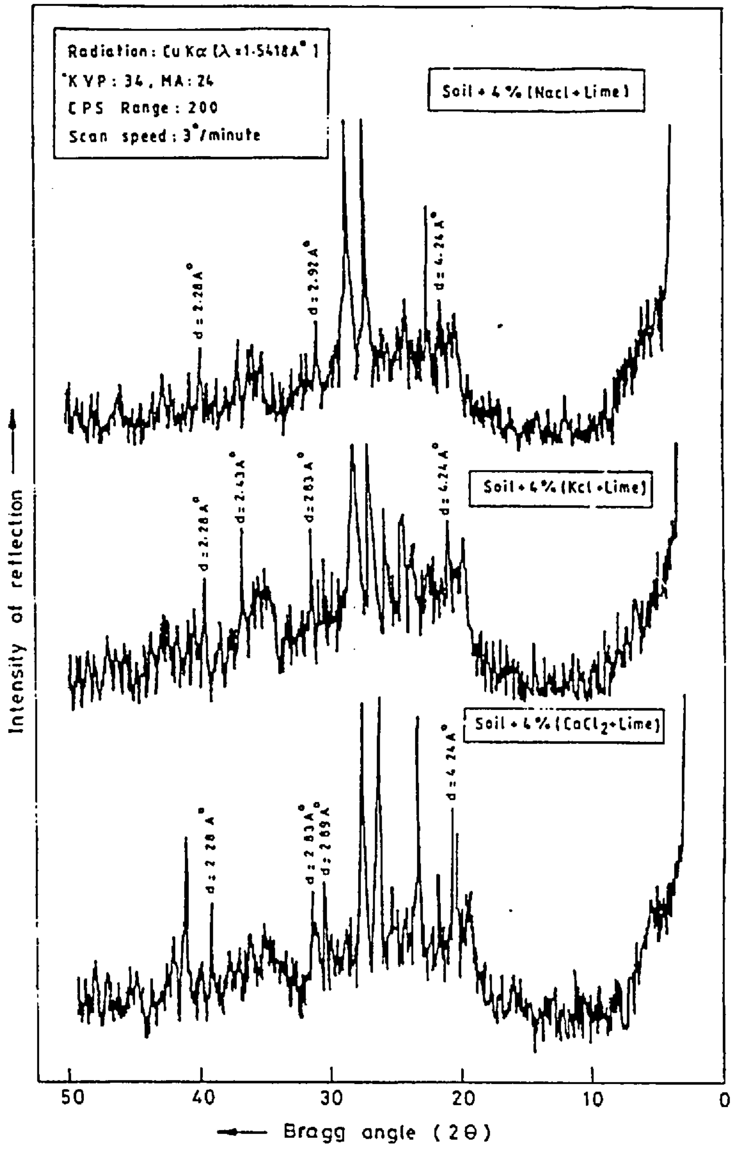

FIG. 3. X-ray diffractogramme of lime pile treated soil samples (first phase).

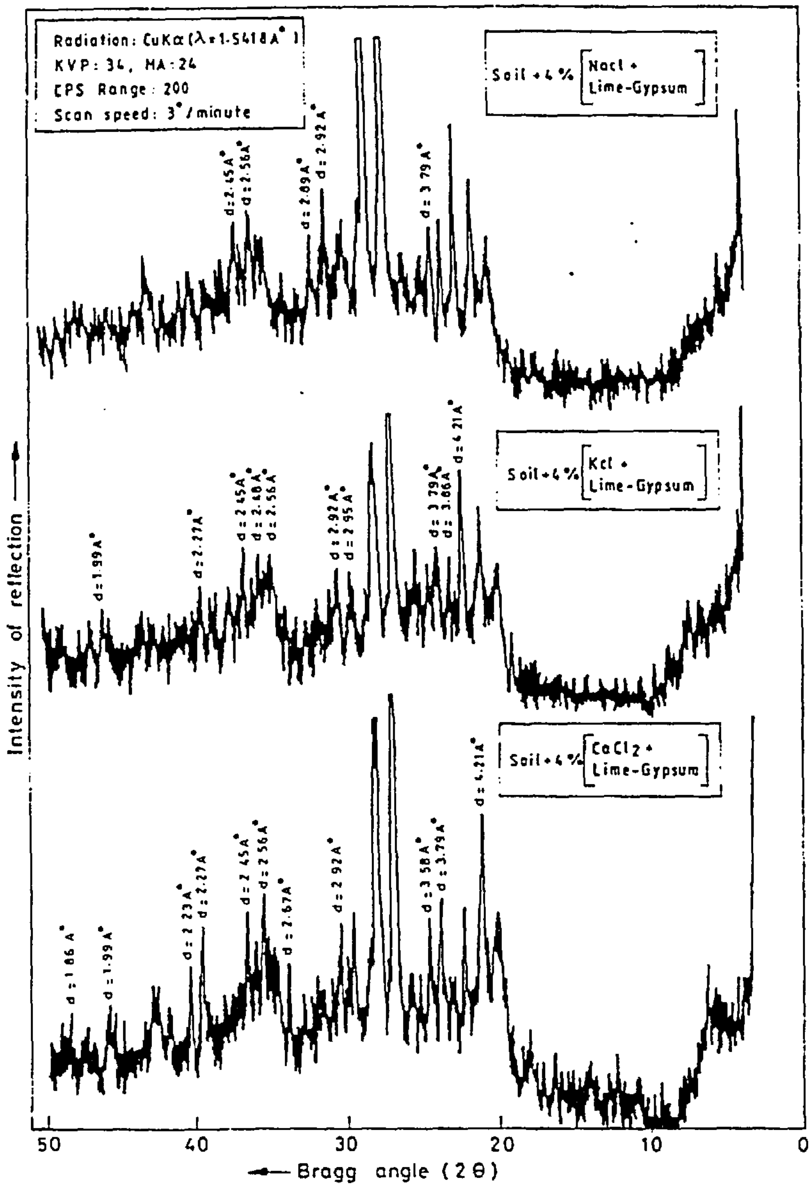

Fig. 4. X-ray diffractogramme of lime-gypsum pile treated soil samples (first phase).

4. CONCLUSIONS

Based on the above test results, the following conclusions can be drawn:

Due to electro-osmosis in the presence of the inorganic additives, there is an improvement of 10–15% in the plasticity characteristics of the soil and this has been confirmed

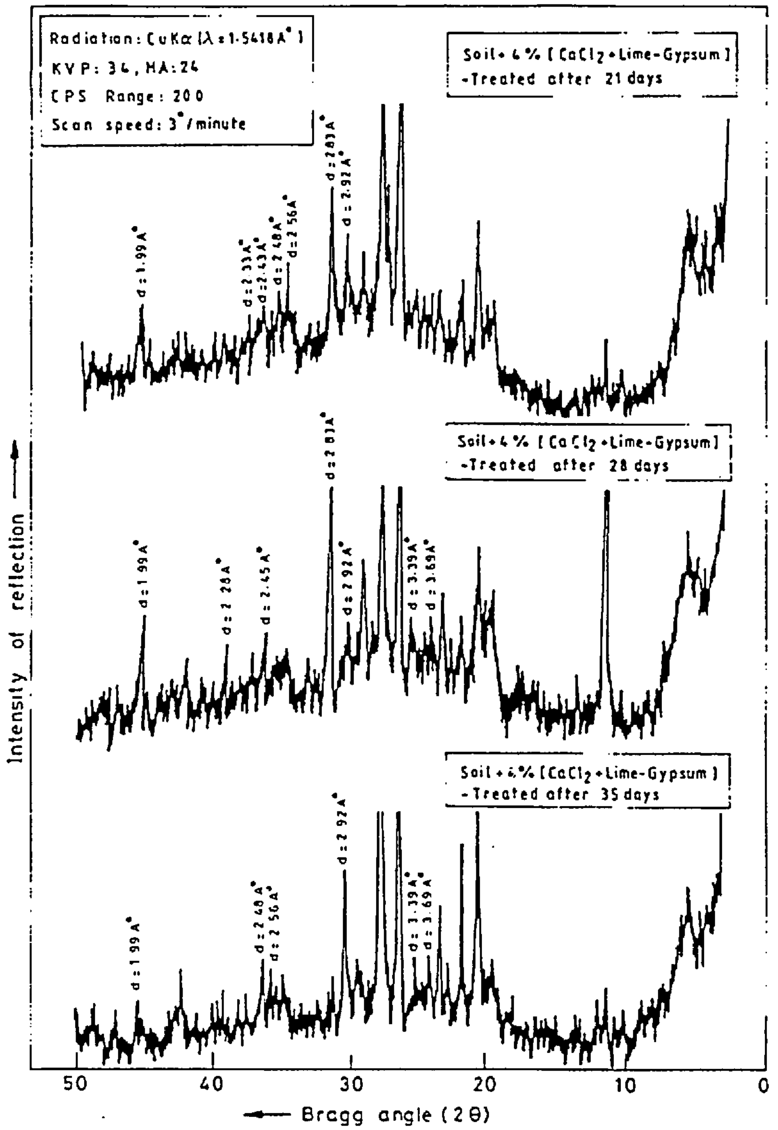

FIG. 5. X-ray diffractogramme of lime-gypsum pile treated soil samples (second phase).

from Atterberg limit tests. The diffusion of chemicals into the soils has been confirmed by pH measurements of the soil samples. A threefold to eightfold improvement in the strength of the soil was noticed and this has been mainly due to the formation of certain cementation compounds. These various compounds have been identified and confirmed using the XRD technique. The chemical calcium chloride gives good results with strength property of the soil compared to other chloride salts with lime and

TABLE 6. REACTION PRODUCTS FORMED DUE TO ELECTRO-OSMOTIC STABILIZATION WITH INORGANIC ADDITIVES (AS IDENTIFIED BY X-RAY DIFFRACTION DATA) (PHASE I)

Sample No.	Sample duration	Basal spacing *d* (Å)	Name of the new compound formed/ modified
1.	*After 3 days (lime pile treatment)*		
	(i) Soil + sodium chloride treatment	2.28	Tobermorite
		2.92	Hillebrandite
		3.16	Anorthite
		4.24	Calcium Silicate Hydrate (CSH)
	(ii) Soil + potassium chloride treatment	2.28	Tobermorite
		2.43	Calcium Aluminate
		2.83	Calcium Silicate Hydrate. CSH (I)
		4.24	Calcium Silicate Hydrate. CSH (I)
	(iii) Soil + calcium chloride treatment	2.28	Tobermorite
		2.83	Calcium Silicate Hydrate. CSH (I)
		2.89	Anorthite
		4.24	Calcium Silicate Hydrate. CSH (I)
2.	*After 3 days (lime-gypsum pile treatment)*		
	(i) Soil – sodium chloride treatment	2.45	Albite
		2.56	Calcium Aluminate
		2.89	Anorthite
		2.92	Hillebrandite
		3.79	Anorthite
	(ii) Soil – potassium chloride treatment	1.99	Calcium Silicate Hydrate. CSH (II)$^{-*}$
		2.27	Tobermorite
		2.45	Albite
		2.48	Tobermorite
		2.56	Calcium Aluminate
		2.92	Hillebrandite
		2.95	Tobermorite
		3.79	Anorthite
		3.86	Calcium carbonate
		4.21	Calcium carbonate
	(iii) Soil – calcium chloride treatment	1.86	Unsubstituted Tobermorite
		1.99	Calcium Silicate Hydrate. CSH (II)$^{-*}$
		2.23	Unsubstituted Tobermorite
		2.27	Tobermorite
		2.45	Albite
		2.56	Calcium Aluminate
		2.67	Calcium carbonate
		2.92	Hillebrandite
		3.58	Calcium carbonate
		3.79	Anorthite
		4.21	Calcium carbonate

lime-gypsum piles. In addition, the lime-gypsum pile improves the characteristics of the soil very well with inorganic additives compared to the lime pile. The combination of calcium chloride with lime-gypsum pile yields the best results in improving the soil properties with time. Hence, it may be concluded that the electro-osmotic technique

TABLE 7. REACTION PRODUCTS FORMED DUE TO ELECTRO-OSMOTIC STABILIZATION WITH INORGANIC ADDITIVES (AS IDENTIFIED BY X-RAY DIFFRACTION DATA) (PHASE II—LONG DURATION TEST)

Sample No.	Sample duration	Basal spacing *d* (Å)	Name of the new compound formed/modified
1.	After 21 days	1.99	Calcium Silicate Hydrate, CSH (I)**
		2.33	Albite
		2.43	Calcium Aluminate
		2.48	Tobermorite
		2.56	Calcium Aluminate
		2.83	Calcium Silicate Hydrate, CSH (I)
		2.92	Hillebrandite
2.	After 28 days	1.99	Calcium Silicate Hydrate, CSH (II)**
		2.28	Tobermorite
		2.45	Albite
		2.83	Calcium Silicate Hydrate, CSH (I)
		2.92	Hillebrandite
		3.39	Calcium carbonate
		3.69	Calcium carbonate
3.	After 35 days	1.99	Calcium Silicate Hydrate, CSH (II)**
		2.48	Tobermorite
		2.56	Calcium Aluminate
		2.92	Hillebrandite
		3.39	Calcium carbonate
		3.69	Calcium carbonate

with inorganic additives can be adopted for weak marine clay deposits to improve their shear strength properties.

Acknowledgement—The authors wish to express their sincere thanks to Dr S. Narasimha Rao, Professor and Head, Ocean Engineering Centre, Indian Institute of Technology, Madras, for his valuable suggestions in connection with the XRD work reported in this paper.

REFERENCES

BALASUBRAMANIAN, N. 1969. Electro-kinetics of a Bombay marine clay. M.Tech. thesis, Indian Institute of Technology, Bombay, India.

BJERRUM, L., MOUM, J. and EIDE, O. 1967. Application of electro-osmosis to a foundation problem in Norwegian quick clay. *Geotechnique* XVII, 214–235.

BROMS, B. and BOMAN, P. 1975. Lime stabilized columns. *Proceedings of the 5th Asian Regional Conference on Soil Mechanics and Foundation Engineering, Bangalore, India*, Vol. 1, pp. 227–234.

BROMS, B. and BOMAN, P. 1976. Stabilization of deep cuts with lime columns. *Proceedings of the 5th European Conference on Soil Mechanics and Foundation Engineering*, Vol. 1, pp. 207–210.

CASAGRANDE, L. 1952. Electro-osmotic stabilization of soil. *J. Boston Soc. civ. Engrs* 9, 51–83.

CASAGRANDE, L., LOUGHNEY, R. and MATRICH, M.A. 1961. Electro-osmotic stabilization of a high slope in loose saturated silt. *Proceedings of the International Conference on Soil Mechanics and Foundation Engineering, Paris*, pp. 555–561.

GLENN, G.R. 1967. X-ray studies of lime bentonite reaction products. *J. Am. Soc.* 50, 312–316.

JACKSON, M.L. 1958. *Soil Chemical Analysis*. Prentice-Hall, London.

KATTI, R.K. 1967. Stabilization of Bombay marine clay with various inorganic additives. *Proceedings of the 2nd South East Asian Conference on Soil Engineering*, pp. 589–599.

KATTI, R.K. and PAVATE, T.V. 1980. Studies on electrochemical hardening of marine clay at IIT Bombay. *Proceedings of the Conference on Geotechnical Engineering, Bombay, India*, pp. 365–368.

LEES, G., ABDELKADER, M.O. and HAMDANI, S.K. 1983. Reaction in lime-sodium chloride treated soils. *J. Institution Highways Transportation*, pp. 8–16.

LO, K.Y., INCULET, I.I. and HO, K.S. 1991. Electro-osmotic strengthening of soft sensitive clays. *Canadian geotech. J.* 28, 62–73.

Mitchell, J.K. 1970. In-place treatment of foundation soils. *J. Soil Mech. Foundation Engng. ASCE* 96, 73–143.

Mitchell, J.K. and Banerjee, S. 1980. *In-situ* volume change properties by electro-osmosis evaluation. *J. Geotech. Div., ASCE* 106, No. 674, 367–384.

Okumara, T. and Terashi, M. 1975. Deep lime mixing method of stabilization for marine clays. *Proceedings of the 5th Asian Regional Conference on Soil Mechanics and Foundation Engineering*, Vol. 1, pp. 69–75.

Patwardhan, S.H. 1969. Further studies on the use of calcium chloride piles on the electrochemical hardening of marine clay. M.Tech. thesis, Indian Institute of Technology, Bombay, India.

Somayazulu, J.R. 1987. Experimental studies on lime columns in soils. Ph.D. thesis, Indian Institute of Technology, Madras, India.

Subba Rao, K.V. 1976. Physico-chemical experimental studies on lime treated soils. Ph.D. thesis, Indian Institute of Technology, Madras, India.

Yanase, S. 1968. Stabilization of alluvial clays with quick lime. Report of the Ports and Harbour Research Institute, Vol. 7, No. 4 (in Japanese).

ELSEVIER

Engineering Geology 44 (1996) 107–120

ENGINEERING GEOLOGY

Stabilization of swelling clays by $Mg(OH)_2$. Changes in clay properties after addition of Mg-hydroxide

G.S. Xeidakis

Department of Civil Engineering, Democritus University of Thrace, GR-67100 Xanthi, Greece

Received 29 August 1995; accepted 26 February 1996

Abstract

Stabilization of the swelling clay structure is attempted by intercalation of $Mg(OH)_2$ and the development of a brucite interlayer between the clay layers. The properties of the product obtained by applying the technique, formulated as described in a previous work, are considered here. The materials used were Wyoming bentonite (USA), Fuller's Earth (UK), kaolinite, illite, lignite, and silica gels. The $Mg(OH)_2$-clay products were examined by the methylene blue dye test, X-ray diffraction analysis (XRD), differential thermal analysis (DTA), and derivative thermogravimetry analysis (DTGA). From the results obtained it is concluded that: the Mg-hydroxide is adsorbed by swelling clays both on their external and internal surface, whereas it is adsorbed on the external surface by non-swelling clays. The internally adsorbed phase of Mg-hydroxide forms an ill-defined interlayer of brucite, retarding swelling, whereas the external phase covers the particles modifying drastically their surface properties, like the adsorption of the MB dye. The material produced after precipitation of Mg-hydroxide on swelling clays (smectites) did not re-expand on wetting or after glycolation. The adsorption of MB dye was also reduced by some 80–90%, due to coating effect, preventing the measurements of the external surface area of the clay by polar molecules. The principal forces involved in the process are believed to be physical adsorption on the external surface, along with chemisorption and some chemical bonding, mostly in the internal surface. Cementation due to crystallization and, in the long term, some pozzolanic reactions take also place. Internal adsorption of the Mg-hydroxide is postulated to be in the form of positively charged mono- and/or small polymers and it is, chiefly, diffusion controlled. Since Mg-hydroxide is internally adsorbed by swelling clays, whereas Ca-hydroxide(lime) is not, and the (Mg, Ca)-clay aggregates are more stable than the Ca-clay or the Mg-one, the combination of the two hydroxides could give better results in soil stabilization than each hydroxide alone.

Key words: Hydroxy-Mg-interlayers; Clay swelling; Clay stabilization; Surface area; Methylene Blue test

1. Introduction

The various factors affecting the intercalation of the $Mg(OH)_2$ into swelling clay structure were investigated and the best conditions for hydroxide adsorption were established. This was presented in a previous paper (Xeidakis, 1996). These conditions are: the use of a dilute and well-dispersed clay suspension (about 1% clay); pH between 10 and 12; around 12 meq Mg^{2-} as $MgCl_2$ (or other Mg-salt) per gram of clay, added inside the clay suspension before the base and followed by drop-wise titration of 1–2 N NaOH solution, to give a molar ratio OH/Mg of about 1.5; vigorous agita-

PII S0013-7952(96)00047-6

tion of the suspension during the titration of the reagents; centrifugation and decantation of the supernatant liquid and drying at 250°C. Similar results are obtained by fast titration of the NaOH solution and drying at 105°C until dry (Xeidakis, 1979, 1996).

The method was applied to swelling and non-swelling clay minerals and other materials for studying the degree of the structure stabilization and the possibility of measuring the external surface area of the clay. The products formed after the precipitation of the Mg-hydroxide on the various clays examined were studied by the Methylene Blue test, X-ray diffraction analysis (XRD), differential thermal analysis (DTA), and derivative thermogravimetry analysis (DTGA) methods. The results of this study are presented and discussed in the following sections.

2. Surface area of clays after the treatment with Mg-hydroxide

The treatment described above was applied to some clays, swelling and non-swelling, common in soils. The $Mg(OH)_2$ precipitation took place at $pH = 10.5$, which was the pH obtained after dispersion of the clay with 33% Na_2CO_3 by weight of clay in suspension. The surface area of the initial minerals and the product, after drying, was measured by the Methylene Blue adsorption test; The surface area of the dye was taken to be 130 $Å^2$ for this study (Xeidakis, 1979). The results are shown in Table 1.

It is apparent from the results obtained that the $Mg(OH)_2$ precipitate reduces drastically the surface properties of all clay minerals and other materials, e.g., silica gels, lignite, etc. The reduction in clay minerals amounts to 82–98% (average $91 \pm 6\%$) but for other materials the reduction is lower, i.e., about 60%. The apparent surface area (ASA) obtained after the treatment was about 5 $m^2\ g^{-1}$ for kaolinite, 8 $m^2\ g^{-1}$ $[(12+4)/2]$ for illite, and 25 $m^2\ g^{-1}$ for montmorillonite and ~ 3 $m^2\ g^{-1}$ for halloysite. These figures undoubtedly show that the property measured is not really the external SA of the mineral itself but of the product obtained after precipitation. For example, illite and kaolinite have no internal SA, thus their values of SA should remain the same, before and after the treatment. The same applies to other materials like lignite, silica gels, etc. It seems that during the treatment the $Mg(OH)_2$ precipitates on the external surfaces of the non-swelling minerals, forming a more or less complete coating around the clay particles (aggregation). It should be noted that the $Mg(OH)_2$ (or brucite) layer, covering the clay particles, does not adsorb the dye; therefore the values of SA obtained do not represent the external SA of the mineral itself, but the degree to which the mineral has been covered by the $Mg(OH)_2$ precipitate. Some reactions may also happen between $Mg(OH)^+$ and the Al^{3+} and Si^{4+} of the clay structure, producing Mg-aluminosilicate minerals; these minerals also precipitate on the clay surface.

Consequently, although the method, as has been formulated, gives satisfactory results regarding the collapse of the montmorillonite structure and the stabilization of clays or soils, it can hardly be applied, as it stands, for measurements of the external surface area of these materials. This is because, such a method should collapse completely and irreversibly any expanding layer but, at the same time, must not alter the original external SA of the other minerals present in soil; and it is beyond any doubt, from the results obtained here, that such a treatment affects seriously (reduces) the surface properties of all minerals in soil.

In the search for a suitable treatment to overcome this problem, ultrasonic treatment has been employed to redisperse the $Mg(OH)_2$-treated kaolinite, assuming that, if the coating of the clay is simply a precipitation and aggregation phenomenon, without any further bonding of the hydroxide on the clay surface it would be possible to free the clay surface and restore the dye adsorption. Unfortunately, even after 30 min ultrasonic irradiation with a high frequency probe, the clay was not redispersed and the results acquired were the same as before, i.e., 5–6 $m^2\ g^{-1}$ for kaolinite.

Reduction of the pH of the suspension was then employed as a possible substitute, supposing that by reducing the pH at about 5 with an acid, e.g., HCl, the stronger H^+ would exchange or dissolve the weakly charged particles of the $Mg(OH)_2$ and remove them, at least, from the external surfaces of the clay particles.

Table 1
Apparent surface area (ASA) (m^2 g^{-1}) of clays with methylene blue dye subject to various treatments

		ASA before treatment with $Mg(OH)_2$, pH = 10.5 (1)	ASA after treatment with $Mg(OH)_2$, pH = 10.5 (2)	% Reduction of ASA (3)	ASA of the product column (2) + HCl, pH = 5 (4)
1	Fuller's Earth (montmorillonite)	1100	30	97	108
2	Wyoming bentonite (montmorillonite)	950	18	98	80
3	China clay (kaolinite)	36	5	86	10
4	Fifthian illite, API No. 35	95	12	87	39
5	Morris illite, API No. 36	120	4	97	36
6	Ball clay (illite + kaolinite)	168	30	82	25
7	Oxford clay (illite + kaolinite)	158	27	83	35
8	Halloysite (Utah)	60	3	95	–
9	Lignite	215	77	64	–
10	Silica gels	135	58	57	–
11	Fuller's Earth (kaolinite 1:1)	520	23	95	–
12	Fuller's Earth (ball clay 1:1)	580	33	94	–

The results of some preliminary tests of the acid treatment are also included in Table 1. They show that the dye adsorption (or SA) of the minerals did increase but it was still far below its original values. Nevertheless, this increase of the dye adsorption by clays after acidification is believed to come from the dissolution of the $Mg(OH)_2$ coating the particles by the HCl, rather than its exchange by hydrogen ions. This is quite possible, since even very dilute solutions (~5%) of HCl is capable of dissolving completely the artificially produced hydroxy-Mg-interlayers from both the external and the internal surfaces of the clay (Caillere and Henin, 1949; Diamond and Kinter, 1958).

It is therefore obvious from the results obtained and the foregoing discussion that the precipitation of $Mg(OH)_2$ at the clay surface is not a simple reversible phenomenon resulting from physical adsorption and/or cation exchange only; it appears to be more complicated, involving complexing of the hydroxide with the clay surface ions.

3. X-ray diffraction and thermal analyses

3.1. *Swelling clays (smectites)*

3.1.1. *X-ray diffraction analysis*

XRD has been carried out both on the original clays and on the hydroxy-Mg-clay system obtained after the precipitation of the hydroxide in a Phillips PW 1310 model X-ray apparatus, with CuKa and Ni-filters, and λ = 1.540 Å. Selected XRD diagrams for Wyoming bentonite (USA), and Fuller's Earth (an ill-crystalized English bentonite) are presented in Figs. 1 and 2. The diagrams for the treated clays represent samples obtained under the best conditions of $Mg(OH)_2$ precipitation as described in the previous section.

From the X-ray diagrams in Figs. 1 and 2, it is shown that the product obtained from montmorillonite, after the precipitation of the Mg-hydroxide, resembles the chlorite and/or vermiculite structures. Almost all the rational series of the chlorite (001) peaks are present. In Wyoming bentonite, even better diagrams, with sharper peaks than in Fig. 1, have been obtained. The new product has been checked with the ASTM standards and is close to F.No. 10-412, Penninite, and/or F.No. 16-351, Chlorite 1b.

On the other hand, in Fuller's Earth (Fig. 2) and notronite (results not shown here), the diffractograms are not so clear. Usually distinct peaks of any new mineral were not obtained in the region $2\theta = 0$–$20°$; only small shoulders like those in Fig. 2, or even worse, testified the presence of brucite. In a few cases a single sharp peak at 0.93 nm (9.3 Å) was obtained, recalling the structure of mica. This may be attributed to poor crystallinity of both the clay and/or the brucite

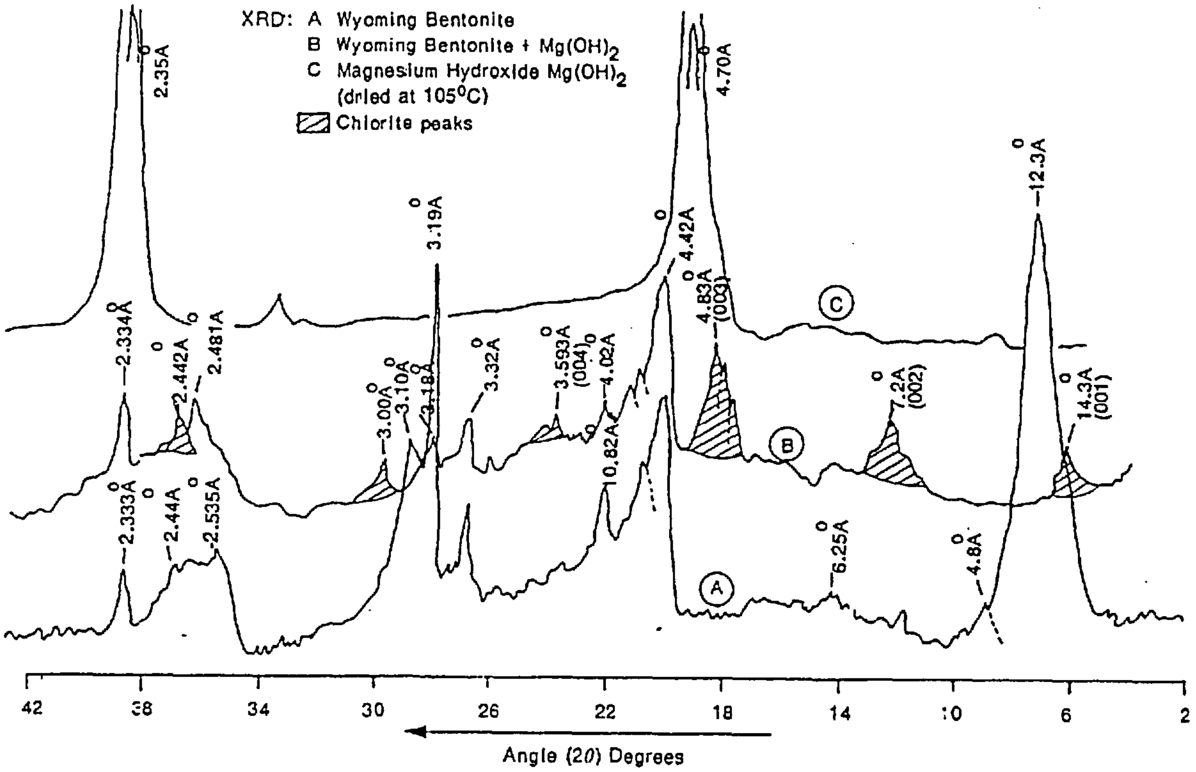

Fig. 1. X-ray diffractograms of Wyoming bentonite (USA), before and after treatment with magnesium hydroxide precipitate ($Mg(OH)_2$).

interlayer. Nonetheless, the material obtained after the clay treatment with $Mg(OH)_2$, in both cases, Wyoming bentonite and Fuller's earth, was not re-expanded on wetting or glycolation. The big basal reflection peak (001) of montmorillonite at 1.2–1.5 nm (12–15 Å) completely disappeared from the X-ray diagrams after the treatment.

It is worthwhile mentioning that in all experiments the X-ray patterns closely followed the dye adsorption, or the apparent surface area, ASA, measured by the MB dye; that is, when the SA of the product was more than about 100 m^2 g^{-1}, indicating incomplete collapse of the clay, the basal peak (001) at about 6° (2θ) of the clay reappeared in the X-ray diagrams and the product re-expanded in water or after glycolation. This means that the dye adsorption is a good indicator of the degree of collapse of the swelling clay structure. On the other hand, whereas the basal reflections of the clay after the hydroxide treatment were absent from the X-ray diagrams, the non-basal ones, such as that at about 0.445–0.225 nm (4.45–2.50 Å), etc., were almost unaltered. It seems, therefore, that the basic structure of the clay changed after the precipitation of the $Mg(OH)_2$ but was not destroyed; so no, at least identifiable, degradation in the clay structure appears in the X-ray diagrams. This was also confirmed by the XRD, DTA, and DTGA diagrams from the same samples, tested about 15 months after their preparation. The samples were kept under room conditions.

3.1.2. *Thermal analyses*

Differential thermal analysis (DTA) and derivative thermogravimetry (DTGA) analysis conducted on both clays, Fuller's Earth and Wyoming bentonite before and after the $Mg(OH)_2$ precipitation, showed very similar patterns. The main

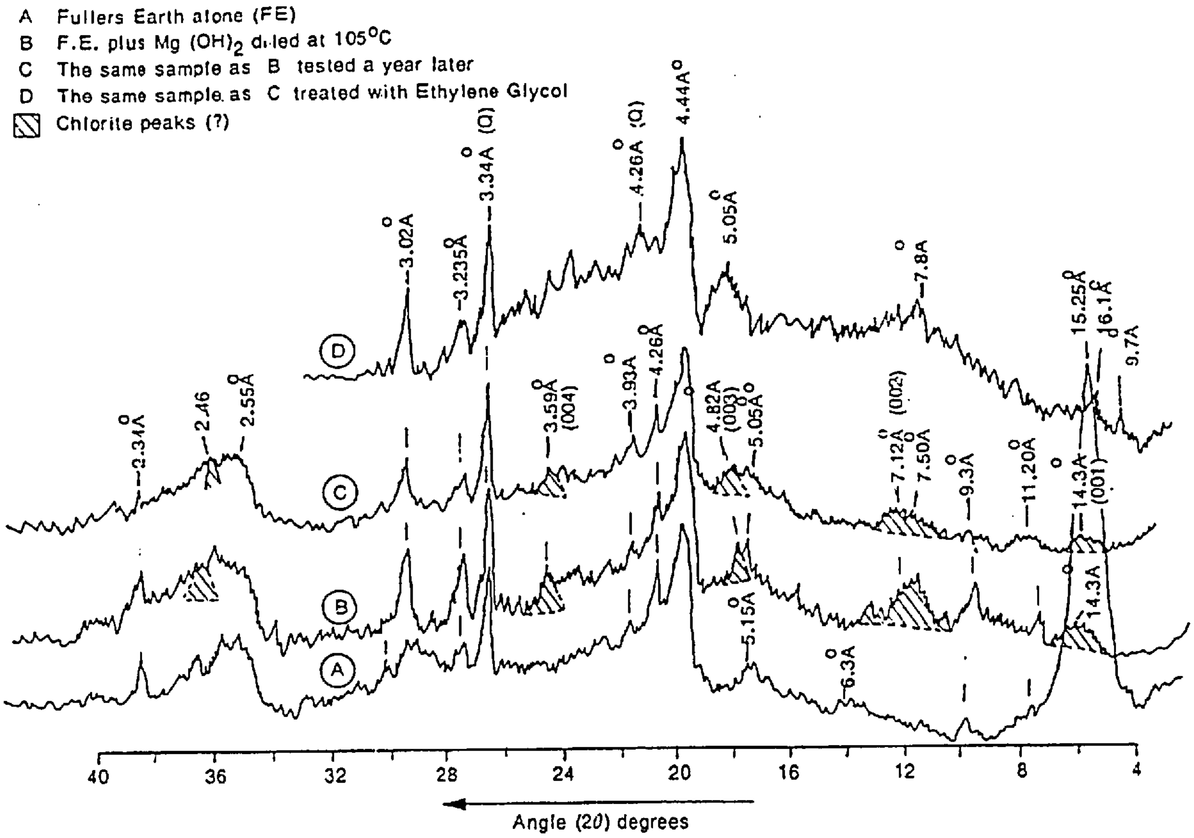

Fig. 2. X-ray diffractograms of Fuller's Earth (UK), before and after treatment with magnesium hydroxide precipitate ($Mg(OH)_2$

difference in DTA curves, between the two clays after the precipitation of the hydroxide, was that the Fuller's Earth–Mg-hydroxy product exhibited smaller and broader thermal peaks than the Wyoming bentonite. Some selected diagrams of DTA are presented in Fig. 3 and for DTGA in Fig. 4.

The DTA curves of the montmorillonite–$Mg(OH)_2$ showed, in general, a small endothermic peak at about 105°C representing absorbed water; a very broad peak starting at about 350°C and ending at around 700°C; this "peak zone" exhibits two smaller peaks within it. The first at about 400°C (390°C) representing, possibly, the dehydroxylation of some unreacted $Mg(OH)_2$ and/or the brucite formed as a separate phase, or precipitated on the external surface of the clay. The second small peak at 600°C could be attributed partly to the $Mg(OH)_2$ intercalated in the interlayer space of the clay and forming a brucite layer in the chlorite structure, and partly to the dehydroxylation of mica sheets.

The broadness of this endothermic peak in the region of 400–700°C may represent a gradual decomposition of the poorly-crystallized brucite layers. This could also account for the small and very broad diffraction peaks obtained in X-ray diagrams, particularly in the case of Fuller's Earth. The small endothermic peak at about 800°C preceding a very large exothermic peak, represents the second dehydroxylation peak of Wyoming bentonite at about 900°C. According to Caillere and Henin (1960) (see also MacKenzie, 1957, p. 215), this endothermic-exothermic inversion in the region of 800–900°C appears to be characteristic of pseudo-chlorites. Finally the crystallization

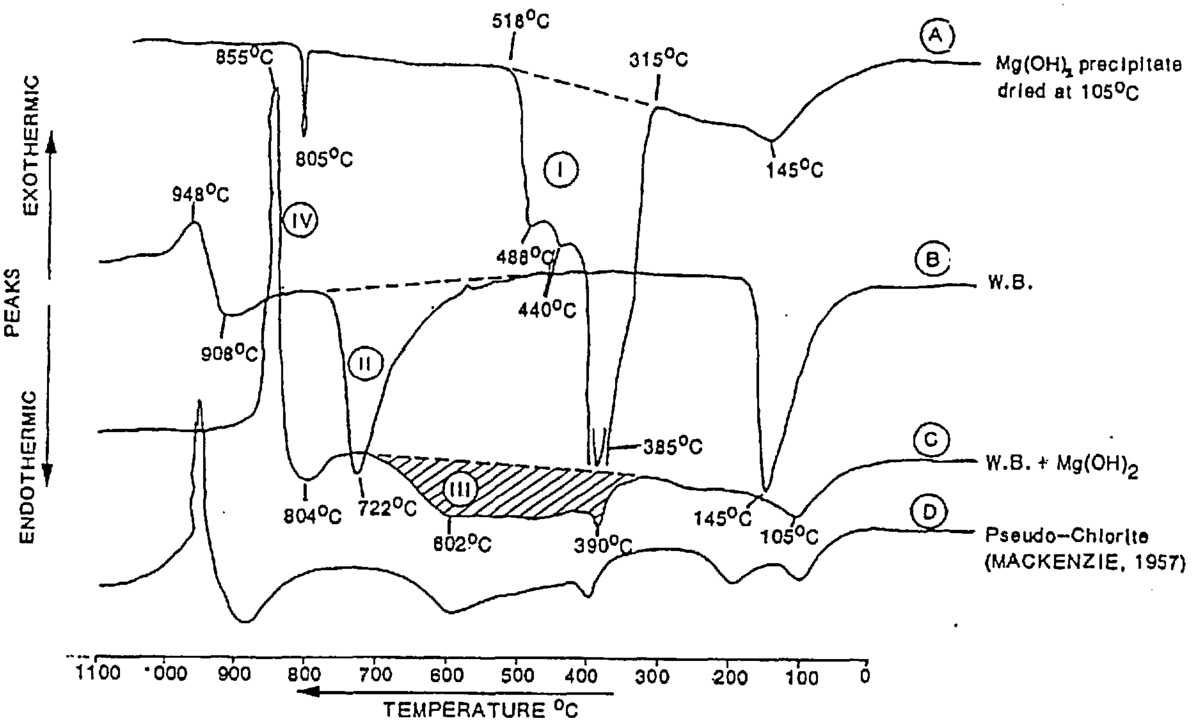

Fig. 3. Differential thermal analysis (DTA) curves of Wyoming bentonite (W.B.), before and after treatment with $Mg(OH)_2$ precipitate.

of enstatite ($Mg_2Si_2O_6$) and/or olivine ($(Mg,Fe)_2 SiO_4$) follows. Some authorities proposed that spinel ($MgAl_2O_4$) may also form at this temperature. The size of this peak varies according to the apparatus used, the heating rate, the cations present, etc. (MacKenzie, 1957, pp. 202, 216; MacKenzie, 1970; Dixon and Jackson, 1960; Grim, 1968, p. 342; McKenzie, 1989; Borchardt, 1989, pp. 682, 702; Barnhisel and Bertsch, 1989, pp. 738, 749). In Fig. 3, a DTA curve of a typical pseudochlorite has also been redrawn from MacKenzie (1957) (p. 214), for comparison. Apart from the endoexothermic peaks at 800–900°C, which in our case are at lower temperatures, the general features of the two curves (C, D in Fig. 3) are very similar. The low temperature peak at about 110°C varies considerably, depending upon the preparation of the hydroxy-interlayer and the drying conditions.

The DTGA curves shown in Fig. 4 have the general pattern of the DTA curves in both Wyoming bentonite and Fuller's Earth. The curves of the product exhibit a weight loss in the region of 50–200°C, representing presumably the hygroscopic water loss; a very broad peak between 300 and 700°C attributable to gradual dehydroxylation of the $Mg(OH)_2$ plus brucite sheet, and/or the mica layers; another small weight loss at about 800°C ascribed also to dehydroxylation of the mica layers and the decomposition of some carbonate impurity in the clay. The thermal curves of the original minerals, clays and $Mg(OH)_2$ are also included in these figures for comparison. In all experiments, i.e. X-ray diffraction, DTA, DTGA, and dye adsorption, the dramatic change of the properties of montmorillonite treated with $Mg(OH)_2$ is clearly apparent.

3.2. *Kaolinite–illite minerals*

Besides the experimental work performed in swelling clay minerals described above, other clays of the kaolinite group (China clay, halloysite) and

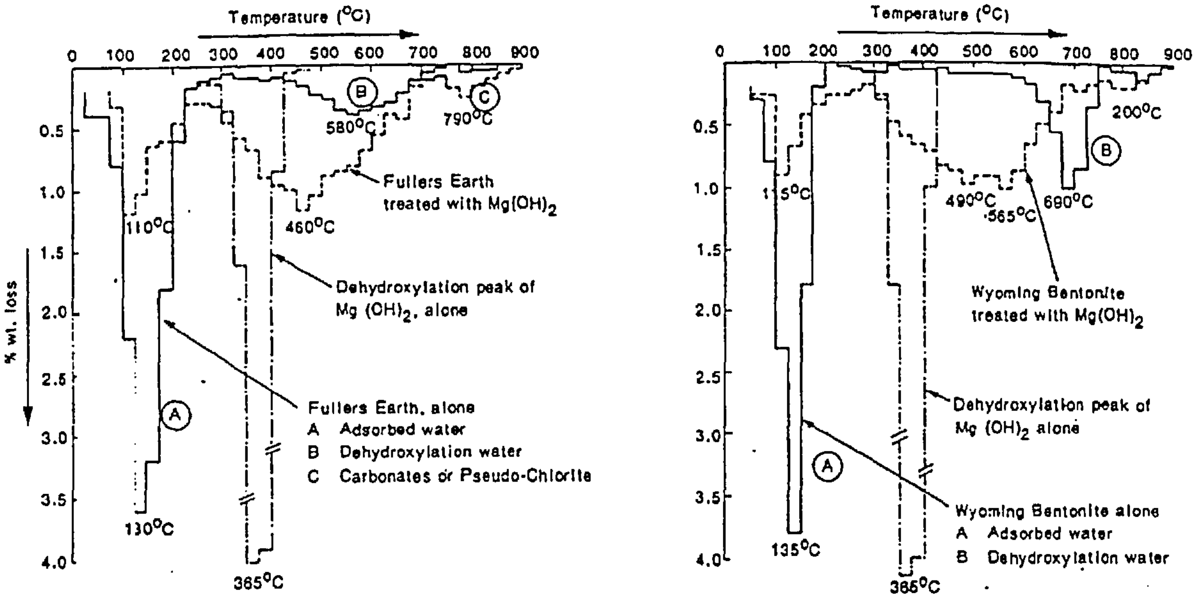

Fig. 4. Derivative thermogravimetry (DTGA) curves of Fuller's Earth (1) and Wyoming bentonite before and after treatment with $Mg(OH)_2$. In both diagrams the magnesium hydroxide peak is included for comparison.

the Mica group (Morris and Fithian illites) have been tested with the same technique. Ball clay and Oxford clay, which contain mainly disordered kaolinite and illite, and two non-clay materials, lignite and silica gel, were also included in the study. The purpose was to decipher the mechanism(s) taking place during the precipitation of $Mg(OH)_2$ on the clay particles and the degree of alteration of the clay surface. The results are presented in Table 1, for the dye adsorption, and in Figs. 5–7 for XRD and thermal analysis.

The tests with Methylene Blue adsorption, described already (Table 1), showed a marked alteration on the clay surface, with a reduction of dye adsorption, after the treatment, of up to 80–90%. However, the XRD, DTA, and DTGA investigations (Figs. 6 and 7) revealed that the $Mg(OH)_2$ had not attacked, seriously, the clay structure but had chiefly coated the particles, inhibiting the adsorption of the dye and the water. The results from all these clays were very similar and are exemplified by Fig. 6 which shows the X-ray diffractograms and by Fig. 7 which shows the DTGA curves of China clay (kaolinite), before and after treatment.

It is clear from the X-ray diagrams (Fig. 6) that all the diffraction peaks of the clay, basal and non-basal, are present in the treated sample as well; in addition the stronger peaks of the magnesium hydroxide at 0.47 nm (4.70 Å) (001) and 0.235 nm (2.35 Å) (002) are present. The only difference observed in the X-ray diagrams was the significant reduction of the height of the diffraction peaks in the treated sample. This strongly suggests that the two phases, clay and hydroxide, retained, basically, their identity in the product. The reduction of the diffraction peaks is certainly due to particle coating by $Mg(OH)_2$. No new minerals, at least identifiable by the methods used, were observed either in the fresh product or, a year later, when the same samples were re-examined.

The results of this study also showed how much the X-ray diffractograms and the measurement of the surface area by polar molecules, like Methylene Blue, can be affected by the coating and aggregation of the soil minerals by various amounts and kinds of oxides and/or hydroxides. They also stress how important it is to clean the mineral surfaces before such measurements take place. In Fig. 6 the reduction of the XRD peaks is not clearly shown,

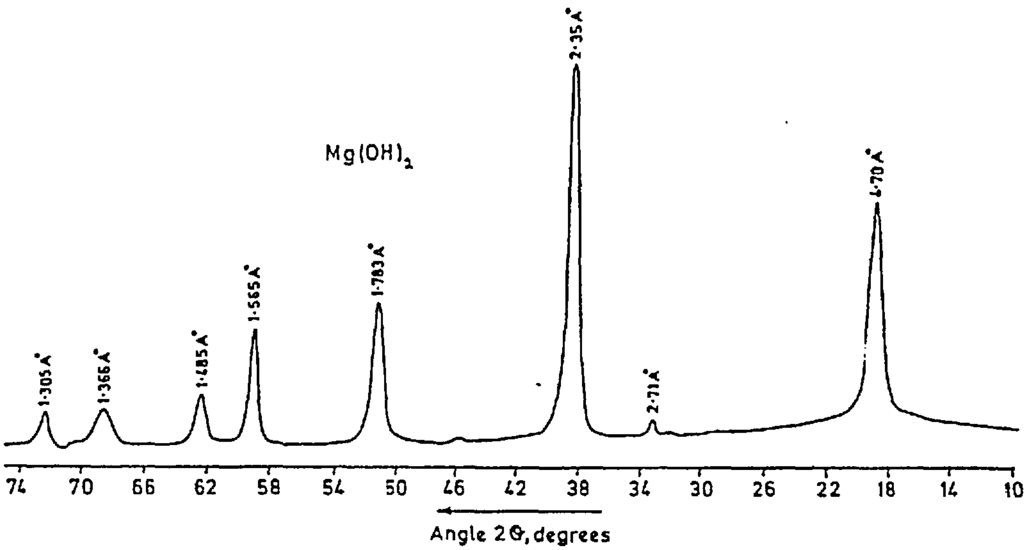

Fig. 5. X-ray diffrctograms of magnesium hydroxide precipitated from ($MgCl_2 + NaOH$) and dried at 105°C.

because the sensitivity of the apparatus (counts per minute, CPS), in the treated samples, was doubled for the identification of the magnesium hydroxide peaks.

Fig. 7 presents the DTGA curves of kaolinite. Apparently the dehydroxylation peaks of the two minerals are quite separate. There should, however, be a small interaction between hydroxide and clay, represented by the broad peak in the region of 400–500°C. Nonetheless, this interaction seems not to affect significantly the clay structure. Such an interaction was observed in most of the XRD, DTA, and DTGA diagrams of kaolinite. The results for illite are not shown as they were very similar to those of kaolinite.

4. Discussion

It is perhaps surprising how the negatively charged clay particles can adsorb the almost neutral $Mg(OH)_2$ molecules in the interlayer space to form the brucite layer. If a Mg-clay is considered, then it must be assumed that the negative hydroxyl ions (OH^-) penetrate between the negative structural sheets of the clay to allow precipitation of the $Mg(OH)_2$ there. Although cases are reported in the literature where negative ions, such as the chlorine ions (Cl^-), penetrated the lattice of an Ag-montmorillonite and precipitated AgCl there, this seems not to be the case with $Mg(OH)_2$. The only plausible explanation which has been advanced so far is hydrolysis and polymerization of the hydroxide's molecules $(Mg_v(OH)_{2v-x})^{+x}$ near the clay surface. This has already been proved for other hydroxy-interlayers such as Al, Fe, and Cr (Caillere and Henin, 1949; Slaughter and Milne, 1960; Carstea, 1968; Rich, 1968; Sawnhey, 1968, 1989; El-Swaify and Emerson, 1975; Brindley and Sempels, 1977; Keren et al., 1977; Rengasamy and Oades, 1978; Cabrera and Nwakanma, 1979; Xeidakis, 1979; Barnhisel and Bertsch, 1989, p. 774; Hsu, 1989; McKenzie, 1989; Keren, 1991; Lou and Huang, 1994, etc.).

The basic monomers and small polymers, produced during the reaction, near the clay surface, diffuse into the interlayer space forming the first "islands" of the brucite sheets; the process proceeds until a more or less continuous "brucite" layer is formed. Under normal conditions, both hydrolysis and polymerization near the clay surface must be very slow and quite complex processes; this is, perhaps, the reason why fully developed "brucite" layers between the clay platelets are

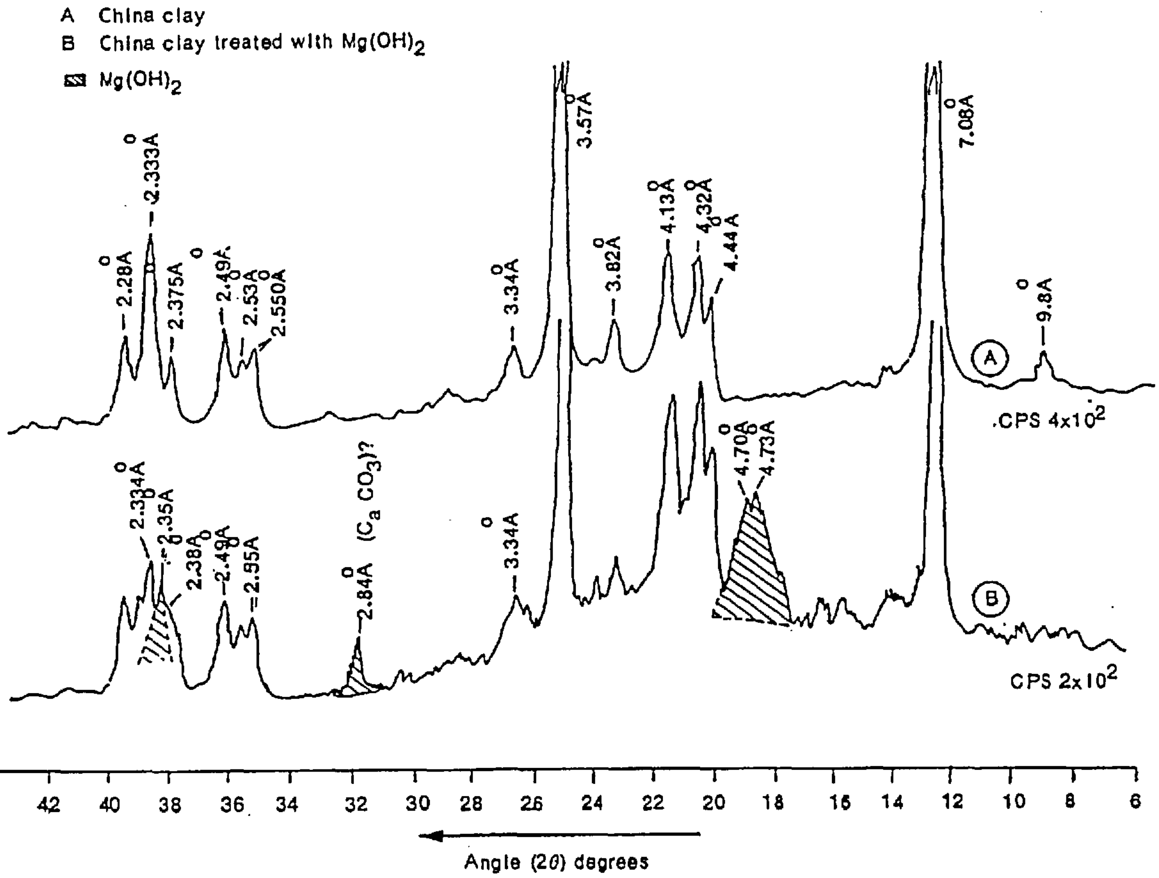

Fig. 6. Supreme China clay (kaolinite) before (A) and after (B) treatment with $Mg(OH)_2$ precipitate.

seldom formed. The external covering of the clay particles by the hydroxide, which retards internal adsorption, and the very slow diffusion process can also account for the almost negligible change in the samples after a year ageing at room conditions. Nevertheless, the diffusion mechanism increases markedly when energy is supplied to the system, e.g., by heating and/or agitation. This process agrees closely with the observations discussed in the previous sections, i.e. the high temperature, the slow rate of reagent titration and the vigorous agitation promotes the formation of hydroxy-interlayers in swelling clays (Worrall, 1975; Barnhisel and Bertsch, 1989, p. 774; Borchardt, 1989, p. 702; Sawnhey, 1989; Xeidakis, 1996).

The increase of the temperature, besides increasing the diffusion rate of the $Mg(OH)_2$ mono- and/or polymers, removes water from the clay surface, brings more closely the clay particles and promotes crystallization and association of the hydroxide with the clay surface, possibly through hydrogen bonding with the surface oxygens, e.g. {>-Si-O}-{H-O-Mg-}. The initially formed chemical bonds seem to be weak and/or very few in number; by the time both the number and the strength of the chemical bonding increases, along with the crystallinity and the strength of the reaction product. Such a process can, conceivably, explain why the brucite layers and the chlorite structure do not develop before complete dryness. The formation, therefore, of the $Mg(OH)_2$ interlayers seems to be a dynamic process which exhibits significant changes with the time and

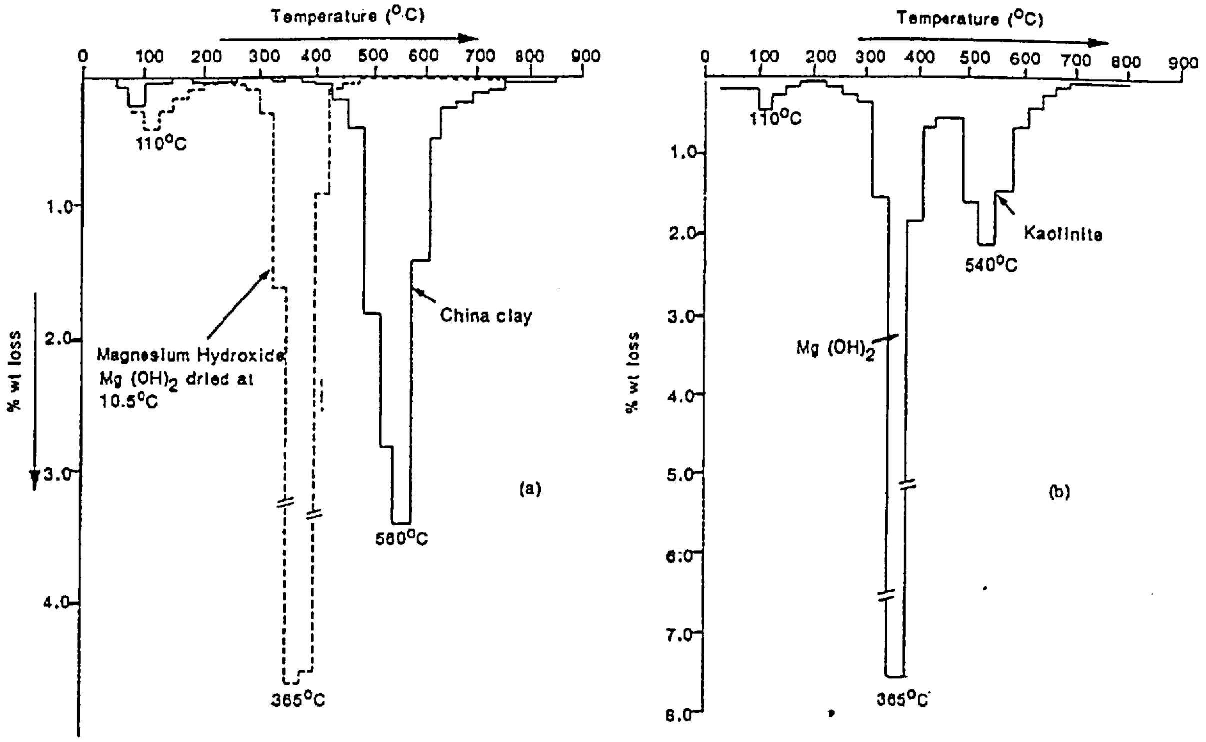

Fig. 7. Derivative thermogravimetry (DTGA) curves of (a) magnesium hydroxide precipitate and Supreme China clay alone, and (b) China clay after mixing with $Mg(OH)_2$.

environmental conditions. Nonetheless, other factors such as the charge density and the structure of the clay, the pH of the reaction, the degree of crystallization, the surface area, the desaggregation of the particles are all involved, to a certain degree, in the formation of hydroxy-interlayers. Some hydrated Mg-Al (MAH) and Mg-Si (MSH) silicates (cementing agents) are certainly produced, over time, on the surface of the platelets, as in the clay-$Ca(OH)_2$ system (Chou, 1987, p. 3).

The adsorption of the metal hydroxides by the clays is basically the same; thus, the observations made in this study could be applied to explain the mechanism of adsorption of other hydroxides by clays and/or soils and, especially, to $Ca(OH)_2$ (lime) extensively used in soil stabilization. When both these hydroxides are present in the soil the Mg^{2+} reacts faster than Ca^{2+} with the clay, but ultimately the Ca forms more stable aggregates than the Mg (Keren et al., 1977; Keren, 1991). On the other hand, dolomite (MgCa) CO_3 is less soluble in water and acids than $MgCO_3$ and CaCO $_3$ themselves. Surprisingly, $Ca(OH)_2$ has been found not to intercalate the swelling mineral structure, and it is adsorbed only in the external surface of the clay forming a monclayer. Thus, theoretically, it would be better to use a mixture of the two hydroxides for soil stabilization. This has been applied in practice by the use of the so-called dolomic lime (MgO+CaO), which has been proven to be more effective than calcium lime CaO alone (Stocker, 1972; Ormsby and Kinter, 1973; Chou, 1987; Sweeney et al., 1988; Borchardt, 1989, p. 711; Borden and Baez, 1991; Nelson and Miller, 1992; Athanasopoulou, 1995, etc.).

If the aforementioned mechanism(s) of hydroxides adsorption is accepted, then the magnesium hydroxide should be adsorbed mostly by physical processes on external surface of the clay, and by chemisorption of the positively charged monomers or small polymers, in the internal one; in the last case some hydrogen bonding may develop between clay oxygens and the hydroxide's molecules. The charged hydroxide polymers have quite a strong affinity with the clay surface and can easily be adsorbed. The forces involved in the process certainly include diffusion, Van Der Waals forces, hydrogen bonding, cementation forces due to crystallization of the precipitate on the clay surface and, in the long term, some pozzolanic reactions.

Of course, not all montmorillonite particles are intercalated simultaneously, and to the same degree, by $Mg(OH)_2$ to form chlorite. Some platelets will be entirely intercalated to form a complete brucite layer, some will be partly intercalated, and some will not be intercalated at all. These cases are schematically represented by the particle stacking model of Fig. 8. This model is similar to that proposed by Nadeau for interstratified clays (Nadeau et al., 1984b; Nadeau and Bain, 1986). At the end of the process the clay particles are covered by $Mg(OH)_2$ and/or MgAlH, MgSiH, $MgCO_3$, forming aggregates (Fig. 9).

5. Conclusions

From the results obtained and the foregoing discussion the following can be deduced.

The intercalation of magnesium hydroxide between the fundamental units (layers) of the clay swelling structure and the formation of the chlo-

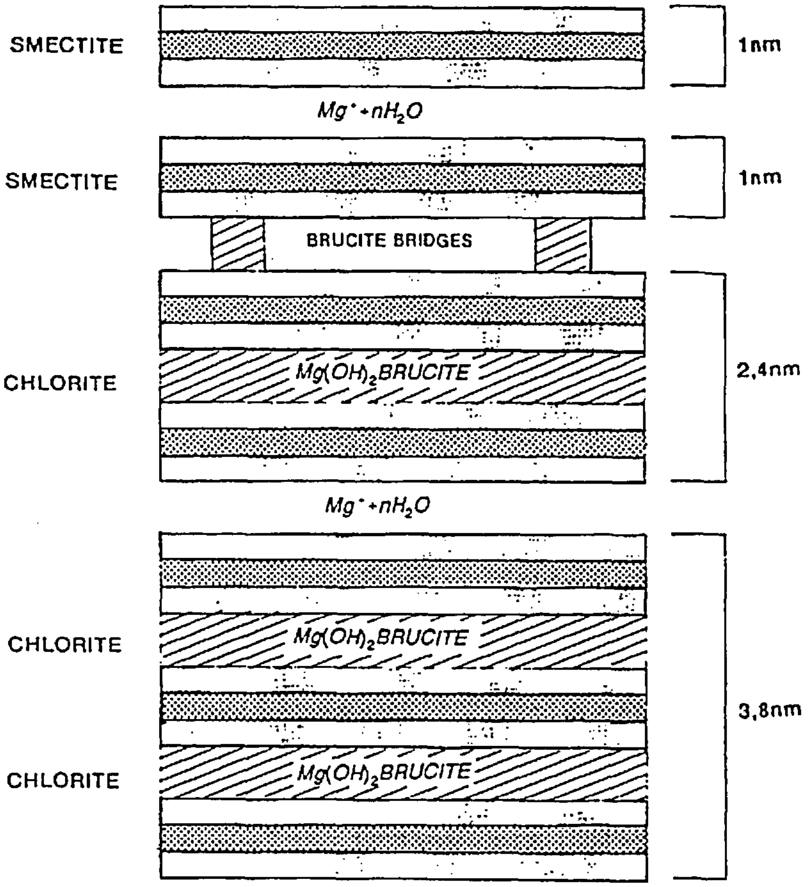

Fig. 8. Schematic representation of the one-dimensional structure of magnesium–hydroxy-interlayers (brucite) formation in smectite, and the development of chloride structure (1 nm = 10 Å).

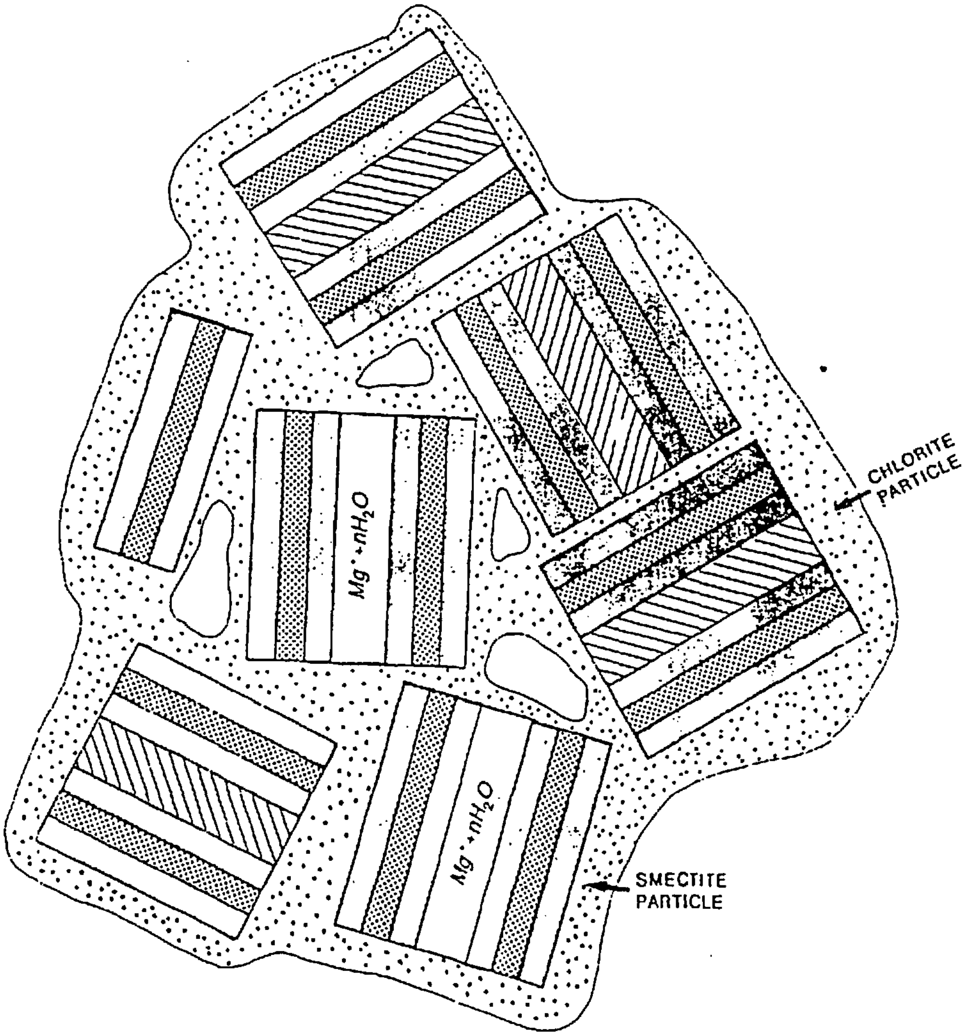

Fig. 9. Aggregation–cementation of clay particles by $Mg(OH)_2$ precipitate and/or other cementing agents like MgAlH, MgSiH, $MgCO_3$, etc.

rite-like structure, under the conditions described, is beyond any doubt. The dramatic modification of the clay properties (physical and technical), after the precipitation of the $Mg(OH)_2$ and the stabilization of the swelling mineral structure, has also been proven.

The mechanism of adsorption of $Mg(OH)_2$ by clays is basically the same for all clay minerals; it involves physical adsorption along with some chemical bonding; cementation due to crystallization and, in the long term, some pozzolanic reactions are also taking place. However, in swelling clays, like smectites, the precipitation takes place on both the external and the internal surfaces, whereas in non-swelling ones, such as kaolinite and illite, the precipitation occurs principally on the external surface, and mostly on the edges rather than on the planar surfaces of the clay. The internal adsorption of the hydroxide is believed to be mainly diffusion controlled.

The stabilization of the swelling mineral structures seems to be a combined process involving:

bonding of the clay particles faces by semi-organized brucite layers developed in the interlayer space; and coating, aggregation and cementation of the clay particles by the external phase of the $Mg(OH)_2$ precipitate.

The adsorption of the metal hydroxides by the clays are basically the same; thus, the results obtained in this study could be applied to elucidate the mechanism of adsorption of other hydroxides by clays and/or soils and especially to $Ca(OH)_2$ used extensively in soil stabilization. Since $Ca(OH)_2$ is not adsorbed in the interlayer space of the clay, whereas $Mg(OH)_2$ is, Mg^{2+} is more difficult to leach off the clay than Ca^{2+}; and since dolomite $(MgCa)CO_3$ is less soluble in water and in acids than $MgCO_3$ and $CaCO_3$ themselves, a mixture of the two hydroxides (Mg and Ca hydroxide) would be better for clay soil stabilization, than each one alone.

A final conclusion that could be drawn from this work is that, under the conditions described, the intercalation of Mg-hydroxide into the clay layers and the stabilization of the swelling clay structures is beyond any doubt; nevertheless the method, as formulated, is not easily applicable to the field; more research is needed in this direction. Our understanding of the processes involved and the bonding developed during the formation of the hydroxy-metal-interlayers in clays is still a little fuzzy; more work is required to elucidate all these complex phenomena.

Acknowledgment

The author would like to express his appreciation to Dr. W.E. Worrall, formerly Reader, and to the late Dr. D. White, formerly Lecturer, in the University of Leeds, UK, for their advice and fruitful discussions during the experimental work at Leeds University. Thanks are also due to the referees, for their constructive comments and suggestions in the initial version of the paper. The author is also grateful to the State Scholarships Foundation of Greece (IKY) for sponsoring this project.

References

Athanasopoulou, A.G., 1995. Improvement of the engineering properties of embankment materials used in road construction, with lime and fly ash. Application to swelling soils of Thrace, N. Greece. Ph.D thesis, Democritus Univ. Thrace, 67100 Xanthi, Greece, 560 pp. (in Greek).

Barnhisel, R.I. and Bertsch, P.M., 1989. Chlorides and hydroxy-interlayered vermiculite and smectite. In: J.B. Dixon and S.B. Weed (Editors), Minerals in Soil Environments. 2nd edn. SSSA Book Series No 1, SSSA, Madison, WI, USA, pp. 729–788.

Borchardt, G., 1989. Smectites. In: J.B. Dixon and S.B. Weed (Editors), Minerals in Soil Environments. 2nd edn. SSSA Book Series No 1, SSSA, Madison, WI, USA, pp. 675–727.

Borden, R.H. and Baez, J.I., 1991. Testing techniques for evaluating the shear strength of lime/fly ash slurry stabilized soil. Geotech. Test., J. 14: 247–256.

Brindley, G.W. and Sempels, R.E., 1977. Preparation and properties of some hydroxy-aluminum beidellites. Clay Miner., 12: 229–237.

Cabrera, J.G. and Nwakanma, C.A., 1979. Pozzolanic activity and mechanism of reaction of red tropical soil-Lime system. In: Transportation Research Record 702, TRB, National Research Council, Washington, DC, pp. 199–207.

Caillere, S. and Henin, S., 1949. Transformation of Minerals of the montmorillonite family into 10 Å micas; and Experimental formation of chlorites from montmorillonite. Miner. Mag., 28: 606–611 and 612–620.

Caillere, S. and Henin, S., 1960. Relation between the crystallochemical constitution of phyllites and their dehydration temperature. Application in the case of chlorites. Bull. Soc. Fr. Geram., 48: 63–67.

Carstea, D.D., 1968. Formation of hydoxy-Al- and Fe-interlayers in montmorillonite and vermiculite. Influence of particle size and temperature. Clays Clay Miner., 16: 231–238.

Chou, L. (Editor), 1987. Lime Stabilization. Reactions, Properties, Design, and Construction. State of the art report 5. Transportation Research Board, National Research Council, Washington, DC, USA, 59 pp.

Diamond, S. and Kinter, E.B., 1958. Surface area of clay minerals as derived from measurements of glycerol retention. Clays Clay Miner., 5: 334–347.

Dixon, J.D. and Jackson, M.L., 1960. Mineralogical analysis of soil clays involving vermiculite-chlorite-kaolinite diffraction. Proc. 8th Nat. Conf. Clays Clay Miner., 274–286.

El-Swaify, S.A. and Emerson, W.W., 1975. Changes in the physical properties of soil-clays due to precipitated Aluminium and Iron Hydroxides. Parts I and II. Soil Sci. Soc. Am. Proc., 39: 1056–1062; 40: 516–520.

Grim, R.E., 1968. Clay Mineralogy. 2nd ed., McGraw Hill, London.

Hsu, Pa Ho, 1989. Aluminum oxides and oxyhydroxides. In: J.B. Dixon and S.B. Weed (Editors), Minerals in Soil Environments. Soil Sci. Soc. Am., Book Series 1, SSSA, Madison, WI, USA, pp. 331–378.

Keren, R., Gast. R.G. and Barnhisel, R.I., 1977. Ion exchange reactions in non-dried chambers montmorillonite hydroxy-aluminium complex. Soil. Sci. Soc. Am. J., 41: 34–39.

Keren, R., 1991. Specific effect of magnesium on soil erosion and water infiltration. Soil Sci. Soc. Am. J., 55: 783–787.

Lou, G. and Huang, P.M., 1994. Interlayer adsorption of polymeric hydroxy-aluminosilicate ions by montmorillonite. Soil Sci. Soc. Am. J., 58: 745–750

MacKenzie, R.C. (Editor), 1957. The Differtential Thermal Investigation of Clays. Mineralogical Society, London, 300 pp.

MacKenzie, R.C., 1970. Differential Thermal Analysis, Vol. 1, chp. 18. Applied Science Publ., London.

McKenzie, R.M., 1989. Manganese oxides and hydroxides. In: J.B. Dixon and S.B. Weed (Editors), Minerals in Soil Environments. Soil Sci. Soc. Am., Book Series 1, SSSA, Madison, WI, USA, pp. 467–339.

Nadeau, P.H. and Bain, D.C., 1986. Composition of some smectites and diagenetic illitic clays and implications for their origin. Clays Clay Miner., 34: 455–464.

Nadeau, P.H., Wilson, W.J., McHardy, W.J. and Tait, J.M., 1984b. Interparticle diffraction: a new concept for interstratified clays. Clay Miner., 19: 757–769.

Nelson, J.D. and Miller, D.J., 1992. Expansive Soils. Problems and Practice in Foundation and Pavement Engineering. Wiley and Sons, inc., 260 pp.

Ormsby, W.C. and Kinter, E.D., 1973. Strength development and reaction products in lime-montmorillonite-water systems. Public Roads, 37(4): 136–160.

Rengasamy, P. and Oades, J.M., 1978. Interaction of monomeric and polymeric species of metal ions with clay surfaces: Part I. Adsorption of Iron (III) species. Part II. Changes in surface properties of clays after addition of Iron (III). Austral. J. Soil Res., 15: 221–242 Part III. Aluminium (III) and Iron (III). Austral. J. Soil Res., 16: 53-56 (1977).

Rich, C.I., 1968. Hydroxy interlayers in expansive layer silicates. Clays Clay Miner., 16: 15–30.

Sawnhey, B.L., 1968. Aluminium interlayers in layer silicates. Effect of OH/Al ratio of Al-solution, time of reaction and type of structure. Clays Clay Miner., 16: 157–163.

Sawnhey, B.L., 1989. Interstratification in layer silicates. In: J.B. Dixon and S.B. Weed (Editors), Minerals in Soil Environments. SSSA. Book Series No 1, SSSA, Madison, WI, USA.

Sweeney, D.A. Wong, D.K.H. and Fredlund, D.G., 1988. Effect of lime on a highly plastic clay with special emphasis on aging. Transportation Research Record 1190, NRC, Washington, DC, USA, pp. 13–23.

Slaughter, M. and Milne, I.H., 1960 The formation of chlorite-like structure from montmorillonite. Clays Clay Miner., 7: 114–124.

Stocker, P.T., 1972. Diffusion and diffuse cementation in lime and cement stabilized clayey soils Australian Road Research Board, Special report No. 8, 1972, 146 pp.

Worrall, W.E., 1975. Clays and Ceramic Raw Materials. Applied Science Publ., London, 204 pp.

Xeidakis, G.S., 1979. Assessment of the engineering and other properties of expansive soils by various methods. Ph.D. Thesis, Univ. of Leeds, England. 407 pp.

Xeidakis, G.S., 1996. Stabilization of swelling clays by $Mg(OH)_2$. Factors affecting hydroxy-Mg-interlayering in swelling clays. Eng. Geol., 44: 93–106.

Chapter 6

LIME/CEMENT STABILIZATION

6.1 GENERAL

Chemical admixture stabilization has been extensively used in both shallow and deep stabilization in order to improve inherent properties of the soil such as strength and deformation behavior. An increment in strength, a reduction in compressibility, an improvement of the swelling or squeezing characteristics and increasing the durability of soil are the main aims of the admixture stabilization. Lime or cement have commonly been used as chemical admixtures for soil stabilization. The lime/cement mixing method has been used to improve the properties of soils since olden times. These processes were developed in the 1970's simultaneously in Sweden and Japan. However, cement columns, using cement powder, were preliminarily reported to be successfully executed in practice in 1980 and 1982 (DJM Research Group, 1984; Chida, 1982; Miura et al. 1986). The method adopted is known as the DJM (Dry Jet Mixing) Method. Since the mid-80's, lime and cement have been utilized increasingly as stabilizing agents. Deep stabilization of soft soils with lime and/or cement stabilized columns has been the subject of research in Sweden, Japan, and other countries for some time. The Swedish Geotechnical Institute together with Linden-Alimak AB and Professor Bengt Broms have done extensive work on the usage of lime column technique for foundations and earth works both for embankments and excavations in soft clays. Modern application of this method for deep mixing of in-situ soils started in the late 1970's in Japan (Terashi et al. 1979; Kawasaki et al. 1981; Suzuki, 1982). The deep mixing method (DMM) originally was developed to improve the soft ground for port and harbor structures. DMM is now applied to foundation of structures built on land such as embankments, buildings, and storage tanks. However, as suggested by Broms (1986), in Southeast Asia, it is preferable to use cement instead of lime, because of the following reasons: the low cost of cement compared to lime; the difficulty of storing unslaked lime in a hot and humid climate; the greater strength which can be obtained with cement while there is a limit of maximum strength that can be obtained with lime.

Lime and cement treatment has been extensively used for road construction purposes resulting in increased bearing capacity of soft subgrade, enabling a reduction in the thickness of the base course. Treatment with cement or lime has been mainly used in the field of highways, railroads and airport constructions in order to improve the mechanical properties of the bearing layers. The use of lime or cement stabilization has more recently been extended to greater depth in which lime or cement columns act as a type of soil reinforcement. Layers of lime or cement stabilized clays, with their high strength and high modulus, can also function as a rigid crust which is useful in spreading the applied loads to the subsoil. As such, additional applications of the technique have been realized. These present applications include the use of cement or lime column to improve the stability of slopes, trenches, and deep excavations; to increase the bearing capacity and reduce the total and differential settlements below lightly loaded structures; to reduce the negative skin friction on structural piles, to prevent sliding failure of embankments; to reduce the vibrations from traffic loads, blasting, and pile driving; and also to accelerate the consolidation settlements under embankments. Because of the proven versatility of cement and lime stabilization, the methods have gained a wider acceptance in different countries of the world and more recently in Southeast Asia. Some applications of lime/cement columns are illustrated in Fig. 6.1.

6.2 FUNDAMENTAL CONCEPTS OF SOIL-CEMENT STABILIZATION

A Portland cement particle is a heterogeneous substance, containing minute tricalcium silicate (C_3S), dicalcium silicate (C_2S), tricalcium aluminate (C_3A), and a solid solution described as tetracalcium alumino-ferrite (C_4A) [Lea, 1956]. These four main constituents are major strength producing compounds. When the pore water of the soil encounters with the cement, hydration of the cement occurs rapidly and the major hydration (primary cementitous) products are hydrated calcium silicates (C_2SH_x, $C_3S_2H_x$), hydrated calcium aluminates (C_3AH_x, C_4AH_x), and hydrated lime $Ca(OH)_2$. The first two of the hydration products listed above are the main cementitious products formed and the hydrated lime is deposited as a separate crystalline solid phase. These cement particles bind the adjacent cement grains together during hardening and form a hardened skeleton matrix, which encloses unaltered soil particles. The silicate and aluminate phases are internally mixed, so it is most likely that none is completely crystalline. Part of the $Ca(OH)_2$ may also be mixed with other hydrated phases, being only partially crystalline. In addition, the hydration of cement leads to a rise of pH value of the pore water, which is caused by the dissociation of the hydrated lime. The strong bases dissolve the soil silica and alumina (which are inherently acidic) from both the clay minerals and amorphous materials on the clay particle surfaces, in a manner similar to the reaction between a weak acid and strong base. The hydrous silica and alumina will then gradually react with the calcium ions liberated from the hydrolysis of cement to form insoluble compounds (secondary cementitious products), which harden when cured to stabilize the soil. This secondary reaction is known as the pozzolanic reaction. The composition of hydrated cements is still not clearly defined by a chemical formula, so considerable variations are feasible. The compounds in the Portland Cement are transformed on the addition of water as follows:

$$\underset{\text{(tricalcium silicate)}}{2(3CaO.SiO_2)} + \underset{\text{(water)}}{6H_2O} = \underset{\text{(tobermorite gel)}}{3CaO.2SiO_2.3H_2O} + \underset{\text{(calcium hydroxide)}}{3Ca(OH)_2} \text{--------(6.1)}$$

$$\underset{\text{(bicalcium silicate)}}{2(2CaO.SiO_2)} + \underset{\text{(water)}}{4H_2O} = \underset{\text{(tobermorite gel)}}{3CaO.2SiO_2.3H_2O} + \underset{\text{(calcium hydroxide)}}{Ca(OH)_2} \text{--------(6.2)}$$

$$\underset{\text{(tetracalciumaluminoferite)}}{4CaO.Al_2O_3.Fe_2O_3} + 10H_2O + 2Ca(OH)_2 = \underset{\text{(calcium aluminoferrite hydrate)}}{6CaO.Al_2O_3.Fe_2O_3.12H_2O} \text{--------(6.3)}$$

$$\underset{\text{(tricalcium aluminate)}}{3CaO.Al_2O_3} + 12H_2O + Ca(OH)_2 = \underset{\text{(tetracalcium aluminate hydrate)}}{3CaO.Al_2O_3.Ca(OH)_2.12H_2O} \text{---(6.4)}$$

$$\underset{\text{(tricalcium aluminate)}}{3CaO.Al_2O_3} + 10H_2O + \underset{\text{(gypsum)}}{CaSO_4.2H_2O} = \underset{\text{(calcium monosulfoaluminate)}}{3CaO.Al_2O_3.Ca(OH)_2.12H_2O} \text{-----(6.5)}$$

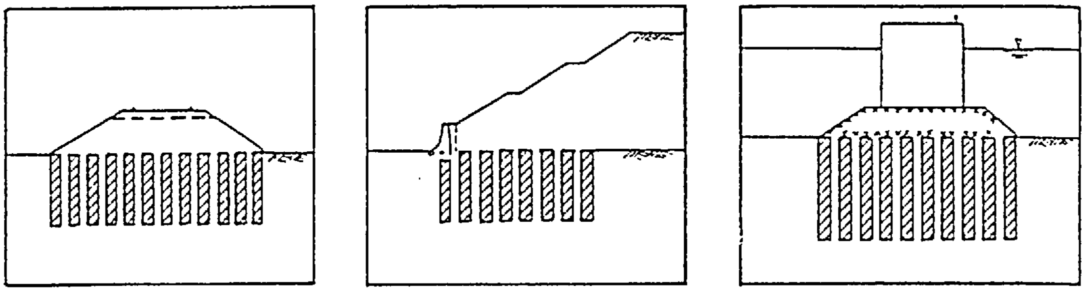

Prevent slope failures and reduce settlement in embankments and structures

Increase the stability of slopes

Increase the bearing capacity of soils and used as foundation to structures

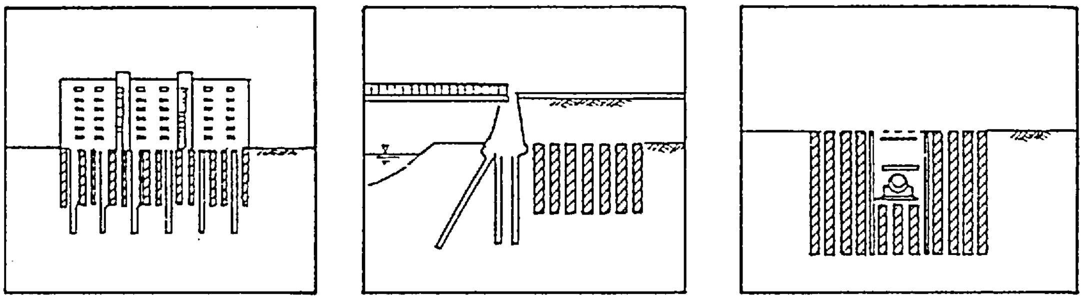

Increase the horizontal resistance of structures

Reduce settlement and prevent slope failure of the abutments bridges

Prevent heaving and reduce the penetration length of sheet piles in excavations

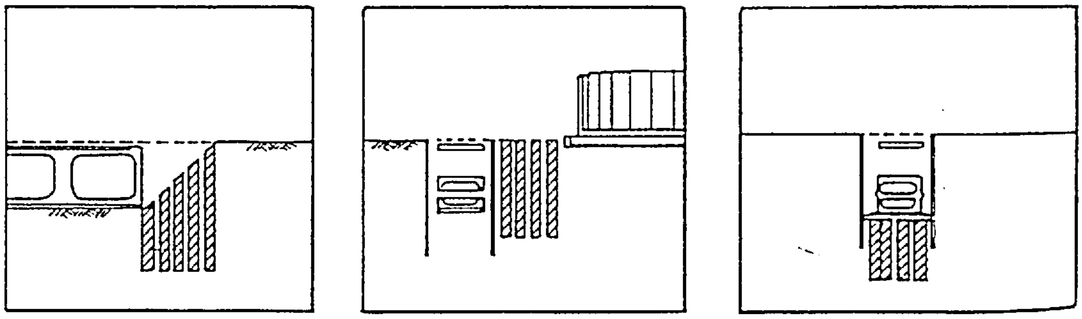

Stabilize cut slopes

Prevent damage to the adjacent structures of construction sites

Prevent settlement of underground embedded structures

Fig. 6.1 Some Applications of Cement Columns (DJM Research Group. 1984)

The first two equations (Eqs. 1 and 2), whose materials constitute 75% of the Portland cement, show that the hydration of the two calcium silicate types produces new compounds: lime and tobermorite gel, with latter playing the leading role with regards to strength, since bondage, strength, and volume variations are mainly governed by them. The reactions which take place in soil-cement stabilization can be represented in the equation given below. The reactions given here are for tricalcium silicate (C_3S) only, because they are the most important constituents of Portland cement:

$$C_3S + \quad H_2O \longrightarrow \underbrace{C_3S_2H_x \text{ (hydrated gel)} \quad + \quad Ca(OH)_2}_{\text{primary cementitious products}} \text{ ------------------ } (6.6)$$

$$Ca(OH)_2 \longrightarrow Ca^{++} + 2(OH)^- \text{ -------------------------} (6.7)$$

$$Ca^{++} + 2(OH)^- + SiO_2 \text{ (soil silica)} \longrightarrow \underset{\text{(secondary cementitious product)}}{CSH} \text{ ------------------------} (6.8)$$

$$Ca^{++} + 2(OH)^- + Al_2O_3 \text{ (soil alumina)} \longrightarrow \underset{\text{(secondary cementitious product)}}{CAH} \text{ ----------------------} (6.9)$$

When pH < 12.6, then the following reaction occurs:

$$C_3S_2H_x \longrightarrow C_3S_2H_x \text{ (hydrated gel)} + Ca(OH)_2 \text{ ------------------------ } (6.10)$$

In order to have additional bonding forces produced in the cement-clay mixture, the silicates and aluminates in the material must be soluble. The solubility of the clay minerals is equally affected by the impurities present, the crystalline degree of the materials involved, the grain size, etc. In the above equations, the cementation strength of the primary cementitous products is much stronger than that of the secondary ones. At low pH values (pH < 12.6), the reactions given by the Eq. 6.10 will occur. However, the pH drops during pozzolanic reaction and a drop in the pH tends to promote the hydrolysis of $C_3S_2H_x$, to form CSH. The formation of CSH is beneficial only if it is formed by the pozzolanic reaction of lime and soil particles, but it is detrimental when CSH is formed at the expense of the formation of the $C_3S_2H_x$, whose strength generating characteristics are superior to those of CSH. The cement hydration and the pozzolanic reaction can last for months, or even years, after the mixing, and so the strength of cement treated clay is expected to increase with time.

Thus, it means that in the soil cement containing fine clay particles, primary and secondary cementing substances are formed. The primary products harden into high-strength additives and differ from the normal cement hydrated in concrete. The secondary processes increase the strength and durability of the soil cement by producing an additional cementing substance to further enhance the bond strength between the particles.

6.3 MECHANISM OF LIME STABILIZATION

The major strength gain of lime treated clay is mainly derived from three reactions, namely: dehydration of soil, ion exchange, and pozzolanic reaction. Other mechanisms such as carbonation cause minor strength increase and can be neglected. Short term reactions include hydration (for quicklime) and flocculation (ion exchange). Longer term reactions are cementation and carbonation. The use of lime as a stabilizing additive is mainly due to its well-known effects when mixed with soils. The natural stabilizing agent for cohesive soils is calcium hydroxide, hydrated lime, or slaked lime. Calcium hydroxide is not itself a binder, but will produce a binder (consisting mainly of calcium silicate hydrates) by slow chemical reactions principally with the silicates in the clay mineral of cohesive soils (Assarson et al., 1974).

6.3.1 Hydration

A large amount of heat is released when quicklime (CaO) is mixed with clay. This is due to the hydration of quicklime with the pore water of the soil. The increase in temperature can, at times, be so high that the pore water starts to boil (Broms, 1984). An immediate reduction of natural water contents occurs when quicklime is mixed with cohesive soil, as water is consumed in the hydration process. Assarson et al. (1974) reported that at the slakening of the lime, a part of the soil water, about 0.3 kg/kg CaO, is consumed. Moreover, a considerably larger amount of the pore water evaporates because of the heavy heat release, i.e., as the hydration of the quicklime proceeds and the temperature increases, the amount of pore water is reduced. This drying action is particularly beneficial in the treatment of the moist clays. Thus, if a reduction of the natural water content in a cohesive soil is desirable, quicklime (or unslaked lime) instead of calcium hydroxide is used. It is important that the water content of the base clay must be sufficient for the complete slakening of the quicklime. Furthermore, to make the ion exchange possible between calcium ions of hydrated lime and the alkali ions of the clay minerals, there must be enough water after the evaporation caused by the heat release at the slakening of the quicklime. During the placement of lime columns and layers, the heat generation and the expansion of lime further affect the consolidation phenomena.

$$CaO + H_2O \longrightarrow Ca(OH)_2 + \text{HEAT (280 Cal/gm of CaO)} \text{---------(6.11)}$$

The calcium hydroxide, $Ca(OH)_2$, from the hydration of quicklime or when using calcium hydroxide as the stabilizer, dissociates in the water, increasing the electrolytic concentration and the pH of the pore water, and dissolving the SiO_2 and Al_2O_3 from the clay particles.

$$Ca(OH)_2 \longrightarrow Ca^{++} + 2(OH)^- \text{---------------------(6.12)}$$

These processes will result in ion exchange, flocculation, and pozzolanic reactions.

6.3.2 Ion Exchange and Flocculation

When lime is mixed with clay, sodium and other cations adsorbed to the clay mineral surfaces are exchanged with calcium. This change in cation complex affects the structural component of the clay mineral. Within a period of a couple of minutes up to some hours after mixing, the calcium hydroxide is transformed again due to the presence of carbonic acid (H_2CO_3) in the soil (Kezdi, 1979). The presence of carbonic acid in the soil is due to the reaction of carbon dioxide of the air in the soil and the free water. The reaction results in the dissociation of the lime into Ca^{++} (or Mg^{++}) and $(OH)^-$ which modifies the electrical surface forces of the clay minerals. A transformation of the soil structure begins, i.e., flocculation and coagulation of soil particles into larger sized aggregates or grains and an associated increase in the plastic limit. Lime causes the clay to coagulate, aggregate or flocculate. The clay plasticity (measured in terms of Atterberg Limits) is reduced making it more easily workable and potentially increasing its strength and stiffness. The change in the soil structure is a consequence of cation exchange caused by dissociated bivalent calcium ions in the pore water replacing such univalent alkali ions that normally are attracted to the negatively charged clay particles (Assarson et al. 1974). This results in the flocculation of the clay particles.

$$Ca^{++} + \text{Clay} \longrightarrow Ca^{++} \text{ exchanged with monovalent ions } (K^{+}, Na^{+}) \text{----(6.13)}$$

In general, the order of replaceability of common cations associated with soils follows the lyotropic series (or Hofmeister series): $Na^{+} < K^{+} < Ca^{++} < Mg^{++}$, with highly metallic ions replacing the weaker one on the surface of clay particles. The crowding of Ca^{++} ions onto the surface of the clay particles (adsorption) brings about flocculation (Herrin and Mitchell, 1961). The cation exchange capacity highly depends on the pH of the soil water and on the type of clay mineral in the soil. Among the types of clay mineral, Montmorillonites have the highest and Kaolinites have the lowest cation exchange capacities (Assarson et al. 1974). Brandl (1981) concluded that cation exchange capacity of a soil is not a criterion for its reactivity with lime, and instead suggested that the amount of semi-removable silica is a useful criterion of lime reactivity for practical purposes.

The fact that flocculation of clay occurs as a consequence of the addition of lime is a well-known phenomenon, but the achievement of flocculation is not necessarily a main mechanism by which lime stabilizes the soils. Diamond and Kinter (1965) argued that although calcium saturation is required for stabilization, many natural soils which are largely saturated still exhibit deficiencies associated with problematic soil for use as subgrades, and thus require stabilization. Furthermore, many chemical agents other than lime induce immediate flocculation when mixed with clays (Brandl, 1981), yet are valueless for stabilization.

6.3.3 Pozzolanic Reaction

The shear strength of the stabilized soil gradually increases with time mainly due to pozzolanic reactions. Calcium hydroxide in the soil water reacts with the silicates and aluminates (pozzolans) in the clay to form cementing materials or binders, consisting of calcium silicates and/or aluminate hydrates (principally dihydrates) (Diamond and Kinter, 1965). The dissolved dissociated Ca^{++} ions react with the dissolved SiO_2 and Al_2O_3 from the clay particle's surface and form hydrated gels, resulting in the combination of the soil particles (Diamond and Kinter, 1965).

$$Ca^{++} + 2(OH)^{-} + SiO_2 \longrightarrow CSH \text{ ---------------------------(6.14)}$$

$$Ca^{++} + 2(OH)^{-} + Al_2O_3 \longrightarrow CAH \text{ ---------------------------(6.15)}$$

The gel of calcium silicates (and/or aluminate hydrates) cements the soil particles in a manner similar to the effect produced by the hydration of Portland cement, but the lime cementing process is a much slower reaction which requires considerably longer time than the hydration of cement. The main part of the reaction does not start until a couple of days after the mixing of lime (Assarson et al. 1974). As a rule, it is not finished until one to five years later (Diamond and Kinter, 1965). The solubility of the pozzolans and thus their inclination to react with lime depends on the pH of the soil water. The rate of reaction also increases with increased soil temperature (Broms, 1984).

6.3.4 Carbonation

Lime reacts with carbon dioxide in the atmosphere or in the soil to form relatively weak cementing agent, such as calcium carbonate or magnesium carbonate (Ingles and Metcalf, 1972). The strength of calcium carbonate which is formed by this process can be discounted, and its significance on the soil lime stabilization can be dismissed (Broms, 1984). Diamond and Kinter (1965) even suggested that carbonation is probably a deleterious rather than helpful phenomenon in the soil stabilization.

6.4 SCHEMATIC ILLUSTRATIONS OF CEMENT-IMPROVED SOIL

With the schematic diagrams shown in Fig. 6.2, it was proposed to illustrate the conditions of hardening (Saitoh et al. 1985). Figure 6.2(a) shows the condition immediately after mixing a cohesive soil and a hardening agent slurry. It is considered that even if the cohesive soil and hardening agent slurry are thoroughly mixed, clay particles will form to a cluster which will be surrounded by the slurry. Figure 6.2(b) shows the condition of the cohesive soil and hardening agent slurry that have formed a hardened body. Here the hardening agent slurry [shown in Fig. 6.2(a)] produces hydrated calcium silicates, hydrated calcium aluminates, $Ca(OH)_2$, etc., and forms hardened cement bodies. The pozzolanic reaction between the clay and the $Ca(OH)_2$ obtained from the cement hydration reaction produces hardened soil bodies. It is considered that the strength of the improved soil will depend upon the strength characteristics of both types of hardened bodies.

6.5 PREDOMINANT FACTORS THAT CONTROL HARDENING CHARACTERISTICS OF CEMENT TREATED CLAY MATERIALS

The hardening characteristics of cement treated soil mixtures are developed by a number of factors. Owing to the large number of alternatives and combinations, it is impossible to tabulate the various mechanical properties as functions of these factors, so the experimental determination is indispensable in most cases. There are, nevertheless, some predominant factors presented below, but they only provide information outlining order-of-dominance value, and illustrating the effect of these factors on the strength and stiffness of the cemented clay. An outline of some superficial factors exerting an influence on the properties of cement treated soils are illustrated in Fig. 6.3.

6.5.1 Type of Cement

The differences in improvement of cement treated clays by using different types of Portland cement have been investigated. The stabilization by Type III Portland cement renders better improvement of soil than the Type I cement does. However, the Type I Portland cement is the most popular cement used in soil stabilization. This is because it is the most readily available and cheapest compared with other types of cement.

6.5.2 Cement Content

In general, it has been found that the greater the cement content, the greater is the strength of the cement treated clay (Broms, 1984). This behavior is different in the case of lime treated clay. In the case of lime, there is a maximum strength limit that can be obtained at the optimum lime content.

6.5.3 Curing Time

In a manner similar to that of concrete and lime treated soils, the shear strength of cement treated clay increases with time. The rate of increase of strength is generally rapid in the early stages of the curing period. Thereafter, the rate of increase of strength decreases with time. The rate of increase of strength for cement treated clay is greater than that of lime treated clay at the early stage.

6.5.4 Soil Type

The effectiveness of cement and lime decreases with increasing water content and organic content. The improvement decreases generally with increasing plasticity index of the clay (Broms, 1986). The strength increase of cement treated clay on organic soils is offen very low. However, cement is more effective than lime in the stabilization of organic soils (Miura et al. 1986).

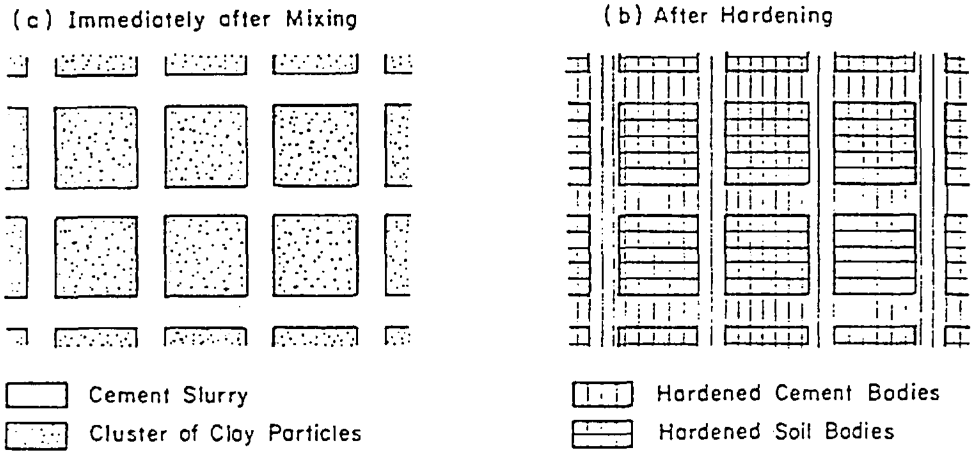

Fig. 6.2 Schematic Illustrations of Improved Soil (Saitoh et al. 1985)

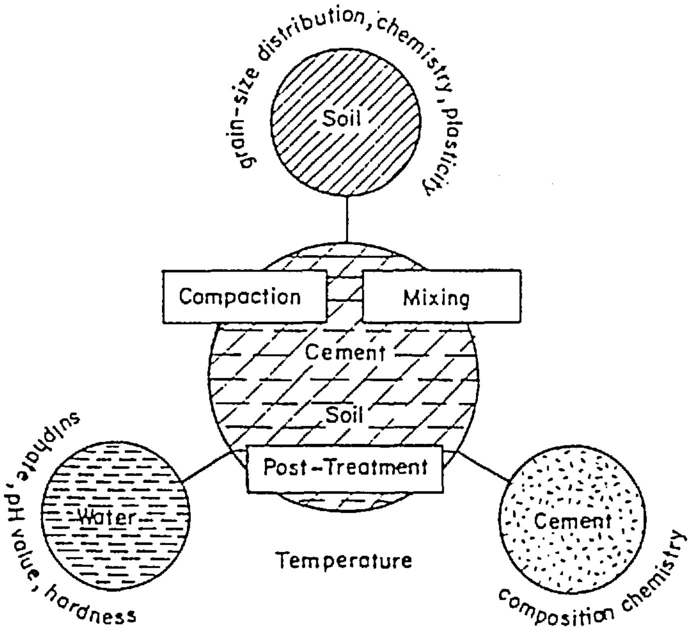

Fig. 6.3 Factors Affecting the Properties of Cement Soils (Kezdi. 1979)

The effects of cement gradually decrease with increasing clay content and increasing plasticity index (Woo, 1971). In general, when the activity of a soil is very high, the increase of the shear strength of the soil treated with cement, is low. However, these are in the reverse order in the case of lime, since the strength of the lime treated clay depends mainly on the participation of the clay particles in the pozzolanic reactions. But for cement treated clay, it depends mainly on the cementation from the cement hydration. The increase of the shear strength due to the flocculation is often relatively small for marine clays deposited in salt water, since these clays already have a flocculated structure (Broms, 1984).

6.5.5 Curing Temperature

The increase of temperature accelerates the chemical reactions and solubility of the silicates and aluminates, thus increasing the rate of strength gain of the treated soil.

6.5.6 Soil Minerals

In the case of soil with the property of higher pozzolanic reactivity, the strength characteristic of the treated soil is governed by the strength behavior of the hardened cement bodies. But in the case of soils having lower pozzolanic reactivity, the strength characteristics of the treated soils are governed by the strength characteristics of the hardened soil bodies (Saitoh et al. 1985). Therefore, if improvement conditions are equal, greater strength is obtained from the soil with higher pozzolanic reactivity. Hilt and Davidson (1960) observed that montmorillonitic and kaolinitic clayey soils were found to be effective pozzolanic agents, as compared to clays which contain illite, chlorite or vermiculite. Wissa et al. (1965) also explained that the amount of secondary cementitious materials that are produced during pozzolanic reaction of the clay particles and hydrated lime ($Ca(OH)_2$) is dependent on the amount and mineral composition of the clay fraction as well as the amorphous silica and the alumina present in the soil. The montmorillonite clay mineral will probably react more readily than the illites and kaolins because of their poorly defined crystallinity.

6.5.7 Soil pH

The long-term pozzolanic reactions are favored by high pH values, since the reactions are accelerated due to the increased solubility of the silicates and the aluminates of the clay particles. When the pH value of the treated clay is lower than 12.6, the reaction of the Eq. 6.10 occurs, where $C_3S_2H_x$ is used up to produce the CSH and the hydrated lime [$Ca(OH)_2$]. This will reduce the strength of the treated clay at the expense of stronger cementitious material, $C_3S_2H_x$, to produce the weaker cementitious material, CSH.

6.6 PREDOMINANT FACTORS THAT CONTROL HARDENING CHARACTERISTICS OF LIME TREATED CLAY

6.6.1 Type of Lime

The efficiency of lime stabilization depends in part on the type of lime material used. Quicklime is generally more effective than hydrated lime (Kezdi, 1979), but generally it needs care in handling for soils with high moisture contents. Unslaked lime or quicklime is more effective since water will be absorbed from the soil and more importantly, the hydration will cause an increase in temperature which is favorable to strength gain (Broms, 1984).

6.6.2 Lime Content

The strength of lime soil mixtures, provided they are properly cured, increases as the lime content is increased. There appears to be no optimum lime content which produces a maximum strength in a lime stabilized soil under all conditions. However, it can be stated that for a particular condition of curing time and soil type, there is a corresponding optimum lime content which causes the maximum strength increase (Herrin and Mitchell, 1961).

6.6.2.1 Lime Fixation Point

The lime fixation point is defined as the point at which the percentage of lime is such that additional increments of lime produce no appreciable increase in the plastic limit. Handy et al. (1965) referred to this point as the "lime retention point". Based on extensive investigations at Iowa State University, the concept of the lime fixation point was suggested. Lime contents equal to the lime fixation point for a soil will generally contribute to the improvement in soil workability, but may not result in sufficient strength increases (Hilt and Davidson, 1960).

6.6.2.2 Optimum Lime Content

Methods of determining the optimum lime requirement for lime stabilization have been proposed. Eades and Grim (1966) suggested that the amount of lime consumed by a soil after one hour affords a quick method of determining the percentage of lime required for stabilization, i.e., the lowest percentage of lime required to maintain a pH of 12.6 is the percentage required to stabilize the soil. However, a strength test is still necessary to show the percentage of strength increase. McDowell (1959) pointed out that short-time or quick tests probably will not identify optimum lime contents, but are essential in checking against the use of non-reactive soils for treatment of lime. On the other hand, while long-term tests would do a better job of identifying optimum lime contents, they may be impractical from the standpoint of time, and may even suggest the use of insufficient amounts of lime due to the ideal conditions under which they are run. Hilt and Davidson (1960) gave a correlation which showed that the amount of lime fixation is in proportion to the type and amount of clay present and is independent of the absorbed cation present in the clays. The relationship is given as:

$$\text{Optimum Lime Content} = \frac{\%\text{ of clay}}{35} + 1.25 \text{ --------------------(6.16)}$$

6.6.3 Curing Time

Broms (1984) reported that the shear strength of stabilized clays will normally be higher than that of untreated clay after mixing. Figure 6.4 shows a typical plot of the increase of shear strength with time for various types of soils. The shear strength of clay stabilized with lime will normally be higher than that of undisturbed clay about one to two hours after mixing even when the sensitivity of the clay is relatively high (Broms, 1984). The undrained final shear strength of stabilized clay can be, under favorable conditions, as high as 10 to 50 times the initial shear strength (Assarson et al. 1974). The shear strength of the stabilized soil gradually increases with time through pozzolanic reactions when the lime reacts with the silicates and aluminates in the soil (Broms, 1984). The rate of increase is generally rapid at the early stage of curing time; thereafter, the rate of increase in strength decreases with time. Lime has an initial reaction with soil taking place during the first 48-72 hours after mixing, and a secondary reaction which starts after this period and continues indefinitely (Taylor and Arman, 1960).

Several attempts have been made to express the strength of lime stabilized soils as a function of curing time. Broms (1984) found that the shear strength of stabilized soils as determined by unconfined compression tests increased linearly with time when plotted in log-log scale (log C_u, log t). Brandl (1981) and Okamura and Terashi (1975), however, found that the time-dependent increase in shear strength was approximately linear with the logarithm of time.

6.6.4 Type of Soil

For lime treatment to be successful, the clay content of the soil should not be less than 20% and the sum of the silt and clay fractions should preferably exceed 35%, which is normally the case when the plasticity index of the soil is larger than 10 (Broms, 1984). The shear strength increase of the stabilized soil is highly dependent on pozzolanic reactions, i.e., the reactions of lime with the silicates and aluminates in the soil.

6.6.4.1 Grain Size Distribution

Figure 6.5 shows the effect of grain size distribution on the lime stabilization method. The increase in strength with time is in general highest for normally consolidated silty clays, with low plasticity index and a low water content. The strength increase in lime treated organic soils is often very low; even a relatively small amount of organic material can have a large effect on the strength increase (Broms, 1984). Gypsum has often been used together with unslaked lime to stabilize organic soils when lime alone is not effective (Broms and Anttikoski, 1983). Generally, the effect of lime decreases with increasing water content (Holm et al. 1983; Miura et al. 1987).

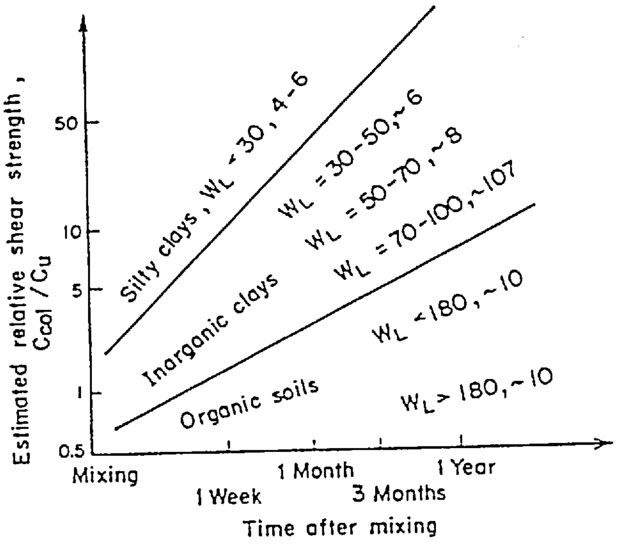

Fig. 6.4 Increase of Shear Strength with Time

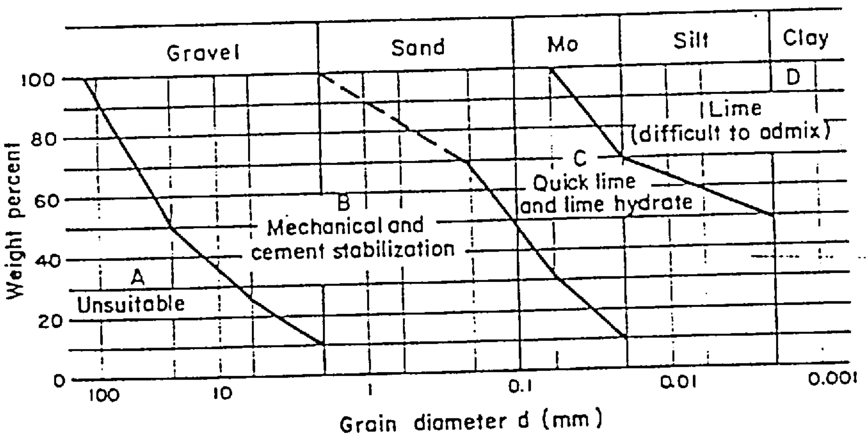

Fig. 6.5 Effect of Grain Size Distribution on the Applicability of Lime Stabilization (Kezdi, 1979)

6.6.5 Clay Minerals

Eades and Grim (1966) reported that the quantity of lime needed to effectively treat a clay is dependent on the type of clay mineral present. Eades and Grim (1966) observed that although kaolinites, illites, montmorillonites and other mixed-layered clays all react with lime to give greater strengths, the quantity of lime needed to treat a clay is dependent on the type of mineral present. Hilt and Davidson (1960) found that from the unconfined compression test results, kaolinitic and montmorillonitic clayey soils are effectively stabilized with lime alone. Whereas illitic clays require addition of fly-ash to obtain a significant strength gain. Lee et al. (1982) found that in terms of strength increase, lime treatment has a greater effect in montmorillonites than kaolinitic soils.

6.6.6 Soil pH

Lime addition will increase the pH of the water content in the soil, and give rise to increased solubility. The base exchange is low when the pH-value is less than 7. The long-term chemical reactions in lime stabilized soils are favored by a high pH-value (pH > 12) since the reactions are accelerated due to the increased solubility of the silicates and aluminates (pozzolans) present in the clays (Broms, 1984). Davidson et al. (1965) suggested that a minimum pH of approximately 10.5 is necessary for pozzolanic reaction to take place, while Eades and Grim (1966) suggested that the lowest percentage of lime required to maintain a pH of 12.40 is the percentage required to stabilize a soil. Broms (1984) pointed out that the pH of the treated soil will normally exceed 12 even when only a few percent of lime has been added to the soil.

6.6.7 Curing Temperature

The chemical reactions in the soil are favored by a high temperature (Broms, 1984). For lime-soil mixture at the same age, the effect of increasing the curing temperature is to increase strength (Ruff and Ho, 1966). The curing temperature has been found to affect the long term reactions between lime and clay. Broms (1984) attributed the favorable effects of high curing temperature to the increased solubility of the silicates and aluminates (pozzolans) in the clay at high temperatures. For lime stabilized clays, Metcalf (1964) found that the curves (UC strength versus temperature) were different for different clays, and that there was an abrupt change in the slope in the vicinity of 45°C. Ruff and Ho (1966) extended the work of Metcalf (1964), and suggested that different reaction products are formed at different curing temperatures and that the cut-off temperature is from 23°C to 40°C. Furthermore, it was found that there was increase of strength with time at all temperatures, with greater rate of increase at the higher temperature. Chaudry (1966) reported that the compacted lime stabilized Bangkok clay cured at 100°F had higher strength values than those cured at 70°F.

6.7 RELEVANT CHARACTERISTICS OF SOFT BANGKOK CLAY

The relevant soil properties for the soft Bangkok clay at Nong Ngu Hao is given in Fig. 6.6. For typical soft Bangkok clay, the percentage of clay varies from 30% to 70%, silt from 20% to 60%, and sand from 0 to 15% (Balasubramaniam and Bergado, 1984). Typical values of natural water content range from 40% to 130%. The liquid limit varies in the range of 50% to 130%, while plastic limit ranges from 20% to 60%. The plasticity index ranges from 20% to 80% and the liquidity index from 0.4 to 1.2. The organic and salt contents are also given in Fig. 6.6. The organic contents seemed to vary from 2% to 5% with occasional maximum value of 9%. Balasubramaniam et al. (1985) reported salt contents of 0 to 0.5% (0 to 5 g/liter) in the upper portions in the weathered crust and 0.5% to 2% (5 to 20 g/ liter) in the lower soft clay portions. The sensitivity of Bangkok clay can sometimes be as high as 8 and averaging about 5 or 6. Regarding the clay minerals, illites seemed to dominate, ranging from 20% to 70%, while montmorrillonite ranged from 5% to 30% and kaolinites about 10%.

6.8 EFFECTS OF QUICKLIME, NATURAL WATER CONTENT, SALT, AND ORGANIC CONTENTS

Miura et al. (1986) previously reported that the improvement mixing with quicklime is more effective for clays located nearshore than onshore locations for soft Ariake clay in Japan. One reason for this difference is the amounts of natural moisture contents being larger in the latter than the former (Fig. 6.7). However, it was suggested that the salt content of clay may have influenced the degree of improvement. Ariizumi (1977) described the improvement effect of quicklime on clay that was accelerated by addition of salts. Tests were made where small amounts of salts were added to the clay sample together with quicklime and the results are shown in Fig. 6.8. In these tests, salt up to 5 percent of quicklime weight and quicklime at 5, 7.5, and 10 percent of dry soil weight were added and then mixed. As seen in Fig. 6.8, the strength of improved soil increased with the increase in salt content up to a certain limit. According to Ariizumi (1977), the addition of salt, NaCl, may act as catalyzer and the ions Cl^-, Na^+, Mg^{+2} may have accelerated the pozzolanic reaction. The effects of quicklime and natural water contents are demonstrated in Fig. 6.9. For clays with high organic contents of more than 8%, the use of cement instead of quicklime becomes advantageous (Miura et al. 1987). This is probably because high organic clay generally requires much amount of quicklime and hence there may remain non-reacted excess admixture.

6.9 STRENGTH OF CEMENT TREATED CLAY

A most comprehensive review of the strength properties of cement stabilization was presented by Mitchell et al. (1974). The unconfined compressive strength, q_u, is generally described as increasing linearly with the cement content percentage, A_w. This increase is more pronounced for coarse-grained soil than for silt and clays. Like q_u, other strength parameters such as cohesion intercept and the friction angle increase with A_w and curing time. Mitchell et al. (1974) gave the following relationships between curing time and q_u.

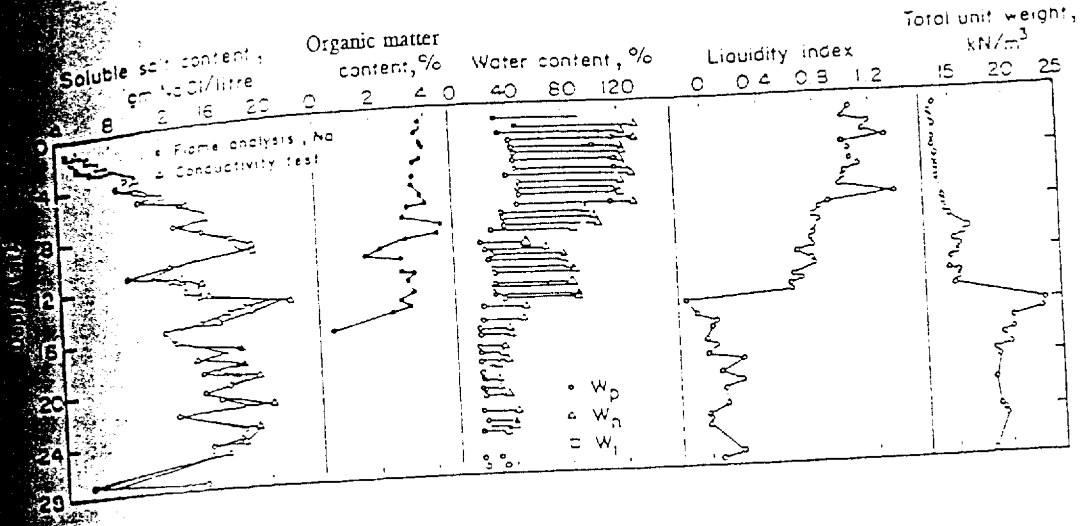

Fig. 6.6 Variation of Soluble Salt Content, Organic Matter Content, Water Content, Liquidity Index, and Total Unit Weight at Nong Ngu Hao (Bangkok Clay)

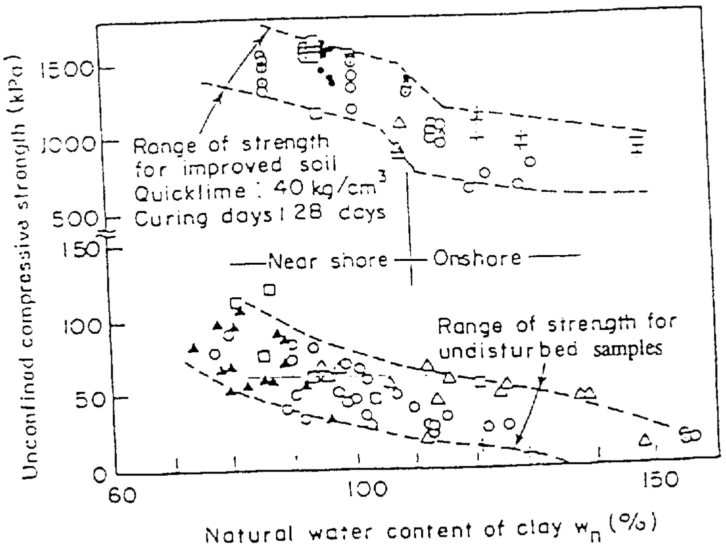

Fig. 6.7: Relationship Between Natural Water Content and Unconfined Compressive Strength of Undisturbed Sample and Improved Soil

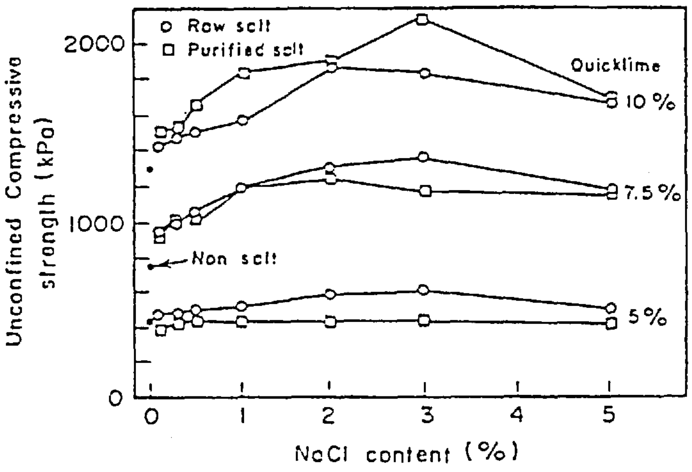

Fig. 6.8 Influences of NaCl Content on the Quicklime Improvement Effect of Ariake Clay (Hasuike Area)

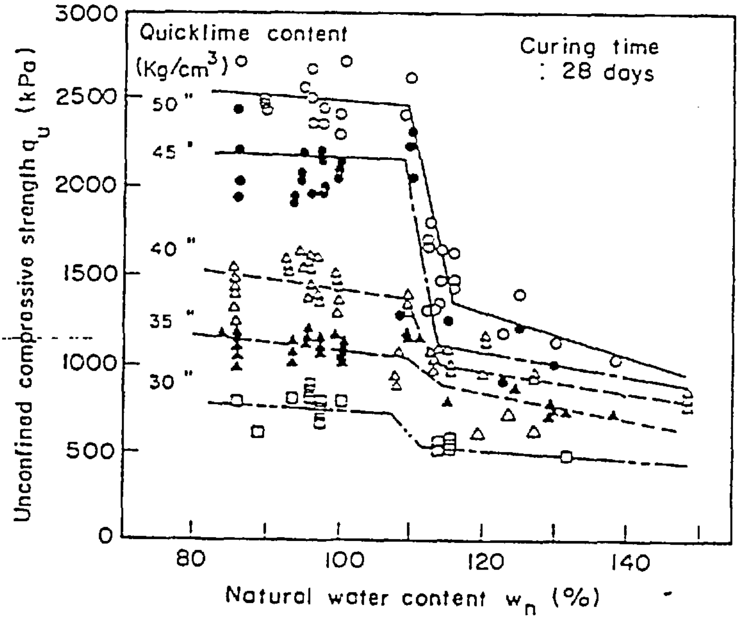

Fig. 6.9 Influences of Natural Water and Quicklime Content on the Improvement Effect

$$q_u = q_u(t_o) + K.\log\frac{t}{t_o} \qquad (6.17)$$

where: q_u (t) = Unconfined compressive strength at t days, kPa
q_u (t_o) = Unconfined compressive strength at t_o days, kPa
A_w = Cement content, % by mass
K = 480 A_W for granular soils and 70 A_W for fine grain soil
t = Curing time

6.10 LIME STABILIZATION OF SOFT BANGKOK CLAY

Bangkok clay is well known for its low strength and high compressibility. In this region, there are extensive deposits of soft marine clay which encounter problems in settlement and stability. The sub-soil conditions in the Bangkok area are typical of deltaic plains. The geotechnical problems encountered there are often associated with the presence of a relatively thick layer of soft clay (about 10 metres) with low strength and high compressibility. Various ground improvement techniques are increasingly being explored for the construction works in this area in order to achieve the desired engineering properties of the soil and to minimize the settlement to within the tolerable values.

Extensive laboratory studies on the use of lime stabilized columns have been carried out at the Asian Institute of Technology (Balasubramaniam et al. 1988, 1989). Addition of 5 to 10% quicklime is the optimum mix proportions for the soft Bangkok clay. The addition of quicklime increased the unconfined compressive strength to about 5 times and increased the preconsolidation by as much as 3 times. The vertical coefficient of consolidation also increased by 10 to 40 times and the effective strength parameters also increased, especially the angle of internal friction from 24^o to 40^o.

6.11 CEMENT TREATMENT OF SOFT BANGKOK CLAY

Broms (1984) has suggested that in Southeast Asia, it is preferable to use cement rather than lime because of the following reasons: low cost of cement compared to lime; difficulty of storing unslaked lime in a humid and hot climate; higher strength can be obtained while there is a limit for maximum strength for lime. At the Asian Institute of Technology, Kamaluddin (1995) conducted studies on the strength and deformation characteristics of cement treated soft Bangkok clay under unconfined compression, oedometer, constant stress ratio tests, and triaxial drained and undrained tests. The study addressed the effect of the variability in terms of quantity of the hardening agent, the pre-shear consolidation pressure, the stress conditions imposed during testing, the drainage condition, and the time dimension. The Oedometer Tests revealed that the cement treatment caused substantial improvement of consolidation properties. Normalized intrinsic compression curves offered confirmation of the hardening effect in the void index plane. The prevalent role of pre-shear consolidation pressure was manifested to annihilate the cementation effects attributing ductility to the treated matrix. Kamaluddin (1995) observed that the main effect of cement treatment is to modify the behavior of the soft clay from normally consolidated to overconsolidated state. The existence of a small strain domain denoted as 'Initial Small Strain Phase' was ascertained based on the characteristics of undrained stress paths and from the (q, ε_v) relationships of drained tests, establishing a family of loci in the (q, p) stress space which governs the onset phase transformation of the treated clays. Beyond the small strain domain and up to the curved failure envelope, a work hardening and elasto-plastic type of behavior with large strain is observed. The stress-dilatancy relations on the Spatial Mobilized Plane (SMP) exhibit a remarkable phenomenon such that the stress ratio, τ/σ_N, and the normal and shear strain increment vector, $-d\varepsilon_N/d\gamma$, constitute a specific correlation between treated and untreated clays. In Constant Stress Ratio (CSR) Tests, strain paths produced sets of stress-dilatancy relationships. Heavily overconsolidated (rigid) behavior was observed inside the loci of the transition points of bilinear strain paths obtained from CSR tests . A composite conceptual model to describe the mechanical behavior of cement treated clay is proposed in which three zones and four subzones have been envisaged. The treated clays have been found to be strain-softened after failure in an 'Unstable Phase' with the residual stress state lying on a failure envelope identified as 'Destructured Envelope', which is close to the critical state line of the untreated clay. At this envelope, the cohesion is destroyed and the treated clay then behaves as purely frictional material.

6.11.1 Fundamental Behavior of Cement Treated Clay

The base soil used in the study was soft Bangkok clay taken from a site within the AIT campus, obtained from depths of 3-4 m. The properties of this clay are shown in Table 6.1. The sample preparation was done by mixing the cement slurry and the base clay thoroughly. Organic matter content of the base clay was 5.6%; whereas organic carbon was 2.87. A considerable amount of cement was required to neutralize the large reserve of potential acidity or buffering capacity of the clay. The properties of the treated samples after curing are listed in Table 6.2.

Table 6.1 Physical Properties of the Soft Bangkok Clay

Liquid Limit	103%	Sand	3%
Plastic Limit	43%	Total Unit Wt., (kN/m^3)	14.3
Plasticity Index	60%	Dry Unit Wt.,(kN/m^3)	7.73
Water Content	76-84%	Initial Void Ratio, e	2.2
Liquidity Index	0.62	Activity	0.87
Silt	28%	Sensitivity	7.3
Clay	69%		

Table 6.2 Properties of Cement Treated Soft Bangkok Clays

Cement Content (%)	Curing Time (month)	Total Unit Weight (kN/m^3)	Dry Unit Weight (kN/m^3)	Void Ratio	Water Content (%)	Degree of Saturation (%)
5	1	14.85-15.12	8.16-8.67	2.03-2.22	73.35-83.77	95.77-100.00
7.5	1	14.90-15.25	8.31-8.76	1.99-2.15	772.92-81.4	96.75-100.00
10	1	14.95-15.43	8.44-8.90	1.93-2.09	69.33-78.53	95.56-99.95
12.5	1	15.03-15.52	8.49-9.21	1.90-2.06	68.51-77.70	95.96-99.96
15	1	15.04-15.40	8.60-9.05	1.87-2.02	66.79-75.37	94.65-98.88
5	2	14.90-15.51	8.28-8.98	1.99-2.16	71.66-80.89	96.15-100.00
7.5	2	14.97-15.55	8.32-9.10	1.92-2.12	70.92-79.98	97.89-100.00
10	2	15.00-15.48	8.62-9.15	1.91-2.05	69.19-77.46	98.78-99.87
12.5	2	15.05-15.60	8.68-9.22	1.85-1.98	67.67-74.22	96.57-98.97
15	2	15.28-15.61	8.81-9.31	1.82-1.95	67.06-73.49	97.67-99.87
Untreated	0, 1 and 3	14.1-14.96	7.74-8.24	2.20-2.44	81.60-86.00	99.81-100.00

The effect of cement content and curing time on the liquid limit was insignificant. It was the plastic limit which was increased with cement content (A_w) and curing time (t). The reduction of plasticity index was due to an increase of plastic limit. The immediate decrease in the water content after mixing cement with clay was from 5% to 10%. Sharp reduction of water content occurred up to the vicinity of 12.5% cement content (reduced by 8.3% to 17.3%), and then the effect of the reduction to a cement content of 40% was small (4.8% to 9.1%). Water content reduces with curing time rapidly up to 10 weeks and then slows down, but continues for a longer time. Cement causes significant reduction in specific gravity and this change is dependent on cement content and curing time. Variation of specific gravity with cement content follows a pattern; the curvilinear variation of lowest curing time gradually turns into a linear variation at the longest curing time. The influence of curing time is larger at the initial stage of curing. After 3 months, the influence becomes minor. A comparative study with untreated base clay revealed that cement treated samples have lower void ratio, higher degree of saturation, and higher unit weight. An investigation showed that the slopes of the lines in the unit weight vs. cement content (γ_t, A_w) plane were found to be almost constant, but the intercepts increased sharply up to 12 weeks curing period and thereafter decreased. In the relationship of unit weight versus curing time (γ_t, t), curvilinear variation was observed up to 8 weeks, then the variation was of linear pattern.

6.11.2 Unconfined Compression Tests

Stress-strain curves for treated samples were found to increase abruptly until the peak compressive strengths, then suddenly decreased to very low residual values upon further straining. Zonal demarcation showing the effectiveness of cement treatment has been illustrated in Fig. 6.10. The q_u (unconfined compressive strength), A_w (percentage of cement by weight) plane was sub-divided into 3 regions (A, B and C) on the basis of gradient development. The properties of the treated soil exhibited significant increase in strength and modulus of deformation, but simultaneously the clay material was changed mainly to brittle and quasi-brittle materials. In general, stress-strain curves of the treated samples were found to increase abruptly to peak values, then suddenly decreased to low residual values. From the aspect of stress-strain relationships, the overall behavior was categorized into brittle, quasi-brittle and ductile. Higher strain, low strength and mild peak were found to be associated with ductile behavior, whereas low strain, higher strength, and sharp peak exhibited brittle behavior. Since the reduction of water content is a function of A_w in the clay matrix, it was concluded that strength gain due to decrease in water content is smaller for low cement content such as 5%; whereas, for higher cement content, a part of the strength increase is due to reduction of water content. From the aspect of unconfined compression condition, 15% to 20% cement content and 1 to 2 months curing period were regarded as optimum. In (ε_f, q_u) relationships, the samples with higher strength produce lower values of failure strain which corresponds to brittle behavior. Ductile samples were found to be more scattered than the brittle samples. For the case of ductile samples, significant reduction of failure strain was observed with curing time without substantial development of strength. Failure strain reduces significantly as the cement content and curing time increase. The (ε_f, A_w) relationships showed that substantial reduction of failure strain occurred up to A_w=20%. On the other hand, failure strain reduced tremendously with a curing period up to 8 weeks, and beyond 16 weeks, the failure strain reaches an asymptotic value. The initial tangent modulus vs. unconfined compressive strength (E_u, q_u) relationships produced a straight band of narrow scatter. In the (E_u, A_w) relationship, sharp increase of the modulus can be noticed up to cement content of 20%. An asymptotic value is reached at about 35% to 40%. A similar type of trend can be noticed in (E_u, t) relationship. Shear type of failure mode was noticed in the case of treated samples. The higher the values of A_w and t, the greater is the degree of stiffness and brittleness of the treated clay. Though the effect of curing time is similar to that of cement content, the result shows that the curing hardening has less influence on failure mode and brittleness than that of cement.

6.11.3 Consolidation Behavior

6.11.3.1 Oedometer Tests

The void ratio-axial stress plot (Fig. 6.11) shows the similarity in the shapes of the void ratio-axial stress curves for 1 to 6 month curing period. The (e, log σ_v) relationships show that the treated curve crosses the untreated curve much before its preconsolidation pressure and then is displaced from untreated curve with increasing values of σ_v, indicating instinct characteristics of lower compressibility than the untreated one. The higher the value of cement content, the greater is the enhancement of the preconsolidation pressure and the decrease of compression index accompanied with gradual reduction of compressibility. The gradual reduction process of compressibility of treated clay with time is quite obvious from the test results. But it was observed that at low value of A_w such as 5%, the increase of curing time could not help in developing significant hardening effect in the clay matrix. The results show that the hardening potential gained by increasing cement content (e.g., 5% to 7.5%) is much greater than that of enhancing curing time (e.g., 1 month to 2 months). With low cement content, the curing time parameter becomes latent. It can be postulated that the value of A_w in

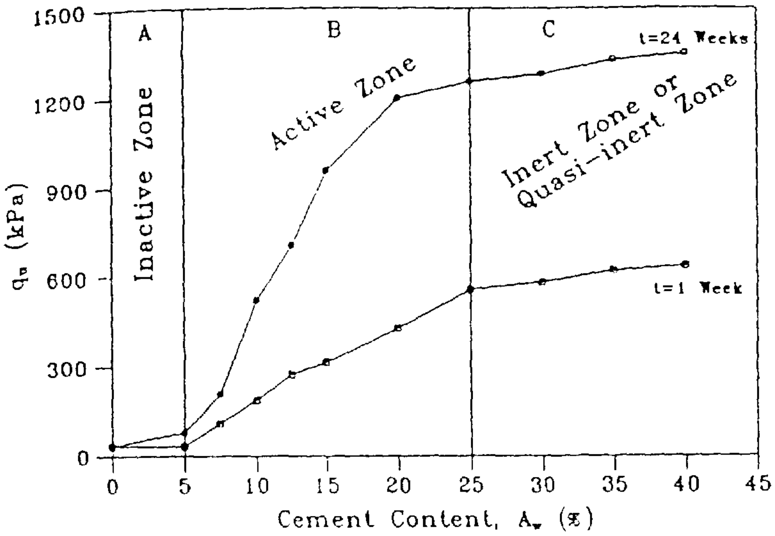

Fig. 6.10 Influence of Cement Content on Unconfined Compressive Strength

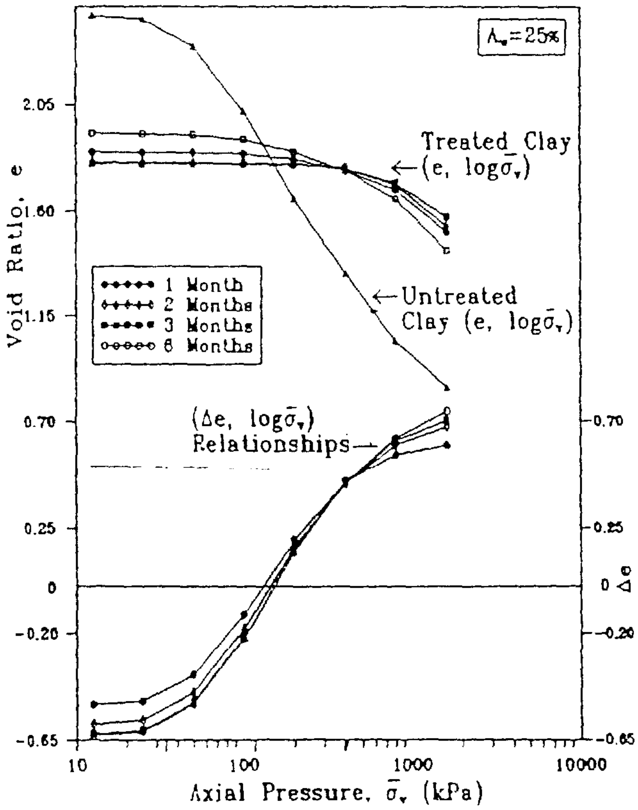

Fig. 6.11 (Δe, log σ_v) Relationship at 25% Cement Content

a sample is a more active parameter than curing time which is a secondary and auxiliary parameter of the former. The swelling ratio (SR) is reduced greatly due to cement treatment, implying a rigid mechanism that is employed during the swelling process. The high pressure tests [σ_v (max)=6000 kPa] showed that the (e, log σ_v) relationships at the highest range of stress tend to proceed nearly parallel with the normally consolidated line of untreated base clay. At large strains, the cohesion of the clay is destroyed and the treated material then behaves as purely frictional material. At a higher stress level, a breakage in (e, log σ_v) relationship was discernible. At this point, a (e, log σ_v) relationship possessing lower values of compression index (C_C) evolved. At sufficiently higher stress level, the relation of (e, log σ_v) treated clay tends to run parallel to that of untreated clay. This stage can be referred to as normally compressed response of the treated clay. Thus, a postulation can be made that the Δe, log σ_v) relationship (Fig. 6.11) reaches an asymptotic value when the treated clay will reach the state of normally compressed response. The initial part of the compression plane (Initial Compression Line) deviates upward for low cement content and curing time. On the other hand, the later part of the compression plane displaces with increasing value of σ_v gradually as the cement content and curing time increase. A way of finding the value of σ_v at which treated clay reaches the normally compressed response is to extrapolate the (Δe, log σ_v) plot to asymptotic value where the axial pressure is the required σ_v.

The void index, I_V, versus log σ_v plot (Fig. 6.12) renders excellent confirmation of the overconsolidation effect of the treated clays. The untreated clay proceeds with ICL (Intrinsic Compression Line). As the cement content increases, the curve is displaced with an increasing value of σ_v. A method can be explored to find the equivalent consolidation pressure, p_e, from the shifted ICL. The intersecting point of the shifted ICL and the horizontal line drawn at the void index of the sample is the value of σ_e for the said sample. One important effect of cement treatment is to increase the values of coefficient of consolidation. The Cv value generally decreases approximately linearly with increasing consolidation pressure. Results show that the higher the cement content, the greater the value of Cv. The highest enhancement of Cv value with cement content occurs in the vicinity of 15% cement content. Curing period of 1 to 2 months is found to be the most effective length of time for enhancement of Cv values and can be designated as optimum curing time. The compression index (C_c) value was found to decrease with cement content. After a certain reduction of C_C value with 5% cement content, gradual reduction was noticed up to 15% cement content and, thereafter, changes were very minor. Substantial reduction of C_C value occurred during the period of 1 to 2 months, and thereafter the C_C values were almost the same. High pressure oedometer tests render similar compressibility characteristics as those of other tests [σ_v (max)=1600 kPa], having approximately identical C_C values.

6.11.3.2 Constant Stress Ratio (CSR) Tests

Application of higher stress ratio exhibited greater compressibility characteristics. The effect of variation of stress ratio on the (e, ln p) relationships (Fig. 6.13) is small for higher cement content and curing time. Higher volumetric strains are associated with low cement

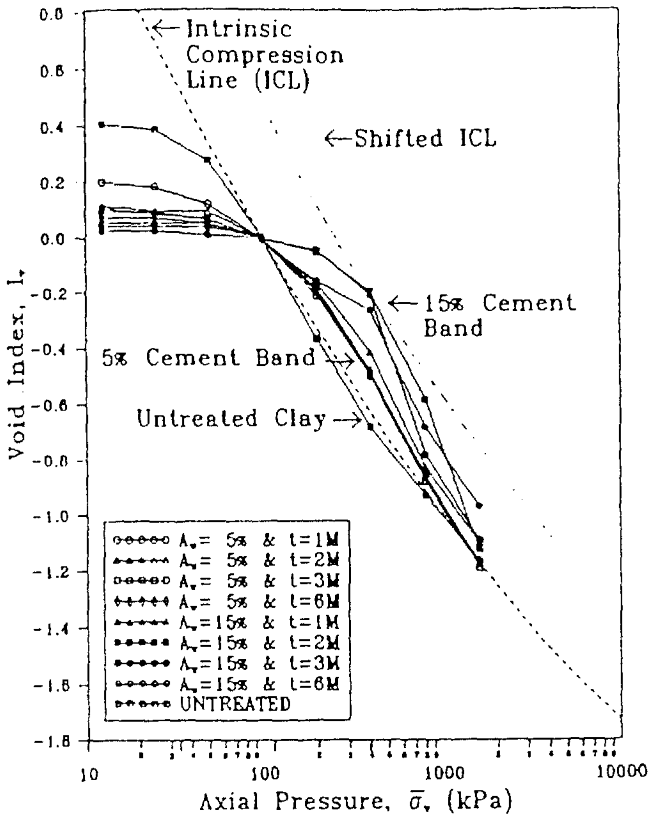

Fig. 6.12 Normalized Intrinsic Compression Curves of the Treated Clays

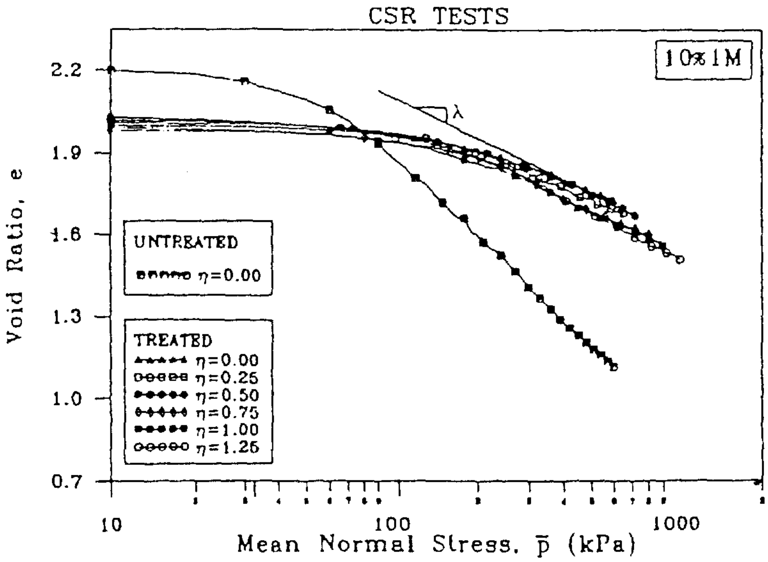

Fig. 6.13 (e - log p) Relationships from CSR Tests (10% Cement and 1 Month Curing)

content and curing time and higher stress ratio. The locus of the transition point between small strain and large strain is influenced by the cement content and curing time. It was found that the higher the stress ratio, the greater is the shear strain incurred by the sample. The variation of shear strain with stress ratio is much larger at low cement content and curing time. The strain path showed (Fig. 6.14) bilinear characteristics. The loci of the transition points of small strain and large strain of the bilinear relationships (Fig. 6.15) are affected by the cement content and curing time; higher cement content and curing time expand the loci considerably.

The strain increment ratio was considered in two parts, inside and outside the transition point. It was found that higher cement content and curing time render greater values of dilatancy at both inside and outside the transition points. The stress-dilatancy relationship (Fig. 6.16) of Modified Cam Clay provides the relationship at lower strain than the experimental curves.

6.11.4 CIU Triaxial Compression Tests

6.11.4.1 Deviator Stress-Shear Strain Relationships

The effect of equivalent pressure, p_e, is very gradual for low range of A_W such as 5% (Fig. 6.17) since pre-shear consolidated volumes are affected largely by the p_o, which in turn affect the (q, ε_S) relationship. On the other hand, for higher cement content such as 15%, the (q, ε_S) relationship (Fig. 6.18) is largely affected by the p_o when it is at the higher range. The ε_S is found to be linearly dependent on deviator stress for the values of q up to 60% to 70% of q_{max}. Beyond this linear elastic portion, the deviation takes place at varying rates according to p_o. Generally, the shear strain at maximum deviator stress is reduced as the curing time increases. With higher curing time, q value rises sharply toward well-defined peak followed by greater amount of strain softening. The (q, ε_S) relationships were found to plot under varying rates depending on the parameter A_W; maximum deviator stress increases with increasing value of A_W. The ε_S at q_{max} is reduced when cement content is increased. Low A_W (5% and 7.5%) results in mild peak and low strain softening beyond peak; whereas sharper peak and larger strain softening can be observed from higher A_W.

6.11.4.2 Excess Pore Pressure-Shear Strain Relationships

Cement treatment modifies pore pressure response behavior by reducing the strain at peak pore pressure (Figs. 6.19 and 6.20). For low p_o values, the maximum pore pressure occurs prior to the failure of the sample, whereas for higher values of p_o, the maximum pore pressure occurs after the failure of the sample. The strain at peak pore pressure keeps on increasing as p_o increases. Lower p_o render greater value of negative pore pressure. Reduction of strains at peak pore pressure occurs when samples are cured for a longer curing time. Moreover, in (Δu, ε_S) relation, a distinct peak and significant amount of pore pressure dissipation after peak are common criteria for longer curing time. Secondly, long term cured specimens tend to develop greater negative pore pressure than that of short term cured specimens. The higher A_W mobilizes lower values of strain at Δu_{max}. As A_W increases, the

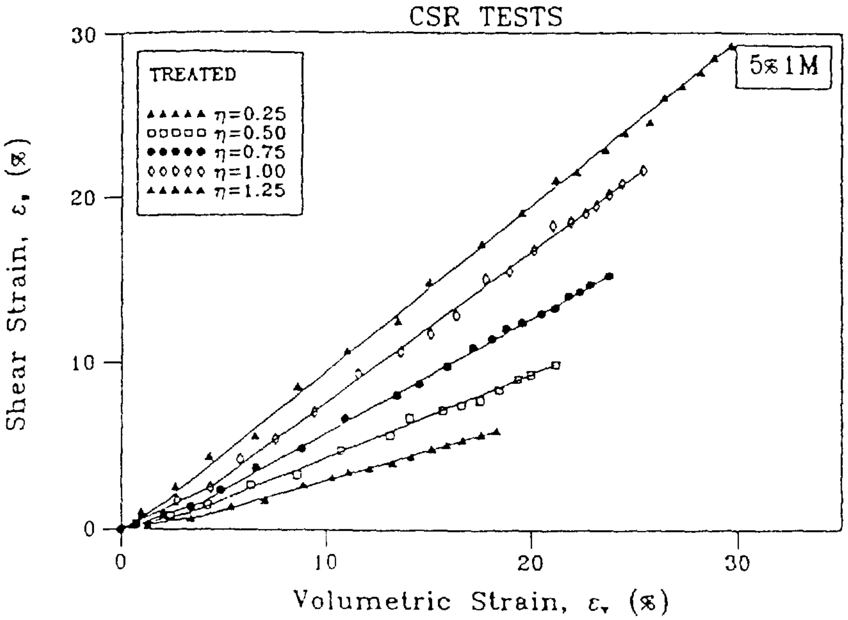

Fig. 6.14 Bilinear Relationship of (ε_s, ε_v)Plot
(5% Cement and 1 Month Curing)

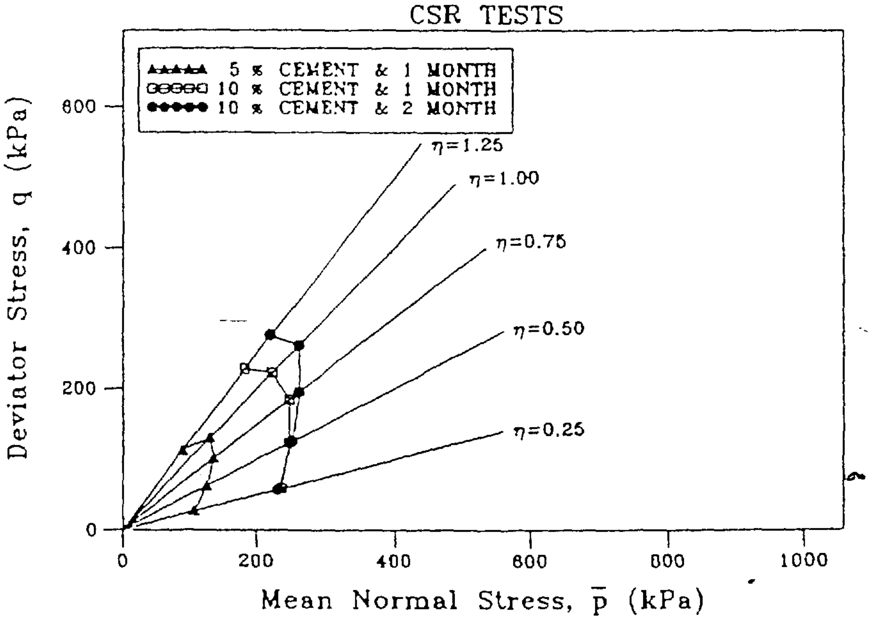

Fig. 6.15 Locus of Transition Points of Bilinear Strain Paths

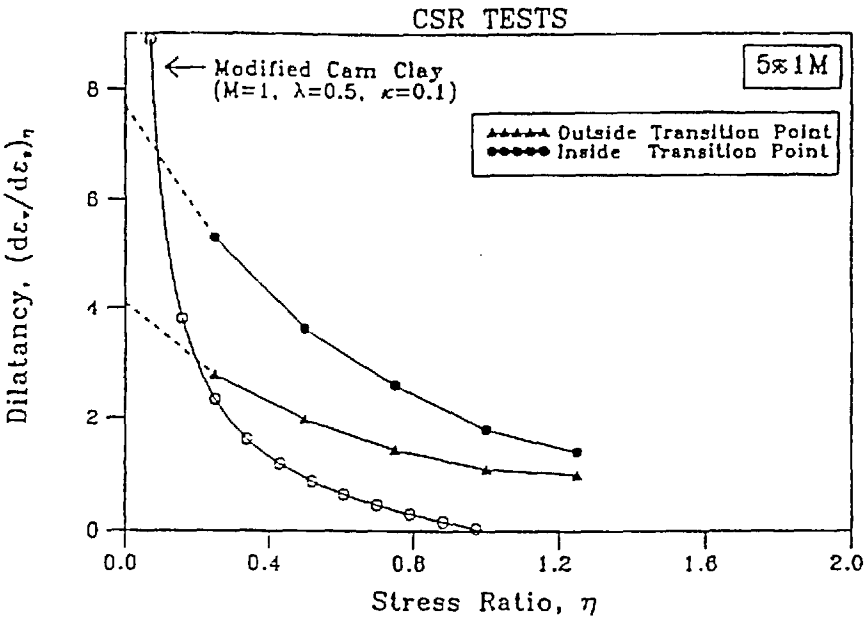

Fig. 6.16 Variation of Strain Increment Ratio with Stress Ratio (5% Cement and 1 Month Curing)

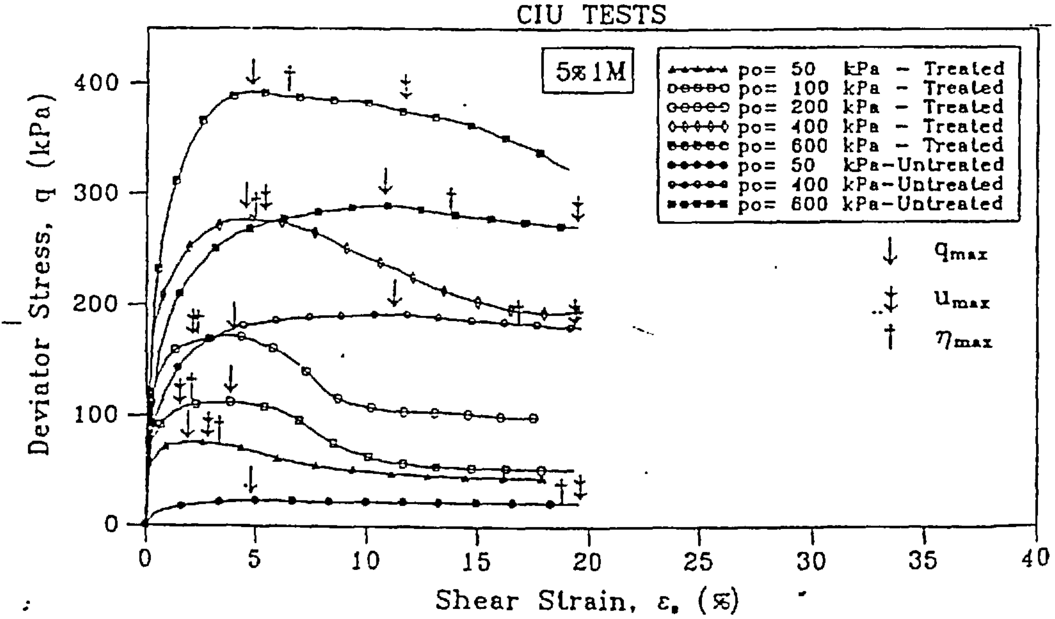

Fig. 6.17 q vs. ϑ_s Plot for Cement Treated Samples (5% Cement Content and 1 Month Curing)

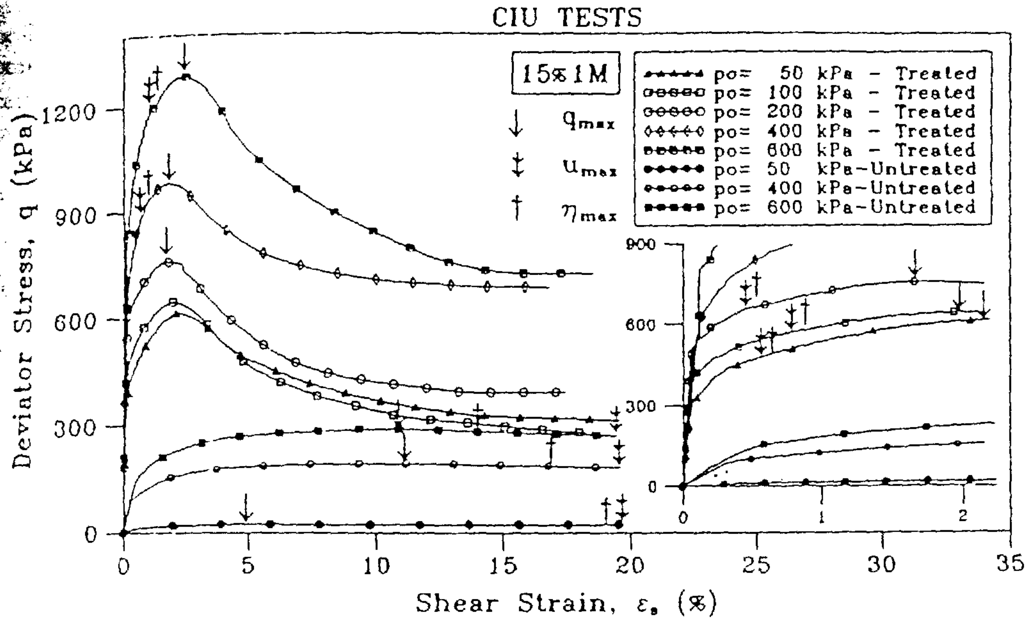

Fig. 6.18 q vs. ε_s Plot for Cement Treated Samples
(15% Cement Content and 1 Month Curing)

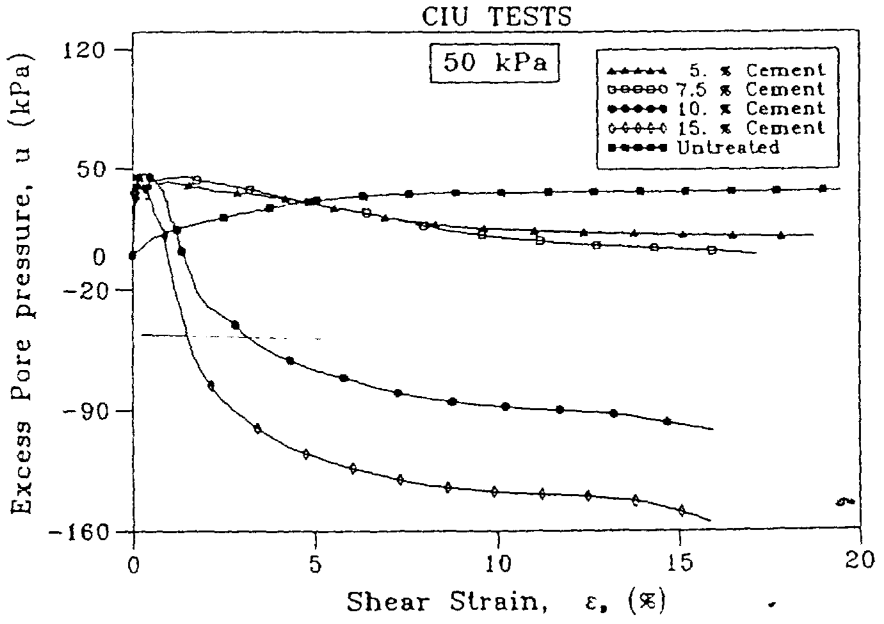

Fig. 6.19 u vs. ε_s Plot for Cement Treated Clay
(p_o=50 kPa and 2 Months Curing)

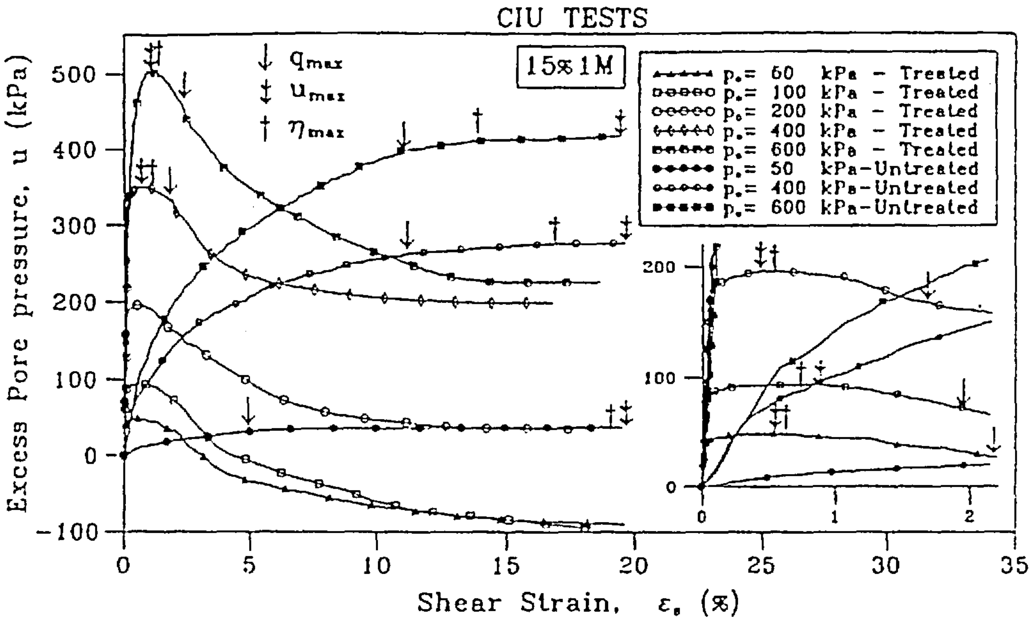

Fig. 6.20 u vs. ε_s Plot for Cement Treated Clay
(15% Cement Content and 1 Month Curing)

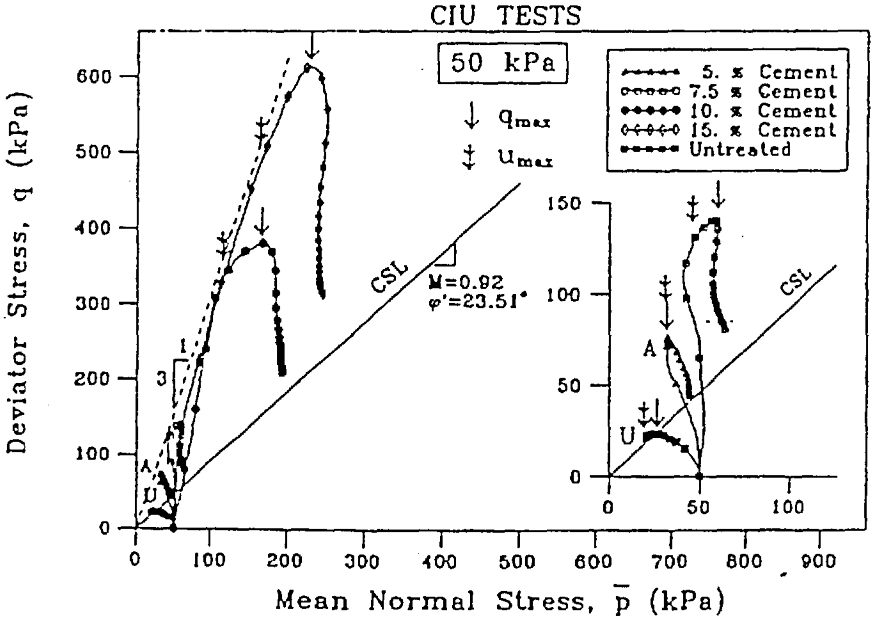

Fig. 6.21 Undrained Stress Paths of Cement Treated Clay
(p_c = 50 kPa and 1 Month Curing Time)

peak pore pressure tends to develop at lower strain. For higher values of A_W, the maximum pore pressure mobilization occurs much before failure. On the other hand, sample with low cement content, Δu_{max} occurs after failure state. The higher the A_W, the greater the negativity of pore pressure.

6.11.4.3 Undrained Stress Paths

The effective stress paths (Figs. 6.21 to 6.23) of treated clays raise several interesting aspects on the undrained behavior of the cement treated clays. It was observed that cement treatment changes the initial normally consolidated characteristics of the clay to that of overconsolidated, rendering more stiffness and rigidity of the clay. A lower A_W value such as 5% and lower does not make a greater alteration of the physico-chemical aspect of the base clays. An 'Initial Small Strain Phase' with constant-p path was found to be followed by large strain phase and generation of greater pore pressure. A conforming picture of phase transformation emerged. Outside the small strain domain and up to the curved failure envelope, a work-hardening, elasto-plastic type of behavior was observed. The phase transformation occurs below the angle of contraflexure. The angle of contraflexure has been defined as an arc tangent of the stress ratio at which the stress path in the (q, p) space change its direction from decreasing p-value to increasing p-value. A very high A_W (e.g., 15%) accompanied by higher t (e.g., 2 months) exhibited rigid behavior and did not show any phase transformation all through. The A_W has been found as the principal hardening parameter that controls the stiffness and rigidity of the treated clay as a prime factor. The hardening effects are influenced mainly by the parameters A_W and t. At the curing period of 1 month, the values of A_W=5% to 15% were found to have completely different effects; the cement content as low as 5% renders less beneficial effects. The curing time also plays a role in increasing the rigidity of the treated samples; but for samples of A_W=5% and lower, the influence of curing time is nominal. The curing time has been marked as secondary hardening parameter in the soft clay solidification process by cementation, whereas A_W has been found as primary parameter. The third variable p_o was also found to influence markedly the behavior of the treated clays. It was seen that higher p_o tends to reduce the beneficial effects of cement treatment by reducing the overconsolidation ratio of the soil. So, it is possible to transform a heavily overconsolidated clay to a normally consolidated clay by employing a sufficiently higher p_o, whose magnitude is a dependent function of A_W and t mainly, among others. It was observed that at low levels of pre-shear consolidation pressure, cement treatment resulted in the samples having stress paths that rise parallel to q-axis, indicating that the mean normal stress p, does not vary much during shear. This behavior can be considered to be a manifestation of the elastic wall concept used extensively in the critical state concepts (Calladine,1963). The stress paths of heavily overconsolidated samples that resulted from cement treatment indicate that samples remaining on the dry side, first move on a constant-p line, then approach Hvorslev strength envelope and tend to seek failure state either moving on the Hvorslev envelope or moving parallel along the tension cut-off line at 1:3 line until they reach the failure envelope of the corresponding treated clay. After reaching the q_{max} level, the stress path incurs strain softening by falling in a line sub-parallel to the q-axis; at this level the sample possesses destructured state. The stress paths of the treated samples follow paths that

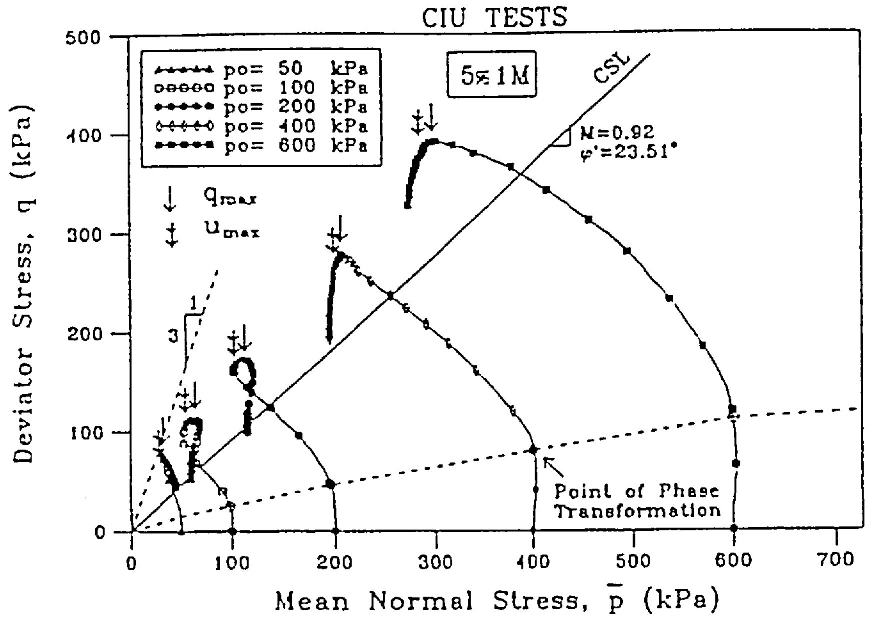

Fig. 6.22 Undrained Stress Paths of Cement Treated Clay (5% Cement Content and 1 Month Curing Time)

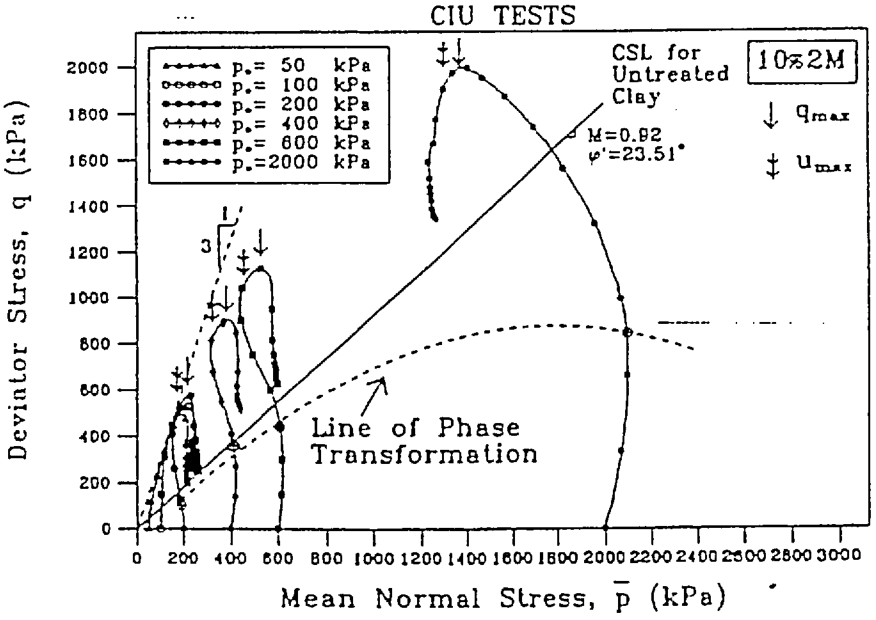

Fig. 6.23 Undrained Stress Paths of Cement Treated Clay (10% Cement Content and 2 Months Curing)

rise to maximum value of the deviator stress, and then return to a lower value of q at the end of the tests. This falling characteristic of the undrained stress paths beyond the peak value of the deviator stress is a remarkable aspect. The treated clay strain-softened with the residual states lying close to the CSL of the untreated clay.

6.11.4.4 Some Salient Aspects of Undrained Behavior

The overall aspects of undrained behavior discussed so far can be put into a framework as illustrated in Fig. 6.24. The undrained behavior of cement treated clay can be explained by sub-dividing (q, p) space into 3 zones. The behavior after the q_{max} condition can be regarded as unstable; strain softening occurs in constant-p route. The residual points of treated clay do not fall exactly on CSL, rather they plot above the CSL in a manner that they constitute an envelope referred as Destructured Envelope. It was postulated that if complete destructuration of the treated clay were achieved, and neglecting any permanent changes in the soil structure due to cement treatment, a destructured envelope would be achieved. At this envelope, cohesion is destroyed and the treated clay then behaves as purely frictional material. The failure envelopes were found to be curved. The overall curvature depends on range of p_o applied. The envelopes shift upward as the values of A_W and t go higher. The normalized pore pressure exhibited bilinear trend with stress ratio, η propounding the possibility of predicting undrained stress path and pore pressure development. The value of η_{tp} increases and slopes of first and second linear portions decrease as A_W and t go higher. A linear type of variation of the relationship (u_f, p_o) exists where all the data fall within a narrow band of scatter. The influence of A_W and t on u_f is not large at low level of p_o. Higher A_W and t shows lower values of shear strain at failure (ε_{sf}); but it reaches asymptotic value at about $A_W = 15\%$. Larger consolidation stress results in greater values of ε_{sf}. An increase of A_W reduces the strain at which η_{max} occurs. With a higher value of p_o, the (η, ε_s) relationship tends to be close to untreated clay. A transitional phase (from N.C. to O.C. state) can be clearly discerned in this relationship. Shear strain is found to increase with stress ratio. Increase of cement content attributes rigidity in the sample which manifests lower range of shear strain. Generally, the greater the pre-shear consolidation stress, the larger is the shear strain and ductility. During strain softening, the shear strain increases with the reduction of stress ratio. Higher cement content exhibits lower pore pressure generation. Enhancement of consolidation pressure results in the generation of higher pore pressure. Reduction of pore pressure can be noticed when the stress ratio decreases during the strain softening process resulting in even negative pore pressure. c and ϕ were found to be increased with cement content and curing time but seems to reach an asymptotic value at the vicinity of $A_W = 15\%$. The curved nature of the failure envelopes obtained from CIU tests indicated that increase of p_o tends to reduce the positive effect of cement treatment. It is observed that failure envelopes are affected by the A_W, t, and p_o. The initial, peak and residual stress states have curved projections on the (q, p) and (e, log p) planes (Fig. 6.25), which refer to the characteristics generally associated with overconsolidated behavior. The stress path of treated clay was found to be initially sub-parallel to q-axis. Phase transformation was manifested by the abrupt change in curvature of the stress paths (Figs. 6.22 and 6.23). A family of curved loci was obtained from these transformation points.

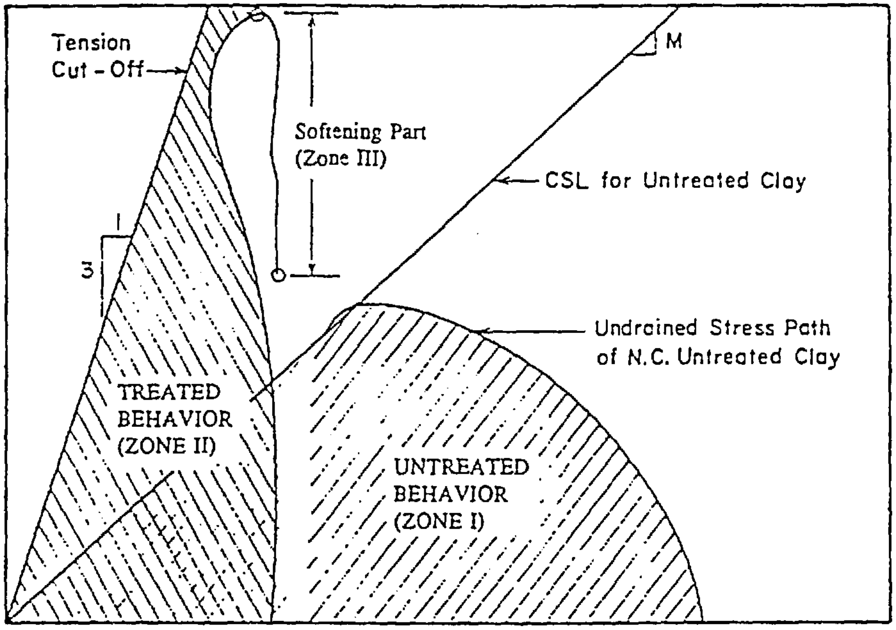

Fig. 6.24 Undrained Behavior of Treated and Untreated Clays in (q, p) Stress Space

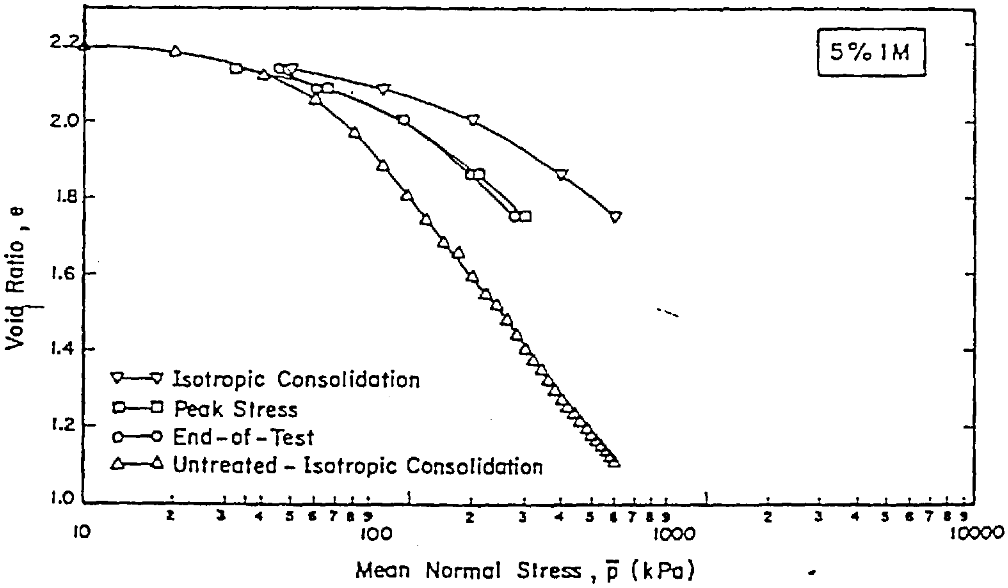

Fig. 6.25 (e, In p) Relationships from CIU Tests Showing Consolidation Curves (A_w = 5% and t = 1 Month)

6.11.5 CID Triaxial Compression Tests

6.11.5.1 Stress - Strain Relationships

Higher values of A_W and t render potential in developing q values and modulus with substantial low strains showing brittle behavior especially at low p_o (Fig. 6.26). The samples with higher cement content showed dilative nature at the residual states. The (q, ε_S) relationships show that they contain an initial linear relationship where the stress states possess low strains followed by a break point and, thereafter, the sample is subjected to higher strain. The (ε_V, p) relationships (Fig. 6.27) during strain hardening showed bilinear characteristics with a transition point of small strain and large strain. (q, ε_V) relationships showed that lower p_o produces smaller ε_V of the treated samples. A transition stress state exists which make demarcation between initial small strain phase and the remaining large strain phase. For higher A_W and low p_o, sample's dilation occurred with negative volumetric strains. With the increase of pre-shear consolidation pressure, the dilatant nature of the samples diminishes. Thus, the role of p_o is to eradicate the cementation effect. At low p_o, the indication of phase transformation is not observed.

6.11.5.2 Stress Ratio - Shear Strain Relationship

From experimental results, it was found that higher p_o reduces the magnitude of η_{max}, increases the shear strain at which $(\sigma_1/\sigma_3)_{max}$ occurs and tends to lessen the hardening potential of cement treatment. The stress ratio for specimens with low p_o increased at a greater rate with increasing strain. The samples at higher curing period reach higher values of stress ratios accompanied by lower values of strain at which η_{max} occur.

6.11.5.3 Some Salient Aspects of Drained Behavior

The treated soil initially shows a stiff and low strained response on drained compression until it reaches the transition point of small strain and large strain. The curved nature of the failure envelopes reveals that pre-shear consolidation stress tends to reduce the cementation effects. During strain hardening, maximum volumetric deformation is attained with stress ratio at the level of the failure envelope. Enhancement of consolidation stress attributes ductility to the sample. Higher cement content produces greater value of η_{max}. Minor reduction of volumetric strain was noticed during strain softening as the η decreased from η_{max}. Higher values of A_W render greater potentiality in the increase of q_{max} with curing time and consolidation stress. For low A_W values, the (q_{max}, p_o) relationships are almost linear but become curved at higher A_W values. Further, the rate of increase of q_{max} is greater in the region of higher p_o. Drained failure envelopes were found to be curved and are influenced by A_W and t. In general, the higher the value of A_W, the farther is the envelope above the CSL of untreated clay. A majority of the end-of-test stress states did not reach the failure envelope of the untreated clay even at much larger strains; rather they were found to cluster on an envelope referred to as the destructured envelope. It is found that an increase of A_W and t lessens the

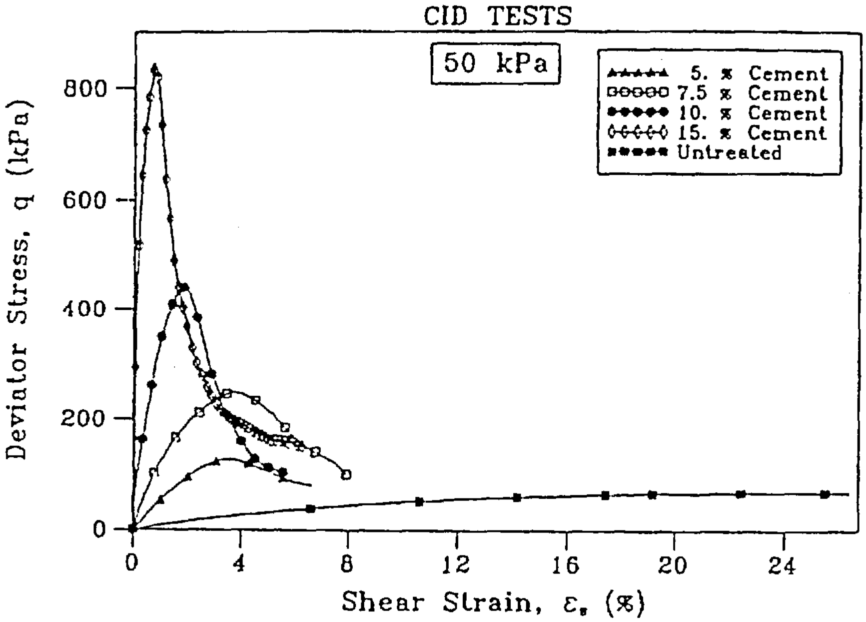

Fig. 6.26 q vs. ε_s Plot for Cement Treated Clay
(p_o = 50 kPa and 1 Month Curing)

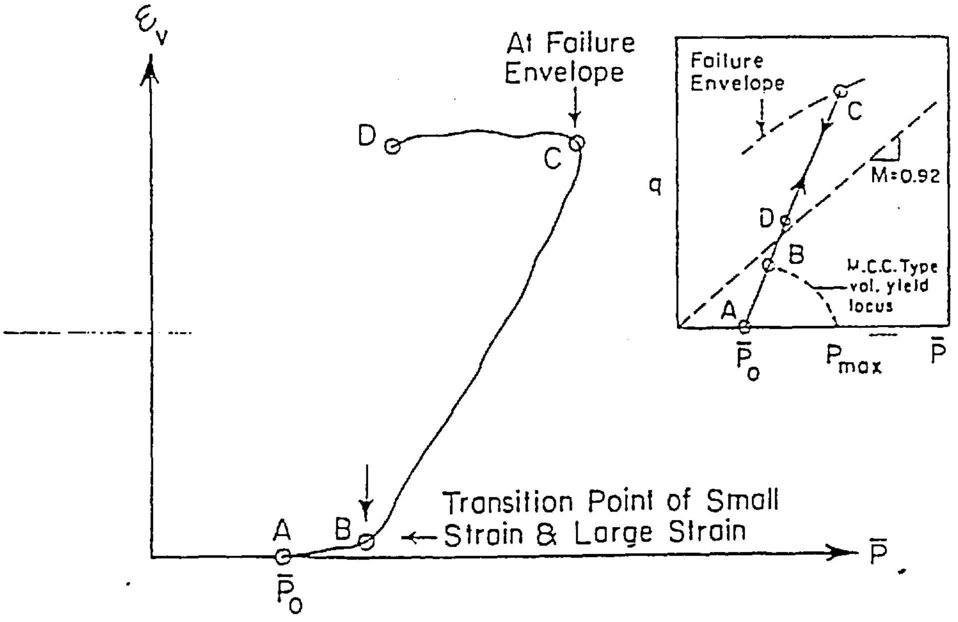

Fig. 6.27 Schematic Diagram of (ε_v, p) Relationship
Showing Transition Point

volumetric failure strain. Furthermore, due to enhancement of p_o, the values of ε_{vf} increase at higher rate at the low level of p_o. The values of ε_{vf} are somewhat unaffected by the value of cement content and curing time at higher values of p_o. The (e, ln p) and (e, ln q) plots indicate that the states at the peak and end-of-test conditions have projections which are curved. It is found that the curves for CID tests are different than those of CIU tests. It is noticed that the relationships (q, ε_s) and (q, ε_v) from drained test exhibit the existence of a small strain region referred to as 'Initial Small Strain Phase' at the outset of the drained shearing. This phase can be clearly discerned in (q, ε_v) relationships. The stress state at transition point has been found to be affected mainly by cement content and curing time. The stress-dilatancy relationships (Figs. 6.28 and 6.29) for the treated and untreated clay show some specific pattern in the plane of (τ/σ_N, $d\varepsilon_N/d\gamma$) relationship. The variation of the relationship between stress ratio (τ/σ_N) and strain increment ratio ($-d\varepsilon_N/d\gamma$) can be categorized with respect to cement content and curing time. The stress-dilatancy for untreated normally consolidated clay is linear and that for treated clay is expressed by the dotted line at the initial stage of shearing and then the relation coincides with the untreated line XY after the dotted line intersects with the solid line. The larger the cement content and curing time are, the higher the stress ratio at the intersection is, as shown in Fig. 6.29 (lines A, B, C)..

6.12 DRY JET MIXING METHOD

Deep mixing method may be classified into two categories, namely: a) mechanical mixing method and b) slurry jet mixing method. Chida (1982) proposed a method that uses cement powder or quicklime instead of slurry called the "Dry Jet Mixing Method (DJM method)." In this method, the cement or quicklime powder is injected into the deep ground through a nozzle pipe with the aid of compressed air and then the powder is mixed mechanically by rotating wings. The detail of this equipment is given in Fig. 6.30. In the DJM method, no water is added to the ground, and hence, much higher improvement is expected than using slurry. When quicklime is used, the hydration process generates some amounts of heat resulting in additional drying effects to the surrounding clay and the improvement can be done more effectively (Yamanouchi et al. 1982).

For the design of dike foundations on the Ariake clay in Japan improved by DJM method, a tentative code has been proposed (Miura et al. 1986). The code states that the unconfined compression strength of improved soil in-situ should be larger than 400 kPa at 28 days curing. It is necessary to carry out a series of laboratory tests in order to estimate the appropriate percentage of quicklime to be mixed in practice that satisfies the design strength. Considering the difficulties of quality control in the deep mixing method, the strength of improved ground may be significantly lower than the laboratory test. Miura et al. (1986) showed that the laboratory strength should not be less than 4 times the design strength required in the field for a certain content of quicklime.

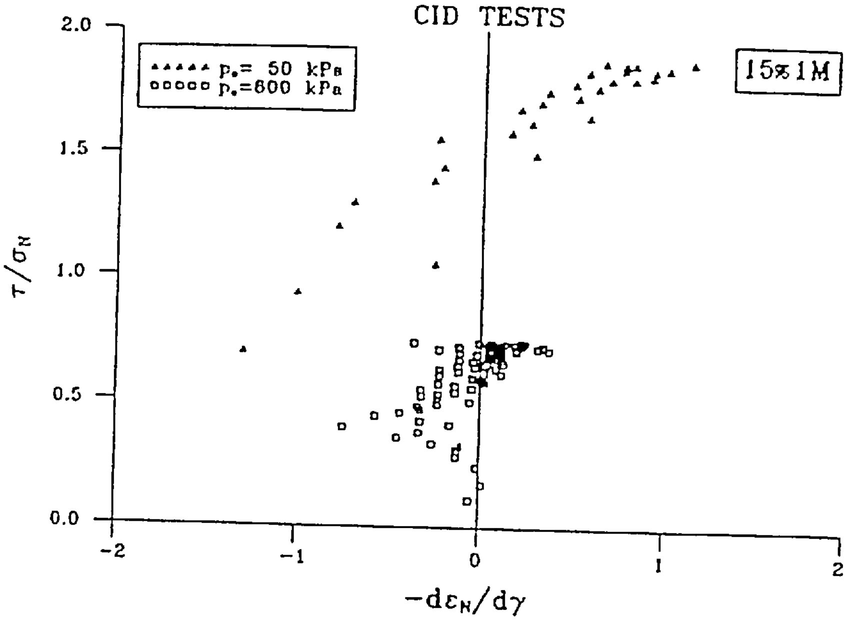

Fig. 6.28 Stress-Dilatancy Relationships on Spatial Mobilized Plane (A_w = 15% and t = 1 Month)

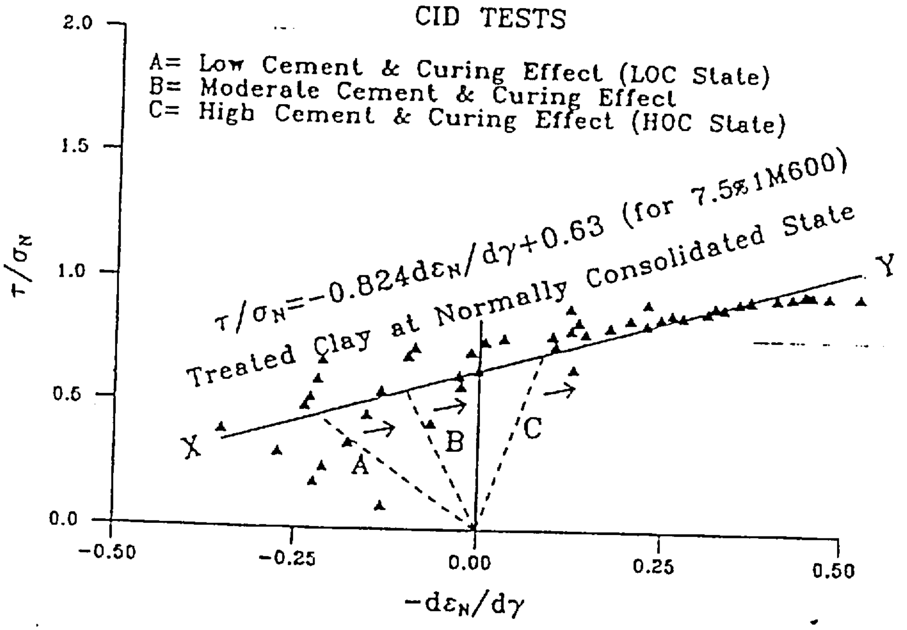

Fig. 6.29 Generalized Stress-Dilatancy Relationships on Spatial Mobilized Plane

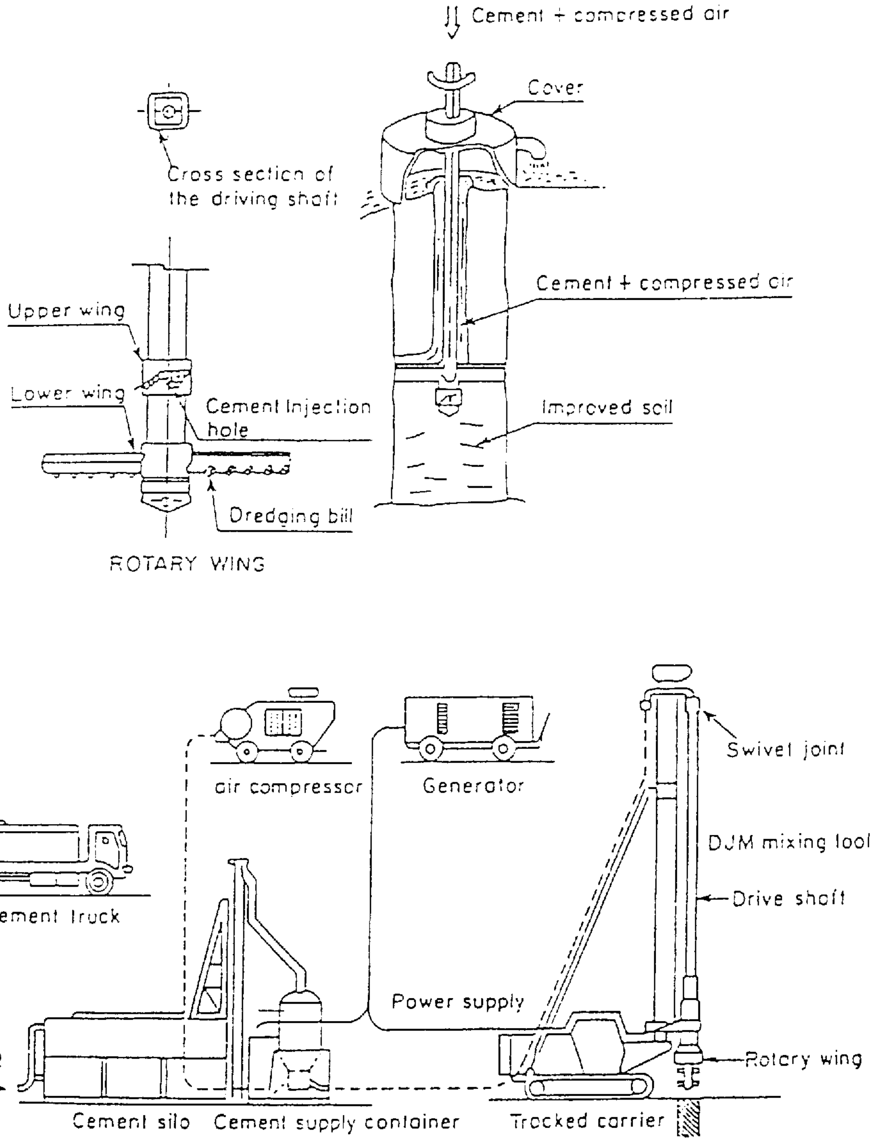

Fig. 6.30 Installation of Cement Column by DJM (DJM Research Group. 1984)

6.13 WET JET MIXING METHOD

Another improvement method is the Wet Jet Mixing (WJM) method or slurry jet grouting method in which slurry lime/cement is jetted into the clay by a pressure of 20 MPa from a rotating nozzle (Chida, 1982). In this method, the machine is relatively light and easy to carry to the project site. A jet grouting system is shown in Fig. 6.31. The main disadvantage is that the diameter of improved column tends to vary with depth according to the variations of the subsoil shear strengths.

A case study is presented by Miura et al. (1987) concerning a site in Ariake clay, Japan. Table 6.3 presents the basic properties of the clay and Fig. 6.32 shows the relevant soil properties with depth. It was found that the field to laboratory strength ratio averaged to about 70 percent. In this case, it was decided to add 190 kg of cement per cubic meter of clay in slurry of water/cement ratio of 2.3.

Table 6.3 Physical Properties of Ariake Clay

Depth (m)	Water Content (%)	Liquid Limit (%)	Plastic Limit (%)	Plastic Index (%)	Liquidity Index
2.5	162	125	55	70	1.57
6.5	122	97	43	54	1.46
10.5	108	79	39	40	1.73

A case of jet grouting work on soft Bangkok clay to stabilize an excavation project is shown in Fig. 6.33. An schematic diagram of the equipment for jet grouting is shown in Fig. 6.34. In this project, 150 kg of cement per cubic meter of clay was added for a water/cement ratio of 1.11. The average diameter of the resulting cement columns was 1.6 m with center to center spacing of 1.4 m. Up to 40 m of cement stabilized columns can be completed in one day.

6.14 TEST EMBANKMENT ON DMM IMPROVED SOFT BANGKOK CLAY

A full scale test embankment, 5.0 m high, was constructed on soft Bangkok clay improved with deep mixing method (dry method) using cement powder by Honjo et al. (1991). The plan and sections of the test embankment is shown in Fig. 6.35. The cement piles were constructed in two different patterns such as the wall type (south side) and the pile type (north side). The lateral movements and settlements of the wall type improved ground are less than that of pile type improved ground when subjected to the same loading conditions as shown in Figs. 6.36 and 6.37, respectively. Furthermore, the deformation pattern of the pile type is tilting, i.e. simple shear deformation. On the other hand, the deformation pattern of the wall type was sliding. Thus, the wall type is more effective in reducing the lateral and vertical deformation. The unconfined compressive strength in the laboratory-mixed stabilized soil was up to 20 times the original value for 28 days curing for cement content of 10 percent (100 kg of Portland cement to 1.0 cubic meter of clay). The in-situ strength was found to be one-half

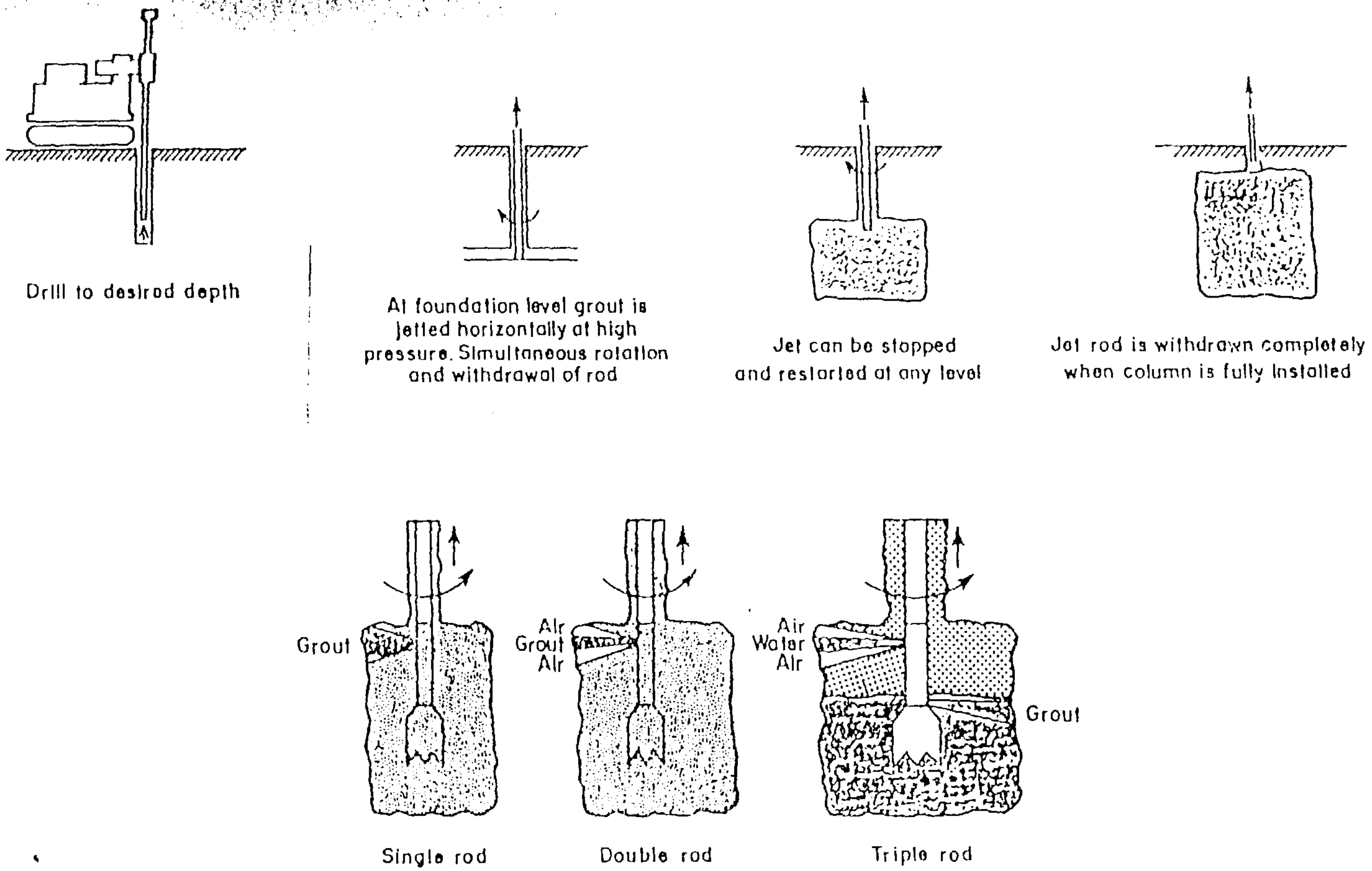

Fig. 6.31 Jet Grouting Systems

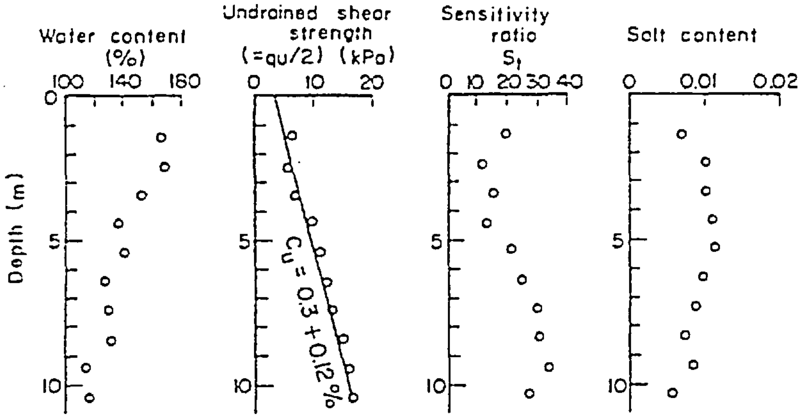

Fig. 6.32 The Properties of the Clay in Ariake District

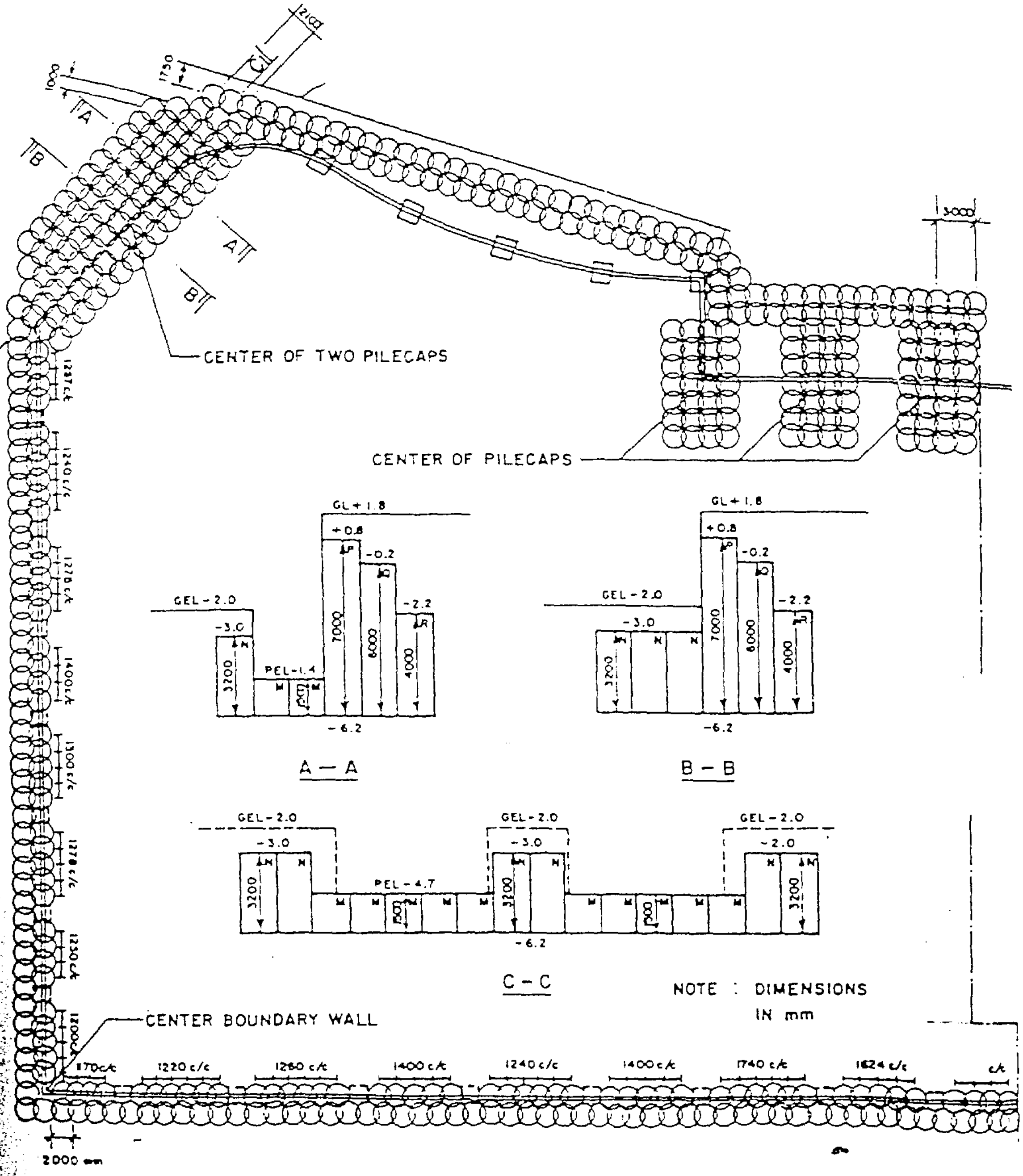

Fig. 6.33 Jet Grouting Layout

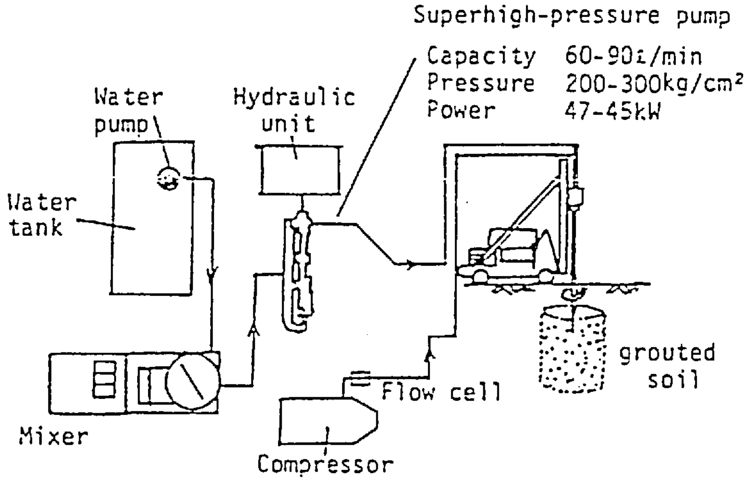

Fig. 6.34 Equipment Used for Jet Grouting

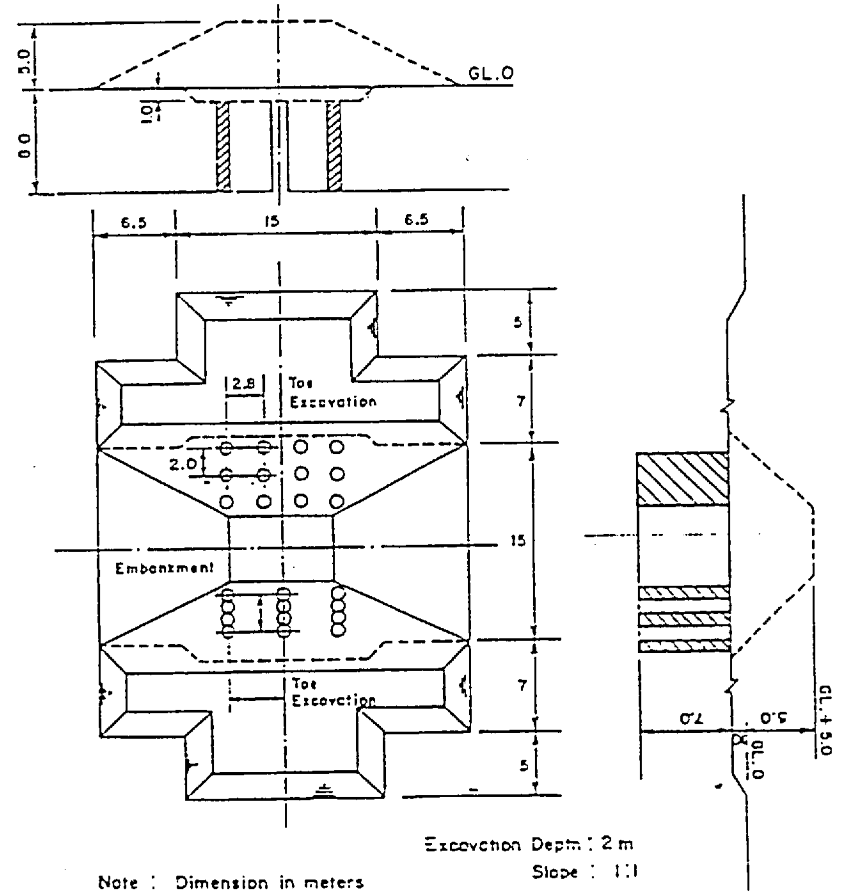

Excavation Depth : 2 m
Slope : 1:1

Note : Dimension in meters

Fig. 6.35 Plan and Section of the Test Embankment with Soil-Cement Piles

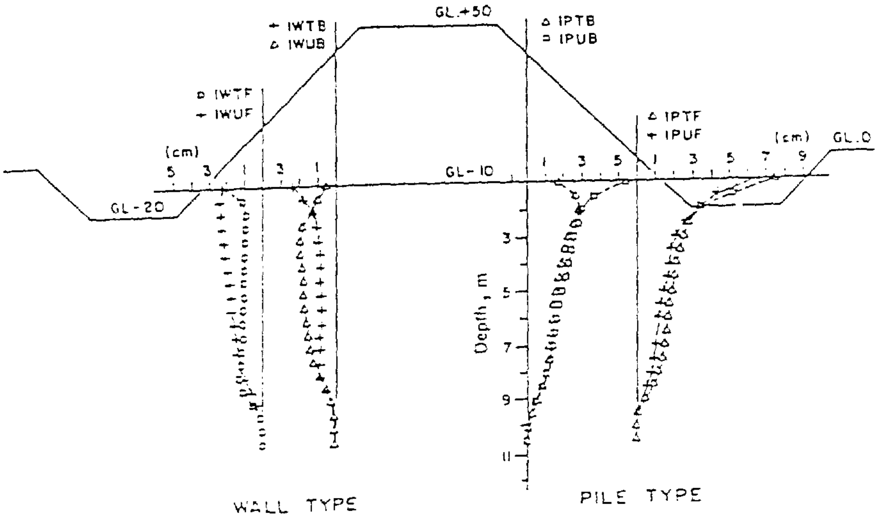

Fig. 6.36 Comparison of Lateral Movement on Improved and Unimproved Ground (71 days)

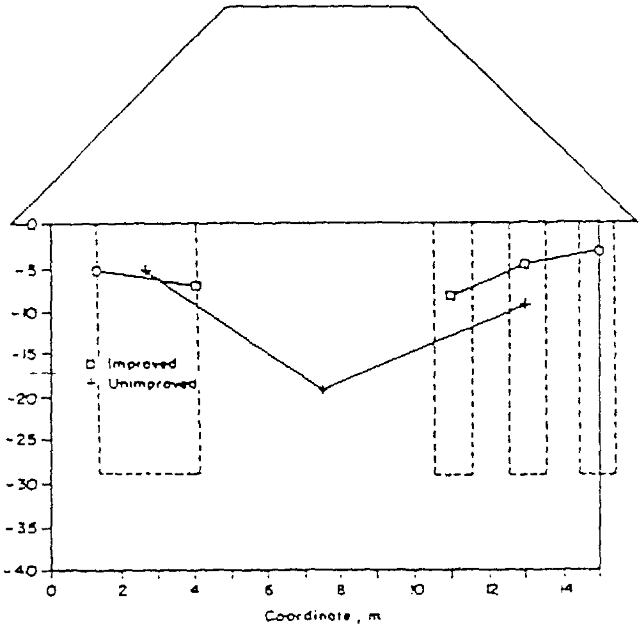

Fig. 6.37 Comparison of Settlement of Improved and Unimproved Parts at 1 m Depth (71 days)

of the corresponding laboratory test results. Figure 6.38 shows a photograph of the equipment to install the cement piles using DMM method.

6.15 CALCULATION METHODS FOR LIME COLUMNS

6.15.1 Ultimate Bearing Capacity of Single Lime Column

The bearing capacity of a single lime column is either governed by the shear strength of the surrounding soft clay (soil failure) or by the shear strength of the column material (column failure). The former mode of failure depends on both the skin friction resistance along the surface of the column and on the point resistance, while the later depends on the shear strength of the column material. The short-term ultimate bearing capacity of a single column in soft clay at soil failure can be calculated from the given expression:

$$Q_{ult,soil} = (\pi d H_{col} + 2.25\pi d^2)C_u \qquad (6.18)$$

where d is the diameter of the column, H_{col} is the column length, and C_u is the average undrained shear strength of the surrounding soft clay as determined by field tests, e.g., fall-cone and vane shear tests. It has been assumed that the skin resistance is equal to the undrained strength of the clay (C_u) and that the point resistance corresponds to 9 C_u. Experience with driven piles indicated that the skin friction resistance of the single column corresponds to at least the undrained shear strength of the surrounding soft clay when C_u is less than 30 kPa. When the undrained shear strength exceeds 30 kPa, a reduced shear strength, e.g. 0.5 C_u, should be used in the calculation of skin resistance. The point resistance of floating columns which do not penetrate the compressible strata is generally low compared with the skin resistance. A high point resistance is expected when the column extends through the compressible strata down to the underlying firm layer with high bearing capacity. A large part of the applied load will be transferred to the underlying soil through the bottom of the column. However, the point resistance cannot exceed the compressive strength of the column.

For the case where bearing capacity is governed by column failure, the behavior of the column material is considered to be similar to that of a stiff fissured clay. This was observed based from load tests on single excavated columns which indicated that failure takes place along the joint planes in unconfined columns and that the shear strength along the joints or fissures will govern the compressive strength rather than the shear strength of the clay matrix in the lumps or aggregates. The shear strength of the clay matrix in the lumps or aggregates represents an upper limit. This limit as determined by fall-cone or vane shear tests is about two or four times the shear strength along the joints as determined by unconfined compression tests. The corresponding failure envelope is shown in Fig. 6.39. The short term ultimate bearing capacity at column failure at depth z can be estimated from the relationship:

$$Q_{ult,col} = A_{col}(3.5C_{col} + 3\sigma_h) \qquad (6.19)$$

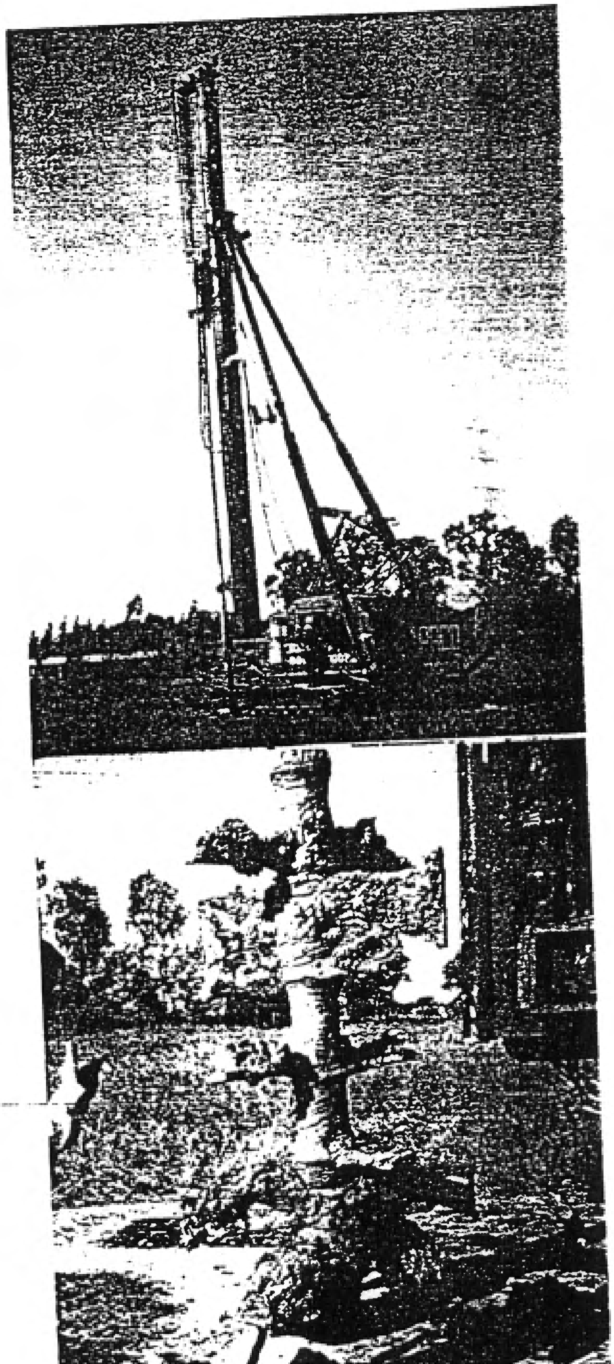

Fig. 6.38 Installation of Cement Piles by DMM Method

where C_{col} is the cohesion of the column material and σ_h is the total lateral pressure acting on the column at critical section. It has been assumed that the angle of internal friction of the soil is 30°. The factor 3 corresponds to the coefficient of passive pressure, K_p, at $\phi_{u,col} = 30^o$. It has also been assumed that $\sigma_h = \sigma_v + 5\ C_u$, where σ_v is the total overburden pressure and C_u is the undrained shear strength of the surrounding unstabilized clay. It is proposed for the time being that only the total overburden pressure should be used in design because of the large lateral displacement required to mobilize the passive earth pressure.

The long-term ultimate strength of the columns may be lower than the short-term strength due to creep. The creep strength of the columns $Q_{creep,col}$ is 65% to 85% of $Q_{ult,col}$. The load-deformation relationship shown in Fig. 6.40 is normally used to calculate the load distribution assuming that the load-deformation relationship is linear up to the creep, $Q_{creep,col}$of the columns and that the slope corresponds to the compression modulus of the column material. When the creep strength is exceeded, the load in the columns assumed to be constant.

6.15.2 Ultimate Bearing Capacity of Lime Column Groups

The ultimate bearing capacity of lime column groups depends on both the shear strength of the untreated soil between the columns and on the shear strength of the column material. Failure is either governed by the bearing capacity of the block with lime columns (Fig. 6.41a) or by the local bearing capacity of the block along the edge (Fig. 6.41b) when the spacing of the lime column is large. In certain cases, shear resistance along a failure surface which cuts through a whole block may govern the bearing capacity. The ultimate bearing capacity of the lime column group at block failure is given as:

$$Q_{ult,group} = 2C_uH[B+L]+(6\ \text{to}\ 9)C_uBL \qquad (6.20)$$

where B, L, and H is the width, length and height of the column group, respectively. The factor 6 corresponds for a rectangular foundation where the length is large compared with the width (i.e. L > > B), while the factor 9 corresponds for a square foundation. It is suggested that end bearing resistance should not be utilized in the design because a relatively large deformation of about 5-10% of the width of the loaded area is required to mobilize the maximum bearing resistance. The ultimate bearing capacity with respect to a local failure along the edge of the lime column block depends on the average shear strength of the soil along the approximately circular failure surface as shown in Fig. 6.41b. This average shear strength can be calculated in the same way as for the slope stability (see Eq. 6.29). The ultimate bearing capacity with respect to local failure can be estimated from the expression:

$$q_{ult} = 5.5C_{av}(1+0.2\frac{b}{l}) \qquad (6.21)$$

where b and l are the width and the length of the locally loaded area, respectively, and C_{av} is the average shear strength along the assumed failure surface. The average shear strength of the

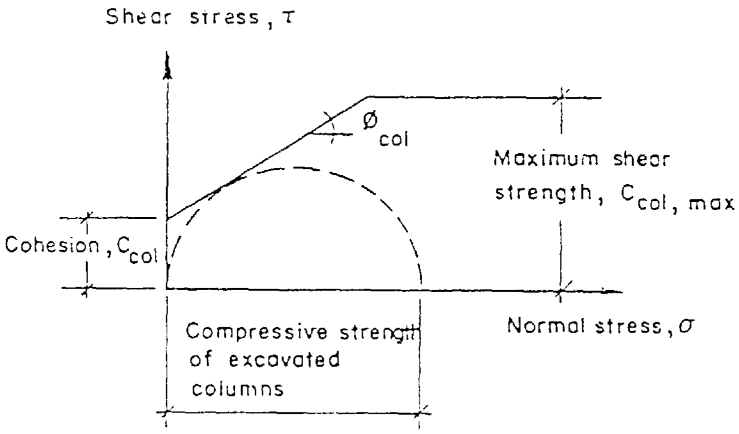

Fig. 6.39 Assumed Failure Diagram of Lime Stabilized Soil

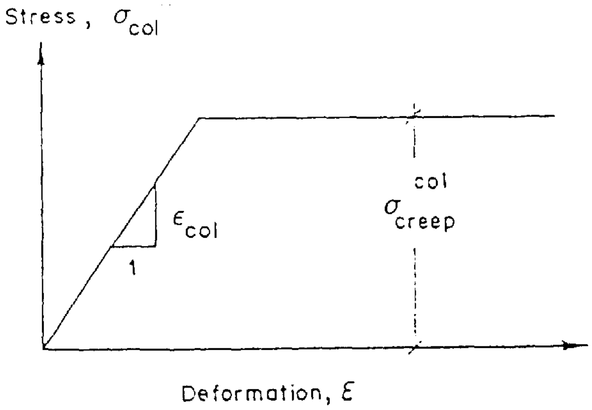

Fig. 6.40 Assumed Stress-Strain Relationship of Lime Stabilized Soil

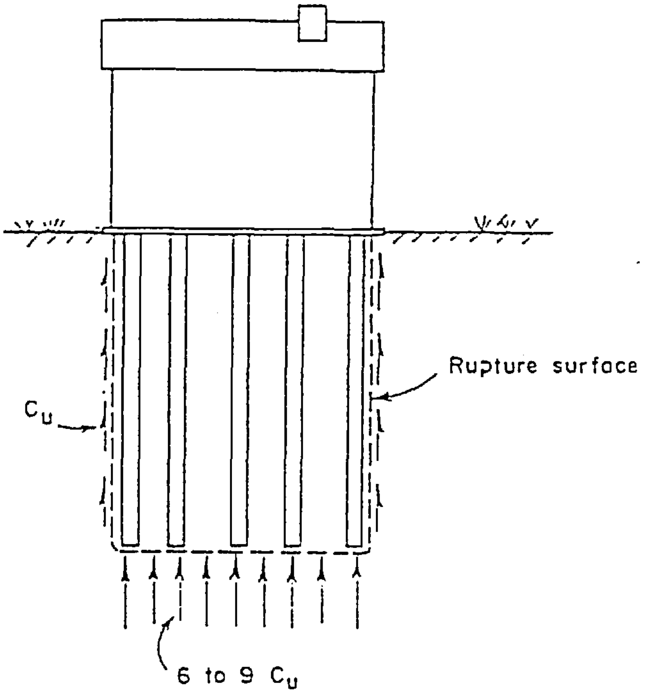

a) Block failure

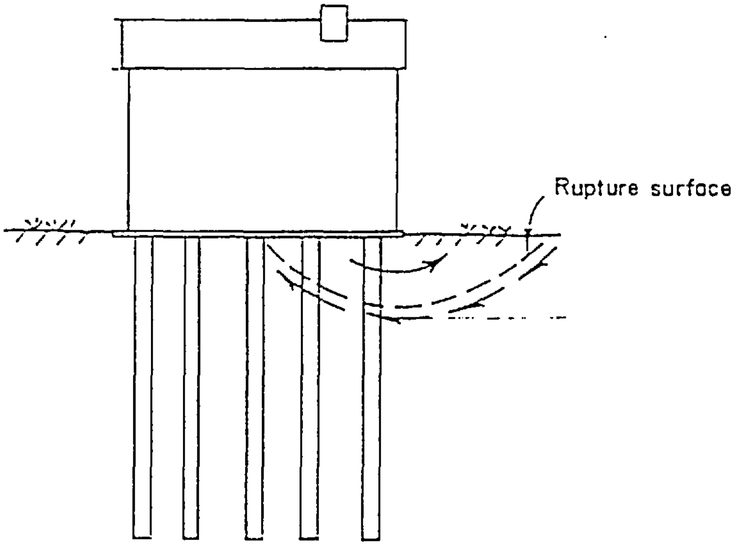

b) Local shear failure

Fig. 6.41 Failure Modes of Lime Column Foundations stabilized area is affected by the relative column area, a, (b x 1) and by the shear strength of the column material. A factor of safety equal to 2.5 is proposed to be used in the design calculations.

6.15.3 Total Settlements

The total settlement of a structure supported on lime columns can be calculated as illustrated in Fig. 6.42. The maximum total settlement is taken equal to the sum of the local settlement of the reinforced block (Δh_1) and the local settlement of the unstabilized soil below the block (Δh_2). Two cases have to be investigated for the calculation of total settlement. In the first case (case A), the applied load is relatively low and the creep of the columns will not be exceeded. In the second case (case B), the applied load is relatively high and the axial load in the columns will correspond to the creep limit.

Previous studies indicate that the columns and the untreated soil between the columns deform as a unit and that the axial shortening of the columns corresponds to the settlement of the surrounding soil. However, it was also reported that the vertical deformation of the surrounding soil closed to the ground surface has been somewhat larger than the axial deformation of the columns. The maximum difference, though, is only a few percent of the total settlement even when the spacing of the columns is 3 to 4 diameters (1.5 to 2 m). When the axial shortening of the column corresponds to the settlement of the surrounding soil, the load distribution will depend on the relative stiffness of the column material with respect to the surrounding untreated soil as long as the axial stress in the columns (σ_{col}) is less than the creep limit of the material of the lime column ($\sigma_{col,creep}$). The load distribution will then depend on the compression modulus of the column material and of the stabilized soil. At the same relative deformation, the axial stress in the columns is expressed as:

$$\sigma_{col} = \frac{Q_{col}}{A_{col}} = \frac{q}{a + (\frac{M_{soil}}{M_{col}})(1-a)} \qquad (6.22)$$

where q is the average contact pressure, a is the relative column area, (NA_{col}/BL) which is the ratio of the total area of the columns (NA_{col}) and the stabilized area (BL), M_{soil} and M_{col} are the compression moduli of the surrounding soil and of the column material, respectively.

<u>Case A</u>: In this case the relative stiffness of the columns with respect to the unstabilized soil will govern the load distribution between the columns and the enclosed unstabilized soil. The relationship M_{col} = 50 to 100 C_{col} is often used to estimate the settlements where M_{col} is the compression modulus and C_{col} is the cohesion of the column material. It is preferable, however, to evaluate M_{col} from oedometer tests. Normally, the modulus is 15 to 25 MPa. For rough calculations, a value of 20 MPa may be used. The average axial stress in the columns is governed by the compression modulus ($M = \Delta\sigma/\Delta\varepsilon$) of the surrounding unstabilized clay. When the clay is overconsolidated and the preconsolidation pressure will not be exceeded, the compression modulus can be estimated from the empirical relationship, $M_{soil} = 250C_u$, where C_u is the undrained shear strength of the surrounding clay as determined by field vane tests. When the soil is normally consolidated or slightly overconsolidated, the compression

modulus should be estimated from oedometer tests. For soft Bangkok clay, the empirical relationship based from back-analyzed data, $M_{soil} = 150C_u$, may be used.

The stress increase, q, caused by a structure or a fill, is carried partly by the columns (q_1) and partly by the surrounding soil (q_2). At the same relative displacement, the following relationship can be derived:

$$\frac{q_1(BL)}{NA_{col}(M_{col})} = \frac{q_2(BL)}{(BL - NA_{col})M_{soil}} \tag{6.23}$$

which is simplified to:

$$\frac{q_1}{aM_{col}} = \frac{q_2}{(1-a)M_{soil}} \tag{6.24}$$

The local settlement, Δh_1 (see Fig. 6.42), can then be calculated by the expression:

$$\Delta h_1 = \frac{qH}{aM_{col} + (1-a)M_{soil}} \tag{6.25}$$

The stress increase, q, is assumed constant throughout the height of the block and that the load in the block is not reduced by the perimeter shear stress. This is a conservative assumption.

The local settlement, Δh_2, below the block can be calculated in the same way as at a standard settlement calculation. The increase in stress at any point below the block can be estimated by the 2:1 method as illustrated in Fig. 6.42. The settlement reduction ratio (β) which is the ratio of the total settlements down to the bottom of the reinforced block with and without lime columns can be estimated from the relationship:

$$\beta = \frac{M_{soil}}{aM_{col} + (1-a)M_{soil}} \tag{6.26}$$

Case B: In this case the applied load is so high that the axial load in the columns corresponds to the creep limit. The settlement, Δh_1, can be calculated as illustrated in Fig. 6.43. The applied load is divided into one part, q_1, which is carried by the columns and a second part, q_2, which is carried by the surrounding soil, exactly the same as Case A. The part q_1, is governed by the creep load of the columns given as:

$$q_1 = \frac{NQ_{creep\ col}}{BL} \tag{6.27}$$

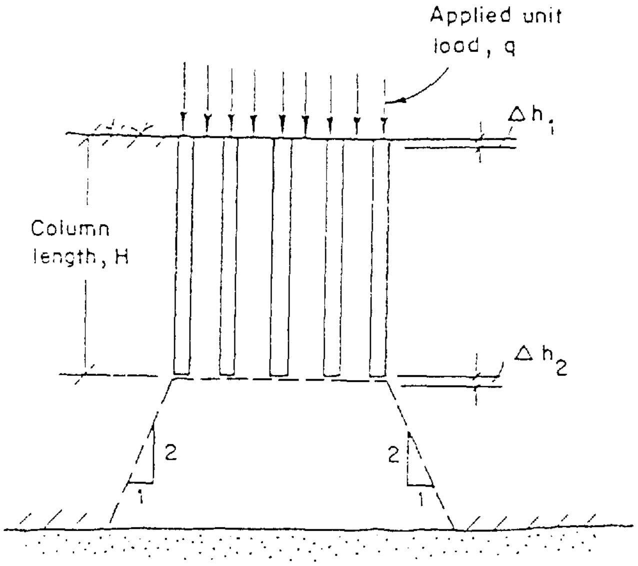

Fig. 6.42 Calculation of Settlement When the Creep Strength of Lime Columns is Not Exceeded

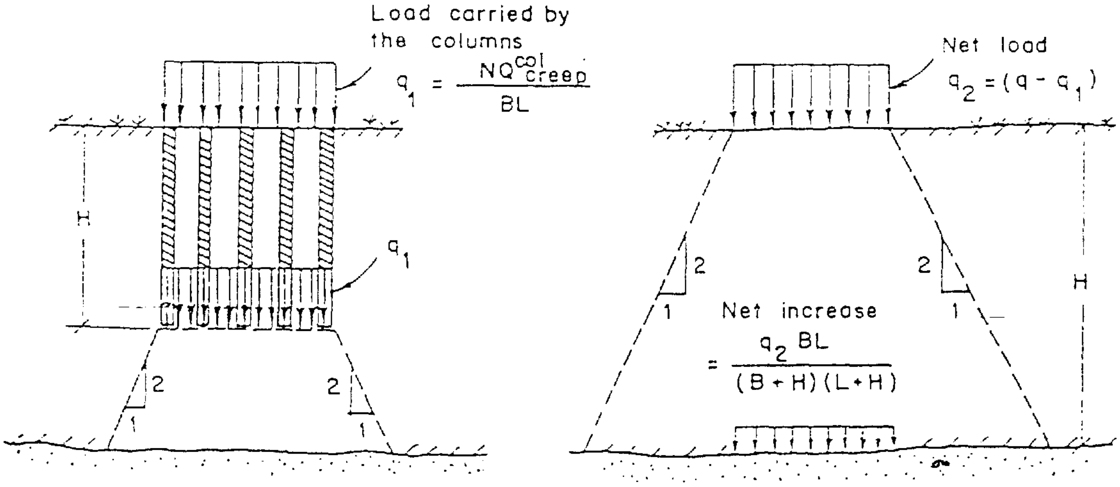

a. Load carried by the lime columns

b. Load carried by the unstabilized clay between columns

Fig. 6.43 Calculation of Settlement When the Creep Strength of Lime Columns is Exceeded where N is the total number of columns. The part $q_2 = q - q_1$, can be used to calculate the local settlement, Δh_1, down to the bottom of the reinforced block. This settlement can be determined by dividing the block into layers. The settlement of each layer is calculated separately.

The settlement, Δh_2, below the reinforced block can be calculated from the assumption that load q_1 is transferred down to the bottom of the reinforced block, while load q_2 is acting at the ground surface.

6.15.4 Differential Settlements

The differential settlements will be small as long as the average shear stress along the perimeter of the reinforced block is less than the average shear strength of the surrounding clay. The angle change (α) between two column rows (refer Fig. 6.44) will be proportional to the average shear stress (τ_{ave}) along the perimeter of the column reinforced block and an average shear modulus (G_{soil}) as expressed by the relationship:

$$\alpha = \frac{\tau_{ave}}{G_{soil}} \tag{6.28}$$

The above expression has been based on the assumption that the columns are stiff in comparison with the surrounding soil and that the contribution of the axial shortening of the columns is small and negligible. The soil between two adjacent column rows will behave in a similar way as in direct shear test. The two rows correspond to the top and the bottom parts of a direct shear box. The average shear stress in the soil corresponds to the average shear stress along the perimeter of the reinforced block.

6.15.5 Settlement Rate and Slope Stability

The rate of settlement can be estimated similar to that for vertical drains. The stability of a slope in soft clay can be improved with lime columns as illustrated in Fig. 6.45. The techniques used for stability analysis of granular piles-improved ground can be used for lime columns-stabilized ground. The average shear strength along a potential failure or rupture surface in the soil can be estimated using the following equation:

$$C_{ave} = C_u (1 - a) + S_{col}\, a \tag{6.29}$$

where S_{col} and C_u are the average strength of the column and the initial shear strength of the surrounding clay, respectively.

6.15.6 Stability of Excavation and Trenches

Lime columns can be used instead of sheet piles in deep trenches and excavations to increase the stability as illustrated in Fig. 6.46. Failure by overturning or by bottom heave

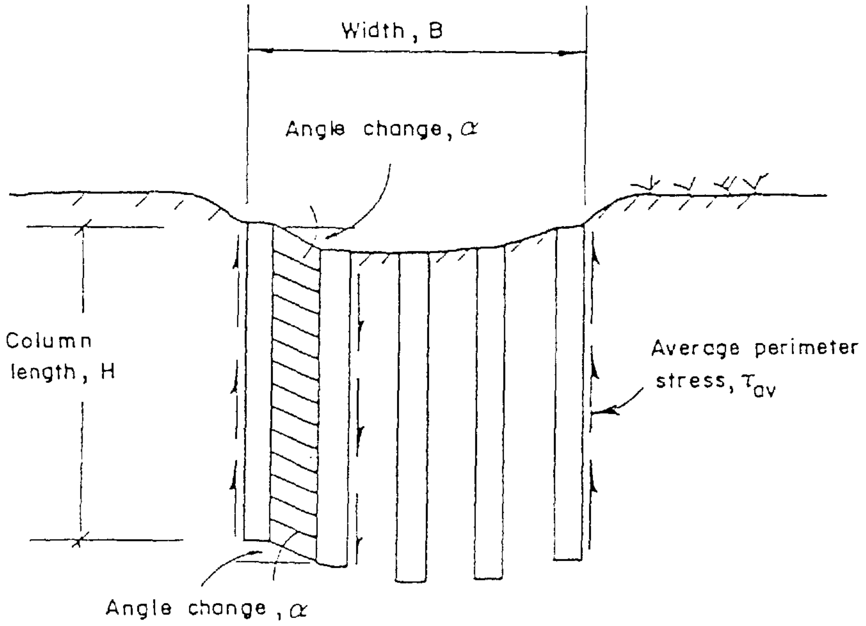

Fig. 6.44 Calculation of Differential Settlement

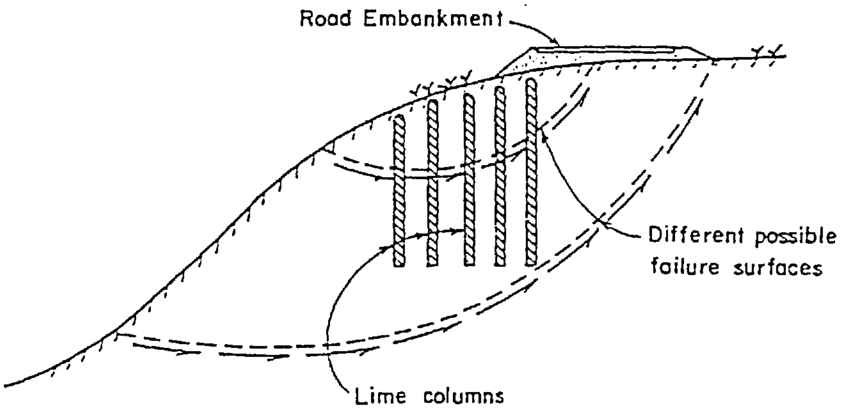

Fig. 6.45 Stabilization of a Slope with Lime Columns

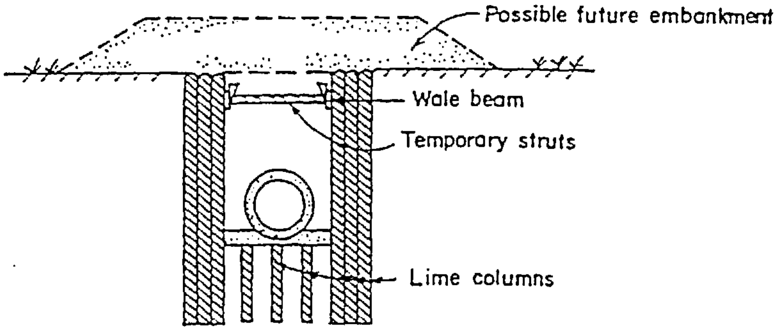

Fig. 6.46 Trench Stabilized with Lime Columns

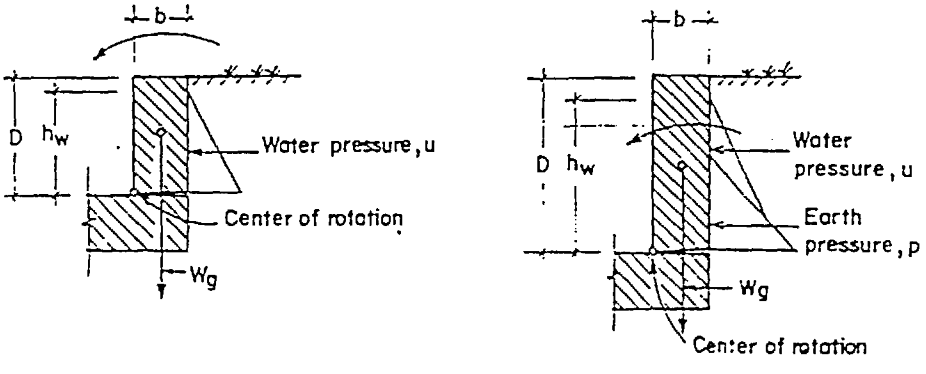

(a) $D \leq \frac{2C_u}{\rho_{soil}}$ (b) $D > \frac{2C_u}{\rho_{soil}}$

Fig. 6.47 Failure by Overturning

should be considered as well as shear failure of the lime column wall with respect to a circular or plain failure surface through the columns.

6.15.6.1 Overturning

The water and earth pressures causing failure of the column wall by overturning are resisted by the weight of the wall in the same way as gravity retaining wall. The moment preventing failure with respect to the centre of rotation should be larger than the earth pressure behind the wall as illustrated in Fig. 6.47. The centre of rotation is located at the bottom of the excavation close to the surface of the wall. When the wall is loaded by water pressure only, the following relationship had to be satisfied (Fig. 6.47a)

$$0.5\, W_g\, b > 1/6\, h_w^3 \rho_w \tag{6.30}$$

where W_g and b are the weight and width of the wall, respectively, h_w is the water level in the crack behind the wall with respect to the bottom of the excavation and ρ_w is the unit weight of water. When h_w is equal to the depth D of the excavation Eq. 6.30 is simplified to

$$b / D \geq 0.58\sqrt{\rho_w / \rho_{col}} \tag{6.31}$$

where ρ_{col} is the unit weight of the column material.

6.15.6.2 Shear Failure

The stability of a lime column wall with respect to shear failure must also be considered in the design. The stability can be calculated by assuming that failure takes place along an inclined rupture surface as illustrated in Fig. 6.48 or along a horizontal plane through the bottom of the excavation. If the cracks behind the wall are completely filled with water, the following relationship can be derived

$$h_w / b \leq \sqrt{3} + \sqrt{\frac{4c_{col}}{b\rho_w} + \frac{\rho_{col}}{\rho_w} - \frac{2D\rho_{col}}{3b\rho_w}} \tag{6.32}$$

where c_{col} is the cohesion of the column material. When (D-1.7b) is larger than $(2c_u/\rho_{soil})$, the earth pressure behind the wall will also affect the stability as illustrated in Fig. 6.48b.

6.15.6.3 Bottom Heave

Failure by bottom heave can occur when the depth of the excavation is larger than the value of $6c_u/\rho_{soil}$ and the length of the excavation is larger compared with the depth. The bottom can be stabilized with lime columns as illustrated in Fig. 6.49. When the columns overlap the undrained shear strength c_{col} of the stabilized soils in the columns will govern.

The length of the columns (H_d) which is required to prevent failure by bottom heave can be calculated from the relationship

$$H_d > \frac{BD\rho_{soil}}{2s_{col}} - \frac{3c_u B}{s_{col}} \qquad (6.33)$$

The shear strength s_{col} is affected by the normal pressure along failure surface.

6.15.7 Transfer Length and Perimeter Stress for Lime Column

The length which is required to transfer the load in a single column to the surrounding soil is relatively small due to the large surface area and high skin friction resistance in comparison with the axial load in the columns (Fig. 6.50). The lime columns and the soil enclosed by the columns act as a rigid block (Fig. 6.51) when the spacing between the individual lime columns does not exceed 1.5 -2.0 m. The columns will then function as vertical reinforcement in the soil. The interaction of the 'reinforced block' and the surrounding soil is primarily governed by the relative dimension of the block, the magnitude of the applied load and the shear strength of the surrounding untreated soil. At low load levels, the load on the block is transferred to the surrounding soil mainly through the periphery of the block (Fig. 6.51) since a very small relative displacement is required to mobilize the shear strength of the soil. The differential settlements will be small if the columns are long and the average shear stress along the perimeter of the block is less than the average shear strength (C_u) of the surrounding soil. The average shear stress along the perimeter of the reinforced block (τ_{per}) can be calculated from the expression

$$\tau_{per} = \frac{0.8W_g}{2(B+L)H} < \frac{c_u}{f_c} \qquad (6.34)$$

where B, L, and H are the width, length and height, respectively, of the block, W_g is the total weight of the structure. and f_c is a partial safety factor which should be at least 1.5.

6.16 CALCULATION METHODS FOR DEEP CEMENT MIXING (DCM)

The following methods of calculation are employed on the design procedure of wall-shaped cement pile-stabilized ground for bulkhead foundation as shown in Fig. 6.52.

6.16.1 Sliding

The factor of safety against sliding (Fig. 6.53) should exceed 1.20 in static condition and 1.0 in seismic condition.

$$FS_s = \frac{Rf + F_a + P_p(E)}{H} \qquad (6.35)$$

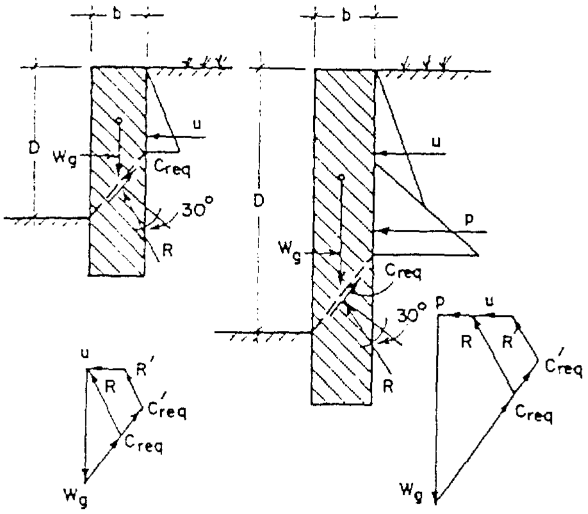

(a) $D \le \dfrac{2C_u}{\rho_{soil}} + b\sqrt{3}$ (b) $D > \dfrac{2C_u}{\rho_{soil}} + b\sqrt{3}$

Fig. 6.48 Shear Failure

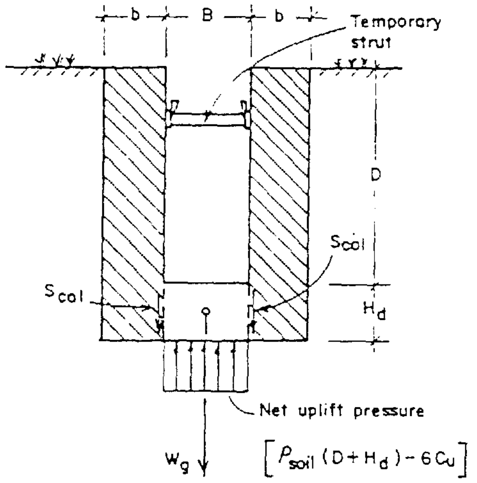

Fig. 6.49 Bottom Heave

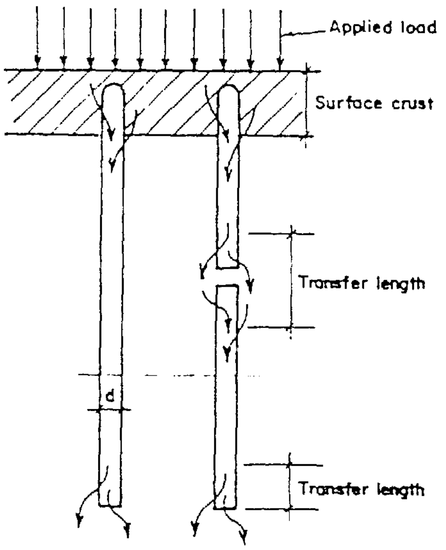

Fig. 6.50 Transfer Length for Lime Columns with Imperfections

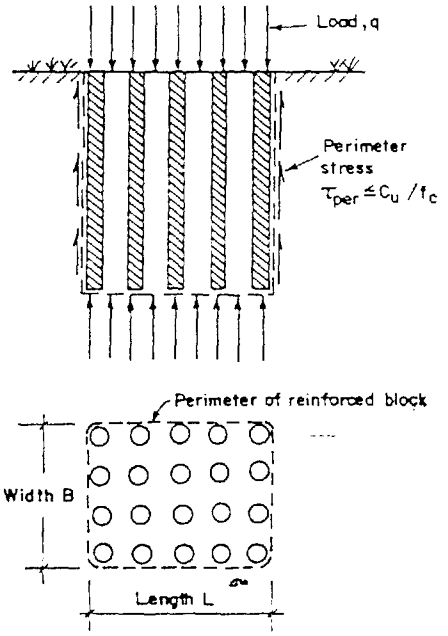

Fig. 6.51 Perimeter Shear Stress

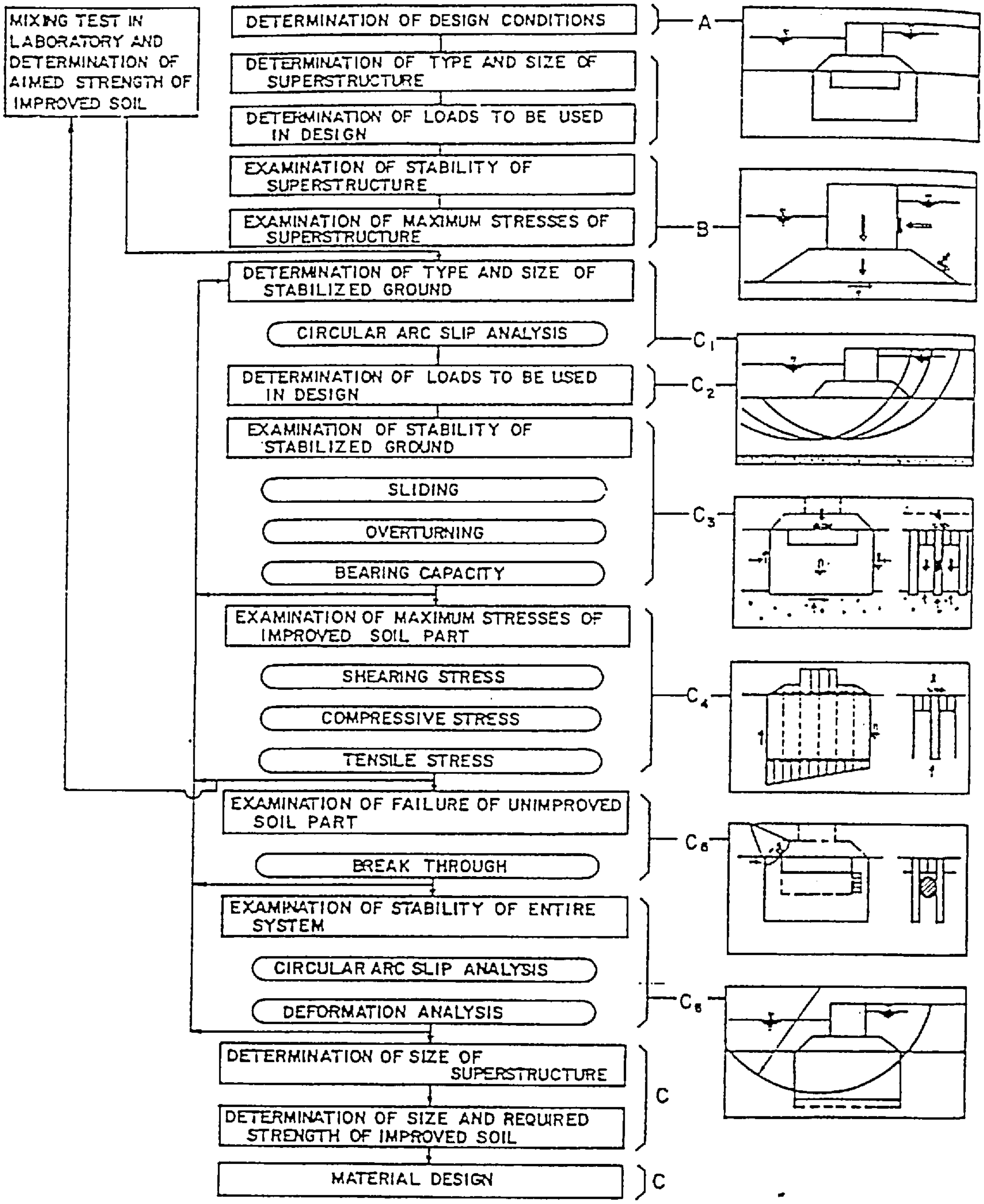

Fig. 6.52 Outline of Simplified Design Procedure

where:

N_{wt} = summation of vertical load on bottom surface of long wall
= $W_{s(E)} + W_T + P_{AV(E)}$
H = summation of horizontal loads
= $P_{AS(E)} + P_{AH(E)}$ $[+H_{WT} + H_{WS} + H_{WU}]$
( ): only in seismic condition
Rf = $N_{WT} \tan \phi$
F_u = minimum value ($W_u \tan \phi$ or $C_{(Z = D)}BLS$)
ϕ = angle of shear resistance of stiff soil layer
$C_{(Z=D)}$ = undrained shear strength of soft clayey soil at the depth of D

6.16.2 Overturning

The factor of safety against overturning should exceed 1.2 in static condition and 1.1 in seismic condition. The loads are shown in Fig. 6.54.

$$\mathbf{FS_t} = \frac{\mathbf{M_{RWT} + M_{WU}}}{\mathbf{M_D}} \tag{6.36}$$

where:

M_{RWT} = summation of resistance moments against overturning
= $M_{WT} + M_{WS(E)} + M_{pp(E)}$
M_D = summation of driving/overturning moments
= $M_{PAH(E)}$ $(M_{HWS} + M_{HWT} + M_{HWV})$
( ): only in seismic condition
M_{WT} = moment of load W_T around point o
$M_{WS(E)}$ = moment of load $W_{S(E)}$ around point o
$M_{PAV(E)}$ = moment of load $P_{AV(E)}$ around point o
$M_{PAS(E)}$ = moment of load $P_{AS(E)}$ around point o
$M_{PAH(E)}$ = moment of load $P_{AH(E)}$ around point o
M_{HWS} = moment of load H_{WS} around point o
M_{WHT} = moment of load H_{WT} around point o
M_{HWU} = moment of load H_{WU} around point o
M_{WU} = moment of load W_U around point o

6.16.3 Allowable Bearing Capacity

The allowable bearing capacity should exceed the maximum contact pressure. The contact pressures, q_1, and q_2 (see Fig. 6.55) are given as:

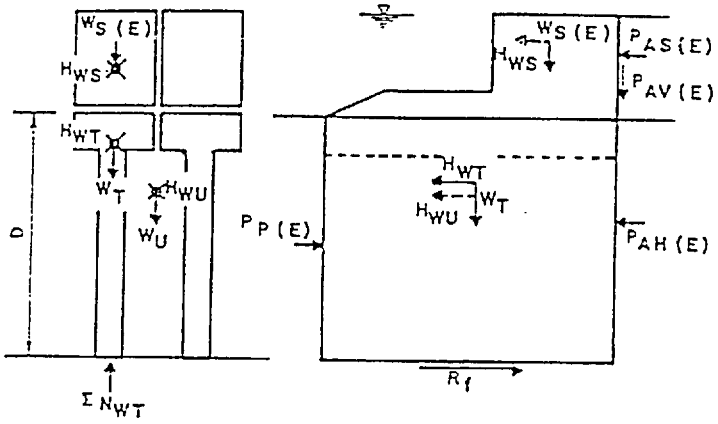

Fig. 6.53 Sliding of Stabilized Ground

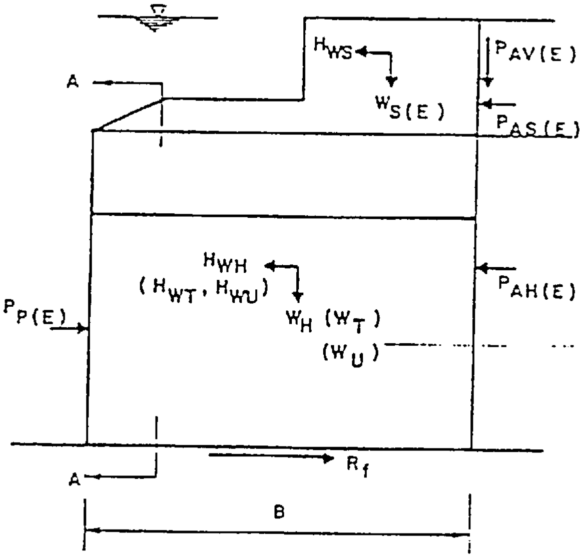

Fig. 6.54 Overturning and Resisting Loads

a) if $e_1 \leq B/6$:

$$q_1 = -\frac{N_{WT}}{BL_1}(1 \pm \frac{6e_1}{B}) \qquad (6.37)$$

b) if $e_1 > B/6$:

$$q_1 = \frac{2N_{WT}}{3d_1L_1} \qquad (6.38)$$

where:

d_1 = distance of resultant load of contact pressure $= \frac{N_{RWT} - M_D}{N_{WT} + W_U}$

e_1 = eccentric distance of resultant load of contact pressure = $B/2 - d_1$

L_1 = thickness of long wall

The allowable bearing capacity is expressed as:

$$Q_A = \frac{1}{FS}(\beta\gamma_1 L_1 N_\gamma + \gamma_2 D N_q) + \gamma_2 D \qquad (6.39)$$

where the geometric dimensions are shown in Fig. 6.56 and the parameters are defined as follows:

FS = factor of safety = 2.5 in static condition and 1.5 in seismic condition

γ_1 = total unit weight of original soil above the plane of contact pressure (bouyant unit weight below the underground water level)

γ_2 = total unit weight of original soil below the plane of contact pressure (bouyant unit weight below the underground water level)

N_γ, N_q = bearing capacity factors

ß = shape factor (0.50)

6.16.4 Maximum Vertical and Horizontal Shear Stresses

Both maximum vertical and horizontal shear stresses should not exceed the strength of the improved soil. The maximum vertical shear stress (Fig. 6.57) is given as:

$$\tau_x = \frac{Q - W}{A} \qquad (6.40)$$

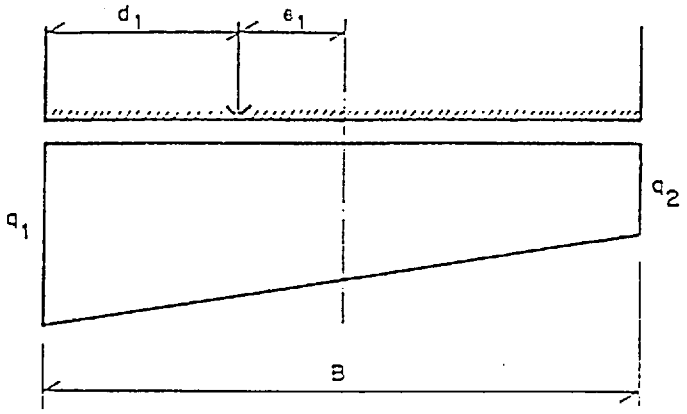

Fig. 6.55 Contact Pressure on Bottom Surface of Stabilized Ground

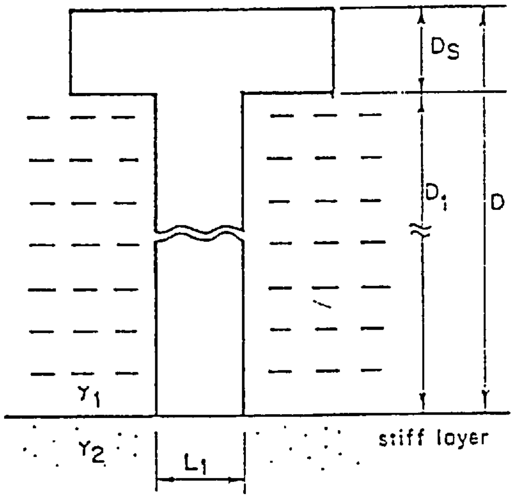

Fig. 6.56 Bearing Capacity of Stiff Layer

where:

Q = resultant load of pressure in the offshore-side vertical surface = $\dfrac{B_x(q_1 + q_x)L_1}{2}$

W = total weights of improved parts and the superstructure which is included in distance B_X

A = vertical cross-sectional area
= $LD - L_SD_1$

The maximum horizontal shear stress (Fig. 6.58) is expressed as:

$$\tau_y = \frac{P_{AS} + P_A - P_P}{A} \qquad (6.41)$$

where:

P_{AS} = horizontal load acting on superstructure

P_A = resultant load of active earth pressure and additional water pressure
$= D_y \dfrac{(P_{A1} + P_{Ay})}{2} L$

A = horizontal cross-sectional area = L_1B

6.16.5 Breakthrough of Unimproved Soil

The examination of the stability of breadthrough in the unimproved soil is shown in Fig. 6.59. It is assumed that the breakthrough of the unimproved soil between piles forms a tunnel-shaped with oval section in direction to the offshore-side. The factor of safety against this type of failure must exceed 2.5 in static condition and 1.5 in seismic condition. The factor of safety is expressed as:

$$FS_b = \frac{P_r}{P_d} \qquad (6.42)$$

where:

P_r = resistant force = B_S (πa + 2ma) [C_0 + C_1 (D_S + 2(m + 1)/2]

P_d = breakthrough force = ΔP ($\pi a^2/4 + ma^2$)

ΔP = lateral force increment on backfill side of stabilized ground

B_S = width of short wall

D_S = height of short wall

a = thickness of unimproved part (soft original soil between improved soil parts)

m = shape factor = $\dfrac{\pi}{4}\sqrt{1 + \dfrac{8}{a}(\dfrac{C_0}{C_1} + D_s - \dfrac{\pi - 2}{4}a)} - 1$

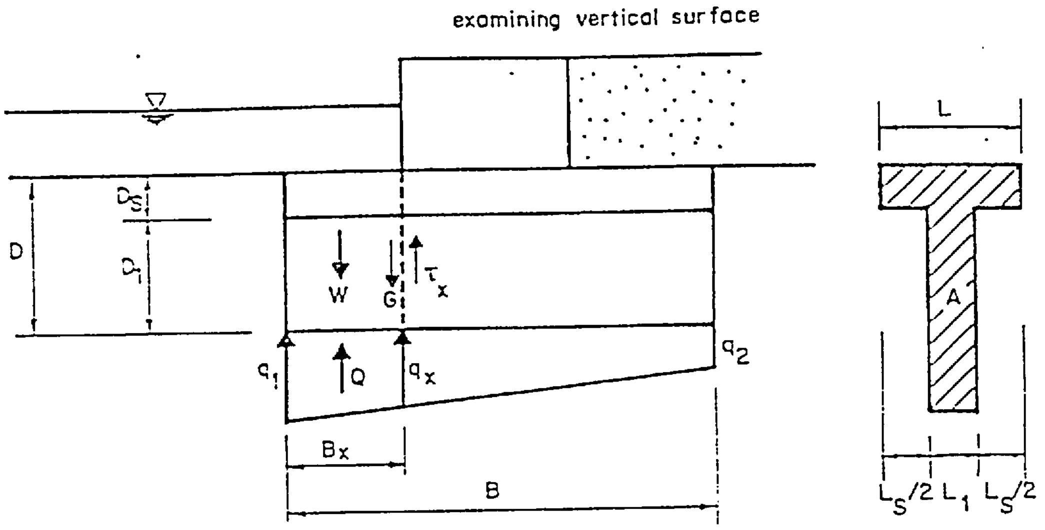

Fig. 6.57 Examination of Vertical Shear Stress

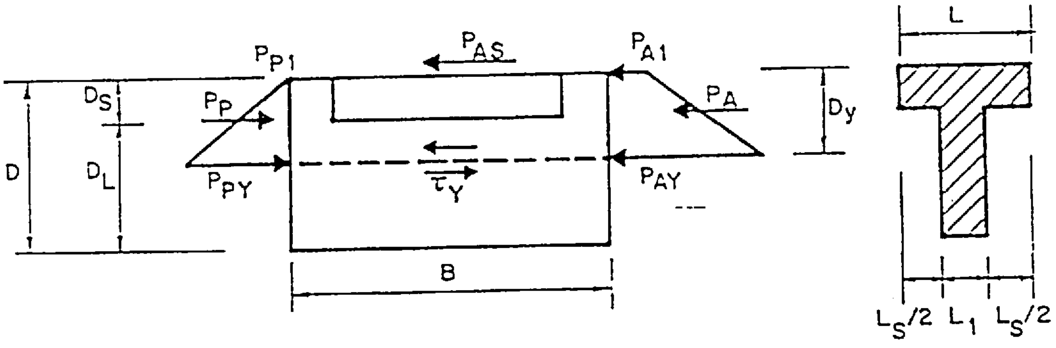

Fig. 6.58 Examination of Horizontal Shear Stress

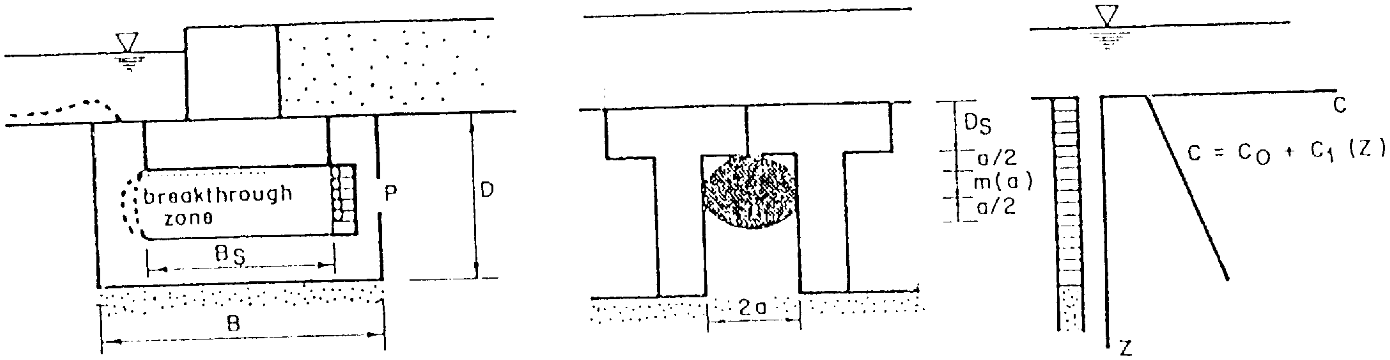

Fig. 6.59 Examination of Breakthrough of Unimproved Part

6.17 CONCLUSIONS

The use of lime and/or cement deep mixing method proved to be effective methods of improving the properties of the soft Bangkok clay. With the addition of 5 to 10% quicklime, which is the optimum mix proportions, the unconfined compressive strength increased to about 5 times. Moreover, the preconsolidation pressure improved to as much as 3 times while the coefficient of consolidation increased by 10 to 40 times. The effective strength parameters also increased wherein the angle of internal friction increased by about 67%. Mixing 10% of cement with soft Bangkok clay improved the unconfined compression strength and the preconsolidation pressure up to 10 to 20 times and by 2 to 4 times, respectively. The coefficient of consolidation increased by 10 to 40 times. From UC tests, overall consideration suggested that the percentage of cement (by weight) of 10% to 15% and and curing time of 1 to 2 months can be treated as optimum. Oedometer test results showed that cement treatment caused substantial improvement of consolidation properties, enhancement of preconsolidation pressure, reduction of compression index and simultaneously raised the value of coefficient of consolidation (Cv). The normalized intrinsic compression curves of the treated clays and the plot of (I_V, log σ_v) in the void index plane confirmed of the hardening effect brought about by cement treatment.

The strain paths from constant stress ratio (CSR) tests showed bilinear characteristics. The locus of transition point of strain paths are similar to the limit state curves for natural clays. The configuration and orientation of these loci of transition points are mainly controlled by the cement content and the curing time. Heavily overconsolidated behavior was observed inside the locus of transition points. The stress-dilatancy relationships showed that Modified Cam Clay provides a relationship at lower stress ratio than the experimental curves. From triaxial tests, it was observed that cement treatment causes transformation of the initial normally consolidated characteristics of the base clay to lightly overconsolidated and then to heavily overconsolidated rendering more stiffness and rigidity of the clay with increasing cement content, Aw, and time, t. The degree of overconsolidation was noticed to be affected by the A_W, t, p_o and applied stress path. In the initial small strain phase, the generation of pore pressure remains very small and concurrently shear strain is small and recoverable. The phase is followed by large strain phase with greater pore pressure, which is extended up to the curved failure envelope. A consistent picture of the phase transformation emerged evolving a family of loci. Outside the small strain domain, a work-hardening, elasto-plastic type of behaviour was observed. The prevalent role of p_o is to annihilate the cementation effects attributing ductility to the treated matrix. The behavior after the maximum deviator stress condition i.e. during strain softening can be regarded as an unstable phase where the stress paths fall along approximately in constant-p path up to residual states and the shear strain increases with the reduction of stress ratio. It was postulated that if complete destructuration of the treated clay could be achieved, and neglecting any permanent changes in the soil structure due to cement treatment, a destructured envelope would be achieved. At this envelope, cohesion is destroyed and the treated clay then behaves as purely frictional material. The pre-shear failure and end-of-test stress states for cement treated clays have curved projection on the (q, p) and (e, ln p) planes, showing characteristics which are typical of overconsolidated clays.

A consistent set of transition points of small strain and large strain was derived from relationships of (ε_v, p) of drained tests. The existence of the initial small strain phase is also observed at the outset part of the drained tests during strain hardening, as was discerned from the transition stress state in the relationship of (q, ε_v) which governs onset propagation of large strain of treated clays. The transition stress state was found to be affected mainly by cement content and curing time. The stress-dilatancy relationships on the spatial mobilized plane (SMP) exhibit a remarkable phenomenon such that the stress ratio, τ/σ_N, and the normal and shear strain increment vector, $-d\varepsilon_N/d\gamma$, constitute a specific correlation between treated and untreated clays. The pattern manifests gradual transformation behavior in the (τ/σ_N, $-d\varepsilon_N/d\gamma$) plane as the degree of overconsolidation of the treated mass changes. The enhancement of effective strength parameters (ϕ, c) was discerned to occur substantially after cement treatment for both the drained and undrained conditions.

The in-situ strength of the cement stabilized soft Bangkok clay was found to be one-half of the corresponding laboratory test results. Based on full-scale test embankment on soil-cement piles, the deformation of the improved ground depends on the type of construction pattern. The lateral movements and settlements of the wall type construction were lower than that of the pile type. Thus, the wall type is more effective in reducing the lateral and vertical deformation.

The method of calculating the bearing capacity of lime columns either for single column and column groups, total and differential settlements, and slope stability are presented. Methods of calculation for the design procedure of bulkhead foundation stabilized with cement piles using the Deep Cement Mixing (DCM) method is also outlined.

6.18 REFERENCES

Ariizumi, M. (1977), Mechanism of lime stabilization, J. of Japan Soc. Soil Mech. and Found. Eng'g., Tsuchi-to-Kiso, Vol. 25, pp. 9-16.

Assarson, K., Broms, B., Granholm, S., and Paus, K. (1974), Deep stabilization of soft cohesive soils, Linden Alimark, Sweden.

Balasubramaniam, A.S., and Bergado, D.T. (1984), Geotechnical problems related to construction activities in soft Bangkok clays, Proc. Symp. on Soil Improvement and Construction Techniques in Soft Ground, pp. 174-185.

Balasubramaniam, A.S., Bergado, D.T., and Sivandran, C. (1985), Engineering behavior of soils in Southeast Asia, In Geotechnical Engineering in Southeast Asia - A Commemorative Volume of the Southeast Asian Geotechnical Society, pp. 25-96, A.A. Balkema Printers.

Balasubramaniam, A.S.,Phien-wej, N., and Kuhananda, M. (1988), Coastal development in soft clay deposits, Proc. Kozai Club Seminar 1988, Bangkok, Thailand.

Balasubramaniam, A.S., Honjo, Y, Law, K.H., Phien-wej, N., and Bergado, D.T. (1989), Ground improvement techniques in Bangkok subsoils, Proc. Kozai Club Seminar 1989, Bangkok, Thailand.

Kawasaki, T., Niina, A., Saitoh, S., Suzuki, Y., and Honjo, Y. (1981), Deep mixing method using cement hardening agent, Proc. 10th. Int'l. Conf. Soil Mech. Found. Eng'g., Stockholm, pp. 721-724.

Kezdi, A. (1979), Stabilization with lime, Development in Geotechnical Eng., Vol. 19, Elsevier Scientific Publ. Co., Amsterdam, pp. 163-174.

Lea, F.M. (1956), The chemistry of cement and concrete, Edward Arnod (Publishers) Ltd., London.

Lee, H.J. (1983), Lime columns stabilization of Bangkok clay, M. Eng. Thesis, Asian Institute of Technology, Bangkok, Thailand.

Lee, S. L., Ramaswamy, S. D., and Aziz, M. A. (1982), A study of the soil type suitable for stabilization with lime, Proc. 7th Southeast Asian Geotech. Conf., Hongkong, pp. 615-629.

Law, K.H. (1989), Strength and deformation characteristics of cement treated clay, M. Eng. Thesis, Asian Institute of Technology, Bangkok, Thailand.

McDowell, C. (1959), Stabilization of soils with lime, lime flyash and other lime flyash materials, Bulletin 231, Highway Research Board, Washington, D.C., pp. 60-66.

Metcalf, J. B. (1964), The effect of high curing temperatures on the unconfined compressive strength of a heavy clay stabilized with lime and with cement, Proc. Australia-New Zealand Conf. Soil Mech. and Found. Eng'g., Vol. 4, pp. 126-130.

Mitchell, J. K., Veng, T. S., and Monismith, C. L (1974), Behavior of stabilized soils under repeated loading, Dept. of Civil Eng'g., Univ. of California, Berkeley, Calif.

Miura, N., Koga, Y., and Nishida, K. (1986), Application of a deep mixing method with quicklime for the Ariake clay ground, J. of Japan Soc. Soil Mech. and Found. Eng'g., Vol. 34, no. 4, pp. 5-11.

Miura, N., Bergado, D.T., Sakai, A., and Nakamura, R. (1987), Improvements of soft marine clays by special admixtures using dry and wet jet mixing methods Proc. 9th Southeast Asian Geotech. Conf., Bangkok, Thailand, pp. 8-35 to 8-46.

Okamura, T., and Terashi, M. (1975), Deep lime mixing method of stabilization for marine clays, Proc. 5th Asian Reg. Conf. Soil Mech. and Found. Eng'g., Bangalore, India, Vol. 1, pp. 69-75.

Roscoe, K. H., Schofield, A. N., and Thurairajah, A. (1963), Yielding of clays in states wetter than critical, Geotechnique, Vol. 13, pp. 211-240.

Ruff, C. G., and Ho, C. (1966), Time-temperature strength-reaction product relationships in lime-bentonite-water mixtures, Highway Research Record No. 139, Behavior Characteristics of Lime-Soil Mixtures, Highway Research Board, Washington, D.C., pp. 42.60.

Saitoh, S., Suzuki, Y., and Shirai, K. (1985), Hardening of soil improvement by deep mixing method, Proc. 11th Intl. Conf. Soil Mech. and Found. Eng'g., Helsinki, Finland, pp. 947-950.

Suzuki, Y. (1982), Deep chemical mixing method using cement as hardening agent, Proc. Symp. on Soil and Rock Improvement Techniques Including Geotextiles, Reinforced Earth and Modern Piling Method, AIT, Bangkok, Thailand.

Taylor, W. H., and Arman, A. (1960), Lime stabilization using preconditioned soils, Bulletin No. 262, Highway Research Board, Washington, D.C., pp. 1-11.

Chapter 7

MECHANICALLY STABILIZED EARTH (MSE)

7.1 GENERAL

Mechanical stabilization of soils by reinforcement with foreign materials is not a new idea, but has been used since time immemorial. The quality of adobe bricks has been improved by adding straw. Mechanically stabilized earth (MSE) consists of reinforcing the soil using polymer, steel, or natural materials. The reinforcement which is strong in tension effectively combines with the soil which is strong in compression, forming a semi-rigid composite material. A French engineer, Henry Vidal, was the first to formalize the rational design of modern reinforced earth with his patented "Reinforced Earth" technique (Vidal, 1969). In this technique, a strip metal reinforcement usually made of galvanized steel is inserted into high quality backfill soil materials consisting of sand and gravel (Fig. 7.1). The strip reinforcements are usually associated with the use of relatively high quality but expensive clean sands and gravel backfill to be able to generate the required frictional resistance between backfill soil and reinforcements. The use of grid type of reinforcements has become necessary because grids have more pullout resistance than strip reinforcements (Fig. 7.2). In so doing, cheaper low-quality, locally available, and cohesive-frictional backfill soils can be used. Steel grids were started to be used in California (Chang et al. 1977). Another type of grid reinforcements is the welded wire mats made of galvanized welded steel wires or welded steel bars patented by an American engineer, Bill Hilfiker, in the late 1970s (Peterson and Anderson, 1980). Subsequently, production of strong polymer grids called Tensar and also Tenax, with high extension stiffness and resistance to corrosion, had increased the use of grid reinforcement with cohesive-frictional backfill soil. Later on, the utilization of polymer geotextiles, both woven or non-woven, as reinforcing materials has further popularized the construction of MSE embankments.

7.2 RELEVANCE TO DEVELOPMENT

MSE construction is quite relevant to developed and developing countries. Easy to construct with no need of specialized equipment, the reinforced earth wall can lead to savings up to 50% in comparison to concrete gravity retaining wall or anchored sheet pile wall construction (Cheney, 1990). Construction of MSE embankments/walls is simple, quick, and labor intensive. It can be built in several stages if necessary and does not demand skilled labor. It involves erecting a layer of facing elements connected to the reinforcement, placing the fill, and compacting adequately. The process is repeated until the entire structure reaches the required height.

Clean granular soils with not more than 15% smaller than 0.074 mm in particle diameter, are considered as ideal backfill materials. However, in the coastal plains including Chao Phraya Plain of Bangkok, Thailand, clean sands and gravel are not readily available, and thus expensive due to large transportation costs from far away sources. Savings in construction costs can be

1993 OMAE — Volume I, Offshore Technology
ASME 1993

MICROSTRUCTURE STUDIES OF LIME TREATED MARINE CLAYS

S. Narasimha Rao
Ocean Engineering Centre
K. V. Subba Rao
Department of Civil Engineering
G. Rajasekaran
Ocean Engineering Centre
Indian Institute of Technology
Madras, India

ABSTRACT

Weak marine clay deposits are extensively located both on and off the coastal areas in many parts of the world. Due to their poor engineering characteristics, severe foundation problems are commonly faced in the construction of coastal and offshore structures. Such deposits can be stabilized to suit the requirements of the foundations. Of the various stabilizing methods developed, chemical stabilization has been found to be more suitable to clayey deposits because of their reactive nature of the clay minerals. In the present investigation, an experimental programme was carried out to bring out the influence of lime treatment on the engineering behaviour of the soil at the particulate level. Using the x-ray diffraction (XRD) and scanning electron microscopy (SEM) techniques, the stability of the newly formed reaction products on long duration was also confirmed. The formation of cementation compounds such as Calcium Aluminate Hydrate (CAH) and Calcium Silicate Hydrate (CSH) was confirmed by XRD and SEM. The formation of these compounds are mainly responsible for the improvement in the engineering behaviour of the soil. This investigation clearly confirms that the lime induced effects on the soil are permanent.

INTRODUCTION

Many soft clay marine deposits are extensively located both on land and off the coast of several parts of the world. These are characterised by low strength and high compressibility. There are several foundation problems in these deposits and these are mainly arising out of excessive settlement. Treatment of the clayey soils with chemical additives to improve their engineering behaviour and make them less sensitive to environmental factors has been in practice for several years. Of the several chemical methods of soil stabilization, lime stabilization is extensively used. There are several mechanisms proposed to bring out the eneficial effects induced by the addition of lime. When lime is added to the soil three basic reactions are known to occur. They are, cation exchange, flocculation and/or aggregation and pozzolanic reaction Clare and Cruchley, 1957; Verhasselt, 1990). The first two reactions are known to occur rapidly as soon as the lime is mixed or diffused with the soil whereas the third reaction is a time-dependent, temperature-dependent long term reaction. However, it is known that most of the improvement in the engineering behaviour is attributed to the cementation and aggregation reactions. The soil-lime reactions produce compounds of two classes mainly, Calcium Silicate Hydrates (CSH) and Calcium Aluminate Hydrates (CAH). The formation of new products like dicalcium silicate hydrates of the hillebrandite type and anorthite are also reported (Diamond et al., 1965; Willoughby et al., 1968). Davidson et al.(1960) and Glenn and Handy (1963) identified the CSH and CAH compounds in the lime treated Kaolinite systems. Because of the reported success of lime stabilization in the field of highway engineering, this technique was, extended to deep in-situ treatment of soft clayey deposits. For the first time, the deep lime mixing method was used to stabilize thick soft marine clayey deposits by Yanese (1968). Subsequently, this technique was utilized by Okumara and Terashi (1975) for stabilizing soft clays in some of the Japanese harbour areas. In the present investigation, an attempt has been made to confirm the formation and stability of these compounds in the marine environment.

EXPERIMENTAL INVESTIGATION

Soil Used

In this investigation, three different soils were used and these soils were procurred from the various places of east coast of India. These soils are referred as soil 1, soil 2 and soil in this investigation. The physical and chemical properties of the soils used are given in Table 1.

Test Programme

In both soil 1 and soil 2, the lime mixing was used primarily to investigate the formation of the cementation compounds and their stability in the marine environment. Lime in different percentages of dry weight, 1%, 2% and 5% were added and thoroughly mixed.

Table 1 Untreated soil properties

S. No.	Properties	Test values		
		Soil 1	Soil 2	Soil 3
1.	Liquid limit (%)	83	47	85
2.	Plasticity index (%)	46	28	53
3.	Shrinkage limit (%)	10	14	-
4.	Specific gravity	2.70	2.61	-
5.	Organic content (%)	1.68	1.0	1.4
6.	Base exchange capacity (m.eq/100g of soil)	61	25	42

These samples were cured over a period of 90 days and were tested for XRD and SEM analysis to examine the nature of new products formed. After the confirmation of the reaction products, lime injection technique was adopted to suit the underwater treatment of soft clays. This was carried out with soil 3 in model test tank of size 1000 mm x 1030 mm x 750 mm. The details of the experimental test setup and the location of sampling points are shown in Fig.1. Hydrated lime slurry of 40% concentration was injected into a homogeneous soft clay bed using a perforated injection pipe. The injection was carried out under a pressure of 0 to 0.8 N/mm^2 in three stages by injecting slurry at top, middle and bottom layers. To maintain constant water content in the soil deposit, a layer of 50 mm sea water was always maintained at the top of soil bed. The diffusibility of lime with time was established by taking samples at various time intervals of 15, 30 and 45 days and investigated for the stability of new reaction products. The samples taken out were used for XRD and SEM analysis.

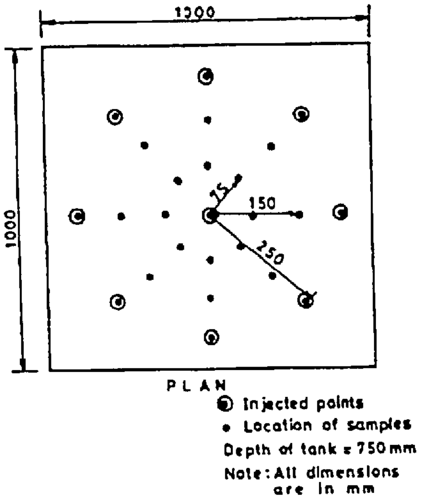

Fig 1. Details of the experimental set-up.

RESULTS AND DISCUSSIONS

X-Ray Analysis of Soils

The success of lime stabilization mainly depends on the mineralogical content of the soil. To investigate the formation of various new products due to soil-lime treatment, it is essential to identify the various clay minerals present in the soil. For all the XRD analysis, air-dried powdered samples were used. The XRD pattern of the untreated soil for soil 1 clearly indicates the presence of clay minerals like albite, kaolinite, montmorillonite, quartz and alumina. The diffractogram for soil 2 reveals the presence of Montmorillonite, Kaolinite, albite and feldspar. The XRD of the untreated soil (soil 3) is shown in Fig.2. This soil contains montmorillonite, kaolinite, sepiolite, quartz and vermiculite. The mineralogical analysis was carried out by comparing with the index card as per Brown (1961) and the standard ASTM powder diffraction file (1991). The same XRD analysis was used by several researchers to bring out the formation of cementation compounds resulting from the reaction of lime with soil (Kantro et al., 1959 and Sabry et al., 1981). Many of the reaction products formed such as CSH and CAH are cementitious in nature and these help in the aggregation of the particles. The XRD patterns of the treated soils for soil 1 and soil 2 are given in Tables 2 and 3. The diffractograms of the lime injection treated soil is shown in Fig.3. These clearly indicate the presence of cementation compounds such as CSH including tobermorite, calcium aluminate hydrate and anorthite etc. And also, quartz is presumed to have reacted with lime to give rise to CSH and this was earlier confirmed by Glenn (1967). Apart from these products which are identified, there can be several other non-crystalline products which cannot be identified using x-ray diffraction techniques.

Further, to investigate the stability of the new reaction products for long duration in maine environment, a series of leaching tests were carried out. In these tests, samples were leached at a pressure of 0.4 N/mm^2. The XRD and SEM analysis carried out on these leached samples indicate no mineralogical changes. The reaction products formed were quite stable.

Scanning Electron Microscopic Studies

Figs.4, 5 and 8 show the micrographs of the different untreated soil samples. These photographs

Fig 9. Micrograph of lime injection treated soil (soil 3 after 45 days)

Strength and Compressibility behaviour of soils

Limited strength tests were carried out to investigate the effect of lime stabilization for all soil systems. For soil 1, triaxial shear tests were carried out to bring out the improvement in the strength. The test results are shown in Fig. 10 and these results clearly indicate that there is an improvement in the strength of the soil by 2 to 4 times that of untreated soil. Similar such type of variation in the strength of the soil (soil 2) was observed. For soil 3, a specially fabricated cone penetrometer was used to study the improvement in the strength of the soils. The test results are plotted in Fig. 11 and they clearly reveal that the lime injection treatment has increased the strength by 5 to 8 times that of origin soil.

CONCLUSIONS

The following conclusions can be drawn based on the above experimental investigation.

The formation of the cementation compounds such as CSH and CAH were confirmed using the XRD analysis. The stability of these compounds in marine environment for long duration was also confirmed from the leaching test series carried out and the SEM studies also confirm these changes.

Table 2 Reaction products formed in Soil 1 due to lime treatment

Sl. No.	Percentage of lime added	Lattice spacing of new peak, d (A^{o})	Product believed to have been formed
1.	2.	3.	4.
1.	1	5.35	Tobermorite
2.	1	3.26	CSH (I)
3.	1	1.99	CSH (II)
4.	3	4.04	Hillebrandite
5.	3	3.26	CSH (I)
6.	3	2.84	CSH (II)
7.	3	1.55	Calcium aluminate
8.	5	13.08	CSH (I)
9.	5	3.26	CSH (I)
10.	5	2.95	Unsubstituted tobermorite
11.	5	2.56	Calcium aluminate
12.	5	2.43	Calcium aluminate
13.	5	2.26	Unsubstituted tobermorite

CSH (I) and CSH (II) are Calcium Silcate Hydrate with slight difference in their chemical compositions.

Table 3 Reaction products formed in Soil 2 due to lime treatment

Sl. No.	Percentage of lime added	Lattice spacing of new peak, d (A°)	Product believed to have been formed
1.	2.	3.	4.
1.	1.5	2.92	Hillebrandite
2.	1.5	2.13	Calcium aluminate
3.	2	3.14	Albite
4.	2	2.24	Unsubstituted tobermorite

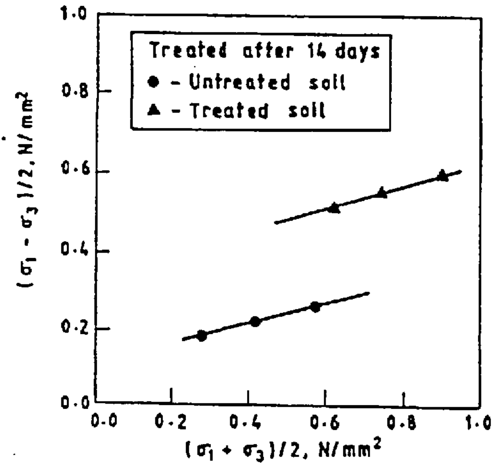

Fig 10. Influence of curing period on strength envelopes for soil 1.

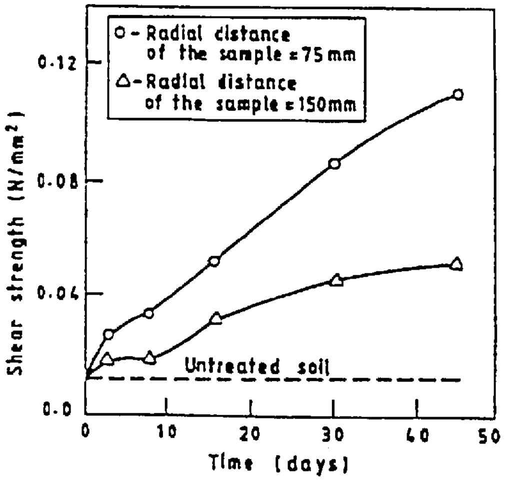

Fig 11. Variation of strength with time (soil 3).

The improvement in the strength of the soil due to the formation of cementation products was also confirmed strength tests and these tests indicate that there is a 3 to 5 fold increase in the strength of the soil. These studies confirm that the lime induced beneficial effects are stable under marine environment and lime stabilization technique can be very well adopted for improving the engineering behaviour of the soil.

REFERENCES

ASTM x-ray card file and index (1962), "Annual book of ASTM standards", Philadelphia, Pa.

Broms, B. and Boman, P. (1975), "Lime stabilized columns", 5th Asian Regional Conference on SM and FE, Bangalore, India, Vol.1, pp.227-234.

Brown, G. (1961), "The x-ray identification and crystal structures of clay minerals", Mineralogical Society (Clay Minerals Group), London.

Clare, K.E. and Cruchley, A.F. (1957), "Laboratory experiments in the stabilization of clays with hydrated lime', Geotechnique, Vol.7, pp.97-111.

Davidson, D.F. Mateas, M. and Barnes, H.F. (1960) "Improvement of lime stabilization of montomrillonite clay soil with chemical addtives", HRB No.262, pp.33-50.

Diamond, S. White, J.L. and Dolch, W.L. (1965), "Transformation of clay minerals by calcium hydroxide attack", Proc. of 12th National Conf. on Clays and Clay Minerals, New York, Pengamon Press.

Gillot, J.E. (1968),"Clay in engineering geology", Elsevier Publishing Company, London.

Glenn, G.12 (1967), "X-ray studies of lime bentonite reaction products", Journal of American Ceramic Society, Vol.50, No.6, pp.312-316.

Glenn, G.R. and Handy, R.L. (1963), "Lime - clay mineral reaction products", HRB No.29, pp.70-82.

Kantro, D.L., Wrunaver, S. and Weise, C.H. (1959), "The ball-mill hydration of tricalcium silicate at room temperature", Journal of Colloid Science, Vol.14, pp. 363-376.

Lambe, T.W. (1953),"The structure of inorganic soil", Proc. of ASCE, Vol.79, p.315.

Okumara, T. and Terashi, M. (1975), "Deep lime mixing method of stabilization for marine clays', 5th Asian Reg. Conf. on SM & FE, Vol.1, pp.65-75.

Sabry, M.A, Reed, L.W. and Parcher, J.V. (1981). "Mineralogy of compacted clay-lime mixtures," Soil science society of American Journal, Vol.45, pp.144-150.

Verhasselt, A.F. (1990), "Physico-chemical aspects of soil and related materials", ASTM:STP 1095, pp.7-17.

Willoughby, D.R., Gross, K.A., Ingles, O.G. Silva, S.R. and Veronica, M.S. (1968),"The identification of reaction products in alkali stabilized clay by electron microscopy, x-ray and electron diffraction". Proc. of 4th Conf. Austriallan Road Research Board, Vol.4, Part 2, pp.1386-1408.

Yanase, S. (1968),"Stabilization of alluvial clay with quick lime", Rept. of Ports and Harbour Research Institute, Vol.7, No.4 (in Japanese)

Yong, R.N. and Warkentin, B.P. (1966), "Introduction to soil behaviour", The Macmillan Co., New York.

ANNEXE C

LISTE DES CONTACTS À EFFECTUER

- ↪ MANUFACTURIERS/FOURNISSEURS (ÉQUIPEMENTS)
- ↪ ASSOCIATIONS (EXPERTS)
- ↪ CONSULTANTS (EXPERTS)
- ↪ INSTITUTIONS (EXPERTS)

↪ *Boart Longyear Inc.*
Box 330, 1111 Main St. W.
North Bay (Ontario) P1B 8H6
Canada

Contact : Sales Manager
Tél. : 1-705-474-2800
Téléc. : 1-705-474-2373

↪ *Conmico Inc.*
11-140 Bradwick Drive
Concord (Ontario) L4K 1K8
Canada

Contact : Sales Manager
Tél. : 1-905-660-7262
Téléc. : 1-905-660-1843

↪ *Consortium Promercan inc.*
138, chemin des Boises
Dubuisson (Québec) J9P 4N7
Canada

Contact : Directeur des ventes
Tél. : 1-819-738-5435 / 800-738-6232
Téléc. : 1-819-736-5624

↪ *Denver Sala Canada*
3136 Mavis Road
Mississauga (Ontario) L5C 1T8
Canada

Contact : Sales Manager
Tél. : 1-905-270-2170
Téléc. : 1-905-270-9996

↪ *Drillex Int'l of Canada*
P.O. Box 2097 Stn. A.
Sudbury, P3A 4R8
Canada

Contact : Sales Manager
Tél. : 1-705-692-3661
Téléc. : 1-705-692-4850

↪ ***Ferinox Ltd***
1900, Marie-Victorin
Saint-Bruno (Québec) J3V 6B9
Canada

Contact : Directeur des ventes
Tél. : 1-514-653-6139
Téléc. : 1-514-653-1133
E-Mail : ferinox@microsoft.com

↪ ***Finning Ltd***
555 Great Northern Way
Vancouver (BC) V5T 1E2
Canada

Contact : Sales Manager
Tél. : 1-604-872-4444
Téléc. : 1-604-872-2994

↪ ***Hydro Dynamics Ltd***
3360 Sartelon St
Saint-Laurent (Québec) H4R 1E4
Canada

Contact : Directeur des ventes
Tél. : 1-514-332-0443
Téléc. : 1-514-745-0345

↪ ***Ingersoll-Dresser Pump Canada Inc.***
15 Worthington Drive, P.O. Box 40
Brantford (Ontario) N3T 5M5
Canada

Contact : Sales Manager
Tél. : 1-519-753-7381
Téléc. : 1-519-753-0845
E-Mail : peter_williams@idpump.com

↪ ***ITT Flygt***
300, Labrosse Avenue
Pointe-Claire (Québec) H9R 4V5
Canada

Contact : Directeur des ventes
Tél. : 1-514-695-0100
Téléc. : 1-514-697-0602

↳ *JF Comer Inc.*
10 Cardico Drive
Gormely (Ontario) L0H 1G0
Canada

Contact : Sales Manager
Tél. : 1-905-888-1164
Téléc. : 1-905-888-1659

↳ *Maclean Engineering*
100 Moutain Rd
Collingwood (Ontario) L9Y 3Z9
Canada

Contact : Sales Manager
Tél. : 1-705-445-5707
Téléc. : 1-705-445-3214

↳ *Minpro Ltd.*
2125 Wyecroft Rd.
Oakville (Ontario)
Canada

Contact : Sales Manager
Tél. : 1-905-847-9140
Téléc. : 1-905-847-9052

↳ *Peacock Inc.*
2360 Millrace Court
Mississauga (Ontario) L5N 1W2
Canada

Contact : Sales Manager
Tél. : 1-905-812-7100
Téléc. : 1-905-812-7203

↳ *Reedrill Canada Inc./Gardner-Denver*
159A Fielding Rd
Lively (Ontario) P3Y 1L7
Canada

Contact : Sales Manager
Tél. : 1-705-682-4141 / 800-461-4077
Téléc. : 1-705-682-4300

↳ ***Robbins & Myers Canada Ltd.***
8032 Torbram Rd
Brampton (Ontario) L6T 3T2
Canada

Contact : Sales Manager
Tél. : 1-416-793-6800
Téléc. : 1-416-793-9434

↳ ***Svedala Pumps & Process***
3136 Mavis Rd
Mississauga (Ontario) L5C 1T8
Canada

Contact : Sales Manager
Tél. : 1-905-270-2170
Téléc. : 1-905-270-9996

↳ ***Tamrock Canada Ltd***
100 Magill St.
Lively (Ontario) P3Y 1K7
Canada

Contact : Sales Manager
Tél. : 1-705-692-5881
Téléc. : 1-705-692-2313

↳ ***Westpro Sales Inc.***
P.O. Box 91777
West Vancouver (BC) V7V 4S1
Canada

Contact : Sales Manager
Tél. : 1-604-685-6311
Téléc. : 1-604-685-6374

↳ ***York Fluid Controls Ltd***
2 Westwyn Court
Brampton (Ontario) L6T 4T5
Canada

Contact : Sales Manager
Tél. : 1-905-454-4013 / 800-509-YORK
Téléc. : 1-905-454-8423

↳ *Concentrall-Ateliers de Carspach*
41, rue du Gazon, B.P. 3
Carspac 68130
France

Contact : Directeur des ventes
Tél. : 011 33 3 89 40 93 03
Téléc. : 011 33 3 89 40 68 71

↳ *Fapmo*
35-37 rue Roger Salengro
F-62230 Outreau
France

Contact : Directeur des ventes
Tél. : 011 33 3 21 31 72 00
Téléc. : 011 33 3 21 80 46 88

↳ *Montabert S.A.*
203, route de Grenoble, B.P. 67
Saint Priest Cedex 69805
France

Contact : Directeur des ventes
Tél. : 011 33 4 72 229 797
Téléc. : 011 33 4 72 229 779

↳ *SMF Int'l*
7 rue des Frères Lumière, B.P. 45
582 02 Cosne/Loire
France

Contact : Directeur des ventes
Tél. : 011 33 3 86 39 52 00
Téléc. : 011 33 3 86 39 52 01

↳ *Salzgitter Maschinenbau GmbH*
Windmuhlenbergstr. 20-22
D-3320, Salzgitter 51
Germany

Contact : Sales Manager
Tél. : 011 49 5341 3021
Téléc. : 011 49 5341 302 424

↳ *Westfalia Becorit Industrietec*
Postfach 1409
D-44504 Lunen
Germany

Contact : Sales Manager
Tél. : 011 49 2306 578 0

↳ ***Wirth Maschinen-u. Bohrgerate***
P.O. Box 1327/1329
D-41812 Erkelenz
Germany

Contact : Sales Manager
Tél. : 011 49 2431 830
Téléc. : 011 49 2431 83 267

↳ ***Geho Pumps-Enviro Tech Pump-Systems***
P.O. Box 249
5900 AE, Venlo
Netherlands

Contact : Sales Manager
Tél. : 011 31 77 895 200
Téléc. : 011 31 77 824 844

↳ ***Robot Pompen B.V.***
Produktieweq 5, P.O. Box 140
Alphen A/D Rijn, NL-2400 AC
Netherlands

Contact : Sales Manager
Tél. : 011 31 1720 315 41
Téléc. : 011 31 1720 424 52

↳ ***Allis Mineral Systems***
P.O. Box 4004
203 11 Malmo
Sweden

Contact : Sales Manager
Tél. : 011 46 40 24 58 00
Téléc. : 011 46 40 78475

↳ *Grindex ab*
Box 538
S-13625 Haninge
Sweden

Contact : Sales Manager
Tél. : 011 46 8 606 66 00
Téléc. : 011 46 8 745 53 28

↳ *Morgardshammar AB*
S-777 82 Smedjebacke
Sweden

Contact : Sales Manager
Tél. : 011 46 240 668 500
Téléc. : 011 46 240 668 501

↳ *Sandvik Rock Tools*
S-811 81 Sandviken
Sweden

Contact : Sales Manager
Tél. : 011 46 26 262 000
Téléc. : 011 46 26 270 794

↳ *Wilfley Mining Machinery*
Cambridge St., Wellingborough
Northamptonshire, NN8 1DW
United Kingdom

Contact : Sales Manager

↳ *Atlas Copco Robbins Inc.*
Box 97027
Kent, WA 98064
USA

Contact : Sales Manager
Tél. : 1-206-872-0500
Téléc. : 1-206-872-0199

↳ ***Baker Hughes Mining Tools Inc.***
P.O. Box 531226
Grande Prairie, TX 75053
USA

Contact : Sales Manager
Tél. : 1-214-988-3322 / 800-527-1632
Téléc. : 1-214-602-3135

↳ ***Barrett, Haentjens & Co.***
225 N. Cedar St.
Hazleton, PA 18201
USA

Contact : Sales Manager
Tél. : 1-717-455-7711
Téléc. : 1-717-459-2586

↳ ***Cowin & Co. Inc.***
P.O. Box 19009
Birmingham, AL 35219
USA

Contact : Sales Manager
Tél. : 1-205-945-1300
Téléc. : 1-205-945-1441

↳ ***D & D Machine & Hydraulics Inc.***
10945 Metro Pkwy. SE
Fort Myers, FL 33912
USA

Contact : Sales Manager
Tél. : 1-813-275-7177 / 800-282-1236
Téléc. : 1-813-275-5350

↳ ***Denver Thomas***
P.O. Box 96
Birmingham, AL 35201
USA

Contact : Sales Manager
Tél. : 1-205-599-6600 / 800-776-2278
Téléc. : 1-205-599-6610

↳ *Dynatec Mining Ltd*
200-9555 Younge St.
Richmond Hill (Ontario) M8W 4K6
USA

Contact : Sales Manager
Tél. : 1-905-780-1980 / 800-892-8293
Téléc. : 1-905-780-1990

↳ *GIW Industries Inc.*
5000 Wrightsboro Rd.
Grevetown, GA 30813-9750
USA

Contact : Sales Manager
Tél. : 1-706-863-1011
Téléc. : 1-706-860-5897

↳ *Gorman-Rupp of CDA Ltd*
70 Burwell Rd
St Thomas (Ontario) N5P 3R7
USA

Contact : Sales Manager
Tél. : 1-519-631-2870
Téléc. : 1-519-631-4624

↳ *Hayward Gordon Ltd*
6660 Campobella Rd
Mississauga (Ontario) L5N 2L9
USA

Contact : Sales Manager
Tél. : 1-905-567-6116
Téléc. : 1-905-567-1706

↳ *IMO Industries Canada Inc.*
1401 Meyerside Drive
Mississauga (Ontario) L5T 1G8
USA

Contact : Sales Manager
Tél. : 1-905-564-3344
Téléc. : 1-905-564-3577

↳ *Inductotherm Corp.*
10 Indel Avenue
Rancocas, NJ 08073
USA

Contact : Sales Manager
Tél. : 1-609-267-9000 / 800-257-9527
Téléc. : 1-609-267-3537

↳ *ITT-A-C Pump*
1150 Tennessee Ave.
Cincinnati, OH 45229
USA

Contact : Sales Manager
Tél. : 1-513-482-2500
Téléc. : 1-513-482-2569

↳ *Lawrence Pumps Inc.*
371 Market St.
Lawrence, MA 01843
USA

Contact : Sales Manager
Tél. : 1-508-682-5248
Téléc. : 1-508-975-4291

↳ *Lightning Industries Inc.*
801 Woodswether Rd.
Kansas City, MO 64105
USA

Contact : Sales Manager
Tél. : 1-816-842-3800
Téléc. : 1-816-842-6736

↳ *Linatex Corp. of America*
P.O. 899
Gallatin, TN 37066
USA

Contact : Sales Manager
Tél. : 1-615-230-2100
Téléc. : 1-615-230-2101

↳ *Mineral Deposits (America) Inc.*
14818 W. 6th Ave., Unit 10A
Golden, CO 80401
USA

Contact : Sales Manager
Tél. : 1-303-279-8932
Téléc. : 1-303-279-7702

↳ *Minerals Equip.*
P.O. Box 57038
Salt Lake City, UT 84157
USA

Contact : Sales Manager
Tél. : 1-801-262-5471
Téléc. : 1-801-269-1775

↳ *Mining Technologies International Inc.*
145 Magill St
Lively (Ontario) P3Y 1K6
USA

Contact : Sales Manager
Tél. : 1-705-692-3661 / 800-461-4094
Téléc. : 1-705-692-4850
E-Mail :

↳ *Mud Cat, Ellicott Machine Corp.*
1611 Bush
Baltimore, MD 21230
USA

Contact : Sales Manager
Tél. : 1-410-837-7900
Téléc. : 1-410-752-3294
E-Mail :

↳ *Nagle Pumps Inc.*
1249 Center Ave.
Chicago Heights, IL 60411
USA

Contact : Sales Manager
Tél. : 1-708-754-2940
Téléc. : 1-708-754-2944

↳ ***Pekor Pumps Inc.***
P.O. Box 8508
Columbus, GA 31908
USA

Contact : Sales Manager
Tél. : 1-706-685-1200 / 800-277-7867
Téléc. : 1-706-685-4355

↳ ***Robbins & Myers Inc.***
Fluids Handling Div.
Box 960
Springfield, OH 45501
USA

Contact : Sales Manager
Tél. : 1-513-327-3553
Téléc. : 1-513-327-3530

↳ ***SRS Crisafulli Inc.***
Crissaufulli Dr., P.O. Box 1051
Glendive, MT 59330-1051
USA

Contact : Sales Manager
Tél. : 1-406-365-3393 / 800-442-7867
Téléc. : 1-406-365-8088

↳ ***The Gorman-Rupp Co.***
P.O. Box 1217
Mansfield, OH 44902
USA

Contact : Sales Manager
Tél. : 1-419-755-1011
Téléc. : 1-419-755-1251

↳ ***The Robbins Co.***
Box 97027
Kent, WA 98064
USA

Contact : Sales Manager
Tél. : 1-206-872-0500
Téléc. : 1-206-872-0199

↳ *Tsurumi (America) Inc.*
845 N. Dillon Dr.
Wood Dale, IL 60191
USA

Contact : Sales Manager
Tél. : 1-708-766-5900 / 800-423
Téléc. : 1-708-766-6445

↳ *Warman Int'l Inc.*
P.O. Box 7610
Madison, WI 53707
USA

Contact : Sales Manager
Tél. : 1-608-221-2261
Téléc. : 1-608-221-5810

↳ *Warren Pumps Inc.*
783 Bridges Ave.
Warren, MA 01083
USA

Contact : Sales Manager
Tél. : 1-413-436-7711
Téléc. : 1-413-436-5605

↳ *Warren Rupp Inc.*
A Unit of IDEX, P.O. Box 1568
Mansfield, OH 44901
USA

Contact : Sales Manager
Tél. : 1-419-524-8388
Téléc. : 1-419-522-7867

↳ *West Virginia & Pump & Supply Co. G*
P.O. Box 2081
Huntington, WV 25721
USA

Contact : Sales Manager
Tél. : 1-304-529-4161
Téléc. : 1-304-522-9361

↪ *Westfalia Mining Progress*
255 Berry Road
Washington, PA 15301
USA

Contact : Sales Manager
Tél. : 1-412-225-4049
Téléc. : 1-412-228-2177

↪ *Zeni Orilling Co.*
R.R. 13 Box 100
Morgantown, WV 26505-8522
USA

Contact : Sales Manager
Tél. : 1-304-328-5665
Téléc. : 1-304-328-5805

↳ *Australasian Institute of Mining and Metallurgy*
Level 3, 15-31 Pelham Street
Carlton VIC 3053
Australia

Contact : G.E. Edwards or Director
Tél. : 011-61-3-662-3166
Téléc. : 011-61-3-662-3662

↳ *Australian Geological Survey Organisation*
GPO Box 378
Canberra ACT 2601
Australia

Contact : Neil Williams or Director
Tél. : 011-61-6-249-9111
Téléc. : 011-61-6-249-9999

↳ *Australian Mines and Metals Association*
10-16 Queen Street, 7th Floor
Melbourne VIC 3000
Australia

Contact : N.A. Amos or Director
Tél. : 011-61-3-9614-4777
Téléc. : 011-61-3-9614-3970

↳ *Australian Mining Industry Council*
P.O. Box 363
Dickson ACT 2602
Australia

Contact : D. A. Buckingham or Director
Tél. : 011-61-6-279-3600
Téléc. : 011-61-6-279-3699

↳ *International Society of Soil Science (ISSS)*
Institut fur Bodenforschung
Gregor-Mendel-Str. 33
A-1180 Vienna
Austria

Contact : W.E.H. Blum or Director
Tél. : 011 43 1 310 6026
Téléc. : 011 43 1 310 6027

↳ ***Australasian Institute of Mining and Metallurgy***
Level 3, 15-31 Pelham Street
Carlton VIC 3053
Australia

Contact : G.E. Edwards or Director
Tél. : 011-61-3-662-3166
Téléc. : 011-61-3-662-3662

↳ ***Australian Geological Survey Organisation***
GPO Box 378
Canberra ACT 2601
Australia

Contact : Neil Williams or Director
Tél. : 011-61-6-249-9111
Téléc. : 011-61-6-249-9999

↳ ***Australian Mines and Metals Association***
10-16 Queen Street, 7th Floor
Melbourne VIC 3000
Australia

Contact : N.A. Amos or Director
Tél. : 011-61-3-9614-4777
Téléc. : 011-61-3-9614-3970

↳ ***Australian Mining Industry Council***
P.O. Box 363
Dickson ACT 2602
Australia

Contact : D. A. Buckingham or Director
Tél. : 011-61-6-279-3600
Téléc. : 011-61-6-279-3699

↳ ***International Society of Soil Science (ISSS)***
Institut fur Bodenforschung
Gregor-Mendel-Str. 33
A-1180 Vienna
Austria

Contact : W.E.H. Blum or Director
Tél. : 011 43 1 310 6026
Téléc. : 011 43 1 310 6027

↳ *Miner's International Federation (MIF)*
109, ave. Emile de Beco
B-1050 Brussels
Belgique

Contact : Peter Michalzik ou Directeur
Tél. : 011 32 2 646 2120
Téléc. : 011 32 2 646 4723

↳ *Instituto Brasileiro de Mineracao (IBRAM)*
SCS 1 Bloco F, Ed. Camargo Correa, 9-Andar
Brasilia D.F. 70397 900
Brazil

Contact : Jose Souza or Director
Tél. : 011-55-61-226-9367
Téléc. : 011-55-61-226-9580

↳ *APEGGA*
15th Floor, Tower One, Scotia Place, 10060 Jasper Avenue
Edmonton (AB) T5J 4A2
Canada

Contact : Director
Tél. : 1-403-426-3990
Téléc. : 1-403-426-1877
E-Mail : email@apegga.com

↳ *Association of Exploration Geochemists*
P.O. Box 26099, 72 Robertson Rd
Nepean (Ontario) K2H 9R0
Canada

Contact : Director
Tél. : 1-613-828-0199
Téléc. : 1-613-828-9288
E-Mail : aeg@synapse.net

↳ *Association of Professional Engineers and Geoscientists*
P.O. Box 21207
St. John's (NF) A1A 5B2
Canada

Contact : Director
Tél. : 1-709-753-7714
Téléc. : 1-709-753-6131
E-Mail : apegn@public.compusult.nf.ca

- *Association of Professionnal Engineers, Geologist and Geophysicists of The Northwest Territories*

4807 - 49th St, Ste 5
Yellowknife, NT X1A 3T5
Canada

Contact : Robert W. Spence or Director
Tél. : 1-403-920-4055
Téléc. : 1-403-873-4058

- *Association of Professionnal Geologists and Geophysicists of Quebec*

2903, 7e Rue
Val d'or (Québec) J9P 6P6
Canada

Contact : Jacques Trottier ou Directeur
Tél. : 1-819-874-1293
Téléc. : 1-819-874-5264

- *British Columbia and Yukon Chamber of Mines*

840 W Hastings St
Vancouver (BC) V6C 1C8
Canada

Contact : Jack M. Patterson or Director
Tél. : 1-604-681-5328
Téléc. : 1-604-681-2363

- *Canadian Association of Mining equipment and Services for Export*

345 Renfrew Dr, Ste 101
Markham (Ontario) L3R 9S9
Canada

Contact : Director
Tél. : 1-905-513-0046
Téléc. : 1-905-513-1834

- *Canadian Drilling Association*

222 McIntyre St W, Ste 306
North Bay (Ontario) P1B 2Y8
Canada

Contact : J.E. Neils or Director
Tél. : 1-705-476-6992
Téléc. : 1-705-476-9494

- *Association of Professionnal Engineers, Geologist west Territories*
  4807 - 49th St, Ste 5
  Yellowknife, NT X1A 3T5
  Canada

  Contact : Robert W. Spence or Director
  Tél. : 1-403-920-4055
  Téléc. : 1-403-873-4058

- *Association of Professionnal Geologists and Geoph*
  2903, 7e Rue
  Val d'or (Québcc) J9P 6P6
  Canada

  Contact : Jacques Trottier ou Directeur
  Tél. : 1-819-874-1293
  Téléc. : 1-819-874-5264

- *British Columbia and Yukon Chamber of Mines*
  840 W Hastings St
  Vancouver (BC) V6C 1C8
  Canada

  Contact : Jack M. Patterson or Director
  Tél. : 1-604-681-5328
  Téléc. : 1-604-681-2363

- *Canadian Association of Mining equipment and Ser*
  345 Renfrew Dr, Ste 101
  Markham (Ontario) L3R 9S9
  Canada

  Contact : Director
  Tél. : 1-905-513-0046
  Téléc. : 1-905-513-1834

- *Canadian Drilling Association*
  222 McIntyre St W, Ste 306
  North Bay (Ontario) P1B 2Y8
  Canada

  Contact : J.E. Neils or Director
  Tél. : 1-705-476-6992
  Téléc. : 1-705-476-9494

↳ ***Canadian Geoscience Council, The***
Department of Earth Sciences
University of Waterloo
Waterloo (Ontario) N2L 3G1
Canada

Contact : Director
Tél. : 1-519-885-1211
Téléc. : 1-519-746-7484

↳ ***Canadian Geotechnical Society (CGS)***
170 Atwell Dr., No. 501
Rexdale (Ontario) M9W 5Z5
Canada

Contact : A.G. Stermac or Director
Tél. : 1-416-674-0366
Téléc. : 1-416-674-9507

↳ ***Canadian Mining Contractors Association***
120 Railroad St
Brampton (Ontario) L6X 1G8
Canada

Contact : Director
Tél. : 1-905-456-0734
Téléc. : 1-905-456-3784

↳ ***Geological Association of Canada, The***
Department of Earth Sciences
Memorial University
Newfoundland (St. John's) A1B 3X5
Canada

Contact : Director
Tél. : 1-709-737-7660
Téléc. : 1-709-737-2532
E-Mail : gac@sparky2.esd.mun.ca

↳ ***Geological Survey of Canada***
3303 33rd Street NW
Calgary AB T2L 2A7
Canada

Contact : Grant Mossop or Director
Tél. : 1-403-292-7000
Téléc. : 1-403-292-5377

↳ *MITEC (Mining Industry T*
1105, 350 Sparks Street
Ottawa ON K1R 7S8
Canada

Contact : Christine Galipe
Tél. : 1-613-233-9835
Téléc. : 1-613-233-0579

↳ *Ontario Mining Association*
110 Yonge Street, Suite 1501
Toronto ON M5C 2A5
Canada

Contact : Patrick Reid or D
Tél. : 1-416-364-9301
Téléc. : 1-416-364-5986

↳ *Prospectors and Developers*
34 King Street East, 9th Floo
Toronto ON M5C 2X8
Canada

Contact : John Hansuld or
Tél. : 1-416-362-1969
Téléc. : 1-416-362-0101

↳ *Prospectors and Developers*
34 King Street East, 9th Floo
Toronto (Ontario) M5C 2X8
Canada

Contact : Rita Plaskett or D
Tél. : 1-416-362-1969
Téléc. : 1-416-372-0101

↳ *Quebec Mining Association*
2600, boul. Laurier, Tour de
Sainte-Foy (Québec) G1V 4
Canada

Contact : Dan Tolgyesi ou
Tél. : 657-2016
Téléc. : 657-2154

- ***MITEC (Mining Industry Technology Council of Canada)***
  1105, 350 Sparks Street
  Ottawa ON K1R 7S8
  Canada

  Contact : Christine Galipeau or Director
  Tél. : 1-613-233-9835
  Téléc. : 1-613-233-0579

- ***Ontario Mining Association***
  110 Yonge Street, Suite 1501
  Toronto ON M5C 2A5
  Canada

  Contact : Patrick Reid or Director
  Tél. : 1-416-364-9301
  Téléc. : 1-416-364-5986

- ***Prospectors and Developers Association of Canada***
  34 King Street East, 9th Floor
  Toronto ON M5C 2X8
  Canada

  Contact : John Hansuld or Director
  Tél. : 1-416-362-1969
  Téléc. : 1-416-362-0101

- ***Prospectors and Developers Association of Canada***
  34 King Street East, 9th Floor
  Toronto (Ontario) M5C 2X8
  Canada

  Contact : Rita Plaskett or Director
  Tél. : 1-416-362-1969
  Téléc. : 1-416-372-0101

- ***Quebec Mining Association inc.***
  2600, boul. Laurier, Tour de la Cité, bureau 942
  Sainte-Foy (Québec) G1V 4W2
  Canada

  Contact : Dan Tolgyesi ou Directeur
  Tél. : 657-2016
  Téléc. : 657-2154

↳ *University of Ottawa*
Civil Engineering
161 Louis Pasteur Street, (A-112), P.O. Box 450, Station A
Ottawa (Ontario) K1N 6N5
Canada

Contact : Vinod Garga or Director
Tél. : 1-613-562-5919
Téléc. : 1-613-562-5173
E-Mail : garga@eng.uottawa.ca

↳ *University of Toronto*
Faculty of Applied Science and Engineering
Galbraith Building, 35 St. George Street
Toronto (Ontario) M5S 1A4
Canada

Contact : Steven D. Scott or Director
Tél. : 1-416-978-6554
Téléc. : 1-416-978-4820

↳ *University of Toronto*
Department of Civil Engineering
35 St. George Street
Toronto (Ontario) M5S 1A4
Canada

Contact : Barry J. Adams or Director
Tél. : 1-416-978-3096
Téléc. : 1-416-978-6813

↳ *University of Waterloo*
Geotechnical Engineering Group
Department of Civil Engineering
Waterloo (Ontario) N2L 3G1
Canada

Contact : Leo Rothenburg or Director
Tél. : 1-519-888-4567, ext. 3759
Téléc. : 1-519-888-6197
E-Mail : leoroth@uwaterloo.ca

↳ *University of Ottawa*
Civil Engineering
161 Louis Pasteur Street, (A-112), P.O. Box 450, Station A
Ottawa (Ontario) K1N 6N5
Canada

Contact : Vinod Garga or Director
Tél. : 1-613-562-5919
Téléc. : 1-613-562-5173
E-Mail : garga@eng.uottawa.ca

↳ *University of Toronto*
Faculty of Applied Science and Engineering
Galbraith Building, 35 St. George Street
Toronto (Ontario) M5S 1A4
Canada

Contact : Steven D. Scott or Director
Tél. : 1-416-978-6554
Téléc. : 1-416-978-4820

↳ *University of Toronto*
Department of Civil Engineering
35 St. George Street
Toronto (Ontario) M5S 1A4
Canada

Contact : Barry J. Adams or Director
Tél. : 1-416-978-3096
Téléc. : 1-416-978-6813

↳ *University of Waterloo*
Geotechnical Engineering Group
Department of Civil Engineering
Waterloo (Ontario) N2L 3G1
Canada

Contact : Leo Rothenburg or Director
Tél. : 1-519-888-4567, ext. 3759
Téléc. : 1-519-888-6197
E-Mail : leoroth@uwaterloo.ca

↳ *Danish Geological Survey*
Thoravej 8
Copenhagen, NV 2400
Denmark

Contact : Erik Thomsen or Technical Advisor
Tél. : 011-45-31-10-66-00
Téléc. : 011-45-31-19-68-68

↳ *Geological Survey of Finland*
Betonimiehenkuja 4, P.O. Box 96
FIN-02151 Espoo
Finland

Contact : Matti Saarnisto or Director
Tél. : 011 358 205 50 11
Téléc. : 011 358 205 50 12

↳ *Geological Survey of Finland*
Betonimiehenkuja 402150
Espoo SF-02150
Finland

Contact : Veikko Lappalainen or Technical Advisor
Tél. : 011-358-0-46931
Téléc. : 011-358-0-462205

↳ *Bureau de Recherches Geologiques et Minieres*
B.P. 6009, Cedex 2
Orleans 45060
France

Contact : Francois Le Lann ou Conseiller technique
Tél. : 011-33-38-64-33-05
Téléc. : 011-33-38-64-35-15

↳ *CEMAGREF Antony Research Group*
B.P. 121
92185 Antony Cedex
France

Contact : Directeur
Tél. : 011 33 1 4096 6121
Téléc. : 011 33 1 4096 6036

↳ *Danish Geological Survey*
Thoravej 8
Copenhagen, NV 2400
Denmark

Contact : Erik Thomsen or Technical Advisor
Tél. : 011-45-31-10-66-00
Téléc. : 011-45-31-19-68-68

↳ *Geological Survey of Finland*
Betonimiehenkuja 4, P.O. Box 96
FIN-02151 Espoo
Finland

Contact : Matti Saarnisto or Director
Tél. : 011 358 205 50 11
Téléc. : 011 358 205 50 12

↳ *Geological Survey of Finland*
Betonimiehenkuja 402150
Espoo SF-02150
Finland

Contact : Veikko Lappalainen or Technical Advisor
Tél. : 011-358-0-46931
Téléc. : 011-358-0-462205

↳ *Bureau de Recherches Geologiques et Minieres*
B.P. 6009, Cedex 2
Orleans 45060
France

Contact : Francois Le Lann ou Conseiller technique
Tél. : 011-33-38-64-33-05
Téléc. : 011-33-38-64-35-15

↳ *CEMAGREF Antony Research Group*
B.P. 121
92185 Antony Cedex
France

Contact : Directeur
Tél. : 011 33 1 4096 6121
Téléc. : 011 33 1 4096 6036

↳ *Institute of Soil Science*
Department of Agriculture
Von-Siebold-Str. 4
37075 Göttingen
Germany

Contact :	Christian Ahl or Director
Tél. :	011 49 551 395 504
Téléc. :	011 49 551 395 502
E-Mail :	cahl@gwdg.de

↳ *National Technical University of Athens*
Department of Mining Engineering and Metallurgy
Zographous Campus
GR-15780 Athens
Greece

Contact :	Athanasia Economou or Director
Tél. :	011 30 1 772 2193
Téléc. :	011 30 1 772 2194

↳ *Geological Survey of the Netherlands*
Richard Hlkade 10, Postbus 157
2000 AD Haarlem
Netherlands

Contact :	Chris Staudt or Technical Advisor
Tél. :	011-31-23-5300-300
Téléc. :	011-31-23-5351-614

↳ *Staatstoezicht op de Mijnen*
P.O. Box 90
2280 AB Rijswijk
Netherlands

Contact :	A.K. van der Tuin or Technical Advisor
Tél. :	011-31-70-3956500
Téléc. :	011-31-70-3956555

- ***Centre de géologie de l'ingénieur***
  60 blvd. Saint-Michel
  F-75272 Paris Cedex 06
  France

  Contact : Michel Deveughèe ou Directeur
  Tél. : 011 33 1 4051 9162
  Téléc. : 011 33 1 4326 3656

- ***Centre d'études des tunnels - CETU***
  109 ave. Salvador Allende, B.P. 48
  69674 Bron Cedex
  France

  Contact : Michel Marec ou Directeur
  Tél. : 011 33 4 7841 8125
  Téléc. : 011 33 4 7237 8111

- ***Laboratoire Central des ponts et chaussées***
  58, blvd. Lefebvre
  75732 Paris Cedex 15
  France

  Contact : François Coste ou Directeur
  Tél. : 011 33 1 4043 5000
  Téléc. : 011 33 1 4043 5498
  E-Mail : lcpc10@calvacom.fr

- *Faculty of geoscience, geotechnics and mining*
  Institute of Meneralogy
  D-09596 Freiberg/Saxony
  Brennhausgasse 14
  Germany

  Contact : Director
  Tél. : 011 49 3731 39 2342
  Téléc. : 011 49 3731 39 2524

- *Institute for Mineralogy and Mineral Resources*
  Adloph-Roemer-Str. 2A
  D-38678 Clausthal-Zellerfeld
  Germany

  Contact : Director
  Tél. : 011 49 5323

↳ *St. Petersburg Mining Institute*
Department of Mineralogy, Crystallography and Petrology
21st Line 2
199026 St. Petersburg
Russia

Contact : Yu. B. Marin or Director
Tél. : 011 7 812 218- 8240
Téléc. : 011 7 812 327 7359
E-Mail : mkp@mineral.ras.spb.ru / mkp@mineral.spb.su

↳ *Australian Mineral Foundation Inc.*
63 Conyngham Street
Glenside 5065
South Australia

Contact : Geoff Hudson or Director
Tél. : 011 61 8 8379 0444
Téléc. : 011 61 8 8379 4634
E-Mail : amf@amf.com.au

↳ *Sveriges Geologiska Undersokning*
Box 670
S-75128 Uppsala
Sweden

Contact : Naz Ahmed Shaikh or Technical Advisor
Tél. : 011-46-18-179000
Téléc. : 011-46-18-179210

↳ *Swedish Geotechnical Society*
S-581 93 Linköping
Sweden

Contact : Bengt Rydell or Director
Tél. : 011 46 13 20 18 00
Téléc. : 011 46 13 20 19 14
E-Mail : martre@geotek.se

↳ ***St. Petersburg Mining Institute***
Department of Mineralogy, Crystallography and Petrology
21st Line 2
199026 St. Petersburg
Russia

Contact : Yu. B. Marin or Director
Tél. : 011 7 812 218- 8240
Téléc. : 011 7 812 327 7359
E-Mail : mkp@mineral.ras.spb.ru / mkp@mineral.spb.su

↳ ***Australian Mineral Foundation Inc.***
63 Conyngham Street
Glenside 5065
South Australia

Contact : Geoff Hudson or Director
Tél. : 011 61 8 8379 0444
Téléc. : 011 61 8 8379 4634
E-Mail : amf@amf.com.au

↳ ***Sveriges Geologiska Undersokning***
Box 670
S-75128 Uppsala
Sweden

Contact : Naz Ahmed Shaikh or Technical Advisor
Tél. : 011-46-18-179000
Téléc. : 011-46-18-179210

↳ ***Swedish Geotechnical Society***
S-581 93 Linköping
Sweden

Contact : Bengt Rydell or Director
Tél. : 011 46 13 20 18 00
Téléc. : 011 46 13 20 19 14
E-Mail : martre@geotek.se

↳ *Research in Mining and Environmental Engineering*
Department of Earth Resources Engineering
Prince Consort Road
London SW7 2BP
United Kingdom

Contact : Sevket Durucan or Director
Tél. : 011 44 171 594 7354
Téléc. : 011 44 171 594 7444

↳ *University of Cambridge*
Department of Civil Engineering
United Kingdom

Contact : FH Lee or Director
Tél. : 011 44 772 2274
Téléc. : 011 44 779 1635
E-Mail : cveleefh@nus.sg

↳ *University of Nottingham*
Department of Mineral Resources Engineering
Nottingham, England, NG7 2RD
United Kingdom

Contact : Richard K. Dunham or Director
Tél. : 011 44 115 951 4078
Téléc. : 011 44 115 951 4115

↳ *American Geological Institute*
4220 King Street
Alexandria, VA 22302-1502
USA

Contact : Director
Tél. : 1-703-379-2480

↳ *American Geological Institute*
4220 King Street
Alexandria, VA 22302-1502
USA

Contact : Director
Tél. : 1-703-379-2480
Téléc. : 1-703-379-7563
E-Mail : webmaster@agi.umd.edu

↳ ***Research in Mining and Environmental Engineering***
Department of Earth Resources Engineering
Prince Consort Road
London SW7 2BP
United Kingdom

Contact : Sevket Durucan or Director
Tél. : 011 44 171 594 7354
Téléc. : 011 44 171 594 7444

↳ ***University of Cambridge***
Department of Civil Engineering
United Kingdom

Contact : FH Lee or Director
Tél. : 011 44 772 2274
Téléc. : 011 44 779 1635
E-Mail : cveleefh@nus.sg

↳ ***University of Nottingham***
Department of Mineral Resources Engineering
Nottingham, England, NG7 2RD
United Kingdom

Contact : Richard K. Dunham or Director
Tél. : 011 44 115 951 4078
Téléc. : 011 44 115 951 4115

↳ ***American Geological Institute***
4220 King Street
Alexandria, VA 22302-1502
USA

Contact : Director
Tél. : 1-703-379-2480

↳ ***American Geological Institute***
4220 King Street
Alexandria, VA 22302-1502
USA

Contact : Director
Tél. : 1-703-379-2480
Téléc. : 1-703-379-7563
E-Mail : webmaster@agi.umd.edu

↳ ***St. Petersburg Mining Institute***
Department of Mineralogy, Crystallography and Petrology
21st Line 2
199026 St. Petersburg
Russia

Contact : Yu. B. Marin or Director
Tél. : 011 7 812 218- 8240
Téléc. : 011 7 812 327 7359
E-Mail : mkp@mineral.ras.spb.ru / mkp@mineral.spb.su

↳ ***Australian Mineral Foundation Inc.***
63 Conyngham Street
Glenside 5065
South Australia

Contact : Geoff Hudson or Director
Tél. : 011 61 8 8379 0444
Téléc. : 011 61 8 8379 4634
E-Mail : amf@amf.com.au

↳ ***Sveriges Geologiska Undersokning***
Box 670
S-75128 Uppsala
Sweden

Contact : Naz Ahmed Shaikh or Technical Advisor
Tél. : 011-46-18-179000
Téléc. : 011-46-18-179210

↳ ***Swedish Geotechnical Society***
S-581 93 Linköping
Sweden

Contact : Bengt Rydell or Director
Tél. : 011 46 13 20 18 00
Téléc. : 011 46 13 20 19 14
E-Mail : martre@geotek.se

↳ *St. Petersburg Mining Institute*
Department of Mineralogy, Crystallography and Petrology
21st Line 2
199026 St. Petersburg
Russia

Contact : Yu. B. Marin or Director
Tél. : 011 7 812 218- 8240
Téléc. : 011 7 812 327 7359
E-Mail : mkp@mineral.ras.spb.ru / mkp@mineral.spb.su

↳ *Australian Mineral Foundation Inc.*
63 Conyngham Street
Glenside 5065
South Australia

Contact : Geoff Hudson or Director
Tél. : 011 61 8 8379 0444
Téléc. : 011 61 8 8379 4634
E-Mail : amf@amf.com.au

↳ *Sveriges Geologiska Undersokning*
Box 670
S-75128 Uppsala
Sweden

Contact : Naz Ahmed Shaikh or Technical Advisor
Tél. : 011-46-18-179000
Téléc. : 011-46-18-179210

↳ *Swedish Geotechnical Society*
S-581 93 Linköping
Sweden

Contact : Bengt Rydell or Director
Tél. : 011 46 13 20 18 00
Téléc. : 011 46 13 20 19 14
E-Mail : martre@geotek.se

↳ *Research in Mining and Environmental Engineering*
Department of Earth Resources Engineering
Prince Consort Road
London SW7 2BP
United Kingdom

Contact : Sevket Durucan or Director
Tél. : 011 44 171 594 7354
Téléc. : 011 44 171 594 7444

↳ *University of Cambridge*
Department of Civil Engineering
United Kingdom

Contact : FH Lee or Director
Tél. : 011 44 772 2274
Téléc. : 011 44 779 1635
E-Mail : cveleefh@nus.sg

↳ *University of Nottingham*
Department of Mineral Resources Engineering
Nottingham, England, NG7 2RD
United Kingdom

Contact : Richard K. Dunham or Director
Tél. : 011 44 115 951 4078
Téléc. : 011 44 115 951 4115

↳ *American Geological Institute*
4220 King Street
Alexandria, VA 22302-1502
USA

Contact : Director
Tél. : 1-703-379-2480

↳ *American Geological Institute*
4220 King Street
Alexandria, VA 22302-1502
USA

Contact : Director
Tél. : 1-703-379-2480
Téléc. : 1-703-379-7563
E-Mail : webmaster@agi.umd.edu

- *Research in Mining and Environmental Engineering*
  Department of Earth Resources Engineering
  Prince Consort Road
  London SW7 2BP
  United Kingdom

  Contact : Sevket Durucan or Director
  Tél. : 011 44 171 594 7354
  Téléc. : 011 44 171 594 7444

- *University of Cambridge*
  Department of Civil Engineering
  United Kingdom

  Contact : FH Lee or Director
  Tél. : 011 44 772 2274
  Téléc. : 011 44 779 1635
  E-Mail : cveleefh@nus.sg

- *University of Nottingham*
  Department of Mineral Resources Engineering
  Nottingham, England, NG7 2RD
  United Kingdom

  Contact : Richard K. Dunham or Director
  Tél. : 011 44 115 951 4078
  Téléc. : 011 44 115 951 4115

- *American Geological Institute*
  4220 King Street
  Alexandria, VA 22302-1502
  USA

  Contact : Director
  Tél. : 1-703-379-2480

- *American Geological Institute*
  4220 King Street
  Alexandria, VA 22302-1502
  USA

  Contact : Director
  Tél. : 1-703-379-2480
  Téléc. : 1-703-379-7563
  E-Mail : webmaster@agi.umd.edu

↳ *Canadian Geoscience Council, The*
Department of Earth Sciences
University of Waterloo
Waterloo (Ontario) N2L 3G1
Canada

Contact : Director
Tél. : 1-519-885-1211
Téléc. : 1-519-746-7484

↳ *Canadian Geotechnical Society (CGS)*
170 Atwell Dr., No. 501
Rexdale (Ontario) M9W 5Z5
Canada

Contact : A.G. Stermac or Director
Tél. : 1-416-674-0366
Téléc. : 1-416-674-9507

↳ *Canadian Mining Contractors Association*
120 Railroad St
Brampton (Ontario) L6X 1G8
Canada

Contact : Director
Tél. : 1-905-456-0734
Téléc. : 1-905-456-3784

↳ *Geological Association of Canada, The*
Department of Earth Sciences
Memorial University
Newfoundland (St. John's) A1B 3X5
Canada

Contact : Director
Tél. : 1-709-737-7660
Téléc. : 1-709-737-2532
E-Mail : gac@sparky2.esd.mun.ca

↳ *Geological Survey of Canada*
3303 33rd Street NW
Calgary AB T2L 2A7
Canada

Contact : Grant Mossop or Director
Tél. : 1-403-292-7000
Téléc. : 1-403-292-5377

↳ *Wyoming Mining Association*
1720 W. Linconlnway
Cheyenne, WY 82003
USA

Contact : Director
Tél. : 1-307-635-0331
Téléc. : 1-307-778-6420

↳ *Excavation Engineering and Earth Mechanics Institute*
Department of Mining Engineering
Golden, CO 80401
USA

Contact : Director
Tél. : 1-303-273-3419
Téléc. : 1-303-273-3719

↳ *Global Environmental Institute (GEI)*
P.O. Box 610361
Newton, MA 02161-0361
USA

Contact : Director
Tél. : 1-617-325-6970
Téléc. : 1-617-325-4970

↳ *Kentucky Department of Mines & Minerals*
P.O. Box 14080
Lexington KY 40512-4080
USA

Contact : Burl S. Scott or Technical Advisor
Tél. : 1-606-254-0367
Téléc. : 1-606-233-4243

↳ *MAMTC*
P.O. Box 3362 University Station
Laramie, WY 82071-3362
USA

Contact : Larry R. Stewart or Director
Tél. : 1-307-766-4811
Téléc. :

↳ *Mineral Information Institute*
475, 17th Street, Suite 510
Denver CO 80202
USA

Contact : Jacqueline R. Evanger or Technical Advisor
Tél. : 1-303-297-3226
Téléc. : 1-303-295-6463

↳ *North Dakota Soil Conservation Committee*
600 E. Boulevard Avenue, 18th Floor
Bismarck ND 58505-0790
USA

Contact : Blake Vander Vorst or Technical Advisor
Tél. : 1-701-328-2650
Téléc. : 1-701-328-4143

↳ *Society for Mining, Metallurgy and Exploration Inc.*
P.O. Box 625002
Littleton, C 80162
USA

Contact : Director
Tél. : 1-303-973-9550
Téléc. : 1-303-973-3845
E-Mail : smenet@aol.com

↳ *Source Clay Minerals Repository*
University of Missouri
101 Geological Sciences Bldg.
Columbia, MO 65211
USA

Contact : Director
Tél. : 1-573-882-3785 / 882-6785
Téléc. : 1-314-882-5458

↳ *The Clay Minerals Society*
P.O. Box 4416
Boulder, CO 80306
USA

Contact : Director
Tél. : 1-303-444-6405
Téléc. : 1-303-444-2260
E-Mail : peberl@clays.org

↳ *Mineralogical Society of America*
1015 Eighteenth Street N.W., Suite 601
Washington, DC 20036
USA

Contact : Director
Tél. : 1-202-775-4344
Téléc. : 1-202-775-0018
E-Mail : business@minsocam.org

↳ *Mining and Metallurgical Society of America*
9 Escalle Lane
Larkspur, CA 94939
USA

Contact : Director
Tél. : 1-415-924-7441
Téléc. : 1-415-924-7463

↳ *Montana Bureau of Mines and Geology*
1300 W Park Street
Butte, MT 59701-8997
USA

Contact : Director
Tél. : 1-406-496-4687

↳ *Nevada Bureau of Minses and Geology*
University of Nevada
Mail Stop 178
Reno, NV 89557-0088
USA

Contact : Director
Tél. : 1-702-784-1709

↳ *New Mexico Tech*
Department of Mineral and Environmental Engineering
801 Leroy Place
Socorro, NM 87801
USA

Contact : Director
Tél. : 1-505-835-5345
E-Mail : caimone@nmt.edu

↳ ***University of Alabama***
Department of Geology
202 Bevill Research Building, P.O. Box 870338
Tuscaloosa, Alabama 35487
USA

Contact : Chunmiao Zheng or Director
Tél. : 1-205-348-0579
Téléc. : 1-205-348-0818
E-Mail : czheng@wgs.geo.ua.edu

↳ ***University of Florida***
Department of Geology
1112 Turlington Hall
Gainesville, FL 32611
USA

Contact : Jerry Daughtry or Director
Tél. : 1-352-392-2231
Téléc. : 1-352-392-9294
E-Mail : ufgeoly@nervm.nerdc.ufl.edu

↳ ***University of Oklahoma***
School of Geology and Geophysics
810 Sarkeys Energy Center
Norman, OK 73069
USA

Contact : Director
Tél. : 1-405-325-3253

↳ *North Dakota Soil Conservation Committee*
600 E. Boulevard Avenue, 18th Floor
Bismarck ND 58505-0790
USA

Contact : Blake Vander Vorst or Technical Advisor
Tél. : 1-701-328-2650
Téléc. : 1-701-328-4143

↳ *Society for Mining, Metallurgy and Exploration Inc.*
P.O. Box 625002
Littleton, C 80162
USA

Contact : Director
Tél. : 1-303-973-9550
Téléc. : 1-303-973-3845
E-Mail : smenet@aol.com

↳ *Source Clay Minerals Repository*
University of Missouri
101 Geological Sciences Bldg.
Columbia, MO 65211
USA

Contact : Director
Tél. : 1-573-882-3785 / 882-6785
Téléc. : 1-314-882-5458

↳ *The Clay Minerals Society*
P.O. Box 4416
Boulder, CO 80306
USA

Contact : Director
Tél. : 1-303-444-6405
Téléc. : 1-303-444-2260
E-Mail : peberl@clays.org

Mineralogi
1015 Eight
Washingto
USA

Contact :
Tél. :
Téléc. :
E-Mail :

Mining an
9 Escalle L
Larkspur, (
USA

Contact :
Tél. :
Téléc. :

Montana B
1300 W Pa
Butte, MT
USA

Contact :
Tél. :

Nevada Bu
University (
Mail Stop 1
Reno, NV 8
USA

Contact :
Tél. :

New Mexic
Department
801 Leroy F
Socorro, NM
USA

Contact :
Tél. :
E-Mail :

↪ ***North Dakota Soil Co***
600 E. Boulevard Ave
Bismarck ND 58505-
USA

Contact : Blake Va
Tél. : 1-701-328
Téléc. : 1-701-328

↪ ***Society for Mining, M***
P.O. Box 625002
Littleton, C 80162
USA

Contact : Director
Tél. : 1-303-973
Téléc. : 1-303-973
E-Mail : smenet@

↪ ***Source Clay Minerals***
University of Missouri
101 Geological Scienc
Columbia, MO 65211
USA

Contact : Director
Tél. : 1-573-882
Téléc. : 1-314-882

↪ ***The Clay Minerals So***
P.O. Box 4416
Boulder, CO 80306
USA

Contact : Director
Tél. : 1-303-444
Téléc. : 1-303-444
E-Mail : peberl@cl

↳ ***Associated Mining Consultants Ltd***
910 7th Avenue SW, Suite 1401
Calgary AB T2P 3N8
Canada

Contact : A. L. Craven or Sales Manager
Tél. : 1-403-264-9496
Téléc. : 1-403-269-7640

↳ ***Bechtel Canada Inc.***
200-12 Concorde PI
North York, ON M3C 3T1
Canada

Contact : Sales Manager
Tél. : 1-416-441-4900
Téléc. : 1-416-441-4941

↳ ***Behre Dolbear & Company, Inc.***
145 King Street, Suite 1002
Toronto, Ontario M5H 3X6
Canada

Contact : Sales Manager
Tél. : 1-416-369-9011
Téléc. : 1-416-367-1954

↳ ***Bharti Laamanen Mining Inc.***
131 Fielding Road
Lively, ON P3Y 1L7
Canada

Contact : Sales Manager
Tél. : 1-705-682-3211
Téléc. : 1-705-682-2718

↳ ***Boart Longyear Inc.***
521, ave. Lepine
Dorval PQ H9P
Canada

Contact : Sales Manager
Tél. : 1-514-422-8211
Téléc. : 1-514-422-8212

↳ *Dynatec International*
2 E. Beaver Cr. Road, Unit # 2
Richmond Hill ON L4B 2N3
Canada

Contact : W. M. Shaver or Sales Manager
Tél. : 1-905-886-6950
Téléc. : 1-905-886-8891

↳ *Geostat Systems International Inc.*
500 Tower C, 800 Chomedey Blvd.
Laval, PQ H7V 3Y4
Canada

Contact : Sales Manager
Tél. : 1-514-973-6561 or 800-474-6561
Téléc. : 1-514-973-6070

↳ *Geostat Systems International Inc.*
800 Chomedey Blvd., Tower C, Suite 500
Laval PQ H8V 3Y4
Canada

Contact : Claude Duplessis or Sales Manager
Tél. : 1-514-973-6561
Téléc. : 1-514-973-6070

↳ *Golder Associates ltd*
213-2550 Argentia
Mississauga, ON L5N 5R1
Canada

Contact : Sales Manager
Tél. : 1-905-819-0600
Téléc. : 1-905-819-9922

↳ *HA Simons Ltd*
400-111 Dunsmuit St
Vancouver, BC V6B 5W3
Canada

Contact : Sales Manager
Tél. : 1-604-664-3300
Téléc. : 1-604-664-3301

er
Wackley Road
va ON K1G 3P5
da

ct : Greg Hodges or Sales Manager
1-613-731-9571
: 1-613-731-0453

rn Engineering and Construction Limited
Lake Shore Blvd. West
to ON M8V 1A4
da

ct : J. Calwell or Sales Manager
1-416-252-5311
: 1-416-231-5356

n Tecsult Inc.
e St. Catherine West
éal PQ H2X 3P4
a

ct : Ray Legault or Sales Manager
1-514-287-8520
: 1-514-287-8669

ner Davy Canada
niversity Ave.
to, ON M5G 1V2
a

t : Sales Manager
1-416-340-1145
: 1-416-343-9300

eld Research
ncession St. P.O. Box 430
ld ON K0L 2H0

t : K. Sarbutt or Sales Manager
1-705-652-2000
1-705-652-6365

↳ ***Met-Chem Canada Inc.***
401-425 de Maisonneuve Blvd W.
Montréal, PQ H3A 3G5
Canada

Contact : Sales Manager
Tél. : 1-514-288-5211
Téléc. : 1-514-288-7937

↳ ***Micon International Ltd***
900-390 Bay St
Toronto ON M5H 2Y2
Canada

Contact : Sales Manager
Tél. : 1-416-362-5135
Téléc. : 1-416-362-5763
E-Mail : micon@idirect.com

↳ ***Neil & Gunter Ltd***
PO Box 713
Fredericton, NB E3B 5B4
Canada

Contact : Sales Manager
Tél. : 1-506-452-7000
Téléc. : 1-506-452-0112
E-Mail : ngl@ngl.ca

↳ ***Piteau Associates Engineering Ltd***
215-260 W Esplanade
North Vancouver, BC V7M 3G7
Canada

Contact : Sales Manager
Tél. : 1-604-986-8551
Téléc. : 1-604-985-7286

↳ ***Richard Brummer Associates***
305 St Charles Lake Rd
Sudbury, ON P3E 5G6
Canada

Contact : Sales Manager
Tél. : 1-705-523-8039
Téléc. : 1-705-623-2543
E-Mail : Richard_Brummer@msn.com

↳ *Roberts & Schaefer Co.*
120 South Riverside Plaza
Chicago IL 60606, United States
Canada

Contact : L. R. Johnson or Sales Manager
Tél. : 1-312-236-7292
Téléc. : 1-312-726-2872

↳ *Rust Environment & Infrastructure Inc.*
12 Metro Park Road
Albany NY 12205, United States
Canada

Contact : William Cutcliffe or Sales Manager
Tél. : 1-518-458-1313
Téléc. : 1-518-458-2472

↳ *Stanley Associates Engineering Ltd*
10160 112th St
Edmonton, AB T5K 2L6
Canada

Contact : Sales Manager
Tél. : 1-403-917-7000
Téléc. : 1-403-917-7330

↳ *VB Cook Ltd*
PO Box 936
Thunder Bay, ON P7C 4X8
Canada

Contact : Sales Manager
Tél. : 1-807-625-6700
Téléc. : 1-807-623-4491

↳ *Almes & Associates, Inc., Consulting Engineers*
RD #1, Box 520, PV Road
Trafford PA 15085
USA

Contact : Richard G. Almes or Sales Manager
Tél. : 1-412-744-3610
Téléc. : 1-412-744-3631

- *Colliers & Associates, Inc.*
114 Dennis Drive, Suite A
Lexington KY 40503, United States
USA

Contact : Thomas, W. McClain or Sales Manager
Tél. : 1-606-278-4100
Téléc. : 1-606-277-7843

- *D'Appolonia*
275 Center Road
Monroeville PA 15146-1451, United States
USA

Contact : Eugene C. Palmer or Sales Manager
Tél. : 1-412-856-9440
Téléc. : 1-412-856-9535

- *Dredge Technology Corp.*
P.O. Box 1520
Wayne NJ 07474-1520, United States
USA

Contact : M. Rudd Ouwerkerk or Sales Manager
Tél. : 1-201-696-1559
Téléc. : 1-201-696-3572

- *GZA GeoEnvironmental Technologies, Inc.*
4 Free Street
Portland, ME 04101
USA

Contact : Robert J. Grillo or Sales Manager
Tél. : 1-207-879-9190
Téléc. : 1-207-879-0099

↳ *Société canadienne de génie civil - SCGC*
2050, rue Mansfield, Suite 700
Montréal (Québec) H3A 1Z2
Canada

Contact : E. Gormley ou Directeur
Tél. : 1-514-842-5653
Téléc. : 1-514-842-8123

↳ *European Union of Geosciences (EUG)*
5, rue René Descartes
F-67084 Strasbourg Cedex
France

Contact : M.I. Johnson ou Directeur
Tél. :
Téléc. : 011 33 3 88 353 063

↳ *ICDA*
45, rue de Lisbonne
Paris
France

Contact : Ann Fitzgerald ou Directeur
Tél. : 011-33-140-76-06-89
Téléc. : 011-33-140-76-06-87

↳ *Societe de l'Indsutrie Minerale*
41-47, rue de la Grange aux Belles
Paris 75010
France

Contact : C. Beaumont ou Directeur
Tél. : 011-33-1-4202-0792
Téléc. : 011-33-1-4206-6930

↳ *European Geophysical Society (EGS)*
Max-Planck-Strasse 1
37191 Katlenburg-Lindau
Germany

Contact : Arne K. Richter or Director
Tél. : 011 49 5556 1440
Téléc. : 011 49 55 56 4709

↪ *German Association of International Mining*
Zitelmannstrasse 9-11, D-53113 Bonn
Postfach 12 02 80, Bonn D-53044
Germany

Contact : P. Kausch or Director
Tél. : 011-49-228-23 56 36
Téléc. : 011-49-228-540 02 35

↪ *European Association of Exploration Geophysicists (EAEG)*
Postbus 298
NL-3700 AG Zeist
Netherlands

Contact : E.H. Bornkamp or Director
Tél. : 011 31 3404 626 55
Téléc. : 011 31 3404 626 40

↪ *New Zealand Minerals Industry Association*
P.O. Box 5039, 117-125 Lambton QY
5th Floor, Public Trust Bldg, Wellington
New Zealand

Contact : Douglas Gordon or Director
Tél. : 011 64 4 499 9871
Téléc. : 011 64 4 499 9873

↪ *Bergindustriens Landsforening*
Essendrops gt. 6, 0368
Oslo 0368
Norway

Contact : Niels Chr. Hald or Director
Tél. : 011-47-22965070
Téléc. : 011-47-22965072

↪ *Australian Mineral Foundation inc.*
63, Conyngham St.
Glenside SA 5065
South Australia

Contact : David Pollard or Director
Tél. : 011-61-8-379-0444
Téléc. : 011-61-8-379-4634

↳ *Nordic Association of Applied Geophysics (NAAG)*
University of Lulea
S-951 87 Lulea
Sweden

Contact : Lena Nilsson or Director
Tél. :
Téléc. : 011 46 920 911 99

↳ *Association of British Mining Equipment Companies (ABMEC)*
Royal Victoria Hotel, Station Rd.
Sheffield, S. Yorkshire S4 7YE
United Kingdom

Contact : Director
Tél. : 011 44 114 273 7334
Téléc. : 011 44 114 273 0194

↳ *Association of Geotechnical and Geoenvironmental Specialists*
39 Upper Elmers End Rd.
Beckenham, Kent BR3 3QY
United Kingdom

Contact : D. Jennings or Director
Tél. : 011 44 44 1816 588 212
Téléc. : 011 44 1816 630 949

↳ *British Drilling Association Ltd.*
P.O. Box 113, Brentwood
Essex CM 15 9DS
United Kingdom

Contact : Barry Johnson or Director
Tél. : 011-44-277-373456
Téléc. : 011-44-277-374405

↳ *Council of Mining & Metallurgical Institutions*
44 Portland Place
London W1N 4BR
United Kingdom

Contact : Brian Loton or Director
Tél. : 011-44-171-580-3802
Téléc. : 011-44-171-436-5388

↳ ***Institution of Civil Engineering Surveyors***
26 Market St.
Altrincham WA14 1PF
United Kingdom

Contact : Director
Tél. : 011 44 161 928 8074
Téléc. : 011 44 161 941 6134

↳ ***Institution of Civil Engineers (ICE)***
1 Great George St.
London SW1P 3AA
United Kingdom

Contact : Director
Tél. : 011 44 171 222 7722
Téléc. : 011 44 171 222 7500

↳ ***Institution of Mining Engineers***
Danum House
6A South Parade
Doncaster DN1 2DY
United Kingdom

Contact : D. L. Copeland
Tél. : 011-44-1302-320486
Téléc. : 011-44-1302-340554

↳ ***Minerals Engineering Society***
2 Ryton Close, Blyth
Notts. S81 8DN
United Kingdom

Contact : Andrew Howells or Director
Tél. : 011-44-909-591-787
Téléc. :

↳ ***Association of Engineering Geologists***
323 Boston Post Road, Suite 2D
Sudbury, MA 01776
USA

Contact : Director
Tél. : 1-508-443-4639
Téléc. : 1-508-443-2948
E-Mail : aeghq@aol.com

- *Colorado Mining Association*
  1600 Broadway # 1770
  Denver, CO 80202
  USA

  Contact : Director
  Tél. : 1-303-894-0536
  Téléc. : 1-303-894-8416

- *Expanded Shale, Clay & Slate Institute*
  2225 E. Murray Holladay Rd., #102
  Salt Lake City UT 84117
  USA

  Contact : John Ries or Director
  Tél. : 1-801-272-7070
  Téléc. : 1-801-272-3377

- *Institute of Shaft Drilling Technology*
  1352 SW 175Th
  Seattle, WA 98166
  USA

  Contact : James Friant or Director
  Tél. : 1-206-243-2558
  Téléc. : 1-206-244-7994

- *Mineral Information Institute*
  475, 17th Street, Suite 510
  Denver CO 80202-4015
  USA

  Contact : Jacqueline R. Evanger or Director
  Tél. : 1-303-297-3226
  Téléc. : 1-303-295-6463

- *Mineral Information Institute*
  475 - 17th St, Ste 510
  Denver, CO 80202
  USA

  Contact : Director
  Tél. : 1-303-297-3226
  Téléc. : 1-303-295-6463

↳ *Mining and Metallurgical Society of America*
9 Escalle Lane
Lakespur CA 94939
USA

Contact : Director
Tél. : 1-415-924-7441
Téléc. : 1-415-924-7463

↳ *National Mining Association*
1130, 17th St. NW
Washington DC 20036-4677
USA

Contact : Richard L. Lawson or Director
Tél. : 1-202-463-2625
Téléc. : 1-202-463-6152

↳ *National Mining Association*
1130 17th Street NW
Washington, DC 20036-4677
USA

Contact : Director
Tél. : 1-202-463-2625
Téléc. : 1-202-833-1965

↳ ***Society for Mining, Metallurgy and Exploration, inc.***
P.O. Box 625002, 8307 S. Shaffer Parkway
Littleton CO 80162-5002
USA

Contact : Gary D. Howell or Director
Tél. : 1-303-973-9550
Téléc. : 1-303-973-3845

↳ ***Utah Mining Association inc.***
Kearns bldg., Suite 825, 136 S. Main Street
Salt Lake City UT 84101
USA

Contact : Alexander H. Jordan or Director
Tél. : 1-801-364-1874
Téléc. : 1-801-359-7561

↳ *Centre de géologie de l'ingénieur*
60 blvd. Saint-Michel
F-75272 Paris Cedex 06
France

Contact : Michel Deveughèe ou Directeur
Tél. : 011 33 1 4051 9162
Téléc. : 011 33 1 4326 3656

↳ *Centre d'études des tunnels - CETU*
109 ave. Salvador Allende, B.P. 48
69674 Bron Cedex
France

Contact : Michel Marec ou Directeur
Tél. : 011 33 4 7841 8125
Téléc. : 011 33 4 7237 8111

↳ *Laboratoire Central des ponts et chaussées*
58, blvd. Lefebvre
75732 Paris Cedex 15
France

Contact : François Coste ou Directeur
Tél. : 011 33 1 4043 5000
Téléc. : 011 33 1 4043 5498
E-Mail : Icpc10@calvacom.fr

↳ *Faculty of geoscience, geotechnics and mining*
Institute of Meneralogy
D-09596 Freiberg/Saxony
Brennhausgasse 14
Germany

Contact : Director
Tél. : 011 49 3731 39 2342
Téléc. : 011 49 3731 39 2524

↳ *Institute for Mineralogy and Mineral Resources*
Adloph-Roemer-Str. 2A
D-38678 Clausthal-Zellerfeld
Germany

Contact : Director
Tél. : 011 49 5323

il Science
Agriculture
Str. 4
gen

hristian Ahl or Directo
1 49 551 395 504
1 49 551 395 502
hl@gwdg.de

nical University of At
Mining Engineering a
Campus
thens

Athanasia Economou or
011 30 1 772 2193
011 30 1 772 2194

urvey of the Netherlan
ade 10, Postbus 157
aarlem
s

Chris Staudt or Technica
011-31-23-5300-300
011-31-23-5351-614

icht op de Mijnen
90
Rijswijk
ds

A.K. van der Tuin or Te
011-31-70-3956500
011-31-70-3956555

c

- *University of Ottawa*
  Civil Engineering
  161 Louis Pasteur Street, (A-112), P.O. Box 450, St
  Ottawa (Ontario) K1N 6N5
  Canada

  Contact : Vinod Garga or Director
  Tél. : 1-613-562-5919
  Téléc. : 1-613-562-5173
  E-Mail : garga@eng.uottawa.ca

- *University of Toronto*
  Faculty of Applied Science and Engineering
  Galbraith Building, 35 St. George Street
  Toronto (Ontario) M5S 1A4
  Canada

  Contact : Steven D. Scott or Director
  Tél. : 1-416-978-6554
  Téléc. : 1-416-978-4820

- *University of Toronto*
  Department of Civil Engineering
  35 St. George Street
  Toronto (Ontario) M5S 1A4
  Canada

  Contact : Barry J. Adams or Director
  Tél. : 1-416-978-3096
  Téléc. : 1-416-978-6813

- *University of Waterloo*
  Geotechnical Engineering Group
  Department of Civil Engineering
  Waterloo (Ontario) N2L 3G1
  Canada

  Contact : Leo Rothenburg or Director
  Tél. : 1-519-888-4567, ext. 3759
  Téléc. : 1-519-888-6197
  E-Mail : leoroth@uwaterloo.ca

- *Danish Geological Survey*
  Thoravej 8
  Copenhagen, NV 2400
  Denmark

  Contact : Erik Thomsen or Techn
  Tél. : 011-45-31-10-66-00
  Téléc. : 011-45-31-19-68-68

- *Geological Survey of Finland*
  Betonimiehenkuja 4, P.O. Box 96
  FIN-02151 Espoo
  Finland

  Contact : Matti Saarnisto or Direc
  Tél. : 011 358 205 50 11
  Téléc. : 011 358 205 50 12

- *Geological Survey of Finland*
  Betonimiehenkuja 402150
  Espoo SF-02150
  Finland

  Contact : Veikko Lappalainen or
  Tél. : 011-358-0-46931
  Téléc. : 011-358-0-462205

- *Bureau de Recherches Geologiques*
  B.P. 6009, Cedex 2
  Orleans 45060
  France

  Contact : Francois Le Lann ou Co
  Tél. : 011-33-38-64-33-05
  Téléc. : 011-33-38-64-35-15

- *CEMAGREF Antony Research Gro*
  B.P. 121
  92185 Antony Cedex
  France

  Contact : Directeur
  Tél. : 011 33 1 4096 6121
  Téléc. : 011 33 1 4096 6036

↳ *Canada Centre of Mineral and Energy Technology*
Mining and Mineral Sciences Lab
555 Booth Street
Ottawa (Ontario) K1A 0G1
Canada

Contact : Lesley Dawes or Director
Tél. : 1-613-992-1285
Téléc. : 1-613-947-6606

↳ *Carleton University*
Department of Civil & Environmental Engineering
1125 Colonel By Drive
Ottawa (Ontario) K1S 5B6
Canada

Contact : J.L. Humar or Director
Tél. : 1-613-520-5784
Téléc. : 1-613-520-3951
E-Mail : jhumar@ccs.carleton.ca

↳ *Centre de recherche géotechnique*
McGill University
817, rue Sherbrooke O.
Montréal (Québec) H3A 2K6
Canada

Contact : Directeur
Tél. : 1-514-398-6672
Téléc. : 1-514-398-7361

↳ *Centre d'études sur les ressources minérales*
555, boul. de l'Université
Chicoutimi (Québec) G7H 2B1
Canada

Contact : Directeur
Tél. : 545-5045
Téléc. : 545-5012

↳ *University of Ottawa*
Civil Engineering
161 Louis Pasteur Street, (A-112), P.O. Box 450, Station A
Ottawa (Ontario) K1N 6N5
Canada

Contact : Vinod Garga or Director
Tél. : 1-613-562-5919
Téléc. : 1-613-562-5173
E-Mail : garga@eng.uottawa.ca

↳ *University of Toronto*
Faculty of Applied Science and Engineering
Galbraith Building, 35 St. George Street
Toronto (Ontario) M5S 1A4
Canada

Contact : Steven D. Scott or Director
Tél. : 1-416-978-6554
Téléc. : 1-416-978-4820

↳ *University of Toronto*
Department of Civil Engineering
35 St. George Street
Toronto (Ontario) M5S 1A4
Canada

Contact : Barry J. Adams or Director
Tél. : 1-416-978-3096
Téléc. : 1-416-978-6813

↳ *University of Waterloo*
Geotechnical Engineering Group
Department of Civil Engineering
Waterloo (Ontario) N2L 3G1
Canada

Contact : Leo Rothenburg or Director
Tél. : 1-519-888-4567, ext. 3759
Téléc. : 1-519-888-6197
E-Mail : leoroth@uwaterloo.ca

- *University of Ottawa*
  Civil Engineering
  161 Louis Pasteur Street, (A-112), P.O. Box 450, Station A
  Ottawa (Ontario) K1N 6N5
  Canada

  Contact : Vinod Garga or Director
  Tél. : 1-613-562-5919
  Téléc. : 1-613-562-5173
  E-Mail : garga@eng.uottawa.ca

- *University of Toronto*
  Faculty of Applied Science and Engineering
  Galbraith Building, 35 St. George Street
  Toronto (Ontario) M5S 1A4
  Canada

  Contact : Steven D. Scott or Director
  Tél. : 1-416-978-6554
  Téléc. : 1-416-978-4820

- *University of Toronto*
  Department of Civil Engineering
  35 St. George Street
  Toronto (Ontario) M5S 1A4
  Canada

  Contact : Barry J. Adams or Director
  Tél. : 1-416-978-3096
  Téléc. : 1-416-978-6813

- *University of Waterloo*
  Geotechnical Engineering Group
  Department of Civil Engineering
  Waterloo (Ontario) N2L 3G1
  Canada

  Contact : Leo Rothenburg or Director
  Tél. : 1-519-888-4567, ext. 3759
  Téléc. : 1-519-888-6197
  E-Mail : leoroth@uwaterloo.ca